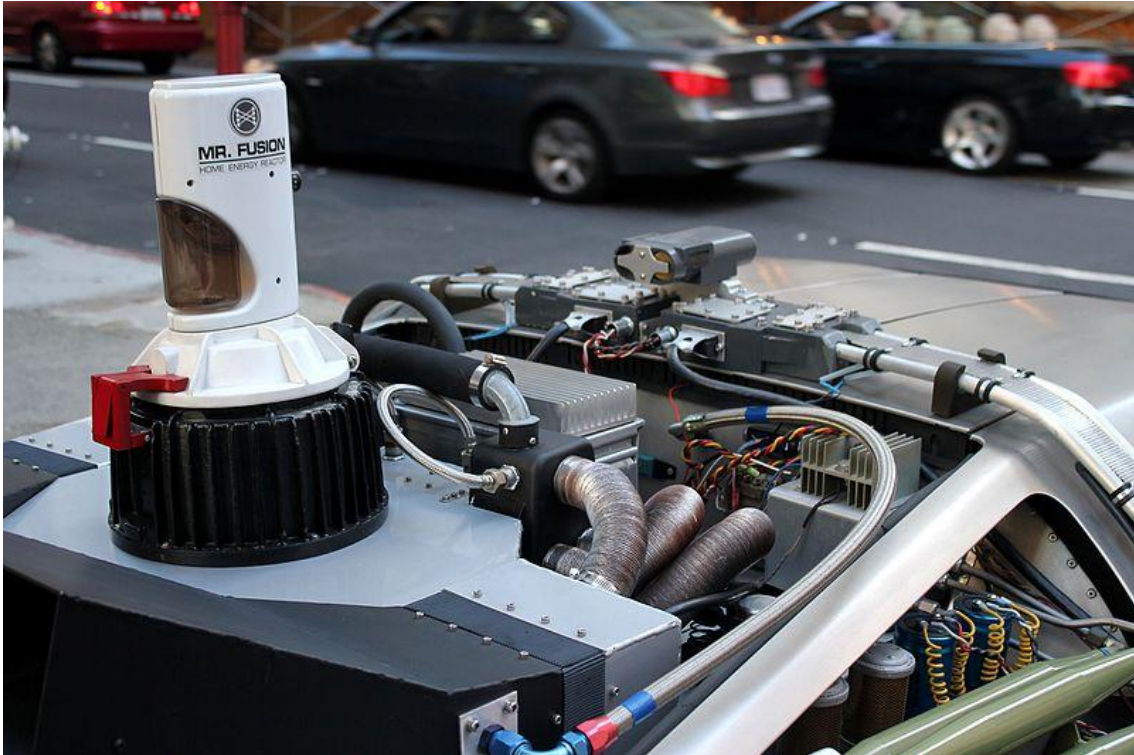


Energy Density



https://upload.wikimedia.org/wikipedia/commons/b/bd/DeLorean_DMC-12_Time_Machine_-_Mr._Fusion.JPG

© 2016-9 Robert A. Freitas Jr. All Rights Reserved.

Cite as: Robert A. Freitas Jr., “Energy Density,” IMM Report No. 50, 25 June 2019;
<http://www.imm.org/Reports/rep050.pdf>.

Table of Contents

Preface.....	5
Chapter 1. Introduction	6
Chapter 2. Energy and Power Density in Natural and Engineered Systems	12
Chapter 3. Thermochemical Energy Storage.....	23
3.1 Sensible Heat	24
3.1.1 Heat Capacity of Solids	28
3.1.2 Heat Capacity of Liquids	32
3.1.3 Heat Capacity of Gases.....	37
3.2 Latent Heat	40
3.2.1 Heat of Fusion.....	41
3.2.2 Heat of Vaporization.....	47
3.2.3 Heat of Sublimation.....	56
3.3 Thermochemical Phase Changes	57
3.3.1 Heat of Solution.....	58
3.3.2 Heat of Crystallization	61
3.3.3 Photoisomer Conversion Energy	64
3.3.4 Allotropic Transition Energy	65
3.3.5 Crystal Structure Phase Transition Energy	67
3.3.6 Other Phase-Change Enthalpies.....	69
3.4 Thermochemical Power Density	71
Chapter 4. Chemical Energy Storage.....	82
4.1 Electrochemical Batteries and Fuel Cells	83
4.1.1 Electrochemical Batteries	84
4.1.2 Fuel Cells	88
4.2 Chemical Fuels and High-Energy Materials	101
4.2.1 Chemical Decomposition and Explosives	104
4.2.2 Nonambient Chemical Combustion.....	111
4.2.3 Ambient Chemical Combustion.....	122
4.2.4 Power Density of Chemical Fuels	133
4.3 Molecular Recombination Energy.....	136
4.3.1 Hydrogen Recombination Energy	138
4.3.1.1 Spin-Polarized Atomic Hydrogen	140
4.3.1.2 Frozen Matrix Trapping	142
4.3.1.3 Endohedral Trapping.....	143
4.3.1.4 Charged Ion Plasma	146
4.3.1.5 Metallic Hydrogen.....	151
4.3.2 Nitrogen Recombination Energy	159
4.3.3 Oxygen Recombination Energy.....	162
4.3.4 Halogen and Other Recombination Energies.....	164

4.4 Excited States, Free Radicals, and Ion Recombination	168
4.4.1 Electronically Excited Metastable States	169
4.4.1.1 Spin-Polarized Triplet Helium	170
4.4.1.2 Other Metastable Species	173
4.4.1.3 Rydberg Matter	178
4.4.2 Free Radical Species	180
4.4.3 Ionized States	182
4.4.3.1 Singly-Ionized Atomic and Molecular Cations	183
4.4.3.2 Multiply-Ionized Atomic and Molecular Cations	188
4.4.3.3 Electron Affinity in Atomic and Molecular Anions	194
4.4.3.4 Ion-Pair Molecules	198
4.5 Atomistic Formation of Solids	200
4.5.1 Covalent Solids	201
4.5.2 Ionic Solids	207
4.5.3 Metallic Solids	209
4.5.4 Hydrogen-Bonded Solids	211
4.5.5 Van der Waals Solids	213
Chapter 5. Mechanical Energy Storage	214
5.1 Pressure	215
5.1.1 Compression of Solids	216
5.1.2 Compression of Liquids	221
5.1.3 Compression of Gases	223
5.1.4 Compression of Plasma	226
5.1.5 Acoustic Waves	227
5.2 Springs	231
5.3 Kinetic Energy	235
5.3.1 Translational Motion	236
5.3.2 Rotational Motion	239
5.4 Thermomechanical Stress	247
Chapter 6. Electromagnetic Energy Storage	251
6.1 Magnetic Fields	252
6.2 Electric Fields	256
6.3 Ambient Electromagnetic Energy	262
6.4 Beamed Electromagnetic Energy	267
6.5 Casimir Effect and Vacuum Energy	269
Chapter 7. Nuclear Energy Storage	271
7.1 Radionuclides	275
7.2 Fission	290
7.3 Fusion	297
7.3.1 Conventional Nuclear Fusion	298
7.3.2 Muon-Catalyzed Fusion	303
7.3.3 Low-Temperature Nuclear Fusion Reactions	307
7.4 Metastable Nuclear Isomers	312

7.5 Exotic Particles and Atoms, and Degenerate Matter	318
7.5.1 Quasiparticles	319
7.5.2 Exotic Atoms	320
7.5.2.1 Muonic Atoms and Muonium	321
7.5.2.2 Hadronic Atoms and Hypernuclear Atoms	324
7.5.3 Double-Charm and Double-Bottom Baryon Fusion	328
7.5.4 Degenerate Matter	329
7.5.4.1 Electron Degenerate Matter (White Dwarf Matter).....	330
7.5.4.2 Neutron Degenerate Matter (Neutronium)	332
7.5.4.3 Quark Degenerate Matter (Quarkium)	334
7.5.4.4 Fully Degenerate Matter.....	337
7.6 Antimatter	338
7.6.1 Annihilation Energy.....	339
7.6.2 Antiparticles and Antielements.....	342
7.6.3 Onium Atoms.....	345
7.6.4 Antimatter Energy Storage	347
Chapter 8. Gravitational Energy Storage	350
8.1 Masses, Orbits, and Pendulums	351
8.2 Extreme Gravity	354
8.2.1 Energy Extraction from Microscale Black Holes	355
8.2.2 Energy Extraction from Stellar Black Holes	358
8.2.3 Supermassive Black Holes.....	361
8.2.4 White Holes	363
8.3 Theoretical and Speculative Forms of Matter	364
Chapter 9. Summary of the Data	370
Appendix A. Compendium of Data Tables	381
A.1 Data on Energy Storage in Nature	382
A.2 Data on Power Generation in Nature	389
A.3 Data on Energy Storage in Chemical Decomposition	402
A.4 Data on Energy Storage in Chemical Combustion Fuels	442
A.5 Data on Energy Storage in Radionuclides	512
A.6 Data on Energy Storage in Spontaneous Fission	515

Preface

The primary purpose of this book is to survey a wide range of energy and power sources, including current, near-term, proposed, bleeding-edge, and speculative (fun!) possibilities. The focus is almost exclusively on two principal performance measures – energy per unit mass (specific energy) and energy per unit volume (energy density) – as opposed to other practical energy-related measures such as cost, safety, ease of use with existing technologies, or regulatory approval.

This book differs from standard engineering reference materials that emphasize current commercial methods for energy storage. It is intended as a much broader survey, including such exotic methods as molecular recombination energy, metastable nuclear isomers, and antimatter, in addition to more conventional energy storage options such as batteries, combustibles and explosives.

A number of examples from nanoengineering (e.g., nanorobotics) are included because one of the motivations of writing the book is to survey opportunities for future nanotechnology development. This work is in some ways an extension of previously-published material on energy sources for atomically precise molecular machine systems,¹ providing a much more comprehensive survey of possible design choices and identifying a few particularly good candidates for nanomachine applications. Another motivation is to establish the operational energy limits, within known science, of proposed power supplies for future macroscale applications (e.g., flying cars, self-sufficient houses, closed-cycle space suits, etc.).

The book includes 62 numerical tables and 15 charts, many with extensive explanatory information and references for each item listed. There is an attempt to calculate energy density and specific energy data in an internally consistent manner and to present that data in a format that allows easy “apples to apples” comparisons. Other sources (e.g., Wikipedia,² Google,³ Google Scholar,⁴ WolframAlpha⁵) may be less consistent, less transparent, less convenient, or less comprehensive in their coverage of the possibilities.

Acknowledgements. The author thanks Tad Hogg and Michael Shawn Marshall for useful comments, suggestions, bits of information, and critiques of earlier versions of this manuscript. Any remaining errors or other shortcomings of this text are solely the responsibility of the author.

¹ Freitas RA Jr., Nanomedicine, Volume I: Basic Capabilities, Landes Bioscience, Georgetown, TX, 1999, Chapter 6, “Power”; <http://www.nanomedicine.com/NMI/6.1.htm>.

² https://en.wikipedia.org/wiki/Energy_density#Table_of_energy_content,
https://en.wikipedia.org/wiki/Energy_density_Extended_Reference_Table.

³ <https://www.google.com/search?q=%22energy+density%22>.

⁴ <https://scholar.google.com/scholar?hl=en&q=energy+density>.

⁵ <https://www.wolframalpha.com/input/?i=%22energy+density%22>.

Chapter 1. Introduction

Energy is the ultimate driver of all physical action. Power, the time rate at which energy is released or consumed, determines the magnitude of physical action that can occur in a given time period. The more energy that is available, the more physical action can be sustained. The more power that is available, the larger the magnitude of physical action that can occur in a given time period, or the longer a given physical action can be maintained.

Energy can be stored in, or released from storage by, physical systems. All physical systems have volume and mass.⁶ Hence all energy storage systems⁷ can be characterized by their energy/volume or energy/mass ratios, and all power generating systems can be characterized by their power/volume or power/mass ratios. Physical systems with higher ratios represent more resource-efficient energy storage or power generating systems for the given volume or mass employed. Note that some power generating systems must be paired with an energy storage system in order to function (e.g., an internal combustion engine and a tank of gasoline) while other power generating systems need not be (e.g., photoelectric solar panels).

The mass requirement for an energy storage or power generating system is important to minimize in many applications. For example, in the case of cars, trucks, trains, watercraft, aircraft and spacecraft – wherein the energy store and the power generator must be moved along with the transportation device – the combined system can move for greater total distances and attain higher accelerations if energy per unit mass and power per unit mass is maximized. In other applications, the volume requirement may be more important to minimize. For example, immobile power supplies such as backup generators or batteries inside PCs may be more constrained by available volume than the need to minimize mass. Machines that must locomote in fluids will generally prefer to minimize powerplant mass when the Reynolds number is high (i.e., inertial forces \gg viscous forces, as in submarines) but to minimize powerplant volume when Reynolds number is low (i.e., inertial forces \ll viscous forces, as in microscale swimmers). Onboard volume may be a scarce resource in medical nanorobots because devices that must pass through bloodstream capillaries cannot much exceed ~ 3 microns in size in at least two of three dimensions, favoring maximum powerplant energy/volume and power/volume ratios.⁸

This book surveys all major fundamental classes of energy storage and primary power generation, identifying in each class the physical systems possessing the highest **energy density**⁹ (energy/volume ratio, measured in megajoules per liter or MJ/L), **specific energy**¹⁰ (energy/mass

⁶ Energy can be stored in the form of massless particles such as photons (**Chapter 6**), but as far as we know it is not possible to create physical systems (e.g., machines) comprised entirely of such particles, able to store the energy contained in such particles, with the possible theoretical exception of geons (**Section 8.3**).

⁷ https://en.wikipedia.org/wiki/Energy_storage.

⁸ Freitas RA Jr., Nanomedicine, Volume I: Basic Capabilities, Landes Bioscience, Georgetown, TX, 1999, Section 6.5.4, “Selection of Principal Power Source”; <http://www.nanomedicine.com/NMI/6.5.4.htm>.

⁹ https://en.wikipedia.org/wiki/Energy_density.

¹⁰ https://en.wikipedia.org/wiki/Specific_energy.

ratio, measured in megajoules per kilogram or MJ/kg), **power density**¹¹ (power/volume ratio, measured in megawatts per liter or MW/L), or **specific power**¹² (power/mass ratio, measured in megawatts per kilogram or MW/kg).¹³ For energy storage or power systems composed of ordinary solid matter ($\rho_{\text{normal}} \sim 1 \text{ kg/L}$), specific energy or power per kg will be numerically similar to energy and power densities per liter.

As a point of reference for nanoengineers interested in molecular machine systems, operating nanomechanical systems may dissipate power in the **0.1-1000 MW/L** power density range. For example, a simple nanosieve¹⁴ for separating molecules based on size and shape may have a power density of **~0.08 MW/L** for large molecules ($\sim 10 \text{ nm}$ molecules, $\sim 5.9 \times 10^7$ molecules/sec) or **~0.8 MW/L** for small molecules ($\sim 0.64 \text{ nm}$ molecules, $\sim 1.5 \times 10^9$ molecules/sec); each unit of a diffusion cascade system,¹⁵ if held to a **~1 MW/L** limit, can process $\sim 10^6$ small molecules/sec; telescoping nanorobotic manipulators¹⁶ $\sim 100 \text{ nm}$ in length may dissipate **~1 MW/L** ($\sim 0.96 \text{ MW/kg}$) in continuous operation at a $\sim 1 \text{ cm/sec}$ arm speed; classic sorting rotors¹⁷ typically dissipate up to **~10 MW/L** ($\sim 6.9 \text{ MW/kg}$) when operated at full speed ($\sim 10^5 \text{ rev/sec}$); a nanomechanical apparatus for performing production mechanosynthetic chemical transformations¹⁸ may require $\sim 8 \text{ MW/kg}$ (**~12 MW/L**); transporter pumps¹⁹ transporting $\sim 10^6$ molecules/sec may draw $\sim 30 \text{ MW/kg}$ (**~45 MW/L**); a $\sim 1 \text{ GHz}$ rod-logic-based mechanical

¹¹ aka. “volume power density”; https://en.wikipedia.org/wiki/Power_density.

¹² See also the closely-related “power-to-weight” ratio; https://en.wikipedia.org/wiki/Power-to-weight_ratio.

¹³ These units were chosen to be intuitively meaningful to the reader. To convert energy or power density in MJ/L or MW/L to standard mks units, simply multiply by 10^9 to obtain J/m^3 or W/m^3 . To convert specific energy or specific power in MJ/kg or MW/kg to standard mks units, multiply by 10^6 to obtain J/kg or W/kg .

¹⁴ Freitas RA Jr., Nanomedicine, Volume I: Basic Capabilities, Landes Bioscience, Georgetown, TX, 1999, Section 3.3.1, “Simple Nanosieving”; <http://www.nanomedicine.com/NMI/3.3.1.htm>.

¹⁵ Freitas RA Jr., Nanomedicine, Volume I: Basic Capabilities, Landes Bioscience, Georgetown, TX, 1999, Section 3.2.4, “Diffusion Cascade Sortation”; <http://www.nanomedicine.com/NMI/3.2.4.htm>.

¹⁶ Freitas RA Jr., Nanomedicine, Volume I: Basic Capabilities, Landes Bioscience, Georgetown, TX, 1999, Section 9.3.1.4, “Telescoping Manipulators”; <http://www.nanomedicine.com/NMI/9.3.1.4.htm>. Drexler KE. Nanosystems: Molecular Machinery, Manufacturing, and Computation, John Wiley & Sons, New York, 1992, pp. 406-7; http://e-drexler.com/d/09/00/Drexler_MIT_dissertation.pdf.

¹⁷ Freitas RA Jr., Nanomedicine, Volume I: Basic Capabilities, Landes Bioscience, Georgetown, TX, 1999, Section 3.4.2, “Sorting Rotors”; <http://www.nanomedicine.com/NMI/3.4.2.htm>.

¹⁸ Drexler KE. Nanosystems: Molecular Machinery, Manufacturing, and Computation, John Wiley & Sons, New York, 1992, p. 397; http://e-drexler.com/d/09/00/Drexler_MIT_dissertation.pdf.

¹⁹ Freitas RA Jr., Nanomedicine, Volume I: Basic Capabilities, Landes Bioscience, Georgetown, TX, 1999, Section 3.4.1, “Transporter Pumps”; <http://www.nanomedicine.com/NMI/3.4.1.htm>.

nanocomputer²⁰ may draw **~1000 MW/L** (~640 MW/kg) of power; and a nanocentrifuge²¹ dissipates up to **~1500 MW/kg** (**~1200 MW/L**) when operated at ~20% of its bursting speed. Cooling systems for macroscopic volumes of nanomachinery have been proposed to deal with power densities up to **~100 MW/L**.²²

Macroscale systems and products containing atomically precise components may have power densities ranging from as low as **~5 x 10⁻⁷ MW/L** (~0.00010 MW/kg) for seagoing carbon-capture paddleboats²³ to **~2.6 x 10⁻⁵ MW/L** (~0.00130 MW/kg) for a mature desktop nanofactory,²⁴ **~2.9 x 10⁻⁵ MW/L** (~0.00005 MW/kg) for a whiskey-synthesizing machine,²⁵ and, for medical nanorobots, **~0.00605 MW/L** (resting) to **~0.12 MW/L** (peak) for respirocytes (artificial red cells),²⁶ up to **~0.032 MW/L** (~0.03140 MW/kg) for microbivores (artificial white cells),²⁷ and up to **~0.0029 MW/L** (~0.00253 MW/kg) for chromalloytes (cell repair machines).²⁸

Leaving aside operating speed, assembling larger diamondoid structures from atomically precise 1-nm precursor cubes may require a specific energy up to **~9 MJ/kg**, although energy recovery techniques might reduce the cost of block assembly of larger structures to as low as **~0.5-1.0**

²⁰ Freitas RA Jr., *Nanomedicine, Volume I: Basic Capabilities*, Landes Bioscience, Georgetown, TX, 1999, Section 10.2.1, "Nanomechanical Computers"; <http://www.nanomedicine.com/NMI/10.2.1.htm>. Drexler KE. *Nanosystems: Molecular Machinery, Manufacturing, and Computation*, John Wiley & Sons, New York, 1992, p. 370; http://e-drexler.com/d/09/00/Drexler_MIT_dissertation.pdf.

²¹ Freitas RA Jr., *Nanomedicine, Volume I: Basic Capabilities*, Landes Bioscience, Georgetown, TX, 1999, Section 3.2.5, "Nanocentrifugal Sortation"; <http://www.nanomedicine.com/NMI/3.2.5.htm>.

²² Drexler KE. *Nanosystems: Molecular Machinery, Manufacturing, and Computation*, John Wiley & Sons, New York, 1992; Sec.11.5 "Convective cooling systems," pp. 330-332; http://e-drexler.com/d/09/00/Drexler_MIT_dissertation.pdf.

²³ Freitas RA Jr. *The Nanofactory Solution to Global Climate Change: Atmospheric Carbon Capture*. IMM Report No. 45, Dec 2015; <http://www.imm.org/Reports/rep045.pdf>.

²⁴ Drexler KE. *Nanosystems: Molecular Machinery, Manufacturing, and Computation*, John Wiley & Sons, New York, 1992; Sec.14.4 "An exemplar manufacturing system architecture," pp. 425-426; http://e-drexler.com/d/09/00/Drexler_MIT_dissertation.pdf.

²⁵ Freitas RA Jr. *The Whiskey Machine: Nanofactory-Based Replication of Fine Spirits and Other Alcohol-Based Beverages*. IMM Report No. 47, May 2016; <http://www.imm.org/Reports/rep047.pdf>.

²⁶ Freitas RA Jr. *Exploratory Design in Medical Nanotechnology: A Mechanical Artificial Red Cell*. *Artif Cells Blood Subst Immobil Biotech*. 1998;26:411-430; <http://www.foresight.org/Nanomedicine/Respirocytes.html>.

²⁷ Freitas RA Jr. *Microbivores: Artificial Mechanical Phagocytes using Digest and Discharge Protocol*. *J Evol Technol*. 2005 Apr;14:55-106; <http://www.jetpress.org/volume14/freitas.pdf>.

²⁸ Freitas RA Jr. *The Ideal Gene Delivery Vector: Chromalloytes, Cell Repair Nanorobots for Chromosome Replacement Therapy*. *J Evol Technol*. 2007 Jun;16:1-97; <http://jetpress.org/v16/freitas.pdf>.

MJ/kg.²⁹ The mechanosynthetic production of such precursor cubes may require between **~0.1 MJ/kg** (using fully reversible chemical transformations) and **~100 MJ/kg** (fully irreversible); depending on computation, materials handling, and other requirements in a particular implementation. Assembling prefabricated diamondoid part-like or module-like components into larger structures will probably cost **~13 MJ/kg** of energy.³⁰

It is of great interest to examine the practical upper limits to controllable energy storage and power generation, especially given the future availability of molecular manufacturing and the coming ability to build machines composed of atomically precise materials and mechanisms. However, we usually will not focus on the efficiency of energy storage, production, or conversion, which is an entirely different question than raw energy density or power density.

We also do not explore technologies for energy recovery³¹ (e.g., regenerative braking)³² or issues involving the thermodynamically reversible³³ operation of machines (for which there is an extensive literature in the field of computation),³⁴ but focus almost exclusively on irreversible³⁵ or dissipative energy use. That is, the discussion is usually concerned with thermodynamically “free energy” that can, in principle, be extracted and put to use, i.e., to perform work.³⁶ Of course, energy storage can be useful to temporarily hold recoverable energy, such as the gravitational potential energy stored in an elevator counterweight when the elevator is on the ground floor and the counterweight is near the top of the building (**Section 8.1**), or in capacitors in electric circuits (**Section 6.2**). In some nanoscale machine systems,³⁷ the energy required to go over potential barriers (recoverable) can be 100-fold higher than the energy lost to friction (unrecoverable).

²⁹ Freitas RA Jr., *Nanomedicine, Volume I: Basic Capabilities*, Landes Bioscience, Georgetown, TX, 1999, Section 6.5.6, “Power Analysis in Design”; <http://www.nanomedicine.com/NMI/6.5.6.htm>.

³⁰ Freitas RA Jr., *Nanomedicine, Volume I: Basic Capabilities*, Landes Bioscience, Georgetown, TX, 1999, Section 6.5.6, “Power Analysis in Design”; <http://www.nanomedicine.com/NMI/6.5.6.htm>.

³¹ https://en.wikipedia.org/wiki/Energy_recovery.

³² https://en.wikipedia.org/wiki/Regenerative_brake.

³³ [https://en.wikipedia.org/wiki/Reversible_process_\(thermodynamics\)](https://en.wikipedia.org/wiki/Reversible_process_(thermodynamics)).

³⁴ https://en.wikipedia.org/wiki/Reversible_computing.

³⁵ https://en.wikipedia.org/wiki/Irreversible_process.

³⁶ For example, an ocean of room-temperature water has lots of internal energy that is not extractable at room temperature, whereas it would have lots of recoverable energy in a cryogenic environment – a case where (recoverable) energy density depends on the circumstances rather than being “intrinsic” to the system.

³⁷ Hogg T, Moses M, Allis D. Evaluating the friction in rotary joints in molecular machines. *Mol Syst Des Eng.* 2017;2:235-252; <http://pubs.rsc.org/en/content/articlehtml/2017/me/c7me00021a>.

Energy density is an intrinsic property,³⁸ a scale-invariant property³⁹ of a given quantity of matter.⁴⁰ Power density, on the other hand, is an extrinsic property, varying according to the circumstances under which the latent energy is released (thus requiring assumptions about system size and geometry). Consider a molecule of gasoline (e.g., octane hydrocarbon). It has a mass of m and releases energy E when combusted with oxygen, a chemical reaction that requires a time t to complete. The specific energy of a single molecule of gasoline under combustion is then E/m (MJ/kg) and the specific power of a single molecule of gasoline is E/mt (MW/kg). Now consider a gallon of gasoline, containing N ($\sim 10^{25}$) molecules of gasoline. The specific energy of gasoline remains the same, at E/m , because specific energy is an intrinsic property. However, the specific power of the gallon of gasoline depends entirely on the circumstances under which the combustion occurs. If all of the gasoline molecules are ignited simultaneously, then the maximum specific power is attained, at $NE/Nmt = E/mt$ (MW/kg). But if the molecules are ignited sequentially, one at a time, then a much lower specific power is attained, at E/Nmt (MW/kg). Similarly, the energy density of a wire carrying electrical current is a constant regardless of the length of the wire (**Section 6.2**), whereas the power density is a function of the length of the wire.

Fission power is one exception to this general rule, since isolated or subcritical masses of radionuclides decay with a particular half-life, giving rise to an intrinsic power density for the material. Of course, fission reactions can be artificially suppressed or enhanced – the best example of which is the nuclear chain reaction, wherein packing large numbers of $^{235}\text{U}_{92}$ atoms into a dense ball may cause its power generation to rise astronomically, even explosively (**Section 7.1**). Hence a more general rule may be stated: When energy can be released from a stored source independently of time, then no intrinsic power density or specific power exists because the energy can be released on any schedule desired, enabling a higher power density over a shorter duration or vice versa. An intrinsic power density or specific power can be specified only when stored energy must be released on a fixed schedule (or within narrow limits of time).

³⁸ “Intrinsic” and “extrinsic” properties as used in engineering (https://en.wikipedia.org/wiki/Intrinsic_and_extrinsic_properties) can be distinguished from “intensive” and “extensive” properties as used in thermodynamics (https://en.wikipedia.org/wiki/Intensive_and_extensive_properties). Thermodynamic variables can be “intensive” variables (e.g., temperature, pressure, density, specific heat) that don’t depend on the amount of material, or “extensive” variables (e.g., volume, mass, heat capacity) that do. Lemons DS, Mere Thermodynamics, JHU Press, 2009, pp. 14, 64-5, 73, 91, 122; <https://books.google.com/books?hl=en&lr=&id=WFZf2G80tNcC&oi=fnd&pg=PA122>.

³⁹ That is, not dependent upon the size or volume of the object, or upon how much material (e.g., mass) is present; https://en.wikipedia.org/wiki/Intrinsic_and_extrinsic_properties.

⁴⁰ Density is an example of an “intrinsic” property of an object that can vary with temperature or pressure, hence altering the energy per unit volume or energy density of that object. Definitionally, we could consider kinetic energy to be an example of an extrinsic property that depends on another object (https://en.wikipedia.org/wiki/Intrinsic_and_extrinsic_properties), since the kinetic energy of an object depends on how fast it is moving relative to the user of that energy.

Batteries are another special case. Batteries typically have a characteristic optimal discharge rate and capacity. As noted in **Section 4.1.1**, batteries can often be discharged more quickly but at the cost of lower capacity (the total amount of charge delivered).⁴¹

The fundamental major classes of energy storage and primary generation surveyed in this book include energy and power density in various natural and engineered systems (**Chapter 2**) and in specific classes of energy storage systems including thermochemical energy (**Chapter 3**), chemical energy (**Chapter 4**), mechanical energy (**Chapter 5**), electromagnetic energy (**Chapter 6**), nuclear energy (**Chapter 7**), and gravitational energy (**Chapter 8**).

The book concludes with a summary of the data in **Chapter 9**. Summary scatterplot charts of energy density vs. specific energy are provided for thermochemical (**Figure 2**), chemical (**Figure 3**), mechanical (**Figure 4**), and nuclear (**Figure 5**) energy storage, with a collective chart in **Figure 6**. Similar summary charts of power density vs. specific power are provided for batteries and fuel cells (**Figure 7**), alpha-emitting radionuclides (**Figure 8**), spontaneous fission and RTGs (**Figure 9**), nuclear isomers (**Figure 10**), and nuclear bombs and catalyzed fusion (**Figure 11**), with a collective chart in **Figure 12**. Scatterplot charts comparing specific energy vs. specific power (**Figure 13**) and energy density vs power density (**Figure 14**), along with bar charts summarizing specific energy (**Figure 15**) and energy density (**Figure 16**) for most of the major energy storage modalities described in this book, are also provided in **Chapter 9**.

Some excellent recent literature is available on the related subject of high energy density physics, which is an area of active current research.⁴²

⁴¹ https://en.wikipedia.org/wiki/Peukert's_law.

⁴² Fortov VA. Extreme States of Matter. High Energy Density Physics. Second Edition, Springer, 2018; <https://www.amazon.com/Extreme-States-Matter-Springer-Materials/dp/3319792636/>.

Chapter 2. Energy and Power Density in Natural and Engineered Systems

In this Chapter, we briefly summarize energy storage and power generation in various familiar natural systems, including nuclear and atomic systems (e.g., radionuclide atoms), biological systems (e.g., plants, animals, and microbes), planet-wide physical systems (e.g., weather, geological events), and astronomical systems (e.g., planets, stars, galaxies, and beyond) to provide some context and appropriate comparisons. Data are included below for the energy density (**Table 1**), specific energy (**Table 2**), power density (**Table 3**), and specific power (**Table 4**) of natural systems. This is followed by a brief summary of the energy density, specific energy, and specific power attained in conventional contemporary engineered systems including a variety of engines, batteries, and vehicles (**Table 5**).

A few observations:

(1) Conventional wind energy (including hurricanes and tornadoes), tidal energy (marine tidal oscillations), geothermal energy (including tidal and radioactive internal heating, earthquakes, and volcanoes), and gravitational hydroelectric energy (dam reservoirs) generally have extremely low ratios, thus are poor candidates for maximizing energy or power density.

(2) Lightning bolts exhibit good power density but are too short-lived to provide a reliable energy source.

(3) Cosmic rays provide high energy density but their flux is too low to provide a useful power source. For example, low-energy 10^{11} eV cosmic rays have a local flux of $1 \text{ ray/m}^2\text{-sec}$,⁴³ a surface power density of only $2 \times 10^{-8} \text{ W/m}^2$ or $\sim 10^{-11}$ the intensity of sunlight. High-energy 10^{19} eV cosmic rays have a local flux of $3 \times 10^{-14} \text{ ray/m}^2\text{-sec}$, a surface power density of only $5 \times 10^{-14} \text{ W/m}^2$ or $\sim 10^{-17}$ the intensity of sunlight.⁴⁴

(4) Biological systems have higher power densities than normal astronomical stars of all classes, but both systems provide unimpressive ratios.

(5) Not surprisingly, the cosmic egg or “ylem” that initiated the Big Bang has the highest estimated theoretical energy and power density.

⁴³ https://en.wikipedia.org/wiki/Cosmic_ray.

⁴⁴ The Greisen-Zatsepin-Kuzmin Limit (aka. GZK Limit) is a theoretical limit on the energy of cosmic ray nuclei traveling from other galaxies through the intergalactic medium to our galaxy, wherein cosmic rays exceeding the energy limit would interact with cosmic microwave background photons, producing pions that would rapidly decay into other particles, slowly draining the cosmic ray energies until they fell below the limit (https://en.wikipedia.org/wiki/Greisen-Zatsepin-Kuzmin_limit). The GZK Limit is 5×10^{19} eV (~ 8 J) for protons and 2.8×10^{21} eV (450 J) for iron nuclei (the heaviest abundant element in cosmic rays); either limit corresponds to a specific energy of $5 \times 10^{21} \text{ MJ/kg}$ for ultra-high-energy cosmic rays (https://en.wikipedia.org/wiki/Ultra-high-energy_cosmic_ray).

It is perhaps amusing to consider the theoretical measurable limits of our ratios of concern, assuming physics as we currently understand it is fundamentally correct.⁴⁵ In this case, the smallest measurable energy E_{\min} might be defined by Heisenberg's uncertainty principle as $E_{\min} = h / 4 \pi t_{\max} = 1.2117 \times 10^{-32}$ J, where $h = 6.6261 \times 10^{-34}$ J/sec (Planck's constant)⁴⁶ and t_{\max} is the longest measurable time $\sim 4.3517 \times 10^{17}$ sec, the estimated current age of the Universe.⁴⁷ (This conveniently defines the minimum measurable mass as $M_{\min} = E_{\min}/c^2 = 1.3482 \times 10^{-69}$ kg, where $c = 2.9979 \times 10^8$ m/sec, the speed of light.⁴⁸)

A similar calculation for the smallest measurable time yields $t_{\min} = h / 4 \pi E_{\max} = 4.06 \times 10^{-105}$ sec, taking E_{\max} as the estimated total mass-energy of the universe $\sim M_U c^2 = 1.31 \times 10^{70}$ J, where the maximum measurable mass $M_{\max} = M_U = 1.46 \times 10^{53}$ kg (the total mass of the observable baryonic universe).⁴⁹ However, it can be argued that the smallest measurable time in our physical universe may be governed by a more restrictive constraint – the speed of light – which implies that the smallest measurable time is that which is required for the fastest known particle (the photon, travelling at the speed of light) to traverse the Planck length⁵⁰ ($L_{\text{Planck}} = 1.616 \times 10^{-35}$ m), which is sometimes asserted to be the shortest measurable length, giving a revised estimated of $t_{\text{Planck}} = 5.39 \times 10^{-44}$ sec, aka. the Planck time.⁵¹ The minimum measurable volume V_{\min} is then the Planck volume or $V_{\text{Planck}} = L_{\text{Planck}}^3 = 4.22 \times 10^{-105}$ m³, and the maximum measurable volume is that of the observable universe,⁵² or $V_{\max} = V_{\text{Universe}} \sim 3.58 \times 10^{80}$ m³. These estimates suggest the following ultimate measurable limits for our ratios of interest:

$$\begin{aligned} \text{Minimum energy density } E_{D,\min} &= E_{\min} / V_{\max} = 3.38 \times 10^{-142} \text{ MJ/L} \\ \text{Maximum energy density } E_{D,\max} &= E_{\max} / V_{\min} = 3.10 \times 10^{165} \text{ MJ/L} \end{aligned}$$

$$\begin{aligned} \text{Minimum specific energy } E_{S,\min} &= E_{\min} / M_{\max} = 8.30 \times 10^{-112} \text{ MJ/kg} \\ \text{Maximum specific energy } E_{S,\max} &= E_{\max} / M_{\min} = 9.72 \times 10^{132} \text{ MJ/kg} \end{aligned}$$

$$\begin{aligned} \text{Minimum power density } P_{D,\min} &= E_{D,\min} / t_{\max} = 7.77 \times 10^{-160} \text{ MW/L} \\ \text{Maximum power density } P_{D,\max} &= E_{D,\max} / t_{\text{Planck}} = 5.75 \times 10^{208} \text{ MW/L} \end{aligned}$$

$$\begin{aligned} \text{Minimum specific power } P_{S,\min} &= E_{S,\min} / t_{\max} = 1.92 \times 10^{-129} \text{ MW/kg} \\ \text{Maximum specific power } P_{S,\max} &= E_{S,\max} / t_{\text{Planck}} = 1.80 \times 10^{176} \text{ MW/kg} \end{aligned}$$

It is unknown if these ultimate measurable limits, spanning more than 300 orders of magnitude, have any direct or practical consequences.

⁴⁵ We're also assuming that the total mass-energy of the universe is not essentially zero – e.g., because positive values from matter are counterbalanced by negative gravitational potential, or because of the existence of large amounts of antimatter or negative matter (**Section 8.3**) beyond our observational horizon.

⁴⁶ https://en.wikipedia.org/wiki/Planck_constant.

⁴⁷ https://en.wikipedia.org/wiki/Age_of_the_universe (13.799 x 10⁹ years).

⁴⁸ https://en.wikipedia.org/wiki/Speed_of_light.

⁴⁹ https://en.wikipedia.org/wiki/Observable_universe#Estimates_based_on_critical_density.

⁵⁰ https://en.wikipedia.org/wiki/Planck_length.

⁵¹ https://en.wikipedia.org/wiki/Planck_time.

⁵² https://en.wikipedia.org/wiki/Observable_universe#Estimates_based_on_critical_density.

Table 1. Energy density of natural systems ⁵³			
Natural Systems	Energy Density (MJ/L)	Natural Systems	Energy Density (MJ/L)
<u>Nuclear and Atomic</u>		<u>Astronomical</u>	
Most energetic cosmic ray known	1.82×10^{37}	Ylem (cosmic egg)	3.10×10^{165}
Polonium-210 radionuclide	2.24×10^7	Quantum vacuum energy (Planck)	5.80×10^{102}
Gadolinium-148 radionuclide	1.64×10^7	Evap BH: ~10-m boulder ($\sim 10^{-24} M_{\text{solar}}$)	6.43×10^{75}
Europium-147 radionuclide	1.00×10^7	Evap BH: ~1 km meteor ($\sim 10^{-18} M_{\text{solar}}$)	6.43×10^{63}
Francium-215 radionuclide	9.16×10^6	Evap BH: Asteroidal ($\sim 10^{-12} M_{\text{solar}}$)	6.43×10^{51}
Neodymium-144 radionuclide	8.59×10^6	Evap BH: Planetary ($\sim 10^{-6} M_{\text{solar}}$)	6.43×10^{39}
Rest mass energy of one H ₂ molecule	8.12×10^6	Quark nova	1.00×10^{28}
Chemical bond energy, H ₂ molecule	1.93×10^2	Quark nova	1.00×10^{28}
Thermal energy, H ₂ molecule at STP	1.52×10^4	Evap BH: Stellar ($\sim 1 M_{\text{solar}}$)	6.43×10^{27}
<u>Biological</u>		Quantum vacuum energy (Compton)	1.30×10^{23}
Fat (oxidation, excluding O ₂)	4.11×10^1	Binary black hole merger	1.38×10^{22}
Glucose (oxidation, excluding O ₂)	2.47×10^1	Evap BH: Galactic core ($\sim 10^6 M_{\text{solar}}$)	6.43×10^{15}
Human body (typical, male, fasting)	9.62×10^0	Type Ia supernova	1.00×10^{14}
ATP (1 mole, full conversion to AMP)	1.56×10^{-1}	Brown dwarf (W0607+24)	7.07×10^{10}
Glucose (oxidation, incl. O ₂ @ STP)	2.14×10^{-2}	Type M9 star	1.44×10^9
Fat (oxidation, including O ₂ @ STP)	1.84×10^{-2}	Sun (typical G2 star)	1.28×10^9
Resilin pad of the flea (<i>Spilopsyllus</i>)	3.00×10^{-3}	Jupiter mass (as fusion fuel)	1.19×10^9
Apple falling from a tree	8.79×10^{-6}	Type O9 star	7.16×10^7
Electric eel (<i>Electrophorus electricus</i>)	8.50×10^{-8}	Type II supernova	3.33×10^7
Electric eel (<i>Electrophorus electricus</i>)	6.00×10^{-8}	Type II supernova	1.00×10^7
<u>Planet-wide</u>		Solar flare (Sun)	1.73×10^5
Asteroid impact, ext. level (Chicxulub)	2.80×10^3	Sun rotational energy	1.16×10^0
Meteoroid impact (Meteor Crater, AZ)	1.62×10^3	Earth rotational energy	2.36×10^{-1}
Earthquake, mag. 9.5 (Valdivia, 1960)	8.46×10^2	Moon orbiting Earth (kinetic energy)	1.01×10^{-5}
Lightning bolt (average neg discharge)	2.50×10^{-1}	Earth orbiting Sun (kinetic energy)	5.36×10^{-8}
Volcanic eruption, Class 8 (La Garita)	2.00×10^{-1}	Globular cluster (M15)	4.17×10^{-13}
Volcanic eruption, Class 5 (St. Helens)	2.38×10^{-2}	Milky Way galaxy	2.28×10^{-13}
Tornado (maximum EF5)	9.52×10^{-4}	Rest mass of observable universe	3.67×10^{-20}
Hydroelectric dam reservoir (Hoover)	7.91×10^{-4}	Universe	3.67×10^{-22}
Lightning bolt (average neg discharge)	6.25×10^{-4}		
Hurricane (typical)	1.24×10^{-5}	<i>Theoretical maximum (measurable)</i>	3.10×10^{165}
Tsunami (typical)	1.67×10^{-8}	<i>Theoretical minimum (measurable)</i>	3.38×10^{-142}

⁵³ Data from Table A1 in Appendix A.1.

Table 2. Specific energy of natural systems ⁵⁴			
Natural Systems	Specific Energy (MJ/kg)	Natural Systems	Specific Energy (MJ/kg)
<u>Nuclear and Atomic</u>		<u>Astronomical</u>	
Most energetic cosmic ray known	3.05×10^{22}	Quantum vacuum energy (Compton)	9.29×10^{10}
Rest mass energy of one H ₂ molecule	9.01×10^{10}	Quantum vacuum energy (Planck)	9.06×10^{10}
Francium-215 radionuclide	4.90×10^6	Evap BH: ~10-m rock ($\sim 10^{-24} M_{\text{solar}}$)	9.00×10^{10}
Polonium-210 radionuclide	2.44×10^6	Evap BH: ~1 km meteor ($\sim 10^{-18} M_{\text{solar}}$)	9.00×10^{10}
Gadolinium-148 radionuclide	2.07×10^6	Evap BH: Asteroidal ($\sim 10^{-12} M_{\text{solar}}$)	9.00×10^{10}
Europium-147 radionuclide	1.91×10^6	Evap BH: Planetary ($\sim 10^{-6} M_{\text{solar}}$)	9.00×10^{10}
Neodymium-144 radionuclide	1.23×10^6	Evap BH: Stellar ($\sim 1 M_{\text{solar}}$)	9.00×10^{10}
Chemical bond energy, H ₂ molecule	2.14×10^2	Evap BH: Galactic core ($\sim 10^6 M_{\text{solar}}$)	9.00×10^{10}
Thermal energy, H ₂ molecule at STP	1.69×10^0	Ylem (cosmic egg)	8.97×10^{10}
<u>Biological</u>		Rest mass of observable universe	8.97×10^{10}
Fat (oxidation, excluding O ₂)	3.70×10^1	Quark nova	3.33×10^{10}
Glucose (oxidation, excluding O ₂)	1.60×10^1	Quark nova	2.78×10^{10}
Fat (oxidation, including O ₂ @ STP)	9.56×10^0	Binary black hole merger	4.16×10^9
Human body (typical, male, fasting)	9.25×10^0	Type O9 star	9.12×10^8
Glucose (oxidation, incl. O ₂ @ STP)	7.73×10^0	Globular cluster (M15)	9.09×10^8
ATP (1 mole, full conversion to AMP)	1.50×10^{-1}	Sun (typical G2 star)	9.05×10^8
Resilin pad of the flea (<i>Spilopsyllus</i>)	2.26×10^{-3}	Brown dwarf (W0607+24)	9.00×10^8
Apple falling from a tree	1.93×10^{-5}	Jupiter mass (as fusion fuel)	8.95×10^8
Electric eel (<i>Electrophorus electricus</i>)	8.50×10^{-8}	Universe	8.97×10^8
Electric eel (<i>Electrophorus electricus</i>)	6.00×10^{-8}	Milky Way galaxy	8.88×10^8
<u>Planet-wide</u>		Type M9 star	8.72×10^8
Earthquake, mag. 9.5 (Valdivia, 1960)	3.14×10^2	Type II supernova	6.25×10^8
Lightning bolt (average neg discharge)	2.50×10^2	Type II supernova	1.25×10^8
Meteoroid impact (Meteor Crater, AZ)	2.17×10^2	Type Ia supernova	7.14×10^7
Asteroid impact, ext. level (Chicxulub)	1.24×10^2	Solar flare (Sun)	1.19×10^5
Tornado (maximum EF5)	8.70×10^{-1}	Sun rotational energy	8.20×10^{-1}
Lightning bolt (average neg discharge)	5.68×10^{-1}	Earth rotational energy	4.29×10^{-2}
Volcanic eruption, Class 8 (La Garita)	7.69×10^{-2}	Moon orbiting Earth (kinetic energy)	6.30×10^{-3}
Hurricane (typical)	1.11×10^{-2}	Earth orbiting Sun (kinetic energy)	1.33×10^{-3}
Volcanic eruption, Class 5 (St. Helens)	9.09×10^{-3}		
Hydroelectric dam reservoir (Hoover)	7.91×10^{-4}	<i>Theoretical maximum (measurable)</i>	9.72×10^{132}
Tsunami (typical)	1.61×10^{-8}	<i>Theoretical minimum (measurable)</i>	8.30×10^{-112}

⁵⁴ Data from Table A1 in Appendix A.1.

Table 3. Power density of natural systems⁵⁵

Natural Systems	Power Density (MW/L)	Natural Systems	Power Density (MW/L)
<u>Nuclear and Atomic</u>			
Francium-215 radionuclide	1.81×10^{15}	Brown fat cell (resting)	3.00×10^{-7}
Europium-147 radionuclide	3.34×10^0	Evergreen trees (pine, fir, larch)	2.75×10^{-7}
Polonium-210 radionuclide	1.30×10^0	Protists (phytoplankton, algae)	9.00×10^{-8}
Gadolinium-148 radionuclide	4.82×10^{-3}	Erythrocyte (red blood cell)	8.51×10^{-8}
Neodymium-144 radionuclide	8.24×10^{-17}	Osteocyte (bone)	6.67×10^{-8}
		Global photosynthesis (all plants)	5.00×10^{-8}
<u>Biological</u>		<u>Animals</u>	
Honeybee flight muscle	2.64×10^{-3}	Fungi (<i>Saccharomyces</i> sp)	5.56×10^{-5}
Platelet (activated)	2.33×10^{-3}	Bacterium (<i>Sarcina lutea</i>)	3.80×10^{-5}
Myosin muscle motor	2.00×10^{-3}	Nematode (<i>Plectus</i>)	7.90×10^{-6}
Bacterial flagellar motor	2.00×10^{-3}	Rat, adult male	7.50×10^{-6}
<i>E. faecalis</i> bacterium (max. growth)	1.15×10^{-3}	Nematode (<i>Plectus</i>)	5.60×10^{-6}
Skeletal muscle cell (max. tetanic)	1.15×10^{-3}	Chicken, adult male	4.62×10^{-6}
Mitochondrion organelle	1.10×10^{-3}	Guinea pig, adult male	3.00×10^{-6}
Flea jumping	6.67×10^{-4}	Goat, adult	2.00×10^{-6}
T-cell lymphocyte (antigen response)	6.50×10^{-4}	Protozoa (<i>Chaos chaos</i>)	1.40×10^{-6}
Heart muscle cell (max.)	6.25×10^{-4}	Horse, adult male	1.22×10^{-6}
Heart muscle cell (max.)	4.38×10^{-4}	Pig, adult male	1.16×10^{-6}
<i>A. maculatum</i> florets	4.00×10^{-4}	<i>Diptera</i> (flies; larvae of <i>Tipula</i> sp)	1.16×10^{-6}
Brown fat cell (thermogenic)	3.20×10^{-4}	Beef cattle, adult male	1.02×10^{-6}
Platelet (activated)	2.33×10^{-4}	Protozoa (<i>Chaos chaos</i>)	9.20×10^{-7}
T-cell lymphocyte (basal)	2.00×10^{-4}	Mollusc (garden snail; <i>Helix aspersa</i>)	4.90×10^{-7}
Bee hummingbird in flight	1.48×10^{-4}	Annelid (earthworm; <i>Lum. terrestris</i>)	3.40×10^{-7}
Mitochondrion organelle	1.00×10^{-4}	Mollusc (garden snail; <i>Helix aspersa</i>)	2.40×10^{-7}
<i>E. coli</i> bacterium (basal)	7.69×10^{-5}		
<i>Philodendron</i> spadix at 10 °C ambient	7.20×10^{-5}	<u>Planet-wide</u>	
Typical human tissue cell (max.)	6.00×10^{-5}	Meteoroid impact (Meteor Crater, AZ)	7.69×10^5
Skeletal muscle cell (max. voluntary)	5.65×10^{-5}	Asteroid impact, ext. level (Chicxulub)	8.67×10^3
Kidney cell	4.33×10^{-5}	Lightning bolt (average neg discharge)	5.00×10^2
Electric eel (<i>Electrophorus electricus</i>)	4.30×10^{-5}	Earthquake, mag 9.5 (Valdivia, 1960)	1.42×10^0
Heart muscle cell (typical)	3.63×10^{-5}	Lightning bolt (average neg discharge)	1.25×10^0
Platelet (resting)	3.00×10^{-5}	Volcanic eruption, Class 5 (St. Helens)	3.10×10^{-4}
Electric eel (<i>Electrophorus electricus</i>)	2.50×10^{-5}	Tornado (maximum EF5)	4.05×10^{-7}
Neutrophil (white blood cell, activated)	2.43×10^{-5}	Tsunami (typical)	3.33×10^{-10}
Human body (max.)	2.38×10^{-5}	Hurricane (typical)	3.53×10^{-11}
Neuron (max.)	2.36×10^{-5}		
Kidney cell	1.94×10^{-5}	<u>Astronomical</u>	
Adrenal cell	1.88×10^{-5}	Ylem (cosmic egg)	5.75×10^{208}
Testicular cell	1.86×10^{-5}	Evap BH: ~10-m boulder ($\sim 10^{-24} M_{\text{solar}}$)	2.57×10^{73}
Neuron (max.)	1.82×10^{-5}	Evap BH: ~1 km meteor ($\sim 10^{-18} M_{\text{solar}}$)	2.57×10^{43}
Hepatocyte (liver cell)	1.80×10^{-5}	Quark nova	3.00×10^{26}
Human brain	1.67×10^{-5}	Quark nova	3.00×10^{26}
Thyroid cell	1.63×10^{-5}	Binary black hole merger	6.93×10^{22}
Pancreatic islet (multi-cell)	1.13×10^{-5}	Type Ia supernova	5.00×10^{13}
Heart muscle cell (typical)	1.09×10^{-5}	Evap BH: Asteroidal ($\sim 10^{-12} M_{\text{solar}}$)	2.57×10^{13}
Spleen cell	1.00×10^{-5}	X-ray pulsar, ex. star (Centaurus X-3)	2.94×10^{10}

⁵⁵ Data from Table A2 in Appendix A.2.

Diaphragm muscle cell	1.00×10^{-5}	X-ray pulsar, ex. star (Centaurus X-3)	2.94×10^7
Lung cell	9.75×10^{-6}	Type II supernova	3.33×10^6
Thymus cell	9.25×10^{-6}	Type II supernova	1.00×10^6
Pancreatic cell	9.00×10^{-6}	Radio pulsar, first (PSR B1919+21)	5.90×10^5
Neuron (basal)	7.86×10^{-6}	Solar flare (Sun)	5.45×10^1
Neutrophil (white blood cell, resting)	7.83×10^{-6}	Superlum. supernova (ASASSN-15lh)	2.20×10^{-1}
Spleen cell	7.50×10^{-6}	White dwarf star (Procyon B)	7.09×10^{-8}
Hepatocyte (liver cell)	7.03×10^{-6}	Type O9 star	9.45×10^{-9}
Lung cell	7.00×10^{-6}	Sun (typical G2 star)	2.71×10^{-10}
Intestine/stomach cell	6.50×10^{-6}	Hyperluminous quasar (S5 0014+81)	1.43×10^{-11}
Pancreatic islet (multi-cell)	6.25×10^{-6}	Blue supergiant star (Deneb)	6.25×10^{-12}
Intestine/stomach cell	5.75×10^{-6}	Brown dwarf (W0607+24)	6.00×10^{-12}
Testicular cell	5.75×10^{-6}	Type M9 star	6.38×10^{-13}
Bone marrow cell	5.63×10^{-6}	Red supergiant star (Betelgeuse)	2.83×10^{-14}
Skeletal muscle cell (resting)	5.00×10^{-6}	Red supergiant star (Betelgeuse)	2.38×10^{-14}
Typical human tissue cell (basal)	3.75×10^{-6}	Tidal heating of Jovian moon Io	6.32×10^{-15}
Skin cell	3.00×10^{-6}	Marine tidal oscillations (Earth-Moon)	2.75×10^{-15}
Heart muscle cell (resting)	2.00×10^{-6}	Tidal heating of Jovian moon Io	2.37×10^{-15}
<i>E. faecalis</i> bacterium (basal)	1.75×10^{-6}	Jovithermal heat (whole planet, Jupiter)	2.34×10^{-16}
Neutrophil (white blood cell, resting)	1.74×10^{-6}	Geothermal heat (whole planet, Earth)	4.08×10^{-17}
Firefly (e.g., <i>Photinus pyralis</i>)	1.63×10^{-6}	Evap BH: Planetary ($\sim 10^{-6} M_{\text{solar}}$)	2.57×10^{-17}
Human body (basal)	1.49×10^{-6}	Globular cluster (M15)	5.83×10^{-32}
Temperate zone herbs (wheat, tomato)	1.35×10^{-6}	Milky Way galaxy	3.74×10^{-33}
Osteocyte (bone)	1.27×10^{-6}	Milky Way galaxy	2.68×10^{-33}
Skin cell	1.00×10^{-6}	Universe	7.82×10^{-41}
Platelet (resting)	1.00×10^{-6}	Evap BH: Stellar ($\sim 1 M_{\text{solar}}$)	2.57×10^{-47}
Tropical grasses (maize, sugarcane)	8.97×10^{-7}	Evap BH: Galactic core ($\sim 10^6 M_{\text{solar}}$)	2.57×10^{-77}
Deciduous trees (oak, beech)	5.04×10^{-7}		
Skeletal muscle cell (resting)	5.00×10^{-7}	<i>Theoretical maximum (measurable)</i>	5.75×10^{208}
Chondrocyte	4.48×10^{-7}	<i>Theoretical minimum (measurable)</i>	7.77×10^{-160}

Table 4. Specific power of natural systems⁵⁶

Natural Systems	Specific Power (MW/kg)	Natural Systems	Specific Power (MW/kg)
<u>Nuclear and Atomic</u>			
Francium-215 radionuclide	9.69×10^{14}	Chondrocyte	4.48×10^{-7}
Europium-147 radionuclide	6.35×10^{-1}	Brown fat cell (resting)	3.33×10^{-7}
Polonium-210 radionuclide	1.41×10^{-1}	Protists (phytoplankton, algae)	9.00×10^{-8}
Gadolinium-148 radionuclide	6.10×10^{-4}	Erythrocyte (red blood cell)	7.27×10^{-8}
Neodymium-144 radionuclide	1.18×10^{-17}	Global photosynthesis (all plants)	7.06×10^{-8}
		Osteocyte (bone)	6.67×10^{-8}
<u>Biological</u>			
Pancreatic cell	9.00×10^{-3}	<u>Animals</u>	
Honeybee flight muscle	2.40×10^{-3}	Fungi (<i>Saccharomyces</i> sp)	5.56×10^{-5}
Platelet (activated)	2.19×10^{-3}	Bacterium (<i>Sarcina lutea</i>)	3.80×10^{-5}
Myosin muscle motor	2.00×10^{-3}	Nematode (<i>Plectus</i>)	7.90×10^{-6}
Bacterial flagellar motor	2.00×10^{-3}	Rat, adult male	7.50×10^{-6}
<i>E. faecalis</i> bacterium (max. growth)	1.15×10^{-3}	Nematode (<i>Plectus</i>)	5.60×10^{-6}
Skeletal muscle cell (max. tetanic)	1.05×10^{-3}	Chicken, adult male	4.62×10^{-6}
Mitochondrion organelle	9.24×10^{-4}	Guinea pig, adult male	3.00×10^{-6}
Flea jumping	6.67×10^{-4}	Goat, adult	2.00×10^{-6}
T-cell lymphocyte (antigen response)	6.19×10^{-4}	Protozoa (<i>Chaos chaos</i>)	1.40×10^{-6}
Heart muscle cell (max.)	5.68×10^{-4}	Horse, adult male	1.22×10^{-6}
<i>A. maculatum</i> florets	4.00×10^{-4}	Pig, adult male	1.16×10^{-6}
Heart muscle cell (max.)	3.98×10^{-4}	Diptera (flies; larvae of <i>Tipula</i> sp)	1.16×10^{-6}
Brown fat cell (thermogenic)	3.56×10^{-4}	Beef cattle, adult male	1.02×10^{-6}
Bee hummingbird in flight	2.37×10^{-4}	Protozoa (<i>Chaos chaos</i>)	9.20×10^{-7}
Platelet (activated)	2.19×10^{-4}	Mollusc (garden snail; <i>Helix aspersa</i>)	4.90×10^{-7}
T-cell lymphocyte (basal)	1.90×10^{-4}	Annelid (earthworm; <i>Lum. terrestris</i>)	3.40×10^{-7}
Mitochondrion organelle	8.40×10^{-5}	Mollusc (garden snail; <i>Helix aspersa</i>)	2.40×10^{-7}
<i>Philodendron</i> spadix at 10 °C ambient	7.20×10^{-5}	<u>Planet-wide</u>	
<i>E. coli</i> bacterium (basal)	6.94×10^{-5}	Lightning bolt (average neg discharge)	5.00×10^5
Typical human tissue cell (max.)	6.00×10^{-5}	Meteoroid impact (Meteor Crater, AZ)	1.03×10^5
Hepatocyte (liver cell)	5.75×10^{-5}	Lightning bolt (average neg discharge)	1.14×10^3
Skeletal muscle cell (max. voluntary)	5.14×10^{-5}	Asteroid impact, ext. level (Chicxulub)	3.82×10^2
Kidney cell	4.33×10^{-5}	Earthquake, mag 9.5 (Valdivia, 1960)	5.29×10^{-1}
Electric eel (<i>Electrophorus electricus</i>)	4.30×10^{-5}	Tornado (maximum EF5)	3.70×10^{-4}
Heart muscle cell (typical)	3.63×10^{-5}	Volcanic eruption, Class 5 (St. Helens)	1.18×10^{-4}
Platelet (resting)	2.81×10^{-5}	Hurricane (typical)	3.16×10^{-8}
Electric eel (<i>Electrophorus electricus</i>)	2.50×10^{-5}	Tsunami (typical)	3.23×10^{-10}
Neuron (max.)	2.36×10^{-5}	<u>Astronomical</u>	
Human body (max.)	2.29×10^{-5}	Ylem (cosmic egg)	1.66×10^{54}
Hepatocyte (liver cell)	2.25×10^{-5}	Binary black hole merger	2.09×10^{10}
Neutrophil (white blood cell, activated)	2.24×10^{-5}	Quark nova	1.00×10^9
Kidney cell	1.94×10^{-5}	Quark nova	8.33×10^8
Adrenal cell	1.88×10^{-5}	Evap BH: ~10-m boulder ($\sim 10^{-24} M_{\text{solar}}$)	3.60×10^8
Testicular cell	1.86×10^{-5}	Type II supernova	6.25×10^7
Neuron (max.)	1.82×10^{-5}	Type Ia supernova	3.57×10^7
Thyroid cell	1.63×10^{-5}	Type II supernova	1.25×10^7
Human brain	1.43×10^{-5}	Solar flare (Sun)	3.75×10^1
Pancreatic islet (multi-cell)	1.13×10^{-5}		

⁵⁶ Data from Table A2 in Appendix A.2.

Heart muscle cell (typical)	1.09×10^{-5}	Superlum. supernova (ASASSN-15lh)	2.75×10^0
Spleen cell	1.00×10^{-5}	Red supergiant star (Betelgeuse)	2.48×10^{-6}
Diaphragm muscle cell	1.00×10^{-5}	Blue supergiant star (Deneb)	1.97×10^{-6}
Lung cell	9.75×10^{-6}	Red supergiant star (Betelgeuse)	1.48×10^{-6}
Thymus cell	9.25×10^{-6}	Hyperlum. quasar (S5 0014+81)	1.25×10^{-6}
Neuron (basal)	7.86×10^{-6}	Type O9 star	1.20×10^{-7}
Spleen cell	7.50×10^{-6}	X-ray pulsar, ex. star (Centaurus X-3)	4.17×10^{-8}
Neutrophil (white blood cell, resting)	7.20×10^{-6}	Evap BH: ~1 km meteor ($\sim 10^{-18} M_{\text{solar}}$)	3.60×10^{-10}
Lung cell	7.00×10^{-6}	Sun (typical G2 star)	1.92×10^{-10}
Intestine/stomach cell	6.50×10^{-6}	Globular cluster (M15)	1.27×10^{-10}
Pancreatic islet (multi-cell)	6.25×10^{-6}	X-ray pulsar, ex. star (Centaurus X-3)	4.17×10^{-11}
Intestine/stomach cell	5.75×10^{-6}	Milky Way galaxy	1.46×10^{-11}
Testicular cell	5.75×10^{-6}	Milky Way galaxy	1.04×10^{-11}
Bone marrow cell	5.63×10^{-6}	Universe	9.24×10^{-12}
Skeletal muscle cell (resting)	4.55×10^{-6}	Radio pulsar, first (PSR B1919+21)	8.21×10^{-13}
Typical human tissue cell (basal)	3.75×10^{-6}	Type M9 star	3.85×10^{-13}
Skin cell	3.00×10^{-6}	White dwarf star (Procyon B)	1.57×10^{-13}
Tropical grasses (maize, sugarcane)	2.25×10^{-6}	Brown dwarf (W0607+24)	7.64×10^{-14}
Heart muscle cell (resting)	1.82×10^{-6}	Marine tidal oscillations (Earth-Moon)	2.63×10^{-15}
<i>E. foecalis</i> bacterium (basal)	1.75×10^{-6}	Tidal heating of Jovian moon Io	1.79×10^{-15}
Firefly (e.g., <i>Photinus pyralis</i>)	1.63×10^{-6}	Tidal heating of Jovian moon Io	6.72×10^{-16}
Neutrophil (white blood cell, resting)	1.60×10^{-6}	Jovithermal heat (whole planet, Jupiter)	1.76×10^{-16}
Human body (basal)	1.43×10^{-6}	Geothermal heat (whole planet, Earth)	7.40×10^{-18}
Temperate zone herbs (wheat, tomato)	1.35×10^{-6}	Evap BH: Asteroidal ($\sim 10^{-12} M_{\text{solar}}$)	3.60×10^{-28}
Osteocyte (bone)	1.27×10^{-6}	Evap BH: Planetary ($\sim 10^{-6} M_{\text{solar}}$)	3.60×10^{-46}
Skin cell	1.00×10^{-6}	Evap BH: Stellar ($\sim 1 M_{\text{solar}}$)	3.60×10^{-64}
Platelet (resting)	9.38×10^{-7}	Evap BH: Galactic core ($\sim 10^6 M_{\text{solar}}$)	3.60×10^{-82}
Deciduous trees (oak, beech)	7.20×10^{-7}		
Evergreen trees (pine, fir, larch)	5.50×10^{-7}	<i>Theoretical maximum (measurable)</i>	1.80×10^{176}
Skeletal muscle cell (resting)	4.55×10^{-7}	<i>Theoretical minimum (measurable)</i>	1.92×10^{-129}

Table 5 below provides a brief summary of energy density, specific energy, and the power-to-weight ratio,⁵⁷ or specific power, in a variety of conventional contemporary engineered systems. The specific power for most complete systems is surprisingly low, including fighter jets at only **~0.0015 MW/kg**. The energy densities of complete machines are reduced in part because those machines devote only a fraction of their mass to energy storage. For example, the hydrocarbon fuel Jet A-1 used in fighter jets has a specific energy of $E_S \sim 43 \text{ MJ/kg}$ but the specific energy of an entire F-22 fighter jet is only $E_S \sim 9.3 \text{ MJ/kg}$.⁵⁸ Interestingly, this is essentially identical to the energy storage in the average human body: **~9.3 MJ/kg (Table 2)** and **~9.6 MJ/L (Table 1)**.

High rates of energy consumption are difficult to maintain for long periods of time in commonplace machines. For example, a 1000 kg automobile with a 200 horsepower (0.15 MW) engine and a 16-gallon gas tank (**~33 MJ/L** for gasoline; **Table 30**) has a fully-fueled whole-machine specific energy of $E_S \sim 2 \text{ MJ/kg}$ but a specific power of $P_S \sim 0.00015 \text{ MW/kg}$. In this case, the stated power level can only be maintained for $\tau_{\text{duration}} \sim E_S / P_S \sim 13,333 \text{ sec}$ (3.7 hr).⁵⁹ Similarly, the Saturn V moon rocket with LH_2/LOX fuel (**5.74 MJ/L; Table 28**) and an overall energy density of **2.1 MJ/L** had a fully-fueled specific energy of $E_S = 4.34 \text{ MJ/kg}$ but a specific power of only $P_S = 0.00423 \text{ MW/kg}$, allowing the average power level of 12.6 GW to be maintained for only $\tau_{\text{duration}} \sim E_S / P_S \sim 1028 \text{ sec}$.⁶⁰

The power density of our ordinary surroundings are normally quite low. For instance, a 2000 SF house drawing 2 kilowatts continuously (~20 light bulbs, each rated at 100 watts) has an overall power density of $P_D \sim 3 \times 10^{-9} \text{ MW/L}$. Inside the house, a ~1 m³ refrigerator drawing 200 watts has $P_D \sim 2 \times 10^{-7} \text{ MW/L}$ and a single incandescent 100-watt light bulb measuring 6 cm in diameter has $P_D \sim 9 \times 10^{-4} \text{ MW/L}$. The ~10 m³ 200-horsepower car parked in the garage will draw $P_D \sim 1.5 \times 10^{-5} \text{ MW/L}$ when accelerating at maximum load, while its ~67.3-liter volume human occupant draws only $P_D \sim 1.5 \times 10^{-6} \text{ MW/L}$ at the 100-watt basal metabolic rate.

⁵⁷ https://en.wikipedia.org/wiki/Power-to-weight_ratio.

⁵⁸ Total mass of fully-loaded F-22 fighter jet is 37,869 kg and total fuel mass 8163 kg (https://en.wikipedia.org/wiki/Thrust-to-weight_ratio#Fighter_aircraft); specific energy of Jet A-1 is similar to kerosene at 43.086 MJ/kg (**Table 29**); so the net specific energy of a fully-fueled F-22 fighter jet is ~9.29 MJ/kg.

⁵⁹ Amusingly, a 16-gallon fillup at a gas station that requires ~1 minute to complete at the pump represents a chemical energy transfer rate of (16 gallons)(3.78 L/gallon)(33 MJ/L)/(60 sec) ~ 33 MW.

⁶⁰ Saturn V data (https://en.wikipedia.org/wiki/Saturn_V): **Stage 1:** mass $2.29 \times 10^6 \text{ kg}$, volume 3373 m^3 , density 0.679 kg/L , burn time 168 sec, specific impulse 263 sec, total energy $7.62 \times 10^6 \text{ MJ}$, thrust power $4.54 \times 10^4 \text{ MW}$, $E_S = 3.33 \text{ MJ/kg}$, $E_D = 2.26 \text{ MJ/L}$. **Stage 2:** mass $4.96 \times 10^5 \text{ kg}$, volume 1987 m^3 , density 0.250 kg/L , burn time 360 sec, specific impulse 421 sec, total energy $4.23 \times 10^6 \text{ MJ}$, thrust power $1.18 \times 10^4 \text{ MW}$, $E_S = 8.53 \text{ MJ/kg}$, $E_D = 2.13 \text{ MJ/L}$. **Stage 3:** mass $1.23 \times 10^5 \text{ kg}$, volume 643 m^3 , density 0.191 kg/L , burn time 500 sec, specific impulse 421 sec, total energy $1.05 \times 10^6 \text{ MJ}$, thrust power $2.10 \times 10^3 \text{ MW}$, $E_S = 8.53 \text{ MJ/kg}$, $E_D = 1.63 \text{ MJ/L}$. **Whole rocket with payload:** mass $2.97 \times 10^6 \text{ kg}$, volume 6129 m^3 , density 0.485 kg/L , burn time 1028 sec, total energy $1.29 \times 10^7 \text{ MJ}$, average thrust power $1.26 \times 10^4 \text{ MW}$, $E_S = 4.34 \text{ MJ/kg}$, $E_D = 2.10 \text{ MJ/L}$, $P_S = 4.23 \times 10^{-3} \text{ MW/kg}$, $P_D = 2.05 \times 10^{-3} \text{ MW/L}$.

Table 5. Energy density (MJ/L) and specific energy (MJ/kg) (at top), and specific power (MW/kg) (at bottom), in conventional contemporary engineered systems

Conventional Contemporary Engineered System	MJ/L	MJ/kg
Springs ⁶¹	0.000004-9.0	0.0000005-8.0
Capacitors and supercapacitors ⁶²	0.00001-0.06	0.00001-0.036
Hydropower (water dams) ⁶³	0.001	0.001
Compressed air storage systems ⁶⁴	0.015-0.2	0.5
Thermal energy ⁶⁵	0.1-0.8	0.03-0.25
Flywheels (steel or composite materials) ⁶⁶	0.1-5.3	0.03-0.5
Electrochemical batteries ⁶⁷	0.1-4.3	0.04-1.8
Chemical fuels (ambient combustion, excl. oxygen) ⁶⁸		
Liquid hydrogen	8.6	121
Dry wood	10-16	12.5-20
Crude oil, coal, methanol, ethanol	17-42	21-42
Passenger automobile ⁶⁹	0.2	2
Saturn V moon rocket ⁷⁰	2.10	4.34
F-22 fighter jet (<i>supra</i>)	---	9.3
Trinity A-bomb (fission) ⁷¹	52,000	19,000
Tsar Bomba H-bomb (fusion) ⁷²	7,580,000	7,780,000
HERCULES 300 TW laser (530 nm; beam energy only) ⁷³	670,000,000	---

⁶¹ **Section 5.2.**

⁶² https://en.wikipedia.org/wiki/Energy_density#Table_of_energy_content.

⁶³ https://www.engineeringtoolbox.com/energy-density-d_1362.html.

⁶⁴ https://www.engineeringtoolbox.com/energy-density-d_1362.html,
https://en.wikipedia.org/wiki/Energy_density#Table_of_energy_content.

⁶⁵ https://www.engineeringtoolbox.com/energy-density-d_1362.html.

⁶⁶ https://www.engineeringtoolbox.com/energy-density-d_1362.html,
https://en.wikipedia.org/wiki/Energy_density#Table_of_energy_content.

⁶⁷ https://www.engineeringtoolbox.com/energy-density-d_1362.html,

https://en.wikipedia.org/wiki/Energy_density#Table_of_energy_content.

⁶⁸ https://www.engineeringtoolbox.com/energy-density-d_1362.html, **Table 29**, and **Table 30**.

⁶⁹ A 1000 kg, 10 m³ car with a full 16-gallon gas tank has an overall energy density of $E_D \sim (16 \text{ gallons})(3.78 \text{ L/gallon})(33 \text{ MJ/L})/(10,000 \text{ L}) = 0.2 \text{ MJ/L}$ and specific energy $E_S \sim E_D / (0.1 \text{ kg/L}) = 2 \text{ MJ/kg}$. If the car generates 200 hp (149 kW), then $P_D \sim 1.5 \times 10^{-5} \text{ MW/L}$ and $P_S \sim 1.5 \times 10^{-4} \text{ MW/kg}$.

⁷⁰ **Whole rocket with payload:** mass $2.97 \times 10^6 \text{ kg}$, volume 6129 m^3 , density 0.485 kg/L , burn time 1028 sec, total energy $1.29 \times 10^7 \text{ MJ}$, average thrust power $1.26 \times 10^4 \text{ MW}$, $E_S = 4.34 \text{ MJ/kg}$, $E_D = 2.10 \text{ MJ/L}$, $P_S = 4.23 \times 10^{-3} \text{ MW/kg}$, $P_D = 2.05 \times 10^{-3} \text{ MW/L}$; https://en.wikipedia.org/wiki/Saturn_V.

⁷¹ **Section 7.2.**

⁷² **Section 7.3.1.**

⁷³ <https://cuos.engin.umich.edu/researchgroups/hfs/facilities/hercules-petawatt-laser/> and **Section 6.4.**

Conventional Contemporary Engineered System	Specific Power (MW/kg)
Closed cell batteries ⁷⁴	0.000002-0.0214
Steam-, diesel-, and electric locomotives ⁷⁵	0.000004-0.000041
Batteries and fuel cells (Table 24)	0.000004-0.00632
Electrostatic, electrolytic and electrochemical capacitors ⁷⁶	0.000005-0.00804
Vestas V164 8 MW wind turbine ⁷⁷	0.0000062
Fuel cell stacks and flow cell batteries ⁷⁸	0.000006-0.0015
Photovoltaics ⁷⁹	0.000006-0.002
Abrams battle tank ⁸⁰	0.00002
Heat engines and heat pumps ⁸¹	0.00003-0.153
Fluid engines and fluid pumps ⁸²	0.000047-0.0057
Common passenger automobiles ⁸³	0.000053-0.000114
800 KW diesel generator ⁸⁴	0.000057
Aircraft (propeller) ⁸⁵	0.000117-0.000361
Performance luxury, roadster, and mild sports automobiles ⁸⁶	0.000124-0.000174
Sports vehicles (automobiles) ⁸⁷	0.000179-0.000763
Electric motors and electromotive generators ⁸⁸	0.00029-0.0101
Sports vehicles (race cars and racing motorcycles) ⁸⁹	0.0005-0.00572
Aircraft (jet fighters, max load), ⁹⁰ using $P_S \sim (200 \text{ m/sec})(\text{thrust})/(\text{mass})$	0.00114-0.00176
Jet and rocket engines, ⁹¹ using $P_S \sim (200 \text{ m/sec})(\text{thrust})/(\text{mass})$	0.00352-0.0353
Thermoelectric generators and electrothermal actuators ⁹²	0.00509-0.165
Nuclear reactor fission core ⁹³	0.0077

⁷⁴ [https://en.wikipedia.org/wiki/Power-to-weight_ratio#\(Closed_cell\)_batteries](https://en.wikipedia.org/wiki/Power-to-weight_ratio#(Closed_cell)_batteries).

⁷⁵ https://en.wikipedia.org/wiki/Power-to-weight_ratio#Notable_low_ratio.

⁷⁶ https://en.wikipedia.org/wiki/Power-to-weight_ratio#Electrostatic,_electrolytic_and_electrochemical_capacitors.

⁷⁷ https://en.wikipedia.org/wiki/Vestas_V164.

⁷⁸ https://en.wikipedia.org/wiki/Power-to-weight_ratio#Fuel_cell_stacks_and_flow_cell_batteries.

⁷⁹ https://en.wikipedia.org/wiki/Power-to-weight_ratio#Photovoltaics.

⁸⁰ https://en.wikipedia.org/wiki/Power-to-weight_ratio#Notable_low_ratio.

⁸¹ https://en.wikipedia.org/wiki/Power-to-weight_ratio#Heat_engines_and_heat_pumps.

⁸² https://en.wikipedia.org/wiki/Power-to-weight_ratio#Fluid_engines_and_fluid_pumps.

⁸³ https://en.wikipedia.org/wiki/Power-to-weight_ratio#Common_power.

⁸⁴ <http://www.generac.com/Industrial/products/diesel-generators/configured/800kw-diesel-generator>.

⁸⁵ https://en.wikipedia.org/wiki/Power-to-weight_ratio#Aircraft.

⁸⁶ https://en.wikipedia.org/wiki/Power-to-weight_ratio#Performance_luxury_roadsters_and_mild_sports.

⁸⁷ https://en.wikipedia.org/wiki/Power-to-weight_ratio#Sports_vehicles.

⁸⁸ https://en.wikipedia.org/wiki/Power-to-weight_ratio#Electric_motors_and_electromotive_generators.

⁸⁹ https://en.wikipedia.org/wiki/Power-to-weight_ratio#Sports_vehicles.

⁹⁰ https://en.wikipedia.org/wiki/Thrust-to-weight_ratio#Fighter_aircraft.

⁹¹ https://en.wikipedia.org/wiki/Thrust-to-weight_ratio#Jet_and_rocket_engines.

⁹² https://en.wikipedia.org/wiki/Power-to-weight_ratio#Thermoelectric_generators_and_electrothermal_actuators.

⁹³ Sun H, Wang C, Liu X, Tian W, Qiu S, Su G. Reactor core design and analysis for a micronuclear power source. Front Energy Res 2018 Mar 22; 6:14;

<https://www.frontiersin.org/articles/10.3389/fenrg.2018.00014/full>.

Chapter 3. Thermochemical Energy Storage

In this Chapter we survey the specific energy (MJ/kg) and energy density (MJ/L) available from various sources of stored thermochemical energy.

Section 3.1 surveys the energy storage densities that are available using “sensible heat” sources that involve a change in temperature, including the heat capacity of solids (**Section 3.1.1**), liquids (**Section 3.1.2**), and gases (**Section 3.1.3**). Similarly, **Section 3.2** surveys storage densities available using “latent heat” sources that occur without a change in temperature, including the heat of fusion that is evolved when a material transforms from the liquid to the solid state (**Section 3.2.1**), the heat of vaporization generated when a material transforms from the gaseous to the liquid state (**Section 3.2.2**), and the heat of sublimation that is released when a material transforms from the gaseous to the solid state (**Section 3.2.3**). **Section 3.3** reviews a wide variety of other thermochemical phase changes that can store and release energy, including the heat of solution (**Section 3.3.1**), the heat of crystallization (**Section 3.3.2**), photoisomer conversion energy (**Section 3.3.3**), allotropic transition energy (**Section 3.3.4**), crystal structure phase transition energy (**Section 3.3.5**), and a few other phase-change enthalpies (**Section 3.3.6**). **Figure 2 (Chapter 9)** provides a chart that summarizes much of this data.

Section 3.4 reiterates the point that, unlike storage energy density, storage power density is not an intrinsic material property. Nevertheless, one can estimate the maximum thermochemical specific power (MW/kg) and power density (MW/L) for various materials by making certain reasonable assumptions regarding storage container size and the rate of resupply of recharged storage containers to the source energy system. Practical modern-day heat engines generally achieve power/weight ratios in the range of **0.001-0.1 MW/kg**.⁹⁴

The second law of thermodynamics says that it is impossible to convert heat into useful work if the heat reservoir and the device are both at the same temperature, as demonstrated by Feynman’s classic example of the Brownian motor using an isothermal ratchet and pawl machine,⁹⁵ although nonequilibrium fluctuations, whether generated by macroscale electric fields or chemical reactions far from equilibrium, can drive a Brownian motor.⁹⁶ Astumian estimates that even a crudely designed chemically-driven Brownian motor could move in 10-nm steps at ~3 microns/sec, developing ~0.5 pN of force, ~3 x 10⁻⁶ pW of power, and a power density of ~**0.001 MW/L**.⁹⁷ Still higher power densities might be possible but seem highly speculative.⁹⁸

⁹⁴ https://en.wikipedia.org/wiki/Power-to-weight_ratio#Heat_engines_and_heat_pumps.

⁹⁵ Feynman RP. “Ratchet and pawl,” Volume I, Chapter 46, The Feynman Lectures on Physics, Addison-Wesley Publishing Company, Reading, MA, 1963.

⁹⁶ Astumian RD. Thermodynamics and kinetics of a Brownian motor. Science 1997 May 9;276(5314):917-922; http://mcb.berkeley.edu/labs/krantz/pdf/astumian-thermo%26kinetics_brownian_motor-science-1997.pdf.

⁹⁷ Astumian RD. Thermodynamics and kinetics of a Brownian motor. Science 1997 May 9;276(5314):917-922; http://mcb.berkeley.edu/labs/krantz/pdf/astumian-thermo%26kinetics_brownian_motor-science-1997.pdf.

3.1 Sensible Heat

“Sensible heat” is the heat exchanged by a body or thermodynamic system that results in a change in temperature. For example, heat capacity is a measurable physical quantity of matter that can be defined as the quantity of thermal energy added to (or removed from) a material object when the temperature of that object changes by a given amount. Specific heat capacity (or, more commonly, specific heat)⁹⁹ is the joules of thermal energy needed to raise the temperature of one kilogram of matter by 1 degree kelvin at constant pressure ($c_p(T)$; see ranked **Table 6**, below, with data sources in **Sections 3.1.1-3**). (Volumetric heat capacity¹⁰⁰ is the joules of thermal energy needed to raise the temperature of one liter of matter by 1 degree kelvin.) Specific heat varies by material, by temperature, and by physical state (solid, liquid, gas) of the material, but only very slightly with pressure¹⁰¹ for most solids and liquids.

High capacity provides an exploitable store of energy when a given mass of hot matter at one temperature is brought into contact with a cold sink at a lower temperature. Energy flows from the hot source to the cold sink until the temperature of the source reaches the temperature of the sink, at which point the stored thermal energy has been drained from the source.¹⁰² For energy storage via heat capacity, we assume the source material does not change its physical state (i.e., solid, liquid, gas) and the cold sink does not warm up during the energy transfer. We also ignore the rate at which energy leaks away from the hot source by radiation, convection, or other means, as this leakage rate is highly implementation-dependent.

⁹⁸ It has been alleged that reversible-energy-fluctuation converters can obtain useful electrical work from thermal Nyquist noise, up to power densities of 10^6 - 10^7 MW/L at ~ 300 K. See: Yater JC. Power conversion of energy fluctuations. Phys Rev A 1974 Oct;10(4):1361-1369; <https://journals.aps.org/pr/abstract/10.1103/PhysRevA.10.1361>. Yater JC. Physical basis of power conversion of energy fluctuations. Phys Rev A 1982 Jul;26(1):522-538; <http://adsabs.harvard.edu/abs/1982PhRvA..26..522Y>. See also: <https://patents.google.com/patent/US4004210A/en>, Phys Rev A 1978 Aug;18:767-772, Phys Rev A 1979 Aug;20:623-627, and Phys Rev A 1979 Oct;20:1614-1618.

⁹⁹ https://en.wikipedia.org/wiki/Heat_capacity#Specific_heat_capacity.

¹⁰⁰ https://en.wikipedia.org/wiki/Volumetric_heat_capacity.

¹⁰¹ For the specific heat of liquid water, heating water causes it to expand, doing work against the surrounding pressure, and this expansion takes a bit more work at higher pressure. For example, heating 1 kg of water from 10 °C to 30 °C decreases density from 999.7026 kg/m³ to 995.6502 kg/m³, an expansion of 4.071×10^{-6} m³ that does a very small **0.413 J** of work at 1 atm (101,325 N/m²) or **1.24 J** at 3 atm, compared to the vastly larger **~84,360 J** (~ 4218 J/kg-K x 1 kg x 20 K) of energy that is needed to heat the water; <http://physics.stackexchange.com/questions/100044/does-specific-heat-change-with-pressure-if-so-why>.

¹⁰² Of course, this process would completely waste the energy, maximally increasing entropy and doing no work unless a heat engine is interposed between the hot and cold objects, allowing extraction of useful energy from that flow, i.e., to perform work. See: <http://demonstrations.wolfram.com/IrreversibleAndReversibleTemperatureEquilibration/>.

Table 6. Specific heat capacity (“specific heat”) data for various materials								
Material	Phase	Specific Heat (J/kg-K)	Material	Phase	Specific Heat (J/kg-K)	Material	Phase	Specific Heat (J/kg-K)
Hydrogen	gas	10800	1-heptanol	liq	2671	Ethyl ether	liq	2220
Hydrogen	liq	9780	1-hexanol	liq	2662	Decane	liq	2210
Helium	gas	5193	1-octanol	liq	2641	Aniline	liq	2180
Ammonia	liq	4700	1-pentanol	liq	2632	Iodine	liq	2150
Lithium	liq	4246	1-butanol	liq	2599	Acetone	liq	2150
Water	liq	4218	Methanol	liq	2522	Water-ice	solid	2100
Lithium	solid	3602	1-propanol	liq	2515	Graphite	solid	2081
Beryllium	liq	3270	Ethanol	liq	2446	Diamond	solid	2081
Calcium chloride	liq	3060	Glycerine	liq	2430	Lithium nitrate	liq	2074
Graphite	liq	3000	Ethylene glycol	liq	2360	Acetic acid	liq	2043
Paraffin wax	solid	2900	Boron	solid	2313	Nitrogen	liq	2028
Propylene	liq	2850	Polyethylene	solid	2303	Ether	gas	1950
1-nonanol	liq	2820	n-butane	liq	2300	Benzene	liq	1920
1-undecanol	liq	2789	Hexane	liq	2260	Basaltic magma ¹⁰³	liq	1450
Beryllium	solid	2774	Heptane	liq	2240			
1-decanol	liq	2725	Octane	liq	2220			

The maximum exploitable amount of energy that can be stored via heat capacity varies according to the physical state of the storage material. In the case of **solids** (Section 3.1.1), the maximum temperature change would occur when the hot source temperature is at the melting point ($T_{m.p.}$) of the material and the cold sink is at 4 K,¹⁰⁴ e.g., $\Delta T_{solid} = T_{m.p.} - 4$ K. In the case of **liquids** (Section 3.1.2), the maximum temperature change occurs when the hot source is at its boiling point ($T_{b.p.}$) and the cold sink is at its melting point, e.g., $\Delta T_{liquid} = T_{b.p.} - T_{m.p.}$ ¹⁰⁵ In the case of **gases** (Section 3.1.3), the cold sink must be at the boiling point but the maximum temperature of the source is indeterminate, since the temperature of matter can in theory rise without limit.

¹⁰³ <http://magma.geol.ucsb.edu/papers/EoV%20chapter%205%20Leshher&Spera.pdf>.

¹⁰⁴ A microkelvin sink near absolute zero (0 K) could extract a bit more energy, but would require the expenditure of additional energy to keep the sink cooled to below the ~4 K natural background temperature of the universe.

¹⁰⁵ Higher pressures may allow a larger range for ΔT_{liquid} . The use of still higher pressures above the critical point to avoid boiling (i.e., no abrupt transition from liquid to gas with increasing temperature) might provide even larger usable temperature ranges.

Rather than choosing some arbitrary uppermost source temperature,¹⁰⁶ we estimate the energy storage of gases in energy units per kilokelvin (1000 K) of temperature differential between source and sink, e.g., $\Delta T_{\text{gas}} \sim 1000 \text{ K}$.

Depending on the particular application, it is a matter of design and engineering to determine how best to extract the energy differential between a hot source and a cold sink. The extraction process will generally consist of some means by which the stored energy can be converted into some other form of energy that can do something useful in the context of the application. The specification or design of such conversion systems is beyond the scope of the present work, but a few representative approaches can be mentioned.

For example, extracted energy can be converted into mechanical work by various classes of heat engines, including the steam engine,¹⁰⁷ the Stirling engine,¹⁰⁸ or the Ericsson engine,¹⁰⁹ all of which require a working fluid that remains either gaseous or liquid throughout the entire range of operation.¹¹⁰ (Nakajima¹¹¹ has built and operated a 50 mm³ Stirling engine working at 10 Hz between 273-373 K producing 10² watts yielding a power density of $P_D = 0.0002 \text{ MW/L}$, and has demonstrated the theoretical engineering feasibility of microscale Stirling engines.) The Banks engine¹¹² is another heat engine that uses nitinol¹¹³ to produce mechanical energy from hot and cold heat sources, though the operating temperature is narrow¹¹⁴ and a practical full-range system would need to include a variety of different “shape memory” materials¹¹⁵ to optimize energy extraction in multiple overlapping temperature bands. Energy from a hot source and cold sink

¹⁰⁶ For example, one could choose (a) the maximum solid temperature of any known material that could serve as a physical container for the source material (e.g., tungsten at 3695 K, graphite carbon (1 atm) at 3915 K, tantalum hafnium carbide or Ta₄HfC₅ at 4215 K, and the recently computationally discovered tantalum nitrogen carbon alloy (Ta_{0.53}N_{0.20}C_{0.27}) at ~4400 K; Hong QJ, van de Walle A. Prediction of the material with highest known melting point from *ab initio* molecular dynamics calculations. Phys. Rev. B 2015 Jul 20;92:020104; <http://authors.library.caltech.edu/59499/1/PhysRevB.92.020104.pdf>); (b) the first ionization temperature of the source material ($T_{\text{ionization}} \sim E_{\text{ionization}} / k_B$, for Boltzmann constant $k_B = 1.38 \times 10^{-23} \text{ J/K}$; e.g., $T_{\text{ionization}} = 116,000 \text{ K}$ for $E_{\text{ionization}} = 10 \text{ eV}$; see **Section 4.4.3.1**), whereupon the material changes physical state from gas to plasma); or (c) various other alternatives.

¹⁰⁷ https://en.wikipedia.org/wiki/Steam_engine.

¹⁰⁸ https://en.wikipedia.org/wiki/Stirling_engine.

¹⁰⁹ https://en.wikipedia.org/wiki/Ericsson_cycle#Ericsson_engine.

¹¹⁰ From 4-20 K, the only available gaseous working fluid is helium, with hydrogen gas available over 20 K and neon gas above 27 K; [https://en.wikipedia.org/wiki/Boiling_points_of_the_elements_\(data_page\)](https://en.wikipedia.org/wiki/Boiling_points_of_the_elements_(data_page)).

¹¹¹ Nakajima N, Ogawa K, Fujimasa I. Study on Microengines: Miniaturizing Stirling Engines for Actuators. Sensors and Actuators 1989;20:75-82; <https://ieeexplore.ieee.org/abstract/document/77979>.

¹¹² Banks R. The Banks Engine. Die Naturwissenschaften. 1975 Jul;62(7):305-308; <http://link.springer.com/article/10.1007/BF00608890>.

¹¹³ https://en.wikipedia.org/wiki/Nickel_titanium.

¹¹⁴ “Nitinol Heat Engine Kit”; <http://www.imagesco.com/nitinol/heat-engine.html>.

¹¹⁵ https://en.wikipedia.org/wiki/Shape-memory_alloy.

can also be converted into acoustic energy using a thermoacoustic heat engine,¹¹⁶ or into electrical energy using a Seebeck effect¹¹⁷ thermoelectric generator¹¹⁸ or thermopile¹¹⁹, pyroelectric generator,¹²⁰ thermogalvanic cell,¹²¹ or thermophotovoltaic generator.¹²²

In the ideal case of a reversible heat engine,¹²³ we would extract the maximum possible work without increasing the entropy.

¹¹⁶ https://en.wikipedia.org/wiki/Thermoacoustic_heat_engine.

¹¹⁷ https://en.wikipedia.org/wiki/Thermoelectric_effect#Seebeck_effect.

¹¹⁸ https://en.wikipedia.org/wiki/Thermoelectric_generator.

¹¹⁹ <https://en.wikipedia.org/wiki/Thermopile>.

¹²⁰ https://en.wikipedia.org/wiki/Pyroelectricity#Power_generation.

¹²¹ https://en.wikipedia.org/wiki/Thermogalvanic_cell.

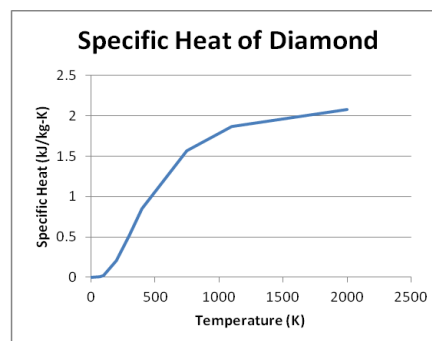
¹²² <https://en.wikipedia.org/wiki/Thermophotovoltaic>.

¹²³ Leff HS. Reversible and irreversible heat engine and refrigerator cycles. Am J Phys. 2018 Apr 19;86:344; <https://www.cpp.edu/~hsleff/Leff%202018a.pdf>. “Reversible Heat Engine,” ScienceDirect, 2019; <https://www.sciencedirect.com/topics/engineering/reversible-heat-engine>.

3.1.1 Heat Capacity of Solids

A classical rule, described by Lewis and Gibson¹²⁴ following the law of Dulong and Petit,¹²⁵ says that the heat capacity of solid pure elements very roughly approaches a maximum of ~ 25 J/K per mole of atoms¹²⁶ at room temperature and above. The natural element with the heaviest atoms (^{238}U) has almost the lowest specific heat of any solid material, at 116 J/kg-K (2010 J/L-K),¹²⁷ very close to the rule-predicted value of 105 J/kg-K. Lithium, the lightest solid element at room temperature, has the highest room temperature specific heat (for solids) at 3580 J/kg-K (1910 J/L-K) at 298 K, also very close to the rule-predicted maximum of 3600 J/kg-K.

A few substances, particularly the hard high-melting crystals of the light atoms of beryllium, boron, and carbon (both graphite and diamond), have specific heats much smaller than this rule predicts across a wide temperature range. For example, diamond (crystalline carbon) at 298 K has a specific heat of 509 J/kg-K (1790 J/L-K), only a quarter of the rule-predicted 2080 J/kg-K maximum; by 1100 K, the specific heat of diamond has risen to 1870 J/kg-K (6580 J/L-K), much closer to the rule-predicted maximum (see chart, right).



The specific heat capacity of solids is generally highest just below the melting point, declining slightly as temperature falls but then falling more rapidly at very low temperatures ($\propto T^3$),¹²⁸ eventually reaching zero in the limit at 0 K.¹²⁹ As a result, applying the maximum specific heat estimate to the full temperature differential $\Delta T_{\text{solid}} = T_{\text{m.p.}} - 4$ K may overestimate the exploitable energy storage that is potentially available by up to a factor of ~ 2 , but at least provides a useful crude upper limit.

Table 7 shows a ranked list of the maximum specific energy of heat capacity for the solid elements and a few other representative solids (range **0.029-8.1 MJ/kg**), mostly computed by multiplying the rule-predicted maximum specific heat capacity with the maximum exploitable

¹²⁴ Lewis GN, Gibson GE. The entropy of the elements and the third law of thermodynamics. J Am Chem Soc 1917;39:2554-2581; <http://pubs.acs.org/doi/abs/10.1021/ja02257a006>.

¹²⁵ Petit AT, Dulong PL. Recherches sur quelques points importants de la Théorie de la Chaleur. Annales de Chimie et de Physique. 1819;10:395-413 (in French); <http://web.lemoyne.edu/~giunta/PETIT.html>.

¹²⁶ This is $\sim 3R$, where $R = 8.31446$ J/mole-K; https://en.wikipedia.org/wiki/Gas_constant.

¹²⁷ [https://en.wikipedia.org/wiki/Heat_capacities_of_the_elements_\(data_page\)](https://en.wikipedia.org/wiki/Heat_capacities_of_the_elements_(data_page)).

¹²⁸ https://en.wikipedia.org/wiki/Debye_model.

¹²⁹ Daniels F, Alberty RA. Physical Chemistry, 3rd Ed., John Wiley & Sons, New York, NY, 1966, p. 46.

temperature range ΔT_{solid} as defined earlier.¹³⁰ The average density of the solid at room temperature is then used to compute the maximum energy density of heat capacity (range **0.10-18 MJ/L**) as shown in **Table 8**. (The density of most solids doesn't change dramatically with temperature.)

The specific heat and density for the representative non-elemental solids of anhydrous calcium chloride,¹³¹ concrete,¹³² fused silica,¹³³ glucose,¹³⁴ granite,¹³⁵ naphthalene,¹³⁶ paraffin wax,¹³⁷ and polyethylene¹³⁸ are taken at room temperature. The specific heat for water-ice is taken as the maximum near-melting-point value of ~ 2100 J/kg-K,¹³⁹ with ice density taken as the mean ~ 928 kg/m³ over the entire available ΔT for ice.¹⁴⁰ (An integration of interpolated specific heat data over the entire $\Delta T_{\text{solid}} = 269$ K temperature range for water-ice¹⁴¹ gives a total exploitable specific heat capacity of 1123 J/kg-K, about 53% of the maximum value of ~ 2100 J/kg-K used in our tables.) The values for beryllium, boron, diamond and graphite are similarly overestimated. For example, an integration of interpolated specific heat data, taken from both below¹⁴² and above¹⁴³ room temperature, over the entire $\Delta T_{\text{solid}} \sim 2000$ K temperature range for solid diamond¹⁴⁴ gives a total exploitable specific heat capacity of 1461 J/kg-K, or about 70% of the maximum value of

¹³⁰ There are quantum models of the heat capacity of solids that include the decrease at low temperatures (e.g., https://en.wikipedia.org/wiki/Debye_model), which could be integrated over the indicated temperature range for various solids if more realistic estimates are required.

¹³¹ https://en.wikipedia.org/wiki/Calcium_chloride.

¹³² Kodur V. Properties of concrete at elevated temperatures. ISRN Civil Engineering 2014;2014:1-15; <https://www.hindawi.com/journals/isrn/2014/468510/>.

¹³³ https://en.wikipedia.org/wiki/Silicon_dioxide; https://en.wikipedia.org/wiki/Heat_capacity.

¹³⁴ <https://en.wikipedia.org/wiki/Glucose>.

¹³⁵ <https://en.wikipedia.org/wiki/Granite>; <http://hyperphysics.phy-astr.gsu.edu/hbase/Tables/sphtt.html#c1>.

¹³⁶ <https://en.wikipedia.org/wiki/Naphthalene>.

¹³⁷ https://en.wikipedia.org/wiki/Paraffin_wax.

¹³⁸ <https://en.wikipedia.org/wiki/Polyethylene>; https://en.wikipedia.org/wiki/Heat_capacity.

¹³⁹ [https://en.wikipedia.org/wiki/Water_\(data_page\)#Thermodynamic_properties](https://en.wikipedia.org/wiki/Water_(data_page)#Thermodynamic_properties).

¹⁴⁰ [https://en.wikipedia.org/wiki/Properties_of_water#/media/File:Density_of_ice_and_water_\(en\).svg](https://en.wikipedia.org/wiki/Properties_of_water#/media/File:Density_of_ice_and_water_(en).svg).

¹⁴¹ [https://en.wikipedia.org/wiki/Water_\(data_page\)](https://en.wikipedia.org/wiki/Water_(data_page)) and https://en.wikipedia.org/wiki/Properties_of_water.

¹⁴² Pitzer KS. The heat capacity of diamond from 70 to 300 K. J Chem Phys 1938 Feb;6:68-70; http://www.colorado.edu/physics/phys4340/phys4340_sp15/hw/JChemPhys_6_68_1938_Diamond.pdf.

¹⁴³ Victor AC. Heat capacity of diamond at high temperatures, J Chem Phys 1962 Apr 1;36(7):1903-1911; http://www.colorado.edu/physics/phys4340/phys4340_sp15/hw/JChemPhys36_1903_1962_Diamond.pdf.

¹⁴⁴ Above ~ 2000 K, diamond graphitizes at ordinary pressure. Evans T, James PF. A study of the transformation of diamond to graphite. Proc Roy Soc A 1964 Jan 21;277:260-269; <http://rspa.royalsocietypublishing.org/content/277/1369/260.short>.

2081 J/kg-K used in the tables. The maximum Carnot efficiency¹⁴⁵ $\eta_{\text{Carnot}} = \Delta T_{\text{solid}} / T_{\text{m.p.}} > 98.3\%$ in all cases if we assume that a low-cost 4 K cold sink is readily available. If a higher-temperature cold sink must be used, the Carnot efficiency will decline and the values estimated in **Table 7** and **Table 8** must be reduced accordingly.

Table 7. Maximum exploitable specific energy in heat capacity for solids					
Atom or Molecule In Solid Phase	Specific Energy (MJ/kg)	Atom or Molecule In Solid Phase	Specific Energy (MJ/kg)	Atom or Molecule In Solid Phase	Specific Energy (MJ/kg)
Carbon (graphite)	8.140	Cobalt	0.748	Strontium	0.298
Boron	5.423	Niobium	0.739	Arsenic	0.295
Beryllium	4.316	Nickel	0.734	Silver	0.285
Carbon (diamond)	4.155	Calcium	0.693	Zinc	0.263
Beryllium oxide	2.832	Manganese	0.689	Platinum	0.261
Boron nitride (cubic)	2.574	Calcium chloride	0.685	Gadolinium	0.251
Lithium	1.620	Zirconium	0.582	Thorium	0.218
Concrete	1.569	Water-ice	0.565	Potassium	0.213
Silicon	1.498	Rhodium	0.542	Antimony	0.185
Silicon dioxide (fused)	1.393	Copper	0.533	Gold	0.169
Granite	1.208	Yttrium	0.505	Selenium	0.155
Vanadium	1.069	Glucose	0.503	Uranium	0.147
Chromium	1.046	Tungsten	0.502	Tellurium	0.141
Titanium	1.012	Tantalum	0.454	Cadmium	0.131
Scandium	1.007	Naphthalene	0.452	Gallium	0.107
Paraffin wax	0.977	Osmium	0.434	Tin (white)	0.106
Magnesium	0.945	Palladium	0.428	Rubidium	0.090
Polyethylene	0.930	Germanium	0.415	Iodine	0.075
Aluminum	0.861	Sodium	0.399	Lead	0.072
Wood	0.843	Iridium	0.353	Bismuth	0.065
Iron	0.809	Hafnium (hexagonal)	0.350	Cesium	0.056
Molybdenum	0.754	Sulfur (rhombohedral)	0.299	Mercury	0.029

Carbon, boron and beryllium top both lists in terms of theoretical total exploitable energy storage, though tungsten and osmium are also in the top five on the energy density list (**Table 8**) due to their very high densities and melting points, and many other heavy metals are also high on the energy density list. It appears that maximum exploitable specific energies in the **4-8 MJ/kg** range and energy densities in the **8-18 MJ/L** range might be possible to achieve using the heat capacity of solids. Note that while the highest heat capacities per degree K are available at the highest

¹⁴⁵ [https://en.wikipedia.org/wiki/Carnot%27s_theorem_\(thermodynamics\)](https://en.wikipedia.org/wiki/Carnot%27s_theorem_(thermodynamics)). Note that “the Carnot efficiency is invariably far above the efficiency of real heat engines...because the reversible conditions under which heat engines would have to operate to achieve Carnot efficiency correspond to zero power output.” Chen J. The maximum power output and maximum efficiency of an irreversible Carnot heat engine. J Phys D: Appl Phys. 1994;27:144-1149; <https://core.ac.uk/download/pdf/41373385.pdf>.

temperatures, this is also where the Carnot efficiencies are lowest, so a proper design must seek the optimum balance of these factors for the particular application.

Table 8. Maximum exploitable energy density in heat capacity for solids					
Atom or Molecule In Solid Phase	Energy Density (MJ/L)	Atom or Molecule In Solid Phase	Energy Density (MJ/L)	Atom or Molecule In Solid Phase	Energy Density (MJ/L)
Carbon (graphite)	18.45	Titanium	4.158	Cadmium	1.049
Carbon (diamond)	14.60	Manganese	4.102	Polyethylene	0.893
Boron	12.85	Silicon	3.850	Paraffin wax	0.880
Boron nitride (cubic)	8.881	Concrete	3.609	Tellurium	0.879
Tungsten	8.834	Zirconium	3.376	Lithium	0.865
Osmium	8.679	Granite	3.261	Glucose	0.775
Beryllium oxide	8.523	Silicon dioxide (fused)	3.060	Lead	0.768
Beryllium	7.295	Gold	2.929	Tin (white)	0.738
Molybdenum	7.030	Scandium	2.818	Strontium	0.709
Tantalum	6.810	Silver	2.659	Bismuth	0.650
Iridium	6.709	Uranium	2.546	Gallium	0.634
Cobalt	6.630	Thorium	2.545	Sulfur (rhombic)	0.620
Chromium	6.591	Germanium	2.212	Selenium	0.619
Niobium	6.333	Yttrium	2.140	Water-ice	0.525
Vanadium	5.882	Aluminum	2.044	Wood	0.506
Rhodium	5.805	Gadolinium	1.986	Naphthalene	0.463
Nickel	5.735	Zinc	1.731	Mercury	0.388
Iron	5.646	Arsenic	1.687	Iodine	0.372
Platinum	5.161	Magnesium	1.497	Sodium	0.370
Palladium	5.152	Calcium chloride	1.473	Potassium	0.176
Hafnium (hexagonal)	4.664	Antimony	1.207	Rubidium	0.132
Copper	4.272	Calcium	1.074	Cesium	0.103

3.1.2 Heat Capacity of Liquids

The heat capacity of a liquid at constant pressure (C_p) usually varies relatively little across the entire liquid temperature range $\Delta T_{\text{liquid}} (= T_{\text{b.p.}} - T_{\text{m.p.}})$, so the assumption that it is constant is generally adequate as a first approximation. The heat capacity of high-temperature liquid metals and molten oxides is essentially constant with temperature. The variation in heat capacity with temperature for lower-temperature liquid elements and other liquid materials is also relatively small but varies in shape according to the substance involved. For example, the C_p of the liquid elements Au, Bi, Ga, Hg, In, Li, Pb, and Rb is highest at $T_{\text{m.p.}}$ and decreases toward $T_{\text{b.p.}}$; the C_p for liquefied gases such as Ar, H_2 , N_2 , Ne, and Xe is lowest at $T_{\text{m.p.}}$ and increases toward $T_{\text{b.p.}}$, exactly the reverse; the C_p for liquid S is convex-shaped between $T_{\text{m.p.}}$ and $T_{\text{b.p.}}$; and the C_p for liquid Cs, H_2O , K, Na, and O_2 is concave-shaped between $T_{\text{m.p.}}$ and $T_{\text{b.p.}}$.¹⁴⁶

Among liquids generally, the specific heat of water is extremely high and varies little with temperature at standard pressure, falling from 4217 J/kg-K at 0 °C to a low of 4178 J/kg-K at 34 °C,¹⁴⁷ then rising back to 4219 J/kg-K at 100 °C,¹⁴⁸ a variation of less than 1% with an average of ~4200 J/kg-K over the full $\Delta T_{\text{liquid}} = 100$ K range at 1 atm. Unfortunately, this ΔT_{liquid} is relatively small compared to other possible energy storage liquids, so the greatest specific heat energy that can be stored in 100 °C liquid water, then extracted by cooling it to 0 °C without a change in phase, is only (4200 J/kg-K) (100 K) = **0.42 MJ/kg**.¹⁴⁹ (Near the boiling point, the specific heat capacity at constant volume for water only varies from these numbers by up to 0.0005 MJ/kg-K at pressures up to 400 atm.¹⁵⁰) Taking 958 kg/m³ as the water density at 100 °C, the greatest extractable energy density is **0.404 MJ/L**.

Table 9 shows a ranked list of the Carnot-adjusted maximum specific energy of heat capacity for various liquid elements and other representative organic and inorganic liquids (range **0.005-8.4 MJ/kg**), calculated as the product of the heat capacity at constant pressure (C_p), estimated either

¹⁴⁶ Fegley B Jr. Practical Chemical Thermodynamics for Geoscientists, Academic Press, 2012, p. 83; <https://books.google.com/books?id=CzHRZBolGR4C&pg=PA83>.

¹⁴⁷ "Heat capacity of liquid water from 0 °C to 100 °C"; http://www.vaxasoftware.com/doc_eduen/qui/caloresph2o.pdf.

¹⁴⁸ http://www.engineeringtoolbox.com/water-thermal-properties-d_162.html.

¹⁴⁹ Higher pressures, extending even to above the critical point pressure, may allow a larger range for ΔT_{liquid} .

¹⁵⁰ http://www.ems.psu.edu/~radovic/Watson_IEC_1943.pdf.

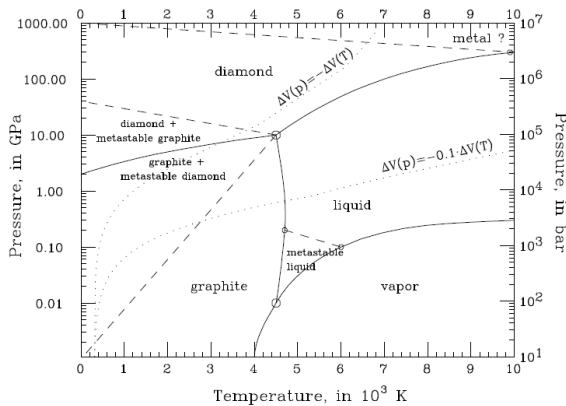
as the average of the values at $T_{m.p.}$ and $T_{b.p.}$ or as a representative value from several data sources,¹⁵¹ and the maximum exploitable temperature range ΔT_{liquid} as defined earlier.

Table 9. Maximum exploitable specific energy in heat capacity for liquids

Atom or Molecule In Liquid Phase	Specific Energy (MJ/kg)	Atom or Molecule In Liquid Phase	Specific Energy (MJ/kg)	Atom or Molecule In Liquid Phase	Specific Energy (MJ/kg)
Carbon (graphite)	8.427	1-nonanol	0.280	n-butane	0.158
Lithium	3.499	1-decanol	0.276	Lead	0.155
Calcium chloride	1.870	1-undecanol	0.271	Bismuth	0.150
Beryllium	1.666	1-heptanol	0.263	Acetone	0.148
Aluminum	1.409	Ethanol	0.258	Xylene	0.144
Silicon	0.881	1-hexanol	0.258	Antimony	0.137
Sodium	0.715	1-octanol	0.251	Osmium	0.119
Titanium	0.582	Propylene	0.239	Iridium	0.116
Vanadium	0.530	Manganese	0.239	Water	0.113
Tin	0.469	Sulfuric acid	0.235	Cesium	0.104
Iron	0.461	Ethylene glycol	0.222	Carbon disulfide	0.077
Cobalt	0.442	Heptane	0.215	Zinc	0.076
Uranium	0.408	Decane	0.205	Selenium	0.072
Nickel	0.395	Methanol	0.196	Naphthalene	0.066
Copper	0.377	Magnesium	0.190	Strontium	0.066
Potassium	0.374	Toluene	0.190	Acetic acid	0.054
Thorium	0.365	Chromium	0.186	Cadmium	0.050
Niobium	0.359	Platinum	0.186	Chloroform	0.049
Zirconium	0.343	Octane (~gasoline)	0.185	Ammonia	0.039
1-propanol	0.339	Yttrium	0.185	Mercury	0.035
Plutonium	0.326	Hexane	0.178	Benzene	0.030
Glycerine	0.320	Tantalum	0.177	Carbon tetrachloride	0.025
Scandium	0.316	Aniline	0.173	Iodine	0.023
Molybdenum	0.306	Tungsten	0.172	Hydrogen (LH ₂)	0.019
1-pentanol	0.299	Gold	0.168	Sodium nitrate	0.013
Rhodium	0.295	Silver	0.166	Potassium nitrate	0.009
1-butanol	0.286	Ethyl ether	0.164	Bromine	0.006
Lithium nitrate	0.283	Rubidium	0.163	Nitrogen (LN ₂)	0.005

¹⁵¹ Data sources: C1-C18 1-alkanols <https://www.nist.gov/sites/default/files/documents/srd/jpcrd390.pdf>, alkali metal liquids <https://www.nist.gov/sites/default/files/documents/srd/jpcrd474.pdf>, liquid iron <http://webbook.nist.gov/cgi/cbook.cgi?ID=C7439896&Units=SI&Mask=2#Thermo-Condensed>, liquid nitrogen <https://www.bnl.gov/magnets/staff/gupta/cryogenic-data-handbook/Section6.pdf>, liquid hydrogen <http://technifab.com/cryogenic-resource-library/cryogenic-fluids/liquid-hydrogen/>, molten nitrate salts <http://energy.sandia.gov/wp-content/gallery/uploads/Thermodynamic-Properties-of-Molten-Nitrate-Salts-Cordaro.pdf>, and other liquids http://www.engineeringtoolbox.com/specific-heat-fluids-d_151.html and http://www.engineeringtoolbox.com/liquid-metal-boiling-points-specific-heat-d_1893.html.

The Carnot efficiency of heat energy extraction ($\eta_{\text{Carnot}} = \Delta T_{\text{liquid}} / T_{\text{b.p.}}$) ranges from 15%-82% for these liquids, so the available specific energy must be reduced by this percentage in each case to accord with the Second Law of Thermodynamics.¹⁵² This gives the maximum exploitable specific energy in heat capacity for liquids. The density of most liquids doesn't change dramatically with temperature, so the average density of the liquid is used to compute the maximum energy density of heat capacity (range **0.001-15.2 MJ/L**) as shown in **Table 10**.



Liquid carbon is at the top of both lists but requires some explanation. At normal pressure, graphite sublimates at ~ 3900 K. The operating pressure must be raised to at least 10.8 MPa (107 atm) to obtain liquid carbon at the triple point, and even higher into the 0.1-10 GPa range (1000-100,000 atm) to obtain a substantial liquid operating range between ~ 4700 K and 10,000 K (or higher)¹⁵³ as indicated in the phase diagram of carbon¹⁵⁴ (chart, left). The experimentally-determined specific heat capacity of ~ 3000 J/kg-K for liquid carbon

near the melting point,¹⁵⁵ coupled with a mean density of ~ 1800 kg/m³ in the pressurized liquid state,¹⁵⁶ along with a potentially very large $\Delta T_{\text{liquid}} \geq 5300$ K operating range, yield the highest theoretical values for specific energy and energy density shown in the tables.

Liquid lithium has the highest exploitable specific energy at normal pressures because it has the second-highest average specific heat of 4246 J/kg-K between $T_{\text{m.p.}}$ and $T_{\text{b.p.}}$ and a very high ΔT_{liquid} of 1149 K giving a very high Carnot efficiency of 72%. (Only liquid ammonia has a higher specific heat of 4700 J/kg-K on this list, but ammonia's ΔT_{liquid} is a miniscule 44 K, giving a Carnot efficiency of only 18%.) Similarly, liquid uranium has the highest exploitable energy density because it has the second-largest ΔT_{liquid} of 2999 K (giving the fifth-highest Carnot efficiency of 68.1%) and the sixth-largest mass density (17,300 kg/m³) on the list, even though its

¹⁵² [https://en.wikipedia.org/wiki/Carnot%27s_theorem_\(thermodynamics\)](https://en.wikipedia.org/wiki/Carnot%27s_theorem_(thermodynamics)).

¹⁵³ Ghiringhelli LM, Meijer EJ. Chapter 1. Liquid Carbon: Freezing Line and Structure Near Freezing. In: Colombo L, Fasolino A, eds., Computer-Based Modeling of Novel Carbon Systems and Their Properties, Carbon Materials: Chemistry and Physics 3, Springer, 2010, pp. 1-36; http://th.fhi-berlin.mpg.de/site/uploads/Publications/Ghiringhelli-Meijer_LiquidCarbon.pdf.

¹⁵⁴ Zazula JM. On Graphite Transformations at High Temperature and Pressure Induced by Absorption of the LHC Beam. CERN LHC Project Note 78/97, 1997 Jan 18; <http://citeseerx.ist.psu.edu/viewdoc/download?doi=10.1.1.617.810&rep=rep1&type=pdf>.

¹⁵⁵ Korobenko VN, Savvatimskiy AI, Cheret R. Graphite melting and properties of liquid carbon. Int. J. Thermophys. 1999 Jul;20(4):1247-1256; <http://link.springer.com/article/10.1023/A:1022679509593>.

¹⁵⁶ Savvatimskiy A. Measurements of the melting point of graphite and the properties of liquid carbon (a review for 1963-2003). Carbon. 2005;43(6):1115; <http://www.sciencedirect.com/science/article/pii/S0008622305000291>

average specific heat is very poor (200 J/kg-K). It appears that exploitable specific energies around **~3-8 MJ/kg** and exploitable energy densities around **~7-15 MJ/L** might be possible to achieve using the heat capacity of liquids.

Table 10. Maximum exploitable energy density in heat capacity for liquids

Atom or Molecule In Liquid Phase	Energy Density (MJ/L)	Atom or Molecule In Liquid Phase	Energy Density (MJ/L)	Atom or Molecule In Liquid Phase	Energy Density (MJ/L)
Carbon (graphite)	15.17	Bismuth	1.507	Ethanol	0.204
Uranium	7.066	Manganese	1.422	Cesium	0.192
Plutonium	5.419	Chromium	1.174	Aniline	0.177
Thorium	4.267	Antimony	0.897	Toluene	0.165
Calcium chloride	4.020	Scandium	0.885	Strontium	0.156
Cobalt	3.918	Yttrium	0.785	Methanol	0.156
Platinum	3.674	Lithium nitrate	0.673	Decane	0.150
Aluminum	3.347	Sodium	0.662	Propylene	0.147
Tin	3.278	Zinc	0.498	Heptane	0.147
Iron	3.216	Mercury	0.469	Octane (~gasoline)	0.130
Rhodium	3.151	Sulfuric acid	0.432	Xylene	0.125
Nickel	3.086	Glycerine	0.403	Ethyl ether	0.117
Niobium	3.073	Cadmium	0.398	Acetone	0.116
Tungsten	3.034	n-butane	0.392	Hexane	0.116
Copper	3.024	Potassium	0.310	Iodine	0.115
Vanadium	2.914	Magnesium	0.301	Water	0.108
Gold	2.909	Selenium	0.289	Carbon disulfide	0.098
Molybdenum	2.856	1-propanol	0.272	Chloroform	0.068
Beryllium	2.816	Ethylene glycol	0.247	Naphthalene	0.064
Tantalum	2.651	1-pentanol	0.242	Acetic acid	0.057
Titanium	2.391	Rubidium	0.237	Carbon tetrachloride	0.039
Osmium	2.371	1-nonanol	0.233	Sodium nitrate	0.030
Silicon	2.265	1-butanol	0.232	Benzene	0.026
Iridium	2.203	1-decanol	0.229	Ammonia	0.026
Zirconium	1.991	1-undecanol	0.225	Bromine	0.019
Lithium	1.792	1-heptanol	0.215	Potassium nitrate	0.019
Lead	1.650	1-hexanol	0.210	Nitrogen (LN ₂)	0.004
Silver	1.543	1-octanol	0.207	Hydrogen (LH ₂)	0.001

The heat capacity of molten salt can be used as a thermal energy storage method “to retain thermal energy collected by a solar tower¹⁵⁷ or solar trough of a concentrated solar power plant, so that it can be used to generate electricity in bad weather or at night.”¹⁵⁸ With proper insulation

¹⁵⁷ e.g., https://en.wikipedia.org/wiki/Crescent_Dunes_Solar_Energy_Project.

¹⁵⁸ https://en.wikipedia.org/wiki/Thermal_energy_storage#Molten_salt_technology and https://en.wikipedia.org/wiki/Thermal_energy_storage#Solar_energy_storage.

on the tank, the thermal energy can be usefully stored for up to a week.¹⁵⁹ The most widely employed fusible salts include the nitrates of lithium, potassium, and sodium,¹⁶⁰ which unfortunately have low ΔT_{liquid} and therefore low η_{Carnot} as well. Low-capacity storage heaters using solid bricks, concrete, earth, or water for diurnal¹⁶¹ or longer-term¹⁶² heat storage are also commonplace.

¹⁵⁹ “13.1.2.2. Thermal storage,” in Ehrlich R. Renewable Energy: A First Course, CRC Press, 2013, p. 375; <https://www.crcpress.com/Renewable-Energy-A-First-Course/Ehrlich/p/book/9781439861158>, <http://www.gbv.de/dms/ilmenau/toc/726403032.PDF> (TOC).

¹⁶⁰ A mixture of 60% NaNO_3 + 40% KNO_3 (“Molten salts properties; http://www.archimedesolarenergy.com/molten_salt.htm), sometimes called “solar salt” (https://en.wikipedia.org/wiki/Eutectic_system#Others), may be used for thermal energy storage in concentrated solar power plants.

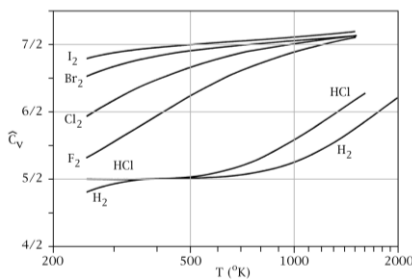
¹⁶¹ https://en.wikipedia.org/wiki/Storage_heater and https://en.wikipedia.org/wiki/Solar_pond.

¹⁶² https://en.wikipedia.org/wiki/Seasonal_thermal_energy_storage.

3.1.3 Heat Capacity of Gases

For gases, we shall use heat capacity at constant volume (C_V) because a practical tank or container for stored energy will normally possess some particular volume. (The constant pressure value C_P ($\approx C_V + R$) only makes sense if the containment has variable volume and can expand as the storage material is heated, allowing pressure to remain constant as work is done during the expansion. When heat is added to a gas confined to a constant volume, the pressure rises but no work is done.)

The C_V of a gas may be thought of as the sum of four separate components. The first component is the **translational kinetic energy** due to the three-dimensional motion of the gas molecule through space, or $1.5R$ per mole (~ 12.47 J/mole-K) taking $0.5R$ per translational degree of freedom. This is the sole contribution for monatomic gases. The second component is the **rotational energy** of the gas molecule. Ideal diatomic molecules effectively have two degrees of rotational freedom, contributing another R per mole (~ 8.31 J/mole-K), and rotations are excited at temperatures below the boiling point for virtually all gases except H_2 , for which rotational energy only becomes significant over ~ 85 K due to the molecule's small moment of inertia which causes a wide spacing of its rotational energy levels. The third component is **vibrational energy**, whose modes (typically excited at temperatures ≥ 1000 K) contribute another R per mole (~ 8.31 J/mole-K) for ideal diatomic molecules having two degrees of freedom. (Triatomic and larger polyatomic molecules have still more rotational and vibrational degrees of freedom and can store



still more energy.) In practice the contributions from these latter two sources bring the total to less than $\sim 3.5R$ (see chart, left; C_V in units of R),¹⁶³ in part because vibrational states, and to a lesser extent rotational states, are quantized, and in part because vibrational modes are generally not completely excited before the dissociation temperature is reached except for diatomic molecules where both atoms are very heavy. The fourth component is **electronic energy** modes, which normally are not excited below $\sim 10,000$ K.¹⁶⁴

To avoid the effort of compiling and integrating comprehensive $C_V(T)$ curves over the entire $\Delta T_{\text{gas}} = 1000$ K temperature range for every gas of interest, we can generate a reasonable comparative estimate of the potential for energy storage with each material by simply multiplying the C_V at NTP (i.e., “Normal Temperature and Pressure”; $20^\circ\text{C} \sim 293$ K, 1 atm)¹⁶⁵ by ΔT_{gas} and

¹⁶³ https://en.wikipedia.org/wiki/Heat_capacity#Diatomic_gas.

¹⁶⁴ Fegley B Jr. Practical Chemical Thermodynamics for Geoscientists, Academic Press, 2012, p. 82-3; <https://books.google.com/books?id=CzHRZBolGR4C&pg=PA83>.

¹⁶⁵ Data sources: Gas densities at STP and NTP from http://www.engineeringtoolbox.com/gas-density-d_158.html, “Gases - Specific Heat Capacities and Individual Gas Constants” <http://catalog.conveyorspneumatic.com/Asset/FLS%20Specific%20Heat%20Capacities%20of%20Gases.pdf>, <https://en.wikipedia.org/wiki/Chloromethane>; https://en.wikipedia.org/wiki/Nitrous_oxide, <http://scorecard.goodguide.com/chemical-profiles/html/carbondisulfide.html>,

by the Carnot efficiency of heat energy extraction $\eta_{\text{Carnot}} = \Delta T_{\text{gas}} / (\Delta T_{\text{gas}} + T_{\text{b.p.}})$, yielding the Carnot-adjusted exploitable specific heat capacity per kilokelvin (range **0.04-10 MJ/kg**) in **Table 11**.

Table 11. Exploitable specific energy per kilokelvin in heat capacity for gases at 1 atm pressure

Atom or Molecule In Gas Phase	Specific Energy (MJ/kg)	Atom or Molecule In Gas Phase	Specific Energy (MJ/kg)	Atom or Molecule In Gas Phase	Specific Energy (MJ/kg)
Hydrogen (H ₂)	10.59	Propylene (Propene)	1.069	Nitrous oxide	0.582
Helium	5.171	Ethylene	1.052	Carbon dioxide	0.548
Methane	1.529	Acetone	0.993	Hydrogen chloride	0.480
Ether	1.491	Sodium (@ 1200 K)	0.779	Carbon disulfide	0.417
Ammonia	1.339	Benzene	0.732	Chloroform	0.412
Ethane	1.249	Nitrogen (N ₂)	0.690	Sulfur dioxide	0.404
Ethanol	1.236	Methyl chloride	0.669	Chlorine (Cl ₂)	0.291
Propane	1.202	Carbon monoxide	0.666	Argon	0.287
Butane	1.202	Hydrogen sulfide	0.645	Hydrogen bromide	0.213
Acetylene	1.152	Nitric oxide	0.640	Bromine (Br ₂)	0.150
Methanol	1.144	Nitrogen dioxide	0.630	Krypton	0.133
Water	1.092	Oxygen (O ₂)	0.604	Xenon	0.082
Ozone	1.095	Neon	0.602	Mercury	0.038

Multiplying the specific heat by the density of each gas at NTP gives the exploitable energy density of heat capacity per kilokelvin (range **0.0001-0.007 MJ/L** at 1 atm) as shown in **Table 12**. Of course, increasing the pressure while maintaining constant volume will increase the exploitable energy density per kilokelvin simply because the gas density goes up. For example, sodium vapor¹⁶⁶ at 1 atm near $T_{\text{b.p.}} \sim 1200$ K with a mass density of 0.394 kg/m^3 has a specific heat of 1680 J/kg-K , yielding a Carnot-adjusted energy density of **0.0003 MJ/L** per kilokelvin. If we now increase the temperature by $\Delta T_{\text{gas}} = 1000$ K up to 2200 K at constant volume, the pressure rises to ~ 70 atm with a mass density of 27.7 kg/m^3 while the specific heat falls slightly to 1340 J/kg-K , but the Carnot-adjusted energy density rises 56-fold to **0.0172 MJ/L** per kilokelvin.

http://www.thermalfuidscentral.org/encyclopedia/index.php/Thermophysical_Properties:_Ethanol,
http://www.thermalfuidscentral.org/encyclopedia/index.php/Thermophysical_Properties:_Acetone,
<http://encyclopedia2.thefreedictionary.com/Bromine+vapor>, <http://scorecard.goodguide.com/chemical-profiles/html/chloroform.html>, https://en.wikipedia.org/wiki/Nitrogen_dioxide (NO₂),
http://www.chemicalbook.com/chemicalproductproperty_en_cb6853949.htm (diethyl ether),
<https://en.wikipedia.org/wiki/Helium>, <http://www.ne.anl.gov/eda/ANL-RE-95-2.pdf> (sodium),
<https://www.bnl.gov/magnets/staff/gupta/cryogenic-data-handbook/Section3.pdf> (hydrogen gas), and
<https://books.google.com/books?id=CzHRZBoLGR4C&pg=PA68> (O₃, HBr, Kr, Xe).

¹⁶⁶ Fink JK, Leibowitz L. Thermodynamic and Transport Properties of Sodium Liquid and Vapor. Argonne National laboratory, Reactor Engineering Division, ANL/RE-95/2, Jan 1995, pp. 15, 87;
<http://www.ne.anl.gov/eda/ANL-RE-95-2.pdf>.

Table 12. Exploitable energy density per kilokelvin in heat capacity for gases at 1 atm pressure

Atom or Molecule In Gas Phase	Energy Density (MJ/L)	Atom or Molecule In Gas Phase	Energy Density (MJ/L)	Atom or Molecule In Gas Phase	Energy Density (MJ/L)
Ether	0.0046	Nitrous oxide	0.0012	Oxygen (O ₂)	0.0008
Butane	0.0030	Bromine (Br ₂)	0.0011	Hydrogen bromide	0.0008
Benzene	0.0026	Methane	0.0010	Carbon monoxide	0.0008
Ozone	0.0023	Carbon dioxide	0.0010	Hydrogen chloride	0.0007
Propane	0.0023	Ammonia	0.0010	Neon	0.0005
Chloroform	0.0020	Hydrogen (H ₂)	0.0010	Krypton	0.0005
Propylene (Propene)	0.0019	Hydrogen sulfide	0.0009	Xenon	0.0005
Ethane	0.0016	Sulfur dioxide	0.0009	Argon	0.0005
Methyl chloride	0.0015	Water	0.0009	Sodium (@ 1200 K)	0.0003
Ethylene	0.0013	Chlorine (Cl ₂)	0.0009	Acetone	0.0003
Carbon disulfide	0.0013	Helium	0.0009	Methanol	0.0002
Acetylene	0.0013	Nitric oxide	0.0008	Ethanol	0.0001
Nitrogen dioxide	0.0012	Nitrogen (N ₂)	0.0008		

Gaseous hydrogen has the highest exploitable specific energy because it has the highest specific heat of the listed materials at NTP (10,160 J/kg-K) and the second-highest Carnot efficiency (98%) because only helium's $T_{b.p.}$ is lower than hydrogen's. Nitrogen dioxide has the second highest specific heat (4600 J/kg-K) on the list. However, gaseous hydrogen has very poor exploitable energy density because it has the lowest mass density at STP (0.09 kg/m³) on the list. It appears that exploitable specific energies of **3-10 MJ/kg** and exploitable energy densities of **~0.007 MJ/L** per kilokelvin per atm of pressure might be possible to achieve using the heat capacity of gases.

3.2 Latent Heat

“Latent heat” is the energy released by, or absorbed by, a material body at some constant temperature, most typically during a phase change from solid to liquid or gas, or from liquid to gas, or the reverse. Also known as the “heat of transition” or “enthalpy of transition”, the latent heat of fusion (melting) or the latent heat of vaporization (boiling) are processes that require an energy input. A similar amount of energy is released during a transition in the opposite direction.

The specific latent heat is the latent heat per unit mass of the storage material (MJ/kg), and the latent heat energy density is the latent heat per unit volume (MJ/L), normally measured at 1 atm pressure. Energy release occurs only at a specific temperature – i.e., the melting point $T_{m.p.}$ or boiling point $T_{b.p.}$, as measured at 1 atm. The heat may be used to increase the temperature of another material which can serve as the hot source, after which the energy can be extracted via heat engine as described in **Section 3.1**. Alternatively, the release of latent heat may involve a significant change in pressure or volume of the energy storage material, which can be converted to mechanical energy as described in **Section 5**.

The heat of fusion is only negligibly affected by increasing pressure because liquids are relatively incompressible. But gases are highly compressible, so raising pressure causes the heat of vaporization to fall, eventually reaching zero at the critical point (e.g., at 218 atm and 647 K for water)¹⁶⁷ where the liquid and vapor phases become thermodynamically indistinguishable.

¹⁶⁷ [https://en.wikipedia.org/wiki/Critical_point_\(thermodynamics\)#Overview](https://en.wikipedia.org/wiki/Critical_point_(thermodynamics)#Overview).

3.2.1 Heat of Fusion

Latent heat energy storage systems exploit the energy that is released during a phase change in the storage material. Existing systems (almost exclusively solid/liquid) typically use paraffin wax or fatty acid materials with specific heats of fusion in the range of **0.072-0.214 MJ/kg**,¹⁶⁸ or hydrated salt materials yielding in the range of **0.115-0.492 MJ/kg**.¹⁶⁹ There is interest in using encapsulated phase change materials, e.g., aluminum and sodium chloride,¹⁷⁰ for this purpose. Ice storage is also used commercially for the reverse purpose – to provide the ability to absorb energy upon demand, as in air conditioning systems for buildings.¹⁷¹

Table 13 shows a ranked list of the specific heat of fusion for the solid elements, oxides, organics, and other representative solids (range **0.011-8.74 MJ/kg**),¹⁷² while **Table 14** presents a

¹⁶⁸ Kenisarin M, Mahkamov K. Solar Energy Storage Using Phase Change Materials. *Renewable and Sustainable Energy Reviews* 2007;11:1913-1965.

¹⁶⁹ Zalba B, Marin JM, Cabeza LF, Mehling H. Review on Thermal Energy Storage with Phase Change: Materials, Heat Transfer Analysis and Applications. *Applied Thermal Engineering* 2003;23:251-283.

¹⁷⁰ Solomon LD. The use of Sodium Chloride & Aluminum as Phase Change materials for High Temperature Thermal Energy Storage Characterized by Calorimetry. Lehigh University Masters Thesis, Paper 1364, 2013; <http://preserve.lehigh.edu/cgi/viewcontent.cgi?article=2364&context=etd>.

¹⁷¹ At nighttime in the office tower at 1 Bryant Park in New York, a large refrigerator in the basement chills a water+glycol solution to below the freezing point of water using cheap overnight electricity from the grid. The system pumps the mixture into two miles of tubing coiled inside each of nearly four dozen 750-gallon tanks full of water at ~27 °F, freezing the water. The next day, the glycol solution flows out of the coils and into a closed-loop air-conditioning system. Combining with water and air, it helps to chill the building's 2.35 million square feet for as many as 10 hours during the day, when power is typically pricier. <https://www.nytimes.com/2017/06/03/business/energy-environment/biggest-batteries.html>.

¹⁷² Data Sources: Handbook of Chemistry and Physics, 49th edition (1969):D-33 to D-37, Wikipedia, Air Liquide <http://encyclopedia.airliquide.com/Encyclopedia.asp>, Engineering Toolbox (http://www.engineeringtoolbox.com/fusion-heat-metals-d_1266.html, http://www.engineeringtoolbox.com/latent-heat-melting-solids-d_96.html, heat of fusion for elements (<http://periodictable.com/Properties/A/FusionHeat.an.html>), boron <http://periodictable.com/Elements/005/data.html>, carbon <http://periodictable.com/Elements/006/data.html>, HF <http://pubs.acs.org/doi/abs/10.1021/ja01101a066>, formic acid <https://cameochemicals.noaa.gov/chris/FMA.pdf>, naphthalene <https://cameochemicals.noaa.gov/chris/NTM.pdf>, isopropyl alcohol (https://www.alibaba.com/product-detail/we-can-supply-iso-propyl-alcohol_1276438951.html), XeF4 (<http://chemister.ru/Database/properties-en.php?dbid=1&id=595>), XeF2 (http://www.chemicaldictionary.org/dic/X/Xenon-difluoride_198.html), PH3 (http://www.concoa.com/phosphine_properties.html), germane (<https://books.google.com/books?id=fmc-pXKkslkC&pg=PA536>), NaCl [https://en.wikipedia.org/wiki/Sodium_chloride_\(data_page\)](https://en.wikipedia.org/wiki/Sodium_chloride_(data_page)), and BeO <https://books.google.com/books?id=Xn8KbsgeFrwC&pg=PA479>.

similar materials list ranked by heat of fusion energy density (range **0.002-11.98 MJ/L**), calculated using the mass density near $T_{m.p.}$ in almost all cases.

Carbon tops both lists, but to repeatedly cycle between solid and liquid graphite to extract (or recharge) the latent heat of fusion will require continuous pressurization of the storage materials to at least 10.8 MPa (107 atm) to obtain liquid carbon at the triple point¹⁷³ (see carbon phase diagram chart, **Section 3.1.2**). Liquid graphite has a density of about 1370 kg/m³ at the triple point,¹⁷⁴ and the very high required operating temperature of $T_{m.p.} \sim 4700$ K at pressures ≥ 107 atm will make it very challenging to find a suitable container.

The next most useful heat of fusion-based energy storage material is boron, which provides the highest specific heat of fusion and the highest heat density of fusion at normal pressure. The operating temperature will be a lot lower than for graphite, with $T_{m.p.} = 2349$ K at 1 atm. Elemental boron has low toxicity, similar to that of table salt.¹⁷⁵ A preliminary design for a phase transition energy storage system using molten boron with a per-cycle storage efficiency of 75% has been published.¹⁷⁶

Beryllium oxide at normal pressure provides the next highest energy density both by mass and by volume, with a reasonably modest operating temperature of $T_{m.p.} = 2780$ K at 1 atm. While BeO is carcinogenic and can cause beryllium disease in particle form, once confined to solid form it should be safe to handle if not subjected to subsequent machining that releases dust.¹⁷⁷

Note that it is possible to “supercool” a liquid to below its melting point and not observe the heat evolved by the phase change from liquid to solid as long as the material remains liquid. The latent heat of fusion appears instantly when the liquid freezes. Explains one source:¹⁷⁸ “A liquid crossing its standard freezing point will crystallize in the presence of a seed crystal or nucleus

¹⁷³ Zazula JM. On Graphite Transformations at High Temperature and Pressure Induced by Absorption of the LHC Beam. CERN LHC Project Note 78/97, 1997 Jan 18; <http://citeseerx.ist.psu.edu/viewdoc/download?doi=10.1.1.617.810&rep=rep1&type=pdf>.

¹⁷⁴ Haaland D. Graphite-liquid-vapor triple point pressure and the density of liquid carbon. Carbon 1976;14(6):357; <http://www.sciencedirect.com/science/article/pii/0008622376900105?via%3Dihub>. Sekine T. An evaluation of the equation of state of liquid carbon at very high pressure. Carbon 1993;31:227.

¹⁷⁵ https://en.wikipedia.org/wiki/Boron#Health_issues_and_toxicity.

¹⁷⁶ Gilpin MR, Scharfe DB, Young MP, Pancotti AP. Molten boron phase-change thermal energy storage: Containment and applicability to microsatellites. 42nd AIAA Plasmadynamics and Laser Conference, held in Honolulu, HI, 27-30 June 2011; <http://www.dtic.mil/dtic/tr/fulltext/u2/a546871.pdf>.

¹⁷⁷ Beryllia ceramic MSDS; http://web.archive.org/web/20160118131605/http://americanberyllia.com/lit/Beryllium_Oxide_MSDS.pdf.

¹⁷⁸ Mishima O, Stanley HE. The relationship between liquid, supercooled and glassy water. Nature 1998;396:329-335; <http://www.nims.jp/water/Publications/MS1998nature-b.pdf>. See also <https://en.wikipedia.org/wiki/Supercooling#Explanation>.

around which a crystal structure can form creating a solid. Lacking any such nuclei, the liquid phase can be maintained all the way down to the temperature at which crystal homogeneous nucleation occurs. Homogeneous nucleation can occur above the glass transition temperature, but if homogeneous nucleation has not occurred above that temperature, an amorphous (non-crystalline) solid will form.” For example, pure nucleation-site-free liquid water ($T_{m.p.} = 273.15$ at 1 atm) can be supercooled down to its crystal nucleation temperature of 224.8 K.

In summary: Prior to any consideration of the attainable per-cycle storage efficiency in real physical systems, it appears that exploitable specific energies of **4-8 MJ/kg** and exploitable energy densities of **8-11 MJ/L** might be possible to achieve using the latent heat of fusion by cycling between solid and liquid phases of a suitable storage material.

Table 13. Maximum exploitable specific heat of fusion for solid/liquid latent heat cycling

Material Cycling Between Solid and Liquid Phases	Specific Energy (MJ/kg)	Material Cycling Between Solid and Liquid Phases	Specific Energy (MJ/kg)	Material Cycling Between Solid and Liquid Phases	Specific Energy (MJ/kg)
Carbon (C)	8.743	Iron (Fe)	0.272	Acetone (C ₃ H ₆ O)	0.098
Boron (B)	4.625	Manganese (Mn)	0.268	Diethyl ether (C ₄ H ₁₀ O)	0.093
Beryllium oxide	2.844	Uranium dioxide	0.259	Strontium (Sr)	0.091
Lithium oxide	1.960	Plutonium dioxide	0.255	Chlorine (Cl ₂)	0.090
Magnesium oxide	1.921	Zirconium (Zr)	0.230	Isopropyl alcohol (C ₃ H ₈ O)	0.088
Silicon (Si)	1.787	Dry granite ¹⁸⁰	0.220	Propane (C ₃ H ₈)	0.080
Calcium oxide	1.343	Dodecane (C ₁₂ H ₂₆)	0.216	Xenon tetrafluoride (XeF ₄)	0.079
Aluminum oxide	1.067	Calcium (Ca)	0.213	Methylpropane (C ₄ H ₁₀)	0.078
Magnesium fluoride	0.940	Copper (Cu)	0.205	Chloroform (CHCl ₃)	0.077
Vanadium monoxide	0.938	Decane (C ₁₀ H ₂₂)	0.201	Nitric oxide	0.077
Beryllium (Be)	0.882	Glycerol (C ₃ H ₈ O ₃)	0.201	Toluene (C ₇ H ₈)	0.072
Titanium dioxide	0.838	Stearic acid (C ₁₈ H ₃₆ O ₂)	0.199	Thorium (Th)	0.071
Manganese monoxide	0.767	Hydrogen fluoride (HF)	0.196	Propylene (C ₃ H ₆)	0.070
Zirconium dioxide	0.706	Uranium carbide	0.196	Selenium (Se)	0.067
Titanium sesquioxide	0.699	Tungsten (W)	0.193	Bromine (Br ₂)	0.067
Scandium sesquioxide	0.698	Silicon dioxide (quartz)	0.188	Gold (Au)	0.063
Nickel monoxide	0.678	Carbon dioxide (CO ₂)	0.184	Iodine (I ₂)	0.062
Strontium oxide	0.674	Acetic acid (C ₂ H ₄ O ₂)	0.181	Potassium (K)	0.061
Cobalt monoxide	0.670	Ethylene glycol (C ₂ H ₆ O ₂)	0.181	Tin (Sn)	0.059
Vanadium sesquioxide	0.670	Octane (C ₈ H ₁₈)	0.181	Methane (CH ₄)	0.058
Lithium (Li)	0.669	Carbon tetrachloride (CCl ₄)	0.174	Barium (Ba)	0.058
Niobium monoxide	0.615	Tantalum (Ta)	0.172	Hydrogen (H ₂)	0.058
Peridotite ¹⁷⁹	0.580	Rhodium (Rh)	0.167	Carbon disulfide (CS ₂)	0.058
Sodium chloride	0.478	Palmitic acid (C ₁₆ H ₃₂ O ₂)	0.164	Cadmium (Cd)	0.055
Potassium fluoride	0.468	Sulfuric acid (H ₂ SO ₄)	0.163	Bismuth (Bi)	0.052
Yttrium sesquioxide	0.463	Antimony (Sb)	0.161	Uranium (U)	0.050
Cerium dioxide	0.462	Hexane (C ₆ H ₁₄)	0.152	Sulfur (S)	0.039
Germanium (Ge)	0.438	Naphthalene (C ₁₀ H ₈)	0.147	Phosphine (PH ₃)	0.033
Iron monoxide	0.437	Osmium (Os)	0.142	Carbon monoxide (CO)	0.030
Titanium (Ti)	0.419	Heptane (C ₇ H ₁₆)	0.140	Argon (Ar)	0.030
Vanadium (V)	0.410	Iridium (Ir)	0.138	Nitrogen (N ₂)	0.026
Aluminum (Al)	0.398	Cyclopropane (C ₃ H ₈)	0.129	Rubidium (Rb)	0.026
Magnesium (Mg)	0.368	Benzene (C ₆ H ₆)	0.127	Lead (Pb)	0.023
Scandium (Sc)	0.356	Phenol (C ₆ H ₆ O)	0.121	Xenon (Xe)	0.017
Water (H₂O)	0.334	Ethylene (C ₂ H ₄)	0.119	Neon (Ne)	0.016
Ammonia (NH ₃)	0.332	Aniline (C ₆ H ₇ N)	0.114	Cesium (Cs)	0.016
Chromium (Cr)	0.331	Sodium (Na)	0.113	Oxygen (O ₂)	0.014
Boron trioxide	0.317	Zinc (Zn)	0.113	Fluorine (F ₂)	0.013
Nickel (Ni)	0.297	Silver (Ag)	0.111	Plutonium (Pu)	0.013
Molybdenum (Mo)	0.289	Ethanol (C ₂ H ₅ OH)	0.108	Helium (He)	0.012
Niobium (Nb)	0.285	Xenon difluoride (XeF ₂)	0.100	Mercury (Hg)	0.011
Formic acid (CH ₂ O ₂)	0.276	Platinum (Pt)	0.100	Germane (GeH ₄)	0.011
Cobalt (Co)	0.276	Methanol (CH ₃ OH)	0.099		

¹⁷⁹ <http://magma.geol.ucsb.edu/papers/EoV%20chapter%205%20Lesh%20Spera.pdf>.¹⁸⁰ <http://magma.geol.ucsb.edu/papers/EoV%20chapter%205%20Lesh%20Spera.pdf>.

Table 14. Maximum exploitable heat of fusion energy density for solid/liquid latent heat cycling

Material Cycling Between Solid and Liquid Phases	Energy Density (MJ/L)	Material Cycling Between Solid and Liquid Phases	Energy Density (MJ/L)	Material Cycling Between Solid and Liquid Phases	Energy Density (MJ/L)
Carbon (C)	11.98	Peridotite ¹⁸¹	1.560	Mercury (Hg)	0.153
Boron (B)	9.620	Beryllium (Be)	1.491	Decane (C ₁₀ H ₂₂)	0.147
Beryllium oxide	8.560	Zirconium (Zr)	1.335	Naphthalene (C ₁₀ H ₈)	0.141
Magnesium oxide	6.875	Potassium fluoride	1.161	Chlorine (Cl ₂)	0.141
Vanadium monoxide	5.398	Gold (Au)	1.091	Palmitic acid (C ₁₆ H ₃₂ O ₂)	0.140
Silicon (Si)	4.593	Antimony (Sb)	1.051	Phenol (C ₆ H ₆ O)	0.129
Nickel monoxide	4.521	Sodium chloride	1.036	Octane (C ₈ H ₁₈)	0.127
Niobium monoxide	4.487	Silver (Ag)	1.035	Chloroform (CHCl ₃)	0.120
Calcium oxide	4.486	Scandium (Sc)	0.997	Aniline (C ₆ H ₇ N)	0.116
Aluminum oxide	4.374	Boron trioxide	0.996	Benzene (C ₆ H ₆)	0.112
Cobalt monoxide	4.315	Aluminum (Al)	0.945	Sodium (Na)	0.105
Manganese monoxide	4.164	Uranium (U)	0.865	Hexane (C ₆ H ₁₄)	0.100
Zirconium dioxide	4.012	Thorium (Th)	0.832	Heptane (C ₇ H ₁₆)	0.095
Lithium oxide	3.946	Zinc (Zn)	0.742	Carbon disulfide (CS ₂)	0.089
Titanium dioxide	3.546	Magnesium (Mg)	0.583	Cyclopropane (C ₃ H ₈)	0.088
Tungsten (W)	3.397	Bismuth (Bi)	0.522	Ethanol (C ₂ H ₅ OH)	0.085
Cerium dioxide	3.333	Dry granite ¹⁸²	0.517	Methanol (CH ₃ OH)	0.078
Vanadium sesquioxide	3.263	Silicon dioxide (quartz)	0.498	Acetone (C ₃ H ₆ O)	0.077
Strontium oxide	3.169	Cadmium (Cd)	0.440	Sulfur (S)	0.071
Titanium sesquioxide	3.136	Xenon difluoride (XeF ₂)	0.434	Isopropyl alcohol (C ₃ H ₈ O)	0.069
Magnesium fluoride	2.959	Tin (Sn)	0.412	Ethylene (C ₂ H ₄)	0.068
Plutonium dioxide	2.922	Lithium (Li)	0.343	Diethyl ether (C ₄ H ₁₀ O)	0.066
Osmium (Os)	2.840	Formic acid (CH ₂ O ₂)	0.337	Toluene (C ₇ H ₈)	0.063
Uranium dioxide	2.839	Water (H₂O)	0.333	Xenon (Xe)	0.051
Molybdenum (Mo)	2.696	Xenon tetrafluoride (XeF ₄)	0.318	Potassium (K)	0.051
Scandium sesquioxide	2.694	Carbon tetrachloride (CCl ₄)	0.315	Methylpropane (C ₄ H ₁₀)	0.046
Uranium carbide	2.666	Iodine (I ₂)	0.307	Propane (C ₃ H ₈)	0.046
Iridium (Ir)	2.622	Sulfuric acid (H ₂ SO ₄)	0.300	Propylene (C ₃ H ₆)	0.043
Tantalum (Ta)	2.580	Calcium (Ca)	0.294	Argon (Ar)	0.041
Iron monoxide	2.509	Carbon dioxide (CO ₂)	0.287	Rubidium (Rb)	0.037
Germanium (Ge)	2.452	Ammonia (NH ₃)	0.271	Cesium (Cs)	0.029
Cobalt (Co)	2.445	Selenium (Se)	0.267	Methane (CH ₄)	0.025
Niobium (Nb)	2.442	Glycerol (C ₃ H ₈ O ₃)	0.253	Phosphine (PH ₃)	0.025
Yttrium sesquioxide	2.321	Lead (Pb)	0.245	Carbon monoxide (CO)	0.024
Nickel (Ni)	2.320	Strontium (Sr)	0.217	Nitrogen (N ₂)	0.022
Vanadium (V)	2.255	Plutonium (Pu)	0.210	Oxygen (O ₂)	0.022
Chromium (Cr)	2.085	Bromine (Br ₂)	0.207	Fluorine (F ₂)	0.020
Platinum (Pt)	1.977	Ethylene glycol (C ₂ H ₆ O ₂)	0.201	Neon (Ne)	0.020
Iron (Fe)	1.899	Barium (Ba)	0.195	Germane (GeH ₄)	0.015
Rhodium (Rh)	1.787	Acetic acid (C ₂ H ₄ O ₂)	0.190	Hydrogen (H ₂)	0.004
Titanium (Ti)	1.722	Hydrogen fluoride (HF)	0.188	Helium (He)	0.002
Copper (Cu)	1.644	Stearic acid (C ₁₈ H ₃₆ O ₂)	0.168		
Manganese (Mn)	1.595	Dodecane (C ₁₂ H ₂₆)	0.162		

¹⁸¹ <http://magma.geol.ucsb.edu/papers/EoV%20chapter%205%20Leshner&Spera.pdf>.¹⁸² <http://magma.geol.ucsb.edu/papers/EoV%20chapter%205%20Leshner&Spera.pdf>.

Among existing practical systems, ice storage air conditioning makes use of the heat of fusion of water by using cheaper electricity at night to freeze water into ice, then using warm daytime ice melting to reduce electricity demands during the more expensive afternoon peak demand period.¹⁸³ “Pumpable ice” technology uses 5-10,000 μm ice particles in a slush or slurry as a refrigerant fluid.¹⁸⁴

Molten silicon energy storage systems currently under investigation in Spain¹⁸⁵ and Australia¹⁸⁶ are claimed to be able to store more than $\sim 3.6 \text{ MJ/L}$ at 1400 °C, with conversion efficiencies over 50%.

Immiscible metal alloys used in Miscibility Gap Alloy storage systems¹⁸⁷ also rely on the phase change of a metallic material to store thermal energy,¹⁸⁸ and are claimed to achieve energy storage densities in the range $0.2\text{-}2.2 \text{ MJ/L}$.¹⁸⁹

A number of fairly low-performance solid/liquid phase change materials¹⁹⁰ are already in widespread commercial use.

¹⁸³ https://en.wikipedia.org/wiki/Ice_storage_air_conditioning.

¹⁸⁴ https://en.wikipedia.org/wiki/Pumpable_ice_technology.

¹⁸⁵ “Molten silicon used for thermal energy storage,” The Engineer, 18 Oct 2016; <https://www.theengineer.co.uk/molten-silicon-used-for-thermal-energy-storage/>.

¹⁸⁶ “Energy storage system based on silicon from sand,” Power Engineering International, 17 Nov 2015; <http://www.powerengineeringint.com/articles/2015/11/australian-company-develops-energy-storage-system-based-on-silicon-from-sand.html>.

¹⁸⁷ https://en.wikipedia.org/wiki/Thermal_energy_storage#Miscibility_Gap_Alloy_technology_.28MGA.29.

¹⁸⁸ Rawson A, Kisi E, Sugo H, Fiedler T. Effective conductivity of Cu–Fe and Sn–Al miscibility gap alloys. International Journal of Heat and Mass Transfer 2014 Oct 1;77:395-405; <http://www.sciencedirect.com/science/article/pii/S0017931014004244>.

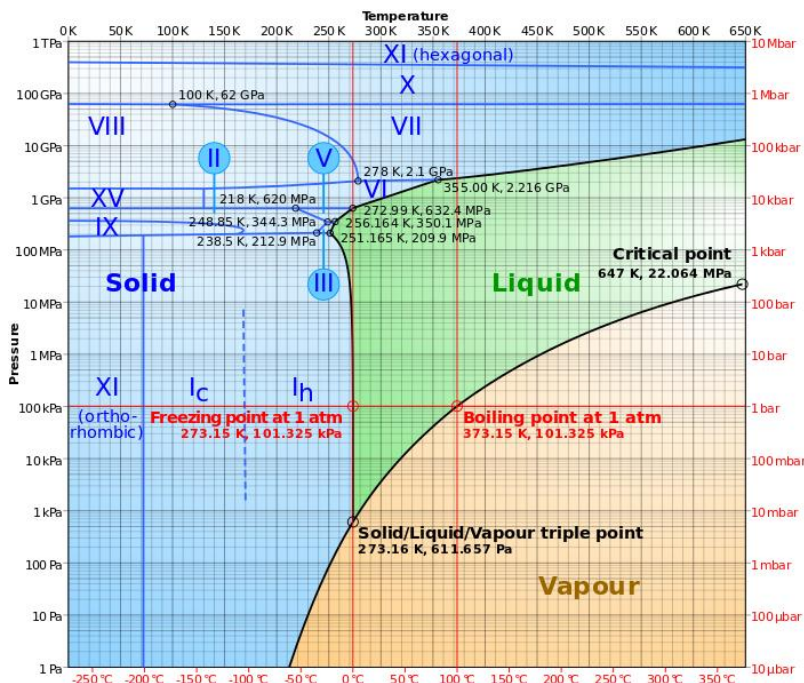
¹⁸⁹ Sugo H, Kisi E, Cuskelly D. Miscibility gap alloys with inverse microstructures and high thermal conductivity for high energy density thermal storage applications. Applied Thermal Engineering. 2013 Mar 1;51(1-2):1345-1350; <http://www.sciencedirect.com/science/article/pii/S1359431112007818>.

¹⁹⁰ https://en.wikipedia.org/wiki/Phase-change_material.

3.2.2 Heat of Vaporization

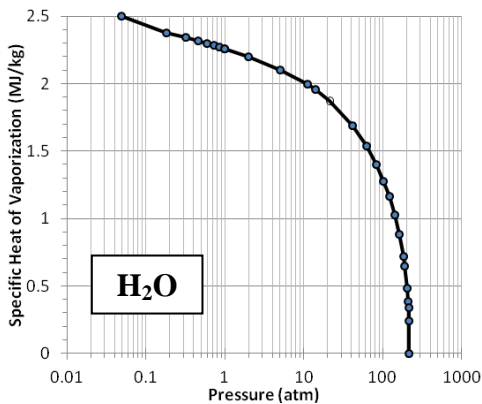
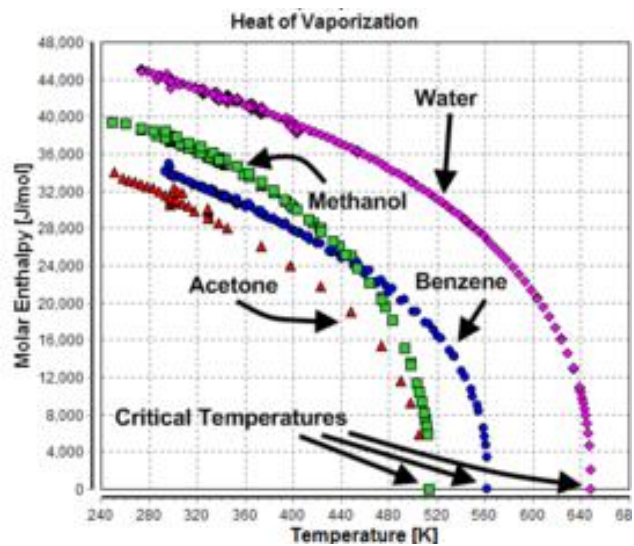
Latent heat energy storage systems that exploit the energy that released during a phase change between liquid and vapor in the storage material have not been widely explored. The heat of vaporization (aka. “enthalpy of vaporization” or “heat of condensation” during the energy extraction half of the cycle) is most commonly reported at a normal pressure of 1 atm. This presents an interesting issue in storage system design, because the volume of a vapor at 1 atm will normally be a thousand-fold larger than the volume of the same mass of storage material in liquid form. A practical storage system will require, in most circumstances, a more compact volume in which to store the vapor portion of the cycle.

To deal with this issue, let us first consider the exemplar phase diagram for water in the chart, below.¹⁹¹ The vaporization or condensation of water takes place along the “phase boundary” separating the liquid and vapor phases, starting from the triple point at 273 K and 0.006 atm (0.0061 MPa) and ending at the critical point at 647 K and 218 atm (22 MPa). The conventional boiling point of 373 K is reported at the normal atmospheric pressure of 1 atm. At temperatures below the triple point temperature of 273 K, the liquid form of water does not exist and solid ice sublimates directly into vapor form without boiling. At temperatures above the critical point temperature of 647 K, boiling also cannot occur because the liquid and vapor phases have become thermodynamically indistinguishable.



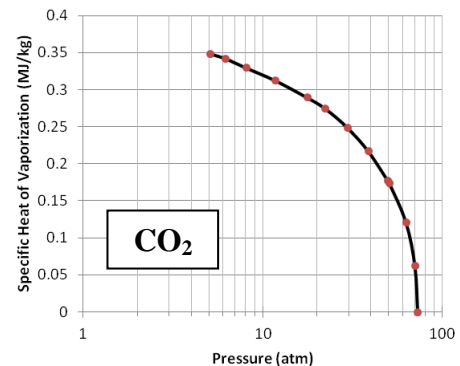
¹⁹¹ [https://en.wikipedia.org/wiki/Water_\(data_page\)#Phase_diagram](https://en.wikipedia.org/wiki/Water_(data_page)#Phase_diagram).

The chart at right¹⁹² shows what happens to the heat of vaporization at various temperatures along the liquid/vapor phase boundary (the purple curve on the chart). Because vapor is highly compressible, the heat of vaporization (reported here as J/mole) is highest at the triple point temperature (which happens to be just 0.01 K above the melting point for water) and falls when temperature and pressure rises as we follow the phase boundary upward, eventually reaching zero at the critical point temperature and pressure. Three other common liquid materials shown on the chart exhibit similar behavior.



The chart at left shows the specific heat of vaporization (MJ/kg) for **water** as a function of pressure (atm) along the liquid/vapor phase boundary.¹⁹³ The specific heat is a maximum (**2.502 MJ/kg**) at the triple point (273.16 K, 0.006 atm) very near the freezing point, only slightly lower (**2.256 MJ/kg**) at the conventional boiling point (373.15 K, 1 atm), but falling to **0 MJ/kg** at the critical point (647 K, 218 atm). However, heat of vaporization data is usually reported at the normal boiling temperature for the

substance at 1 atm, not at the triple point where the value would be at its highest. Hence the use of conventional boiling-point data for the heat of vaporization will often somewhat underestimate the maximum specific heat of vaporization that is actually available at the triple point, yielding a “conservative” estimate of the energy storage capacity of the material. In a few cases such as **carbon dioxide** (chart, right),¹⁹⁴ the material can only sublime at



¹⁹² https://en.wikipedia.org/wiki/Enthalpy_of_vaporization.

¹⁹³ Data sources: “Saturated Steam Table” <http://www.systhermique.com/steam-condensate/tables/saturated-steam-table/>; Handbook of Chemistry and Physics, 49th edition (1969):E-12.

¹⁹⁴ Data sources: Heat of vaporization http://www.ddbst.com/en/EED/PCP/HVP_C1050.php and density http://www.peacesoftware.de/einigewerte/co2_e.html for CO₂ as a function of pressure and temperature.

1 atm, and the pressure must be raised to the triple point pressure of 5.117 atm before the substance can be liquefied and made to boil. In this case, the heat of vaporization is reported at the triple point (215.58 K), giving the true maximum value of **0.3482 MJ/kg** for the specific heat of vaporization.

Table 15 shows a ranked list of the specific heat of vaporization for the pure elements, various oxides, organics and other representative liquids (range **0.02-50.8 MJ/kg**),¹⁹⁵ “conservatively” estimated using the conventional heat of vaporization at the boiling temperature at 1 atm in almost all cases, as described above. Once again carbon tops the list, but to repeatedly cycle between liquid and vapor graphite to extract (or recharge) the latent heat of vaporization will require continuous pressurization of the storage materials to at least 10.8 MPa (107 atm) to obtain liquid or vapor carbon at the triple point¹⁹⁶ (see carbon phase diagram chart, **Section 3.1.2**). The very high required operating temperature of $T_{b,p} \sim 4700$ K at pressures ≥ 107 atm will make it very challenging to find a suitable container.

¹⁹⁵ Data Sources: Handbook of Chemistry and Physics, 49th edition (1969):D-33 to D-37, Wikipedia, Air Liquide <http://encyclopedia.airliquide.com/Encyclopedia.asp>, Heat of Vaporization of the elements (Wolfram Research) <http://periodictable.com/Properties/A/VaporizationHeat.an.html>, Engineering Toolbox (http://www.engineeringtoolbox.com/melting-boiling-temperatures-d_390.html, http://www.engineeringtoolbox.com/fluids-evaporation-latent-heat-d_147.html), Al₂O₃ <http://www.matweb.com/search/datasheet.aspx?matguid=c8c56ad547ae4cfabad15977bfb537f1&ckck=1>, boron <http://periodictable.com/Elements/005/data.html>, CaO <https://books.google.com/books?id=ZJk3BQAAQBAJ&pg=PA137>, CO₂, [https://en.wikipedia.org/wiki/Carbon_dioxide_\(data_page\)](https://en.wikipedia.org/wiki/Carbon_dioxide_(data_page)), formic acid <https://cameochemicals.noaa.gov/chris/FMA.pdf>, HF <http://pubs.acs.org/doi/abs/10.1021/ja01101a066>, isopropyl alcohol (https://www.alibaba.com/product-detail/we-can-supply-iso-propyl-alcohol_1276438951.html), KF <http://chemister.ru/Database/properties-en.php?dbid=1&id=530>, MgF₂ <http://chemister.ru/Database/properties-en.php?dbid=1&id=641>, MgO <http://www.microkat.gr/msdspd90-99/Magnesium%20oxide.htm>, NaCl and KCl <https://books.google.com/books?id=qMQ6AQAAAJ&pg=PA615>, naphthalene <https://cameochemicals.noaa.gov/chris/NTM.pdf>, palmitic acid (https://pubchem.ncbi.nlm.nih.gov/compound/palmitic_acid), phenol (<https://pubchem.ncbi.nlm.nih.gov/compound/phenol>), PuO₂ (p.43), UC (p.53), and BeO (p.131) [Kirillov PL, ed. Thermophysical Properties of materials for Nuclear Engineering, Obninsk, 2006; https://www.google.com/url?sa=t&rct=j&q=&esrc=s&source=web&cd=24&ved=0ahUKEwjB48PNI-7SAhUHwIQKHY1kBJg4FBAWCCowAw&url=http%3A%2F%2Ftherpro.hanyang.ac.kr%2Fcontent%2Fattach_down.jsp%3Fdispos%3Dy%26b%3D130890718532272%26n%3D1%26&usq=AFQjCNFxECD4Tq3rk4f2Yrv6aCbN_Jtg&bvm=bv.150475504,d.cGw&cad=rjastearic acid (http://www.chemicalbook.com/ProductMSDSDetailCB4853859_EN.htm), SiO <http://onlinelibrary.wiley.com/doi/10.1111/j.1151-2916.1967.tb15135.x/abstract>, TiO₂ http://www.chemicalbook.com/ProductMSDSDetailCB7461626_EN.htm, and ZrO₂ https://archive.org/stream/DTIC_AD0018364/DTIC_AD0018364_djvu.txt. Regarding carbon, the book (Barrett J, Malati MA. *Fundamentals of Inorganic Chemistry*, Horwood Publishing, 1998, p. 162; <https://books.google.com/books?id=pwEDm8u5PVsC&pg=PA102>) reports 715 kJ/mole (59.529 MJ/kg) as the heat of sublimation for graphite; subtracting 8.743 MJ/kg as our previously reported latent heat of fusion to melt graphite gives an estimate of 50.786 MJ/kg for the latent heat of vaporization for carbon.

¹⁹⁶ Zazula JM. On Graphite Transformations at High Temperature and Pressure Induced by Absorption of the LHC Beam. CERN LHC Project Note 78/97, 1997 Jan 18; <http://citeseerx.ist.psu.edu/viewdoc/download?doi=10.1.1.617.810&rep=rep1&type=pdf>.

Table 15. Exploitable specific heat of vaporization for liquid/vapor latent heat cycling

Material Cycling Between Liquid and Vapor Phases	Specific Energy (MJ/kg)	Material Cycling Between Liquid and Vapor Phases	Specific Energy (MJ/kg)	Material Cycling Between Liquid and Vapor Phases	Specific Energy (MJ/kg)
Carbon (C)	50.79	Tin (Sn)	2.492	Cyclopropane (C ₃ H ₈)	0.472
Boron (B)	46.90	Germanium dioxide	2.440	Aniline (C ₆ H ₇ N)	0.450
Beryllium (Be)	32.45	Silver (Ag)	2.323	Hydrogen (H ₂)	0.448
Lithium (Li)	21.03	Potassium chloride	2.270	Propylene (C ₃ H ₆)	0.439
Beryllium oxide	19.60	Water (H₂O)	2.257	Phosphine (PH ₃)	0.429
Aluminum oxide	19.38	Thorium (Th)	2.217	Propane (C ₃ H ₈)	0.426
Calcium oxide	10.97	Uranium carbide	2.120	Acetic acid (C ₂ H ₄ O ₂)	0.402
Silicon (Si)	10.68	Tin dioxide	2.080	Benzene (C ₆ H ₆)	0.390
Aluminum (Al)	10.50	Potassium (K)	2.043	Hydrogen fluoride (HF)	0.374
Vanadium (V)	8.873	Uranium (U)	1.765	Methylpropane (C ₄ H ₁₀)	0.365
Titanium (Ti)	8.795	Zinc (Zn)	1.764	Hexane (C ₆ H ₁₄)	0.365
Magnesium oxide	8.205	Gold (Au)	1.698	Diethyl ether (C ₄ H ₁₀ O)	0.353
Lithium oxide	7.840	Gallium trioxide	1.670	Palmitic acid (C ₁₆ H ₃₂ O ₂)	0.351
Titanium dioxide	7.667	Strontium (Sr)	1.643	Carbon disulfide (CS ₂)	0.351
Niobium (Nb)	7.498	Uranium dioxide	1.530	Toluene (C ₇ H ₈)	0.351
Scandium (Sc)	6.989	Ammonia (NH ₃)	1.371	Carbon dioxide (CO ₂)	0.348
Silicon monoxide	6.880	Plutonium dioxide	1.365	Naphthalene (C ₁₀ H ₈)	0.338
Chromium (Cr)	6.622	Plutonium (Pu)	1.332	Selenium (Se)	0.333
Cobalt (Co)	6.389	Indium trioxide	1.280	Heptane (C ₇ H ₁₆)	0.318
Zirconium (Zr)	6.376	Niobium pentoxide	1.260	Octane (C ₈ H ₁₈)	0.298
Nickel (Ni)	6.311	Praseodymium sesquioxide	1.140	Mercury (Hg)	0.295
Molybdenum (Mo)	6.232	Zirconium dioxide	1.140	Chlorine (Cl ₂)	0.288
Iron (Fe)	6.090	Methanol (CH ₃ OH)	1.104	Decane (C ₁₀ H ₂₂)	0.263
Silicon dioxide (quartz)	6.050	Chromium trioxide	1.050	Dodecane (C ₁₂ H ₂₆)	0.256
Magnesium (Mg)	5.242	Barium (Ba)	1.034	Chloroform (CHCl ₃)	0.247
Rhodium (Rh)	4.791	Cerium sesquioxide	1.020	Xenon tetrafluoride (XeF ₄)	0.230
Copper (Cu)	4.726	Glycerol (C ₃ H ₈ O ₃)	0.974	Stearic acid (C ₁₈ H ₃₆ O ₂)	0.224
Germanium (Ge)	4.599	Samarium sesquioxide	0.960	Carbon monoxide (CO)	0.215
Tungsten (W)	4.482	Cadmium (Cd)	0.890	Oxygen (O ₂)	0.213
Vanadium monoxide	4.380	Lead (Pb)	0.858	Xenon difluoride (XeF ₂)	0.204
Magnesium fluoride	4.370	Rubidium (Rb)	0.845	Nitrogen (N ₂)	0.198
Sodium (Na)	4.218	Ethanol (C ₂ H ₅ OH)	0.841	Carbon tetrachloride (CCl ₄)	0.194
Manganese (Mn)	4.114	Ethylene glycol (C ₂ H ₆ O ₂)	0.800	Bromine (Br ₂)	0.187
Tantalum (Ta)	4.106	Isopropyl alcohol (C ₃ H ₈ O)	0.732	Germane (GeH ₄)	0.184
Calcium (Ca)	3.833	Antimony (Sb)	0.634	Fluorine (F ₂)	0.171
Cobalt monoxide	3.406	Phenol (C ₆ H ₆ O)	0.614	Iodine (I ₂)	0.164
Boron trioxide	3.310	Acetone (C ₃ H ₆ O)	0.539	Argon (Ar)	0.161
Osmium (Os)	3.299	Sulfuric acid (H ₂ SO ₄)	0.510	Xenon (Xe)	0.096
Iron monoxide	3.200	Cesium (Cs)	0.510	Neon (Ne)	0.086
Sodium chloride	3.170	Formic acid (CH ₂ O ₂)	0.502	Sulfur (S)	0.054
Iridium (Ir)	3.142	Bismuth (Bi)	0.501	Helium (He)	0.021
Potassium fluoride	2.974	Ethylene (C ₂ H ₄)	0.482		
Platinum (Pt)	2.614	Methane (CH ₄)	0.481		

Second on the list and almost as good as graphite is elemental boron, a low-toxicity substance that provides the highest specific heat of vaporization at normal pressure. The operating temperature will be somewhat lower than for graphite at $T_{b.p.} = 4200$ K at 1 atm, just low enough that a viable physical container conceivably might be made of some high melting point material such as tantalum hafnium carbide (Ta_4HfC_5 , $T_{m.p.} = 4215$ K) or perhaps the recently computationally-discovered tantalum nitrogen carbon alloy ($Ta_{0.53}N_{0.20}C_{0.27}$, $T_{m.p.} \sim 4400$ K)¹⁹⁷ if it can be manufactured. The triple point of boron is presently unknown,¹⁹⁸ but might provide a somewhat lower operating temperature and a slightly higher specific heat of vaporization.

Elemental beryllium provides the second-highest specific heat of vaporization at normal pressure, with a quite reasonable operating temperature of $T_{b.p.} = 2742$ K at 1 atm that should make containerization relatively easy. The 35 μ g of Be normally present in the average human body is not considered harmful, but any dust or fumes that are released and inhaled can cause berylliosis¹⁹⁹ or acute beryllium poisoning.²⁰⁰

The specific heat of vaporization of **~21 MJ/kg** for elemental lithium is reported at the relatively modest boiling point of $T_{b.p.} = 1603$ K at 1 atm, but its triple point²⁰¹ is an even lower 453.7 K at 2×10^{-13} atm (an excellent vacuum), potentially an extremely low operating temperature for an energy storage system at which the heat of vaporization of lithium rises slightly to **22.40 MJ/kg**.²⁰² Both beryllium oxide (see **Section 3.2.1**) and aluminum oxide also provide over **19 MJ/kg** of energy storage capacity but again at the cost of very high operating temperatures ($T_{b.p.} = 4170$ K and 3250 K, respectively, at 1 atm).²⁰³

¹⁹⁷ Hong QJ, van de Walle A. Prediction of the material with highest known melting point from *ab initio* molecular dynamics calculations. Phys. Rev. B 2015 Jul 20;92:020104; <http://authors.library.caltech.edu/59499/1/PhysRevB.92.020104.pdf>.

¹⁹⁸ Young DA. Phase Diagrams of the Elements, Lawrence Livermore Laboratory, UCRL-51902, 1975 Sep 11, p. 7; http://www.iaea.org/inis/collection/NCLCollectionStore/_Public/07/255/7255152.pdf?r=1. Parakhonskiy G, Dubrovinskaia N, Bykova E, Wirth R, Dubrovinsky L. Experimental pressure-temperature phase diagram of boron: resolving the long-standing enigma. Scientific Reports 2011 Sep 19;1:96; <http://www.nature.com/articles/srep00096>.

¹⁹⁹ <https://en.wikipedia.org/wiki/Berylliosis>.

²⁰⁰ https://en.wikipedia.org/wiki/Acute_beryllium_poisoning.

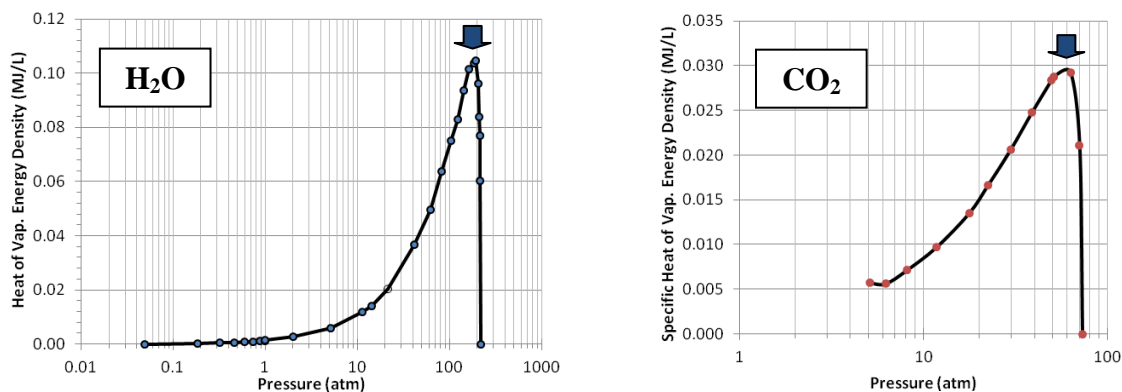
²⁰¹ "Table III. Some Thermodynamic Properties of Lithium," in D. Gruen. ed., The Chemistry of Fusion Technology: Proceedings of a Symposium on the Role of Chemistry in the Development of Controlled Fusion, an American Chemical Society Symposium, held in Boston, Massachusetts, April 1972, Springer Science & Business Media, 2012, p. 96; <https://books.google.com/books?id=oEnhBwAAQBAJ&pg=PA96>.

²⁰² Williams RK, Coleman GL, Yarbrough DW. An Evaluation of Some Thermodynamic and Transport Properties of Solid and Liquid Lithium over the Temperature range 200-1700 K, Oak Ridge National Laboratory, ORNL/TM-10622, March 1988, p. 8; <http://web.archive.org/web/20170127012232/http://web.ornl.gov/info/reports/1988/3445602747393.pdf>.

²⁰³ https://en.wikipedia.org/wiki/Beryllium_oxide and https://en.wikipedia.org/wiki/Aluminium_oxide.

These estimates for the specific heat of vaporization (MJ/kg) of various materials are relatively straightforward, but similar estimates for the heat of vaporization energy density (MJ/L) are not so simple. This is because, as noted earlier, the volume of a vapor at 1 atm may be a thousand-fold larger than the volume of the same mass of storage material in liquid form, leading to impractically low values of MJ/L. One possible solution to this problem is to seek a more compact volume in which to store the vapor portion of the cycle.

To release the stored condensation energy, a system's pressure and temperature must lie somewhere on the gas/liquid phase boundary and must traverse that boundary by, for example, bringing a cold sink into contact with the hot vapor source. The chart of the heat of vaporization (H_{vap} , in MJ/kg) of water as a function of pressure presented earlier shows that H_{vap} is highest at the lowest pressure on the gas/liquid phase boundary and falls to zero at the highest pressure. However, the density (ρ_{vap} , in kg/L) of the vaporous storage material responds oppositely, rising linearly with increasing pressure. As a result, the heat of vaporization energy density ($E_{\text{Dvap}} \sim \rho_{\text{vap}} H_{\text{vap}}$, in MJ/L), which is the product of these two pressure-dependent variables, falls to lows at the highest and lowest pressures but reaches a maximum value at some intermediate pressure on the gas/liquid phase boundary, as shown by the arrows in the charts for water (below, left) and carbon dioxide (below, right). An energy storage system would be operated at that pressure.



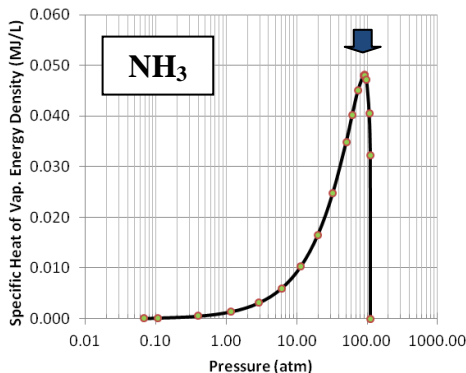
“Steam tables” and fluid density along the gas/liquid phase boundary for most materials can be difficult or impossible to find. However, a simple power formula²⁰⁴ for estimating the heat of vaporization as a function of temperature along the gas/liquid phase boundary shows that the shapes of the curves are basically the same for a wide variety of inorganic liquids, hydrocarbons, water, CO₂, NH₃, and several elemental metals and gases, varying only by a scalar slope parameter that provides an excellent estimate with an average error of only 0.94%. Can we find a method for at least coarsely estimating the maximum value of the heat of vaporization energy density, or E_{DvapMax} , at the peaks of the above two charts?

In the case of liquid water at $T_{\text{b.p.}} = 373.15$ K and 1 atm pressure, $E_{\text{Dvap}} \sim \mathbf{0.001}$ MJ/L, and is 0 MJ/L at 647 K and 218 atm (critical point), but rises to a peak of **0.105 MJ/L** at 636 K and 192 atm. Since $H_{\text{vap}}(192 \text{ atm}) = \mathbf{0.649}$ MJ/kg and $H_{\text{vap}}(1 \text{ atm}, T_{\text{b.p.}}) = \mathbf{2.256}$ MJ/kg, E_{Dvap} is a

²⁰⁴ Martin JJ, Edwards JB. Correlation of the latent heats of vaporization. A.I.Ch.E. Journal 1965 Mar;11(2):331-333; <https://deepblue.lib.umich.edu/bitstream/handle/2027.42/37333/690110226ftp.pdf>.

maximum at $0.288 H_{\text{vap}}$ (1 atm, $T_{\text{b.p.}}$); also, since ρ_{vap} (192 atm) = 0.161 kg/L and ρ_{liq} (1 atm, $T_{\text{b.p.}}$) = 0.958 kg/L, E_{Dvap} is a maximum at $0.168 \rho_{\text{liq}}$ (1 atm, $T_{\text{b.p.}}$); therefore, $E_{\text{DvapMax}} \sim 0.29 H_{\text{vap}}$ (1 atm, $T_{\text{b.p.}}$) x **0.17** ρ_{liq} (1 atm, $T_{\text{b.p.}}$) for water.

In the case of liquid carbon dioxide at $T_{\text{t.p.}} = 216$ K (triple point) and 5.12 atm pressure, $E_{\text{Dvap}} \sim 0.006$ MJ/L, and is **0 MJ/L** at 304 K and 72.8 atm (critical point), but rises to a peak of **0.0293 MJ/L** at 298 K and 62.7 atm. Since H_{vap} (62.7 atm) = **0.121 MJ/kg** and H_{vap} (5.12 atm, $T_{\text{t.p.}}$) = **0.348 MJ/kg**, E_{Dvap} is a maximum at $0.348 H_{\text{vap}}$ (5.12 atm, $T_{\text{t.p.}}$); also, since ρ_{vap} (62.7 atm) = 0.242 kg/L and ρ_{liq} (5.12 atm, $T_{\text{t.p.}}$) = 1.179 kg/L, E_{Dvap} is a maximum at $0.205 \rho_{\text{liq}}$ (5.12 atm, $T_{\text{t.p.}}$); therefore, $E_{\text{DvapMax}} \sim 0.35 H_{\text{vap}}$ (5.12 atm, $T_{\text{t.p.}}$) x **0.21** ρ_{liq} (5.12 atm, $T_{\text{t.p.}}$) for carbon dioxide.



For further confirmation, the above analysis was repeated for the case of liquid ammonia²⁰⁵ at $T_{\text{t.p.}} = 195.4$ K (triple point) and 6060 Pa (0.0598 atm) pressure, where $E_{\text{Dvap}} \sim 0.00011$ MJ/L, and is **0 MJ/L** at 405.5 K and 111.3 atm (critical point), but rises to a peak of **0.0481 MJ/L** at 394 K and 91.5 atm (see chart, left). Since H_{vap} (91.5 atm) = **0.466 MJ/kg** and H_{vap} (0.0598 atm, $T_{\text{t.p.}}$) = **1.485 MJ/kg**, E_{Dvap} is a maximum at $0.314 H_{\text{vap}}$ (0.0598 atm, $T_{\text{t.p.}}$); also, since ρ_{vap} (91.5 atm) = 0.103 kg/L and ρ_{liq} (0.0598 atm, $T_{\text{t.p.}}$) = 0.732 kg/L, E_{Dvap} is a maximum at $0.141 \rho_{\text{liq}}$ (0.0598 atm, $T_{\text{t.p.}}$); therefore, $E_{\text{DvapMax}} \sim 0.31 H_{\text{vap}}$

(5.12 atm, $T_{\text{t.p.}}$) x **0.14** ρ_{liq} (5.12 atm, $T_{\text{t.p.}}$) for ammonia, largely consistent with the previous two examples, above.

Table 16 shows a ranked list of the maximum heat of vaporization energy density for the pure elements, various oxides, organics and other representative liquids (range **0.0001-5.27 MJ/L**), as crudely estimated using the parameters derived from the water, carbon dioxide and ammonia examples above, employing the consensus formula: $E_{\text{DvapMax}} \sim 0.30 H_{\text{vap}} \times 0.18 \rho_{\text{liq}}$, where H_{vap} is the heat of vaporization reported under boiling conditions (normally at 1 atm) and ρ_{liq} is the liquid density reported under boiling conditions (normally at 1 atm)²⁰⁶. The values reported for H₂O, CO₂ and NH₃ in **Table 16** are the “actual” numbers calculated as described using the charts above. The other values should be validated prior to use for engineering purposes.

Of the top three materials on the list – specifically boron ($T_{\text{b.p.}} = 4200$ K at 1 atm), aluminum oxide ($T_{\text{b.p.}} = 3250$ K at 1 atm), and tungsten ($T_{\text{b.p.}} = 6203$ K at 1 atm) – aluminum oxide will be the easiest storage material for which to provide physical containment. Tungsten is even more problematic than graphite vapor ($T_{\text{b.p.}} \sim 4700$ K at ≥ 107 atm; see above).

²⁰⁵ Haar L, Gallagher JS. Thermodynamic Properties of Ammonia. J Phys Chem Ref Data 1978; 7(3):635-792, see pp. 684-689; <https://srd.nist.gov/JPCRD/jpcrd119.pdf>.

²⁰⁶ Average liquid density is used when boiling point density is not readily available, overestimating E_{DvapMax} by no more than ~10% because most liquids expand relatively little when heated to $T_{\text{b.p.}}$.

Table 16. Exploitable heat of vaporization energy density for liquid/vapor latent heat cycling

Material Cycling Between Liquid and Vapor Phases	Energy Density (MJ/L)	Material Cycling Between Liquid and Vapor Phases	Energy Density (MJ/L)	Material Cycling Between Liquid and Vapor Phases	Energy Density (MJ/L)
Boron (B)	5.268	Silicon monoxide	0.7913	Formic acid (CH ₂ O ₂)	0.0331
Aluminum oxide	4.291	Tin dioxide	0.7694	Bromine (Br ₂)	0.0314
Tungsten (W)	4.260	Magnesium fluoride	0.7429	Isopropyl alcohol (C ₃ H ₈ O)	0.0311
Carbon (C)	3.757	Zinc (Zn)	0.6257	Carbon dioxide (CO ₂)	0.0293
Osmium (Os)	3.563	Lithium (Li)	0.5813	Aniline (C ₆ H ₇ N)	0.0248
Niobium (Nb)	3.470	Gallium trioxide	0.5808	Chlorine (Cl ₂)	0.0243
Tantalum (Ta)	3.326	Boron trioxide	0.5623	Carbon disulfide (CS ₂)	0.0240
Iridium (Ir)	3.224	Germanium dioxide	0.5571	Acetone (C ₃ H ₆ O)	0.0228
Beryllium oxide	3.186	Indium trioxide	0.4962	Acetic acid (C ₂ H ₄ O ₂)	0.0228
Molybdenum (Mo)	3.140	Lead (Pb)	0.4937	Hydrogen fluoride (HF)	0.0194
Cobalt (Co)	3.057	Magnesium (Mg)	0.4484	Chloroform (CHCl ₃)	0.0186
Beryllium (Be)	2.961	Samarium sesquioxide	0.4327	Benzene (C ₆ H ₆)	0.0185
Platinum (Pt)	2.791	Praseodymium sesquioxide	0.4248	Naphthalene (C ₁₀ H ₈)	0.0176
Rhodium (Rh)	2.768	Potassium fluoride	0.3983	Cyclopropane (C ₃ H ₈)	0.0173
Nickel (Ni)	2.662	Cadmium (Cd)	0.3841	Phosphine (PH ₃)	0.0171
Vanadium (V)	2.635	Sodium chloride	0.3706	Carbon tetrachloride (CCl ₄)	0.0166
Iron (Fe)	2.295	Zirconium dioxide	0.3497	Toluene (C ₇ H ₈)	0.0165
Chromium (Cr)	2.253	Cerium sesquioxide	0.3415	Palmitic acid (C ₁₆ H ₃₂ O ₂)	0.0162
Copper (Cu)	2.047	Niobium pentoxide	0.3130	Xenon (Xe)	0.0153
Zirconium (Zr)	1.997	Calcium (Ca)	0.2852	Ethylene (C ₂ H ₄)	0.0148
Calcium oxide	1.979	Bismuth (Bi)	0.2722	Propylene (C ₃ H ₆)	0.0145
Titanium (Ti)	1.952	Potassium chloride	0.2432	Fluorine (F ₂)	0.0139
Titanium dioxide	1.751	Antimony (Sb)	0.2234	Diethyl ether (C ₄ H ₁₀ O)	0.0136
Uranium (U)	1.648	Mercury (Hg)	0.2158	Germane (GeH ₄)	0.0135
Gold (Au)	1.587	Sodium (Na)	0.2111	Propane (C ₃ H ₈)	0.0133
Magnesium oxide	1.586	Strontium (Sr)	0.2108	Oxygen (O ₂)	0.0131
Uranium carbide	1.560	Barium (Ba)	0.1864	Hexane (C ₆ H ₁₄)	0.0129
Silicon (Si)	1.482	Chromium trioxide	0.1531	Argon (Ar)	0.0122
Thorium (Th)	1.404	Water (H₂O)	0.1047	Methylpropane (C ₄ H ₁₀)	0.0117
Germanium (Ge)	1.391	Potassium (K)	0.0913	Heptane (C ₇ H ₁₆)	0.0117
Vanadium monoxide	1.362	Selenium (Se)	0.0718	Octane (C ₈ H ₁₈)	0.0113
Aluminum (Al)	1.347	Rubidium (Rb)	0.0666	Methane (CH ₄)	0.0110
Manganese (Mn)	1.322	Glycerol (C ₃ H ₈ O ₃)	0.0663	Decane (C ₁₀ H ₂₂)	0.0104
Plutonium (Pu)	1.196	Cesium (Cs)	0.0507	Dodecane (C ₁₂ H ₂₆)	0.0104
Cobalt monoxide	1.185	Sulfuric acid (H ₂ SO ₄)	0.0507	Stearic acid (C ₁₈ H ₃₆ O ₂)	0.0103
Silver (Ag)	1.169	Xenon tetrafluoride (XeF ₄)	0.0502	Carbon monoxide (CO)	0.0092
Scandium (Sc)	1.057	Ammonia (NH ₃)	0.0481	Nitrogen (N ₂)	0.0086
Iron monoxide	0.9927	Ethylene glycol (C ₂ H ₆ O ₂)	0.0481	Neon (Ne)	0.0056
Tin (Sn)	0.9405	Xenon difluoride (XeF ₂)	0.0475	Sulfur (S)	0.0053
Uranium dioxide	0.9055	Methanol (CH ₃ OH)	0.0472	Hydrogen (H ₂)	0.0017
Silicon dioxide (quartz)	0.8651	Iodine (I ₂)	0.0436	Helium (He)	0.0001
Lithium oxide	0.8522	Ethanol (C ₂ H ₅ OH)	0.0358		
Plutonium dioxide	0.8477	Phenol (C ₆ H ₆ O)	0.0355		

Prior to any consideration of the attainable per-cycle storage efficiency in real physical systems, it appears that maximum exploitable specific energies of **30-50 MJ/kg** and maximum exploitable energy densities of **3-5 MJ/L** might be possible to achieve using the latent heat of vaporization by cycling between liquid and vapor phases of a suitable storage material.

Interestingly, liquid/vapor conversion energy storage systems, aka. “cryogenic energy storage”,²⁰⁷ are already being investigated to replace batteries for renewable power generation buffering,²⁰⁸ with the current 25% efficiency potentially improvable to 70% with extensive engineering. This idea has a long history: a vehicle powered by a liquid nitrogen engine,²⁰⁹ with the brand name Liquid Air,²¹⁰ was first demonstrated in 1902.

²⁰⁷ https://en.wikipedia.org/wiki/Cryogenic_energy_storage.

²⁰⁸ Highview Power Storage; <http://www.highview-power.com/>. “Liquid air offers energy storage hope,” BBC News, 2 Oct 2012; <http://www.bbc.com/news/science-environment-19785689>.

²⁰⁹ https://en.wikipedia.org/wiki/Liquid_nitrogen_engine.

²¹⁰ https://en.wikipedia.org/wiki/Liquid_Air.

3.2.3 Heat of Sublimation

Sublimation is the phase transition of a material directly from solid to vapor form without passing through an intermediate liquid phase.²¹¹ For example, at room temperature and normal pressure, solid carbon dioxide or “dry ice” sublimates directly into CO₂ vapor, because the liquid form cannot exist below the triple point pressure of 5.12 atm.

Sublimation is an endothermic process that occurs at temperatures and pressures below a substance’s triple point in its phase diagram. The reverse (exothermic) process of sublimation is called deposition or desublimation,²¹² in which a warm substance passes directly from a gas phase to a solid phase upon exposure to a cold sink. These complementary processes define a potentially exploitable thermal energy storage cycle.

The heat of sublimation, aka. enthalpy of sublimation, can be calculated by summing the heat of fusion and the heat of vaporization, taken at the temperature and pressure at which the sublimation takes place. We will not here present separate data tables for sublimation-based storage materials because the specific energies for heat of vaporization are much larger than for heat of fusion (the two of which are being summed), so the former (**Table 15**) should be fairly representative of a similar materials list ranked by specific heat of sublimation (MJ/kg), and the numbers in that table should be fairly close to the sublimation numbers that we are not repeating here. Similarly, the heat of fusion energy densities are generally higher than heat of vaporization energy density, so the former (**Table 14**) may be fairly representative of a similar materials list ranked by heat of sublimation energy density (MJ/L).

²¹¹ [https://en.wikipedia.org/wiki/Sublimation_\(phase_transition\)](https://en.wikipedia.org/wiki/Sublimation_(phase_transition)).

²¹² Boreyko JB, Hansen RR, Murphy KR, Nath S, Retterer ST, Collier CP. Controlling condensation and frost growth with chemical micropatterns. *Scientific Reports* 2016 Jan 22;6(19131); <http://www.nature.com/articles/srep19131>.

3.3 Thermochemical Phase Changes

Any kind of reversible phase change in which energy repeatedly enters and leaves the system is potentially exploitable for energy storage purposes. Single-use energy storage modalities are also useful, but less so.

In this Section, we discuss possible energy storage using reversible enthalpies of solution (**Section 3.3.1**) and crystallization (**Section 3.3.2**), photoisomer conversion energy (**Section 3.3.3**), allotropic transition energy (**Section 3.3.4**), crystal structure phase transition energy in polymorphs (**Section 3.3.5**), and several other phase-change enthalpies (**Section 3.3.6**).

Heat engines can be used to convert the heat released during these processes by means previously described.

3.3.1 Heat of Solution

The heat of solution, aka. enthalpy of solution or enthalpy of dissolution, is the amount of heat that is absorbed or evolved during the dissolution of a solute material in a solvent at a constant pressure. Heat of solution (J/mole or J/kg of solute) is usually reported at the initial solvent temperature (e.g., 25 °C) and at “infinite dilution” (where the addition of solvent produces no further thermal effect).

Dissolution occurs in three steps: (1) the endothermic breaking of solute-solute attractions (e.g., enthalpy of crystallization or lattice energy in solid salts), (2) the endothermic breaking of solvent-solvent attractions (e.g., of hydrogen bonding in water), and (3) the exothermic formation of solute-solvent attractions during solvation (e.g., the energy of hydration).²¹³ The heat of solution is the sum of the enthalpies attributable to these three steps. For solid solutes, dissolution can heat or cool the solvent, depending on the material. Dissolution of gases in water usually releases heat; adding heat to a saturated solution causes most gases to come out of solution. This establishes the physical basis for a cyclable energy storage system: Add solvent to an exothermic solute and heat is released; add heat to the resulting solution, evaporating or boiling off the solvent, and heat is absorbed.

Table 17 shows a ranked list of the specific heat of solution (MJ/kg) and heat of solution energy density (MJ/L) for a number of solids and gases placed into pure aqueous solution²¹⁴ (range **0-3.1 MJ/kg** and **0-6.1 MJ/L**).²¹⁵ Negative numbers indicate that the solute releases heat as it dissolves; positive numbers indicate cooling during dissolution. Density for gaseous solutes was taken as the density of the liquid form of the solute, as seemed appropriate for a compact energy storage system.

²¹³ https://en.wikipedia.org/wiki/Enthalpy_change_of_solution.

²¹⁴ It is more difficult to find data for potentially useful nonaqueous solvents such as liquid ammonia, liquid nitrogen, liquid SO₂ (Elving PJ, Markowitz JM. Chemistry of solutions in liquid sulfur dioxide. J Chem Educ. 1960 Feb;37(2):75-81; <http://www.sciencemadness.org/talk/files.php?pid=597011&aid=73447>), or pressurized liquid CO₂ (https://en.wikipedia.org/wiki/Supercritical_carbon_dioxide#Solvent). But note that the solubility of, e.g., LiCl, is much higher in water than in methanol, ethanol, acetone, liquid ammonia, or formic acid; https://en.wikipedia.org/wiki/Lithium_chloride.

²¹⁵ Data sources: “Enthalpy of solution of Electrolytes” http://sites.chem.colostate.edu/diverdi/all_courses/CRC%20reference%20data/enthalpies%20of%20solution%20of%20electrolytes.pdf, Wikipedia https://en.wikipedia.org/wiki/Enthalpy_change_of_solution, Mg and Ca halides, nitrate and sulfate http://chem.libretexts.org/LibreTexts/Howard_University/General_Chemistry%3A_An_Atoms_First_Approach/Unit_4%3A_Thermochemistry/09%3A_Thermochemistry/Chapter_9.05%3A_Enthalpies_of_Solution, HCl, NaOH, and H₂SO₄ <https://books.google.com/books?id=gJ7KNvbMtREC&pg=PA28>, AlCl₃ <http://www.science.uwaterloo.ca/~cchieh/cact/applychem/hydration.html>, and FeCl₃ <https://cameochemicals.noaa.gov/chris/FCL.pdf>.

Table 17. Exploitable specific heat of solution and heat of solution energy density in aqueous solution cycling, including solute only (solute + solvent water figure in parens)

Material Cycling Between Hydrated and Unhydrated	Specific Energy (MJ/kg)	Material Cycling Between Hydrated and Unhydrated	Specific Energy (MJ/kg)	Material Cycling Between Hydrated and Unhydrated	Specific Energy (MJ/kg)
Hydrogen fluoride	-3.07	Lithium hydroxide	-0.99 (-0.11)	Lithium bromide	-0.56 (-0.35)
Aluminum chloride	-2.80 (-0.87)	Sulfuric acid (liq)	-0.98	Calcium bromide	-0.52 (-0.30)
Hydrogen chloride	-2.06	Lithium chloride	-0.87 (-0.40)	Cesium hydroxide	-0.48 (-0.36)
Ammonia	-1.79 (-0.42)	Ferric chloride	-0.84 (-0.40)	Calcium iodide	-0.41 (-0.16)
Magnesium chloride	-1.68 (-0.59)	Magnesium iodide	-0.77 (-0.46)	Acetic acid	-0.03
Sodium hydroxide	-1.07 (-0.56)	Magnesium sulfate	-0.76 (-0.20)	Glucose	+0.06
Hydrogen bromide	-1.05 (-0.69)	Calcium chloride	-0.73 (-0.24)	Sodium chloride	+0.07
Potassium hydroxide	-1.03 (-0.56)	Hydrogen iodide	-0.64 (-0.45)		
Magnesium bromide	-1.01 (-0.51)	Magnesium nitrate	-0.61 (-0.34)		
Material Cycling Between Hydrated and Unhydrated	Energy Density (MJ/L)	Material Cycling Between Hydrated and Unhydrated	Energy Density (MJ/L)	Material Cycling Between Hydrated and Unhydrated	Energy Density (MJ/L)
Aluminum chloride	-6.95 (-1.07)	Magnesium sulfate	-2.02 (-0.23)	Hydrogen iodide	-1.45 (-0.75)
Magnesium chloride	-3.90 (-0.74)	Lithium bromide	-1.95 (-0.63)	Lithium hydroxide	-1.44 (-0.12)
Magnesium bromide	-3.75 (-0.81)	Lithium chloride	-1.81 (-0.52)	Magnesium nitrate	-1.41 (-0.50)
Magnesium iodide	-3.40 (-0.85)	Sulfuric acid (liq)	-1.80	Ammonia	-1.22 (-0.38)
Hydrogen fluoride	-3.04	Cesium hydroxide	-1.75 (-0.79)	Acetic acid	-0.03
Hydrogen chloride	-2.46	Calcium bromide	-1.73 (-0.52)	Glucose	+0.09
Ferric chloride	-2.44 (-0.58)	Hydrogen bromide	-1.72 (-0.93)	Sodium chloride	+0.14
Sodium hydroxide	-2.28 (-0.78)	Calcium iodide	-1.61 (-0.23)		
Potassium hydroxide	-2.18 (-0.79)	Calcium chloride	-1.58 (-0.29)		

Hydrogen fluoride gives the best specific heat of solution for heat generation. Aluminum chloride (AlCl_3) gives the best heat of solution energy density and might be safer to work with than HF. However, the hydration enthalpy of the Al^{3+} ion is so large that after dissolution in water, evaporation of the water does not yield the solid AlCl_3 but rather a solid containing the hydrated aluminum ion and chloride ions $[\text{Al}(\text{H}_2\text{O})_6]\text{Cl}_3$, which upon further heating goes to $[\text{Al}(\text{H}_2\text{O})_3]\text{Cl}_3$, and with still more heating HCl is lost rather than H_2O , yielding $\text{Al}(\text{OH})_3 + 3\text{HCl}$ instead of the original AlCl_3 .²¹⁶

Note that solvent mass and volume are not included in calculating the energy ratios given in the table, on the assumption that solvent water might be provided free from the environment. If we include solvent mass and volume, this gives the lower ratios shown in parens in the table.

Commercially available heat-of-solution single-use “heat packs” employ calcium chloride or magnesium sulfate in dry crystal form, surrounding a small pouch filled with water.²¹⁷ Breaking the pouch allows the chemical salt to dissolve in the water, producing heat in either of two temperature ranges, 120°- 130° F (49°-54°C) and 150-160°F (66°-71°C).²¹⁸

A fully reversible heat-of-solution system announced in 2013 by the Dutch technology developer TNO uses sodium hydroxide (NaOH) solvation in water to store heat in a container containing 50% NaOH solution. Energy is stored by heating the solution using a solar collector on a rooftop or any other heat source, and evaporating the water in an endothermic reaction. Energy is extracted by adding water back, causing heat release in an exothermic reaction at 50 °C. A container with a few cubic meters of salt could store enough thermochemical energy to heat a house through the winter in a temperate climate like that of the Netherlands, operating at 60% efficiency and able to store energy from a few months to years.²¹⁹ Current systems only achieve **0.18 MJ/L**, but with “further optimization of the selected reaction and architecture” the energy density might be improved to **1 MJ/L**.

²¹⁶ House JE. Inorganic Chemistry, pp. 231-2; <https://books.google.com/books?id=ocKWuxOur-kC&pg=PA231>.

²¹⁷ <http://sciencing.com/chemicals-used-heat-packs-7441567.html>.

²¹⁸ <http://apbrwww5.apsu.edu/robertsonr/TSTA%20Presentation/CACL2LB.pdf>.

²¹⁹ De Jong A-J, Van Vliet L, Hoegaerts C, Roelands M, Cuypers R Ruud. Thermochemical Heat Storage – from Reaction Storage Density to System Storage Density. Energy Procedia. 2016;91:128-37; <https://dx.doi.org/10.1016%2Fj.egypro.2016.06.187>. Klose Rainer. Seasonal energy storage: Summer heat for the winter. Zurich, Switzerland: Empa; <https://www.empa.ch/web/s604/naoh-heat-storage>.

3.3.2 Heat of Crystallization

The heat of crystallization, aka. enthalpy of crystallization, is the amount of heat that is absorbed or evolved during the crystallization of a solute material out of solution in a solvent at a constant pressure. Heat of crystallization (J/mole or J/kg of solute) is usually reported at the initial solution temperature (e.g., 25 °C) and starting from “infinite dilution.” For example, potassium nitrate (KNO₃) is a salt that dissolves more at higher temperature. To recharge a cyclable energy storage system, we add heat to a slush of crystalline solid particles and solvent; the crystals absorb heat and go into solution. To extract energy, we cool the solution and the solid material crystallizes out, releasing heat.

Table 18 shows a ranked list of the specific heat of crystallization (MJ/kg) and heat of crystallization energy density (MJ/L) for a number of solids placed into pure aqueous solution (range **0-0.4 MJ/kg** and **0-2.9 MJ/L**),²²⁰ with positive heat of solution numbers indicating that the solute releases heat as it crystallizes out of solution. Note that including solvent mass and volume makes a huge difference in calculating the energy ratios given in the table (in parens), becoming significantly smaller than if solvent mass and volume are excluded from the calculation on the assumption that solvent water might be provided free from the environment.

Potassium perchlorate provides the greatest heat of crystallization if we could ignore the mass and volume storage requirements of solvent provided as needed from the environment, but including solvent ruins the ratios for all the perchlorates because of their low solubility in water. Taking solvent into account, the best performers are ammonium nitrate, ammonium thiocyanate, sodium nitrate, and sodium chlorate, and the best ratios are around **0.2 MJ/kg** and **0.3 MJ/L**.

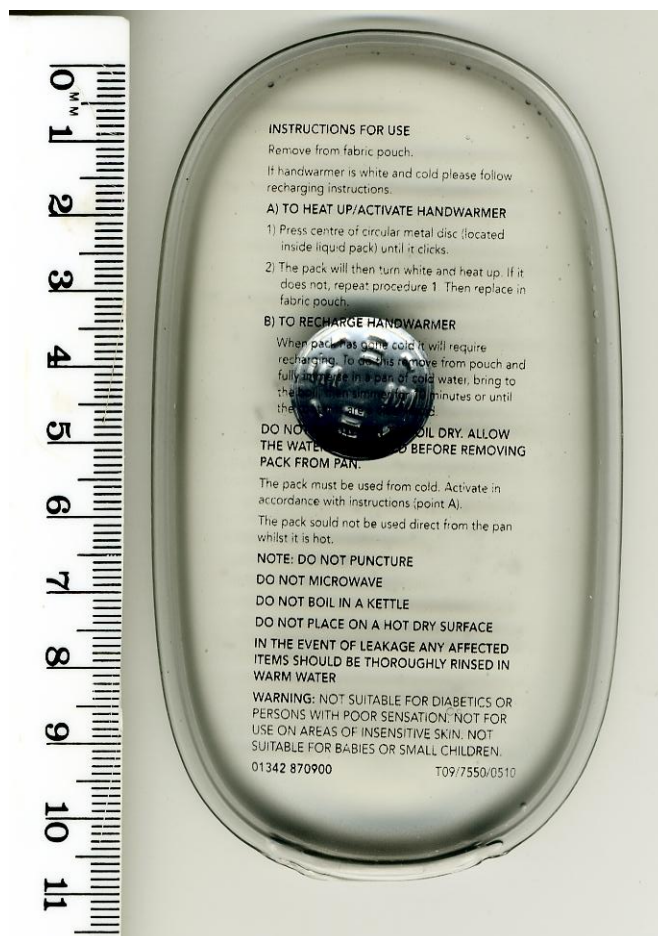
²²⁰ Data sources: “Enthalpy of solution of Electrolytes”

http://sites.chem.colostate.edu/diverdi/all_courses/CRC%20reference%20data/enthalpies%20of%20solution%20of%20electrolytes.pdf, RbClO₃ http://rubidium.atomistry.com/rubidium_chlorate.html, and Wikipedia.

Table 18. Exploitable specific heat of crystallization and heat of crystallization energy density in aqueous solution cycling, including solute only (solute + solvent water figure in parens)

Material Cycling Between Hydrated and Unhydrated	Specific Energy (MJ/kg)	Material Cycling Between Hydrated and Unhydrated	Specific Energy (MJ/kg)	Material Cycling Between Hydrated and Unhydrated	Specific Energy (MJ/kg)
KClO ₄ KNO ₃ KClO ₃ NH ₄ NO ₃ RbClO ₄ NH ₄ CNS NaCNO	+0.37 (+0.005) +0.35 (+0.08) +0.34 (+0.03) +0.32 (+0.19) +0.31 (+0.004) +0.30 (+0.17) +0.30 (+0.03)	RbClO ₃ KMnO ₄ KBrO ₃ NaNO ₃ AgNO ₂ C ₂ H ₃ NaO ₂ • 3H ₂ O CsClO ₄	+0.28 (+0.01) +0.28 (+0.02) +0.25 (+0.02) +0.24 (+0.12) +0.24 (+0.001) +0.24 (+0.08) +0.24 (+0.005)	KCl NaClO ₃ NaBrO ₃ NaCl Glucose	+0.23 (+0.05) +0.20 (+0.11) +0.18 (+0.05) +0.07 (+0.02) +0.06 (+0.03)
Material Cycling Between Hydrated and Unhydrated	Energy Density (MJ/L)	Material Cycling Between Hydrated and Unhydrated	Energy Density (MJ/L)	Material Cycling Between Hydrated and Unhydrated	Energy Density (MJ/L)
AgNO ₂ KClO ₄ RbClO ₃ RbClO ₄ KBrO ₃ CsClO ₄ KClO ₃	+1.07 (+0.001) +0.93 (+0.005) +0.90 (+0.01) +0.88 (+0.004) +0.81 (+0.02) +0.79 (+0.005) +0.78 (+0.03)	KMnO ₄ KNO ₃ NaBrO ₃ NaCNO NH ₄ NO ₃ NaNO ₃ NaClO ₃	+0.75 (+0.02) +0.73 (+0.09) +0.60 (+0.06) +0.56 (+0.03) +0.55 (+0.26) +0.54 (+0.16) +0.52 (+0.15)	KCl NH ₄ CNS C ₂ H ₃ NaO ₂ • 3H ₂ O NaCl Glucose	+0.46 (+0.05) +0.39 (+0.19) +0.35 (+0.08) +0.14 (+0.02) +0.09 (+0.03)

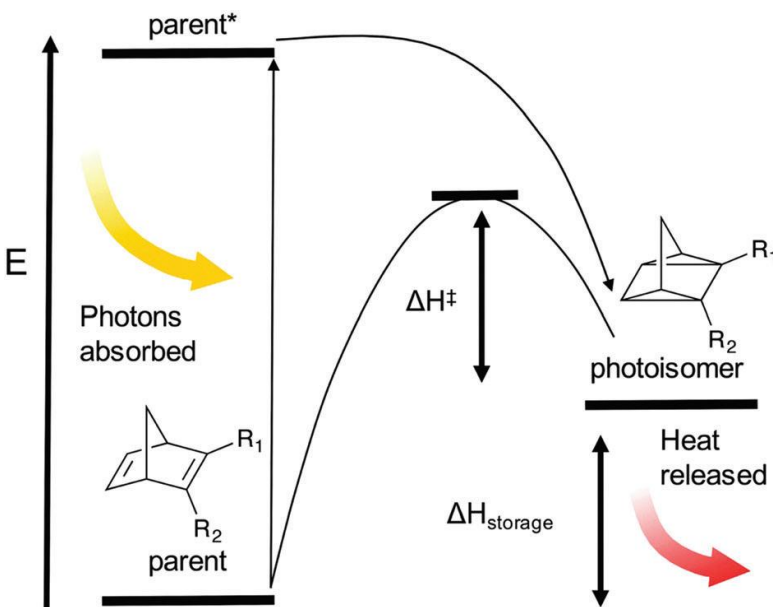
There are a few examples of commercial use of heat of crystallization energy storage. The best-known is sodium acetate trihydrate ($C_2H_3NaO_2 \cdot 3H_2O$) which is used in heat packs that are fully reversible (see image, right).²²¹ When heated, these crystals melt at $58\text{ }^\circ\text{C}$ and dissolve in their water of crystallization; if subsequently allowed to cool, the aqueous solution becomes supersaturated that is stable as low as room temperature without forming crystals. By pressing on a metal disc within the heating pad, a nucleation center is formed, causing the solution to crystallize back into solid sodium acetate trihydrate – a bond-forming process of crystallization that is exothermic by **0.264-0.289 MJ/kg (0.383-0.419 MJ/L)**. This heat pack can be reused by immersing the pack in boiling water for a few minutes until the crystals are completely dissolved, then allowing the pack to slowly cool back to room temperature.



²²¹ https://en.wikipedia.org/wiki/Sodium_acetate#Heating_pad.

3.3.3 Photoisomer Conversion Energy

In this scheme, solar (or other photonic) energy is stored as latent chemical energy in a photo-induced isomer of an otherwise stable molecule. The photoisomer is kinetically stable but can be triggered to re-isomerize back to the parent molecule, releasing heat. The parent molecule is then ready to repeat the cycle with the absorption of another photon. The energy release can be triggered using either thermal activation²²² or catalysts,²²³ and specific energies up to **0.966 MJ/kg** have been demonstrated, with storage times exceeding several months.²²⁴ Various molecules have been explored in this context, including norbornadienes (see diagram, at right),²²⁵ ruthenium compounds, azobenzenes, and other systems.²²⁶



²²² Gray V, Lennartson A, Ratanalert P, Borjesson K, Moth-Poulsen K, Karl B. Diaryl-substituted norbornadienes with red-shifted absorption for molecular solar thermal energy storage. *Chem Commun (Camb)*. 2014 May 25;50(40):5330-2; <https://www.ncbi.nlm.nih.gov/pubmed/24280803>.

²²³ Miki S, Maruyama T, Ohno T, Tohma T, Toyama S, Yoshida Z. Alumina-anchored cobalt (II) Schiff base catalyst for the isomerization of trimethyldicyanoquadricyclane to the norbornadiene. *Chem Lett*. 1988:861-864; <http://www.journal.csj.jp/doi/pdf/10.1246/cl.1988.861>.

²²⁴ Dubonosov AD, Bren VA, Chernoiivanov VA. Norbornadiene-quadricyclane as an abiotic system for the storage of solar energy. *Russ Chem Rev*. 2002;71: 917-927; <http://pubs.rsc.org/-/content/articlelanding/2002/rc/rc020917#!divAbstract>.

²²⁵ Dreos A, Borjesson K, Wang Z, Roffey A, Norwood Z, Kushnird D, Moth-Poulsen K. Exploring the potential of a hybrid device combining solar water heating and molecular solar thermal energy storage. *Energy Environ. Sci*. 2017;10:728-734; <http://pubs.rsc.org/en/content/articlepdf/2017/ee/c6ee01952h>

²²⁶ Lennartson A, Roffey A, Moth-Poulsen K. Designing photoswitches for molecular solar thermal energy storage. *Tetrahedron Lett*. 2015 Mar 18;56:1457-1465; <http://www.sciencedirect.com/science/article/pii/S0040403915002373>.

3.3.4 Allotropic Transition Energy

Allotropy is the property of some chemical elements to exist in two or more different forms in the same physical state (gas, liquid, or solid), and can exhibit quite different physical properties and chemical behaviors. The change between allotropic forms may be triggered by pressure, light, or temperature, and such change usually involves a change in system energy that is often reversible. At least 38 natural elements have two or more allotropes at ambient pressure.²²⁷

By far the largest heat of allotropy is likely possessed by ozone (O₃), an allotrope of oxygen (O₂) that is produced following the absorption of a 241 nm photon by a dioxygen molecule. The bond energy of O₃ (364 kJ/mole or **7.58 MJ/kg**) is lower than the bond energy of O₂ (498 kJ/mole or **15.56 MJ/kg**),²²⁸ so O₃ is thermodynamically favored to transform back to O₂ with the release of **7.98 MJ/kg** of heat. However, it will be difficult to design an O₂/O₃-based energy storage system because ozone cannot easily be stored and transported like other industrial gases, as it quickly decays into the dioxygen allotrope at any significant ozone concentration;²²⁹ its liquid and solid forms are very unstable. NASA's predecessor agency studied using ozone as rocket propellant starting in the late 1940s.²³⁰ Princeton researchers found that ozone concentrations of 10-15% were stable but concentrations exceeding ~28% in O₃/O₂ mixtures were unstably explosive,²³¹ and NASA researchers found that "explosions were encountered when equipment or procedure permitted ozone to concentrate locally."²³²

Graphite can be converted into diamond by applying very high pressure (>GPa), and diamond can be converted back into graphite by applying very high temperature (~2000 K), so it might be possible to design an energy storage system that cycles between these two carbon allotropes that

²²⁷ https://en.wikipedia.org/wiki/Allotropy#List_of_allotropes.

²²⁸ "Bond Energy: Ozone"; <http://butane.chem.uiuc.edu/pshapley/GenChem2/A4/2.html>.

²²⁹ <https://en.wikipedia.org/wiki/Ozone>.

²³⁰ Miller RO, Ordin PM. Theoretical Performance of Some Rocket Propellants Containing Hydrogen, Nitrogen, and Oxygen. NACA Research Memorandum No. E8A30, Washington DC, 26 May 1948.

²³¹ Palaszewski BA, Bennett GL. Propulsion Estimates for High Energy Lunar Missions Using Future Propellants, 52nd AIAA/SAE/ASEE Joint Propulsion Conference, 2016, p. 4989, Appendix B: Propellant Chemistry, Reference 19; <https://ntrs.nasa.gov/archive/nasa/casi.ntrs.nasa.gov/20170001563.pdf>.

²³² Miller RO, Brown DD. Effect of Ozone Addition on Combustion Efficiency of Hydrogen - Liquid-Oxygen Propellant in Small Rockets. NASA Lewis Research Center Memo 5-26-59E, Cleveland OH, June 1959.

differ in free energy by **0.241 MJ/kg (0.538 MJ/L** at $\rho_{\text{graphite}} \sim 2.23 \text{ kg/L}$).²³³ Carbon has the largest number of allotropes of any element, currently estimated around 300, due to its valency.²³⁴

Most transitions have a much lower energy density. Nitinol, aka. shape-memory alloy with equal parts pure nickel and titanium metals,²³⁵ transforms between cubic and monoclinic crystalline structures at a transformation temperature range (due to hysteresis) between 290-320 K (20-50 °C), with a latent heat of $0.05 \text{ k}_B/\text{atom}$ ²³⁶ or **0.047 MJ/kg (0.30 MJ/L)** at 300 K. Sulfur, which has perhaps the second largest number (~50) of identified allotropes,²³⁷ exhibits a reversible transition between the two most common α -orthorhombic and β -monoclinic forms at 368 K, which at 1 atm and 298 K have a free energy differential of just **~0.0025 MJ/kg (0.005 MJ/L)**.²³⁸

²³³ <https://books.google.com/books?id=53QoRNEjlrkC&pg=PA13>.

²³⁴ Hoffmann R, Kabanov AA, Golov AA, Proserpio DM. Homo Citans and Carbon Allotropes: For an Ethics of Citation. *Angew chemie* 2016 Sep 5; 55(37):10962-10976; <http://onlinelibrary.wiley.com/doi/10.1002/anie.201600655/full>.

²³⁵ https://en.wikipedia.org/wiki/Nickel_titanium.

²³⁶ <https://books.google.com/books?id=czADBAAAQBAJ&pg=PA380>.

²³⁷ https://en.wikipedia.org/wiki/Allotropes_of_sulfur.

²³⁸ <https://www.cpp.edu/~tknguyen/che303/Homework/set5ans-09.doc>.

3.3.5 Crystal Structure Phase Transition Energy

Many solids change, often reversibly, from one crystal structure to another structure upon being heated or compressed past a transition point, although the enthalpy changes are modest, usually under 0.0075 MJ/mole (**~0.04 MJ/kg**) for organic molecule crystals.²³⁹ This ability of a solid material to exist in more than one form or crystal structure, analogous to allotropy for the chemical elements, is generally known as polymorphism.²⁴⁰

For example, beryllium oxide (BeO) crystallizes in the “alpha phase” hexagonal wurtzite structure at low temperatures, but upon heating above the 2050 °C alpha-beta phase transition temperature, the crystal structure undergoes a polymorphic transformation to the “beta phase” tetragonal form,²⁴¹ with a heat of phase transition of **0.0021 MJ/kg (0.0063 MJ/L)**.²⁴² Similarly with high pressure: above 55 GPa, the BeO wurtzite structure transforms to a zincblende structure with a phase transition energy of **0.022 MJ/kg (0.065 MJ/L)**.²⁴³ A similar wurtzite to tetragonal transformation has been reported for ZnO²⁴⁴ and lithium aluminum oxide.²⁴⁵

Polymorphs are often encountered in the pharmaceutical industry. For instance, the drug acetazolamide has two polymorphic forms, called A and B. These differ in free energy by only **0.0016 MJ/kg** while the activation energy to create the higher temperature form at the transition temperature of 78 °C is **1.11 MJ/kg**,²⁴⁶ so the cost is probably too high even for an extremely efficient system to be worth the trouble.

²³⁹ Nyman J, Day GM. Static and lattice vibrational energy differences between polymorphs. *Cryst Eng Comm* 2015; 17:5154-5165; <http://pubs.rsc.org/en/content/articlehtml/2015/ce/c5ce00045a>.

²⁴⁰ [https://en.wikipedia.org/wiki/Polymorphism_\(materials_science\)](https://en.wikipedia.org/wiki/Polymorphism_(materials_science)).

²⁴¹ Smith DK, Cline CF, Austerman SB. *Acta Crystallogr.* 1965;18:393. Wells AF. *Structural Inorganic Chemistry*, 5th ed, Oxford Science Publications, 1984.

²⁴² Kirillov PL, ed. *Thermophysical Properties of materials for Nuclear Engineering*, Obninsk, 2006, p. 131; https://www.google.com/url?sa=t&rct=j&q=&esrc=s&source=web&cd=24&ved=0ahUKEwjB48PNI-7SAhUHwlQKHY1kBJg4FBAWCCowAw&url=http%3A%2F%2Ftherpro.hanyang.ac.kr%2Fcontent%2Fattach_down.jsp%3Fdispos%3Dy%26b%3D130890718532272%26n%3D1%26&usg=AFQjCNFxECD4ITq3rk4f2Yrv6aCbN_Jtg&bvm=bv.150475504,d.cGw&cad=rja.

²⁴³ Van Camp PE, Van Doren VE. Ground-state properties and structural phase transformation of beryllium oxide. *J Phys: Condensed Matter* 8(19).

²⁴⁴ Wang J, Xiao P, Zhou M, Wang ZR, Ke FJ. Wurtzite-to-tetragonal structure phase transformation and size effect in ZnO nanorods. *J Appl Phys* 2010;107:023512; http://dprl2.me.gatech.edu/sites/default/files/PDFpub/JAPIAU1072023512_1.pdf

²⁴⁵ Marezio M, Remeika JP, *J. Chem. Phys.* 1966;44:3348.

²⁴⁶ Umeda T, Ohnishi N, Yokoyama T, Kuroda T, Kita Y, Kuroda K, Tatsumi E, Matsuda Y. Physico-chemical Properties and Isothermal Transition of Acetazolamide Polymorphs. *Chem Pharm Bull (Tokyo)*. 1985 Aug;33(8):3422-8; https://www.jstage.jst.go.jp/article/cpb1958/33/8/33_8_3422/article.

Interestingly, there are 15 known phases of water ice, among which at 1 atm pressure are normal hexagonal crystalline ice (Ih) and metastable cubic ice (Ic) which undergo transformation based on temperature.²⁴⁷ The phase transition energy between Ih and Ic is only **0.0007-0.009 MJ/kg (0.0007-0.008 MJ/L)**.²⁴⁸ The 150 K transition between amorphous and hexagonal ice is **~0.061 MJ/kg (~0.061 MJ/L)**.²⁴⁹

²⁴⁷ While it was previously thought that Ic transforms to Ih at temperatures above 180-200 K, recent studies indicate that Ic remains stable for hours at up to 228 K with complex time and temperature dependences. Murray BJ, Bertram AK. Formation and stability of cubic ice in water droplets. *Phys Chem Chem Phys*. 2006;8:186;

<https://open.library.ubc.ca/cIRcle/collections/facultyresearchandpublications/52383/items/1.0041852>.

²⁴⁸ Raza Z. Proton ordering and reactivity of ice. PhD Thesis, University College London, Sep 2012, p. 23; http://discovery.ucl.ac.uk/1369753/1/Raza.Redacted_1369753_thesis-final.pdf.

²⁴⁹ Speedy RJ, Debenedetti PG, Smith RS, Huang C, Kay BD. The evaporation rate, free energy, and entropy of amorphous water at 150 K. *J Chem Phys*. 1996;105:240-244.

3.3.6 Other Phase-Change Enthalpies

The **heat of mixing** is the enthalpy liberated or absorbed from a substance upon mixing with another substance (often, both are liquids).²⁵⁰ Because it is so small, the enthalpy of mixing can often be ignored in calculations for mixtures where other heat terms exist, or in cases where the mixture is ideal.²⁵¹ For example, mixing liquid water and ethanol at 25 °C yields the largest heat of mixing (**-0.0350 MJ/kg**)²⁵² at a 16% ethanol concentration, whereupon the solution warms slightly. The heat of mixing at the same temperature was found to be **0.0013 MJ/kg** for a solution of 48% ethyl acetate in benzene and **0.0010 MJ/kg** for 60% ethyl acetate in toluene.²⁵³

The glass-liquid transition²⁵⁴ is “the reversible transition in amorphous materials (or in amorphous regions within semicrystalline materials) from a hard and relatively brittle glassy state into a viscous or rubbery state as the temperature is increased. An amorphous solid that exhibits a glass transition is called a glass. The reverse transition, achieved by supercooling a viscous liquid into the glass state, is called vitrification. The glass-transition temperature of a material characterizes the range of temperatures over which this glass transition occurs, which is always lower than the melting temperature of the crystalline state of the material, if one exists.” A material could be cycled back and forth through the glass transition region, creating a rechargeable energy store, but this energy is typically too small to be useful. For instance, the **glass-liquid transition enthalpy** for the chalcogenide glass arsenic triselenide²⁵⁵ (As_2Se_3) at the glass transition temperature between 150-190 °C is **~0.017 MJ/kg (0.079 MJ/L)**.²⁵⁶ Cycling the glass-liquid transition in low-density amorphous ice at 137-149 K has an even lower enthalpy, **~0.001 MJ/kg (~0.001 MJ/L)**.²⁵⁷

²⁵⁰ https://en.wikipedia.org/wiki/Enthalpy_of_mixing.

²⁵¹ An ideal mixture is a solution with thermodynamic properties analogous to those of a mixture of ideal gases, in which the volume change upon mixing is zero, yielding an enthalpy of mixing of zero. https://en.wikipedia.org/wiki/Ideal_solution.

²⁵² Boyne JA, Williamson AG. Enthalpies of mixing of ethanol and water at 25 °C. J Chem Eng Data. 1967 Jul; 12(3):318-318; <http://pubs.acs.org/doi/abs/10.1021/je60034a008>.

²⁵³ Shivabasappa KL, Babu PN, Rao YJ. Enthalpy of mixing and heat of vaporization of ethyl acetate with benzene and toluene at 298.15 K and 308.15 K. Braz J Chem Eng. 2008 Mar; 25(1); http://www.scielo.br/scielo.php?script=sci_arttext&pid=S0104-66322008000100017.

²⁵⁴ https://en.wikipedia.org/wiki/Glass_transition.

²⁵⁵ https://en.wikipedia.org/wiki/Arsenic_triselenide.

²⁵⁶ Cernošek Z, Holubová J, Cernošková E, Liška M. Enthalpic relaxation and the glass transition. J Optoelectronics Adv Mater. 2002 Sep; 4(3):489-503; https://joam.inoe.ro/arhiva/pdf4_3/Cernosek.pdf.

²⁵⁷ Elsaesser MS, Winkel K, Mayer E, Loerting T. Reversibility and isotope effect of the calorimetric glass → liquid transition of low-density amorphous ice. Phys Chem Chem Phys. 2010(3); <http://pubs.rsc.org/en/Content/ArticleLanding/2010/CP/B917662D#!divAbstract>.

Other thermodynamic phase changes such as heat of adsorption,²⁵⁸ eutectic transformation,²⁵⁹ liquid crystal phase transitions,²⁶⁰ metallic transition in highly compressed covalent or ionic solids,²⁶¹ magnetic material demagnetization at the Curie temperature,²⁶² spinodal decomposition (rapid unmixing of mixture of solids or liquids, such as oil and water),²⁶³ superconductivity below the critical temperature,²⁶⁴ and even the DNA or protein coil-globule transition²⁶⁵ in biological systems, all might provide opportunities for energy storage via cyclable enthalpic changes, but the changes are unlikely to be high enough in magnitude to be of interest to us here.

²⁵⁸ https://en.wikipedia.org/wiki/Adsorption#Adsorption_enthalpy.

²⁵⁹ https://en.wikipedia.org/wiki/Eutectic_system.

²⁶⁰ https://en.wikipedia.org/wiki/Liquid_crystal.

²⁶¹ e.g., room-temperature cesium iodide becomes metallic when compressed to ~1.15 million atmospheres; Eremets MI, Shimizu K, Kobayashi TC, Amaya K. Metallic CsI at pressures of up to 220 gigapascals. Science 1998 Aug 28;281(5381):1333-1335; <http://science.sciencemag.org/content/281/5381/1333>.

²⁶² https://en.wikipedia.org/wiki/Curie_temperature.

²⁶³ https://en.wikipedia.org/wiki/Spinodal_decomposition.

²⁶⁴ <https://en.wikipedia.org/wiki/Superconductivity>.

²⁶⁵ Wu C, Wang X. Globule-to-coil transition of a single homopolymer chain in solution. Phys Rev Lett. 1998 May 4; 80(18):4092-4094; https://web.archive.org/web/20110721022738/http://ludfc39.u-strasbg.fr/pdflib/polymers/collapse/1998_wu_wang.pdf.

3.4 Thermochemical Power Density

While thermochemical energy density is an intrinsic property of a material given particular conditions of pressure, temperature, and phase, power density depends not just on intrinsic material properties of a substance but also on extrinsic factors such as physical size (scale) and geometry. The duration over which the power density can be continuously maintained also depends on the replacement rate of the energy storage containers.

Consider the case of heat capacity energy that is stored in a cubic box of edge length L_{box} (m), filled with a solid or liquid energy storage material of density ρ (kg/m^3), melting point $T_{\text{m.p.}}$ (K), boiling point $T_{\text{b.p.}}$ (K), heat capacity C_p (J/kg-K), and thermal conductivity K_t (W/m-K). As long as the box remains in full contact with a heat source at $T_{\text{m.p.}}$, the material remains fully charged with stored energy. The instant the box is removed from full contact with the heat source and is placed in full contact with a cold sink at some lower temperature T_{cold} , heat energy immediately begins to drain away from the box.

A box that was surrounded by a perfect thermal insulator could remain charged indefinitely, and the rate of energy extraction – that is, the power draw – by any of the means described in **Section 3.1** could be as slow as desired, or even zero. But in any real system, insulation is not perfect and thermal energy begins to leak away at some finite rate, with faster leakage if: (a) the insulation material is more thermally conductive, (b) the $T_{\text{m.p.}} - T_{\text{cold}}$ differential is larger, (c) the box is immersed in a gas or fluid that permits convective heat losses, or (d) the geometry of the box has a larger surface/volume ratio.

If the entire thermal energy content of the storage box could be usefully drained almost instantly before any leakage occurs, then exploitable power density would be maximized, but only for an infinitesimal period of time; replacement storage boxes would then have to arrive in every succeeding infinitesimal time period in order to maintain the same power draw at continuous levels. As drainage time increases, some of the energy in the box will leak away before it can be extracted for useful work. When drainage time is about equal to the thermal equilibration time for conduction ($t_{\text{EQ}} = \rho L_{\text{box}}^2 C_p / K_t$) for the storage material, about the same amount of energy may leak away as can be usefully harvested, i.e., the theoretical extraction efficiency should be ~50%. At still longer extraction times, even more stored energy leaks away, whereupon power density plunges because the amount extracted is falling while the draw time is lengthening. For purposes of comparison here, we compute the “equilibrium specific power” and the “equilibrium power density” for various materials by taking the extraction time as $\sim t_{\text{EQ}}$.

Physical size affects the thermal leakage rate and thus the computed power density. Assuming a cubical box immersed in a vacuum, there are two main leakage sources: radiative power loss $P_{\text{radiative}} = 6 L^2 e_r \sigma (T_{\text{hot}}^4 - T_{\text{cold}}^4)$, and conductive power loss $P_{\text{conductive}} = \rho L_{\text{box}}^3 C_p (T_{\text{hot}} - T_{\text{cold}}) / t_{\text{EQ}} = L_{\text{box}} K_t (T_{\text{hot}} - T_{\text{cold}})$, with $P_{\text{radiative}} = P_{\text{conductive}}$ at box size $L_{\text{crit}} = K_t (T_{\text{hot}} - T_{\text{cold}}) / [6 e_r \sigma (T_{\text{hot}}^4 - T_{\text{cold}}^4)]$, where emissivity $e_r = 0.02$ for polished silver, $\sigma = 5.67 \times 10^{-8} \text{ W/m}^2\text{-K}^4$ (Stefan-Boltzmann constant), $T_{\text{hot}} = T_{\text{m.p.}}$ for solids or $T_{\text{b.p.}}$ for liquids, and $T_{\text{cold}} = 4 \text{ K}$ for solids or $T_{\text{m.p.}}$ for liquids. Because $P_{\text{radiative}} \propto L_{\text{box}}^2$ and $P_{\text{conductive}} \propto L_{\text{box}}$, the former dominates at box sizes $L_{\text{box}} > L_{\text{crit}}$ and the latter dominates at $L_{\text{box}} < L_{\text{crit}}$. With the exception of liquid graphite ($L_{\text{crit}} \sim 0.002 \text{ m}$), L_{crit} for solid materials ranges from 0.02-400 m; L_{crit} for liquids ranges from 0.05-15 m (excepting the much larger values for LHe and LH₂). For purposes of comparison here, we compute the “equilibrium specific power” and the “equilibrium power density” for various materials by taking the storage box size as $L_{\text{box}} = 0.001 \text{ m}$ (1 mm) $\ll L_{\text{crit}}$ where conductive

power losses strongly dominate for all materials. Note that power density P_D (W/m^3) $\propto 1 / L_{\text{box}}^2$ for conductive energy extraction is maximized at the smallest possible L_{box} , but maintaining a constant power output requires importing fresh storage containers continuously at a circulation velocity of $v_{\text{circ}} \geq K_t / \rho L_{\text{box}} C_p$ which is minimized at the largest possible L_{box} . Choosing $L_{\text{box}} = 0.001$ m provides the highest possible power density while conveniently keeping v_{circ} near or below ~ 1 m/sec for most materials examined. If higher circulating velocities can be conveniently engineered, then container size could be much smaller and a much higher continuously-available system power density could be achieved.

Making these assumptions allows us to directly compare the equilibrium specific power P_S (W/kg) = $K_t (T_{\text{hot}} - T_{\text{cold}}) / \rho L_{\text{box}}^2$ (**Table 19**) and equilibrium power density P_D (W/m^3) = ρP_S (**Table 20**) for a variety of potential solid and liquid thermal energy storage materials,²⁶⁶ along

²⁶⁶ Data sources for thermal conductivity:

[https://en.wikipedia.org/wiki/Thermal_conductivities_of_the_elements_\(data_page\)](https://en.wikipedia.org/wiki/Thermal_conductivities_of_the_elements_(data_page)),
https://en.wikipedia.org/wiki/List_of_thermal_conductivities, Wikipedia entries for specific compounds,
http://www.engineeringtoolbox.com/thermal-conductivity-d_429.html, liquids
http://chemistry.mdma.ch/hiveboard/rhodium/pdf/chemical-data/thermcond_liquids.pdf, MgO
https://en.wikipedia.org/wiki/Magnesium_oxide, ceramics
<http://global.kyocera.com/fcworld/charact/heat/thermalcond.html>, mercury
http://mercury.atomistry.com/physical_properties.html, CaCl_2
<http://www.porousmedialab.by/seminar/light/33.pdf>, liquid naphthalene
http://www.ddbst.com/en/EED/PCP/TCN_C123.php, solid naphthalene
<https://books.google.com/books?id=rUTL9liIfkC&pg=PA22>, cubic boron nitride (Slack GA, J Phys Chem Solids 1973;34:321), liq Li <https://ntrs.nasa.gov/archive/nasa/casi.ntrs.nasa.gov/19680018893.pdf>, 9 liquid metals <https://books.google.com/books?id=gyWDAMo0Q6cC&pg=PA168>, liq Be <https://books.google.com/books?id=3-GbhmsfyeYC&pg=PA43>, organic liquids
http://www.engineersedge.com/heat_transfer/thermal_conductivity_of_liquids_9921.htm, LH_2
<https://www2.mathesongas.com/industrialgas/pdfs/Bulk-Hydrogen.pdf>, cryogenic liqs
<https://technifab.com/cryogenic-resource-library/cryogenic-fluids/>, ethanol vapor
<https://books.google.com/books?id=DYtgBwAAQBAJ&pg=PA568>, liq Si and Ge
https://www.researchgate.net/publication/223794570_Thermal_Conductivities_of_Silicon_and_Germanium_in_Solid_and_Liquid_States_Measured_by_Non-Stationary_Hot_Wire_Method_with_Silica_Coated_Probe, liq n-butane
<https://books.google.com/books?id=DFo1sZBwdNgC&pg=PA164>, liq NH_3
<http://pubs.acs.org/doi/abs/10.1021/je60019a014>, liq alkali metals
<https://books.google.com/books?id=DFo1sZBwdNgC&pg=PA77>, undecanol
<https://cameochemicals.noaa.gov/chris/UND.pdf>, liq propylene
<https://books.google.com/books?id=ViyrmRy2xWoC&pg=PA332>, liq iron
<http://nvlpubs.nist.gov/nistpubs/Legacy/NSRDS/nbsnrsds8.pdf>, liq copper
https://www.researchgate.net/publication/256773519_Thermal_conductivity_of_liquid_metals_and_metallurgical_alloys, and liq graphite @ 4700 K (Zazula JM. On Graphite Transformations at High Temperature and Pressure Induced by Absorption of the LHC Beam. CERN LHC Project Note 78/97, 1997 Jan 18; <http://citeseerx.ist.psu.edu/viewdoc/download?doi=10.1.1.617.810&rep=rep1&type=pdf>). Additional sources for heat capacity data: Al_2O_3 http://nvlpubs.nist.gov/nistpubs/jres/057/jresv57n2p67_A1b.pdf, Si_3N_4 <https://www.memnet.org/material/siliconnitridesi3n4bulk/>, ZrO_2 <http://pubs.acs.org/doi/abs/10.1021/ie50412a022>, liq Ge <https://books.google.com/books?id=b83PO5B88HMC&pg=PA309>, sodium nitrate <https://dspace.mit.edu/bitstream/handle/1721.1/39261/173660389-MIT.pdf>, Li and K nitrate liqs https://www.researchgate.net/profile/Murat_Kenisarin/publication/223742922_High-temperature_phase_change_materials_for_thermal_energy_storage/links/0c96053037798a176d000000.pdf.

with the estimated circulation velocity required to maintain a continuous power draw assuming the circulating storage containers are 1 mm^3 in size. The thermal conductivity of both metals and nonmetals is approximately constant at high temperatures, though conductivity can drop at cryogenic temperatures in both cases.²⁶⁷ Thermal conductivity can also change somewhat during a phase change, e.g., from 0.56 W/m-K for liquid water at $0 \text{ }^\circ\text{C}$ to 2.18 W/m-K for water-ice at $0 \text{ }^\circ\text{C}$.²⁶⁸

Solid diamond ($T_{\text{graphitize}} \sim 2000 \text{ K}$) and cubic boron nitride ($T_{\text{m.p.}} = 3246 \text{ K}$) appear to be the highest ranking substances on both lists. Containment materials such as tungsten ($T_{\text{m.p.}} = 3695 \text{ K}$), graphite carbon ($T_{\text{m.p.}} = 3915 \text{ K}$, 1 atm), and tantalum hafnium carbide or Ta_4HfC_5 ($T_{\text{m.p.}} = 4215 \text{ K}$) are available up to the high end of the heat capacity operating temperature range for both substances.

²⁶⁷ https://en.wikipedia.org/wiki/Thermal_conductivity#Temperature.

²⁶⁸ https://en.wikipedia.org/wiki/Thermal_conductivity#Chemical_phase.

Table 19. Comparison of heat capacity equilibrium specific power and continuous-power circulating velocity for solids or liquids in (1 mm)³ storage containers

Material	Phase	Specific Power P _S (MW/kg)	Circulat. Velocity (mm/sec)	Material	Phase	Specific Power P _S (MW/kg)	Circulat. Velocity (mm/sec)
Carbon (diamond)	solid	1306	314.4	Lead	liq	2.7	12.1
Boron nitride (cubic)	solid	1222	474.6	Cadmium	liq	2.5	21.6
Silicon carbide	solid	336	4123.1	Bismuth	liq	2.3	10.9
Carbon (graphite)	solid	285	35.0	Uranium	solid	2.2	15.1
Beryllium oxide	solid	277	97.7	Gadolinium	solid	2.1	8.4
Aluminum nitride	solid	216	119.0	Gallium	solid	2.1	19.2
Beryllium	solid	184	42.7	Manganese	solid	2.0	2.9
Calcium	solid	144	207.9	Lead	solid	2.0	27.4
Silica (fused)	solid	126	90.7	Zirconium dioxide	solid	1.6	1.2
Lithium	liq	122	25.0	Calcium chloride	solid	1.2	1.7
Silicon	solid	98	65.1	Granite	solid	1.0	0.8
Aluminum	solid	93	107.7	Concrete	solid	0.8	0.5
Magnesium	solid	91	95.7	Water-ice	solid	0.5	0.8
Aluminum	liq	80	37.5	Bismuth	solid	0.4	6.6
Lithium	solid	71	44.1	Mercury	solid	0.4	14.8
Copper	solid	68	127.1	Tellurium	solid	0.4	2.8
Sodium	liq	59	56.3	Mercury	liq	0.2	4.4
Carbon (liq. graphite)	liq	59	3.7	Polyethylene	solid	0.2	0.2
Silver	solid	57	198.6	Naphthalene	solid	0.1	0.3
Sodium	solid	56	140.9	Paraffin wax	solid	0.1	0.1
Magnesium oxide	solid	52	17.9	Sulfuric acid	liq	0.1	0.2
Beryllium	liq	49	12.7	Wood	solid	0.1	0.1
Molybdenum	solid	43	56.8	Lithium nitrate	liq	0.1	0.1
Potassium	solid	41	193.6	Selenium	solid	0.1	0.4
Silicon	liq	41	24.4	Water	liq	0.1	0.2
Tungsten	solid	36	72.3	Glycerine	liq	0.1	0.1
Potassium	liq	34	60.4	Glucose	solid	0.1	0.1
Chromium	solid	32	31.0	Ethylene glycol	liq	0.05	0.1
Copper	liq	31	43.3	1-decanol	liq	0.04	0.1
Rhodium	solid	31	57.7	1-undecanol	liq	0.04	0.1
Boron	solid	27	5.0	Methanol	liq	0.04	0.1
Gold	solid	24	144.7	1-propanol	liq	0.04	0.1
Silver	liq	23	69.0	1-nonanol	liq	0.04	0.1
Iridium	solid	21	59.5	Ethanol	liq	0.04	0.1
Iron	solid	21	25.7	1-octanol	liq	0.04	0.1
Nickel	solid	20	27.3	1-heptanol	liq	0.04	0.1
Cobalt	solid	20	26.6	1-pentanol	liq	0.04	0.1
Aluminum oxide	solid	19	11.1	1-butanol	liq	0.04	0.1
Niobium	solid	17	23.3	Sulfur (rhombic)	solid	0.04	0.1
Strontium	solid	16	52.2	1-hexanol	liq	0.04	0.1
Germanium	liq	15	20.2	Decane	liq	0.04	0.1
Osmium	solid	14	33.3	Iodine	solid	0.03	0.5
Germanium	solid	14	32.9	Heptane	liq	0.03	0.1
Silicon nitride	solid	14	8.8	Octane (~gasoline)	liq	0.03	0.1
Tantalum	solid	13	27.7	Aniline	liq	0.03	0.1
Rubidium	solid	12	136.3	Ammonia	liq	0.03	0.2
Vanadium	solid	12	11.4	Toluene	liq	0.03	0.1
Zinc	solid	12	46.2	Acetone	liq	0.03	0.1
Tin	liq	12	20.9	Hexane	liq	0.03	0.1
Palladium	solid	11	25.4	Propylene	liq	0.03	0.1
Titanium	solid	10	10.2	Xylene	liq	0.03	0.1
Rubidium	liq	10	42.4	Ethyl ether	liq	0.03	0.1
Scandium	solid	10	10.1	Carbon disulfide	liq	0.02	0.1

Thorium	solid	9.3	42.8	Naphthalene	liq	0.02	0.1
Zirconium	solid	8.3	14.2	Sodium nitrate	liq	0.02	0.1
Arsenic	solid	7.7	26.3	Acetic acid	liq	0.02	0.1
Platinum	solid	7.4	28.3	Benzene	liq	0.01	0.1
Yttrium	solid	7.3	14.4	Potassium nitrate	liq	0.01	0.1
Cadmium	solid	7.1	54.3	Chloroform	liq	0.01	0.1
Iron	liq	6.6	6.1	Hydrogen (LH ₂)	liq	0.01	0.2
Cesium	liq	5.9	38.8	n-butane	liq	0.01	<0.1
Cesium	solid	5.8	103.6	Carbon tetrachloride	liq	0.01	0.1
Tin (white)	solid	4.8	45.4	Bromine	liq	0.003	0.1
Hafnium (hexagonal)	solid	4.3	12.3	Nitrogen (LN ₂)	liq	0.002	0.1
Zinc	liq	4.1	22.2	Helium	liq	0.001	<0.1
Antimony	solid	3.4	18.2	Argon	liq	0.0003	0.1

Table 20. Comparison of heat capacity equilibrium power density and continuous-power circulating velocity for solids or liquids in (1 mm)³ storage containers

Material	Phase	Power Density P _D (MW/L)	Circulat. Velocity (mm/sec)	Material	Phase	Power Density P _D (MW/L)	Circulat. Velocity (mm/sec)
Carbon (diamond)	solid	4591	314.4	Cadmium	liq	20	21.6
Boron nitride (cubic)	solid	4215	474.6	Rubidium	solid	18	136.3
Silicon carbide	solid	1079	4123.1	Gadolinium	solid	17	8.4
Beryllium oxide	solid	833	97.7	Rubidium	liq	15	42.4
Aluminum nitride	solid	703	119.0	Gallium	solid	12	19.2
Carbon (graphite)	solid	645	35.0	Manganese	solid	12	2.9
Tungsten	solid	639	72.3	Cesium	liq	11	38.8
Copper	solid	543	127.1	Cesium	solid	11	103.6
Silver	solid	528	198.6	Zirconium dioxide	solid	9.0	1.2
Gold	solid	424	144.7	Mercury	solid	5.7	14.8
Molybdenum	solid	399	56.8	Bismuth	solid	4.3	6.6
Iridium	solid	399	59.5	Mercury	liq	3.3	4.4
Rhodium	solid	335	57.7	Granite	solid	2.6	0.8
Beryllium	solid	311	42.7	Calcium chloride	solid	2.5	1.7
Osmium	solid	289	33.3	Tellurium	solid	2.4	2.8
Silica (fused)	solid	277	90.7	Concrete	solid	1.9	0.5
Copper	liq	251	43.3	Water-ice	solid	0.4	0.8
Silicon	solid	251	65.1	Selenium	solid	0.3	0.4
Calcium	solid	223	207.9	Polyethylene	solid	0.2	0.2
Aluminum	solid	220	107.7	Lithium nitrate	liq	0.2	0.1
Silver	liq	216	69.0	Iodine	solid	0.2	0.5
Chromium	solid	204	31.0	Sulfuric acid	liq	0.2	0.2
Aluminum	liq	190	37.5	Naphthalene	solid	0.1	0.3
Tantalum	solid	189	27.7	Glucose	solid	0.1	0.1
Magnesium oxide	solid	187	17.9	Paraffin wax	solid	0.1	0.1
Cobalt	solid	176	26.6	Glycerine	liq	0.1	0.1
Nickel	solid	157	27.3	Sulfur (rhombic)	solid	0.1	0.1
Niobium	solid	147	23.3	Water	liq	0.1	0.2
Platinum	solid	146	28.3	Ethylene glycol	liq	0.1	0.1
Iron	solid	145	25.7	Wood	solid	0.05	0.1
Magnesium	solid	143	95.7	1-decanol	liq	0.04	0.1
Palladium	solid	131	25.4	Sodium nitrate	liq	0.04	0.1
Thorium	solid	109	42.8	1-undecanol	liq	0.04	0.1
Carbon (liq. graphite)	liq	106	3.7	1-nonanol	liq	0.04	0.1
Silicon	liq	106	24.4	1-propanol	liq	0.03	0.1
Tin	liq	83	20.9	Methanol	liq	0.03	0.1
Beryllium	liq	83	12.7	1-octanol	liq	0.03	0.1
Germanium	liq	81	20.2	1-heptanol	liq	0.03	0.1
Zinc	solid	80	46.2	1-pentanol	liq	0.03	0.1
Aluminum oxide	solid	75	11.1	Aniline	liq	0.03	0.1
Germanium	solid	73	32.9	Ethanol	liq	0.03	0.1
Vanadium	solid	67	11.4	1-butanol	liq	0.03	0.1
Boron	solid	64	5.0	1-hexanol	liq	0.03	0.1
Lithium	liq	62	25.0	Potassium nitrate	liq	0.03	0.1
Hafnium (hexagonal)	solid	58	12.3	Toluene	liq	0.03	0.1
Cadmium	solid	57	54.3	Decane	liq	0.03	0.1
Sodium	liq	55	56.3	Xylene	liq	0.02	0.1
Sodium	solid	52	140.9	Acetone	liq	0.02	0.1
Zirconium	solid	48	14.2	Carbon disulfide	liq	0.02	0.1
Iron	liq	46	6.1	Octane (~gasoline)	liq	0.02	0.1
Arsenic	solid	44	26.3	Heptane	liq	0.02	0.1
Silicon nitride	solid	43	8.8	Ammonia	liq	0.02	0.2
Titanium	solid	42	10.2	n-butane	liq	0.02	<0.1

Uranium	solid	39	15.1	Hexane	liq	0.02	0.1
Lithium	solid	38	44.1	Ethyl ether	liq	0.02	0.1
Strontium	solid	37	52.2	Propylene	liq	0.02	0.1
Potassium	solid	34	193.6	Naphthalene	liq	0.02	0.1
Tin (white)	solid	33	45.4	Acetic acid	liq	0.02	0.1
Yttrium	solid	31	14.4	Chloroform	liq	0.01	0.1
Scandium	solid	29	10.1	Benzene	liq	0.01	0.1
Lead	liq	28	12.1	Carbon tetrachloride	liq	0.01	0.1
Potassium	liq	28	60.4	Bromine	liq	0.01	0.1
Zinc	liq	27	22.2	Nitrogen (LN ₂)	liq	0.002	0.1
Bismuth	liq	23	10.9	Hydrogen (LH ₂)	liq	0.001	0.2
Antimony	solid	22	18.2	Argon	liq	0.0004	0.1
Lead	solid	21	27.4	Helium	liq	0.0001	<0.1

A similar analysis can be applied to a thermochemical power source that derives its energy from the release of heat during a phase change at a particular temperature or narrow temperature range, such as latent heat-based systems. For example, a material that releases a heat of fusion H_{fusion} (J/kg)²⁶⁹ upon transforming from the liquid to the solid state can be estimated to generate an equilibrium specific power P_S (W/kg) = $H_{\text{fusion}} K_t / \rho L_{\text{box}}^2 C_P$ (**Table 21**) and equilibrium power density P_D (W/m³) = ρP_S (**Table 22**) for a variety of potential solid thermal energy storage materials,²⁷⁰ along with the estimated circulation velocity $v_{\text{circ}} \geq K_t / \rho L_{\text{box}} C_P$ required to maintain a continuous power draw assuming the circulating storage containers are 1 mm³ in size, the same as we used in the earlier analysis of a heat capacity-based power storage system. These figures and rankings should be viewed as approximations because reliable data for liquid phase material at the melting point was often not readily available and required the substitution of solid-phase data, introducing some small unknown error in the estimates. As before, if higher circulating velocities can be conveniently engineered, then container size can be much smaller in which case a much higher continuously-available system power density can be achieved.

The maximum specific power and power density for heat of fusion-based systems appears to be achieved by using beryllium oxide,²⁷¹ which has a reasonable operating temperature of $T_{\text{m.p.}} = 2780$ K at 1 atm. In second place is aluminum nitride,²⁷² which provides about one-third as much power per unit mass or volume with a slightly lower operating temperature ($T_{\text{m.p.}} = 2470$ K). Both substances are easily containable by known high-melting-point metal or ceramic materials.

²⁶⁹ Heat of fusion data from **Section 3.2.1**.

²⁷⁰ Additional data sources for heat of fusion: yttrium <http://periodictable.com/Elements/039/data.html>, 1-propanol <https://books.google.com/books?id=ORQeCgAAQBAJ&pg=PT406>, 1-pentanol https://books.google.com/books?id=fio_Ah_hh_OC&pg=PA110, 1-butanol http://www.dbst.com/en/EED/PCP/HFS_C39.php, 1-decanol <https://toxnet.nlm.nih.gov/cgi-bin/sis/search/a?dbs+hsdb:@term+@DOCNO+1072>, 1-hexanol <https://webwisser.nlm.nih.gov//getSubstanceData.do?substanceId=176&displaySubstanceName=1-Hexanol&STCCID=&UNNAID=2282&selectedDataMenuItemID=44>, 1-octanol <http://webbook.nist.gov/cgi/cbook.cgi?ID=C111875&Mask=6F>, lithium nitrate <http://chemister.ru/Database/properties-en.php?dbid=1&id=609>, n-butane http://www.engineeringtoolbox.com/butane-d_1415.html, xylene <http://webbook.nist.gov/cgi/cbook.cgi?ID=C106423&Mask=4>, sodium nitrate <https://cameochemicals.noaa.gov/chris/SDN.pdf>, calcium chloride <https://cameochemicals.noaa.gov/chris/CLC.pdf>, silicon nitride <http://www.azom.com/properties.aspx?ArticleID=53>, silicon carbide <http://www.azom.com/properties.aspx?ArticleID=42>, aluminum nitride <http://www.azom.com/properties.aspx?ArticleID=610>, and boron nitride <http://www.azom.com/properties.aspx?ArticleID=78>. Additional data sources for thermal conductivity: lithium oxide <http://www-ferp.ucsd.edu/LIB/PROPS/PANOS/li2o.html>, magnesium fluoride <http://www.makeitfrom.com/compare/Fluorosilicone-Rubber-FVMQ/Magnesium-Fluoride-MgF2-Optical-Material/>, stearic acid https://www.researchgate.net/publication/222073101_Thermal_conductivity_improvement_of_stearic_acid_using_expanded_graphite_and_carbon_fiber_for_energy_storage_applications, platinum http://www.engineeringtoolbox.com/thermal-conductivity-metals-d_858.html, and barium <http://periodictable.com/Properties/A/ThermalConductivity.v.log.html>.

²⁷¹ https://en.wikipedia.org/wiki/Beryllium_oxide.

²⁷² https://en.wikipedia.org/wiki/Aluminium_nitride.

Table 21. Comparison of heat of fusion equilibrium specific power and continuous-power circulating velocity for liquid/solid materials in (1 mm)³ storage containers

Material	Specific Power P _S (MW/kg)	Circulat. Velocity (mm/sec)	Material	Specific Power P _S (MW/kg)	Circulat. Velocity (mm/sec)
Beryllium oxide	277.9	97.7	Zirconium dioxide	0.9	1.2
Aluminum nitride	90.9	65.4	Cesium (Cs)	0.6	38.8
Calcium (Ca)	44.3	207.9	Bismuth (Bi)	0.6	10.9
Silicon (Si)	43.6	24.4	Manganese (Mn)	0.4	1.6
Boron nitride (cubic)	35.4	19.7	Uranium (U)	0.4	7.9
Magnesium oxide	34.3	17.9	Calcium chloride	0.4	1.7
Carbon (liq. graphite)	32.4	3.70	Lead (Pb)	0.3	12.1
Magnesium (Mg)	27.0	73.5	Water (H₂O)	0.1	0.2
Boron (B)	23.1	5.0	Ammonia (NH ₃)	0.05	0.2
Silicon nitride	18.6	12.0	Mercury (Hg)	0.05	4.4
Silicon dioxide (quartz)	17.0	90.7	Stearic acid (C ₁₈ H ₃₆ O ₂)	0.04	0.2
Lithium (Li)	16.7	25.0	Lithium nitrate	0.04	0.1
Aluminum (Al)	14.9	37.5	Sulfuric acid (H ₂ SO ₄)	0.03	0.2
Aluminum oxide	11.9	11.1	Selenium (Se)	0.03	0.4
Molybdenum (Mo)	11.6	40.0	Sodium nitrate	0.02	0.1
Beryllium (Be)	11.2	12.7	Glycerol (C ₃ H ₈ O ₃)	0.02	0.1
Tungsten (W)	11.2	57.8	Ethylene glycol (C ₂ H ₆ O ₂)	0.02	0.1
Copper (Cu)	8.9	43.3	1-decanol	0.02	0.1
Germanium (Ge)	8.8	20.2	Decane (C ₁₀ H ₂₂)	0.02	0.1
Magnesium fluoride	8.5	9.0	Octane (C ₈ H ₁₈)	0.01	0.1
Gold (Au)	7.7	122.5	1-octanol	0.01	0.1
Silver (Ag)	7.7	69.0	Xylene	0.01	0.1
Cobalt (Co)	7.3	26.6	Acetic acid (C ₂ H ₄ O ₂)	0.01	0.1
Sodium (Na)	6.4	56.4	Carbon tetrachloride (CCl ₄)	0.01	0.1
Lithium oxide	6.1	3.1	Hexane (C ₆ H ₁₄)	0.01	0.1
Rhodium (Rh)	6.0	35.9	Benzene (C ₆ H ₆)	0.01	0.1
Iridium (Ir)	5.9	43.0	Heptane (C ₇ H ₁₆)	0.01	0.1
Chromium (Cr)	5.2	15.9	Naphthalene (C ₁₀ H ₈)	0.01	0.1
Niobium (Nb)	5.1	17.9	1-hexanol	0.01	0.1
Nickel (Ni)	4.7	15.9	Methanol (CH ₃ OH)	0.01	0.1
Strontium (Sr)	4.5	49.5	Hydrogen (H ₂)	0.01	0.2
Osmium (Os)	3.9	27.4	Ethanol (C ₂ H ₅ OH)	0.009	0.1
Tantalum (Ta)	3.9	22.5	Acetone (C ₃ H ₆ O)	0.009	0.1
Potassium (K)	3.7	60.5	1-butanol	0.009	0.1
Zirconium (Zr)	3.6	15.5	Aniline (C ₆ H ₇ N)	0.009	0.1
Scandium (Sc)	3.4	9.6	1-pentanol	0.009	0.1
Titanium (Ti)	2.8	6.7	Diethyl ether (C ₄ H ₁₀ O)	0.008	0.1
Vanadium (V)	2.6	6.4	Carbon disulfide (CS ₂)	0.007	0.1
Zinc (Zn)	2.5	22.2	1-propanol	0.007	0.1
Silicon carbide	2.4	6.6	Toluene (C ₇ H ₈)	0.006	0.1
Antimony (Sb)	2.3	14.4	Chloroform (CHCl ₃)	0.006	0.1
Platinum (Pt)	2.1	20.5	Bromine (Br ₂)	0.006	0.1
Yttrium	1.7	13.5	Propylene (C ₃ H ₆)	0.005	0.1
Sodium chloride	1.7	3.6	Sulfur (S)	0.005	0.1
Iron (Fe)	1.7	6.1	Iodine (I ₂)	0.003	<0.1
Thorium (Th)	1.6	23.1	Argon (Ar)	0.002	0.1
Barium (Ba)	1.5	26.4	Nitrogen (N ₂)	0.002	0.1
Tin (Sn)	1.2	20.9	n-butane	0.001	<0.1
Cadmium (Cd)	1.2	21.6	Helium (He)	0.001	<0.1
Rubidium (Rb)	1.1	42.5			

Table 22. Comparison of heat of fusion equilibrium power density and continuous-power circulating velocity for liquid/solid materials in (1 mm)³ storage containers

Material	Power Density P _D (MW/L)	Circulat. Velocity (mm/sec)	Material	Power Density P _D (MW/L)	Circulat. Velocity (mm/sec)
Beryllium oxide	836.4	97.7	Sodium chloride	3.7	3.6
Aluminum nitride	300.0	65.4	Potassium (K)	3.1	60.5
Tungsten (W)	196.4	57.8	Lead (Pb)	3.0	12.1
Gold (Au)	133.6	122.5	Manganese (Mn)	2.5	1.6
Magnesium oxide	122.9	17.9	Rubidium (Rb)	1.6	42.5
Iridium (Ir)	112.7	43.0	Cesium (Cs)	1.1	38.8
Silicon (Si)	111.9	24.4	Calcium chloride	0.8	1.7
Molybdenum (Mo)	107.8	40.0	Mercury (Hg)	0.7	4.4
Boron nitride (cubic)	81.4	19.7	Selenium (Se)	0.1	0.4
Osmium (Os)	77.7	27.4	Lithium nitrate	0.1	0.1
Silver (Ag)	71.4	69.0	Sulfuric acid (H ₂ SO ₄)	0.1	0.2
Copper (Cu)	71.1	43.3	Sodium nitrate	0.1	0.1
Calcium (Ca)	68.7	207.9	Water (H₂O)	0.05	0.2
Cobalt (Co)	65.1	26.6	Ammonia (NH ₃)	0.03	0.2
Rhodium (Rh)	64.2	35.9	Stearic acid (C ₁₈ H ₃₆ O ₂)	0.03	0.2
Silicon nitride	60.6	12.0	Glycerol (C ₃ H ₈ O ₃)	0.02	0.1
Carbon (liq. graphite)	58.3	3.70	Carbon tetrachloride (CCl ₄)	0.02	0.1
Tantalum (Ta)	58.2	22.5	Ethylene glycol (C ₂ H ₆ O ₂)	0.02	0.1
Boron (B)	54.8	5.0	Bromine (Br ₂)	0.02	0.1
Germanium (Ge)	49.5	20.2	1-decanol	0.01	0.1
Aluminum oxide	47.6	11.1	Acetic acid (C ₂ H ₄ O ₂)	0.01	0.1
Niobium (Nb)	43.7	17.9	Iodine (I ₂)	0.01	<0.1
Magnesium (Mg)	42.8	73.5	Xylene	0.01	0.1
Platinum (Pt)	40.6	20.5	Decane (C ₁₀ H ₂₂)	0.01	0.1
Silicon dioxide (quartz)	37.4	90.7	1-octanol	0.01	0.1
Nickel (Ni)	37.0	15.9	Benzene (C ₆ H ₆)	0.01	0.1
Aluminum (Al)	35.4	37.5	Octane (C ₈ H ₁₈)	0.01	0.1
Chromium (Cr)	33.1	15.9	Naphthalene (C ₁₀ H ₈)	0.01	0.1
Magnesium fluoride	26.6	9.0	Sulfur (S)	0.01	0.1
Zirconium (Zr)	20.7	15.5	Aniline (C ₆ H ₇ N)	0.01	0.1
Thorium (Th)	19.2	23.1	Carbon disulfide (CS ₂)	0.01	0.1
Beryllium (Be)	18.9	12.7	Chloroform (CHCl ₃)	0.01	0.1
Zinc (Zn)	16.5	22.2	1-hexanol	0.01	0.1
Antimony (Sb)	15.1	14.4	Methanol (CH ₃ OH)	0.01	0.1
Vanadium (V)	14.5	6.4	Hexane (C ₆ H ₁₄)	0.01	0.1
Lithium oxide	12.2	3.1	Heptane (C ₇ H ₁₆)	0.01	0.1
Silicon carbide	11.8	6.6	Ethanol (C ₂ H ₅ OH)	0.01	0.1
Titanium (Ti)	11.6	6.7	1-butanol	0.01	0.1
Iron (Fe)	11.5	6.1	Acetone (C ₃ H ₆ O)	0.01	0.1
Strontium (Sr)	10.7	49.5	1-pentanol	0.01	0.1
Scandium (Sc)	9.6	9.6	Toluene (C ₇ H ₈)	0.01	0.1
Cadmium (Cd)	9.5	21.6	Diethyl ether (C ₄ H ₁₀ O)	0.01	0.1
Tin (Sn)	8.6	20.9	1-propanol	0.01	0.1
Lithium (Li)	8.6	25.0	Argon (Ar)	0.003	0.1
Yttrium	7.3	13.5	Propylene (C ₃ H ₆)	0.003	0.1
Uranium (U)	6.9	7.9	n-butane	0.003	<0.1
Sodium (Na)	5.9	56.4	Nitrogen (N ₂)	0.002	0.1
Bismuth (Bi)	5.7	10.9	Hydrogen (H ₂)	0.001	0.2
Barium (Ba)	5.1	26.4	Helium (He)	0.0001	<0.1
Zirconium dioxide	4.9	1.2			

Macroscale masses of working nanodevices may grow extremely hot, placing major scaling limits on large-scale nanomachinery aggregates. As a somewhat fanciful example,²⁷³ consider a macroscopic ball of radius R consisting of N tightly-packed nanodevices each of mass density ρ and whole-nanorobot power density $P_D \sim 1 \text{ MW/L}$, of which nanodevices some fraction f_n are active, all suspended in mid-air. The ball grows hotter as R ($\sim N^{1/3}$) rises, until at some “critical combustible mass” $M_{\text{crit}} = (4/3) \pi \rho R_{\text{crit}}^3$ the surface temperature exceeds the maximum combustion point for diamond in air ($T_{\text{burn}} = 1070 \text{ K}$)²⁷⁴ and the solid ball of nanorobots bursts into flame. (Sapphire devices cannot burn, but have a $T_{\text{melt}} \sim 2310 \text{ K}$;²⁷⁵ as a practical matter, nanomachinery may fail at temperatures significantly below T_{burn} .) From simple geometry and neglecting $\sim 2\%$ air conduction losses, the maximum noncombustible aggregate radius R_{crit} is:

$$R_{\text{crit}} \sim 3 \sigma e_r (T_{\text{burn}}^4 - T_{\text{environ}}^4) / f_n P_D$$

For emissivity $e_r = 0.97$ (e.g., carbon black) to maximize heat emission at the lowest possible temperature, $\sigma = 5.67 \times 10^{-8} \text{ W/m}^2\text{-K}^4$ (Stefan-Boltzmann constant), and environmental temperature $T_{\text{environ}} = 300 \text{ K}$, then $R_{\text{crit}} = 0.22 \text{ mm}$ for $f_n = 100\%$. Assuming a full cold start, critical time to incineration is $t_{\text{crit}} \sim C_V (T_{\text{burn}} - T_{\text{environ}}) / f_n P_D = 1.4 \text{ sec}$ for $f_n = 100\%$ at $R \sim R_{\text{crit}}$ if nanorobot heat capacity $C_V = 1.8 \times 10^6 \text{ joules/m}^3\text{-K}$ (\sim diamond). Decreasing whole-nanorobot P_D to **0.01 MW/L** or simply switching off 99% of the nanorobots ($f_n = 1\%$) increases R_{crit} to $\sim 22 \text{ cm}$.

²⁷³ Freitas RA Jr., Nanomedicine, Volume I: Basic Capabilities, Landes Bioscience, Georgetown, TX, 1999, Section 6.5.3, “Nanorobot Power Scaling”; <http://www.nanomedicine.com/NMI/6.5.3.htm>.

²⁷⁴ Cotton FA, Wilkinson G. Advanced Inorganic Chemistry: A Comprehensive Text, Second Edition, John Wiley & Sons, New York, 1966.

²⁷⁵ Richard W. Hughes, Ruby & Sapphire, RWH Publishing, Boulder CO, 1997.

Chapter 4. Chemical Energy Storage

Chemical energy generally refers to the potential of atoms in normal matter to share, exchange, or excite their electrons. Energy is usually stored or released “chemically” either when electrons are transferred between a “reactant” and a “product” during a chemical reaction, or when the electrons associated with an atom are excited from their lowest electronic ground state into higher and more energetic electronic states, or are even removed from the atom altogether as occurs during ionization.

The discussion here evaluates various materials that store or release energy, largely ignoring any possible infrastructure that may be necessary for harnessing the stored energy for some useful purpose. Including such infrastructure components – which may include tankage, insulation, regulators, controllers, wiring, pipes, and so forth – will reduce the net energy density of the energy processing and utilization system to some unknown degree, depending on the particular system design that is chosen.

In this Chapter we survey the specific energy (MJ/kg) and energy density (MJ/L) available from various material stores of chemical energy. In particular, we examine the limits of chemical energy storage densities that are currently available, or could theoretically become available in the future, from the following modalities: Electrochemical batteries and fuel cells (**Section 4.1**), chemical decomposition and explosives (**Section 4.2.1**), nonambient chemical combustion in which fuel and oxidizer are contained within the system (**Section 4.2.2**), ambient chemical combustion in which the oxidizer is provided from the environment (**Section 4.2.3**), molecular recombination energy (**Section 4.3**), electronically metastable molecules (**Section 4.4.1**), free radical species (**Section 4.4.2**), ion recombination energy (**Section 4.4.3**), and finally the atomistic formation of solids having covalent, ionic, metallic, hydrogen, or van der Waals bonding (**Section 4.5**).

Figure 3 (Chapter 9) provides a chart that summarizes much of this data.

A few interesting points of note:

(1) TNT burned in ambient air releases almost three times more energy (**14.5 MJ/kg, 24.1 MJ/L**) than if it is allowed to explode (**5.4 MJ/kg, 9.0 MJ/L**). This behavior is typical for most explosives.

(2) Boron has the highest energy density of any combustible burned in ambient air (**271 MJ/L**), much higher than the energy density of solid molecular hydrogen burned in ambient air (**73 MJ/L**) and even higher than the vaunted molecular recombination energy of monatomic hydrogen (**~216 MJ/L**) that might possibly be available using metallic hydrogen (**Section 4.3.1.5**).

(3) The maximum *theoretical* energy densities for purely chemical systems are **~82 MJ/L** for batteries, **~177 MJ/L** for explosives, **~271 MJ/L** for combustion in ambient air, **~288 MJ/L** for hypothetical crystals of metastable-state atoms, and up to **~31,500 MJ/L** for fully ionized heavy atoms in a **~9000 tesla** magnetic field.

4.1 Electrochemical Batteries and Fuel Cells

An electrochemical battery generally consists of one or more electrochemical cells whose negative terminal (the anode) serves as a source of electrons which can flow through an external circuit, providing energy to some external device, and then return to the positive terminal (the cathode).²⁷⁶ Ions move inside the battery so as to complete an electrochemical reaction in which ions may be created or neutralized at separate terminals. The movement of these ions through an electrolyte allows current to flow out of the battery to perform work. The electrolyte is an ionically (but not electronically) conductive material acting as a medium for the flow of charge carriers.²⁷⁷

Primary or non-rechargeable batteries such as the alkaline batteries used in flashlights are used once and then discarded because the electrode materials are irreversibly chemically changed during discharge. Secondary or rechargeable batteries – such as lead-acid batteries in cars, or lithium-ion batteries in laptops and smartphones – can be discharged and recharged multiple times (e.g., from wall socket current) because the original composition of the electrodes can be restored by reverse current.

Fuel cells convert the chemical energy of a fuel that is flowing through them into electricity, usually via a chemical reaction reaction of positively charged hydrogen ions with oxygen or another oxidizing agent.²⁷⁸ Fuel cells require a continuous source of fuel and oxygen or air to sustain the chemical reaction. A few high-temperature variants employ oxygen ions (solid oxide fuel cells) or carbonate ions (molten carbonate fuel cells). While batteries typically have at least one solid metal electrode that is slowly consumed as electricity is produced, in a fuel cell the electrode is not consumed and the cell produces electricity as long as fuel and oxidizer are pumped through it.²⁷⁹

Note that Carnot's theorem limiting the efficiency of heat engines does not apply to batteries and fuel cells,²⁸⁰ which can generate useful power when all components of the system are at the same temperature by converting chemical energy to work. Carnot's theorem only applies only to engines that convert thermal energy to work by exploiting a temperature differential. However, the Second Law may still restrict the efficiency of energy conversion in batteries and fuel cells.²⁸¹

Figure 7 (Chapter 9) provides a chart that summarizes power density vs. specific power for batteries and fuel cells.

²⁷⁶ [https://en.wikipedia.org/wiki/Battery_\(electricity\)](https://en.wikipedia.org/wiki/Battery_(electricity)).

²⁷⁷ <https://en.wikipedia.org/wiki/Electrolyte>.

²⁷⁸ https://en.wikipedia.org/wiki/Fuel_cell.

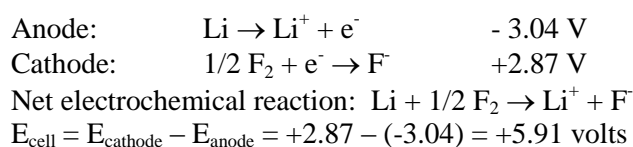
²⁷⁹ https://www.nasa.gov/centers/glenn/technology/fuel_cells.html.

²⁸⁰ [https://en.wikipedia.org/wiki/Carnot%27s_theorem_\(thermodynamics\)#Applicability_to_fuel_cells_and_batteries](https://en.wikipedia.org/wiki/Carnot%27s_theorem_(thermodynamics)#Applicability_to_fuel_cells_and_batteries).

²⁸¹ Jacob KT, Jain S. Fuel cell efficiency redefined : Carnot limit reassessed. Q1 - Ninth International Symposium on Solid Oxide Fuel Cells (SOFC IX), USA, July 2005; <http://eprints.iisc.ernet.in/42739/>.

4.1.1 Electrochemical Batteries

The basis for an electrochemical cell is a redox reaction consisting of two half-reactions – “oxidation” (electron loss) at the anode and “reduction” (electron gain) at the cathode – with the electric potential difference between the two electrodes generating the electrical energy.²⁸² The highest energy density battery will use electrodes with the largest possible electrode potential difference and atoms having the smallest possible atomic mass. Consulting a table of standard electrode potentials (**Table 23**, below),²⁸³ we find that the elemental reducing agent with highest reducing-agent potential and the lightest atoms is **lithium** ($\text{Li}^+ + \text{e}^- \rightarrow \text{Li(s)}$ at -3.04 volts per e^-) and the elemental oxidizing agent with the highest oxidizing-agent potential and the lightest atoms is **fluorine** ($\text{F}_2(\text{g}) + 2\text{e}^- \rightarrow 2\text{F}^-$ at +2.87 volts per e^-). Hence we have:



For a lithium-fluorine galvanic cell in which a spontaneous redox reaction drives the cell to produce an electric potential, the Gibbs free energy of electrochemical power generated by the cell $\Delta G^\circ_{\text{cell}} = -n F_c E_{\text{cell}} = -5.70 \times 10^5$ joules/mole, where $n = 1$ mole of reactants, electrical potential $E_{\text{cell}} = +5.91$ volts, and the Faraday constant $F_c = 96,485$ coul/mole.²⁸⁴ Since the reactants include 1 mole of Li (mass = 0.00694 kg, volume 0.0130 L, taking density $\rho_{\text{Li}} = 534$ kg/m³) and 0.5 mole of F₂ (mass = 0.019 kg, volume = 0.00965 L taking density $\rho_{\text{F}_2} = 1970$ kg/m³ for solid $\alpha\text{-F}_2$)²⁸⁵, the reactants have mass = 0.02594 kg and volume 0.0227 L, yielding a specific energy of **22.0 MJ/kg** and an energy density of **25.1 MJ/L**. This is essentially identical to the specific energy of **23.784 MJ/kg** for Li + F₂ nonambient chemical combustion (see **Section 4.2.2, Table 27**).

A reduction reaction like $\text{Sr}^+ + \text{e}^- \rightleftharpoons \text{Sr}$ in which a singly-ionized strontium atom²⁸⁶ is reduced to strontium metal might yield a slightly higher net reaction voltage, but strontium ions are so heavy that the specific energy of a theoretical Sr-F₂ battery (net electrochemical reaction: $\text{Sr} + 1/2 \text{ F}_2 \rightarrow \text{Sr}^+ + \text{F}^-$) would only reach **6.29 MJ/kg**.

²⁸² https://en.wikipedia.org/wiki/Standard_electrode_potential.

²⁸³ [https://en.wikipedia.org/wiki/Standard_electrode_potential_\(data_page\)](https://en.wikipedia.org/wiki/Standard_electrode_potential_(data_page)).

²⁸⁴ https://en.wikipedia.org/wiki/Faraday_constant.

²⁸⁵ https://en.wikipedia.org/wiki/Phases_of_fluorine.

²⁸⁶ Divalent strontium ions are the norm, but monovalent strontium (Sr^+) ions exist under certain exotic conditions, e.g., Tang IN, Lian MS, Castleman AW. Mass Spectrometric Study of Gas - Phase Clustering Reactions: Hydration of the Monovalent Strontium Ion. J Chem Phys. 1976;65(10):4022; <http://aip.scitation.org/doi/abs/10.1063/1.432854>; Gapeev A, Dunbar RC. Binding of Alkaline Earth Halide Ions MX^+ to Benzene and Mesitylene. J Phys Chem A 2000;104(17):4084-4088; <http://pubs.acs.org/doi/abs/10.1021/jp9943934>.

Table 23. Standard Electrode Potentials (E°) for Reducing/Oxidizing Half-Reactions (aqueous, 298 K)

Reducing Agent Half-Reaction			Oxidizing Agent Half-Reaction		
Oxidant	Reductant	E° (volts)	Oxidant	Reductant	E° (volts)
$\text{Sr}^+ + \text{e}^-$	\rightleftharpoons Sr	-4.10	$\text{KrF}_2(\text{aq}) + 2\text{e}^-$	\rightleftharpoons Kr(g) + $2\text{F}^-(\text{aq})$	+3.27
$\text{Ca}^+ + \text{e}^-$	\rightleftharpoons Ca	-3.80	$\text{F}_2(\text{g}) + 2\text{H}^+ + 2\text{e}^-$	\rightleftharpoons 2HF(aq)	+3.05
$\text{Pr}^{3+} + \text{e}^-$	\rightleftharpoons Pr ²⁺	-3.10	$\text{F}_2(\text{g}) + 2\text{e}^-$	\rightleftharpoons 2F ⁻	+2.87
$3\text{N}_2(\text{g}) + 2\text{H}^+ + 2\text{e}^-$	\rightleftharpoons 2HN ₃ (aq)	-3.09	$\text{H}_4\text{XeO}_6(\text{aq}) + 2\text{H}^+ + 2\text{e}^-$	\rightleftharpoons XeO ₃ (aq) + 3H ₂ O	+2.42
$\text{Li}^+ + \text{e}^-$	\rightleftharpoons Li(s)	-3.04	$\text{XeF}_2(\text{aq}) + 2\text{H}^+ + 2\text{e}^-$	\rightleftharpoons Xe(g) + 2HF(aq)	+2.32
$\text{N}_2(\text{g}) + 4\text{H}_2\text{O} + 2\text{e}^-$	\rightleftharpoons 2NH ₂ OH(aq) + 2OH ⁻	-3.04	$\text{FeO}_4^{2-} + 3\text{e}^- + 8\text{H}^+$	\rightleftharpoons Fe ³⁺ + 4H ₂ O	+2.20
$\text{Cs}^+ + \text{e}^-$	\rightleftharpoons Cs(s)	-3.03	$\text{H}_4\text{XeO}_6(\text{aq}) + 8\text{H}^+ + 8\text{e}^-$	\rightleftharpoons Xe(g) + 6H ₂ O	+2.18
$\text{Ca}(\text{OH})_2 + 2\text{e}^-$	\rightleftharpoons Ca + 2OH ⁻	-3.02	$\text{XeO}_3(\text{aq}) + 6\text{H}^+ + 6\text{e}^-$	\rightleftharpoons Xe(g) + 3H ₂ O	+2.12
$\text{Er}^{3+} + \text{e}^-$	\rightleftharpoons Er ²⁺	-3.00	$\text{HMnO}_4^- + 3\text{H}^+ + 2\text{e}^-$	\rightleftharpoons MnO ₂ (s) + 2H ₂ O	+2.09
$\text{Ba}(\text{OH})_2 + 2\text{e}^-$	\rightleftharpoons Ba + 2OH ⁻	-2.99	$\text{O}_3(\text{g}) + 2\text{H}^+ + 2\text{e}^-$	\rightleftharpoons O ₂ (g) + H ₂ O	+2.08
$\text{Rb}^+ + \text{e}^-$	\rightleftharpoons Rb(s)	-2.98	$\text{S}_2\text{O}_8^{2-} + 2\text{e}^-$	\rightleftharpoons 2SO ₄ ²⁻	+2.01
$\text{K}^+ + \text{e}^-$	\rightleftharpoons K(s)	-2.93	$\text{Ag}^{2+} + \text{e}^-$	\rightleftharpoons Ag ⁺	+1.98
$\text{Ba}^{2+} + 2\text{e}^-$	\rightleftharpoons Ba(s)	-2.91	$\text{BrO}_4^- + 2\text{H}^+ + 2\text{e}^-$	\rightleftharpoons BrO ₃ ⁻ + H ₂ O	+1.85
$\text{La}(\text{OH})_3(\text{s}) + 3\text{e}^-$	\rightleftharpoons La(s) + 3OH ⁻	-2.90	$\text{Au}^+ + \text{e}^-$	\rightleftharpoons Au(s)	+1.83
$\text{Fr}^+ + \text{e}^-$	\rightleftharpoons Fr	-2.90	$\text{Co}^{3+} + \text{e}^-$	\rightleftharpoons Co ²⁺	+1.82
$\text{Sr}^{2+} + 2\text{e}^-$	\rightleftharpoons Sr(s)	-2.90	$\text{H}_2\text{O}_2(\text{aq}) + 2\text{H}^+ + 2\text{e}^-$	\rightleftharpoons 2H ₂ O	+1.78
$\text{Sr}(\text{OH})_2 + 2\text{e}^-$	\rightleftharpoons Sr + 2OH ⁻	-2.88	$\text{AgO}(\text{s}) + 2\text{H}^+ + \text{e}^-$	\rightleftharpoons Ag ⁺ + H ₂ O	+1.77
$\text{Ca}^{2+} + 2\text{e}^-$	\rightleftharpoons Ca(s)	-2.87	$\text{MnO}_4^- + 4\text{H}^+ + 3\text{e}^-$	\rightleftharpoons MnO ₂ (s) + 2H ₂ O	+1.70
$\text{Mg}^{2+} + 2\text{e}^-$	\rightleftharpoons Mg(s)	-2.38	$\text{SbO}^+ + 2\text{H}^+ + 3\text{e}^-$	\rightleftharpoons Sb(s) + H ₂ O	+0.20
$2\text{H}^+ + 2\text{e}^-$	\rightleftharpoons H ₂ (g)	0			

Despite many efforts since the 1960s,²⁸⁷ no one has ever made an Li-F₂ battery and it's unclear if one is even possible, given the extreme toxicity and chemical reactivity of F₂ gas, the vigorous reactivity of Li with water and F₂, and the fact that: (A) cells with aqueous electrolytes are limited to <2 volts because the oxygen and hydrogen in water dissociate above this voltage,²⁸⁸ (B)

²⁸⁷ Scrosati B, Abraham KM, van Schalkwijk WA, Hassoun J, eds. Lithium Batteries: Advanced Technologies and Applications, Wiley, 2013.

²⁸⁸ Perhaps some non-water electrolyte, such as a liquefied noble gas, could be used to mobilize Li and F ions. F₂ melts at 53.5 K and boils at 85.0 K. Argon melts at 83.8 K and boils at 87.3 K, and liquid Ar can be used as a solvent – e.g., hydrocarbons (<http://link.springer.com/article/10.1023/A:1015825102964>) and fluorocarbons (<http://www.sciencedirect.com/science/article/pii/0584853973801758>) are at least weakly soluble in liquid argon. The solubility of F₂ is unknown, but xenon has a measured solubility in liquid fluorine of 0.015 mole fraction at 80 K and the lighter krypton has a measured solubility in liquid fluorine of 0.3 mole fraction at 80 K (Seaver RE. Cryogenic solutions and solubilities in liquid fluorine. NASA Technical Note TN D-2286, June 1964, p. 8; <https://ntrs.nasa.gov/archive/nasa/casi.ntrs.nasa.gov/19640013319.pdf>). This progression suggests that the next lightest noble gas, argon, might be quite soluble in liquid F₂, hence also *vice versa*. As for reactivity, a mixture of Ar and F₂ generally requires high pressure and electrical stimulation to temporarily combine into ArF (as in an excimer laser; https://en.wikipedia.org/wiki/Argon_fluoride_laser); the difference between the ground and excited state of ArF is 6.3 eV, at least somewhat above the 5.91 volt electrode potential of the putative Li-F battery.

Li-F₂ cells seem unlikely to be rechargeable, and (C) lithium fluoride can crystallize and stop conducting electricity.²⁸⁹ Note that if you could operate a lithium battery in a pure fluorine atmosphere and freely draw F₂ from the external environment, then it would be possible to exclude the mass and volume of fluorine from the energy density calculations, yielding a specific energy of (5.70 x 10⁵ joules / 0.00694 kg =) **82.1 MJ/kg** and an energy density of (5.70 x 10⁵ joules / 0.0130 L =) **43.8 MJ/L** for the lithium-fluorine battery. We probably can't do much better than this with any electrochemical battery – and, of course, no one knows how to safely build a battery using frozen solid fluorine, or under what circumstances one might safely operate an Li-F₂ battery in a pure F₂ atmosphere.

The only other high energy density battery systems are metal-air batteries drawing ambient air, allowing the mass of reactant oxygen to be excluded from the energy density calculations.²⁹⁰ For example, a metal-air electrochemical cell uses an anode made from pure metal and an external cathode of ambient air, typically with an aqueous electrolyte. The best case is the lithium-air battery discharge reaction (4Li + O₂ → 2Li₂O at 2.91 volts) with a nominal specific energy of **18.8 MJ/kg** (~**19.86 MJ/kg** for Li/O₂ nonambient chemical combustion; **Section 4.2.2, Table 27**), giving a theoretical specific energy of **40.1 MJ/kg** when oxygen is excluded because O₂ is not stored in the battery.²⁹¹ This is essentially the same result as we get for ambient air combustion of lithium (~**42.557 MJ/kg**; **Section 4.2.3, Table 29**) and is almost as high as the **47.9 MJ/kg** we get for the ambient air combustion of octane, the main hydrocarbon component of gasoline (**Section 4.2.3 and Table A4**). Present-day experimental lithium-air batteries remain in a fairly primitive state, and are said to have “low power, poor cyclability, and need pure O₂ which requires an oxygen tank.”²⁹² One of the best lithium-based might be the Innolith Energy Battery, announced in April 2019 as “the world’s first 1000 Wh/kg rechargeable battery” incorporating non-flammable all-inorganic electrolytes for use in electric vehicles,²⁹³ stores only **3.6 MJ/kg**.

Note, however, that battery power density is very low, using current technologies. For example, the Tesla Model 3 battery for electric cars stores 5.3 KW-hr and weighs 25.6 kg, giving a specific energy of **0.745 MJ/kg**,²⁹⁴ but in a car the Model 3 produces 211 kW of power (283 hp)²⁹⁵ using a 478 kg battery pack,²⁹⁶ giving a specific power of only **0.00044 MW/kg** for the battery pack.

²⁸⁹ Alice J. Friedemann, *When Trucks Stop Running: Energy and the Future of Transportation*, Springer 2015, p. 60; <https://books.google.com/books?id=jBUUpCwAAQBAJ&pg=PA60>.

²⁹⁰ Chen-Xi Zu, Hong Li. Thermodynamic analysis on energy densities of batteries. *Energy Environ Sci.* 2011;4:2614-2624; <http://pubs.rsc.org/en/Content/ArticleLanding/2011/EE/c0ee00777c#!divAbstract>.

²⁹¹ https://en.wikipedia.org/wiki/Metal%E2%80%93air_electrochemical_cell#Types.

²⁹² Alice J. Friedemann, *When Trucks Stop Running: Energy and the Future of Transportation*, Springer 2015, p. 60; <https://books.google.com/books?id=jBUUpCwAAQBAJ&pg=PA60>.

²⁹³ “Innolith energy technology brings 1000 km EV within range,” Innolith AG, 4 Apr 2019; <https://innolith.com/innolith-energy-technology-brings-1000km-ev-within-range/>.

²⁹⁴ “Tesla Model 3 Battery Cell Has World’s Highest Energy Density,” 3 May 2018; <https://insideevs.com/tesla-claims-model-3-battery-has-highest-energy-density-of-any-electric-car/>.

²⁹⁵ https://en.wikipedia.org/wiki/Tesla_Model_3#Specifications.

Batteries usually have a characteristic optimal discharge rate and capacity. A battery's "capacity", typically measured in ampere-hours, is the amount of electric charge it can deliver at the rated voltage. (Capacity is ampere-hours multiplied by the voltage, which gives the total energy stored in the battery, e.g., in joules.) Capacity is higher when more electrode material is contained in the cell. The rated capacity of a battery is often expressed as the product of 20 hours multiplied by the current that a new battery can consistently supply for 20 hours at 68 °F (20 °C), while remaining above a specified terminal voltage per cell.²⁹⁷ The higher the discharge rate, the lower the capacity of the battery, according to Peukert's law.²⁹⁸

Batteries that are stored for a long period of time or that are discharged to only a small fraction of their capacity lose capacity due to the presence of irreversible side reactions that consume charge carriers without producing current, a phenomenon known as internal self-discharge. When batteries are recharged, additional side reactions can occur that reduce capacity for subsequent discharges. After enough recharges, all capacity may be lost and the battery stops producing power.²⁹⁹

²⁹⁶ "Battery Expert: Tesla Model 3 has most advanced large scale lithium battery ever produced," 27 Jun 2018; <https://evannex.com/blogs/news/tesla-s-battery-pack-is-both-mysterious-and-alluring-work-in-progress>.

²⁹⁷ https://en.wikipedia.org/wiki/Electric_battery#Capacity_and_discharge.

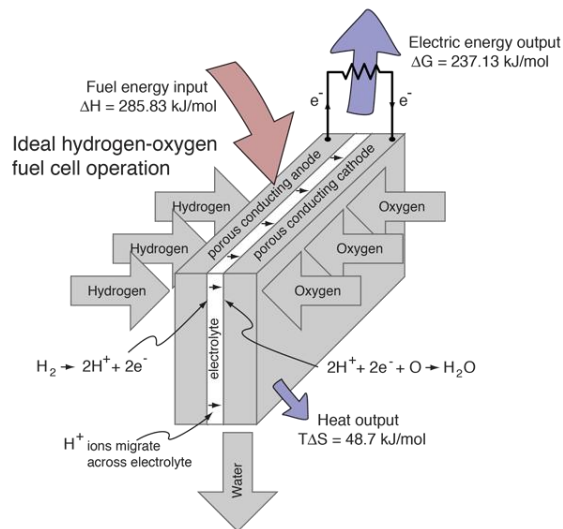
²⁹⁸ https://en.wikipedia.org/wiki/Peukert's_law.

²⁹⁹ https://en.wikipedia.org/wiki/Electric_battery#Capacity_and_discharge.

4.1.2 Fuel Cells

A fuel cell is an electrochemical cell that converts the chemical energy from a fuel into electricity through an electrochemical reaction of hydrogen fuel with oxygen or another oxidizing agent.³⁰⁰ Fuel cells require a continuous source of fuel and oxygen (e.g., from air) to sustain the chemical reaction, whereas in a battery the chemical energy comes from chemicals already present in the battery. Fuel cells produce electricity continuously as long as fuel and oxygen are supplied. They include three adjacent segments (the anode, the electrolyte, and the cathode). At the anode a catalyst oxidizes the fuel (e.g., H₂), turning the fuel into a positively charged ion and a negatively charged electron. The electrolyte is a substance specifically designed so that ions, but not electrons, can pass through it. The freed electrons travel through a wire, creating an electric current flowing through a load. The ions travel through the electrolyte to the cathode where they are reunited with the electrons, whereupon the two react with a third chemical (e.g., O₂) to create waste product (e.g., H₂O).

An H₂/O₂ fuel cell can produce electrical energy at a higher efficiency than just burning the hydrogen to produce heat to drive a generator because it is not subject to the thermal bottleneck³⁰¹ from the second law of thermodynamics.³⁰² Following the fuel cell example provided by R. Nave,³⁰³ combining a mole of H₂ gas and a half-mole of O₂ gas produces a mole of H₂O. At an operating pressure of P = 1 atm and T = 298 K, the heat of formation for H₂O product from the elements is $\Delta H = -285.83$ KJ/mole, system work is $W = P\Delta V = (101.3 \times 10^3 \text{ N/m}^2)(1.5 \text{ moles})(-22.4 \times 10^{-3} \text{ m}^3/\text{mol})(298\text{K}/273\text{K}) = -3715 \text{ J}$, the change in internal energy is $\Delta U = \Delta H - P\Delta V = -285.83 \text{ KJ} + 3.715 \text{ KJ} = -282.1 \text{ KJ}$, the entropy of the gases decreases by $T\Delta S = 298 [(1 \text{ mole H}_2)(130.68 \text{ J/K}) + (0.5 \text{ mole O}_2)(205.14 \text{ J/K}) - (1 \text{ mole H}_2\text{O})(69.91 \text{ J/K})] = 48.7 \text{ KJ}$ in the process of combination, hence the amount of energy per mole of hydrogen which can be provided as electrical energy is the change in the Gibbs free energy $\Delta G = \Delta H - T\Delta S = -285.83 \text{ KJ} + 48.7 \text{ KJ} = -237.1 \text{ KJ}$. Thus this fuel cell allows extracting 237 KJ as electric energy while dumping 48.7 KJ to the environment, a maximum theoretical energy efficiency of 83%. Present-day fuel cells don't yet approach that ideal efficiency, typically achieving 40%-60% efficiency.³⁰⁴



³⁰⁰ https://en.wikipedia.org/wiki/Fuel_cell.

³⁰¹ <http://hyperphysics.phy-astr.gsu.edu/hbase/thermo/seclaw2.html>.

³⁰² <http://hyperphysics.phy-astr.gsu.edu/hbase/thermo/seclaw.html>.

³⁰³ <http://hyperphysics.phy-astr.gsu.edu/hbase/thermo/electrol.html>.

³⁰⁴ https://www.energy.gov/sites/prod/files/2015/11/f27/fcto_fuel_cells_fact_sheet.pdf.

In this example using 1 mole (0.002 kg) of H₂ and 0.5 mole (0.016 kg) of O₂ reactants, the specific energy of this fuel cell is $E_S = (0.2371 \text{ MJ}) / (0.018 \text{ kg}) = \mathbf{13.17 \text{ MJ/kg}}$ for a gas mixture of both reactants (similar to the **13.444 MJ/kg** for H₂/O₂ nonambient chemical combustion; **Section 4.2.2, Table 27**), or $E_S = (0.2371 \text{ MJ}) / (0.002 \text{ kg}) = \mathbf{118.6 \text{ MJ/kg}}$ if the mass of the oxygen is excluded when it can be readily extracted from the ambient environment (similar to the **121.0 MJ/kg** for H₂/O₂ ambient chemical combustion; **Section 4.2.3, Table 29**). If the reactants are stored at STP,³⁰⁵ then the energy density is very low: $E_D = (0.2371 \text{ MJ}) / (33.4 \text{ L}) = \mathbf{0.0071 \text{ MJ/L}}$ for the H₂/O₂ mixture or $E_D = (0.2371 \text{ MJ}) / (22.3 \text{ L}) = \mathbf{0.0106 \text{ MJ/L}}$ for the H₂ gas alone, at STP. But if the reactants can be cooled or pressurized to liquid densities,³⁰⁶ then the energy density rises to $E_D = (0.2371 \text{ MJ}) / (0.0426 \text{ L}) = \mathbf{5.57 \text{ MJ/L}}$ for the H₂/O₂ mixture and $E_D = (0.2371 \text{ MJ}) / (0.0286 \text{ L}) = \mathbf{8.29 \text{ MJ/L}}$ for the H₂ reactant alone.

Assuming an ideal fuel cell could be designed that would achieve a similar specific energy as nonambient chemical combustion of the same reactants, we could in theory obtain fuel cells achieving up to a maximum limit of **~13.4 MJ/kg** for H₂/O₂, **~13.7 MJ/kg** for H₂/F₂, **~19.9 MJ/kg** for Li/O₂, **~21.5 MJ/kg** for Be/F₂, **~23.8 MJ/kg** for Li/F₂, or **~24.0 MJ/kg** for Be/O₂.

What about power density? Many kinds of fuel cells have been developed for power applications including proton exchange membrane fuel cells (PEMFCs),³⁰⁷ phosphoric acid fuel cells (PAFCs),³⁰⁸ solid acid fuel cells (SAFCs),³⁰⁹ alkaline anion exchange membrane fuel cells³¹⁰ and alkaline fuel cells (AFCs);³¹¹ high-temperature solid oxide fuel cells (SOFCs),³¹² molten carbonate fuel cells (MCFCs),³¹³ direct carbon fuel cells (DCFCs),³¹⁴ and protonic ceramic fuel cells (PCFCs)³¹⁵; and enzymatic biofuel cells³¹⁶ and microbial fuel cells (MFCs).³¹⁷ Fuel cells typically have a good energy density but poor power density. For example, a new flexible PEMFC has a specific energy of **1.88 MJ/kg** but a power density of only **0.00519 MW/L** (which

³⁰⁵ The density of H₂ gas at STP is 0.08988 g/L (<https://en.wikipedia.org/wiki/Hydrogen>) and the density of O₂ gas at STP is 1.429 g/L (<https://en.wikipedia.org/wiki/Oxygen>), hence the STP volume of the H₂/O₂ mixture is $[(0.002 \text{ kg}) / (0.08988 \times 10^{-3} \text{ kg/L})] + [(0.016 \text{ kg}) / (1.429 \times 10^{-3} \text{ kg/L})] = 33.4 \text{ L}$; the STP volume of the H₂ alone is $[(0.002 \text{ kg}) / (0.08988 \times 10^{-3} \text{ kg/L})] = 22.3 \text{ L}$.

³⁰⁶ The density of liquid H₂ is 70 g/L (<https://en.wikipedia.org/wiki/Hydrogen>) and the density of liquid O₂ is 1141 g/L (<https://en.wikipedia.org/wiki/Oxygen>), hence the liquid volume of the H₂/O₂ mixture is $[(0.002 \text{ kg}) / (0.07 \text{ kg/L})] + [(0.016 \text{ kg}) / (1.141 \text{ kg/L})] = 0.0426 \text{ L}$; the liquid volume of the H₂ alone is $[(0.002 \text{ kg}) / (0.07 \text{ kg/L})] = 0.0286 \text{ L}$.

³⁰⁷ https://en.wikipedia.org/wiki/Proton_exchange_membrane_fuel_cell.

³⁰⁸ https://en.wikipedia.org/wiki/Phosphoric_acid_fuel_cell.

³⁰⁹ https://en.wikipedia.org/wiki/Solid_acid_fuel_cell.

³¹⁰ https://en.wikipedia.org/wiki/Alkaline_anion_exchange_membrane_fuel_cells.

³¹¹ https://en.wikipedia.org/wiki/Alkaline_fuel_cell.

³¹² https://en.wikipedia.org/wiki/Solid_oxide_fuel_cell.

³¹³ https://en.wikipedia.org/wiki/Molten_carbonate_fuel_cell.

³¹⁴ https://en.wikipedia.org/wiki/Direct_carbon_fuel_cell.

³¹⁵ https://en.wikipedia.org/wiki/Protonic_ceramic_fuel_cell.

³¹⁶ https://en.wikipedia.org/wiki/Enzymatic_biofuel_cell.

³¹⁷ https://en.wikipedia.org/wiki/Microbial_fuel_cell.

has been described as “amazing”),³¹⁸ while a Nissan Fuel Cell Stack for electric cars delivered $E_D = 9 \text{ MJ/L}$ but only $P_D = 0.0025 \text{ MW/L}$.³¹⁹ The specific power for just the isolated membrane electrode assembly in a PEM currently only achieves $\sim 0.1 \text{ MW/kg}$.³²⁰ Increasing power density generally reduces fuel cell efficiency.³²¹

Table 24 summarizes the specific energy (range **0.005-118 MJ/kg**)³²² and energy density (range **0.03-44 MJ/L**) for a wide variety of batteries and fuel cells, both practical/experimental and theoretical. Some limited data for both specific power (range **0.0000002-0.006 MW/kg**) and power density (range **0.000001-0.02 MW/L**) of existing systems are listed, but all are abysmally low because they are for large macroscale systems whereas power density (as noted in **Section 3.4**) can be a function of scale and refresh rate. All else equal, the smaller the system the higher the available power density but the higher the refresh rate that is required to maintain continuous power.

The application of nanotechnology to battery technology is still in its infancy, currently relying entirely on bulk-processed or self-assembled nanoscale materials.³²³ The first reported nanobattery in 1992 was a “nanometer-scale galvanic cell” that used a scanning tunneling microscope to assemble copper and silver pillars in close proximity, whereupon the copper plating solution acted as an electrolyte, causing the copper to anodically dissolve and plate onto the silver pillars – the first example of a system with a nanoscale (<70 nm) anode, cathode, and electrolyte.³²⁴ In 1999, Fendler³²⁵ used self-assembly to construct an entire thin-film lithium-ion nanoscaled battery system with a specific capacity of 1232 mA-h/gm ($\sim 4 \text{ MJ/kg}$, assuming ~ 1

³¹⁸ Ning F., *et al.* Flexible and Lightweight Fuel Cell with High Specific Power Density. ACS Nano. 2017 Jun 27;11(6):5982-5991; http://www.mscatalysis.net/my_papers/mscatalysis/2017/Flexible%20and%20Lightweight%20Fuel%20Cell%20with%20High%20Specific%20Power%20Density.pdf.

³¹⁹ Mike Hanlon, “Nissan doubles power density with new Fuel Cell Stack,” New Atlas, 13 Oct 2011; <https://newatlas.com/nissan-doubles-power-density-with-new-fuel-cell-stack/20156/>.

³²⁰ Kadyk T, Winnefeld C, Hanke-Rauschenbach R, Krewer U. Analysis and design of fuel cell systems for aviation. Energies 2018;11:375-300; <https://www.mdpi.com/1996-1073/11/2/375/pdf>.

³²¹ Benziger JB, *et al.* The power performance curve for engineering analysis of fuel cells. J Power Sources 2006;155:272-285; http://pemfc.princeton.edu/Documents/Publications/PowerPerf_2006.pdf.

³²² To convert units of MJ/kg or MJ/L to the more commonly reported units of watt-hours/kg (Wh/kg) or watt-hours/liter (Wh/L), simply multiply by $0.0036^{-1} \sim 278$.

³²³ e.g., https://en.wikipedia.org/wiki/Nanoarchitectures_for_lithium-ion_batteries and <https://en.wikipedia.org/wiki/Nanobatteries>.

³²⁴ Li W, Virtanen JA, Penner RM. A nanometer-scale galvanic cell. J Phys Chem. 1992;96:6529-6532; <http://cat.inist.fr/?aModele=afficheN&cpsid=5581104>.

³²⁵ Fendler JH. Colloid chemical approach to the construction of high energy density rechargeable lithium-ion batteries. J Dispersion Science Technol. 1999;20(1-2):13-25; <http://www.tandfonline.com/doi/abs/10.1080/01932699908943776>.

volt operation). In the early 2000s the first nanoporous alumina galvanic cells appeared, the pores filled with a polymer electrolyte and capped with various electrode materials creating arrays of individual nanobatteries with electrodes <200 nm in size, with a volumetric capacity of $45 \mu\text{A}\cdot\text{h}/\mu\text{m}\cdot\text{cm}^2$ (~**1.62 MJ/L**, assuming ~1 volt operation).³²⁶ Sakti3 reports a thin-film solid-state battery “that could leapfrog lithium-ion” with an energy density of **4.11 MJ/L**.³²⁷ Many other concepts are being tried, including a vesicle-based battery using ferrocyanide-containing polymerized 45-nm vesicles tethered to gold current collectors via disulfide bonds.³²⁸

When we can construct molecular machine systems, including fuel cells and batteries, using the techniques of atomically precise manufacturing with every structural atom fixed in exactly the right place,³²⁹ it seems conceivable that improvements in power density of up to 4-5 orders of magnitude over current macroscale systems may become possible. For example, in 1999 the author performed a simple scaling study of a glucose/O₂ fuel cell analyzing hypothetical nanoscale proton-exchange nanomembranes ~1 nm thick and ~1 nm³ pores with a central channel ~0.1 nm wide that is just wide enough to admit protons, with the resulting device estimated to provide a specific power >**200 MW/kg** and a power density on the order of ~**700 MW/L**.³³⁰ Heat management and refresh rates will become critical design issues at the high power levels available in macroscale systems composed of nanoscale power components of this caliber.

Quantum batteries³³¹ and other quantum heat engines³³² have been proposed for useful energy storage, but the ultimate efficiency of quantum systems appears to be subject to tighter

³²⁶ Vullum F, Teeters D. Investigation of lithium battery nanoelectrode arrays and their component nanobatteries. *J Power Sources* 2005 Aug 26;146(1-2):804-808; <http://www.sciencedirect.com/science/article/pii/S0378775305004994>. Vullum F, Teeters D, Nyten A, Thomas J. Characterization of lithium nanobatteries and lithium battery nanoelectrode arrays that benefit from nanostructure and molecular self-assembly. *Solid State Ionics* 2006 Oct 31;177(26-32):2833-2838; http://www.academia.edu/download/44223629/Characterization_of_lithium_nanobatterie20160330-27935-1239shz.pdf.

³²⁷ “Secretive Company Claims Battery Breakthrough.” 20 Aug 2014; <https://www.scientificamerican.com/article/secretive-company-claims-battery-breakthrough/>.

³²⁸ Stanish I, Lowy DA, Hung CW, Singh A. Vesicle-based rechargeable batteries. *Adv Mater.* 2005 Apr 25;17(9):1194-1198; <http://onlinelibrary.wiley.com/doi/10.1002/adma.200401132/full>.

³²⁹ Freitas RA Jr., Merkle RC. A Minimal Toolset for Positional Diamond Mechanochemistry. *J Comput Theor Nanosci.* 2008 May;5:760-861; <http://www.molecularassembler.com/Papers/MinToolset.pdf>. Freitas RA Jr. Chapter 6. Diamondoid Nanorobotics, in: Mavroidis C, Ferreira A, eds. *NanoRobotics: Current Approaches and Techniques*, Springer, New York, 2013; <http://www.molecularassembler.com/Papers/DiamondoidNanorobotics2013.pdf>.

³³⁰ Freitas RA Jr. *Nanomedicine, Volume I: Basic Capabilities*, Landes Bioscience, Georgetown TX, 1999, p. 153; <http://www.nanomedicine.com/NMI/6.3.4.5.htm#p8>.

³³¹ Campaioli F, Pollock FA, Binder FC, Céleri LC, Goold J, Vinjanampathy S, Modi K. Enhancing the charging power of quantum batteries. *Phys Rev Lett.* 2017 Apr 14;118(15):150601; <https://arxiv.org/pdf/1612.04991>.

fundamental limits than those imposed by the second law of thermodynamics which governs the efficiency of classical systems.³³³

³³² Klatzow J, Becker JN, Ledingham PM, Weinzetl C, Kaczmarek KT, Saunders DJ, Nunn J, Walmsley IA, Uzdin R, Poem E. Experimental demonstration of quantum effects in the operation of microscopic heat engines. Phys Rev Lett 2019; <https://arxiv.org/pdf/1710.08716.pdf>.

³³³ Abah O, Lutz E. Energy efficiency quantum machines. Europhys Lett. 2017 Jul 26;118(4):40005; <http://iopscience.iop.org/article/10.1209/0295-5075/118/40005>.

Table 24. Specific energy, energy density, specific power and power density for batteries and fuel cells (theoretical systems indicated in red)

Battery or Fuel Cell Type	Specific Energy (MJ/kg)	Energy Density (MJ/L)	Specific Power (MW/kg)	Power Density (MW/L)
Hydrogen-oxygen fuel cell (theoretical) (excl. oxygen) ³³⁴	118.6	8.29		
Lithium-fluorine battery (theoretical) (excl. fluorine) ³³⁵	82.1	43.80		
Lithium-air battery (theoretical) (excl. oxygen) ³³⁶	40.1			
Silicon-air battery (theoretical) (excl. oxygen) ³³⁷	32.5	7.59		
Aluminum-air battery (theoretical) (excl. oxygen) ³³⁸	29.3			
Germanium-air battery (theoretical) (excl. oxygen) ³³⁹	28.3			
Magnesium-air battery (theoretical) (excl. oxygen) ³⁴⁰	23.3			
Tin-air @ 1000 K battery (theoretical) (excl. oxygen) ³⁴¹	22.5			
Lithium-fluorine battery (theoretical) ³⁴²	22.0	25.10		
Lithium-air battery (theoretical) (w/oxygen) ³⁴³	18.8	37.80		
Aluminum-air battery (theoretical) (w/oxygen) ³⁴⁴	15.5			
Silicon-air battery (theoretical) (w/oxygen) ³⁴⁵	15.2			
Calcium-air battery (theoretical) (excl. oxygen) ³⁴⁶	15.0			
Hydrogen-oxygen fuel cell (theoretical) (w/oxygen) ³⁴⁷	13.2	5.57		
Calcium-air battery (theoretical) (w/oxygen) ³⁴⁸	10.8			
Magnesium-air battery (theoretical) (w/oxygen) ³⁴⁹	10.0			
Lithium-sulfur battery (theoretical) ³⁵⁰	9.18	10.30		
Sodium-air battery (theoretical) (excl. oxygen) ³⁵¹	8.14			

³³⁴ See discussion in text.

³³⁵ See discussion in text.

³³⁶ https://en.wikipedia.org/wiki/Metal-air_electrochemical_cell#Types.

³³⁷ https://en.wikipedia.org/wiki/Metal-air_electrochemical_cell#Types and https://en.wikipedia.org/wiki/Silicon-air_battery#Storage.

³³⁸ Theoretical specific energy 6000-8000 Wh/kg; https://en.wikipedia.org/wiki/Aluminium-air_battery; and https://en.wikipedia.org/wiki/Metal-air_electrochemical_cell#Types.

³³⁹ https://en.wikipedia.org/wiki/Metal-air_electrochemical_cell#Types.

³⁴⁰ https://en.wikipedia.org/wiki/Metal-air_electrochemical_cell#Types.

³⁴¹ https://en.wikipedia.org/wiki/Metal-air_electrochemical_cell#Types.

³⁴² See discussion in text.

³⁴³ https://en.wikipedia.org/wiki/Metal-air_electrochemical_cell#Types; <http://science.sciencemag.org/content/sci/361/6404/777.full.pdf>.

³⁴⁴ https://en.wikipedia.org/wiki/Metal-air_electrochemical_cell#Types.

³⁴⁵ https://en.wikipedia.org/wiki/Metal-air_electrochemical_cell#Types.

³⁴⁶ https://en.wikipedia.org/wiki/Metal-air_electrochemical_cell#Types.

³⁴⁷ See discussion in text.

³⁴⁸ https://en.wikipedia.org/wiki/Metal-air_electrochemical_cell#Types.

³⁴⁹ https://en.wikipedia.org/wiki/Metal-air_electrochemical_cell#Types.

³⁵⁰ "Lithium Sulfur Rechargeable battery Data Sheet," Sion Power, 3 Oct 2008; <http://www.sionpower.com/pdf/articles/LIS%20Spec%20Sheet%2010-3-08.pdf>.

³⁵¹ https://en.wikipedia.org/wiki/Metal-air_electrochemical_cell#Types.

Iron-air battery (theoretical) (excl. oxygen) ³⁵²	7.36			
Aluminum-air battery (projected) ³⁵³	7.20			
Lithium-air battery (practical) ³⁵⁴	6.48	5.76		
Strontium-fluorine battery (theoretical) ³⁵⁵	6.29	15.70		
Magnesium/sulfur battery (theoretical) ³⁵⁶	6.20			
Potassium-air battery (theoretical) (excl. oxygen) ³⁵⁷	6.12			
Sodium-air battery (theoretical) (w/oxygen) ³⁵⁸	6.04			
Germanium-air battery (theoretical) (w/oxygen) ³⁵⁹	5.33			
Iron-air battery (theoretical) (w/oxygen) ³⁶⁰	5.15			
Hydrogen-lithium chlorate flow battery ³⁶¹	5.04			
Zinc-air battery (theoretical) (excl. oxygen) ³⁶²	4.93			
Aluminum/sulfur battery (theoretical) ³⁶³	4.82			
Aluminum-air battery (practical) ³⁶⁴	4.68		0.000200	
Lithium-ion seawater battery ³⁶⁵	4.68			
URI 1418Ah replaceable anode aluminum-air battery ³⁶⁶	4.68		0.000130	
Zinc-air battery (theoretical) (w/oxygen) ³⁶⁷	3.92			
Aluminum-ion battery ³⁶⁸	3.82			
Vanadium pentoxide borate powder battery ³⁶⁹	3.60			
Innolith inorganic rechargeable lithium battery ³⁷⁰	3.60			
Potassium-air battery (theoretical) (w/oxygen) ³⁷¹	3.37			

³⁵² https://en.wikipedia.org/wiki/Metal-air_electrochemical_cell#Types.

³⁵³ The design battery energy density is 2000 Wh/kg (projected). Yang S, Knickle H. Design and analysis of aluminum/air battery system for electric vehicles. J Power Sources 2002 Oct 24;112(1):162-173; <http://www.sciencedirect.com/science/article/pii/S0378775302003701>.

³⁵⁴ https://en.wikipedia.org/wiki/Lithium-air_battery and https://en.wikipedia.org/wiki/Lithium_battery.

³⁵⁵ See discussion in text.

³⁵⁶ https://en.wikipedia.org/wiki/Magnesium_battery#Secondary_cells.

³⁵⁷ https://en.wikipedia.org/wiki/Metal-air_electrochemical_cell#Types.

³⁵⁸ https://en.wikipedia.org/wiki/Metal-air_electrochemical_cell#Types.

³⁵⁹ https://en.wikipedia.org/wiki/Metal-air_electrochemical_cell#Types.

³⁶⁰ https://en.wikipedia.org/wiki/Metal-air_electrochemical_cell#Types and

https://en.wikipedia.org/wiki/Metal-air_electrochemical_cell#Iron-air.

³⁶¹ https://en.wikipedia.org/wiki/Flow_battery#Chemistries.

³⁶² https://en.wikipedia.org/wiki/Zinc-air_battery and https://en.wikipedia.org/wiki/Metal-air_electrochemical_cell#Types.

³⁶³ https://en.wikipedia.org/wiki/Aluminium-ion_battery#University_of_Maryland.

³⁶⁴ The design battery energy density is 1300 Wh/kg (present). Yang S, Knickle H. Design and analysis of aluminum/air battery system for electric vehicles. J Power Sources 2002 Oct 24;112(1):162-173; <http://www.sciencedirect.com/science/article/pii/S0378775302003701>. Specific power is 200 W/kg; https://en.wikipedia.org/wiki/Aluminium-air_battery.

³⁶⁵ https://en.wikipedia.org/wiki/Research_in_lithium-ion_batteries#Seawater.

³⁶⁶ https://en.wikipedia.org/wiki/Power-to-weight_ratio#.28Closed_cell.29_batteries.

³⁶⁷ https://en.wikipedia.org/wiki/Metal-air_electrochemical_cell#Types.

³⁶⁸ https://en.wikipedia.org/wiki/Aluminium-ion_battery#Oak_Ridge_National_Laboratory.

³⁶⁹ https://en.wikipedia.org/wiki/Research_in_lithium-ion_batteries#Disordered_materials.

³⁷⁰ "Innolith energy technology brings 1000 km EV within range," Innolith AG, 4 Apr 2019; <https://innolith.com/innolith-energy-technology-brings-1000km-ev-within-range/>.

Tin-air @ 1000 K battery (theoretical) (w/oxygen) ³⁷²	3.10			
Lithium-carbon monofluoride battery ³⁷³	2.81	5.32	0.000080	0.000151
Hydrogen-lithium bromate flow battery ³⁷⁴	2.70			
Lithium-thionyl chloride battery ³⁷⁵	2.52	4.32		
Smart Fuel Cell Jenny 1200 50W DMFC + M5 Fuel Cartridge ³⁷⁶	2.37	1.36	0.000007	0.000004
Sugar biobattery @ 1 volt ³⁷⁷	2.15			
Thin film lithium manganese oxide (battery cathode material) ³⁷⁸	2.13			
Thin film lithium cobalt oxide (battery cathode material) ³⁷⁹	2.09			
Thin film lithium iron phosphate (battery cathode material) ³⁸⁰	2.08			
Lithium sulfur battery ³⁸¹	1.80	1.26		
Lithium battery (nonrechargeable) ³⁸²	1.80	4.32		
Zinc-air battery (practical) ³⁸³	1.69	6.02	0.000100	0.000356
NanoFlowCell redox flow cell electrolyte (for electric car) ³⁸⁴	1.66	2.16		
Energizer 675 Mercury Free Zinc-air battery ³⁸⁵	1.64	6.25	0.000004	0.000014
Sodium-ion (battery cathode material) ³⁸⁶	1.44			
Lithium-thionyl chloride with bromine chloride battery ³⁸⁷	1.26	2.77		

³⁷¹ https://en.wikipedia.org/wiki/Metal-air_electrochemical_cell#Types.

³⁷² https://en.wikipedia.org/wiki/Metal-air_electrochemical_cell#Types. See also: HyungKuk J, Jaeyoung L. High-temperature liquid Sn-air energy storage cell. *J Energy Chem.* 2015 Sep;24(5):614-619; <http://www.sciencedirect.com/science/article/pii/S2095495615000534>.

³⁷³ https://en.wikipedia.org/wiki/Comparison_of_battery_types.

³⁷⁴ https://en.wikipedia.org/wiki/Flow_battery#Chemistries.

³⁷⁵ https://en.wikipedia.org/wiki/Lithium_battery.

³⁷⁶ “Smart Fuel Cell Jenny 1200 50W DMFC fuel cell (Direct Methane Fuel Cell),” http://www.sfc-defense.com/sites/default/files/160530_produktdatenblatt_jenny_1200_en_online.pdf. Data: 4.32 MJ charging capacity/day = 50 W; 50 W x 100 hr x 3600 sec/hr = 18 MJ; mass = 7.6 kg, volume = 13.24 L; therefore 2.37 MJ/kg, 1.36 MJ/L, 6.58 W/kg, 3.78 W/L.

³⁷⁷ Sugar biobattery has a storage density of 596 ampere-hours/kg; ~1 volt implies 596 Wh/kg = 2.15 MJ/kg. Zhu Z, *et al.* A high-energy-density sugar biobattery based on a synthetic enzymatic pathway. *Nat Commun.* 2014 Jan 21;5:3026; <https://www.nature.com/articles/ncomms4026>.

³⁷⁸ https://en.wikipedia.org/wiki/Thin_film_lithium-ion_battery#Cathode_materials.

³⁷⁹ https://en.wikipedia.org/wiki/Thin_film_lithium-ion_battery#Cathode_materials.

³⁸⁰ https://en.wikipedia.org/wiki/Thin_film_lithium-ion_battery#Cathode_materials.

³⁸¹ https://en.wikipedia.org/wiki/Lithium-sulfur_battery.

³⁸² https://en.wikipedia.org/wiki/Energy_density#Energy_densities_of_common_energy_storage_materials.

³⁸³ https://en.wikipedia.org/wiki/Zinc-air_battery.

³⁸⁴ bi-ION dual-electrolyte flow cell for the Quant 48 Volt electric car; electrolyte energy density 600 W-hr/liter (<https://nanoflowcell.com/what-we-do/innovation-research/bi-ion/>); “ionic liquid” electrolyte with organic and inorganic salts dissolved in water, density assumed ~1.3 kg/L.

³⁸⁵ “ENERGIZER 675 size - Mercury Free Product Datasheet,” <http://data.energizer.com/pdfs/675.pdf>. Data: 1.4 V x 0.620 amp-hours x 3600 sec/hr = 3125 J; service time = 125 hours = 450,000 sec, which implies 0.00694 W; mass = 1.9 gm, so 3125 J / 0.0019 kg = 1.64 MJ/kg and 0.00694 W / 0.0019 kg = 3.65 W/kg; volume = 0.0005 L, so 3125 J / 0.0005 L = 6.25 MJ/L, and 0.00694 W / 0.0005 L = 13.9 W/L.

³⁸⁶ https://en.wikipedia.org/wiki/Sodium-ion_battery.

³⁸⁷ https://en.wikipedia.org/wiki/Lithium_battery.

Planar sodium-nickel chloride battery ³⁸⁸	1.26			
Sion Power 2.5Ah Li-S Lithium-ion battery ³⁸⁹	1.26	0.86	0.000053	0.000036
Lithium-sulfuryl chloride battery ³⁹⁰	1.19	2.59		
Lithium-manganese dioxide battery ³⁹¹	1.19	2.60	0.000400	0.000874
Lithium-iron disulfide battery ³⁹²	1.07	2.10		
Molten salt battery (generally) ³⁹³	1.04	0.58	0.000220	0.000122
Lithium polymer battery ³⁹⁴	0.95	2.63		
Lithium-ion battery ³⁹⁵	0.95	2.43	0.000340	0.000867
Lithium-vanadium pentoxide battery ³⁹⁶	0.94	2.38		
Lithium-sulfur dioxide battery ³⁹⁷	0.90	1.44		
Electric Fuel Battery Corp. BA-8180/U Zinc-air battery ³⁹⁸	0.90	0.70	0.000009	0.000007
Lithium-carbon dioxide battery (est.) ³⁹⁹	0.81		0.00045	
Lithium nickel cobalt aluminum oxide battery ⁴⁰⁰	0.79	2.20		
Tesla Model 3 battery (for electric car) ⁴⁰¹	0.75			

³⁸⁸ Planar sodium-nickel chloride batteries can be operated at an intermediate temperature of 190 °C with ultra-high energy density. A specific energy density of 350 Wh kg⁻¹, higher than that of conventional tubular sodium–nickel chloride batteries (280 °C), is obtained for planar sodium-nickel chloride batteries operated at 190 °C over long-term cell test (1,000 cycles), which implies 350 watt-hours/kg = 1.26 MJ/kg. Guosheng L, *et al.* Advanced intermediate temperature sodium–nickel chloride batteries with ultra-high energy density. *Nat Commun.* 2016;7:10683; <https://www.nature.com/articles/ncomms10683>.

³⁸⁹ “Lithium Sulfur Rechargeable Battery Data Sheet,” 3 Oct 2008; <http://web.archive.org/web/20140202101643/http://sionpower.com/pdf/articles/LIS%20Spec%20Sheet%2010-3-08.pdf>. Data: 350 Wh/kg = 1.26 MJ/kg; 0.016 kg x 1.26 MJ/kg = 0.0202 MJ capacity; volume = 55 mm x 37 mm x 11.5 mm = 0.0234L, so 0.0202 MJ / 0.0234L = 0.863 MJ/L; discharge time = 400 min = 24,000 sec, so 0.0202 MJ / 24,000 sec = 0.842 W; therefore 0.842 W / 0.016 kg = 52.6 W/kg and 0.842 W / 0.0234L = 36.0 W/L.

³⁹⁰ https://en.wikipedia.org/wiki/Lithium_battery.

³⁹¹ https://en.wikipedia.org/wiki/Comparison_of_battery_types.

³⁹² https://en.wikipedia.org/wiki/Comparison_of_battery_types.

³⁹³ https://en.wikipedia.org/wiki/Molten_salt_battery.

³⁹⁴ https://en.wikipedia.org/wiki/Lithium_polymer_battery.

³⁹⁵ https://en.wikipedia.org/wiki/Lithium-ion_battery.

³⁹⁶ https://en.wikipedia.org/wiki/Lithium_battery.

³⁹⁷ https://en.wikipedia.org/wiki/Lithium_battery.

³⁹⁸ “EFB Zinc Air Batteries: Electric Fuel Battery Corp. BA-8180/U Zinc-air battery,” <http://www.efbpower.com/userfiles/Sheet-Batteries%20and%20Chargers%20Chart.pdf>. Data: 56 amp-hr x 3600 sec/hr x 12V = 2.42 MJ; max current = 2 amp, so 56 amp-hr/2 amp = 28 hours = 100,800 sec, which implies 24.01 W; mass = 2.7 kg and volume = 31.0 x 18.5 x 6.0 cm = 3.441 L; therefore 0.896 MJ/kg, 0.703 MJ/L, 8.89 W/kg, 6.98 W/L.

³⁹⁹ Qiao Y, Yi J, Wu S, Liu Y, Yang S, He P, Zhou H. Li-CO₂ Electrochemistry: A New Strategy for CO₂ Fixation and Energy Storage. *Joule* 2017 Oct 11;1:359-370; [https://www.cell.com/joule/pdf/S2542-4351\(17\)30008-9.pdf](https://www.cell.com/joule/pdf/S2542-4351(17)30008-9.pdf).

⁴⁰⁰ https://en.wikipedia.org/wiki/Comparison_of_battery_types.

⁴⁰¹ “Tesla Model 3 Battery Cell Has World’s Highest Energy Density,” 3 May 2018; <https://insideevs.com/tesla-claims-model-3-battery-has-highest-energy-density-of-any-electric-car/>

Lithium nickel manganese cobalt oxide battery ⁴⁰²	0.74	2.10		
Lithium cobalt oxide battery ⁴⁰³	0.70	2.00		
Alkaline battery ⁴⁰⁴	0.68	1.56	0.000050	0.000115
Panasonic CGA103450A 1.95Ah LiCoO ₂ Lithium-ion battery ⁴⁰⁵	0.67	1.44	0.000035	0.000076
EFB Corp. 120 Ah Zinc–air fuel cell for underwater propulsion ⁴⁰⁶	0.63		0.000500	
MR2791 Rechargeable Lithium-Ion Military Battery ⁴⁰⁷	0.62	0.95	0.000023	0.000035
ClaytonPower 400Ah Lithium-ion battery ⁴⁰⁸	0.62		0.000086	
Saft 45E Fe Super-Phosphate Lithium iron phosphate battery ⁴⁰⁹	0.56	1.05	0.000177	0.000332
Lithium manganese oxide battery ⁴¹⁰	0.54	1.50		
Sodium-sulfur battery ⁴¹¹	0.54			
LG Chemical/CPI E2 6Ah LiMn ₂ O ₄ Li-ion polymer battery ⁴¹²	0.53	0.96	0.000071	0.000129
LG Chemical/CPI E2 6Ah LiMn ₂ O ₄ Li-ion polymer battery ⁴¹³	0.51	0.93	0.000138	0.000249

⁴⁰² https://en.wikipedia.org/wiki/Comparison_of_battery_types.

⁴⁰³ https://en.wikipedia.org/wiki/Comparison_of_battery_types.

⁴⁰⁴ https://en.wikipedia.org/wiki/Comparison_of_battery_types.

⁴⁰⁵ “LITHIUM ION BATTERIES: INDIVIDUAL DATA SHEET CGA103450A: Prismatic Model,” https://web.archive.org/web/20090327125952/http://www.panasonic.com/industrial/battery/oem/images/pdf/Panasonic_LiIon_CGA103450A.pdf. Data: standard current 0.370 amp, voltage 3.7 V, power = 1.37 W; capacity 1.95 amp-hours @ 3.7 V = 25,974 J; mass = 0.039 kg and volume = 34 mm x 50 mm x 10.6 mm = 18,020 mm³ = 0.01802 L; therefore 0.666 MJ/kg, 1.44 MJ/L, 35.1 W/kg, 76.0 W/L.

⁴⁰⁶ “EFB Corp. 120Ah Zinc–air fuel cell for underwater propulsion,” <http://www.efbpower.com/userfiles/UVS02.pdf>. Data: 175 Wh/kg = 0.63 MJ/kg, 500 W/kg.

⁴⁰⁷ “EFB - MR2791 Rechargeable Lithium - Ion Military Battery,” <http://www.efbpower.com/userfiles/MR2791-Spec-Sheet.pdf>. Data: 222 Wh = 799200 J, or 14.8V x 15 amp-hr x 3600 sec/hr = 799200 J; capacity = 15 amp-hr @ 2 amps = 7.5 hours; 799200 J / 7.5 hours = 29.6 W; mass = 1.28 kg, volume = 186.2 mm x 69.5 mm x 65.0 mm = 841,159 mm³ = 0.841 L; therefore 0.624 MJ/kg, 0.950 MJ/L, 23.1 W/kg, 35.2 W/L.

⁴⁰⁸ https://en.wikipedia.org/wiki/Power-to-weight_ratio#28Closed_cell.29_batteries.

⁴⁰⁹ Saft 45E Fe Super-Phosphate Lithium iron phosphate battery; <http://web.archive.org/web/20120312075212/http://www.saftbatteries.com/doc/Documents/defence/Cube769/VL45EFe.e3741a09-74fd-4df4-8687-12997f445ef5.pdf>. Data: 3.3V x 44 amp-hr x 3600 sec/hr = 0.523 MJ, but use 140 Wh = 0.504 MJ; 44 amp-hr / 50 amp = 0.88 hr = 3168 sec; 0.504 MJ / 3168 sec = 159.1 W; mass = 0.9 kg and volume = 0.48 L; therefore 0.56 MJ/kg, 1.05 MJ/L, 177 W/kg, 331 W/L.

⁴¹⁰ https://en.wikipedia.org/wiki/Comparison_of_battery_types.

⁴¹¹ https://en.wikipedia.org/wiki/Rechargeable_battery#Experimental_types.

⁴¹² “LG Chemical/CPI E2 6Ah LiMn₂O₄ Lithium-ion polymer battery,” [http://web.archive.org/web/20130421061814/http://www.lgchem.com/upload/02_Ko/e2%20cell%20specsheet\(6ah\).pdf](http://web.archive.org/web/20130421061814/http://www.lgchem.com/upload/02_Ko/e2%20cell%20specsheet(6ah).pdf). Data: 3.8V x 6.2 Ah x 3600 sec/hr = 84,816 J; draws 3 amp, so 6.2 Ah/3A = 2.07 hr = 7440 sec, and 84,816 J / 7440 sec = 11.4 W; mass = 0.160 kg and volume = 4.7 x 93.6 x 201.5 mm = 0.0886 L; therefore 0.530 MJ/kg, 0.957 MJ/L, 71.3 W/kg, 129 W/L.

Silver-oxide battery ⁴¹⁴	0.47	1.80		
Energizer 522 Prismatic Zn-MnO ₂ Alkaline battery ⁴¹⁵	0.44	0.96	0.000005	0.000011
Mercury oxide-zinc battery ⁴¹⁶	0.44	1.80		
Lithium iron phosphate battery ⁴¹⁷	0.40	0.79	0.000200	0.000400
Lithium-titanate battery ⁴¹⁸	0.40	0.64		
GE Durathon™ NaMx Type A2 UPS Molten salt battery ⁴¹⁹	0.39	0.69	0.000016	0.000028
A123 Systems 26650 Cell 2.3Ah LiFePO ₄ Lithium ion battery ⁴²⁰	0.39	0.75	0.000047	0.000091
Nickel-zinc battery ⁴²¹	0.36	1.01	0.003000	0.008400
Nickel-metal hydride battery ⁴²²	0.36	1.44	0.001000	0.004000
Panasonic BK450A 4.5Ah Nickel-metal hydride battery ⁴²³	0.32	1.11		
A123 Systems 26650 Cell 2.3Ah LiFePO ₄ Lithium ion battery ⁴²⁴	0.31	0.59	0.001471	0.002841

⁴¹³ “LG Chemical/CPI E2 6Ah LiMn₂O₄ Lithium-ion polymer battery,”
[http://web.archive.org/web/20130421061814/http://www.lgchem.com/upload/02_Ko/e2%20cell%20specsheet\(6ah\).pdf](http://web.archive.org/web/20130421061814/http://www.lgchem.com/upload/02_Ko/e2%20cell%20specsheet(6ah).pdf). Data: 3.8V x 6.0 Ah x 3600 sec/hr = 82,080 J; draws 6 amp, so 6.2 Ah/3A = 1.03 hr = 3720 sec, and 82,080 J / 3720 sec = 22.06 W; mass = 0.160 kg and volume = 4.7 x 93.6 x 201.5 mm = 0.0886 L; therefore 0.513 MJ/kg, 0.926 MJ/L, 138 W/kg, 249 W/L.

⁴¹⁴ https://en.wikipedia.org/wiki/Silver-oxide_battery.

⁴¹⁵ “Energizer 522 Prismatic Zn–MnO₂ Alkaline battery,” <http://data.energizer.com/PDFs/522.pdf>. Data: 9V, 0.0456 kg, 0.0211 L; @ 0.025A: 9V x 0.625 Ah x 3600 sec/hr = 20250 J; 0.625 Ah/.025 A = 25 hr = 90000 sec; 20250 J / 90000 sec = 0.225 W; therefore 0.444 MJ/kg, 0.960 MJ/L, 4.93 W/kg, 10.7 W/L.

⁴¹⁶ https://en.wikipedia.org/wiki/Comparison_of_battery_types.

⁴¹⁷ https://en.wikipedia.org/wiki/Lithium_iron_phosphate_battery.

⁴¹⁸ https://en.wikipedia.org/wiki/Lithium-titanate_battery.

⁴¹⁹ “GE Durathon™ NaMx Type A2 UPS Molten salt battery,”
<http://web.archive.org/web/20160304110120/http://www.personal.psu.edu/klm5709/plugin-GE-NaMx-Batteries-ss.pdf>. Data: stored energy 24.8 kWh = 102.24 MJ; 6 hr discharge at 456 Ah implies 76 amps, 54.2 V x 76 amps = 4119 W; mass = 260 kg, volume = 320 x 530 x 870 mm = 147.5 L (0.147 m³); therefore 0.393 MJ/kg, 0.693 MJ/L, 15.8 W/kg, 27.9 W/L.

⁴²⁰ “A123 Systems 26650 Cell 2.3Ah LiFePO₄ Lithium ion battery,”
https://web.archive.org/web/20100601144233/http://www.a123systems.com/cms/product/pdf/1/_ANR26650M1A.pdf. Data: 3.3V x 2.3 Ah x 3600 sec/hr = 27,324 J; 1A discharge implies 2.3 hr = 8280 sec implies 3.3 W; mass = 0.070 kg, volume = 26.62 mm diam x 65.15 mm tall = 36,259 mm³ = 0.0363 L; therefore 0.390 MJ/kg, 0.753 MJ/L, 47.1 W/kg, 90.9 W/L.

⁴²¹ https://en.wikipedia.org/wiki/Nickel-zinc_battery.

⁴²² https://en.wikipedia.org/wiki/Nickel-metal_hydride_battery.

⁴²³ Panasonic BK450A 4.5Ah Nickel–metal hydride battery,
<https://na.industrial.panasonic.com/sites/default/pidsa/files/downloads/files/battery-energy-catalog.pdf>. Data: 1.2V x 4.5 Ah x 3600 sec/hr = 19,440 J; mass = 0.060 kg, volume = 18.2 mm diam x 67.5 mm length = 0.01756 L; therefore 0.324 MJ/kg, 1.105 MJ/L.

⁴²⁴ “A123 Systems 26650 Cell 2.3Ah LiFePO₄ Lithium ion battery,”
https://web.archive.org/web/20100601144233/http://www.a123systems.com/cms/product/pdf/1/_ANR26650M1A.pdf. Data: 2.7V x 2.2 Ah x 3600 sec/hr = 21384 J; 40A discharge implies 0.0575 hr = 207 sec implies 103 W; mass = 0.070 kg, volume = 26.62 mm diam x 65.15 mm tall = 36,259 mm³ = 0.0363 L; therefore 0.305 MJ/kg, 0.589 MJ/L, 1471 W/kg, 2837 W/L.

Ionix Power Systems LiMn ₂ O ₄ Lithium-ion lab model battery ⁴²⁵	0.27		0.001700	
Nickel-hydrogen battery ⁴²⁶	0.27	0.22	0.000220	0.000176
Toshiba SCiB cell 4.2Ah Li ₂ TiO ₃ Lithium-ion battery cell ⁴²⁷	0.24	0.47	0.000400	0.000783
Saft VL 6Ah Lithium-ion battery ⁴²⁸	0.23	0.50	0.006324	0.013435
Nickel-cadmium battery ⁴²⁹	0.22	0.54	0.000150	0.000375
Energizer 522 Prismatic Zn-MnO ₂ Alkaline battery ⁴³⁰	0.21	0.46	0.000099	0.000214
Zinc-bromine battery ⁴³¹	0.19	0.14		
Toshiba SCiB cell 4.0Ah Li ₂ TiO ₃ Lithium-ion battery pack ⁴³²	0.17	0.23	0.000096	0.000127
Lead-acid battery ⁴³³	0.15	0.40	0.000180	0.000472
Energizer CH35 C 1.8Ah Nickel-cadmium battery ⁴³⁴	0.14	0.29	0.000008	0.000016
Firefly Energy Oasis FF12D1-G31 6-cell 105Ah VRLA battery ⁴³⁵	0.14		0.000004	

⁴²⁵ “Ionix Power Systems LiMn₂O₄ Lithium-ion lab model battery,”
http://web.archive.org/web/20130307031336/http://www.ionixpower.com/lithium_ion_battery.htm. Data: 1700 W/kg, delivers 75 Wh/kg = 0.270 MJ/kg.

⁴²⁶ https://en.wikipedia.org/wiki/Nickel-hydrogen_battery and
https://en.wikipedia.org/wiki/Comparison_of_battery_types.

⁴²⁷ “Toshiba SCiB cell 4.2Ah Li₂TiO₃ Lithium-ion battery pack,”
<http://web.archive.org/web/20120312013930/http://www.scib.jp/en/product/spec.htm>. Data: 2.4V x 4.2 Ah x 3600 sec/hr = 36,288 J; max discharge current = 25 amps implies 4.2 Ah / 25 A = 0.168 hr = 605 sec, 36,288 J / 605 sec = 60.0 W; mass = 0.150 kg, volume = 62 x 95 x 13 mm = 0.07657 L; therefore 0.242 MJ/kg, 0.474 MJ/L, 400 W/kg, 784 W/L.

⁴²⁸ Saft VL 6Ah Lithium-ion battery
http://web.archive.org/web/20120312075223/http://www.saftbatteries.com/doc/Documents/defence/Cube769/VL6A_data_sheet.9ea09188-84ad-4c54-989b-a2206dc28da2.pdf stores 79.2 kJ, continuous power output 2150 W, mass 0.34 kg, volume 0.16 L, which yields 0.233 MJ/kg, 0.495 MJ/L, 6324 W/kg, and 0.0134 MW/L.

⁴²⁹ https://en.wikipedia.org/wiki/Nickel-cadmium_battery.

⁴³⁰ “Energizer 522 Prismatic Zn–MnO₂ Alkaline battery,” <http://data.energizer.com/PDFs/522.pdf>. Data: 9V, 0.0456 kg, 0.0211 L; @ 0.500A: 9V x 0.300 Ah x 3600 sec/hr = 9720 J; 0.300 Ah/.5 A = 0.6 hr = 2160 sec; 9720 J / 2160 sec = 4.5 W; therefore 0.213 MJ/kg, 0.461 MJ/L, 98.7 W/kg, 213 W/L.

⁴³¹ https://en.wikipedia.org/wiki/Zinc-bromine_battery.

⁴³² “Toshiba SCiB cell 4.2Ah Li₂TiO₃ Lithium-ion battery pack,”
<http://web.archive.org/web/20120312013930/http://www.scib.jp/en/product/spec.htm>. Data: 12V x 4.0 Ah x 3600 sec/hr = 172,800 J; continuous discharge current = 8.0 A implies 4.0 Ah / 8.0 A = 0.5 hr = 1800 sec, 172,800 J / 1800 sec = 96 W; mass = 1.0 kg, volume = 145 x 109 x 48 mm = 0.7586 L; therefore 0.1728 MJ/kg, 0.228 MJ/L, 96 W/kg, 127 W/L.

⁴³³ https://en.wikipedia.org/wiki/Lead-acid_battery.

⁴³⁴ “Energizer CH35 C 1.8Ah Nickel–cadmium battery,” <http://data.energizer.com/PDFs/CH35.pdf>. Data: 1.2V x 1.8 Ah x 3600 sec/hr = 7776 J; 360 mA discharge rate implies 1800 mAh / 360 mA = 5 hr = 18,000 sec, 7776 J / 18,000 sec = 0.432 W; mass = 0.054 kg, volume = 0.0269 L; therefore 0.144 MJ/kg, 0.289 MJ/L, 8 W/kg, 16.1 W/L.

Zinc-carbon “dry cell” battery ⁴³⁶	0.13	0.33	0.000027	0.000069
Nickel-iron battery ⁴³⁷	0.09	0.45	0.000100	0.000500
Vanadium-vanadium sulfate flow battery ⁴³⁸	0.08	0.09		
Vanadium-vanadium bromide flow battery ⁴³⁹	0.08	0.18		
Vanadium redox battery ⁴⁴⁰	0.07	0.09		
Stanford Prussian Blue durable potassium-ion battery ⁴⁴¹	0.05		0.000693	
Ionix Power Systems LiMn ₂ O ₄ Lithium-ion lab model battery ⁴⁴²	0.03		0.004900	
Firefly Energy Oasis FF12D1-G31 6-cell 105Ah VRLA battery ⁴⁴³	0.01		0.000300	
Firefly Energy Oasis FF12D1-G31 6-cell 105Ah VRLA battery ⁴⁴⁴	0.01		0.000234	
Penny battery ⁴⁴⁵	0.005	0.03	0.0000002	0.000001
Flexible air-breathing PEMFC (fuel cell) ⁴⁴⁶			0.00223	0.00519

⁴³⁵ “Firefly Energy Oasis FF12D1-G31 6-cell 105Ah VRLA battery,” <http://fireflyenergy.com/products/12v-g31-battery/>; data originally from <http://www.fireflyenergy.com/images/stories/pdfs/Group%2031%20Spec%20Sheet%20REV%20-%20110909.pdf>.

⁴³⁶ https://en.wikipedia.org/wiki/Zinc-carbon_battery.

⁴³⁷ https://en.wikipedia.org/wiki/Nickel-iron_battery and https://en.wikipedia.org/wiki/Comparison_of_battery_types.

⁴³⁸ https://en.wikipedia.org/wiki/Flow_battery#Chemistries.

⁴³⁹ https://en.wikipedia.org/wiki/Flow_battery#Chemistries.

⁴⁴⁰ https://en.wikipedia.org/wiki/Vanadium_redox_battery.

⁴⁴¹ Pasta M, *et al.* Full open-framework batteries for stationary energy storage. Nat Commun 2014 Jan 6;5:3007; <http://www.nature.com/articles/ncomms4007>.

⁴⁴² “Ionix Power Systems LiMn₂O₄ Lithium-ion lab model battery,” http://web.archive.org/web/20130307031336/http://www.ionixpower.com/lithium_ion_battery.htm. Data: 4900 W/kg, delivers 8.1 Wh/kg = 0.0292 MJ/kg.

⁴⁴³ “Firefly Energy Oasis FF12D1-G31 6-cell 105Ah VRLA battery,” <http://fireflyenergy.com/products/12v-g31-battery/>; data originally from <http://www.fireflyenergy.com/images/stories/pdfs/Group%2031%20Spec%20Sheet%20REV%20-%20110909.pdf>.

⁴⁴⁴ “Firefly Energy Oasis FF12D1-G31 6-cell 105Ah VRLA battery,” <http://fireflyenergy.com/products/12v-g31-battery/>; data originally from <http://www.fireflyenergy.com/images/stories/pdfs/Group%2031%20Spec%20Sheet%20REV%20-%20110909.pdf>.

⁴⁴⁵ “Penny battery” (https://en.wikipedia.org/wiki/Penny_battery#Energy), aka. a “voltaic pile”: 5 pennies @ 0.0005 watts and 0.6 volts, over duration of 6.5 hours (23,400 sec) implies energy of 11.7 J. From [https://en.wikipedia.org/wiki/Penny_\(United_States_coin\)](https://en.wikipedia.org/wiki/Penny_(United_States_coin)), one penny weighs 2.5 gm and has a volume of $\pi(19.05\text{ mm})^2(1.62\text{ mm}) = 461.7\text{ mm}^3 = 4.617 \times 10^{-4}\text{ L}$, hence: 4680 J/kg, 25.3 kJ/L, 0.2 W/kg, 1.08 W/L.

⁴⁴⁶ Julien Happich, “Thin flexible fuel cell ha record specific volume power density,” EE News Europe, 20 Jun 2017; <http://www.eenewseurope.com/news/thin-flexible-fuel-cell-has-record-specific-volume-power-density>.

4.2 Chemical Fuels and High-Energy Materials

Chemical fuels⁴⁴⁷ are the most common source of chemical energy in everyday life. Chemical fuels undergo combustion with an oxidant, typically an oxygen-rich material or ambient oxygen drawn from the air, releasing significant amounts of energy on demand, usually as heat, which is subsequently converted into mechanical energy (e.g., gasoline-powered automobiles), electrical energy (e.g., diesel-powered electric generators), or other useful forms of energy. Energy release may be triggered by heat, electric spark, open combustion, catalysis,⁴⁴⁸ or by other means.⁴⁴⁹ In the case of hypergolics,⁴⁵⁰ no energy trigger is required because simply mixing the reactants spontaneously initiates combustion.

High-energy materials⁴⁵¹ also release energy via chemical transformation, but without combustion or an oxidant. Rather, these “unstable” materials (e.g., explosives) just decompose into simpler molecules, ions, or atoms, usually triggered by the application of heat, friction, shock, electric

⁴⁴⁷ <https://en.wikipedia.org/wiki/Fuel#Chemical>.

⁴⁴⁸ e.g., via catalytic combustion

(<http://www.netl.doe.gov/File%20Library/Research/Coal/energy%20systems/turbines/handbook/3-2-2.pdf>), the use of metals (Mn, Fe, Cu, Ba, Ce, Ca, Pt) to catalyze combustion of hydrocarbon fuels (https://energy.gov/sites/prod/files/2014/03/f9/2005_deer_hirs.pdf), or the contact process using platinum or vanadium (https://en.wikipedia.org/wiki/Contact_process).

⁴⁴⁹ Nanoscale systems can easily use mechanical pressure to surmount the activation barrier and ignite the reactants. For example, the activation energy of a stoichiometric mixture of glucose and oxygen has been estimated at $\sim 8.7 \times 10^7 \text{ J/m}^3$, which can be supplied to the reactants by applying a mechanical pressure of $\sim 860 \text{ atm}$; <http://www.nanomedicine.com/NMI/6.3.4.4.htm#p7>.

⁴⁵⁰ “A hypergolic propellant combination used in a rocket engine is one whose components spontaneously ignite when they come into contact with each other. The two propellant components usually consist of a fuel and an oxidizer. Although commonly used hypergolic propellants are difficult to handle because of their extreme toxicity and/or corrosiveness, they can be stored as liquids at room temperature and hypergolic engines are easy to ignite reliably and repeatedly. [Common examples include] dinitrogen tetroxide plus hydrazine, and/or its relatives monomethylhydrazine and unsymmetrical dimethylhydrazine.” https://en.wikipedia.org/wiki/Hypergolic_propellant. See update and references at: Titi *et al.* Hypergolic zeolitic imidazolate frameworks (ZIFs) as next-generation solid fuels: Unlocking the latent energetic behavior of ZIFs. *Science Advances* 2019 Apr 5;5(4); <https://advances.sciencemag.org/content/5/4/eaav9044>.

⁴⁵¹ Agrawal JP. *High Energy Materials: Propellants, Explosives and Pyrotechnics*. Wiley-VCH, 2010; <https://www.amazon.com/High-Energy-Materials-Propellants-Pyrotechnics/dp/3527326103>, available online at https://exploders.info/Files/Library/eng/explosives/high_energy_materials_-_propellants_eksplives_and_pyrotechnitss_agrawal_i.p._2010_g._464_s..pdf. Klapötke TM. *Chemistry of High-Energy Materials*, 3rd Edition, De Gruyter, 2015; <https://www.amazon.com/Chemistry-High-Energy-Materials-Gruyter-Textbook/dp/3110439328>. Sabatini JJ, Oyler KD. Recent advances in the synthesis of high explosive materials. *Crystals* 2016;6(5):1-22; <https://www.mdpi.com/2073-4352/6/1/5/pdf>.

spark, or some other modest energy input that moves enough of the energetic material over its activation energy barrier to enable wholesale energy release from the bulk to proceed. “High explosives” (e.g., TNT, C-4 plastic explosive⁴⁵²) are energetic materials that “detonate” – i.e., the explosive shock front passes through the material at supersonic speed (e.g., 3000-9000 m/sec), propagating via shock compression.⁴⁵³ “Low explosives” (aka. propellants, propane, gasoline, gunpowder, and fireworks) propagate via thermal activity at subsonic speeds (e.g., 0.03-400 m/sec), a process commonly called “deflagration.”⁴⁵⁴ There is an entire field of research dedicated to the study of high energy density materials (HEDM).⁴⁵⁵

As a general rule, chemical decomposition yields the lowest energy density, with combustion of fuel-oxidant mixtures giving higher energy densities and the combustion of fuels using ambient oxidant providing the highest energy density since only fuel mass must be included in the calculation. For example, a given mass of the high explosive TNT (trinitrotoluene)⁴⁵⁶ generates several times more energy when it is combusted in ambient air (**14.5 MJ/kg**) than when it decomposes explosively (**5.4 MJ/kg**). However, the rate of energy release during combustion of a fuel-oxidant mixture is relatively slow when compared to the often-explosive release rate that occurs during the decomposition of high-energy materials. For example, a 1 gm cube of coal may take ~60 sec to burn (generating ~500 W of power during that time), while a 1 gm cube of the high explosive HMX takes only $\sim 10^{-6}$ sec to decompose (but generating $\sim 6 \times 10^9$ W during the explosion).⁴⁵⁷

In this Section, we survey the specific energy and energy density for a variety of chemically energetic materials, including the chemical decomposition of explosive materials (**Section 4.2.1**), the chemical combustion of fuel-oxidant mixtures (**Section 4.2.2**), and the chemical combustion of pure fuels using oxidants that are freely available from the ambient environment (**Section 4.2.3**). Practical modern-day automobiles and aircraft using engines that generate energy via the ambient combustion of petroleum-based fuels generally achieve very poor power densities in the range of **0.00005-0.006 MW/kg**,⁴⁵⁸ though these figures are for the entire system and not just the powerplant.

The figures given in the data tables in the following subsections should not be regarded as definitive for every substance and circumstance. Most importantly, heat-of-formation-derived reaction enthalpies can vary depending upon the temperature at which the heat of formation was calculated and on the presumed states of the reactants and products (e.g., gas, liquid, or solid).

⁴⁵² [https://en.wikipedia.org/wiki/C-4_\(explosive\)](https://en.wikipedia.org/wiki/C-4_(explosive)).

⁴⁵³ https://en.wikipedia.org/wiki/Explosive_material#High_explosives.

⁴⁵⁴ https://en.wikipedia.org/wiki/Explosive_material#Low_explosives.

⁴⁵⁵ Klapötke TM (ed.), High Energy Density Materials (Structure and Bonding), Springer, 2007; <http://www.springer.com/us/book/9783540722014>.

⁴⁵⁶ <https://en.wikipedia.org/wiki/TNT>.

⁴⁵⁷ Venugopalan S. Demystifying Explosives: Concepts in High Energy Materials, Elsevier, 2015; Table 2.1, p. 19; <https://books.google.com/books?id=u-ucBAAQBAJ&pg=PA19>.

⁴⁵⁸ https://en.wikipedia.org/wiki/Power-to-weight_ratio#Vehicles.

Different choices will produce somewhat different results than those tabulated in the table, altering individual absolute energies though probably not dramatically changing the relative rankings or overall results and conclusions. The biggest such effect may occur for reactions involving water, a common combustion product for fuels containing hydrogen. The data tables assume that water (H₂O) and carbon dioxide (CO₂) product molecules remain in the gaseous state, even though some additional energy could be extracted by exposing them to a cold sink, transferring a bit more energy as they condense into liquid or solid form. If H₂O(l) is used in place of H₂O(g), an additional extractable energy of -44 kJ/mole (**2.44 MJ/kg** or **2.44 MJ/L** of product water) is theoretically available. In the case of oxides such as aluminum oxide or silicon dioxide, or other common solids, energy extraction to the usual room temperature solid state is assumed except where indicated. Additional variation in the tabulated figures may arise when the density (kg/m³) of an energetic material is not reported in the literature and must be estimated, guessed, or assumed. We also neglect the net work done by product gases (resulting from decomposition or combustion of nongaseous reactants) in expanding the surrounding medium – though this is usually relatively small (e.g., ~1% in the case of the explosive PETN)⁴⁵⁹ compared to the heat liberated at constant pressure. Finally, many of the entries are not corrected for strain energy, an omission which is usually small in magnitude but which in some instances could yield a computed reaction energy that is underreported by as much as 10%-20% in the case of highly strained molecules.

In this Section, we will not consider methods which are only used to extract a bit more performance from chemical fuels. For example, “endothermic fuels” may be employed in hypersonic aircraft,⁴⁶⁰ wherein heat generated by the passage of the aircraft through the air is used to thermally crack, depolymerize, dehydrogenate, or dehydrocyclize hydrocarbons thus increasing the available combustion energy of the fuel, but mainly providing a necessary cooling function for the powerplant.⁴⁶¹

⁴⁵⁹ https://en.wikipedia.org/wiki/Chemical_explosive#Example_of_thermochemical_calculations.

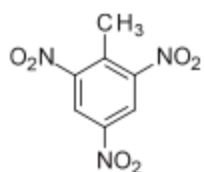
⁴⁶⁰ Lander H, Nixon AC. Endothermic fuels for hypersonic vehicles. *J Aircraft* 1971 Apr;8(4):200-7; <https://arc.aiaa.org/doi/abs/10.2514/3.44255>.

⁴⁶¹ Method of cooling with an endothermic fuel, 15 May 1991; <https://www.google.com/patents/US5176814>. Endothermic fuel system, 15 May 1993; <https://www.google.com/patents/US5232672>. Yong-sheng G, Rui-sen L. Investigation of heat sink of endothermic hydrocarbon fuels. *J Zhejiang University-SCIENCE A*. 2005 Jul;6(7):632-5; <http://citeseerx.ist.psu.edu/viewdoc/download?doi=10.1.1.584.7474&rep=rep1&type=pdf>. Hydrocarbon-fueled rocket engine with endothermic fuel cooling, 15 Aug 2006; <https://www.google.com/patents/US20100257839>. Srinivas J, Manjunath P. Experimental Demonstration of the Concept of Endothermic Fuels for Providing Efficient Cooling to Scramjet Combustors. In: INTERNATIONAL CONFERENCE ON ADAPTIVE TECHNOLOGIES FOR SUSTAINABLE GROWTH, 16 Jun 2011, Namakkal, Tamil Nadu, India; <http://nal-ir.nal.res.in/11779/1/cp83.pdf>. Deam AM, Bogin GE, Kee RJ, Lobo RF, Vlachos DG, Colket MB, Opalka SM. AFOSR BRI: Heterogeneously Catalyzed Endothermic Fuel Cracking. 5th Annual Fuels Res Review, Sandia Natl lab, 17-20 Sep 2012; http://kinetics.nist.gov/RealFuels/maccr/maccr2012/MACCCR_2012_Dean.pdf. Mikhaylov AM. The use of supercritical endothermic fuel. *J Phys: Conf Ser*. 2013;461:012035; <http://iopscience.iop.org/article/10.1088/1742-6596/461/1/012035/pdf>.

4.2.1 Chemical Decomposition and Explosives

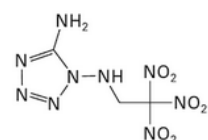
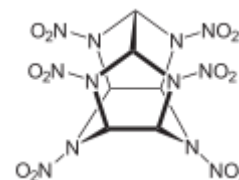
Energetic chemical decomposition involves no combustion. The material is simply unstable and explosive energy is released by carrying the molecules over an activation energy barrier using heat, shock, irradiation, or other means. The explosive shock front in a high explosive material is supersonic, typically 3000-9000 m/sec, e.g., ~5800 m/sec for TNT.

As noted by the German explosives expert Thomas Klapötke⁴⁶² in his landmark textbook,⁴⁶³ high explosives are covalent or ionic homogenous substances that can store and evolve chemical



energy in three different ways. First, **oxidation of the carbon backbone:** fuel and oxidizer must be combined in each single molecule of explosive – e.g., in TNT ($C_6H_2(NO_2)_3CH_3$, at left), the three nitro groups represent the oxidizer while the C-H backbone acts as the fuel.

Second, there is **bond strain:** While in TNT all of the C-C bonds have almost the ideal angles for a normal sp^2 or sp^3 hybridized atom, the explosive molecule CL-20 ($C_6H_6N_{12}O_{12}$, at right) contains considerable ring or cage strain – so its explosive decomposition to CO, CO₂, H₂O and N₂ releases more energy (by ~0.319 MJ/mole) than would occur in an unstrained system (i.e., ~2.96 MJ/mole).⁴⁶⁴ Third, there are the **nitrogen-rich molecules:** The element nitrogen is unique in that its bond energy per two-electron covalent bond increases from a single to a double to a triple bond. The huge bond energy of the N≡N triple bond explains why all nitrogen-rich and polynitrogen compounds show a strongly exothermic decomposition when N₂ is formed – such reactions are strongly “downhill,” energetically. (Unlike nitrogen, carbon bond energies go in the opposite direction, and oxygen doesn't even have a triple bond.) Klapötke notes that nitrogen-rich explosives



(with N ideally $\geq 50\%$ of all heavy atoms, e.g., the explosive TTD, at left) lie at the forefront of high-energy explosives research: “Researchers have already realized the energy content limit for CHNO based molecules. Materials with a high nitrogen content ($>50\%$) offer...the potential for vastly increased energy content.”

The specific energy (**Table 25**; range **0.3-23.4 MJ/kg** experimental, up to **43.7 MJ/kg** theoretical) and energy density (**Table 26**; range **0.6-38.9 MJ/L** experimental, up to **177.2 MJ/L** theoretical) of explosive materials during chemical decomposition are grouped into three classes: monopropellants (chemicals that release energy through exothermic chemical decomposition, often triggered using a catalyst), polynitrogen and binary nitrogen explosives (nitrogen-rich explosives, including both pure nitrogen molecules and nitrogen in combination with one other

⁴⁶² <http://www.hedm.cup.uni-muenchen.de/index.html>.

⁴⁶³ Klapotke TM. Chemistry of High-Energy Materials, Walter de Gruyter GmbH, 2015, Ch. 9 (https://books.google.com/books?id=p_roBQAAQBAJ&pg=PA153).

⁴⁶⁴ Bumpus JA. A Theoretical Investigation of the Ring Strain Energy, Destabilization Energy, and Heat of Formation of CL-20. Adv Phys Chem 2012:175146; <http://downloads.hindawi.com/journals/apc/2012/175146.pdf>

element), and decomposing explosives (standard high explosives).⁴⁶⁵ The original data supporting the numbers listed in both tables are compiled in **Table A3** in **Appendix A**. Materials that have at least some theoretical support but have not yet been synthesized experimentally are indicated in red.

Which explosive is the most energetic? Above 110 GPa and ~2000 K, nitrogen forms a network solid, bound by single covalent bonds in a “cubic-gauche” structure, abbreviated as cg-N, that has been synthesized experimentally. This material is very stiff with a bulk modulus similar to diamond, and is the highest-energy non-nuclear pure material currently known.⁴⁶⁶ Cubic gauche nitrogen is metastable when pressure is released at least down to 25 GPa but is predicted possibly to be metastable down to atmospheric pressures,⁴⁶⁷ below which its decomposition to N₂ would release the entire **27.92 MJ/kg (102.19 MJ/L)** heat of formation.

Imidogen (NH) has the next highest specific energy (**23.4 MJ/kg**) of any experimentally-verified molecule on the list, but has a short stable lifetime at room temperature; pentanitrogen (N₅⁺), aka. pentazenium cation, has the second-highest verified energy density (**38.9 MJ/L**); neither seems likely to be useful in bulk-power applications. Nitrogen-rich compounds tend to be the most energy-dense materials in both tables. Single-bonded polynitrogen is alleged to possess an energy capacity of 4.6 eV/mol or (444 kJ/mole) / (0.014 kg/mole N) = **31.7 MJ/kg** though its stability remains unknown,⁴⁶⁸ and many possible higher-cage molecules of pure nitrogen have been investigated for stability including various cage isomers of N₁₄ and N₁₆,⁴⁶⁹ N₁₈,⁴⁷⁰ N₂₄, N₃₀, and N₃₆,⁴⁷¹ and even N₆₀.

Using the techniques of atomically precise molecular manufacturing, it may be possible to build otherwise highly endoergic molecules, atom by atom, forcing energy into the molecules

⁴⁶⁵ The work done by the creation and expansion of gaseous products during chemical decomposition explosions contributes relatively little to the total energy release (**Section 5.1.3**).

⁴⁶⁶ https://en.wikipedia.org/wiki/Solid_nitrogen#Cubic_gauche.

⁴⁶⁷ Eremets MI, Gavriliuk AG, Trojan IA, Dzivenko DA, Boehler R. Single-bonded cubic form of nitrogen. *Nat Mater*. 2004 Aug;3(8):558-63; https://www.researchgate.net/profile/A_Gavriliuk/publication/8472556_Single-bonded_cubic_form_of_nitrogen/links/0fcfd50a001fe74989000000.pdf.

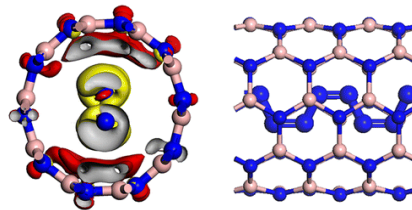
⁴⁶⁸ Uddin J, Barone V, Scuseria GE. Energy storage capacity of polymeric nitrogen. *Molecular Physics* 2006;104:745-749; <http://www.tandfonline.com/doi/abs/10.1080/00268970500417325>.

⁴⁶⁹ Strout DL. Cage Isomers of N₁₄ and N₁₆: Nitrogen Molecules That Are Not a Multiple of Six. *J Phys Chem A* 2004 Dec;108(49):10911-10916; https://www.researchgate.net/profile/Douglas_Strout/publication/239721938_Cage_Isomers_of_N_14_and_N_16_Nitrogen_Molecules_That_Are_Not_a_Multiple_of_Six/links/55ae8b1b08aee0799220e26d.pdf.

⁴⁷⁰ Sturdivant SE, Nelson FA, Strout DL. Trends in stability for N₁₈ cages. *J Phys Chem A* 2004;108:7087-7090; https://www.researchgate.net/publication/231639366_Trends_in_Stability_for_N18_Cages.

⁴⁷¹ Strout DL. Isomer Stability of N₂₄, N₃₀, and N₃₆ Cages: Cylindrical versus Spherical Structure. *J Phys Chem A* 2004;108(13):2555-2558; <http://pubs.acs.org/doi/abs/10.1021/jp0378889>.

mechanically. However, one would still need to ensure that the now-highly energetic and unhappy molecules would not decompose as soon as compressive forces were withdrawn. Packing them into a container at high pressure to avoid decompression losses could be a viable option in some cases, though in other cases extreme pressurization may cause a rearrangement of bonds or even an explosion as some of these highly-compressed materials might be acutely shock-, impact-, or pressure-sensitive. One recent theoretical analysis of polymeric nitrogen chains forced to reside inside a boron nitride BNNT (5,5) nanotube (image, right) suggests that this material is stable in ambient conditions and that the trapped nitrogen polymer could “release tremendous energy” above 1400 K upon dissociation into N₂ molecules.⁴⁷²



Ballotechnics⁴⁷³ are another class of materials that undergo a mechanochemical reaction⁴⁷⁴ when quickly subjected to extreme pressures on the order of tens of thousands of atmospheres, with these reactions initiated by shock waves transmitted through the material. The shock-initiated chemical reaction progresses with little change in volume and is therefore not “explosive” since the energy is released in the form of heat rather than work (e.g., no product gases to expand).⁴⁷⁵ Examples include highly-compressed powder mixtures of nickel and aluminum,⁴⁷⁶ nickel and titanium,⁴⁷⁷ titanium and silicon,⁴⁷⁸ and thermitite.⁴⁷⁹

⁴⁷² Liu S, Yao M, Ma F, Liu B, Yao Z, Liu R, Cui T, Liu B. High Energetic Polymeric Nitrogen Stabilized in the Confinement of Boron Nitride Nanotube at Ambient Conditions. *J Phys Chem C*. 2016 Jul 19;120(30):16412-16417; <http://pubs.acs.org/doi/abs/10.1021/acs.jpcc.6b04374>.

⁴⁷³ <https://en.wikipedia.org/wiki/Ballotechnics>.

⁴⁷⁴ Graham RA, Anderson MU, Holman GT, Baer MR. Prediction of violent mechanochemical processes. SAND Report, SAND97-0038; 1997 Jan 1; http://infoserve.sandia.gov/sand_doc/1997/970038.pdf.

⁴⁷⁵ Boslough MB. A thermochemical model for shock-induced chemical reactions in porous solids: Analogs and contrasts to detonation. *Proc 9th Symp (Intl) Detonation (CONF-890811-26)*, Vol. II, 28 Aug – 1 Sep 1989, pp. 1199-1216; <http://www.dtic.mil/dtic/tr/fulltext/u2/a247996.pdf>.

⁴⁷⁶ Boslough MB. Shock-induced chemical reactions in nickel-aluminum powder mixtures: Radiation pyrometer measurements. *Chem Phys Lett*. 1989;160(5-6):618. Taylor PA, Boslough MB, Horle Y. Modeling of shock-induced chemistry in nickel-aluminum systems. *Shock Waves in Condensed Matter – 1987*, Monterey CA, 20-23 Jul 1987, pp. 395-8.

⁴⁷⁷ Xu X, Thadhani NN. Investigation of shock-induced reaction behavior of as-blended and ball-milled Ni+ Ti powder mixtures using time-resolved stress measurements. *J Appl Phys*. 2004 Aug 15;96(4):2000-9; <http://aip.scitation.org/doi/abs/10.1063/1.1773380>.

⁴⁷⁸ Graham RA, Anderson MU, Horie Y, You SK, Holman GT. Pressure measurements in chemically reacting powder mixtures with the Bauer piezoelectric polymer gauge. *Shock Waves*. 1993 Sep 1;3(2):79-82; <https://link.springer.com/article/10.1007/BF02115887>.

⁴⁷⁹ Hornig H, Kury J, Simpson R, Helm F, von Holle W. Shock ignition of pyrotechnic heat powders. *Proc 11th Intl Pyrotech Seminar*, Vail CO, 7-11 Jul 1986, pp. 699-719.

Table 25. Specific energy of explosive materials during chemical decomposition (theoretical materials indicated in red)⁴⁸⁰

High-Energy Material	Specific Energy (MJ/kg)	High-Energy Material	Specific Energy (MJ/kg)
Monopropellants		CL-20	7.489
Nitromethane monopropellant	10.328	Diazirone	7.464
Guanidine nitrate monopropellant	7.172	BNO ₂ (theoretical)	7.394
Sodium ozonide decomposition	6.324	Hexanitrobenzene	7.356
Cyclic ozone (O ₃) decomposition (theoretical)	5.688	Tetradecanitrobicubane (theoretical)	7.335
Propylene glycol dinitrate monopropellant	4.578	Prismane	7.262
Hydrogen peroxide monopropellant	3.118	Hydroperoxymethane	7.208
Octaoxygen (O ₈) decomposition	3.070	TNAZ	7.188
Hydrazine (N ₂ H ₄) monopropellant	2.981	Methylene dinitramine	6.801
Ozone (O ₃) decomposition	2.979	NAATO (theoretical)	6.786
Ammonium dinitramide monopropellant	2.710	BDNM-TN-TABO (theoretical)	6.707
Nitrous oxide (N ₂ O) monopropellant	1.855	EGDN	6.645
Hydroxylammonium nitrate	1.094	1,1'-Azobis-1,2,3-triazole	6.463
Ammonium nitrate monopropellant	0.455	BTAT	6.461
		DTTO (theoretical)	6.320
Polynitrogen and Binary Nitrogen Explosives		PETN	6.266
N ₁₀ , azaadamantane (theoretical)	30.886	RDX	6.216
N ₈ , cubic gauche nitrogen (theoretical at STP)	27.920	Nitroglycerine	6.211
N ₈ , octaazacubane (theoretical)	26.964	1,1'-Azobis(tetrazole)	6.205
NH, imidogen	23.433	HMX	6.182
N ₅ , pentanitrogen	20.986	DNBTT	6.181
N ₄ , tetranitrogen	20.000	TMETN	6.118
N ₂₀ , eicosaaza[20]fullerene (theoretical)	19.321	Tetryl	5.993
N ₄ , tetraazatetrahedrane (theoretical)	17.250	TKX-50	5.975
N ₆ , hexaazaprismane (theoretical)	16.429	MTO3N (theoretical)	5.907
N ₁₈ , cage isomer 2063A (theoretical)	13.687	DDNP	5.905
N ₁₆ C ₂ cage "Isomer B" (theoretical)	13.500	Composition C-4	5.900
N ₁₀ C ₂ cage "Isomer B" (theoretical)	13.476	TNTA	5.889
N ₄ , tetrazete (theoretical)	13.339	FOX-7	5.872
N ₁₂ , cage isomer 2060 (theoretical)	13.244	Mannitol hexanitrate	5.863
N ₁₈ H ₆ (theoretical)	11.290	DEGDN	5.816
N ₆ , hexaazabenzene (theoretical)	10.850	HHTDD	5.812
N ₂ O ₃ , dinitrogen trioxide (theoretical)	10.724	TNGU	5.807
N ₂ Be ₃ , beryllium nitride	10.653	Chromium pentazolate (theoretical)	5.778
N ₈ , octanitrogen (theoretical)	9.714	LLM-105	5.741
N ₃ F, fluorine azide	9.262	TNB	5.728
N ₆ , diazide (theoretical)	9.205	Hexanitrostilbene	5.667
N ₁₀ , triazidamine (theoretical)	9.029	MEKP	5.667
N ₇ H, diazidamine (theoretical)	8.406	Composition H6	5.650
N ₈ , pentaazapentalene (theoretical)	8.402	Composition B	5.560
N ₄ H ₄ (theoretical)	8.383	1,4-Bis(dihydroperoxymethyl)benzene	5.500
N ₂₃ P	8.357	PYX	5.435
N ₁₇ B	8.353	Nitrocellulose	5.421
N ₂ O ₂ , dinitrogen dioxide	8.333	TNT	5.419
N ₁₂ C, tetraazidomethane	8.333	Picric acid	5.328
N ₃ H ₃ , triaziridine	8.111	DAAF	5.297

⁴⁸⁰ Data from Table A3 in Appendix A.3.

N ₆₀ , hexacontaazo[60]fullerene (theoretical)	8.083	Dynamite	5.263
N ₁₀ , dipentazole (theoretical)	7.771	HMTD	5.240
N ₈ , azidopentazole (theoretical)	7.348	Hexamine peroxide	5.240
N ₁₀ C ₃ , planar NAA (theoretical)	6.875	Propyne (methylacetylene)	5.237
N ₁₄ C ₂ , azidotetrazole	6.795	TEGDN	5.167
N ₁₀ C ₂ , planar DAT	6.634	3,5-Dihydroperoxy-3,5-dimethyl-1,2-dioxolane	5.133
N ₂ C ₄ , dicyanoacetylene	6.576	FNO ₂ (theoretical)	5.077
N ₂₀ C ₆	6.168	HNF	5.060
N ₃ H, hydrogen azide	6.140	DAAT	5.045
N ₄ O, nitrosyl azide (theoretical)	6.097	ADNQ	5.024
N ₁₂ P ₆ (N ₁₈ isomer 2063A analog) (theoretical)	5.845	Tetranitrotetrahydrane (C ₄ (NO ₂) ₄)	4.871
N ₅ H, hydrogen pentazole	5.761	ANG	4.866
N ₃ B, boron azide (theoretical)	5.341	TEX	4.809
N ₃ Cl, chlorine azide	5.032	Dihydrazinium 5,5'-azidotetrazolate dihydrazinate	4.804
N ₂ H, polymeric hydronitrogen (theoretical)	4.414	Hydroxylammonium azidotetrazolate	4.743
N ₂ C, penta-CN ₂ (theoretical)	4.400	DAB	4.713
N ₂ B ₂ , dinitrogen diboride (theoretical)	4.355	DNAN	4.707
N ₄ O ₂ , nitryl azide (theoretical)	4.284	Krypton hydrogen fluoride, HKrF (theoretical)	4.599
N ₃ H ₃ , triazene	4.267	TTD	4.596
N ₃ Ag, silver azide	4.140	TATB	4.496
N ₃ H ₅ , hydrazinium azide	3.800	sil-a-PETN	4.488
N ₂₀ Ti (theoretical)	3.720	BNCP	4.405
N ₁₂ C ₃ , cyanuric triazide	3.458	PETNC	4.324
N ₅ B ₃ , triboron pentanitride (theoretical)	3.438	Tetranitratocarbon (theoretical)	4.305
N ₂ H ₂ , diimine	3.280	Aluminum pentazolate (theoretical)	4.266
N ₆ Cu, copper(II) azide	3.000	Methylammonium nitrate	4.231
N ₆ O ₈ , tetranitrohydrazine (theoretical)	2.764	CLCP	4.063
N ₃ Li, lithium pentanitride (theoretical)	2.714	NTO (nitrotriazolon)	3.892
N ₄ S ₄ , tetrasulfur tetranitride	2.609	BTATz	3.863
N ₄ O ₆ , trinitramine (theoretical)	2.480	Hydrazine mononitrate	3.832
NCl ₃ , nitrogen trichloride	1.910	Copper acetylde	3.828
N ₆ Pb, lead azide	1.589	Nitroguanidine	3.740
N ₆ Cu ₂ , copper(I) azide	1.200	Nitrourea	3.709
NAg ₃ , silver nitride	0.932	TAG-AT	3.663
N ₅ Na, sodium pentazolate (theoretical)	0.908	NONA	3.510
N ₆ Cs, cesium pentanitride (theoretical)	0.747	CTA	3.458
NI ₃ , nitrogen triiodide	0.734	sil-a-PETNC	3.373
N ₃ Na, sodium azide	0.334	Xenon tetroxide	3.297
		Xenon dioxide	2.988
		Xenon trioxide	2.950
Decomposing Explosives		AAT	2.851
Carbon tetroxide, bicyclic (theoretical)	43.658	DADP	2.838
Helium hydrogen fluoride, HHeF (theoretical)	28.146	Urea nitrate	2.756
Carboxycubane, C ₄ O ₄ (theoretical)	13.071	TATP	2.743
Carbonyl oxide	11.298	Silver fulminate	2.507
BAFDAONAB	11.057	Carbon tetroxide, monocyclic	2.488
Bicyclo-dioxydiazamethane (theoretical)	11.042	Nitramide	2.456
Heptanitrocubane	10.372	HAA	2.399
ONC (octanitrocubane)	10.366	Ammonium permanganate	2.336
HN ₃ O (theoretical)	10.153	GAT	2.232
Carbenium triazidoperchlorate	9.873	Polymeric CNO (theoretical)	2.200
Hexanitroprismane (theoretical)	9.741	Mercury fulminate	2.130
Argon hydrogen fluoride, HArF (theoretical)	9.583	Tetranitromethane	1.888
Erythritol tetranitrate	9.305	BHDBT	1.819
Acetylene	8.727	Lead styphnate	1.693
TACOT	8.660	Chlorine dioxide	1.519
HNO ₂ (theoretical)	8.447	Silver acetylde	1.492
Polymeric CO	8.000	Tetradecanitrofullerene	1.481
TTTO	7.900	Tetrazene	0.632
DNAF/DDF	7.778	Antimony trisulfide	0.515
BTTN	7.635		

Table 26. Energy density of explosive materials during chemical decomposition (theoretical materials indicated in red)⁴⁸¹

High-Energy Material	Energy Density (MJ/L)	High-Energy Material	Energy Density (MJ/L)
Monopropellants		Polymeric CO	13.201
Nitromethane monopropellant	20.064	NAATO (theoretical)	12.881
Guanidine nitrate monopropellant	10.294	DTTO (theoretical)	12.515
Sodium ozonide decomposition	10.113	MTO3N (theoretical)	12.410
Cyclic ozone (O ₃) decomposition (theoretical)	9.820	TNTA	12.350
Propylene glycol dinitrate monopropellant	5.630	BTAT	12.198
Octaoxygen (O ₈) decomposition	5.527	HHTDD	12.035
Ozone (O ₃) decomposition	5.144	HMX	11.806
Ammonium dinitramide monopropellant	5.106	TNGU	11.688
Hydrogen peroxide monopropellant	4.530	Prismane	11.623
Hydrazine (N ₂ H ₄) monopropellant	3.038	BTTN	11.572
Nitrous oxide (N ₂ O) monopropellant	2.279	RDX	11.311
Hydroxylammonium nitrate	2.000	TKX-50	11.190
Ammonium nitrate monopropellant	0.784	PETN	11.124
		FOX-7	11.056
Polynitrogen and Binary Nitrogen Explosives		1,1'-Azobis(tetrazole)	11.004
N ₁₀ , azaadamantane (theoretical)	177.213	LLM-105	10.973
N ₈ , cubic gauche nitrogen (theoretical at STP)	102.190	1,1'-Azobis-1,2,3-triazole	10.600
N ₈ , octaazacubane (theoretical)	72.422	Methylene dinitramine	10.488
N ₂₀ , eicosaaza[20]fullerene (theoretical)	45.083	Tetryl	10.361
N ₄ , tetraazatetrahedrane (theoretical)	39.753	Composition C-4	10.190
N ₅ , pentanitrogen	38.862	Mannitol hexanitrate	10.153
N ₄ , tetrazete (theoretical)	36.798	TNB	10.083
N ₄ , tetranitrogen	35.000	Nitroglycerine	9.930
N ₆ , hexaazaprismane (theoretical)	32.857	EGDN	9.902
N ₂ Be ₃ , beryllium nitride	28.916	Silver fulminate	9.869
N ₁₇ B	28.809	Composition H6	9.725
N ₈ , octanitrogen (theoretical)	25.361	Hexanitrostilbene	9.623
N ₁₈ H ₆ (theoretical)	23.729	PYX	9.615
N ₁₆ C ₂ cage "Isomer B" (theoretical)	23.250	DDNP	9.612
N ₂₃ P	23.228	TEX	9.545
N ₁₀ C ₂ cage "Isomer B" (theoretical)	23.214	Mercury fulminate	9.425
N ₆₀ , hexacontaazo[60]fullerene (theoretical)	21.556	HNF	9.411
N ₈ , pentaazapentalene (theoretical)	20.150	Picric acid	9.385
N ₂₀ Ti (theoretical)	19.427	DAAF	9.281
N ₆ , diazide (theoretical)	19.330	Composition B	9.175
N ₃ Ag, silver azide	18.319	TMETN	9.070
N ₁₀ , dipentazole (theoretical)	14.763	TNT	8.978
N ₁₀ , triazidamine (theoretical)	14.266	DAAT	8.952
N ₁₂ C, tetraazidomethane	13.636	Nitrocellulose	8.944
N ₆ , hexaazabenzene (theoretical)	13.563	1,4-Bis(dihydroperoxymethyl)benzene	8.815
N ₇ H, diazidamine (theoretical)	13.118	ADNQ	8.715
N ₁₀ C ₃ , planar NAA (theoretical)	12.235	TATB	8.657
N ₃ F, fluorine azide	12.047	ANG	8.603
N ₅ B ₃ , triboron pentanitride (theoretical)	11.852	TTD	8.418
N ₁₄ C ₂ , azidotetrazole	11.680	DEGDN	8.201

⁴⁸¹ Data from **Table A3** in **Appendix A.3**.

N ₁₀ C ₂ , planar DAT	11.429	DNBTT	8.051
N ₂₀ C ₆	10.590	CLCP	7.991
N ₄ O, nitrosyl azide (theoretical)	9.380	Hydroxylammonium azidotetrazolate	7.824
NAg ₃ , silver nitride	8.400	PETNC	7.617
N ₆ Cu, copper(II) azide	7.803	sil-a-PETN	7.450
N ₃ Cl, chlorine azide	7.544	NTO (nitrotriazolon)	7.430
N ₄ O ₂ , nitryl azide (theoretical)	7.540	3,5-Dihydroperoxy-3,5-dimethyl-1,2-dioxolane	7.346
N ₆ Pb, lead azide	7.481	Hydroperoxymethane	7.193
N ₃ H, hydrogen azide	6.684	DAB	7.163
N ₅ H, hydrogen pentazole	6.283	TEGDN	6.889
N ₁₂ C ₃ , cyanuric triazide	6.271	BTATz	6.794
N ₆ O ₈ , tetranitrohydrazine (theoretical)	5.998	Silver acetylde	6.667
N ₂ C ₄ , dicyanoacetylene	5.964	MEKP	6.648
N ₄ S ₄ , tetrasulfur tetranitride	5.847	Tetranitrotoxicarbon (theoretical)	6.630
N ₄ O ₆ , trinitramine (theoretical)	5.332	Nitroguanidine	6.388
N ₅ Li, lithium pentanitride (theoretical)	4.976	Acetylene	6.356
NCl ₃ , nitrogen trichloride	3.159	DNAN	6.297
N ₆ Cu ₂ , copper(I) azide	3.117	Hydrazine mononitrate	6.287
NI ₃ , nitrogen triiodide	2.900	Tetranitrotetrahydrane (C ₄ (NO ₂) ₄)	6.278
N ₆ Cs, cesium pentanitride (theoretical)	2.613	NONA	6.261
N ₅ H ₅ , hydrazinium azide	2.591	Dynamite	6.250
N ₂ H ₂ , diimine	2.236	Methylammonium nitrate	6.008
N ₅ Na, sodium pentazolate (theoretical)	1.675	CTA	5.968
N ₃ Na, sodium azide	0.616	TAG-AT	5.880
Decomposing Explosives		Nitrourea	5.777
Carbenium triazidoperchlorate	24.684	sil-a-PETNC	5.537
Chromium pentazolate (theoretical)	29.467	Ammonium permanganate	5.212
BAFDAONAB	21.361	Lead styphnate	4.916
Heptanitrocubane	20.995	Dihydrazinium 5,5'-azotetrazolate dihydrazinate	4.722
ONC (octanitrocubane)	20.556	Urea nitrate	4.657
Hexanitroprismane (theoretical)	19.483	HMTD	4.619
TTTO	18.810	Hexamine peroxide	4.599
Diazirone	16.392	Polymeric CNO (theoretical)	4.400
TACOT	16.000	AAT	4.360
DNAF/DDF	15.664	HAA	4.069
CL-20	15.327	DADP	3.784
Xenon tetroxide	14.953	BHDBT	3.489
Erythritol tetranitrate	14.868	TATP	3.460
Aluminum pentazolate (theoretical)	14.868	GAT	3.427
Hexanitrobenzene	14.629	Nitramide	3.384
BDNM-TN-TABO (theoretical)	13.975	Antimony trisulfide	3.346
Xenon dioxide	13.528	Tetranitromethane	3.058
Xenon trioxide	13.435	Propyne (methylacetylene)	2.774
TNAZ	13.398	Chlorine dioxide	2.494
Tetradecanitrobicubane (theoretical)	13.275	Tetradecanitrofullerene	2.443
Bicyclo-dioxydiamethane (theoretical)	13.250	BNCP	1.325
		Tetrazene	1.073

4.2.2 Nonambient Chemical Combustion

Chemical fuels undergo combustion with an oxidant, typically an oxygen-rich material or ambient oxygen drawn from the air. In nonambient combustion, both fuel and oxidant are contained entirely within the energy storage system, and no material inputs are provided from the environment. Hence the mass of the energy storage material is the sum of the mass of the fuel and the mass of the oxidant. Rockets are one example of such a system. The most common oxidants used for combustion in chemical energy storage systems are pure oxygen, chlorine, fluorine, chlorine trifluoride, nitrous oxide, or nitric acid. (Hydrogen burns in chlorine to form hydrogen chloride, liberating the heat and light of combustion, though at very low energy density.)⁴⁸²

The specific energy (**Table 27**; range **1.2-30.9 MJ/kg**) and energy density (**Table 28**; range **2.7-47.8 MJ/L**) of fuel-oxidant materials during nonambient combustion are grouped into 18 classes for greater clarity:

- (1) metals and elements (**1.2-24.0 MJ/kg; 3.0-31.7 MJ/L**);
- (2) hydrides (**2.1-30.9 MJ/kg; 5.1-22.7 MJ/L**);
- (3) boranes (**10.8-27.4 MJ/kg; 10.8-18.3 MJ/L**);
- (4) silanes (**14.7-15.1 MJ/kg; 12.7-13.8 MJ/L**);
- (5) phosphanes (**11.1-14.0 MJ/kg; 11.0-15.8 MJ/L**);
- (6) metal borides (**19.8-28.8 MJ/kg; 26.7-39.0 MJ/L**);
- (7) solid nitrides (**7.7-15.3 MJ/kg; 13.4-29.2 MJ/L**);
- (8) organics (**3.4-15.2 MJ/kg; 5.0-17.9 MJ/L**);
- (9) organometallics (**4.6-13.6 MJ/kg; 5.9-13.5 MJ/L**);
- (10) other oxygen combustibles (**3.8-15.3 MJ/kg; 5.4-22.0 MJ/L**);
- (11) nitrogen combustibles (**2.0-10.3 MJ/kg; 2.7-12.1 MJ/L**);
- (12) carbon dioxide combustibles (**6.0-9.0 MJ/kg; 14.2-17.4 MJ/L**);
- (13) water combustibles (**2.1-9.8 MJ/kg; 3.0-12.8 MJ/L**);
- (14) nonambient combustibles with halogen oxidants (**1.8-23.8 MJ/kg; 3.2-41.7 MJ/L**);
- (15) nonambient combustibles with O_n-allotrope oxidants (**5.9-26.4 MJ/kg; 10.5-47.8 MJ/L**);
- (16) nonambient combustibles with nitrate oxidants (**9.4-19.0 MJ/kg; 16.8-38.5 MJ/L**);
- (17) nonambient thermitic combustibles (**2.9-14.1 MJ/kg; 10.6-36.5 MJ/L**); and
- (18) nonambient combustible propellants & explosives (**2.1-17.4 MJ/kg; 3.2-39 MJ/L**).

Whenever possible, the most compact liquid or solid form of the reactants was used to compute the energy density of the fuel-oxidant materials, on the assumption that these materials can be stored compactly even if they must later be heated or gasified prior to actual use. The original data supporting the numbers listed in both tables are compiled in **Table A4** in **Appendix A**. Materials that have at least some theoretical support but have not yet been synthesized experimentally are indicated in red.

⁴⁸² <https://en.wikipedia.org/wiki/Combustion>.

The fuel-oxidant material with the highest specific energy for nonambient combustion is beryllium monohydride + liquid oxygen (BeH+LOX) at **30.9 MJ/kg**, but this is likely impractical because BeH is a metastable monoradical species that has only been observed in gas phase to date, so this must be considered highly “theoretical”. Discounting the still-theoretical diberyllium diboride (Be₂B₂+LOX) at **28.8 MJ/kg** and dilithium diboride (Li₂B₂+LOX) at **26.4 MJ/kg**, and the gaseous-only-known boron monohydride radical (BH+LOX) at **27.4 MJ/kg**, the highest practical prospect may be beryllium + octaoxygen at **26.4 MJ/kg**. Octaoxygen (O₈), aka. “red oxygen,” is a rhomboid cluster of oxygen atoms that can be obtained by compressing oxygen to 10 GPa at room temperature, producing a deep red solid ε-phase that is subsequently stable over a wide pressure range (at least 8-96 GPa).⁴⁸³ Beryllium + ozone (**26.3 MJ/kg**) might be impractical because ozone appears difficult to stably liquefy or solidify,⁴⁸⁴ but the next two highest candidates are quite practical: lithium + fluorine (Li+F₂) at **23.8 MJ/kg** and beryllium dihydride (BeH₂+LOX) at **23.7 MJ/kg**. Of course, all mixtures involving beryllium can be quite toxic⁴⁸⁵ and the element is very rare.⁴⁸⁶ The very safe-burning conventional liquid hydrogen (LH₂+LOX) mixture provides only **13.4 MJ/kg**.

The fuel-oxidant material with the highest energy density for nonambient combustion is again Be+O₈, at **47.8 MJ/L**. Setting aside Be+O₃ for impracticality, the next most energy-dense combination is beryllium + fluorine (Be+F₂) at **41.7 MJ/L**, and the safest energy-dense fuel-oxidant combination is probably aluminum + octaoxygen (Al+O₈) at **39.0 MJ/L**. Once again, the energy density of the traditional liquid rocket fuel LH₂+LOX is extremely disappointing in comparison, yielding only **5.7 MJ/L**. (Using solid hydrogen⁴⁸⁷ and solid oxygen improves H₂+O₂ energy density to **17.7 MJ/L**, but we assume LOX in all energy calculations here because it is

⁴⁸³ Fujihisa H, Akahama Y, Kawamura H, Ohishi Y, Shimomura O, Yamawaki H, Sakashita M, Gotoh Y, Takeya S, Honda K. O₈ cluster structure of the epsilon phase of solid oxygen. Phys Rev Lett. 2006 Aug 25;97(8):085503; <https://www.ncbi.nlm.nih.gov/pubmed/17026315>. Lundegaard LF, Weck G, McMahon MI, Desgreniers S, Loubeyre P. Observation of an O₈ molecular lattice in the epsilon phase of solid oxygen. Nature. 2006 Sep 14;443(7108):201-4; <https://www.ncbi.nlm.nih.gov/pubmed/16971946>. See also: <http://www.azonano.com/article.aspx?ArticleID=1797>.

⁴⁸⁴ Hanson D, Mauersberger K. The vapor pressures of solid and liquid ozone. J Chem Phys 1986 Jul;85(8):4669; <http://aip.scitation.org/doi/abs/10.1063/1.451740>. Allison DK. Apparatus and method for producing liquid ozone. U.S Patent 2704274A, 15 Mar 1955; <https://www.google.com/patents/US2704274>.

⁴⁸⁵ <https://en.wikipedia.org/wiki/Beryllium#Precautions> and https://en.wikipedia.org/wiki/Acute_beryllium_poisoning.

⁴⁸⁶ Beryllium is only the 50th most abundant element out of 92, occurring at ~2 ppm vs. 460,000 ppm for oxygen in the Earth’s crust; https://en.wikipedia.org/wiki/Abundance_of_elements_in_Earth%27s_crust.

⁴⁸⁷ Palaszewski B. Solid hydrogen experiments for atomic propellants: Particle formation energy and imaging analysis. NASA/TM-2002-211915, AIAA-2002-4092, Dec 2002; <http://web.archive.org/web/20110927045420/http://gltrs.grc.nasa.gov/reports/2002/TM-2002-211915.pdf>.

almost as dense as solid oxygen and apparently safer and easier to store and handle.⁴⁸⁸) Note that even the most highly-strained carbon cage compounds such as pyramidane, tetrahedrane and cubane, whether theoretical or experimentally validated, only achieve energy densities of no more than ~18 MJ/L when the volume of the oxidant is included in the calculation.

Activation Energy. It should be noted that almost all chemical reactions (that do not involve free radicals) require the reactants to receive a minimum amount of energy, called the activation energy, before the indicated reaction can proceed to completion, releasing the indicated energy. Typically the activation energy is a modest fraction of the total reaction energy. In practice, this means that some reactions that will readily take place at room temperature will not occur at all if the reactants are maintained at cryogenic temperatures – for example, it was first observed in 1885 that cold metallic sodium or potassium would not react with liquid oxygen,⁴⁸⁹ nor will it react with metallic lithium unless ignited with flame.⁴⁹⁰

Specific Impulse. In rockets employing nonambient combustion of fuel + oxidizer, equating the chemical energy stored in the fuel (E_{fuel}) with the kinetic energy of the exhaust (of mass m_e and average velocity v_e) gives $E_{\text{fuel}} = (1/2) m_e v_e^2$, hence specific energy $E_S = E_{\text{fuel}} / m_e = v_e^2 / 2$. The specific impulse (I_{sp})⁴⁹¹ is a measure of how efficiently the rocket uses its propellant – the change in momentum delivered per unit mass of propellant consumed – most commonly defined as $I_{\text{sp}} = F_{\text{thrust}} / g \dot{m} = v_e / g = (2 E_S)^{1/2} / g$, or $E_S = (g I_{\text{sp}})^2 / 2$ and $F_{\text{thrust}} = 2^{1/2} \dot{m} E_S^{1/2}$, where F_{thrust} is the thrust obtained from the rocket engine in newtons, $g = 9.81 \text{ m/sec}^2$ (the gravity at Earth's surface, i.e., taking the weight of the propellant at sea level), and \dot{m} is the mass flow rate of the propellant in kg/sec (the negative of the time rate of change of the rocket's mass, since the propellant is being expelled). Thus a rocket burning liquid $\text{H}_2 + \text{O}_2$ with $E_S = 13.4 \text{ MJ/kg}$ (Table 27) has $I_{\text{sp}} = 528 \text{ sec}$ and generates $F_{\text{thrust}} = 5177 \text{ N}$ of thrust for every $\dot{m} = 1 \text{ kg/sec}$ of propellant consumed. I_{sp} measured in seconds is the length of time a rocket engine can generate thrust burning a quantity of propellant whose sea-level weight is equal to the engine's thrust.⁴⁹²

⁴⁸⁸ There are indications that contact between solid oxygen and the carbon fiber in the rocket fuel tank caused the launch-pad explosion of SpaceX's Falcon 9 rocket in September 2016. The LOX may have inadvertently froze due to contact with adjacent liquid helium pressure vessels. "SpaceX explosion was caused by frozen oxygen," 9 Nov 2016; <http://www.nextbigfuture.com/2016/11/spacex-explosion-was-caused-by-frozen.html>.

⁴⁸⁹ McGee HA Jr. Chemical Reactivity and Synthesis at Cryogenic Temperatures. In: Timmerhaus KD, Advances in Cryogenic Engineering, Vol. 9, Proceedings of the 1963 Cryogenic Engineering Conference, Springer, 1964, pp. 1-10; <https://books.google.com/books?id=dn3SBwAAQBAJ&pg=PA2>. Early experiments in cryogenic chemistry found that "hydrogen gas would ignite when bubbled beneath the surface of liquid fluorine at 85 K, and liquid hydrogen at 20 K and solid fluorine would explode on contact." Solutions of ozone difluoride (O_3F_2) in liquid oxygen are hypergolic (igniting on contact) with hydrocarbon fuels (e.g., UDMH) and with liquid hydrogen under certain conditions.

⁴⁹⁰ "Awesome liquid oxygen and lithium metal explosion," 25 Apr 2016; <https://www.youtube.com/watch?v=Mtb87I3xKUU>.

⁴⁹¹ https://en.wikipedia.org/wiki/Specific_impulse.

⁴⁹² https://en.wikipedia.org/wiki/Specific_impulse#General_definition.

Table 27. Specific energy of fuel-oxidant materials during nonambient combustion (theoretical materials indicated in red)⁴⁹³

Fuel-Oxidant Materials	Specific Energy (MJ/kg)	Fuel-Oxidant Materials	Specific Energy (MJ/kg)
Metals and Elements		Nitromethane CH ₃ NO ₂ , liquid (with LOX)	7.572
Beryllium Be (with LOX)	23.960	Glucose C ₆ H ₁₂ O ₆ , solid (with LOX)	7.554
Lithium Li (with LOX)	19.860	1-nitroprismane C ₆ H ₅ NO ₂ (theor.) (with LOX)	6.788
Boron B (with LOX)	18.017	1,1-dinitropropane C ₃ H ₆ N ₂ O ₄ , liquid (w/LOX)	6.763
Aluminum Al (with LOX)	16.431	Tetranitratroxy carbon (theoretical) (with LOX)	3.365
Silicon Si (with LOX)	15.183		
Magnesium Mg (with LOX)	14.804	Organometallics	
Scandium Sc (with LOX)	13.841	Methyl lithium LiCH ₃ (with LOX)	13.605
Solid hydrogen H ₂ (with solid O ₂)	13.444	Trimethylaluminum Al(CH ₃) ₃ , liquid (w/LOX)	12.048
Liquid molecular hydrogen H ₂ (with LOX)	13.444	Ethyl lithium LiC ₂ H ₅ (with LOX)	11.757
Carbon, as C ₂₀ fullerene (with LOX)	12.534	Dimethylberyllium Be(CH ₃) ₂ (with LOX)	11.251
Titanium Ti (with LOX)	11.827	Butyllithium LiC ₄ H ₉ (with LOX)	11.117
Calcium Ca (with LOX)	11.339	Diethylzinc Zn(C ₂ H ₅) ₂ , liquid (with LOX)	9.704
Phosphorus P (with LOX)	10.507	Dimethylzinc Zn(CH ₃) ₂ (with LOX)	9.038
Carbon, as C ₆₀ fullerene (with LOX)	9.886	Triethylaluminum Al ₂ (C ₂ H ₅) ₆ , liquid (w/LOX)	5.676
Carbon, as diamond C (with LOX)	8.984	Dimethylmercury Hg(CH ₃) ₂ , liquid (w/LOX)	4.651
Carbon, as graphite C (with LOX)	8.943	Trimethylmercury Hg(CH ₃) ₃ , liquid (w/LOX)	4.636
Zirconium Zr (with LOX)	8.766		
Vanadium V (with LOX)	8.564	Other Oxygen Combustibles	
Chromium Cr (with LOX)	7.421	Octasilacubane Si ₈ H ₈ (theoretical) (with LOX)	15.306
Sodium Na (with LOX)	6.603	BN-prismane B ₃ N ₃ H ₆ (theoretical) (with LOX)	13.915
Cerium Ce (with LOX)	6.337	Diborane + Hydrazine (with LOX)	13.570
Strontium Sr (with LOX)	5.714	N ₁₈ H ₆ (theoretical) (with LOX)	11.520
Hafnium Hf (with LOX)	5.439	Borazine B ₃ N ₃ H ₆ , liquid (with LOX)	10.474
Iron Fe (with LOX)	5.161	Hydrazine N ₂ H ₄ , liquid (with LOX)	9.720
Sulfur S (with LOX)	4.633	Ammonia NH ₃ , liquid (with LOX)	9.341
Tantalum Ta (with LOX)	4.631	Hydronitrogen polymer N ₁₀ H ₁₂ (with LOX)	8.871
Zinc Zn (with LOX)	4.306	Tetrazene H ₂ N-NH-N=NH solid (with LOX)	8.533
Uranium U (with LOX)	4.246	Ammonium azide NH ₄ N ₃ solid (with LOX)	6.511
Neptunium Np (with LOX)	4.011	Nickel tetracarbonyl Ni(CO) ₄ (with LOX)	5.821
Potassium K (with LOX)	4.008	Cobalt octacarbonyl Co ₂ (CO) ₈ (with LOX)	3.762
Plutonium Pu (with LOX)	3.826		
Tungsten W (with LOX)	3.636	Nitrogen Combustibles	
Nickel Ni (with LOX)	3.213	Beryllium Be (with LN ₂)	10.309
Cobalt Co (with LOX)	3.178	Boron B (with LN ₂)	10.161
Rubidium Rb (with LOX)	2.372	Aluminum Al (with LN ₂)	7.756
Cesium Cs (with LOX)	1.736	Titanium Ti (with LN ₂)	5.460
Lead Pb (with LOX)	1.158	Silicon Si (with LN ₂)	5.311
		Lithium Li (with LN ₂)	4.703
Hydrides		Magnesium Mg (with LN ₂)	4.569
Beryllium monohydride BeH (theor.) (with LOX)	30.941	Zirconium Zr (with LN ₂)	3.470
Beryllium dihydride BeH ₂ (with LOX)	23.651	Cerium Ce (with LN ₂)	2.123
Aluminum monohydride AlH (with LOX)	20.333	Phosphorus P (with LN ₂)	1.982
Lithium borohydride LiBH ₄ (with LOX)	19.857		
Beryllium borohydride Be(BH ₄) ₂ (with LOX)	16.437	Carbon Dioxide Combustibles	
Lithium octahydride LiH ₈ (theor.) (with LOX)	15.075	Aluminum Al (with CO ₂ (s))	9.000

⁴⁹³ Data from Table A4 in Appendix A.4.

Silane SiH ₄ (with LOX)	14.880	Magnesium Mg (with CO ₂ (s))	8.747
Alane AlH ₃ (with LOX)	14.744	Titanium Ti (with CO ₂ (s))	6.007
Magnesium borohydride Mg(BH ₄) ₂ (with LOX)	14.066		
Lithium hydride LiH (with LOX)	13.695	Water Combustibles	
Germane GeH ₄ (with LOX)	8.179	Lithium Li (with H ₂ O)	9.840
Sulfanyl HS (with LOX)	7.396	Aluminum Al (with H ₂ O)	8.796
Sodium hydride NaH (with LOX)	6.708	Magnesium Mg (with H ₂ O)	8.511
Arsine AsH ₃ (with LOX)	6.021	Chlorine trifluoride ClF ₃ (with H ₂ O)	2.066
Potassium hydride KH (with LOX)	4.547	Cesium Cs (with H ₂ O)	1.163
Uranium hydride UH ₃ (with LOX)	4.444		
Rubidium hydride RbH (with LOX)	2.833	Nonambient Combustibles: Halogen Oxidants	
Cesium hydride CsH (with LOX)	2.131	Lithium + Fluorine	23.784
		Beryllium + Fluorine	21.489
Boranes		Beryllium + Fluorine perchlorate (FCIO ₄)	19.767
Boron monohydride BH (theor.) (with LOX)	27.397	Beryllium + Perchloryl fluoride (FCIO ₃)	18.497
Borane BH ₃ (with LOX)	17.638	Lithium + Fluorine perchlorate (FCIO ₄)	18.371
Decaborane B ₁₀ H ₁₄ (with LOX)	16.913	Magnesium + Fluorine	18.042
Pentaborane B ₅ H ₉ (with LOX)	16.739	Beryllium + Dioxygen difluoride (O ₂ F ₂ , aka. FOOF)	18.041
Diborane B ₂ H ₆ (with LOX)	16.492	Beryllium + Tetrafluorohydrazine (N ₂ F ₄)	16.803
closo-2,4-C ₂ B ₃ H ₇ carborane (with LOX)	15.257	Boron + Fluorine	16.770
1,7-C ₂ B ₁₀ H ₁₁ -1-CH ₃ carborane (with LOX)	14.719	Beryllium + Oxygen difluoride (OF ₂)	15.972
Iminoborane HNBH (with LOX)	13.997	Silicon + Fluorine	15.514
Trimethylborane B(CH ₃) ₃ (with LOX)	12.061	Boron + Fluorine perchlorate (FCIO ₄)	14.573
Triethylborane B(C ₂ H ₅) ₃ (with LOX)	11.475	Aluminum + Fluorine perchlorate (FCIO ₄)	14.443
Ammonia borane H ₃ NBH ₃ (with LOX)	10.787	Aluminum + Tetrafluorohydrazine (N ₂ F ₄)	14.357
		Aluminum + Fluorine	14.345
Silanes		Sodium + Fluorine	13.667
Disilane Si ₂ H ₆ (with LOX)	15.098	Hydrogen + Fluorine	13.665
Silane SiH ₄ (with LOX)	14.727	Aluminum + Dichlorine heptoxide (Cl ₂ O ₇)	13.561
		Aluminum + Chlorine trifluoride (ClF ₃)	12.651
Phosphanes		Scandium + Fluorine	12.225
Phosphine PH ₃ (with LOX)	14.033	Aluminum + Dioxygen difluoride (O ₂ F ₂ , aka. FOOF)	10.692
Trisilylphosphine P(SiH ₃) ₃ (with LOX)	13.963	Carbon + Fluorine	10.609
Diphosphane P ₂ H ₆ (with LOX)	11.130	Aluminum + Dibromine pentoxide (Br ₂ O ₅)	9.848
		Beryllium + Nitrosyl tetrafluorochlorate (NOClF ₄)	9.191
Metal Borides		Beryllium + Chlorine pentafluoride (ClF ₅)	8.217
Diberyllium diboride Be ₂ B ₂ (theor.) (w/LOX)	28.763	Aluminum + Oxygen difluoride (OF ₂)	8.102
Dilithium diboride Li ₂ B ₂ (theor.) (with LOX)	26.358	Beryllium + Chlorine trifluoride (ClF ₃)	7.747
Beryllium diboride BeB ₂ (with LOX)	19.767	Aluminum + Diiodine hexoxide (I ₂ O ₆)	7.118
		Hydrazine + Fluorine	6.532
Solid Nitrides		Uranium + Fluorine	6.099
Beryllium nitride Be ₃ N ₂ (with LOX)	15.297	Dimethylmercury HgC ₂ H ₆ + FOOF (O ₂ F ₂)	5.972
Lithium nitride Li ₃ N (with LOX)	12.398	Tungsten + Fluorine	5.782
Silicon nitride Si ₃ N ₄ (with LOX)	8.347	Thorium + Fluorine	5.711
Aluminum nitride AlN (with LOX)	8.000	Hydrogen + Chlorine trifluoride (ClF ₃)	4.386
Boron nitride BN (with LOX)	7.725	Cesium + Fluorine	3.645
		Boron + Chlorine	3.643
Organics		Hydrogen + Chlorine	2.648
Pyramidane C ₅ H ₄ (theoretical) (with LOX)	15.234	Chlorine + Fluorine	1.764
Tetrahdrane C ₄ H ₄ (theoretical) (with LOX)	14.906	Nonambient Combustibles: O_n-allotrope Oxidants	
[3.3.3]fenestrane C ₅ H ₆ (with LOX)	13.869	Beryllium + Octaoxygen	26.360
Bihexaplane C ₁₇ H ₁₆ (with LOX)	13.487	Beryllium + Ozone	26.280
Cyclobutadiene C ₄ H ₄ (with LOX)	13.019	Lithium + Ozone	21.533
Cubane C ₆ H ₆ , solid (with LOX)	12.811	Boron + Ozone	20.345
[1.1.1]Propellane C ₅ H ₆ (with LOX)	12.774	Aluminum + Octaoxygen	17.843
Bicyclobutane C ₄ H ₆ , liquid (with LOX)	12.130	Aluminum + Ozone	17.824
RP-1 rocket fuel ~kerosene (with LOX)	12.103	Beryllium nitride + Ozone	17.750
Diazatetrahdrane C ₂ N ₂ H ₂ (theor.) (w/LOX)	12.015	Magnesium + Ozone	16.104
Acetylene C ₂ H ₂ (with LOX)	11.830	Hydrogen + Ozone	16.056
Diacetylene C ₄ H ₂ (with LOX)	11.701	Acetylene + Octaoxygen (O ₈)	14.151
Tetrapropargylammonium tetraethynylborate (w/LOX)	11.603	Acetylene + Ozone (O ₃)	14.057

Triacetylene C ₆ H ₂ (with LOX)	11.525	Lithium borohydride + Ozone	9.112
Prismane C ₆ H ₆ , liquid (with LOX)	11.487	Hafnium + Ozone	5.891
Tetraacetylene C ₈ H ₂ (with LOX)	11.486		
Butatriene C ₄ H ₄ (with LOX)	11.368	Nonambient Combustibles: Nitrate Oxidants	
Cyclobutene C ₄ H ₆ , liquid (with LOX)	11.217	Beryllium + Trinitramide	18.980
Ethylene C ₂ H ₄ (with LOX)	11.201	Lithium + Trinitramide	16.327
Cyclopropane C ₃ H ₆ , liquid (with LOX)	11.177	Boron + Trinitramide	14.303
Methane CH ₄ , liquid (with LOX)	11.138	Aluminum + Trinitramide	13.846
Propadiene C ₃ H ₄ (with LOX)	11.012	Beryllium + Hydroxylammonium nitrate	12.018
Propyne C ₃ H ₄ (with LOX)	11.005	Hydrogen + Trinitramide	10.366
Ethane C ₂ H ₆ , liquid (with LOX)	10.988	Beryllium + Hydrazinium nitroformate	9.389
Benzvalene C ₆ H ₆ (with LOX)	10.893		
Propane C ₃ H ₈ , liquid (with LOX)	10.877	Nonambient Combustibles: Thermite/Thermitic	
Ethanol C ₂ H ₅ OH, liquid (with LOX)	10.873	NO ₂ + Al	14.065
Tripropargyl amine C ₉ H ₉ N (with LOX)	10.855	NO + Al	13.542
Cyclobutane C ₄ H ₈ , liquid (with LOX)	10.802	H ₂ O ₂ + Al	13.238
Butane C ₄ H ₁₀ , liquid (with LOX)	10.785	BO + Al (theoretical)	13.060
Dipropargylammonium C ₆ H ₇ N (with LOX)	10.762	MgO ₂ + Al	12.708
Butyne C ₄ H ₆ (with LOX)	10.648	NO ₂ + Sc	12.327
1,2-nitroprismane C ₆ H ₄ (NO ₂) ₂ (theor.) (w/LOX)	10.640	P ₂ O ₅ + Al	11.007
Octane C ₈ H ₁₈ ~ gasoline (with LOX)	10.623	C ₃ O ₂ + Al	9.872
1,2-Butadiene C ₄ H ₆ (with LOX)	10.604	CO + Al	9.710
Ethylene oxide C ₂ H ₄ O, liquid (with LOX)	10.524	NaO ₂ + Al	9.451
Quadricyclane C ₇ H ₈ , liquid (with LOX)	10.447	Mn ₂ O ₇ + Al	9.128
1,3-Butadiene C ₄ H ₆ (with LOX)	10.387	SO ₃ + Al	9.104
Propylene C ₃ H ₆ (with LOX)	10.371	CO ₂ + Al	9.050
Dodecane C ₁₂ H ₂₆ (with LOX)	10.363	H ₂ O (ice) + Al	8.796
Adamantane C ₁₀ H ₁₆ (with LOX)	10.322	RuO ₄ + Al	8.427
Propylene oxide C ₃ H ₆ O, liquid (with LOX)	10.317	B ₂ O ₂ + Al	7.418
Octanol C ₈ H ₁₇ OH, liquid (with LOX)	10.288	SeO ₃ + Al	6.409
Dimethyl ether H ₃ COCH ₃ , liquid (with LOX)	10.282	ZnO ₂ + Al	6.200
Syntin rocket fuel C ₁₀ H ₁₆ (with LOX)	10.274	RaO ₂ + Al (theoretical)	5.941
Benzene C ₆ H ₆ , liquid (with LOX)	10.273	Li ₂ O ₂ + Al	5.886
Diethyl ether C ₄ H ₁₀ O, liquid (with LOX)	10.259	OsO ₄ + Al	5.633
Cholesterol C ₂₇ H ₄₆ O (with LOX)	10.208	Ag ₂ O ₂ + Al	5.430
Pagodane C ₂₀ H ₂₀ (with LOX)	10.189	MoO ₃ + Al	4.702
Dicyanoacetylene C ₄ N ₂ , liquid (with LOX)	10.142	Rh ₂ O ₃ + Al	4.318
Cyclopentane C ₅ H ₁₀ , liquid (with LOX)	10.094	CuO + Al (Copper Thermite)	4.096
1,2,4,5-nitroprismane C ₆ H ₂ (NO ₂) ₄ (theor.) (w/LOX)	10.089	Fe ₂ O ₃ + Al (Iron Thermite)	3.981
Butyraldehyde C ₄ H ₈ O, liquid (with LOX)	10.036	CoO + Al	3.448
Butanol C ₄ H ₉ OH, liquid (with LOX)	10.034	NiO + Al	3.439
Fuel Oil #2, liquid (with LOX)	9.931	PdO + Al	3.381
Napalm-B, liquid (with LOX)	9.903	FeO + Al	3.197
Propanol C ₃ H ₇ OH, liquid (with LOX)	9.897	WO ₃ + Al	2.913
1,2,3,4,5-nitroprismane C ₆ H(NO ₂) ₅ (theor.) (w/LOX)	9.883		
Methylcyclohexane C ₇ H ₁₄ , liquid (with LOX)	9.804	Nonambient Combustibles: Propellants/Explosives	
Diesel fuel ~C ₁₂ H ₂₃ (with LOX)	9.796	LiClO ₄ + Be	17.394
Fat (oxidation, with LOX)	9.691	Aerozine 50 + Nitrogen tetroxide	13.333
Tetracene C ₁₈ H ₁₂ , solid (with LOX)	9.672	Diborane + Nitric oxide	12.788
UDMH C ₂ H ₈ N ₂ (with LOX)	9.569	LiClO ₄ + B	12.772
Pyridine C ₅ H ₅ N, liquid (with LOX)	9.566	LiClO ₄ + Al	12.687
DMAZ C ₄ H ₁₀ N ₄ (with LOX)	9.565	Aluminum + Carbenium triazidoperchlorate	12.045
Dipropyl ether C ₆ H ₁₄ O, liquid (with LOX)	9.534	KClO ₄ + Al (Flash powder)	10.617
Acetone C ₃ H ₆ O, liquid (with LOX)	9.522	AgClO ₄ + Be	10.412
Cyanogen C ₂ N ₂ , liquid (with LOX)	9.483	KClO ₃ + Al (Flash powder)	9.683
Propargyl alcohol C ₃ H ₄ O, liquid (with LOX)	9.408	Aluminum + Ammonium dinitramide	9.063
Hydroperoxymethane CH ₃ O ₂ (with LOX)	9.238	Acetylene + Nitrogen tetroxide	9.007
Diethylenetriamine C ₄ H ₁₃ N ₃ (with LOX)	9.194	Space Shuttle Solid Rocket Booster (SRB) propellant	8.502
Dimethylfuran C ₆ H ₈ O, liquid (with LOX)	9.088	Ammonal	8.415
Methanol CH ₃ OH, liquid (with LOX)	8.938	Hydrazine + Nitrogen tetroxide	7.500
Picryl propyl ether C ₉ H ₉ N ₃ O ₇ (with LOX)	8.902	UDMH + Nitrogen tetroxide	7.459
HMTD C ₆ H ₁₂ N ₂ O ₆ (with LOX)	8.625	KNO ₃ + Mg (Flash powder)	7.346

Heptanitrocubane $C_8H_7N_7O_{14}$ (with LOX)	8.519	Hydrogen + Nitrous oxide	7.022
Nitroethane $C_2H_5NO_2$, liquid (with LOX)	8.484	Armstrong's mixture	5.512
Benzyne C_6H_4 (theoretical) (with LOX)	8.454	ANNM	4.530
DNAN $C_7H_6N_2O_5$ (with LOX)	8.436	Panclastites	4.292
TNT, burned (with LOX)	8.354	ANFO	3.789
HNS $C_{14}H_6N_6O_{12}$ (with LOX)	8.342	Gunpowder (black powder)	3.000
TACOT $C_{12}H_4N_8O_8$ (with LOX)	7.781	Rocket candy	2.178
1,2,3-nitroprismane $C_6H_3(NO_2)_3$ (theor.) (w/LOX)	7.638	ZS propellants	2.113

Table 28. Energy density of fuel-oxidant materials during nonambient combustion (theoretical materials indicated in red)⁴⁹⁴

Fuel-Oxidant Materials	Energy Density (MJ/L)	Fuel-Oxidant Materials	Energy Density (MJ/L)
Metals and Elements		1-nitroprismane C ₆ H ₅ NO ₂ (theoretical) (with LOX)	8.180
Beryllium Be (with LOX)	31.693	Tetranitratocarbon (theoretical) (with LOX)	5.018
Hafnium Hf (with LOX)	27.590		
Aluminum Al (with LOX)	26.989	Organometallics	
Boron B (with LOX)	26.852	Dimethylmercury Hg(CH ₃) ₂ , liquid (with LOX)	15.737
Neptunium Np (with LOX)	26.774	Methylithium LiCH ₃ (with LOX)	13.510
Scandium Sc (with LOX)	26.454	Ethyllithium LiC ₂ H ₅ (with LOX)	12.429
Plutonium Pu (with LOX)	26.139	Trimethylaluminum Al(CH ₃) ₃ , liquid (with LOX)	12.053
Zirconium Zr (with LOX)	25.714	Diethylzinc Zn(C ₂ H ₅) ₂ , liquid (with LOX)	11.278
Titanium Ti (with LOX)	24.419	Dimethylberyllium Be(CH ₃) ₂ (with LOX)	11.190
Uranium U (with LOX)	23.833	Butyllithium LiC ₄ H ₉ (with LOX)	10.921
Silicon Si (with LOX)	22.718	Dimethylzinc Zn(CH ₃) ₂ (with LOX)	10.919
Cerium Ce (with LOX)	22.382	Trimethylmercury Hg(CH ₃) ₃ , liquid (with LOX)	8.748
Tantalum Ta (with LOX)	22.288	Triethylaluminum Al ₂ (C ₂ H ₅) ₆ , liquid (with LOX)	5.921
Magnesium Mg (with LOX)	21.307		
Chromium Cr (with LOX)	19.965	Other Oxygen Combustibles	
Vanadium V (with LOX)	17.876	N ₁₈ H ₆ (theoretical) (with LOX)	22.031
Solid hydrogen H ₂ (with solid O ₂)	17.664	Octasilacubane Si ₈ H ₈ (theoretical) (with LOX)	20.105
Carbon, as C ₂₀ fullerene (with LOX)	17.316	BN-prismane B ₃ N ₃ H ₆ (theoretical) (with LOX)	17.547
Tungsten W (with LOX)	16.335	Hydronitrogen polymer N ₁₀ H ₁₂ (with LOX)	13.750
Phosphorus P (with LOX)	16.043	Diborane + Hydrazine (with LOX)	12.199
Calcium Ca (with LOX)	15.955	Tetrazene H ₂ N-NH-N=NH solid (with LOX)	10.813
Zinc Zn (with LOX)	15.108	Hydrazine N ₂ H ₄ , liquid (with LOX)	10.473
Iron Fe (with LOX)	14.639	Borazine B ₃ N ₃ H ₆ , liquid (with LOX)	10.294
Carbon, as diamond C (with LOX)	12.549	Ammonia NH ₃ , liquid (with LOX)	8.326
Strontium Sr (with LOX)	12.542	Ammonium azide NH ₄ N ₃ solid (with LOX)	8.251
Lithium Li (with LOX)	12.491	Nickel tetracarbonyl Ni(CO) ₄ (with LOX)	7.516
Carbon, as C ₆₀ fullerene (with LOX)	12.316	Cobalt octacarbonyl Co ₂ (CO) ₈ (with LOX)	5.448
Carbon, as graphite C (with LOX)	11.781		
Nickel Ni (with LOX)	11.650	Nitrogen Combustibles	
Cobalt Co (with LOX)	11.553	Titanium Ti (with LN ₂)	12.071
Sodium Na (with LOX)	6.812	Zirconium Zr (with LN ₂)	11.661
Sulfur S (with LOX)	6.812	Aluminum Al (with LN ₂)	11.648
Lead Pb (with LOX)	5.983	Beryllium Be (with LN ₂)	11.501
Liquid molecular hydrogen H ₂ (with LOX)	5.735	Boron B (with LN ₂)	11.455
Potassium K (with LOX)	3.883	Cerium Ce (with LN ₂)	8.605
Rubidium Rb (with LOX)	3.322	Silicon Si (with LN ₂)	7.081
Cesium Cs (with LOX)	2.954	Magnesium Mg (with LN ₂)	6.018
		Lithium Li (with LN ₂)	2.908
Hydrides		Phosphorus P (with LN ₂)	2.669
Beryllium dihydride BeH ₂ (with LOX)	22.650		
Uranium hydride UH ₃ (with LOX)	18.565	Carbon Dioxide Combustibles	
Lithium borohydride LiBH ₄ (with LOX)	18.529	Aluminum Al (with CO ₂ (s))	17.363
Alane AlH ₃ (with LOX)	18.429	Magnesium Mg (with CO ₂ (s))	14.413
Beryllium borohydride Be(BH ₄) ₂ (with LOX)	15.568	Titanium Ti (with CO ₂ (s))	14.227
Magnesium borohydride Mg(BH ₄) ₂ (with LOX)	15.329		

⁴⁹⁴ Data from **Table A4** in **Appendix A.4**.

Lithium hydride LiH (with LOX)	13.554	Water Combustibles	
Silane SiH ₄ (with LOX)	12.883	Aluminum Al (with H ₂ O)	12.838
Germane GeH ₄ (with LOX)	10.268	Magnesium Mg (with H ₂ O)	11.250
Arsine AsH ₃ (with LOX)	8.460	Lithium Li (with H ₂ O)	7.935
Sodium hydride NaH (with LOX)	8.429	Chlorine trifluoride ClF ₃ (with H ₂ O)	3.009
Potassium hydride KH (with LOX)	5.805	Cesium Cs (with H ₂ O)	2.019
Rubidium hydride RbH (with LOX)	5.355		
Cesium hydride CsH (with LOX)	5.120	Nonambient Combustibles: Halogen Oxidants	
Boranes		Beryllium + Fluorine	41.736
Decaborane B ₁₀ H ₁₄ (with LOX)	18.269	Boron + Fluorine	33.940
closo-2,4-C ₂ B ₅ H ₇ carborane (with LOX)	16.478	Magnesium + Fluorine	33.754
1,7-C ₂ B ₁₀ H ₁₁ -1-CH ₃ carborane (with LOX)	15.900	Aluminum + Dibromine pentoxide (Br ₂ O ₅)	32.773
Pentaborane B ₅ H ₉ (with LOX)	15.815	Silicon + Fluorine	31.917
Diborane B ₂ H ₆ (with LOX)	13.973	Aluminum + Diiodine hexoxide (I ₂ O ₆)	31.107
Trimethylborane B(CH ₃) ₃ (with LOX)	11.589	Aluminum + Fluorine	30.977
Triethylborane B(C ₂ H ₅) ₃ (with LOX)	11.344	Uranium + Fluorine	30.541
Ammonia borane H ₃ NBH ₃ (with LOX)	10.777	Thorium + Fluorine	30.120
		Beryllium + Oxygen difluoride (OF ₂)	30.105
		Beryllium + Fluorine perchlorate (FCIO ₄)	29.633
Silanes		Aluminum + Dichlorine heptoxide (Cl ₂ O ₇)	29.201
Disilane Si ₂ H ₆ (with LOX)	13.842	Scandium + Fluorine	28.341
Silane SiH ₄ (with LOX)	12.655	Beryllium + Perchloryl fluoride (FCIO ₃)	28.163
		Beryllium + Dioxygen difluoride (O ₂ F ₂ , aka. FOOF)	27.822
Phosphanes		Beryllium + Tetrafluorohydrazine (N ₂ F ₄)	27.443
Trisilylphosphine P(SiH ₃) ₃ (with LOX)	15.782	Lithium + Fluorine	27.257
Phosphine PH ₃ (with LOX)	11.623	Aluminum + Chlorine trifluoride (ClF ₃)	26.000
Diphosphane P ₂ H ₆ (with LOX)	11.006	Aluminum + Tetrafluorohydrazine (N ₂ F ₄)	25.670
		Tungsten + Fluorine	25.564
Metal Borides		Aluminum + Fluorine perchlorate (FCIO ₄)	25.508
Diberyllium diboride Be ₂ B ₂ (theoretical) (with LOX)	39.047	Hydrogen + Fluorine	24.186
Beryllium diboride BeB ₂ (with LOX)	26.714	Carbon + Fluorine	22.229
		Boron + Fluorine perchlorate (FCIO ₄)	22.059
Solid Nitrides		Aluminum + Dioxygen difluoride (O ₂ F ₂ , aka. FOOF)	18.398
Beryllium nitride Be ₃ N ₂ (with LOX)	29.227	Beryllium + Nitrosyl tetrafluorochlorate (NOClF ₄)	17.226
Aluminum nitride AlN (with LOX)	15.476	Sodium + Fluorine	17.186
Silicon nitride Si ₃ N ₄ (with LOX)	15.391	Aluminum + Oxygen difluoride (OF ₂)	16.667
Lithium nitride Li ₃ N (with LOX)	15.062	Lithium + Fluorine perchlorate (FCIO ₄)	16.047
Boron nitride BN (with LOX)	13.369	Beryllium + Chlorine pentafluoride (ClF ₅)	15.542
		Beryllium + Chlorine trifluoride (ClF ₃)	14.533
Organics		Dimethylmercury HgC ₂ H ₆ + FOOF (O ₂ F ₂)	11.813
Pyramidane C ₅ H ₄ (theoretical) (with LOX)	17.890	Hydrazine + Fluorine	11.328
1,2,3,4,5-nitroprismane C ₆ H(NO ₂) ₅ (theor.) (w/LOX)	17.656	Hydrogen + Chlorine trifluoride (ClF ₃)	7.581
Tetrahdrane C ₄ H ₄ (theoretical) (with LOX)	17.459	Cesium + Fluorine	7.057
[3.3.3]fenestrane C ₅ H ₆ (with LOX)	17.040	Boron + Chlorine	5.873
1,2,4,5-nitroprismane C ₆ H ₂ (NO ₂) ₄ (theor.) (w/LOX)	16.394	Hydrogen + Chlorine	3.922
Heptanitrocubane C ₈ HN ₇ O ₁₄ (with LOX)	16.157	Chlorine + Fluorine	3.163
Bihexaplane C ₁₇ H ₁₆ (with LOX)	16.126	Nonambient Combustibles: O_n-allotrope Oxidants	
Cubane C ₆ H ₆ , solid (with LOX)	15.047	Beryllium + Octaoxygen	47.754
Tetrapropargylammonium tetraethynylborate (w/LOX)	14.647	Beryllium + Ozone	46.596
1,2-nitroprismane C ₆ H ₄ (NO ₂) ₂ (theoretical) (w/LOX)	14.542	Aluminum + Octaoxygen	38.972
Diazatetrahdrane C ₂ N ₂ H ₂ (theoretical) (with LOX)	14.375	Hafnium + Ozone	38.871
Prismane C ₆ H ₆ , liquid (with LOX)	14.108	Beryllium nitride + Ozone	38.046
Tripropargyl amine C ₉ H ₉ N (with LOX)	13.358	Aluminum + Ozone	38.033
[1.1.1]Propellane C ₅ H ₆ (with LOX)	13.208	Boron + Ozone	37.068
Dipropargylammonium C ₆ H ₇ N (with LOX)	13.154	Magnesium + Ozone	27.854
Benzvalene C ₆ H ₆ (with LOX)	12.833	Hydrogen + Ozone	22.937
Tetraacetylene C ₈ H ₂ (with LOX)	12.649	Lithium + Ozone	18.249
Pagodane C ₂₀ H ₂₀ (with LOX)	12.544	Acetylene + Octaoxygen (O ₈)	17.281
RP-1 rocket fuel ~kerosene (with LOX)	12.381	Acetylene + Ozone (O ₃)	16.798
Triacetylene C ₆ H ₂ (with LOX)	12.311	Lithium borohydride + Ozone	10.512
Picryl propyl ether C ₉ H ₉ N ₃ O ₇ (with LOX)	12.255		

Bicyclobutane C ₄ H ₆ , liquid (with LOX)	12.237	Nonambient Combustibles: Nitrate Oxidants	
HNS C ₁₄ H ₆ N ₆ O ₁₂ (with LOX)	11.846	Beryllium + Trinitramide	38.521
TNT, burned (with LOX)	11.620	Aluminum + Trinitramide	32.028
Adamantane C ₁₀ H ₁₆ (with LOX)	11.618	Boron + Trinitramide	29.957
Tetracene C ₁₈ H ₁₂ , solid (with LOX)	11.484	Beryllium + Hydroxylammonium nitrate	22.026
Quadricyclane C ₇ H ₈ , liquid (with LOX)	11.474	Hydrogen + Trinitramide	18.377
Cholesterol C ₂₇ H ₄₆ O (with LOX)	11.396	Beryllium + Hydrazinium nitroformate	17.447
TACOT C ₁₂ H ₄ N ₈ O ₈ (with LOX)	11.385	Lithium + Trinitramide	16.842
Cyclobutene C ₄ H ₆ , liquid (with LOX)	11.316		
Acetylene C ₂ H ₂ (with LOX)	11.097	Nonambient Combustibles: Thermite/Thermite	
Cyclopropane C ₃ H ₆ , liquid (with LOX)	11.064	MgO ₂ + Al	36.515
Benzene C ₆ H ₆ , liquid (with LOX)	10.930	P ₂ O ₅ + Al	34.537
Diacetylene C ₄ H ₂ (with LOX)	10.913	Ag ₂ O ₂ + Al	30.769
Cyclobutane C ₄ H ₈ , liquid (with LOX)	10.894	RaO ₂ + Al (theoretical)	26.899
Ethylene oxide C ₂ H ₄ O, liquid (with LOX)	10.883	Rh ₂ O ₃ + Al	26.078
Syntin rocket fuel C ₁₀ H ₁₆ (with LOX)	10.850	RuO ₄ + Al	26.042
Fuel Oil #2, liquid (with LOX)	10.843	NO ₂ + Al	25.554
Propyne C ₃ H ₄ (with LOX)	10.756	H ₂ O ₂ + Al	25.181
Octanol C ₈ H ₁₇ OH, liquid (with LOX)	10.730	NO ₂ + Sc	25.160
Ethanol C ₂ H ₅ OH, liquid (with LOX)	10.703	Mn ₂ O ₇ + Al	25.139
Propadiene C ₃ H ₄ (with LOX)	10.694	OsO ₄ + Al	23.390
Octane C ₈ H ₁₈ ~ gasoline (with LOX)	10.602	NaO ₂ + Al	22.435
Dodecane C ₁₂ H ₂₆ (with LOX)	10.590	PdO + Al	22.153
Butatriene C ₄ H ₄ (with LOX)	10.570	NO + Al	21.595
Dicyanoacetylene C ₄ N ₂ , liquid (with LOX)	10.561	CuO + Al (Copper Thermite)	20.725
Propylene oxide C ₃ H ₆ O, liquid (with LOX)	10.492	SeO ₃ + Al	20.387
1,2,3-nitroprismane C ₆ H ₃ (NO ₂) ₃ (theor.) (with LOX)	10.485	SO ₃ + Al	19.902
Butyne C ₄ H ₆ (with LOX)	10.470	MoO ₃ + Al	18.363
Napalm-B, liquid (with LOX)	10.451	NiO + Al	17.836
Pyridine C ₅ H ₅ N, liquid (with LOX)	10.430	CoO + Al	17.523
1,2-Butadiene C ₄ H ₆ (with LOX)	10.427	CO ₂ + Al	17.432
DNAN C ₇ H ₆ N ₂ O ₅ (with LOX)	10.411	Fe ₂ O ₃ + Al (Iron Thermite)	16.871
Ethylene C ₂ H ₄ (with LOX)	10.373	WO ₃ + Al	15.897
DMAZ C ₄ H ₁₀ N ₄ (with LOX)	10.370	FeO + Al	14.957
Cyclopentane C ₅ H ₁₀ , liquid (with LOX)	10.330	Li ₂ O ₂ + Al	14.538
Fat (oxidation, with LOX)	10.323	H ₂ O (ice) + Al	12.838
Diesel fuel ~C ₁₂ H ₂₃ (with LOX)	10.300	ZnO ₂ + Al	10.973
Propane C ₃ H ₈ , liquid (with LOX)	10.278	CO + Al	10.635
Butanol C ₄ H ₉ OH, liquid (with LOX)	10.269		
Butane C ₄ H ₁₀ , liquid (with LOX)	10.250	Nonambient Combustibles: Propellants/Explosives	
Butyraldehyde C ₄ H ₈ O, liquid (with LOX)	10.205	LiClO ₄ + Be	39.021
Ethane C ₂ H ₆ , liquid (with LOX)	10.203	LiClO ₄ + Al	32.136
Propargyl alcohol C ₃ H ₄ O, liquid (with LOX)	10.188	LiClO ₄ + B	30.641
Methylcyclohexane C ₇ H ₁₄ , liquid (with LOX)	10.088	Aluminum + Carbenium triazidoperchlorate	30.286
Propanol C ₃ H ₇ OH, liquid (with LOX)	10.050	KClO ₄ + Al (Flash powder)	27.388
Diethyl ether C ₄ H ₁₀ O, liquid (with LOX)	10.037	AgClO ₄ + Be	27.117
1,3-Butadiene C ₄ H ₆ (with LOX)	10.000	KClO ₃ + Al (Flash powder)	23.489
Dimethyl ether H ₃ COCH ₃ , liquid (with LOX)	9.932	Aluminum + Ammonium dinitramide	17.726
Cyanogen C ₂ N ₂ , liquid (with LOX)	9.910	Space Shuttle Solid Rocket Booster (SRB) propellant	17.635
Diethylenetriamine C ₄ H ₁₃ N ₃ (with LOX)	9.904	Ammonal	15.828
Propylene C ₃ H ₆ (with LOX)	9.897	KNO ₃ + Mg (Flash powder)	14.337
Glucose C ₆ H ₁₂ O ₆ , solid (with LOX)	9.860	Aerzine 50 + Nitrogen tetroxide	14.187
Hydroperoxymethane CH ₄ O ₂ (with LOX)	9.711	Armstrong's mixture	13.816
Dimethylfuran C ₆ H ₈ O, liquid (with LOX)	9.639	Diborane + Nitric oxide	13.084
UDMH C ₂ H ₈ N ₂ (with LOX)	9.574	Acetylene + Nitrogen tetroxide	10.410
Dipropyl ether C ₆ H ₁₄ O, liquid (with LOX)	9.563	Hydrazine + Nitrogen tetroxide	9.213
Acetone C ₃ H ₆ O, liquid (with LOX)	9.527	UDMH + Nitrogen tetroxide	8.922
Methane CH ₄ , liquid (with LOX)	9.479	ZS propellants	8.340
Benzyne C ₆ H ₄ (theoretical) (with LOX)	9.446	Hydrogen + Nitrous oxide	8.261
Nitroethane C ₂ H ₅ NO ₂ , liquid (with LOX)	9.313	ANNM	6.667
Methanol CH ₃ OH, liquid (with LOX)	8.677	Panclastites	5.862
Nitromethane CH ₃ NO ₂ , liquid (with LOX)	8.627	Gunpowder (black powder)	5.254

HMTD $C_6H_{12}N_2O_6$ (with LOX)	8.519	Rocket candy	4.120
1,1-dinitropropane $C_3H_6N_2O_4$, liquid (with LOX)	8.507	ANFO	3.184

4.2.3 Ambient Chemical Combustion

Chemical fuels may undergo combustion with an oxidant that is present in excess quantities in the external environment in which the energy storage system is embedded. In ambient combustion, only the fuel is contained entirely within the energy storage system, and the oxidant is provided from the environment. Hence the mass of the energy storage material is the mass of the fuel alone. An automobile that burns gasoline while drawing oxygen from ambient air is one commonplace example of such a system; fuel-air explosives⁴⁹⁵ and food⁴⁹⁶ are additional examples.

The specific energy (**Table 29**; range **1.3-121 MJ/kg**) and energy density (**Table 30**; range **4.2-271 MJ/L**) of fuel materials during ambient combustion are grouped into 16 classes for greater clarity:

- (1) metals and elements (**1.3-121.0 MJ/kg; 4.2-271.4 MJ/L**);
- (2) hydrides (**2.7-105.2 MJ/kg; 9.2-83.6 MJ/L**);
- (3) boranes (**34.9-101.7 MJ/kg; 28.0-61.7 MJ/L**);
- (4) silanes (**42.3-43.2 MJ/kg; 25.2-28.7 MJ/L**);
- (5) phosphanes (**20.1-37.3 MJ/kg; 14.9-41.4 MJ/L**);
- (6) metal borides (**10.4-86.9 MJ/kg; 102.9-191.1 MJ/L**);
- (7) intermetallics (**17.5-27.5 MJ/kg; 51.4-100.0 MJ/L**);
- (8) solid carbides (**6.4-51.6 MJ/kg; 43.8-130.1 MJ/L**);
- (9) solid nitrides (**12.7-22.0 MJ/kg; 26.6-59.6 MJ/L**);
- (10) metal phosphides (**6.0-27.0 MJ/kg; 35.1-80.1 MJ/L**);
- (11) organics (**3.7-60.9 MJ/kg; 5.7-92.0 MJ/L**);
- (12) organometallics (**7.2-53.2 MJ/kg; 18.7-41.6 MJ/L**);
- (13) other oxygen combustibles (**6.9-39.0 MJ/kg; 9.1-60.0 MJ/L**);
- (14) nitrogen combustibles (**2.3-23.3 MJ/kg; 4.2-54.5 MJ/L**);
- (15) carbon dioxide combustibles (**11.5-20.0 MJ/kg; 28.9-54.0 MJ/L**); and
- (16) water combustibles (**2.9-35.4 MJ/kg; 5.1-47.5 MJ/L**).

Here we have combustion requiring a fuel and oxidizer, but the oxidizer is provided free from the environment (e.g., oxygen in the air). The original data supporting the numbers listed in both tables are compiled in **Table A4** in **Appendix A**; fuel materials that have at least some theoretical support but have not yet been synthesized experimentally are indicated in red. Note that the reaction energies used to compile the energy density figures assume the use of high-density LOX, but the ambient oxygen molecules would have to be extracted from the air (20.95%

⁴⁹⁵ https://en.wikipedia.org/wiki/Thermobaric_weapon.

⁴⁹⁶ A 0.146 kg ham and cheese sandwich has 352 kilocalories of metabolizable chemical energy (https://www.google.com/search?ei=p6x9XLm8OaS6ggeTgpTgDQ&q=calories+in+ham+and+cheese+sandwich&oq=calories+in+ham+and+cheese+sandwich&gs_l=psy-ab.3.0.0i4j0i22i30i4j0i22i10i30j0i22i30.24520.29710..31830...0.0..0.173.1064.0j7.....0....1..gws-wiz.....0i71j33i10.Qj7Ly2SLSK4.), hence a specific energy of $E_s \sim 10.1 \text{ MJ/kg}$.

O₂) for a minimum separation cost of **0.111 MJ/kg**,⁴⁹⁷ and then be compressed to liquid form for an additional energy cost of **0.727 MJ/kg**,⁴⁹⁸ for a total “air-LOXing deduction” of **0.838 MJ/kg** which should be subtracted from the specific energy of fuels undergoing combustion while drawing oxygen from room temperature ambient air, usually a very small correction of ~1%. A slightly smaller deduction (~**0.75 MJ/kg**) should similarly be made for fuels that are combustible in nitrogen, since nitrogen can also be freely extracted in pure form from ambient air but is present at almost four times higher concentration than oxygen (~**0.02 MJ/kg** for N₂ extraction, but a similar compression cost as for O₂). A slightly larger deduction should be made for fuels that burn in carbon dioxide, which is only 0.04% of air⁴⁹⁹ – CO₂ is extractable directly from the atmosphere using nanoscale sorting devices at an energy cost of ~88 zJ/molecule⁵⁰⁰ or ~**1.2 MJ/kg** CO₂. Water combustibles will require a slightly larger or smaller deduction than for oxygen, depending on circumstances – H₂O is present in air⁵⁰¹ at 0.001%-5% for use during air-breathing combustion, but is available much more abundantly in seawater (~96.5%)⁵⁰² or freshwater (~99.95%)⁵⁰³ in the case of underwater operation.

The fuel with the highest specific energy for ambient combustion is liquid (or solid) H₂+O₂ at **121.0 MJ/kg**. This is great for any application in which minimum mass without regard to volume is a design objective, such as aircraft that use the stored energy to oppose the force of gravity that acts upon the mass of the fuel. However, this fuel-oxidant combination may be a poor choice in applications where minimum volume is a design objective (e.g., medical nanorobots), since the energy density of H₂+O₂ even in the difficult-to-use frozen solid form (**72.7 MJ/L**) is poorer than at least 52 other fuels on the list, and the liquid form (**8.6 MJ/L**) has the 6th lowest energy density on the list. Two other fuels that exceed 100 MJ/kg are BeH (**105.2 MJ/kg**) and BH (**101.7 MJ/kg**), but both are only known in gaseous form and thus may be impractical, so we must consider them highly “theoretical”. The next best is beryllium dihydride (BeH₂)⁵⁰⁴ at **92.2 MJ/kg**, an amorphous white solid that decomposes above 523 K and releases beryllium oxide

⁴⁹⁷ The minimum energy cost of extracting O₂ from room temperature air is approximately $(N_A/MW) k_B T \ln(100/23.20) = 0.111 \text{ MJ/kg}$, where $k_B = 1.381 \times 10^{-23} \text{ J/K}$ (Boltzmann constant), $T = 293 \text{ K}$, $N_A = 6.022 \times 10^{23} \text{ molecules/mole}$, $MW = 0.032 \text{ kg/mole}$ for O₂, and O₂ is 23.20% of air by weight (20.95% by volume) (http://www.engineeringtoolbox.com/air-composition-d_212.html).

⁴⁹⁸ The minimum energy cost of compressing pure O₂ from gas at 1 atm to liquid form may be estimated as the sum of the concentration cost from 1.33 kg/m³ at 293 K to 1141 kg/m³ at the boiling point, or $(N_A/MW) k_B T \ln(1141/1.33) = 0.514 \text{ MJ/kg}$, plus the heat of vaporization at the boiling point (0.213 MJ/kg; <http://www.airproducts.com/~media/files/pdf/company/safetygram-6.pdf>), or 0.727 MJ/kg.

⁴⁹⁹ https://en.wikipedia.org/wiki/Atmosphere_of_Earth#Composition.

⁵⁰⁰ Freitas RA Jr. The Nanofactory Solution to Global Climate Change: Atmospheric Carbon Capture. IMM Report No. 45, Dec 2015, “Section 4 Molecular Filters”; <http://www.imm.org/Reports/rep045.pdf>.

⁵⁰¹ https://en.wikipedia.org/wiki/Atmosphere_of_Earth#Composition.

⁵⁰² <https://en.wikipedia.org/wiki/Seawater>.

⁵⁰³ https://en.wikipedia.org/wiki/Fresh_water#Numerical_definition.

⁵⁰⁴ https://en.wikipedia.org/wiki/Beryllium_hydride.

(BeO)⁵⁰⁵ and water when burned in an excess of oxygen at high temperature.⁵⁰⁶ Discounting the still-theoretical lithium octahydride (LiH₈) at **87.9 MJ/kg**, diberyllium diboride (Be₂B₂) at **86.9 MJ/kg**, and dilithium diboride (Li₂B₂) at **74.0 MJ/kg**, and also disregarding borane (BH₃) at **79.0 MJ/kg** which is only known in the gaseous state, the next two highest specific energy candidates are liquid diborane (B₂H₆)⁵⁰⁷ at **73.6 MJ/kg** and solid beryllium borohydride (Be(BH₄)₂) at **70.8 MJ/kg**.

The fuel with the highest energy density for ambient combustion with oxygen is elemental boron at **271.4 MJ/L**. While boron can be difficult to burn with high efficiency in combustion chambers of conventional length, it can be oxidized at reasonable efficiency if the boron particle size is very small, and can be used as a propellant in combination rocket-air-burning engines where there is adequate combustion volume and oxygen from the air.⁵⁰⁸ Micron-size boron particles will burn in oxygen⁵⁰⁹ with an ignition temperature of ~2100 K.⁵¹⁰ Atomic boron has

⁵⁰⁵ “[Particulate] BeO is carcinogenic and may cause chronic beryllium disease. Once fired into solid form, it is safe to handle if not subjected to machining that generates dust. Beryllium oxide ceramic is not a hazardous waste under federal law in the USA.” https://en.wikipedia.org/wiki/Beryllium_oxide#Safety.

⁵⁰⁶ Baumgartner WE, Butts PG. Propellant Composition Containing Beryllium Hydride, Nitrocellulose and Nitrate Co-Plasticizers. U.S. Patent 3861970A, 21 Jan 1975; <https://www.google.com/patents/US3861970>.

⁵⁰⁷ Diborane+oxygen combustion is hypergolic, the boric oxide (B₂O₃) ash is harmless, and the combustion and explosive characteristics of diborane have been extensively studied at least since the early 1950s (e.g., Gammon BE, Genco RS, Gerstein M. A preliminary and analytical evaluation of diborane as a ram-jet fuel, NACA Research Memorandum, Washington DC, 22 Dec 1950; <http://naca.central.cranfield.ac.uk/reports/1950/naca-rm-e50j04.pdf>; Roth W, Bauer WH. Combustion of diborane-oxygen mixtures at the second explosion limit. Symp Intl on Combustion 1955;5(1):710-717; <http://www.sciencedirect.com/science/article/pii/S0082078455800987>). “Diborane ... rocket propellant [has been] experimentally fired but not used in any in service rocket, [and also has been used] as a flame-speed accelerator.” https://en.wikipedia.org/wiki/Diborane#Other_uses. “The toxic effects of diborane are primarily due to its irritant properties”; <https://en.wikipedia.org/wiki/Diborane#Safety>.

⁵⁰⁸ Sutton GP, Biblarz O. Rocket Propulsion Elements, Wiley, 2011; <https://books.google.com/books?id=pFktw0GYSX8C&pg=PT556>. However, under certain conditions its oxidation may not yield B₂O₃ alone owing to the equilibrium with gaseous HBO₂ (Beckstead M, Culick FE, Brill TB, Seitzman J. Investigations of Novel Energetic Materials to Stabilize Rocket Motors. California Institute of Technology Jet Propulsion Center, ONR Contract No. N00014-95-1-1338, 30 Apr 2002, p. 38; https://www.researchgate.net/publication/235121677_Investigations_of_Novel_Energetic_Materials_to_Stabilize_Rocket_Motors).

⁵⁰⁹ King MK. Ignition and combustion of boron particles and clouds. J Spacecraft Rockets 1982;19(4):294-306; <https://arc.aiaa.org/doi/abs/10.2514/3.62256>. Particle sizes 0.05 μm, 3.5 μm, 5 μm: Li SC. Ignition and combustion of boron particles. Intl J Energetic Mater Chem Propulsion 1993;2(1-6):248-271; <http://www.dl.begellhouse.com/journals/17bbb47e377ce023,181301e53c3359b9,5ced96055d5e4f6b.html>. Particle size 3 μm: Yeh CL, Kuo KK. Ignition and combustion of boron particles. Progress in Energy and Combustion Science. 1996;22(6):511-541; <http://www.sciencedirect.com/science/article/pii/S0360128596000123>.

⁵¹⁰ King MK. Boron particle ignition in hot gas streams. Combustion Sci Technol. 1974;8:255-273; <http://www.dtic.mil/dtic/tr/fulltext/u2/a003731.pdf>.

been investigated as a potential rocket fuel,⁵¹¹ and particulate boron has informally been proposed as an alternative fuel for automobiles.⁵¹² Monatomic boron atoms can also be stably added to frozen molecular parahydrogen (p-H₂) at up to 15% concentration⁵¹³ to boost the energy content of solid hydrogen fuel when burned in oxygen.

Leaving aside the still-theoretical diberyllium diboride (Be₂B₂) at **191.1 MJ/L**, the next most energy dense fuels for ambient combustion with oxygen are elemental carbon in the form of the smallest known stable fullerene (C₂₀) at **145.3 MJ/L**, several existing beryllium borides (e.g., BeB₂ (**134.5 MJ/L**), Be₂B (**133.8 MJ/L**), BeB₆ (**133.4 MJ/L**), boron carbide (B₄C) at **130.1 MJ/L**, elemental beryllium (Be) at **123.0 MJ/L**, and elemental carbon as diamond (C) at **115.6 MJ/L**. The most energy-dense organic chemical fuel on the list is [3.3.3]fenestrane (C₅H₆) at **92.0 MJ/L**, a bridged spiro-pentane molecule believed to have the highest strain energy per carbon atom of any observed hydrocarbon to date.⁵¹⁴ Many metal borides produce **103-133 MJ/L**, and pure particulate metals (U, Ta, V, Ti, Np, W, Hf) yield **85-96 MJ/L**, when burned in oxygen. Because of its very low specific gravity, liquid hydrogen (LH₂) at **8.6 MJ/L** has nearly the lowest energy density on the list.

Far lower in energy are dust-air explosions,⁵¹⁵ whose energy release rises as particle size declines below ~350 μm though plateauing at ~1 μm particle size, with a maximum explosive overpressure of, e.g., 6.7 bar (**0.00066 MJ/L**) for zinc dust, 9.1 bar (**0.0009 MJ/L**) for flour dust, and 17.5 bar (**0.0017 MJ/L**) for magnesium dust.⁵¹⁶

An interesting question in nanomedical applications is the maximum energy density of a solution of fuel molecules dissolved in water (e.g., glucose, in the bloodstream) that might be accessible to medical nanorobots to provide onboard power. As shown in **Table 31**, the common solute molecule that provides, after extraction, the highest chemical energy per weight of solution at sublethal concentrations in human blood is acetylene, at **0.052 MJ/kg (0.052 MJ/L)**.

⁵¹¹ Palaszewski B. Launch Vehicle Performance for Bipropellant Propulsion using Atomic Propellants with Oxygen. NASA/TM-2000-209443, Nov 2000; <https://ntrs.nasa.gov/archive/nasa/casi.ntrs.nasa.gov/20010016350.pdf>.

⁵¹² Cowan GRL. Boron: A Better Energy Carrier than Hydrogen? 2009; http://www.eagle.ca/~gcowan/boron_blast.html.

⁵¹³ Jang S, Jang S, Voth GA. Quantum molecular dynamic simulations of low-temperature high energy density matter: solid p-H₂/Li and p-H₂/B. J Phys Chem A.1999;103:9512-9520; <http://www.dtic.mil/dtic/tr/fulltext/u2/a372629.pdf#page=139>. (Para-hydrogen is one of two nuclear spin isomers of hydrogen (https://en.wikipedia.org/wiki/Spin_isomers_of_hydrogen)).

⁵¹⁴ Rasmussen DR. A Theoretical Approach to Molecular Design: Planar-Tetracoordinate Carbon. Ph.D. thesis, Research School of Chemistry, Australian National University, April 2000, Table 4-14, p. 187; <https://openresearch-repository.anu.edu.au/bitstream/1885/48020/19/07Chapter4b.pdf>.

⁵¹⁵ https://en.wikipedia.org/wiki/Dust_explosion.

⁵¹⁶ "Dust Explosions – the basics," 2016; <http://www.dustexplosion.info/dust%20explosions%20-%20the%20basics.htm>.

Table 29. Specific energy of fuel materials during ambient combustion (theoretical materials indicated in red)⁵¹⁷

Fuel Materials	Specific Energy (MJ/kg)	Fuel Materials	Specific Energy (MJ/kg)
Metals and Elements		Organics	
Solid hydrogen H ₂ (excl. O ₂)	121.000	Pyramidane C ₅ H ₄ (theoretical) (excl. O ₂)	60.938
Liquid molecular hydrogen H ₂ (excl. O ₂)	121.000	Tetrahydrene C ₄ H ₄ (theoretical) (excl. O ₂)	60.653
Beryllium Be (excl. O ₂)	66.556	Benzynes C ₆ H ₄ (theoretical) (excl. O ₂)	58.289
Boron B (excl. O ₂)	58.056	[3.3.3]fenestrane C ₅ H ₆ (excl. O ₂)	57.576
Carbon, as C ₂₀ fullerene (excl. O ₂)	45.958	Methane CH ₄ , liquid (excl. O ₂)	55.688
Lithium Li (excl. O ₂)	42.557	Bihexaplane C ₁₇ H ₁₆ (excl. O ₂)	54.682
Carbon, as C ₆₀ fullerene (excl. O ₂)	36.214	[1.1.1]Propellane C ₅ H ₆ (excl. O ₂)	53.030
Carbon, as diamond C (excl. O ₂)	32.942	Cyclobutadiene C ₄ H ₄ (excl. O ₂)	52.975
Carbon, as graphite C (excl. O ₂)	32.792	Cubane C ₆ H ₆ , solid (excl. O ₂)	52.231
Silicon Si (excl. O ₂)	32.536	Ethane C ₂ H ₆ , liquid (excl. O ₂)	51.912
Aluminum Al (excl. O ₂)	31.037	Bicyclobutane C ₄ H ₆ , liquid (excl. O ₂)	51.571
Magnesium Mg (excl. O ₂)	24.551	Propane C ₃ H ₈ , liquid (excl. O ₂)	50.340
Phosphorus P (excl. O ₂)	24.065	Ethylene C ₂ H ₄ (excl. O ₂)	49.466
Scandium Sc (excl. O ₂)	21.222	Cyclopropane C ₃ H ₆ , liquid (excl. O ₂)	49.406
Titanium Ti (excl. O ₂)	19.729	Butane C ₄ H ₁₀ , liquid (excl. O ₂)	49.398
Calcium Ca (excl. O ₂)	15.875	Acetylene C ₂ H ₂ (excl. O ₂)	48.231
Vanadium V (excl. O ₂)	15.295	Octane C ₈ H ₁₈ ~ gasoline (excl. O ₂)	47.895
Zirconium Zr (excl. O ₂)	11.842	Cyclobutane C ₄ H ₈ , liquid (excl. O ₂)	47.772
Sodium Na (excl. O ₂)	11.196	Cyclobutene C ₄ H ₆ , liquid (excl. O ₂)	46.689
Chromium Cr (excl. O ₂)	10.846	Prismane C ₆ H ₆ , liquid (excl. O ₂)	46.786
Sulfur S (excl. O ₂)	9.252	Dodecane C ₁₂ H ₂₆ (excl. O ₂)	46.389
Cerium Ce (excl. O ₂)	7.786	Butatriene C ₄ H ₄ (excl. O ₂)	46.346
Iron Fe (excl. O ₂)	7.379	Propyne C ₃ H ₄ (excl. O ₂)	46.135
Potassium K (excl. O ₂)	7.289	Propadiene C ₃ H ₄ (excl. O ₂)	46.135
Strontium Sr (excl. O ₂)	6.758	Propylene C ₃ H ₆ (excl. O ₂)	45.843
Hafnium Hf (excl. O ₂)	6.415	Diacetylene C ₄ H ₂ (excl. O ₂)	45.400
Tantalum Ta (excl. O ₂)	5.655	Butyne C ₄ H ₆ (excl. O ₂)	45.287
Zinc Zn (excl. O ₂)	5.359	1,2-Butadiene C ₄ H ₆ (excl. O ₂)	45.102
Uranium U (excl. O ₂)	5.007	Cyclopentane C ₅ H ₁₀ , liquid (excl. O ₂)	44.650
Tungsten W (excl. O ₂)	4.586	Fuel Oil #2, liquid (excl. O ₂)	44.381
Neptunium Np (excl. O ₂)	4.553	Benzvalene C ₆ H ₆ (excl. O ₂)	44.366
Plutonium Pu (excl. O ₂)	4.328	Tetrapropargylammonium tetraethynylborate (ex. O ₂)	44.306
Nickel Ni (excl. O ₂)	4.089	Adamantane C ₁₀ H ₁₆ (excl. O ₂)	44.273
Cobalt Co (excl. O ₂)	4.041	1,3-Butadiene C ₄ H ₆ (excl. O ₂)	44.177
Rubidium Rb (excl. O ₂)	3.260	Syntin rocket fuel C ₁₀ H ₁₆ (excl. O ₂)	44.118
Cesium Cs (excl. O ₂)	2.153	Triacetylene C ₆ H ₂ (excl. O ₂)	43.919
Lead Pb (excl. O ₂)	1.337	Tetraacetylene C ₈ H ₂ (excl. O ₂)	43.367
		Methylcyclohexane C ₇ H ₁₄ , liquid (excl. O ₂)	43.350
Hydrides		Diesel fuel ~C ₁₂ H ₂₃ (excl. O ₂)	43.114
Beryllium monohydride BeH (theor.) (excl. O ₂)	105.200	Quadricyclane C ₇ H ₈ , liquid (excl. O ₂)	43.105
Beryllium dihydride BeH ₂ (excl. O ₂)	92.220	RP-1 rocket fuel ~kerosene (excl. O ₂)	43.086
Lithium octahydride LiH ₈ (theor.) (excl. O ₂)	87.919	Cholesterol C ₂₇ H ₄₆ O (excl. O ₂)	42.731
Beryllium borohydride Be(BH ₄) ₂ (excl. O ₂)	70.801	Napalm-B, liquid (excl. O ₂)	41.750
Lithium borohydride LiBH ₄ (excl. O ₂)	63.578	Benzene C ₆ H ₆ , liquid (excl. O ₂)	41.844
Dialuminum borohydride Al ₂ H ₂ (BH ₄) ₄ (excl. O ₂)	58.174	Pagodane C ₂₀ H ₂₀ (excl. O ₂)	41.538

⁵¹⁷ Data from Table A4 in Appendix A.4.

Aluminum borohydride $\text{Al}(\text{BH}_4)_3$, liquid (excl. O_2)	57.730	Tripropargyl amine $\text{C}_9\text{H}_9\text{N}$ (excl. O_2)	40.687
Magnesium borohydride $\text{Mg}(\text{BH}_4)_2$ (excl. O_2)	47.495	Octanol $\text{C}_8\text{H}_{17}\text{OH}$, liquid (excl. O_2)	40.630
Silane SiH_4 (excl. O_2)	44.548	Dietary lipid	39.500
Aluminum monohydride AlH (excl. O_2)	43.571	Dipropargylammonium $\text{C}_6\text{H}_7\text{N}$ (excl. O_2)	39.462
Lithium hydride LiH (excl. O_2)	41.258	Tetracene $\text{C}_{18}\text{H}_{12}$, solid (excl. O_2)	38.180
Lithium aluminum hydride LiAlH_4 (excl. O_2)	39.261	Fat (oxidation, excl. O_2)	37.471
Alane AlH_3 (excl. O_2)	38.333	Diethyl ether $\text{C}_4\text{H}_{10}\text{O}$, liquid (excl. O_2)	36.842
Magnesium hydride MgH_2 (excl. O_2)	29.132	Dipropyl ether $\text{C}_6\text{H}_{14}\text{O}$, liquid (excl. O_2)	36.399
Titanium dihydride TiH_2 (excl. O_2)	21.436	Butanol $\text{C}_4\text{H}_9\text{OH}$, liquid (excl. O_2)	36.032
Sulfanyl HS (excl. O_2)	19.909	Butyraldehyde $\text{C}_4\text{H}_8\text{O}$, liquid (excl. O_2)	34.535
Germane GeH_4 (excl. O_2)	15.013	Pyridine $\text{C}_5\text{H}_5\text{N}$, liquid (excl. O_2)	33.755
Sodium hydride NaH (excl. O_2)	13.417	Propanol $\text{C}_3\text{H}_7\text{OH}$, liquid (excl. O_2)	33.611
Zirconium hydride ZrH_2 (excl. O_2)	12.442	Dimethylfuran $\text{C}_6\text{H}_8\text{O}$, liquid (excl. O_2)	33.299
Arsine AsH_3 (excl. O_2)	9.730	Propylene oxide $\text{C}_3\text{H}_6\text{O}$, liquid (excl. O_2)	33.046
Potassium hydride KH (excl. O_2)	8.628	Dimethyl ether H_3COCH_3 , liquid (excl. O_2)	31.739
Uranium hydride UH_3 (excl. O_2)	5.477	Propargyl alcohol $\text{C}_3\text{H}_4\text{O}$, liquid (excl. O_2)	30.873
Rubidium hydride RbH (excl. O_2)	4.012	Acetone $\text{C}_3\text{H}_6\text{O}$, liquid (excl. O_2)	30.499
Cesium hydride CsH (excl. O_2)	2.704	Hexamine $\text{C}_6\text{H}_{12}\text{N}_4$, solid (excl. O_2)	30.000
Boranes		UDMH $\text{C}_2\text{H}_8\text{N}_2$ (excl. O_2)	29.950
Boron monohydride BH (theor.) (excl. O_2)	101.695	Diethylenetriamine $\text{C}_4\text{H}_{13}\text{N}_3$ (excl. O_2)	29.903
Borane BH_3 (excl. O_2)	78.986	Diazatetrahydrane $\text{C}_2\text{N}_2\text{H}_2$ (theoretical) (excl. O_2)	29.815
Diborane B_2H_6 (excl. O_2)	73.646	Ethanol $\text{C}_2\text{H}_5\text{OH}$, liquid (excl. O_2)	29.783
Pentaborane B_5H_9 (excl. O_2)	67.670	Ethylene oxide $\text{C}_2\text{H}_4\text{O}$, liquid (excl. O_2)	29.615
Decaborane $\text{B}_{10}\text{H}_{14}$ (excl. O_2)	65.630	1-nitroprismane $\text{C}_6\text{H}_5\text{NO}_2$ (theoretical) (excl. O_2)	28.862
closo-2,4- $\text{C}_2\text{B}_3\text{H}_7$ carborane (excl. O_2)	58.284	Dicyanoacetylene C_4N_2 , liquid (excl. O_2)	27.201
1,7- $\text{C}_2\text{B}_{10}\text{H}_{11}$ -1- CH_3 carborane (excl. O_2)	56.456	DMAZ $\text{C}_4\text{H}_{10}\text{N}_4$ (excl. O_2)	27.018
Trimethylborane $\text{B}(\text{CH}_3)_3$ (excl. O_2)	53.488	Dietary protein	23.600
Triethylborane $\text{B}(\text{C}_2\text{H}_5)_3$ (excl. O_2)	50.816	Methanol CH_3OH , liquid (excl. O_2)	22.344
Ammonia borane H_3NBH_3 (excl. O_2)	35.922	Cyanogen C_2N_2 , liquid (excl. O_2)	21.154
Iminoborane HNBH (excl. O_2)	34.888	1,2-nitroprismane $\text{C}_6\text{H}_4(\text{NO}_2)_2$ (theoretical) (ex. O_2)	20.774
Silanes		Dietary carbohydrate	17.600
Silane SiH_4 (excl. O_2)	43.202	Picryl propyl ether $\text{C}_9\text{H}_9\text{N}_3\text{O}_7$ (excl. O_2)	17.048
Disilane Si_2H_6 (excl. O_2)	42.283	Nitroethane $\text{C}_2\text{H}_5\text{NO}_2$, liquid (excl. O_2)	16.618
Phosphanes		DNAN $\text{C}_7\text{H}_6\text{N}_2\text{O}_5$ (excl. O_2)	16.616
Trisilylphosphine $\text{P}(\text{SiH}_3)_3$ (excl. O_2)	37.329	HMTD $\text{C}_6\text{H}_{12}\text{N}_2\text{O}_6$ (excl. O_2)	16.587
Diphosphane P_2H_6 (excl. O_2)	30.308	1,2,3-nitroprismane $\text{C}_6\text{H}_3(\text{NO}_2)_3$ (theoretical) (ex. O_2)	16.244
Phosphine PH_3 (excl. O_2)	20.145	Glucose $\text{C}_6\text{H}_{12}\text{O}_6$, solid (excl. O_2)	15.611
Metal Borides		Hydroperoxymethane CH_4O_2 (excl. O_2)	15.396
Diberyllium diboride Be_2B_2 (theoretical) (excl. O_2)	86.869	TNT, burned (excl. O_2)	14.537
Dilithium diboride Li_2B_2 (theoretical) (excl. O_2)	74.011	1,1-dinitropropane $\text{C}_3\text{H}_6\text{N}_2\text{O}_4$, liquid (excl. O_2)	14.030
Be_3B (excl. O_2)	62.824	HNS $\text{C}_{14}\text{H}_6\text{N}_6\text{O}_{12}$ (excl. O_2)	13.978
Beryllium diboride BeB_2 (excl. O_2)	61.111	TACOT $\text{C}_{12}\text{H}_4\text{N}_8\text{O}_8$ (excl. O_2)	13.557
Be_2B (excl. O_2)	60.333	1,2,4,5-nitroprismane $\text{C}_6\text{H}_2(\text{NO}_2)_4$ (theor.) (ex. O_2)	13.217
BeB_6 (excl. O_2)	57.255	1,2,3,4,5-nitroprismane $\text{C}_6\text{H}(\text{NO}_2)_5$ (theor.) (ex. O_2)	11.188
AlB_{12} (excl. O_2)	52.071	Nitromethane CH_3NO_2 , liquid (excl. O_2)	10.551
MgB_{12} (excl. O_2)	51.870	Cyanuric triazide C_3N_3 , solid (excl. O_2)	10.439
B_6Si (excl. O_2)	48.521	Heptanitrocubane $\text{C}_8\text{HN}_7\text{O}_{14}$ (excl. O_2)	9.332
MgB_6 (excl. O_2)	47.656	Tetranitratocarbon (theoretical) (excl. O_2)	3.714
MgB_4 (excl. O_2)	44.553	Organometallics	
B_3Si (excl. O_2)	43.952	Methyl lithium LiCH_3 (excl. O_2)	53.182
MgB_2 (excl. O_2)	38.319	Ethyl lithium LiC_2H_5 (excl. O_2)	48.333
AlB_2 (excl. O_2)	37.983	Dimethylberyllium $\text{Be}(\text{CH}_3)_2$ (excl. O_2)	48.082
TiB_2 (excl. O_2)	27.043	Butyllithium LiC_4H_9 (excl. O_2)	47.192
VB_2 (excl. O_2)	23.842	Tributylaluminum $\text{Al}(\text{C}_4\text{H}_9)_3$ (excl. O_2)	45.618
ZrB_2 (excl. O_2)	17.901	Diisobutylaluminum hydride (i- C_4H_9) $_2\text{AlH}$ (ex. O_2)	45.091
TaB_2 (excl. O_2)	10.416	Trimethylaluminum $\text{Al}(\text{CH}_3)_3$, liquid (excl. O_2)	44.133
		Triethylphosphine $\text{P}(\text{C}_2\text{H}_5)_3$ (excl. O_2)	43.790
		Trimethylamine $\text{N}(\text{CH}_3)_3$ (excl. O_2)	42.030
		Triethylgallium $\text{Ga}(\text{C}_2\text{H}_5)_3$ (excl. O_2)	31.549
		Diethylzinc $\text{Zn}(\text{C}_2\text{H}_5)_2$, liquid (excl. O_2)	27.304
		Trimethylgallium $\text{Ga}(\text{CH}_3)_3$ (excl. O_2)	25.549

Intermetallics		Trimethylarsine $\text{As}(\text{CH}_3)_3$ (excl. O_2)	23.158
Al_3Mg_4 (excl. O_2)	27.499	Triethylaluminum $\text{Al}_2(\text{C}_2\text{H}_5)_6$, liquid (excl. O_2)	22.383
Mg_2Si (excl. O_2)	26.463	Dimethylzinc $\text{Zn}(\text{CH}_3)_2$ (excl. O_2)	21.152
VSi_2 (excl. O_2)	22.594	Trimethylstibine $\text{Sb}(\text{CH}_3)_3$ (excl. O_2)	17.501
V_2Si (excl. O_2)	17.543	Trimethylbismuthine $\text{Bi}(\text{CH}_3)_3$ (excl. O_2)	11.460
		Dimethylmercury $\text{Hg}(\text{CH}_3)_2$, liquid (excl. O_2)	7.232
		Trimethylmercury $\text{Hg}(\text{CH}_3)_3$, liquid (excl. O_2)	7.210
Solid Carbides		Other Oxygen Combustibles	
B_4C (excl. O_2)	51.574	Diborane + Hydrazine (excl. O_2)	39.028
Be_2C (excl. O_2)	43.711	Octasilacubane Si_8H_8 (theoretical) (excl. O_2)	36.326
Li_2C_2 (excl. O_2)	33.773	BN-prismane $\text{B}_3\text{N}_3\text{H}_6$ (theoretical) (excl. O_2)	34.658
SiC (excl. O_2)	30.923	Borazine $\text{B}_3\text{N}_3\text{H}_6$, liquid (excl. O_2)	26.087
Al_4C_3 (excl. O_2)	30.010	Ammonia NH_3 , liquid (excl. O_2)	22.529
CaC_2 (excl. O_2)	21.217	Hydrazine N_2H_4 , liquid (excl. O_2)	19.441
TiC (excl. O_2)	19.195	Hydronitrogen polymer $\text{N}_{10}\text{H}_{12}$ (excl. O_2)	14.474
VC (excl. O_2)	15.886	N_{18}H_6 (theoretical) (excl. O_2)	13.663
ZrC (excl. O_2)	12.399	Tetrazene $\text{H}_2\text{N}-\text{NH}-\text{N}=\text{NH}$ solid (excl. O_2)	13.083
Fe_3C (excl. O_2)	6.739	Carbon monoxide, CO (excl. O_2)	10.100
TaC (excl. O_2)	6.633	Ammonium azide NH_4N_3 solid (excl. O_2)	9.983
Ni_3C (excl. O_2)	6.378	Cobalt octacarbonyl $\text{Co}_2(\text{CO})_8$ (excl. O_2)	6.930
		Nickel tetracarbonyl $\text{Ni}(\text{CO})_4$ (excl. O_2)	6.913
Solid Nitrides		Nitrogen Combustibles	
Beryllium nitride Be_3N_2 (excl. O_2)	21.960	Boron B (excl. N_2)	23.333
Lithium nitride Li_3N (excl. O_2)	20.948	Beryllium Be (excl. N_2)	21.000
Boron nitride BN (excl. O_2)	15.202	Aluminum Al (excl. N_2)	11.778
Silicon nitride Si_3N_4 (excl. O_2)	14.071	Silicon Si (excl. N_2)	8.851
Aluminum nitride AlN (excl. O_2)	12.683	Lithium Li (excl. N_2)	7.838
		Titanium Ti (excl. N_2)	7.056
		Magnesium Mg (excl. N_2)	6.324
		Zirconium Zr (excl. N_2)	4.002
Metal Phosphides		Phosphorus P (excl. N_2)	3.473
BP (excl. O_2)	27.046	Cerium Ce (excl. N_2)	2.336
AlP (excl. O_2)	23.810		
MgP_2 (excl. O_2)	20.867	Carbon Dioxide Combustibles	
Mg_3P_2 (excl. O_2)	21.352	Aluminum Al (excl. CO_2)	20.000
TiP (excl. O_2)	17.370	Magnesium Mg (excl. CO_2)	16.667
ZrP_2 (excl. O_2)	14.755	Titanium Ti (excl. CO_2)	11.524
FeP_2 (excl. O_2)	12.564		
FeP (excl. O_2)	9.744	Water Combustibles	
Ni_3P_2 (excl. O_2)	7.855	Lithium Li (excl. H_2O)	35.447
Zn_3P_2 (excl. O_2)	7.711	Aluminum Al (excl. H_2O)	17.593
Fe_2P (excl. O_2)	7.500	Magnesium Mg (excl. H_2O)	14.815
Ni_2P (excl. O_2)	6.941	Chlorine trifluoride ClF_3 (excl. H_2O)	2.871
Fe_3P (excl. O_2)	6.750	Cesium Cs (excl. H_2O)	1.320
Ni_3P (excl. O_2)	5.987		

Table 30. Energy density of fuel materials during ambient combustion (theoretical materials indicated in red)⁵¹⁸

Fuel Materials	Energy Density (MJ/L)	Fuel Materials	Energy Density (MJ/L)
Metals and Elements			
Boron B (excl. O ₂)	271.429	Bihexaplane C ₁₇ H ₁₆ (excl. O ₂)	76.624
Carbon, as C ₂₀ fullerene (excl. O ₂)	145.323	Prismane C ₆ H ₆ , liquid (excl. O ₂)	74.877
Beryllium Be (excl. O ₂)	122.998	Pagodane C ₂₀ H ₂₀ (excl. O ₂)	67.500
Carbon, as diamond C (excl. O ₂)	115.585	Cubane C ₆ H ₆ , solid (excl. O ₂)	67.395
Uranium U (excl. O ₂)	95.588	Tripropargyl amine C ₉ H ₉ N (excl. O ₂)	63.986
Tantalum Ta (excl. O ₂)	94.286	Dipropargylammonium C ₆ H ₇ N (excl. O ₂)	59.194
Vanadium V (excl. O ₂)	91.588	Benzynes C ₆ H ₄ (theoretical) (excl. O ₂)	58.289
Titanium Ti (excl. O ₂)	89.151	Benzvalene C ₆ H ₆ (excl. O ₂)	57.654
Neptunium Np (excl. O ₂)	88.443	Tetracene C ₁₈ H ₁₂ , solid (excl. O ₂)	51.509
Tungsten W (excl. O ₂)	88.262	Adamantane C ₁₀ H ₁₆ (excl. O ₂)	47.857
Plutonium Pu (excl. O ₂)	85.854	Cholesterol C ₂₇ H ₄₆ O (excl. O ₂)	44.902
Hafnium Hf (excl. O ₂)	85.448	Tetraacetylene C ₈ H ₂ (excl. O ₂)	43.367
Aluminum Al (excl. O ₂)	83.800	1-nitroprismane C ₆ H ₅ NO ₂ (theoretical) (excl. O ₂)	42.720
Chromium Cr (excl. O ₂)	77.793	[1.1.1]Propellane C ₃ H ₆ (excl. O ₂)	42.424
Zirconium Zr (excl. O ₂)	77.143	Quadricyclane C ₇ H ₈ , liquid (excl. O ₂)	42.324
Silicon Si (excl. O ₂)	75.917	Fuel Oil #2, liquid (excl. O ₂)	42.143
Carbon, as graphite C (excl. O ₂)	73.141	Hexamine C ₆ H ₁₂ N ₄ , solid (excl. O ₂)	40.000
Solid hydrogen H ₂ (excl. O ₂)	72.673	Triacetylene C ₆ H ₂ (excl. O ₂)	39.538
Phosphorus P (excl. O ₂)	64.729	Diazatetrahedrane C ₂ N ₂ H ₂ (theoretical) (excl. O ₂)	38.333
Scandium Sc (excl. O ₂)	63.245	Bicyclobutane C ₄ H ₆ , liquid (excl. O ₂)	37.805
Carbon, as C ₆₀ fullerene (excl. O ₂)	59.748	Synton rocket fuel C ₁₀ H ₁₆ (excl. O ₂)	37.500
Iron Fe (excl. O ₂)	58.042	Benzene C ₆ H ₆ , liquid (excl. O ₂)	36.678
Cerium Ce (excl. O ₂)	52.657	Diesel fuel ~C ₁₂ H ₂₃ (excl. O ₂)	35.821
Magnesium Mg (excl. O ₂)	42.614	Dietary lipid	35.586
Zinc Zn (excl. O ₂)	38.264	Napalm-B, liquid (excl. O ₂)	35.532
Nickel Ni (excl. O ₂)	36.419	Cyclobutene C ₄ H ₆ , liquid (excl. O ₂)	34.959
Cobalt Co (excl. O ₂)	35.952	RP-1 rocket fuel ~kerosene (excl. O ₂)	34.907
Calcium Ca (excl. O ₂)	24.612	1,2-nitroprismane C ₆ H ₄ (NO ₂) ₂ (theoretical) (ex. O ₂)	34.900
Sulfur S (excl. O ₂)	19.161	Dodecane C ₁₂ H ₂₆ (excl. O ₂)	34.802
Strontium Sr (excl. O ₂)	17.831	Cyclobutane C ₄ H ₈ , liquid (excl. O ₂)	34.403
Lithium Li (excl. O ₂)	17.680	Octanol C ₈ H ₁₇ OH, liquid (excl. O ₂)	33.910
Lead Pb (excl. O ₂)	15.137	Fat (oxidation, excl. O ₂)	33.684
Sodium Na (excl. O ₂)	10.842	Cyclopentane C ₅ H ₁₀ , liquid (excl. O ₂)	33.548
Liquid molecular hydrogen H ₂ (excl. O ₂)	8.582	Cyclopropane C ₃ H ₆ , liquid (excl. O ₂)	33.494
Potassium K (excl. O ₂)	6.278	Methylcyclohexane C ₇ H ₁₄ , liquid (excl. O ₂)	33.258
Rubidium Rb (excl. O ₂)	4.995	Pyridine C ₅ H ₅ N, liquid (excl. O ₂)	33.127
Cesium Cs (excl. O ₂)	4.154	Octane C ₈ H ₁₈ ~ gasoline (excl. O ₂)	33.091
		Propyne C ₃ H ₄ (excl. O ₂)	31.092
		Butyne C ₄ H ₆ (excl. O ₂)	30.702
Hydrides		1,2-Butadiene C ₄ H ₆ (excl. O ₂)	30.500
Titanium dihydride TiH ₂ (excl. O ₂)	83.594	Propadiene C ₃ H ₄ (excl. O ₂)	30.378
Zirconium hydride ZrH ₂ (excl. O ₂)	70.732	Dimethylfuran C ₆ H ₈ O, liquid (excl. O ₂)	29.630
Beryllium dihydride BeH ₂ (excl. O ₂)	60.178	Acetylene C ₂ H ₂ (excl. O ₂)	29.575
Uranium hydride UH ₃ (excl. O ₂)	60.000	Butane C ₄ H ₁₀ , liquid (excl. O ₂)	29.346
Alane AlH ₃ (excl. O ₂)	56.650	Propane C ₃ H ₈ , liquid (excl. O ₂)	29.249
Magnesium borohydride Mg(BH ₄) ₂ (excl. O ₂)	46.972	Butanol C ₄ H ₉ OH, liquid (excl. O ₂)	29.180

⁵¹⁸ Data from **Table A4** in **Appendix A.4**.

Beryllium borohydride $\text{Be}(\text{BH}_4)_2$ (excl. O_2)	42.746	Picryl propyl ether $\text{C}_9\text{H}_9\text{N}_3\text{O}_7$ (excl. O_2)	29.057
Lithium borohydride LiBH_4 (excl. O_2)	42.385	Propargyl alcohol $\text{C}_3\text{H}_4\text{O}$, liquid (excl. O_2)	29.012
Magnesium hydride MgH_2 (excl. O_2)	41.459	1,2,3-nitroprismane $\text{C}_6\text{H}_3(\text{NO}_2)_3$ (theor.) (ex. O_2)	28.833
Lithium aluminum hydride LiAlH_4 (excl. O_2)	36.077	Dietary protein	28.780
Dialuminum borohydride $\text{Al}_2\text{H}_2(\text{BH}_4)_4$ (excl. O_2)	32.163	Diethylenetriamine $\text{C}_4\text{H}_{13}\text{N}_3$ (excl. O_2)	28.519
Lithium hydride LiH (excl. O_2)	32.157	1,3-Butadiene C_4H_6 (excl. O_2)	28.284
Aluminum borohydride $\text{Al}(\text{BH}_4)_3$, liquid (excl. O_2)	31.288	Ethane C_2H_6 , liquid (excl. O_2)	28.279
Silane SiH_4 (excl. O_2)	25.953	Propylene C_3H_6 (excl. O_2)	28.134
Germane GeH_4 (excl. O_2)	20.426	Ethylene C_2H_4 (excl. O_2)	28.081
Sodium hydride NaH (excl. O_2)	18.721	Diacetylene C_4H_2 (excl. O_2)	27.819
Arsine AsH_3 (excl. O_2)	15.958	Butyraldehyde $\text{C}_4\text{H}_8\text{O}$, liquid (excl. O_2)	27.697
Potassium hydride KH (excl. O_2)	12.357	Dipropyl ether $\text{C}_6\text{H}_{14}\text{O}$, liquid (excl. O_2)	27.353
Rubidium hydride RbH (excl. O_2)	10.420	Butatriene C_4H_4 (excl. O_2)	27.262
Cesium hydride CsH (excl. O_2)	9.235	Propylene oxide $\text{C}_3\text{H}_6\text{O}$, liquid (excl. O_2)	27.119
Boranes		Dietary carbohydrate	27.119
Decaborane $\text{B}_{10}\text{H}_{14}$ (excl. O_2)	61.692	Propanol $\text{C}_3\text{H}_7\text{OH}$, liquid (excl. O_2)	27.005
closo-2,4- $\text{C}_2\text{B}_5\text{H}_7$ carborane (excl. O_2)	54.807	DMAZ $\text{C}_4\text{H}_{10}\text{N}_4$ (excl. O_2)	26.783
1,7- $\text{C}_2\text{B}_{10}\text{H}_{11}$ -1- CH_3 carborane (excl. O_2)	53.095	Diethyl ether $\text{C}_4\text{H}_{10}\text{O}$, liquid (excl. O_2)	26.250
Pentaborane B_5H_9 (excl. O_2)	41.863	Ethylene oxide $\text{C}_2\text{H}_4\text{O}$, liquid (excl. O_2)	26.120
Triethylborane $\text{B}(\text{C}_2\text{H}_5)_3$ (excl. O_2)	34.345	TACOT $\text{C}_{12}\text{H}_4\text{N}_8\text{O}_8$ (excl. O_2)	25.048
Trimethylborane $\text{B}(\text{CH}_3)_3$ (excl. O_2)	33.445	1,2,4,5-nitroprismane $\text{C}_6\text{H}_2(\text{NO}_2)_4$ (theor.) (ex. O_2)	24.710
Diborane B_2H_6 (excl. O_2)	32.903	Dicyanoacetylene C_4N_2 , liquid (excl. O_2)	24.672
Ammonia borane H_3NBH_3 (excl. O_2)	28.030	TNT, burned (excl. O_2)	24.088
Silanes		Glucose $\text{C}_6\text{H}_{12}\text{O}_6$, solid (excl. O_2)	24.017
Disilane Si_2H_6 (excl. O_2)	28.743	Acetone $\text{C}_3\text{H}_6\text{O}$, liquid (excl. O_2)	23.914
Silane SiH_4 (excl. O_2)	25.176	HNS $\text{C}_{14}\text{H}_6\text{N}_6\text{O}_{12}$ (excl. O_2)	23.736
Phosphanes		UDMH $\text{C}_2\text{H}_8\text{N}_2$ (excl. O_2)	23.684
Trisilylphosphine $\text{P}(\text{SiH}_3)_3$ (excl. O_2)	41.429	Methane CH_4 , liquid (excl. O_2)	23.509
Diphosphane P_2H_6 (excl. O_2)	24.231	Ethanol $\text{C}_2\text{H}_5\text{OH}$, liquid (excl. O_2)	23.499
Phosphine PH_3 (excl. O_2)	14.919	Dimethyl ether H_3COCH_3 , liquid (excl. O_2)	23.323
Metal Borides		DNAN $\text{C}_4\text{H}_6\text{N}_2\text{O}_5$ (excl. O_2)	22.230
Diberyllium diboride Be_2B_2 (theoretical) (excl. O_2)	191.111	1,2,3,4,5-nitroprismane $\text{C}_6\text{H}(\text{NO}_2)_5$ (theor.) (ex. O_2)	21.592
Beryllium diboride BeB_2 (excl. O_2)	134.532	Cyanogen C_2N_2 , liquid (excl. O_2)	20.110
Be_2B (excl. O_2)	133.846	1,1-dinitropropane $\text{C}_3\text{H}_6\text{N}_2\text{O}_4$, liquid (excl. O_2)	19.748
BeB_6 (excl. O_2)	133.438	Heptanitrocubane $\text{C}_8\text{HN}_7\text{O}_{14}$ (excl. O_2)	18.889
AlB_{12} (excl. O_2)	132.683	Cyanuric triazide C_3N_{12} , solid (excl. O_2)	18.016
Be_5B (excl. O_2)	131.955	Methanol CH_3OH , liquid (excl. O_2)	17.698
MgB_{12} (excl. O_2)	126.624	Nitroethane $\text{C}_2\text{H}_5\text{NO}_2$, liquid (excl. O_2)	17.504
TiB_2 (excl. O_2)	122.078	Hydroperoxymethane CH_4O_2 (excl. O_2)	15.364
VB_2 (excl. O_2)	121.831	HMTD $\text{C}_6\text{H}_{12}\text{N}_2\text{O}_6$ (excl. O_2)	14.557
AlB_2 (excl. O_2)	121.233	Nitromethane CH_3NO_2 , liquid (excl. O_2)	12.007
B_6Si (excl. O_2)	119.947	Tetranitratroxy carbon (theoretical) (excl. O_2)	5.720
MgB_6 (excl. O_2)	117.080	Organometallics	
TaB_2 (excl. O_2)	115.934	Ethyllithium LiC_2H_5 (excl. O_2)	41.627
MgB_4 (excl. O_2)	111.481	Methylithium LiCH_3 (excl. O_2)	38.235
B_3Si (excl. O_2)	110.833	Tributylaluminum $\text{Al}(\text{C}_4\text{H}_9)_3$ (excl. O_2)	37.226
ZrB_2 (excl. O_2)	109.189	Diisobutylaluminum hydride (i- C_4H_9) $_2\text{AlH}$ (ex. O_2)	36.022
MgB_2 (excl. O_2)	102.924	Triethylphosphine $\text{P}(\text{C}_2\text{H}_5)_3$ (excl. O_2)	35.211
Intermetallics		Triethylgallium $\text{Ga}(\text{C}_2\text{H}_5)_3$ (excl. O_2)	33.673
VSi_2 (excl. O_2)	100.000	Dimethylberyllium $\text{Be}(\text{CH}_3)_2$ (excl. O_2)	33.631
V_2Si (excl. O_2)	96.203	Trimethylaluminum $\text{Al}(\text{CH}_3)_3$, liquid (excl. O_2)	33.180
Al_3Mg_4 (excl. O_2)	59.107	Diethylzinc $\text{Zn}(\text{C}_2\text{H}_5)_2$, liquid (excl. O_2)	33.059
Mg_2Si (excl. O_2)	51.392	Butyllithium LiC_4H_9 (excl. O_2)	32.078
Solid Carbides		Trimethylgallium $\text{Ga}(\text{CH}_3)_3$ (excl. O_2)	29.040
B_4C (excl. O_2)	130.137	Diethylaluminum chloride $(\text{C}_2\text{H}_5)_2\text{AlCl}$ (excl. O_2)	28.616
SiC (excl. O_2)	99.200	Trimethylamine $\text{N}(\text{CH}_3)_3$ (excl. O_2)	28.163
		Dimethylzinc $\text{Zn}(\text{CH}_3)_2$ (excl. O_2)	27.785
		Trimethylstibine $\text{Sb}(\text{CH}_3)_3$ (excl. O_2)	26.555
		Trimethylbismuthine $\text{Bi}(\text{CH}_3)_3$ (excl. O_2)	26.473
		Trimethylarsine $\text{As}(\text{CH}_3)_3$ (excl. O_2)	25.972
		Dimethylmercury $\text{Hg}(\text{CH}_3)_2$, liquid (excl. O_2)	21.413

TiC (excl. O ₂)	94.262	Trimethylmercury Hg(CH ₃) ₃ , liquid (excl. O ₂)	21.348
TaC (excl. O ₂)	92.086	Triethylaluminum Al ₂ (C ₂ H ₅) ₆ , liquid (excl. O ₂)	18.650
VC (excl. O ₂)	91.743		
ZrC (excl. O ₂)	83.660	Other Oxygen Combustibles	
Be ₂ C (excl. O ₂)	83.051	Octasilacubane Si ₈ H ₈ (theoretical) (excl. O ₂)	60.028
Al ₄ C ₃ (excl. O ₂)	70.820	BN-prismane B ₃ N ₃ H ₆ (theoretical) (excl. O ₂)	51.955
Fe ₃ C (excl. O ₂)	51.931	N ₁₈ H ₆ (theoretical) (excl. O ₂)	29.873
Ni ₃ C (excl. O ₂)	50.847	Hydronitrogen polymer N ₁₀ H ₁₂ (excl. O ₂)	28.947
CaC ₂ (excl. O ₂)	47.059	Diborane + Hydrazine (excl. O ₂)	24.973
Li ₂ C ₂ (excl. O ₂)	43.836	Borazine B ₃ N ₃ H ₆ , liquid (excl. O ₂)	21.127
		Hydrazine N ₂ H ₄ , liquid (excl. O ₂)	19.875
Solid Nitrides		Tetrazene H ₂ N-NH-N=NH solid (excl. O ₂)	17.601
Beryllium nitride Be ₃ N ₂ (excl. O ₂)	59.606	Ammonia NH ₃ , liquid (excl. O ₂)	15.382
Boron nitride BN (excl. O ₂)	52.434	Ammonium azide NH ₄ N ₃ solid (excl. O ₂)	13.430
Silicon nitride Si ₃ N ₄ (excl. O ₂)	44.977	Cobalt octacarbonyl Co ₂ (CO) ₈ (excl. O ₂)	12.951
Aluminum nitride AlN (excl. O ₂)	41.270	Nickel tetracarbonyl Ni(CO) ₄ (excl. O ₂)	9.147
Lithium nitride Li ₃ N (excl. O ₂)	26.606		
		Nitrogen Combustibles	
Metal Phosphides		Boron B (excl. N ₂)	54.545
BP (excl. O ₂)	80.142	Beryllium Be (excl. N ₂)	38.836
FeP ₂ (excl. O ₂)	75.510	Titanium Ti (excl. N ₂)	31.887
ZrP ₂ (excl. O ₂)	70.405	Aluminum Al (excl. N ₂)	31.800
TiP (excl. O ₂)	68.500	Zirconium Zr (excl. N ₂)	26.071
FeP (excl. O ₂)	59.161	Silicon Si (excl. N ₂)	20.596
AlP (excl. O ₂)	57.500	Cerium Ce (excl. N ₂)	15.797
Fe ₂ P (excl. O ₂)	50.952	Magnesium Mg (excl. N ₂)	11.002
Ni ₂ P (excl. O ₂)	50.000	Phosphorus P (excl. N ₂)	9.335
Fe ₃ P (excl. O ₂)	48.029	Lithium Li (excl. N ₂)	4.188
Ni ₃ P ₂ (excl. O ₂)	47.103		
Ni ₃ P (excl. O ₂)	46.097	Carbon Dioxide Combustibles	
Mg ₃ P ₂ (excl. O ₂)	43.902	Aluminum Al (excl. CO ₂)	54.000
MgP ₂ (excl. O ₂)	41.763	Titanium Ti (excl. CO ₂)	52.075
Zn ₃ P ₂ (excl. O ₂)	35.097	Magnesium Mg (excl. CO ₂)	28.929
Organics		Water Combustibles	
[3.3.3]fenestrane C ₅ H ₆ (excl. O ₂)	92.010	Aluminum Al (excl. H ₂ O)	47.500
Tetrapropargylammonium tetraethynylborate (ex. O ₂)	79.808	Magnesium Mg (excl. H ₂ O)	25.714
Pyramidane C ₅ H ₄ (theoretical) (excl. O ₂)	78.629	Lithium Li (excl. H ₂ O)	18.923
Tetrahydrane C ₄ H ₄ (theoretical) (excl. O ₂)	78.218	Chlorine trifluoride ClF ₃ (excl. H ₂ O)	5.084
		Cesium Cs (excl. H ₂ O)	2.547

Table 31. Specific energy of a solution of water-solvated fuel molecules (MJ/kg of solution) at 1 atm and 298 K, assuming combustion of extracted solute with ambient oxygen

Water-Solvated Fuel Molecule (the solute)	Solute Concentration in Water (gm/L)	Characterization of this Concentration	Ambient O ₂ Combustion Energy of Solute Fuel, from Table 29 (MJ/kg)	Specific Energy of the Solution (MJ/kg)	Basis of Blood-Stream Lethality in Humans at the Indicated Concentration
Amantadine (C ₁₀ H ₁₅ NH ₂)	0.00032	max. blood dose ⁵¹⁹	~44.000	0.000014	FDA-approved drug
Hydrogen (H ₂) *	0.00157	max. solubility	121.000	0.000191	none
Amantadine (C ₁₀ H ₁₅ NH ₂)	0.00480	lethal blood level ⁵²⁰	~44.000	0.000212	FDA-approved drug
Adamantane (C ₁₀ H ₁₆)	0.00491	max. solubility ⁵²¹	44.273	0.000218	none
Carbon monoxide (CO) *	0.02698	max. solubility	10.100 ⁵²⁵	0.000273	Hemoglobin poison
Ammonia (NH ₃)	0.03300	lethal blood level ⁵²²	22.529	0.000746	metabolic poison
Methane (CH ₄) *	0.02131	max. solubility	55.688	0.001190	none
Ethane (C ₂ H ₆) *	0.05493	max. solubility	51.912	0.002860	none
Ethylene (C ₂ H ₄) *	0.13508	max. solubility	49.466	0.006701	none
Glucose (C ₆ H ₁₂ O ₆)	1.00000	normal blood level	15.611	0.015642	none
Acetone (CH ₃) ₂ CO)	0.55000	lethal blood level	30.499	0.016816	metabolic poison
Ethanol (C ₂ H ₅ OH)	1.00000	drunk blood level	29.783	0.029843	none
Acetylene (C ₂ H ₂) *	1.08104	max. solubility	48.231	0.052240	inhal. anesthetic ⁵²⁶
Ethanol (C ₂ H ₅ OH)	4.00000	lethal blood level ⁵²³	29.783	0.119013	metabolic poison
Amantadine (C ₁₀ H ₁₅ NH ₂)	6.29000	max. solubility ⁵²⁴	~44.000	0.275852	metabolic poison
Ammonia (NH ₃) *	424.21953	max. solubility	22.529	6.724677	metabolic poison
Glucose (C ₆ H ₁₂ O ₆)	909.00000	max. solubility	15.611	7.445120	metabolic poison
Ethanol (C ₂ H ₅ OH)	997.00000	max. solubility (50%)	29.783	14.891500	metabolic poison

* Maximum solubility (Henry's Law constants) from NMI.⁵²⁷

⁵¹⁹ https://www.accessdata.fda.gov/drugsatfda_docs/label/2009/016023s041,018101s016lbl.pdf.

⁵²⁰ <https://www.ncbi.nlm.nih.gov/pmc/articles/PMC3580721/>.

⁵²¹ <https://www.drugbank.ca/drugs/DB03627>.

⁵²² [https://yosemite.epa.gov/sab/sabproduct.nsf/0/2FE334E0BEC7A3CF85257B65005C500B/\\$File/Ammonia_ToxReview-Supplemental_SAB+review+draft_080713_HERO+\(2\).pdf](https://yosemite.epa.gov/sab/sabproduct.nsf/0/2FE334E0BEC7A3CF85257B65005C500B/$File/Ammonia_ToxReview-Supplemental_SAB+review+draft_080713_HERO+(2).pdf) (page E-2).

⁵²³ <https://www.ncbi.nlm.nih.gov/pmc/articles/PMC3580721/>.

⁵²⁴ <https://pubchem.ncbi.nlm.nih.gov/compound/amantadine#section=Solubility>.

⁵²⁵ https://nvlpubs.nist.gov/nistpubs/jres/6/jresv6n1p37_A2b.pdf.

⁵²⁶ Acetylene has a very low acute toxicity (<https://scialert.net/fulltext/?doi=jms.2005.21.25>). The gas is an inhalation anesthetic when administered at 10%-40% in air; at such high air concentrations, the blood concentration is probably near saturation at the maximum solubility in water (https://stacks.cdc.gov/view/cdc/19368/cdc_19368_DS1.pdf). There are rare cases of death due to abuse via inhalation (<https://www.ncbi.nlm.nih.gov/pubmed/11327229>) or ill effects due to inhaling 100% pure gas (<https://www.ncbi.nlm.nih.gov/pubmed/11244734>), but "acetylene rebreathing" is a commonly used and medically safe technique for measuring cardiac output in sports medicine (<https://www.ncbi.nlm.nih.gov/pubmed/9156963>) and in pulmonary medicine (<https://www.ncbi.nlm.nih.gov/pubmed/10894104>).

⁵²⁷ Freitas RA Jr., Nanomedicine, Volume I: Basic Capabilities, Landes Bioscience, Georgetown, TX, 1999, Table 9.2; <http://www.nanomedicine.com/NMI/Tables/9.2.jpg>.

4.2.4 Power Density of Chemical Fuels

As was the case with thermochemical energy, the energy density of chemical fuels is an intrinsic property of a material but power density also depends on extrinsic factors such as physical size (scale) and geometry.⁵²⁸ The duration over which a given chemical power density can be continuously maintained also depends on the replacement rate of the energy storage containers.⁵²⁹ Unlike thermochemical energy, however, chemical energy can be stored indefinitely and triggered upon demand, whenever and wherever it is needed. Two cases are readily distinguished: (1) episodic or one-time power generation, and (2) continuous power generation.

First, consider the case of a one-time release of stored chemical energy in which the energetic materials are stored in a cubic box of edge length L_{box} (m), filled with an energy storage material of material density ρ (kg/L) and energy density E_D (MJ/L) that can be independently ignited upon demand to release energy in a wave of combustion or detonation with a burn velocity of v_{burn} (m/sec). Combustion of all the material inside the box is completed in a time $t_{\text{burn}} \sim L_{\text{box}} / v_{\text{burn}}$, demonstrating a power density of $P_D = E_D / t_{\text{burn}} = E_D v_{\text{burn}} / L_{\text{box}}$ (MW/L) and a specific energy $P_S = P_D / \rho$ (MW/kg).

The maximum energy density for ambient combustion appears to be **39 MJ/L (177 MJ/L theoretical)** for explosive decomposition (**Section 4.2.1**), **48 MJ/L** for nonambient chemical combustion (**Section 4.2.2**), and **271 MJ/L** for ambient chemical combustion (**Section 4.2.3**). The highest explosive detonation velocities⁵³⁰ are 10,100 m/sec for octanitrocubane (ONC)⁵³¹ and 10,000 m/sec for 4,4'-dinitro-3,3'-diazonofuroxan (DDF).⁵³² Taking E_D (max) \sim **100 MJ/L** and v_{burn} (max) \sim 10,000 m/sec, the maximum power density appears to be $P_{D,\text{max}} = E_D v_{\text{burn}} / L_{\text{box}} \sim$ **10^9 MW/L** at $L_{\text{box}} = 1$ mm, **$\sim 10^{12}$ MW/L** at $L_{\text{box}} = 1$ μm , and finally **10^{15} MW/L (10^{24} W/m³)** at $L_{\text{box}} = 1$ nm, or **$\sim 10^{15}$ MW/kg** taking material density $\rho \sim 1$ kg/L. A box size of 1 nm is roughly the scale of individual chemical fuel-oxidant molecules, e.g., (0.716 nm)³ per molecule of ONC. This may represent the theoretical upper limit for chemical fuel power density in the extreme limiting case where each molecule can be ignited individually and in unison with all the others, releasing all the stored energy in a single burst of duration $t_{\text{burn}} \sim L_{\text{box}} / v_{\text{burn}} = (1 \text{ nm}) / (10,000 \text{ m/sec}) = 10^{-13}$ sec. It's not clear how closely we can approach this theoretical maximum, since even ONC, one of the best high explosives that has been synthesized to date, has $E_D =$ **20.6 MJ/L** \ll 100 MJ/L, and most low explosives and propellants are far inferior in both combustion

⁵²⁸ For example, while traditional thermites have slow energy release rates, nanothermites with much smaller 10-100 nm particles have much higher energy release rates; <https://en.wikipedia.org/wiki/Nano-thermite>. See also: Miziolek A. Nanoenergetics: An Emerging Technology Area of National Importance. AMPTIAC Quarterly 2002;6(1); <http://infohouse.p2ric.org/ref/34/33115.pdf>.

⁵²⁹ Of course, the material can be supplied not just in container boxes, but in arrays of boxes moving in parallel, or in fluid form through pipes, etc. Containerization is used here solely as an aid to conceptualization and computation.

⁵³⁰ https://en.wikipedia.org/wiki/Table_of_explosive_detonation_velocities.

⁵³¹ <https://en.wikipedia.org/wiki/Octanitrocubane>.

⁵³² <https://en.wikipedia.org/wiki/4,4%27-Dinitro-3,3%27-diazonofuroxan>.

velocity and energy density (e.g., $v_{\text{burn}} \sim 10$ m/sec,⁵³³ and $E_D \sim 5.3$ MJ/L, for gunpowder). Also, the simultaneous ignition of every energy molecule may require a significant volume of intrusively interpenetrating hardware that will reduce the practical attainable energy density.⁵³⁴

Second, let's consider the challenge of continuous release of stored chemical energy to maintain a given power level, which requires the arrival and combustion of a fresh box of chemical energy every t_{burn} seconds and thus a container circulating velocity of $v_{\text{circ}} = L_{\text{box}} / t_{\text{burn}}$. A system in which the circulating velocity is $v_0 < v_{\text{circ}}$ will yield a reduced power density of $\sim P_D (v_0 / v_{\text{burn}})$. Supersonic movement of energy storage materials (whether encapsulated or fluidic) also consumes a lot of extra energy. For example, the energy cost of nanoscale containerized transport⁵³⁵ on rollers or conveyor belts in vacuum is $\propto v_{\text{circ}}^2$,⁵³⁶ and a diamond-crushing pressure of ~ 55 GPa (550,000 atm) would be required to force liquid water through a 2 nm wide tube that is 1 nm long at $v_{\text{circ}} \sim 10,000$ m/sec assuming laminar Poiseuille flow.⁵³⁷

Of course, thermal management is the overriding consideration at such high power densities (potentially up to 10^{24} W/m³). In a continuous-release scenario we must pay close attention to the ability of the surrounding infrastructure and environment to nondestructively transport the chemically-generated heat away from the site of energy release. The maximum power density that can be continuously radiated by an energy storage system of size L_{system} without thermally destroying itself is $P_{D,\text{rad}} \sim 3 \sigma \epsilon_r (T_{\text{destroy}}^4 - T_{\text{environ}}^4) / L_{\text{system}}$, where $\sigma = 5.67 \times 10^{-8}$ W/m²-K⁴ (Stefan-Boltzmann constant), emissivity $\epsilon_r = 0.97$ (e.g., carbon black, to maximize heat emission at the lowest possible temperature), T_{destroy} is the temperature at which the infrastructure material will destroy itself or become nonfunctional in the local environment, and the temperature of the local environment $T_{\text{environ}} \sim 300$ K.⁵³⁸ Considering a thermal management infrastructure operated in air and made of diamond (a material having a combustion temperature in air of $T_{\text{destroy}} \sim T_{\text{burn,diamond}} \sim 1070$ K),⁵³⁹ $P_{D,\text{rad}} = 0.21$ MW/L for $L_{\text{system}} = 1$ mm and **215** MW/L for $L_{\text{system}} = 1$ μm . An infrastructure operated in air but made of sapphire (almost as strong as diamond) cannot

⁵³³ <https://en.wikipedia.org/wiki/Gunpowder#Corning>.

⁵³⁴ Jun F, Xinghai F, Guanren Z. Experimental studies on the detonation of an explosive by multi-point initiation. Proc 9th Symp (Intl) Detonation (CONF-890811-26), Vol. II, 28 Aug – 1 Sep 1989, pp. 1360-1363; <http://www.dtic.mil/dtic/tr/fulltext/u2/a247996.pdf>.

⁵³⁵ Freitas RA Jr., Nanomedicine, Volume I: Basic Capabilities, Landes Bioscience, Georgetown, TX, 1999, Section 9.2.7.7; <http://www.nanomedicine.com/NMI/9.2.7.7.htm>.

⁵³⁶ Freitas RA Jr., Nanomedicine, Volume I: Basic Capabilities, Landes Bioscience, Georgetown, TX, 1999, Section 3.4.3; <http://www.nanomedicine.com/NMI/3.4.3.htm>.

⁵³⁷ Freitas RA Jr., Nanomedicine, Volume I: Basic Capabilities, Landes Bioscience, Georgetown, TX, 1999, Section 9.2.5; <http://www.nanomedicine.com/NMI/9.2.5.htm>.

⁵³⁸ Freitas RA Jr., Nanomedicine, Volume I: Basic Capabilities, Landes Bioscience, Georgetown, TX, 1999, Section 6.5.3; <http://www.nanomedicine.com/NMI/6.5.3.htm>.

⁵³⁹ Cotton FA, Wilkinson G. Advanced Inorganic Chemistry: A Comprehensive Text, Second Edition, John Wiley & Sons, New York, 1966.

burn but will melt⁵⁴⁰ at $T_{m.p.} = 2310 \text{ K} = T_{\text{destroy}}$, yielding $P_{D,\text{rad}} = 4.7 \text{ MW/L}$ for $L_{\text{system}} = 1 \text{ mm}$ and **4,700 MW/L** for $L_{\text{system}} = 1 \text{ }\mu\text{m}$.

However, from **Section 3.4**, conductive power losses dominate radiative power losses in a powerplant of size $L_{\text{system}} < L_{\text{crit}} = K_t (T_{\text{destroy}} - T_{\text{environ}}) / [6 e_r \sigma (T_{\text{destroy}}^4 - T_{\text{environ}}^4)] = 3.6 \text{ m}$ for diamond (thermal conductivity $K_t \sim 2000 \text{ W/m-K}$ at $T_{\text{environ}} \sim 300 \text{ K}$), or $L_{\text{crit}} = 0.4 \text{ mm}$ for sapphire ($K_t \sim 20 \text{ W/m-K}$). Hence for $L_{\text{system}} \leq \sim 1 \text{ m}$, the dominant loss mechanism will be the conductive power loss $P_{\text{conductive}} = L_{\text{system}} K_t (T_{\text{destroy}} - T_{\text{environ}})$ which allows the maximum nondestructive power density to rise to $P_{D,\text{cond}} = P_{\text{conductive}} / L_{\text{system}}^3 = K_t (T_{\text{destroy}} - T_{\text{environ}}) / L_{\text{system}}^2 = 1540 \text{ MW/L}$ at $L_{\text{system}} = 1 \text{ mm}$ and **1,540,000,000 MW/L at $L_{\text{system}} = 1 \text{ }\mu\text{m}$** for diamond (thermal conductivity $K_t \sim 2000 \text{ W/m-K}$ at $T_{\text{environ}} \sim 300 \text{ K}$), and **40 MW/L** at $L_{\text{system}} = 1 \text{ mm}$ and **40,000,000 MW/L** at $L_{\text{system}} = 1 \text{ }\mu\text{m}$ for sapphire ($K_t \sim 20 \text{ W/m-K}$).

We conclude that conventional chemical energy powerplants $\sim 1 \text{ }\mu\text{m}$ in size probably have a theoretical upper limit on continuously-deliverable power density of $\sim 10^9 \text{ MW/L}$, or $\sim 10^9 \text{ MW/kg}$ at $\rho \sim 1 \text{ kg/L}$. Somewhat higher continuous power densities may be possible if complete sub-micron powerplants can be built together with all necessary supportive molecular machine infrastructure.

Similar considerations apply to other chemical power sources such as molecular recombination (**Section 4.3**) or excited states, radicals and ion recombination (**Section 4.4**) – sources that are described below.

⁵⁴⁰ Hughes RW. Ruby & Sapphire, RWH Publishing, Boulder CO, 1997.

4.3 Molecular Recombination Energy

Molecules are composed of two or more atoms that are joined by covalent bonds formed from the sharing of electrons. The bond energy is the measure of bond strength in a chemical bond. For diatomic molecules, the bond energy is the same as the bond dissociation energy – the same amount of energy must be added to break a bond (bond dissociation) as is released when the bond is created between the two atoms (bond formation). In the case of the 7 diatomic molecular elements, the energy that is released when two monatomic atoms combine to form a single diatomic molecule is called the molecular recombination energy (**Table 32**).⁵⁴¹

Table 32. Recombination energies for the diatomic molecular elements ⁵⁴²		
Diatomic Molecular Element	Recombination Energy	Specific Energy
Hydrogen (H ₂)	436 kJ/mole (4.53 eV)	216 MJ/kg H
Nitrogen (N ₂)	945 kJ/mole	33.7 MJ/kg N
Oxygen (O ₂)	498 kJ/mole	15.6 MJ/kg O
Fluorine (F ₂)	159 kJ/mole	4.18 MJ/kg F
Chlorine (Cl ₂)	242 kJ/mole	3.41 MJ/kg Cl
Bromine (Br ₂)	192 kJ/mole	1.20 MJ/kg Br
Iodine (I ₂)	151 kJ/mole	0.59 MJ/kg I

The **216 MJ/kg** molecular recombination energy of monatomic hydrogen ($H + H \rightarrow H_2$) is clearly of greatest interest, since it potentially provides a specific energy roughly twice as high as the 121 MJ/kg available from the ambient combustion of solid or liquid molecular hydrogen (**Table 29**), and is much higher than the experimentally-available **~6 MJ/kg** for batteries, **~23 MJ/kg** for explosives, and **~31 MJ/kg** for nonambient combustibles. Monatomic hydrogen (H), comprising 73.9% of the elemental mass of the universe,⁵⁴³ is readily generated from molecular hydrogen (H₂) via electric arc or ultraviolet light and already has some limited practical utility. For instance, the atomic hydrogen torch⁵⁴⁴ uses monatomic hydrogen to create very high

⁵⁴¹ This should be distinguished from the ion recombination energy – the energy released when an electron is added to an ionized molecule or atom, making it more or less charged or rendering it electrically neutral (**Section 4.4**).

⁵⁴² Bond dissociation energies at 298 K https://en.wikipedia.org/wiki/Bond-dissociation_energy; bond energy for F₂ https://en.wikipedia.org/wiki/Compounds_of_fluorine#Difluorine. Note that these values represent the bond dissociation energy or BDE (based on ΔH , the change in enthalpy), not the bond dissociation free energy or BDFE (based on ΔG , the change in Gibbs energy) that would include effects from entropy changes (https://en.wikipedia.org/wiki/Bond-dissociation_energy#Definitions_and_related_parameters).

⁵⁴³ https://en.wikipedia.org/wiki/Abundance_of_the_chemical_elements.

⁵⁴⁴ https://en.wikipedia.org/wiki/Atomic_hydrogen_welding.

temperatures near 4,000°C for welding. NASA has investigated the use of atomic hydrogen as a rocket propellant: if stored in liquid helium to prevent it from recombining into molecular hydrogen, vaporization of the helium unleashes the atomic hydrogen which can then recombine back to molecular hydrogen with the release of energy, creating an intensely hot stream of hydrogen and helium gas suitable for rocket propulsion.⁵⁴⁵

In this Section we review the current status of energy generation from monatomic recombination reactions of hydrogen (**Section 4.3.1**), nitrogen (**Section 4.3.2**), oxygen (**Section 4.3.3**), and halogens and other molecules (**Section 4.3.4**).

⁵⁴⁵ Palaszewski BA. Atomic Hydrogen Propellants: Historical Perspectives and Future Possibilities, NASA Lewis Research Center, NASA/TM-106053, 1993;
<https://ntrs.nasa.gov/archive/nasa/casi.ntrs.nasa.gov/19930011425.pdf>.

4.3.1 Hydrogen Recombination Energy

Hydrogen has received the greatest attention among all of the proposed molecular recombination energy sources. Starting in 1943,⁵⁴⁶ Fritz Zwicky at Aerojet Engineering Corporation circulated concepts for novel propellants exemplifying “meta-chemistry” that dealt with the “study, production and the use of quantum mechanically metastable particles, molecules or states of matter in general,” including the high-energy $H + H \rightarrow H_2$ recombination reaction.⁵⁴⁷ Since the 1950s, the idea of monatomic hydrogen propellants has received a fair amount of attention from the propulsion engineering community.⁵⁴⁸

Amusingly, monatomic hydrogen and ozone were employed as the hypothetical high-powered rocket fuel in the 1950 science fiction movie *Rocketship X-M*.⁵⁴⁹ (Willy Ley⁵⁵⁰ noted that to undergo combustion ozone (O_3) must transform into oxygen (O_2) and additionally release its allotropic transition energy (**Section 3.3.4**) of **7.98 MJ/kg.**)

⁵⁴⁶ Zwicky F. Fundamentals of Propulsive Power. Presentation to the International Congress for Applied Mechanics, Paris, 22-29 Sep 1946. Zwicky F. Chemical Kinetics and Jet Propulsion. Chem Eng News 1950 Jan 16;28(3):156-158.

⁵⁴⁷ Zwicky F. Propellants for tomorrow's rockets. Astronautics. 1957 Aug;2(1):45-49, 95.

⁵⁴⁸ McKinley JD Jr, Garvin D. The Reactions of Atomic Hydrogen with Ozone and with Oxygen. J Am Chem Soc. **1955**;77(22):5802-5805. Giguère PA, Chin D. Reaction Products of Atomic Hydrogen with Solid Ozone. J Chem Phys. **1959**; 31:1685-1685. Nicolet N. Aeronomic Reactions of Hydrogen and Ozone. In: Fiocco G (ed.). Mesospheric Models and Related Experiments, Vol. 25, Astrophysics and Space Science Library, D. Reidel Publishing Company, **1971**, pp. 1-51. Rosen G. Manufacture and deflagration of an atomic hydrogen propellant. AIAA Journal **1974** Oct;12(10):1325-1330. Howard CJ, Finlayson-Pitts BJ. Yields of HO_2 in the reaction of hydrogen atoms with ozone. J Chem Phys. **1980**;72(6):3842-3843. Palaszewski B. Atomic Hydrogen as a Launch Vehicle Propellant. NASA Lewis Research Center, AIAA 90-0715, NASA/TM-102459, Jan **1990**; <https://ntrs.nasa.gov/archive/nasa/casi.ntrs.nasa.gov/19900004968.pdf>. Palaszewski BA. Atomic Hydrogen Propellants: Historical Perspectives and Future Possibilities, NASA Lewis Research Center, NASA/TM-106053, **1993**; <https://ntrs.nasa.gov/archive/nasa/casi.ntrs.nasa.gov/19930011425.pdf>. Palaszewski B. Launch Vehicle Performance for Bipropellant Propulsion using Atomic Propellants with Oxygen. NASA/TM-2000-209443, Nov **2000**; <https://ntrs.nasa.gov/archive/nasa/casi.ntrs.nasa.gov/20010016350.pdf>. Palaszewski BA, Bennett GL. Propulsion Estimates for High Energy Lunar Missions Using Future Propellants, 52nd AIAA/SAE/ASEE Joint Propulsion Conference, **2016**, p. 4989; <https://ntrs.nasa.gov/archive/nasa/casi.ntrs.nasa.gov/20170001563.pdf>.

⁵⁴⁹ *Rocketship X-M*, Lippert Productions, Inc., 1950; https://en.wikipedia.org/wiki/Rocketship_X-M. Theoretical and experimental studies of $H+O_3$ propellant, which provides the desired attributes of high combustion temperature and low reactant mass, were conducted beginning in the late 1940s and may have provided screenwriters with the idea for an atomic hydrogen-ozone rocket engine for the film.

⁵⁵⁰ Ley W. *Rockets, Missiles, and Space Travel*. Revised edition, Viking Press, New York, 1957.

There are at least five possible methods for making, storing, and exploiting the large recombination energy of monatomic hydrogen, including spin polarization (**Section 4.3.1.1**), frozen matrix trapping (**Section 4.3.1.2**), endohedral trapping (**Section 4.3.1.3**), charged ion plasma (**Section 4.3.1.4**), and metallic hydrogen (**Section 4.3.1.5**).

4.3.1.1 Spin-Polarized Atomic Hydrogen

The hydrogen atom consists of a nucleus containing one proton surrounded by an electron cloud containing a single electron. The electron may have one of two possible “spin” states, either “up” ($H\uparrow$) or “down” ($H\downarrow$). Hydrogen atoms interact via the attractive singlet or repulsive triplet potential depending on whether the electron spins are aligned antiparallel or parallel, respectively, so a collection of hydrogen atoms whose spins are all polarized into just one spin state will not readily recombine to make an H_2 molecule and thus will remain monatomic. At very low temperatures (≤ 1 K) and in high magnetic fields (~ 10 T), monatomic H can be stabilized by separation of the $H\uparrow$ and $H\downarrow$ states and subsequent magnetic confinement of $H\downarrow$ at the maximum of the field.⁵⁵¹ Electron-spin-polarized $H\downarrow$ is the only system in nature that remain stable in the gaseous state even at absolute zero temperature up until ~ 54 atm, whereupon it is calculated that the gas condenses into a solid. (Spin-polarized monatomic tritium $T\downarrow$ is estimated to liquefy at 3.28 K⁵⁵² with a solidification pressure of 5 atm, and to be stable against rapid recombination.⁵⁵³)

To date, spin-polarized $H\downarrow$ gas densities as high as $\sim 5 \times 10^{18} \text{ cm}^{-3}$ at temperatures 0.2-0.6 K have been achieved on LHe-cooled surfaces using a liquid helium piston,⁵⁵⁴ and magnetic traps for $H\uparrow$ atoms have also been demonstrated but at somewhat lower density.⁵⁵⁵ Silvera and Walraven

⁵⁵¹ Silvera IF, Walraven JTM. Chapter 3. Spin-polarized atomic hydrogen. In: Brewer DF, ed., Progress in Low Temperature Physics, Vol. X, Elsevier Science Publishers B.V., 1986, pp. 139-370; [https://staff.fnwi.uva.nl/j.t.m.walraven/walraven/Publications_files/Progr.%20Low%20Temp.%20Phys.%20X%20\(1986\)%20139-370.pdf](https://staff.fnwi.uva.nl/j.t.m.walraven/walraven/Publications_files/Progr.%20Low%20Temp.%20Phys.%20X%20(1986)%20139-370.pdf).

⁵⁵² Hecht CE. Predicted critical-point values for the isotopes of spin-polarized atomic hydrogen. Phys Rev B. 1981 Apr 1;23:3547; <https://journals.aps.org/prb/abstract/10.1103/PhysRevB.23.3547>.

⁵⁵³ Bešlić I, Markić LV, Boronat J. Stability limits of mixed spin-polarised tritium clusters. J Phys Conf Ser. 2009; 150(3):032010; <http://iopscience.iop.org/article/10.1088/1742-6596/150/3/032010>.

⁵⁵⁴ Bell DA, Hess HF, Kochanski GP, Buchman S, Pollack L, Xiao YM, Kleppner D, Greytak TJ. Relaxation and recombination in spin-polarized atomic hydrogen. Phys Rev B 1986 Dec 1;34:7670-97; <https://journals.aps.org/prb/abstract/10.1103/PhysRevB.34.7670>. Vainio O, Ahokas J, Järvinen J, Lehtonen L, Novotny S, Sheludiakov S, Suominen KA, Vasiliev S, Zvezdov D, Khmelenko VV, Lee DM. Bose-Einstein condensation of magnons in atomic hydrogen gas. Phys Rev Lett. 2015 Mar 27;114:125304; <https://arxiv.org/pdf/1502.03963.pdf>.

⁵⁵⁵ Kleppner's group has produced spin-polarized hydrogen “in quantities large enough to cause damaging explosions in cryogenic glassware.” Hess HF, Kochanski GP, Doyle JM, Masuhara N, Kleppner D, Greytak TJ. Magnetic trapping of spin-polarized atomic hydrogen. Phys Rev Lett. 1987 Aug 10;59:672-5; <https://journals.aps.org/prl/abstract/10.1103/PhysRevLett.59.672>. Van Roijen R, Berkhout JJ, Jaakkola S, Walraven JT. Experiments with Atomic Hydrogen in a Magnetic Trapping Field. Phys Rev Lett. 1988 Aug 22;61:931-4; <http://repository.naturalis.nl/document/43048>. van Roijen R. Atomic hydrogen in a magnetic trap. PhD thesis, 1989; http://www.iaea.org/inis/collection/NCLCollectionStore/_Public/20/066/20066588.pdf. Fried DG, Killian TC, Willmann L, Landhuis D, Moss SC, Kleppner D, Greytak TJ. Bose-Einstein Condensation of Atomic Hydrogen. Phys Rev Lett. 1998 Nov 2;81:3811-4; http://ultracold.rice.edu/publications/HBEC_vol81_num18.pdf.

believe that $\sim 2 \times 10^{19} \text{ cm}^{-3}$ may be attainable using current techniques, but also that “the rapidly increasing recombination rate with increasing density will make it difficult to dissipate the heat generated by recombination” at still higher densities⁵⁵⁶ – e.g., three-body recombination would occur in ~ 1 sec in spin-polarized hydrogen gas at a density of $1.2 \times 10^{19} \text{ cm}^{-3}$ in a magnetic field of $\sim 7.6 \text{ T}$.⁵⁵⁷

Assuming an attainable number density of $\sim 10^{19} \text{ cm}^{-3} = 1.7 \times 10^{-5} \text{ kg/L}$, a recombination energy of 436 kJ/mole yields a very high specific energy of $E_s = \mathbf{216 \text{ MJ/kg}}$ but an energy density of only $E_D = \mathbf{0.004 \text{ MJ/L}}$. Note that the highest gas densities occur on surfaces; if multiple surfaces could be vertically stacked very closely together using the techniques of molecular manufacturing, energy density might be boosted significantly. Higher energy densities might also be possible at even colder sub-kelvin temperatures, perhaps even solidifying at somewhere close to solid molecular hydrogen densities (e.g., $\sim 0.086 \text{ kg/L}$,⁵⁵⁸ implying $E_D \sim \mathbf{18.6 \text{ MJ/L}}$). Triggered recombination times on the order of $\sim 10^{-9}$ sec could yield very impressive power densities.

Another hypothetical idea for boosting energy density in spin-polarized hydrogen is to cool the trap to such a low temperature that a significant fraction of the H atoms would lack the energy to recombine if they were unable to surmount a theoretical activation barrier for the recombination reaction – if such a barrier exists. One paper⁵⁵⁹ has proposed that a very small recombination energy barrier of this kind might exist (0.005-0.018 eV), but most authors assume that there is no such barrier to recombination.⁵⁶⁰ One paper attributes this conclusion to tunneling effects: “Quantum-mechanical barrier penetration would easily overcome the activation barrier even at zero temperature. We therefore assume that an [H] atom bound to an enhanced site...can recombine with an adjacent atom without hindrance.”⁵⁶¹

⁵⁵⁶ The lifetime of spin-polarized hydrogen atoms decreases sharply with increasing density due to an increase in the number of three-body recombination collisions.

⁵⁵⁷ Hess HF, Bell DA, Kochanski GP, Kleppner D, Greytak TJ. Temperature and magnetic field dependence of three-body recombination in spin-polarized hydrogen. *Phys Rev Lett*. 1984 Apr 23;52:1520-3; <https://journals.aps.org/prl/abstract/10.1103/PhysRevLett.52.1520>.

⁵⁵⁸ https://en.wikipedia.org/wiki/Solid_hydrogen.

⁵⁵⁹ Pirronello V, Biham O, Liu C, Shen L, Vidali G. Efficiency of molecular hydrogen formation on silicates. *Astrophys J Lett*. 1997 Apr 24;483(2):L131-L134; <http://citeseerx.ist.psu.edu/viewdoc/download?doi=10.1.1.337.670&rep=rep1&type=pdf>.

⁵⁶⁰ Katz N, Furman I, Biham O, Pirronello V, Vidali G. Molecular hydrogen formation on astrophysically relevant surfaces. *Astrophys J*. 1999 Sep 1;522(1):305-312; <http://iopscience.iop.org/article/10.1086/307642/fulltext/>; Biham O, Furman I, Pirronello V, Vidali G. Master Equation for Hydrogen Recombination on Grain Surfaces. *Astrophys J*. 2001 Jun 1;553:595-603; <http://iopscience.iop.org/article/10.1086/320975/fulltext/>.

⁵⁶¹ Hollenbach D, Salpeter EE. Surface recombination of hydrogen molecules. *Astrophys J*. 1971 Jan 1;163:155-164; <http://articles.adsabs.harvard.edu/full/1971ApJ...163..155H/0000160.000.html>.

4.3.1.2 Frozen Matrix Trapping

Monatomic hydrogen can also be embedded in an ultracold matrix of frozen material. For example, $\sim 10^{18}$ atoms/cm³ of spin-polarized hydrogen atoms embedded in a frozen H₂ matrix underneath a superfluid helium film at 0.15 K are “very stable against recombination during two weeks of observations, indicating a high degree of localization of the atoms in the H₂ matrix.”⁵⁶² The H atoms were created using a miniature radio-frequency dissociator to generate electrons that bombarded the solid H₂ film, obtaining atomic concentrations approaching 1%. A few years later the same group boosted atomic H density to 2×10^{19} atoms/cm³ with strong suppression of recombination into H₂ molecules, which was explained by “the increasing role of energy level mismatch at near distances as the atoms approach each other and the temperature is lowered.”⁵⁶³ The authors were confident they could exceed 10^{20} atoms/cm³, which others⁵⁶⁴ had calculated should be stable against recombination, “by the method of cold atomic H and molecular H₂ beam epitaxy, when the two beams are simultaneously condensed on a cold substrate.” By 2009 a Russian group had achieved a peak density of 6×10^{19} atoms/cm³ in stable concentrations of H atoms in frozen krypton nanoclusters (~5 nm) immersed in superfluid helium, with mean distance ~1.4 nm between H atoms on the surface.⁵⁶⁵

A number density of $\sim 10^{20}$ cm⁻³ = 1.7×10^{-4} kg/L with a hydrogen atom recombination energy of 436 kJ/mole yields a very high specific energy of $E_S = \mathbf{216 \text{ MJ/kg}}$ but a still unimpressive energy density of only $E_D = \mathbf{0.04 \text{ MJ/L}}$.

⁵⁶² Ahokas J, Järvinen J, Khmelenko VV, Lee DM, Vasiliev S. Exotic Behavior of Hydrogen Atoms in Solid H₂ at Temperatures below 1 K. Phys. Rev. Lett. 2006 Aug 31;97:095301; <https://journals.aps.org/prl/abstract/10.1103/PhysRevLett.97.095301>.

⁵⁶³ Ahokas J, Vainio O, Järvinen J, Khmelenko VV, Lee DM, Vasiliev S. Stabilization of high-density atomic hydrogen in H₂ films at T < 0.5 K. Phys Rev B Cond Mat. 2009 Jun;79:220505; https://www.researchgate.net/profile/Vladimir_Khmelenko/publication/238971408_Stabilization_of_high-density_atomic_hydrogen_in_H-2_films_at_T_05_K/links/0912f50aa7286254c5000000/Stabilization-of-high-density-atomic-hydrogen-in-H-2-films-at-T-05-K.pdf.

⁵⁶⁴ Rosen G. Storage and recombination of atomic H in solid H₂. J Chem Phys. 1976;65:1735; <http://aip.scitation.org/doi/abs/10.1063/1.433318>.

⁵⁶⁵ Boltnev RE, Bernard EP, Järvinen J, Khmelenko VV, Lee DM. Stabilization of hydrogen atoms in aggregates of krypton nanoclusters immersed in superfluid helium. Phys Rev B. 2009;79:180506; https://www.researchgate.net/profile/Vladimir_Khmelenko/publication/233529484_Stabilization_of_hydrogen_atoms_in_aggregates_of_krypton_nanoclusters_immersed_in_superfluid_helium/links/09e4150aa72257d74f000000.pdf.

4.3.1.3 Endohedral Trapping

The trapping of individual atoms inside a fullerene cage molecule (e.g., C₆₀), called endohedral trapping, has been demonstrated experimentally since the early 1990s for metal atoms such as Ca, Co, La, Li, Sc, U and Y, aka. the metallofullerenes, and for a variety of small molecules such as CO and CN.⁵⁶⁶ Endohedral trapping of H₂ molecules inside the C₆₀ cage has been achieved using a molecular surgery method⁵⁶⁷ and laser excitation.⁵⁶⁸

Although challenging to manufacture,⁵⁶⁹ monatomic hydrogen trapped inside small carbon fullerene cages might provide a better effective H atom number density – and thus an acceptable energy density – perhaps in the form of a macroscale solid fullerene powder, especially if modestly compressed⁵⁷⁰ (but not highly compressed⁵⁷¹ which might overcome the 2.57 eV barrier to H passage through a hexagonal ring in the fullerene wall).⁵⁷² Endohedral trapping of

⁵⁶⁶ Moro L, Ruoff RS, Becker CH, Lorents DC, Malhotra R. Studies of metallofullerene primary soots by laser and thermal desorption mass spectrometry. *J Phys Chem.* 1993 Jul;97(26):6801-5; <http://pubs.acs.org/doi/abs/10.1021/j100128a009>. Bethune DS, Johnson RD, Salem JR, De Vries MS, Yannoni CS. Atoms in carbon cages: the structure and properties of endohedral fullerenes. *Nature.* 1993 Nov 11;366(6451):123-8; http://www.chem.ucsb.edu/devriesgroup/sites/secure.lsit.ucsb.edu.chem.d7_devries/files/sitefiles/lab/54.pdf. Gromov A, Krätschmer W, Krawez N, Tellgmann R, Campbell EE. Extraction and HPLC purification of Li@C60/70. *Chem Commun.* 1997(20):2003-4; <http://pubs.rsc.org/en/content/articlelanding/1997/cc/a704609j>.

⁵⁶⁷ Komatsu K, Murata M, Murata Y. Encapsulation of molecular hydrogen in fullerene C60 by organic synthesis. *Science.* 2005 Jan 14;307(5707):238-40; <http://science.sciencemag.org/content/307/5707/238>.

⁵⁶⁸ Oksengorn B. Preparation of endohedral complexes of molecular hydrogen-fullerene C60, together with hydrogenated C60. *CR Chimie.* 2003 Apr 1;6:467; <http://www.sciencedirect.com/science/article/pii/S163107480300064X>.

⁵⁶⁹ Beardmore K, Smith R, Richter A, Mertesacker B. The interaction of C₆₀ with hydrogen plasma. *Vacuum.* 1995 Aug 1;46(8-10):1091-6; <http://www.sciencedirect.com/science/article/pii/0042207X95001131>. Long Z, Zhou X, Cai H, Chen C, Miao L, Allen RE. Breathing-trap mechanism for encapsulation of atomic hydrogen in C₆₀. *Chem Phys Lett.* 2013 Sep 17;583:114-8; <http://people.physics.tamu.edu/allen/Long-Zhou-July3.pdf>.

⁵⁷⁰ <https://en.wikipedia.org/wiki/Buckminsterfullerene#Solid>.

⁵⁷¹ Kozlov ME, Hirabayashi M, Nozaki K, Tokumoto M, Ihara H. Superhard form of carbon obtained from C₆₀ at moderate pressure. *Synthetic Metals.* 1995 Mar 15;70(1):1411-2; <http://www.sciencedirect.com/science/article/pii/037967799402900J>.

⁵⁷² Vehviläinen TT, Ganchenkova MG, Oikkonen LE, Nieminen RM. Hydrogen interaction with fullerenes: From C₂₀ to graphene. *Phys Rev B.* 2011 Aug 30;84(8):085447; https://aaltodoc.aalto.fi/bitstream/handle/123456789/17264/A1_vehvil%C3%A4inen_t_t_2011.pdf.

individual H atoms⁵⁷³ has been studied theoretically, both in pure carbon fullerenes and in other cage molecules such as deuterated fullerenes (C₂₀D₂₀),⁵⁷⁴ dodecahedral nitrogen cages (N₂₀),⁵⁷⁵ beryllium cluster cages (Be_n, n = 5-9)⁵⁷⁶ and octasilsesquioxane (Si₈O₁₂H₈),⁵⁷⁷ but has not yet

⁵⁷³ Connerade JP, Dolmatov VK, Lakshmi PA, Manson ST. Electron structure of endohedrally confined atoms: atomic hydrogen in an attractive shell. *J Phys B: Atom Molec Optical Phys.* 1999 May 28;32(10):L239; https://www.researchgate.net/profile/Valeriy_Dolmatov/publication/231143527_Electron_structure_of_endohedrally_confined_atoms_atomic_hydrogen_in_an_attractive_shell/links/00b7d5272a152d2ba4000000.pdf. Varshni YP. Critical cage radii for a confined hydrogen atom. *J Phys B: Atomic Molec Optical Phys.* 1998 Jul 14;31(13):2849; <http://iopscience.iop.org/article/10.1088/0953-4075/31/13/005/meta>. Hao-Xue QI, Bai-Wen LI. Spectral properties of endohedrally confined hydrogen atom and hydrogen-like ions obtained by using B-spline basis set. *Commun Theoret Phys.* 2002 Apr 15;37(4):475; <http://iopscience.iop.org/article/10.1088/0253-6102/37/4/475/meta>. Neek-Amal M, Tayebirad G, Asgari R. Ground-state properties of a confined simple atom by C₆₀ fullerene. *J Phys B: Atomic Molec Optical Phys.* 2007 Mar 26;40(8):1509; https://www.researchgate.net/profile/Reza_Asgari3/publication/1861625_Ground_state_properties_of_a_confined_simple_atom_by_C_60_fullerene/links/0deec51683e4cb4723000000.pdf. Gryzlova EV, Grum-Grzhimailo AN, Strakhova SI. Ionization of endohedrals H@C₆₀ and H@C₃₆ by intense VUV femtosecond pulses. *J Phys: Conf Series* 2012;388(3):032047; http://www.academia.edu/download/43776292/Ionization_of_endohedrals_HC60_and_HC36_20160316-17279-141bdx.pdf. Lin CY, Ho YK. Photoionization of endohedral atoms in fullerene cages. *Few-Body Systems.* 2013 Mar 1:1-5; http://www.iams.sinica.edu.tw/project/ykho/files/2013_3.pdf. Javan MB, Ganji MD. Theoretical investigation on the encapsulation of atomic hydrogen into heterofullerene nanocages. *Curr Appl Phys.* 2013 Sep 30;13(7):1525-31; https://www.researchgate.net/profile/M_Ganji/publication/260672335_Theoretical_investigation_on_the_encapsulation_of_atomic_hydrogen_into_heterofullerene_nanocages/links/55990b3a08ae21086d237bd2.pdf.

⁵⁷⁴ Javan MB, Ganji MD. Theoretical investigation on the encapsulation of atomic hydrogen into heterofullerene nanocages. *Curr Appl Phys.* 2013 Sep 30;13(7):1525-31; https://www.researchgate.net/profile/M_Ganji/publication/260672335_Theoretical_investigation_on_the_encapsulation_of_atomic_hydrogen_into_heterofullerene_nanocages/links/55990b3a08ae21086d237bd2.pdf.

⁵⁷⁵ Wright JS, McKay DJ, DiLabio GA. Dodecahedral molecular nitrogen (N₂₀) and related structures. *J Molec Struct: THEOCHEM.* 1998 Feb 9;424(1):47-55; <http://www.sciencedirect.com/science/article/pii/S0166128097002248>.

⁵⁷⁶ Naumkin FY, Wales DJ. Hydrogen trapped in Be_n cluster cages: The atomic encapsulation option. *Chem Physics Lett.* 2012 Aug 30;545:44-9; http://myweb.science.uoit.ca/~fnaumkin/papers/cpl_545_44.pdf. Naumkin FY, Wales DJ. Trapping of hydrogen atoms inside small beryllium clusters and their ions. *Chem Phys Lett.* 2016 Aug 16;659:282-8; <http://www.sciencedirect.com/science/article/pii/S0009261416305450>.

⁵⁷⁷ Mattori M, Mogi K, Sakai Y, Isobe T. Studies on the trapping and detrapping transition states of atomic hydrogen in octasilsesquioxane using the density functional theory B3LYP method. *J Phys Chem A.* 2000 Nov 23;104(46):10868-72; <http://pubs.acs.org/doi/abs/10.1021/jp0015269>. Päch M, Macrae RM, Carmichael I. Hydrogen and deuterium atoms in octasilsesquioxanes: Experimental and computational studies. *J Amer Chem Soc.* 2006 May 10;128(18):6111-25; https://www.researchgate.net/profile/Michael_Paech/publication/7110309_Hydrogen_and_deuterium_atoms_in_octasilsesquioxanes_Experimental_and_computational_studies/links/0deec52036d23dbf67000000.pdf.

been achieved experimentally – although endohedral tritium ($^3\text{H}@C_{60}$) has been reported.⁵⁷⁸ It is possible that monatomic hydrogen can tunnel through the five-member rings in the fullerene cage⁵⁷⁹ or destabilize the fullerene cage bond structure,⁵⁸⁰ so success with $\text{H}@C_{60}$ is not assured. Cryogenic temperatures may be required if atomic hydrogen in C_{60} is not stable at room temperature.⁵⁸¹

A C_{60} buckyball with an atom trapped inside has a nominal diameter of 1 nm; with a volumetric packing factor of $f_{\text{sph}} = (3\pi^2 / 64)^{1/2} = 0.68017$ for closely-packed spheres of equal radius,⁵⁸² we can pack together $N_{C_{60}} \sim 10^{24} f_{\text{sph}} = 6.8 \times 10^{23}$ buckyballs/liter. Taking one H atom per buckyball and $E_{\text{H}} = 3.59 \times 10^{-19}$ J/atom of recombination energy, the implied energy density would be $E_{\text{D}} = N_{C_{60}} E_{\text{H}} = \mathbf{0.24 \text{ MJ/L}}$.

⁵⁷⁸ Khong A, Cross RJ, Saunders M. From $^3\text{He}@C_{60}$ to $^3\text{H}@C_{60}$: Hot-Atom Incorporation of Tritium in C_{60} . *J Phys Chem A*. 2000 May 4;104(17):3940-3; <http://pubs.acs.org/doi/abs/10.1021/jp994289m>.

⁵⁷⁹ Nanbu S, Ishida T, Nakamura H. Atomic hydrogen transmission through five-membered carbon ring by the mechanism of non-adiabatic tunneling. *Chem Phys*. 2006 May 31;324(2):721-32; http://www-old.ac.nctu.edu.tw/files/users/research/127_879b14ea.pdf.

⁵⁸⁰ Berber S, Tománek D. Hydrogen-induced disintegration of fullerenes and nanotubes: An ab initio study. *Phys Rev B*. 2009 Aug 24;80(7):075427; <http://www.pa.msu.edu/cmp/csc/eprint/DT200.pdf>.

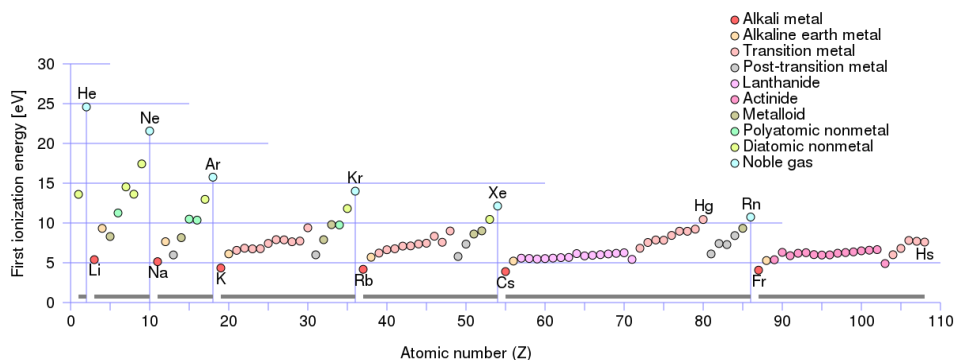
⁵⁸¹ Waiblinger M, Pietzak B, Lips K, Dennis TJ, Weidinger A, Päch M, Stösser R. Atomic hydrogen in the Si_8O_{12} cage. In Kuzmany H, Mehring M, Roth S, editors. *AIP Conference Proceedings* 1999 Sep 30;486(1):148-151; <http://aip.scitation.org/doi/abs/10.1063/1.59774>.

⁵⁸² Gasson PC. *Geometry of Spatial Forms*, John Wiley & Sons, New York, 1983.

4.3.1.4 Charged Ion Plasma

If a single hydrogen atom is fully ionized⁵⁸³ by the removal of its sole electron at an energy cost of 1312 kJ/mole or 13.60 eV (the first ionization potential), the monoatom becomes a positively charged H^+ hydrogen ion, aka. a naked proton.⁵⁸⁴ Aggregated into a charged plasma cloud, such monatomic ions experience Coulombic (electrostatic) repulsion and cannot recombine with neighboring ions into molecular hydrogen until one electron per ion is injected into the cloud, leading to H^+ deionization followed by molecular recombination to H_2 which releases **216 MJ/kg** of stored recombination energy. (The deionization event also releases additional energy, equivalent in magnitude to the first ionization potential, usually as photons.)

The higher the ionization energy, the harder it is to remove the first electron from the atom. Thus the walls of our physical container that must store the naked protons should consist of a material with the highest possible first ionization potential. That way, electrons will prefer to stay bound to neutral wall atoms and not jump to the naked proton and neutralize it, which would produce a higher total energy for the proton/neutral-atom system. Only 7 elements have higher first ionization potentials than hydrogen (chart, below):⁵⁸⁵ He (24.6 eV), Ne (21.6 eV), F (17.4 eV), Ar (15.8 eV), N (14.5 eV), Kr (14.0 eV), and O (13.62 eV). Ignoring He which solidifies <0.95 K and >25 atm and is mechanically weak,⁵⁸⁶ Ne solidifies <25 K with mechanical yield strength 0.2 MPa at 8-21 K.⁵⁸⁷



⁵⁸³ Adiabatic ionization is a form of ionization in which an electron is removed from or added to an atom or molecule in its lowest energy state to form an ion in its lowest energy state; https://en.wikipedia.org/wiki/Ionization#Production_of_ions.

⁵⁸⁴ Most of the fast ions in the magnetosphere and in the solar wind are protons; <https://www-spo.gsfc.nasa.gov/Education/Ielect.html>.

⁵⁸⁵ https://en.wikipedia.org/wiki/Ionization#/media/File:First_Ionization_Energy.svg.

⁵⁸⁶ https://en.wikipedia.org/wiki/Helium#Liquid_helium;
<https://web.archive.org/web/20080531145546/http://www.phys.ualberta.ca/~therman/lowtemp/projects1.htm>.

⁵⁸⁷ Shirron PJ, *et al.* Mechanical properties of solid neon and structural modeling of the XRS solid neon dewar. *Cryogenics* 1999 Apr;39(4):405-414; <http://www.sciencedirect.com/science/article/pii/S0011227599000405>.

The first ionization energy of a neon atom is $\Delta E = 8.0 \text{ eV}$ ($1.28 \times 10^{-18} \text{ J}$) higher than for hydrogen, so a naked proton impacting a neon wall with less than 8.0 eV of translational kinetic energy ($T_{\text{TKE}} \sim 2 \Delta E / 3 k_B = 61,800 \text{ K}$) would be unlikely to extract an electron from the Ne atom and thus recombine into a neutral H atom. The electric potential energy of n_p protons placed in a box of size L_{box} with a mean interproton separation of $r_{\text{mean}} = (L_{\text{box}}^3/n_p)^{1/3}$ is just the sum of the energies of each unique pair of particles,⁵⁸⁸ or $E_{\text{cloud}} \sim q^2 C(n_p, 2) / 4\pi\epsilon_0 r_{\text{mean}}$; setting $E_{\text{cloud}}/n_p \leq \Delta E$, then $L_{\text{box}} \geq q^2 C(n_p, 2) / 4\pi\epsilon_0 n_p^{2/3} \Delta E$, the minimum box size into which n_p protons can be packed without exceeding an electric potential energy of ΔE per proton, where proton charge $q = 1.60 \times 10^{-19} \text{ coul}$, permittivity constant $\epsilon_0 = 8.85 \times 10^{-12} \text{ coul}^2/\text{Nm}^2$, and electrostatic energy density $E_D = E_{\text{cloud}} / L_{\text{box}}^3$. For $n_p = 207$ protons, $E_D = \mathbf{0.0002 \text{ MJ/L}}$ for $L_{\text{box}} \geq 110 \text{ nm}$ and an electrostatic pressure of 0.2 MPa, the strength limit for solid neon box walls.⁵⁸⁹ If the neon walls can be reinforced from behind with diamond having a tensile strength of $\sim 100 \text{ GPa}$,⁵⁹⁰ then for $n_p = 4$ protons, $E_D = \mathbf{65 \text{ MJ/L}}$ for $L_{\text{box}} \geq 0.4 \text{ nm}$ and an electrostatic pressure of 65 GPa.⁵⁹¹ The combined specific energy for deionization + molecular recombination is **984 MJ/kg** in both cases.

Note that hydrogen is one of the few elements whose atoms can readily form both cations (H^+) and anions (H^-). Rather than injecting electrons into a charged cationic plasma to trigger energy release as described earlier, we could instead imagine a hypergolic system with separate tanks of cationic and anionic hydrogen ions which spontaneously form neutral H_2 molecules when mixed at a controlled rate, simultaneously releasing the combined **984 MJ/kg** energy of deionization and the energy of molecular recombination.

Of course, the trapping and storing of charged ions – e.g., in magnetic bottles or ion traps using a combination of electric or magnetic fields – is hardly a new concept in physics, but the ion densities achieved to date are not impressive. For example, a **Penning trap** stores cold charged particles using a strong homogeneous axial magnetic field to confine particles radially and a

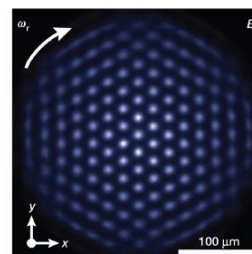
⁵⁸⁸ The combination number (binomial coefficient) of unique groupings of k items drawn from a total population of n items is $C(n, k) = n! / k!(n-k)!$; https://en.wikipedia.org/wiki/Binomial_coefficient.

⁵⁸⁹ While 207 protons in a $(110 \text{ nm})^3$ neon box might not sound like much, it equates to **1.56×10^{17}** protons/cm³, which exceeds current storage densities of **1×10^{10}** protons/cm³ for a 50 T Penning trap, **4.3×10^{14}** protons/cm³ for the 2016 record confinement in a Tokamak fusion reactor, and **1.9×10^{14}** protons/cm³ in the Large Hadron Collider proton beam as of 2016 (see below). Four protons in a $(0.6 \text{ nm})^3$ box equates to **6.3×10^{22}** protons/cm³.

⁵⁹⁰ Luo X, Liu Z, Xu B, Yu D, Tian Y, Wang HT, He J. Compressive Strength of Diamond from First-Principles Calculation. J Phys Chem C. 2010 Oct 21;41(114):17851-3; https://www.researchgate.net/profile/Xiaoguang_Luo/publication/225376850_Compressive_Strength_of_Diamond_From_First-Principles_Calculation/links/0fcfd5126365a800dc000000.pdf.

⁵⁹¹ Given some average group energy, a collection of free particles will develop a distribution of individual energies, many of which may be much higher than the group average. Assuming a simple Maxwell-Boltzmann distribution, to ensure that fewer than 1 of 207 particles in the box will have an energy of 8 eV or higher requires the group mean electric potential energy should not exceed 1.14 eV ($T_{\text{TKE}} \sim 8820 \text{ K}$), or 3.72 eV ($T_{\text{TKE}} \sim 28,800 \text{ K}$) for 4 particles, using a modified Jeans escape formula (<http://sci.esa.int/science-e/www/object/doc.cfm?fobjectid=50647>).

quadrupole electric field to confine the particles axially. Early systems could trap just a single proton in a $\sim 1.4 \text{ mm}^3$ volume,⁵⁹² but the theoretical limit for a Penning trap is apparently $\sim 2.4 \times 10^8$ protons/cm³ at 9.4 tesla and $\sim 10^{10}$ protons/cm³ at 50 tesla.⁵⁹³ The TRAP experiment at CERN successfully stored a single antiproton for 57 days, the current world record for a Penning trap.⁵⁹⁴ A typical **Paul trap** (a type of quadrupole ion trap that uses static direct current and radio frequency oscillating electric fields to trap ions) might store $\sim 10^6$ ions in a $\sim 500 \text{ mm}^3$ trap over storage times of $\sim 10^4$ sec in vacuums pumped down to $\sim 10^{-13}$ atm,⁵⁹⁵ with a theoretical maximum of $\sim 3 \times 10^9$ protons/cm³ for a Paul trap at ~ 1 MHz and ~ 10 kilovolts.⁵⁹⁶ Atomic ions can form “ion Coulomb crystals” inside ion traps (e.g., image, right, shows a single plane of Be⁺ ions in a Penning trap), with ion-ion separations of $\sim 10 \text{ }\mu\text{m}$ with a number density on the order of $\sim 10^9$ ions/cm³.⁵⁹⁷ A $\sim 10^{10}$ proton/cm³ number density would correspond to a very poor molecular recombination energy density of $3.6 \times 10^{-6} \text{ MJ/L}$, while specific energy remains at **216 MJ/kg**.



The prospect of fusion energy has inspired a great deal of experimental effort to confine hot plasma ions (usually deuterium and tritium, not hydrogen) for sufficiently long confinement times to allow nuclear fusion to occur. In late 2016, the Alcator C-Mod tokamak at MIT set a new world confinement pressure record⁵⁹⁸ of 2.05 atm ($\sim 4.3 \times 10^{14}$ ions/cm³) for deuterium-tritium plasma using a 5.7 tesla magnetic field and a particle temperature of 3.5×10^7 K while sustaining fusion for ~ 2 seconds,⁵⁹⁹ with the French ITER reactor expected to reach only a slightly better 2.6 atm (1.4×10^{14} ions/cm³)⁶⁰⁰ when in full operation in 2032. (Maximum magnetic field pressure is $\sim B^2/2\mu_0 = 128$ atm for magnetic field strength $B = 5.7$ tesla with permeability constant $\mu_0 = 1.26 \times 10^{-6}$ N/A².)

⁵⁹² Brown LS, Gabrielse G. Geonium theory: Physics of a single electron or ion in a Penning trap. Rev Mod Phys. 1986 Jan;58(1):233-311; <http://gabrielse.physics.harvard.edu/gabrielse/papers/1986/Review.pdf>.

⁵⁹³ Li GZ, Guan S, Marshall AG. Comparison of Equilibrium Ion Density Distribution and Trapping Force in Penning, Paul, and Combined Ion Traps. J Amer Soc Mass Spectrometry 1998 May;9(5):473-481; <http://www.sciencedirect.com/science/article/pii/S1044030598000051>.

⁵⁹⁴ <http://angelsanddemons.web.cern.ch/antimatter/trapping-antimatter>.

⁵⁹⁵ http://www.springer.com/cda/content/document/cda_downloaddocument/9783540922605-c1.pdf?SGWID=0-0-45-793331-p173876933.

⁵⁹⁶ Li GZ, Guan S, Marshall AG. Comparison of Equilibrium Ion Density Distribution and Trapping Force in Penning, Paul, and Combined Ion Traps. J Amer Soc Mass Spectrometry 1998 May;9(5):473-481; <http://www.sciencedirect.com/science/article/pii/S1044030598000051>.

⁵⁹⁷ Thompson RC. Ion Coulomb Crystals. Contemporary Physics 2015 Jan;56(1):63-79; <https://arxiv.org/pdf/1411.4945.pdf>.

⁵⁹⁸ <http://news.mit.edu/2016/alcator-c-mod-tokamak-nuclear-fusion-world-record-1014>.

⁵⁹⁹ https://en.wikipedia.org/wiki/Alcator_C-Mod.

⁶⁰⁰ In operation, ITER (International Thermonuclear Experimental Reactor) will use 0.5 gm of ionized D/T mixture in an 840 m³ reaction chamber; <https://en.wikipedia.org/wiki/ITER>.

10^{-6} henry/meter.⁶⁰¹) It has been hypothesized that the minimum reactor size for tokamaks might be on the order of centimeters, not meters.⁶⁰²

A great variety of hot confinement schemes are being explored,⁶⁰³ but the general range of “confinement quality” either already achieved or expected soon to be achieved, most commonly using magnetic or inertial confinement, is 10^{11} - 10^{16} particle-sec/cm³ for hot 0.1-100 KeV charged particles.⁶⁰⁴ If the 10^{16} particle-sec/cm³ figure can be taken to apply to protons, then we could confine 10^{16} protons/cm³ for 1 second, still yielding only a very poor molecular recombination energy density of $E_D = (10^{19} \text{ protons/L}) (1.67 \times 10^{-27} \text{ kg/proton}) (216 \text{ MJ/kg}) = 3.6 \times 10^{-6} \text{ MJ/L}$, and with a storage lifetime of only 1 second.⁶⁰⁵

Particle accelerators also confine charged ions in dense collimated beams using enormous magnets inside “storage rings” (circular particle accelerators) “in which a continuous or pulsed particle beam may be kept circulating typically for many hours.”⁶⁰⁶ For example, CERN’s **Intersecting Storage Rings** (ISR), the world’s first hadron collider, produced beams of 28 GeV protons with a number density of 1.5×10^{10} protons/cm³ in 1973, which could circulate for up to 36 hours before requiring a refill.⁶⁰⁷ The **Large Hadron Collider** (LHC), currently the world’s largest hadron collider, produces beams of 6.5 TeV protons with a number density of 1.9×10^{13}

⁶⁰¹ McMillan BF. The physics of fusion. Warwick University, 10 Feb 2014, p. 25;
http://www2.warwick.ac.uk/fac/sci/physics/current/teach/module_home/px438/lecture_distributed_2014.pdf.

⁶⁰² Rostoker N, Binderbauer MW, Monkhurst HJ. Colliding beam fusion reactor. Science. 1997 Nov 21;278(5342):1419-22;
https://www.researchgate.net/profile/Michl_Binderbauer/publication/3835752_Colliding_beam_fusion_reactor/links/55d71ee308ae9d65948d339e.pdf.

⁶⁰³ https://en.wikipedia.org/wiki/Fusion_power#Approaches.

⁶⁰⁴ https://en.wikipedia.org/wiki/Fusion_power#Confinement and
https://upload.wikimedia.org/wikipedia/commons/0/0e/IFE_and_MFE_parameter_space.svg.

⁶⁰⁵ Gravitational confinement seems more effective but may be difficult to exploit. For example, the Sun gravitationally traps a 90% H / 9% He (by atom count) charged ion plasma with a mean density of 1.408 kg/L (<https://en.wikipedia.org/wiki/Sun>), so a specific energy of 216 MJ/kg for molecular recombination would equate to an energy density of ~300 MJ/L. Barnard’s Star, a hydrogen-rich red dwarf with ~19 times the mean density of the Sun (https://en.wikipedia.org/wiki/Barnard's_Star), may exhibit superlative proton confinement (among Main Sequence stars) that would equate to a recombination energy density of ~5700 MJ/L. However, mining these high energy density materials may prove technically challenging.

⁶⁰⁶ https://en.wikipedia.org/wiki/Storage_ring.

⁶⁰⁷ ISR ring circumference 942.66 m, beam height ~3 mm or 2.8×10^{-5} m² cross-sectional area, proton beam current ~20 amps or 4×10^{14} protons/beam, with nominal beam “luminosity” of 2×10^{30} protons/cm²-sec; Johnsen K. CERN Intersecting Storage Ring (ISR). PNAS 1973 Feb;70(2):619-626;
<http://www.pnas.org/content/70/2/619.full.pdf>.

protons/cm³ in 2016,⁶⁰⁸ with a beam storage lifetime (i.e., intensity falls to 1/e) of ~45 hr due to proton collisions with other protons and with gas molecules in the imperfect vacuum.⁶⁰⁹ (There are also synchrotron radiation losses,⁶¹⁰ which at a 6.5 TeV beam energy amounts to $\sim 1.6 \times 10^{-11}$ W that would drain the proton's kinetic energy in $\tau_{\text{synch}} \sim 18$ hr, improving to $\tau_{\text{synch}} \sim 136,000$ yr at a 0.1 MeV beam energy.) This implies a molecular recombination energy density of only $E_{D,\text{mre}} = (1.9 \times 10^{13} \text{ protons/cm}^3) (1.67 \times 10^{-27} \text{ kg/proton}) (216 \text{ MJ/kg}) = \mathbf{7 \times 10^{-9} \text{ MJ/L}}$ for the LHC beamline, which is dwarfed by the LHC proton beamline kinetic energy density of $E_{D,\text{kinetic}} \sim (1.9 \times 10^{13} \text{ protons/cm}^3) (6.5 \text{ TeV}) (1.60 \times 10^{-7} \text{ J/TeV}) = \mathbf{20,000 \text{ MJ/L}}$.⁶¹¹

Since a lower beam energy permits higher beam density at a much smaller device radius or a lower magnetic field strength, might a compact ion beamline energy storage be possible using low-energy high-current storage rings? A stellarator-type magnetic storage ring for an $I_{\text{beam}} \sim 10$ ampere, 0.1 MeV proton beam has been studied for research on the p+¹¹B fusion reaction.⁶¹² With a B = 1 tesla field,⁶¹³ a beam of E = 0.1 MeV protons of mass $m_p = 1.67 \times 10^{-27}$ kg and charge $q_p = 1.60 \times 10^{-19}$ coul/proton could circulate at a radius as small as $R_{\text{ring}} = (2 m_p E)^{1/2} / q_p B = 4.6$ cm. An LHC-like beam cross-sectional area of $A_{\text{beam}} = 8 \times 10^{-10} \text{ m}^2$ would yield a proton number density of $n_p = I_{\text{beam}} / c q_p A_{\text{beam}} = 2.6 \times 10^{14} \text{ protons/cm}^3$, storing $E_{D,\text{kinetic}} = (2.6 \times 10^{14} \text{ protons/cm}^3) (0.1 \text{ MeV/proton}) (1.60 \times 10^{-13} \text{ J/MeV}) = \mathbf{4.2 \times 10^{-3} \text{ MJ/L}}$ of kinetic energy, $E_{D,\text{mre}} = (2.6 \times 10^{14} \text{ protons/cm}^3) (1.67 \times 10^{-27} \text{ kg/proton}) (216 \text{ MJ/kg}) = \mathbf{9 \times 10^{-8} \text{ MJ/L}}$ of molecular recombination energy, and $E_{D,\text{ire}} = (2.6 \times 10^{14} \text{ protons/cm}^3) (13.6 \text{ eV/proton}) (1.6 \times 10^{-19} \text{ J/eV}) = \mathbf{6 \times 10^{-7} \text{ MJ/L}}$ of ion recombination energy (**Section 4.4.3.2**), for a total system energy density of only $\sim \mathbf{0.004 \text{ MJ/L}}$ which is still almost exclusively due to the kinetic energy component. Beam densities in excess of $\sim 10^{18}$ protons/cm³ are probably required for a practical molecular recombination energy storage system.

⁶⁰⁸ LHC ring circumference 27,000 m, beam height $\sim 16 \mu\text{m}$ or $8 \times 10^{-10} \text{ m}^2$ cross-sectional area, proton beam current $\sim 3.2 \times 10^{14}$ protons/beam, with year-end 2016 beam “luminosity” of 1.4×10^{34} protons/cm²-sec; https://en.wikipedia.org/wiki/Large_Hadron_Collider and https://www.lhc-closer.es/taking_a_closer_look_at_lhc/0.luminosity.

⁶⁰⁹ “Beam Lifetime,” https://www.lhc-closer.es/taking_a_closer_look_at_lhc/0.beam_lifetime.

⁶¹⁰ “Synchrotron Radiation,” https://www.lhc-closer.es/taking_a_closer_look_at_lhc/0.synchrotron_radiation.

⁶¹¹ The total stored kinetic beam energy in the LHC proton beam at 6.5 TeV is ~ 360 MJ; https://www.lhc-closer.es/taking_a_closer_look_at_lhc/0.energy. A 6.5 TeV proton is traveling at $\sim 0.99999999c$; https://en.wikipedia.org/wiki/Large_Hadron_Collider#Design.

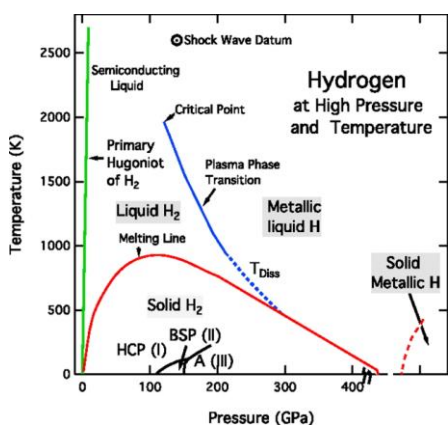
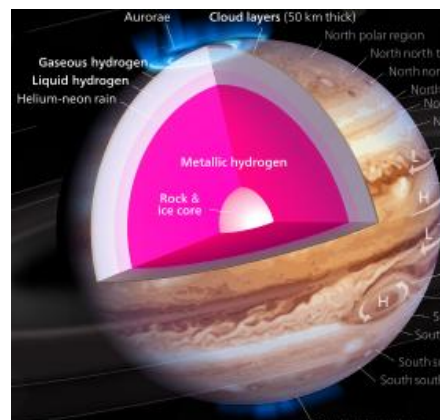
⁶¹² Droba M, Joshi N, Ratzinger U. Magnetic high current ion storage ring. In: Plasma Science 2008, ICOPS 2008, IEEE 35th Intl Conf on 2008 Jun 15; <http://ieeexplore.ieee.org/document/4590870/>.

⁶¹³ https://en.wikipedia.org/wiki/Neodymium_magnet.

4.3.1.5 Metallic Hydrogen

Another way to improve the energy density of monatomic hydrogen might be to apply ultrahigh pressure to compact it to a higher physical density. To this end, it has been asserted that metallic hydrogen would make an ideal high-energy rocket fuel.⁶¹⁴

While elemental hydrogen is often placed atop the alkali metal column in the periodic table,⁶¹⁵ it does not normally exhibit metallic properties at atmospheric pressure but rather forms gaseous diatomic H_2 molecules that liquefy (20 K) or solidify (14 K) only at very low temperature. In 1935, Wigner and Huntington⁶¹⁶ first predicted that hydrogen might display metallic properties



if subjected to pressures exceeding 25 GPa (~250,000 atm). Instead of discrete H_2 molecules having two electrons bound between two protons, a bulk phase would form consisting of a liquid or solid lattice of protons, with electrons delocalized throughout as occurs in conductive metals. The first existence proof for this prediction came from planetary astronomy, as most of the mass of the planet Jupiter (image, above) is now believed to consist of liquid metallic hydrogen at ~200 GPa and ~10,000 K.⁶¹⁷ Laboratory investigations confirm⁶¹⁸ that the original estimated metallization pressure was too low. Proposed phase diagrams of hydrogen (image, left) suggest 100-600 GPa pressure may be required for metallization.⁶¹⁹

⁶¹⁴ Silvera IF, Cole JW. Metallic hydrogen: The most powerful rocket fuel yet to exist. *J Phys: Conf Ser.* 2010; 215:012194; <http://iopscience.iop.org/article/10.1088/1742-6596/215/1/012194/pdf;jsessionid=9E441ED29B79EBE9627B0EBE4230C7BA.c3.iopscience.cld.iop.org>.

⁶¹⁵ https://en.wikipedia.org/wiki/Periodic_table.

⁶¹⁶ Wigner E, Huntington HB. On the possibility of a metallic modification of hydrogen. *J Chem Phys.* 1935;3(12):764-770; <http://aip.scitation.org/doi/abs/10.1063/1.1749590>.

⁶¹⁷ Guillot T, Stevenson DJ, Hubbard WB, Saumon D. "Chapter 3: The Interior of Jupiter," in: Bagenal F, Dowling TE, McKinnon WB, eds. *Jupiter: The Planet, Satellites and Magnetosphere*. Cambridge University Press, 2004; see also https://en.wikipedia.org/wiki/Jupiter#Internal_structure.

⁶¹⁸ Loubeyre P, *et al.* X-ray diffraction and equation of state of hydrogen at megabar pressures. *Nature.* 1996 Oct 24;383(6602):702-704; <https://www.nature.com/nature/journal/v383/n6602/abs/383702a0.html>.

⁶¹⁹ Silvera I. The insulator-metal transition in hydrogen. *PNAS* 2010;107(29):12743-12744; <http://www.pnas.org/content/107/29/12743.full>.

Once H₂ has been dissociated under extreme pressurization, releasing the pressure on the metallic hydrogen (and possibly heating to above some as yet unknown critical temperature⁶²⁰) would allow the free protons, immersed in a degenerate electron sea (**Section 7.5.4.1**), to recombine into hydrogen molecules, releasing **216 MJ/kg** of stored recombination energy.⁶²¹

One interesting question is whether or not any energy barrier to recombination exists,⁶²² raising the possibility of a metastable metallic hydrogen material. For example, CO₂ compressed to 40 GPa at 1800 K forms a translucent quartzlike extended covalent solid that remains metastable even when cooled down to room temperature and depressurized as low as ~1 GPa.⁶²³ (Diamond is also a metastable phase of graphite.) If a barrier exists for metallic hydrogen, it might be possible to store “metastable”⁶²⁴ or “quenched”⁶²⁵ metallic hydrogen at ordinary pressures over long periods of time for more convenient use as a fuel. There is one experimental 1972 report of

⁶²⁰ Cole JW, Silvera IF. Metallic hydrogen propelled launch vehicles for lunar missions. AIP Conf Proceedings 2009; 1103(1):117; https://www.researchgate.net/profile/Isaac_Silvera/publication/234979364_Metallic_Hydrogen_Propelled_Launch_Vehicles_for_Lunar_Missions/links/54ac2ef20cf2479c2ee77a59.pdf.

⁶²¹ A fuel releasing this much energy, if used in a rocket engine, could raise the reaction chamber temperature to >6000 K, much higher than current materials can withstand. One proposed method to reduce reaction temperature is to dilute the metallic hydrogen with water, hydrocarbons or molecular hydrogen, still providing a marked increase in efficiency over traditional rocket fuel even with significant dilutions (Cole JW, Silvera IF. Future Propellants for Launch Vehicles – Metallic Hydrogen with Water and Hydrocarbon Diluents. AIP Conference Proceedings, 2010;1208(1):107-120).

⁶²² Nellis WJ. Metastable solid metallic hydrogen. J Phil Mag Part B. 1999;79(4):655-661; https://www.researchgate.net/profile/W_Nellis/publication/252786756_Metastable_solid_metallic_hydrogen/links/55a2840508aec9ca1e64f591.pdf.

⁶²³ Iota V, Yoo CS, Cynn H. Quartzlike carbon dioxide: an optically nonlinear extended solid at high pressures and temperatures. Science 1999 Mar 5;283(5407):1510-1513; <http://www.hpcat.aps.anl.gov/highlights/Sci-1999.pdf>.

⁶²⁴ Ashcroft NW. Metallic hydrogen: A high-temperature Superconductor? Phys Rev Lett. 1968 Dec 23;21:1748; <https://journals.aps.org/prl/abstract/10.1103/PhysRevLett.21.1748>. Brovamn EG, Kagan Y, Kholas A. Structure of metallic hydrogen at zero pressure. Soviet Physics JETP 1972 Jun;34(6):1300-1315; http://jetp.ac.ru/cgi-bin/dn/e_034_06_1300.pdf. Brovamn EG, Kagan Y, Kholas A, Pushkarev VV. Role of electron-electron interaction in the formation of a metastable state of metallic hydrogen. ZhETF Pis. Red. 1973 Aug 20;18(4):269-273; http://www.jetpletters.ac.ru/ps/1562/article_23921.pdf. Cole JW, Silvera IF, Foote JP. Conceptual launch vehicles using metallic hydrogen propellant. AIP Conf Proceedings 2008;969(1):977; <http://aip.scitation.org/doi/abs/10.1063/1.2845066>. Vorob'ev VS, Novikov VG. Melting line and new metastable state of hydrogen at megabar pressures. Europhys Lett. 2010 Mar 11;89(4):69902; <http://iopscience.iop.org/article/10.1209/0295-5075/89/40014/meta>.

⁶²⁵ Nellis WJ. Metastable solid metallic hydrogen. J Phil Mag Part B. 1999;79(4):655-661; https://www.researchgate.net/profile/W_Nellis/publication/252786756_Metastable_solid_metallic_hydrogen/links/55a2840508aec9ca1e64f591.pdf.

possible metastability at 20 K,⁶²⁶ but early theoretical calculations suggested that the metastability time of hydrogen might be short (10^{-3} - 10^2 sec) due to surface evaporation,⁶²⁷ bulk effects,⁶²⁸ or a tunneling mechanism in which atoms on the atomic lattice tunnel into molecular states.⁶²⁹ Many are skeptical about the metastability of metallic hydrogen generally,⁶³⁰ but the metastable lifetime could increase a little⁶³¹ or a lot⁶³² with higher pressure. Most recently, theory work by two Russian authors suggests that metallic hydrogen might remain in a long-lived metastable state down to 10-20 GPa, but would decay instantly at lower pressures.⁶³³ Actual parameters for experimentally accessible metastability in liquid or solid metallic hydrogen remain unknown at the present time.

Given that 1000 GPa static pressures have been demonstrated experimentally,⁶³⁴ and given theoretical predictions of a liquid-liquid-solid multiphase coexistence point in the hydrogen phase diagram as low as ~290 GPa at 550 K corresponding to the intersection of the liquid-liquid/metal-insulator phase transition with the melting curve,⁶³⁵ it should be possible to manufacture metallic hydrogen using currently available laboratory equipment. Metallization pressure is theoretically

⁶²⁶ Vereshchagin LF, Arkhipov RG. Production of metallic hydrogen. *Priroda* 1972;3:9-12, transl. JPRS 56130 (1972); cited in <http://citeseerx.ist.psu.edu/viewdoc/download?doi=10.1.1.561.8506&rep=rep1&type=pdf>.

⁶²⁷ Chapline GF Jr. Metal-insulator transition in solid hydrogen. *Phys Rev B*. 1972 Sep 15;6(6):2067-2070; <https://journals.aps.org/prb/abstract/10.1103/PhysRevB.6.2067>.

⁶²⁸ Estrin EI. Temperature stability of the metallic modification of hydrogen. *Soviet Phys JETP Letters* 1971 Jun;13:510-511; http://www.jetpletters.ac.ru/ps/1588/article_24384.pdf.

⁶²⁹ Salpeter EE. Evaporation of Cold Metallic Hydrogen. *Phys Rev Lett* 1972 Feb 28;28(9):560-2; [http://documents.htracyhall.org/ocr/HTH-Archives/Cabinet%204/Drawer%202%20\(POU-ROB\)/Salpeter,%20E.E%20\(linked\)/Salpeter,%20E.E.-309_OCR.pdf](http://documents.htracyhall.org/ocr/HTH-Archives/Cabinet%204/Drawer%202%20(POU-ROB)/Salpeter,%20E.E%20(linked)/Salpeter,%20E.E.-309_OCR.pdf).

⁶³⁰ Harris FE, Delhalle J. Structure and stability of metallic hydrogen. *Phys Rev Lett* 1977 Nov 21;39(21):1340-1342; <https://journals.aps.org/prl/abstract/10.1103/PhysRevLett.39.1340>.

⁶³¹ Chapline GF Jr. Metal-insulator transition in solid hydrogen. *Phys Rev B*. 1972 Sep 15;6(6):2067-2070; <https://journals.aps.org/prb/abstract/10.1103/PhysRevB.6.2067>.

⁶³² Salpeter EE. On convection and gravitational layering in Jupiter and in stars of low mass. *Astrophys J*. 1973 Apr 15;181:L83-L86; <http://articles.adsabs.harvard.edu/full/1973ApJ...181L..83S/L000083.000.html>.

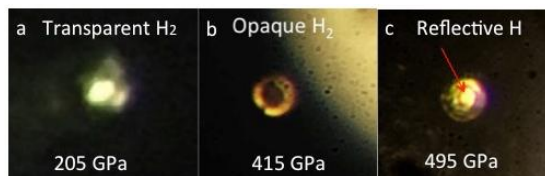
⁶³³ Burmistrov SN, Dubovskii LB. On the lifetime of metastable metallic hydrogen. 2016 Nov; <https://arxiv.org/pdf/1611.02593.pdf>.

⁶³⁴ Dubrovinskaia N, *et al*. Terapascal static pressure generation with ultrahigh yield strength nanodiamond. *Science Advances* 2016 Jul 20;2(7):e1600341; <http://advances.sciencemag.org/content/2/7/e1600341.full>.

⁶³⁵ Morales MA, Pierleoni C, Schwegler E, Ceperley DM. Evidence for a first-order liquid-liquid transition in high-pressure hydrogen from ab initio simulations. *PNAS* 2010 Jul 20;107(29):12799-12803; <http://www.pnas.org/content/107/29/12799.full.pdf>.

predicted to be ~ 300 GPa at 0 K⁶³⁶ and is observed to lie >340 GPa at 300 K.⁶³⁷ With an estimated mass density of ~ 1 kg/L at 250 GPa compression,⁶³⁸ metallic hydrogen might achieve a much-improved energy density of $E_D \sim 216$ MJ/L along with a specific energy of $E_S = 216$ MJ/kg.

The most straightforward technique for making liquid metallic hydrogen is simple compression of molecular hydrogen at constant temperature (moving from left to right in the phase diagram above). Over the decades there have been many claimed observations of metallic hydrogen,⁶³⁹ though none have yet been widely accepted by the high-pressure physics community. Most recently in 2016, Dias and Silvera⁶⁴⁰ reported that under increasing pressure in a diamond anvil apparatus, a cryogenic molecular hydrogen sample at 15 K was observed (image, right) to transform from transparent, to black, to a reflective metal at an applied pressure of 495 GPa. (The extrapolated hydrogen liquid metal density near ~ 500 GPa would be ~ 1300 kg/m³, based on DFT quantum chemistry simulations.⁶⁴¹) At the time of the experiment, the authors were maintaining their (1.5 μm thick, 10 μm diameter) sample at LN₂ temperature in a cryostat, and were planning to see if it survived warming to room temperature, and alternatively were considering cooling the sample back to liquid helium temperatures and then slowly releasing the pressure load to see if the metallic hydrogen was metastable. Unfortunately in Feb 2017 the



⁶³⁶ Ashcroft NW. Pairing instabilities in dense hydrogen. Phys Rev B Condens Matter. 1990 Jun 1;41(16):10963-10971; <https://journals.aps.org/prb/abstract/10.1103/PhysRevB.41.10963>.

⁶³⁷ Narayana C, Luo H, Orloff J, Ruoff AL. Solid hydrogen at 342 GPa: no evidence for an alkali metal. Nature 1998 May 7;393:46-49; <http://www.nature.com/nature/journal/v393/n6680/abs/393046a0.html>.

⁶³⁸ Morales MA, Pierleoni C, Schwegler E, Ceperley DM. Evidence for a first-order liquid-liquid transition in high-pressure hydrogen from *ab initio* simulations. PNAS 2010 Jul 20;107(29):12799-12803; <http://www.pnas.org/content/107/29/12799.full.pdf>.

⁶³⁹ e.g., Weir ST, Mitchell AC, Nellis WJ. Metallization of fluid molecular hydrogen at 140 GPa (1.4 Mbar). Phys Rev Lett. 1996 Mar 11;76(11):1860-1863; https://www.researchgate.net/profile/W_Nellis/publication/13229096_Metallization_of_Fluid_Molecular_Hydrogen_at_140_GPa_14_Mbar/links/02e7e538723ad8ab7b000000.pdf. Eremets MI, Troyan IA. Conductive dense hydrogen. Nature Mater. 2011 Nov 13;10:927-931; <http://www.nature.com/nmat/journal/v10/n12/abs/nmat3175.html>. Eremets MI, Troyan IA, Drozdov AP. Low temperature phase diagram of hydrogen at pressures up to 380 GPa. A possible metallic phase at 360 GPa and 200 K. 2016 Jan 18; <https://arxiv.org/abs/1601.04479>.

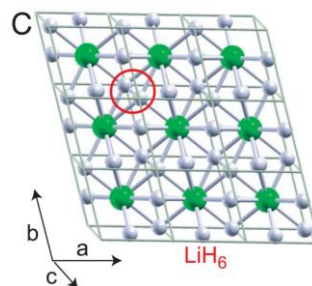
⁶⁴⁰ Dias R, Silvera IF. Observation of the Wigner-Huntington Transition to Solid Metallic Hydrogen. Science 2017 Feb 17;355(6326):715-718; <http://science.sciencemag.org/content/355/6326/715/tab-pdf>. See also: <https://arxiv.org/ftp/arxiv/papers/1610/1610.01634.pdf>.

⁶⁴¹ Morales MA, Pierleoni C, Schwegler E, Ceperley DM. Evidence for a first-order liquid-liquid transition in high-pressure hydrogen from *ab initio* simulations. PNAS 2010 Jul 20;107(29):12799-12803; <http://www.pnas.org/content/107/29/12799.full.pdf>.

sample was destroyed⁶⁴² during a low-powered laser irradiation experiment before either of these tests could be run. The validity of the effort has been challenged by competing groups,⁶⁴³ and defended,⁶⁴⁴ in the literature. Presumably the authors, who are long-term researchers in this field, will eventually attempt a replication experiment.

It might also be possible to obtain liquid metal hydrogen by heating molecular hydrogen at constant pressure (moving from bottom to top in the hydrogen phase diagram above). However, according to one review,⁶⁴⁵ this has not been possible “because hydrogen is optically transparent, electrically insulating, and hydrogen at high temperatures has an enormous mass diffusion coefficient and high chemical reactivity with solids [so that] at static high temperatures and pressures hydrogen either diffuses out of and/or reacts chemically with its container before an accurate measurement can be made above ~500 K.”

Other methods for manufacturing metallic hydrogen have been suggested. One proposal is to catalyze the transformation to the metallic state by “inject[ing] electrons into solid molecular hydrogen under pressure ... weaken[ing] the intermolecular bonds, enabling metallization at a much lower pressure than required for a pure hydrogen sample.”⁶⁴⁶ Another method is to dope the hydrogen with an electropositive element such as lithium – e.g., the H₂ sublattice of LiH₆ is computationally predicted to become metallic at only ~100 GPa, about one quarter of the pressure believed to be required for pure hydrogen.⁶⁴⁷ The LiH₆ lattice (image, right), with Li atoms in green and H atoms in white, shows that about half of the H atoms are monatomic in this material and thus should remain available to yield up their stored molecular recombination energy upon decompression. Another approach is to mix silane (SiH₄) with molecular hydrogen, which interact strongly at high pressure to induce bond weakening in the H₂



⁶⁴² <http://www.sciencealert.com/the-world-s-only-metallic-hydrogen-sample-has-disappeared>.

⁶⁴³ Goncharov AF, Struzhkin V. Comment on Observation of the Wigner-Huntington transition to metallic hydrogen. 2017 Feb 13; <https://arxiv.org/abs/1702.04246>. Eremets MI, Drozdov AP. Comments on the claimed observation of the Wigner-Huntington Transition to Metallic Hydrogen. 2017 Feb 16; <https://arxiv.org/abs/1702.05125>. Loubeyre P, Occelli F, Dumas P. Comment on: Observation of the Wigner-Huntington transition to metallic hydrogen. 2017 Feb 23; <https://arxiv.org/abs/1702.07192>.

⁶⁴⁴ Silvera I, Dias R. Response to critiques on Observation of the Wigner-Huntington transition to metallic hydrogen. 2017 Mar 8; <https://arxiv.org/abs/1703.03064>.

⁶⁴⁵ Nellis WJ. Metastable solid metallic hydrogen. J Phil Mag Part B. 1999;79(4):655-661; https://www.researchgate.net/profile/W_Nellis/publication/252786756_Metastable_solid_metallic_hydrogen/links/55a2840508aec9ca1e64f591.pdf.

⁶⁴⁶ Silvera IF. Metallic Hydrogen: A Game Changing Rocket Propellant. Final Report, Phase I NASA NIAC, 25 Jul 2016; <https://ntrs.nasa.gov/archive/nasa/casi.ntrs.nasa.gov/20160010446.pdf>.

⁶⁴⁷ Zurek E, Hoffmann R, Ashcroft NW, Oganov AR, Lyakhov AO. A little bit of lithium does a lot for hydrogen. PNAS 2009 Oct 20;105(42):17640-17643; <http://www.pnas.org/content/106/42/17640.full.pdf>.

due to intermolecular interactions between the two molecules, with the phase of the high-pressure structures of $\text{SiH}_4(\text{H}_2)_2$ predicted to become metallic near 120 GPa.⁶⁴⁸ Electric field induced nucleation could also reduce the pressures required for metallization, and could create metastable metallic hydrogen once removed from the external field and the high pressure environment.⁶⁴⁹ Other theory work predicts that di-phosphine may form a 2D lattice with metallic hydrogen trapped in it, stabilized by phosphorus atoms under high hydrostatic pressure of 50-250 GPa.⁶⁵⁰ However, none of these approaches has yet been tested experimentally.⁶⁵¹



The curious reader might wonder if we could attempt to mine recombination-energy-rich liquid metallic hydrogen from its huge naturally-occurring reservoir inside the gravitationally compressed interior of Jupiter, perhaps by lowering a hermetically-sealable “bucket” on a long cable from a fuel depot (image, left)⁶⁵² in jovisynchronous orbit ($R_{js} = 1.61 \times 10^8 \text{ m}$)⁶⁵³ down to the top of the metallic hydrogen layer ($R_{mh} = 5.45 \times 10^7 \text{ m}$ or $\sim 78\%$ of the $6.99 \times 10^7 \text{ m}$ mean Jovian radius⁶⁵⁴), filling the bucket, then retracting the cable to return the bucket to the depot, or alternatively by using a scoop bucket mounted on an atmospheric penetrator missile. The minimum extraction energy using a perfectly efficient lift system with 100% regenerative capture during cable extension and a massless bucket and cable is $E_{\text{cable}} / m_{\text{mh}} = G M_J (1/R_{\text{mh}} - 1/R_{\text{js}}) = \mathbf{1540 \text{ MJ/kg}}$, taking $G = 6.67 \times 10^{-11} \text{ Nm}^2/\text{kg}^2$ (gravitation constant), Jovian mass $M_J = 1.90 \times 10^{27} \text{ kg}$,⁶⁵⁵ and $m_{\text{mh}} = 1 \text{ kg}$ of liquid metal hydrogen payload. Unfortunately, both the cable-based extraction energy of **1540 MJ/kg** and the kinetic energy of a missile-bound payload at Jovian escape velocity ($v_{\text{Jesc}} = 59.5 \text{ km/sec}$)⁶⁵⁶ of $\sim v_{\text{Jesc}}^2/2 = \mathbf{1770 \text{ MJ/kg}}$ greatly exceed the **216 MJ/kg** of recombination energy available from the metallic hydrogen payload.⁶⁵⁷

⁶⁴⁸ Yao Y, Klug DD. Silane plus molecular hydrogen as a possible pathway to metallic hydrogen. PNAS 2010 Dec;107(49):20893-20898; <http://www.pnas.org/content/107/49/20893.full>.

⁶⁴⁹ Nardone M, Karpov VG. Electric field induced nucleation: an alternative pathway to metallic hydrogen. arXiv.org, e-Print Arch., Condens. Matter, 2011 Mar; https://www.researchgate.net/profile/Marco_Nardone/publication/50235447_Electric_field_induced_nucleation_An_alternative_pathway_to_metallichydrogen/links/54008f850cf23d9765a3ed7d.pdf.

⁶⁵⁰ Degtyarenko NN, Mazur EA. Quasi-two-dimensional metallic hydrogen inside di-phosphide at high pressure. J Physics: Conf Series 2016;747:012029; <http://iopscience.iop.org/article/10.1088/1742-6596/747/1/012029/pdf>.

⁶⁵¹ There is one questionable claim that atomic metallic hydrogen was formed inside of metal-ceramic oxide-nickel electrodes of a nickel-cadmium battery during a long period of electrochemical hydrogenation, the powder “composed by 97.5% of hydrogen atoms and 2.5% of nickel atoms, hence the powder is not nickel hydride, but dense hydrogen with small impurity of nickel atoms.” Galushkin NE, Yazvinskaya NN, Galushkin DN. Possibility of obtaining atomic metallic hydrogen by electrochemical method. 2013 Dec; <https://arxiv.org/ftp/arxiv/papers/1312/1312.6851.pdf>.

⁶⁵² image courtesy of Steve Bowers; <http://www.orionsarm.com/eg-article/4f181b2caecff>.

⁶⁵³ https://tap.iop.org/fields/gravity/403/file_46832.pdf.

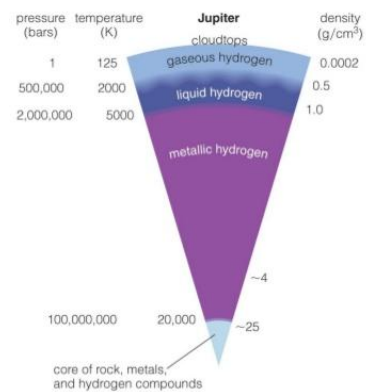
⁶⁵⁴ https://en.wikipedia.org/wiki/Jupiter#Internal_structure.

⁶⁵⁵ https://en.wikipedia.org/wiki/Jupiter#Physical_characteristics.

⁶⁵⁶ https://en.wikipedia.org/wiki/Jupiter#Physical_characteristics.

Is there an alternative method that might harvest more energy than it consumes? Consider a massless bucket of volume $V_{\text{bucket}} = 1 \text{ L}$ attached to a massless balloon of maximum inflatable volume V_{balloon} and a ballast weight with a mass equal to $m_{\text{mh}} = 1 \text{ kg}$ that is tossed into the Jovian atmosphere with its balloon fully deflated. The bucket falls until the density of the surroundings equals the density of the bucket or $m_{\text{mh}}/(V_{\text{bucket}} + V_{\text{balloon}}) = 1 \text{ gm/cm}^3$, the approximate density at the top of the liquid metallic hydrogen layer on Jupiter. The bucket is filled with the metallic hydrogen payload as the ballast is jettisoned, holding bucket density constant. The walls of the balloon are then mechanically expanded to create a vacuum inside of volume $V_{\text{balloon}} = 1 \text{ L}$, causing bucket density to fall to 0.5 gm/cm^3 which allows the bucket to rise to the top of the liquid hydrogen layer where environmental density is only 0.5 gm/cm^3 . The energy cost of expanding the balloon is approximately the pressure energy density at the top of the liquid metallic hydrogen layer (image, below right),⁶⁵⁸ which is $2,000,000 \text{ bars} = 2 \times 10^{11} \text{ N/m}^2 = \mathbf{200 \text{ MJ/L}}$, slightly less than the $\mathbf{216 \text{ MJ/kg}}$ of recombination energy available from the metallic hydrogen payload. If the balloon is inflated in two steps, to 0.5 L and then to 1 L , the total energy requirement for the two steps drops from $\mathbf{200 \text{ MJ/L}}$ to $\mathbf{150 \text{ MJ/L}}$, and continues to drop to an even lower minimum in the limit where the balloon is inflated in tiny infinitesimal steps (not calculated here). So far, so good.

However, previous literature suggests that a vacuum-filled balloon generally cannot generate buoyant lift on Earth because its walls must be too massive to resist crushing.⁶⁵⁹ Consider a spherical balloon of radius R_{balloon} and wall thickness t_{balloon} , with wall material of density ρ_{balloon} and compressive strength σ_{balloon} of mass $M_{\text{balloon}} = 4\pi R_{\text{balloon}}^2 t_{\text{balloon}} \rho_{\text{balloon}}$ with an external crushing pressure $P_{\text{ext}} = 2 t_{\text{balloon}} \sigma_{\text{balloon}} / R_{\text{balloon}}$. The balloon generates positive lift if the mass (M_{displace}) of metallic hydrogen of density ρ_{mh} that the expanded balloon displaces with vacuum is $M_{\text{displace}} = (4/3)\pi R_{\text{balloon}}^3 \rho_{\text{mh}} \geq M_{\text{balloon}}$, which reduces to the



⁶⁵⁷ Assuming a frictionless pulley, a cable holding a bucket with 1 kg of metallic hydrogen could be counterbalanced by a 1 kg ballast at the other end of the cable; as one descends, the other ascends, and *vice versa*, neutralizing the gravitational energy cost of lifting the payload. However, the maximum length of a Jovian self-supporting untapered physical cable made of diamond, the strongest known material, is $L_{\text{max}} \sim \sigma_{\text{diamond}} / \rho_{\text{diamond}} g_{\text{Jupiter}} = 5.7 \times 10^5 \text{ m} = 570 \text{ km}$, about 100-fold short of the needed 54,500 km length, taking working stress $\sigma_{\text{diamond}} = 5 \times 10^{10} \text{ N/m}^2$, $\rho_{\text{diamond}} = 3510 \text{ kg/m}^3$, and $g_{\text{Jupiter}} \sim 24.8 \text{ m/sec}^2$.

⁶⁵⁸ Image modified from "Chapter 11 Lecture: Jovian Planet Systems," The Cosmic Perspective, 7th Edition, Pearson Education, Inc.; <https://image.slidesharecdn.com/11lectureoutline-16040220743/95/11-lecture-outline-13-638.jpg>.

⁶⁵⁹ Freitas RA Jr. Nanomedicine, Volume I: Basic Capabilities, Landes Bioscience, Georgetown TX, 1999, p. 331; <http://www.nanomedicine.com/NMI/9.5.3.3.htm#p2>.

narrowly failed buoyancy condition: $1 \geq B_C = 3 \rho_{\text{balloon}} P_{\text{ext}} / (2 \rho_{\text{mh}} \sigma_{\text{balloon}}) = 2.2$, taking $\rho_{\text{balloon}} = 3510 \text{ kg/m}^3$ and $\sigma_{\text{balloon}} = 470 \text{ GPa}$ for flawless diamond,⁶⁶⁰ $P_{\text{ext}} = 200 \text{ GPa}$ (2,000,000 bars), and $\rho_{\text{mh}} \sim 1 \text{ gm/cm}^3$ at the top of the metallic hydrogen layer. B_C does fall to 1.1 at the top of the liquid hydrogen layer, and probably dips below 1 (generating positive buoyancy) somewhere low in the gaseous hydrogen layer because Jovian environmental pressure falls faster than density with increasing altitude, improving buoyancy as the balloon rises.

Another difficult challenge is that the temperature at the top of the liquid metallic hydrogen layer is $\sim 5000 \text{ K}$, which is hotter than the melting points of any known high-strength material including diamond (graphitizes at 2000 K), cubic boron nitride (3246 K), tungsten (3695 K), or graphite (3915 K). Perhaps one or more shaped nuclear charges could punch a hole through the Jovian liquid/metallic interface, releasing a brief harvestable spout of metallic hydrogen from below, cooling as it rose, that could be scooped up and collected at lower temperature if the predicted⁶⁶¹ long-lived metastable state down to pressures as low as 10-20 GPa actually exists. Note that a bucket filled with metallic hydrogen that was cable-lifted to a depot floating $\leq 5740 \text{ km}$ above the metallic layer in the upper liquid H_2 region, about one-third of the way to the top of the Jovian cloud deck, would consume an extraction energy $\leq 216 \text{ MJ/L}$ and thus could produce net energy. Many possible container materials could be employed at the cooler 2500-3000 K temperatures encountered at the altitude of such a depot.

⁶⁶⁰ The calculated uniaxial ideal compressive strength of flawless diamond, using pseudopotential density functional theory, is -223.1 GPa, -469.0 GPa, and -470.4 GPa along the $\langle 100 \rangle$, $\langle 110 \rangle$, and $\langle 111 \rangle$ crystal lattice directions, respectively. Luo X, Liu Z, Xu B, Yu D, Tian Y, Wang HT, He J. Compressive Strength of Diamond from First-Principles Calculation. J Phys Chem C. 2010 Oct 21;41(114):17851-3; https://www.researchgate.net/profile/Xiaoguang_Luo/publication/225376850_Compressive_Strength_of_Diamond_From_First-Principles_Calculation/links/0fcfd5126365a800dc000000.pdf.

⁶⁶¹ Burmistrov SN, Dubovskii LB. On the lifetime of metastable metallic hydrogen. 2016 Nov; <https://arxiv.org/pdf/1611.02593.pdf>.

4.3.2 Nitrogen Recombination Energy

Monatomic nitrogen has the highest molar recombination energy (0.945 MJ/mole) of any element but only the second-highest specific energy of recombination (**33.7 MJ/kg**) after hydrogen (**216 MJ/kg**), though its higher mass density may improve its energy density compared to hydrogen.

Frozen Matrix Trapping. As with atomic hydrogen (**Section 4.3.1.2**), monatomic nitrogen can also be embedded in an ultracold matrix of frozen material, isolating the atoms from one another and thus preventing or vastly inhibiting their chemical recombination. Early interest in high-energy rocket fuels in the late 1950s led NIST to study inert-matrix trapping of monatomic nitrogen.⁶⁶² Many experiments were performed with nitrogen atoms embedded in a matrix of frozen molecular nitrogen, but only very low concentrations ($\leq 0.1\%$) of monatomic nitrogen were obtained, with the recombining N atoms producing a green phosphorescent glow.⁶⁶³ These early efforts were abandoned after theoretical calculations⁶⁶⁴ suggested that recombination chain reactions would frustrate any attempts to achieve higher concentrations.

Subsequent efforts used a new approach⁶⁶⁵ in which a mixture of helium gas and an impurity gas such as molecular and monatomic nitrogen was injected into superfluid helium, forming a solid consisting of the impurity molecules surrounded by frozen helium.⁶⁶⁶ Examination of the resulting matrix material using electron spin resonance techniques found that very high ($\sim 50\%$) concentrations of monatomic nitrogen could be stored in the N-N₂-He impurity helium solids, producing total spin densities as high as 4×10^{20} atoms/cm³,⁶⁶⁷ as long as the impurity-helium solid is maintained below the lambda temperature (2.17 K) of liquid helium.⁶⁶⁸

⁶⁶² Bass AM, Brodia HP (eds). Formation and Trapping of Free Radicals. Academic Press, NY, 1960.

⁶⁶³ Brodia H, Pellam J. Phosphorescence of Atoms and Molecules of Solid Nitrogen at 4.2 K. Phys Rev. 1954 Aug 1;95(3):845-846; <https://journals.aps.org/pr/abstract/10.1103/PhysRev.95.845>.

⁶⁶⁴ Jackson JL. Free radical trapping-theoretical aspects. In: Bass AM, Brodia HP (eds). Formation and Trapping of Free Radicals. Academic Press, NY, 1960, p. 327.

⁶⁶⁵ Gordon EB, Mezhov-Deglin LP, Pugachev OF. Stabilization of nitrogen atoms in superfluid helium. JETP Lett. 1974 Jan 1;19:63-65; http://www.jetpletters.ac.ru/ps/1772/article_26955.pdf.

⁶⁶⁶ Gordon EB, Khmelenko VV, Pelmenov AA, Popov EA, Pugachev OF. Impurity-helium van der Waals crystals. Chem Phys Lett. 1989 Mar 3;155(3):301-304; <http://www.sciencedirect.com/science/article/pii/0009261489853291>. Gordon EB, Khmelenko VV, Pelmenov AA, Popov EA, Pugachev OF, Shestakov AF. Metastable impurity-helium solid phase. Experimental and theoretical evidence. Chem Phys. 1993 Mar 15;170(3):411-426; https://www.researchgate.net/profile/Vladimir_Khmelenko/publication/223670865_Metastable_impurity-helium_solid_phase_Experimental_and_theoretical_evidence/links/00463528af23bfd09000000/Metastable_impurity-helium_solid_phase_Experimental_and_theoretical_evidence.pdf.

⁶⁶⁷ Khmelenko VV, Kiselev SI, Lee DM, Lee CY. Impurity-helium solids – quantum gels? Physica Scripta 2002;T102:118-127; https://www.nobelprize.org/nobel_organizations/nobelfoundation/symposia/physics/ncs-2001-1/lee.pdf.

A number density of 4×10^{20} N atoms/cm³ = 0.0093 kg/L with a nitrogen atom recombination energy of 945 kJ/mole yields a specific energy of $E_S = 33.7$ MJ/kg but a still-unimpressive energy density of only $E_D = 0.31$ MJ/L. Ground-state nitrogen atoms have also been stably trapped in solid molecular hydrogen⁶⁶⁹ and deuterium⁶⁷⁰ matrices at temperatures <5 K, with rapid recombination observed above this temperature.

Endohedral Trapping. Individual nitrogen atoms can be implanted into fullerenes by simultaneous ion bombardment and fullerene evaporation onto a target.⁶⁷¹ For example, nuclear implantation techniques using 18 MeV ions can convert almost 6% of a ~40 μm fullerene layer into endohedral compounds.⁶⁷² The resulting endohedrals are very thermally⁶⁷³ and chemically stable⁶⁷⁴ at ambient conditions, not decomposing until temperatures reach 400-600 K. In low-energy implanted samples only ~0.01% of the cages are actually filled, but the more massive N@C₆₀ molecules can be concentrated using high-pressure chromatography.⁶⁷⁵ Atomic nitrogen endohedral dimers (N@C₆₀)₂ have also been synthesized.⁶⁷⁶

⁶⁶⁸ Kiselev SI, Khmelenko VV, Lee DM, Kiryukhin V, Boltnev RE, Gordon EB, Keimer B. Structural studies of impurity-helium solids. *Phys Rev B*. 2001 Dec 19;65(2):024517; http://www.academia.edu/download/41776907/Structural_studies_of_impurity-helium_so20160130-15209-e11b71.pdf.

⁶⁶⁹ Fajardo ME, Tam S, Thompson TL, Cordonnier ME. Spectroscopy and reactive dynamics of atoms trapped in molecular hydrogen matrices. *Chem Phys*. 1994 Dec 1;189(2):351-65; <http://www.sciencedirect.com/science/article/pii/0301010494002320>.

⁶⁷⁰ Thompson TL, Cordonnier ME, Fajardo ME. Thermoluminescence studies of atomic nitrogen in cryogenic solid deuterium. In: Thompson TL, Rodgers SL (eds). *Proceedings of the High Energy Density Matter (HEDM) Contractors' Conference held 5-7 June 1994 in Crystal Bay NV, Dec 1994*, pp. 183-184; <http://www.dtic.mil/cgi-bin/GetTRDoc?AD=ADA292988#page=192>.

⁶⁷¹ Harneit W. Fullerene-based electron-spin quantum computer. *Phys Rev A*. 2002 Feb 27;65(3):032322; https://www.researchgate.net/profile/Wolfgang_Harneit/publication/257976907_Fullerene-based_electron-spin_quantum_computer/links/566a9d6208aea0892c4a257d.pdf.

⁶⁷² Ray A, Das P, Saha SK, Das JJ, Madhavan N, Center VE. Change of ⁷Be decay rate in exohedral and endohedral C₆₀ fullerene. *NSTI Nanotech-2006*, Vol. 2; <http://www.nsti.org/publications/Nanotech/2006/pdf/637.pdf>.

⁶⁷³ Waiblinger M, Lips K, Harneit W, Weidinger A, Dietel E, Hirsch A. Corrected Article: Thermal stability of the endohedral fullerenes N@C₆₀, N@C₇₀, and P@C₆₀ [*Phys. Rev. B* 63, 045421 (2001)]. *Phys Rev B*. 2001 Sep 28;64(15):159901; <https://journals.aps.org/prb/abstract/10.1103/PhysRevB.64.159901>.

⁶⁷⁴ Pietzak B, Waiblinger M, Murphy TA, Weidinger A, Höhne M, Dietel E, Hirsch A. Buckminsterfullerene C₆₀: a chemical Faraday cage for atomic nitrogen. *Chem Phys Lett*. 1997 Nov 21;279(5-6):259-63; <http://www.sciencedirect.com/science/article/pii/S0009261497011007>.

⁶⁷⁵ Goedde B, Waiblinger M, Jakes P, Weiden N, Dinse KP, Weidinger A. Nitrogen doped C₆₀ dimers (N@C₆₀-C₆₀). *Chem Phys Lett*. 2001 Feb 2;334(1):12-7; https://www.researchgate.net/profile/Klaus-Peter_Dinse/publication/239160377_Nitrogen_doped_C_60_dimers_NC_60-60/links/570b990608ae8883a1ffcd40.pdf.

Charged Ion Plasma. Monatomic nitrogen has an even higher first ionization potential than hydrogen, but still less than neon which could be used for box walls (**Section 4.3.1.4**). For a box with $n_p = 177$ nitrogen atoms, $E_D = 0.0002 \text{ MJ/L}$ for $L_{\text{box}} \geq 100 \text{ nm}$ and an electrostatic pressure of 0.2 MPa, the strength limit for solid neon box walls. If the neon walls are reinforced from behind with diamond having a tensile strength of $\sim 100 \text{ GPa}$, then for $n_p = 4$ nitrogen atoms, $E_D = 40 \text{ MJ/L}$ for $L_{\text{box}} \geq 0.5 \text{ nm}$ and an electrostatic pressure of 40 GPa. The combined specific energy for deionization + molecular recombination is **83 MJ/kg** in both cases.

Metallic Nitrogen. Nitrogen is theoretically estimated to enter a metallic state starting at a pressure of $\sim 460 \text{ GPa}$ at 0 K,⁶⁷⁷ but metallic nitrogen at high pressure has not yet been made. Semiconducting “non-molecular” nitrogen has been observed between 140-240 GPa and stably recovered to ambient pressure at temperatures below 100 K.⁶⁷⁸ It is presently unknown if this material releases the theoretical specific energy of $E_S = 33.7 \text{ MJ/kg}$ during recombination to N_2 ; if so, a mass density close to that of solid nitrogen ($\sim 1.03 \text{ kg/L}$)⁶⁷⁹ for this material might also imply an available energy density of **34.7 MJ/L**.

⁶⁷⁶ Farrington BJ, Jevric M, Rance GA, Ardavan A, Khlobystov AN, Briggs GA, Porfyraakis K. Chemistry at the nanoscale: synthesis of an $\text{N}@C_{60}\text{-N}@C_{60}$ endohedral fullerene dimer. *Angew Chemie Int Ed.* 2012 Apr 10;51(15):3587-90;

https://www.researchgate.net/profile/George_Briggs/publication/262861363_Chemistry_at_the_Nanoscale_Synthesis_of_an_NC60-NC60_Endohedral_Fullerene_Dimer/links/5669c45408ae1a797e376ff4.pdf.

⁶⁷⁷ Wang X, *et al.* Predicted novel metallic metastable phases of polymeric nitrogen at high pressures. *New J Phys.* 2013 Jan;15:013010; <http://iopscience.iop.org/article/10.1088/1367-2630/15/1/013010/pdf>. Earlier theoretical estimates suggested somewhat lower metallization pressures, e.g., $\sim 100 \text{ GPa}$ (Nellis WJ, Holmes NC, Mitchell AC, Van Thiel M. Phase transition in fluid nitrogen at high densities and temperatures. *Phys Rev Lett.* 1984 Oct 22;53(17):1661-1664; https://www.researchgate.net/profile/W_Nellis/publication/252407856_Phase_Transition_in_Fluid_Nitrogen_at_High_Densities_and_Temperatures/links/0046352070b171736e000000.pdf).

⁶⁷⁸ Eremets MI, Hemley RJ, Mao HK, Gregoryanz E. Semiconducting non-molecular nitrogen up to 240 GPa and its low-pressure stability. *Nature.* 2001 May 10;411(6834):170-4; <http://www.nature.com/nature/journal/v411/n6834/full/411170a0.html>.

⁶⁷⁹ Dewar J. Physical Constants at Low Temperatures. (1)--The Densities of Solid Oxygen, Nitrogen, Hydrogen, etc. *Proc Roy Soc London.* 1904 Jan 1;73:251-261; <https://ia800502.us.archive.org/9/items/philtrans01167503/01167503.pdf>.

4.3.3 Oxygen Recombination Energy

Monatomic oxygen has the second highest molar recombination energy (0.498 MJ/mole) of any substance but only the third-highest specific energy of recombination (**15.6 MJ/kg**) after hydrogen (**216 MJ/kg**) and nitrogen (**33.7 MJ/kg**).

Frozen Matrix Trapping. Monatomic oxygen was first trapped in a matrix of solid oxygen as early as 1954.⁶⁸⁰ Oxygen atoms have been trapped in solid molecular hydrogen⁶⁸¹ and deuterium⁶⁸² matrices, and neutral oxygen atoms stored in cryogenic krypton matrix appear indefinitely stable against recombination below ~ 10 K at concentrations at least as high as 1:30,000 (O/Kr)⁶⁸³ or $\sim 0.003\%$ ($\sim 6 \times 10^{20}$ O atoms/L), which would equate to a recombination energy density $E_D \sim (6 \times 10^{20} \text{ O atoms/L}) (2.66 \times 10^{-26} \text{ kg/O atom}) (15.6 \text{ MJ/kg}) = 2.5 \times 10^4 \text{ MJ/L}$ at the recombination specific energy of $E_S = 15.6 \text{ MJ/kg}$.

Endohedral Trapping. Trapping of oxygen atoms inside C_{60} fullerenes has been studied theoretically using semi-empirical⁶⁸⁴ and density-functional⁶⁸⁵ methods, but has not yet been achieved experimentally.

⁶⁸⁰ Brodia H, Pellam J. Phosphorescence of Atoms and Molecules of Solid Nitrogen at 4.2 K. Phys Rev. 1954 Aug 1;95(3):845-846; <https://journals.aps.org/pr/abstract/10.1103/PhysRev.95.845>.

⁶⁸¹ Fajardo ME, Tam S, Thompson TL, Cordonnier ME. Spectroscopy and reactive dynamics of atoms trapped in molecular hydrogen matrices. Chem Phys. 1994 Dec 1;189(2):351-65; <http://www.sciencedirect.com/science/article/pii/0301010494002320>.

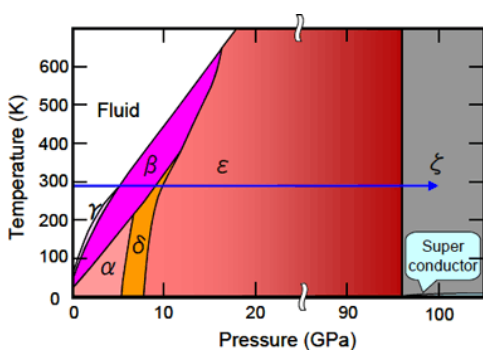
⁶⁸² Apkarian VA. Photodynamics in cryogenic solids. In: Thompson TL, Rodgers SL (eds). Proceedings of the High Energy Density Matter (HEDM) Contractors' Conference held 5-7 June 1994 in Crystal Bay NV, Dec 1994, pp. 140-143; <http://www.dtic.mil/cgi-bin/GetTRDoc?AD=ADA292988#page=147>. Fajardo ME, Tam S, Boatz J, Cordonnier ME, Thompson TL, Macler M. Progress on atom doped cryogenic solid propellants. In: Thompson TL, Rodgers SL (eds). Proceedings of the High Energy Density Matter (HEDM) Contractors' Conference held 5-7 June 1994 in Crystal Bay NV, Dec 1994, pp. 65-67; <http://www.dtic.mil/cgi-bin/GetTRDoc?AD=ADA292988#page=72>.

⁶⁸³ Danilychev AV, Apkarian VA. Temperature induced mobility and recombination of atomic oxygen in crystalline Kr and Xe. I. Experiment. J Chem Phys. 1993 Dec 1;99(11):8617-8627; <http://chem.ps.uci.edu/~aapkaria/manuscripts/55.pdf>.

⁶⁸⁴ Mauser H, Clark T, Hirsch A. Stabilisation of atomic elements inside C_{60} . In Kuzmany H, Fink J, Mehring M, Roth S, eds., AIP Conf Proc 1998 Aug 11;442(1):392-395; <http://www.dtic.mil/cgi-bin/GetTRDoc?AD=ADA359278#page=395>.

⁶⁸⁵ Tománek D, Li YS. Ionicity of the MC_{60} bond in $M@C_{60}$ endohedral complexes. Chem Phys Lett. 1995 Sep 8;243(1-2):42-4; <http://www.sciencedirect.com/science/article/pii/000926149500839V>. Lu J, Zhang X, Zhao X. Electronic structures of endohedral $N@C_{60}$, $O@C_{60}$ and $F@C_{60}$. Chem Phys Lett. 1999 Oct 2;312(2):85-90; <http://www.sciencedirect.com/science/article/pii/S0009261499009136>. Park JM, Tarakeshwar P, Kim KS, Clark T. Nature of the interaction of paramagnetic atoms ($A = {}^4N, {}^4P, {}^3O, {}^3S$) with π systems and C_{60} : A theoretical investigation of $A \cdots C_6H_6$ and endohedral fullerenes $A@C_{60}$. J Chem Phys. 2002 Jun 22;116(24):10684-91; <http://oasis.postech.ac.kr/bitstream/2014.oak/10777/1/OAIR001520.pdf>.

Charged Ion Plasma. Monatomic oxygen has a first ionization potential almost identical to that of hydrogen, so the neon walls (Section 4.3.1.4) still provide a $\Delta E = 8.0$ eV. For a box with $n_p = 207$ oxygen atoms, $E_D = 0.0002$ MJ/L for $L_{\text{box}} \geq 110$ nm and an electrostatic pressure of 0.2 MPa, the strength limit for solid neon box walls. If the neon walls are reinforced from behind with diamond having a tensile strength of ~ 100 GPa, then for $n_p = 4$ oxygen atoms, $E_D = 65$ MJ/L for $L_{\text{box}} \geq 0.4$ nm and an electrostatic pressure of 65 GPa. The combined specific energy for deionization + molecular recombination is **64 MJ/kg** in both cases.



Metallic Oxygen. Molecular oxygen (O_2) enters the metallic state at a pressure ~ 96 GPa,⁶⁸⁶ accompanied by a structural transition,⁶⁸⁷ and this metallic phase becomes superconducting⁶⁸⁸ at a pressure of ~ 100 GPa and a temperature of 0.6 K (see O_2 phase diagram⁶⁸⁹ at left). A further transformation of metallic O_2 into an atomic metal is believed to occur only at much higher pressures, probably above 250 GPa based on density-functional theory calculations extending the pressure range of metallic molecular oxygen.⁶⁹⁰ However, metallic atomic oxygen has not

yet been demonstrated experimentally. Such a material, if it could be made, would release the theoretical specific energy of $E_S = 15.6$ MJ/kg during recombination to O_2 ; and if that material had a mass density similar to that of solid oxygen (~ 1.43 kg/L)⁶⁹¹ then it might offer a recombination energy density of **~ 22.3 MJ/L**.

⁶⁸⁶ Desgreniers S, Vohra YK, Ruoff AL. Optical response of very high density solid oxygen to 132 GPa. J Phys Chem. 1990;94(3):1117-1122; <http://pubs.acs.org/doi/pdf/10.1021/j100366a020>.

⁶⁸⁷ Akahama Y, Kawamura H, Häusermann D, Hanfland M, Shimomura O. New high-pressure structural transition of oxygen at 96 GPa associated with metallization in a molecular solid. Phys Rev Lett. 1995 Jun 5;74(23):4690-4693; <https://journals.aps.org/prl/abstract/10.1103/PhysRevLett.74.4690>.

⁶⁸⁸ Shimizu K, Suhara K, Ikumo M, Eremets MI. Superconductivity in oxygen. Nature. 1998 Jun 25;393(6687):767-769; <http://www.nature.com/nature/journal/v393/n6687/abs/393767a0.html>.

⁶⁸⁹ <http://www.azonano.com/article.aspx?ArticleID=1797>.

⁶⁹⁰ Ma Y, Oganov AR, Glass CW. Structure of the metallic ζ -phase of oxygen and isosymmetric nature of the ϵ - ζ phase transition: *Ab initio* simulations. Phys Rev B. 2007 Aug 1;76(6):064101; <http://uspx.stonybrook.edu/pdfs/YMa-PRB-2007.pdf>.

⁶⁹¹ Dewar J. Physical Constants at Low Temperatures. (1)--The Densities of Solid Oxygen, Nitrogen, Hydrogen, etc. Proc Roy Soc London 1904 Jan 1;73:251-261; <https://ia800502.us.archive.org/9/items/philtrans01167503/01167503.pdf>.

4.3.4 Halogen and Other Recombination Energies

Monatomic halogens provide the lowest recombination energies of all the diatomic elements, including monatomic fluorine (**4.2 MJ/kg**), chlorine (**3.4 MJ/kg**), bromine (**1.2 MJ/kg**), and iodine (**0.6 MJ/kg**).

Of these, the only experimentally-reported metalized atomic halogens are metallic atomic iodine and metallic atomic bromine, but not metallic fluorine or chlorine, “presumably due to their formidably high transition pressures above 500 GPa.”⁶⁹²

The application of pressure causes the dissociation of molecular iodine (I_2) into **metallic atomic iodine** (I) at about 21 GPa;⁶⁹³ at 55 GPa, metallic iodine (I) undergoes a further transition from the face-centered-tetragonal to a face-centered-cubic phase in its monatomic metallic state.⁶⁹⁴ Molecular bromine (Br_2) undergoes the molecular-to-monatomic phase transition to **atomic metallic bromine** (Br) at ~80 GPa.⁶⁹⁵ However, the achievable molecular recombination energy densities for atomic metallic bromine ($E_D \sim 4.9 \text{ MJ/L}$) and atomic metallic iodine ($E_D \sim 2.9 \text{ MJ/L}$) are not very impressive.

Moving beyond the halogens, there appear to be no high-energy single-element triatomic molecules that are suitable candidates for molecular recombination energy storage. Ozone (O_3), for instance, lies energetically “uphill” from molecular oxygen (O_2) by +142.67 kJ/mole,⁶⁹⁶ so monatomic oxygen atoms would recombine to form molecular O_2 and would not further recombine to form O_3 . Neutral triatomic hydrogen (H_3), observed experimentally,⁶⁹⁷ has a

⁶⁹² Kim M, Debessai M, Yoo CS. Two- and three-dimensional extended solids and metallization of compressed XeF_2 . *Nature Chem.* 2010 Sep 1;2(9):784-788; <http://www.nature.com/nchem/journal/v2/n9/full/nchem.724.html>.

⁶⁹³ Takemura K, Minomura S, Shimomura O, Fujii Y. Observation of molecular dissociation of iodine at high pressure by X-ray diffraction. *Phys Rev Lett.* 1980 Dec 8;45(23):1881-1884; <https://journals.aps.org/prl/abstract/10.1103/PhysRevLett.45.1881>. Kenichi T, Kyoko S, Hiroshi F, Mitsuko O. Modulated structure of solid iodine during its molecular dissociation under high pressure. *Nature.* 2003 Jun 26;423(6943):971-974; <http://www.nature.com/nature/journal/v423/n6943/abs/nature01724.html>.

⁶⁹⁴ Fujii Y, Hase K, Hamaya N, Ohishi Y, Onodera A, Shimomura O, Takemura K. Pressure-induced face-centered-cubic phase of monatomic metallic iodine. *Phys Rev Lett.* 1987 Feb 23;58(8):796-799; <https://journals.aps.org/prl/abstract/10.1103/PhysRevLett.58.796>.

⁶⁹⁵ Fujihisa H, Fujii Y, Takemura K, Shimomura O. Structural aspects of dense solid halogens under high pressure studied by X-ray diffraction—molecular dissociation and metallization. *J Phys Chem Solids.* 1995 Oct 1;56(10):1439-1444; <http://www.sciencedirect.com/science/article/pii/002236979500081X>.

⁶⁹⁶ <https://en.wikipedia.org/wiki/Ozone>.

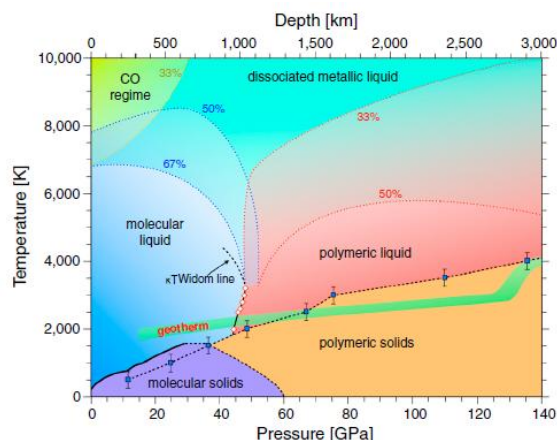
⁶⁹⁷ Herzberg G. A spectrum of triatomic hydrogen. *J Chem Phys.* 1979 May 15;70(10):4806-7; <http://aip.scitation.org/doi/abs/10.1063/1.437272>.

lifetime of only $<10^{-6}$ sec;⁶⁹⁸ trihydrogen cation (H_3^+) is energetically favored over H_2^+ by -2.65 eV (**84.8 MJ/kg**) but is stable against spontaneous dissociation only in isolation, and is formed in the reaction $H_2^+ + H_2 \rightarrow H_3^+$ but not via serial monatomic recombination.⁶⁹⁹ Triatomic nitrogen (N_3) is a weakly bound molecule,⁷⁰⁰ and thiozone (S_3 , sulfur analog of ozone), is unstable under normal conditions.⁷⁰¹ Neutral trihalogens are unknown, but gas-phase trifluoride anion (F_3^-) is exoergically formed by $F_2 + F^- \rightarrow F_3^- + 1.02$ eV or $F + F_2^- \rightarrow F_3^- + 1.30$ eV (**6.6 MJ/kg**).⁷⁰²

The dissociation of triatomic molecular **carbon dioxide** (CO_2) into a metalized phase of unbonded carbon and oxygen atoms has been suggested by at least one research group,⁷⁰³ whose theoretical studies and pressurization experiments concluded that CO_2 begins to break down into various molecular species including CO and O_2 at high temperatures ~ 4000 - 6000 K under compression above ~ 30 GPa (2.4-2.5 kg/L density) but by ~ 70 GPa (~ 3.2 kg/L) “the system has completely dissociated into atomic C and O.”

Taking the recombination energy as ~ 643 kJ/mole, equal to the heat of formation of CO_2 from C and O_2 (393.5 kJ/mole) plus half the dissociation energy of O_2 into 2O (249.2 kJ/mole), the recombination energy density would then be **14.6 MJ/kg**, or **46.8 MJ/L** assuming a 3.2 kg/L mass density for metallic atomic CO_2 .

Another theory research group⁷⁰⁴ proposes a phase diagram for CO_2 (chart, right) that shows a region identified as “dissociated metallic



⁶⁹⁸ https://en.wikipedia.org/wiki/Triatomic_hydrogen.

⁶⁹⁹ Martin DW, McDaniel EW, Meeks ML. On the possible occurrence of H_3^+ in interstellar space. *Astrophys J.* 1961 Nov;134:1012-1013; <http://articles.adsabs.harvard.edu/full/1961ApJ...134.1012M/0001012.000.html>.

⁷⁰⁰ Peyron M, Hörl EM, Brown HW, Broida HP. Spectroscopic Evidence for Triatomic Nitrogen in Solids at Very Low Temperature. *J Chem Phys.* 1959 May;30(5):1304-10; <http://aip.scitation.org/doi/abs/10.1063/1.1730176>.

⁷⁰¹ <https://en.wikipedia.org/wiki/Trisulfur>.

⁷⁰² Artau A, Nizzi KE, Hill BT, Sunderlin LS, Wenthold PG. Bond dissociation energy in trifluoride ion. *Journal of the American Chemical Society.* 2000 Nov 1;122(43):10667-70; <http://pubs.acs.org/doi/abs/10.1021/ja001613e>.

⁷⁰³ Root S, Cochrane KR, Carpenter JH, Mattsson TR. Carbon dioxide shock and reshock equation of state data to 8 Mbar: Experiments and simulations. *Phys Rev B.* 2013 Jun 4;87(22):224102; <https://journals.aps.org/prb/abstract/10.1103/PhysRevB.87.224102>.

⁷⁰⁴ Boates B, Teweldeberhan AM, Bonev SA. Stability of dense liquid carbon dioxide. *PNAS* 2012 Sep 11;109(37):14808-14812; <http://www.pnas.org/content/109/37/14808.full.pdf>.

liquid,” while nonetheless arguing that liquid CO₂ “does not decompose into carbon and oxygen up to at least 200 GPa and 10,000 K.” Some who performed laser-heating DAC experiments on solid samples concluded that CO₂ dissociates into carbon and molecular oxygen at $P > 34$ GPa and temperatures over 2000 K;⁷⁰⁵ and yet other experimental work claims to show the onset of metallic conductivity >200 GPa, “consistent with dissociation to metallic oxygen”.⁷⁰⁶ More research will be needed to resolve these conflicting claims and results.⁷⁰⁷

Another triatomic example may be **xenon difluoride** (XeF₂), a transparent linear insulating molecule that, according to one research group,⁷⁰⁸ transforms into a reddish two-dimensional graphite-like hexagonal layered structure of semiconducting XeF₄ at ~ 50 GPa, and then further transforms above ~ 70 GPa into a black three-dimensional fluorite-like structure representing the first observed metallic XeF₈ polyhedron; when pressure is withdrawn, ~ 1 MJ/kg (or ~ 8.6 MJ/L, assuming the XeF₈ material has twice the 4.32 kg/L STP density of the solid⁷⁰⁹) of recombination energy is released.⁷¹⁰ However, the nature of this transformation is disputed by another highly-regarded research group,⁷¹¹ whose theoretical calculations suggests that molecular XeF₂ simply dissociates into an ionic solid [XeF]⁺F⁻ at 200 GPa.

⁷⁰⁵ Tschauner O, Mao HK, Hemley RJ. New transformations of CO₂ at high pressures and temperatures. *Phys Rev Lett*. 2001 Jul 31;87(7):075701; <http://www.bnl.gov/isd/documents/23813/section%206%20abstracts/tsch142.pdf>. Litasov KD, Goncharov AF, Hemley RJ. Crossover from melting to dissociation of CO₂ under pressure: Implications for the lower mantle. *Earth Planet Sci Lett*. 2011 Sep 15;309(3):318-23; https://www.researchgate.net/profile/Konstantin_Litasov2/publication/232363531_Crossover_from_melting_to_dissociation_of_CO2_under_pressure_Implications_for_the_lower_mantle/links/00b7d5384ad703326b000000.pdf.

⁷⁰⁶ Spaulding DK, Rygg JR, Eggert J, Uhlich S, Collins G. Laser-Driven Shock Studies of Precompressed CO₂ in the Diamond Anvil Cell. In AGU Fall Meeting Abstracts 2010 Dec; <http://adsabs.harvard.edu/abs/2010AGUFMMR11C1884S>.

⁷⁰⁷ Wu M, Tse JS, Pan Y. Stability and properties of liquid CO₂ at high pressure and high temperature: Implications for electrical conductivities in Earth's lower mantle. *Geophysical Research Letters*. 2015 Jul 28;42(14):5820-7; <http://onlinelibrary.wiley.com/doi/10.1002/2015GL064522/full>.

⁷⁰⁸ Kim M, Debessai M, Yoo CS. Two- and three-dimensional extended solids and metallization of compressed XeF₂. *Nature Chem*. 2010 Sep 1;2(9):784-8; <http://www.nature.com/nchem/journal/v2/n9/full/nchem.724.html>.

⁷⁰⁹ https://en.wikipedia.org/wiki/Xenon_difluoride.

⁷¹⁰ Christopher Mims, “New ‘Ultra-Battery’ as Energy-Dense as High Explosives: Metallized xenon difluoride heralds a new class of solid fuels,” MIT Technology Review, 9 Jul 2010; <https://www.technologyreview.com/s/419767/new-ultra-battery-as-energy-dense-as-high-explosives/>.

⁷¹¹ Kurzydłowski D, Zaleski-Ejgierd P, Grochala W, Hoffmann R. Freezing in resonance structures for better packing: XeF₂ becomes (XeF⁺)(F⁻) at large compression. *Inorg Chem*. 2011 Apr 18;50(8):3832-40; http://www.roaldhoffmann.com/sites/all/files/554.-freezing-in-resonance_0.pdf.

Venturing into still larger polyatomic recombination reactions, there have been experiments in which monatomic H and monatomic N were cryogenically trapped in an N₂ matrix at 10-30 K and allowed to recombine into NH₃,⁷¹² a tetratomic molecule with a recombination energy of 1167 kJ/mole (the enthalpy of formation from atomic hydrogen and nitrogen)⁷¹³ or **68.5 MJ/kg**. However, only trace amounts were present in the 1995 experiment so the energy density was very low, and no efforts appear to have been made to study the reaction at higher concentrations.

⁷¹² Hiraoka K, Yamashita A, Yachi Y, Aruga K, Sato T, Muto H. Ammonia formation from the reactions of H atoms with N atoms trapped in a solid N₂ matrix at 10-30 K. *Astrophys J.* 1995 Apr;443:363-370; <http://articles.adsabs.harvard.edu/full/1995ApJ...443..363H/0000363.000.html>.

⁷¹³ <https://socratic.org/questions/what-is-the-standard-enthalpy-of-formation-of-nh3-gas-standard-heat-of-atomisati>.

4.4 Excited States, Free Radicals, and Ion Recombination

Energy can be stored in molecules as kinetic or potential energy. Translation energy (the energy of motion through space at some velocity) is one example of purely kinetic energy storage that is discussed later in **Section 5.3.1**. Rotational energy is the kinetic energy associated with the tumbling motion of molecules (typically of order ~ 0.0001 eV between quantized rotational energy levels), and vibrational energy involves potential/kinetic energy exchange during the oscillatory motion of atoms or atom groups within a molecule (typically of order ~ 0.1 eV between quantized vibrational energy levels).

The highest energy densities are obtained from electronic states, in which quantized energy is stored as potential energy in excited electronic configurations (typically of order ~ 1 eV and higher). Such excited configurations include excited states in which the energies of existing electrons have been raised above the lowest-level ground state (**Section 4.4.1**), free radicals in which free valences are present among the existing electrons (**Section 4.4.2**), and ionized states in which orbital electrons have been added or removed (**Section 4.4.3**).

4.4.1 Electronically Excited Metastable States

Metastable states of atoms and molecules are excited states that are energetically unstable with respect to decay processes such as dissociation, ionization or the emission of a photon, but do not decay on the μsec time scale because the decay processes are hindered by selection rules or by the nature of the potential energy landscape.⁷¹⁴

The most-investigated metastable species for energy storage is metastable triplet helium (**Section 4.4.1.1**) but several other potentially useful metastable species may also be available (**Section 4.4.1.2**), including the exotic highly-excited states found in Rydberg matter (**Section 4.4.1.3**).

⁷¹⁴ Raunhardt M. Generation and spectroscopy of atoms and molecules in metastable states. PhD thesis, ETH Zurich, Diss. ETH No. 18260, 2009; <http://e-collection.library.ethz.ch/eserv/eth:41903/eth-41903-02.pdf>.

4.4.1.1 Spin-Polarized Triplet Helium

Perhaps the most-studied metastable species for possible energy storage is the $1s2s\ ^3S_1$ triplet state⁷¹⁵ of helium (^4He), aka. He^* , that possesses “radiative metastability” preventing immediate photon emission and decay to the $1s^2\ ^1S_0$ ground state⁷¹⁶ via the transition: $1s2s\ ^3S_1 \rightarrow 1s^2\ ^1S_0$. The half-life of this transition, initially estimated as $7860\ \text{sec}^{717}$ - $8300\ \text{sec}^{718}$ theoretically, was initially measured experimentally⁷¹⁹ to be $\sim 9100\ \text{sec}$ and most recently refined to $7870\ \text{sec}$ (2.2 hr).⁷²⁰ Isolated triplet ^4He atoms lie $19.82\ \text{eV}$ (**478.2 MJ/kg**) above the ground state in energy.⁷²¹ He^* has been prepared using high-energy (10-100 keV) electron bombardment of liquid helium, with only low metastable populations of 10^{12} - $10^{13}\ \text{He}^*/\text{cm}^3$ produced so far.⁷²² Energy can also be lost via collisions, reducing lifetime. The first Bose-Einstein condensate (BEC)⁷²³ of He^* was

⁷¹⁵ aka. the “ 2^3S_1 ”, “ 2^3S ”, “ $\text{He}^*(^3S)$ ” or “ He^* ” state. The 2^3S_1 triplet state of the helium atom has two electrons with the same spin, occupying the 1s and 2s orbitals.

⁷¹⁶ aka. the “ 1^1S_0 ” or $\text{He}(^1S)$ ground state.

⁷¹⁷ Drake GW. Theory of Relativistic Magnetic Dipole Transitions: Lifetime of the Metastable 2^3S State of the Heliumlike Ions. *Phys Rev A*. 1971 Mar 1;3(3):908-915; <http://scholar.uwindsor.ca/cgi/viewcontent.cgi?article=1113&context=physicspub>.

⁷¹⁸ Feinberg G, Sucher J. Calculation of the decay rate for $2^3S_1 \rightarrow 1^1S_0 + \text{one photon}$ in helium. *Phys Rev Lett*. 1971 Mar 22;26, 681-684; <https://journals.aps.org/prl/abstract/10.1103/PhysRevLett.26.681>; errata *Phys Rev A*. 1971 Apr 26;26(17):1084; <https://journals.aps.org/prl/pdf/10.1103/PhysRevLett.26.1084.2>.

⁷¹⁹ Woodworth JR, Moos HW. Experimental determination of the single-photon transition rate between the 2^3S_1 and 1^1S_0 states of He I. *Phys Rev A*. 1975 Dec 1;12(6):2455-2463; <https://journals.aps.org/prl/abstract/10.1103/PhysRevA.12.2455>.

⁷²⁰ Hodgman SS, Dall RG, Byron LJ, Baldwin KG, Buckman SJ, Truscott AG. Metastable helium: A new determination of the longest atomic excited-state lifetime. *Phys Rev Lett*. 2009 Jul 30;103(5):053002; https://openresearch-repository.anu.edu.au/bitstream/10440/978/1/Hodgman_Metastable2009.pdf.

⁷²¹ Rosen G. Current status of free radicals and electronically excited metastable species as high energy propellants. NASA-CR-136938, N74-17496, Aug 1973; <https://ntrs.nasa.gov/archive/nasa/casi.ntrs.nasa.gov/19740009383.pdf>.

⁷²² Dennis WS, Durbin Jr E, Fitzsimmons WA, Heybey O, Walters GK. Spectroscopic identification of excited atomic and molecular states in electron-bombarded liquid helium. *Phys Rev Lett*. 1969 Nov 10;23(19):1083-1086; <https://journals.aps.org/prl/abstract/10.1103/PhysRevLett.23.1083>. Hill JC, Heybey O, Walters GK. Evidence of metastable atomic and molecular bubble states in electron-bombarded superfluid liquid helium. *Phys Rev Lett*. 1971 May 17;26(20):1213-1216; <https://journals.aps.org/prl/abstract/10.1103/PhysRevLett.26.1213>. Watkins JL, Zmuidzinas JS, Williams GA. Electron beam excitation of the liquid helium surface. *Physica B+C*. 1981 Aug 1;108(1):1313-1314; <http://www.sciencedirect.com/science/article/pii/0378436381909554>.

⁷²³ https://en.wikipedia.org/wiki/Bose%E2%80%93Einstein_condensate.

reported in 2001 using a magnetic trap at 0.001 K at a number density of 2×10^8 $^4\text{He}^*/\text{cm}^3$ but for only ~ 60 sec,⁷²⁴ and a BEC of $\sim 10^6$ $^3\text{He}^*/\text{cm}^3$ was reported in 2006.⁷²⁵

As previously described in connection with spin-polarized atomic hydrogen (**Section 4.3.1.1**), stability should be maximized when the spins of all electrons in a macroscale collection of He^* atoms are aligned in one direction by applying an external magnetic field. Spin polarization is necessary (but not sufficient) to prevent destruction of He^* by autoionization or radiative decay.⁷²⁶ Low-density ($\sim 10^{12}$ cm^{-3} , $\sim 3 \times 10^{-9}$ MJ/L) He^* in liquid He can probably be spin-polarized via strong magnetic fields at low temperatures, and it might be possible to use optical pumping to reach densities as high as $\sim 10^{18}$ cm^{-3} (~ 0.003 MJ/L).⁷²⁷

Starting in 1973⁷²⁸ and continuing at least until 1984,⁷²⁹ key proponent Jonas Zmuidzinas of JPL proposed that attractive forces between spin-polarized He^* might bind these species into a classical solid that he called “He IV-A”. At normal temperatures and pressures, Zmuidzinas suggested that an assembly of spin-polarized $\text{He}^*\uparrow$ atoms would form a non-autoionizing insulator having properties similar to those of rare gas solids,⁷³⁰ with a ~ 4.2 Å nearest-neighbor atom separation, a preferred fcc crystal structure with a number density of 1.3×10^{22} cm^{-3} (mass density 0.086 kg/L), and a melting point of ~ 580 K, with a recoverable specific energy of **478.2 MJ/kg (41 MJ/L)**. In a metallic phase, claimed to be preferred energetically, He IV-A might better be represented as a system composed of spin-polarized helium ions ($\text{He}^+\uparrow$) and spin-polarized electrons ($e^-\uparrow$) and would have a mass density of 0.89 kg/L and a recoverable specific

⁷²⁴ Robert A, Sirjean O, Browaeys A, Poupard J, Nowak S, Boiron D, Westbrook CI, Aspect A. A Bose-Einstein condensate of metastable atoms. *Science*. 2001 Apr 20;292(5516):461-4; <http://science.sciencemag.org/content/292/5516/461/tab-pdf>.

⁷²⁵ McNamara JM, Jeltens T, Tychkov AS, Hogervorst W, Vassen W. Degenerate Bose-Fermi mixture of metastable atoms. *Phys Rev Lett*. 2006 Aug 24;97(8):080404; http://www.nat.vu.nl/en/sec/atom/Publications/pdf/PRL_Mac.pdf.

⁷²⁶ The decay takes place via a slow relativistic magnetic-dipole (M1) transition; if this transition could somehow be inhibited, He^* would have a lifetime of $2.48\text{-}2.88 \times 10^8$ sec (7.9-9.2 yr) as determined by the next-dominant two-photon electric-dipole (2E1) transition; Bely O, Faucher P. The Two-Photon Transition Probabilities from the Metastable 2^3S_1 State in the Helium Like Series. *Astron Astrophys*. 1969 Jan;1:37-41; <http://articles.adsabs.harvard.edu/full/1969A%26A.....1...37B/0000037.000.html>.

⁷²⁷ Zmuidzinas JS. Spin-Polarized Triplet Helium. Air Force Rocket Propulsion Laboratory, AFRPL TR-84-027 (AD-A141054), April 1984; <http://www.dtic.mil/cgi-bin/GetTRDoc?AD=ADA141054>.

⁷²⁸ Zmuidzinas JS. Energy Storage in Solid Helium. JPL Technical Memorandum 33-653 (NASA-CR-135716, N73-32541), 15 Sep 1973; <https://ntrs.nasa.gov/archive/nasa/casi.ntrs.nasa.gov/19730023808.pdf>.

⁷²⁹ Zmuidzinas JS. Spin-Polarized Triplet Helium. Air Force Rocket Propulsion Laboratory, AFRPL TR-84-027 (AD-A141054), April 1984; <http://www.dtic.mil/cgi-bin/GetTRDoc?AD=ADA141054>.

⁷³⁰ Liquid helium only solidifies above 2.5 MPa with a density of 0.19 kg/L; Henshaw DG. Structure of Solid Helium by Neutron Diffraction. *Phys Rev*. 1958 Jan 15;109(2):328-330; <https://journals.aps.org/pr/abstract/10.1103/PhysRev.109.328>.

energy of **324 MJ/kg (288 MJ/L)**.⁷³¹ The metastable character of He* is apparently not much impaired when suspended in liquid helium,⁷³² and Manykin's theory of the condensed excited state might allow an extended lifetime of an He* assembly beyond the normal lifetime of an isolated excited atom.⁷³³ Frustrated by the lack of progress, Zmuidzinis left the field in the late 1980s, leaving it to others to complete future research on using He* for energy storage – although general experimental interest in metastable triplet helium continues to this day.

⁷³¹ For conventional high-pressure metallization, the insulator-to-metal transition in solid helium is predicted to occur at a density of 21.3 kg/L and a super-high pressure of 25,700 GPa; Khairallah SA, Militzer B. First-principles studies of the metallization and the equation of state of solid helium. *Phys Rev Lett.* 2008 Sep 5;101(10):106407; http://greif.geo.berkeley.edu/papers/HeMetalv9_header.pdf.

⁷³² Hickman AP, Lane NF. Localized excited states of helium in liquid helium. *Phys Rev Lett.* 1971 May 17;26(20):1216-1219; <https://journals.aps.org/prl/abstract/10.1103/PhysRevLett.26.1216>. Swaminathan PK, Murthy CS. Simulations of high-pressure condensed helium. *J Phys Chem.* 1990 Aug;94(16):6479-6483; <http://pubs.acs.org/doi/abs/10.1021/j100379a059?journalCode=jpchax>.

⁷³³ Manykin EA, Ozhovan MI, Poluektov PP. Theory of the condensed state in a system of excited atoms. *Zh. Eksp. Teor. Fiz.* 1983 Feb;84(2):442-53 [*Sov Phys JETP* 1983;57:256]; http://www.jetp.ac.ru/cgi-bin/dn/e_057_02_0256.pdf.

4.4.1.2 Other Metastable Species

Electronically excited metastable species of possible interest for energy storage must have sufficient resistance to spontaneous electromagnetic decay (i.e., a sufficiently long radiative lifetime) in addition to having a high specific energy content. An atomic or molecular species is generally considered “metastable” if its radiative lifetime $> 1 \mu\text{sec}$, but longer lifetimes are clearly required for a useful energy storage system.

Table 33 is a representative list of experimentally accessible metastable species with transition energy $\geq 1 \text{ eV}$ and radiative lifetimes $\geq 1 \text{ msec}$.⁷³⁴ Metastable triplet helium (**478.2 MJ/kg**, 7870 sec \sim 2.2 hr half-life; blue data in table) has the fourth-highest specific energy and the third longest radiative lifetime, probably the best combination, on the list – which explains the great interest in the $^4\text{He } 2^3\text{S}_1$ species (**Section 4.4.1.1**). Additional electronically excited metastable species that might be of practical interest for energy storage include $^3\text{P}_2$ neon (**80.2 MJ/kg**, 400 sec \sim 0.1 hr half-life), ^2D atomic nitrogen (**16.6 MJ/kg**, 140,000 sec \sim 38.9 hr half-life), $^3\text{P}_2$ magnesium (**10.8 MJ/kg**, 2050 sec \sim 0.6 hr half-life), ^1P atomic carbon (**10.1 MJ/kg**, 5000 sec \sim 1.4 hr half-life), and a $^1\Delta_g$ molecular oxygen (**3.0 MJ/kg**, 3000 sec \sim 0.8 hr half-life). The metastable atom with the highest specific energy – hydrogen $2^2\text{S}_{1/2}$ (**978.6 MJ/kg**) – is another

⁷³⁴ Muschlitz EE Jr. Metastable Atoms and Molecules. *Science* 1968 Feb 9;159(3815):599-604; <http://science.sciencemag.org/content/159/3815/599/tab-pdf>. Rosen G. Current status of free radicals and electronically excited metastable species as high energy propellants. NASA-CR-136938, N74-17496, Aug 1973; <https://ntrs.nasa.gov/archive/nasa/casi.ntrs.nasa.gov/19740009383.pdf>. Noerdlinger PD, Dynan SE. Ultraviolet absorption lines arising on metastable states. *The Astrophysical Journal Supplement Series*. 1975 Jun;29:185-91; <http://articles.adsabs.harvard.edu/full/1975ApJS...29..185N/0000185.000.html>. Zmuidzinas JS. Spin-Polarized Triplet Helium. Air Force Rocket Propulsion Laboratory, AFRPL TR-84-027 (AD-A141054), April 1984; <http://www.dtic.mil/cgi-bin/GetTRDoc?AD=ADA141054>. Yarkony DR. Theoretical studies of nonadiabatic processes relevant to the stability and detection of energetic species. In: Thompson TL, Rodgers SL. *Proceedings of the High Energy Density Matter (HEDM) Contractors' Conference held 5-7 June 1994 in Crystal Bay NV, Dec 1994*, pp. 39-45; <https://www.google.com/url?sa=t&rct=j&q=&esrc=s&source=web&cd=2&ved=0ahUKEwin5N-93vXTAhUJzGMKHTnD1MOFggpMAE&url=http%3A%2F%2Fwww.dtic.mil%2Fcgi-bin%2FGetTRDoc%3FLocation%3DU2%26doc%3DGetTRDoc.pdf%26AD%3DADA292988&usq=AFQjCNHhKvoIXSOpcRnJpZQL2mHL8OqQIA&cad=rja>. Dunning FB, Hulet RG (eds). *Atomic, Molecular, and Optical Physics: Atoms and Molecules*. Academic Press, 1996; “Table 1. Selected Metastable States of Atoms and Molecules”; <https://books.google.com/books?id=0chPSpRpio0C&pg=PA206>. Fridman A, Kennedy LA. *Plasma Physics and Engineering*, CRC Press, 2004; “Table 3.1 Lowest Electronically Excited States and Lowest Metastable States for Excited Atoms with Their Radiative Lifetimes” and “Table 3.5 Lifetimes and Energies of Metastable Diatomic Molecules”; https://books.google.com/books?id=9wqtYiy_gloC&pg=PA75. Santra R, Christ KV, Greene CH. Properties of metastable alkaline-earth-metal atoms calculated using an accurate effective core potential. *Phys Rev A*. 2004 Apr 14;69(4):042510; <https://arxiv.org/pdf/physics/0312033.pdf>.

interesting target, but only if its short 0.12 sec radiative lifetime can somehow be increased several orders of magnitude, by some means currently unknown.⁷³⁵

⁷³⁵ Zmuidzinas and Rosen speculate that to preserve the shorter-lived metastable species, “it may be possible to interfere destructively with the quantum mechanical probability amplitude for spontaneous electromagnetic radiative decay of an atomic metastable state, e.g., by imposing a standing-wave electromagnetic field of critical amplitude and wavelength on metastables in a lattice.” Rosen G. Current status of free radicals and electronically excited metastable species as high energy propellants. NASA-CR-136938, N74-17496, Aug 1973, p. 5 (footnote); <https://ntrs.nasa.gov/archive/nasa/casi.ntrs.nasa.gov/19740009383.pdf>.

Table 33. Specific energy and radiative lifetime of the longest-lived high-energy atomic and molecular electronic metastable species

Atomic or Molecular Species	Electronic Metastable State →	Electronic Ground State	Energy (eV)	Radiative Lifetime (sec)	Specific Energy (MJ/kg)
H	$2^2S_{1/2}$	$2^2S_{1/2}$	10.2	0.12	978.6
H ₂	$c^3\Pi_u$	$1^1\Sigma_g^+$	11.86	0.001	572.3
He	2^1S_0	1^1S_0	20.61	0.02	497.3
He	2^3S_1	1^1S_0	19.82	7870	478.2
He ₂	$a^3\Sigma_u^+$		18.1	0.1	218.0
Ne	3^3P_0	1^1S_0	16.71	20	80.6
Ne	3^3P_2	1^1S_0	16.62	400	80.2
N ₂	$E^3\Sigma_g^+$		11.9	300	41.0
N ₂	$a^1\Sigma_u^-$		8.4	0.7	28.9
Ar	2^2P_0	1^1S_0	11.72	1.3	28.3
Ar	2^2P_2	1^1S_0	11.55	40	27.9
O	1^1S_0	3^3P_2	4.17	1.31	25.1
N	$2^2P_{3/2}$	$4^4S_{3/2}$	3.6	170	24.9
N	$2^2P_{1/2}$	$4^4S_{3/2}$	3.58	40	24.7
C	1^1P	1^1S	2.68	2	21.6
N ₂	$A^3\Sigma_u^+$	$1^1\Sigma_g^+$	6.16	13	21.2
CO	$a^3\Pi$	$1^1\Sigma^+$	6.01	0.004	20.7
N	$2^2D_{5/2}$	$4^4S_{3/2}$	2.4	140,000	16.6
N	$2^2D_{3/2}$	$4^4S_{3/2}$	2.38	61,000	16.4
NO	$a^4\Pi$	$2^2\Pi$	4.7	0.2	15.1
Kr	3^3P_0	1^1S_0	10.6	1	12.2
O	1^1D_2	3^3P_2	1.97	110	11.9
Kr	3^3P_2	1^1S_0	9.9	2	11.4
Mg	3^3P_2	1^1S_0	2.72	2050	10.8
BH	$a^3\Pi$	$X^1\Sigma^+$	1.3	16	10.5
C	1^1P	1^1D	1.26	5000	10.1
S	1^1P	1^1S	2.75	2.8	8.3
CH ₂	\bar{a}^1A_1	$3^3\Sigma_g^-$	1	0.01	6.9
Si	1^1P	1^1S	1.91	1.2	6.6
¹³² Xe	3^3P_2	1^1S_0	8.32	150	6.1
O ₂	$b^1\Sigma_g^+$		1.6	7	4.8
C ₆ H ₆	\bar{a}^3B_u	1^1A_{1g}	3.8	28	4.7
Ca	3^3P_2	1^1S_0	1.90	7700	4.6
S	1^1P	1^1D	1.14	28	3.4
O ₂	$a^1\Delta_g$	$3^3\Sigma_g^-$	0.98	3000	3.0
Si	1^1F	1^1D	0.78	270	2.7
Hg	3^3P_2	1^1S_0	5.43	1	2.6
Hg	3^3P_0	1^1S_0	4.64	1	2.2

Excited tetrahydrogen (H_4^*) – a tetrahedron-shaped molecule in the $^1A'$ excited state – was once proposed⁷³⁶ as a possible high energy density molecule (~ 6.66 eV, **159 MJ/kg**) that could be embedded in NaCl-type crystals such as AgF and RbI.⁷³⁷ It was initially believed to be both synthesizable⁷³⁸ and stable,⁷³⁹ but more extensive theoretical calculations determined that the cluster has a fast-acting decay channel leading to a 10^{-13} sec lifetime.⁷⁴⁰

Photoluminescence⁷⁴¹ is a related phenomena in which the atomic or molecular absorption of photons creates an excited state, storing energy in a “trapping site” from which it is later released by photon re-emission. Two variants, fluorescence⁷⁴² and Raman emission,⁷⁴³ occur on nanosecond timescales and thus are not useful for energy storage applications. Another variant, **phosphorescence**,⁷⁴⁴ occurs as a result of triplet–singlet electronic relaxation. While most phosphorescent compounds are relatively fast emitters with triplet lifetimes on the order of milliseconds, a few materials have triplet lifetimes up to minutes or even hours, allowing these substances to effectively store light energy in the form of very slowly degrading excited electron states.

⁷³⁶ Nicolaides CA, Theodorakopoulos G, Petsalakis ID. Theory of chemical reactions of vibronically excited $H_2(B^1\Sigma_u^+)$. I. Prediction of a strongly bound excited state of H_4 . J Chem Phys. 1984 Feb 15;80(4):1705-6; <http://aip.scitation.org/doi/abs/10.1063/1.446874>.

⁷³⁷ Nicolaides CA, Valtazanos P, Bacalis NC. Excited molecules and clusters in solid media. Hydrogen and tetrahydrogen in ionic crystals. Chem Phys Lett. 1988 Oct 7;151(1-2):22-6; <http://www.sciencedirect.com/science/article/pii/0009261488800617>.

⁷³⁸ Kuppermann A. Experimental Studies of the Properties of Trihydrogen and Tetrahydrogen. California Inst Of Tech Pasadena, D-A228869, AL-TR-90-038, 1990 Oct; <http://www.dtic.mil/cgi-bin/GetTRDoc?AD=ADA228869>.

⁷³⁹ Metropoulos A, Nicolaides CA. On the stability of excited tetrahydrogen. J Phys B: Atomic, Molecular and Optical Physics. 1988 Feb 28;21(4):L77-L81; <http://iopscience.iop.org/article/10.1088/0953-4075/21/4/002/meta>.

⁷⁴⁰ Petsalakis ID, Metropoulos A, Theodorakopoulos G, Nicolaides CA. An estimate of the lifetime of excited tetrahydrogen. Chem Phys Lett. 1989 Jun 9;158(3-4):229-32; <http://www.sciencedirect.com/science/article/pii/0009261489873269>. Valtazanos P, Bacalis NC, Nicolaides CA. Hydrogen molecule and tetrahydrogen cluster embedded in ionic crystals. Chem Phys. 1990 Jul 15;144(3):363-70; <http://www.sciencedirect.com/science/article/pii/0301010490801013>.

⁷⁴¹ <https://en.wikipedia.org/wiki/Photoluminescence>.

⁷⁴² Fluorescence (<https://en.wikipedia.org/wiki/Fluorescence>) is a form of photoluminescence resulting from singlet–singlet electronic relaxation; excited state decay times are 0.5-20 nanoseconds for photon emission from UV to near infrared for commonly used fluorescent compounds including laser dyes (https://en.wikipedia.org/wiki/Dye_laser), fluorophores (<https://en.wikipedia.org/wiki/Fluorophore>), and fluorescent brightening agents (https://en.wikipedia.org/wiki/Optical_brightener).

⁷⁴³ Raman emission (https://en.wikipedia.org/wiki/Raman_scattering) is a form of photoluminescence that results from inelastic light scattering, with a typical lifetime of ~nanoseconds.

⁷⁴⁴ <https://en.wikipedia.org/wiki/Phosphorescence>.

For example, strontium aluminate doped with europium and dysprosium ions ($\text{SrAl}_2\text{O}_4:\text{Eu}^{2+},\text{Dy}^{3+}$) has a luminescence lifetime exceeding 10 hours,⁷⁴⁵ believed to involve emission of a 3.44 eV photon as the dopant europium ion falls from a triplet into its singlet $^8\text{S}_{7/2}$ electronic state.⁷⁴⁶ The dopant ions are present at ~3-4% concentration,⁷⁴⁷ so the specific energy is only ~**0.06 MJ/kg**, illustrating that overall energy densities for phosphorescing materials are generally rather low.

⁷⁴⁵ Matsuzawa T, Aoki Y, Takeuchi N, Murayama Y. A New Long Phosphorescent Phosphor with High Brightness, $\text{SrAl}_2\text{O}_4:\text{Eu}^{2+},\text{Dy}^{3+}$. J Electrochem Soc. 1996 Aug 1;143(8):2670-73; <http://jes.ecsdl.org/content/143/8/2670.short>.

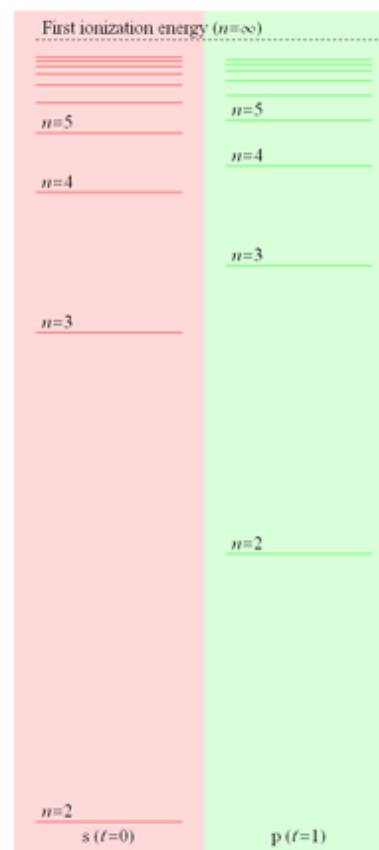
⁷⁴⁶ Aitasalo T, Dereń P, Hölsä J, Jungner H, Krupa JC, Lastusaari M, Legendziewicz J, Niittykoski J, Stręk W. Persistent luminescence phenomena in materials doped with rare earth ions. J Solid State Chem. 2003 Mar 1;171(1):114-22; <http://www.sciencedirect.com/science/article/pii/S0022459602001949>.

⁷⁴⁷ Bamfield P. Chromic Phenomena: The Technological Applications of Colour Chemistry, Royal Society of Chemistry, 2001; <http://chemistry-chemists.com/chemister/Physchemie/chromic-phenomena.pdf>.

4.4.1.3 Rydberg Matter

A Rydberg atom⁷⁴⁸ is an excited atom in which one or more outer electrons are excited to a high principal quantum number (quantum state) but without quite being ionized (image, right), resulting in an atom with a large-diameter electron cloud.⁷⁴⁹ Rydberg atoms can be extremely big – e.g., the $n = 137$ state of hydrogen has an atomic radius $\sim 1 \mu\text{m}$, with the outermost electron said to occupy a planar circular orbit with lifetimes up to several hours.⁷⁵⁰ Rydberg atoms can also form Rydberg molecules,⁷⁵¹ such as dihelium (He_2^*).⁷⁵²

Condensation of Rydberg atoms forms Rydberg matter,⁷⁵³ most often observed in the form of long-lived clusters of up to 91 H_2^* molecules⁷⁵⁴ with cluster radiative lifetimes of, for example, ~ 25 sec for $n = 12$.⁷⁵⁵ Rydberg matter – a condensed state of highly excited atoms – can be created by desorbing alkali metals from nonmetal surfaces.⁷⁵⁶ Rydberg matter has been used as the active medium for a laser, widely tunable in the IR, whose excitation is entirely thermal.⁷⁵⁷



⁷⁴⁸ https://en.wikipedia.org/wiki/Rydberg_atom.

⁷⁴⁹ Gallagher TF. Rydberg Atoms. Cambridge University Press, 1994.

⁷⁵⁰ Sorochenko RL. Postulation, detection and observations of radio recombination lines. In: Gordon MA, Sorochenko RL. Radio recombination lines: 25 years of investigation. Kluwer, 1990, p. 1; http://link.springer.com/chapter/10.1007/978-94-009-0625-9_1#page-1.

⁷⁵¹ Bendkowsky V, Butscher B, Nipper J, Shaffer JP, Löw R, Pfau T. Observation of ultralong-range Rydberg molecules. Nature. 2009 Apr 23;458(7241):1005-8; http://www.physics.uoguelph.ca/~rbrooks/phys4930/nature458_1005.pdf.

⁷⁵² https://en.wikipedia.org/wiki/Helium_dimer.

⁷⁵³ https://en.wikipedia.org/wiki/Rydberg_matter.

⁷⁵⁴ Wang J, Holmlid L. Rydberg Matter clusters of hydrogen (H_2) N^* with well-defined kinetic energy release observed by neutral time-of-flight. Chem Phys. 2002 Mar 15;277(2):201-10; <http://cemunsel.unse.edu.ar/Pdf/r1541.pdf>.

⁷⁵⁵ https://en.wikipedia.org/wiki/Rydberg_matter#Lifetime.

⁷⁵⁶ Holmlid L. Complex kinetics of desorption and diffusion. Field reversal study of K excited-state desorption from graphite layer surfaces. J Phys Chem A. 1998 Dec 24;102(52):10636-46; <http://pubs.acs.org/doi/abs/10.1021/jp9823796>.

A cloud of Rydberg matter consisting partially of neutral H atoms produced using a hydrogen gas pressure of 10^{-9} atm has been experimentally observed to release fragments having 9.4 eV (**~902 MJ/kg**) of kinetic energy after irradiation with a 5 nsec laser pulse;⁷⁵⁸ these fragments were found to be H* atoms in Rydberg states with principal quantum number >28 .⁷⁵⁹ However, given the large size of Rydberg clusters, their highest available number densities (up to $\sim 10^9$ clusters/cm³ in the lab)⁷⁶⁰ may be too small for practical high-density energy storage.

⁷⁵⁷ Holmlid L. Optical stimulated emission transitions in Rydberg matter observed in the range 800-14,000 nm. *J Phys B: Atomic Molec Optical Phys.* 2003 Dec 17;37(2):357; <http://iopscience.iop.org/article/10.1088/0953-4075/37/2/005/meta>. Badiei S, Holmlid L. Stimulated emission in Rydberg Matter—a thermal ultra-broadband tunable laser. *Chem Physics Lett.* 2003 Jul 31;376(5):812-7; <http://www.sciencedirect.com/science/article/pii/S0009261403011266>.

⁷⁵⁸ Badiei S, Holmlid L. Lowest state $n=1$ of H atom Rydberg matter: many eV energy release in Coulomb explosions. *Phys Lett A.* 2004 Jun 28;327(2):186-91; <http://www.sciencedirect.com/science/article/pii/S0375960104006826>.

⁷⁵⁹ Badiei S, Holmlid L. Experimental studies of fast fragments of H Rydberg matter. *J Phys B: Atomic Molec Optical Phys.* 2006 Oct 10;39(20):4191-4212; <http://iopscience.iop.org/article/10.1088/0953-4075/39/20/017/meta>.

⁷⁶⁰ Holmlid L. The diffuse interstellar band carriers in interstellar space: all intense bands calculated from He doubly excited states embedded in Rydberg Matter. *Mon Not R Astron Soc.* 2008 Feb 21;384(2):764-74; http://www.academia.edu/download/44257507/The_diffuse_interstellar_band_carriers_i20160331-21865-zknm76.pdf.

4.4.2 Free Radical Species

A free radical species is an electrically neutral atom or molecule with one or more unpaired valence electrons or “dangling bonds”. For practical use as an energy store, a free radical species should be a stable (ground-state) quantum mechanical structure with a high energy of reaction per unit mass, which implies that the free radical should have relatively low molecular weight. Quantum mechanical analysis shows that a host of free radical species are likely to have adequate ground-state stability and sufficient specific energy to warrant further consideration.⁷⁶¹

The best practical candidates for free radical energy storage are shown in **Table 34**, all of which have been extensively studied experimentally except for three species (HLi,⁷⁶² He₂O,⁷⁶³ and H₂Li) that have been only lightly studied by quantum mechanical analysis.⁷⁶⁴ Three of the entries – monatomic H, N, and O – involve recombination reactions that have already been extensively discussed in **Section 4.3**.

At present, free radical species can only be stored in solid cryogenic matrices,⁷⁶⁵ which ultimately limits their concentrations to at most 1-10% using current techniques. Experimental radical production is currently limited to relatively low densities because the radicals are so chemically

⁷⁶¹ “The object of this investigation was the determination of those molecules in this group which appeared most likely to be sufficiently stable and energetic to merit attention as possible high-energy chemical propellants. Initial emphasis was placed upon a preliminary quantum mechanical screening of the possible molecular electronic states in an attempt to predict, a priori, those states most worthy of further investigation. Several thousand states of the diatomic molecules and well over 10,000 states of the triatomics were screened and, of these, about 100 of each type were selected as being most interesting. Quantum mechanical energy calculations were then performed for 43 states of the diatomic molecules and 11 of the triatomic molecules and the performance potential of each of these was estimated.”
Schneiderman SB. Theoretical Investigation of High-Energy Metastable Compounds. AFRPL-TR-66-228, Sep 1966; <http://oai.dtic.mil/oai/oai?verb=getRecord&metadataPrefix=html&identifier=AD0377319>.

⁷⁶² Jain M, Gupta A. Diamagnetic susceptibility of HLi. In: Diamagnetic Susceptibility and Anisotropy of Inorganic and Organometallic Compounds, Springer Berlin Heidelberg, 2007, pp. 1098-1098; http://link.springer.com/chapter/10.1007/978-3-540-44694-1_1049. Yongjian ZZ, Daqiao M. Two-Photon Excitation for H₂O and HLi [J]. Acta Optica Sinica. 2012;1:049; http://en.cnki.com.cn/Article_en/CJFDTOTAL-GXXB201201049.htm.

⁷⁶³ Hogreve H. A theoretical study of the dications HeO²⁺ and He₂O²⁺. Molec Phys. 2004 Mar 10;102(5):461-70; <http://www.tandfonline.com/doi/abs/10.1080/00268970410001668444>. Tulub AV, Panin AI, Khait YG. Theoretical Study of Possible Decay Channels and Lifetime of the Metastable Triplet State of the He₂O²⁺ Ion. Optics Spectrosc. 1998 Jan 1;84(1):29-33.

⁷⁶⁴ Rosen G. Current status of free radicals and electronically excited metastable species as high energy propellants. NASA-CR-136938, N74-17496, Aug 1973; <https://ntrs.nasa.gov/archive/nasa/casi.ntrs.nasa.gov/19740009383.pdf>.

⁷⁶⁵ e.g., Langford VS, Williamson BE. Magnetic circular dichroism of the CH radical in an argon matrix. J Phys Chem A. 1998 Jan 1;102(1):138-45; <http://pubs.acs.org/doi/abs/10.1021/jp9728823>.

reactive – e.g., in one experiment,⁷⁶⁶ a hydrocarbon flame burner generated a peak ground-state methylidyne (CH) number density of only 1.53×10^{13} molecules/cm³ ($\sim 1.5 \times 10^{-8}$ MJ/L).

Table 34. Known and conjectured ground-state free radical species for energy storage			
Free Radical Species	Ground State	Chemical Reaction	Specific Energy (MJ/kg)
H	$^2S_{1/2}$	$2H \rightarrow H_2$	216.0
CH	$^4\Sigma^-$	$2CH \rightarrow 2C$ (solid phase) + H_2	45.6
N	$^4S_{3/2}$	$2N \rightarrow N_2$	33.7
BH	$^3\Pi$	$2BH \rightarrow 2B + H_2$	25.9
HLi	$^1\Sigma^+$	$2HLi \rightarrow H_2 + 2Li$	22.8
CH ₂	$^3\Sigma_g^-$	$CH_2 \rightarrow C$ (solid phase) + H_2	22.1
NH	$^1\Delta$	$2NH \rightarrow N_2 + H_2$	22.0
BH ₂	2A_1	$BH_2 \rightarrow B + H_2$	21.7
He ₂ O	$^1\Sigma_g^+$	$2He_2O \rightarrow 4He + O_2$	18.2
H ₂ Li	$^2\Sigma_u^+$	$H_2Li \rightarrow H_2 + Li$	16.5
O	3P	$2O \rightarrow O_2$	15.6

⁷⁶⁶ Walsh KT, Long MB, Tanoff MA, Smooke MD. Experimental and computational study of CH, CH*, and OH* in an axisymmetric laminar diffusion flame. Symposium (International) on Combustion 1998 Jan 1;27(1):615-623; <http://guilford.eng.yale.edu/pdfs/ch.pdf>.

4.4.3 Ionized States

An ionized state occurs when an atom or molecule has gained or lost one or more electrons, changing from an electrically neutral species to an electrically charged ion. A positively charged ion is called a “cation”; a negatively charged ion is called an “anion”.⁷⁶⁷

The largest reserve of stored energy in ions is the propensity of cations to absorb one or more electrons to regain charge neutrality, a process called ion recombination.⁷⁶⁸ Ion recombination energy – the energy released when an electron is added to an ionized molecule or atom, reducing its positive charge – is distinguished from molecular recombination energy (**Section 4.3**). Ion recombination energy is the exact inverse of the ionization energy: the amount of energy required to remove the most loosely bound remaining electron, e.g., the valence electron of an isolated gaseous electrically neutral atom, to form a positive ion.⁷⁶⁹

In this Section we review the specific energies and energy densities potentially available from the ion recombination of singly-ionized atomic and molecular cations (**Section 4.4.3.1**) and multiply-ionized atomic and molecular cations (**Section 4.4.3.2**). We then consider the energy storage possibilities of electron autodetachment from negatively-ionized atomic and molecular anions (**Section 4.4.3.3**).

Finally, because of their opposite charges, a cation and an anion can be induced to combine into an “ion-pair molecule” (**Section 4.4.3.4**), accompanied by the release of energy. Ion-pair molecules are a usually gaseous form of an crystalline ionic solid (**Section 4.5.2**).

⁷⁶⁷ pronounced “CAT-ion” and “AN-ion”.

⁷⁶⁸ Hahn Y. Electron-ion recombination processes-an overview. Rep Prog Phys. 1997 Jul;60(7):691-759; <http://iopscience.iop.org/article/10.1088/0034-4885/60/7/001/meta>. See also: https://en.wikipedia.org/wiki/Plasma_recombination.

⁷⁶⁹ https://en.wikipedia.org/wiki/Ionization_energy.

4.4.3.1 Singly-Ionized Atomic and Molecular Cations

The energy that is released upon ion recombination of a free cation with a free electron, expressed in the chart as the specific energy of ion recombination in MJ/kg, is the negative value of the first ionization energy of the elements⁷⁷⁰ – the energy required to remove the outermost valence electron from the atom. The ten elements with the highest ion recombination specific energy for singly-ionized cations are listed in **Table 35**. Hydrogen cations (H⁺), aka. hydrons,⁷⁷¹ are the highest at **1302 MJ/kg** because of their low mass. Helium cations (He⁺) yield almost twice the ion recombination energy per atom, but only half as much per unit mass (**593 MJ/kg**).

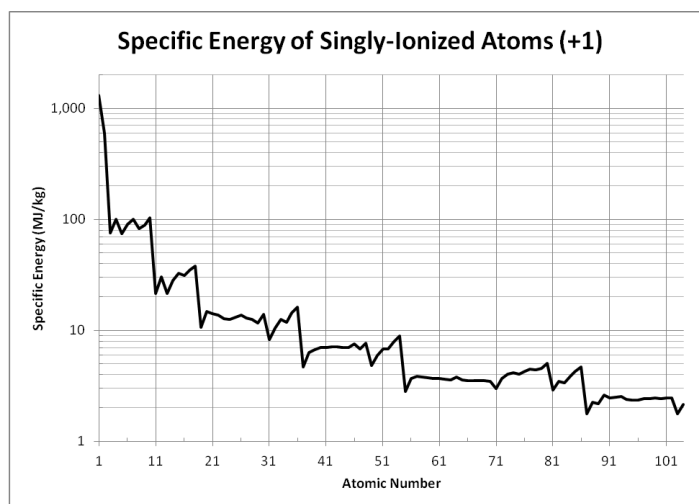


Table 35. The ten highest specific energies (> 40 MJ/kg) for ion recombination of singly-ionized atoms, for $X^+ + e^- \rightarrow X + \text{energy}$

Atomic Cation	Ion Recombination Energy (eV)	Specific Energy (MJ/kg)	Atomic Cation	Ion Recombination Energy (eV)	Specific Energy (MJ/kg)
H ⁺	-13.60	1312	C ⁺	-11.26	90.5
He ⁺	-24.59	593	F ⁺	-17.42	88.5
Ne ⁺	-21.56	103	O ⁺	-13.62	82.1
N ⁺	-14.53	100	Li ⁺	-5.39	75.0
Be ⁺	-9.32	99.8	B ⁺	-8.30	74.1

⁷⁷⁰ Data source: “Section 10, Atomic, Molecular, and Optical Physics; Ionization Potentials of Atoms and Atomic Ions,” in: Lide DR (ed). CRC Handbook of Chemistry and Physics, 84th Edition, CRC Press, Boca Raton FL, 2003; [https://en.wikipedia.org/wiki/Ionization_energies_of_the_elements_\(data_page\)](https://en.wikipedia.org/wiki/Ionization_energies_of_the_elements_(data_page)).

⁷⁷¹ [https://en.wikipedia.org/wiki/Hydron_\(chemistry\)](https://en.wikipedia.org/wiki/Hydron_(chemistry)).

Table 36 is a complete list of all elements in the first three rows of the periodic table, and a selection of elements in later rows which have ion recombination energies between 10-14 eV, that are singly- or doubly-ionized and could in principle be contained in the same frozen neon-lined box previously described in **Section 4.3.1.4** for the containment of the H^+ cation.⁷⁷² The Li^+ , Be^+ , C^+ , O^+ , and B^+ cations offer fairly impressive ion recombination energy storage values, though all are an order of magnitude below H^+ .

Table 36. Specific energy for singly- or doubly-ionized atoms that could be stored in a neon-ice-walled containment vessel, for $X^+ + e^- \rightarrow X + \text{energy}$					
Atomic Cation	Ion Recombination Energy (eV)	Specific Energy (MJ/kg)	Atomic Cation	Ion Recombination Energy (eV)	Specific Energy (MJ/kg)
H^+	-13.60	1312.0	Xe^+	-12.13	8.91
Li^+	-5.39	173.4	I^+	-10.45	7.95
Be^+	-9.32	99.81	La^{2+}	-11.06	7.68
C^+	-11.26	90.45	Lu^{2+}	-13.90	7.66
O^+	-13.62	82.13	Ce^{2+}	-10.85	7.47
B^+	-8.30	74.06	Pm^{2+}	-10.90	7.25
Cl^+	-12.97	35.29	Pr^{2+}	-10.55	7.22
P^+	-10.49	32.67	Nd^{2+}	-10.73	7.18
S^+	-10.36	31.18	Eu^{2+}	-11.24	7.14
Mg^+	-7.65	30.35	Sm^{2+}	-11.07	7.10
Ca^{2+}	-11.87	28.57	Gd^{2+}	-12.09	7.42
Si^+	-8.15	28.00	Tb^{2+}	-11.52	6.99
Sc^{2+}	-12.80	27.47	Dy^{2+}	-11.67	6.93
Na^+	-5.14	21.57	Ho^{2+}	-11.80	6.90
Al^+	-5.99	21.41	Er^{2+}	-11.93	6.88
Kr^+	-14.00	16.12	Tm^{2+}	-12.05	6.88
Ca^+	-6.11	14.72	Yb^{2+}	-12.18	6.79
Br^+	-11.81	14.26	Re^{2+}	-12.99	6.73
Sc^+	-6.56	14.08	Ac^{2+}	-12.10	5.14
Zr^{2+}	-13.13	13.89	Hg^+	-10.44	5.02
Y^{2+}	-12.24	13.28	Th^{2+}	-11.50	4.78
Sr^{2+}	-11.03	12.15	Rn^+	-10.75	4.67
K^+	-4.34	10.71	Ra^{2+}	-10.15	4.33

⁷⁷² Data source: "Section 10, Atomic, Molecular, and Optical Physics; Ionization Potentials of Atoms and Atomic Ions," in: Lide DR (ed). CRC Handbook of Chemistry and Physics, 84th Edition, CRC Press, Boca Raton FL, 2003; [https://en.wikipedia.org/wiki/Ionization_energies_of_the_elements_\(data_page\)](https://en.wikipedia.org/wiki/Ionization_energies_of_the_elements_(data_page)).

In principle, singly-ionized molecules could also be employed for high-density energy storage (Table 37). The simplest molecular ion is the dihydrogen cation⁷⁷³ (H_2^+) with an ion recombination energy of 15.43 eV (744 MJ/kg), the highest specific energy of any molecule. With only one bonding electron, the molecular ion can be dissociated into an H atom and an H cation by adding only 1.8 eV to break the bond. The isolated dihydrogen cation is relatively stable because it has a large number of bound states in which neither of the protons can escape to infinity leaving behind an H atom,⁷⁷⁴ but it is an extremely reactive molecule that will even react with itself.

Table 37. Specific energies for ion recombination of singly-ionized molecules, for $\text{X}^+ + \text{e}^- \rightarrow \text{X} + \text{energy}$

Atomic Cation	Ion Recombination Energy (eV)	Specific Energy (MJ/kg)	Atomic Cation	Ion Recombination Energy (eV)	Specific Energy (MJ/kg)
Hydrogen, H_2^+	-15.6	752.6	(E)-2-Butene, C_4H_8^+	-9.1	15.7
Trihydrogen, H_3^+	-5.3	170.5	Chlorine, Cl_2^+	-11.5	15.6
Methane, CH_4^+	-12.618	76.1	Ethanethiol, $\text{C}_2\text{H}_6\text{S}^+$	-9.3	14.5
Nitrogen, N_2^+	-15.58	53.7	Pentane, $n\text{-C}_5\text{H}_{12}^+$	-10.3	13.8
Carbon monoxide, CO^+	-14	48.2	Dimethylsulfide, $\text{C}_2\text{H}_6\text{S}^+$	-8.7	13.5
Fluorine, F_2^+	-15.7	39.9	Benzene, C_6H_6^+	-9.2	11.4
Ethane, C_2H_6^+	-11.5	37.0	Hexane, $n\text{-C}_6\text{H}_{14}^+$	-10.1	11.3
Oxygen, O_2^+	-12.1	36.5	Toluene, C_6H_8^+	-8.8	10.6
Ethene, C_2H_4^+	-10.5	36.2	Aniline, $\text{C}_6\text{H}_7\text{N}^+$	-7.7	8.0
Hydrohelium, HeH^+	-1.68	32.4	Indene, C_9H_8^+	-8.6	7.2
Carbon dioxide, CO_2^+	-13.8	30.3	Decane, $n\text{-C}_{10}\text{H}_{22}^+$	-9.7	6.6
Propane, $n\text{-C}_3\text{H}_8^+$	-10.9	23.9	Bromine, Br_2^+	-10.5	6.3
Propene, C_3H_6^+	-9.7	22.3	Biphenyl, $\text{C}_{12}\text{H}_{10}^+$	-8.2	5.1
Ethanol, $\text{C}_2\text{H}_6\text{O}^+$	-10.5	22.0	Naphthalene, $\text{C}_{14}\text{H}_{10}^+$	-8.1	4.4
Dimethyl ether $\text{C}_2\text{H}_6\text{O}^+$	-10	21.0	Anthracene, $\text{C}_{14}\text{H}_{10}^+$	-7.4	4.0
Dimethylamine, $\text{C}_2\text{H}_7\text{N}^+$	-8.2	17.6	Iodine, I_2^+	-9.3	3.5
Butane, $n\text{-C}_4\text{H}_{10}^+$	-10.5	17.5	Triphenylamine, $\text{C}_{18}\text{H}_{15}\text{N}^+$	-6.8	2.7

⁷⁷³ https://en.wikipedia.org/wiki/Dihydrogen_cation.

⁷⁷⁴ Armour EA, Brown WB. The stability of three-body atomic and molecular ions. Acc Chem Res. 1993 Apr;26(4):168-73; <http://pubs.acs.org/doi/abs/10.1021/ar00028a006?journalCode=achre4>.

The trihydrogen cation,⁷⁷⁵ aka. protonated molecular hydrogen (H_3^+) is the simplest triatomic molecule and the simplest example of a three-center two-electron bond system with a 4.5 eV bond energy and an estimated ion recombination energy⁷⁷⁶ of ~5.3 eV (**170 MJ/kg**) to an unstable molecular trihydrogen⁷⁷⁷ H_3 Rydberg state. It is apparently the most abundantly produced interstellar molecule, second only to H_2 , and acts as a universal proton donor via $\text{H}_3^+ + \text{X} \rightarrow \text{HX}^+ + \text{H}_2$ because the 4.4 eV proton affinity of H_2 is lower than that of almost all atoms and molecules except He, N, and O_2 ; in diffuse interstellar clouds with 10^2 - 10^4 ions/ cm^3 it is destroyed mainly by ion recombination with electrons released from the photoionization of C.⁷⁷⁸ Hence it is stable in isolation, but is very reactive. Laboratory experiments have been conducted with H_3^+ ions using cold ion traps,⁷⁷⁹ but the ion density achieved in these apparatuses is very low.⁷⁸⁰

Methane cation (CH_4^+) has the next-highest specific energy (**76 MJ/kg**) but suffers dissociative recombination with low energy electrons between 10-1000 K (0.001-0.1 eV), returning almost no neutral methane but instead breaking one or more C-H bonds and producing reactive radicals in the following yields: $\bullet\text{CH}_3 + \text{H}\bullet$ (18%), $\text{:CH}_2 + 2\text{H}\bullet$ (51%), $\text{:CH}_2 + \text{H}_2$ (6%), $\text{:}\cdot\text{CH} + \text{H}_2 + \text{H}\bullet$ (23%), and $\text{:}\cdot\text{CH} + 2\text{H}_2$ (2%).⁷⁸¹ In part this is because the recombination energy so greatly exceeds the ~4.2 eV bond energy of a single C-H bond. N_2^+ cations⁷⁸² and O_2^+ cations⁷⁸³ exposed to electrons also undergo dissociative recombination.⁷⁸⁴

⁷⁷⁵ https://en.wikipedia.org/wiki/Trihydrogen_cation.

⁷⁷⁶ Tashiro M, Kato S. Quantum dynamics study on predissociation of H_3 Rydberg states: importance of indirect mechanism. J Chem Phys. 2002 Aug 1;117(5):2053-62; https://www.researchgate.net/profile/Motomichi_Tashiro/publication/252861436_Quantum_dynamics_study_on_predissociation_of_H3_Rydberg_states_Importance_of_indirect_mechanism/links/00b495181b37a2dfd0000000.pdf.

⁷⁷⁷ https://en.wikipedia.org/wiki/Triatomic_hydrogen.

⁷⁷⁸ Oka T. Interstellar H_3^+ . PNAS. 2006 Aug 15;103(33):12235-42; <http://www.pnas.org/content/103/33/12235.full>.

⁷⁷⁹ Wester R. Radiofrequency multipole traps: tools for spectroscopy and dynamics of cold molecular ions. J Phys B: Atomic Molec Opt Phys. 2009 Jul 15;42(15):154001; <https://arxiv.org/pdf/0902.0475.pdf>.

⁷⁸⁰ In these experiments, H_3^+ cation is created by the exothermic reaction: $\text{H}_2^+ + \text{H}_2 \rightarrow \text{H}_3^+ + \text{H} + 1.7 \text{ eV}$.

⁷⁸¹ Thomas RD, Kashperka I, Vigren E, Geppert WD, Hamberg M, Larsson M, Af Ugglas M, Zhaunerchyk V. Dissociative Recombination of CH_4^+ . J Phys Chem A. 2013 May 29;117(39):9999-10005; <http://pubs.acs.org/doi/abs/10.1021/jp400353x?journalCode=jpcfah>.

⁷⁸² Kasner WH, Biondi MA. Electron-ion recombination in nitrogen. Phys Rev. 1965 Jan 18;137(2A):317-329; <https://journals.aps.org/pr/abstract/10.1103/PhysRev.137.A317>.

⁷⁸³ <https://en.wikipedia.org/wiki/Dioxygenyl>.

⁷⁸⁴ Sheehan CH, St-Maurice JP. Dissociative recombination of N_2^+ , O_2^+ , and NO^+ : Rate coefficients for ground state and vibrationally excited ions. J Geophys Res: Space Phys. 2004 Mar 1;109:A03302; <http://onlinelibrary.wiley.com/doi/10.1029/2003JA010132/pdf>.

In general, collision with an electron converts a molecular cation into a neutral molecule in an excited state, which may then dump the recombination energy by radiative recombination (neutral molecule plus photon emission, the most convenient outcome for energy extraction), dissociative recombination (scission into an excited and neutral components), dissociative excitation (scission into excited and cationic components plus an electron), or ion pair formation (scission into anionic and cationic components).⁷⁸⁵ These many possible recombination products complicate the process of extracting all of the ionization potential energy from the molecular cation by simply injecting an electron.

Perhaps somewhat simpler is the hydrohelium cation⁷⁸⁶ (HeH^+), aka. helium hydride ion or helium-hydride molecular ion, which forms from the reaction of a proton with a helium atom in the gas phase or via tritium decay.⁷⁸⁷ The predicted ion recombination energy (electron affinity) of HeH^+ cation is 1.68 eV (**32 MJ/kg**)⁷⁸⁸ though a resulting neutral ground-state HeH molecule would be unstable⁷⁸⁹ and would dissociate in $\sim 10^{-8}$ sec,⁷⁹⁰ with the additional release of its molecular binding energy of 0.626 meV (**0.012 MJ/kg**).⁷⁹¹

⁷⁸⁵ Sheehan CH, St-Maurice JP. Dissociative recombination of N_2^+ , O_2^+ , and NO^+ : Rate coefficients for ground state and vibrationally excited ions. *J Geophys Res: Space Phys.* 2004 Mar 1;109:A03302; <http://onlinelibrary.wiley.com/doi/10.1029/2003JA010132/pdf>.

⁷⁸⁶ https://en.wikipedia.org/wiki/Helium_hydride_ion.

⁷⁸⁷ HeH^+ is formed during the decay of tritium in the molecules HT or T_2 ; the cation is excited by the recoil from the beta decay but remains intact. Mannone F. *Safety in Tritium Handling Technology*, Springer, 1993, p. 92.

⁷⁸⁸ Szabo A, Ostlund NS. *Modern Quantum Chemistry: Introduction to Advanced Electronic Structure Theory*, Courier Corp., 2012; <https://books.google.com/books?id=KQ3DAgAAQBAJ&pg=PA169>.

⁷⁸⁹ Release of the ion recombination energy by electron absorption normally pushes the neutral HeH molecule into one of its electronically excited states, creating a stable excimer molecule (HeH^*). Möller T, Beland M, Zimmerer G. Observation of fluorescence of the HeH molecule. *Phys Rev Lett.* 1985 Nov 11;55(20):2145-8; <https://journals.aps.org/prl/abstract/10.1103/PhysRevLett.55.2145>; and Ketterle W, Figger H, Walther H. Emission spectra of bound helium hydride. *Phys Rev Lett.* 1985 Dec 30;55(27):294; <https://journals.aps.org/prl/abstract/10.1103/PhysRevLett.55.294>.

⁷⁹⁰ Gray J, Tomlinson RH. Molecular beam studies of HeH and H_3 molecules. *Chem Phys Lett.* 1969 Nov 15;4(5):251-4; <http://www.sciencedirect.com/science/article/pii/0009261469801764>.

⁷⁹¹ Partridge H, Bauschlicher JR CW. The dissociation energies of He_2 , HeH, and ArH: a bond function study. *Molec Phys.* 1999 Feb 1;96(4):705-10; <http://www.tandfonline.com/doi/abs/10.1080/00268979909483006>.

4.4.3.2 Multiply-Ionized Atomic and Molecular Cations

The estimated lifetimes of many doubly-ionized isolated diatomic molecular cations against tunneling decay from the lowest metastable ground state can be extremely long, e.g., O_2^{2+} (1×10^{12} sec), NO^{2+} (2×10^{30} sec), N_2^{2+} (5×10^{82} sec), and Ba_2^{2+} (2×10^{197} sec), though only $\sim 20,000$ sec for He_2^{2+} .⁷⁹²

The last of these, the helium dication dimer (He_2^{2+}),⁷⁹³ is the simplest stable molecule with a double positive charge and the shortest known bond length (0.703 \AA)⁷⁹⁴. The helium dication dimer has been proposed as a possible rocket fuel additive.⁷⁹⁵ He_2^{2+} is extremely repulsive and upon autodissociation of the $v=0$ vibrational level of the $^1\Sigma_g^+$ state according to $\text{He}_2^{2+} \rightarrow \text{He}^+ + \text{He}^+$ releases 835.9 kJ/mol (8.66 eV or **104.5 MJ/kg**).⁷⁹⁶ The ion has long been predicted to be dynamically stable,⁷⁹⁷ with an energy barrier of 138.9 kJ/mol (1.44 eV) preventing immediate decay (for 4-5 hr).⁷⁹⁸

Other helium molecular ions, including HeH^{2+} and He_2^{3+} , are unstable;⁷⁹⁹ the ion recombination energy (negative ionization potential) of HeH^{2+} is 43.47 eV (**838.8 MJ/kg**),⁸⁰⁰ but unfortunately the lifetime of the isolated HeH^{2+} dication is only 3.9 nsec .⁸⁰¹

⁷⁹² Sramek SJ, Macek JH, Gallup GA. Very-long-lived metastable vibrational states of Ba_2^{++} . *Phys Rev A*. 1980 May 1;21(5):1361-3; <http://digitalcommons.unl.edu/cgi/viewcontent.cgi?article=1012&context=physicsgallup>.

⁷⁹³ https://en.wikipedia.org/wiki/Helium_dimer#Molecular_ions.

⁷⁹⁴ Yagisawa H, Sato H, Watanabe T. Accurate electronic energies of He_2^{++} . *Phys Rev A*. 1977 Oct 1;16(4):1352-7; <https://journals.aps.org/pr/abstract/10.1103/PhysRevA.16.1352>.

⁷⁹⁵ Nicolaides CA. Energy generation from volcanic ground states. Application to cold He_2^{2+} . *Chem Phys Lett*. 1989;161(6):547-553; <http://www.sciencedirect.com/science/article/pii/0009261489870368>.

⁷⁹⁶ Guilhaus M, Brenton AG, Beynon JH, Rabrenović M, von Ragué Schleyer P. He_2^{2+} , the experimental detection of a remarkable molecule. *J Chem Soc Chem Commun*. 1985(4):210-1; <http://pubs.rsc.org/is/content/articlelanding/1985/c3/c39850000210>.

⁷⁹⁷ Pauling L. The Normal State of the Helium Molecule-Ions He_2^+ and He_2^{++} . *J Chem Phys*. 1933 Jan;1(1):56-9; <http://authors.library.caltech.edu/2619/1/PAUjcp33a.pdf>.

⁷⁹⁸ Radom L, Gill PM, Wong MW, Nobes RH. Multiply-charged cations: remarkable structures and stabilities. *Pure Appl Chem*. 1988 Jan 1;60(2):183-8; <http://rscweb.anu.edu.au/~pgill/papers/008MultCat.pdf>.

⁷⁹⁹ Rebane TK. Stability of molecular ions. *J Struct Chem*. 1991 Sep 1;32(5):734-5; <http://docslide.net/documents/stability-of-molecular-ions.html>.

⁸⁰⁰ Szabo A, Ostlund NS. *Modern Quantum Chemistry: Introduction to Advanced Electronic Structure Theory*, Courier Corp., 2012, p. 177; <https://books.google.com/books?id=KQ3DAgAAQBAJ&pg=PA177>.

The still smaller molecular hydrogen dication (H_2^{2+}) is also unstable; removal of the last electron from the H_2^+ cation leads automatically to the dissociation and the subsequent Coulomb explosion of the molecule, with the release of ~ 9.5 eV of energy (**458 MJ/kg**) if the two protons make a vertical Franck–Condon transition from the molecular ground state.⁸⁰²

A few other highly energetic helium-based cations might also be stable, such as the HeCO^{2+} dication which is predicted to be both kinetically and thermodynamically stable with dissociation energetically uphill by $+0.77$ eV, and the HeCF^{3+} trication which releases 973 kJ/mole (**27.8 MJ/kg**) upon fragmentation but has a 132 kJ/mole (1.4 eV) barrier to fragmentation.⁸⁰³ Some potentially useful heliocarbocations predicted by theory may include the triheliummethyl trication (CHe_3^{3+}) with fragmentation energy 1030 kJ/mole (10.7 eV, **42.9 MJ/kg**) and fragmentation barrier 152 kJ/mole (1.58 eV), and the tetraheliummethane tetracation (CHe_4^{4+}) with fragmentation energy 1605 kJ/mole (16.6 eV, **57.3 MJ/kg**) and fragmentation barrier 72 kJ/mole (0.75 eV).⁸⁰⁴

In general, however, multiply-ionized molecules have so much energy in excess of normal chemical bond energy that dissociative recombination can occur even more easily than for singly-ionized molecules, further complicating the energy extraction process and making reversible energy storage cycling much more difficult. The rest of this Section will consider the energy-storage prospects for multiply-ionized atoms.⁸⁰⁵

⁸⁰¹ Ben-Itzhak I, Chen Z, Esry BD, Gertner I, Heber O, Lin CD, Rosner B. Mean lifetime of the bound $2p\sigma$ state of HeH^{2+} . *Phys Rev A*. 1994 Mar 1;49:1774;
<https://journals.aps.org/pr/abstract/10.1103/PhysRevA.49.1774>.

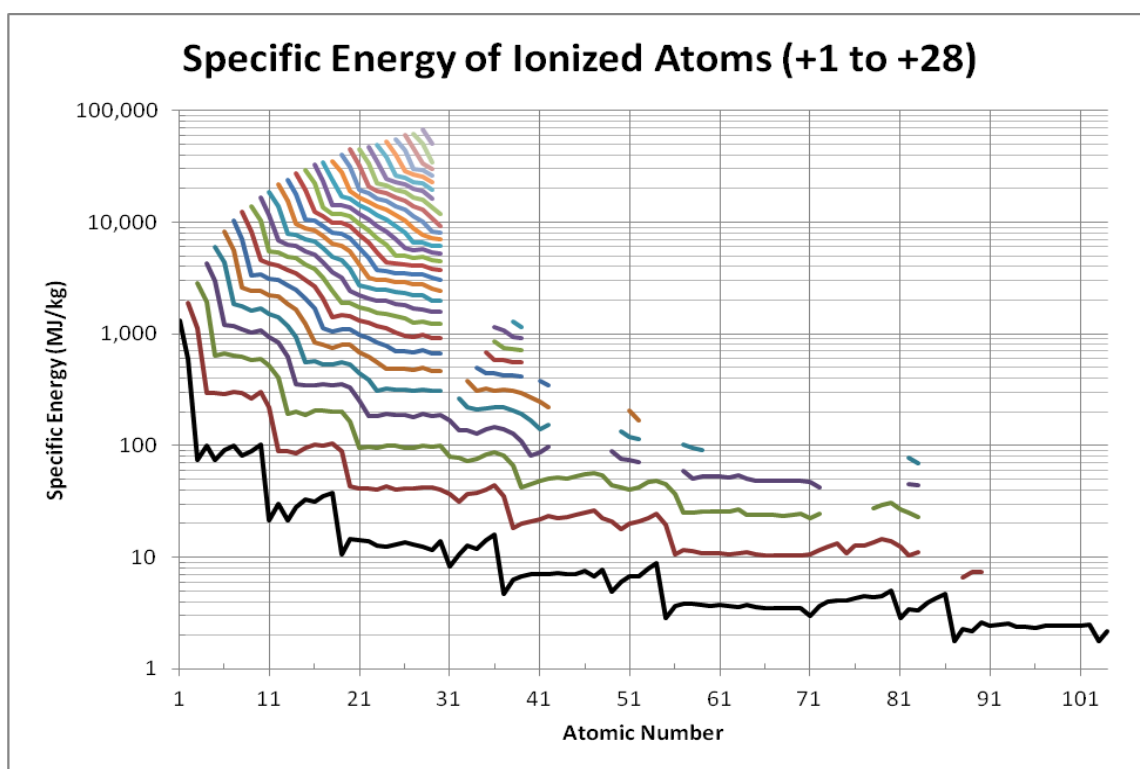
⁸⁰² Frémont F, Bedouet C, Tarisien M, Adoui L, Cassimi A, Dubois A, Chesnel JY, Husson X. Fragmentation of H_2^{2+} ions following double electron capture in slow Xe^{23+} and $\text{O}^{5+} + \text{H}_2$ collisions. *J Phys B: Atomic Molec Optical Phys*. 2000 Apr 14;33(7):L249-L258;
https://www.researchgate.net/profile/Francois_Fremont/publication/231018807_Fragmentation_of_H22_ions_following_double_electron_capture_in_slow_Xe23_and_O5H2_collisions/links/54abad990cf2bce6aa1d9636.pdf.

⁸⁰³ Wong MW, Nobes RH, Radom L. Multiply-charged helium-containing cations: HeCO^{2+} , HeCF^{3+} and HeCNe^{4+} . *Rapid Commun Mass Spectrom*. 1987 May 1;1(1):3-5;
<http://docslide.net/download/link/multiply-charged-helium-containing-cations-heco2-hecf3-and-hecne4>.

⁸⁰⁴ Radom L, Gill PM, Wong MW, Nobes RH. Multiply-charged cations: remarkable structures and stabilities. *Pure Appl Chem*. 1988 Jan 1;60(2):183-8;
<http://rscweb.anu.edu.au/~pgill/papers/008MultCat.pdf>.

⁸⁰⁵ A solar spectroscopy experiment conducted during a full eclipse on 7 Aug 1869 found an unknown spectral line in the solar corona that was initially thought to originate from a new element, dubbed coronium (Gruenwald A. On Remarkable Relations Between the Spectrum of Watery Vapour and the Line Spectra of Hydrogen and Oxygen. *Chemical News* 2 Dec 1887;LVI(1462):232;
<https://books.google.ca/books?id=6ybOAAAAMAAJ&pg=PA232>), but was later found to be emitted from Fe^{13+} – an ion species that could only occur naturally at temperatures in excess of 2,000,000 K.

The chart below shows the cumulative specific energy for atoms that have been stripped of one, two, or more electrons, up to 28 electrons.⁸⁰⁶ **Table 38** lists the cumulative cation recombination energy for fully ionized or “stripped” atoms, which is the negative of the sum of all the ionization energies needed to remove all electrons from the atom, leaving a naked positively-charged nucleus.⁸⁰⁷ These energies, expressed as specific energies (MJ/kg), are astonishingly large, reaching a high of **308,800 MJ/kg** for a fully-stripped uranium atom ($^{238}\text{U}^{92+}$), the highest ionization energy for a naturally-occurring element.



⁸⁰⁶ Data source: “Section 10, Atomic, Molecular, and Optical Physics; Ionization Potentials of Atoms and Atomic Ions,” in: Lide DR (ed). CRC Handbook of Chemistry and Physics, 84th Edition, CRC Press, Boca Raton FL, 2003; [https://en.wikipedia.org/wiki/Ionization_energies_of_the_elements_\(data_page\)](https://en.wikipedia.org/wiki/Ionization_energies_of_the_elements_(data_page)).

⁸⁰⁷ Data sources: “Section 10, Atomic, Molecular, and Optical Physics; Ionization Potentials of Atoms and Atomic Ions,” in: Lide DR (ed). CRC Handbook of Chemistry and Physics, 84th Edition, CRC Press, Boca Raton FL, 2003; [https://en.wikipedia.org/wiki/Ionization_energies_of_the_elements_\(data_page\)](https://en.wikipedia.org/wiki/Ionization_energies_of_the_elements_(data_page)). Data for Au, Pb, and U from: Brown KA, Gardner C, Thieberger P. Rest Mass of Fully Stripped Ions in RHIC: Updated Values, Collider-Accelerator Department, Brookhaven National Laboratory, C-A/AP/#293, Oct 2007; <http://public.bnl.gov/docs/cad/Documents/Rest%20Mass%20of%20Fully%20Stripped%20Ions%20in%20RHIC%20Updated%20Values.pdf>.

The current maximum experimentally-achieved density for highly-stripped uranium cations appears to be $\sim 10^9$ ions/cm³ using a 200 mA stripping beam of 198-keV electrons, although “the total yield of highly charged uranium ions could be increased with a more intense electron beam, and the fractional abundance of U⁹²⁺ could be significantly increased with a higher-energy electron beam.”⁸⁰⁸

Table 38. Specific energy for cumulative ion recombination of fully-ionized “stripped” atoms, for $X^{n+} + e^- \rightarrow X^{(n-1)+} + \text{energy}$					
Atomic Cation	Specific Energy (MJ/kg)	Atomic Cation	Specific Energy (MJ/kg)	Atomic Cation	Specific Energy (MJ/kg)
Hydrogen, H ⁺	1302	Magnesium, Mg ¹²⁺	21,636	Vanadium, V ²³⁺	48,904
Helium, He ²⁺	1904	Aluminum, Al ¹³⁺	23,620	Chromium, Cr ²⁴⁺	53,039
Lithium, Li ³⁺	2830	Silicon, Si ¹⁴⁺	27,095	Manganese, Mn ²⁵⁺	55,351
Beryllium, Be ⁴⁺	4273	Phosphorus, P ¹⁵⁺	28,991	Iron, Fe ²⁶⁺	59,782
Boron, B ⁵⁺	5989	Sulfur, S ¹⁶⁺	32,682	Cobalt, Co ²⁷⁺	62,077
Carbon, C ⁶⁺	8276	Chlorine, Cl ¹⁷⁺	34,171	Nickel, Ni ²⁸⁺	68,027
Nitrogen, N ⁷⁺	10,234	Argon, Ar ¹⁸⁺	34,773	Copper, Cu ²⁹⁺	68,379
Oxygen, O ⁸⁺	12,325	Potassium, K ¹⁹⁺	40,419	Gold, Au ⁷⁹⁺	253,200
Fluorine, F ⁹⁺	13,791	Calcium, Ca ²⁰⁺	44,557	Lead, Pb ⁸²⁺	264,700
Neon, Ne ¹⁰⁺	16,790	Scandium, Sc ²¹⁺	44,607	Uranium, U ⁹²⁺	308,800
Sodium, Na ¹¹⁺	18,550	Titanium, Ti ²²⁺	46,803		

Fully-stripped U⁹²⁺ cations have been stored and cooled in the ESR storage ring of the heavy ion SIS-ESR facility at the GSI in Darmstadt, Germany.⁸⁰⁹ Spontaneous radiative recombination energy can be recovered by adding 92 cold electrons⁸¹⁰ per cation to the uranium cation population,⁸¹¹ or by related techniques such as induced radiative electron capture.⁸¹² Direct

⁸⁰⁸ A 198 keV electron beam system produced ~ 500 hydrogenlike $^{238}\text{U}^{91+}$ ions and ~ 10 bare $^{238}\text{U}^{92+}$ ions. In this apparatus, the ionization and recombination of U⁹¹⁺ ions has a characteristic time of ~ 1 sec. Marrs RE. Production of U⁹²⁺ with an EBIT. UCRL-JC-122132, Lawrence Livermore Natl Lab, 1995; http://www.iaea.org/inis/collection/NCLCollectionStore/_Public/27/032/27032790.pdf. See also: Marrs RE, Elliott SR, Knapp DA. Production and trapping of hydrogenlike and bare uranium ions in an electron beam ion trap. Phys Rev Lett. 1994 Jun 27;72(26):4082-5; <https://www-ebit.lbl.gov/publications/PRL-1994-72:4082-marrs.pdf>.

⁸⁰⁹ Banaś D, Pajek M, Stöhlker T, Beyer HF, Böhm S, Bosch F, Brandau C, Czarnota M, Chatterjee S, Dousse JC, Fritzsche S. The enhancement effect in K-shell radiative recombination of ions with cooling electrons. Eur Phys J-Special Topics. 2009 Mar 1;169(1):15-8; <http://web-docs.gsi.de/~fritzsche/pub/p263.b09.epjst-darrek-rec-enhancement-original.pdf>.

⁸¹⁰ The rate coefficient climbs rapidly as electron temperature is reduced, e.g., to a relatively “cold” 100-1000 K and below; <https://books.google.com/books?id=-XD1BwAAQBAJ&pg=PA53>.

⁸¹¹ Shi W, Böhm S, Böhme C, Brandau C, Hoffknecht A, Kieslich S, Schippers S, Müller A, Kozuharov C, Bosch F, Franzke B. Recombination of U 92+ ions with electrons. Eur Phys J D. 2001 Aug 19;15(2):145-54; <https://link.springer.com/article/10.1007/s100530170160>.

radiative recombination will release the stored energy as a series of photons of various frequencies, from X-ray down to optical. However, an energy storage system with $\sim 10^9$ $^{238}\text{U}^{92+}$ cations/cm³ could only store an ion recombination energy density of $E_{D,\text{ire}} = (10^9 \text{ }^{238}\text{U}^{92+} \text{ cations/cm}^3) (3.97 \times 10^{-25} \text{ kg/cation}) (308,800 \text{ MJ/kg}) = \mathbf{1 \times 10^{-7} \text{ MJ/L}}$. Ion densities in excess of $\sim 10^{18}$ protons/cm³ are probably required for a practical heavy ion recombination energy storage system.

Purely physical containment of dense collections of such highly charged ions appears difficult. The neon icebox approach (**Section 4.3.1.4**) only works for cryogenic cations with an ionization potential under ~ 14 eV (**Table 36**). The much higher ionization potentials of most multiply-ionized cations will rip electrons out of the surface atoms of any normal container wall material with which they come into contact, causing the disintegration of that material along with neutralization of the stored cations. The only solid material that would probably be able to physically contain fully-stripped $^{238}\text{U}^{92+}$ cations would be pure neutronium,⁸¹³ given that (1) the cation-induced beta decay⁸¹⁴ of an isolated wall neutron would release 0.782 MeV of binding energy,⁸¹⁵ slightly higher than the available 0.762 MeV ion recombination energy that one $^{238}\text{U}^{92+}$ cation could provide, and (2) the $^{238}\text{U}^{92+}$ cation would have to strip electrons from 92 neutrons to become fully electrically neutralized.

If practical physical containment of $^{238}\text{U}^{92+}$ cations is ruled out, then field containment such as magnetic bottles or beamline magnets must be employed. The electric potential energy of n_{U} stripped $^{238}\text{U}^{92+}$ cations placed in a box of size L_{box} with a mean intercation separation of $r_{\text{mean}} = (L_{\text{box}}^3/n_{\text{U}})^{1/3}$ is the sum of the energies of each unique pair of particles,⁸¹⁶ or $E_{\text{cloud}} \sim q^2 C(n_{\text{U}},2) / 4\pi\epsilon_0 r_{\text{mean}}$, where $^{238}\text{U}^{92+}$ cation charge $q = 92e$, elementary charge $e = 1.60 \times 10^{-19}$ coul, and permittivity constant $\epsilon_0 = 8.85 \times 10^{-12}$ coul²/Nm². Assuming that a given magnetic field pressure would be sufficient to contain a cation-derived electrostatic field of equal pressure, then cation energy density $E_{\text{cloud}}/L_{\text{box}}^3 \sim B^2 / 2\mu_0$ (the energy density of a magnetic containment with field strength B and permeability constant $\mu_0 = 1.26 \times 10^{-6}$ henry/meter). We should also insist that the cation recombination energy density must be at least as large as the energy density of the magnetic containment field, otherwise the device merely exemplifies magnetic field energy storage (**Section 6.1**). With these assumptions, 25 $^{238}\text{U}^{92+}$ cations contained in a $0.005 \mu\text{m}^3$ volume (**0.64 MJ/L** of ion recombination energy density) requires a 40 tesla field, comparable to the strongest continuous magnetic field (45 T) ever created in a lab,⁸¹⁷ 21 $^{238}\text{U}^{92+}$ cations

⁸¹² Poth H. Electron cooling: theory, experiment, application. Phys Reports. 1990 Nov 1;196(3-4):135-297; <http://cds.cern.ch/record/204690/files/cer-000116390.pdf>.

⁸¹³ <https://en.wikipedia.org/wiki/Neutronium>.

⁸¹⁴ In neutron beta decay, an electron is removed from a neutron, leaving a proton behind.

⁸¹⁵ https://en.wikipedia.org/wiki/Neutron#Free_neutron_decay.

⁸¹⁶ The combination number (binomial coefficient) of unique groupings of k items drawn from a total population of n items is $C(n,k) = n! / k!(n-k)!$; https://en.wikipedia.org/wiki/Binomial_coefficient.

⁸¹⁷ "World's Most Powerful Magnet Tested Ushers in New Era for Steady High Field Research," 17 Dec 1999; <http://legacywww.magnet.fsu.edu/mediacenter/news/pressreleases/1999december17.html>.

contained in a $800,000 \text{ nm}^3$ volume (**3.2 MJ/L**) requires a 90 tesla field, comparable to the strongest nondestructive pulsed magnetic field (100 T) produced in a lab to date;⁸¹⁸ and $12 \text{ }^{238}\text{U}^{92+}$ cations contained in a 31 nm^3 volume (**31,500 MJ/L**) requires an 8900 tesla field, comparable to the strongest (destructive) pulsed magnetic field (9000 T) ever created in a lab.⁸¹⁹

Extremely dense gravitational containment of ions does occur in nature but may be challenging to arrange in a technological energy storage device. For example, hydrogen ions undergoing fusion in the solar core are compacted to a density of $\sim 150 \text{ kg/L}$,⁸²⁰ which is $\sim 9 \times 10^{28}$ ions/L or $\sim 90,000$ ions/ nm^3 . In this case the average separation between two adjacent ions is $\sim 0.022 \text{ nm}$, representing a repulsive electrostatic potential energy of $q^2/4\pi\epsilon_0 r \sim 10^{-17} \text{ J}$ which is equivalent to a specific energy of $\sim 3100 \text{ MJ/kg}$ and an energy density of $\sim 470,000 \text{ MJ/L}$ at solar core densities.

One final consideration for the prospects of stripped-atom energy storage is that stripping all the electrons from a heavy unstable nucleus (thus producing a bare nucleus) can reduce the lifetime of the nucleus. For example, neutral ^{187}Re undergoes β -decay with a half-life of 42×10^9 years, but for fully ionized $^{187}\text{Re}^{75+}$ this half-life is shortened by a factor of 10^9 to only 32.9 years.⁸²¹ Similarly, the nucleus of a stable neutral atom can also become unstable after stripping – e.g., the ^{163}Dy nucleus is stable as a neutral atom,⁸²² but when fully ionized $^{163}\text{Dy}^{66+}$ β -decays to $^{163}\text{Ho}^{66+}$ with a half-life of 47 days.⁸²³

⁸¹⁸ Pulsed Field Facility, National High Magnetic Field Laboratory, 28 Feb 2017; <https://nationalmaglab.org/user-facilities/pulsed-field-facility>.

⁸¹⁹ “Z machine makes progress toward nuclear fusion,” 10 Oct 2014; <http://www.sciencemag.org/news/2014/10/z-machine-makes-progress-toward-nuclear-fusion>.

⁸²⁰ https://en.wikipedia.org/wiki/Solar_core.

⁸²¹ Bosch F, *et al.* Observation of bound-state beta minus decay of fully ionized ^{187}Re : $^{187}\text{Re} \rightarrow ^{187}\text{Os}$ Cosmochronometry. *Phys Rev Lett* 1996;77(26):5190-5193; <https://2014.f.a0z.ru/04/06-3430949-physrevlett.77.5190-1996.pdf>.

⁸²² Audi G, Wapstra AH. The 1995 update to the atomic mass evaluation. *Nucl Phys A* 1995 Dec 25;595(4):409-480; <https://www.sciencedirect.com/science/article/abs/pii/0375947495004459>.

⁸²³ Jung M, Bosch F, Beckert K, Eickhoff H, Folger H, Franzke B, Gruber A, Kienle P, Klepper O, Koenig W, Kozhuharov C, Mann R, Moshhammer R, Nolden F, Schaaf U, Soff G, Spädtke P, Steck M, Stöhlker T, Sümmerer K. First observation of bound-state β^- decay. *Phys Rev Lett*. 1992 Oct 12;69(15):2164-2167; <https://journals.aps.org/prl/abstract/10.1103/PhysRevLett.69.2164>.

4.4.3.3 Electron Affinity in Atomic and Molecular Anions

Positive Electron Affinity Species. Neutral atoms or molecules forced to accept one or more excess electrons become negatively charged ions, or anions. In the case of gaseous species with a positive electron affinity, the addition of an electron via radiative electron attachment ($X + e^- \rightarrow X^- + \text{energy}$), aka. radiative electron capture, is thermodynamically preferred and releases energy, after which energy must be pumped into the resulting anion (e.g., via photodetachment) to remove the extra electron and convert the anion back to an electrically neutral species. **Table 39** provides a list of isolated atoms and gaseous molecules with positive electron affinity,⁸²⁴ ranked in descending order of the amount of energy that is released when the species absorbs an electron to become an anion.

Theory predicts⁸²⁵ and surveys confirm⁸²⁶ that H^- , Li^- , B^- , C^- , O^- , F^- , Na^- , Al^- , Si^- , P^- , S^- , Cl^- are stable ions, many of which can retain their extra electron for an indefinite amount of time barring photodetachment⁸²⁷ or collisional detachment events, whereas He^- , Be^- , N^- , Ne^- , Mg^- are unstable ions. The hydrogen anion (H^-), aka. hydride ion or negative hydrogen ion, has a weakly bound singlet ground state,⁸²⁸ and H has the highest electron affinity specific energy of any anion (**72.2 MJ/kg**). Ground-state fluorine anion F^- ($2p^6\ ^1S$), isoelectronic with the inert gas neon, gives F the second highest electron affinity specific energy (**17.3 MJ/kg**). Ground-state $^{32}S^-$ anions (**6.3 MJ/kg**) have been stored in an electrostatic ion storage ring at very low density ($\sim 20,000$ ions/cm³ at 13 K) with a lifetime of 939 sec.⁸²⁹ Electronically excited anion states are unstable against electron detachment with lifetimes in the 10^{-11} - 10^{-16} sec range, with the notable exception

⁸²⁴ Data sources: Andersen T. Atomic negative ions: structure, dynamics and collisions. Phys Rep. 2004 May 31;394(4):157-313; https://www.physics.uoguelph.ca/~rbrooks/phys710/PhysRep394_157.pdf. Scheller MK, Compton RN, Cederbaum LS. Gas-phase multiply charged anions. Science. 1995 Nov 17;270(5239):1160-7; <http://science.sciencemag.org/content/270/5239/1160/tab-pdf>. See also: [https://en.wikipedia.org/wiki/Electron_affinity_\(data_page\)](https://en.wikipedia.org/wiki/Electron_affinity_(data_page)).

⁸²⁵ Kais S, Neirotti JP, Serra P. Phase transitions and the stability of atomic and molecular ions. Intl J Mass Spectrom. 1999 Mar 1;182:23-9; <http://www.famaf.unc.edu.ar/~serra/ijms99.pdf>.

⁸²⁶ Andersen T, Haugen HK, Hotop H. Binding energies in atomic negative ions: III. J Phys Chem Ref Data. 1999 Nov;28(6):1511-33; <https://www.nist.gov/sites/default/files/documents/srd/jpcrd570.pdf>.

⁸²⁷ For example, the solar photon flux at the radius of Earth's orbit limits the lifetime of free H^- anions to ~ 0.5 sec via photodetachment. Wekhof A. Negative ions in the ionospheres of planetary bodies without atmospheres. Moon Planets 1981 Feb;24:45-52; <http://articles.adsabs.harvard.edu/full/1981M%26P....24...45W/0000051.000.html>.

⁸²⁸ Armour EA, Brown WB. The stability of three-body atomic and molecular ions. Acc Chem Res. 1993 Apr;26(4):168-73; <http://pubs.acs.org/doi/abs/10.1021/ar00028a006?journalCode=achre4>.

⁸²⁹ Bäckström E, Hanstorp D, Hole OM, Kaminska M, Nascimento RF, Blom M, Björkhage M, Källberg A, Löfgren P, Reinhd P, Rosén S. Storing keV Negative Ions for an Hour: The Lifetime of the Metastable $^2P_{1/2}^o$ level in $^{32}S^-$. Phys Rev Lett. 2015 Apr 6;114(14):143003; <https://physics.aps.org/featured-article-pdf/10.1103/PhysRevLett.114.143003>.

of a few elements in which excited bound states lie below the the ground state of the parent neutral atom thus preventing decay via electron emission, e.g., the anions of Os⁻,⁸³⁰ Ce⁻,⁸³¹ and La⁻,⁸³² the latter having a predicted lifetime of ~300 sec.⁸³³ From an energy storage perspective, technical challenges in extracting the electron affinity energy would include safely storing the relatively fragile non-ionized radical species (**Section 4.4.2**) at some reasonable density, and ensuring a sufficiently high electron capture cross-section to elicit the energy release.

Other molecular anions have extremely short lifetimes against autodetachment or dissociation and thus are probably unsuitable for energy storage purposes. Examples include H₂⁻ (8.2 μsec) and D₂⁻ (23 μsec),⁸³⁴ and He₂⁻ (350 μsec).⁸³⁵ However, singly-ionized molecular anions have been considered for high-density energy storage. For example, Matsunaga⁸³⁶ notes that PH₄⁻ → PH₃ + H⁻ dissociation releases 1.45 eV (**4.01 MJ/kg**) and there is a 0.24 eV barrier to dissociation with ionization potential 0.32 eV, suggesting the possibility of a reasonable lifetime; NH₄⁻ → NH₃ + H⁻ dissociation releases 0.38 eV (**2.05 MJ/kg**), but since the 1.41 eV barrier to dissociation is far above the 0.39 eV ionization potential, “it is likely the molecule with autoionize before it has a chance to dissociate.” Unfortunately, the hypervalent NH₄⁻ anion has been observed⁸³⁷ but the phosphorus analog PH₄⁻ has not.

⁸³⁰ Bilodeau RC, Haugen HK. Experimental studies of Os⁻: observation of a bound-bound electric dipole transition in an atomic negative ion. *Phys Rev Lett*. 2000 Jul 17;85(3):534-7; <http://www.naomib.ca/Os-PRL.pdf>.

⁸³¹ Walter CW, Gibson ND, Li YG, Matyas DJ, Alton RM, Lou SE, Field III RL, Hanstorp D, Pan L, Beck DR. Experimental and theoretical study of bound and quasibound states of Ce⁻. *Phys Rev A*. 2011 Sep 21;84(3):032514; http://digitalcommons.cedarville.edu/cgi/viewcontent.cgi?article=1178&context=science_and_mathematics_publications.

⁸³² Walter CW, Gibson ND, Matyas DJ, Crocker C, Dungan KA, Matola BR, Rohlén J. Candidate for laser cooling of a negative ion: observations of bound-bound transitions in La⁻. *Phys Rev Lett*. 2014 Aug 5;113(6):063001; <https://journals.aps.org/prl/abstract/10.1103/PhysRevLett.113.063001>.

⁸³³ O'Malley SM, Beck DR. Lifetimes and branching ratios of excited states in La⁻, Os⁻, Lu⁻, Lr⁻, and Pr⁻. *Phys Rev A*. 2010 Mar 5;81(3):032503; <https://journals.aps.org/pra/abstract/10.1103/PhysRevA.81.032503>.

⁸³⁴ Heber O, Golser R, Gnaser H, Berkovits D, Toker Y, Eritt M, Rappaport ML, Zajfman D. Lifetimes of the negative molecular hydrogen ions: H₂⁻, D₂⁻, and HD⁻. *Phys Rev A*. 2006 Jun 7;73(6):060501; <http://www.weizmann.ac.il/particle/molecule/publications/92.pdf>.

⁸³⁵ Andersen T. Lifetimes of negative ions determined in a storage ring. *Physica Scripta*. 1995;1995(T59):230-5; <http://iopscience.iop.org/article/10.1088/0031-8949/1995/T59/031/meta>.

⁸³⁶ Matsunaga N. Theoretical studies of possible high energy density materials, PhD thesis, Iowa State University, 1995, pp.11-36; <http://lib.dr.iastate.edu/cgi/viewcontent.cgi?article=12016&context=rtd>.

⁸³⁷ Kleingeld JC, Ingemann S, Jalonen JE, Nibbering NM. Formation of the NH₄⁻ ion in the gas phase. *J Am Chem Soc*. 1983 Apr;105(8):2474-5; <http://pubs.acs.org/doi/abs/10.1021/ja00346a061?journalCode=jacsat>.

Table 39. Electron affinity specific energies for single-electron anion generation in atoms and molecules, for $X + e^- \rightarrow X^- + \text{energy}$ (theoretical species noted in red)

Atomic or Molecular Cation	Electron Affinity (eV)	Specific Energy (MJ/kg)	Atomic or Molecular Cation	Electron Affinity (eV)	Specific Energy (MJ/kg)
Hydrogen, H	0.75	72.19	Sodium, Na	0.55	2.30
Fluorine, F	3.40	17.27	Iron oxide, FeO	1.50	2.01
Lithium difluoride, LiF ₂	6.70	14.39	Nickel, Ni	1.16	1.90
Dicarbon, C ₂	3.27	13.14	Copper, Cu	1.24	1.88
Beryllium trifluoride, BeF ₃	7.85	11.47	Sulfur dioxide, SO ₂	1.11	1.67
Hydroxyl, OH	1.83	10.37	Germanium, Ge	1.23	1.64
Carbon, C	1.26	10.14	Aluminum, Al	0.43	1.55
Chlorine, Cl	3.61	9.83	Dibromine, Br ₂	2.53	1.53
Trilithium Li ₃	1.95	9.04	Tellurium, Te	1.97	1.49
Boron oxide, BO	2.51	8.96	Uranium hexafluoride, UF ₆	5.06	1.39
Oxygen, O	1.46	8.81	Chromium, Cr	0.68	1.25
Lithium, Li	0.62	8.59	Potassium, K	0.50	1.24
Difluorine, F ₂	3.08	7.82	Iodine bromide, IBr	2.51	1.17
Beryllium hydride, BeH	0.70	6.74	Tungsten hexafluoride, WF ₆	3.50	1.13
Sulfhydryl, SH	2.32	6.77	Gold, Au	2.31	1.13
Sulfur, S	2.08	6.25	Cobalt, Co	0.66	1.08
Silicon, Si	1.39	4.77	Platinum, Pt	2.13	1.05
Nitrogen dioxide, NO ₂	2.27	4.77	Vanadium, V	0.53	1.00
Ozone, O ₃	2.10	4.23	Diiodine, I ₂	2.52	0.96
Vinyloxy, CH ₂ CHO	1.82	4.09	Osmium, Os	1.08	0.55
Bromine, Br	3.36	4.06	Cerium, Ce	0.63	0.43
Boron trifluoride, BF ₃	2.65	3.76	Tungsten, W	0.82	0.43
Dichlorine, Cl ₂	2.35	3.20	Scandium, Sc	0.19	0.40
Boron, B	0.28	2.50	Lanthanum, La	0.55	0.38
Selenium, Se	2.02	2.47	Fullerene, C ₆₀	2.68	0.36
Tetracyanoethylene, C ₂ (CN) ₄	3.17	2.39	Iron, Fe	0.15	0.26
Phosphorus, P	0.75	2.33	Titanium, Ti	0.08	0.17
Iodine, I	3.06	2.33	Calcium, Ca	0.02	0.06

What about multiply-charged atomic and molecular anions? Some large molecular systems can hold many extra electrons because these electrons can stay well-separated,⁸³⁸ and smaller multiply-negatively-charged molecular dianions (e.g., CO₃²⁻, CrO₄²⁻, Cr₂O₇²⁻, HPO₄²⁻, SO₄²⁻, SO₃²⁻, S₂O₃²⁻, S₂O₆²⁻, S₂O₈²⁻)⁸³⁹ and trianions (e.g., PO₄³⁻) are commonly found in aqueous solution

⁸³⁸ Wang XB, Ding CF, Wang LS. Photodetachment spectroscopy of a doubly charged anion: direct observation of the repulsive Coulomb barrier. Phys Rev Lett. 1998 Oct 19;81(16):3351-4; <http://casey.brown.edu/chemistry/misspelled-research/LSWang/publications/64.pdf>.

⁸³⁹ Blades AT, Kebarle P. Study of the Stability and Hydration of Doubly Charged Ions in the Gas Phase: SO₄²⁻, S₂O₆²⁻, S₂O₈²⁻, and Some Related Species. J Am Chem Soc. 1994 Nov;116(23):10761-6; <http://pubs.acs.org/doi/abs/10.1021/ja00102a046?journalCode=jacsat>.

where they can be stabilized via solvation and other electrostatic interactions, even though they are unstable against autodetachment in the gas phase. There have been no experimental observations of thermodynamically stable isolated atomic dianions or trianions to date.⁸⁴⁰ While most theoretical studies conclude that atomic anions cannot exist,⁸⁴¹ there is at least one theoretical prediction⁸⁴² that many atomic dianions might become stable in the presence of huge magnetic fields such as might occur in “magnetic white dwarf stellar atmospheres,” e.g., Be²⁻ (444,000 T), B²⁻ (383,000 T), N²⁻ (465,000 T), O²⁻ (400,000 T), Mg²⁻ (790,000 T), and S²⁻ (296,000 T). However, the energy density of such large magnetic fields is $E_D = B^2 / 2 \mu_0 = 4 \times 10^7 \text{ MJ/L}$ for $B = 300,000 \text{ T}$ and permeability constant $\mu_0 = 1.26 \times 10^{-6} \text{ henry/meter}$, dwarfing the likely electron affinity energy densities of any putative atomic dianions by ~6 orders of magnitude, hence hardly seems worth the effort.

Negative Electron Affinity Species. In the case of species with a negative electron affinity, energy must be added to force a neutral species to accept an additional electron, with capture occurring only when the impinging electron has a kinetic energy large enough to excite a resonance of the atom-plus-electron system ($X + e^- + \text{energy} \rightarrow X^-$). After such an anion is formed, energy is spontaneously released by electron autodetachment from these negatively-charged atomic and molecular anions, returning them to electrical neutrality, with the energy carried off in the kinetic energy of the freed electron, e.g., $X^- \rightarrow X + e^- + \text{energy}$. Negative ions formed in these cases are always unstable, usually with lifetimes of the order of microseconds to milliseconds before autodetachment occurs – examples include He⁻ (350 μsec), Be⁻ (43 μsec), N⁻ (<1 μsec), and Ar⁻ (0.26 μsec).⁸⁴³ Since there is no obvious way to artificially extend the short lifetimes or to trigger electron detachment at will, these species seem unlikely to be useful for energy storage purposes.

⁸⁴⁰ Scheller MK, Compton RN, Cederbaum LS. Gas-phase multiply charged anions. *Science*. 1995 Nov 17;270(5239):1160-7; <http://science.sciencemag.org/content/270/5239/1160/tab-pdf>.

⁸⁴¹ Hogreve H. On the maximal electronic charge bound by atomic nuclei. *J Phys B: Atom Molec Opt Phys*. 1998 May 28;31(10):L439-L446; <http://iopscience.iop.org/article/10.1088/0953-4075/31/10/001/meta>.

⁸⁴² Sergeev AV, Kais S. Critical Nuclear Charges for N-Electron Atoms. *Intl J Quantum Chem*. 1999;75:533-542;; <http://www.sergeev.org/papers/model/jpaper.pdf>.

⁸⁴³ [https://en.wikipedia.org/wiki/Electron_affinity_\(data_page\)](https://en.wikipedia.org/wiki/Electron_affinity_(data_page)).

4.4.3.4 Ion-Pair Molecules

An ion-pair molecule⁸⁴⁴ consists of a weakly bound positive ion and negative ion orbiting their common center of mass. The extremely large separation between the two components of an ion-pair molecule results in an almost perfect $1/r$ hydrogenic potential seen by each ion, with the positive ion analogous to the nucleus of a hydrogen atom and the negative ion analogous to the electron.⁸⁴⁵ The lightest ion-pair molecule is H^+H^- ,⁸⁴⁶ consisting of a naked proton bound to an H^- ion, but H^+F^- ,⁸⁴⁷ H^+SH^- ,⁸⁴⁸ and others have been investigated. The energy required to dissociate a neutral H_2 into separate H^+ and H^- ions is ~ 14.36 eV,⁸⁴⁹ much higher than the energy required to dissociate H_2 into two neutral monatomic H atoms (4.52 eV); the similar ion-pair threshold for $HF \rightarrow H^+ + F^-$ is 13.32 eV.⁸⁵⁰

Once the separate cation and anion are formed, the two can join to form a weakly-bound ionic ion-pair molecule. For example, the H^+F^- molecule has a relatively low binding energy of ~ 3 meV (**0.014 MJ/kg**) which is released when the molecule subsequently decays after a lifetime of

⁸⁴⁴ aka. “heavy Bohr atom,” “heavy Rydberg state,” “heavy Rydberg system,” or “heavy Rydberg atom,” not to be confused with a Rydberg molecule which is simply a molecule with one or more highly excited electrons; https://en.wikipedia.org/wiki/Heavy_Rydberg_system.

⁸⁴⁵ Reinhold E, Ubachs W. Heavy Rydberg states. *Molec Phys*. 2005 May 20;103(10):1329-52; https://www.physics.uoguelph.ca/~rbrooks/phys710/mphys103_1329.pdf.

⁸⁴⁶ Reinhold E, Ubachs W. Observation of coherent wave packets in a heavy Rydberg system. *Phys Rev Lett*. 2001 Dec 14;88(1):013001; <http://dare.ubvu.vu.nl/bitstream/handle/1871/31548/H+H-.pdf>. Kirrander A. Communication: Heavy Rydberg states: The H^+H^- system. *J Chem Phys*. 2010;133(12):121103; http://www.research.ed.ac.uk/portal/files/8893598/Communication_Heavy_Rydberg_states.pdf. Vogel JS. H^- formation by neutral resonant ionization of H ($n=2$) atoms. In: Kraus W, McNeely P (eds). *AIP Conf Proc* 2015 Apr 8;1655(1): 020015); <http://aip.scitation.org/doi/pdf/10.1063/1.4916424>.

⁸⁴⁷ Shiell RC, Reinhold E, Magnus F, Ubachs W. Control of diabatic versus adiabatic field dissociation in a heavy Rydberg system. *Phys Rev Lett*. 2005 Nov 17;95(21):213002; <http://dare.ubvu.vu.nl/bitstream/handle/1871/31561/HF-Control.pdf?sequence=2>.

⁸⁴⁸ Shiell RC, Hu XK, Hu QJ, Hepburn JW. A Determination of the Bond Dissociation Energy ($D^0(H-SH)$): Threshold Ion-Pair Production Spectroscopy (TIPPS) of a Triatomic Molecule. *J Phys Chem A*. 2000 May 18;104(19):4339-42; <http://pubs.acs.org/doi/abs/10.1021/jp000025k>.

⁸⁴⁹ Kirrander A. Communication: Heavy Rydberg states: The H^+H^- system. *J Chem Phys*. 2010;133(12):121103; http://www.research.ed.ac.uk/portal/files/8893598/Communication_Heavy_Rydberg_states.pdf.

⁸⁵⁰ Shiell RC, Reinhold E, Magnus F, Ubachs W. Control of diabatic versus adiabatic field dissociation in a heavy Rydberg system. *Phys Rev Lett*. 2005 Nov 17;95(21):213002; <http://dare.ubvu.vu.nl/bitstream/handle/1871/31561/HF-Control.pdf?sequence=2>.

$\sim 10 \mu\text{sec}$.⁸⁵¹ The binding energy of the H^+H^- ion-pair molecule is 1.1-3.2 meV (**0.053-0.15 MJ/kg**),⁸⁵² with a lifetime of only $\sim 0.4 \mu\text{sec}$.⁸⁵³ These times are probably too brief for a practical energy storage system unless the lifetime can be significantly extended, by some means currently unknown. Also, current production of ion-pair molecules relies on vacuum ultraviolet laser⁸⁵⁴ or multi-photon transition⁸⁵⁵ excitation, both of which are inefficient and produce low number densities.

⁸⁵¹ Shiell RC, Reinhold E, Magnus F, Ubachs W. Control of diabatic versus adiabatic field dissociation in a heavy Rydberg system. *Phys Rev Lett*. 2005 Nov 17;95(21):213002; <http://dare.ubv.uu.nl/bitstream/handle/1871/31561/HF-Control.pdf?sequence=2>.

⁸⁵² Reinhold E, Ubachs W. Observation of coherent wave packets in a heavy Rydberg system. *Phys Rev Lett*. 2001 Dec 14;88(1):013001; <http://dare.ubv.uu.nl/bitstream/handle/1871/31548/H+H-.pdf>.

⁸⁵³ Reinhold E, Ubachs W. Heavy Rydberg states. *Molec Phys*. 2005 May 20;103(10):1329-52; https://www.physics.uoguelph.ca/~rbrooks/phys710/mphys103_1329.pdf.

⁸⁵⁴ Suits AG, Hepburn JW. Ion pair dissociation: spectroscopy and dynamics. *Annu Rev Phys Chem*. 2006 May 5;57:431-65; <http://annualreviews.org/doi/abs/10.1146/annurev.physchem.56.092503.141209>.

⁸⁵⁵ Kung AH, Page RH, Larkin RJ, Shen YR, Lee YT. Rydberg spectroscopy of H_2 via stepwise resonant two-photon ion-pair ($\text{H}^+ + \text{H}^-$) production. *Phys Rev Lett*. 1986 Jan 27;56(4):328. <https://journals.aps.org/prl/abstract/10.1103/PhysRevLett.56.328>.

4.5 Atomistic Formation of Solids

“Chemical” energy generally involves the making or breaking of covalent, ionic, metallic hydrogen, or van der Waals bonds between atoms or molecules.

In this Section, we briefly review the energy storage capacities of ions or atoms as they are individually assembled into covalent solids (**Section 4.5.1**), ionic solids (**Section 4.5.2**), metallic solids (**Section 4.5.3**), hydrogen-bonded solids (**Section 4.5.4**), or van der Waals solids (**Section 4.5.5**).

4.5.1 Covalent Solids

Covalent bonds⁸⁵⁶, which involve the sharing of electrons among two or more atoms, are the strongest of the chemical bonds. Two or more bulk reactants can always be mixed to produce covalently-bonded product molecules with significant energy release (**Section 4.2.2**). But covalent bonds have directionality and multiple connectivity among specific atoms, a feature that can be exploited while assembling covalently-bonded solids using the techniques of atomically precise molecular manufacturing.

At the most primitive level of atomically precise manufacturing, covalent solids can be built atom by atom using “mechanosynthesis.” Mechanosynthesis, involving molecular positional fabrication, is the formation of covalent chemical bonds using precisely applied mechanical forces to build diamondoid⁸⁵⁷ or other structures. Mechanosynthesis employs chemical reactions driven by the mechanically precise positioning of extremely reactive chemical species in an ultra-high vacuum environment. Mechanosynthesis may be automated via computer control, enabling programmable molecular positional fabrication.

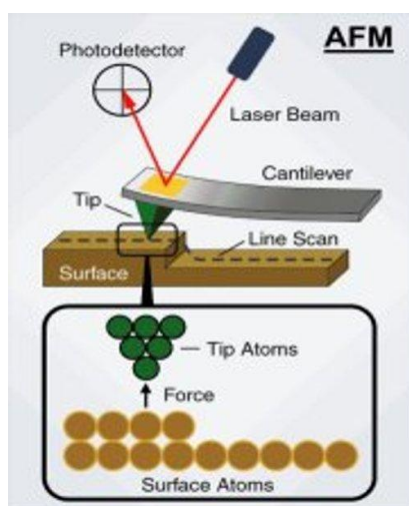
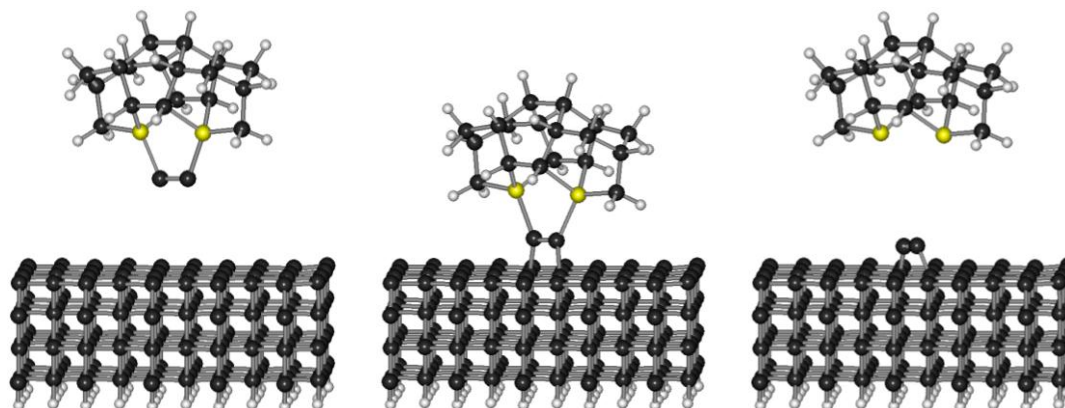
Atomically precise fabrication may involve holding feedstock atoms or molecules (e.g., bound to a scanning probe microscope tip), and a growing nanoscale workpiece, in the proper relative positions and orientations so that when they touch they will chemically bond in the desired manner. During this process, a mechanosynthetic tool is brought up to the surface of a workpiece. One or more transfer atoms are added to, or removed from, the workpiece by the tool (**Figure 1**). Then the tool is withdrawn and recharged. This process is repeated until the workpiece (e.g., a growing nanopart) is completely fabricated to molecular precision with each atom in exactly the right place. Note that the transfer atoms are under positional control at all times to prevent unwanted side reactions from occurring. Side reactions are also prevented using proper reaction sequence design so that the interaction energetics help to avoid undesired pathological intermediate structures.⁸⁵⁸

⁸⁵⁶ https://en.wikipedia.org/wiki/Covalent_bond.

⁸⁵⁷ Most diamondoids resemble ceramics. First and foremost, diamondoid materials include pure diamond, the crystalline allotrope of carbon. Among other exceptional properties, diamond has extreme hardness, high thermal conductivity, low frictional coefficient, chemical inertness, a wide electronic bandgap, and is the strongest and stiffest material presently known at ordinary pressures. Diamondoid materials also may include any stiff covalent solid that is similar to diamond in strength, chemical inertness, or other important material properties, and which possesses a dense three-dimensional network of bonds. Examples of such materials are carbon nanotubes and fullerenes, several strong covalent ceramics such as silicon carbide, silicon nitride, and boron nitride, and a few very stiff ionic ceramics such as sapphire (monocrystalline aluminum oxide) that can be covalently bonded to purely covalent structures such as diamond.

⁸⁵⁸ Freitas RA Jr., Merkle RC. A minimal toolset for positional diamond mechanosynthesis. *J Comput Theor Nanosci*. 2008;5:760-861; <http://www.molecularassembler.com/Papers/MinToolset.pdf>.

Figure 1. Three frames at the top show the DCB6Ge tooltip depositing two carbon atoms on a diamond surface. The tooltip is attached to a much larger tool handle structure (not shown) which is attached, in turn, to the macroscale tip of a laboratory-scale scanning probe microscope (e.g., see schematic, lower left, and image, lower right, of a UHV scanning probe microscope).



Positionally-controlled mechanosynthesis has been extensively discussed in the theoretical literature, starting in 1992,⁸⁵⁹ with the first theoretical quantitative systems-level study of a complete suite of reaction pathways for scanning-probe based ultrahigh-vacuum diamond mechanosynthesis published by Freitas and Merkle in 2008.⁸⁶⁰ Atomically precise positional

⁸⁵⁹ Drexler KE. *Nanosystems: Molecular Machinery, Manufacturing, and Computation*, John Wiley & Sons, New York, 1992, Chapter 8 http://e-drexler.com/d/09/00/Drexler_MIT_dissertation.pdf.

⁸⁶⁰ Freitas RA Jr., Merkle RC. A minimal toolset for positional diamond mechanosynthesis. *J Comput Theor Nanosci.* 2008;5:760-861; <http://www.molecularassembler.com/Papers/MinToolset.pdf>.

mechanosynthesis was first demonstrated experimentally in 2003 using silicon (Si) atoms,⁸⁶¹ and subsequently with other neutral atoms such as germanium (Ge)⁸⁶² and tin (Sn),⁸⁶³ and with charged anions such as chlorine (Cl⁻) and bromine (Br⁻).⁸⁶⁴ The first U.S. patent on positional mechanosynthesis was issued to Freitas in 2010,⁸⁶⁵ and other patents on positional mechanosynthesis have followed.⁸⁶⁶ At this writing mechanosynthesis has not yet achieved widespread commercial acceptance because historically it has proven experimentally challenging to accomplish, but it is currently performed using cryogenic UHV scanning probe technology of the kind illustrated in **Figure 1** above.

Table 40 shows the specific energy of bonds created between two or more atoms using very simple mechanosynthetic tools – in particular, a substituted adamantane molecule tooltip to which a transfer moiety (usually a single atom) is bonded, and a substituted adamantane workpiece to receive the transfer atoms, wherein the transfer moiety moves from the tooltip to the workpiece during the reaction.⁸⁶⁷ The reported specific energy assigns the reaction energy to the masses of the transfer moiety plus the recipient atom with which the bond is formed.

⁸⁶¹ Oyabu N, Custance O, Yi I, Sugawara Y, Morita S. Mechanical vertical manipulation of selected single atoms by soft nanoindentation using near contact atomic force microscopy. *Phys Rev Lett*. 2003 May 2;90(17):176102;

https://www.researchgate.net/profile/Seizo_Morita/publication/10726137_Mechanical_vertical_manipulation_of_selected_single_atoms_by_soft_nanoindentation_using_near_contact_atomic_force_microscopy/links/0912f4fc41f5127627000000.pdf.

⁸⁶² Oyabu N, Custance O, Abe M, Moritabe S. Mechanical vertical manipulation of single atoms on the Ge(111)-c(2x8) surface by noncontact atomic force microscopy. Abstracts of Seventh International Conference on Non-Contact Atomic Force Microscopy, Seattle, Washington, USA, 12-15 Sep 2004, p. 34; <http://www.engr.washington.edu/epp/afm/abstracts/15Oyabu2.pdf>.

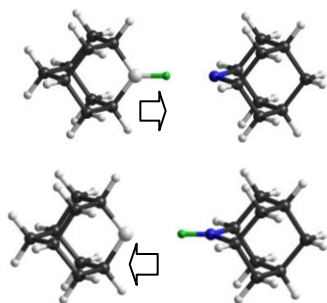
⁸⁶³ Sugimoto Y, Pou P, Custance O, Jelinek P, Abe M, Perez R, Morita S. Complex patterning by vertical interchange atom manipulation using atomic force microscopy. *Science*. 2008;322(5900):413-417; <http://www.sciencemag.org/cgi/content/full/322/5900/413>.

⁸⁶⁴ Kawai S, Foster AS, Canova FF, Onodera H, Kitamura S, Meyer E. Atom manipulation on an insulating surface at room temperature. *Nat Commun*. 2014 Jul 15;5:4403; <https://users.aalto.fi/~asf/publications/Nature%20Comm%20manip.pdf>.

⁸⁶⁵ Freitas RA Jr. Simple Tool for Positional Diamond Mechanosynthesis, and its Method of Manufacture. U.S. Patent 7,687,146, 30 Mar 2010; <http://www.freepatentsonline.com/7687146.pdf>.

⁸⁶⁶ e.g., Freitas RA Jr., Merkle RC. Positional Diamond Mechanosynthesis. U.S. Patent 8,171,568, 1 May 2012; <http://www.freepatentsonline.com/9676677.pdf>. Freitas RA Jr., Merkle RC. Build sequences for mechanosynthesis. U.S. Patent 9,676,677, 1 May 2012; <http://www.freepatentsonline.com/9676677.pdf>.

⁸⁶⁷ Data sources: Freitas RA Jr., Merkle RC. A minimal toolset for positional diamond mechanosynthesis. *J Comput Theor Nanosci*. 2008;5:760-861; <http://www.molecularassembler.com/Papers/MinToolset.pdf>. Freitas RA Jr., Merkle RC. Mechanosynthetic tools for atomic-scale fabrication. U.S. Patent 9,244,097, 26 Jan 2016; <http://www.freepatentsonline.com/9244097.pdf>.



For example, the illustrated reaction at left illustrates the most energy-dense reaction listed in the table – the creation of a particular boron-nitrogen bond (**13.2 MJ/kg**). Specifically, in the topmost two images, an Al-sidewall adamantane tooltip with a B (green) transfer atom bonded to the Al (top, left) approaches an N atom (blue) that has been substituted into the sidewall position of an adamantane workpiece (top, right). These are the mechanochemical reactants. In the bottommost two post-reaction images, the Al-sidewall adamantane tooltip (bottom, left) is retracted away from the N-sidewall adamantane workpiece (bottom, right) to which the B transfer atom has now become covalently bonded. These are the products of this thermodynamically-favored purely mechanochemical reaction. A sequence of similar reactions can build a covalently-bonded solid material.

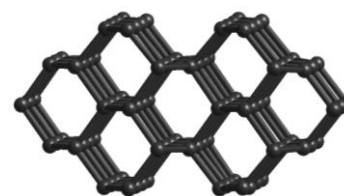
Table 40. Specific energy of mechanochemical covalent bonds

Tooltip/Transfer Atom → Recipient Workpiece	Bond Created	Reactn. Energy (eV)	Spec. Energy (MJ/kg)	Tooltip/Transfer Atom → Recipient Workpiece	Bond Created	Reactn. Energy (eV)	Spec. Energy (MJ/kg)
C ₉ H ₁₄ Al/B → NC ₉ H ₁₄	B-N	-3.40	13.22	C ₉ H ₁₅ C/Cl → SiC ₉ H ₁₅	Cl-Si	-1.02	1.55
C ₉ H ₁₆ C/H → CCC ₁₀ H ₁₅	H-C	-1.59	11.78	C ₉ H ₁₄ Al/Mg → NC ₉ H ₁₄	Mg-N	-0.61	1.54
C ₉ H ₁₄ Al/Be → NC ₉ H ₁₄	Be-N	-2.71	11.36	C ₉ H ₁₅ C/Mg → NC ₉ H ₁₄	Mg-N	-0.61	1.54
C ₉ H ₁₅ Ge/O → BC ₉ H ₁₄	O-B	-2.96	10.65	C ₉ H ₁₅ Ge/CH ₂ → CC ₉ H ₁₅	H ₂ C-C	-0.41	1.52
C ₉ H ₁₅ C/O → BC ₉ H ₁₄	O-B	-2.68	9.65	C ₉ H ₁₅ C/S → AlC ₉ H ₁₄	S-Al	-0.88	1.44
C ₉ H ₁₄ Al/H → BC ₉ H ₁₄	H-B	-1.05	8.57	C ₉ H ₁₅ Si/P → BC ₉ H ₁₄	P-B	-0.54	1.25
C ₉ H ₁₄ Al/N → BC ₉ H ₁₄	N-B	-1.73	6.73	C ₉ H ₁₅ Ge/H → SiC ₉ H ₁₅	H-Si	-0.35	1.16
C ₉ H ₁₄ Al/Be → CC ₉ H ₁₅	Be-C	-1.46	6.70	C ₉ H ₁₅ C/Br → AlC ₉ H ₁₄	Br-Al	-1.23	1.11
C ₉ H ₁₄ Al/H → CC ₉ H ₁₅	H-C	-0.90	6.67	C ₉ H ₁₅ Ge/C → SiC ₉ H ₁₅	C-Si	-0.46	1.11
C ₉ H ₁₅ Ge/F → BC ₉ H ₁₄	F-B	-1.79	5.79	C ₉ H ₁₅ Ge/Cl → AlC ₉ H ₁₄	Cl-Al	-0.71	1.10
C ₉ H ₁₄ B/Be → NC ₉ H ₁₄	Be-N	-1.26	5.28	C ₉ H ₁₄ N/S → AlC ₉ H ₁₄	S-Al	-0.65	1.06
C ₉ H ₁₅ C/Li → NC ₉ H ₁₄	Li-N	-1.06	4.88	C ₉ H ₁₅ C/S → SiC ₉ H ₁₅	S-Si	-0.63	1.01
C ₉ H ₁₅ Si/B → CC ₉ H ₁₅	B-C	-1.12	4.74	C ₉ H ₁₅ Ge/Br → BC ₉ H ₁₄	Br-B	-0.90	0.96
C ₉ H ₁₅ Ge/C → CC ₉ H ₁₅	C-C	-1.15	4.62	C ₉ H ₁₄ Al/P → NC ₉ H ₁₄	P-N	-0.42	0.90
C ₉ H ₁₅ Si/H → BC ₉ H ₁₄	H-B	-0.56	4.57	C ₉ H ₁₅ C/Br → SiC ₉ H ₁₅	Br-Si	-1.01	0.90
C ₉ H ₁₆ Ge/H → CC ₉ H ₁₅	H-C	-0.60	4.45	C ₉ H ₁₅ Ge/Cl → SiC ₉ H ₁₅	Cl-Si	-0.51	0.77
C ₉ H ₁₅ C/S → BC ₉ H ₁₄	S-B	-1.78	4.01	C ₉ H ₁₄ P/Mg → BC ₉ H ₁₄	Mg-B	-0.27	0.74
C ₉ H ₁₄ P/Al → NC ₉ H ₁₄	Al-N	-1.67	3.93	C ₉ H ₁₄ N/S → SiC ₉ H ₁₅	S-Si	-0.41	0.66
C ₉ H ₁₄ B/Li → NC ₉ H ₁₄	Li-N	-0.78	3.59	C ₉ H ₁₅ Si/Al → CC ₉ H ₁₅	Al-C	-0.25	0.62
C ₉ H ₁₄ Al/Li → NC ₉ H ₁₄	Li-N	-0.76	3.50	C ₉ H ₁₄ Al/Mg → BC ₉ H ₁₄	Mg-B	-0.22	0.60
C ₉ H ₁₄ N/S → BC ₉ H ₁₄	S-B	-1.55	3.49	C ₉ H ₁₅ Ge/Br → AlC ₉ H ₁₄	Br-Al	-0.63	0.57
C ₉ H ₁₅ Ge/S → BC ₉ H ₁₄	S-B	-1.54	3.47	C ₉ H ₁₅ Si/Br → BC ₉ H ₁₄	Br-B	-0.49	0.52
C ₉ H ₁₅ C/Cl → BC ₉ H ₁₄	Cl-B	-1.62	3.38	C ₉ H ₁₅ C/Br → BC ₉ H ₁₄	Ir-B	-1.07	0.51
C ₉ H ₁₅ Si/Li → NC ₉ H ₁₄	Li-N	-0.57	2.63	C ₉ H ₁₅ Ge/Si → CC ₉ H ₁₅	Si-C	-0.21	0.51
C ₉ H ₁₅ Si/S → BC ₉ H ₁₄	S-B	-1.14	2.57	C ₉ H ₁₅ C/S → NC ₉ H ₁₄	S-N	-0.23	0.48
C ₉ H ₁₅ Ge/F → AlC ₉ H ₁₄	F-Al	-1.08	2.27	C ₉ H ₁₅ C/Cl → GeC ₉ H ₁₅	Cl-Ge	-0.52	0.46
C ₉ H ₁₄ N/Br → AlC ₉ H ₁₄	Br-Al	-2.48	2.24	C ₉ H ₁₅ C/Br → GeC ₉ H ₁₅	Br-Ge	-0.60	0.38
C ₉ H ₁₅ Ge/Li → NC ₉ H ₁₄	Li-N	-0.46	2.12	C ₉ H ₁₅ Ge/Br → SiC ₉ H ₁₅	Br-Si	-0.41	0.37
C ₉ H ₁₅ Ge/O → SiC ₉ H ₁₅	O-Si	-0.96	2.10	C ₉ H ₁₄ Al/P → SiC ₉ H ₁₅	P-Si	-0.21	0.34
C ₉ H ₁₄ Al/S → BC ₉ H ₁₄	S-B	-0.90	2.03	C ₉ H ₁₄ B/Na → NC ₉ H ₁₄	Na-N	-0.13	0.34
C ₉ H ₁₄ P/P → BC ₉ H ₁₄	P-B	-0.87	2.01	C ₉ H ₁₄ B/Al → CC ₉ H ₁₅	Al-C	-0.13	0.32
C ₉ H ₁₅ C/Cl → AlC ₉ H ₁₄	Cl-Al	-1.22	1.89	C ₉ H ₁₅ Si/Si → CC ₉ H ₁₅	Si-C	-0.11	0.26
C ₉ H ₁₅ Ge/P → BC ₉ H ₁₄	P-B	-0.79	1.82	C ₉ H ₁₅ C/S → GeC ₉ H ₁₅	S-Ge	-0.24	0.22
C ₉ H ₁₄ Al/P → BC ₉ H ₁₄	P-B	-0.75	1.73	C ₉ H ₁₅ Ge/Ir → SiC ₉ H ₁₅	Ir-Si	-0.33	0.14
C ₉ H ₁₄ Al/H → SiC ₉ H ₁₅	H-Si	-0.49	1.63	C ₉ H ₁₅ C/Ir → SiC ₉ H ₁₅	Ir-Si	-0.29	0.13
C ₉ H ₁₅ C/Br → BC ₉ H ₁₄	Br-B	-1.50	1.60	C ₉ H ₁₄ P/Mg → AlC ₉ H ₁₄	Mg-Al	-0.05	0.09
C ₉ H ₁₄ Al/Al → CC ₉ H ₁₅	Al-C	-0.64	1.58	C ₉ H ₁₅ Si/Ge → CC ₉ H ₁₅	Ge-C	-0.08	0.09
C ₁₈ H ₂₂ Ge ₂ /C ₂ → CCC ₂₀ H ₂₄	C ₂ -C ₂	-0.78	1.57	C ₉ H ₁₅ Ge/Ir → CC ₉ H ₁₅	Ir-C	-0.04	0.02

The specific energy of these covalent bond-making reactions is relatively low because in each case, the transfer atom must break one covalent bond and then re-form a second one that is more thermodynamically favored, i.e., lower in energy. If it were possible to build covalent solids starting from individual monatomic transfer atoms – perhaps by manipulating unbonded atoms using electric or magnetic fields or by other means – then the specific energy that could be derived from those atoms when forming a covalent solid could be much higher, by avoiding incurring the debonding energy cost.

Table 41 lists the specific energy equivalents of the bond dissociation energies of various covalent bonds at 298 K (which is released when the bonds are formed), considering only the masses of the two atoms directly involved in making the bond.⁸⁶⁸ The bond dissociation energy can vary depending on which other atoms are already bonded to the two bonding atoms of interest; figures in the table generally reflect a larger value within the range of possibilities. Setting aside the diatomic molecular elements H₂, N₂, O₂, and F₂ already previously discussed (**Section 4.3**), many of the most energy-dense covalent bonds involve the elements carbon, hydrogen, and nitrogen. An energy storage system that made use of monatomic feedstock delivered atom by atom to build a covalent solid would require the stable storage of monatomic species, usually radicals (**Section 4.4.2**), and at a high enough concentration to provide a useful energy density from the device.

Diamond is a covalent solid with perhaps the highest bond density of any covalently material. The cleavage energy⁸⁶⁹ of the C(110) surface (image, right) is 6.5 J/m²; the minimum single-cage thickness of this surface is ~0.25 nm, giving an energy density of $E_{D,cleaveC110} = 26.0 \text{ MJ/L}$ and a specific energy of **91.3 MJ/kg** taking $\rho_{diamond} = 3.51 \text{ kg/L}$.⁸⁷⁰ Since fully dehydrogenated C(110) surfaces do not reconstruct, in principle an energy storage device could be made that stored individual C(110) sheets at a separation of, say, double the sheet thickness or 0.50 nm, that could release stored cleavage energy of (0.25 nm /0.50 nm) $E_{D,cleaveC110} \sim 13 \text{ MJ/L}$ (~**46 MJ/kg**) upon compression of the stack, seamlessly bonding the sheets into a single block of C(100) crystal.



Of course, joining flat plates of C(110) diamond into a solid block releases only a one-time burst of energy. A reversible energy storage mechanism might employ flat plates of alternating boron- and nitrogen-substituted C(110) to create inter-plate BN dative bonds (more easily torn apart, but

⁸⁶⁸ Data source: Dean JA. Lange's Handbook of Chemistry, 15th Edition, McGraw-Hill, NY, 1999, "Table 4.11 Bond Dissociation Energies";

https://www.google.com/url?sa=t&rct=j&q=&esrc=s&source=web&cd=1&ved=0ahUKEwj54G8-6rUAhUBRT4KHx-SATUQFggiMAA&url=http%3A%2F%2Fchemistry-chemists.com%2Fchemister%2FSpravocniki%2Fdean.pdf&usg=AFQjCNEzR-Bj_uqaR43wj2pVUixvZbk7yA&cad=rja.

⁸⁶⁹ Field JE. Chapter 9. Strength and Fracture Properties of Diamond. In: Field JE (ed). The Properties of Diamond, Academic Press, NY, 1979, Table 9.1, p. 284.

⁸⁷⁰ The C(111) diamond surface cleaves at 5.3 J/m² and 0.21 nm thick, giving **25.2 MJ/L (88.5 MJ/kg)**; the C(100) diamond surface has 9.2 J/m² and 0.35 nm thick, giving **26.3 MJ/L (92.3 MJ/kg)**.

with lower energy density). Silicon or germanium atoms, or even strategically-placed lattice defects, might deliver a higher energy density. Plates should be as thin as possible to maximize energy density, but thick enough to allow the plates to be pulled apart without destroying them while recovering the original undisturbed interfacial structure. This “mechanochemical battery” system could then be cycled endlessly between charged (plates separated) and discharged (plates together) states.

Table 41. Specific energy for bond dissociation of covalent bonds

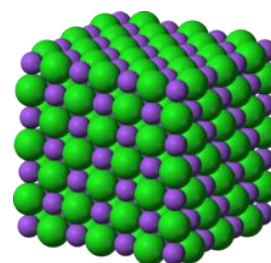
Bond	Dissoc. Energy (eV)	Specific Energy (MJ/kg)	Bond	Dissoc. Energy (eV)	Specific Energy (MJ/kg)	Bond	Dissoc. Energy (eV)	Specific Energy (MJ/kg)
H-H	4.52	216.27	B-B	3.08	13.74	Si-Se	5.50	4.96
HC≡CH	9.97	40.05	N-P	6.39	13.72	Ni-H	3.00	4.84
C-O	11.16	38.43	FAl-O	6.03	13.54	Pr-O	7.80	4.80
C≡O	11.14	38.38	P-O	6.18	12.70	Nd-O	7.29	4.39
HC≡N	9.71	36.01	C-P	5.32	11.93	Gd-O	7.42	4.13
N≡N	9.80	33.77	Al-O	5.31	11.91	F-F	1.63	4.13
N-N	9.80	33.74	Si-F	5.60	11.47	Ta-O	8.34	4.09
Li-H	2.56	31.08	Sc-O	6.99	11.06	Sn-O	5.68	4.07
B-O	8.35	30.06	S-O	5.41	10.86	Hf-O	8.20	4.07
C-N	7.98	29.59	Si-C	4.51	10.85	Tb-O	7.33	4.04
C=O	7.76	26.74	Mg-F	4.79	10.67	Al-Al	1.93	3.45
CIB-O	7.41	26.67	Ti-O	6.86	10.37	Th-O	8.85	3.44
C-H	3.49	25.90	Si-S	6.42	10.29	Dy-O	6.33	3.42
B-F	7.94	25.70	V-O	6.67	9.62	Be-Be	0.61	3.27
C-C	6.29	25.27	K-F	5.16	8.56	W-O	6.77	3.27
O-H	4.44	25.17	Ti-F	5.90	8.51	Tb-F	5.81	3.15
NC-CN	6.25	25.10	Li-Li	1.10	7.64	U-O	7.89	3.00
H ₂ C=NH	6.67	24.75	Ge-O	6.86	7.47	Ge-Si	3.12	2.99
OB-BO	5.24	23.40	Zr-O	7.88	7.09	Hf-C	5.68	2.88
Be-H	2.34	22.55	Nb-O	7.80	6.91	Cm-O	7.63	2.80
Li-F	5.98	22.25	Y-O	7.41	6.82	V-V	2.51	2.38
N-O	6.54	21.01	Ga-F	5.98	6.50	Pt-B	4.95	2.32
Be-F	5.98	20.60	Cr-O	4.43	6.28	Ir-Si	4.80	2.10
B-C	4.64	19.63	Cr-F	4.53	6.16	Ge-Ge	2.84	1.89
Si-O	8.27	18.10	Si-Si	3.39	5.82	Au-S	4.33	1.83
Be-O	4.64	17.91	Mn-F	4.38	5.72	Pb-O	3.92	1.69
C-F	5.56	17.29	Fe-O	4.24	5.69	Ir-O	3.65	1.69
OAl-F	7.89	16.55	Ni-F	4.51	5.60	Al-Au	3.38	1.46
H ₃ C-C ₆ H ₅	4.03	16.19	Co-F	4.51	5.58	H ₃ C-HgCH ₃	2.49	1.13
C-S	7.24	15.86	Zr-C	5.81	5.43	Hg-S	2.21	0.92
B-N	4.03	15.67	Mo-O	6.29	5.42	Sn-Sn	2.02	0.82
F-C ₆ H ₅	5.03	15.64	Ni-O	4.06	5.24	Pb-Pb	3.51	0.82
O-O	5.16	15.57	Cu-F	4.47	5.22	Kr-F	0.56	0.53
Li-O	3.53	14.87	La-O	8.28	5.16	Xe-O	0.38	0.25
Al-F	6.88	14.44	Ce-O	8.24	5.09	Hg-Hg	0.18	0.04

A simple stack-of-plates system provides a predominantly thermal energy release, but it should be possible to design a device whose structure requires a succession of single bonding events to occur, the completion of one event overcoming the barrier to forming the next, resulting in a mechanical energy output such as a linear tractor or a helical system that generates rotational torque. Such devices may be reversible if the system can be mechanically forced to move in the opposite direction, sequentially unzipping all the covalent bonds previously formed during the discharge cycle, and requiring the input of mechanical energy to execute the recharge cycle.

4.5.2 Ionic Solids

Ionic solids are composed of atoms joined by ionic bonding,⁸⁷¹ which involves the electrostatic attraction between oppositely charged ions (e.g., Na^+ and Cl^- ions, which combine to form the ionic solid NaCl) and not the sharing of valence electrons as occurs in covalent solids. When ionic bonding occurs in the solid (or liquid) state, it is not correct to consider that a single “ionic bond” has formed between two individual atoms because the cohesive forces that keep the lattice together are of a more collective nature – unlike in covalent bonding, which involves the formation of a distinct bond localized between two particular atoms.

The lattice formation enthalpy of an ionic solid is the amount of energy that is released when a lattice comprising an ionic solid is formed from the constituent gaseous ions. For example, if a mole of gaseous sodium ions (Na^+) is mixed with a mole of gaseous chlorine atoms (Cl^-), then about -787 kJ/mole or **~ 13.5 MJ/kg** of energy would be released upon the subsequent formation of 1 mole of NaCl salt crystal (image, right).⁸⁷² **Table 42**⁸⁷³ shows a large selection of inorganic ionic solids, ranked in descending order of their specific energy of lattice formation enthalpy. Beryllium oxide and aluminum oxide have the highest specific energies, at **177.7 MJ/kg** and **156.1 MJ/kg**, respectively. These are comparable or superior to the best specific energies attainable by the ambient combustion of covalent chemical fuels (**Section 4.2.3**).



The chief practical obstacle to attaining this performance will be the challenge of long-term stable storage of the separate reactive ions at sufficient density. Endohedral trapping (**Section 4.3.1.3**) or particle storage rings (**Section 4.3.1.4**) may provide possible solutions to this problem.

⁸⁷¹ https://en.wikipedia.org/wiki/Ionic_bonding.

⁸⁷² Note that some energy must be expended to prepare the sodium ion by removing one valence electron from a neutral sodium atom via ionization, creating an Na^+ , and some additional energy must be expended to prepare the chlorine atom by dissociating the molecular Cl_2 to monatomic chlorine, and then to ionize the atom by adding an extra electron to its valence shell, creating a Cl^- . Adding these endoergic energy costs drops the energy store for ion-assembled NaCl from -787 kJ/mole (**13.5 MJ/kg**) down to the standard enthalpy of formation for NaCl of -411 kJ/mole (**7.03 MJ/kg, 15.2 MJ/L**) – the amount of energy released when neutral metallic sodium (Na) is “burned” in an atmosphere of pure molecular chlorine (Cl_2).

⁸⁷³ Data sources: Chemistry@TutorVista.com; “Table 6.3 Lattice Energies of Some Ionic Solids (kJ/mol),” Laboratory Manual for Chemistry, 6th Edition, <http://www.chegg.com/homework-help/look-lattice-energies-table-63-calculate-energy-change-kiloj-chapter-6-problem-63p-solution-9780321727206-exc>; “Table 8.2 Lattice Energies for Some Ionic Compounds,” Chapter 8, Chemistry: The Central Science, <http://wps.prenhall.com/wps/media/objects/3311/3391006/blb0802.html>; CRC Handbook of Chemistry and Physics (2004), cited in Averill & Eldredge, Chemistry, “Table 8.3.1: Representative Calculated Lattice Energies,” [https://chem.libretexts.org/Textbook_Maps/General_Chemistry_Textbook_Maps/Map%3A_Chemistry_\(Averill_and_Eldredge\)/08%3A_Ionic_versus_Covalent_Bonding/8.3_Lattice_Energies_in_Ionic_Solids;_Lattice_Energies](https://chem.libretexts.org/Textbook_Maps/General_Chemistry_Textbook_Maps/Map%3A_Chemistry_(Averill_and_Eldredge)/08%3A_Ionic_versus_Covalent_Bonding/8.3_Lattice_Energies_in_Ionic_Solids;_Lattice_Energies),” Wired Chemist, <http://www.wiredchemist.com/chemistry/data/lattice-energies>.

Table 42. Specific energy of lattice formation for ionic solids

Ionic Solid	Lattice Formation Enthalpy (kJ/mole)	Specific Energy (MJ/kg)	Ionic Solid	Lattice Formation Enthalpy (kJ/mole)	Specific Energy (MJ/kg)
BeO	4443	177.65	BeBr ₂	2914	17.26
Al ₂ O ₃	15916	156.10	HgS	3573	15.36
ScN	7547	128.00	BaH ₂	2121	15.22
LiH	906	113.96	KF	821	14.13
Li ₂ O	2925	97.89	NaCl	787	13.47
MgO	3791	94.06	SrCl ₂	2127	13.42
Ga ₂ O ₃	15,600	83.22	BaF ₂	2352	13.41
BeF ₂	3505	74.56	MgBr ₂	2440	13.25
Al(OH) ₃	5627	72.14	AlI ₃	5218	12.80
AlF ₃	5215	62.10	CaBr ₂	2176	10.89
CaO	3401	60.65	BeI ₂	2800	10.65
Mg(OH) ₂	3006	51.54	CuCl	979	9.89
MgF ₂	2957	47.46	BaCl ₂	2056	9.87
Na ₂ O	2695	43.48	KCl	715	9.59
CaS	3093	42.87	LiBr	807	9.29
AlCl ₃	5492	41.19	NaNO ₃	755	8.88
LiF	1036	39.94	MgI ₂	2327	8.37
BeCl ₂	3020	37.79	AgF	969	7.64
ZnS	3619	37.13	RbF	785	7.51
Ca ₃ (PO ₄) ₂	10,602	34.18	NaBr	747	7.26
NaH	811	33.79	CaI ₂	2074	7.06
CaF ₂	2630	33.69	CuBr	976	6.80
TiF ₂	2749	32.02	BaBr ₂	1985	6.68
CrF ₂	2879	31.99	AgCl	916	6.39
VF ₂	2812	31.62	KBr	682	5.73
NiF ₂	3046	31.50	RbCl	689	5.70
FeF ₂	2912	31.03	LiI	757	5.66
SrO	3200	30.88	CuI	958	5.03
CoF ₂	2962	30.56	CsF	740	4.87
CuF ₂	3042	29.96	BaI ₂	1877	4.80
MnF ₂	2770	29.81	AgBr	900	4.79
ZnF ₂	2971	28.73	NaI	704	4.70
CaCO ₃	2804	28.02	AuCl	1042	4.48
MgCl ₂	2524	26.51	RbBr	660	3.99
K ₂ O	2360	25.05	KI	649	3.91
CdS	3402	23.55	CsCl	659	3.91
NaOH	900	22.50	AgI	895	3.81
NaF	923	21.98	AuI	1050	3.24
CaCl ₂	2258	20.35	TlCl	748	3.12
LiCl	853	20.12	RbI	630	2.97
AlBr ₃	5361	20.10	CsBr	631	2.97
BaO	3000	19.57	CsI	604	2.32

4.5.3 Metallic Solids

Solid metals are held together by metallic bonds – a type of chemical bonding that arises from the electrostatic attractive force between conduction electrons (in the form of an electron cloud of delocalized electrons) and positively charged metal ions, and involves the sharing of free electrons among a lattice of positively charged ions (cations).⁸⁷⁴ While the standard state of a metal is the neutral atom and the standard enthalpy of formation of a metal is zero, the addition of a metal atom to an existing metallic solid releases energy with the formation of the metallic bond. Thus, a collection of isolated metal atoms can be considered as storing a metallic bonding energy when they “condense” into a bonded solid material. **Table 43** gives the specific energy of neutral metal atoms that are assembled into a pure metallic solid.⁸⁷⁵

Table 43. Specific energy of solid metal formation from neutral metal atoms					
Metal	Metallic Bond Energy (kJ/mole)	Specific Energy (MJ/kg)	Metal	Metallic Bond Energy (kJ/mole)	Specific Energy (MJ/kg)
Be	324	35.95	Mn	279	5.08
Li	159.3	22.96	Na	107.5	4.68
Al	324	12.01	W	849	4.62
V	515	10.11	Ca	177.8	4.44
Ti	473	9.88	Ga	272	3.90
Cr	398	7.65	K	89.6	2.29
Sc	342	7.61	Zn	131	2.00
Fe	418	7.49	Sr	164.4	1.88
Ni	423	7.21	Ba	180	1.31
Co	383	6.50	Rb	80.9	0.95
Mg	147.1	6.05	Cs	76.5	0.58
Cu	339	5.33	Hg	68	0.34
Ge	377	5.19			

⁸⁷⁴ https://en.wikipedia.org/wiki/Metallic_bonding.

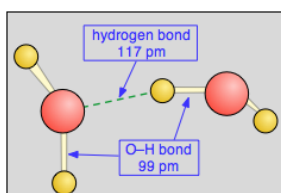
⁸⁷⁵ Data sources: “Table 3. Enthalpies of formation of Group 1 and Group 2 metal ions,” in: Lang PF, Smith BC. *Metallic Structure and Bonding*. World J Chem Educ 2015;3(2):30-35; <http://pubs.sciepub.com/wjce/3/2/1/>. “Table 2.8. Bonding energies, melting points, and electron configurations of the fourth-period metals of the Periodic Table,” Slide 28, <https://www.slideshare.net/mizakamaruzzaman/phy351-ch-2-27831741>. “Bonding Energies and Melting Temperature of Various Substance,” Slide 13, <https://www.slideshare.net/TechnicalReport/1-15110135>.

The available energy storage is generally less than is available for covalent or ionic bonding, but is greater than that available for hydrogen-bonded material or van der Waals solids. Beryllium appears to possess the highest specific energy for metallic bonding, releasing **~36 MJ/kg** as Be atoms are added to solid beryllium metal. As with ionic solids, the chief practical obstacle to extracting this energy will be the challenge of long-term stable storage of separated individual metal atoms at a sufficient density.

4.5.4 Hydrogen-Bonded Solids

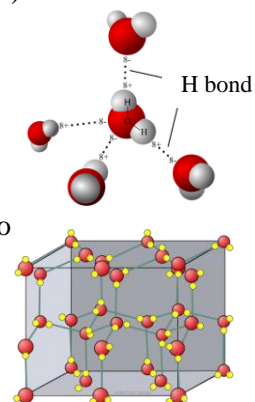
The hydrogen bond is an electrostatic attraction between two polar groups that occurs when a hydrogen (H) atom that is covalently bound to a highly electronegative atom such as nitrogen (N), oxygen (O), or fluorine (F) experiences the electrostatic field of another highly electronegative atom nearby.⁸⁷⁶ This type of bond can occur in inorganic molecules such as water and in organic molecules like DNA and proteins. Depending on geometry and environment, the hydrogen bond free energy content is usually between 4-20 kJ/mole,⁸⁷⁷ which is stronger than the van der Waals attractive force (Section 4.5.5) but weaker than covalent bonds (Section 4.5.1), ionic bonds (Section 4.5.2) or metallic bonds (Section 4.5.3). Typical hydrogen bond strengths include:⁸⁷⁸

N-H···O	(8 kJ/mole, 0.46 MJ/kg)	N-H···N	(13 kJ/mole, 0.87 MJ/kg)
HO-H···OH ₃ ⁺	(18 kJ/mole, 1.0 MJ/kg)		
O-H···O	(21 kJ/mole, 1.2 MJ/kg)	O-H···N	(29 kJ/mole, 1.9 MJ/kg)



Of course, most solids that contain hydrogen bonds (e.g., DNA base pairs, beta sheet formation in folded proteins, nylon polymers, etc.) do not consist mostly of hydrogen bonds. Perhaps one of the most heavily hydrogen-bonded materials is solid water-ice, as well as liquid water. The H₂O molecule is electrically neutral overall, but because the oxygen atom has nonbonding electrons (two lone pairs) the molecule

becomes an electric dipole, slightly more positive on the hydrogen side and slightly more negative on the oxygen side. This creates a weak attraction – a hydrogen bond – between the oxygen of one water molecule and the hydrogens of a neighboring water molecule. Note that the hydrogen bond (shown by the dashed green line in the above image at left)⁸⁷⁹ is somewhat longer than the covalent O-H bond and is also much weaker, about 21 kJ/mole per hydrogen bond (~**1.2 MJ/kg**, counting one hydrogen bond per H···O pair) as compared to the O-H covalent bond strength of 428 kJ/mole (**25.2 MJ/kg**; Table 41). When water freezes into ice, each molecule is surrounded by four other molecules (image at right, top) and the hydrogen bonds form a rigid and stable network with crystals having a hexagonal lattice structure (image at right, bottom). At the surface of a liquid, the surface molecules experience fewer



⁸⁷⁶ https://en.wikipedia.org/wiki/Hydrogen_bond.

⁸⁷⁷ A very few unusually strong hydrogen bonds are known, including the 161.5 kJ/mole (~**4.1 MJ/kg**) F-H···F bond in the HF₂⁻ ion (Emsley J. Very strong hydrogen bonding. Chem Soc Rev. 1980;9(1):91-124; <http://pubs.rsc.org/en/content/articlelanding/1980/cs/cs9800900091>), but it is unclear how best to take advantage of this to build a high specific energy storage system.

⁸⁷⁸ https://en.wikipedia.org/wiki/Hydrogen_bond#Bonding.

⁸⁷⁹ [https://chem.libretexts.org/Textbook_Maps/General_Chemistry_Textbook_Maps/Map%3A_ChemI_\(Lower\)/07%3A_Solids_and_Liquids/7.03%3A_Hydrogen-Bonding_and_Water](https://chem.libretexts.org/Textbook_Maps/General_Chemistry_Textbook_Maps/Map%3A_ChemI_(Lower)/07%3A_Solids_and_Liquids/7.03%3A_Hydrogen-Bonding_and_Water).

hydrogen bonds so the cohesive forces are weaker. The 0.072 J/m^2 surface tension of water⁸⁸⁰ in air at $25 \text{ }^\circ\text{C}$ represents an energy density of only $\sim 0.3 \text{ MJ/L}$,⁸⁸¹ taking the thickness of a single molecular sheet of water molecules as $\sim 2.4 \text{ \AA}$ or twice the covalent radius of the oxygen atom.⁸⁸² Molecular receptors or binding sites for small and large molecules in water, whether using hydrogen bonding or van der Waals forces (**Section 4.5.5**) to establish physical affinity, may have energy densities in the range of **0.006-0.04 MJ/L**.⁸⁸³

⁸⁸⁰ https://en.wikipedia.org/wiki/Surface_tension#Data_table.

⁸⁸¹ This **0.3 MJ/L** energy density for the surface tension of hydrogen-bonded water stands intermediate between the comparable energy density of **1.6 MJ/L** for liquid mercury (0.487 J/m^2 , $\sim 3.0 \text{ \AA}$), where bonding is predominantly metallic (**Section 4.5.3**), and **0.0013 MJ/L** for liquid helium II (0.00037 J/m^2 , $\sim 2.8 \text{ \AA}$; Brouwer W, Pathria RK. On the surface tension of liquid helium II. Phys Rev. 1967 Nov 5;163(1):200-5; <https://journals.aps.org/pr/abstract/10.1103/PhysRev.163.200>), where bonding is predominantly van der Waals (**Section 4.5.5**).

⁸⁸² https://en.wikipedia.org/wiki/Atomic_radius#Empirically_measured_atomic_radius.

⁸⁸³ Freitas RA Jr. Nanomedicine, Volume I: Basic Capabilities, Landes Bioscience, Georgetown TX, 1999, Section 3.5, "Molecular Receptor Engineering"; <http://www.nanomedicine.com/NMI/3.5.htm>.

4.5.5 Van der Waals Solids

Intermolecular van der Waals forces⁸⁸⁴ create non-electronic “bonds” that are weakest of all the chemical bonds, hence produce the lowest energy densities. For example, the helium dimer (He_2) is a van der Waals molecule⁸⁸⁵ with a bond so weak that it can only exist at extreme cryogenic temperatures and breaks if the molecule rotates or vibrates too much. Two isolated helium atoms will join to form a dimer molecule with the release of only 9.5×10^{-8} eV,⁸⁸⁶ a specific energy of **1.1×10^{-6} MJ/kg**.

Frozen argon (~ 0.078 eV, **~ 0.19 MJ/kg**)⁸⁸⁷ is a more typical van der Waals solid. As a nonpolar noble gas with a full octet and no charge, it cannot readily participate in covalent, ionic, or metallic bonds and can only be held together in solid form by weak van der Waals forces at temperatures below 84 K.

Other materials can also form van der Waals solids in ambient conditions,⁸⁸⁸ including high-pressure $\text{He}(\text{N}_2)_{11}$ crystal⁸⁸⁹ and solid C_{60} ,⁸⁹⁰ but there is relatively little energy stored in these intermolecular attractions.⁸⁹¹

⁸⁸⁴ https://en.wikipedia.org/wiki/Van_der_Waals_force.

⁸⁸⁵ https://en.wikipedia.org/wiki/Van_der_Waals_molecule.

⁸⁸⁶ Grisenti RE, Schollkopf W, Toennies JP, Hegerfeldt GC, Kohler T, Stoll M. Determination of the bond length and binding energy of the helium dimer by diffraction from a transmission grating. *Phys Rev Lett*. 2000 Sep 11;85(11):2284-7; http://isites.harvard.edu/fs/docs/icb.topic105883.files/deBroglie_wavelength/He2_Molecular_Diffraction.pdf.

⁸⁸⁷ Serway RA, Moses CJ, Moyer CA. *Modern Physics*, Thomson Learning, 2005, p. 410; <https://books.google.com/books?id=uTM8AAAAQBAJ&pg=PA410>.

⁸⁸⁸ Lin YC, Lu N, Perea-Lopez N, Li J, Lin Z, Peng X, Lee CH, Sun C, Calderin L, Browning PN, Bresnehan MS. Direct synthesis of van der Waals solids. *ACS Nano*. 2014 Mar 27;8(4):3715-23; http://www.academia.edu/download/35351462/ACS_Nano_2014_Lin.pdf. Choi B, Yu J, Paley DW, Trinh MT, Paley MV, Karch JM, Crowther AC, Lee CH, Lalancette RA, Zhu X, Kim P. van der Waals Solids from Self-Assembled Nanoscale Building Blocks. *Nano Lett*. 2016 Feb 1;16(2):1445-9; <http://pubs.acs.org/doi/abs/10.1021/acs.nanolett.5b05049>.

⁸⁸⁹ Vos WL, Finger LW, Hemley RJ, Hu JZ, Mao HK, Schouten JA. A high-pressure van der Waals compound in solid nitrogen-helium mixtures. *Nature*. 1992 Jul 2;358(6381):46-8; <http://cops.nano-cops.com/sites/default/files/nature358vanderwaals1992.pdf>.

⁸⁹⁰ Hoen S, Chopra NG, Xiang XD, Mostovoy R, Hou J, Vareka WA, Zettl A. Elastic properties of a van der Waals solid: C_{60} . *Phys Rev B*. 1992 Nov 15;46(19):12737; <https://journals.aps.org/prb/abstract/10.1103/PhysRevB.46.12737>.

Chapter 5. Mechanical Energy Storage

In this Chapter we survey the specific energy (MJ/kg) and energy density (MJ/L) available from various sources of stored mechanical energy.

Section 5.1 describes the energy that may be stored by compressing matter while it is in the solid (**Section 5.1.1**), liquid (**Section 5.1.2**), gaseous (**Section 5.1.3**), or plasma (**Section 5.1.4**) state, along with the special case of acoustic waves (**Section 5.1.5**). **Section 5.2** describes the spring energy that may be stored in mechanical systems to which a mechanical stress has been applied, including compression, tension, torsion, or bending. **Section 5.3** describes the energy content of a mass in translational (**Section 5.3.1**) or rotational (**Section 5.3.2**) motion. The energy that can be stored in materials due to thermomechanical stress is discussed in **Section 5.4**.

Figure 4 (Chapter 9) provides a chart that summarizes much of this data.

⁸⁹¹ The “van der Waals” force is often used to include a variety of weak interactions. Michael Marshall notes that the attraction in many of the included examples is specifically induced dipole-induced dipole attraction. In computational chemistry, this interaction is referred to as dispersion. This clarification is important because approximations in many levels of theory (including density functional theory, unless time-dependent) cannot describe this interaction because of how electron density is treated in an averaged way. Symmetry-adapted perturbation theory or SAPT (https://en.wikipedia.org/wiki/Symmetry-adapted_perturbation_theory), a methodology in electronic structure theory developed to describe non-covalent interactions between atoms and/or molecules. treats attractive interactions as combinations of electrostatics, dispersion, and induction effects (e.g., Burns LA, Faver JC, Zheng Z, Marshall MS, Smith DGA, Vanommeslaeghe K, MacKerell AD Jr, Merz KM Jr, Sherrill CD. The BioFragment Database (BFDdb): An open-data platform for computational chemistry analysis of noncovalent interactions. *J Chem Phys.* 2017 Oct 28;147(16):161727; https://www.ncbi.nlm.nih.gov/pmc/articles/PMC5656042/pdf/JCPSA6-000147-161727_1.pdf).

5.1 Pressure

Energy can be stored in materials simply by compressing or tensioning them to a pressure above the ambient level. The compressed material can be containerized and stored indefinitely. Allowing the material to exit the container and return to ambient pressure releases the stored energy as the expansion of the material performs mechanical work.

In the Section we briefly review the capacity for compressive and tensile energy storage in solids (**Section 5.1.1**), liquids (**Section 5.1.2**), gases (**Section 5.1.3**), and plasmas (**Section 5.1.4**).

5.1.1 Compression of Solids

Solids have the poorest compression energy densities of all the four states of matter because, in general, they are incompressible and thus cannot store much “PV” (pressure/volume) energy. Among the solid elements, frozen helium (0.95 K @ ~25 atm,⁸⁹² 1.15 K @ 66 atm,⁸⁹³ ~300 K @ 114,000 atm⁸⁹⁴ to solidify) is the most compressible, being ~80 times more compressible than water (bulk modulus $K_{\text{He}} \sim 2.7 \times 10^7 \text{ N/m}^2$,⁸⁹⁵ vs. $K_{\text{H}_2\text{O}} \sim 2.2 \times 10^9 \text{ N/m}^2$ for water) and with a volume compressibility of 0.224 at 10 GPa pressure.⁸⁹⁶ Diamond is generally regarded as the least compressible solid,⁸⁹⁷ with an estimated volume compressibility of 0.979 at 10 GPa.⁸⁹⁸

If a solid or liquid is compressed by increasing physical pressure from P_1 to P_2 ($\Delta P = P_2 - P_1$), causing the compressed material to shrink in volume from V_1 to V_2 ($\Delta V = V_1 - V_2$), increasing its density from ρ_1 to ρ_2 , then the stored energy may be approximated (using a variation of one form of the Rankine-Hugoniot equation)⁸⁹⁹ as the product of the change in applied pressure and the relative change in volume ($\Delta V/V_1$): specific energy $E_S \sim (\Delta P / \rho_2) (\Delta V/V_1) = (\Delta P / \rho_2) (1 - V_2/V_1)$ and the stored energy density $E_D \sim (\Delta P) (\Delta V/V_1) = (\Delta P) (1 - V_2/V_1)$ for compressed solid materials in the elastic regime where the bonding structure has not been permanently dislocated

⁸⁹² “Solid Helium,” Department of Physics, University of Alberta. 2005 Oct 5; <https://web.archive.org/web/20080531145546/http://www.phys.ualberta.ca/~therman/lowtemp/projects1.htm>.

⁸⁹³ Henshaw DB. Structure of Solid Helium by Neutron Diffraction. Phys Rev Lett. 1958 Jan 15;109(2):328-330; <https://journals.aps.org/pr/abstract/10.1103/PhysRev.109.328>.

⁸⁹⁴ “Facts about helium,” chemicool.com, 7 Jun 2017; <http://www.chemicool.com/elements/helium-facts.html>.

⁸⁹⁵ Grilly ER. Pressure-volume-temperature relations in liquid and solid ^4He . J Low Temp Phys. 1973 Apr 21;11(1-2):33-52; <https://link.springer.com/article/10.1007%2F00655035>.

⁸⁹⁶ Mao HK, Hemley RJ, Wu Y, Jephcoat AP, Finger LW, Zha CS, Bassett WA. High-pressure phase diagram and equation of state of solid helium from single-crystal X-ray diffraction to 23.3 GPa. Phys Rev Lett. 1988 Jun 20;60(25):2649-52; <https://legacy.gl.ciw.edu/static/users/rhemley/037MaoPRL1988.pdf>.

⁸⁹⁷ At low pressure, solid osmium metal is less compressible than diamond, but with increasing pressure osmium becomes more compressible than diamond. Hebbache M, Zenzemi M. *Ab initio* study of high-pressure behavior of a low compressibility metal and a hard material: Osmium and diamond. Phys Rev B. 2004 Dec 21;70(22):224107; <https://journals.aps.org/prb/abstract/10.1103/PhysRevB.70.224107>.

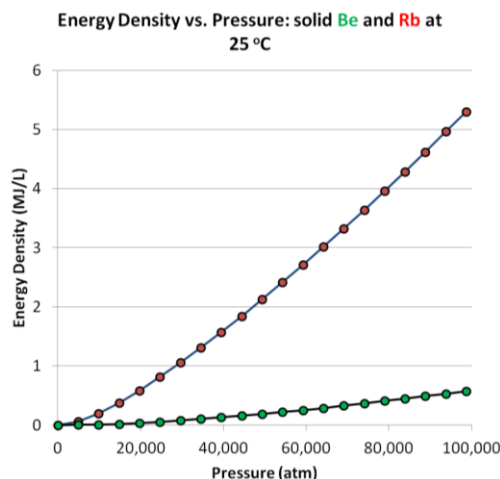
⁸⁹⁸ Cumberland RW, Weinberger MB, Gilman JJ, Clark SM, Tolbert SH, Kaner RB. Osmium diboride, an ultra-incompressible, hard material. J Am Chem Soc. 2005 May 25;127(20):7264-5; <http://tolbert.chem.ucla.edu/Publication/jacsmay2005.pdf>.

⁸⁹⁹ Salas MD. The curious events leading to the theory of shock waves. 17th Shock Interaction Symposium, Rome, Italy, 4-8 Sep 2006; <https://ntrs.nasa.gov/archive/nasa/casi.ntrs.nasa.gov/20060047586.pdf>. See also: https://en.wikipedia.org/wiki/Rankine-Hugoniot_conditions.

or altered by the application of pressure. (Metals can sustain pressures up to 10-30 GPa (~100,000-300,000 atm) and remain elastic.⁹⁰⁰)

Table 44 shows that solids, even after being very highly compressed to 10 GPa (~100,000 atm), can only store **0.01-10 MJ/kg** and **0.1-10 MJ/L**.⁹⁰¹ Most of the V_2/V_1 data⁹⁰² for this table were drawn from the work of the celebrated high-pressure researcher P.W. Bridgman, dating from 1911-1955, and thus are somewhat variable in consistency according to the 1972 AIP Handbook in which they were republished.

The chart at right shows that energy storage is a nearly linear function of pressure, at high pressures. Energy density reaches **~5 MJ/L** for rubidium metal (red dots) compressed to 100,000 atm (~10 GPa), but only about one-tenth as much (**~0.5 MJ/L**) for beryllium (green dots) – a much harder metal – at the same pressure.



The energy density of compressed solids at lower pressures such as ~1000 atm (the highest recommended pressure for some biology-interfacing molecular machine applications, e.g., medical nanorobotics) would likely be in the **0.0001-0.004 MJ/L (0.00004-0.002 MJ/kg)** range – which may be too low for practical use in most situations.

⁹⁰⁰ Lubarda V. Finite compression of solids – second order thermoelastic analysis. Int J Solids Structures. 1986;22(12):1517-24; <http://maeresearch.ucsd.edu/~vlubarda/research/pdfpapers/ijss-86.pdf>.

⁹⁰¹ Interestingly, the compression energy that would be stored in monatomic metallic hydrogen at an estimated pressure of ~500 GPa (~5,000,000 atm) and density of ~1.3 kg/L (**Section 4.3.1.5**) starting from solid molecular hydrogen of density 0.086 kg/L at ordinary pressure, using the V_2/V_1 method above, represents an energy density of $E_D \sim 467$ MJ/L and a specific energy of $E_S \sim 359$ MJ/kg.

⁹⁰² Data sources for volume compressibility V_2/V_1 : “Section 44. Compressibility / Table 4d-1. V/V_0 of Elements,” American Institute of Physics Handbook, Third Edition, McGraw-Hill, 1972, pp.4-38–4-45. Helium: Mao HK, Hemley RJ, Wu Y, Jephcoat AP, Finger LW, Zha CS, Bassett WA. High-pressure phase diagram and equation of state of solid helium from single-crystal X-ray diffraction to 23.3 GPa. Phys Rev Lett. 1988 Jun 20;60(25):2649-52; <https://legacy.gi.ciw.edu/static/users/rhemley/037MaoPRL1988.pdf>. Diamond: Cumberland RW, Weinberger MB, Gilman JJ, Clark SM, Tolbert SH, Kaner RB. Osmium diboride, an ultra-incompressible, hard material. J Am Chem Soc. 2005 May 25;127(20):7264-5; <http://tolbert.chem.ucla.edu/Publication/jacsmay2005.pdf>. Water-ice: Martin Chaplin, “Amorphous Ice and Glassy Water,” 9 May 2017; http://www1.lsbu.ac.uk/water/amorphous_ice.html.

Table 44. Approximate pressure energy storage in the solid chemical elements, when compressed to $\Delta P = 10$ GPa ($\sim 100,000$ atm)

Material	Initial Density ρ_1 (kg/L)	Compressed Density ρ_2 (kg/L)	Volume Compressibility V_2/V_1	Stored Specific Energy E_s (MJ/kg)	Stored Energy Density E_D (MJ/L)	Axial Strain Energy Density E_D' (MJ/L)	Bulk Modulus Energy Density E_D'' (MJ/L)
He	0.187	0.834	0.224	9.30	7.76	---	---
Cs @ 25 °C	1.930	5.245	0.368	1.21	6.32	---	---
Rb @ 25 °C	1.532	3.260	0.470	1.63	5.30	---	---
K	0.862	1.727	0.499	2.90	5.01	---	---
Ice (H ₂ O)	0.917	1.630	0.562	2.68	4.38	9.88	---
Ba	3.510	6.094	0.576	0.70	4.24	6.68	9.04
Na	0.968	1.608	0.602	2.48	3.98	8.31	13.18
Ce	6.770	10.304	0.657	0.33	3.43	2.24	3.46
Li	0.534	0.798	0.669	4.15	3.31	15.25	6.79
Ca	1.550	2.217	0.699	1.36	3.01	3.58	4.21
Se @ 25 °C	4.390	6.254	0.702	0.48	2.98	7.12	8.58
S @ 25 °C	2.070	2.855	0.725	0.96	2.75	3.87	8.96
Te @ 25 °C	6.240	8.548	0.730	0.32	2.70	1.59	1.05
Bi @ 25 °C	9.780	13.270	0.737	0.20	2.63	2.12	2.19
P (black)	2.690	3.375	0.797	0.60	2.03	1.20	5.70
La	6.162	7.722	0.798	0.26	2.02	1.69	2.24
Pr	6.770	8.379	0.808	0.23	1.92	1.35	2.13
Sm	7.520	9.284	0.810	0.20	1.90	1.23	1.62
Sb @ 25 °C	6.697	8.237	0.813	0.23	1.87	1.12	1.46
Nd	7.010	8.549	0.820	0.21	1.80	1.49	1.91
Tl	11.850	14.294	0.829	0.12	1.71	7.54	1.40
In @ 25 °C	7.310	8.702	0.840	0.18	1.60	5.41	1.69
Mg	1.738	2.057	0.845	0.75	1.55	1.31	1.31
Cd	8.650	10.165	0.851	0.15	1.49	1.18	1.40
Pb @ 25 °C	11.340	13.310	0.852	0.11	1.48	3.91	1.28
Zn	7.140	8.235	0.867	0.16	1.33	0.53	0.82
As	5.727	6.486	0.883	0.18	1.17	7.08	2.57
C (graphite)	2.267	2.564	0.884	0.45	1.16	2.05	1.71
Th	11.700	13.220	0.885	0.09	1.15	0.72	1.05
Pu	19.816	21.993	0.901	0.05	0.99	0.58	0.78
Zr	6.520	7.173	0.909	0.13	0.91	0.81	0.60
Al	2.700	2.954	0.914	0.29	0.86	0.78	0.72
Mn	7.210	7.880	0.915	0.11	0.85	0.28	0.46
Ge	5.323	5.805	0.917	0.14	0.83	0.68	0.73
Ti	4.506	4.814	0.936	0.13	0.64	0.46	0.49
Si	2.329	2.475	0.941	0.24	0.59	0.30	0.53
U	19.100	20.298	0.941	0.03	0.59	0.26	0.53
Be	1.850	1.962	0.943	0.29	0.57	0.18	0.41
C (diamond)	3.515	3.590	0.979	0.06	0.21	0.05	0.12

As a simple reality check, the second rightmost column in **Table 44** reports the axial strain energy⁹⁰³ that occurs when an isotropic elastic rod is axially compressed by a change in pressure ΔP , adjusted to the higher density of the post-compression rod, with $E_D' = [(1/2) \Delta P^2 / E_{rod}] / (V_2/V_1)$, where E_{rod} is Young's modulus for linear stress.⁹⁰⁴ The rightmost column in **Table 44** reports a similar energy density E_D'' calculated with the same formula⁹⁰⁵ but using the bulk modulus⁹⁰⁶ for uniform compression of a 3D block of material on all sides. Given the data inconsistencies and the crude approximations employed here, the reasonably close agreement among the three energy density estimates E_D , E_D' , and E_D'' is remarkable. Note that other kinds of mechanical strain can be imposed on solids to store energy in them, including bending, shearing, and torsion stresses – alternate forms of mechanical energy storage that are reviewed in **Section 5.2**, below.

Energy density can also be stored in solids via tensile pressure (negative pressure) loading, but to a lesser degree in part because the compressive strength for materials is generally higher than their tensile strength. For example, diamond has an estimated tensile strength of ~100 GPa which is 2-4 times lower than its calculated uniaxial ideal compressive strengths of 223.1 GPa (C(100) crystal lattice face), 469.0 GPa (C(110) face), and 470.4 GPa (C(111) face).⁹⁰⁷

Tensile pressure storage is also less effective because isotropic solid materials, when elastically stretched in one direction, tend to contract in the directions transverse to the direction of stretching, reducing the increase in volume that otherwise might occur. (If stretched in tension beyond the yield stress, the material permanently deforms plastically, rendering some of the stored energy unrecoverable.) For small changes in length (L) during stretching, the relative change in volume $\Delta V/V \sim (1 - 2\nu) (\Delta L/L) \sim 0$ for a Poisson ratio $\nu = 0.5$ (resulting in zero tensile energy storage due to zero volume change upon application of tensile pressure) and $\Delta V/V \sim \Delta L/L$ for a Poisson ratio $\nu = 0$ (volume change equal to relative length change upon application of

⁹⁰³ https://en.wikipedia.org/wiki/Strain_energy.

⁹⁰⁴ Data sources for Young's modulus: <http://www.periodictable.com/Properties/A/YoungModulus.html>; <http://www.nanomedicine.com/NMI/Tables/9.3.jpg>; P: <https://arxiv.org/abs/1503.00200>; Ge: http://www.knowledgedoor.com/2/elements_handbook/germanium.html; S: http://www.knowledgedoor.com/2/elements_handbook/sulfur.html; water-ice: <http://www.lpi.usra.edu/meetings/europa2004/pdf/7005.pdf>.

⁹⁰⁵ Dana Swift, "Calculation of Potential Energy Stored in Compressed Water," Pressure Test Vessel Operations Guidelines, 4 Feb 2004; <http://runt.ocean.washington.edu/swift/PTV-manual/node27.html>.

⁹⁰⁶ Bulk modulus data sources: <http://www.periodictable.com/Properties/A/BulkModulus.html>; In: <http://documents.indium.com/qdynamo/download.php?docid=358>; Ge: <https://en.wikipedia.org/wiki/Germanium>; Zr: <https://en.wikipedia.org/wiki/Zirconium>; Pu: <https://journals.aps.org/prb/abstract/10.1103/PhysRevB.71.172101>.

⁹⁰⁷ Luo X, Liu Z, Xu B, Yu D, Tian Y, Wang HT, He J. Compressive Strength of Diamond from First-Principles Calculation. J Phys Chem C. 2010 Oct 21;41(114):17851-3; https://www.researchgate.net/profile/Xiaoguang_Luo/publication/225376850_Compressive_Strength_of_Diamond_From_First-Principles_Calculation/links/0fcfd5126365a800dc000000.pdf.

tensile pressure, and energy storage levels like those tabulated in **Table 44**, adjusted for the lower material tensile strength, become available).⁹⁰⁸

In general, $\Delta V/V > 0$ and a material undergoing tensile elastic deformation exhibits at least some increase in volume and thus stores some “PV” energy. Most engineering materials have $\nu = 0.2$ - 0.5 – for example, $\nu \sim 0.21$ (Cr), 0.30 (carbon steel), 0.31 (graphite), and 0.4999 (natural rubber) – with only a few very hard materials such as α -beryllium ($\nu \sim 0.02$ - 0.12), cubic boron nitride ($\nu \sim 0.14$ - 0.18), and diamond ($\nu \sim 0.07$ - 0.10) falling outside this range.⁹⁰⁹ For diamond, $\Delta V/V \sim 0.8$ ($\Delta L/L$) so we might estimate tensile $E_D \sim (0.8) (0.21 \text{ MJ/L}) (100 \text{ GPa} / 470.4 \text{ GPa}) \sim \mathbf{0.035 \text{ MJ/L}}$.

The energy that can be stored in materials due to thermomechanical stress is reviewed in **Section 5.4**, below.

⁹⁰⁸ https://en.wikipedia.org/wiki/Poisson's_ratio#Volumetric_change.

⁹⁰⁹ Mott PH, Roland CM. Limits to Poisson's ratio in isotropic materials. Phys Rev B. 2009 Oct 20;80:132104; http://polymerphysics.net/pdf/PhysRevB_80_132104_09.pdf.

5.1.2 Compression of Liquids

Like solids, liquids have poor compression energy densities because they are largely incompressible and cannot store much “PV” energy. Mercury is the least compressible liquid in the temperature range -30 °C to +200 °C; glycerine is one of the least compressible organic liquids.⁹¹⁰

Following **Section 5.1.1**, we approximate the specific energy as $E_S \sim (\Delta P / \rho_2) (\Delta V / V_1) = (\Delta P / \rho_2) (1 - V_2 / V_1)$ and the energy density as $E_D \sim (\Delta P) (\Delta V / V_1) = (\Delta P) (1 - V_2 / V_1)$, stored due to pressurization in a liquid that is compressed from pressure P_1 to P_2 ($\Delta P = P_2 - P_1$), causing the liquid to shrink in volume from V_1 to V_2 ($\Delta V = V_1 - V_2$) and increasing its density from ρ_1 to ρ_2 .

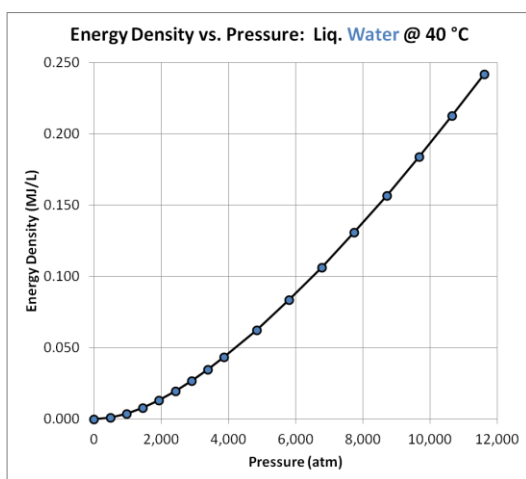


Table 45 tabulates the estimated stored pressure energy in a few pure liquids at ~1 GPa (~10,000 atm).⁹¹¹ At this pressure, the range of energy density is only **0.03-0.3 MJ/L**.

The chart at left shows that the compression storage energy density for liquid water at 40 °C as a function of pressure becomes almost linear above ~7,000 atm. Above ~10,000 atm, the relative volume change with pressure for all liquids is about the same.⁹¹² At ~13,900 atm, 40 °C water solidifies to Ice VI.⁹¹³ Temperature effects are relatively modest. If water is cooled from 100 °C to 0 °C at ~2000 atm pressure, the resulting

increase in density is about the same as for a ~1500 atm pressure increase at 40 °C, equivalent to just a minor change in energy density of ~**0.04 MJ/L**.

So much for liquid compression. What about liquid tension? Capillary flow⁹¹⁴ of liquids in narrow tubes is caused by the interaction between the surface tension in the liquid (due to internal molecular cohesion) and the adhesive forces between the liquid and tube walls. For example, the smallest reasonable glass nanocapillary with a radius of 2 nm dipped into pure water could generate an estimated capillary pressure of ~700 atm (~**0.07 MJ/L**).⁹¹⁵

⁹¹⁰ American Institute of Physics Handbook, Third Edition, McGraw-Hill, 1972, p. 2-168.

⁹¹¹ Data source: American Institute of Physics Handbook, Third Edition, McGraw-Hill, 1972, pp. 2-171 to 2-181.

⁹¹² American Institute of Physics Handbook, Third Edition, McGraw-Hill, 1972, p. 2-168.

⁹¹³ [https://en.wikipedia.org/wiki/Water_\(data_page\)#Phase_diagram](https://en.wikipedia.org/wiki/Water_(data_page)#Phase_diagram).

⁹¹⁴ https://en.wikipedia.org/wiki/Capillary_action.

⁹¹⁵ Freitas RA Jr. Nanomedicine, Volume I: Basic Capabilities, Landes Bioscience, Georgetown TX, 1999, p. 279; <http://www.nanomedicine.com/NMI/9.2.4.htm#p6>.

Table 45. Approximate pressure energy storage in pure liquids, when compressed to $\Delta P \sim 1$ GPa ($\sim 10,000$ atm).

Material	Initial Density ρ_1 (kg/L)	Compressed Density ρ_2 (kg/L)	Volume Compressibility V_2/V_1	Stored Specific Energy E_S (MJ/kg)	Stored Energy Density E_D (MJ/L)
Octane @ 95 °C †	0.8905	1.2634	0.705	0.229	0.289
Diethyl ether @ 20 °C	0.9695	1.3550	0.715	0.213	0.288
Acetone @ 40 °C	0.9447	1.2975	0.728	0.212	0.276
Pentane @ 0 °C †	1.0000	1.3904	0.719	0.198	0.275
Methanol @ 20 °C	0.9768	1.2994	0.752	0.194	0.252
Ethanol @ 20 °C	0.9792	1.3036	0.751	0.193	0.252
Carbon disulfide @ 20 °C	0.9770	1.2863	0.760	0.189	0.244
Water (H₂O) @ 40 °C †	0.9922	1.2216	0.812	0.151	0.184
Heavy water (D ₂ O) @ 40 °C †	1.1005	1.3563	0.811	0.136	0.185
Glycerine @ 50 °C †	0.9741	1.1167	0.872	0.112	0.125
Mercury (Hg) @ 10 °C	13.571	14.040	0.967	0.002	0.034

† 9,678 atm instead of 10,000 atm

Entirely aside from capillary forces, continuous liquids in tubes exhibit pure tensile strength due to molecular cohesion,⁹¹⁶ a phenomenon to which has been attributed the ability of tall trees to pull sap as high as 115 meters,⁹¹⁷ with a maximum recorded arboreal tensile pressure of 120 atm (~ 0.012 MJ/L).⁹¹⁸ It has been estimated that a continuous narrow column of water may exhibit a tensile strength on the order of ~ 300 atm (~ 0.03 MJ/L).⁹¹⁹

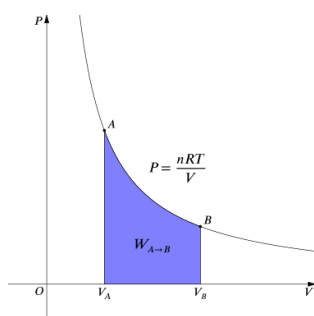
⁹¹⁶ Plesset MS. Tensile strength of liquids. Office of Naval Research, Report No. 85-47, April 1967; <http://authors.library.caltech.edu/46061/1/Report%20No.85-47.pdf>. Debenedetti PG. Physics of water: Stretched to the limit. Nature Physics. 2013 Jan 1;9(1):7-8; <https://www.nature.com/nphys/journal/v9/n1/full/nphys2496.html>.

⁹¹⁷ Holman RM, Robbins WW. A Textbook of General Botany, Second Edition, John Wiley & Sons, NY, 1928.

⁹¹⁸ Schlesinger WH, Gray JT, Gill DS, Mahall BE. *Ceanothus megacarpus* chaparral: a synthesis of ecosystem processes during development and annual growth. The Botanical Review. 1982 Jan 1;48(1):71-117; <https://link.springer.com/article/10.1007%2FBF02860536>. Zimmermann MH. Xylem Structure and the Ascent of Sap, Springer-Verlag, Berlin, 1983.

⁹¹⁹ Harvey NE, McElroy WD, Whiteley AH. On cavity formation in water. J Appl Phys. 1947 Feb;18(2):162-172; <http://aip.scitation.org/doi/abs/10.1063/1.1697598>. J.S. Rowlinson, B. Widom, Molecular Theory of Capillarity, Clarendon Press, Oxford, 1982.

5.1.3 Compression of Gases



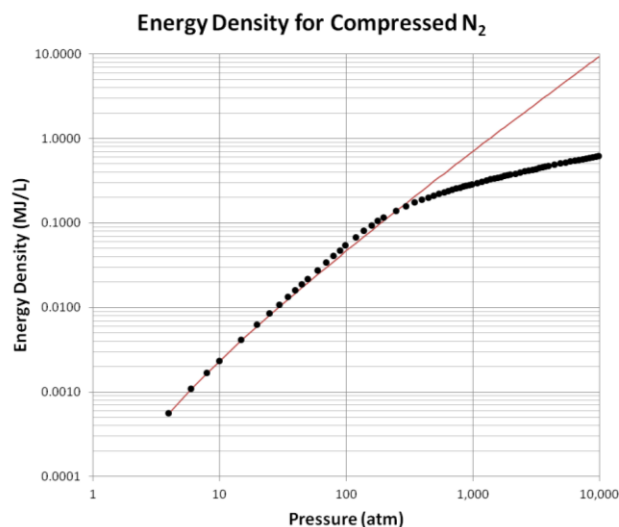
Gases can have a higher pressurized energy density than solids or liquids because they are more readily compressible. Consider a rigid container of volume V filled with n moles of a compressed ideal gas at pressure P and temperature T . Following an isothermal expansion process (wherein compression work could be completely recovered as expansion work with $\sim 100\%$ efficiency), the ideal gas law predicts that volume increases to V_{final} while the pressure decreases to P_{final} at constant temperature T . Since $PV = P_{\text{final}}V_{\text{final}} = nR_{\text{gas}}T$ (for universal gas constant R_{gas}), the reversible isothermal expansion work is the purple area under the PV curve at left,⁹²⁰ or:

$$W_{\text{exp}} = \int_V^{V_{\text{final}}} p \, dV = nR_{\text{gas}}T \int_V^{V_{\text{final}}} V^{-1} \, dV = nR_{\text{gas}}T \ln(V_{\text{final}}/V) = PV \ln(P/P_{\text{final}})$$

and the stored energy density in the gas container of volume V is $E_{D,\text{ideal}} = W_{\text{exp}}/V = P \ln(P/P_{\text{final}})$.

Most gases obey the ideal gas law to within a few percent at low pressure. But finite molecular volumes and intermolecular attractions cause significant deviation from the ideal gas law for real gases at high pressure – a real gas cannot compress to quite as small a volume as that predicted by the ideal gas law. For example, the published⁹²¹ molar volumes of nitrogen gas between 1-10,000 bar at 200 K allow us to calculate the actual ratio V_{final}/V for isothermal expansion at each pressure and then recalculate $E_D \sim P_{\text{equiv}} \ln(P/P_{\text{final}})$ to estimate the actual potential energy stored in compressed N_2 , where $P_{\text{equiv}} \sim P_{\text{final}}$ (V_{final}/V). This is shown in the chart at

right as a series of black data points, with the ideal gas prediction ($E_{D,\text{ideal}}$) indicated by a thin red line. Other gases show the same results at low pressures where they are all essentially ideal, and



⁹²⁰ Daniels F, Alberty RA. Physical Chemistry, Third Edition, John Wiley & Sons, 1966, pp. 34-36. See also: https://en.wikipedia.org/wiki/Compressed_air_energy_storage#Isothermal_Storage and https://en.wikipedia.org/wiki/Isothermal_process#Calculation_of_work.

⁹²¹ Jacobsen RT, Stewart RB. Thermodynamic properties of nitrogen including liquid and vapor phases from 63 K to 2000 K with pressures to 10,000 bar. J Phys Chem Ref Data. 1973 Oct;2(4):757-922; <https://srdata.nist.gov/JPCRD/jpcrd39.pdf>.

exhibit comparable falloffs in energy density at higher pressures. At 1000 atm real gases can store only about 50% of the ideal gas compression energy density, falling to ~5% at 10,000 atm (~0.65 MJ/L). Above 10,000 atm, gases don't compress very much more because they're already at near-liquid/solid density, hence can't store a lot more PV energy if further pressure is applied.

A few industrial-scale compressed air energy storage (CAES) systems are already in operation around the world. The first utility-scale CAES project in 1978 used an underground salt dome near the 290 MW Huntorf power plant in Germany,⁹²² and in 1991 a 110 MW plant with 26-hour storage capacity was built in McIntosh, Alabama, using a 540,000 m³ solution-mined salt cavern to store compressed air at up to 75 atm (~0.008 MJ/L).⁹²³ Both systems employ isothermal pressure storage. City-wide CAES distribution systems have been deployed in Europe and Argentina.⁹²⁴ On a smaller scale, compressed air has been used to provide onboard stored power to operate mining locomotives,⁹²⁵ trains,⁹²⁶ ships,⁹²⁷ aircraft,⁹²⁸ submarines,⁹²⁹ torpedoes,⁹³⁰ bazookas,⁹³¹ catapults,⁹³² rifles,⁹³³ brakes,⁹³⁴ hand tools,⁹³⁵ toys,⁹³⁶ postal delivery systems,⁹³⁷ logic circuits,⁹³⁸ and automobiles⁹³⁹ including at least one car powered by liquid nitrogen⁹⁴⁰ (though it is alleged⁹⁴¹ that carbon dioxide might provide slightly higher energy density in this application because CO₂ is more compressible than N₂ when it transitions from gaseous to supercritical form).

⁹²² “The Biggest, Strangest Batteries: Compressed Air in a Cavern,” New York Times, 3 Jun 2017; <https://www.nytimes.com/2017/06/03/business/energy-environment/biggest-batteries.html>.

⁹²³ https://en.wikipedia.org/wiki/Compressed_air_energy_storage#Storage_2.

⁹²⁴ https://en.wikipedia.org/wiki/Compressed_air_energy_storage#Transmission.

⁹²⁵ https://en.wikipedia.org/wiki/Fireless_locomotive.

⁹²⁶ https://en.wikipedia.org/wiki/Atmospheric_railway.

⁹²⁷ https://en.wikipedia.org/wiki/Compressed_air_energy_storage#Ships.

⁹²⁸ https://en.wikipedia.org/wiki/Victor_Tatin.

⁹²⁹ https://en.wikipedia.org/wiki/French_submarine_Plongeur.

⁹³⁰ https://en.wikipedia.org/wiki/Torpedo#Compressed_air.

⁹³¹ https://en.wikipedia.org/wiki/Holman_Projector.

⁹³² https://en.wikipedia.org/wiki/Aircraft_catapult#Steam_catapult.

⁹³³ https://en.wikipedia.org/wiki/Air_gun#Pneumatic.

⁹³⁴ [https://en.wikipedia.org/wiki/Air_brake_\(road_vehicle\)](https://en.wikipedia.org/wiki/Air_brake_(road_vehicle)).

⁹³⁵ https://en.wikipedia.org/wiki/Pneumatic_tool & https://en.wikipedia.org/wiki/Pneumatic_motor#Tools.

⁹³⁶ https://en.wikipedia.org/wiki/Water_rocket & https://en.wikipedia.org/wiki/Air_Hogs.

⁹³⁷ https://en.wikipedia.org/wiki/Pneumatic_tube#Pneumatic_post.

⁹³⁸ https://en.wikipedia.org/wiki/Pneumatic_circuit.

⁹³⁹ https://en.wikipedia.org/wiki/Compressed_air_car.

⁹⁴⁰ Knowlen C, Mattick AT, Bruckner AP, Hertzberg A. High efficiency energy conversion systems for liquid nitrogen automobiles. SAE Technical Paper 1998 Aug 11; <http://large.stanford.edu/publications/coal/references/docs/sae98.pdf>. See also: https://en.wikipedia.org/wiki/Liquid_nitrogen_engine.

⁹⁴¹ Oldenburg CM. Carbon dioxide as cushion gas for natural gas storage. Energy & Fuels. 2003 Jan 15;17(1):240-6; <http://www2.lbl.gov/ttd/publications/2570pub.pdf>.

It is worth noting that the work done by the creation and expansion of gaseous products during chemical explosions contributes relatively little to the total energy release, which is why we ignored this factor in our discussion of chemical explosives in **Section 4.2.1**. Consider an open-air explosion creating product gases that push back the air as they expand and cool, returning to ~ 1 atm ambient pressure at $T \sim 300$ K ambient temperature, representing a work energy of $W_{\text{gas}} \sim R_{\text{gas}}T \sim 2500$ J/mole.⁹⁴² As a representative example: The most common formulation of the decomposition reaction for TNT ($\text{C}_7\text{H}_5\text{N}_3\text{O}_6 \rightarrow 1.5 \text{ N}_2 + 3.5 \text{ CO} + 2.5 \text{ H}_2\text{O} + 3.5 \text{ C}$) liberates $n = 7.5$ moles of gas at detonation representing expansion work of only $nW_{\text{gas}} = 0.019$ MJ per mole of TNT, or just $\sim 2\%$ of the total 0.930 MJ per mole of TNT of chemical energy released during the explosion.

⁹⁴² [https://en.wikipedia.org/wiki/Strength_\(explosive\)](https://en.wikipedia.org/wiki/Strength_(explosive)).

5.1.4 Compression of Plasma

Because a plasma consists of charged particles that are electrostatically mutually repulsive, a relatively small number density of such particles trapped in a confined space can produce relatively large pressures. For example, a box with frozen neon walls at ~ 20 K measuring 110 nm on a side that contains only 207 protons ($\sim 1.6 \times 10^{17}$ protons/cm³) produces an electrostatic pressure of ~ 2 atm (**0.0002 MJ/L**; **Section 4.3.1.4**); those same protons, if suddenly converted to neutral hydrogen by adding one electron each (and ignoring molecular recombination), would exhibit a static gas pressure of only ~ 0.0004 atm at ~ 20 K, or ~ 5000 times less pressure than the electrostatic case.⁹⁴³

Charged ion plasmas are typically contained and compressed via magnetic fields. The strongest continuous magnetic field ($B \sim 45$ T) ever created in a lab⁹⁴⁴ can create a magnetic field pressure of $P_{\text{mag}} \sim B^2/2\mu_0 = 7930$ atm ($E_D = \mathbf{0.8 MJ/L}$), taking permeability constant $\mu_0 = 1.26 \times 10^{-6}$ henry/meter.⁹⁴⁵ The strongest nondestructive pulsed magnetic field (100 T) produced in a lab to date⁹⁴⁶ represents a magnetic field pressure energy density of **3.1 MJ/L**, and the strongest short-term (destructive) pulsed magnetic field (9000 T) ever created in a lab⁹⁴⁷ would represent an instantaneous magnetic field pressure energy density of **32,000 MJ/L**.

⁹⁴³ A similar box of singly-ionized He atoms under similar conditions would give the same results without having to “ignore” molecular recombination.

⁹⁴⁴ “World’s Most Powerful Magnet Tested Ushers in New Era for Steady High Field Research,” 17 Dec 1999; <http://legacywww.magnet.fsu.edu/mediacenter/news/pressreleases/1999december17.html>.

⁹⁴⁵ McMillan BF. The physics of fusion. Warwick University, 10 Feb 2014, p. 25; http://www2.warwick.ac.uk/fac/sci/physics/current/teach/module_home/px438/lecture_distributed_2014.pdf.

⁹⁴⁶ Pulsed Field Facility, National High Magnetic Field Laboratory, 28 Feb 2017; <https://nationalmaglab.org/user-facilities/pulsed-field-facility>.

⁹⁴⁷ “Z machine makes progress toward nuclear fusion,” 10 Oct 2014; <http://www.sciencemag.org/news/2014/10/z-machine-makes-progress-toward-nuclear-fusion>.

5.1.5 Acoustic Waves

Acoustic waves in solid, liquid, gaseous or plasma media can store a mechanical energy density E_D similar to the fairly modest values described in the preceding sections for most physical media. Acoustic energy density may be estimated by dividing the acoustic energy intensity $(I_{\text{sound}})^{948}$ by the speed of sound (v_{sound}), i.e., $E_D \sim I_{\text{sound}} / v_{\text{sound}}$. Using the decibel notation, $\text{dB} = 10 \log_{10}(I_{\text{sound}} / I_0)$, where $I_0 \sim 5 \times 10^{-13} \text{ W/m}^2$ in air and $I_0 \sim 1 \times 10^{-16} \text{ W/m}^2$ in water, hence $I_{\text{sound}} = I_0 \cdot 10^{\text{dB}/10}$ with $v_{\text{sound}} = v_{\text{air}} = 331.4 \text{ m/sec}$ for the speed of sound in STP air and $v_{\text{sound}} = v_{\text{water}} = 1482 \text{ m/sec}$ for the speed of sound in 20 °C fresh water.

Gas. The minimum audible sound intensity in dry STP air⁹⁴⁹ is 0 dB ($I_{\text{sound}} = 5 \times 10^{-13} \text{ W/m}^2$, $E_D = 1.5 \times 10^{-24} \text{ MJ/L}$), the threshold of acoustic pain for humans⁹⁵⁰ is 120 dB ($I_{\text{sound}} = 0.5 \text{ W/m}^2$, $E_D = 1.5 \times 10^{-12} \text{ MJ/L}$), and the maximum possible sound pressure in air⁹⁵¹ is 200 dB ($I_{\text{sound}} = 5 \times 10^7 \text{ W/m}^2$, $E_D = 0.00015 \text{ MJ/L}$).

Liquid. In medical ultrasound, the maximum safe acoustic power that may be applied to the human body continuously for unlimited durations is $P_{\text{acoustic}} \sim 1000 \text{ W/m}^2$.⁹⁵² Taking the speed of sound in human tissue as roughly the same as for water ($v_{\text{sound}} \sim 1482 \text{ m/sec}$), the energy density of the acoustic field during an ultrasound scan of maximum safe continuous intensity is $E_D \sim P_{\text{acoustic}} / v_{\text{sound}} = 6.7 \times 10^{-10} \text{ MJ/L}$. The maximum possible sound pressure in water is 280 dB ($I_{\text{sound}} = 1 \times 10^{12} \text{ W/m}^2$, $E_D = 0.67 \text{ MJ/L}$).

Solid. The maximum acoustic energy density that could be sustained in a rigid crystalline solid is bounded by the energy required to break the chemical bonds between the atoms in the solid – for example, estimated as $E_D \sim 28 \text{ MJ/L}$ and $E_S \sim 8 \text{ MJ/kg}$ for solid diamond lattice (**Section 5.2**).

As previously described elsewhere,⁹⁵³ power can also be transmitted by fluids inside physical tubes. For example, a virtually leakproof thick-walled fullerene nanotube measuring $2r_{\text{tube}} = 1 \mu\text{m}$ in diameter and $L_{\text{tube}} = 1$ meter long could safely transport pressurized fluid of absolute viscosity $\eta_{\text{tube}} = 6.9 \times 10^{-4} \text{ kg/m-sec}$ (310 K water)⁹⁵⁴ at a fluid pressure $p_{\text{tube}} = 5 \text{ atm}$ to drive a mechanical turbine or valved reciprocating piston system, establishing an continuous (DC) energy density of

⁹⁴⁸ https://en.wikipedia.org/wiki/Sound_intensity#Sound_intensity_level.

⁹⁴⁹ https://en.wikipedia.org/wiki/Absolute_threshold_of_hearing.

⁹⁵⁰ https://en.wikipedia.org/wiki/Threshold_of_pain.

⁹⁵¹ https://en.wikipedia.org/wiki/Sound_pressure#Examples_of_sound_pressure.

⁹⁵² American Institute of Ultrasound in Medicine, “Bioeffects considerations for the safety of diagnostic ultrasound,” J. Ultrasound Med. 7(September 1988):suppl. See also: “American Institute of Ultrasound in Medicine Guidelines,” J. Ultrasound Med. 11(April 1992):171-172.

⁹⁵³ Freitas RA Jr. Nanomedicine, Volume I: Basic Capabilities, Landes Bioscience, Georgetown TX, 1999; Sec. 6.4.3.3 “Hydraulic and Acoustic Tethers”; <http://www.nanomedicine.com/NMI/6.4.3.3.htm>.

⁹⁵⁴ Freitas RA Jr. Nanomedicine, Vol. I: Basic Capabilities, Landes Bioscience, Georgetown TX, 1999; Table 9.4; <http://www.nanomedicine.com/NMI/Tables/9.4.jpg>.

$E_{D,tube} = p_{tube} / L_{tube} = \mathbf{0.0005 \text{ MJ/L}}$ and delivering $P_{tube} = \pi r_{tube}^4 p_{tube}^2 / 8 \eta_{tube} L_{tube} \sim 10 \text{ pW}$ to a $V_{tube} = 1 \mu\text{m}^3$ nanorobot power plant at a fluid flow velocity of $v_{fluid} = r_{tube}^2 p_{tube} / 8 \eta_{tube} L_{tube} \sim 20 \mu\text{m/sec}$ and producing a continuous (DC) power density of $P_{D,tube} = P_{tube} / V_{tube} \sim \mathbf{0.01 \text{ MW/L}}$, assuming Poiseuille flow.⁹⁵⁵

Time-varying pressure waves (i.e., acoustic waves) can also transmit power. Consider a water-filled pipe with dimensions as defined in the previous paragraph which is excited at one end by a vibrating piston operating at a frequency $\nu_p \ll v_{sound}/r_{tube}$ ($\sim 3 \text{ GHz}$ for $2r_{tube} = 1 \mu\text{m}$). For such small tubes, the inertia and kinetic reaction of the fluid may be neglected in favor of the frictional force (e.g., Poiseuille flow),⁹⁵⁶ since the compressions and rarefactions of the fluid are practically isothermal⁹⁵⁷ because of the almost perfect heat conduction due to the small tube size.⁹⁵⁸ The power transmission is then given by $P_{trans} = P_0 \exp(-2 \alpha_{tube} L_{tube})$ (watts) with the attenuation coefficient given by Rayleigh's classical formulation⁹⁵⁹ $\alpha_{tube} = (8\pi \gamma \eta_{tube} \nu_p / \rho v_{sound}^2 r_{tube}^2)^{1/2}$, where P_0 is the input power, γ is the ratio of specific heats (1.004 for water, 1.009 for seawater), $v_{sound} = 1500 \text{ m/sec}$, and $\rho = 993.4 \text{ kg/m}^3$ for water at 310 K.⁹⁶⁰ Maximum energy transfer (as in a rigid bar) occurs at integral multiples of half-wavelengths of the incident sonic waves, in other words, at $\nu_p = n v_{sound} / 2 L_{tube}$, where $n = 1$ is the fundamental frequency or first harmonic, $n = 2$ is the first overtone or second harmonic, and so forth. Minimum attenuation occurs at $n = 1$, the first harmonic. Assuming a periodic source pulse must be of an intensity low enough to avoid cavitation in pure water ($P_{source} \leq 10^4 \text{ W/m}^2$),⁹⁶¹ then applying an input power of $P_{source} = 10^4 \text{ W/m}^2$ across a tube area of πr_{tube}^2 with $r_{tube} = 0.5 \text{ mm}$ and $L_{tube} = 1 \text{ m}$ produces an output power of $P_{trans} \sim 0.00578 \text{ W}$ at $\nu_p = n v_{sound} / 2 L_{tube} = 750 \text{ Hz}$ with $P_0 = \pi r_{tube}^2 P_{source} \sim 0.00785 \text{ W}$ and $\alpha_{tube} \sim 0.153 \text{ m}^{-1}$, representing a usable transferred power density of $P_{D,tube} \sim P_{trans} / \pi r_{tube}^2 L_{tube} \sim \mathbf{0.0000074 \text{ MW/L}}$ and a dissipated power density of $P_{D,diss} \sim (P_0 - P_{trans}) / \pi r_{tube}^2 L_{tube} \sim$

⁹⁵⁵ Freitas RA Jr. Nanomedicine, Vol. I: Basic Capabilities, Landes Bioscience, Georgetown TX, 1999; Sec. 9.2.5 "Pipe Flow"; <http://www.nanomedicine.com/NMI/9.2.5.htm>.

⁹⁵⁶ Freitas RA Jr. Nanomedicine, Vol. I: Basic Capabilities, Landes Bioscience, Georgetown TX, 1999; Eqn. 9.25; <http://www.nanomedicine.com/NMI/9.2.5.htm#Eqn9p25>.

⁹⁵⁷ https://en.wikipedia.org/wiki/Isothermal_process.

⁹⁵⁸ This is in contrast to typical sound waves in larger systems that are adiabatic (https://en.wikipedia.org/wiki/Adiabatic_process), with oscillations occurring faster than heat can be conducted from high to low pressure regions.

⁹⁵⁹ Stewart GW, Lindsay RB. Acoustics: A Text on Theory and Applications, D. Van Nostrand Company, New York, 1930. Wood AB. A Textbook of Sound, G. Bell and Sons Ltd., London, 1960.

⁹⁶⁰ Freitas RA Jr. Nanomedicine, Volume I: Basic Capabilities, Landes Bioscience, Georgetown TX, 1999; Sec. 6.4.3.3 "Hydraulic and Acoustic Tethers"; <http://www.nanomedicine.com/NMI/6.4.3.3.htm#2>.

⁹⁶¹ Freitas RA Jr. Nanomedicine, Vol. I: Basic Capabilities, Landes Bioscience, Georgetown TX, 1999; Sec. 6.4.1 "Acoustic Power Transmission"; <http://www.nanomedicine.com/NMI/6.4.1.htm>.

0.0000026 MW/L, yielding an $\epsilon_{\text{tube}} = P_{\text{trans}} / P_0 \sim 74\%$ transfer efficiency.⁹⁶² **Table 46** shows the usable transferred power density for a variety of water-filled tube radii and lengths.

Table 46. Usable transferred power density (MW/L) of longitudinal acoustic waves in a 310 K water-filled pipe of radius r_{tube} and length L_{tube}, with power input $P_{\text{source}} = 10^4 \text{ W/m}^2$ applied to the source end of the pipe; transfer efficiency ϵ_{tube} noted in parens.									
L_{tube}	r_{tube}								
	0.5 m	50 mm	5 mm	0.5 mm	50 μm	5 μm	0.5 μm	50 nm	5 nm
1 m	0.00001 (99.97%)	1×10^{-7} (99.7%)	1×10^{-7} (97.0%)	7×10^{-6} (73.7%)	5×10^{-7} (4.7%)				
0.1 m		1×10^{-6} (99.9%)	1×10^{-6} (99.0%)	0.00009 (90.8%)	0.00004 (38.0%)	6×10^{-9} (0.01%)			
10 mm			0.001 (99.7%)	0.001 (97.0%)	0.0007 (73.7%)	0.00005 (4.7%)			
1 mm				0.01 (99.0%)	0.009 (90.8%)	0.004 (38.0%)	6×10^{-7} (~0%)		
0.1 mm					0.1 (97.0%)	0.07 (73.7%)	0.005 (4.7%)		
10 μm						0.9 (90.8%)	0.4 (38.0%)	0.00006 (0.01%)	
1 μm							7.4 (73.7%)	0.5 (4.7%)	
0.1 μm								38 (38.0%)	0.006 (~0%)
10 nm									47 (5.0%)

Diamond rods can also make nearly lossless acoustic power transmission lines,⁹⁶³ in part because of the extreme stiffness of diamond. Consider a rod of volume V_{rod} at temperature T_{rod} , made of a material with a thermal coefficient of volume expansion β and constant-volume heat capacity C_V , to which a pressure pulse ΔP is applied at one end that travels at velocity $v_{\text{sound}} \sim 17,300 \text{ m/sec}$ (for diamond) to the other end at some frequency ν_{pulse} . In the worst-case thermodynamic cycle, the total energy dissipation per pulse ΔW_{max} due to thermoelastic damping of a mechanical compression wave⁹⁶⁴ is a modest $\Delta W_{\text{max}} = T_{\text{rod}} V_{\text{rod}} \beta^2 \Delta P^2 / C_V = 2 \times 10^{-6} \text{ zJ/cycle}$ when a $\Delta P = 1$

⁹⁶² A three-phase “alternating current” acoustical power transmission system using 100 Hz waves traversing three water-filled pipes was patented by M. Constantinesco in 1920. Wood AB. A Textbook of Sound, G. Bell and Sons Ltd., London, 1960.

⁹⁶³ Freitas RA Jr. Nanomedicine, Vol. I: Basic Capabilities, Landes Bioscience, Georgetown TX, 1999; Sec. 7.2.5.3 “Acoustic Cables and Transmission Lines”; <http://www.nanomedicine.com/NMI/7.2.5.3.htm>.

⁹⁶⁴ Drexler KE. Nanosystems: Molecular Machinery, Manufacturing, and Computation, John Wiley & Sons, NY, 1992; Sec. 7.4.1 “Thermoelastic damping”; http://e-drexler.com/d/09/00/Drexler_MIT_dissertation.pdf.

atm ($\Delta E_{\text{pulse}} = \Delta P^2 A_{\text{rod}} / 2 \rho_{\text{diam}} v_{\text{sound}} v_{\text{pulse}} \sim 8 \times 10^{-3} \text{ zJ/cycle}$) input pulse is applied to a diamond rod 1 μm in length and 10 nm x 10 nm in width (cross-sectional area $A_{\text{rod}} = 10^{-16} \text{ m}^2$; volume $V_{\text{rod}} \sim 10^{-22} \text{ m}^3$) at $v_{\text{pulse}} = 1 \text{ GHz}$, with $\rho_{\text{diam}} = 3510 \text{ kg/m}^3$, $\beta = 3.5 \times 10^{-6} \text{ K}^{-1}$ and $C_V = 1.7 \times 10^6 \text{ J/K-m}^3$ for diamond at $T_{\text{rod}} = 310 \text{ K}$. In the above example, the usable transferred power density is $P_{\text{D,rod}} = (\Delta E_{\text{pulse}} - \Delta W_{\text{max}}) v_{\text{pulse}} / V_{\text{rod}} \sim \mathbf{0.08 \text{ MW/L}}$. Under smooth mechanical cycling, nanomechanical systems may approach the isothermal limit and significantly reduce dissipation still further to $\sim 1\% \Delta W_{\text{max}}$ at $\sim 1 \text{ GHz}$.⁹⁶⁵

⁹⁶⁵ Drexler KE. Nanosystems: Molecular Machinery, Manufacturing, and Computation, John Wiley & Sons, NY, 1992; Sec. 7.4.1 "Thermoelastic damping"; http://e-drexler.com/d/09/00/Drexler_MIT_dissertation.pdf.

5.2 Springs

A simple helical spring of mass m_{spring} made of a material of density ρ_{spring} having a spring constant k_{spring} can be linearly compressed or extended by a distance x_{displace} by applying a force of $F = -k_{\text{spring}}x_{\text{displace}}$, storing potential energy $E_{\text{spring}} = (1/2) k_{\text{spring}} x_{\text{displace}}^2$ with a specific energy of $E_S = E_{\text{spring}} / m_{\text{spring}} = k_{\text{spring}} x_{\text{displace}}^2 / 2m_{\text{spring}}$ and an energy density of $E_D = \rho_{\text{spring}} E_S = \rho_{\text{spring}} k_{\text{spring}} x_{\text{displace}}^2 / 2m_{\text{spring}}$. Such a “Hooke’s Law” spring⁹⁶⁶ applies to any type of linear spring kept within its elastic limit (i.e., not stretched or compressed beyond the point of permanent deformation). Energy density is maximized by using spring materials with the highest possible spring constant (i.e., the stiffest possible spring). For example, a simple stainless steel coil spring of mass $m_{\text{spring}} = 1$ kg, density $\rho_{\text{spring}} = 7800$ kg/m³ and spring constant $k_{\text{spring}} = 100$ N/m that is displaced by $x_{\text{displace}} = 0.1$ m would store an energy density of $E_D = 4 \times 10^{-6}$ MJ/L ($\sim 5 \times 10^{-7}$ MJ/kg).

Conveniently, there is a widely-tabulated engineering parameter called the elastic modulus, aka. Young’s modulus Y , that measures stiffness as the applied stress (force per unit area) needed to produce a given strain (proportional linear deformation) in an elastic solid material.⁹⁶⁷ If we consider the strongest spring configuration⁹⁶⁸ – a simple tensioned bar or rod of length $L = L_{\text{spring}}$ and cross-sectional area $A = L_{\text{spring}}^2$ – then $k_{\text{spring}} = Y A / L = Y L_{\text{spring}}$ and energy density is:

$$E_D = k_{\text{spring}} x_{\text{displace}}^2 / 2 L_{\text{spring}}^3 = (1/2) Y \epsilon_{\text{spring}}^2$$

where fractional strain $\epsilon_{\text{spring}} = x_{\text{displace}}/L_{\text{spring}}$ and $Y =$ Young’s modulus.⁹⁶⁹ Assuming a moderate permissible linear elastic fractional strain of $\epsilon_{\text{spring}} \sim 10\%$ and taking $\rho_{\text{diamond}} = 3510$ kg/m³ and $Y = 1.05 \times 10^{12}$ N/m² for diamond (one of the stiffest materials with the highest known Young’s modulus),⁹⁷⁰ then $E_D = 5.3$ MJ/L and $E_S = E_D / \rho_{\text{diamond}} = 1.5$ MJ/kg. However, strains may be applied in three dimensions as well as in tension, shear, or torsion, so total energy storage may be somewhat higher. The fracture surface energy of the weakest {111} diamond plane is $E_{\text{fracture}} =$

⁹⁶⁶ https://en.wikipedia.org/wiki/Hooke's_law.

⁹⁶⁷ For example, in a simple compression coil spring, $k_{\text{spring}} = G d^4 / (8 n D^3)$, where the modulus of rigidity of the spring material $G = (Y/2) / (1 + \nu)$, $\nu =$ Poisson’s ratio of the spring material (https://en.wikipedia.org/wiki/Poisson%27s_ratio), $d =$ wire diameter, $D =$ mean coil diameter (= outer diameter – wire diameter), and $n =$ number of active coils, which is the number of coils subjected to flexure (always less than the total number of coils); https://www.engineersedge.com/spring_comp_calc_k.htm.

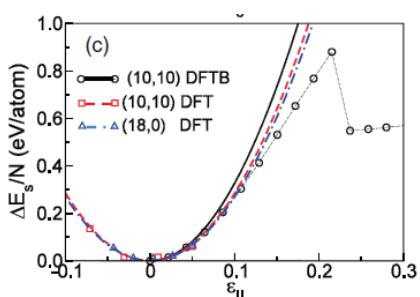
⁹⁶⁸ A tensioned rod produces maximum efficiency because all of the material is equally stressed. However, such springs are regarded as less practical “because of the inherent high stiffness, large loads, and small deflections associated with energy storage in direct tension members.” Collins JA, Busby HR, Staab GH. Mechanical Design of Machine Elements and Machines: A Failure Prevention Perspective, John Wiley & Sons, 2010, p. 584; <https://books.google.com/books?id=909-5C4eyUkC&pg=PA584>.

⁹⁶⁹ https://en.wikipedia.org/wiki/Elastic_energy.

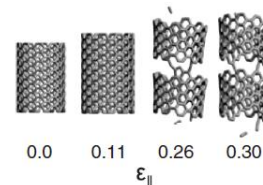
⁹⁷⁰ https://en.wikipedia.org/wiki/Young's_modulus#Approximate_values.

5.3 joules/m^2 ,⁹⁷¹ and the distance between $\{111\}$ planes is $L_{\text{plane}} \sim 0.24 \text{ nm}$ given that there are $\sim 1.8 \times 10^{19} \text{ bonds/m}^2$, so the theoretical maximum mechanical energy storage density in a maximally strained diamond block is $E_D \sim E_{\text{fracture}} / L_{\text{plane}} \sim \mathbf{22 \text{ MJ/L}}$ ($\sim \mathbf{6.3 \text{ MJ/kg}}$).

The maximum theoretical molecular limit for a **tensioned spring** may be estimated by evaluating the Morse potential of a single stretched covalent bond. For example, according to one reference,⁹⁷² a relaxed C-C bond between two carbon atoms ($m_{\text{C-C}} \sim 4 \times 10^{-26} \text{ kg}$) has a bond length of 152 pm whereas the same bond becomes mechanically unstable⁹⁷³ if stretched to 187 pm, beyond which it breaks. The Morse potential energy for the covalent bond between two carbon atoms at this fully-stretched limit ($\epsilon_{\text{spring}} \sim 23\%$) is 138 zJ, implying a maximum energy density $E_D = (1/2) Y \epsilon_{\text{spring}}^2 \sim \mathbf{28 \text{ MJ/L}}$ at maximum specific energy $E_S = E_D / \rho_{\text{diamond}} \sim \mathbf{8 \text{ MJ/kg}}$.



Similar results are obtained using density functional theory (DFT and DFTB) quantum chemistry simulations⁹⁷⁴ of a single-walled (10,10) carbon nanotube that is stretched to the maximum elastic limit of $\epsilon_{\parallel} \sim 12\%$ stretch strain, storing up to $\sim 0.47 \text{ eV}$ per atom of mechanical stretch energy (chart, left) or a specific energy of $E_S \sim \mathbf{3.8 \text{ MJ/kg}}$ ($E_D \sim \mathbf{4.9 \text{ MJ/L}}$, assuming $\rho_{\text{nanotube}} \sim 1.3$



kg/L); nanotubes stretched to 26% strain break up (images, right). **Compressed springs** yield energy storage of similar magnitude, with close-packed nanotube arrays storing up to $\sim 0.58 \text{ eV/atom}$ in the elastic limit,⁹⁷⁵ or $E_S \sim \mathbf{4.6 \text{ MJ/kg}}$ ($E_D \sim \mathbf{6.0 \text{ MJ/L}}$).

Torsion springs can also provide relatively high energy storage. A torsion spring can be a simple rod clamped at one end that is twisted within the elastic limit through a circumferential amplitude of ΔX , storing Hooke's Law torsional energy of $E_{\text{rod}} = (1/2) k_{\text{torsion}} \theta^2$. Stored strain energy per unit volume, or energy density, is $E_D \sim (C_F / 2) \epsilon_{\text{torsion}}^2 G$ for a material with shear

⁹⁷¹ Field JE. Chapter 9. Strength and Fracture Properties of Diamond. In: Field JE (ed). The Properties of Diamond, Academic Press, NY, 1979.

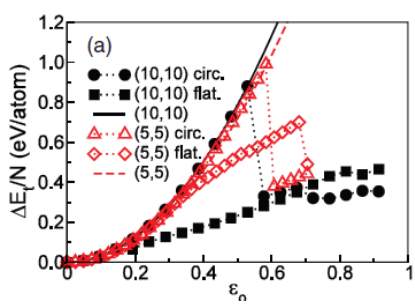
⁹⁷² Drexler KE. Nanosystems: Molecular Machinery, Manufacturing, and Computation, John Wiley & Sons, New York, 1992, Sec. 3.3.3 "Molecular mechanics"; http://e-drexler.com/d/09/00/Drexler_MIT_dissertation.pdf.

⁹⁷³ This is the inflection point in the stiffness, beyond which the stiffness becomes negative.

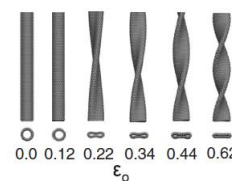
⁹⁷⁴ Fthenakis ZG, Zhu Z, Teich D, Seifert G, Tománek D. Limits of mechanical energy storage and structural changes in twisted carbon nanotube ropes. Phys Rev B. 2013 Dec 2;88(24):245402; <http://www.pa.msu.edu/cmp/csc/eprint/DT225.pdf>.

⁹⁷⁵ Fthenakis ZG, Zhu Z, Teich D, Seifert G, Tománek D. Limits of mechanical energy storage and structural changes in twisted carbon nanotube ropes. Phys Rev B. 2013 Dec 2;88(24):245402; <http://www.pa.msu.edu/cmp/csc/eprint/DT225.pdf>.

modulus G and a geometry-based form coefficient C_F .⁹⁷⁶ Taking $G = 5 \times 10^{11} \text{ N/m}^2$, density $\rho_{\text{diamond}} = 3510 \text{ kg/m}^3$ for solid diamond and assuming a moderate permissible fractional torsion strain $\epsilon_{\text{torsion}} \sim 20\%$, then $E_D = 5 \text{ MJ/L}$ and $E_S = E_D / \rho_{\text{diamond}} = 1.4 \text{ MJ/kg}$ for a solid cylindrical torsion bar with $C_F \sim 0.50$. A thin-walled cylindrical torsion tube has $C_F \sim 0.90$,⁹⁷⁷ giving $E_D = 9 \text{ MJ/L}$ and $E_S = 2.6 \text{ MJ/kg}$. A helical coiled spring using circular cross-section diamond wire has $C_F \sim 0.36$ in compression or extension, yielding only $E_D = 3.6 \text{ MJ/L}$ and $E_S = 1 \text{ MJ/kg}$; the same coil made of steel with $\epsilon_{\text{torsion}} \sim 20\%$ has $G \sim 8 \times 10^{10} \text{ N/m}^2$,⁹⁷⁸ yielding $E_S \sim 0.07 \text{ MJ/kg}$ and $E_D \sim 0.55 \text{ MJ/L}$ for $\rho \sim 7900 \text{ kg/m}^3$.⁹⁷⁹



According to density functional theory (DFTB) quantum chemistry simulations,⁹⁸⁰ a twisted single-walled carbon nanotube can store up to $\sim 0.85 \text{ eV}$ per atom of mechanical torsion energy (chart, left), equivalent to a specific energy $E_S \sim 6.8 \text{ MJ/kg}$, ($\sim 8.8 \text{ MJ/L}$ taking carbon nanotube density as $\sim 1.3 \text{ kg/L}$),⁹⁸¹ for nanotubes near the maximum elastic limit of $\epsilon_0 \sim 52\%$ twist strain for a (10,10) SWCNT where the cross-section



can remain circular; a flattened SWCNT (images, right) can only store about half as much energy per atom or per kg. Single-walled boron nitride nanotubes may exhibit similar torsional stiffness.⁹⁸²

As for **flexure springs**, bending deformations in the elastic regime apparently store much less mechanical energy than does tensioning, compression, or torsioning. A simple cantilever spring

⁹⁷⁶ Collins JA, Busby HR, Staab GH. Mechanical Design of Machine Elements and Machines: A Failure Prevention Perspective, John Wiley & Sons, 2010, p. 584; <https://books.google.com/books?id=909-5C4eyUkC&pg=PA584>.

⁹⁷⁷ “Thin tubes have good energy storage efficiency because the shearing stress is relatively uniform all across the wall. Solid members in bending or torsion have much lower energy storage efficiency because the central material is stressed to much lower levels.” Collins JA, Busby HR, Staab GH. Mechanical Design of Machine Elements and Machines: A Failure Prevention Perspective, John Wiley & Sons, 2010, p. 584; <https://books.google.com/books?id=909-5C4eyUkC&pg=PA584>.

⁹⁷⁸ https://en.wikipedia.org/wiki/Shear_modulus#Explanation.

⁹⁷⁹ https://en.wikipedia.org/wiki/Steel#Material_properties.

⁹⁸⁰ Fthenakis ZG, Zhu Z, Teich D, Seifert G, Tománek D. Limits of mechanical energy storage and structural changes in twisted carbon nanotube ropes. Phys Rev B. 2013 Dec 2;88(24):245402; <http://www.pa.msu.edu/cmp/csc/eprint/DT225.pdf>.

⁹⁸¹ “Mechanical properties of carbon nanotubes”; https://en.wikipedia.org/wiki/Mechanical_properties_of_carbon_nanotubes#Strength.

⁹⁸² Garel J, Leven I, Zhi C, Nagapriya KS, Popovitz-Biro R, Golberg D, Bando Y, Hod O, Joselevich E. Ultrahigh torsional stiffness and strength of boron nitride nanotubes. Nano Lett. 2012 Dec 12;12(12):6347-52; <http://www.weizmann.ac.il/materials/ernesto/pdfs/p48.pdf>.

with a rectangular cross-section beam has $C_F \sim 0.11$ with an energy density of $E_D \sim (C_F / 2) \epsilon_{\text{bending}}^2 Y = \mathbf{0.58 \text{ MJ/L}}$ and $E_S = E_D / \rho_{\text{diamond}} \sim \mathbf{0.16 \text{ MJ/kg}}$, taking $\rho_{\text{diamond}} = 3510 \text{ kg/m}^3$ and $Y = 1.05 \times 10^{12} \text{ N/m}^2$ for diamond, and assuming a moderate permissible linear elastic fractional strain of $\epsilon_{\text{bending}} \sim 10\%$; a flat-strip diamond cantilever has $C_F \sim 0.38$, yielding a somewhat higher strain energy density of $E_D \sim \mathbf{2 \text{ MJ/L}}$ and $E_S \sim \mathbf{0.6 \text{ MJ/kg}}$.⁹⁸³

Thin-walled tubes have higher geometry-based form coefficients than solid rods or beams.⁹⁸⁴ This is borne out by density functional theory (DFTB) quantum chemistry simulations⁹⁸⁵ on hollow-cylinder nanotubes, which reveal that a single-walled (10,10) carbon nanotube bent to the point of kinking at the elastic limit ($\epsilon_{\text{bending}} \sim 21\%$ bending strain) can store $\sim 0.17 \text{ eV}$ per atom of mechanical flexure energy, equivalent to a specific energy of $E_S \sim \mathbf{1.4 \text{ MJ/kg}}$ and $E_D \sim \mathbf{1.8 \text{ MJ/L}}$.

The strongest known material (from which the stiffest possible springs could be fashioned) is theorized to be “nuclear pasta” (neutron star crust material), with a shear modulus of 10^{29} - 10^{29} J/m^3 .⁹⁸⁶

⁹⁸³ Collins JA, Busby HR, Staab GH. Mechanical Design of Machine Elements and Machines: A Failure Prevention Perspective, John Wiley & Sons, 2010, pp. 584-5; <https://books.google.com/books?id=909-5C4eyUkC&pg=PA585>.

⁹⁸⁴ Gavin HP. “Strain Energy in Linear Elastic Solids”, CEE 201L. Uncertainty, Design, and Optimization, Duke University, Spring 2015; <http://people.duke.edu/~hpgavin/cee201/strain-energy.pdf>.

⁹⁸⁵ Fthenakis ZG, Zhu Z, Teich D, Seifert G, Tománek D. Limits of mechanical energy storage and structural changes in twisted carbon nanotube ropes. Phys Rev B. 2013 Dec 2;88(24):245402; <http://www.pa.msu.edu/cmp/csc/eprint/DT225.pdf>.

⁹⁸⁶ Caplan ME, Schneider AS, Horowitz CJ. The elasticity of nuclear pasta. Phys Rev Lett. 2018 Sep 28;121(13-28):132701; <https://arxiv.org/pdf/1807.02557.pdf>.

5.3 Kinetic Energy

Energy can readily be stored by a physical mass in motion.

Translational motion energy (**Section 5.3.1**) is stored in a mass that is traveling along a linear path at some velocity relative to the receiver device. Objects traveling at relativistic speeds can hold enormous amounts of energy, but are not very compact if the path length traveled during the time of storage is regarded as the size of the “storage device”.

Rotational motion energy (**Section 5.3.2**) confines the motion of a mass to a relatively small volume, hence permits more compact energy storage, e.g., as in flywheels. However, rotational energy storage capacity is limited by the maximum strength of materials that are capable of confining the moving mass to its more compact circulating trajectory.

5.3.1 Translational Motion

For a rest mass m (kg) of rest density ρ (kg/m³) traveling along a linear path in free space at a constant nonrelativistic velocity v (m/sec) $\ll c$, where $c = 2.99792458 \times 10^8$ m/sec (the speed of light *in vacuo*),⁹⁸⁷ the kinetic energy of the mass $K_{\text{trans}} = \frac{1}{2} mv^2$ (joules), hence the specific energy $E_S = K_{\text{trans}} / m = \frac{1}{2} v^2$ (MJ/kg) and the energy density $E_D = \rho E_S = \frac{1}{2} \rho v^2$ (MJ/L). Hence a chunk of diamond of density $\rho = \rho_{\text{diamond}} = 3510$ kg/m³ has a kinetic specific energy of **1 MJ/kg** at a velocity of $v = 1410$ m/sec and a kinetic energy density of **1 MJ/L** at $v = 750$ m/sec. Note that the kinetic specific energy and the kinetic energy density are both independent of the mass of the moving object.

For masses moving at high velocities where the assumption of $v \ll c$ does not hold, the corrected formula for relativistic kinetic energy must be used: $K_{\text{trans}} = mc^2 [(1 - v^2/c^2)^{-1/2} - 1]$.⁹⁸⁸ In this case, the relativistic kinetic specific energy becomes $E_S = 10^{-6} c^2 [(1 - v^2/c^2)^{-1/2} - 1]$ (MJ/kg). The relativistic kinetic energy density is $E_D = 10^{-9} \rho_{\text{rel}} c^2 [(1 - v^2/c^2)^{-1/2} - 1]$ (MJ/L), where relativistic density ρ_{rel} is related to the rest density ρ by $\rho_{\text{rel}} = \rho (1 - v^2/c^2)^{-1/2}$ since Lorentz length contraction of one dimension of the chunk parallel to its line of motion reduces the volume as velocity approaches the speed of light. (This definition of relativistic density, just one of several possible,⁹⁸⁹ may be described as “rest mass per unit observer-frame volume”.)

One author⁹⁹⁰ has proposed that fundamental particles have a maximum attainable velocity of $v_{\text{max}} = c (1 - (L_{\text{Planck}}^2 / \bar{\lambda}^2))^{1/2}$, where $\bar{\lambda}$ is the reduced Compton wavelength of the particle being accelerated and L_{Planck} is the Planck length (1.6×10^{-35} meter),⁹⁹¹ arguing that no fundamental particle can attain a relativistic mass higher than the Planck mass (2.2×10^{-8} kg)⁹⁹² and the Planck length is the shortest reduced Compton wavelength that we can observe from length contraction.

Table 47 gives the specific energy and energy density stored in a mass of solid diamond moving at various velocities. E_S and E_D can be increased by another factor of ~ 6 at any given velocity by switching from diamond to a denser material, e.g., osmium at $\rho = 22,600$ kg/m³.⁹⁹³ Translational energy density surpasses the best available energy density for chemical storage when velocity exceeds $\sim 10,000$ m/sec. Note that the kinetic energy of a mass traveling at 86.6% c is exactly

⁹⁸⁷ https://en.wikipedia.org/wiki/Speed_of_light.

⁹⁸⁸ Helliwell TM. An Introduction to Special Relativity. Allyn and Bacon, Boston, 1966, p. 85.

⁹⁸⁹ <https://physics.stackexchange.com/questions/151605/what-is-the-definition-of-density-in-a-relativistic-context>.

⁹⁹⁰ Haug EG. The Ultimate Limits of the Relativistic Rocket Equation. The Planck Photon Rocket. Acta Astronaut. 2017 Jul;136:144-147; <https://www.sciencedirect.com/science/article/pii/S0094576517300371>.

⁹⁹¹ https://en.wikipedia.org/wiki/Planck_length.

⁹⁹² https://en.wikipedia.org/wiki/Planck_mass.

⁹⁹³ <https://en.wikipedia.org/wiki/Osmium>.

equal to its rest mass energy.⁹⁹⁴ Thus the impact of a mass moving at 0.866 c with a stationary object can release as much energy as if that mass was unmoving but experienced “total conversion” to energy in the manner of a perfectly efficient matter-antimatter explosion (**Section 7.6.1**).

Table 47. Relativistic kinetic specific energy and kinetic energy density for a linearly translating chunk of diamond in free space with velocity v and density $\rho = 3510 \text{ kg/m}^3$.

Velocity of Diamond Chunk v			Stored Specific Energy E_s	Stored Energy Density E_D
(m/sec)	(km/hr)	(% of c)	(MJ/kg)	(MJ/L)
1	3.6	3.34×10^{-7}	5.00×10^{-7}	1.76×10^{-6}
10	36	3.34×10^{-6}	5.00×10^{-5}	1.76×10^{-4}
100	360	3.34×10^{-5}	5.00×10^{-3}	1.76×10^{-2}
1000	3600	3.34×10^{-4}	0.500	1.76
3292	11,850	1.10×10^{-3}	5.419 *	19
10,000	36,000	3.34×10^{-3}	50	176
100,000	360,000	3.34×10^{-2}	5000	17,600
1,000,000	3,600,000	0.334	5.00×10^5	1.76×10^6
3,940,000	14,200,000	1.31	7.78×10^6 †	2.73×10^7
10,000,000	36,000,000	3.34	5.00×10^7	1.76×10^8
100,000,000	360,000,000	33.4	5.46×10^9	2.03×10^{10}
149,896,229	539,626,424	50	1.39×10^{10}	5.64×10^{10}
259,620,269	934,632,966	86.6 **	8.94×10^{10}	6.31×10^{11}
269,813,212	971,327,564	90	1.16×10^{11}	9.39×10^{11}
296,794,533	1,068,460,320	99	5.47×10^{11}	1.36×10^{13}
299,492,666	1,078,173,596	99.9	1.92×10^{12}	1.51×10^{14}
299,762,479	1,079,144,924	99.99	6.27×10^{12}	1.56×10^{15}
299,789,460	1,079,242,056	99.999	2.00×10^{13}	1.57×10^{16}
299,792,158	1,079,251,770	99.999 9	6.34×10^{13}	1.57×10^{17}
299,792,428	1,079,252,741	99.999 99	2.01×10^{14}	1.58×10^{18}
299,792,455	1,079,252,838	99.999 999 ‡	6.35×10^{14}	1.58×10^{19}

* Specific energy of TNT (**Table 25**).

† Specific energy of Tsar Bomba, largest fusion bomb (58.6 MT) ever detonated (**Section 7.3.1**).

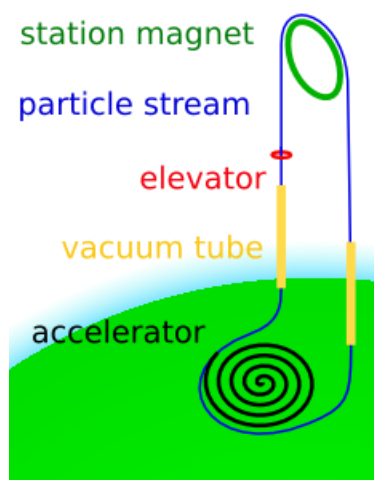
** Speed at which kinetic energy exactly equals rest mass energy (**Section 7.6.1**).

‡ Speed of the fastest man-made physical objects to date: the 6.5 TeV protons circulating in the Large Hadron Collider.⁹⁹⁵

⁹⁹⁴ Setting relativistic kinetic energy $mc^2 [(1 - v^2/c^2)^{-1/2} - 1]$ equal to rest mass energy mc^2 , or $mc^2 [(1 - v^2/c^2)^{-1/2} - 1] = mc^2$, implies $(1 - v^2/c^2)^{-1/2} - 1 = 1$, hence $v = 0.866 c$.

⁹⁹⁵ https://en.wikipedia.org/wiki/Large_Hadron_Collider#Design.

The energy represented in the kinetic energy of the moving mass can be extracted in many ways, including transfer of mechanical energy via elastic collision,⁹⁹⁶ conversion to heat energy via inelastic impact,⁹⁹⁷ conversion to electrical energy via deceleration of a high-velocity conductive metallic mass during axial transit through the coils of an electromagnetic mass driver,⁹⁹⁸ and so forth.



One interesting method for harvesting the kinetic energy in moving masses provides a possible alternative to space elevators,⁹⁹⁹ called the “space fountain” (image, left), a concept pioneered by Robert Forward.¹⁰⁰⁰ According to one description:¹⁰⁰¹ “A space fountain is a proposed form of an extremely tall tower extending into space. A stream of pellets is accelerated upwards at a ground station. At the top it is deflected downwards. The necessary force for this deflection supports the station at the top and payloads going up the structure. Spacecraft could launch from the top without having to deal with the atmosphere. This could reduce the cost of placing payloads into orbit. The lower part of the pellet stream has to be in a vacuum tube to avoid excessive drag in the atmosphere. Similar to the top station this tube can be supported by transferring energy from the upwards going stream

(slowing it) to the downwards going stream (accelerating it). Unlike a space elevator this concept does not need extremely strong materials anywhere and unlike space elevators and orbital rings it does not need a 40,000 km long structure.”

⁹⁹⁶ https://en.wikipedia.org/wiki/Elastic_collision.

⁹⁹⁷ https://en.wikipedia.org/wiki/Kinetic_bombardment.

⁹⁹⁸ <http://www.xenology.info/Xeno/21.4.1.htm>,
https://books.google.com/books?id=oxLBa_8tLHAC&pg=PA402.

⁹⁹⁹ https://en.wikipedia.org/wiki/Space_elevator.

¹⁰⁰⁰ Forward RL, *Starquake*, Del Rey Books, 1985; [https://en.wikipedia.org/wiki/Starquake_\(novel\)](https://en.wikipedia.org/wiki/Starquake_(novel)).
Forward RL, *Indistinguishable from Magic*, Baen Books, 1995;
<http://www.baen.com/chapters/W200602/0671876864.htm>.

¹⁰⁰¹ https://en.wikipedia.org/wiki/Space_fountain.

5.3.2 Rotational Motion

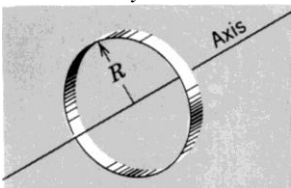
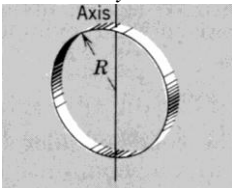
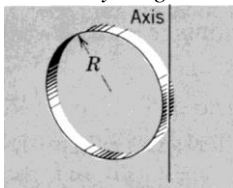
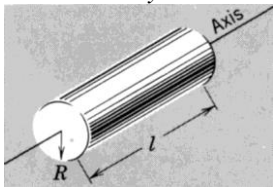
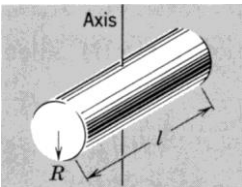
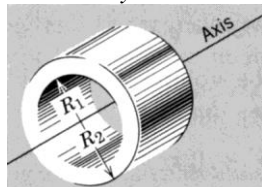
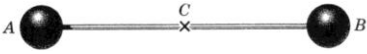
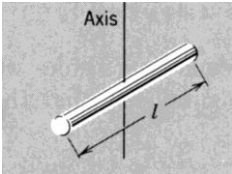
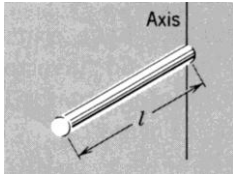
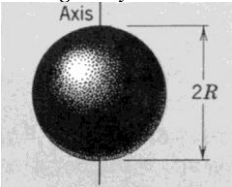
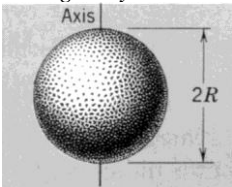
It is difficult to employ the kinetic energy of purely linear motion for energy storage in a compact physical system because of the potentially unlimited scale due to Newton's First Law of Motion. However, if the motion can be curved into a periodic or closed path like a circle, then in principle high velocities could be sustained in a relatively small volume of space, enabling more compact storage of kinetic energy by a mass in motion.¹⁰⁰² Gravitational forces (**Chapter 8**) and electrostatic forces (**Chapter 6**) are two well-known methods for curving the paths of moving masses. The motion of high-velocity masses can also be physically constrained inside curved tubes, tracks, or races, but frictional losses will usually be severe as the mass slides in direct contact with the surfaces that are constraining its motion. The ultimate limit of curved motion is rotation – in particular, the rotation of a high-velocity rigid or tethered mass around an axis or pivot point.

The kinetic energy of a rotating rigid body is $K_{\text{rot}} = (1/2) I_{\text{rot}} \omega^2$, where I_{rot} ($\text{kg}\cdot\text{m}^2$) is the rotational inertia (or moment of inertia) of a rotating body with respect to a particular axis of rotation, and ω is the angular speed of the rotation, measured in radians/sec, with $\omega = v_{\text{tang}} / R_{\text{rot}}$ where v_{tang} is the tangential or rim velocity of the rotating body and R_{rot} is the radial distance from the center of mass to the rim, and rotational frequency $\nu = \omega/2\pi$ (Hz).

Table 48 below gives formulas for the rotational inertia (I_{rot}), specific energy ($E_{\text{S,rot}}$), and energy density ($E_{\text{D,rot}}$) for a variety of common solids of mass M , radius R , length l , and uniform density ρ_{rot} .

¹⁰⁰² Note that electrical charges forced into circular or sinusoidal motion throw off electromagnetic energy, as observed in synchrotrons (https://en.wikipedia.org/wiki/Synchrotron_radiation) and free-electron lasers (https://en.wikipedia.org/wiki/Free-electron_laser).

Table 48. Rotational inertia, specific energy and energy density for various rigid solids

<p><i>Hoop, around cylinder axis</i></p>  $I_{\text{rot}} = M R^2$ $E_{\text{S,rot}} = (1/2) R^2 \omega^2$ $E_{\text{D,rot}} = (1/2) \rho_{\text{rot}} R^2 \omega^2$	<p><i>Hoop, around any diameter</i></p>  $I_{\text{rot}} = (1/2) M R^2$ $E_{\text{S,rot}} = (1/4) R^2 \omega^2$ $E_{\text{D,rot}} = (1/4) \rho_{\text{rot}} R^2 \omega^2$	<p><i>Hoop, around any tangent line</i></p>  $I_{\text{rot}} = (3/2) M R^2$ $E_{\text{S,rot}} = (3/4) R^2 \omega^2$ $E_{\text{D,rot}} = (3/4) \rho_{\text{rot}} R^2 \omega^2$
<p><i>Solid disk/cylinder, around disk/cylinder axis</i></p>  $I_{\text{rot}} = (1/2) M R^2$ $E_{\text{S,rot}} = (1/4) R^2 \omega^2$ $E_{\text{D,rot}} = (1/4) \rho_{\text{rot}} R^2 \omega^2$	<p><i>Solid disk/cylinder, around a central diameter</i></p>  $I_{\text{rot}} = (1/4) M R^2 + (1/12) M l^2$ $E_{\text{S,rot}} = (1/24) (3R^2 + l^2) \omega^2$ $E_{\text{D,rot}} = (1/24) \rho_{\text{rot}} (3R^2 + l^2) \omega^2$	<p><i>Annular ring/disk/cylinder, around cylinder axis</i></p>  $I_{\text{rot}} = (1/2) M (R_1^2 + R_2^2)$ $E_{\text{S,rot}} = (1/4) (R_1^2 + R_2^2) \omega^2$ $E_{\text{D,rot}} = (1/4) \rho_{\text{rot}} (R_1^2 + R_2^2) \omega^2$
<p><i>Barbell w/spherical masses A & B, around axis thru C normal to length</i></p>  <p>(bar has negligible mass)</p> $I_{\text{rot}} = M_A R_{AC}^2 + M_B R_{BC}^2$ $E_{\text{S,rot}} = I_{\text{rot}} \omega^2 / 2 (M_A + M_B)$ $E_{\text{D,rot}} = \rho_{\text{rot}} E_{\text{S,rot}}$	<p><i>Thin rod, around axis through center and normal to length</i></p>  $I_{\text{rot}} = (1/12) M l^2$ $E_{\text{S,rot}} = (1/24) l^2 \omega^2$ $E_{\text{D,rot}} = (1/24) \rho_{\text{rot}} l^2 \omega^2$	<p><i>Thin rod, around axis through one end and normal to length</i></p>  $I_{\text{rot}} = (1/3) M l^2$ $E_{\text{S,rot}} = (1/6) l^2 \omega^2$ $E_{\text{D,rot}} = (1/6) \rho_{\text{rot}} l^2 \omega^2$
<p><i>Solid sphere, through any diameter</i></p>  $I_{\text{rot}} = (2/5) M R^2$ $E_{\text{S,rot}} = (1/5) R^2 \omega^2$ $E_{\text{D,rot}} = (1/5) \rho_{\text{rot}} R^2 \omega^2$	<p><i>Thin spherical shell, through any diameter</i></p>  $I_{\text{rot}} = (2/3) M R^2$ $E_{\text{S,rot}} = (1/3) R^2 \omega^2$ $E_{\text{D,rot}} = (1/3) \rho_{\text{rot}} R^2 \omega^2$	

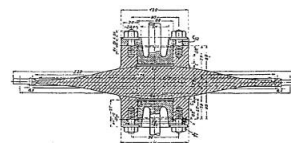
The most energy-dense storage configuration appears to be some form of mechanical flywheel. The maximum rotational energy that can be stored in a spinning flywheel depends on the physical properties of the flywheel material and the shape of the flywheel, with maximum energy density (E_D) for single-material isotropic rotors¹⁰⁰³ given by:

$$E_{Dmax} = K_{rotor} J_{rotor} \sigma_{rotor} / (\rho_{rotor} V_{rotor}) \\ \sim \sigma_{rotor} \text{ (J/m}^3\text{) (for a constant-stress disk)}$$

with maximum specific energy (E_S) of:

$$E_{Smax} = E_{Dmax} / \rho_{rotor} \text{ (J/kg)}$$

where K_{rotor} is the geometric shape factor of the rotor (typical range 0.3-1 m⁻²) which apparently reaches a theoretical maximum of 1.0 m⁻² for the constant-stress solid disk geometry (image, right),¹⁰⁰⁴ J_{rotor} is the rotor's moment of inertia (kg-m²), σ_{rotor} is the tensile strength of the rotor material, ρ_{rotor} is the density of the rotor material (kg/m³), and V_{rotor} is the volume of the rotor (m³). For a solid diamond rotor with an estimated maximum tensile strength of σ_{rotor} ($= \sigma_{diamond}$) \sim 90 GPa for tension parallel to the weakest [111] direction¹⁰⁰⁵ and density ρ_{rotor} ($= \rho_{diamond}$) \sim 3510 kg/m³, maximum flywheel energy density $E_{Dmax} \sim$ **90 MJ/L** and maximum flywheel specific energy $E_{Smax} \sim$ **25.6 MJ/kg**.¹⁰⁰⁶ These values are comparable to the best values for both chemical explosives (**Section 4.2.1**) and nonambient chemical combustion (**Section 4.2.2**), and almost as good as the best values for ambient chemical combustion (**Section 4.2.3**). Diamond rotors¹⁰⁰⁷ are also far superior to disks made of other materials such as standard carbon fiber¹⁰⁰⁸ (longitudinal ultimate tensile strength 1.5 GPa with



¹⁰⁰³ Genta G. Kinetic Energy Storage. Butterworth & Co. Ltd, London, 1985.

¹⁰⁰⁴ Genta G. Some considerations on the constant stress disc profile. Meccanica 1989 Dec;24(4):235-248; <https://link.springer.com/article/10.1007/BF01556455>.

¹⁰⁰⁵ DFT plane wave calculations suggest the maximum tensile strength for defect-free diamond is 225 GPa parallel to [100], 130 GPa parallel to [110], and 90 GPa parallel to [111]. Telling RH, Pickard CJ, Payne MC, Field JE. Theoretical strength and cleavage of diamond. Phys Rev Lett. 2000 May 29;84(22):5160-3; http://www.tcm.phy.cam.ac.uk/~cjp20/old/publications/PRL84_5160.pdf. A fracture tensile strength 60 GPa was first recorded experimentally 40 years ago. Ruoff AL, Wanagel J. High pressures on small areas. Science 1977 Dec 9;198:1037-8; <http://science.sciencemag.org/content/198/4321/1037.full.pdf>.

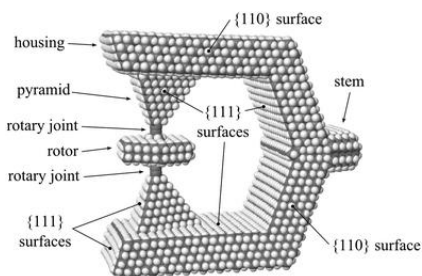
¹⁰⁰⁶ At this energy density, the rotor disc is nearly at its bursting rim speed of $v \sim 2^{1/2} (E_D/\rho)^{1/2} \sim$ 7000 m/sec.

¹⁰⁰⁷ A polyynes (-C≡C-C≡C-)n rod, if bent into a hoop and spun rapidly, could store up to the bond dissociation energy of a single C-C bond (~556 zJ), giving a theoretical maximum specific energy for a polyynes flywheel of ~28 MJ/kg, about the same as estimated for diamond. A hoop made of cumulene (=C=C=C=C-)n spinning at top speed might not break until the dissociation energy of the C=C double bond (1207 zJ) was surpassed, giving a theoretical maximum specific energy for a cumulene flywheel of ~61 MJ/kg, more than double the figure for diamond. However, the stability of large cumulene hoops is presently unknown.

¹⁰⁰⁸ http://www.performance-composites.com/carbonfibre/mechanicalproperties_2.asp.

density 1600 kg/m^3 , hence $E_{D\text{max}} \sim 1.5 \text{ MJ/L}$, $E_{S\text{max}} \sim 0.94 \text{ MJ/kg}$) or high-performance VectranTM UM fiber composite¹⁰⁰⁹ ($E_{D\text{max}} \sim 3.0 \text{ MJ/L}$, $E_{S\text{max}} \sim 2.1 \text{ MJ/kg}$), as well as conventional metals such as stainless steel ($E_{D\text{max}} \sim 2.0 \text{ MJ/L}$, $E_{S\text{max}} \sim 0.25 \text{ MJ/kg}$) and aluminum ($E_{D\text{max}} \sim 0.6 \text{ MJ/L}$, $E_{S\text{max}} \sim 0.21 \text{ MJ/kg}$).

In principle, flywheels can be rapidly charged and discharged, providing high peak power delivered mechanically through the rotor shaft. However, large frictional energy losses may occur in the bearings that support the spinning disk, an effect that becomes increasingly severe in flywheels reduced to micron size or smaller. For example, one published calculation¹⁰¹⁰ estimates that a diamond flywheel disk measuring $1 \mu\text{m}$ in diameter and $1.3 \mu\text{m}$ in height, riding on a well-designed 100 nm diameter diamond bearing, may lose half of its energy due to friction in the bearings in a half-life $\tau_{1/2} \sim 20 \text{ sec}$; an even smaller 400 nm (diam) \times 20 nm disk riding on a 20 nm (diam) diamond bearing loses half its stored energy in only $\tau_{1/2} \sim 0.35 \text{ sec}$.



This source of energy loss can be greatly reduced if the bearing is reduced in size to a single atom. Recent computational work by Hogg, Moses and Allis¹⁰¹¹ analyzed the frictional losses in a spinning diamond rotor supported by an acetylenic ($-\text{C}\equiv\text{C}-$) rotary joint (image, left) in which each face of the disk is bonded to the larger diamond housing through a single C-C bond.

The characteristic damping time for the rotational motion during free spindown is $\gamma^{-1} = J_{\text{disk}} / k_{\text{rd}}$ (sec), hence the energy half-life is $\tau_{1/2} \sim \gamma^{-1} \ln(2) = (J_{\text{disk}} / k_{\text{rd}}) \ln(2)$, where the rotor's moment of inertia $J_{\text{disk}} = M_{\text{disk}} R_{\text{disk}}^2 / 2$ and mass $M_{\text{disk}} = \pi R_{\text{disk}}^2 h_{\text{disk}} \rho_{\text{disk}}$ for a spinning disk of radius R_{disk} , height h_{disk} , and density $\rho_{\text{disk}} = \rho_{\text{diamond}} = 3510 \text{ kg/m}^3$, with a calculated rotational frictional drag coefficient $k_{\text{rd}} = 2.4 \times 10^{-35} \text{ kg-m}^2/\text{sec}$ for the acetylenic rotary joint when the device is operated at room temperature at $\sim 16 \text{ GHz}$. For the modeled rotor, $R_{\text{disk}} \sim 0.9 \text{ nm}$ and $h_{\text{disk}} \sim 0.45 \text{ nm}$, giving $M_{\text{disk}} \sim 4.24 \times 10^{-24} \text{ kg}$, $J_{\text{disk}} \sim 1.76 \times 10^{-42} \text{ kg-m}^2$, and $\gamma^{-1} \sim 70 \text{ nsec}$ as reported in the paper, yielding an energy half-life $\tau_{1/2} \sim 51 \text{ nsec}$. Taking $h_{\text{disk}} \sim R_{\text{disk}}$ for mathematical convenience in scaling, $\tau_{1/2} \sim \pi R_{\text{disk}}^4 h_{\text{disk}} \rho_{\text{disk}} \ln(2) / 2 k_{\text{rd}} \sim \pi R_{\text{disk}}^5 \rho_{\text{disk}} \ln(2) / 2 k_{\text{rd}} \sim (1.6 \times 10^{38}) R_{\text{disk}}^5$ for the modeled rotor.

Hence an acetylenic-mounted diamond flywheel with a serviceable energy half-life of $\tau_{1/2} \geq 10^5 \text{ sec}$ ($\sim 1 \text{ day}$) requires using a rotor of size $R_{\text{disk}} \geq 230 \text{ nm}$. (Larger rotors would leak energy through the acetylenic rotary joint even more slowly.) Rotor rotational frequency $\nu_{\text{disk}} \sim (E_D / \rho_{\text{disk}})^{1/2} / \pi R_{\text{disk}} \sim 7.0 \text{ GHz}$ for a $\sim 230 \text{ nm}$ disk spun up to the maximum rotational energy density of $E_D = 90 \text{ MJ/L}$ for diamond, very close to the maximum rotational frequency of $\sim 5 \text{ GHz}$ at which the stochastic method used in Hogg *et al.* is estimated to remain accurate.

¹⁰⁰⁹ <http://www.vectranfiber.com/properties/tensile-properties/>.

¹⁰¹⁰ Freitas RA Jr. Nanomedicine, Volume I: Basic Capabilities, Landes Bioscience, Georgetown TX, 1999, Sec. 6.2.2.2 "Flywheels"; <http://www.nanomedicine.com/NMI/6.2.2.2.htm#p7>.

¹⁰¹¹ Hogg T, Moses M, Allis D. Evaluating the friction in rotary joints in molecular machines. Mol Syst Des Eng. 2017;2:235-252; <http://pubs.rsc.org/en/content/articlehtml/2017/me/c7me00021a>.

Dynamic rotational stability must be carefully analyzed and engineered since flywheels (like gyroscopes) will tend to precess, nutate, or wobble in response to external forces.¹⁰¹² Large external lateral accelerations (e.g., sudden force shocks) applied to an acetylenic-mounted diamond flywheel could destroy the bearing, leading to catastrophic energy release,¹⁰¹³ and so should be avoided or ameliorated during the design and use of the system. Flywheel design must also avoid any frictional or other energy losses between the rotating mass and any housing in which it might be encased (also a major concern in the case of cables rotating inside sheaths¹⁰¹⁴), even in the case of noncontact magnetic¹⁰¹⁵ or electrostatic¹⁰¹⁶ bearings. Interestingly, the null energy condition¹⁰¹⁷ places a fundamental limit on the specific strength of any material,¹⁰¹⁸ which is bounded to be no greater than $c^2 \sim 9 \times 10^{16}$ N-m/kg where c is the speed of light. This limit is alleged to be achieved by electric and magnetic field lines, QCD flux tubes, and the fundamental strings hypothesized by string theory.¹⁰¹⁹

¹⁰¹² <http://farside.ph.utexas.edu/teaching/336k/Newtonhtml/node71.html>.

¹⁰¹³ Freitas RA Jr. Nanomedicine, Volume I: Basic Capabilities, Landes Bioscience, Georgetown TX, 1999, Sec. 6.2.2.2 “Flywheels”; <http://www.nanomedicine.com/NMI/6.2.2.2.htm#p11>.

¹⁰¹⁴ Freitas RA Jr. Nanomedicine, Volume I: Basic Capabilities, Landes Bioscience, Georgetown TX, 1999, Sec. 6.4.3.4 “Gear Trains and Mechanical Tethers”; <http://www.nanomedicine.com/NMI/6.4.3.4.htm#p2>.

¹⁰¹⁵ Owusu-Ansah P, Justice AF, Agyeman PK, Francis AT, Mensah RA. Effects of Operational Losses in Active Magnetic Bearing Designs. Intl J Engin Res Applic. 2016;6(4):01-04; <http://www.ingentaconnect.com/content/doi/22489622/2016/00000006/00000004/art00003> See also: https://en.wikipedia.org/wiki/Magnetic_bearing.

¹⁰¹⁶ Han F, Wu Q, Gao Z. Initial levitation of an electrostatic bearing system without bias. Sensors Actuators A: Phys. 2006 Aug 14;130-131:513-522; <http://www.sciencedirect.com/science/article/pii/S0924424705007168>.

¹⁰¹⁷ https://en.wikipedia.org/wiki/Energy_condition#Null_energy_condition.

¹⁰¹⁸ Brown AR. Tensile strength and the mining of black holes. Phys Rev Lett. 2013 Nov 22;111(21-22):211301; <https://arxiv.org/pdf/1207.3342v1.pdf>.

¹⁰¹⁹ https://en.wikipedia.org/wiki/Specific_strength#Fundamental_limit_on_specific_strength.

What is the highest flywheel rotational energy storage available using ordinary matter?¹⁰²⁰ Raw energy density can be boosted for a single-use application if diamond flywheels spun up to near-bursting velocity are subsequently combusted using ambient oxygen (**Section 4.2.3**) while still spinning. Maximum total energy density can then approach 90 MJ/L (rotational) + 115.6 MJ/L (ambient combustion, **Table 30**) = **205.6 MJ/L** and maximum total specific energy can approach 25.6 MJ/kg (rotational) + 32.9 MJ/kg (ambient combustion, **Table 29**) = **58.5 MJ/kg**. This energy density is comparable to the best explosives (**Section 4.2.1**) and ambient combustion fuels (**Section 4.2.3**), but the flywheels in this case are destroyed and cannot be re-used.

Torque power may also be transmitted via a long rotating rod or cable,¹⁰²¹ for instance using a “DC” strategy in which a driver end turns the cable at a constant rate (up to the bursting velocity) and the cable is maintained at constant torque (up to the shear strength limit). The maximum surface speed of a spinning diamond rod with radius $R_{\text{rod}} = 1 \mu\text{m}$, density $\rho_{\text{rod}} = 3510 \text{ kg/m}^3$ and conservative working stress $\sigma_w \sim 10^{10} \text{ N/m}^2$ (maximum of $\sim 1\%$ strain) is the bursting rim speed $v_{\text{burst}} = (\sigma_w / \rho_{\text{rod}})^{1/2} \sim 1700 \text{ m/sec}$ at a rotational frequency of $v_{\text{burst}} = \omega_{\text{burst}} / 2\pi = (v_{\text{burst}} / R_{\text{rod}}) / 2\pi \sim 270 \text{ MHz}$. Ignoring friction or other sources of energy dissipation caused by contact with cable sheaths or jackets, an isolated axially rotating rod (**Section 5.3.2**) of angular velocity $\omega_{\text{rod}} = 2\pi v_{\text{rod}}$ has a maximum energy density $E_{\text{D,rot,max}} = (1/4) \rho_{\text{rod}} R_{\text{rod}}^2 \omega_{\text{rod}}^2 = \pi^2 \rho_{\text{rod}} R_{\text{rod}}^2 v_{\text{rod}}^2 \sim (34,600) R_{\text{rod}}^2 v_{\text{rod}}^2 = \mathbf{2.5 \text{ MJ/L}} (\sim \mathbf{0.71 \text{ MJ/kg}})$ for $R_{\text{rod}} = 1 \mu\text{m}$ and $v_{\text{rod}} = v_{\text{burst}} = 270 \text{ MHz}$, regardless of length.

A static cable, secured at one end and twisted through a maximum angle θ_{max} at the other end, acquires at maximum stress an energy density $E_{\text{D,twist,max}} = \sigma_w^2 / G_{\text{rod}} \sim \mathbf{0.2 \text{ MJ/L}} (\sim \mathbf{0.06 \text{ MJ/kg}})$ for diamond shear modulus $G_{\text{rod}} = 5 \times 10^{11} \text{ N/m}^2$ and $\sigma_w \sim 10^{10} \text{ N/m}^2$, with $\theta_{\text{max}} = 2 L_{\text{rod}} \sigma_w / G_{\text{rod}}$ $R_{\text{rod}} = 40$ radians (~ 6.4 complete turns) for $R_{\text{rod}} = 1 \mu\text{m}$ and $L_{\text{rod}} = 1 \text{ mm}$. Thus we see that ~ 10 times more energy can be stored in constant rotational energy than as twist energy in a mechanical cable system.

But now repeat the twist-and-release at some frequency v_{AC} , resulting in the propagation of a repeating torsion wave that looks locally like a shear wave. This “AC” strategy may be thought of as the propagation of a shear sound wave with maximum shear σ_w and maximum strain $s_{\text{max}} = \sigma_w / G_{\text{rod}}$, traveling at $v_{\text{shear}} \sim (G_{\text{rod}} / \rho_{\text{rod}})^{1/2} \sim 11,900 \text{ m/sec}$, the transverse wave velocity in the diamond cable medium. The maximum power passing through a rod with $r_{\text{rod}} = 1 \mu\text{m}$, $L_{\text{rod}} = 1$

¹⁰²⁰ The classical rotational energy density of an electron circling a proton in a hydrogen atom is $E_{\text{D}} = E_{\text{rot}} / V_{\text{H}} \sim \mathbf{3500 \text{ MJ/L}}$ (and $E_{\text{S}} \sim E_{\text{rot}} / (m_{\text{p}} + m_{\text{e}}) \sim \mathbf{1300 \text{ MJ/kg}}$), where $E_{\text{rot}} = (1/2) J \omega^2 = 2.19 \times 10^{-18} \text{ J}$ ($\sim 10^{-8}$ rest mass energy), moment of inertia for 2 point masses $J \sim m_{\text{p}} m_{\text{e}} R_{\text{H}}^2 / (m_{\text{p}} + m_{\text{e}}) = 2.25 \times 10^{-51} \text{ kg}\cdot\text{m}^2$, $\omega = v_{\text{e}} / R_{\text{H}} = 4.14 \times 10^{16} \text{ rad/sec}$, Bohr radius $R_{\text{H}} \sim 5.29 \times 10^{-11} \text{ m}$ (https://en.wikipedia.org/wiki/Bohr_radius), atomic number $Z = 1$, fine structure constant $\alpha \sim 1/137$, speed of light $c = 3 \times 10^8 \text{ m/sec}$, proton mass $m_{\text{p}} = 1.67 \times 10^{-27} \text{ kg}$, electron mass $m_{\text{e}} = 9.11 \times 10^{-31} \text{ kg}$, atomic volume $V_{\text{H}} \sim (4/3) \pi R_{\text{H}}^3 = 6.20 \times 10^{-31} \text{ m}^3$, and $v_{\text{e}} \sim \alpha Zc = 2.19 \times 10^6 \text{ m/sec}$ (e.g., Norrby LJ. Why is mercury liquid? Or, why do relativistic effects not get into chemistry textbooks? J Chem Educ 1991 Feb;68(2):110-3; <https://45180ac4-a-62cb3a1a-sites.googlegroups.com/site/billswebsite100/home/files/172rpint--LiquidMercury.pdf>). The same energy density figures are 10-100 times higher if we sum all 92 electrons in a heavy uranium atom. However, it is unclear how to directly tap this stored energy, whether reversibly or irreversibly.

¹⁰²¹ Freitas RA Jr. Nanomedicine, Volume I: Basic Capabilities, Landes Bioscience, Georgetown TX, 1999; Sec. 6.4.3.4 “Gear Trains and Mechanical Tethers”; <http://www.nanomedicine.com/NMI/6.4.3.4.htm>.

mm, and $V_{\text{rod}} = \pi R_{\text{rod}}^2 L_{\text{rod}} = 3.1 \times 10^{-15} \text{ m}^3$ is $P_{\text{AC}} = \pi R_{\text{rod}}^2 E_{\text{D,twist,max}} v_{\text{shear}} \sim \pi R_{\text{rod}}^2 \sigma_w^2 / \rho_{\text{rod}}^{1/2} G_{\text{rod}}^{1/2} = 7.5 \text{ W}$, yielding a power density of $P_{\text{D,AC}} = P_{\text{AC}} / V_{\text{rod}} = \mathbf{2.4 \times 10^6 \text{ MW/L}}$ with rotational frequency limited to $v_{\text{AC}} \sim G_{\text{rod}}^{1/2} / \rho_{\text{rod}}^{1/2} L_{\text{rod}} \sim 12 \text{ MHz}$. Energy dissipation due to shear deformation¹⁰²² at temperature $T = 310 \text{ K}$ is $\Delta W_{\text{cycle}} \sim (3 T \beta^2 \sigma_w^2 \tau_{\text{relax}} / 2 C_V) v_{\text{AC}} V_{\text{rod}} = \mathbf{1.2 \times 10^{15} \text{ J/cycle}}$ (taking thermal coefficient of volume expansion $\beta = 3.5 \times 10^{-6} \text{ K}^{-1}$ and constant-volume heat capacity $C_V = 1.7 \times 10^6 \text{ J/K-m}^3$ for diamond), well below the driving energy of $E_{\text{cycle}} = P_{\text{AC}} / v_{\text{AC}} = \mathbf{6.3 \times 10^{-7} \text{ J/cycle}}$, where $\tau_{\text{relax}} \sim 10^{-13} \text{ sec}$ for $v_{\text{shear}} \sim 10^4 \text{ m/sec}$ in nanomechanical systems.

A simple gear train also transmits mechanical rotational power from one location to another. In one example,¹⁰²³ a 17 nm^3 steric gear pair transmits 1 nanowatt of mechanical power, giving a power density of $\mathbf{6 \times 10^7 \text{ MW/L}}$ with a mechanical efficiency of 99.997%. Complex 100- μm -scale gear trains have been fabricated.¹⁰²⁴ Sandia's Microelectronics Development Laboratory has been mass-producing 100-micron motors and gears for decades.¹⁰²⁵ Properly designed molecular bearings will have lifetimes that are not limited by wear but only by the static lifetime of the bearing (e.g., due to radiation damage).

Biological motors have much lower power densities – for example, the bacterial flagellar proton-gradient chemomechanical motor develops $\sim 10^{-4} \text{ pW}$ with a power density of $\sim \mathbf{0.002 \text{ MW/L}}$ and a motor efficiency of <5% at low load, 50-99%+ at high load.¹⁰²⁶

Decades-old commercially available micromachined rotors $\sim 1 \text{ micron}$ thick and $\sim 100 \text{ microns}$ in radius respond to electric field intensities $> 10^8 \text{ volts/m}$ producing motive torques of $\sim 10 \text{ pN-m}$ by converting electrical to mechanical energy, achieving power densities in the $\mathbf{10^{-5} - 10^{-4} \text{ MW/L}}$ range with device lifetimes approaching 10^7 rotations.¹⁰²⁷

¹⁰²² Drexler KE. Nanosystems: Molecular Machinery, Manufacturing, and Computation, John Wiley & Sons, NY, 1992; Sec. 7.4.2 "Phonon viscosity"; http://e-drexler.com/d/09/00/Drexler_MIT_dissertation.pdf.

¹⁰²³ Drexler KE. Nanosystems: Molecular Machinery, Manufacturing, and Computation, John Wiley & Sons, NY, 1992; Sec. 10.7.1.b, "Energy dissipation in gear contacts"; http://e-drexler.com/d/09/00/Drexler_MIT_dissertation.pdf.

¹⁰²⁴ Gianchandani Y, Najafi K. Batch fabrication and assembly of micromotor-driven mechanisms with multi-level linkages. Proceedings 5th IEEE Micro Electro Mechanical Systems, IEEE Robotics and Automation Society, 1992, pp. 141-146.

¹⁰²⁵ Howie D. Nanotechnology: Progress and Prospects. Oxford Nanotechnology PLC, Aug 1997; <http://www.oxfordnano.com>.

¹⁰²⁶ Jones CJ, Aizawa S. The bacterial flagellum and flagellar motor: structure, assembly and function. Adv Microbial Physiol. 1991;32:109-172; <https://www.ncbi.nlm.nih.gov/pubmed/1882727>.

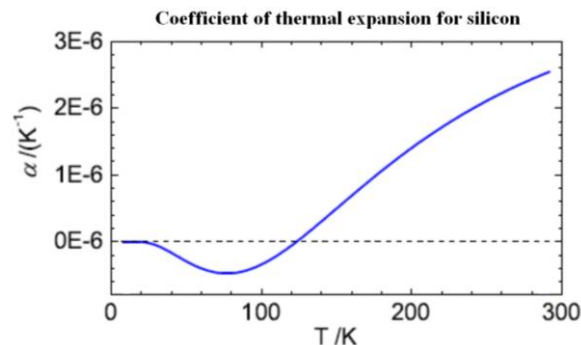
¹⁰²⁷ Mehregany M, Tai YC. Surface micromachined mechanisms and micromotors. J Micromech Microeng. 1991;1:73-85.

ZnO nanowire textured films have been fabricated that can harvest low-frequency mechanical energy with a power density of $\sim 10^{-5}$ MW/L.¹⁰²⁸

¹⁰²⁸ Hu Y, Zhang Y, Xu C, Lin L, Snyder RL, Wang ZL. Self-powered system with wireless data transmission. *Nano Lett.* 2011 Jun 8;11(6):2572-7;
http://www.nanoscience.gatech.edu/paper/2011/11_NL_02.pdf.

5.4 Thermomechanical Stress

Mechanical energy can be stored as materials are heated or cooled and attempt to expand or contract against restraints, according to their coefficient of thermal expansion which is a function of both material composition and temperature. Coefficients of expansion may exist for linear,¹⁰²⁹ areal,¹⁰³⁰ or volumetric¹⁰³¹ expansion, and the coefficients may be positive or negative depending on the thermal response of the particular material. For instance, the coefficient of linear thermal expansion for pure silicon crystal has a negative value below 123 K and a positive value above 123 K (chart, at right).¹⁰³² More familiarly, the coefficient of thermal expansion for water reaches zero at 3.983 °C and becomes negative with further cooling, which explains why water has a maximum density at this temperature. Substances that expand at the same rate in every direction are called isotropic – for such materials, the area and volumetric thermal expansion coefficient are, respectively, approximately two and three times larger than the linear thermal expansion coefficient. For solids, the coefficient values most commonly reported are for linear expansion.



If a heated solid body with a positive thermal expansion coefficient is constrained so that it cannot expand, then internal stress will be caused (or changed) by a change in temperature. This stress can be calculated by considering the strain that would occur if the body were free to expand and the stress that would be required to reduce that strain to zero, through the stress/strain relationship characterized by the elastic or Young's modulus.¹⁰³³ (External ambient pressure does not usually appreciably affect the size of solid materials (**Section 5.1.1**) and so it is not usually necessary to consider the effect of external pressure changes.)

The coefficient of linear thermal expansion α_L is the fractional change in length per degree of temperature change. For example, $\alpha_L \sim 7 \times 10^{-7} \text{ K}^{-1}$ for diamond at room temperature ($\sim 300 \text{ K}$)¹⁰³⁴ but rises to $6 \times 10^{-6} \text{ K}^{-1}$ at $\sim 1700 \text{ K}$ (see solid dots representing experimental data in the

¹⁰²⁹ https://en.wikipedia.org/wiki/Thermal_expansion#Linear_expansion.

¹⁰³⁰ https://en.wikipedia.org/wiki/Thermal_expansion#Area_expansion.

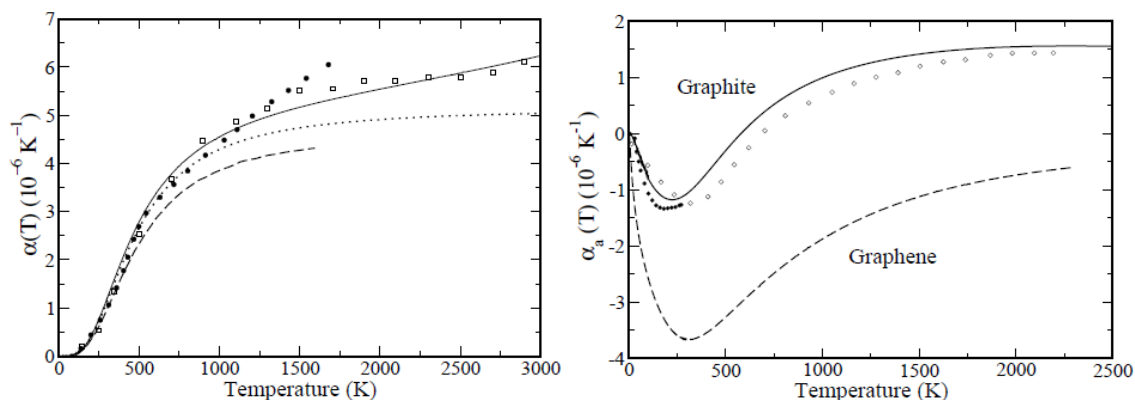
¹⁰³¹ https://en.wikipedia.org/wiki/Thermal_expansion#Volume_expansion.

¹⁰³² Middelmann T, Walkov A, Bartl G, Schödel R. Thermal expansion coefficient of single-crystal silicon from 7 K to 293 K. Phys Rev B. 2015 Nov 1;92(17):174113; <https://arxiv.org/pdf/1507.06822>.

¹⁰³³ https://en.wikipedia.org/wiki/Thermal_expansion#Expansion_in_solids.

¹⁰³⁴ Moelle C, Klose S, Szücs F, Fecht HJ, Johnston C, Chalker PR, Werner M. Measurement and calculation of the thermal expansion coefficient of diamond. Diam Relat Mater. 1997 Apr;6(5-7):839-842; <https://www.sciencedirect.com/science/article/pii/S0925963596006747>.

chart below, at left). Interestingly, graphene exhibits a negative coefficient of linear thermal expansion all the way up to 2300 K (see chart below, at right)¹⁰³⁵ – in other words, it contracts when heated, at all temperatures, which is a rather unusual property.



The material strain on a solid is proportional to the change in length, which in turn is proportional to the change in temperature ΔT , hence the change in strain $\epsilon_{\text{thermal}} = \alpha_L \Delta T$. For isotropic materials subjected to modest deformations, the applied uniaxial stress (the force per unit area), which approximates the density of the energy stored in the strain, is related to stress by the Young's modulus Y , which is the ratio of stress to strain,¹⁰³⁶ hence the stored energy density $E_D = Y \epsilon_{\text{thermal}} = Y \alpha_L \Delta T = \mathbf{0.074 \text{ MJ/L}}$ for a geometrically-constrained diamond rod heated from 300 K to 400 K (i.e., $\Delta T = 100 \text{ K}$), taking $Y = 1.05 \times 10^{12} \text{ N/m}^2$ for diamond.¹⁰³⁷ For aluminum rods in similar circumstances, $\alpha_L \sim 2.34 \times 10^{-5} \text{ K}^{-1}$,¹⁰³⁸ $Y = 6.9 \times 10^{10} \text{ N/m}^2$,¹⁰³⁹ hence $E_D = Y \alpha_L \Delta T = \mathbf{0.16 \text{ MJ/L}}$. The energy density of thermomechanical storage is tabulated for a variety of materials in **Table 49**, below. Dividing by density gives the stored specific energy E_S , which ranges from a low of **0.0004 MJ/kg** for rubber to a high of **0.1862 MJ/kg** for beryllium.

Other thermomechanical architectures that might store thermomechanical energy could include sandwich cantilevers made of composite materials with high coefficients of linear expansion

¹⁰³⁵ Mounet N, Marzar N. High-accuracy first-principles determination of the structural, vibrational and thermodynamical properties of diamond, graphite, and derivatives. Phys Rev B. 2005 May 31;71:205214; <https://arxiv.org/pdf/cond-mat/0412643.pdf>.

¹⁰³⁶ https://en.wikipedia.org/wiki/Young's_modulus.

¹⁰³⁷ https://en.wikipedia.org/wiki/Young's_modulus#Approximate_values.

¹⁰³⁸ Otte HM, Montague WG, Welch DO. X-Ray Diffractometer Determination of the Thermal Expansion Coefficient of Aluminum near Room Temperature. J Appl Phys. 1963 Oct;34(10):3149-3150; <https://apps.dtic.mil/dtic/tr/fulltext/u2/410258.pdf>.

¹⁰³⁹ https://www.engineeringtoolbox.com/young-modulus-d_417.html.

(e.g., heated metal bimorphs),¹⁰⁴⁰ Nitinol or other temperature-sensitive shape-memory alloys,¹⁰⁴¹ thermally-driven phase-change microactuators,¹⁰⁴² thermally-powered contraction turbines,¹⁰⁴³ and even thermally-driven contractile proteins.¹⁰⁴⁴

¹⁰⁴⁰ Riethmuller W, Benecke W, Schnakenberg U, Heuberger A. Micromechanical silicon actuators based on thermal expansion effects. Dig. Int. Conf. Solid-State Sensors and Actuators, Tokyo, Japan, Jun 1987, pp. 834-837.

¹⁰⁴¹ Ikuta K, Tsukamoto M, Hirose S. Mathematical model and experimental verification of shape memory alloy for designing microactuators. Proc. IEEE Micro Electro Mechanical Systems Workshop, Feb 1991, pp. 103-108.

¹⁰⁴² Bergstrom PL, Ji J, Liu Y-N, Kaviany M, Wise KD. Thermally Driven Phase-Change Microactuation. J Microelectromech Syst. 1995 Mar;4:10-17; <https://ieeexplore.ieee.org/abstract/document/365365>.

¹⁰⁴³ Sussmann MV, Katchalsky A. Mechanochemical Turbine: A New Power Cycle. Science 1970 Jan 2;167:45-47; <http://science.sciencemag.org/content/167/3914/45>.

¹⁰⁴⁴ Urry D. Elastic Biomolecular Machines. Sci Amer. 1995 Jan;272:44-49; <https://www.jstor.org/stable/24980141>.

Table 49. Thermomechanical energy density stored in expansion-constrained materials for $\Delta T = 100$ K, using data for coefficient of linear thermal expansion¹⁰⁴⁵ and Young's modulus¹⁰⁴⁶.

Material	Coeff. of Linear Thermal Expansion (K ⁻¹)	Young's Modulus (N/m ²)	Energy Density for $\Delta T = 100$ K (MJ/L)	Material	Coeff. of Linear Thermal Expansion (K ⁻¹)	Young's Modulus (N/m ²)	Energy Density for $\Delta T = 100$ K (MJ/L)
Plutonium	5.05×10^{-5}	9.60×10^{10}	0.4848	Gold	1.42×10^{-5}	7.40×10^{10}	0.1051
Manganese	2.20×10^{-5}	1.58×10^{11}	0.3476	Vanadium	8.00×10^{-6}	1.31×10^{11}	0.1048
Beryllium	1.20×10^{-5}	2.87×10^{11}	0.3444	Tin	2.15×10^{-5}	4.70×10^{10}	0.1011
Iridium	6.40×10^{-6}	5.17×10^{11}	0.3309	Titanium	8.75×10^{-6}	1.10×10^{11}	0.0963
Osmium	5.50×10^{-6}	5.50×10^{11}	0.3025	Cadmium	3.00×10^{-5}	3.17×10^{10}	0.0951
Zinc	3.25×10^{-5}	8.30×10^{10}	0.2698	Granite	1.82×10^{-5}	5.20×10^{10}	0.0944
Iconel	1.21×10^{-5}	2.14×10^{11}	0.2579	Antimony	1.00×10^{-5}	7.79×10^{10}	0.0779
Iron	1.20×10^{-5}	2.10×10^{11}	0.2520	Diamond	7.00×10^{-7}	1.05×10^{12}	0.0735
Cobalt	1.20×10^{-5}	2.07×10^{11}	0.2484	Niobium	7.00×10^{-6}	1.03×10^{11}	0.0721
Monel metal	1.35×10^{-5}	1.79×10^{11}	0.2417	Thorium	1.20×10^{-5}	5.90×10^{10}	0.0708
Rhodium	8.00×10^{-6}	2.89×10^{11}	0.2312	Silicon	4.00×10^{-6}	1.58×10^{11}	0.0630
Sapphire	5.30×10^{-6}	4.35×10^{11}	0.2306	Oak wood	5.40×10^{-5}	1.10×10^{10}	0.0594
Uranium	1.34×10^{-5}	1.70×10^{11}	0.2278	Bismuth	1.33×10^{-5}	3.17×10^{10}	0.0420
Steel	1.18×10^{-5}	1.90×10^{11}	0.2233	Glass	5.90×10^{-6}	7.00×10^{10}	0.0413
Nickel	1.30×10^{-5}	1.70×10^{11}	0.2210	Lead	2.90×10^{-5}	1.40×10^{10}	0.0406
Selenium	3.70×10^{-5}	5.80×10^{10}	0.2146	Polyvinylchloride	8.20×10^{-5}	3.25×10^9	0.0267
Brass	1.85×10^{-5}	1.14×10^{11}	0.2100	Concrete	1.35×10^{-5}	1.70×10^{10}	0.0230
Bronze	1.78×10^{-5}	1.08×10^{11}	0.1917	Acrylic	7.15×10^{-5}	3.20×10^9	0.0229
Copper	1.64×10^{-5}	1.17×10^{11}	0.1913	Polystyrene	7.00×10^{-5}	3.25×10^9	0.0228
Tungsten	4.50×10^{-6}	4.05×10^{11}	0.1823	Nylon	7.00×10^{-5}	3.00×10^9	0.0210
Molybdenum	5.00×10^{-6}	3.29×10^{11}	0.1645	ABS Thermoplastic	9.00×10^{-5}	2.25×10^9	0.0203
Aluminum	2.34×10^{-5}	6.90×10^{10}	0.1615	Chlorinated PVC	6.45×10^{-5}	2.90×10^9	0.0187
Chromium	6.50×10^{-6}	2.48×10^{11}	0.1612	Polycarbonate	6.75×10^{-5}	2.60×10^9	0.0176
Cast iron, gray	1.08×10^{-5}	1.30×10^{11}	0.1404	Polypropylene	8.10×10^{-5}	1.75×10^9	0.0142
Silver	1.94×10^{-5}	7.20×10^{10}	0.1393	Polyethylene	1.54×10^{-4}	8.00×10^8	0.0123
Platinum	9.00×10^{-6}	1.47×10^{11}	0.1323	Chlorinat'd polyether	8.00×10^{-5}	1.10×10^9	0.0088
Silicon carbide	2.77×10^{-6}	4.50×10^{11}	0.1247	PTFE	1.24×10^{-4}	4.00×10^8	0.0049
Tantalum	6.50×10^{-6}	1.86×10^{11}	0.1209	Rubber	8.00×10^{-5}	5.50×10^7	0.0004
Magnesium	2.60×10^{-5}	4.50×10^{10}	0.1168				

¹⁰⁴⁵ https://www.engineeringtoolbox.com/linear-expansion-coefficients-d_95.html.

¹⁰⁴⁶ https://www.engineeringtoolbox.com/young-modulus-d_417.html.

Chapter 6. Electromagnetic Energy Storage

In this Chapter we survey the specific energy (MJ/kg) and energy density (MJ/L) available from various stores of electric and magnetic energy.

Electromagnetic energy is carried in packets of energy called photons. What is the energy density of a photon? The energy contained in a photon is well-defined: $E_{\text{photon}} = h\nu = hc/\lambda$, where ν is the electromagnetic frequency (Hz), λ is photon wavelength (m), $c = 3 \times 10^8$ m/sec (speed of light), and $h = 6.63 \times 10^{-34}$ J-sec (Planck's constant). The volume of a photon is the subject of much confusion and discussion¹⁰⁴⁷ in the technical literature,¹⁰⁴⁸ but if we consider the effective size of a photon as approximately equal to its wavelength,¹⁰⁴⁹ then its volume is $V_{\text{photon}} \sim \lambda^3$; with this assumption, the energy density of a photon would be $E_{\text{D,photon}} \sim E_{\text{photon}} / V_{\text{photon}} = hc/\lambda^4 = h\nu^4/c^3 = 2 \times 10^{-40}$ MJ/L for a 10 MHz radio wave photon, 3×10^{-9} MJ/L for a 600 THz optical photon, and 2×10^{16} MJ/L for a 10^{21} Hz gamma ray photon.

Electromagnetic radiation in a region of space that is at equilibrium with its surroundings can be described by the Planck radiation formula $P/A = \sigma T^4$, relating power (P) per unit area (A) to temperature (T) via the Stefan-Boltzmann constant $\sigma = 5.67 \times 10^{-8}$ W/m²-K⁴. The total energy radiated from an area in this region of space is given by the Stefan-Boltzmann law, and the energy density (E_{D}) associated with the radiation can be related to that law by $P/A = (c/4) E_{\text{D}}$, hence the cumulative energy density for all wavelengths of radiation is $E_{\text{D}} = (4\sigma/c)T^4$.¹⁰⁵⁰ In astronomy and astrophysics texts, the energy density in radiation is typically written $E_{\text{D,rad}} = a_{\text{rad}}T^4$, where $a_{\text{rad}} = 4\sigma/c = 7.57 \times 10^{-16}$ J/m³-K⁴. Thus, for example, the region of space near Earth's orbit (where the mean radiation temperature $T \sim 278$ K)¹⁰⁵¹ has a radiation energy density of $E_{\text{D,rad}} \sim 5 \times 10^{-15}$ MJ/L.

In this Chapter, we first examine the energy that may be stored in magnetic fields (**Section 6.1**) and in electric fields (**Section 6.2**). **Section 6.3** describes the stored energy available in ambient electromagnetic fields, and **Section 6.4** consider beamed electromagnetic energy such as laser beams.

¹⁰⁴⁷ “Just how big is a photon?” <https://www.physicsforums.com/threads/just-how-big-is-a-photon.555379/>. “The shape and size of a photon,” <https://readingfeynman.org/2014/09/16/the-size-and-shape-of-a-photon/>. “How big is a photon,” <https://www.quora.com/How-big-is-a-photon>. What are the dimensions, width and length, of a photon? <https://physics.stackexchange.com/questions/161055/what-are-the-dimensions-width-and-length-of-a-photon>. “Does a photon have physical volume or geometrical size?” <https://www.scienceforums.net/topic/27337-does-a-photon-have-physical-volume-or-geometrical-size/>.

¹⁰⁴⁸ Liu SL. Electromagnetic fields, size, and copy of a single photon. arXiv:1604.03869v3, 30 May 2018; <https://arxiv.org/ftp/arxiv/papers/1604/1604.03869.pdf>.

¹⁰⁴⁹ Brian Koberlein, “That’s about the size of it,” 14 Apr 2015; <https://briankoberlein.com/2015/04/14/thats-about-the-size-of-it/>.

¹⁰⁵⁰ “Radiation Energy Density,” <http://hyperphysics.phy-astr.gsu.edu/hbase/quantum/raddens.html>.

¹⁰⁵¹ https://en.wikipedia.org/wiki/Greenhouse_effect#Mechanism.

6.1 Magnetic Fields

Magnetic fields can be used to store energy. However, stable magnetic fields cannot exist in the absence of a material structure that creates them – e.g., a permanent magnet or an electromagnet.

Since isolated magnetic poles (called magnetic monopoles,¹⁰⁵² analogous to the electron) are not known to exist, magnetic field energy can be stored only in an array of aligned atomic dipoles. For example, the energy density of the static magnetic field of a permanent magnet comprised of atoms with dipole moment M_{dipole} and number density N_{dipole} producing a flux density B at 100% saturation is given by $E_D \sim M_{\text{dipole}} N_{\text{dipole}} B = \mathbf{8 \times 10^6 \text{ MJ/L}}$ for iron atoms, where $M_{\text{dipole}} = 1.8 \times 10^{-23} \text{ amp}\cdot\text{m}^2$ for iron atoms in an iron bar,¹⁰⁵³ $N_{\text{dipole}} = \rho_{\text{iron}} N_A / A_{\text{Fe}} = 8.5 \times 10^{28} \text{ iron atoms/m}^3$ where bulk density $\rho_{\text{iron}} = 7860 \text{ kg/m}^3$, $A_{\text{Fe}} = 0.055845 \text{ kg/mole}$, and $N_A = 6.022 \times 10^{23} \text{ atoms/mole}$ (Avogadro's constant), and $B \sim 0.005 \text{ tesla}$ for a typical refrigerator iron magnet.¹⁰⁵⁴

The strongest permanent magnets are made from alloys that include rare-earth elements. The strongest known permanent magnet is sintered neodymium iron boron ($\text{Nd}_2\text{Fe}_{14}\text{B}$), aka. “FIB” magnets, with a remanence (B_r)¹⁰⁵⁵ and coercivity (H_{cJ})¹⁰⁵⁶ up to 1.3 tesla and $1.99 \times 10^6 \text{ amp/m}$, respectively, giving a magnetic field “maximum energy product” ($BH_{\text{max}} \propto B_r, H_{cJ}$)¹⁰⁵⁷ or maximum energy density $E_D \sim \mathbf{3.1 \times 10^4 \text{ MJ/L}}$, which is a specific energy of $E_S \sim E_D / \rho_{\text{NIB}} = \mathbf{4.2 \times 10^5 \text{ MJ/kg}}$ for $\rho_{\text{NIB}} \sim 7400 \text{ kg/m}^3$.¹⁰⁵⁸ (From the same source, close behind NIB are the sintered SmCo or samarium-cobalt ($\text{Sm}(\text{Co},\text{Fe},\text{Cu},\text{Zr})_7$) magnets, with maximums of 1.16 tesla, $1.59 \times 10^6 \text{ amp/m}$, $E_D \sim \mathbf{2.6 \times 10^4 \text{ MJ/L}}$ and $E_S \sim E_D / \rho_{\text{SmCo}} = \mathbf{3.1 \times 10^5 \text{ MJ/kg}}$ for $\rho_{\text{SmCo}} \sim 8300 \text{ kg/m}^3$.)

Only a negligible amount of magnetic energy is stored in a magnetic field created by a single permanent current loop in a ring of superconducting material. For a wire loop of radius R_{loop} and circular cross-section radius r_{wire} carrying current I_{wire} , peak magnetic flux density is $B = \mu_0 I_{\text{wire}} / 2 R_{\text{loop}}$ at the center of the loop with permeability constant $\mu_0 = 1.26 \times 10^{-6} \text{ henry/m}$, so the peak

¹⁰⁵² https://en.wikipedia.org/wiki/Magnetic_monopole.

¹⁰⁵³ Resnick R, Halliday D. Physics, John Wiley & Sons, New York, 1966, p. 941.

¹⁰⁵⁴ <http://www.nevusnetwork.org/mritech.htm>.

¹⁰⁵⁵ Remanence or residual magnetism is the strength of the magnetic field that remains in a ferromagnetic material when an external magnetic field is removed; <https://en.wikipedia.org/wiki/Remanence>.

¹⁰⁵⁶ Coercivity, aka. intrinsic coercive force, is a material's resistance to becoming demagnetized by an externally-applied magnetic field; <https://en.wikipedia.org/wiki/Coercivity>.

¹⁰⁵⁷ “What is Maximum Energy Product / BHmax and How Does It Correspond to Magnet Grade?” Dura Magnetics Inc., 15 Sep 2014; <https://www.duramag.com/techtalk/tech-briefs/what-is-maximum-energy-product-bhmax-and-how-does-it-correspond-to-magnet-grade/>.

¹⁰⁵⁸ Pyrhonen J, Jokinen T, Hrabovcova, Design of Rotating Electrical Machines, John Wiley & Sons, 2009, p. 206, Table 3.3; https://books.google.com/books?id=_y3LSh1XTJYC&pg=PT206.

energy density is $E_D = B^2 / 2 \mu_0 = \mu_0 I_{\text{wire}}^2 / 8 R_{\text{loop}}^2 = 6.3 \times 10^{12} \text{ MJ/L}$ taking $I_{\text{wire}} = \pi r_{\text{wire}}^2 i_{\text{density}} = 10^4$ amperes for wire radius $r_{\text{wire}} = 50 \text{ nm}$, $R_{\text{loop}} = 0.5 \mu\text{m}$, and current density $i_{\text{density}} \sim 10^{10} \text{ amp/m}^2$.¹⁰⁵⁹

The maximum magnetic field strength for an iron core electromagnet is 1.6-2 tesla.¹⁰⁶⁰

The strongest continuous magnetic field ever created in a lab using an electromagnet is $B = 45 \text{ tesla}$ at the National High Magnetic Field Laboratory (NHMFL) in Florida in 1999 (image, right). According to one description,¹⁰⁶¹ “the total magnet system weighs 34 tons and stands 22 feet tall. An enormous superconducting



magnet forms the outside layer and is the largest cable-in-conduit magnet ever built and operated to such high field. It is cooled to [1.8 K] with the only operating superfluid helium cryogenic system built for magnet applications in the United States. A very large resistive magnet (electromagnet) sits in the center of the superconducting magnet.” The magnet is a “hybrid” type that combines a superconducting magnet of 11.5 tesla with a resistive magnet of 33.5 tesla. The magnetic field has a nominal energy density of $E_{D,\text{nom}} \sim B^2/2\mu_0 = 0.804 \text{ MJ/L}$,¹⁰⁶² but the field cannot exist (or store any magnetic field energy) without the massive enabling material that surrounds it. Taking mass $m_{45T} = 31,752 \text{ kg}$ and volume $V_{45T} \sim (6.7 \text{ m})^3 = 301 \text{ m}^3$, then if the field spanned only the magnetic field bore size $L_{\text{bore}} = 32 \text{ mm}$,¹⁰⁶³ the net magnetic field energy density would be $E_D \sim (L_{\text{bore}}^3 / V_{45T}) E_{D,\text{nom}} \sim 8.8 \times 10^{-8} \text{ MJ/L}$ and specific energy $E_S \sim E_D (V_{45T} / m_{45T}) \sim 8.3 \times 10^{-7} \text{ MJ/kg}$.

¹⁰⁵⁹ Aluminum conductors in integrated circuits are limited to $i_{\text{density}} \sim 3 \times 10^9 \text{ amp/m}^2$ due to electromigration, while thin-film high-temperature superconductors can achieve $i_{\text{density}} > 3 \times 10^{10} \text{ amp/m}^2$; Chu PCW. High-Temperature Superconductors. Sci Amer. 1995 Sep;273:162-165.

¹⁰⁶⁰ https://en.wikipedia.org/wiki/Electromagnet#Magnetic_circuit_.E2.80.93_the_constant_B_field_approximation.

¹⁰⁶¹ “World’s Most Powerful Magnet Tested Ushers in New Era for Steady High Field Research,” 17 Dec 1999; <http://legacywww.magnet.fsu.edu/mediacenter/news/pressreleases/1999december17.html>.

¹⁰⁶² McMillan BF. The physics of fusion. Warwick University, 10 Feb 2014, p. 25; http://www2.warwick.ac.uk/fac/sci/physics/current/teach/module_home/px438/lecture_distributed_2014.pdf.

¹⁰⁶³ “Meet the 45 Tesla Hybrid magnet,” National MagLab, 10 Oct 2016; <https://nationalmaglab.org/about/around-the-lab/meet-the-magnets/meet-the-45-tesla-hybrid-magnet>.



The world's strongest purely resistive (non-superconducting) electromagnet was constructed in 2014 by the High Field Magnet Laboratory at Radboud University Nijmegen (Netherlands).¹⁰⁶⁴

According to specifications, the magnet produces a continuous $B = 37.5$ tesla ($E_{D,nom} \sim 0.67$ MJ/L) with an $L_{bore} = 32$ mm bore at room temperature. From the image of the device behind the people at left, we estimate a cylinder height of ~ 2 m with diameter ~ 1 m, volume $V_{37.5T} \sim 2$ m³ and total system mass $m_{37.5T} \sim 4000$ kg, for a net magnetic field energy density of $E_D \sim (L_{bore}^3 / V_{45T}) E_{D,nom} \sim 1.1 \times 10^5$ MJ/L and

specific energy $E_S \sim E_D (V_{37.5T} / m_{37.5T}) \sim 5.5 \times 10^6$ MJ/kg.

The strongest nondestructive pulsed magnetic field produced in a lab to date resides in the Pulsed Field Facility at the National High Magnetic Field Laboratory, generating 25 millisecond pulses of a 100 tesla magnetic field ($E_{D,nom} \sim 3.1$ MJ/L) which remains 99% homogeneous within a 22 mm radius of the center of the electromagnet (image, right).¹⁰⁶⁵ Assuming $V_{100T} \sim 8$ m³, $m_{100T} \sim 12,000$ kg, and magnetic field volume $V_{field} \sim (22 \text{ mm})^3 \sim 10^{-5}$ m³, then $E_D \sim (V_{field} / V_{100T}) E_{D,nom} \sim 3.9 \times 10^6$ MJ/L and specific energy $E_S \sim E_D (V_{100T} / m_{100T}) \sim 2.6 \times 10^6$ MJ/kg.



The strongest short-term (destructive) pulsed magnetic field ever created in a lab is at the Magnetized Liner Inertial Fusion Z-facility at Sandia National Laboratories (image, left),¹⁰⁶⁶ which by 2014 had reached a one-shot magnetic field intensity of $B \sim 9000$ tesla ($E_{D,nom} \sim 32,000$ MJ/L) in a "tiny metal can 5 mm across and 7.5 mm tall" ($V_{field} \sim 1.9 \times 10^{-7}$ m³) in a single 100 nanosecond pulse.¹⁰⁶⁷ Assuming the electromagnet is cylindrical and roughly 2 m tall and 4 m in diameter, and again assuming the

¹⁰⁶⁴ "HFML sets world record with a new 37.5 tesla magnet," High Field Magnet Laboratory, 31 Mar 2014; <http://www.ru.nl/hfml/news/news/news-items/hfml-sets-world/>.

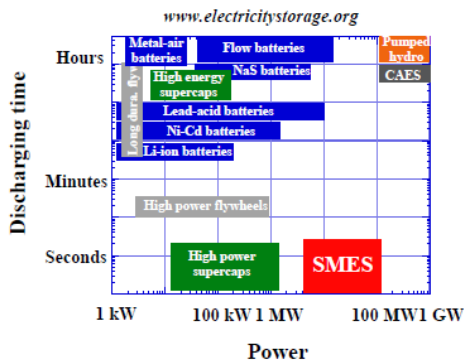
¹⁰⁶⁵ "100 Tesla Multi-Shot Magnet," National High Magnetic Field Laboratory, 20 Jun 2017; <https://nationalmaglab.org/user-facilities/pulsed-field-facility/instruments-pff/100-tesla-multi-shot-magnet>.

¹⁰⁶⁶ https://www.arpa-e.energy.gov/sites/default/files/documents/files/Drivers_Fusion_Sinars_Presentation.pdf.

¹⁰⁶⁷ "Z machine makes progress toward nuclear fusion," 10 Oct 2014; <http://www.sciencemag.org/news/2014/10/z-machine-makes-progress-toward-nuclear-fusion>.

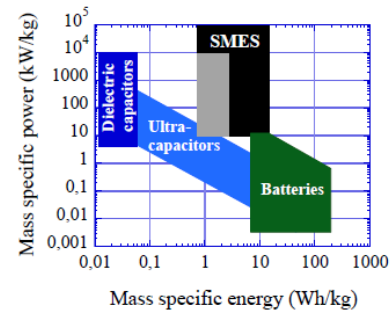
useful field spans only the volume of the “can”, then $V_{9000T} \sim 25 \text{ m}^3$ and $E_D \sim (V_{\text{field}} / V_{9000T})$
 $E_{D,\text{nom}} \sim 2.4 \times 10^{-4} \text{ MJ/L}$. As with the earlier figures above, this is likely an underestimate because some magnetic field (also useful for energy storage) undoubtedly exists outside of the “can” or “bore” volumes.

As we see, magnetic systems generally exhibit low energy storage densities when the mass and volume of the requisite infrastructure is included. For example, existing and proposed superconducting magnetic energy storage (SMES) systems (see illustrations at right and left) are estimated to provide an energy density only on the order of $\sim 0.02 \text{ MJ/L}$ with a



specific energy of $\sim 0.01 \text{ MJ/kg}$.¹⁰⁶⁸

The main advantage of magnetic energy storage is that the charge and discharge cycle times can be very short, enabling very high power outputs for brief periods of time. Specific power up to $\sim 10 \text{ MW/kg}$ for discharge periods of $\sim 0.001 \text{ sec}$ has been achieved experimentally, and a specific power of $\sim 100 \text{ MW/kg}$ at a specific energy of $\sim 0.05 \text{ MJ/L}$ may be possible but will “require more research and development.”¹⁰⁶⁹



What is possible at the extremes? According to one paper,¹⁰⁷⁰ the maximum magnetic field allowed under quantum electrodynamics theory is $B \sim 10^{38}$ tesla, which might correspond to an energy density of $E_{D,\text{max}} \sim B^2/2\mu_0 = 4 \times 10^{34} \text{ MJ/L}$.

¹⁰⁶⁸ Tixador P. Superconducting Magnetic Energy Storage: Status and Perspective. IEEE/CSC & ESAS European Superconductivity News Forum. 2008 Jan; No. 3; http://snf.ieeecsc.org/sites/ieeecsc.org/files/CR5_Final3_012008.pdf. Vulusala G, Suresh V, Madichetty S. Application of superconducting magnetic energy storage in electrical power and energy systems: a review. Intl J Energy Res. 2017 May 16; <http://onlinelibrary.wiley.com/doi/10.1002/er.3773/abstract>. See also: https://en.wikipedia.org/wiki/Superconducting_magnetic_energy_storage.

¹⁰⁶⁹ Tixador P. Superconducting Magnetic Energy Storage: Status and Perspective. IEEE/CSC & ESAS European Superconductivity News Forum. 2008 Jan; No. 3; http://snf.ieeecsc.org/sites/ieeecsc.org/files/CR5_Final3_012008.pdf.

¹⁰⁷⁰ Shabad AE, Usov VV. Positronium Collapse and the Maximum Magnetic Field in Pure QED. Phys Rev Lett. 2006 May 12;96(18):180401; <https://arxiv.org/pdf/hep-th/0605020.pdf>.

6.2 Electric Fields

Pure electric fields can also be used to store energy. As with magnetic fields, stable electric fields cannot exist in the absence of a material structure that creates them – such as a capacitor, electret, van de Graff generator, or other surface or container in which electrical charges are trapped.

The maximum energy density (aka. electrostatic pressure) of a static electric field of strength E traversing a material of dielectric constant κ_e is given by:

$$E_D = (1/2) \epsilon_0 \kappa_e E^2 = 1.01 \times 10^8 \text{ joules/m}^3 (= \mathbf{0.1 \text{ MJ/L}}) \text{ for diamond}$$

where $\epsilon_0 = 8.85 \times 10^{-12}$ farad/m (permittivity constant), dielectric constant $\kappa_e = 5.7$ for diamond, and the maximum dielectric strength or breakdown voltage $E_{\text{breakdown,diamond}} = 2 \times 10^9$ volts/m (= E) for diamond.¹⁰⁷¹ This formula also approximates the energy density of the electric field inside a rectangular waveguide and similar structures.¹⁰⁷² Ideally, vacuum is the best voltage insulator with theoretical electric field stress levels up to $\sim 10^9$ volts/m limited only by emission from electrode surfaces, though practical systems fall far below this level.¹⁰⁷³ For example, the maximum breakdown voltage for vacuum between oxygen-free copper¹⁰⁷⁴ or high-purity molybdenum¹⁰⁷⁵ electrodes is $E_{\text{breakdown}} \sim 2 \times 10^8$ volts/m but the dielectric constant for vacuum is only $\kappa_e = 1$, giving a much lower $E_D \sim 1.77 \times 10^5$ joules/m³ (= **0.0002 MJ/L**) than for diamond. A high breakdown material is ruby mica ($\kappa_e = 5.4$, $E_{\text{breakdown}} = 1.6 \times 10^8$ volts/m, $E_D = \mathbf{0.0006 \text{ MJ/L}}$); a typical high dielectric material is titanium dioxide ($\kappa_e = 100$, $E_{\text{breakdown}} = 6 \times 10^6$ volts/m, $E_D = \mathbf{0.00002 \text{ MJ/L}}$). Extremely high dielectric materials such as the perovskite-related oxide CCTO ($\text{CaCu}_3\text{Ti}_4\text{O}_{12}$) have $\kappa_e \sim 100,000$ between 100-600 K at kilohertz radio frequencies¹⁰⁷⁶ but also tend to have low breakdown voltages, e.g., $E_{\text{breakdown}} \sim 200,000$ volts/m,¹⁰⁷⁷ yielding only modest energy densities of $E_D \sim \mathbf{0.00002 \text{ MJ/L}}$.

¹⁰⁷¹ https://en.wikipedia.org/wiki/Dielectric_strength#Breakdown_field_strength; National Materials Advisory Board, Status and Applications of Diamond and Diamond-Like Materials: An Emerging Technology, Report of the Committee on Superhard Materials, NMAB-445, National Academy Press, 1990.

¹⁰⁷² Orfanidis SJ. "Chapter 9. Waveguides," Electromagnetic Waves and Antennas, Rutgers University, 1 Aug 2016, p. 380; <https://www.ece.rutgers.edu/~orfanidi/ewa/ch09.pdf>.

¹⁰⁷³ Mulcahy MJ, Bolin PC. High-Voltage Breakdown Study, Technical Report ECOM-00394-20, Ion Physics Corporation, March 1971; <http://www.dtic.mil/dtic/tr/fulltext/u2/723107.pdf>.

¹⁰⁷⁴ Saito Y. Breakdown phenomena in vacuum. Proc. 1992 Linear Accelerator Conf., Ottawa ONT, Canada; <https://accelconf.web.cern.ch/accelconf/192/papers/th1-03.pdf>.

¹⁰⁷⁵ Tatarinova NV. Method of improving the dielectric strength of vacuum insulation. Tech. Phys. 2012;57(11):1535-1540; <https://link.springer.com/article/10.1134%2FS1063784212110242>.

¹⁰⁷⁶ Homes CC, Vogt T, Shapiro SM, Wakimoto S, Ramirez AP. Optical response of high-dielectric-constant perovskite-related oxide. Science. 2001 Jul 27;293(5530):673-6; https://www.bnl.gov/cmmsd/esg/docs/pdf/publications/2001/homes_01.pdf.

Commercially available capacitors¹⁰⁷⁸ of various types generally have only modest energy storage capacities – though somewhat better than electret¹⁰⁷⁹ based devices which produce only **0.000001 MJ/kg**¹⁰⁸⁰ or **~0.00002 MW/L**.¹⁰⁸¹ Maximum energy density for high voltage capacitors¹⁰⁸² is typically 0.01-1 J/cm³ (**0.00001-0.001 MJ/L**). Conventional capacitors¹⁰⁸³ provide only **0.0004 MJ/kg** specific energy; aluminum electrolytic capacitors achieve only **0.001 MJ/kg** and **0.1 MW/kg** and supercapacitors reach **0.05 MJ/kg** and **0.06 MJ/L**¹⁰⁸⁴ but only **0.01 MW/kg**,¹⁰⁸⁵ though a U.S. patent has been issued for a barium titanate ultracapacitor with a claimed specific energy of **1.47 MJ/kg**.¹⁰⁸⁶ This may be compared to conventional alkaline batteries at **0.68 MJ/kg** but only **0.00005 MW/kg** and lithium-ion batteries that typically achieve **0.95 MJ/kg** and **0.003 MW/kg** (Section 4.1, Table 24), similar to the lithium-ion-based Tesla Powerwall 2 and Powerpack 2 (**0.4 MJ/kg, 0.4 MJ/L, 0.00004 MW/kg, 0.00004 MW/L**).¹⁰⁸⁷ Coiled “twistron” yarns made of carbon nanotubes, when submerged in or coated with an ionically conducting material or electrolyte (e.g., salt water), can generate **0.00025 MW/kg** of peak electrical power when stretched 30 times per second, essentially acting as mechanical supercapacitors.¹⁰⁸⁸

¹⁰⁷⁷ Tang Z, Wu K, Huang Y, Li J. High Breakdown Field CaCu₃Ti₄O₁₂ Ceramics: Roles of the Secondary Phase and of Sr Doping. *Energies* 2017 Jul;10(7):1031-1040; <https://pdfs.semanticscholar.org/bb1b/8d38cfc437009d4a8d22bed2f2487bc6503d.pdf>.

¹⁰⁷⁸ Capacitors differ from electrochemical batteries and fuel cells in that their energy is usually stored as electrostatic, not chemical, potential energy, although electrostatic, electrolytic, and electrochemical “capacitors” do exist; [https://en.wikipedia.org/wiki/Power-to-weight_ratio#Electrostatic, electrolytic and electrochemical capacitors](https://en.wikipedia.org/wiki/Power-to-weight_ratio#Electrostatic,_electrolytic_and_electrochemical_capacitors).

¹⁰⁷⁹ <https://en.wikipedia.org/wiki/Electret>.

¹⁰⁸⁰ Lagomarsini C, Jean-Mistral C, Monfray S, Sylvestre A. New approach to improve the energy density of hybrid electret-dielectric elastomer generators. *SPIE Proc. Vol. 10163, Electroactive Polymer Actuators and Devices (EAPAD)*, 17 Apr 2017; <https://www.spiedigitallibrary.org/conference-proceedings-of-spie/10163/101632C/New-approach-to-improve-the-energy-density-of-hybrid-electret/10.1117/12.2259933.short?SSO=1>.

¹⁰⁸¹ Ahmed S, Kakkar V. An electret-based angular electrostatic energy harvester for battery-less cardiac and neural implants. *IEEE Access*, 14 Aug 2017; <https://ieeexplore.ieee.org/stamp/stamp.jsp?arnumber=8010270>.

¹⁰⁸² “Very High Voltage Capacitors,” General Atomics, 2018; <http://www.ga.com/very-high-voltage-capacitors>.

¹⁰⁸³ https://en.wikipedia.org/wiki/Capacitor#Energy_storage.

¹⁰⁸⁴ https://en.wikipedia.org/wiki/Energy_density#Energy_densities_of_common_energy_storage_materials.

¹⁰⁸⁵ https://en.wikipedia.org/wiki/Supercapacitor#Comparison_with_other_storage_technologies.

¹⁰⁸⁶ <https://patents.google.com/patent/US7466536B1/>.

¹⁰⁸⁷ https://en.wikipedia.org/wiki/Tesla_Powerwall#Powerwall_specifications.

¹⁰⁸⁸ “No Batteries Required: Energy-Harvesting Yarns Generate Electricity,” Univ. of Texas at Dallas News Center, 25 Aug 2017; https://www.utdallas.edu/news/2017/8/25-32663_No-Batteries-Required-Energy-Harvesting-Yarns-Generate-Electricity.html.

Even higher electric fields than the $E_{\text{breakdown,diamond}} = 2 \times 10^9$ volts/m available with diamond can be briefly generated in special circumstances, though it is challenging to see how such fields could be employed for practical long-term energy storage. For example, plasma wakefield accelerators¹⁰⁸⁹ have briefly generated record-high electric fields of 52×10^9 volts/m at SLAC¹⁰⁹⁰ and have produced peak fields (within small regions inside the waves) of up to 100×10^9 volts/m at CERN,¹⁰⁹¹ the latter implying an energy density of $E_D = 4.4 \times 10^{10}$ joules/m³ (**44 MJ/L**) in vacuum ($\kappa_e = 1$). The HERCULES laser at the University of Michigan holds the 2006-2018 world record for focused laser beam intensity at $I_{\text{laser}} = 2 \times 10^{22}$ W/cm²,¹⁰⁹² giving a laser electric field strength of $E_{\text{laser}} = (2 I_{\text{laser}} / c \epsilon_0)^{1/2} = 390,000 \times 10^9$ volts/m (speed of light $c = 3 \times 10^8$ m/sec),¹⁰⁹³ equivalent to $E_D = I_{\text{laser}} / c = 6.7 \times 10^{17}$ joules/m³ (**6.7 x 10⁸ MJ/L**) in vacuum. Spontaneous e^-e^+ pair creation by static electric fields is expected to set in at the Schwinger critical field strength¹⁰⁹⁴ of $E_{\text{cr}} = m^2c^3/e\hbar \approx 1.32 \times 10^{18}$ volts/m (**7.7 x 10¹⁵ MJ/L** in vacuum). Such a high field cannot be reached by the strongest laser facilities available today, but when achieved will represent the theoretical quantum mechanical upper limit for maximum electric field strength. (Note that a surface-burst EMP from a nuclear explosion achieves only a modest $\sim 10^6$ volts/m,¹⁰⁹⁵ about the maximum field strength of $\sim 3 \times 10^6$ volts/m in sea-level air.¹⁰⁹⁶)

¹⁰⁸⁹ Wakefields are matter waves, oscillations moving through a plasma at 99.997% of the speed of light, created in the wake of an ultra-intense laser pulse; https://en.wikipedia.org/wiki/Plasma_acceleration.

¹⁰⁹⁰ Blumenfeld I, *et al.* Energy doubling of 42 GeV electrons in a metre-scale plasma wakefield accelerator. Nature 2007 Feb 15;445:741-744; <https://www.nature.com/articles/nature05538>.

¹⁰⁹¹ “CERN’s pioneering mini-accelerator passes first test,” Nature, 29 Aug 2018; <https://www.nature.com/articles/d41586-018-06114-9>. “Plasma Accelerator – the 100 Billion Volt Machine”, EUPRAXIA, <http://www.eupraxia-project.eu/plasma-accelerator-the-100-billion-volt-machine.html>. “Fastest Waves Ever Photographed,” Phys.org, 27 Oct 2006, <https://phys.org/news/2006-10-fastest.html>; Physics Central, 31 Oct 2006, <http://physicsbuzz.physicscentral.com/2006/10/fastest-waves-ever-photographed.html>.

¹⁰⁹² Center for Ultrafast Optical Science, University of Michigan, 2018; <https://cuos.engin.umich.edu/>.

¹⁰⁹³ <https://physics.stackexchange.com/questions/246765/what-is-the-amplitude-of-the-electric-field-in-a-laser>.

¹⁰⁹⁴ Wollert A, Bauke H, Keitel CH. Multi-pair states in electron-positron pair creation. Phys Lett B. 2016 Sep 16;760:552-557; <https://www.sciencedirect.com/science/article/pii/S0370269316303781>.

¹⁰⁹⁵ “The Electromagnetic Pulse and its Effects”; https://www.fourmilab.ch/etexts/www/effects/eonw_11.pdf. “Appendix C. Nuclear Burst Effects on Electronics,” GlobalSecurity.org, 2018; https://www.globalsecurity.org/wmd/library/policy/army/fm/3-3-1_2/Appc.htm.

¹⁰⁹⁶ “Dielectric Strength of Air,” The Physics Factbook, 2000; <https://hypertextbook.com/facts/2000/AliceHong.shtml>.

High electrical energy densities may be exhibited by electrons flowing through conductive wires, including isolated carbon nanotube wires. For example, double-walled carbon nanotubes (DWCNTs) having an average outer diameter of ~ 1.4 nm combine the electrical and thermal stability of multi-wall nanotubes (MWNTs) with the flexibility of single-walled nanotubes (SWNTs)¹⁰⁹⁷ and have already been used to make high-current-carrying field-emission displays (FEDs)¹⁰⁹⁸ and field-effect transistors (FETs).¹⁰⁹⁹ DWCNT nanowires ~ 1.6 nm diameter can likely carry $\sim 50 \times 10^{-6}$ amp/wire at 1 volt – consistent with experimental observations¹¹⁰⁰ of individual 10-50 nm long single-walled “metallic” carbon nanotubes conducting $25\text{-}100 \times 10^{-6}$ amp/wire electrical currents before failing, along with a peak burnout threshold of $\sim 1000 \times 10^{-6}$ amp/wire as reported by others.¹¹⁰¹ A “metallic” carbon nanowire $R_{\text{nanotube}} = 0.8$ nm in radius and $L_{\text{nanotube}} = 50$ nm long (volume ~ 100 nm³) carrying $I_{\text{nanowire}} = 50 \times 10^{-6}$ amp at $E_{\text{nanowire}} = 1$ volt has a notional electrical power density of $P_D = E_{\text{nanowire}} I_{\text{nanowire}} / (\pi R_{\text{nanotube}}^2 L_{\text{nanotube}}) = 5 \times 10^{11}$ MW/L, but this number is misleading because it can be made arbitrarily large by decreasing the length of the wire. The areal power density of $E_{\text{nanowire}} I_{\text{nanowire}} / (\pi R_{\text{nanotube}}^2) = 2.5 \times 10^{13}$ W/m² divided by the electron drift velocity $u_{\text{drift}} \sim I_{\text{nanowire}} / n A q_e = 1500$ m/sec (taking nanotube atomic number density $n \sim 10^{29}$ atoms/m³, wire cross-sectional area $A \sim 2 \times 10^{-18}$ m², and ~ 1 free electron per carbon atom with $q_e = 1.6 \times 10^{-18}$ coul)¹¹⁰² gives a length-independent energy density of $E_D \sim E_{\text{nanowire}} I_{\text{nanowire}} / (A u_{\text{drift}}) = \mathbf{17$ MJ/L in the conducting wire.

Similarly, in residential construction $I = 15$ amps of electrical current may flow at $E = 110$ volts through standard white “Romex” insulated copper wiring¹¹⁰³ having $n = 8.5 \times 10^{28}$ electrons/m³ and a cross-sectional area $A = 2.08$ mm², with an electron drift velocity of $u_{\text{drift}} \sim I / n A q_e = 5.3$ x

¹⁰⁹⁷ Yamada T, Namai T, Hata K, Futaba DN, Mizuno K, Fan J, Yudasaka M, Yumura M, Iijima S. Size-selective growth of double-walled carbon nanotube forests from engineered iron catalysts. *Nature Nanotechnology* 2006;1:131-136; <http://www.nature.com/nnano/journal/v1/n2/full/nnano.2006.95.html>.

¹⁰⁹⁸ H. Kurachi *et al.* FED with double-walled carbon nanotube emitters. *IDW Proc.* 2001:1237-1240.

¹⁰⁹⁹ Shimada T, Sugai T, Ohno Y, Kishimoto S, Mizutani T, Yoshida H, Okazaki T, Shinohara H. Double-wall carbon nanotube field-effect transistors: Ambipolar transport characteristics. *Appl Phys Lett.* 2004 Mar 29;84(13):2412-2414; https://www.researchgate.net/profile/Takashi_Shimada2/publication/37509207_Double-wall_carbon_nanotube_field-effect_transistors_Ambipolar_transport_characteristics/links/0912f507f0d101ab36000000.pdf.

¹¹⁰⁰ Javey A, Qi P, Wang Q, Dai H. Ten- to 50-nm-long quasi-ballistic carbon nanotube devices obtained without complex lithography. *PNAS* 2004 Sep 14;101:13408-13410; <http://www.pnas.org/cgi/content/abstract/101/37/13408>.

¹¹⁰¹ Dai H, Wong EW, Lieber CM. Probing Electrical Transport in Nanomaterials: Conductivity of Individual Carbon Nanotubes. *Science* 1996 Apr 26;272:523-526; http://www.academia.edu/download/24927806/science272_523.pdf. Frank S, Poncharal P, Wang ZL, de Heer WA. Carbon Nanotube Quantum Resistors. *Science* 1998 Jun 12;280:1744-1746; http://www.nanoscience.gatech.edu/paper/1998/98_sci_1.pdf.

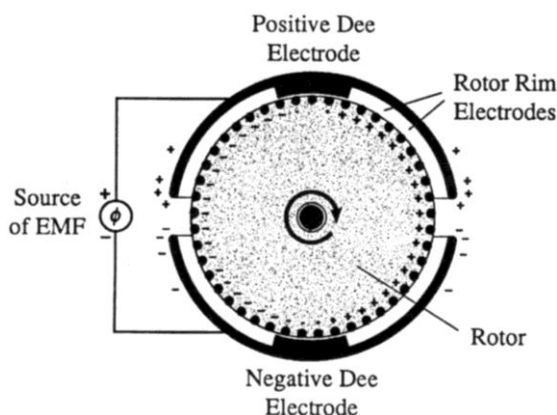
¹¹⁰² https://en.wikipedia.org/wiki/Drift_velocity#Numerical_example.

¹¹⁰³ https://en.wikipedia.org/wiki/Thermoplastic-sheathed_cable#North_America.

10^{-5} m/sec and a length-independent energy density of $E_D \sim E I / (A u_{\text{drift}}) = \mathbf{15,000}$ MJ/L in the conducting wire.

A simple dielectric motor can be operated by drawing a dielectric slab of area A_{slab} and dielectric constant κ_{slab} into a gap d_{gap} between the plates of a charged capacitor at voltage V_{cap} , producing a field-dependent force. Applying a time-varying input voltage of frequency ν_d (Hz) produces a mechanical output power of $P_{\text{slab}} = (\epsilon_0 A_{\text{slab}} / 2 d_{\text{gap}}) (1 - \kappa_{\text{slab}}^{-1}) \nu_d V_{\text{cap}}^2 \sim 5 \times 10^{-15}$ watts, taking vacuum permittivity constant $\epsilon_0 = 8.85 \times 10^{-12}$ coul/N-m², $A_{\text{slab}} = 500$ nm², $d_{\text{gap}} = 2$ nm, $V_{\text{cap}} = 1$ volt, $\kappa_{\text{slab}} = 5.7$ for diamond at 300 K, and $\nu_d = 5000$ Hz. The force applied to the slab during $\Delta x = 1$ nm displacements is $F_{\text{slab}} \sim P_{\text{slab}} / (\Delta x \nu_d) \sim 1$ nN, yielding a power density $P_D \sim P_{\text{slab}} / d_{\text{gap}} A_{\text{slab}} = \mathbf{5}$ MW/L for this device.

A submicron electrostatic motor might achieve much higher power densities. In one implementation (schematic, right), electric charge is placed on the rim of a rotor as the rim passes within a dee electrode. This charge is then transported across a ~ 3 nm gap to the interior of the opposite dee electrode, where it is removed and replaced by a charge of opposite sign. Applying a voltage of proper sign across the dees causes the charges in transit to apply a torque to the rotor (like a Van de Graaff generator¹¹⁰⁴ operating in reverse), converting electrical into mechanical power.



As a specific case,¹¹⁰⁵ a motor $d_{\text{motor}} = 390$ nm in diameter and $t_{\text{motor}} = 25$ nm thick made of diamond with density $\rho_{\text{rod}} = 3510$ kg/m³ and conservative working stress $\sigma_w \sim 10^{10}$ N/m² (maximum of $\sim 1\%$ strain) has a bursting rim speed $v_{\text{burst}} = (\sigma_w / \rho_{\text{rod}})^{1/2} = 1700$ m/sec. A single rotor-embedded diamond electrode of diameter $d_{\text{electrode}} = 3$ nm, length $L_{\text{electrode}} = 20$ nm, and static electric field $E_{\text{electrode}} \sim 0.1 E_{\text{breakdown,diamond}} = 2 \times 10^8$ volts/m requires a surface charge density of $S_q \sim 2 \kappa_e \epsilon_0 E_{\text{electrode}} = 0.0035$ coul/m²,¹¹⁰⁶ taking $\kappa_e \sim 1$ for vacuum, or a charge of $q_{\text{electrode}} \sim$

¹¹⁰⁴ https://en.wikipedia.org/wiki/Van_de_Graaff_generator.

¹¹⁰⁵ Drexler KE. Nanosystems: Molecular Machinery, Manufacturing, and Computation, John Wiley & Sons, New York, 1992; Sec. 11.7 “DC motors and generators”; http://e-drexler.com/d/09/00/Drexler_MIT_dissertation.pdf.

¹¹⁰⁶ The proposed surface charge density of $S_q \sim \mathbf{0.0035}$ coul/m² is well below than the $\sim \mathbf{0.1600}$ coul/m² for charged amino acid molecules and $\sim \mathbf{0.3000}$ coul/m² for “fully ionized surface” [Israelachvili JN. Intermolecular and Surface Forces, Second Edition, Academic Press, NY, 1992] and the $\mathbf{0.0050-0.0200}$ coul/m² recorded experimentally for SiO₂ on mica [Horn RG, Smith DT. Contact Electrification and Adhesion Between Dissimilar Materials. Science 1992 Apr 17;256(5055):362-364; <http://science.sciencemag.org/content/256/5055/362>], but about 10-fold higher than the $\mathbf{0.0002}$ coul/m² figure reported by Lowell and Rose-Innes as typical for “highly charged surfaces” [Lowell J, Rose-Innes AC. Contact electrification. Adv Phys. 1980;29:947-1023; <https://www.tandfonline.com/doi/abs/10.1080/00018738000101466>].

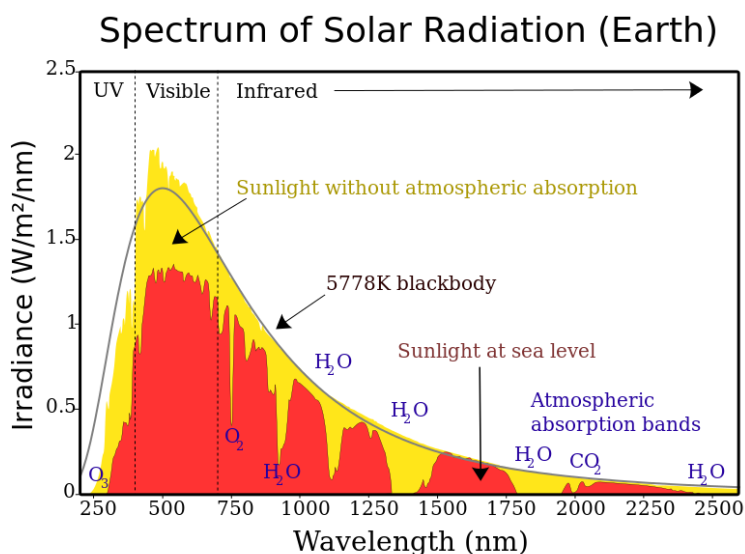
$d_{\text{electrode}} L_{\text{electrode}} S_q = 2.1 \times 10^{-19}$ coul/electrode which gives a charge per unit rotor circumference of $Q_{\text{rim}} = q_{\text{electrode}} / d_{\text{electrode}} = 7 \times 10^{-11}$ coul/m. Taking the motor rim velocity as $v_{\text{rim}} \sim 1000$ m/sec and the charge per unit length as $Q_{\text{rim}} \sim 7 \times 10^{-11}$ coul/m, the current flow is $I_{\text{motor}} = Q_{\text{rim}} v_{\text{rim}} = 7 \times 10^{-8}$ amperes. Imposing an electric potential of $V_{\text{motor}} \sim 10$ volts yields a power output of $P_{\text{motor}} = I_{\text{motor}} V_{\text{motor}} \sim 7 \times 10^{-7}$ watts and a power density of $P_D = 4 P_{\text{motor}} / \pi d_{\text{motor}}^2 t_{\text{motor}} \sim \mathbf{200,000 \text{ MW/L}}$.

6.3 Ambient Electromagnetic Energy

Electromagnetic energy in the form of radio waves, infrared radiation (heat), visible light, gamma rays, cosmic rays, etc. is ubiquitous in the ambient environment. Of these forms, the most plentiful for easy collection in terms of energy per unit volume are the visible photons of light (see chart, right).¹¹⁰⁷

Present-day photovoltaic collectors typically produce a specific power up to **0.000077 MW/kg** for spacecraft-grade devices,¹¹⁰⁸

though the Vanguard THINS thin-film technology achieves **0.0005 MW/kg** and **0.0002 MW/L**.¹¹⁰⁹ Thin-film InP Schottky-type solar cells can produce up to **0.002 MW/kg**,¹¹¹⁰ and in 2016 a thin-film solar cell demonstrated **0.006 MW/kg**.¹¹¹¹ Solar panels for residential use typically achieve only **0.00001-0.00002 MW/kg**.¹¹¹² Biophotovoltaic devices can produce **0.00002 MW/L** power density.¹¹¹³



¹¹⁰⁷ https://upload.wikimedia.org/wikipedia/commons/e/e7/Solar_spectrum_en.svg.

¹¹⁰⁸ Turner MJL. Rocket and Spacecraft Propulsion: Principles, Practice And New Developments. Springer Science, 2005; <https://books.google.com/books?id=ja1ROyh4yPYC&pg=RA1-PA180>.

¹¹⁰⁹ "ParaSol - A Novel Deployable Approach for Very Large Ultra-lightweight Solar Arrays, Phase I", NASA SBIR/STTR, Dec 2014; <https://techport.nasa.gov/view/18152>.

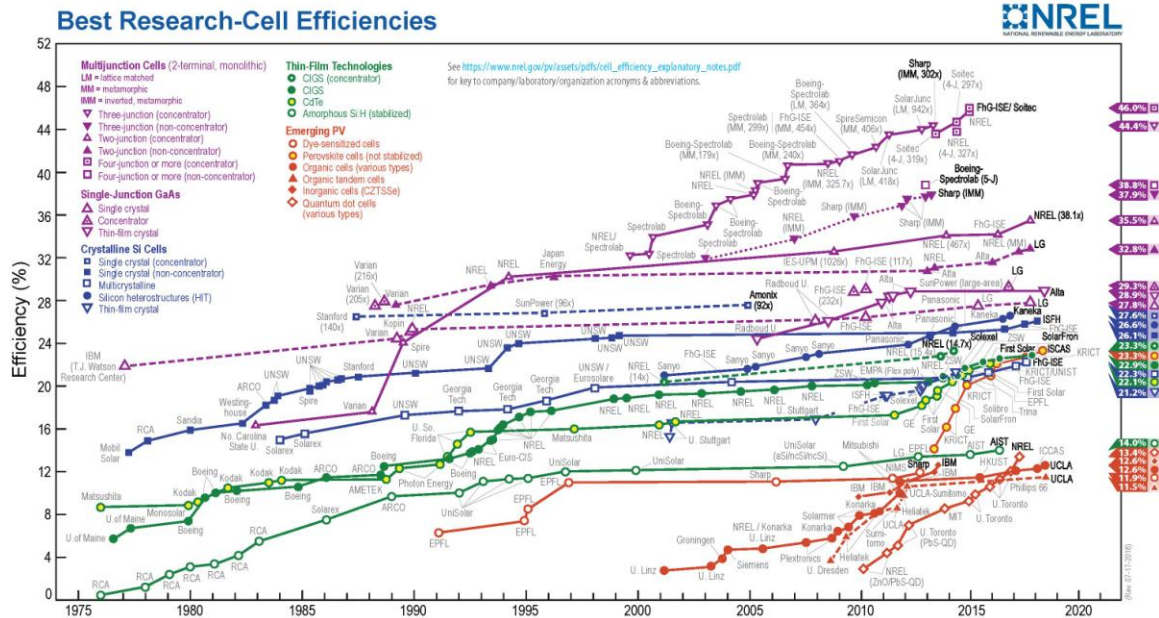
¹¹¹⁰ Shiu KT, Zimmerman J, Wang H, Forrest SR. Ultrathin film, high specific power InP solar cells on flexible plastic substrates. Appl Phys Lett. 2009 Nov;95:223503; <https://aip.scitation.org/doi/10.1063/1.3268805>.

¹¹¹¹ Chandler DL. "Super-skinny solar cells". MIT Technology Review, 26 Apr 2016; <https://www.technologyreview.com/s/601133/super-skinny-solar-cells/>.

¹¹¹² "How many watt/kg do the best commercially available solar panels currently have?" Quora, 20 Nov 2015; <https://www.quora.com/How-many-watt/kg-do-the-best-commercially-available-solar-panels-currently-have>.

¹¹¹³ Bombelli P, Müller T, Herling TW, Howe CJ, Knowles TP. A High Power-Density, Mediator-Free, Microfluidic Biophotovoltaic Device for Cyanobacterial Cells. Adv Energy Mater. 2015 Jan 21;5(2):1-6; <https://www.ncbi.nlm.nih.gov/pmc/articles/PMC4503997/pdf/aenm0005-0001.pdf>.

At the Earth's distance from the Sun where solar insolation (aka. the solar constant) is $I_{\text{Earth}} = 1370 \text{ W/m}^2$ (ambient energy density $E_D \sim I_{\text{Earth}} / c \sim 4.6 \times 10^{-15} \text{ MJ/L}$), a 1 mm thick solar panel with ~50% efficiency (see historical chart of research-grade photovoltaic cell efficiencies, below)¹¹¹⁴ would have a power density of **0.0005 MW/L** (~0.0002 MW/kg for silicon @ 2.329 kg/L). A much thinner 1-micron thick cell would raise the power density of the collector to ~0.5 MW/L (~0.2 MW/kg for silicon), and still thinner cells could have even higher power density.¹¹¹⁵



Power density also might be nearly doubled from the above numbers if nanostructured optical rectennas or nantennas¹¹¹⁶ can be devised with whole-spectrum conversion efficiencies approaching 90%.¹¹¹⁷ More specifically, theory predicts a maximum thermodynamic limit of 85.4% efficiency for a non-energy-selective solar collector with maximal concentration assuming the Sun to be a ~6000 K black body radiator and assuming the surroundings to be at ~300 K, or up to 86.8% assuming an infinite series of frequency-selective filters in the case of a solar

¹¹¹⁴ https://en.wikipedia.org/wiki/Solar_cell_efficiency.

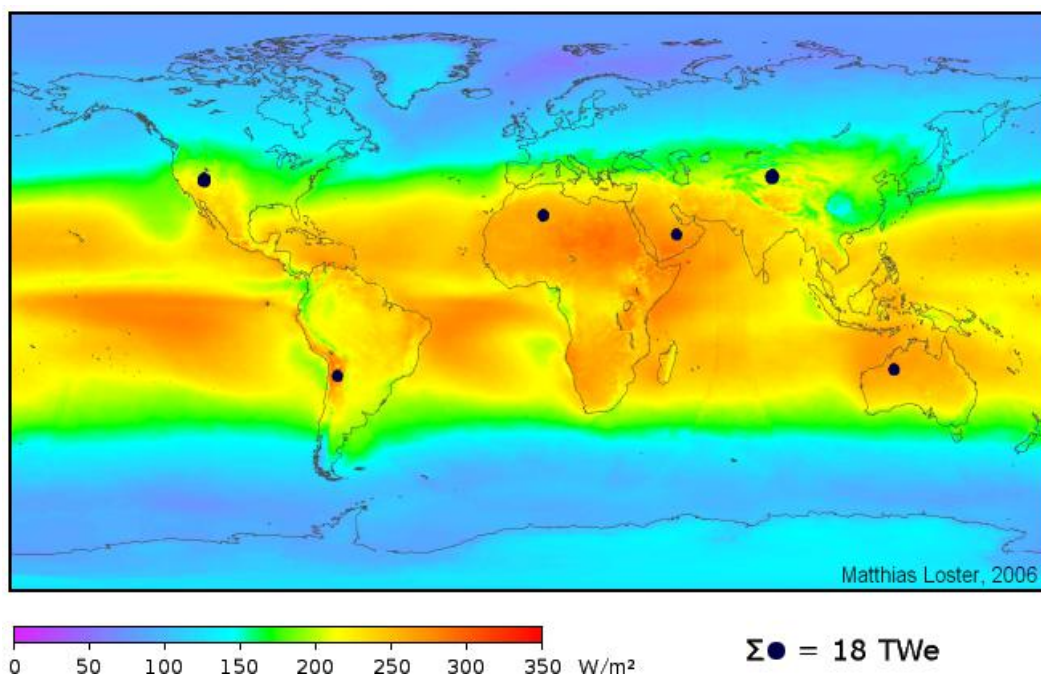
¹¹¹⁵ A detailed analysis of atomically precise diamondoid solar cells measuring ~200 μm in diameter and ~500 nm thick (primary mirror) and massing ~20 $\times 10^{-12}$ kg, should be able to achieve up to ~1 MW/kg when ideally positioned in orbital space at the Earth's distance from the Sun (1 AU). Thomas L. McKendree, Technical and Operational Assessment of Molecular Nanotechnology for Space Operations, Ph.D. Dissertation, University of Southern California, Aug 2001 (Section 3.2.2 and Appendix H); <http://digitallibrary.usc.edu/cdm/ref/collection/p15799coll16/id/166699>.

¹¹¹⁶ https://en.wikipedia.org/wiki/Optical_rectenna.

¹¹¹⁷ Johnson RC. Solar Cells Made Obsolete: 3D rectennas aim at 40%-90% efficiency. EE Times, 28 Sep 2015; https://www.eetimes.com/document.asp?doc_id=1327819.

rectenna.¹¹¹⁸ An optical antenna or nantenna (e.g., using carbon nanotubes¹¹¹⁹) can absorb any wavelength of light efficiently, provided that the size of the antenna is optimized for that specific wavelength. For sunlight, nantennas would absorb light at wavelengths between 0.4-1.6 μm because these wavelengths have higher energy than far-infrared (longer wavelengths) and make up about 85% of the solar radiation spectrum.¹¹²⁰

Note that the “lighting power density” commonly available on the surface of the Earth is considerably less than the 1370 W/m^2 available above the top of the atmosphere – typically only 5-15 W/m^2 inside well-lighted buildings¹¹²¹ but up to 200-300 W/m^2 ($\sim 0.7\text{-}1 \times 10^{15}$ MJ/L) in full daylight sun at the equator.¹¹²² The map below shows worldwide average total solar irradiance at the Earth’s surface, averaged over 3 years from 1991-1993 for 24 hours/day, taking into account the cloud coverage available from weather satellites.¹¹²³ (Solar collector areas defined by the dark disks on the map could collectively provide 18 terawatts (electrical), roughly the world’s total primary energy demand in 2018, assuming only 8% conversion efficiency.)



¹¹¹⁸ Corkish R, Green MA, Puzzer T. Solar energy collection by antennas. *Solar Energy* 2002;73(6):395-401; https://www.univie.ac.at/photovoltaik/vorlesung/ss2013/unit4/solar_antenna.pdf.

¹¹¹⁹ <http://www.novasolix.com/technology/>, <https://www.nextbigfuture.com/2018/11/self-assembled-carbon-nanotube-antennas-for-solar-power-revolution.html>.

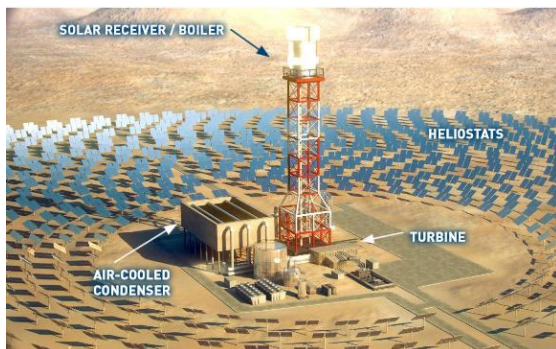
¹¹²⁰ https://en.wikipedia.org/wiki/Optical_rectenna.

¹¹²¹ “Lighting System Assessment Guidelines,” U.S. Dept. of Energy, NREL/BR-7A20-50125, Jun 2011; <https://www.nrel.gov/docs/fy11osti/50125.pdf>.

¹¹²² http://en.wikipedia.org/wiki/File:Solar_land_area.png.

¹¹²³ http://en.wikipedia.org/wiki/File:Solar_land_area.png.

Concentrated solar power (CSP) systems generate solar power by using mirrors or lenses to concentrate a large area of sunlight, or solar thermal energy, onto a small area, whereupon electricity can be generated when the concentrated light (A) is converted to heat that drives a heat engine (usually a steam turbine) connected to an electrical power generator, or (B) powers a thermochemical reaction.¹¹²⁴ The 392 MW Ivanpah Solar Power Facility,¹¹²⁵ second largest such



facility in the world, uses 173,500 heliostats each having two mirrors with 14.05 m² of reflecting area to focus sunlight on boilers located on three centralized solar power towers (image, left). The mirrors focus ambient sunlight onto three cylindrical collectors (boilers) that sit atop three 459 foot tall towers.¹¹²⁶ Assuming the collectors are 25 m tall and 18 m in diameter, the three boilers together receive 759 MW of solar energy distributed over a surface area of 4241 m²,

giving an intensity of $I_{\text{solar,CSP}} = 179 \text{ kW/m}^2$ and an average energy density at the boiler surfaces of $E_D \sim I_{\text{solar,CSP}} / c = 0.6 \times 10^{-12} \text{ MJ/L}$. High concentration photovoltaic (HCPV) systems employ concentrating optics consisting of dish reflectors or Fresnel lenses that converge sunlight to intensities of 1,000 suns or more.¹¹²⁷ Taking $I_{\text{solar,HCPV}} \sim 3 \times 10^5 \text{ W/m}^2$, energy density is still only $E_D \sim I_{\text{solar,HCPV}} / c \sim 1 \times 10^{-12} \text{ MJ/L}$.

One crude upper limit on photovoltaic energy density using a physical collector is that the incident energy converted to waste heat cannot be so intense as to melt the collector.¹¹²⁸ This defines a maximum limit on photovoltaic energy density of $E_{D,\text{max}} = C_V (T_{\text{max}} - T_{\text{ambient}}) / (1 - e\%)$, where C_V is the heat capacity of the collector material, T_{max} is the maximum functional temperature of the collector, T_{ambient} is the initial temperature of the collector before incident energy arrives, and $e\%$ is the efficiency with which incident light is converted into electricity (hence $1 - e\%$ is the incident energy converted into waste heat), assuming that the incident energy arrives too fast for most of the waste heat to be radiated or conducted away from the collector. This crude energy capacity limit yields $E_{D,\text{max}} = 2.3 \text{ MJ/L}$ for silicon ($C_V = 1.64 \times 10^6 \text{ J/m}^3\text{-K}$, $T_{\text{max}} = T_{\text{melt}} = 1687 \text{ K}$), 2.8 MJ/L for diamond ($C_V = 1.82 \times 10^6 \text{ J/m}^3\text{-K}$, $T_{\text{max}} = T_{\text{burn}} = 1070 \text{ K}$), 12 MJ/L for sapphire ($C_V = 2.89 \times 10^6 \text{ J/m}^3\text{-K}$, $T_{\text{max}} = T_{\text{melt}} = 2300 \text{ K}$), and 17 MJ/L for tungsten (if tungsten could somehow perform as a photovoltaic material; $C_V = 2.55 \times 10^6 \text{ J/m}^3\text{-K}$, $T_{\text{max}} = T_{\text{melt}} = 3695 \text{ K}$), assuming ambient room temperature operation at $T_{\text{ambient}} = 300 \text{ K}$ with $e\% = 50\%$.

¹¹²⁴ https://en.wikipedia.org/wiki/Concentrated_solar_power.

¹¹²⁵ https://en.wikipedia.org/wiki/Ivanpah_Solar_Power_Facility.

¹¹²⁶ "Ivanpah Project Facts," Bright Source Limitless; http://www.brightsourceenergy.com/stuff/contentmgr/files/0/8a69e55a233e0b7edfe14b9f77f5eb8d/folder/ivanpah_fact_sheet_3_26_14.pdf.

¹¹²⁷ [https://en.wikipedia.org/wiki/Concentrator_photovoltaics#High_concentration_photovoltaics_\(HCPV\)](https://en.wikipedia.org/wiki/Concentrator_photovoltaics#High_concentration_photovoltaics_(HCPV)).

¹¹²⁸ Sarah Zhang, "A Huge Solar Plant Caught on Fire," Wired, 23 May 2016; <https://www.wired.com/2016/05/huge-solar-plant-caught-fire-thats-least-problems/>.

(The above figures would be 3.79 times higher using $\epsilon = 86.8\%$ instead of 50%.) If the collector can continue to operate in the liquid state, then $T_{\max} = T_{\text{boil}}$ could be substituted for $T_{\max} = T_{\text{melt}}$ but the overall limiting energy density would be largely unchanged in most cases.

Other forms of ambient electromagnetic radiation normally present in the environment are much less intense. For example, radio frequency (RF) exposures in developed countries in the 0.03-3 GHz frequency range are typically $\sim 16 \mu\text{W}/\text{m}^2$ in rural areas, $\sim 270 \mu\text{W}/\text{m}^2$ in urban areas, and $\sim 2400 \mu\text{W}/\text{m}^2$ in city areas, with occasional peak readings as high as $0.1 \text{ W}/\text{m}^2$.¹¹²⁹ The inside of a microwave oven generates ~ 700 watts of 2.45 GHz microwave power over an interior cooking chamber area of $\sim 0.16 \text{ m}^2$ generating a power intensity of $I_{\text{micro}} = 4375 \text{ W}/\text{m}^2$, (energy density $E_D \sim I_{\text{micro}} / c \sim \mathbf{1.5 \times 10^{-14} \text{ MJ/L}}$) but the maximum legally-allowable leakage is only $50 \text{ W}/\text{m}^2$ at 5 cm from the oven surface.¹¹³⁰ (Note that 700 watts flooding a $\sim 25,000 \text{ cm}^3$ microwave oven volume implies a power density $P_D \sim \mathbf{0.000028 \text{ MW/L}}$.) Rectennas for receiving RF radiation between 3-18 GHz for direct conversion to electricity currently achieve at least $\sim 20\%$ efficiency,¹¹³¹ and nanoradios have been constructed using a carbon nanotube¹¹³² or graphene sheet¹¹³³ to receive ambient RF signals in the MHz-GHz range.

Persons standing too close in front of an operating microwave radar dish can experience severe heating and injury.¹¹³⁴ The radiated power of a microwave radar dish is $P_{\text{rad}} = P_{\text{trans}} g_{\text{dish}} A_{\text{dish}} / 4\pi X^2 = (\pi^2 v^2 R_{\text{dish}}^4 / c^2 X^2) P_{\text{trans}}$ at a distance X from a circular antenna with transmitter power P_{trans} , radius R_{dish} , aperture area $A_{\text{dish}} = \pi^2 R_{\text{dish}}^2$, geometric gain $g_{\text{dish}} = (2\pi R_{\text{dish}} v / c)^2$, and microwave frequency v . Energy density $E_D = P_{\text{rad}} / 4\pi X^2 = (\pi v^2 R_{\text{dish}}^4 / 4 c^3 X^4) P_{\text{trans}} = \mathbf{2.9 \times 10^{-10} \text{ MJ/L}}$ taking $v = 10 \text{ GHz}$, $P_{\text{trans}} \sim 10^5$ watts, $R_{\text{dish}} = X = 10 \text{ m}$, and $c = 3 \times 10^8 \text{ m/sec}$ (speed of light).

¹¹²⁹ Hedendahl LK, Carlberg M, Koppel T, Hardell L. Measurements of radiofrequency radiation with a body-borne exposimeter in Swedish schools with Wi-Fi. *Front. Public Health* 2017 Nov 20; <https://www.frontiersin.org/articles/10.3389/fpubh.2017.00279/full>.

¹¹³⁰ https://en.wikipedia.org/wiki/Microwave_oven.

¹¹³¹ Hagerty JA, Helmbrecht FB, McCalpin WH, Zane R, Popovic ZB. Recycling ambient microwave energy with broad-band rectenna arrays. *IEEE Trans Microwave Theory and Techniques*. 2004 Mar;52(3):1014-1024; http://nemes.colorado.edu/microwave/papers/2004/MTT_JHfhWMrzZP_Mar04.pdf.

¹¹³² Jensen K, Weldon J, Garcia H, Zettl A. Nanotube radio. *Nano Lett*. 2007;7(11):3508-3511; <https://pubs.acs.org/doi/10.1021/nl0721113>. Dragoman D, Dragoman M. Tunneling nanotube radio. *J Appl Phys*. 2008 Oct;104(7):074314; <http://adsabs.harvard.edu/abs/2008jap...104g4314d>.

¹¹³³ Dragoman, M, Neculoiu D, Cismaru A, Deligeorgis G, Konstantinidis G, Dragoman D. Graphene radio: Detecting radio waves with a single atom sheet. *Appl Phys Lett*. 2012 Jul;101(3):033109; <https://arxiv.org/pdf/1202.1968>.

¹¹³⁴ <https://www.quora.com/Would-anything-happen-if-you-stand-in-front-of-a-powerful-military-radar-at-the-point-when-its-strength-is-the-greatest>.

6.4 Beamed Electromagnetic Energy

The most common and powerful source of beamed electromagnetic energy is the optical laser. What is the maximum energy density of an optical laser beam? The most powerful continuous-wave lasers are in the 0.1-1 MW range, mostly for military applications.¹¹³⁵ For example, the highest-power continuous laser of any type developed to date is the MIRACL infrared laser ($\lambda = 3600\text{-}4000\text{ nm}$) built by TRW for the U.S. Navy in 1980.¹¹³⁶ MIRACL was a continuous-wave deuterium fluoride based chemical laser that could produce ~ 1 megawatt power levels, emitted through a 21 cm x 3 cm aperture, for up to 70 seconds at a time, accumulating over 3500 sec of total lasing time.¹¹³⁷ The 0.006 m² aperture for MIRACL gives an intensity of $I_{\text{laser}} \sim 160\text{ MW/m}^2$, representing a beamline energy density of only $E_D = I_{\text{laser}} / c \sim \mathbf{5 \times 10^{-9}\text{ MJ/L}}$.

The HERCULES laser at the University of Michigan holds the 2006-2018 world record for focused laser beam intensity at $I_{\text{laser}} = 2 \times 10^{26}\text{ W/m}^2$,¹¹³⁸ giving a laser electric field strength of $E_{\text{laser}} = (2 I_{\text{laser}} / c \epsilon_0)^{1/2} = 3.9 \times 10^{14}\text{ volts/m}$ (speed of light $c = 3 \times 10^8\text{ m/sec}$),¹¹³⁹ equivalent to an energy density of $E_D = I_{\text{laser}} / c = 6.7 \times 10^{17}\text{ joules/m}^3$ (**$6.7 \times 10^8\text{ MJ/L}$**) in vacuum. However, this tremendous field intensity is not a continuous laser source but rather is the result of mere 9-joule pulses produced in 30 femtosecond chirps with a repetition rate of 0.1 Hz.¹¹⁴⁰ The highest-intensity lasers typically operate in the range of $10^{18}\text{-}10^{26}\text{ W/m}^2$ with pulse lengths of $10^{-12}\text{-}10^{-14}\text{ sec}$ and repetition rates of $10^3\text{-}10^6\text{ Hz}$ with average continuous power of 10-100 W.¹¹⁴¹ Laser field strengths up to $m^2c^3/e\hbar \approx 1.32 \times 10^{18}\text{ volts/m}$ (**$7.7 \times 10^{15}\text{ MJ/L}$** in vacuum), the Schwinger critical field strength,¹¹⁴² are theoretically possible but would have to be maintainable for extended durations to be useful for an energy storage device.

¹¹³⁵ “Navy buying two 150 kilowatt combat lasers for \$150 million and 300 kilowatt lasers for another \$800 million,” Next Big Future, 8 Feb 2018; <https://www.nextbigfuture.com/2018/02/navy-buying-two-150-kilowatt-combat-lasers-for-150-million-and-300-kilowatt-lasers-for-another-800-million.html>. See also: https://en.wikipedia.org/wiki/Laser_Weapon_System; https://en.wikipedia.org/wiki/Advanced_Tactical_Laser; https://en.wikipedia.org/wiki/Iron_Beam.

¹¹³⁶ <https://en.wikipedia.org/wiki/MIRACL>.

¹¹³⁷ “MIRACL,” <https://web.archive.org/web/20070808184605/http://helstf-www.wsmr.army.mil/miracl.htm>.

¹¹³⁸ Center for Ultrafast Optical Science, University of Michigan, 2018; <https://cuos.engin.umich.edu/>.

¹¹³⁹ <https://physics.stackexchange.com/questions/246765/what-is-the-amplitude-of-the-electric-field-in-a-laser>.

¹¹⁴⁰ <https://cuos.engin.umich.edu/researchgroups/hfs/facilities/hercules-petawatt-laser/>.

¹¹⁴¹ Sprangle P, Hafizi B. High-power, high-intensity laser propagation and interactions. *Physics of Plasmas* 2014;21:055402; <https://aip.scitation.org/doi/pdf/10.1063/1.4878356>.

¹¹⁴² Wollert A, Bauke H, Keitel CH. Multi-pair states in electron-positron pair creation. *Phys Lett B*. 2016 Sep 16;760:552-557; <https://www.sciencedirect.com/science/article/pii/S0370269316303781>.

In occupational health science, the maximum safe exposure limits of electromagnetic radiation that may be applied to the overall human body continuously for unlimited durations is $P_{\text{electromagnetic}} \sim 100 \text{ W/m}^2$ for the frequency ranges 0.01-1 MHz and 10^3 - 10^6 MHz, and $\sim 10 \text{ W/m}^2$ for 1-1000 MHz.¹¹⁴³ Taking the speed of electromagnetic radiation in human tissue as roughly the same as the speed of light generally ($c \sim 3 \times 10^8 \text{ m/sec}$), the energy density of the electromagnetic field during an exposure at the maximum safe continuous intensity is $E_D \sim P_{\text{electromagnetic}} / c \sim 3 \times 10^{-17} \text{ MJ/L}$ for 1-1000 MHz and $\sim 3 \times 10^{-16} \text{ MJ/L}$ elsewhere in the frequency spectrum.

In biomedical applications, silica fibers are used to conduct photons from excimer lasers, the brightest known sources of UV radiation.¹¹⁴⁴ Typical continuous laser power intensities are $\sim 30,000 \text{ watts/m}^2$ ($\sim 1 \times 10^{-13} \text{ MJ/L}$) for corneal sculpting, $\sim 10^5 \text{ watts/m}^2$ ($\sim 3 \times 10^{-13} \text{ MJ/L}$) for bile duct cholangiocarcinoma tumor surgery, and $\sim 10^6 \text{ watts/m}^2$ ($\sim 3 \times 10^{-12} \text{ MJ/L}$) for arterial debulking, laser dental machining and laser lithotripsy for kidney stones.¹¹⁴⁵

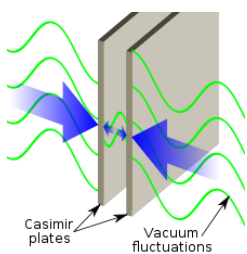
¹¹⁴³ Czerski P. The development of biomedical approaches and concepts in radiofrequency radiation protection. *J Microw Power Electromagn Energy* 1986;21(1):9-23; <https://www.tandfonline.com/doi/abs/10.1080/08327823.1986.11687978>.

¹¹⁴⁴ van Leeuwen TG, Borst C. Fundamental laser-tissue interactions. *Semin Interv Cardiol.* 1996 Jun;1:121-128; see related papers, pp. 129-171. Manche EE, Carr JD, Haw WW, Hersh PS. Excimer laser refractive surgery. *West J Med.* 1998 Jul;169:30-38; <https://www.ncbi.nlm.nih.gov/pmc/articles/PMC1305094/pdf/westjmed00322-0032.pdf>.

¹¹⁴⁵ Gower M. Chapter 12. Excimer Lasers for Surgery and Biomedical Fabrication. In: Coombs RRH, Robinson DW, eds., *Nanotechnology in Medicine and the Biosciences*, Gordon & Breach Publishers, Netherlands, 1996, pp. 169-193. Pearson G. Precision Milling of Teeth for Dental Caries. In: Coombs RRH, Robinson DW, eds., *Nanotechnology in Medicine and the Biosciences*, Gordon & Breach Publishers, Netherlands, 1996, pp. 195-208.

6.5 Casimir Effect and Vacuum Energy

The Dutch physicists Hendrik Casimir and Dirk Polder at Philips Research Labs proposed the existence of a force between two polarizable atoms and between such an atom and a conducting plate in 1947, but after a conversation with Niels Bohr, who suggested it had something to do with zero-point energy, Casimir alone formulated the theory predicting a force between neutral conducting plates in 1948 which is now called the Casimir effect.¹¹⁴⁶ These predictions of quantum electrodynamics theory were verified to within 5% in 1997,¹¹⁴⁷ and again to within 1% in 1998.¹¹⁴⁸



The typical example is of two uncharged conductive plates in a vacuum, placed a few nanometers or microns apart. In a classical description, the lack of an external field means that there is no field between the plates, and no force would be measured between them.¹¹⁴⁹ When this field is instead studied using the quantum electrodynamic vacuum, it is seen that the plates do affect the virtual photons which constitute the field, and generate a net force – either an attraction or a repulsion depending on the specific arrangement of the two plates. The simplest explanation of the Casimir effect is that the two metal plates attract because their reflective surfaces exclude virtual photons of wavelengths longer than the separation distance, reducing the energy density between the plates compared with that outside, and – like external air pressure tending to collapse a slightly evacuated vessel – the Casimir force pulls the plates toward one another.¹¹⁵⁰ The magnitude of the Casimir force F_{Casimir} between two plates per unit area A (equivalent to energy density) separated by a distance d_{plates} is:

$$E_{D,\text{Casimir}} = F_{\text{Casimir}}/A = (\pi/480) (hc/d_{\text{plates}}^4) \text{ (N/m}^2\text{) or (J/m}^3\text{)}$$

The strength of the force falls off rapidly with distance and is measurable only when the distance between the objects is extremely small, becoming the dominant force between uncharged conductors at the submicron scale. For example, at a separation of $d_{\text{plates}} = 10 \text{ nm}$ – about 100

¹¹⁴⁶ https://en.wikipedia.org/wiki/Casimir_effect.

¹¹⁴⁷ Lamoreaux SK. Demonstration of the Casimir Force in the 0.6 to 6 μm Range. Phys Rev Lett. 1997 Jan 6;78(1):5-8; <http://web.mit.edu/~kardar/www/research/seminars/Casimir/PRL-Lamoreaux.pdf>.

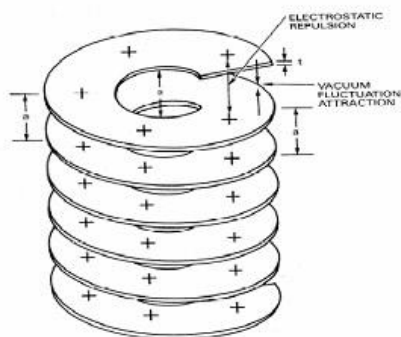
¹¹⁴⁸ Mohideen U, Roy A. Precision Measurement of the Casimir Force from 0.1 to 0.9 μm . Phys Rev Lett 1998 Nov;81:4549; <http://web.mit.edu/kardar/www/research/seminars/PolymerForce/articles/PRL-Mohideen98.pdf>.

¹¹⁴⁹ Genet C, Intravaia F, Lambrecht A, Reynaud S. Electromagnetic vacuum fluctuations, Casimir and Van der Waals forces. Annales de la Fondation Louis de Broglie. 2004;29 (1-2):311-328; <https://arxiv.org/abs/quant-ph/0302072>.

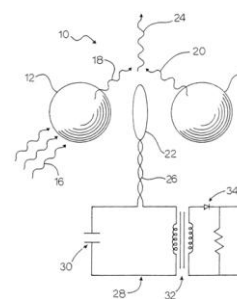
¹¹⁵⁰ Focus: The Force of Empty Space. Phys Rev Focus 1998 Dec;3(2):28; <https://physics.aps.org/story/v2/st28>.

times the typical size of an atom – the Casimir effect produces the equivalent of 1.3 atm of pressure or $E_{D,Casimir} = 1.3 \times 10^{-4} \text{ MJ/L}$, taking $h = 6.63 \times 10^{-34} \text{ J-sec}$ and $c = 3 \times 10^8 \text{ m/sec}$, rising to $\sim 1.3 \text{ MJ/L}$ for a $d_{plates} \sim 1 \text{ nm}$ separation (very close to “contact”, typically taken as $\sim 0.2 \text{ nm}$).

Although the Casimir effect can be expressed in terms of virtual particles interacting with the objects, it is best described and more easily calculated in terms of the zero-point energy (ZPE) or vacuum energy¹¹⁵¹ of a quantized field in the intervening space between the objects. Quantum theory predicts that the vacuum of space in the universe is filled with low-energy electromagnetic waves, random in phase and amplitude and propagating in all possible directions. This is different from the cosmic microwave background radiation and it is referred to as the electromagnetic quantum vacuum since it is the lowest energy state of otherwise empty space. Electromagnetic quantum vacuum energy, aka. zero-point vacuum energy density, has been estimated¹¹⁵² by summing the zero-point energies of all the electromagnetic vibrational modes predicted to exist by quantum theory, giving $E_{D,vacuum} = h \nu_{Planck}^4 / 16 \pi^3 c^3 \sim 5.8 \times 10^{102} \text{ MJ/L}$ (mass-energy $6.4 \times 10^{94} \text{ kg/m}^3$) when integrated over all frequency modes up to the Planck frequency ($\nu_{Planck} = 1.85 \times 10^{43} \text{ Hz}$)¹¹⁵³ as the cutoff, where $h = 6.63 \times 10^{-34} \text{ J-sec}$ and $c = 3 \times 10^8 \text{ m/sec}$.



This energy density is so enormous that most physicists believe that even though zero-point energy seems to be an inescapable consequence of quantum field theory, it cannot be physically real. Nevertheless there have been several proposals for extracting energy from the vacuum zero-point field, including the **Vacuum-Fluctuation Battery** (image, left)¹¹⁵⁴ and the **ZPE Resonant Dielectric Spheres Electrical Power Generator** (image, right).¹¹⁵⁵



¹¹⁵¹ https://en.wikipedia.org/wiki/Vacuum_energy.

¹¹⁵² Davis EW, Teofilo VL, Haisch B, Puthoff HE, Nickisch LJ, Rueda A, Cole DC. Review of Experimental Concepts for Studying the Quantum Vacuum Field. AIP Conf. Proc. 2006;813:1390-1401; http://www.bu.edu/simulation/publications/dcole/PDF/Davis%20et%20al_STAIF06_Log063.pdf.

¹¹⁵³ https://en.wikipedia.org/wiki/Planck_units#Derived_units.

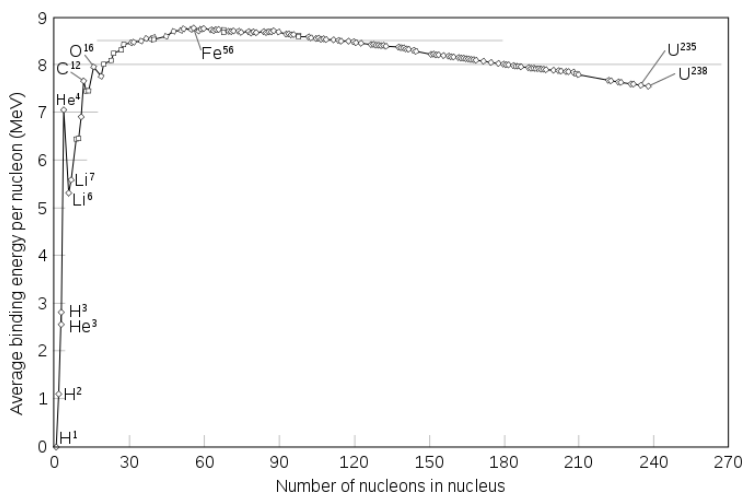
¹¹⁵⁴ Forward RL. Alternate Propulsion Energy Sources, Final Report AFRPL TR-83-067, Air Force Rocket Propulsion Laboratory, Air Force Space Tech. Ctr. Space Div., Air Force Systems Command, Edwards AFB, CA, 1983, pp. A1-A14; <http://www.dtic.mil/dtic/tr/fulltext/u2/b088771.pdf>. Forward RL. Extracting Electrical Energy from the Vacuum by Cohesion of Charged Foliated Conductors. Phys Rev B. 1984 Aug 15;30(4):1700-1702; <https://journals.aps.org/prb/abstract/10.1103/PhysRevB.30.1700>.

¹¹⁵⁵ Mead FB, Nachamkin J. System for converting electromagnetic radiation energy to electrical energy. United States Patent No. 5,590,031, 1996; <https://patentimages.storage.googleapis.com/37/c6/ba/566c00e9b0f513/US5590031.pdf>.

Chapter 7. Nuclear Energy Storage

The atoms of most elements found in nature contain within their nuclei a certain amount of stored or latent nuclear energy that in principle is available to be released. The energy stored in the nuclei of atoms is commonly called the nuclear binding energy. The nuclear binding energy is the minimum energy that would be required to disassemble the nucleus into its constituent nucleons (protons and neutrons). The binding energy is always a positive number because energy must be expended to move these nucleons – which are attracted to each other by the short-range strong nuclear force – away from each other. As a result, the mass of an atomic nucleus is always less than the sum of the individual masses of the free constituent protons and neutrons. This “missing mass” is called the mass defect and represents the energy that was released when the nucleus was formed from its physically separated constituent nucleons.

The potential nuclear energy that is available to be released (E_{nuclear}) can be approximated from the average nuclear binding energy per nucleon for a particular atomic nucleus (chart, below). The largest nuclear binding energy of $E_{\text{bind}} = 8.7948 \text{ MeV/nucleon}$ occurs for the nickel nucleus ^{62}Ni while the smallest mass per nucleon occurs for ^5Fe ($E_{\text{bind}} = 8.7906 \text{ MeV}$), 1156 nuclei that sit at the highest point on the binding energy curve and therefore cannot yield further energy from either fusion or fission. Lighter or heavier nuclei retain at least some potential binding energy that in principle could be released by transmutation to ^{56}Fe or ^{62}Ni , respectively, via fusion or fission.



¹¹⁵⁶ The net binding energy of a nucleus is that of the nuclear attraction, minus the disruptive energy of the electric force. As nuclei get heavier than helium, their net binding energy per nucleon (deduced from the difference in mass between the nucleus and the sum of masses of component nucleons) grows more and more slowly, reaching its peak at iron. As nucleons are added, the total nuclear binding energy always increases – but the total disruptive energy of electric forces (positive protons repelling other protons) also increases, and, past iron, the second increase outweighs the first. ^{56}Fe is the most efficiently bound nucleus with the least average mass per nucleon, while ^{62}Ni is the most tightly bound nucleus in terms of energy of binding per nucleon. The higher energy of binding of ^{62}Ni does not translate to a larger mean mass loss than ^{56}Fe , because ^{62}Ni has a slightly higher ratio of neutrons/protons than does ^{56}Fe , and the presence of the heavier neutrons increases the average mass per nucleon of ^{62}Ni . Photodisintegration of ^{62}Ni to form ^{56}Fe might be energetically possible in an extremely hot star core due to beta decay conversion of neutrons to protons, in which case energy can be released by converting all matter into ^{56}Fe nuclei (ionized atoms) at the pressure and temperature conditions in the cores of large stars.

https://en.wikipedia.org/wiki/Nuclear_binding_energy#The_binding_energy_maximum_and_ways_to_approach_it_by_decay.

The fact that the maximum binding energy is found in medium-sized nuclei is a consequence of the trade-off in the effects of two opposing forces that have different range characteristics. The attractive nuclear force (strong nuclear force), which binds protons and neutrons equally to each other, has a limited range due to a rapid exponential decrease in this force with distance. However, the repelling electromagnetic force, which acts between protons to force nuclei apart, falls off with distance much more slowly (as the inverse square of distance). For nuclei larger than about four nucleons in diameter, the incremental repelling force of additional protons more than offsets any binding energy that results between further added nucleons as a result of additional strong force interactions. Such nuclei become increasingly less tightly bound as their size increases, though most of them are still stable. Finally, nuclei containing more than 209 nucleons (larger than about 6 nucleons in diameter) are all too large to be stable, and are subject to spontaneous decay to smaller nuclei.¹¹⁵⁷

The potential nuclear energy available to be released may be approximated by $E_{\text{nuclear}} \sim \Sigma[E_{\text{bind}}(\text{products})] - \Sigma[E_{\text{bind}}(\text{reactants})]$, where the average binding energy per nucleon for all known nuclei is widely available in tabulated form.¹¹⁵⁸ Taking ^{56}Fe as the endpoint product and using protons (hydrogen nuclei) and neutrons as the minimum-binding-energy reactants, the maximum possible fusion nuclear energy release upon forming a single product nucleus is $E_{\text{nuclear,max}} \sim [E_{\text{bind}}(^{56}\text{Fe})] - [E_{\text{bind}}(26 \text{ protons} + 30 \text{ neutrons})] = [(56)(8.7903 \text{ MeV})] - [(26)(0.0000136 \text{ MeV}) + (30)(0 \text{ MeV})] = 492.256 \text{ MeV} = 7.887 \times 10^{-11} \text{ joules}$. The mass of the reactants is $m_{\text{reactants}} = (26)(1.6726 \times 10^{-27} \text{ kg}) + (30)(1.6749 \times 10^{-27} \text{ kg}) = 9.3735 \times 10^{-26} \text{ kg}$, giving fusion fuel a theoretical maximum specific energy of $E_S = E_{\text{nuclear,max}} / m_{\text{reactants}} = \mathbf{841 \times 10^6 \text{ MJ/kg}}$.

A similar calculation for radioisotopes, assuming it was possible for $^{294}\text{Og}_{118}$ (the experimentally-observed synthetic superheavy element isotope with the lowest-known average binding energy per nucleon of 7.080 MeV)¹¹⁵⁹ to decay all the way to ^{56}Fe , would give an estimated maximum possible nuclear energy release from a single radionuclide nucleus of $E_{\text{nuclear,max}} \sim [E_{\text{bind}}(^{56}\text{Fe})] - [E_{\text{bind}}(^{294}\text{Og}_{118})] = (294)[(8.7903 \text{ MeV})] - [(7.080 \text{ MeV})] = 502.828 \text{ MeV} = 8.056 \times 10^{-11} \text{ joules}$. The mass of the reactants is $m_{\text{reactants}} = (294.213920 \text{ amu})(1.660539 \times 10^{-27} \text{ kg/amu}) = 4.8855 \times 10^{-25} \text{ kg}$, giving radionuclides a theoretical maximum specific energy of $E_S = E_{\text{nuclear,max}} / m_{\text{reactants}} = \mathbf{165 \times 10^6 \text{ MJ/kg}}$.

¹¹⁵⁷ https://en.wikipedia.org/wiki/Nuclear_binding_energy#Binding_energy_and_nuclide_masses.

¹¹⁵⁸ For example: Wang M, Audi G, Wapstra AH, Kondev FG, MacCormick M, Xu X, Pfeiffer B. The AME2012 atomic mass evaluation. (II). Tables, graphs and references. Chinese Phys C 2012 Dec;36(12):1603-2014; <http://amdc.in2p3.fr/masstable/Ame2012/Ame2012b-v2.pdf>.

¹¹⁵⁹ For example: Wang M, Audi G, Wapstra AH, Kondev FG, MacCormick M, Xu X, Pfeiffer B. The AME2012 atomic mass evaluation. (II). Tables, graphs and references. Chinese Phys C 2012 Dec;36(12):1603-2014; <http://amdc.in2p3.fr/masstable/Ame2012/Ame2012b-v2.pdf>.

Nuclear energy is most commonly released by one of three exoergic processes:

* Radioactive decay of radionuclides (**Section 7.1**), where an unstable atomic nucleus spontaneously emits nuclear particles (e.g., p^+ , e^- , e^+ , ${}^4\text{He}^{+2}$, ν , $\bar{\nu}$), electromagnetic radiation (e.g., gamma rays), or both;¹¹⁶⁰

* Fission (**Section 7.2**), involving the breaking of a heavy nucleus into two (or, more rarely, three) lighter nuclei; and

* Fusion (**Section 7.3**), where two atomic nuclei fuse together to form a heavier nucleus.

Nuclear energy can also be stored and released by the decay of nuclear isomers (**Section 7.4**), by a variety of exotic atoms, particles and other materials (**Section 7.5**), and by matter-antimatter annihilation reactions (**Section 7.6.1**).

Figure 5 (Chapter 9) provides a chart that summarizes much of this data.

Once the latent potential nuclear energy of a material has been tapped, it is more difficult but not impossible to “recharge” the nuclear products to restore them as energy-rich reactants, thus reversibly storing energy in nuclear form. For example, a particle accelerator could direct high-energy particles at an ${}^{56}\text{Fe}$ nucleus, adding energy to the system and splitting the ${}^{56}\text{Fe}$ nucleus into smaller fragments. These lighter fragments could then be collected and stored, and would potentially have the ability to undergo fusion back to ${}^{56}\text{Fe}$, releasing the latent nuclear binding energy. If some of these fragments were radioactive, the timing of their stored energy release would be constrained by their radioactive half-lives.

Similarly, ions can be forced to collide with heavier atoms to synthesize more massive nuclei that are much heavier than ${}^{56}\text{Fe}$ – one of the ways that transuranic¹¹⁶¹ and transactinide¹¹⁶² (superheavy) elements are often synthesized.¹¹⁶³ These more massive nuclei would then possess surplus nuclear binding energy relative to ${}^{56}\text{Fe}$ that could in principle later be released for useful purpose. Another example of nuclear energy “recharge” occurs in the process used to manufacture ${}^{239}\text{Pu}$ in a fission breeder reactor. Bombarding ${}^{238}\text{U}$ with slow neutrons causes it to absorb them (becoming ${}^{239}\text{U}$), which subsequently β -decays to ${}^{239}\text{Np}$ and then decays again by the same process to ${}^{239}\text{Pu}$. A tiny bit of energy has now been stored because ${}^{239}\text{Pu}$ has a slightly

¹¹⁶⁰ Note that in radioactive decay, it is not strictly necessary for the binding energy to increase; only a decrease in mass is strictly necessary. For example, if a neutron decays into a proton and the energy of the decay is less than 0.782343 MeV (as when ${}^{87}\text{Rb}$ decays to ${}^{87}\text{Sr}$), the average binding energy per nucleon will actually decrease. https://en.wikipedia.org/wiki/Nuclear_binding_energy#Fission_and_fusion.

¹¹⁶¹ https://en.wikipedia.org/wiki/Transuranium_element.

¹¹⁶² https://en.wikipedia.org/wiki/Transactinide_element.

¹¹⁶³ Kit Chapman, “What it takes to make a new element,” Chemistry World, 30 Nov 2016; <https://www.chemistryworld.com/features/what-it-takes-to-make-a-new-element/1017677.article>.

lower binding energy (7.560310 MeV/nucleon) than the original ^{238}U (7.570120 MeV/nucleon),¹¹⁶⁴ though both lie well below ^{56}Fe (8.7906 MeV/nucleon).

All of these “nuclear recharge” processes seem to require bulky complex mechanisms or high temperatures to carry out and are not “nucleonically precise,” so many practical challenges would have to be overcome to create an efficient reversible nuclear energy storage system.

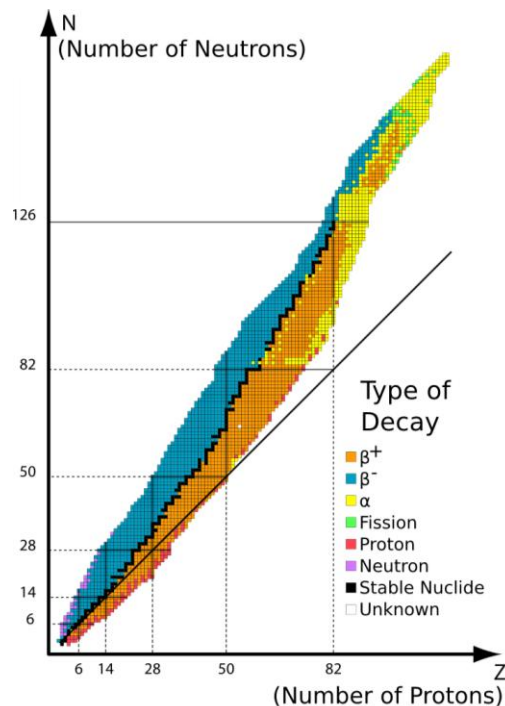
¹¹⁶⁴ Wang M, Audi G, Wapstra AH, Kondev FG, MacCormick M, Xu X, Pfeiffer B. The AME2012 atomic mass evaluation. (II). Tables, graphs and references. Chinese Phys C 2012 Dec;36(12):1603-2014; <http://amdc.in2p3.fr/masstable/Am2012/Am2012b-v2.pdf>.

7.1 Radionuclides

Radioactive decay¹¹⁶⁵ (also known as nuclear decay, radioactivity or nuclear radiation) is the process by which an unstable atomic nucleus loses energy (in terms of mass in its rest frame) by emitting radiation, such as an alpha (α) particle (a naked ${}^4\text{He}$ nucleus), beta (β) particle (an electron e^- or a positron e^+) with neutrino or antineutrino in the case of electron capture or beta decay, or a gamma (γ) ray (a high-energy photon) or electron in the case of internal conversion. A material containing such unstable nuclei is considered radioactive. The nuclei of the atoms of radioactive isotopes of elements are radionuclides.

The total energy emitted when a radionuclide disintegrates produces a specific energy (MJ/kg) and an energy density (MJ/L) that is unique to that radioactive material. Additionally, each radionuclide decays with a characteristic half-life,¹¹⁶⁶ giving rise to an intrinsic specific power (MW/kg) and power density (MW/L) for all radioactive materials.

Typically an α -decay produces 5-10 times more energy than a β -decay.¹¹⁶⁷ For applications in which the radioactive power system must be compatible with biology, selection of the optimum nuclear fuel is often dictated by safety considerations and the requirement for radiation shielding. The mass of the α -particle is ~ 7000 times greater than that of an electron, so the velocity and hence the range of α -particles in matter is considerably less than for β -particles of equal energy. A simple empirical “stopping power” approximation¹¹⁶⁸ for the range of 1-10 MeV α -particles is: R_α (microns) $\sim 430 E_{\text{MeV}}^{1.3} / \rho_{\text{absorb}}^{0.6}$, where E_{MeV} = energy per α decay (MeV) and ρ_{absorb} = absorber density (e.g., 21,450 kg/m³ for Pt). Thus a 3 MeV α -particle (initially traveling at $\sim 0.04c$) has a range of $R_\alpha \sim 2$ cm in air, ~ 30 microns in water, ~ 10 microns in germanium, and ~ 5 microns in platinum, with a fairly sharp



¹¹⁶⁵ https://en.wikipedia.org/wiki/Radioactive_decay.

¹¹⁶⁶ Half-life is the time required for half of the atoms in a sample of radioactive material to disintegrate, releasing their stored nuclear energy; <https://en.wikipedia.org/wiki/Half-life>.

¹¹⁶⁷ For example, ${}^{240}\text{U}$ produces 3.837 MeV α -decays but only 0.4004 MeV β -decays; <http://www.periodictable.com/Isotopes/092.240/index2.full.dm.prod.html>.

¹¹⁶⁸ Gray DE, ed., American Institute of Physics Handbook, Third Edition, McGraw-Hill Book Company, New York, 1972.

cutoff and only ~1% straggling (fluctuation of particle range around mean range). By contrast, as a crude approximation the range of β -particles of equal energy (initially traveling at $\sim 0.99c$) is $R_\beta \sim 10^2 R_\alpha$ and the range of γ photons and fast neutrons of equal energy is $R_\gamma \sim 10^4 R_\alpha$, although “range” for these particles is imprecisely defined because beam intensity is never truly reduced to zero but rather decays exponentially with increased shielding. Since radioactive elements typically decay to progressively lighter elements which may also be radioactive, each of the daughter products of the ideal “safe” radionuclide would also be α -emitters for the entire decay chain down to stable (non-radioactive) nuclei.

The absorption of α -particles in matter results almost entirely from collisions with electrons, or ionization reactions, which create 10^5 - 10^6 ion pairs per \sim MeV α -particle (depending upon absorber material), slowing the particle almost to a halt. For some light-nucleus absorbers, there may also be an extremely small contribution from direct interactions with the nucleus. Alpha particles with energies as low as 4.9 MeV (e.g., from ^{226}Ra) are observed to transmute atoms of all elements from boron up to potassium (except for carbon and oxygen) with the emission of protons.¹¹⁶⁹ Low-energy α -particles can also occasionally transmute light-atom nuclei to produce neutrons – one of the strongest such reactions involves 4.6 MeV α -particles emanating from ^{222}Rn striking a ^9Be absorber, wherein one α -particle out of every 5000 enters the beryllium nucleus and sends out a neutron (with a much longer range than an α -particle of equal energy), a 0.02% reaction probability.¹¹⁷⁰ Thus the worst case (i.e., nuclear and shield materials are very poorly chosen) is one low-energy proton or neutron emitted per 10^9 - 10^{10} ion pairs generated (e.g., ~ 1 every 2000 sec at an α -particle current of 1 picoamp). Most such secondary reactions have vastly lower probabilities.

Naturally emitted α -particles generally cannot penetrate the nuclei of heavier elements and therefore generally cannot create significant secondary radiation in heavy-nucleus absorbers, hence shielding is typically made from heavier elements. To first order, overcoming Coulomb repulsion and entering the nucleus requires an α -particle energy $E_{\text{repulse}} > 2 Z e^2 / (4\pi\epsilon_0 r_{\text{nuc}})$,¹¹⁷¹ where Z is atomic number (the number of protons, or nuclear charge number), the elementary charge $e = 1.60 \times 10^{-19}$ coul, the permittivity constant $\epsilon_0 = 8.85 \times 10^{-12}$ farad/m, and Rutherford’s classical formula for nuclear radius $r_{\text{nuc}} \sim \rho_{\text{nuc}} Z^{1/3}$,¹¹⁷² where $\rho_{\text{nuc}} \sim 1.6 \times 10^{-15}$ m.¹¹⁷³ A Pt

¹¹⁶⁹ Rutherford E, Chadwick J. The artificial disintegration of light elements. *Phil Mag.* 1921;42(251):809-825; <https://www.tandfonline.com/doi/abs/10.1080/14786442108633822>. Also *Phil Mag.* 1922;44:417 and *Proc Phys Soc.* 1924;36:417.

¹¹⁷⁰ Paneth FA, Gluckauf E, Loleit H. Spectroscopic identification and manometric measurement of artificially produced helium. *Proc. Roy. Soc.* 1936 Dec 2;147:412-422; <https://royalsocietypublishing.org/doi/pdf/10.1098/rspa.1936.0204>.

¹¹⁷¹ Cork JM. *Radioactivity and Nuclear Physics*, Second Edition, D. Van Nostrand Company, New York, 1950.

¹¹⁷² Richtmyer FK, Kennard EH. *Introduction to Modern Physics*, Third Edition, McGraw-Hill Book Company, New York, 1942.

¹¹⁷³ Some exotic artificial nuclei such as ^{11}Li do not obey the classical $Z^{1/3}$ rule; Taubes G. Physicists explore the driplines. *Science* 1993 Jun 25;260:1874-1876.

absorber with $Z = 78$ has $r_{\text{nucl}} \sim 7 \times 10^{-15}$ m and $E_{\text{repulse}} > 33$ MeV, while a Ge absorber ($Z = 32$) has $r_{\text{nucl}} \sim 5 \times 10^{-15}$ m and $E_{\text{repulse}} > 18$ MeV, both of which are much higher energy barriers than natural-emission α -particles at 2-7 MeV can likely surmount.

Nuclei with mass numbers greater than ~ 140 are unstable with respect to the emission of an α -particle. **Tables 50-53** list the 70 radionuclides that are known (or predicted) to be pure alpha emitters, or that emit a vast preponderance of α -particles with only very minor emissions of other particles, with a half-life ($\tau_{1/2}$) of at least 1 day.¹¹⁷⁴ All radionuclides are ranked from highest to lowest specific energy (E_S ; **Table 50**), energy density (E_D ; **Table 51**), specific power (P_S ; **Table 52**) and power density (P_D ; **Table 53**), with supporting data provided in **Table A5, Appendix A**.

Figure 8 (Chapter 9) provides a chart that summarizes power density vs. specific power for alpha-emitting radionuclides.

Alpha-emitting radionuclides with $\tau_{1/2} \geq 1$ day can provide a specific energy range of **0.9-2.7 x 10⁶ MJ/kg** and an energy density range of **7-48 x 10⁶ MJ/L**. ²³⁶Pu achieves the second-highest energy density with a conveniently long $\tau_{1/2}$ of almost 3 years. Unfortunately, this stored energy cannot be metered out at some desired faster rate but can only be accessed at the pace dictated by the intrinsic rate of radioactive decay for each radionuclide (see image, right, of red-hot ²³⁸Pu disk due to internal heat generation). Because of this constraint, intrinsic power generation is a more relevant figure of merit for radioactive energy sources. Specifically, alpha-emitting radionuclides with $\tau_{1/2} \geq 1$ day can provide a specific power up to **20 MW/kg** and a power density up to **218 MW/L**. The highest power levels are provided by radioactive materials with the shortest half-lives, typically days, for instance:



- * ²⁵²Fm produces **~20 MW/kg** and **~200 MW/L** but only for $\tau_{1/2} \sim 1$ day;
- * ²²⁵Ac gives **~2 MW/kg** and **~20 MW/L** for $\tau_{1/2} \sim 10$ days;
- * ²⁵⁷Fm generates **~0.2 MW/kg** and **~2 MW/L** for $\tau_{1/2} \sim 100$ days; and
- * ²⁵²Cf yields **~0.02 MW/kg** and **~0.2 MW/L** for $\tau_{1/2} \sim 1000$ days.

¹¹⁷⁴ Radionuclides with $\tau_{1/2} < 1$ day can produce astronomical power densities but only over very short periods of time, hence seem impractical for most energy storage applications. Among the pure alpha-emitters, the most extreme example appears to be ²¹⁹Pa which emits $\sim 100\%$ of 10.0846 MeV α -particles (and $5 \times 10^{-9} \%$ of β^+ particles) with a half-life of 53 nanoseconds, briefly yielding a specific power of **5.8 x 10¹³ MW/kg** and power density of **8.9 x 10¹⁴ MW/L**. (Energy density is a more modest **68 x 10⁶ MJ/L**.) Among the light elements, one of the most extreme examples may be the unstable isotope quadrium or ⁴H (the three-neutron isotope of hydrogen) which decays in 1.39×10^{-22} sec with the release of a 4.6 MeV neutron (https://en.wikipedia.org/wiki/Isotopes_of_hydrogen#Hydrogen-4), implying an instantaneous specific power of **7.9 x 10²⁹ MW/kg** and power density **2.9 x 10²⁹ MW/L**, with energy density **40 x 10⁶ MJ/L** taking cryogenic liquid ⁴H₂ density as ~ 0.36 kg/L as extrapolated from known densities of LH₂ (https://en.wikipedia.org/wiki/Liquid_hydrogen), LD₂ (<https://www.bnl.gov/magnets/staff/gupta/cryogenic-data-handbook/Section4.pdf>), and LT₂ (<https://babel.hathitrust.org/cgi/pt?id=mdp.39015086416230;view=1up;seq=17>) at 21 K.

Most of the best-performing alpha-emitting radionuclides aren't readily available in kg quantities,¹¹⁷⁵ and the amounts currently available in the largest quantities are very expensive. For example, curium is one of the most radioactive isolable elements, produced in small quantities in nuclear reactors (~20 gm per metric tonne of spent fuel). Kilograms of its two most common isotopes (^{242}Cm and ^{244}Cm) have been accumulated: ^{242}Cm ($\tau_{1/2} \sim 163$ days, **0.1 MW/kg, 1.65 MW/L**) costs ~\$2M/kg and ^{244}Cm ($\tau_{1/2} \sim 18.1$ yrs, **0.04 MW/L**) costs ~\$0.2M/kg.¹¹⁷⁶

Radioisotope Power Throttling. The principal shortcoming of radionuclide-based energy is that the rate of power generation cannot be conveniently throttled. The decay rate follows a deterministic declining curve, and the power must be used when generated or transferred to some other energy storage mechanism to prevent it from being wasted – i.e., “use it or lose it”, as illustrated by the continuous purple glow of a lump of radioactive curium metal (image, left). Nothing much seems to alter the natural decay rate. A number of experiments have found that radioisotope decay rates are largely unaffected by external conditions such as temperature, pressure, the chemical environment, and ambient electric, magnetic, or gravitational fields,¹¹⁷⁷ although a few intriguing correlations remain to be investigated.¹¹⁷⁸



However, there are a few modest exceptions, especially regarding **electron capture (EC)** decay rates. For example, the EC half-life in ^7Be is increased by 0.9% if the beryllium atoms are chemically bonded to palladium atoms or by 0.7% if bonded to indium atoms, both at 12 K;¹¹⁷⁹ the EC decay rate for ^7Be is 0.08% greater in BeF_2 than in metallic Be;¹¹⁸⁰ and enclosing the ^7Be atom in a C_{60} buckyball cage reduces the EC half-life by 1.13%.¹¹⁸¹ The observed increase in the

¹¹⁷⁵ For example, in 1954 the total worldwide supply of purified radium amounted to about 2.3 kg and it is still in this range today, while the annual production of pure radium compounds is currently only about 0.1 kg/yr; <https://en.wikipedia.org/wiki/Radium#Production>.

¹¹⁷⁶ https://en.wikipedia.org/wiki/Curium#Isotope_preparation.

¹¹⁷⁷ Emery GT. Perturbation of nuclear decay rates. *Ann Rev Nucl Sci Annual Reviews*. 1972;22:165-202; <https://www.annualreviews.org/doi/abs/10.1146/annurev.ns.22.120172.001121>.

¹¹⁷⁸ Jenkins JH, Fischbach E, Buncher JB, Gruenwald JT, Krause DE, Mattes JJ. Evidence for Correlations Between Nuclear Decay Rates and Earth-Sun Distance. *Astropart Phys*. 2009 Aug;32(1):42-46; <https://arxiv.org/pdf/0808.3283.pdf>. Norman EB, Browne E, Shugart HA, Joshi TH, Firestone RB. Evidence against correlations between nuclear decay rates and Earth–Sun distance. *Astropart Phys*. 2009 Mar;31(2):135-137; <http://donuts.berkeley.edu/papers/EarthSun.pdf>.

¹¹⁷⁹ Wang B, Yan S, Limata B, *et al.* Change of the ^7Be electron capture half-life in metallic environments. *Eur Phys J A*. 2006;28(3):375-377; https://www.researchgate.net/profile/J_Cruz2/publication/225144934_Change_of_the_7Be_electron_capture_half-life_in_metallic_environments/links/0fcfd50747ca07efc9000000.pdf.

¹¹⁸⁰ Daniels F, Alberty RA. *Physical Chemistry*, Third Edition, John Wiley & Sons, New York, NY, 1966, p. 709.

¹¹⁸¹ Ohtsuki T, Hirose K, Ohno K. Electron-capture decay rate of ^7Be encapsulated in C_{60} cages. *J Nuclear Radiochem Sci*. 2007;8(1):A1-A7; <http://www.radiochem.org/en/paper/JN81/jn8101.pdf>.

EC decay constant of ^7Be oxide with pressure is so linear that it may be used as a method of pressure measurement in diamond anvil experiments in which optical access is impossible, and the EC decay rates of ^{99}Tc and ^{131}Ba are measurably altered at a pressure of 100,000 atm.¹¹⁸² The EC half-life of 3.39 min for neutral $^{140}\text{Pr}^0$ atoms with all 59 orbital electrons still present shortens by 10% to 3.04 min for almost fully-ionized $^{140}\text{Pr}^{58+}$ atoms retaining only a single orbital electron.¹¹⁸³ Most impressively, the EC half-life in ^{83}Rb is normally 86.2 days, but the radionuclide can be made to never decay by removing all the orbital electrons.¹¹⁸⁴

It is well-known that the **β -decay** probability of a nucleus is also significantly affected by its ionic charge state. For instance, the β -decay half-life of neutral $^{52}\text{Fe}^0$ is 8.275 hours but increases to 12.5 hours for fully-ionized $^{52}\text{Fe}^{26+}$.¹¹⁸⁵ Perhaps the largest-known such effect is for the β -decay half-life of ^{187}Re into ^{187}Os , which is measurably reduced from 41.6 billion years to only 33 years if the rhenium atom is stripped of all of its orbital electrons.¹¹⁸⁶ Intermediate degrees of ionization produce intermediate declines in half-life, in principle allowing us to throttle the β -decay rate of ^{187}Re between 7×10^{-16} MW/kg ($^{187}\text{Re}^0$) and 9×10^{-7} MW/kg ($^{187}\text{Re}^{75+}$) by increasing or decreasing the ionization level of the atoms. However, the specific power levels for this particular radionuclide are not very impressive, in part because the β -decay energy for ^{187}Re is an anomalously low 2.62 KeV,¹¹⁸⁷ but the charge-based decay-control principle might be applicable to other radionuclides. Ionization control of power output can also be applied to some stable neutral atoms whose nuclei become unstable after stripping – e.g., the ^{163}Dy nucleus is

¹¹⁸² Hensley WK, Bassett WA, Huizenga JR. Pressure dependence of the radioactive decay constant of beryllium-7. *Science* 1973 Sep 21;181(4105):1164-1165; <https://www.ncbi.nlm.nih.gov/pubmed/17744291>.

¹¹⁸³ Litvinov YuA, *et al.* Measurement of the β^+ and orbital electron-capture decay rates in fully-ionized, hydrogen-like, and helium-like ^{140}Pr ions. *Phys Rev Lett*. 2007 Dec 31;99(26):262501; <https://arxiv.org/pdf/0711.3709.pdf>.

¹¹⁸⁴ Christopher S. Baird, “Can the decay half-life of a radioactive material be changed?” West Texas A&M University, 27 Apr 2015; <http://wtamu.edu/~cbaird/sq/2015/04/27/can-the-decay-half-life-of-a-radioactive-material-be-changed/>.

¹¹⁸⁵ Irnich H, *et al.* Half-life measurements of bare, mass-resolved isomers in a storage-cooler ring. CERN GSI-Preprint-95-53, 14 Sep 1995; <http://cds.cern.ch/record/289997/files/SCAN-9510246.pdf>.

¹¹⁸⁶ Bosch F, *et al.* Observation of bound-state beta minus decay of fully ionized ^{187}Re : $^{187}\text{Re} \rightarrow ^{187}\text{Os}$ cosmochronometry. *Phys Rev Lett* 1996;77(26):5190-5193; <https://2014.f.a0z.ru/04/06-3430949-physrevlett.77.5190-1996.pdf>.

¹¹⁸⁷ Brodzinski RL, Conway DC. Decay of Rhenium-187. *Phys Rev* 1965 Jun 21;138:B1368; <https://journals.aps.org/pr/abstract/10.1103/PhysRev.138.B1368>.

stable as a neutral atom;¹¹⁸⁸ but when fully ionized, $^{163}\text{Dy}^{66+}$ β -decays to $^{163}\text{Ho}^{66+}$ with a half-life of 47 days.¹¹⁸⁹ Intermediate levels of ionization would likely produce intermediate decay rates.

Alteration of the electronic environment of **alpha emitters** may also produce some change in the half-life for α -decay, but such changes are not expected to be as great as those that might result for electron capture and β -decay radionuclides, and literature reports of this effect are rare. There is one paper¹¹⁹⁰ claiming that ^{210}Po embedded in copper metal and cooled to 12 K has an α -decay half-life 6.3% shorter than at room temperature, and another theory paper¹¹⁹¹ suggests that heavy-element α -decay half-life might be reduced by several orders of magnitude in ultrastrong magnetic fields (e.g., $\sim 10^{11}$ tesla). Further research is needed to explore these and other possible approaches to α -decay half-life control.

If radioactive power could be throttled at will, then specific energy and energy density would become more relevant performance metrics for this energy source.

One final consideration is that some of the suggested isotopes can sustain a fissile chain reaction (**Section 7.2**) and careless handling could cause a criticality accident.¹¹⁹² Please handle carefully!

¹¹⁸⁸ Audi G, Wapstra AH. The 1995 update to the atomic mass evaluation. Nucl Phys A 1995 Dec 25;595(4):409-480; <https://www.sciencedirect.com/science/article/abs/pii/0375947495004459>.

¹¹⁸⁹ Jung M, Bosch F, Beckert K, Eickhoff H, Folger H, Franzke B, Gruber A, Kienle P, Klepper O, Koenig W, Kozhuharov C, Mann R, Moshhammer R, Nolden F, Schaaf U, Soff G, Spädtke P, Steck M, Stöhlker T, Sümmerer K. First observation of bound-state β^- decay. Phys Rev Lett. 1992 Oct 12;69(15):2164-2167; <https://journals.aps.org/prl/abstract/10.1103/PhysRevLett.69.2164>.

¹¹⁹⁰ Raiola F, *et al.* First hint on a change of the ^{210}Po alpha-decay half-life in the metal Cu. Eur Phys J A 2007 Apr; 32:51; <https://link.springer.com/article/10.1140%2Fepja%2Fi2007-10012-8>.

¹¹⁹¹ Liolios TE. Screened α decay in dense astrophysical plasmas and superstrong magnetic fields. Phys Rev C 2003 Jul 30;68:015804; <https://arxiv.org/pdf/nucl-th/0302021.pdf>.

¹¹⁹² https://en.wikipedia.org/wiki/Criticality_accident.

Table 50. Specific energy (E_s) of α -emitting radionuclides with half-life ≥ 1 day¹¹⁹³

Radionuclide	Half-Life	E_s (MJ/kg)	Radionuclide	Half-Life	E_s (MJ/kg)
²⁵² Fm	1.06 d	2.74×10^6	²³¹ Pa	3.28×10^4 y	2.15×10^6
²⁵⁸ Md	51.5 d	2.72×10^6	¹⁴⁸ Gd	70.9 y	2.13×10^6
²⁴⁶ Cf	1.49 d	2.69×10^6	²³⁹ Pu	2.41×10^4 y	2.12×10^6
²²⁷ Th	18.7 d	2.61×10^6	²⁴⁰ Pu	6560 y	2.11×10^6
²⁵² Es	1.29 y	2.60×10^6	²⁴⁷ Cm	1.56×10^7 y	2.09×10^6
²²³ Ra	11.4 d	2.59×10^6	²²⁶ Ra	1590 y	2.08×10^6
²⁵⁷ Fm	101 d	2.58×10^6	²³³ U	1.59×10^5 y	2.03×10^6
²⁴⁰ Cm	26.6 d	2.57×10^6	²³⁷ Np	2.14×10^6 y	2.02×10^6
²⁵³ Es	20.5 d	2.57×10^6	²⁴⁸ Cm	3.49×10^5 y	2.01×10^6
²²⁵ Ac	9.95 d	2.55×10^6	²³⁰ Th	7.54×10^4 y	2.00×10^6
²³⁰ U	20.8 d	2.51×10^6	²³⁴ U	2.46×10^5 y	2.00×10^6
²⁵⁴ Es	276 d	2.51×10^6	²⁴² Pu	3.74×10^5 y	1.99×10^6
²²⁴ Ra	3.63 d	2.49×10^6	²³⁵ U	7.04×10^8 y	1.92×10^6
²¹⁰ Po	138 d	2.48×10^6	²³⁶ U	2.34×10^7 y	1.87×10^6
²⁴² Cm	163 d	2.48×10^6	¹⁵⁴ Dy	3.01×10^6 y	1.85×10^6
²⁴⁸ Cf	334 d	2.47×10^6	²⁴⁴ Pu	7.93×10^7 y	1.84×10^6
²⁴³ Cm	29.1 y	2.45×10^6	¹⁵⁰ Gd	1.79×10^6 y	1.81×10^6
²⁴⁹ Cf	351 y	2.44×10^6	²³⁸ U	4.47×10^9 y	1.73×10^6
²⁰⁸ Po	2.90 y	2.42×10^6	²³² Th	1.41×10^{10} y	1.70×10^6
²³⁶ Pu	2.86 y	2.40×10^6	¹⁴⁶ Sm	1.03×10^8 y	1.67×10^6
²⁵² Cf	2.65 y	2.38×10^6	¹⁹⁰ Pt	6.50×10^{11} y	1.65×10^6
²⁵⁰ Cf	13.1 y	2.37×10^6	¹⁴⁷ Sm	1.06×10^{11} y	1.52×10^6
²⁵¹ Cf	898 y	2.37×10^6	¹⁸⁶ Os	2.00×10^{15} y	1.46×10^6
²²⁸ Th	1.91 y	2.34×10^6	²⁰⁹ Bi	1.90×10^{19} y	1.45×10^6
²⁴⁴ Cm	18.1 y	2.33×10^6	¹⁵² Gd	1.08×10^{14} y	1.40×10^6
²⁴⁷ Bk	1380 y	2.30×10^6	¹⁷⁴ Hf	2.00×10^{15} y	1.38×10^6
²³⁸ Pu	87.8 y	2.27×10^6	¹⁸⁰ W	1.80×10^{18} y	1.34×10^6
²⁴¹ Am	433 y	2.26×10^6	¹⁴⁸ Sm	6.98×10^{15} y	1.29×10^6
²³² U	68.8 y	2.25×10^6	¹⁴⁴ Nd	2.29×10^{15} y	1.28×10^6
²⁴⁸ Bk	9.51 y	2.25×10^6	¹⁵¹ Eu	5.00×10^{18} y	1.25×10^6
²⁰⁹ Po	102 y	2.21×10^6	¹⁴⁹ Sm	2.01×10^{15} y	1.21×10^6
²⁴⁵ Cm	8560 y	2.21×10^6	¹⁸² W	8.30×10^{18} y	9.39×10^5
²²⁹ Th	7880 y	2.18×10^6	²⁰⁴ Pb	1.40×10^{17} y	9.32×10^5
²⁴³ Am	7390 y	2.16×10^6	¹⁸³ W	1.30×10^{19} y	8.86×10^5
²⁴⁶ Cm	4760 y	2.15×10^6	¹⁸⁴ W	2.90×10^{19} y	8.68×10^5

¹¹⁹³ Data from Table A5 in Appendix A.5.

Table 51. Energy density (E_D) of α -emitting radionuclides with half-life ≥ 1 day¹¹⁹⁴

Radionuclide	Half-Life	E_D (MJ/L)	Radionuclide	Half-Life	E_D (MJ/L)
²³⁰ U	20.8 d	4.80×10^7	²⁴⁸ Cm	3.49×10^5 y	2.71×10^7
²³⁶ Pu	2.86 y	4.75×10^7	²⁴¹ Am	433 y	2.71×10^7
²³⁸ Pu	87.8 y	4.49×10^7	²⁵² Fm	1.06 d	2.66×10^7
²³² U	68.8 y	4.30×10^7	¹⁸⁰ W	1.80×10^{18} y	2.59×10^7
²³⁹ Pu	2.41×10^4 y	4.20×10^7	²⁴³ Am	7390 y	2.59×10^7
²⁴⁰ Pu	6560 y	4.19×10^7	²²⁵ Ac	9.95 d	2.55×10^7
²⁴⁶ Cf	1.49 d	4.06×10^7	²²⁹ Th	7880 y	2.55×10^7
²⁴² Pu	3.74×10^5 y	3.94×10^7	²⁵⁷ Fm	101 d	2.50×10^7
²³⁷ Np	2.14×10^6 y	3.91×10^7	²³⁰ Th	7.54×10^4 y	2.34×10^7
²³³ U	1.59×10^5 y	3.88×10^7	²⁵² Es	1.29 y	2.30×10^7
²³⁴ U	2.46×10^5 y	3.83×10^7	²¹⁰ Po	138 d	2.28×10^7
²⁴⁸ Cf	334 d	3.74×10^7	²⁵³ Es	20.5 d	2.27×10^7
²⁴⁹ Cf	351 y	3.68×10^7	²⁰⁸ Po	2.90 y	2.22×10^7
²³⁵ U	7.04×10^8 y	3.67×10^7	²⁵⁴ Es	276 d	2.22×10^7
²⁴⁴ Pu	7.93×10^7 y	3.66×10^7	²⁰⁹ Po	102 y	2.04×10^7
²⁵² Cf	2.65 y	3.59×10^7	²³² Th	1.41×10^{10} y	1.99×10^7
²⁵¹ Cf	898 y	3.58×10^7	¹⁷⁴ Hf	2.00×10^{15} y	1.84×10^7
²⁵⁰ Cf	13.1 y	3.57×10^7	¹⁸² W	8.30×10^{18} y	1.81×10^7
²³⁶ U	2.34×10^7 y	3.57×10^7	¹⁸³ W	1.30×10^{19} y	1.71×10^7
¹⁹⁰ Pt	6.50×10^{11} y	3.54×10^7	¹⁸⁴ W	2.90×10^{19} y	1.68×10^7
²⁴⁰ Cm	26.6 d	3.47×10^7	¹⁴⁸ Gd	70.9 y	1.68×10^7
²⁴⁷ Bk	1380 y	3.40×10^7	¹⁵⁴ Dy	3.01×10^6 y	1.58×10^7
²⁴² Cm	163 d	3.35×10^7	¹⁵⁰ Gd	1.79×10^6 y	1.43×10^7
²⁴⁸ Bk	9.51 y	3.32×10^7	²²³ Ra	11.4 d	1.42×10^7
²³¹ Pa	3.28×10^4 y	3.31×10^7	²⁰⁹ Bi	1.90×10^{19} y	1.42×10^7
²⁴³ Cm	29.1 y	3.31×10^7	²²⁴ Ra	3.63 d	1.37×10^7
¹⁸⁶ Os	2.00×10^{15} y	3.31×10^7	¹⁴⁶ Sm	1.03×10^8 y	1.26×10^7
²³⁸ U	4.47×10^9 y	3.31×10^7	²²⁶ Ra	1590 y	1.14×10^7
²⁴⁴ Cm	18.1 y	3.15×10^7	¹⁴⁷ Sm	1.06×10^{11} y	1.14×10^7
²²⁷ Th	18.7 d	3.06×10^7	¹⁵² Gd	1.08×10^{14} y	1.10×10^7
²⁴⁵ Cm	8560 y	2.99×10^7	²⁰⁴ Pb	1.40×10^{17} y	1.06×10^7
²⁴⁶ Cm	4760 y	2.90×10^7	¹⁴⁸ Sm	6.98×10^{15} y	9.74×10^6
²⁴⁷ Cm	1.56×10^7 y	2.83×10^7	¹⁴⁹ Sm	2.01×10^{15} y	9.11×10^6
²⁵⁸ Md	51.5 d	2.80×10^7	¹⁴⁴ Nd	2.29×10^{15} y	8.95×10^6
²²⁸ Th	1.91 y	2.73×10^7	¹⁵¹ Eu	5.00×10^{18} y	6.61×10^6

¹¹⁹⁴ Data from Table A5 in Appendix A.5.

Table 52. Specific power (P_S)* of α -emitting radionuclides with half-life ≥ 1 day¹¹⁹⁵

Radionuclide	Half-Life	P_S (MW/kg)	Radionuclide	Half-Life	P_S (MW/kg)
²⁵² Fm	1.06 d	20.8	²⁴³ Am	7390 y	6.42×10^{-6}
²⁴⁶ Cf	1.49 d	14.5	²²⁹ Th	7880 y	6.06×10^{-6}
²²⁴ Ra	3.63 d	5.50	²⁴⁵ Cm	8560 y	5.68×10^{-6}
²²⁵ Ac	9.95 d	2.05	²³⁹ Pu	2.41×10^4 y	1.93×10^{-6}
²²³ Ra	11.4 d	1.82	²³¹ Pa	3.28×10^4 y	1.44×10^{-6}
²²⁷ Th	18.7 d	1.12	²³⁰ Th	7.54×10^4 y	5.83×10^{-7}
²⁵³ Es	20.5 d	1.01	²³³ U	1.59×10^5 y	2.81×10^{-7}
²³⁰ U	20.8 d	0.968	²³⁴ U	2.46×10^5 y	1.79×10^{-7}
²⁴⁰ Cm	26.6 d	0.775	²⁴⁸ Cm	3.49×10^5 y	1.27×10^{-7}
²⁵⁸ Md	51.5 d	0.424	²⁴² Pu	3.74×10^5 y	1.17×10^{-7}
²⁵⁷ Fm	101 d	0.206	¹⁵⁰ Gd	1.79×10^6 y	2.22×10^{-8}
²¹⁰ Po	138 d	0.144	²³⁷ Np	2.14×10^6 y	2.07×10^{-8}
²⁴² Cm	163 d	0.122	¹⁵⁴ Dy	3.01×10^6 y	1.35×10^{-8}
²⁵⁴ Es	276 d	7.32×10^{-2}	²⁴⁷ Cm	1.56×10^7 y	2.94×10^{-9}
²⁴⁸ Cf	334 d	5.96×10^{-2}	²³⁶ U	2.34×10^7 y	1.75×10^{-9}
²⁵² Es	1.29 y	4.43×10^{-2}	²⁴⁴ Pu	7.93×10^7 y	5.12×10^{-10}
²²⁸ Th	1.91 y	2.69×10^{-2}	¹⁴⁶ Sm	1.03×10^8 y	3.56×10^{-10}
²⁵² Cf	2.65 y	1.98×10^{-2}	²³⁵ U	7.04×10^8 y	6.00×10^{-11}
²³⁶ Pu	2.86 y	1.85×10^{-2}	²³⁸ U	4.47×10^9 y	8.51×10^{-12}
²⁰⁸ Po	2.90 y	1.83×10^{-2}	²³² Th	1.41×10^{10} y	2.65×10^{-12}
²⁴⁸ Bk	9.51 y	5.19×10^{-3}	¹⁴⁷ Sm	1.06×10^{11} y	3.15×10^{-13}
²⁵⁰ Cf	13.1 y	3.92×10^{-3}	¹⁹⁰ Pt	6.50×10^{11} y	5.58×10^{-14}
²⁴⁴ Cm	18.1 y	2.83×10^{-3}	¹⁵² Gd	1.08×10^{14} y	2.84×10^{-16}
²⁴³ Cm	29.1 y	1.85×10^{-3}	¹⁸⁶ Os	2.00×10^{15} y	1.61×10^{-17}
²³² U	68.8 y	7.19×10^{-4}	¹⁷⁴ Hf	2.00×10^{15} y	1.52×10^{-17}
¹⁴⁸ Gd	70.9 y	6.60×10^{-4}	¹⁴⁹ Sm	2.01×10^{15} y	1.33×10^{-17}
²³⁸ Pu	87.8 y	5.67×10^{-4}	¹⁴⁴ Nd	2.29×10^{15} y	1.23×10^{-17}
²⁰⁹ Po	102 y	4.77×10^{-4}	¹⁴⁸ Sm	6.98×10^{15} y	4.08×10^{-18}
²⁴⁹ Cf	351 y	1.52×10^{-4}	²⁰⁴ Pb	1.40×10^{17} y	1.46×10^{-19}
²⁴¹ Am	433 y	1.15×10^{-4}	¹⁸⁰ W	1.80×10^{18} y	1.64×10^{-20}
²⁵¹ Cf	898 y	5.81×10^{-5}	¹⁵¹ Eu	5.00×10^{18} y	5.51×10^{-21}
²⁴⁷ Bk	1380 y	3.67×10^{-5}	¹⁸² W	8.30×10^{18} y	2.49×10^{-21}
²²⁶ Ra	1590 y	2.88×10^{-5}	²⁰⁹ Bi	1.90×10^{19} y	1.68×10^{-21}
²⁴⁶ Cm	4760 y	9.92×10^{-6}	¹⁸³ W	1.30×10^{19} y	1.50×10^{-21}
²⁴⁰ Pu	6560 y	7.08×10^{-6}	¹⁸⁴ W	2.90×10^{19} y	6.58×10^{-22}

* $P_S \sim \ln(2) E_S / \tau_{1/2}$ ¹¹⁹⁵ Data from Table A5 in Appendix A.5.

Table 53. Power density (P_D) of α -emitting radionuclides with half-life ≥ 1 day¹¹⁹⁶

Radionuclide	Half-Life	P_D (MW/L)	Radionuclide	Half-Life	P_D (MW/L)
²⁴⁶ Cf	1.49 d	218	²⁴³ Am	7390 y	7.71×10^{-5}
²⁵² Fm	1.06 d	201	²⁴⁵ Cm	8560 y	7.68×10^{-5}
²²⁴ Ra	3.63 d	30.3	²²⁹ Th	7880 y	7.09×10^{-5}
²²⁵ Ac	9.95 d	20.5	²³⁹ Pu	2.41×10^4 y	3.83×10^{-5}
²³⁰ U	20.8 d	18.5	²³¹ Pa	3.28×10^4 y	2.22×10^{-5}
²²⁷ Th	18.7 d	13.1	²³⁰ Th	7.54×10^4 y	6.82×10^{-6}
²⁴⁰ Cm	26.6 d	10.5	²³³ U	1.59×10^5 y	5.36×10^{-6}
²²³ Ra	11.4 d	9.99	²³⁴ U	2.46×10^5 y	3.43×10^{-6}
²⁵³ Es	20.5 d	8.90	²⁴² Pu	3.74×10^5 y	2.31×10^{-6}
²⁵⁸ Md	51.5 d	4.36	²⁴⁸ Cm	3.49×10^5 y	1.71×10^{-6}
²⁵⁷ Fm	101 d	2.00	²³⁷ Np	2.14×10^6 y	4.01×10^{-7}
²⁴² Cm	163 d	1.65	¹⁵⁰ Gd	1.79×10^6 y	1.75×10^{-7}
²¹⁰ Po	138 d	1.32	¹⁵⁴ Dy	3.01×10^6 y	1.15×10^{-7}
²⁴⁸ Cf	334 d	0.899	²⁴⁷ Cm	1.56×10^7 y	3.98×10^{-8}
²⁵⁴ Es	276 d	0.647	²³⁶ U	2.34×10^7 y	3.35×10^{-8}
²⁵² Es	1.29 y	0.391	²⁴⁴ Pu	7.93×10^7 y	1.01×10^{-8}
²³⁶ Pu	2.86 y	0.366	¹⁴⁶ Sm	1.03×10^8 y	2.68×10^{-9}
²²⁸ Th	1.91 y	0.314	²³⁵ U	7.04×10^8 y	1.15×10^{-9}
²⁵² Cf	2.65 y	0.299	²³⁸ U	4.47×10^9 y	1.63×10^{-10}
²⁰⁸ Po	2.90 y	0.169	²³² Th	1.41×10^{10} y	3.10×10^{-11}
²⁴⁸ Bk	9.51 y	7.67×10^{-2}	¹⁴⁷ Sm	1.06×10^{11} y	2.37×10^{-12}
²⁵⁰ Cf	13.1 y	5.92×10^{-2}	¹⁹⁰ Pt	6.50×10^{11} y	1.20×10^{-12}
²⁴⁴ Cm	18.1 y	3.83×10^{-2}	¹⁵² Gd	1.08×10^{14} y	2.25×10^{-15}
²⁴³ Cm	29.1 y	2.50×10^{-2}	¹⁸⁶ Os	2.00×10^{15} y	3.64×10^{-16}
²³² U	68.8 y	1.37×10^{-2}	¹⁷⁴ Hf	2.00×10^{15} y	2.03×10^{-16}
²³⁸ Pu	87.8 y	1.12×10^{-2}	¹⁴⁹ Sm	2.01×10^{15} y	1.00×10^{-16}
¹⁴⁸ Gd	70.9 y	5.21×10^{-3}	¹⁴⁴ Nd	2.29×10^{15} y	8.59×10^{-17}
²⁰⁹ Po	102 y	4.38×10^{-3}	¹⁴⁸ Sm	6.98×10^{15} y	3.07×10^{-17}
²⁴⁹ Cf	351 y	2.30×10^{-3}	²⁰⁴ Pb	1.40×10^{17} y	1.66×10^{-18}
²⁴¹ Am	433 y	1.38×10^{-3}	¹⁸⁰ W	1.80×10^{18} y	3.17×10^{-19}
²⁵¹ Cf	898 y	8.78×10^{-4}	¹⁸² W	8.30×10^{18} y	4.80×10^{-20}
²⁴⁷ Bk	1380 y	5.42×10^{-4}	¹⁵¹ Eu	5.00×10^{18} y	2.90×10^{-20}
²²⁶ Ra	1590 y	1.59×10^{-4}	¹⁸³ W	1.30×10^{19} y	2.89×10^{-20}
²⁴⁰ Pu	6560 y	1.40×10^{-4}	²⁰⁹ Bi	1.90×10^{19} y	1.64×10^{-20}
²⁴⁶ Cm	4760 y	1.34×10^{-4}	¹⁸⁴ W	2.90×10^{19} y	1.27×10^{-20}

¹¹⁹⁶ Data from Table A5 in Appendix A.5.

Radioisotope thermoelectric generators (RTG or RITEG)¹¹⁹⁷ are electrical generators with no moving parts that use an array of thermocouples to convert the heat released by the decay of a suitable radioactive material into electricity by the Seebeck effect. RTGs have been used as practical power sources in satellites, space probes, and unmanned remote facilities. There are at least 1,300 radioactive isotopes, both natural and man-made, that are potentially available for use in RTGs. Many of these isotopes are fission products from the burning of fissile fuel in nuclear fission reactors (**Section 7.2**), while others can be manufactured in particle accelerators:

²¹⁰Po (an α -emitter) was used in prototype RTGs built in 1958 by the U.S. Atomic Energy Commission¹¹⁹⁸ and in the Orion-1 RTGs in the Earth-orbiting USSR satellites Kosmos 84 and Kosmos 90 in 1965 and in the USSR lunar surface landers Lunokhod 201, Lunokhod 1 and Lunokhod 2.¹¹⁹⁹ This isotope has a decay half-life of 138 days and a thermal specific power of **0.14 MW/kg (1.3 MW/L)**. A half-gram sample of ²¹⁰Po reaches a temperature above 500 °C.¹²⁰⁰ Polonium is present in uranium ores at only ~0.1 mg/tonne or ~0.2% of the abundance of radium, making isolation from natural sources a tedious process. Polonium is now made in milligram amounts using the high neutron fluxes found in nuclear reactors, wherein the bombardment of natural ²⁰⁹Bi with neutrons creates ²¹⁰Bi, which then decays to ²¹⁰Po via β^- -emission. Only about 0.1 kg of ²¹⁰Po is produced each year, practically all of it in Russia.¹²⁰¹

¹⁰⁶Ru (a β -emitter) has been considered for RTG applications; it has a decay half-life of 1 year and a specific power of **0.033 MW/kg (0.41 MW/L)**.¹²⁰²

¹⁴⁴Ce and **⁶⁰Co** (both β -emitters with γ emission) have also been considered for RTG applications.¹²⁰³ ⁶⁰Co was once regarded as a useful gamma-ray source, producing 1.17 MeV and 1.33 MeV γ -particles.¹²⁰⁴ ¹⁴⁴Ce has a decay half-life of 285 days and a specific power of **0.026 MW/kg (0.17 MW/L)**, while ⁶⁰Co has a decay half-life of 5.27 years and a specific power of **0.018 MW/kg (0.16 MW/L)**.

²³⁸Pu (an α -emitter) has a decay half-life of 87.7 years and a specific power of **5.7 x 10⁻⁴ MW/kg (0.011 MW/L)**. It has become the most widely used fuel for RTGs, despite its low power density, in part because of its exceptionally low gamma and neutron radiation levels and low

¹¹⁹⁷ https://en.wikipedia.org/wiki/Radioisotope_thermoelectric_generator.

¹¹⁹⁸ https://en.wikipedia.org/wiki/Radioisotope_thermoelectric_generator#210Po.

¹¹⁹⁹ https://en.wikipedia.org/wiki/List_of_nuclear_power_systems_in_space.

¹²⁰⁰ “Polonium,” Argonne National Laboratory, Human Health Fact Sheet, Aug 2005; <https://web.archive.org/web/20120310145431/http://www.ead.anl.gov/pub/doc/polonium.pdf>.

¹²⁰¹ https://en.wikipedia.org/wiki/Polonium#Occurrence_and_production.

¹²⁰² M. Ragheb, “Chapter 3. Radioisotopes Power Production,” course materials, Stanford University, 15 Feb 2011; <http://large.stanford.edu/courses/2011/ph241/yemane1/docs/ragheb.pdf>.

¹²⁰³ M. Ragheb, “Chapter 3. Radioisotopes Power Production,” course materials, Stanford University, 15 Feb 2011; <http://large.stanford.edu/courses/2011/ph241/yemane1/docs/ragheb.pdf>.

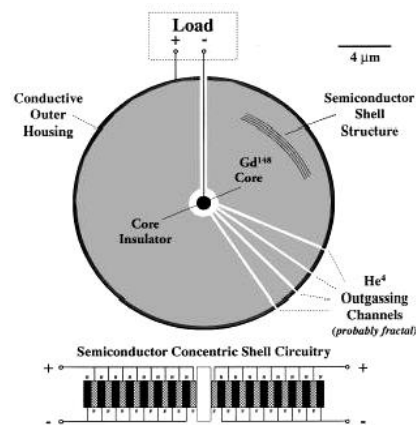
¹²⁰⁴ <https://en.wikipedia.org/wiki/Cobalt#Radioisotopes>.

shielding requirements. ²³⁸Pu-powered Stirling electrical generators¹²⁰⁵ and radioisotope heater units¹²⁰⁶ have been investigated by NASA. ²³⁸Pu must be specifically synthesized and is not abundant as a nuclear waste product. Russia has maintained consistent production, and in 2013 the U.S. restarted production at a 1.5 kg/yr rate.¹²⁰⁷

²⁴¹Am (an α -emitter) has been considered as an RTG fuel by the European Space Agency¹²⁰⁸ and others.¹²⁰⁹ It has a decay half-life of 433 years and a specific power of 1.2×10^{-4} MW/kg (0.0014 MW/L). It is commonly used in ionization-type smoke detectors, is present in aged civilian plutonium fuel sources at 25-50 gm/kg, and exists in kilogram quantities at a price of ~\$1.5M/kg.¹²¹⁰ ²⁴¹Am produces more penetrating radiation through decay chain products than ²³⁸Pu but its shielding requirements are still the second lowest of all possible isotopes; only ²³⁸Pu requires less.

⁹⁰Sr (a β -emitter with minor γ emission) was used by the Soviet Union in terrestrial RTGs. It has a decay half-life of 28.8 years and a specific power of 4.6×10^{-4} MW/kg (0.0012 MW/L).¹²¹¹ ⁹⁰Sr is a product of nuclear fission and is present in significant amounts in spent nuclear fuel and in radioactive waste from nuclear reactors.

Alphavoltaic devices, as first described in connection with medical nanorobotics in 1999 (est. 10^{-5} MW/L; image, right),¹²¹² would use higher-energy alpha particles coupled to a semiconductor p/n junction diode. An attempt by NASA to avoid the observed α -particle damage to the semiconductor material found that an indium gallium phosphide (InGaP) cell damaged by exposure to alpha emissions could be significantly recovered by annealing at 200 °C for 1 hour.¹²¹³ A second proposed approach would use a lateral junction “nipi” device that spatially separates the n and p layers of a cell, permitting charge separation



¹²⁰⁵ https://en.wikipedia.org/wiki/Stirling_radioisotope_generator.

¹²⁰⁶ https://en.wikipedia.org/wiki/Radioisotope_heater_unit.

¹²⁰⁷ https://en.wikipedia.org/wiki/Radioisotope_thermoelectric_generator#238Pu.

¹²⁰⁸ Major S. Chahal. European Space Nuclear Power Programme: UK Activities. UK Space Agency, 9 Feb 2012; <http://www.unoosa.org/pdf/pres/stsc2012/tech-18E.pdf>.

¹²⁰⁹ https://en.wikipedia.org/wiki/Americium-241#RTG_power_generation.

¹²¹⁰ <https://en.wikipedia.org/wiki/Americium-241#Nucleosynthesis>.

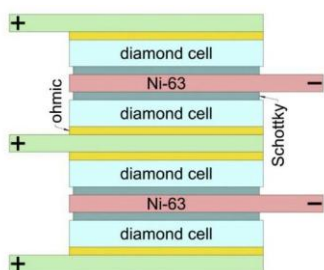
¹²¹¹ https://en.wikipedia.org/wiki/Radioisotope_thermoelectric_generator#90Sr.

¹²¹² Freitas RA Jr. Nanomedicine, Volume I: Basic Capabilities, Landes Bioscience, Georgetown TX, 1999, Section 6.3.7.1 “Radionuclides”; <http://www.nanomedicine.com/NMI/6.3.7.1.htm#p13>.

¹²¹³ Sheila G. Bailey, “Alpha-Voltaic Power Source Designs Investigated,” NASA Glenn Photovoltaic and Space Environments Branch, 16 Oct 2016; <https://web.archive.org/web/20100716172638/http://www.grc.nasa.gov/WWW/RT/2005/RP/RPV-bailey1.html>.

and transport to occur within two separate orthogonal planes thus ensuring a higher radiation tolerance. A third approach would use an intermediate material (e.g., a semiconducting quantum dot) to absorb the incident alpha energy and reemit it as light without undergoing significant radiation damage. A phosphor material would be chosen with emissions tailored to the bandgap of the photovoltaic device to ensure a high conversion efficiency, while the phosphor protects the p/n junction of the device. The projected specific power for a ^{241}Am -powered alpha-voltaic device of this type is said to be $1.7 \times 10^{-6} \text{ MW/kg}$ or about 10^{-5} MW/L .

Betavoltaic devices, also known as betavoltaic cells, use energy from a radioactive source emitting beta particles – commonly the hydrogen isotope tritium (^3H) – to generate electric current by employing a non-thermal conversion process: converting the electron-hole pairs produced by the ionization trail of beta particles traversing a semiconductor p-n junction.¹²¹⁴ These would be mainly used as power sources for equipment that must operate unattended for long periods of time, such as spacecraft, pacemakers, underwater systems and automated scientific stations in remote parts of the world. The Betacel¹²¹⁵ was the first commercially successful betavoltaic battery using ^{147}Pm radioisotope as the electron source coupled to silicon



semiconductor cells for use in a cardiac pacemaker in the 1970s. Most recently in 2018, a betavoltaic cell was fabricated at the Moscow Institute of Physics and Technology using $2 \mu\text{m}$ thick layers of ^{63}Ni (a β -emitter) sandwiched between $10 \mu\text{m}$ thick diamond diodes (image, left), achieving a specific energy of **12 MJ/kg** (which is 2-100 times better than conventional electric batteries; **Section 4.1**) but a minuscule power density of only 10^{-8} MW/L . Following demonstration that a “diamond battery” generates a small electric current when placed in a ^{63}Ni radioactive

field, the next goal of a team at the University of Bristol¹²¹⁶ would incorporate 1 gm of ^{14}C (a β -emitter) into a 20 gm betavoltaic diamond battery yielding a specific power of $\sim 9 \times 10^{-9} \text{ MW/kg}$ ($3 \times 10^{-8} \text{ MW/L}$). The “atomic battery,” “nuclear battery,” “tritium battery” and “radioisotope generator” all use energy from the decay of a radioactive isotope to generate electricity with efficiencies up to 6%-8% for betavoltaics.¹²¹⁷

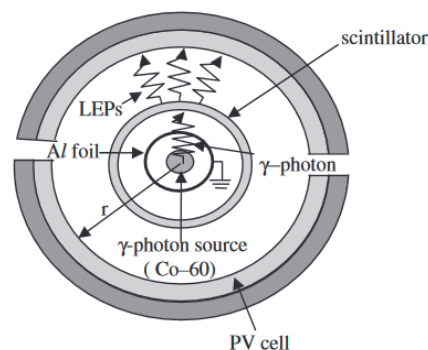
¹²¹⁴ https://en.wikipedia.org/wiki/Betavoltaic_device.

¹²¹⁵ <https://en.wikipedia.org/wiki/Betacel>.

¹²¹⁶ “‘Diamond-age’ of power generation as nuclear batteries developed,” Cabot Institute, University of Bristol, 25 Nov 2016; <http://www.bris.ac.uk/news/2016/november/diamond-power.html>.

¹²¹⁷ https://en.wikipedia.org/wiki/Atomic_battery.

Gammavoltaic devices, also known as gamma ray photovoltaic cells (GRPVCs) or gamma voltaic cells,¹²¹⁸ are now being actively investigated for the direct harvesting of electrical energy from high-energy γ rays.¹²¹⁹ In one design,¹²²⁰ a scintillation material is inserted between a nuclear isomer (**Section 7.4**) or other γ -ray source and the semiconductor material of a photovoltaic cell (image, right). Each high-energy gamma photon is converted by the scintillator into a large number of low-energy photons (LEPs) which in turn illuminate the semiconductor material, which absorbs them. It can be arranged for the LEPs' energy to match the energy gap of existing semiconductor materials in order to achieve optimal operation. An experimental 1.03 cm³ radio-voltaic nuclear battery (FRVB) using ZnS:Cu fluorescent material and an AlGaInP semiconductor PN junction generated only 0.056 mW/L (5.6×10^{-11} MW/L) when irradiated by an X-ray tube,¹²²¹ so there is much room for improvement. Researchers at EPFL found that millimeter-sized single crystals of methylammonium lead iodide exhibited 75% charge-collection efficiency when irradiated with X-rays.¹²²²



Three types of interaction between matter and X-rays or γ -rays can potentially serve as the basis for energy recovery:¹²²³

(1) **Photoelectric effect.** This describes the case in which a gamma photon interacts with and transfers its energy to an atomic electron, ejecting that electron from the atom. The kinetic energy of the resulting photoelectron is equal to the energy of the incident gamma photon minus the binding energy of the electron. The photoelectric effect is the dominant energy transfer

¹²¹⁸ Ryan MD. Gamma Voltaic Cell. United States Patent Application 20180350482, 6 Dec 2018; <http://www.freepatentsonline.com/20180350482.pdf>. Francis Yu-Hei Tsang, *et al.* Nuclear voltaic cell. European Patent Application EP1690308A2, 21 Nov 2003; <https://patents.google.com/patent/EP1690308A2/en>.

¹²¹⁹ Hirota J, Tarusawa K, Kudo K, Uchida M. Proposal for electric power generation by using X-rays and gamma rays. *J Nucl Sci Technol.* 2011;48(1):103-107; <https://www.tandfonline.com/doi/pdf/10.1080/18811248.2011.9711683>.

¹²²⁰ Liakos JK. Gamma-ray-driven photovoltaic cells via a scintillator interface. *J Nucl Sci Technol.* 2011;48(12):1428-1436; <https://www.tandfonline.com/doi/pdf/10.1080/18811248.2011.9711836>.

¹²²¹ Jin Z, Tang X, Guo X, Liu Y, Xu Z, Chen W, Zhou D. Design and performance study of four-layer radio-voltaic and dual-effect nuclear batteries based on γ -ray. *Nucl Instrum Methods Phys Res B.* 2018 Aug;428:47-55; <https://www.sciencedirect.com/science/article/pii/S0168583X18303422>.

¹²²² Náfrádi B, Náfrádi G, Forró L, Horváth E. Methylammonium lead iodide for efficient X-ray energy conversion. *J Phys Chem C.* 2015 Oct 16;119(45):25204-25208; http://www.nafradi.eu/article_pdf/Nafradi_2015_jpcc.pdf.

¹²²³ <https://www.physicsforums.com/threads/can-photovoltaic-cells-capture-gamma-photons.538569/>.

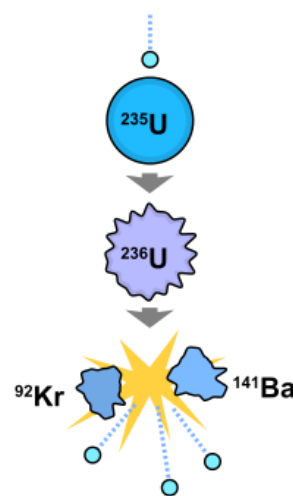
mechanism for X-ray and gamma ray photons with energies below 50 KeV but it is much less important at higher energies.

(2) Compton scattering. This is an interaction in which an incident gamma photon loses enough energy to an atomic electron to cause its ejection, with the remainder of the original photon's energy being emitted as a new, lower energy gamma photon with an emission direction different from that of the incident gamma photon. The probability of Compton scatter decreases with increasing photon energy. Compton scattering is thought to be the principal absorption mechanism for gamma rays in the intermediate energy range 100 KeV to 10 MeV. Compton scattering is relatively independent of the atomic number of the absorbing material, which is why very dense metals like lead are only modestly better shields, on a per weight basis, than are less dense materials.

(3) Pair production. This becomes possible with gamma energies exceeding 1.02 MeV, and becomes important as an absorption mechanism at energies over ~ 5 MeV. By interaction with the electric field of a nucleus, the energy of the incident photon is converted into the mass of an electron-positron pair. Any gamma energy in excess of the equivalent rest mass of the two particles (1.02 MeV) appears as the kinetic energy of the pair and the recoil nucleus. At the end of the positron's range, it combines with a free electron. The entire mass of these two particles is then converted into two gamma photons of at least 0.51 MeV energy each (or higher, according to the kinetic energy of the annihilated particles).

7.2 Fission

While radioactive decay occurs when an unstable atomic nucleus emits small α , β , or γ particles and becomes a different isotope, nuclear fission is a nuclear reaction or radioactive decay process in which a heavy nucleus splits into two (or, more rarely, three) lighter nuclei, often producing free neutrons and gamma photons while releasing a large amount of energy. Fission is a form of nuclear transmutation because the resulting fragments are not the same element as the original atom. The daughter nuclei produced are most often of comparable but slightly different sizes, typically with a mass ratio of products of about 3 to 2 for common fissile isotopes. Most fissions are “binary” fissions (producing two charged fragments), but occasionally (0.2%-0.4% of the time) three positively charged fragments are produced in a “ternary fission” – with the smallest of the ternary fragments ranging in size from a proton to an argon nucleus. The unpredictable composition of the products (which vary in a broad probabilistic and somewhat chaotic manner) distinguishes fission from purely quantum-tunneling processes such as alpha decay which give the same products each time.¹²²⁴



In engineered nuclear devices, essentially all nuclear fission occurs as a nuclear reaction – a bombardment-driven process involving the collision of two subatomic particles.¹²²⁵ In nuclear reactions, a subatomic particle collides with an atomic nucleus and causes changes to it. Nuclear reactions are thus driven by the mechanics of bombardment, not by the relatively constant exponential decay and half-life characteristic of spontaneous radioactive processes. Many types of nuclear reactions are currently known. Nuclear fission differs from other types of nuclear reactions in that it can be amplified and sometimes controlled via a nuclear chain reaction (one type of general chain reaction). In such a reaction, free neutrons released by each fission event can trigger yet more events, which in turn release more neutrons and cause more fission events. Certain substances called nuclear fuels undergo fission when struck by fission neutrons, and in turn emit neutrons when they break apart. This makes a self-sustaining nuclear chain reaction possible, releasing energy at a slow controlled rate in a nuclear reactor or at a very rapid rate in a nuclear weapon.

Nuclear fission can also occur without neutron bombardment as a type of radioactive decay. This type of fission (called spontaneous fission or SF)¹²²⁶ is rare except in a few heavy isotopes. The lightest natural nuclides that are hypothetically subject to SF might be ^{93}Nb and ^{94}Mo ,¹²²⁷ but spontaneous fission hasn't been observed in these naturally occurring isotopes. SF is feasible over practical observation times only for isotopes with atomic mass number $A \geq 232$. These are

¹²²⁴ https://en.wikipedia.org/wiki/Nuclear_fission.

¹²²⁵ https://en.wikipedia.org/wiki/Nuclear_fission#Nuclear_Reaction.

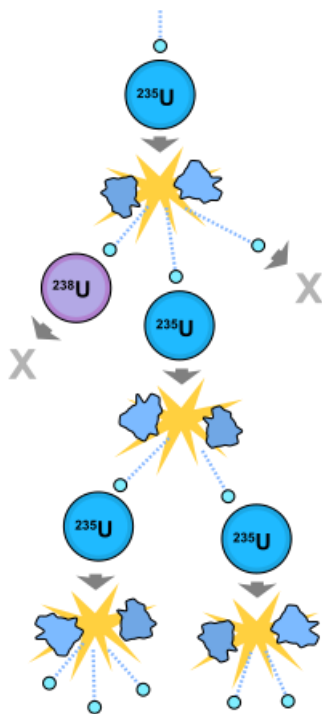
¹²²⁶ https://en.wikipedia.org/wiki/Spontaneous_fission.

¹²²⁷ https://en.wikipedia.org/wiki/List_of_nuclides#Nuclides_that_are_observationally_stable_and_a_theoretical_decay_mode_of_spontaneous_fission.

elements at least as heavy as ^{232}Th – which has a half-life somewhat longer than the age of the universe. For naturally occurring ^{232}Th , ^{235}U and ^{238}U , spontaneous fission occurs rarely (e.g., $\tau_{1/2} = 9 \times 10^{15}$ years for SF in ^{238}U) but the vast majority of decays are α -decay (e.g., $\tau_{1/2} = 4.47 \times 10^9$ years in ^{238}U) or β -decay and so the spontaneous fission of these isotopes is usually negligible. The known elements most susceptible to spontaneous fission are the synthetic high-atomic-number actinides and transactinides with atomic numbers $Z \geq 100$. As in neutronic nuclear fission, each nucleus that undergoes SF releases ~ 0.87 MeV/nucleon of the starting element.

Of the 69 radioisotopes up through atomic number 107 (Bohrium) for which SF disintegrations are known to represent at least 0.1% (= “SF Branch Ratio”) of all radioactive decays experienced by the nucleus, only 12 of these radioisotopes have an SF half-life of at least 1 hour, as tabulated in **Table 54** with supporting data provided in **Table A6** in **Appendix A**. (The table presents only the SF component of the total energy release due to all nuclear disintegrations – isotopes with low SF branch ratios may have substantial additional energy releases from α -emission, β -emission, or other radioactive decay pathways.) For practical applications the two most notable isotopes on the list are ^{260}Md which has a half-life of 27.8 days and throws off **21 MW/kg (216 MW/L)**, and

^{254}Cf with a half-life of 60.5 days and throws off **11 MW/kg (167 MW/L)**. Inconveniently, mendelevium metal of any isotope has not yet been prepared in bulk quantities, and bulk preparation is currently impossible;¹²²⁸ the High Flux Isotope Reactor has produced 0.5 gm/yr of ^{252}Cf for \$10M/gm,¹²²⁹ but bulk Californium-254 has not yet been produced.



The chemical element isotopes that can sustain a fission chain reaction (image, left) are called nuclear fuels and are said to be fissile. These fuels lie in the region of the binding energy curve where a fission chain reaction is possible (i.e., above radium).¹²³⁰

The most common nuclear fuels are ^{235}U and ^{239}Pu . These fuels break apart into a bimodal range of chemical elements (fission products)¹²³¹ with atomic masses centering near $A \sim 95$ and $A \sim 135$. Most nuclear fuels undergo spontaneous fission only very slowly, decaying instead mainly via an alpha-beta decay chain over periods of millennia to eons. In a nuclear reactor or nuclear weapon, the overwhelming majority of fission events are induced by bombardment with another particle, a neutron, which is itself produced by prior fission events.

¹²²⁸ Silva RJ. Fermium, Mendelevium, Nobelium, and Lawrencium. In: Morss LR, Edelstein NM, Fuger J, eds., *The Chemistry of the Actinide and Transactinide Elements*, 3rd edition, Dordrecht: Springer, 2006, pp. 1621-1651, at pp. 1634-1635; <https://web.archive.org/web/20100717155410/http://radchem.nevada.edu/classes/rdch710/files/Fm%20to%20Lr.pdf>.

¹²²⁹ <https://en.wikipedia.org/wiki/Californium#History>.

¹²³⁰ https://en.wikipedia.org/wiki/Fissile_material#Nuclear_fuel.

¹²³¹ [https://en.wikipedia.org/wiki/Fission_products_\(by_element\)](https://en.wikipedia.org/wiki/Fission_products_(by_element)).

Table 54. Estimated specific power (P_S) and power density (P_D), and specific energy (E_S) and energy density (E_D), for spontaneous fission (SF) in radionuclides with half-life ≥ 1 hour¹²³²

Radio-nuclide	SF Branch Ratio	Half-Life (sec)	P_S (MW/kg)	P_D (MW/L)	E_S (MJ/kg)	E_D (MJ/L)
²⁵⁹ Md	98.7 %	5800	9900	102,000	82.9×10^6	853×10^6
²⁵⁶ Fm	91.9 %	9460	5650	54,900	77.1×10^6	748×10^6
²⁶² Lr	10 %	14,400	404	6510	8.39×10^6	135×10^6
²⁵⁶ Md	3 %	4600	379	3910	2.52×10^6	25.9×10^6
²⁵⁷ Md	1 %	19,900	29.2	301	0.84×10^6	8.65×10^6
²⁶⁰ Md	86.5 %	2.40×10^6	21	216	72.6×10^6	748×10^6
²⁵⁴ Cf	99.69 %	5.23×10^6	11.1	167	83.7×10^6	1260×10^6
²⁵² Cf	3.092 %	83.4×10^6	0.0216	0.326	2.60×10^6	39.2×10^6
²⁵⁷ Fm	0.21 %	8.68×10^6	0.0141	0.137	0.18×10^6	1.71×10^6
²⁵⁰ Cm	74 %	0.26×10^{12}	1.65×10^{-4}	2.23×10^{-3}	62.1×10^6	839×10^6
²⁴⁸ Cm	8.39 %	11.0×10^{12}	4.44×10^{-7}	6.00×10^{-6}	7.04×10^6	95.1×10^6
²⁴⁴ Pu	0.121 %	2.50×10^{15}	2.82×10^{-11}	5.58×10^{-10}	0.10×10^6	2.01×10^6

Figure 9 (Chapter 9) provides a chart that summarizes power density vs. specific power for spontaneous fission and RTGs.

Fissile nuclides¹²³³ that can be made to undergo nuclear fission (i.e., are fissionable) and also produce neutrons from such fission that can sustain a nuclear chain reaction (in the correct setting) include ²²⁵Th (likely), ²²⁷Th (likely), ²²⁸Pa (likely), ²²⁹Th (likely), ²³⁰Pa (likely), ²³¹U (likely), ²³²Pa (likely), ²³²U, ²³³U (15.8 kg), ²³⁴Np (likely), ²³⁵U (46.7 kg), ²³⁶Pu, ²³⁶Np (7 kg), ²³⁷Pu, ²³⁷Np (63.6 kg), ²³⁸Np, ²³⁸Pu (9.5 kg), ²³⁹Pu (10 kg), ²⁴⁰Am (likely), ²⁴⁰Pu (35.7 kg), ²⁴¹Pu (12.3 kg), ²⁴¹Am (57.6 kg), ^{242m}Am (8.8 kg), ²⁴²Pu (75-100 kg), ²⁴³Cm (8.4 kg), ²⁴³Pu, ²⁴³Am (180-280 kg), ²⁴⁴Am, ²⁴⁴Cm (26.6 kg), ²⁴⁵Cm (9.1 kg), ²⁴⁶Cm (39-70.1 kg), ²⁴⁶Bk (likely), ²⁴⁷Cm (6.9 kg), ²⁴⁷Bk (75.7 kg), ²⁴⁸Bk (likely), ²⁴⁹Cf (5.9 kg), ²⁴⁹Bk (192 kg), ²⁵⁰Bk, ²⁵¹Cf (5.46 kg), ²⁵²Cf (2.73 kg), ²⁵²Es (likely), ²⁵³Cf, ²⁵⁴Es (9.89 kg), ²⁵⁵Fm (likely), ²⁵⁶Es (likely), ²⁵⁷Fm (likely), and ²⁵⁹Fm (likely). The estimated “bare sphere” critical mass¹²³⁴ for each fissile isotope is indicated in the above listing, in parens.¹²³⁵

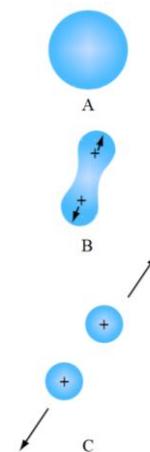
¹²³² Data from **Table A6** in **Appendix A.6**.

¹²³³ https://en.wikipedia.org/wiki/Fissile_material#Fissile_nuclides.

¹²³⁴ “Critical mass is the smallest amount of fissile material needed for a sustained nuclear chain reaction. The critical mass of a fissionable material depends upon its nuclear properties (specifically, the nuclear fission cross-section), its density, its shape, its enrichment, its purity, its temperature, and its surroundings.” https://en.wikipedia.org/wiki/Critical_mass.

¹²³⁵ https://en.wikipedia.org/wiki/Critical_mass#Critical_mass_of_a_bare_sphere;
<https://www.euronuclear.org/info/encyclopedia/criticalmass.htm>.

The fission of a heavy nucleus requires a total input energy of about 7-8 MeV to initially overcome the nuclear force that holds the nucleus in a spherical or nearly spherical shape (i.e., liquid-drop model of fission; image, right). Once initiated, typical heavy-nucleus fission events (or spontaneous fission events) release ~200 MeV of energy, or roughly 0.87 MeV per nucleon of the starting element. When a uranium nucleus fissions into two daughter nuclei fragments, about 0.1% of the mass of the uranium nucleus appears as the fission energy. For ^{235}U with a total mean fission energy of 202.79 MeV,¹²³⁶ typically ~169 MeV appears as the kinetic energy of the daughter nuclei which fly apart at ~3% of the speed of light due to Coulomb repulsion. An average of 2.5 neutrons are emitted with a collective kinetic energy of ~5 MeV, and the fission reaction also releases ~7 MeV in prompt gamma ray photons, ~6 MeV in delayed gamma radiation, and ~8 MeV in anti-neutrinos. Hence a nuclear fission explosion or criticality accident emits about 6.5% of its energy as gamma rays, 2.5% as fast neutrons, 4% as anti-neutrinos, and the remaining ~87% as the kinetic energy of fission fragments. The total prompt fission energy amounts to about 181 MeV, or ~89% of the total energy which is eventually released by fission over time; the remaining ~11% is released in beta decays with various half-lives.¹²³⁷ Assuming full recoverability, the total specific energy of neutron-induced fission of the ^{235}U nucleus is $E_S \sim 202.79 \text{ MeV} / [(235 \text{ nucleons})(1.67 \times 10^{-27} \text{ kg/nucleon})] = 83 \times 10^6 \text{ MJ/kg}$, and ^{235}U fission energy density $E_D = \rho_{\text{U}235} E_S = 1.6 \times 10^9 \text{ MJ/L}$, taking $\rho_{\text{U}235} = 19,100 \text{ kg/m}^3$. The total mean fission energy of ^{239}Pu is 207.1 MeV,¹²³⁸ again giving a specific energy for nuclear fission of $E_S \sim 207.1 \text{ MeV} / [(239 \text{ nucleons})(1.67 \times 10^{-27} \text{ kg/nucleon})] = 83 \times 10^6 \text{ MJ/kg}$ and a fission energy density $E_D = \rho_{\text{Pu}239} E_S = 1.6 \times 10^9 \text{ MJ/L}$, taking $\rho_{\text{Pu}239} = 19,816 \text{ kg/m}^3$. (~8 MeV is neutrinos and is usually considered unrecoverable, which drops the practical specific energy of fission fuels to ~80 x 10⁶ MJ/kg.)



The nuclear reaction fission energy release can be throttled to produce any desired power output by controlling the flux rate and impact energy of the bombarding neutrons or by altering other reaction conditions. For example, packing ^{235}U into a dense ball causes its power generation to



rise astronomically due to the chain reaction (up to and including a high-energy nuclear explosion; see below). Alternatively, inserting a neutron-absorbing material such as boron, silver, indium or cadmium (e.g., a control rod in a nuclear reactor)¹²³⁹ can slow the rate of nuclear fissions and reduce power generation.

Nuclear power plants (image, left) are employed commercially¹²⁴⁰ to convert fission energy into electricity in a

¹²³⁶ Kopeikin V, Mikaelyan L, Sinev V. Reactor as a source of antineutrinos: Thermal fission energy. *Physics of Atomic Nuclei*. 2004 Oct;67(10):1892-1899; <https://arxiv.org/pdf/hep-ph/0410100.pdf>.

¹²³⁷ https://en.wikipedia.org/wiki/Nuclear_fission#Output.

¹²³⁸ https://en.wikipedia.org/wiki/Plutonium-239#Nuclear_properties.

¹²³⁹ https://en.wikipedia.org/wiki/Control_rod.

¹²⁴⁰ https://en.wikipedia.org/wiki/List_of_nuclear_reactors.

highly controlled manner. Critical fission reactors are the most common type of nuclear reactor.¹²⁴¹ In a critical fission reactor, neutrons produced by fission of fuel atoms are used to induce yet more fissions, to sustain a controllable amount of energy release. Critical fission reactors are built for three primary purposes, which typically involve different engineering trade-offs to take advantage of either the heat or the neutrons produced by the fission chain reaction.¹²⁴²

(1) Power reactors¹²⁴³ intended to produce heat for nuclear power, either as part of a generating station or a local power system such as a nuclear submarine;

(2) Research reactors¹²⁴⁴ intended to produce neutrons and/or to activate radioactive sources for scientific, medical, engineering, or other research purposes; and

(3) Breeder reactors¹²⁴⁵ intended to produce nuclear fuels in bulk from more abundant isotopes. The best known fast breeder reactor¹²⁴⁶ makes ²³⁹Pu (a nuclear fuel) from the naturally very abundant ²³⁸U (not a nuclear fuel). Thermal breeder reactors¹²⁴⁷ using ²³²Th to breed the fissile isotope ²³³U (thorium fuel cycle) continue to be studied and developed.

Robert Forward has suggested¹²⁴⁸ that it might be possible to build “subcritical nuclear reactors.” Normally, atomic fission piles must be a certain minimum size because the neutrons which initiate fission reactions arise randomly from within the fissionable material itself. But if some nonstatistical means for controlling neutrons could be found,¹²⁴⁹ neutron emission would no longer be random and vastly improved efficiencies should be possible. Tiny, portable fission reactors could probably be built to service aircraft and surface vehicles, and reactors using nonradioactive lightweight metals such as beryllium or lithium might also be possible.

The energy released in the fission process generates heat, some of which can be converted into usable energy. A common method of harnessing this thermal energy is to use it to boil water to produce pressurized steam which will then drive a steam turbine that turns an alternator¹²⁵⁰ and generates electricity.¹²⁵¹ The mass of the conventionally required infrastructure significantly

¹²⁴¹ Devices that produce engineered but non-self-sustaining fission reactions are “subcritical fission reactors” (https://en.wikipedia.org/wiki/Subcritical_reactor) that use radioactive decay (**Section 7.1**) or particle accelerators to trigger fissions.

¹²⁴² https://en.wikipedia.org/wiki/Nuclear_fission#Fission_reactors.

¹²⁴³ https://en.wikipedia.org/wiki/Nuclear_power_plant.

¹²⁴⁴ https://en.wikipedia.org/wiki/Research_reactor.

¹²⁴⁵ https://en.wikipedia.org/wiki/Breeder_reactor.

¹²⁴⁶ https://en.wikipedia.org/wiki/Breeder_reactor#Fast_breeder_reactor.

¹²⁴⁷ https://en.wikipedia.org/wiki/Breeder_reactor#Thermal_breeder_reactor.

¹²⁴⁸ Forward RL. Far Out Physics. Analog SF/Sci Fact 1975 Aug;95(8):147-166; <http://www.isfdb.org/cgi-bin/title.cgi?115713>.

¹²⁴⁹ And the Neutrons Go Round and Round. Science News 1977 Dec 17;112:407.

¹²⁵⁰ <https://en.wikipedia.org/wiki/Alternator>.

¹²⁵¹ https://en.wikipedia.org/wiki/Nuclear_reactor.

drops the power density for the entire system compared to the pure nuclear fuel. Most commercial nuclear reactors use nuclear fuel enriched in ^{232}Th , ^{233}U , ^{235}U , or ^{239}Pu ,¹²⁵² and the typical power density that is allowed to develop inside a nuclear power plant reactor core is only **0.001-0.150 MW/L**.¹²⁵³ For example, a recently-designed 2.4 MW ^{235}U -burning “micronuclear” power source with a 69-liter reactor core of total mass 310 kg would provide a specific power in the reactor core of **0.0077 MW/kg** and a power density of **0.035 MW/L**.¹²⁵⁴ The power density of a nuclear power plant is substantially less than for the reactor core. For example, the Palo Verde Nuclear Generating Station¹²⁵⁵ in Arizona has a 74,000 m³ containment building surrounding each reactor unit that generates ~1313 MW of nuclear power, giving an overall power density for each generating unit of only $P_D = 1.77 \times 10^{-5}$ MW/L.



What is the maximum fissile power density? An atomic fission bomb (e.g., Trinity, 1945; image, left)¹²⁵⁶ releases all of its energy in a very short time, thus achieving a huge power density. For example, a 1-megaton fission bomb would release $\sim 4.18 \times 10^9$ MJ from the fission of ~ 52 kg of fissile ^{235}U storing **$\sim 80 \times 10^6$ MJ/kg** of nuclear energy. The time required for a supercritical mass of this size to completely chain-react is ~ 1 μsec ,¹²⁵⁷ so the nuclear material in an atomic fission bomb can briefly achieve a specific power of **$\sim 8 \times 10^{13}$ MW/kg** and a power density of **$\sim 1.5 \times 10^{15}$ MW/L**.

The specific power for an entire atomic bomb device, which includes conventional high explosives and other infrastructure surrounding the fissile core, may be ~ 1000 -fold lower than for the pure fissile material. For example, the 22.1-kiloton Trinity test device¹²⁵⁸ nicknamed “Gadget” – the first fission bomb ever detonated – was a 1.5-meter sphere¹²⁵⁹ (volume ~ 1767 L) with an estimated total weight¹²⁶⁰ of ~ 4800 kg that released $\sim 92 \times 10^{12}$ J of energy¹²⁶¹ in ~ 1 μsec ,

¹²⁵² https://en.wikipedia.org/wiki/Nuclear_fuel.

¹²⁵³ International Atomic Energy Agency, “Nuclear Power Plant Design Characteristics,” IAEA-TECDOC-1544, Mar 2007, Table 2; https://www-pub.iaea.org/MTCD/Publications/PDF/te_1544_web.pdf.

¹²⁵⁴ Sun H, Wang C, Liu X, Tian W, Qiu S, Su G. Reactor core design and analysis for a micronuclear power source. *Front Energy Res* 2018 Mar 22; 6:14; <https://www.frontiersin.org/articles/10.3389/fenrg.2018.00014/full>.

¹²⁵⁵ https://en.wikipedia.org/wiki/Palo_Verde_Nuclear_Generating_Station#Description.

¹²⁵⁶ [https://en.wikipedia.org/wiki/Trinity_\(nuclear_test\)](https://en.wikipedia.org/wiki/Trinity_(nuclear_test)).

¹²⁵⁷ “How long does a nuclear explosion take?” 22 Feb 2018; <https://www.quora.com/How-long-does-a-nuclear-explosion-take>.

¹²⁵⁸ [https://en.wikipedia.org/wiki/Trinity_\(nuclear_test\)#The_Gadget](https://en.wikipedia.org/wiki/Trinity_(nuclear_test)#The_Gadget).

¹²⁵⁹ <https://nuclearweaponarchive.org/Nwfaq/Nfaq8.html#nfaq8.1.1>.

¹²⁶⁰ <https://www.atomicheritage.org/history/little-boy-and-fat-man>.

giving $E_S \sim 19,000 \text{ MJ/kg}$, $E_D \sim 52,000 \text{ MJ/L}$, $P_S \sim 1.9 \times 10^{10} \text{ MW/kg}$, and $P_D \sim 5.2 \times 10^{10} \text{ MW/L}$ for the entire device.

¹²⁶¹ Hanson SK, Pollington AD, Waidmann CR, Kinman WS, Wende AM, Miller JL, Berger JA, Oldham WJ, Selby HD. Measurements of extinct fission products in nuclear bomb debris: Determination of the yield of the Trinity nuclear test 70 y later. *Proc Natl Acad Sci U S A*. 2016 Jul 19;113(29):8104-8; <https://www.ncbi.nlm.nih.gov/pmc/articles/PMC4961180/>.

7.3 Fusion

Nuclear fusion is a reaction in which two or more atomic nuclei and/or nucleons are combined to form one or more heavier atomic nuclei and/or nucleons (neutrons or protons). A change in mass between the reactants and products arises due to the difference in their nuclear binding energies (**Section 7.0**), and this change is manifested by the release of fusion energy.¹²⁶²

The following discussion includes energy and power density in conventional nuclear fusion (**Section 7.3.1**), muon-catalyzed fusion (**Section 7.3.2**), and low-energy nuclear fusion reactions (**Section 7.3.3**).

¹²⁶² https://en.wikipedia.org/wiki/Nuclear_fusion.

7.3.1 Conventional Nuclear Fusion

Stars generate power via high-temperature fusion, and stellar fusion produces virtually all of the natural elements via nucleosynthesis.¹²⁶³ As a main-sequence star, the Sun generates its energy by the nuclear fusion of 620 million metric tons of hydrogen nuclei into 606 million metric tons of helium each second.¹²⁶⁴ However, at the temperatures and densities in stellar cores the rates of fusion reactions are surprisingly slow. For example, at the solar core temperature (~15 million K) and density (~150 kg/L),¹²⁶⁵ the power density is only ~**0.0194 W/L** (~0.000129 W/kg)¹²⁶⁶ which is actually less than the ~**1.5 W/L** of the resting human body. Conventional nuclear fusion reaction rates depend on density as well as temperature. Since it is difficult to create artificial plasmas ~150 times more dense than water comparable to the solar core, contemporary fusion reactors are restricted to much lower densities (e.g., ~10⁻⁹ kg/L)¹²⁶⁷ and thus must typically operate at temperatures 10-100 times hotter than the stellar interior (100-1000 million K).

To be a useful energy source, a conventional fusion reaction should satisfy several criteria: (1) be exothermic (which limits the reactants to the low Z (number of protons) side of the binding energy curve, with ⁴He the most common fusion product because of its extraordinarily tight binding); (2) involve low atomic number (Z) nuclei (because the electrostatic repulsion that must be overcome before the nuclei are close enough to fuse is directly related to the number of protons it contains); (3) have two reactants (because at anything less than stellar densities, three body collisions are too improbable); (4) have two or more products (which allows simultaneous conservation of energy and momentum without relying on the electromagnetic force); and (5) conserve both protons and neutrons (because the cross sections for the weak interaction are too small).¹²⁶⁸

The reactions that meet these criteria with the largest cross sections (~ probability of reaction),¹²⁶⁹ along with the foundational p-p reaction, are listed in **Table 55** below, ranked by specific energy of the fusion fuel.

¹²⁶³ <https://en.wikipedia.org/wiki/Nucleosynthesis>.

¹²⁶⁴ https://en.wikipedia.org/wiki/Nuclear_fusion#Astrophysical_reaction_chains.

¹²⁶⁵ https://en.wikipedia.org/wiki/Solar_core.

¹²⁶⁶ About 99% of solar fusion energy is generated in a core of radius $R_{\text{core}} \sim 0.24 R_{\text{solar}} = (0.24) (6.957 \times 10^8 \text{ m}) = 1.67 \times 10^8 \text{ m}$; https://en.wikipedia.org/wiki/Solar_core. Total solar output is $P_{\text{solar}} = 3.828 \times 10^{26} \text{ W}$, hence core power density is $P_{\text{D,core}} = 0.99 P_{\text{solar}} / [(4/3) \pi R_{\text{core}}^3] = 0.0194 \text{ W/L}$.

¹²⁶⁷ For example, in late 2016 the Alcator C-Mod tokamak at MIT (https://en.wikipedia.org/wiki/Alcator_C-Mod) set a new world confinement pressure record (<http://news.mit.edu/2016/alcator-c-mod-tokamak-nuclear-fusion-world-record-1014>) of $\sim 4.3 \times 10^{14}$ deuteron ions/cm³ or $\sim 10^{-9}$ kg/L) for deuterium-tritium plasma using a 5.7 tesla magnetic field and a particle temperature of $3.5 \times 10^7 \text{ K}$ while sustaining fusion for ~2 seconds.

¹²⁶⁸ https://en.wikipedia.org/wiki/Nuclear_fusion#Criteria_and_candidates_for_terrestrial_reactions.

¹²⁶⁹ https://en.wikipedia.org/wiki/Nuclear_cross_section.

Table 55. Exothermic fusion reactions with the highest cross-sections, ranked by specific energy (E_S) of the nuclear fuel¹²⁷⁰

Reactants	Products	Reaction Energy (MeV)	Mass of Reactants (kg)	Specific Energy (MJ/kg)
${}^2\text{D}_1 + {}^3\text{He}_2$	${}^4\text{He}_2 + \text{p}^+$	18.35	8.35×10^{-27}	352×10^6
${}^2\text{D}_1 + {}^3\text{T}_1$	${}^4\text{He}_2 + \text{n}^0$	17.59	8.35×10^{-27}	337×10^6
${}^2\text{D}_1 + {}^6\text{Li}_3$	${}^4\text{He}_2 + {}^4\text{He}_2$	22.40	1.33×10^{-26}	269×10^6
${}^3\text{He}_2 + {}^3\text{T}_1$	${}^4\text{He}_2 + {}^2\text{D}_1$	14.30	1.00×10^{-26}	229×10^6
${}^3\text{He}_2 + {}^3\text{T}_1$	${}^4\text{He}_2 + \text{p}^+ + \text{n}^0$	14.30	1.00×10^{-26}	229×10^6
$\text{p}^+ + {}^7\text{Li}_3$	${}^4\text{He}_2 + {}^4\text{He}_2$	17.35	1.33×10^{-26}	209×10^6
${}^3\text{He}_2 + {}^3\text{He}_2$	${}^4\text{He}_2 + \text{p}^+ + \text{p}^+$	12.86	1.00×10^{-26}	206×10^6
${}^3\text{He}_2 + {}^3\text{T}_1$	${}^4\text{He}_2 + \text{p}^+ + \text{n}^0$	12.10	1.00×10^{-26}	194×10^6
${}^3\text{T}_1 + {}^3\text{T}_1$	${}^4\text{He}_2 + \text{n}^0 + \text{n}^0$	11.33	1.00×10^{-26}	181×10^6
${}^3\text{He}_2 + {}^6\text{Li}_3$	${}^4\text{He}_2 + {}^4\text{He}_2 + \text{p}^+$	16.90	1.50×10^{-26}	181×10^6
${}^2\text{D}_1 + {}^2\text{D}_1$	${}^3\text{T}_1 + \text{p}^+$	4.03	6.69×10^{-27}	96.5×10^6
${}^2\text{D}_1 + {}^2\text{D}_1$	${}^3\text{He}_2 + \text{n}^0$	3.27	6.69×10^{-27}	78.3×10^6
$\text{p}^+ + {}^{11}\text{B}_5$	${}^4\text{He}_2 + {}^4\text{He}_2 + {}^4\text{He}_2$	8.68	2.00×10^{-26}	69.7×10^6
$\text{n}^0 + {}^6\text{Li}_3$	${}^3\text{T}_1 + {}^4\text{He}_2$	4.78	1.17×10^{-26}	65.7×10^6
${}^2\text{D}_1 + {}^6\text{Li}_3$	${}^7\text{Li}_3 + \text{p}^+$	5.00	1.33×10^{-26}	60.1×10^6
$\text{p}^+ + {}^6\text{Li}_3$	${}^4\text{He}_2 + {}^3\text{He}_2$	4.02	1.17×10^{-26}	55.2×10^6
${}^2\text{D}_1 + {}^6\text{Li}_3$	${}^7\text{Be}_4 + \text{n}^0$	3.40	1.33×10^{-26}	40.9×10^6
${}^2\text{D}_1 + {}^6\text{Li}_3$	${}^3\text{He}_2 + {}^4\text{He}_2 + \text{n}^0$	2.56	1.33×10^{-26}	30.8×10^6
$\text{p}^+ + {}^{15}\text{N}_7$	${}^{12}\text{C}_6 + {}^4\text{He}_2$	4.97	2.66×10^{-26}	30.0×10^6
$\text{p}^+ + \text{p}^+$	${}^2\text{D}_1 + \text{e}^+ + \text{v}_e$	0.42	3.35×10^{-27}	20.1×10^6
${}^{12}\text{C}_6 + {}^{12}\text{C}_6$	${}^{20}\text{Na}_{11} + {}^4\text{He}_2$	4.62	3.99×10^{-26}	18.6×10^6
${}^{12}\text{C}_6 + {}^{12}\text{C}_6$	${}^{23}\text{Na}_{11} + \text{p}^+$	2.24	3.99×10^{-26}	9.01×10^6

The most energy-dense exothermic fusion reactions appear to be ${}^2\text{D}_1 + {}^3\text{He}_2 \rightarrow {}^4\text{He}_2 + \text{p}^+$ at $E_S = 352 \times 10^6 \text{ MJ/kg}$ and ${}^2\text{D}_1 + {}^3\text{T}_1 \rightarrow {}^4\text{He}_2 + \text{n}^0$ at $E_S = 337 \times 10^6 \text{ MJ/kg}$. These provide up to ~40% of the theoretical maximum specific energy of $E_S = 841 \times 10^6 \text{ MJ/kg}$ for fusion fuels calculated earlier in **Section 7**.

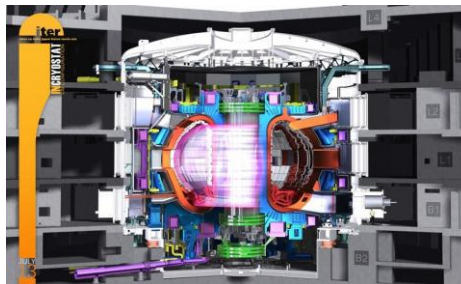
Hydrogen is the most abundant element in many stars, and the fusion of two hydrogen ions (the proton-proton reaction)¹²⁷¹ is the main fusion reaction that converts hydrogen to helium in stars that are less than 1.3 times the mass of the Sun. The low-energy p-p reaction proceeds in two steps, the second of which is so slow (i.e., the half-life of a proton in the stellar interior is ~1

¹²⁷⁰ https://en.wikipedia.org/wiki/Nuclear_fusion#Criteria_and_candidates_for_terrestrial_reactions and <http://www.fisicanucleare.it/documents/0-19-856264-0.pdf>.

¹²⁷¹ https://en.wikipedia.org/wiki/Proton%E2%80%93proton_chain_reaction.

billion years) that the complete conversion of the hydrogen in the core of the Sun is calculated to take more than ten billion years.¹²⁷²

Research into developing controlled thermonuclear fusion for civilian energy purposes began in earnest in the 1940s and continues to this day (image of ITER,¹²⁷³ right). Devices designed to harness this energy are known as fusion reactors.¹²⁷⁴ Fusion reactors generally use hydrogen and helium isotopes such as deuterium, tritium, and ³He which react more easily, and create a confined ion plasma at temperatures of millions of degrees. The plasma is usually confined by one of several leading methods including magnetic confinement,¹²⁷⁵ inertial confinement,¹²⁷⁶ electrostatic confinement,¹²⁷⁷ or magnetic/electric pinch confinement.¹²⁷⁸ As a source of power, nuclear fusion is expected to have several theoretical advantages over fission including reduced radioactivity in operation, little nuclear waste, ample fuel supplies, and increased safety. However, controlled fusion has proven to be extremely difficult to produce in a practical and economical manner. To date, no design has produced more fusion power output than the electrical power input, so all existing designs have had a negative power balance.



Two major challenges in realizing fusion power are to engineer a system that can: (1) confine the plasma long enough at a high enough temperature and density to allow a reaction to occur,¹²⁷⁹ and (2) manage any neutrons released during the reaction, which over time can degrade many common materials used within the reaction chamber. While the specific energy for fusion is very high, devices that must employ a confined ion plasma are seriously constrained by attainable plasma densities. A rough estimate of the power density P (in MW/L) that should be available from several fusion reactions in hot confinement reactors, as a function of ion density, is given by:¹²⁸⁰

$$P_{D,D/D} = 3.3 \times 10^{-22} n_D n_D \langle \sigma v \rangle_{D/D}$$

$$P_{D,D/T} = 5.6 \times 10^{-22} n_D n_T \langle \sigma v \rangle_{D/T}$$

$$P_{D,D/3He} = 2.93 \times 10^{-21} n_D n_{3He} \langle \sigma v \rangle_{D/3He}$$

¹²⁷² Krane KS. Introductory Nuclear Physics, Wiley, 1987, p. 537.

¹²⁷³ <https://en.wikipedia.org/wiki/ITER>.

¹²⁷⁴ https://en.wikipedia.org/wiki/Fusion_power.

¹²⁷⁵ https://en.wikipedia.org/wiki/Fusion_power#Magnetic_confinement.

¹²⁷⁶ https://en.wikipedia.org/wiki/Fusion_power#Inertial_confinement.

¹²⁷⁷ https://en.wikipedia.org/wiki/Fusion_power#Inertial_electrostatic_confinement.

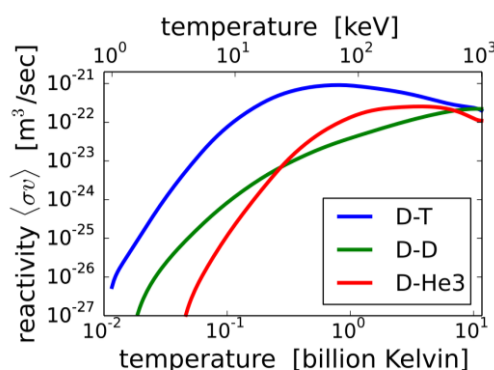
¹²⁷⁸ https://en.wikipedia.org/wiki/Fusion_power#Magnetic_or_electric_pinches.

¹²⁷⁹ https://en.wikipedia.org/wiki/Lawson_criterion#Extension_into_the_%22triple_product%22.

¹²⁸⁰ Teh-Ming Hsieh, "Section VII. Thermonuclear Fusion Technology and its Application in Space Propulsion," JPL Technical Memorandum 33-722, pp. 134-194; <https://ntrs.nasa.gov/archive/nasa/casi.ntrs.nasa.gov/19750014301.pdf>.

where $\langle\sigma v\rangle$ is the average fusion reactivity (m^3/sec), σ is the cross-section (m^2), v is the relative velocity between colliding ions (m/sec), and n is the ion density ($\text{particles}/\text{m}^3$).

Taking the $\text{D}/^3\text{He}$ reaction which has the highest specific energy and the lowest neutron generation of the three, reactivity $\langle\sigma v\rangle_{\text{D}/^3\text{He}} \sim 2 \times 10^{-22} \text{ m}^3/\text{sec}$ near the peak at $T \sim 2$ billion K (chart, right); assuming the record peak ion density of $n_{\text{D}} \sim n_{^3\text{He}} \sim 4.3 \times 10^{20} \text{ ions}/\text{m}^3$ as recently achieved in the Alcator C-Mod tokamak (image below, left),¹²⁸¹ then $P_{\text{D,D}/^3\text{He}} = \mathbf{0.11 \text{ MW/L}}$. Using the same ion density and the peak reactivity particular to each reaction, then $P_{\text{D,D/T}} = \mathbf{0.093 \text{ MW/L}}$ at $T \sim 0.6$ billion K and $P_{\text{D,D/D}} = \mathbf{0.012 \text{ MW/L}}$ at $T \sim 10$ billion K. These fusion reactor



core power densities are comparable to the power densities of fission nuclear power plant reactor cores (**Section 7.2**) and a million-fold higher than the $\sim 2.8 \times 10^{-7} \text{ MW/L}$ observed in the stellar fusion core of the Sun. Unavoidable energy losses due to bremsstrahlung (the generation of X-rays when electrons collide with nuclei)¹²⁸² are claimed to amount to $\sim 24\%$ for $\text{D}-^3\text{He}$, $\sim 0.8\%$ for D-T , and $\sim 47\%$ for D-D , whereas other reactions such as $^3\text{He}-^3\text{He}$ (142%), p^+-^6Li (536%) and p^+-^{11}B (174%) were estimated to have losses exceeding 100% of the fusion power generation,¹²⁸³ hence “there appears to be no way to produce net power with these fuels.”¹²⁸⁴ Nevertheless, a private company called TAE Technologies¹²⁸⁵ is pursuing development of an aneutronic fusion¹²⁸⁶ reactor employing the $\text{p}^+ + ^{11}\text{B}_5 \rightarrow 3\ ^4\text{He}_2 + 8.68 \text{ MeV}$ reaction using a field-reversed toroidal configuration¹²⁸⁷ that produces no neutrons and offers a pure electrical output with α -particle energy harvested via magnetohydrodynamics with 90% efficiency¹²⁸⁸ (needed for

¹²⁸¹ <http://news.mit.edu/2016/alcator-c-mod-tokamak-nuclear-fusion-world-record-1014>.

¹²⁸² <https://en.wikipedia.org/wiki/Bremsstrahlung>.

¹²⁸³ Rider TH. A general critique of inertial-electrostatic confinement fusion systems. *Phys Plasma* 1995 Jun;2(6):1853-1872; <http://fsl.npre.illinois.edu/IEC/Rider,%20Phys.ofPlasmas1995.pdf>.

¹²⁸⁴ Rider TH. Fundamental Limitations on Plasma Fusion Systems not in Thermodynamic Equilibrium. *Physics of Plasma* 1997;4(4):1039-1046; <https://pdfs.semanticscholar.org/fce7/a35629488ec030d983025a44dc00d38d0f68.pdf>.

¹²⁸⁵ https://en.wikipedia.org/wiki/TAE_Technologies.

¹²⁸⁶ https://en.wikipedia.org/wiki/Aneutronic_fusion.

¹²⁸⁷ https://en.wikipedia.org/wiki/Compact_toroid.

¹²⁸⁸ Yoshikawa K, Noma T, Yamamoto Y. Direct-Energy Conversion from High-Energy Ions Through Interaction with Electromagnetic Fields. *Fusion Science and Technology*. 1991 May;19(3P2A):870–875; <https://www.tandfonline.com/doi/abs/10.13182/FST91-A29454>.

conventional thermal conversion) and claiming only 40% bremsstrahlung losses using an X-ray photoelectric converter to capture the emitted photon energy.¹²⁸⁹

According to Hsieh:¹²⁹⁰ “In order not to produce an explosion in the D-T fusion reactor, the density n must be limited to approximately 1000-10,000 times less than that of air (i.e., $n \leq 10^{21}$ - 10^{22} particles/m³), while the confinement time must reach at least a few fractions of a second. For highly compressed laser-induced fusion, in which the energy is released in an explosive mode, densities could be of the order of $\sim 10^{32}$ particles/m³ or more, so that confinement times of picoseconds would be adequate.” (Note: A ~ 150 kg/L plasma density in the stellar core¹²⁹¹ represents an H⁺ particle concentration of $\sim 9 \times 10^{31}$ particles/m³.)

What is the maximum fusion power density? A thermonuclear fusion bomb releases all of its energy in a very short time, thus achieving a huge power density. For example, the 58.6-megaton Tsar Bomba (e.g., Tsar Bomba, 1961; image, right),¹²⁹² the largest bomb ever detonated on Earth, weighed 27,000 kg with a volume of ~ 27.7 m³ and released 210×10^{15} J of fusion energy while converting $\sim 1\%$ of its ~ 230 kg deuterium fusion fuel mass (~ 3300 L) to energy; assuming a ~ 1 μ sec burn time, then the entire device demonstrated a specific energy $E_S \sim 7.78 \times 10^6$ MJ/kg, energy density $E_D \sim 7.58 \times 10^6$ MJ/L, specific power of $P_S \sim 7.8 \times 10^{12}$ MW/kg and a power density $P_D \sim 7.6 \times 10^{12}$ MW/L for the entire device. The nuclear material inside the bomb briefly achieved a specific power of $\sim 9 \times 10^{14}$ MW/kg (~ 10 -fold higher than fissile material) and a power density of $\sim 6 \times 10^{13}$ MW/L (~ 20 -fold lower than fissile material, since liquid hydrogen has very low density).



¹²⁸⁹ https://en.wikipedia.org/wiki/Direct_energy_conversion#X-ray_photoelectric_converter.

¹²⁹⁰ Teh-Ming Hsieh, “Section VII. Thermonuclear Fusion Technology and its Application in Space Propulsion,” JPL Technical Memorandum 33-722, pp. 134-194; <https://ntrs.nasa.gov/archive/nasa/casi.ntrs.nasa.gov/19750014301.pdf>.

¹²⁹¹ https://en.wikipedia.org/wiki/Solar_core.

¹²⁹² https://en.wikipedia.org/wiki/Tsar_Bomba.

7.3.2 Muon-Catalyzed Fusion

Muon-catalyzed fusion¹²⁹³ is a fusion process that can occur at ordinary temperatures.¹²⁹⁴ Here's how it works.

In principle, the two deuterons in a deuterium molecule could spontaneously fuse to form tritium + proton or ${}^3\text{He}$ + neutron, liberating 4.03 MeV (6.46×10^{-13} J) of energy. The two electrons in the D_2 molecule act as a catalyst, holding the deuterons together so they can react. According to quantum mechanics, the deuterons can tunnel toward each other through the classically forbidden region of repulsion until they get so close ($\sim 2 \times 10^{-15}$ m) that the strong force dominates and fusion occurs.¹²⁹⁵ In practice the rate of this reaction is very small, $\sim 10^{-74}$ molecule⁻¹ sec⁻¹.¹²⁹⁶ But if an electron of mass m_e is replaced by a heavier negatively charged particle such as a muon ($m_{\text{muon}} \sim 207 m_e$), forming a muonic molecule, the required tunneling distance shortens by the ratio of the masses – in this case, from 5×10^{-11} m to 2×10^{-13} m, making penetration of the barrier much more likely and dramatically raising the reaction rate to $\sim 10^6$ molecule⁻¹ sec⁻¹.¹²⁹⁷ Assuming liquid deuterium density for the D-D reactants (~ 0.142 kg/L, $\sim 4.25 \times 10^{25}$ molecules/L), then the power density for muonic deuterium is $P_D = (10^6 \text{ reactions/D}_2\text{-sec}) (6.46 \times 10^{-19} \text{ MJ/reaction}) (4.25 \times 10^{25} \text{ D}_2\text{/L}) = \mathbf{2.7 \times 10^{13} \text{ MW/L}}$ and specific power $P_S = P_D / (0.142 \text{ kg/L}) = \mathbf{1.9 \times 10^{14} \text{ MW/kg}}$. These power levels are 25%-50% as large as those of a thermonuclear explosion¹²⁹⁸ (**Section 7.3.1**). (Energy density is about the same as for conventional fusion.)

¹²⁹³ https://en.wikipedia.org/wiki/Muon-catalyzed_fusion.

¹²⁹⁴ Froelich P. Muon catalysed fusion: Chemical confinement of nuclei within the muonic molecule dt μ . *Advances in Physics* 1992 Feb 6;41:405-508; <https://www.tandfonline.com/doi/abs/10.1080/00018739200101533>.

¹²⁹⁵ Zweig G. Quark catalysis of exothermal nuclear reactions. *Science* 1978 Sep 15;201(4360):973-979; <http://science.sciencemag.org/content/201/4360/973.full.pdf>.

¹²⁹⁶ Van Siclen CD, Jones SE. Piezonuclear fusion in isotopic hydrogen molecules. *J Phys G*. 1986 Mar;12(3):213-221; <http://iopscience.iop.org/article/10.1088/0305-4616/12/3/009/meta>.

¹²⁹⁷ Jones SE, Palmer EP, Czirr JB, Decker DL, Jensen GL, Thorne JM, Taylor SF, Rafelski J. Observation of cold nuclear fusion in condensed matter. *Nature* 1989 Apr 27;338:737-740; <http://www.territorioscuola.com/download/fusione-fredda/fusione-fredda-nuclear-matter-condensed.pdf>.

¹²⁹⁸ According to J Rafelski and SE Jones (Cold nuclear fusion. *Sci Am*. 1987 Jul;257(1):84-89; http://pages.erau.edu/~reynodb2/blog/Rafelski_Jones_ColdNuclearFusion.pdf), the resonance mechanism that makes it possible for muomolecular ions to form quickly and to be freed quickly after catalyzing a fusion event works best at ~ 900 °C. At much higher temperatures the resonance mechanism ensures that fusion proceeds more slowly, with two interesting implications: (1) a muon-catalyzed fusion reactor would not be susceptible to runaway reactions or meltdown, and (2) muon-catalyzed fusion cannot be used as the basis for thermonuclear weapons.

Muon catalysis of the proton-deuteron reaction, initially proposed theoretically by Frank in 1947,¹²⁹⁹ was first observed experimentally in 1957 by Alvarez.¹³⁰⁰ It has since been shown to be an effective means of rapidly inducing fusion reactions in low-temperature (<1200 K) mixtures of hydrogen isotopes, with D-T reaction rates of $\sim 10^9 \text{ sec}^{-1}$.¹³⁰¹

Unfortunately, muon catalysis has long been considered impractical for large-scale fusion reactors for two main reasons: (1) short lifetime, and (2) helium capture.

Short Lifetime. First, the muon is relatively short-lived ($\sim 2.2 \mu\text{sec}$). Typically the number of fusions catalyzed by a muon during its lifetime is ~ 150 in liquid D_2/T_2 , but ~ 1000 are needed to achieve energy breakeven¹³⁰² given the energy cost of artificial muon production.¹³⁰³ An artificial source of muons such as a “muon breeder” reactor might remove this constraint. Alternatively, another “free” (energy) muon source is the natural muonic background – more than 70% of the cosmic ray flux at Earth’s surface consists of positive and negative muons – but the cosmic-ray induced fusion rate is still impractically low, capable of inducing only $\sim 10^{17} \text{ MW/L}$ ($10^{26} \text{ W}/\mu\text{m}^3$) in liquid deuterium targets.¹³⁰⁴ The rate-limiting step in muon-catalyzed fusion is the formation of the muonic molecular ion which can take $\sim 0.01 \mu\text{sec}$ or more in liquid D_2 , DT , or T_2 . Effectively, each catalyzing muon spends most of its ephemeral existence searching for suitable deuterons and tritons with which to bind. The fusion reaction rate would be improved if the liquid hydrogen molecule target density could be significantly increased. It would also help if the muons had a longer lifetime. Aside from time dilation effects for relativistic particles, there are few good proposals for artificially extending the muon lifetime. One suggestion is to try to exploit the quantum Zeno effect¹³⁰⁵ for quantum-mechanical systems that can allow a particle’s time evolution to be arrested by measuring it frequently enough with respect to some chosen

¹²⁹⁹ Frank FC. Hypothetical alternative energy sources for the second meson events. *Nature* 1947 Oct 18;160(4068):525-527.

¹³⁰⁰ Alvarez LW, Bradner H, Crawford FS Jr., Crawford JA, Falk-Vairant P, Good ML, Gow JD, Rosenfeld AH, Solmitz F, Stevenson ML, Ticho HK, Tripp RD. Catalysis of nuclear reactions by μ mesons. *Phys Rev.* 1957 Feb 1;105(3):1127-1128; <https://escholarship.org/content/qt5pp2h0qp/qt5pp2h0qp.pdf>.

¹³⁰¹ Rafelski J, Jones SE. *Cold Nuclear Fusion*. *Scientific American* 1987 Jul;257(1):84-89; http://pages.erau.edu/~reynodb2/blog/Rafelski_Jones_ColdNuclearFusion.pdf. Jones SE, Anderson AN, Caffrey AJ, Walter JB, Watts KD, Bradbury JN, Gram PAM, Leon M, Maltrud HR, Paciotti MA. Experimental investigation of muon-catalyzed d-t fusion. *Phys Rev Lett.* 1983 Nov 7;51:1757-1760; <https://journals.aps.org/prl/abstract/10.1103/PhysRevLett.51.1757>. Jones SE. Muon-catalysed fusion revisited. *Nature* 1986 May 8;321(6066):127-133; <https://www.nature.com/articles/321127a0>.

¹³⁰² Eliezer S, Henis Z. Muon-catalyzed fusion – an energy production perspective. *Fusion Technology* 1994 Aug;26:46-73; <https://www.tandfonline.com/doi/abs/10.13182/FST94-A30300>.

¹³⁰³ The electrical energy cost of generating a muon using contemporary particle accelerators is $\sim 6 \text{ GeV}$; https://en.wikipedia.org/wiki/Muon-catalyzed_fusion#Problems_facing_practical_exploitation.

¹³⁰⁴ McCevoy AJ, O’Sullivan CTD. Cold fusion: what’s going on? *Nature* 1989 Apr 27;338(6218):711-712; https://inis.iaea.org/search/search.aspx?orig_q=RN:20070595.

¹³⁰⁵ https://en.wikipedia.org/wiki/Quantum_Zeno_effect.

measurement setting.¹³⁰⁶ More generally, the quantum Zeno effect is the suppression of unitary time evolution in quantum systems provided by a variety of sources (measurement, interactions with the environment, or stochastic fields, among other factors),¹³⁰⁷ and applying a series of sufficiently strong and fast pulses with appropriate symmetry can decouple a system from its decohering environment.¹³⁰⁸

Helium Capture. Second, the muon may be quickly captured by a helium nucleus formed in the fusion reaction.¹³⁰⁹ This “alpha-sticking problem,”¹³¹⁰ which is the ~0.4% probability¹³¹¹ of the muon sticking to an alpha particle created during D-T fusion, forming singly-ionized muonic helium until the muon decays, effectively removes the muon from the muon-catalysis process altogether. The sticking probability is about 10-fold higher for D-D fusion, giving a 10-fold lower reaction rate for muon-catalyzed D-D fusion than for D-T fusion.¹³¹² One suggestion by Andrew Reid for eliminating the sticking problem¹³¹³ – to “make your reaction vessel a conducting superlattice where the photon emitted by the muon when it transitions to the stuck state is forbidden, then you can eliminate sticking” – would be technically challenging.

Tauon-catalyzed fusion. In 1975 an even heavier negatively-charged lepton was discovered, the tauon.¹³¹⁴ The internuclear tunneling distance for a hypothetical tauonic deuterium molecule ($m_{\text{tauon}} \sim 3500 m_e$) is only $\sim 10^{-14}$ m, which should catalyze fusion almost instantaneously. Unfortunately the tauon is even shorter-lived (2.2×10^{-13} sec) than the muon, a lifetime much closer to the typical nuclear reaction time range of 10^{-13} - 10^{-21} sec. A tauon traveling at 10%c would disintegrate after traveling only ~ 7 μm , placing severe constraints on any particle generator and target geometry that was intended to attempt tauon-catalyzed fusion.

¹³⁰⁶ Sudarshan ECG, Misra B. The Zeno’s paradox in quantum theory. *J Math Phys.* 1977;18(4):756-763; <http://repository.ias.ac.in/51139/1/211-pub.pdf>.

¹³⁰⁷ Nakanishi T, Yamane K, Kitano M. Absorption-free optical control of spin systems: the quantum Zeno effect in optical pumping. *Phys Rev A.* 2001;65(1):013404; <https://core.ac.uk/download/pdf/39176091.pdf>.

¹³⁰⁸ Facchi P, Lidar DA, Pascazio S. Unification of dynamical decoupling and the quantum Zeno effect. *Phys Rev A.* 2004;69(3):032314; <http://www.chem.utoronto.ca/staff/dlidar/PRA69.032314.2004.pdf>.

¹³⁰⁹ Zweig G. Quark catalysis of exothermal nuclear reactions. *Science* 1978 Sep 15;201(4360):973-979; <http://science.sciencemag.org/content/201/4360/973.full.pdf>.

¹³¹⁰ Jackson JD. Catalysis of nuclear reactions between hydrogen isotopes by μ^- mesons. *Phys Rev.* 1957 Apr 15;106(2):330-339; <https://journals.aps.org/pr/abstract/10.1103/PhysRev.106.330>.

¹³¹¹ Rafelski J, Jones SE. Cold nuclear fusion. *Sci Am.* 1987 Jul;257(1):84-89; http://pages.erau.edu/~reynodb2/blog/Rafelski_Jones_ColdNuclearFusion.pdf.

¹³¹² [https://en.wikipedia.org/wiki/Muon-catalyzed_fusion#Deuterium-deuterium_\(d-d_or_dd\)_and_other_types](https://en.wikipedia.org/wiki/Muon-catalyzed_fusion#Deuterium-deuterium_(d-d_or_dd)_and_other_types).

¹³¹³ John Baez, “Light hydrogen,” 11 Oct 2015; comment by Andrew Reid, 27 Sep 2016; <https://plus.google.com/+johncbaz999/posts/L7mcLBJuEAp>.

¹³¹⁴ [https://en.wikipedia.org/wiki/Tau_\(particle\)](https://en.wikipedia.org/wiki/Tau_(particle)).

Other fusion catalysts. It is possible that some other particles might also be able to catalyze fusion. For example, George Zweig of the California Institute of Technology has suggested that free quarks (if they are ever found) could catalyze fusion reactions.¹³¹⁵ It might also be possible to induce antimuon-catalyzed fusion in atoms of antihydrogen having an antiproton (p^-) nucleus by replacing the orbital positron (e^+) with an antimuon (μ^+), though the antimuon decay time is still only 2.2 μsec .¹³¹⁶

Small amounts of antimatter (e.g., antiprotons) can initiate fission or fusion in large masses of suitable materials made of regular matter.¹³¹⁷ For example, when an antiproton annihilates in a uranium or plutonium nucleus, the nucleus fissions almost 100% of the time;¹³¹⁸ ~20% of the fission energy is in the fission fragments, and more than a dozen neutrons are emitted which can produce additional fissions. Similarly, numerous authors have proposed using the annihilation of antiprotons or antihydrogen to directly initiate fusion reactions for spacecraft propulsion.¹³¹⁹ Since the antiprotons used to start these reactions are consumed, they cannot properly be considered a catalyst.¹³²⁰

¹³¹⁵ Rafelski J, Jones SE. Cold nuclear fusion. *Sci Am.* 1987 Jul;257(1):84-89;
http://pages.erau.edu/~reynodb2/blog/Rafelski_Jones_ColdNuclearFusion.pdf.

¹³¹⁶ https://en.wikipedia.org/wiki/Muon#Muon_decay.

¹³¹⁷ Cassenti BN, Kammash T, Galbraith DL. Antiproton catalyzed fusion propulsion for interplanetary missions. *J Propulsion and Power* 1997;13(3):428-434;
<http://citeseerx.ist.psu.edu/viewdoc/download?doi=10.1.1.875.8344&rep=rep1&type=pdf>. Smith GA, Kramer KJ, Meyer KJ. Antimatter-initiated microfission/fusion. Space Manufacturing Conference; <https://space.nss.org/media/Space-Manufacturing-conference-13-069-Antimatter-Initiated-Microfission-Fusion.pdf>.

¹³¹⁸ Morgan DL. Annihilation of Antiprotons in Heavy Nuclei. Air Force Rocket Propulsion Laboratory, AFRPL TR 86-011, Edwards Air Force Base, Oct 1986.

¹³¹⁹ Forward RL. Antiproton annihilation propulsion. *J Propulsion and Power.* 1985;1(5):370-374;
<http://www.dtic.mil/get-tr-doc/pdf?AD=ADA160734>. Cassenti BN. Conceptual Designs for Anti-proton Space Propulsion Systems. *J Propulsion and Power.* 1991;7(3):368-373;
<https://arc.aiaa.org/doi/abs/10.2514/6.1989-2333>. Kammash T, Galbraith DL. Antimatter-Driven-Fusion Propulsion for Solar System Exploration. *J Propulsion and Power.* 1992;8(3):644-649;
<https://deepblue.lib.umich.edu/bitstream/handle/2027.42/76531/AIAA-23527-891.pdf;sequence=1>.

¹³²⁰ https://en.wikipedia.org/wiki/Antimatter-catalyzed_nuclear_pulse_propulsion.

7.3.3 Low-Temperature Nuclear Fusion Reactions

Mechanical pressure, laser pressure, electric fields and electric currents can cause fusion reactions to occur at relatively low temperatures (e.g., 100-1000 K). For example:

Mechanical Pressure. It has been suggested that very high pressures could induce fusion.¹³²¹ One experiment in which Pd and Ti immersed in liquid D₂O were bombarded with intense ultrasound apparently produced above-background levels of ⁴He, an expected end product of D-D fusion processes.¹³²²

Femtosecond Laser Pressure. A 2017 paper¹³²³ describes a basic proof-of-principle simulation that shows how, in two dimensions, a 5-femtosecond, near-infrared shaped laser pulse could push an electron-stripped molecule of deuterium and tritium, its nuclei already poised at a much smaller internuclear distance than in a plasma, nearly close enough to fuse. Higher-energy vacuum ultraviolet shaped laser pulses might improve muon-catalyzed fusion (**Section 7.3.2**) enough to achieve breakeven energy generation. In effect, this method could allow a single molecule controlled by a laser pulse to be turned into a nuclear accelerator.

Fracture Deformation. Fracto-fusion¹³²⁴ experiments have detected neutron emission when a crystal of lithium deuteride or heavy ice is mechanically fractured, believed to be the consequence of deuteron acceleration by >10 KeV electric fields generated by a propagating crack in the crystal, consistent with D-D fusion.¹³²⁵ Heating, cooling, or fracturing metal

¹³²¹ Van Siclen CD, Jones SE. Piezonuclear fusion in isotopic hydrogen molecules. *J Phys G*. 1986 Mar;12(3):213-221; <http://iopscience.iop.org/article/10.1088/0305-4616/12/3/009/meta>. Moss WC, Clarke DB, White JW, Young DA. Sonoluminescence and the prospects for table-top micro-thermonuclear fusion. *Phys Lett A*. 1996 Feb 5;211:69-74; <https://pdfs.semanticscholar.org/d637/dbfbde2085d49f573d5507542b7c38dda9f7.pdf>.

¹³²² Stringham R, George R. Cavitation induced solid state production of heat, He³, and He⁴. 209th American Chemical Society (ACS) National Meeting, 2-6 April 1995, Anaheim CA, Book of Abstracts, No. NUCL-044.

¹³²³ Berrios E, Gruebele M, Wolynes PG. Quantum controlled fusion. *Chem Phys Lett*. 2017 Sep 1;683:216-221; <http://repositorio.uchile.cl/bitstream/handle/2250/147731/Quantum-controlled-fusion.pdf?sequence=1>.

¹³²⁴ Tekeda T, Takizuka T. Fractofusion mechanism. *J Phys Soc Japan* 1989 Sep;58:3073-3076; <https://journals.jps.jp/doi/abs/10.1143/JPSJ.58.3073>.

¹³²⁵ Klyuev VA, Lipson AG, Toporov YP, Deryagin BV, Lushchikov VJ, Streikov AV, Shabalin EP. High-energy processes accompanying the fracture of solids. *Sov Tech Phys Lett*. 1986;12:551-552. Golubnichii PI, Kurakin VA, Filonenko AD, Tsarev VA, Tsarik AA. A possible mechanism for cold nuclear fusion. *Sov Phys Dokl*. 1989 Jul;34:628-629. Preparata G. A new look at solid-state fractures, particle emission and cold nuclear fusion. *Il Nuovo Cimento* 1991 Aug;104A(8):1259-1263; <https://link.springer.com/article/10.1007/BF02784502>.

specimens exposed to high-pressure D₂ (e.g., deuterated titanium) frequently produces statistically significant bursts of neutrons and emission of charged particles, RF signals and photons. It is proposed that crack growth results in charge separation on the newly formed crack surfaces, accelerating D⁺ ions in the electric field across the crack tip up to energies >10 KeV which is sufficient to significantly raise the D-D fusion probability.¹³²⁶ Neutrons are reportedly generated when fragments of titanium are crushed with steel balls in a bath of heavy water.¹³²⁷ It has also been speculated that the core of the spherical acoustic shock wave generated during sonoluminescence, if it remains stable to a 10-nm radius, might reach temperatures appropriate to fusion $\geq 10^6$ K.¹³²⁸

Electric Fields. Claytor *et al* at Los Alamos National Laboratory passed a current of 2.5 amperes at 2000 volts through 200-micron diameter palladium wires in a glow discharge tube of D₂ gas at 0.3 atm for ~100 hours apparently producing ~10 nanocuries of tritium, with great care being taken to eliminate possible sources of contamination.¹³²⁹ Deuterium-saturated LiTaO₃ crystals in a 75 KV/cm AC field exhibit elevated neutron emission that have been attributed to D-D fusion.¹³³⁰ Wires of LiD exploded by high current pulses also emit fusion neutrons.¹³³¹ In another experiment, a team at UCLA used a pyroelectric crystal heated from -34 to 7 °C and a tungsten needle to produce an electric field of about 25 GV/m to ionize and accelerate deuterium nuclei into an erbium deuteride target. The D-D fusion reaction may occur at the estimated

¹³²⁶ Dickinson JT, Jensen LC, Langford SC, Ryan RR, Garcia E. Fracto-emission from deuterated titanium: Supporting evidence for a fracto-fusion mechanism. *J Materials Res.* 1990 Jan;5(1):109-122; <https://www.cambridge.org/core/journals/journal-of-materials-research/article/fractoemission-from-deuterated-titanium-supporting-evidence-for-a-fractofusion-mechanism/73B4C906F0F759E7C67CC31D5DA19196>.

¹³²⁷ Derjaguin BV, Lipson AG, Kluev VA, Sakov DM, Toporov YP. Titanium fracture yields neutrons? *Nature* 1989 Oct;341(6242):492; <http://adsabs.harvard.edu/abs/1989Natur.341Q.492D>.

¹³²⁸ Moss WC, Clarke DB, White JW, Young DA. Sonoluminescence and the prospects for table-top micro-thermonuclear fusion. *Phys Lett A.* 1996 Feb 5;211:69-74; <https://pdfs.semanticscholar.org/d637/dbfbde2085d49f573d5507542b7c38dda9f7.pdf>. Moss WC, Clarke DB, Young DA. Calculated pulse widths and spectra of a single sonoluminescing bubble. *Science* 1997 May 30;276:1398-1401, 1348-1349; <https://pdfs.semanticscholar.org/391d/9b8f88f67d09a3c264b059c2e25918a70518.pdf>.

¹³²⁹ Claytor TN, Jackson DD, Tuggle DG. Tritium production from a low voltage deuterium discharge on palladium and other metals. LAUR#95-2687, 1995; <https://web.archive.org/web/20060716074727/http://nde.lanl.gov/cf/tritweb.htm>. See also: Kohn GK. Letters. *Science* 1996 Oct 25;274:481.

¹³³⁰ Jabon VDD, Fedorovich GV, Samsonenko NV. Catalytically induced D-D fusion in ferroelectrics. *Brazilian J Phys.* 1997 Dec;27(4):515-521; http://www.sbfisica.org.br/bjp/files/v27_515.pdf.

¹³³¹ Lochte-Holtgreven W. Research on nuclear reactions in exploding (Li + LiD) wires. *Z. Naturforsch.* 1987;42a:538-542; http://zfn.mpg.de/data/Reihe_A/42/ZNA-1987-42a-0538.pdf.

energy levels,¹³³² producing helium-3 and a 2.45 MeV neutron, though the apparatus was not intended for power generation since it consumes far more energy than it produces.¹³³³

Mechanical Pressure plus Electric Current. Most controversial is the speculative possibility of metallic deuteride catalyzed fusion at temperatures between 300-1100 K,¹³³⁴ first reported (then later partially retracted!) in the years 1926-27.¹³³⁵ Positive results are reported for a comprehensive series of experiments conducted at SRI International for the Electric Power Research Institute (EPRI) during 1989-94,¹³³⁶ and for another comprehensive series of experiments conducted by the U.S. Naval Air Warfare Center at China Lake during 1989-96,¹³³⁷ and U.S. patents have been issued for such devices.¹³³⁸ In another class of experiments,¹³³⁹ a hydrogenophilic metal such as palladium is loaded with deuterium at effective pressures of 10-100 atm, giving molecular loadings of D/Pd = 90%-95%. Palladium deuteride normally exists

¹³³² Naranjo B, Gimzewski JK, Putterman S. Observation of nuclear fusion driven by a pyroelectric crystal. *Nature* 2005;434(7037):1115-1117, supplementary materials; <http://www.nature.com/nature/journal/v434/n7037/supinfo/nature03575.html>.

¹³³³ Schewe P, Stein B. Pyrofusion: a room-temperature, palm-sized nuclear fusion device. *Physics News Update* 2005;729(1); <https://web.archive.org/web/20131112155702/http://www.aip.org/pnu/2005/split/729-1.html>.

¹³³⁴ Fleischmann M, Pons S, Hawkins M. Electrochemically induced nuclear fusion of deuterium. *J Electroanalytical Chem.* 1989;261:301-308; <http://citeseerx.ist.psu.edu/viewdoc/download?doi=10.1.1.380.7906&rep=rep1&type=pdf>. Fleischmann M, Pons S. Calorimetry of the Pd-D₂O system: From simplicity via complications to simplicity. *Phys Lett A* 1993;176:118-129; <https://www.lenr-canr.org/acrobat/Fleischmancalorimetra.pdf>. Miles MH, Bush BF, Stilwell DE. Calorimetric principles and problems in measurements of excess power during Pd-D₂O electrolysis. *J Phys Chem.* 1994 Feb;98(7):1948-1952; <https://pubs.acs.org/doi/abs/10.1021/j100058a038>. Arata Y, Zhang Y-C. Solid-state plasma fusion. *J Japan High-Temp Society* 1997 Jan;23:entire issue. Arata Y, Zhang Y-C. Deuterium nuclear reaction process within solid. *Proc Japan Acad.* 1996 Nov;72B(9):179-184; https://www.jstage.jst.go.jp/article/pjab1977/72/9/72_9_179/pdf.

¹³³⁵ "Fusion in 1926: plus ca change," *Nature* 1989 Apr 27;338:706.

¹³³⁶ McKubre MCH, *et al.* Isothermal flow calorimetric investigations of the D/Pd and H/Pd systems. *J Electroanalytical Chem.* 1994;386:55-66; <http://www.academia.edu/download/42552843/McKubreMCHisothermal.pdf>. McKubre MCH, *et al.* Development of Advanced Concepts for Nuclear Processes in Deuterated Metals. EPRI TR-104195, Research Project 3170-01, Final Report, August 1994.

¹³³⁷ Miles MH, Bush BF, Johnson KB. Anomalous effects in deuterated systems. Research and Technology Division, U.S. Naval Air Warfare Center Weapons Division (China Lake, CA 93555-6100), Report NAWCWPN TP 8302, Sep 1996, 98 pp; <https://apps.dtic.mil/dtic/tr/fulltext/u2/a315020.pdf>.

¹³³⁸ Patterson JA, Cravens D. System for electrolysis. U.S. Patent 5,607,563, 4 Mar 1997; <https://patents.google.com/patent/US5607563A>.

¹³³⁹ Edmund Storms, personal communication with Robert Freitas, 1996.

either as Pd₂D or PdD, but it is believed that the highest loadings¹³⁴⁰ may give rise to significant concentrations of PdD_x (x = 1-2), asserted to be the “nuclear active phase.” Superstoichiometric palladium hydride (x = 1.33) at ~50,000 atm has been observed experimentally in X-ray diffraction studies,¹³⁴¹ although preliminary molecular simulation studies of deuterium-entrained metal lattices had given pessimistic results.¹³⁴²

Upon applying a current of ~1 nanoamp/μm² at ~1-10 volts to a pressurized superstoichiometric metallic deuteride, significant heat energy in excess of the electrical input is said to be developed as the deuterium is consumed, on the order of **0.001-1 MW/L**. ⁴He is claimed to be produced at the expected rate of ~10¹¹ ⁴He atoms/sec-watt,¹³⁴³ with neutrons, tritons (tritium nuclei), γ-rays and X-rays missing or detected in amounts far too small to account for the excess energy, which is asserted to be evidence of a catalyzed D-D aneutronic process at work. If the results of these and related experiments¹³⁴⁴ were confirmed, it might become possible to use diamondoid pistons to maintain continuously high deuterium loadings in an active catalytic crystal and thus to develop 1-1000 pW of aneutronic thermal energy in a precisely nanomanufactured porous 1 μm³ metal-deuteride reactor with ⁴He (23.85 MeV) as the principal (and benign) effluent, achieving energy storage densities >10⁷ MJ/L that would allow a completely self-contained >10 year fuel

¹³⁴⁰ De Ninno A, La Barbera A, Violante V. Deformations induced by high loading ratios in palladium-deuterium compounds. J Alloys and Compounds 1997 May 20;253-254:181-184; https://s3.amazonaws.com/academia.edu.documents/32132168/1997_AURELIO-Journal_of_Alloys_and_Compound_253-254_%281997%29_181-184.pdf?AWSAccessKeyId=AKIAIWOWYYGZ2Y53UL3A&Expires=1546174328&Signature=Ni2YIKI6pTnsQOvIHg0fpO4LvwU%3D&response-content-disposition=inline%3B%20filename%3DDeformations_induced_by_high_loading_rat.pdf. Asami N, Senjuh T, Kamimura H, Sumi M, Kennel E, Sakai T, Mori K, Watanabe H, Matsui K. Material characteristics and behavior of highly deuterium loaded palladium by electrolysis. J Alloys and Compounds 1997 May 20;253-254:185-190; <https://www.sciencedirect.com/science/article/abs/pii/S0925838896030691>. Senjuh T, Kamimura H, Uehara T, Sumi M, Miyasita S, Sigemitsu T, Asami N. Experimental Study of Electrochemical Deuterium Loading of Pd Cathodes in the LiOD/D₂O System. J Alloys and Compounds 1997 May 20;253-254:617-620; <https://www.sciencedirect.com/science/article/abs/pii/S0925838896030757>.

¹³⁴¹ Fukai Y, Okuma N. Formation of superabundant vacancies in Pd hydride under high hydrogen pressures. Phys Rev Lett. 1994 Sep 19;73(12):1640-1643; <https://journals.aps.org/prl/abstract/10.1103/PhysRevLett.73.1640>.

¹³⁴² White CT, Brenner DW, Mowrey RC, Mintmire JW, Schmidt PP, Dunlap BI. D-D (H-H) interactions within the interstices of Pd. Jap J Appl Phys. 1991 Jan;30(1.1):182-189; <http://iopscience.iop.org/article/10.1143/JJAP.30.182/meta>.

¹³⁴³ Miles MH, Bush BF, Johnson KB. Anomalous effects in deuterated systems. Research and Technology Division, U.S. Naval Air Warfare Center Weapons Division (China Lake, CA 93555-6100), Report NAWCWPNS TP 8302, Sep 1996, 98 pp; <https://apps.dtic.mil/dtic/tr/fulltext/u2/a315020.pdf>.

¹³⁴⁴ <https://lenr-canr.org/>.

supply to be carried aboard a 10 pW medical nanorobot¹³⁴⁵ in a $\sim 1 \mu\text{m}^3$ fuel tank (assuming thermal energy can be efficiently harnessed in microscale systems).

¹³⁴⁵ Freitas RA Jr. Nanomedicine, Volume I: Basic Capabilities, Landes Bioscience, Georgetown TX, 1999, Section 6.3.7.3, "Exothermal Nuclear Catalysis"; <http://www.nanomedicine.com/NMI/6.3.7.3.htm#p12>.

7.4 Metastable Nuclear Isomers

A metastable nuclear isomer¹³⁴⁶ is a metastable state of an atomic nucleus caused by the excitation of one or more of its nucleons (protons or neutrons). The nucleus of a nuclear isomer occupies a higher energy state than the non-excited nucleus at ground state, analogous to the excited states of electrons in atoms (**Section 4.4.1**). When excited atomic states decay, energy is released by fluorescence with the emission of light near the visible range, often in the 3-30 eV range. When excited nuclear states decay, energy is usually released by the emission of gamma rays, typically in the 30,000-3,000,000 eV range.

There are more than 2460 known nuclear isomers¹³⁴⁷ with a lower limit on half-life of ~10 nanosec and an upper limit on isomeric decay energy of ~13 MeV.¹³⁴⁸ **Table 56** is a list of known metastable nuclear isomers¹³⁴⁹ that decay at least 1% of the time by isomeric transition (IT) into the parent isotope (ignoring other decay routes such as β -decay, EC-decay, etc.) and with a half-life of at least ~1 day (to allow an isomer-based storage mechanism to have a reasonably useful shelf life). The simplest isomeric energy storage system would employ an isomer with close to 100% IT decay, yielding almost exclusively gamma ray photons as the energetic output product.

Figure 10 (Chapter 9) provides a chart that summarizes power density vs. specific power for nuclear isomers.

¹³⁴⁶ https://en.wikipedia.org/wiki/Nuclear_isomer.

¹³⁴⁷ A different kind of metastable nuclear state is the “fission isomer” or “shape isomer” (https://en.wikipedia.org/wiki/Nuclear_isomer#Metastable_isomers). Most actinide nuclei in their ground states are not spherical, but rather prolate spheroidal, a geometry that can result in quantum-mechanical states where the distribution of protons and neutrons is so much further from spherical geometry that de-excitation to the nuclear ground state is strongly hindered. However, these states usually de-excite to the ground state or they undergo spontaneous fission with half-lives <0.1 sec (<https://www.nucleonica.com/Application/KNC/FissionShapeIsomers.pdf>).

¹³⁴⁸ <https://inis.iaea.org/collection/NCLCollectionStore/Public/47/104/47104610.pdf>. See also: Juraj Tolgyessy, Erno Bujdoso, CRC Handbook of Radioanalytical Chemistry, Volume II, CRC Press, 1991; <https://www.amazon.com/CRC-Handbook-Radioanalytical-Chemistry-II/dp/0849335140>.

¹³⁴⁹ https://en.wikipedia.org/wiki/Isotopes_of_hafnium, etc.

Table 56. Energy density of nuclear isomers that decay via isomeric transition to the parent nuclide with a half-life exceeding ~1 day

Nuclear Isomer	% IT Decay to Parent	Half-life (sec)	Decay Energy (KeV)	Specific Energy (MJ/kg)	Energy Density (MJ/L)	Specific Power (MW/kg)	Power Density (MW/L)
^{93m} Mo ₄₂	99.98%	2.47 x 10 ⁴	2424.89	2,515,772	25,862,138	102.018	1048.748
^{178m2} Hf ₇₂	~100%	9.78 x 10 ⁸	2445.69	1,325,695	17,645,001	0.001	0.018
^{179m2} Hf ₇₂	~100% ?	2.16 x 10 ⁶	1105.84	599,425	7,978,340	0.277	3.686
^{44m2} Sc ₂₁	98.8%	2.11 x 10 ⁵	270.95	594,154	1,773,548	2.816	8.406
^{177m3} Lu ₇₁	21.7%	1.39 x 10 ⁷	970.175	528,858	5,204,491	0.038	0.376
^{198m2} Au ₇₉	100%	1.96 x 10 ⁵	811.7	395,542	7,633,960	2.017	38.923
^{117m1} Sn ₅₀	100%	1.19 x 10 ⁶	314.58	259,422	1,884,704	0.218	1.585
^{95m} Nb ₄₁	94.4%	3.12 x 10 ⁵	235.69	239,376	2,051,448	0.767	6.577
^{121m} Te ₅₂	88.6%	1.33 x 10 ⁷	293.991	234,429	1,462,835	0.018	0.110
^{123m} Te ₅₂	100%	1.03 x 10 ⁷	247.47	194,124	1,211,335	0.019	0.118
^{194m2} Ir ₇₇	?	1.48 x 10 ⁷	370	184,019	4,151,464	0.012	0.281
^{129m} Xe ₅₄	100%	7.67 x 10 ⁵	236.14	176,621	519,619	0.230	0.677
^{133m} Xe ₅₄	100%	1.89 x 10 ⁵	233.221	169,191	497,761	0.894	2.631
^{114m1} In ₄₉	96.75%	4.28 x 10 ⁶	190.29	161,055	1,177,310	0.038	0.275
^{101m} Rh ₄₅	6.4%	3.75 x 10 ⁵	157.32	150,288	1,865,076	0.401	4.974
^{197m} Hg ₈₀	91.4%	8.57 x 10 ⁴	298.93	146,408	1,981,489	1.709	23.127
^{131m} Te ₅₂	22.2%	1.08 x 10 ⁵	182.25	134,233	837,612	1.243	7.756
^{195m} Pt ₇₈	100%	3.46 x 10 ⁵	259.3	128,301	2,752,057	0.370	7.943
^{131m} Xe ₅₄	100%	1.03 x 10 ⁶	163.93	120,739	355,216	0.117	0.345
^{125m} Te ₅₂	100%	4.96 x 10 ⁶	144.772	111,747	697,303	0.023	0.141
^{91m1} Nb ₄₁	93%	5.26 x 10 ⁶	104.6	110,905	950,459	0.021	0.181
^{110m2} Ag ₄₇	1.36%	2.16 x 10 ⁷	117.59	103,143	1,081,970	0.005	0.050
^{184m} Re ₇₅	75.4%	1.46 x 10 ⁷	188.01	98,588	2,072,326	0.007	0.142
^{108m} Ag ₄₇	8.96%	1.32 x 10 ¹⁰	109.44	97,772	1,025,628	7.4 x 10 ⁻⁶	7.8 x 10 ⁻⁵
^{97m} Tc ₄₃	99.66%	7.86 x 10 ⁶	96.56	96,048	1,056,527	0.012	0.134
^{174m1} Lu ₇₁	99.38%	1.23 x 10 ⁷	170.83	94,728	932,216	0.008	0.076
^{148m} Pm ₆₁	5%	3.57 x 10 ⁶	137.9	89,901	652,682	0.025	0.183
^{195m} Hg ₈₀	54.2%	1.50 x 10 ⁵	176.07	87,119	1,179,069	0.582	7.873
^{192m2} Ir ₇₇	?	7.61 x 10 ⁹	168.14	84,495	1,906,212	1.1 x 10 ⁻⁵	2.5 x 10 ⁻⁴
^{129m} Te ₅₂	~100% ?	2.90 x 10 ⁶	105.5	78,909	492,390	0.027	0.170
^{186m} Re ₇₅	90%	6.31 x 10 ¹²	149	77,292	1,624,682	1.2 x 10 ⁻⁸	2.6 x 10 ⁻⁷
^{193m} Pt ₇₈	100%	3.74 x 10 ⁵	149.78	74,879	1,606,150	0.200	4.293
^{119m1} Sn ₅₀	100%	2.53 x 10 ⁷	89.531	72,592	527,381	0.003	0.021
^{127m} Te ₅₂	97.6%	9.42 x 10 ⁶	88.26	67,054	418,415	0.007	0.044
^{180m1} Ta ₇₃	?	1.42 x 10 ²⁴	75.3	40,363	673,660	2.8 x 10 ⁻²⁰	4.7 x 10 ⁻¹⁹
^{193m} Ir ₇₇	100%	9.10 x 10 ⁵	80.24	40,114	904,972	0.044	0.995
^{95m} Tc ₄₃	3.88%	5.27 x 10 ⁶	38.89	39,498	434,479	0.007	0.082
^{156m1} Tb ₆₅	100%	8.78 x 10 ⁴	54	33,399	274,872	0.380	3.129
^{93m} Nb ₄₁	100%	5.09 x 10 ⁸	30.77	31,923	273,582	6.3 x 10 ⁻⁵	0.001
^{242m1} Am ₉₅	99.54%	4.45 x 10 ⁹	48.6	19,377	232,522	4.4 x 10 ⁻⁶	5.2 x 10 ⁻⁵
^{121m1} Sn ₅₀	77.6%	1.39 x 10 ⁹	6.3	5,024	36,497	3.6 x 10 ⁻⁶	2.6 x 10 ⁻⁵
^{229m} Th ₉₀	100%	2.52 x 10 ⁵	0.0076	3	35	0.002	0.019

Table 56 shows that the natural power density remains relatively low despite high energy densities for most nuclear isomers. To be useful for energy storage and supply, it would be necessary to trigger the fast release of the stored isomeric energy, ideally using a relatively small energy input,¹³⁵⁰ greatly boosting the available power density of the isomeric nuclear fuel.

Tantalum. The only natural nuclear isomer is $^{180m1}\text{Ta}_{73}$, present in all tantalum samples at about 1 part in 8300, with an estimated half-life of 4.5×10^{16} years. If $^{180m1}\text{Ta}_{73}$ were to relax via isomeric transition to its ground state of $^{180}\text{Ta}_{73}$, it would release a photon with an energy of 77.1 KeV.¹³⁵¹ In 1988 it was first reported that $^{180m1}\text{Ta}_{73}$ could be forced to release its energy by irradiation with bremsstrahlung X-rays from a linear accelerator with an end-point energy of ~6000 KeV;¹³⁵² the same group reported a trigger energy as low as 2800 KeV by 1990,¹³⁵³ and by 2002 the onset of the de-excitation of ^{180m}Ta via resonant photo-excitation had been observed at an end-point energy of only ~1020 KeV.¹³⁵⁴ In all cases to date, the “trigger” energy input is much larger than the isomeric transition energy output of ~77 KeV – in other words, the energy-triggering process does not achieve energy breakeven.

Hafnium. A nuclear isomer with a lower trigger energy or a higher decay energy – or both – might provide the desired net positive energy output. Most strikingly, $^{178m2}\text{Hf}_{72}$ possesses the unusual combination of a very high decay energy (~2446 KeV), a very high specific energy of

¹³⁵⁰ Collins CB, Lee FW, Shemwell DM, DePaola BD, Olariu S, Popescu II. The coherent and incoherent pumping of a gamma laser with intense optical radiation. *J Appl Phys.* 1982;53:4645; <https://aip.scitation.org/doi/abs/10.1063/1.331291>.

¹³⁵¹ This low excitation energy allows gamma de-excitation to the ^{180}Ta ground state, which itself is radioactive with an 8-hour half-life by β -decay to $^{180}\text{Hf}_{72}$ (86%) or $^{180}\text{W}_{74}$ (14%).

¹³⁵² Collins CB, Eberhard CD, Glesener JW, Anderson JA. Depopulation of the isomeric state $^{180}\text{Ta}^m$ by the reaction $^{180}\text{Ta}^m(\gamma, \gamma')^{180}\text{Ta}$. *Phys Rev C* 1988;37(5):2267-2269; <http://www.hafniumisomer.org/isomer/180ta.pdf>.

¹³⁵³ Collins CB, Carroll JJ, Sinor TW, Byrd MJ, Richmond DG, Taylor KN, Huber M, Huxel N, von Neumann-Cosel P, Richter A, Spieler C, Ziegler W. Resonant excitation of the reaction $^{180}\text{Ta}^m(\gamma, \gamma')^{180}\text{Ta}$. *Phys Rev C.* 1990 Nov;42(5):R1813-R1816; https://www.researchgate.net/profile/Peter_Von_Neumann-Cosel2/publication/255052531_Resonant_excitation_of_the_reaction_sup_180_Ta_sup_m_gamma_gamm_a_prime_sup_180_Ta/links/0c960530677bbbefa4000000.pdf.

¹³⁵⁴ Belic D, Arlandini C, Besserer J, de Boer J, Carroll JJ, Enders J, Hartmann T, Käppeler F, Kaiser H, Kneissl U, Kolbe E, Langanke K, Loewe M, Maier HJ, Maser H, Mohr P, von Neumann-Cosel P, Nord A, Pitz HH, Richter A, Schumann M, Thielemann FK, Volz S, Zilges A. Photo-induced depopulation of the $^{180}\text{Ta}^m$ isomer via low-lying intermediate states: Structure and astrophysical implications. *Phys Rev C* 2002;65:035801; https://www.researchgate.net/profile/Peter_Von_Neumann-Cosel2/publication/235522230_Photo-induced_depopulation_of_the180_Tam_isomer_via_low-lying_intermediate_states_Structure_and_astrophysical_implications/links/0c96051d2ea8a9e648000000.pdf.

~**10⁶ MJ/kg**, and a very long half-life of ~31 years (leading to the claim that the energy-rich isomer can be “safely” stored¹³⁵⁵ for long periods of time).

Military people have taken notice that a stable material with a triggerable energy density of 18 GJ/cm³ might make an excellent explosive munition.¹³⁵⁶ In 1999, a DARPA-supported group at the University of Texas at Dallas claimed¹³⁵⁷ to have triggered complete isomeric energy release from ^{178m2}Hf₇₂ using only soft X-rays generated by a dental X-ray machine via resonant absorption of bremsstrahlung photons: “We have demonstrated that the resonant absorption of an X-ray photon with the energy of the order of 40 KeV can induce the prompt release of the 2446 KeV stored by the isomer into freely radiating states....an energy gain of about 60.” The 2446 KeV energy release seemed to have occurred in ~4 sec, which would give an apparent transient specific power of **331,000 MW/kg** and power density of **4.4 x 10⁶ MW/L**. Unfortunately, some attempts to replicate these results by other research groups have been unsuccessful¹³⁵⁸ and the work remains controversial,¹³⁵⁹ most recently with one Ukrainian group claiming success in

¹³⁵⁵ A device containing large amounts of ^{178m2}Hf₇₂ “would pose an extreme radiation hazard. Radiation is inverse to half-life, and the hafnium isomer, with a 31-year half-life, is vastly more radioactive than U-235 (700 million years) or Pu-239 (24,000 years). Further, hafnium isomer decays emit gamma rays, which are the most penetrating form of ionizing nuclear radiation and the most difficult against which to shield. The shielding required to protect humans in the vicinity of a tangible quantity of hafnium isomer would more than negate its small mass and compact size.” John Walker, “Reading List: Imaginary Weapons,” Fourmilab Change Log, 26 Jun 2006; <https://www.fourmilab.ch/fourmilog/archives/2006-06/000715.html>.

¹³⁵⁶ In May 2003 a Hafnium Isomer Production Panel (HIPP) was assembled to draw up plans for bulk production of the substance, with visions of 2-kiloton nuclear hand grenades and clean bunker-busting fusion bombs to be funded by DARPA, who envisioned a two-year budget of \$30 million for the project. <https://www.fourmilab.ch/fourmilog/archives/2006-06/000715.html>. See also: https://en.wikipedia.org/wiki/Hafnium_controversy.

¹³⁵⁷ Collins CB, Davanloo F, Iosif MC, Dussart R, Hicks JM, Karamian SA, Ur CA, Popescu II, Kirischuk VI, Carroll JJ, Roberts HE, McDaniel P, Crist CE. Accelerated emission of gamma rays from the 31-yr isomer of ¹⁷⁸Hf induced by X-ray irradiation. *Phys Rev Lett*. 1999 Jan 25;82(4):695-698; <http://www.hafniumisomer.org/isomer/PRL00695.pdf>.

¹³⁵⁸ Ahmad I, *et al*. Search for X-ray induced decay of the 31-yr isomer of ¹⁷⁸Hf using synchrotron radiation. Lawrence Livermore National laboratory, UCRL-TR-206598, 16 Sep 2004; <https://e-reports-ext.llnl.gov/pdf/311645.pdf>. See also: Bertram Schwarzschild, “Conflicting Results on a Long-Lived Nuclear Isomer of Hafnium Have Wider Implications,” *PhysicsToday.org*, 2 Jun 2004; <https://web.archive.org/web/20040602192614/http://www.physicstoday.org/vol-57/iss-5/p21.html>.

¹³⁵⁹ Tkalya EV. Induced decay of ¹⁷⁸Hf^{m2}: Theoretical analysis of experimental results. *Phys Rev C* 2005 Feb 24;71:024606; <https://journals.aps.org/prc/abstract/10.1103/PhysRevC.71.024606>. See also: Sharon Weinberger, *Imaginary Weapons*, Nation Books, NY, 2006; <https://www.fourmilab.ch/fourmilog/archives/2006-06/000715.html> and <https://www.fourmilab.ch/fourmilog/archives/2006-07/000716.html>.

2012¹³⁶⁰ and 2015¹³⁶¹ while a Chinese group claimed no replication success in 2013,¹³⁶² both using X-ray triggering. It has been suggested¹³⁶³ that Coulomb excitation of nuclear isomers by channeled relativistic heavy particles at 331 KeV¹³⁶⁴ could also trigger a form of isomer photo-destruction, releasing the full 2446 KeV of ^{178m2}Hf₇₂ stored isomer energy, and other possible means for triggering hafnium isomer decay have been discussed.¹³⁶⁵

Molybdenum. Another interesting case is the energy-level structure of the ^{93m}Mo₄₂ nuclear isomer, which decays in 7 hours releasing 2425 KeV of γ -rays. It has been calculated that in a 4 million K plasma the isomer decay rate could be enhanced by a factor of $\sim 10^6$ (i.e., decay in ~ 0.03 sec) due to a predicted nuclear excitation by electron capture (NEEC) process that could be driven by a 5 KeV energy input to an intermediate energy level lying just above the isomer.¹³⁶⁶ NEEC was first predicted in 1976¹³⁶⁷ but had not been observed experimentally in 2004 when this proposal was originally made, but in 2018 the first observation of NEEC was reported in the

¹³⁶⁰ Kirischuk VI, Strilchuk NV, in: Proc. 4th Int. Conf. “Current Problems in Nuclear Physics and Atomic Energy”, Kyiv, 3-7 Sept. 2012, 2013, p. 396, www.npae2012.kiev.ua/docs/NPAE-Kyiv2012-Part%25202.pdf. Dovbnaya AM, Kandybey SS, Kirischuk VI, *et al.*, in: Proc. 4th Int. Conf. “Current Problems in Nuclear Physics and Atomic Energy”, Kyiv, 3-7 Sept. 2012, 2013, p. 378, www.npae2012.kiev.ua/docs/NPAE-Kyiv2012-Part%25202.pdf.

¹³⁶¹ Kirischuk VI, Ageev VA, Dovbnaya AM, Kandybei SS, Ranyuk YuM. Induced acceleration of the decay of the 31-yr isomer of ^{178m2}Hf using bremsstrahlung radiation. Phys Lett B. 2015;750:89-94; <https://www.sciencedirect.com/science/article/pii/S0370269315006528/pdf>.

¹³⁶² Yang TL, de Ze R, Wu HL, Jiang T, He YH. Search for induced emission from the 178Hfm2 isomer by low-energy x rays. Phys Rev C 2013 Jul 16;88:014312; <https://journals.aps.org/prc/abstract/10.1103/PhysRevC.88.014312>.

¹³⁶³ Walker PM, Carroll JJ. Nuclear Isomers: Recipes from the Past and Ingredients for the Future. Nuclear Physics News 2007;17(2):11-15; <https://pdfs.semanticscholar.org/70e2/cad8638afa5fac15dcc0a7fe35bfd6005684.pdf>.

¹³⁶⁴ Karamian SA, Carroll JJ. Prospects for coherently driven nuclear radiation by Coulomb excitation. Laser Phys. 2007 Feb;17(2):80-86; <https://pdfs.semanticscholar.org/fafb/942c6aacfe2ea2c69e2a44bff08ac27ec880.pdf>.

¹³⁶⁵ Karamian SA, Carroll JJ, Rivlin LA, Zadernovsky AA, Agee FJ. Possible ways for triggering the ^{179m2}Hf isomer. Laser Physics 2004;14(2):166-173; https://www.researchgate.net/profile/Anatoly_Zadernovsky/publication/297579718_Possible_ways_for_triggering_the_Hf-179m2_isomer/links/57e3cbce08ae4d15ffae8c94/Possible-ways-for-triggering-the-Hf-179m2-isomer.pdf.

¹³⁶⁶ Gosselin G, Morel P. Enhanced nuclear level decay in hot dense plasmas. Phys Rev C. 2004;70:064603; <https://journals.aps.org/prc/abstract/10.1103/PhysRevC.70.064603>.

¹³⁶⁷ Goldanskii VI, Namiot VA. On the excitation of isomeric nuclear levels by laser radiation through inverse internal electron conversion. Phys Lett B. 1976;62:393-394; <https://www.sciencedirect.com/science/article/abs/pii/0370269376906651>.

^{93m}Mo₄₂ isomer.¹³⁶⁸ The aforementioned 10⁶-fold rate enhancement, if achieved, would produce an apparent transient specific power of **84 x 10⁶ MW/kg** and power density of **862 x 10⁶ MW/L**.

Lutetium. A few military isomer programs have investigated the use of triggerable nuclear isomers as high-energy-density batteries. For example, one Army-Navy research program has investigated using ^{177m3}Lu₇₁ in a switchable nuclear battery, in which a 300 KeV broadband gamma source irradiates the target material, converting long-lived isomeric states to short-lived radioisotope decaying states.¹³⁶⁹ ^{177m3}Lu₇₁ releases gamma rays by IT decay through a series of internal energy levels within the nucleus, but 78.3% of the total energy release is from β-decay, not IT. Note the researchers: “Optimizing the efficiency of a nuclear battery would require that the decay modes (and decay products α, β, and γ) of these high-energy-density materials be matched to direct energy conversion materials....Samples of SiC have been irradiated with gammas from a 300 KeV bremsstrahlung gamma source and betas from ⁹⁰Sr. Efficiency as high as 2% has been measured from the SiC PIN device (under irradiation from the ⁹⁰Sr)...SiC would appear to be a promising material for the applications of small long-lived (10-year) batteries.”

Americium. It may be possible to trigger the isomeric decay of ^{242m1}Am₉₅ with the application of as little as 4.3 KeV of excitation energy,¹³⁷⁰ but this has yet to be demonstrated experimentally. The result would be an IT specific energy of **~19,000 MJ/kg** and energy density of **~230,000 MJ/L**.

Thorium. Lawrence Livermore National Laboratory has studied the isomeric decay of ^{229m}Th₉₀ with the objective of demonstrating isomer triggering. This isomer is unique in having the only known nucleus whose excitation energy (~7.1 eV)¹³⁷¹ is near optical energies, sufficiently low in energy to allow for direct nuclear optical laser excitation. Thus it may be possible to transition ²²⁹Th₉₀ nuclei between the ground and isomeric states using a table-top laser.¹³⁷² Of course, at **35 MJ/L** the energy density for this metastable nuclear isomer is the poorest on the list.

¹³⁶⁸ Chiara CJ, *et al.* Isomer depletion as experimental evidence of nuclear excitation by electron capture. Nature 2018 Feb 7;554:216-218; <https://www.nature.com/articles/nature25483>.

¹³⁶⁹ Litz MS, Blaine K, Geil B, Merkel G. On-demand high energy density materials. Third International Energy Conversion Engineering Conference, 15-18 Aug 2005, San Francisco CA, AIAA 2005-5740; <https://arc.aiaa.org/doi/pdf/10.2514/6.2005-5740>.

¹³⁷⁰ Karamian SA, Carroll JJ. Possibility of combining nuclear level pumping in plasma with lasing in solid. Hyperfine Interact. 2002 Nov;143(1-4):69-78; <https://inis.iaea.org/collection/NCLCollectionStore/Public/33/061/33061027.pdf>. Karamian SA, Carroll JJ. Hybridization of Atomic-Nuclear Excitations and Pumping of Nuclear Levels. Laser Phys. 2003 Sep;13(9):1182-1187; https://www.researchgate.net/publication/289590680_Hybridization_of_Atomic-Nuclear_Excitations_and_Pumping_of_Nuclear_Levels.

¹³⁷¹ Borisyuk PV, Chubunova EV, Kolachevsky NN, Lebedinskii YY, Vasiliev OS, Tkalya EV. Excitation of ²²⁹Th nuclei in laser plasma: the energy and half-life of the low-lying isomeric state. eprint arXiv, Apr 2018; <https://arxiv.org/abs/1804.00299>.

¹³⁷² Anne Stark, “Researchers move closer to switching nuclear isomer decay on and off,” LLNL News, 6 Apr 2007; https://web.archive.org/web/20100527235502/https://publicaffairs.llnl.gov/news/news_releases/2007/NR-07-04-02.html.

7.5 Exotic Particles and Atoms, and Degenerate Matter

This Section describes the potential for energy storage in quasiparticles (**Section 7.5.1**), exotic atoms (**Section 7.5.2**), dual-quantum-number atoms (**Section 7.5.3**), and degenerate matter (**Section 7.5.4**).

7.5.1 Quasiparticles

Quasiparticles¹³⁷³ (and the related “collective excitations”) are “emergent phenomena that occur when a microscopically complicated system such as a solid behaves as if it contained different weakly interacting particles in free space. For example, as an electron travels through a semiconductor, its motion is disturbed in a complex way by its interactions with all of the other electrons and nuclei; however, it approximately behaves like an electron with a different mass (effective mass) traveling unperturbed through free space. This ‘electron with a different mass’ is called an ‘electron quasiparticle’ [or a polaron¹³⁷⁴ when in a polarizable crystal lattice]. In another example, the aggregate motion of electrons in the valence band of a semiconductor or a hole band in a metal is the same as if the material instead contained positively charged quasiparticles called electron holes.” Quasiparticles and collective excitations are a type of low-lying excited state.¹³⁷⁵

There are many known quasiparticles¹³⁷⁶ but in most cases their capacity for energy storage has limits already addressed elsewhere in this book. For example, electron quasiparticles,¹³⁷⁷ holes,¹³⁷⁸ excitons,¹³⁷⁹ trions,¹³⁸⁰ and dropletions¹³⁸¹ should have maximum energy densities of the same order as electrons moving through wires (**Section 6.2**). Phonons (a collective excitation associated with the vibration of atoms in a rigid crystal structure; a quantum of a sound wave) will have energy densities similar to acoustic waves moving through solids, or through liquids in the case of solitons¹³⁸² (**Section 5.1.5**). Plasmons (a collective excitation of electrons oscillating with respect to the ions; a quantum of a plasma oscillation) will have energy densities similar to compressed electrical plasmas (**Section 5.1.4**).

One interesting special case is the magnetic monopole,¹³⁸³ a hypothetical free-space particle predicted to exist by Paul Dirac¹³⁸⁴ that has been experimentally demonstrated to exist as a quasiparticle,¹³⁸⁵ although the ability of these entities to store energy remains largely unexplored.

¹³⁷³ <https://en.wikipedia.org/wiki/Quasiparticle>.

¹³⁷⁴ <https://en.wikipedia.org/wiki/Polaron>.

¹³⁷⁵ https://en.wikipedia.org/wiki/Quasiparticle#Relation_to_many-body_quantum_mechanics.

¹³⁷⁶ https://en.wikipedia.org/wiki/List_of_quasiparticles.

¹³⁷⁷ https://en.wikipedia.org/wiki/Quasiparticle#More_common_examples.

¹³⁷⁸ https://en.wikipedia.org/wiki/Electron_hole.

¹³⁷⁹ <https://en.wikipedia.org/wiki/Exciton>.

¹³⁸⁰ [https://en.wikipedia.org/wiki/Trion_\(physics\)](https://en.wikipedia.org/wiki/Trion_(physics)).

¹³⁸¹ <https://en.wikipedia.org/wiki/Dropletion>.

¹³⁸² <https://en.wikipedia.org/wiki/Soliton>.

¹³⁸³ https://en.wikipedia.org/wiki/Magnetic_monopole.

¹³⁸⁴ Dirac P. Quantised Singularities in the Electromagnetic Field. Proc Roy Soc (London) A 1931;133:60; <http://rspa.royalsocietypublishing.org/content/133/821/60>.

7.5.2 Exotic Atoms

An exotic atom¹³⁸⁶ is an otherwise normal atom in which one or more subatomic particles have been replaced by other particles of the same charge. For example, electrons may be replaced by other negatively charged particles such as muons (**Section 7.5.2.1**) or hadrons such as kaons or pions (**Section 7.5.2.2**), and nuclei can be partially substituted with baryons other than protons or neutrons, such as hyperons, creating hypernuclear atoms (**Section 7.5.2.2**). These substitute particles are usually unstable, so exotic atoms typically have very short lifetimes in which to participate in an exothermic fusion reaction.

¹³⁸⁵ Morris J. The hunt for the magnetic monopole. IEEE Spectrum, 1 Aug 2013; <https://spectrum.ieee.org/semiconductors/materials/the-hunt-for-the-magnetic-monopole>. “Physicists create synthetic magnetic monopole predicted more than 80 years ago,” PhysOrg, 29 Jan 2014; <https://phys.org/news/2014-01-physicists-synthetic-magnetic-monopole-years.html>. Phatak C, Petford-Long A. Direct Evidence of Topological Defects in Electron Waves through Nanoscale Localized Magnetic Charge. Nano Lett. 2018 Nov 14;18(11):6989-6994; <https://pubs.acs.org/doi/10.1021/acs.nanolett.8b02915>.

¹³⁸⁶ https://en.wikipedia.org/wiki/Exotic_atom.

7.5.2.1 Muonic Atoms and Muonium

In a muonic atoms¹³⁸⁷ (previously called mu-mesic atoms),¹³⁸⁸ an electron in an ordinary atom is replaced by a negative-charged muon,¹³⁸⁹ orbiting one or more ordinary nucleons in the nucleus. Since leptons (e.g., electrons, muons)¹³⁹⁰ are only sensitive to weak, electromagnetic and gravitational forces, the interactions of muonic atoms are governed mostly by the electromagnetic interaction. A muon is ~207 times massive than an electron, so the Bohr orbits are much closer to the nucleus in a muonic atom than in an ordinary atom.

Muonic hydrogen atoms (e.g., $p^+\mu^-$) with a negative muon may undergo nuclear fusion in the process of muon-catalyzed fusion¹³⁹¹ (**Section 7.3.2**), after which the muon may leave the new atom to induce fusion in another hydrogen molecule. The binding energies of muomolecular ions are ~100 larger than the energies of normal molecules. In the case of muonic heavy hydrogen molecules (HD, D₂, DT, or T₂), once the muonic molecular ion forms it becomes unstable against induced fusion via nucleon tunneling, subsequently decaying to fusion products in ~ 1 nanosec with the release of 17.6 MeV in the case of DT (i.e., a 14.1 MeV fast neutron and a 3.5 MeV alpha particle) – a potential technical application of muonic atoms. In muonic hydrogenic molecules the induced D-D fusion rate is only ~1% of the induced D-T rate, and the muon-induced H-D fusion¹³⁹² rate is even less, only ~10⁻⁶ of the D-T rate.¹³⁹³ The energy and power densities available from muon-catalyzed fusion were previously estimated in **Section 7.3.2**.

Muonic hydrogen atoms are much smaller than typical hydrogen atoms, but in multi-electron atoms where only one of the electrons is replaced by a muon, the size of the atom continues to be determined by the other electrons and the atomic size is nearly unchanged although the muon orbital is smaller and far closer to the nucleus than the atomic orbitals of the electrons.

¹³⁸⁷ https://en.wikipedia.org/wiki/Exotic_atom#Muonic_atoms.

¹³⁸⁸ This must be distinguished from muonium (see below), the name assigned by IUPAC to the system of a positive-charged antimuon bound with a negative-charged electron, violating the usual convention in which the suffix -onium denotes a bound state of a particle and its antiparticle (<https://en.wikipedia.org/wiki/Omium>).

¹³⁸⁹ “The muon is an unstable subatomic particle with a mean lifetime of 2.2 μs. Muon decay is slow (by subatomic standards) because the decay is mediated by the weak interaction exclusively (rather than the more powerful strong interaction or electromagnetic interaction), and because the mass difference between the muon and the set of its decay products is small, providing few kinetic degrees of freedom for decay.” <https://en.wikipedia.org/wiki/Muon>.

¹³⁹⁰ <https://en.wikipedia.org/wiki/Lepton>.

¹³⁹¹ https://en.wikipedia.org/wiki/Muon-catalyzed_fusion.

¹³⁹² Alvarez LW, *et al.* Catalysis of nuclear reactions by μ mesons. Phys Rev. 1957;105(3):1127.

¹³⁹³ Jackson JD. Catalysis of nuclear reactions between hydrogen isotopes by μ⁻ mesons. Phys Rev. 1957 Apr 15;106(2):330-339; <https://journals.aps.org/pr/abstract/10.1103/PhysRev.106.330>.

Muonic helium atoms are created by substituting a muon for one of the electrons in ^4He . The muon orbits much closer to the nucleus (mean radius ~ 0.2 pm), so muonic helium can therefore be regarded as an isotope of helium whose nucleus consists of two neutrons, two protons and a muon, with a single electron far outside. Muonic helium, having one unpaired valence electron, could bond with other atoms and behave (chemically) more like a hydrogen atom than an inert helium atom.¹³⁹⁴ One possible alternative fate of negative muons bound to conventional atoms may be to be captured via the weak-force by protons in the nucleus in a process analogous to electron capture, converting the proton to a neutron with emission of a muon neutrino.¹³⁹⁵

Muonium (aka. “muium”)¹³⁹⁶ is an exotic atom comprising a positive-charged antimuon orbited by a negative-charged electron in a Coulombic bound state (e.g., μ^+e^-).¹³⁹⁷ After its discovery in 1960¹³⁹⁸ muonium was given the chemical symbol Mu because of its ability to enter into chemical compounds such as muonium chloride (MuCl) and sodium muonide (NaMu) during its brief 2.2 μs lifetime.¹³⁹⁹ The mass difference between the antimuon and the electron makes muonium (μ^+e^-) more similar to atomic hydrogen (p^+e^-) than to positronium (e^+e^-) – with a Bohr radius and ionization energy within 0.5% of H, D, and T, muonium can usefully be considered as an exotic light isotope of hydrogen with 1/9th the normal mass of H.¹⁴⁰⁰ The muon decays into two

¹³⁹⁴ Fleming DG, Arseneau DJ, Sukhorukov O, Brewer JH, Mielke SL, Schatz GC, Garrett BC, Peterson KA, Truhlar DG. Kinetic Isotope Effects for the Reactions of Muonic Helium and Muonium with H_2 . *Science*. 2011 Jan 28;331(6016):448–450; http://140.123.79.88/~yach932/CH3_Reference/99.Science-2011-Fleming-448-50.pdf. Moncada F, Cruz D, Reyes A. Muonic alchemy: Transmuting elements with the inclusion of negative muons. *Chem Phys Lett*. 2012 Jun 29;539-540:209-13; <http://www.academia.edu/download/36408116/muonsIP.pdf>. Moncada F, Cruz D, Reyes A. Electronic properties of atoms and molecules containing one and two negative muons. *Chem Phys Lett*. 2013 May 10;570:16–21; http://www.academia.edu/download/41803930/Electronic_properties_of_atoms_and_molec20160131-3924-1fde024.pdf.

¹³⁹⁵ https://en.wikipedia.org/wiki/Muon#Negative_muon_atoms.

¹³⁹⁶ <https://en.wikipedia.org/wiki/Muonium>. The name “muonium” was chosen before people had developed a systematic naming scheme for exotic elements. In the modern naming scheme, muonium should really be called “muium”; <https://plus.google.com/+johncbaez999/posts/L7mcLBJuEAp>.

¹³⁹⁷ “Muonium,” IUPAC Compendium of Chemical Terminology, 2nd ed. (the “Gold Book”). Compiled by A. D. McNaught and A. Wilkinson. Blackwell Scientific Publications, Oxford (1997); <http://goldbook.iupac.org/html/M/M04069.html>.

¹³⁹⁸ Hughes VW, McColm DW, Ziock K, Prepost R. Formation of muonium and observation of its Larmor precession. *Phys Rev Lett*. 1960 Jul 15;5(2):63-65; <https://journals.aps.org/prl/abstract/10.1103/PhysRevLett.5.63>. Summary at <http://inspirehep.net/record/1341473/files/C60-08-25-p789.pdf>.

¹³⁹⁹ Koppenol WH. Names for muonium and hydrogen atoms and their ions. *Pure Appl Chem*. 2001;73(2):377-380; <http://www.iupac.org/publications/pac/2001/pdf/7302x0377.pdf>.

¹⁴⁰⁰ Walker DC. *Muon and Muonium Chemistry*, Cambridge University Press, 2009; http://assets.cambridge.org/9780521103374/excerpt/9780521103374_excerpt.pdf.

neutrinos and an electron to which up to 53 MeV of recoverable kinetic energy is imparted.¹⁴⁰¹ A muonium atom has a mass of $\sim 106.169 \text{ MeV}/c^2$ ($1.90 \times 10^{-28} \text{ kg}$) and decays in $2.2 \text{ } \mu\text{sec}$, hence has a specific energy of $E_s \sim 4.5 \times 10^{10} \text{ MJ/kg}$ and an average specific power of $P_s \sim 2.0 \times 10^{16} \text{ MW/kg}$ over the lifetime of this exotic atom.

¹⁴⁰¹ https://web.archive.org/web/20130413042650/https://isnap.nd.edu/Lectures/Laboratory/16_Muon_Lifetime.pdf.

7.5.2.2 Hadronic Atoms and Hypernuclear Atoms

Hadronic atoms¹⁴⁰² are atoms with a regular nucleus in which one or more of the orbital electrons is replaced by a negatively charged hadron.¹⁴⁰³ Possible hadrons include mesons such as the kaon or pion, yielding a kaonic atom or a pionic atom, collectively called mesonic atoms or mesic atoms.

Kaonic hydrogen¹⁴⁰⁴ is another exotic atom consisting of a negatively charged kaon¹⁴⁰⁵ orbiting a proton (i.e., p^+K^-). The negative kaon has a mass 4.67 times larger than the negative muon and a decay time of only 0.01 μsec (177 times faster than the muon), so kaonic hydrogen atoms are even less stable than muonic hydrogen atoms – and yet such particles were first identified, through their X-ray spectrum, at the KEK proton synchrotron in Tsukuba, Japan in 1997.¹⁴⁰⁶ Subsequent observations of kaonic hydrogen (but not kaonic deuterium) have been reported.¹⁴⁰⁷ While electron/proton binding is dominated by the electromagnetic interaction in hydrogen atoms, negative kaons and protons are also affected by the strong interaction at small distances, which in kaonic hydrogen adds a repulsive contribution, shifting the ground state energy by ~ 283 eV and making the system unstable against decay into $\Lambda\pi$ and $\Sigma\pi$.¹⁴⁰⁸ Kaonic helium-3¹⁴⁰⁹ and kaonic helium-4¹⁴¹⁰ (helium atoms with one electron replaced by a negative kaon) have also been observed. Because kaons are heavier than muons, kaonic hydrogen and kaonic helium should

¹⁴⁰² Deloff A. Fundamentals in Hadronic Atom Theory. World Scientific, River Edge NJ, 2003. See also: https://en.wikipedia.org/wiki/Exotic_atom#Hadronic_atoms.

¹⁴⁰³ <https://en.wikipedia.org/wiki/Hadron>.

¹⁴⁰⁴ https://en.wikipedia.org/wiki/Kaonic_hydrogen.

¹⁴⁰⁵ <https://en.wikipedia.org/wiki/Kaon>.

¹⁴⁰⁶ Nakamura SN, *et al.* Observation of kaonic hydrogen atom X-ray. Hyperfine Interactions 1999;118:45-51; https://www.researchgate.net/profile/Tomoki_Terada/publication/227079046_Observation_of_kaonic_hydrogen_atom_X-ray/links/00b7d530c85ae4dc4a000000.pdf. Iwasaki M, Hayano R, Ito T, Nakamura S, Terada T, Gill D, Lee L, Olin A, Salomon M, Yen S, Bartlett K, Beer G, Mason G, Trayling G, Ota H, Taniguchi T, Yamashita Y, Seki R. Observation of Kaonic Hydrogen $K\alpha$ X Rays. Phys Rev Lett. 1997;78(16):3067; <https://journals.aps.org/prl/abstract/10.1103/PhysRevLett.78.3067>.

¹⁴⁰⁷ Bazzi M, *et al.* Kaonic hydrogen X-ray measurement in SIDDHARTA. Nucl Phys A 2012 May 1;881:88-97; <https://arxiv.org/pdf/1201.4635.pdf>.

¹⁴⁰⁸ Yan Y. Kaonic hydrogen atom and kaon-proton scattering length. ArXiv.org, 29 May 2009; <https://arxiv.org/pdf/0905.4818>.

¹⁴⁰⁹ Bazzi M, *et al.* First measurement of kaonic helium-3 X-rays. Phys Lett B. 2011 Mar 7;697(3-2):199-202; <https://www.ncbi.nlm.nih.gov/pmc/articles/PMC3087507/>.

¹⁴¹⁰ Bazzi M, *et al.* Kaonic helium-4 X-ray measurement in SIDDHARTA. Phys Lett B 2009 Nov 9;681(4):310-314; <https://www.sciencedirect.com/science/article/abs/pii/S0370269309012490>.

theoretically be capable of initiating fusion reactions even more readily than the analogous muonic atoms (**Section 7.3.2**) – were it not for the shorter lifetime of kaons compared to muons.

Pionic atoms have been known for many decades.¹⁴¹¹ Pions¹⁴¹² have a mass similar to muons but a short lifetime (0.026 μsec) similar to kaons. Pionic hydrogen¹⁴¹³ and pionic deuterium¹⁴¹⁴ is an atom of hydrogen with one electron replaced by a negative pion and a lifetime of 0.026 μsec . Pionic helium¹⁴¹⁵ is an atom of helium with one electron replaced by a negative pion with the same short decay time; pion mass has been determined in experiments using pionic magnesium ($\pi^{-24}\text{Mg}$)¹⁴¹⁶ and pionic nitrogen.¹⁴¹⁷

Kaonium¹⁴¹⁸ is an exotic atom consisting of a bound state of a positively charged kaon and a negatively charged kaon. Because of its higher mass and shorter decay time, kaonium has not yet been observed experimentally as it is expected to have a lifetime on the order of $\sim 10^{-18}$ seconds.¹⁴¹⁹

Pionium¹⁴²⁰ is an experimentally-observed¹⁴²¹ bound state of two pions, one positive and one negative, with an estimated decay lifetime of 3×10^{-15} sec.¹⁴²²

¹⁴¹¹ Backenstoss G. Pionic atoms. *Ann Rev Nucl Sci* 1970;20:467-508;
http://personal.psu.edu/rq9/HOW/Pionic_atoms.pdf.

¹⁴¹² <https://en.wikipedia.org/wiki/Pion>.

¹⁴¹³ Horvath D. Chemistry of pionic hydrogen atoms. *Radiochimica Acta* 1981; 28(4):241-254;
<https://hungary.pure.elsevier.com/en/publications/chemistry-of-pionic-hydrogen-atoms>.

¹⁴¹⁴ Hauser P, Kirch K, Simons L, Borchert G, Gotta D, Siems T, El-Khoury P, Indelicato P, Augsburger M, Chatellard D, Egger JP, Anagnostopoulos DF. New precision measurement of the pionic deuterium s-wave strong interaction parameters. *Phys Rev C* 1998 Oct 1;58(4):R1869;
<https://journals.aps.org/prc/abstract/10.1103/PhysRevC.58.R1869>.

¹⁴¹⁵ Korobov VI, Bekbaev AK, Aznabayev DT, Zhaugasheva SA. Polarizability of the pionic helium atom. *J. Phys. B: At. Mol. Opt. Phys.* 2015;48:245006;
http://theor.jinr.ru/~korobov/papers/Polarizability_in_pi_He_atom_JPB15.pdf.

¹⁴¹⁶ Jeckelmann B, *et al.* New precision determination of the π^{-} mass from pionic X-rays. *Nucl Phys A* 1986 Sep 15-22;457(3-4):709-730;
<https://www.sciencedirect.com/science/article/abs/pii/0375947486904768>.

¹⁴¹⁷ Lenz S, *et al.* A new determination of the mass of the charged pion. *Phys Lett B* 1998 Jan;416(1-2):50-55; <https://www.sciencedirect.com/science/article/abs/pii/S0370269397013373>.

¹⁴¹⁸ <https://en.wikipedia.org/wiki/Kaonium>.

¹⁴¹⁹ Krewald S, Lemmer RH, Sassen FP. Lifetime of kaonium. *Phys Rev D.* 2004 Jan 29;69(1):016003;
<https://arxiv.org/pdf/hep-ph/0307288>.

¹⁴²⁰ <https://en.wikipedia.org/wiki/Pionium>.

It is an open question if exotic atoms analogous to muonium (**Section 7.5.2.1**) are possible, with a positive pion (i.e., π^+e^-)¹⁴²³ or a positive antikaon (i.e., K^+e^-) orbited by a negative electron – to date, only the nucleus-substituted bound states of e^+e^- (positronium)¹⁴²⁴ and μ^+e^- (muonium)¹⁴²⁵ are known experimentally. The theoretical existence of gravitationally-bound pion stars with π^+e^- composition has been proposed;¹⁴²⁶ such stars would have an energy density $E_D \sim 7 \times 10^{18}$ MJ/L.

Other types of hadronic atoms include antiprotons orbiting a normal nucleus, yielding an antiprotonic atom (e.g., antiprotonic hydrogen or antiprotonic helium; **Section 7.6.3**), or a sigmaonic atom in which a negative sigma (Σ^-) particle orbits a normal nucleus.¹⁴²⁷

A hypernuclear atom¹⁴²⁸ consists of one or more electrons orbiting a hypernucleus. A hypernucleus¹⁴²⁹ is a nucleus that contains normal protons, neutrons, and at least one hyperon carrying the “strangeness” quantum number. Hypernuclei containing the lightest hyperon,¹⁴³⁰ the lambda (Λ) (mass $\sim 1.19 m_p$; proton mass $m_p = 1.67 \times 10^{-27}$ kg),¹⁴³¹ can be observed¹⁴³² because

¹⁴²¹ Batley JR, *et al.* Observation of a cusp-like structure in the $\pi^0\pi^0$ invariant mass distribution from $K^\pm \rightarrow \pi^\pm\pi^0\pi^0$ decay and determination of the $\pi\pi$ scattering lengths. Phys Lett B. 2006;633(2-3):173-182; <https://www.sciencedirect.com/science/article/pii/S0370269305017570>. Batley JR, *et al.* Determination of the S-wave $\pi\pi$ scattering lengths from a study of $K^\pm \rightarrow \pi^\pm\pi^0\pi^0$ decays. Euro Phys J C. 2009;64(4):589-608; <https://arxiv.org/pdf/0912.2165.pdf>.

¹⁴²² Jallouli H, Sazdjian H. Relativistic effects in the pionium lifetime. Phys Rev D. 1998 May 28;58:014011; <https://arxiv.org/pdf/hep-ph/9706450.pdf>.

¹⁴²³ <https://www.quora.com/Would-it-be-possible-for-a-electron-to-orbit-a-positive-pion-and-form-some-sort-of-exotic-particle-with-a-half-life-of-around-150-ns>;
<http://www.alternativephysics.org/book/Particles.htm>.

¹⁴²⁴ <https://en.wikipedia.org/wiki/Positronium>.

¹⁴²⁵ <https://en.wikipedia.org/wiki/Muonium>.

¹⁴²⁶ Brandt BB, Endrödi G, Fraga ES, Hippert M, Schaffner-Bielich J, Schmalzbauer S. New class of compact stars: Pion stars. 27 Nov 2018; <https://arxiv.org/pdf/1802.06685.pdf>.

¹⁴²⁷ Sigmaonic atoms are thought to be possible but have not yet been observed.

¹⁴²⁸ https://en.wikipedia.org/wiki/Exotic_atom#Hypernuclear_atoms.

¹⁴²⁹ <https://en.wikipedia.org/wiki/Hypernucleus>.

¹⁴³⁰ <https://en.wikipedia.org/wiki/Hyperon>.

¹⁴³¹ https://en.wikipedia.org/wiki/Lambda_baryon#Types_of_lambda_baryons.

¹⁴³² Danysz M, Pniewski J. Delayed disintegration of a heavy nuclear fragment: I. Phil. Mag. 1953 Mar 1;44(350):348-350; <https://www.tandfonline.com/doi/abs/10.1080/14786440308520318?journalCode=tphm18>. Nakamura SN, *et al.* Observation of the Helium 7 Lambda hypernucleus by the (e,e'K+) reaction. arXiv:1207.0571, 19 Nov 2012; <https://arxiv.org/pdf/1207.0571.pdf>.

the lifetime of a lambda in a nucleus is ~ 0.2 nanosec.¹⁴³³ The lambda decays into a positive proton and a negative pion with recoverable kinetic energy 38.4 MeV,¹⁴³⁴ hence specific energy $E_s \sim 3.1 \times 10^9$ MJ/kg and average specific power $P_s \sim 1.6 \times 10^{19}$ MW/kg over the brief lifetime of a lambda hypernuclear atom. Hypernuclear atoms incorporating sigma particles (the next heaviest hyperon after the lambda) have also been sought.¹⁴³⁵

All known hadronic and hypernuclear atoms have very short lifetimes, so it is difficult to see how they could be employed in a practical energy storage system or serve as useful catalysts to trigger nuclear fusion unless these lifetimes can be extended by some artificial means, e.g., the quantum Zeno effect¹⁴³⁶ (**Section 7.3.2**).

¹⁴³³ Ota H, Aoki M, Hayano RS, Ishikawa T, Iwasaki M, Sakaguchi A, Takada E, Tamura H, Yamazaki T. Mesonic and non-mesonic decay widths of $\Lambda^4\text{H}$ and $\Lambda^4\text{He}$. Nucl Phys A 1998 Aug 24; 639(1-2):251c-260c; <https://www.sciencedirect.com/science/article/abs/pii/S0375947498002814>.

¹⁴³⁴ <https://www.chegg.com/homework-help/lambda-particle-decays-rest-proton-pion-reaction-p-rest-ener-chapter-rs8-problem-13re-solution-9780071284431-exc>.

¹⁴³⁵ May M. Recent results and directions in hypernuclear and kaon physics. In: A. Pascolini, ed. PAN XIII: Particles and Nuclei, World Scientific, 1994; <https://www.osti.gov/biblio/10107402>. Chrien RE. The story of Sigma hypernuclei – a modern fable. INIS 32(50); https://inis.iaea.org/search/search.aspx?orig_q=RN:32067955.

¹⁴³⁶ https://en.wikipedia.org/wiki/Quantum_Zeno_effect.

7.5.3 Double-Charm and Double-Bottom Baryon Fusion

In 2017, researchers at the Large Hadron Collider (LHC) reported¹⁴³⁷ an experiment in which two particles fused to create a double-charm baryon – analogous to baryon-like protons (made of 2 “up” quarks and 1 “down” quark) or neutrons (2 “down” quarks and 1 “up” quark), but made from 2 “charm” quarks and 1 “up” quark, called the Xi double-charm baryon (Ξ_{cc}^{++}) with a mass of $3621.4 \text{ MeV}/c^2$ ($6.48 \times 10^{-27} \text{ kg}$) and a lifetime of $0.05\text{-}1 \times 10^{-12} \text{ sec}$.¹⁴³⁸ While it took 130 MeV to force the two precursor charm quarks together, there was a net energy release of 12 MeV ($1.9 \times 10^{-12} \text{ J}$) of fusion energy from each reaction event,¹⁴³⁹ representing a specific energy of $E_S \sim \mathbf{293 \times 10^6 \text{ MJ/kg}}$ which is comparable to the most energy-dense light-element exothermic fusion reactions (i.e., $E_S \sim \mathbf{352 \times 10^6 \text{ MJ/kg}}$ for ${}^2\text{D}_1 + {}^3\text{He}_2$; **Table 55**).

When the researchers extrapolated that reaction to another kind of quark, the thrice-heavier “bottom” quark, the energy density greatly exceeded that of conventional light-element fusion. According to calculations,¹⁴⁴⁰ fusing two “bottom” quarks takes about 230 MeV to initiate but the net energy production should be $\sim 138 \text{ MeV}$ ($2.22 \times 10^{-11} \text{ J}$). For a double-bottom baryon weighing $10,162 \text{ MeV}/c^2$ ($1.82 \times 10^{-26} \text{ kg}$) the specific energy released by fusion rises to $E_S \sim \mathbf{1220 \times 10^6 \text{ MJ/kg}}$, or ~ 3.5 times larger than the best light-element fusion reaction. However, this kind of bottom quark fusion has yet to be observed experimentally, and the colliding B^- mesons containing “bottom” quarks will decay to a more stable “up” quark in just $\sim 1.6 \times 10^{-12} \text{ sec}$. In this amount of time, two bottom quark particles sharing 230 MeV would be traveling at $\sim 0.15c$ and could only move a distance of $\sim 72 \mu\text{m}$, defining a relatively small operating volume for a working energy storage system that may prove challenging to implement.

¹⁴³⁷ LHCb Collaboration. Observation of the doubly charmed baryon Ξ_{cc}^{++} . CERN-EP-2017-156, 6 Jul 2017; <http://lhcb-public.web.cern.ch/lhcb-public/Images2017/LHCb-PAPER-2017-018.pdf>.

¹⁴³⁸ <https://en.wikipedia.org/wiki/%CE%9Ecc%2B%2B>.

¹⁴³⁹ Nathaniel Scharping, “Discovered: A (theoretical) fusion technique 8 times stronger than one in H-bomb,” Discover Magazine, 3 Nov 2017; <http://blogs.discovermagazine.com/d-brief/2017/11/03/fusion-technique-hydrogen-bomb/#.XCqbHWI7kZp>.

¹⁴⁴⁰ Karliner M, Rosner JL. Quark-level analogue of nuclear fusion with doubly heavy baryons. Nature 2017 Nov 2;551:89-91; https://www.nature.com/articles/nature24289.epdf?referrer_access_token=O5kwdWIYrf9Jci6eN_2TRdRg_N0jAjWel9jnR3ZoTv0MwVq8cmHLuj5WCtSbfQ6pv5qW_5FS9B6KfsqxMVjlpKGsNlpMfjsuzJSXaWiJt_YDvg5MByZU7iniH4NPkzrURmM11bRRLREnN3c4hLDnbedacpQ1TVCNo9qpZv6uWMrngnm4IY2r0-moIFXIObuEY1gtDhnO2o_DqH3CmjpQM_bXVHccZGiMPce3GBE-iRx_ePY7IVE3pdYMN1ur8X9kljV8jPaoQ2pqE_c6qJNFokisHj6IsTb8ekjdPwjfyX2IE%3D&tracking_referrer=www.newsweek.com.

7.5.4 Degenerate Matter

Degenerate matter¹⁴⁴¹ is a highly dense state of fermionic matter (e.g., quarks, leptons, and baryons)¹⁴⁴² in which particles must occupy high states of kinetic energy in order to satisfy the Pauli exclusion principle.¹⁴⁴³ The description applies to matter composed of electrons, protons, neutrons or other fermions, and is mainly used in astrophysics to refer to dense stellar objects where gravitational pressure is so extreme that quantum mechanical effects are significant. This type of matter is naturally found in stars in their final evolutionary states, like white dwarfs and neutron stars, where thermal pressure alone is not enough to avoid gravitational collapse.

The four general classes of known or hypothesized degenerate matter are electron degenerate matter (**Section 7.5.4.1**), neutron degenerate matter (**Section 7.5.4.2**), quark degenerate matter (**Section 7.5.4.3**), and fully degenerate matter (**Section 7.5.4.4**).

¹⁴⁴¹ https://en.wikipedia.org/wiki/Degenerate_matter.

¹⁴⁴² <https://en.wikipedia.org/wiki/Fermion>.

¹⁴⁴³ https://en.wikipedia.org/wiki/Pauli_exclusion_principle.

7.5.4.1 Electron Degenerate Matter (White Dwarf Matter)

As hydrogen-burning nuclear fusion ends, a normal star¹⁴⁴⁴ of mass 0.5-1.4 M_{solar} becomes a white dwarf¹⁴⁴⁵ – a collection of positively charged ions, largely helium and carbon nuclei, floating in a sea of electrons that have been stripped from the nuclei. As particle density increases, electrons progressively fill the lower energy states and additional electrons are forced to occupy states of higher energy even at low temperatures.¹⁴⁴⁶ Such degenerate gases strongly resist further compression because the electrons cannot move to already-filled lower energy levels due to the Pauli exclusion principle.¹⁴⁴⁷ White dwarf stars are held in hydrostatic equilibrium by degeneracy pressure, also known as Fermi pressure, creating an exotic form of matter known as electron degenerate matter.¹⁴⁴⁸

In a white dwarf – a stellar core remnant composed mostly of electron degenerate matter – matter density reaches $\rho_{\text{wd}} \sim 10^9 \text{ kg/m}^3$,¹⁴⁴⁹ with electrons no longer bound to single nuclei but instead forming a degenerate electron gas with a number density of $\sim 10^{36} \text{ electrons/m}^3$ ($\sim 10^6 \text{ kg/m}^3$ of the total density; the rest of the density is from nuclei).¹⁴⁵⁰ The electron degeneracy pressure¹⁴⁵¹ that resists further compression in a white dwarf is given¹⁴⁵² by $P_{\text{edp}} = (h^2/20m_e m_p^{5/3}) (3/\pi)^{2/3} (\rho_{\text{wd}}/\mu_e)^{5/3} \sim 10^{22} \text{ N/m}^2$, representing an energy density of $E_D \sim 10^{13} \text{ MJ/L}$, taking Planck's constant $h = 6.63 \times 10^{-34} \text{ J-sec}$, electron mass $m_e = 9.11 \times 10^{-31} \text{ kg}$, proton mass $m_p = 1.67 \times 10^{-27} \text{ kg}$, and the electron/proton number ratio $\mu_e = N_e/N_p \sim 1$. Electron degenerate matter is far too highly compressed to allow storage in any ordinary physical container (e.g., diamond can provide at most $\sim 10^{11} \text{ N/m}^2$ of mechanical restraint, or $\sim 10^{11}$ times too little)¹⁴⁵³ or confinement by practical electric or magnetic fields, so probably must be stored using neutronium containment (**Section 7.5.4.2**) or be confined using a strong natural gravitational field (as occurs in a white dwarf star¹⁴⁵⁴ with roughly stellar mass compressed to the volume of Earth) or a high-strength artificial

¹⁴⁴⁴ M_{solar} (mass of Sun) = $1.99 \times 10^{30} \text{ kg}$.

¹⁴⁴⁵ White dwarfs are luminous not because they are generating any energy but rather because they have trapped a large amount of heat which is gradually radiated away;
https://en.wikipedia.org/wiki/Degenerate_matter#Electron_degeneracy.

¹⁴⁴⁶ https://en.wikipedia.org/wiki/Degenerate_matter#Electron_degeneracy.

¹⁴⁴⁷ https://en.wikipedia.org/wiki/Pauli_exclusion_principle#Astrophysics.

¹⁴⁴⁸ https://en.wikipedia.org/wiki/Degenerate_matter.

¹⁴⁴⁹ https://en.wikipedia.org/wiki/White_dwarf#Composition_and_structure.

¹⁴⁵⁰ https://en.wikipedia.org/wiki/Fermi_gas#White_dwarfs.

¹⁴⁵¹ https://en.wikipedia.org/wiki/Electron_degeneracy_pressure.

¹⁴⁵² <http://scienceworld.wolfram.com/physics/ElectronDegeneracyPressure.html>.

¹⁴⁵³ Luo X, Liu Z, Xu B, Yu D, Tian Y, Wang HT, He J. Compressive Strength of Diamond from First-Principles Calculation. J Phys Chem C. 2010 Oct 21;41(114):17851-3;
https://www.researchgate.net/profile/Xiaoguang_Luo/publication/225376850_Compressive_Strength_of_Diamond_From_First-Principles_Calculation/links/0fcfd5126365a800dc000000.pdf.

¹⁴⁵⁴ https://en.wikipedia.org/wiki/White_dwarf.

gravitational field.¹⁴⁵⁵ Electron degenerate matter separated from a white dwarf would rapidly decompress back to ordinary matter, releasing significant stored energy, but extracting energy from this storage modality may be technically challenging. One wild speculation is that hypothetical physical confinement structures made of electron degenerate matter¹⁴⁵⁶ might be stabilized in the absence of strong gravitational forces using dynamic stabilization provided by “incredibly fast, low-amplitude vibrations [of the] subatomic particles”, in the same way that inverted pendulums can be kept vertical via dynamic stabilization.¹⁴⁵⁷

Metallic hydrogen (**Section 4.3.1.5**), believed to exist at the hot gravitationally-compressed core of Jovian-size gas giant planets, is another example of electron-degenerate matter.

Sufficiently dense matter containing protons also experiences proton degeneracy pressure,¹⁴⁵⁸ but in matter with approximately equal numbers of protons and electrons, proton degeneracy pressure is much smaller than electron degeneracy pressure, so proton degeneracy is usually modeled as a correction to the equations of state of electron-degenerate matter.

¹⁴⁵⁵ Markley LC, Lindner JF. Artificial gravity field. *Results in Physics* 2013;3:24-29; <https://www.sciencedirect.com/science/article/pii/S2211379713000041>. Füzfa A. How current loops and solenoids curve spacetime. *Phys Rev D* 2016 Jan 11;93:024014; <https://arxiv.org/pdf/1504.00333.pdf>.

¹⁴⁵⁶ Bolonkin AA. Femtotechnology: Nuclear matter with fantastic properties. *Amer J Engin Appl Sci* 2009;2(2):501-514; <https://core.ac.uk/download/pdf/25754819.pdf>.

¹⁴⁵⁷ Goertzel B. There’s Plenty More Room at the Bottom: Beyond Nanotech to Femtotech. *HPlus Magazine*, 10 Jan 2011; <http://hplusmagazine.com/2011/01/10/theres-plenty-more-room-bottom-beyond-nanotech-femtotech/>.

¹⁴⁵⁸ https://en.wikipedia.org/wiki/Degenerate_matter#Proton_degeneracy.

7.5.4.2 Neutron Degenerate Matter (Neutronium)

Gravity in a normal aging (~post-fusion) star of mass 1.4-2.3 M_{solar} can overcome the electron degeneracy pressure and compress atoms so strongly that the electrons are forced to combine with protons via inverse β -decay, resulting in a superdense conglomeration of “degenerate” neutrons,¹⁴⁵⁹ also as known as “neutron matter”, “neutronium”, or, most commonly, “neutronium”.¹⁴⁶⁰ Free neutrons outside an atomic nucleus normally decay with a half life of ~15 minutes,¹⁴⁶¹ but in a neutron star,¹⁴⁶² the Pauli exclusion principle¹⁴⁶³ prevents further compression of the degenerate neutrons. (The nuclear force becomes repulsive at neutron-neutron separations of less than 0.7 fm.¹⁴⁶⁴) The upper limit to the mass of a neutron-degenerate object (the Tolman-Oppenheimer-Volkoff or TOV limit)¹⁴⁶⁵ is believed to be ~2.2 M_{solar} for a cold nonrotating neutron star¹⁴⁶⁶ and perhaps up to ~2.4 M_{solar} for a rigidly spinning neutron star.¹⁴⁶⁷

Neutron stars have overall average densities of $3.7\text{-}5.9 \times 10^{17} \text{ kg/m}^3$ (similar to the $3 \times 10^{17} \text{ kg/m}^3$ density of an atomic nucleus), varying from a low of $\sim 10^9 \text{ kg/m}^3$ in the crust to a maximum of $6\text{-}8 \times 10^{17} \text{ kg/m}^3$ deeper inside.¹⁴⁶⁸ The neutron degeneracy pressure¹⁴⁶⁹ increases from $3.2 \times 10^{31} \text{ N/m}^2$ (**$3.2 \times 10^{22} \text{ MJ/L}$**) at the inner crust to $1.6 \times 10^{34} \text{ N/m}^2$ (**$1.6 \times 10^{25} \text{ MJ/L}$**) at the center. (A pressure of $\sim 1.6 \times 10^{34} \text{ N/m}^2$ might deform the neutrons into a cubic symmetry allowing tighter packing of neutrons.¹⁴⁷⁰) Neutron stars can have huge magnetic fields up to $B \sim 10^{11}$ tesla¹⁴⁷¹ which in principle could provide a containment pressure of $P_{\text{containment}} \sim B^2/2\mu_0 = 4 \times 10^{27} \text{ N/m}^2$, ~400,000 times more than needed to containerize electron degenerate matter (**Section 7.5.4.1**) but still $10^4\text{-}10^7$ times too low to restrain neutronium. Adequate containment of neutronium may

¹⁴⁵⁹ https://en.wikipedia.org/wiki/Neutron-degenerate_matter.

¹⁴⁶⁰ <https://en.wikipedia.org/wiki/Neutronium>.

¹⁴⁶¹ <https://en.wikipedia.org/wiki/Neutron>.

¹⁴⁶² https://en.wikipedia.org/wiki/Neutron_star.

¹⁴⁶³ https://en.wikipedia.org/wiki/Pauli_exclusion_principle#Astrophysics.

¹⁴⁶⁴ https://en.wikipedia.org/wiki/Nuclear_force.

¹⁴⁶⁵ https://en.wikipedia.org/wiki/Tolman%E2%80%93Oppenheimer%E2%80%93Volkoff_limit.

¹⁴⁶⁶ Rezzolla L, Most ER, Weih LR. Using Gravitational-wave Observations and Quasi-universal Relations to Constrain the Maximum Mass of Neutron Stars. *Astrophys J* 2018 Jan 9;852(2):L25; <https://arxiv.org/abs/1711.00314>.

¹⁴⁶⁷ Cho A. A weight limit emerges for neutron stars. *Science* 2018 Feb 16;359(6377):724-725; <https://www.ncbi.nlm.nih.gov/pubmed/29449468>.

¹⁴⁶⁸ https://en.wikipedia.org/wiki/Neutron_star#Density_and_pressure.

¹⁴⁶⁹ https://en.wikipedia.org/wiki/Degenerate_matter#Neutron_degeneracy.

¹⁴⁷⁰ Llanes-Estrada FJ; Navarro GM. Cubic neutrons. *Modern Phys Lett A*. 2011;27(6):1250033.

¹⁴⁷¹ https://en.wikipedia.org/wiki/Neutron_star#Magnetic_field.

require neutron stars, artificial gravity fields,¹⁴⁷² gravitationally- or electrostatically-bound black hole lattices,¹⁴⁷³ or some other fictional-sounding contrivance.¹⁴⁷⁴

If gravity was suddenly turned off, a neutron star would promptly explode, rapidly releasing the energy that had been stored as neutron degeneracy pressure. A similar outcome would arise if the neutron star was spun rapidly enough to embed a rotational energy comparable in magnitude to the neutron degeneracy energy density of 10^{22} - 10^{25} MJ/L. Neutronium separated from a neutron star would also rapidly decompress back to ordinary matter, converting stable bound neutrons into unstable free neutrons with a 15-min half-life that would β -decay into protons and electrons with the release of $E_{\text{neut}} = 0.782$ MeV (1.26×10^{-13} J) per decay event.¹⁴⁷⁵ Degenerate compressed neutronium at a density of $\rho_{\text{neut}} \sim 5 \times 10^{17}$ kg/m³ contains $N_{\text{neut}} \sim \rho_{\text{neut}}/m_n = 3 \times 10^{44}$ neutrons/m³, taking neutron mass $m_n = 1.67 \times 10^{-27}$ kg, giving a latent β -decay energy density of $E_D \sim N_{\text{neut}} E_{\text{neut}} = 4 \times 10^{22}$ MJ/L (average power density $P_D \sim 2 \times 10^{19}$ MW/L during the first 15-min half-life) which is only $\sim 0.2\%$ of the neutron degeneracy energy density near the center of a neutron star. (Free neutrons released in the presence of ordinary matter could be significantly “consumed” by absorption into nearby atomic nuclei, converting the affected atoms into different isotopes.) While sometimes described as a building material in science fiction,¹⁴⁷⁶ free neutrons and decompressed neutronium are perhaps the most energy-dense fuel or explosive currently known.¹⁴⁷⁷

¹⁴⁷² Markley LC, Lindner JF. Artificial gravity field. *Results in Physics* 2013;3:24-29; <https://www.sciencedirect.com/science/article/pii/S2211379713000041>. Füzfa A. How current loops and solenoids curve spacetime. *Phys Rev D* 2016 Jan 11;93:024014; <https://arxiv.org/pdf/1504.00333.pdf>.

¹⁴⁷³ Bengtsson I, Galstyan I. Black hole lattices under the microscope. *Class Quantum Grav* 2018 Jun 19;35:145004; <https://iopscience.iop.org/article/10.1088/1361-6382/aac7e0/pdf>. Durk J, Clifton T. A quasi-static approach to structure formation in black hole universes. *J Cosmology Astroparticle Phys.* 2017 Oct;2017(10):012; <https://arxiv.org/pdf/1707.08056>.

¹⁴⁷⁴ “Imagine a sphere of di-clad neutronium, shiny with Compton-scattered light. It’s a sort of very large atomic nucleus; a billion-tons of normal matter crushed down to a diameter of three centimeters so that the protons and electrons that comprise it are bonded together into a thick neutron paste. Left to itself it would, within nanoseconds, explode back into a billion tons of protons and electrons, this time with considerable outward momentum. Hence the cladding: crystalline diamond and fibrediamond and then crystalline again, with a bound layer of wellstone on top.” Wil McCarthy, *The Collapsium*, Bantam Books, 2000, p. 5.

¹⁴⁷⁵ https://en.wikipedia.org/wiki/Neutron#Bound_neutron_decay.

¹⁴⁷⁶ e.g., Spock: “Sensors show the object’s hull is solid neutronium. A single ship cannot combat it.” From “The Doomsday Machine,” *Star Trek*, 20 Oct 1967; [https://en.wikipedia.org/wiki/The_Doomsday_Machine_\(Star_Trek:_The_Original_Series\)](https://en.wikipedia.org/wiki/The_Doomsday_Machine_(Star_Trek:_The_Original_Series)).

¹⁴⁷⁷ “The Doomsday Explosive! (The Neutronium Bomb)”, 3 Nov 2012; https://www.youtube.com/watch?v=o_EBqZPCZdw.

7.5.4.3 Quark Degenerate Matter (Quarkium)

In a neutron star, the pressure separating nucleons has been overwhelmed by gravity, causing them to become extremely densely packed neutron matter (**Section 7.5.4.2**). Because these neutrons are made of “up” and “down” quarks, it is hypothesized¹⁴⁷⁸ that under even more extreme conditions, the degeneracy pressure keeping the quarks apart within the neutrons might break down in much the same way, creating an ultra-dense phase of degenerate quarkian matter based on densely packed quarks that could be called “quarkium”,¹⁴⁷⁹ or quark matter¹⁴⁸⁰ (a degenerate Fermi gas of quarks).¹⁴⁸¹ This conversion might be confined to the neutron star’s center or it might transform the entire star into a quark star,¹⁴⁸² depending on the physical circumstances.¹⁴⁸³

At temperatures of $\sim 10^{12}$ K, or at densities high enough to make the average inter-quark separation < 1 fm (quark chemical potential ~ 400 MeV), the hadrons may melt into their constituent quarks and the strong interaction becomes the dominant feature of the physics. Energy density at the transition between the hadronic and quark phase has been estimated to fall between 0.5 - 2 GeV/fm³, or **0.8-3 x 10²⁶ MJ/L**.¹⁴⁸⁴ Quark-gluon plasma or quark soup¹⁴⁸⁵ is the high-temperature phase in which quarks become free and able to move independently in a sea of gluons (subatomic particles that transmit the strong force that binds quarks together), analogous to the liberation of electrons from atoms in a plasma.¹⁴⁸⁶ At high densities but relatively low

¹⁴⁷⁸ Ivanenko DD, Kurdgelaidze DF. Hypothesis concerning quark stars. *Astrophysics*. 1965 Oct;1(4):251-252; <https://link.springer.com/article/10.1007%2FBF01042830>. Ivanenko DD, Kurdgelaidze DF. Remarks on quark stars. *Lettere al Nuovo Cimento*. 1969;2:13-16; <https://link.springer.com/article/10.1007%2FBF02753988>.

¹⁴⁷⁹ Carruthers PA. Quarkium: A bizarre Fermi liquid. *Collect Phenom*. 1974 Jan;1(3):147-161; <https://www.osti.gov/biblio/4224519>.

¹⁴⁸⁰ https://en.wikipedia.org/wiki/QCD_matter.

¹⁴⁸¹ Ruster SB. Phase diagram of neutral quark matter at moderate densities. In: Sedrakian A; Clark JW, Alford MG, eds. *Pairing in Fermionic Systems*, World Scientific, 2007.

¹⁴⁸² https://en.wikipedia.org/wiki/Quark_star.

¹⁴⁸³ Blaschke D, Glendenning NK, Sedrakian A. *Physics of neutron star interiors*. Lecture Notes in Physics, Vol. 578, Springer, 2001. Shapiro SL, Teukolsky SA. *Black Holes, White Dwarfs and Neutron Stars: The Physics of Compact Objects*, Wiley 2008, pp. 238, 323, 325; <https://www.amazon.com/Black-Holes-White-Dwarfs-Neutron/dp/0471873179>.

¹⁴⁸⁴ Burgio GF, Baldo M, Sahu PK, Santra AB, Schulz HJ. Maximum mass of neutron stars with a quark core. *Phys Lett B*. 2002 Jan 31;526(1-2):19-26; <https://www.sciencedirect.com/science/article/pii/S0370269301014794>.

¹⁴⁸⁵ https://en.wikipedia.org/wiki/Quark%E2%80%93gluon_plasma.

¹⁴⁸⁶ https://en.wikipedia.org/wiki/State_of_matter#Quark_matter.

temperatures, quarks are theorized to form a quark liquid with a distinct color-flavor locked (CFL) phase at even higher densities that is superconductive for color charge.¹⁴⁸⁷

Strange matter¹⁴⁸⁸ is a hypothetical quark matter that contains three types of quarks (up, down, and strange), in contrast with nuclear matter¹⁴⁸⁹ (a liquid of neutrons and protons made of up and down quarks) and with non-strange quark matter¹⁴⁹⁰ (a quark liquid containing only up and down quarks). If strange matter is found to exist, strangelets (small bits of strange matter a few fm in diameter with the mass of a light nucleus)¹⁴⁹¹ are predicted to absorb neutrons exothermically without limit,¹⁴⁹² releasing ~20 MeV per neutron with photon emission,¹⁴⁹³ while converting the neutrons to more strange matter. In this scenario the neutrons become a high-energy-density nuclear fuel (possibly provided by a neutron star¹⁴⁹⁴) with specific energy $E_S \sim 20 \text{ MeV}/m_n \sim 2 \times 10^9 \text{ MJ/kg}$ and energy density $E_D \sim (20 \text{ MeV}) N_{\text{neut}} \sim 8 \times 10^{23} \text{ MJ/L}$.

So far only two quark containment modalities have been seriously proposed: (1) for conventional quark matter (containing only up/down quarks), the center of a massive neutron star;¹⁴⁹⁵ and (2) for strange matter (containing up/down/strange quarks), the “strange matter hypothesis” of Bodmer¹⁴⁹⁶ and Witten¹⁴⁹⁷ which proposes that the nuclei we see in the nuclear matter around us are actually metastable against decaying into strange matter; the lifetime for spontaneous decay is very long, so we do not see this decay process happening around us, but given enough time (or the right external stimulus) all nuclear matter would decay into strange matter. If true, strange matter would be stable at low temperature and low external pressure,¹⁴⁹⁸ forming “quark

¹⁴⁸⁷ https://en.wikipedia.org/wiki/State_of_matter#Quark_matter.

¹⁴⁸⁸ https://en.wikipedia.org/wiki/Strange_matter.

¹⁴⁸⁹ https://en.wikipedia.org/wiki/Nuclear_matter.

¹⁴⁹⁰ https://en.wikipedia.org/wiki/OCD_matter.

¹⁴⁹¹ <https://en.wikipedia.org/wiki/Strangelet>.

¹⁴⁹² Farhi E, Jaffe RL. Strange matter. Phys Rev D 1984 Dec 1;30(11):2379-2390;
http://chimera.roma1.infn.it/OMAR/dottorato/papers/jaffe_sqm_1.pdf.

¹⁴⁹³ Shaw GL, Shin M, Dalitz RH, Desai M. Growing drops of strange matter. Nature 1989;337:436-439;
<https://www.nature.com/articles/337436a0>.

¹⁴⁹⁴ Herzog M, Ropke F. Three-dimensional simulations of the burning of a neutron star to a hybrid star. COMPSTAR, Catania, 2011;
<http://agenda.ct.infn.it/event/491/session/17/contribution/37/material/slides/0.pdf>.

¹⁴⁹⁵ Burgio GF, Baldo M, Sahu PK, Santra AB, Schulz HJ. Maximum mass of neutron stars with a quark core. Phys Lett B. 2002 Jan 31;526(1-2):19-26;
<https://www.sciencedirect.com/science/article/pii/S0370269301014794>.

¹⁴⁹⁶ Bodmer AR. Collapsed nuclei. Phys Rev D 1971 Sep 15;4:1601-1606;
<http://chimera.roma1.infn.it/OMAR/dottorato/papers/bodmer.pdf>.

¹⁴⁹⁷ Witten E. Cosmic separation of phases. Phys Rev D 1984 Jul 15;30(2):272-285;
<https://journals.aps.org/prd/abstract/10.1103/PhysRevD.30.272>.

¹⁴⁹⁸ https://en.wikipedia.org/wiki/Strange_matter#Strange_matter_that_is_stable_at_zero_pressure.

nuggets¹⁴⁹⁹ that possibly could be stored in containers of ordinary matter. One paper¹⁵⁰⁰ estimates that the largest bulk strange-matter nuggets that could be supported on the Earth's surface without falling through the crust would be ~1 nm in diameter and would weigh $\sim 10^{-10}$ kg. However, at present the strange matter hypothesis remains unproven and unsupported experimentally.¹⁵⁰¹

¹⁴⁹⁹ Witten E. Cosmic separation of phases. Phys Rev D 1984 Jul 15;30(2):272-285;
<https://journals.aps.org/prd/abstract/10.1103/PhysRevD.30.272>.

¹⁵⁰⁰ Farhi E, Jaffe RL. Strange matter. Phys Rev D 1984 Dec 1;30(11):2379-2390;
http://chimera.roma1.infn.it/OMAR/dottorato/papers/jaffe_sqm_1.pdf.

¹⁵⁰¹ https://en.wikipedia.org/wiki/Strangelet#Debate_about_the_strange_matter_hypothesis.

7.5.4.4 Fully Degenerate Matter

At densities greater than those supported by any degeneracy, gravity overwhelms all other forces and a stellar body collapses to form a black hole¹⁵⁰² (in classical general relativity; **Section 8.2**) or a fuzzball¹⁵⁰³ (in string theory).

¹⁵⁰² https://en.wikipedia.org/wiki/Black_hole.

¹⁵⁰³ [https://en.wikipedia.org/wiki/Fuzzball_\(string_theory\)](https://en.wikipedia.org/wiki/Fuzzball_(string_theory)).

7.6 Antimatter

Antimatter¹⁵⁰⁴ is a material composed of the antiparticles of the corresponding particles of ordinary matter. Particles and their antiparticles have different signs on all charges (e.g., electric charge, spin, magnetic moment, etc.) but otherwise have identical masses, decay lifetimes (if unstable), optical spectrum,¹⁵⁰⁵ response to gravity (probably),¹⁵⁰⁶ and so forth.

Section 7.6.1 describes the energy potentially available from the annihilation of ordinary matter with antimatter. The rest of this Section covers energy density in antiparticles and antielements (**Section 7.6.2**) and “onium” atoms (**Section 7.6.3**), with antimatter storage briefly considered in **Section 7.6.4**.

¹⁵⁰⁴ <https://en.wikipedia.org/wiki/Antimatter>.

¹⁵⁰⁵ “ALPHA observes light spectrum of antimatter for first time,” CERN News, 19 Dec 2016; <https://home.cern/news/news/experiments/alpha-observes-light-spectrum-antimatter-first-time>.

¹⁵⁰⁶ Kalaydzhyan T. Gravitational mass of positron from LEP synchrotron losses. Sci Reports 2016 Jul 27;6(30461); <https://www.nature.com/articles/srep30461>. Kalaydzhyan T. Gravitational mass of relativistic matter and antimatter. Phys Lett B. 2015 Dec 17;751:29-33; <https://www.sciencedirect.com/science/article/pii/S0370269315007650>.

7.6.1 Annihilation Energy

Annihilation¹⁵⁰⁷ is the process that occurs when a subatomic particle collides with its respective antiparticle to produce other particles. The simplest example is an electron (e^-) colliding with a positron (e^+) to produce two photons. The total energy and momentum of the initial pair are conserved in the annihilation process and are distributed among a set of other particles in the final state. A particle and its antiparticle annihilate when they meet – they disappear and their kinetic plus rest-mass energy is converted into other particles ($E = mc^2$).¹⁵⁰⁸ For example, when an electron and a positron annihilate at rest, two gamma rays, each with energy 0.511 MeV, are produced and go off in opposite directions because both energy and momentum must be conserved. Similarly, when a proton (p^+) and an antiproton (p^-) annihilate at rest, other particles are usually produced (see below) but the total kinetic plus rest mass energies of these products adds up to twice the rest mass energy of the proton (2×938.27 MeV) or 1876.5 MeV.

The maximum specific energy that can be derived from matter-antimatter annihilation is $E_{S,max} = mc^2/m = c^2 \sim \mathbf{9 \times 10^{10} \text{ MJ/kg}}$,¹⁵⁰⁹ where m is the total annihilated mass. If packed to the density of ordinary solid matter ($\rho_{normal} \sim 1000 \text{ kg/m}^3 = 1 \text{ kg/L}$), then $E_{D,max} = E_{S,max} \rho_{normal} \sim \mathbf{9 \times 10^{10} \text{ MJ/L}}$; if packed to the maximum possible nuclear density of neutronium ($\rho_{neut} \sim 5 \times 10^{17} \text{ kg/m}^3$; **Section 7.5.4.2**), then $E_{D,neut} = E_{S,max} \rho_{neut} \sim \mathbf{5 \times 10^{25} \text{ MJ/L}}$.

In the case of electron-positron annihilation, the reaction product is pure gamma ray photons which can in principle be collected (e.g., by gammavoltaic devices; **Section 7.1**) and employed to do useful work:



Lepton-antilepton collisions (i.e., electrons, muons, and tauons, with their antiparticles) are among the few annihilation reactions that can produce only gamma rays, thus achieving the maximum specific energy of $E_{S,e-p} \sim \mathbf{9 \times 10^{10} \text{ MJ/kg}}$. These are the only examples of true “total conversion” of matter into energy that has been experimentally demonstrated to date.¹⁵¹⁰ Annihilation reactions involving quark-containing mesons¹⁵¹¹ or hadrons¹⁵¹² usually generate neutrinos or antineutrinos that reduce the attainable specific energy available from antimatter reactions because neutrinos don’t feel the strong force or the electromagnetic force, hence are not readily trapped in energy collectors composed of ordinary matter.

¹⁵⁰⁷ <https://en.wikipedia.org/wiki/Annihilation>.

¹⁵⁰⁸ “Antimatter”; <https://www2.lbl.gov/abc/Antimatter.html>.

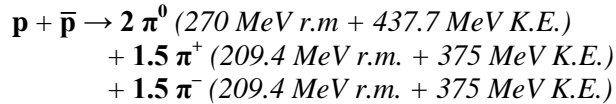
¹⁵⁰⁹ The exact number is $8.987\ 551\ 787 \times 10^{10}$ MJ/kg; https://en.wikipedia.org/wiki/Speed_of_light.

¹⁵¹⁰ An electron and positron at rest can only annihilate into two photons, whereas a muon and antimuon have enough mass-energy to create either two photons or an electron-positron pair when they annihilate.

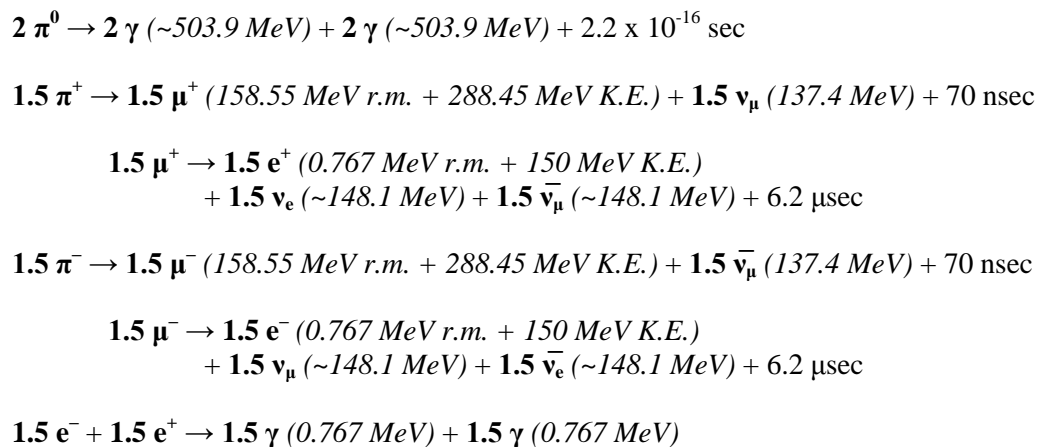
¹⁵¹¹ <https://en.wikipedia.org/wiki/Meson>.

¹⁵¹² <https://en.wikipedia.org/wiki/Hadron>.

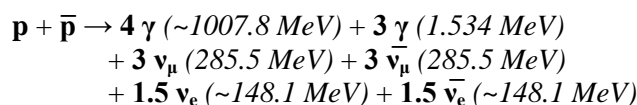
For example, in the case of a zero-velocity proton-antiproton annihilation, a cascade of multiple leptons and mesons may share the total energy and momentum; but the newly created mesons are unstable, and unless they encounter and interact with some other material, they will decay in a series of secondary reactions that ultimately produce only gamma rays, electrons and positrons (which can annihilate to make more gamma rays), and neutrinos.¹⁵¹³ The annihilation reaction:



yields 1876.5 MeV, where “r.m.” designates rest mass energy and “K.E.” designates kinetic energy for each particle, but the secondary particle decays and annihilation reactions break down as follows:¹⁵¹⁴



which nets out to:



or ~1009.3 MeV of gamma ray photons (53.8%) and ~867.2 MeV of neutrinos (ν) and antineutrinos ($\bar{\nu}$) (46.2%). The significant amount of energy that goes into neutrinos and antineutrinos is likely lost because these particles interact very little with ordinary matter making their energy very difficult to collect – thus reducing the maximum available specific energy for the proton-antiproton annihilation reaction to $E_{s,p-ap} = 4.8 \times 10^{10} \text{ MJ/kg}$ with at most 53.8% conversion efficiency. The annihilation of heavier particle-antiparticle combinations generally produces more complex particle cascades with additional intermediates and decay pathways.

¹⁵¹³ https://en.wikipedia.org/wiki/Annihilation#Proton-antiproton_annihilation.

¹⁵¹⁴ Michael R. LaPointe, “Antiproton powered propulsion with magnetically confined plasma engines,” NASA Contractor Report 185131 (N89-27700), AIAA-89-2334, Aug 1989; <https://ntrs.nasa.gov/archive/nasa/casi.ntrs.nasa.gov/19890018329.pdf>.

These pathways are even more tedious to analyze than the simplest proton-antiproton interaction outlined above – which is, nevertheless, fairly representative.

Current particle accelerators have an abysmal 0.000002% efficiency in converting electricity into antimatter,¹⁵¹⁵ but the theoretical maximum efficiency of converting electricity into antimatter is 50% due to the Law of Baryon Number Conservation¹⁵¹⁶ which demands that equal amounts of matter and antimatter must be created when turning energy into matter.

¹⁵¹⁵ http://www.projectrho.com/public_html/rocket/antimatterfuel.php.

¹⁵¹⁶ <https://www.nuclear-power.net/laws-of-conservation/law-conservation-baryon-number/>,
https://en.wikipedia.org/wiki/Baryon_number#Conservation.

7.6.2 Antiparticles and Antielements

A wide range of particles can undergo partial or total annihilation reactions, including (mostly) stable antiparticles and antielements such as:

Antielectron.¹⁵¹⁷ Antielectrons (positrons) annihilate with electrons (see above) and are readily produced experimentally.¹⁵¹⁸

Antiproton. Antiprotons annihilate with protons (see above), whether those protons are isolated or part of the nucleus of an atom. For instance, antiprotons impinging on uranium atoms trigger fission nearly 100% of the time, releasing 180 MeV of fission fragment energy in the target.¹⁵¹⁹ CERN facilities are capable of producing ten million antiprotons per minute.¹⁵²⁰ An antiproton stopped in ordinary matter usually annihilates on an ordinary nucleus within picoseconds.

Antineutron. Antineutrons annihilate with neutrons and were first observed experimentally in 1956.¹⁵²¹

Antihydrogen,¹⁵²² consisting of a positron orbiting an antiproton (p^-e^+), is the simplest antiatom. Upon contact with protium (hydrogen) or other ordinary matter, antihydrogen annihilates with the release of high-energy pions that quickly decay into muons, neutrinos, positrons, and electrons, and ultimately just photons and neutrinos. Low-energy “cold” antihydrogen atoms¹⁵²³ have been produced experimentally since 2002.¹⁵²⁴ Antihydrogen atoms suspended in a perfect vacuum should be stable indefinitely; lacking a perfect vacuum, in 2010 up to 38 antihydrogen atoms were Penning-trapped together for 0.172 sec,¹⁵²⁵ and in 2011 a shifting population of 3

¹⁵¹⁷ <https://en.wikipedia.org/wiki/Positron>.

¹⁵¹⁸ https://en.wikipedia.org/wiki/Positron#Artificial_production.

¹⁵¹⁹ Smith G. Excitation of nuclei by antiproton annihilation at rest. AFOSR-91-0302, 30 Jul 1992; <http://www.dtic.mil/get-tr-doc/pdf?AD=ADA255447>.

¹⁵²⁰ Madsen N. Cold antihydrogen: a new frontier in fundamental physics. *Phil Trans Royal Soc A*. 2010 Aug 13;368(1924):3671-82; <http://citeseerx.ist.psu.edu/viewdoc/download?doi=10.1.1.664.3821&rep=rep1&type=pdf>.

¹⁵²¹ <https://en.wikipedia.org/wiki/Antineutron>.

¹⁵²² <https://en.wikipedia.org/wiki/Antihydrogen>.

¹⁵²³ https://en.wikipedia.org/wiki/Antihydrogen#Low-energy_antihydrogen.

¹⁵²⁴ Madsen N. Cold antihydrogen: a new frontier in fundamental physics. *Phil Trans Royal Soc A*. 2010 Aug 13;368(1924):3671-82; <http://citeseerx.ist.psu.edu/viewdoc/download?doi=10.1.1.664.3821&rep=rep1&type=pdf>.

¹⁵²⁵ Andresen GB, *et al*. Trapped antihydrogen. *Nature*. 2010 Dec 2;468(7324):673-676; http://www2.mpg.de/~rnp/download/Is1415/papers/ALPHA_2010_Trapped_antihydrogen.pdf.

antihydrogen atoms at a time were trapped for up to 1000 sec.¹⁵²⁶ By 2018, one group of researchers at CERN's Antihydrogen Laser Physics Apparatus (ALPHA) reported being able to accumulate ~500 antihydrogen atoms in a trap and holding them there for ~2 hours.¹⁵²⁷

Antideuterium,¹⁵²⁸ consisting of a positron orbiting an antideuteron nucleus, has not yet been produced experimentally, though antideuterons were first created in 1965.¹⁵²⁹

Antitritium – there are unconfirmed claims of experimental observation of the antitritium nucleus¹⁵³⁰ in Russian journals from 1974.

Antihelium.¹⁵³¹ Antihelium-3 nuclei were first observed in the 1970s¹⁵³² and later created in nucleus-nucleus collision experiments.¹⁵³³ Observation of artificially created antihelium-4 nuclei (anti-alpha particles, containing 2 antiprotons and 2 antineutrons) was first reported in 2011.¹⁵³⁴

¹⁵²⁶ Andresen GB, *et al.* Confinement of antihydrogen for 1,000 seconds. *Nature Physics*. 2011 Jul;7(7):558-564; <https://arxiv.org/ftp/arxiv/papers/1104/1104.4982.pdf>.

¹⁵²⁷ Ahmadi M, *et al.* Observation of the 1S-2P Lyman- α transition in antihydrogen. *Nature* 2018 Sep;561(7722):211–215; <https://www.nature.com/articles/s41586-018-0435-1>. “Excited atoms throw light on anti-hydrogen research,” *Phys.org*, 22 Aug 2018; <https://phys.org/news/2018-08-atoms-anti-hydrogen.html>.

¹⁵²⁸ <https://en.wikipedia.org/wiki/Deuterium#Antideuterium>.

¹⁵²⁹ Massam T, Muller Th, Righini B, Schneegans M, Zichichi A. Experimental observation of antideuteron production. *Il Nuovo Cimento*. 1965 Sep;63(1):10-14; <https://link.springer.com/article/10.1007%2FBF02898804>. Dorfan DE, Eades J, Lederman LM, Lee W, Ting CC. Observation of Antideuterons. *Phys. Rev. Lett.* 1965 Jun 14;14(24):1003-1006; <https://journals.aps.org/prl/abstract/10.1103/PhysRevLett.14.1003>.

¹⁵³⁰ Vishnevskij NK, *et al.* Observation of the antitritium nuclei. *Yadernaya Fizika* 1974;20(4):694-708; https://inis.iaea.org/search/search.aspx?orig_q=RN:6184051. Poze D. Observation of antitritium nuclei. *Joint Inst. for Nuclear Research, Dubna (USSR)*; p. 150-163; 1974; 3. international symposium on high energy and elementary particle physics; Sinaia, Romania; 2 Oct 1973; https://inis.iaea.org/search/search.aspx?orig_q=RN:6170749. Baldin BY, *et al.* Observation of antitritium. *Yad. Fiz.* 1974 Apr 3; <http://cds.cern.ch/record/415673>. “In the steps of the proton,” *CERN Courier*, Sep 2015, pp. 21-26; <http://cds.cern.ch/record/2232492/files/vol55-issue7-p021-e.pdf>

¹⁵³¹ <https://en.wikipedia.org/wiki/Antimatter#Antihelium>.

¹⁵³² Antipov YM, *et al.* Observation of antihelium3 (in Russian). *Yadernaya Fizika*. 1974;12:311.

¹⁵³³ Arsenescu R, *et al.* Antihelium-3 production in lead–lead collisions at 158 A GeV/c. *New Journal of Physics*. 2003;5(1):1; <https://iopscience.iop.org/article/10.1088/1367-2630/5/1/301/pdf>.

¹⁵³⁴ Agakishiev H, *et al.* Observation of the antimatter helium-4 nucleus. *Nature*. 2011;473(7347):353-356; <https://arxiv.org/pdf/1103.3312>.

These experimental results provide proof that antimatter can bind together in stable clusters just like ordinary matter. Complete antihelium atoms (with 2 orbiting positrons) have yet to be created.

Antihelium is the heaviest antinucleus made to date, though in principle heavier nuclei and entire whole atoms could be created and, in a perfect vacuum, should behave just like their ordinary matter counterparts.

Each of the above antiatoms or antielements, if brought into contact with their matter equivalent, will annihilate, ultimately producing a mixture of energetic photons, neutrinos, and antineutrinos after everything is fully decayed. They would probably also partially annihilate if brought into contact with any other form of ordinary matter.

7.6.3 Onium Atoms

An onium¹⁵³⁵ is an exotic atom consisting of a particle and its antiparticle in a bound state, but these atoms generally annihilate themselves in too short a time to be useful for energy storage:

Positronium¹⁵³⁶ – a positron orbiting an electron. The singlet state has a lifetime of 0.000125 μsec , the triplet state has a lifetime of 0.142 μsec , and the ^2S state has a lifetime of 1.1 μsec . All three decay via self-annihilation with photon emission, releasing 1.022 MeV total with a specific energy of $E_s \sim 9 \times 10^{10} \text{ MJ/kg}$, the maximum amount for cold (low-velocity) particles. The storage lifetime is likely too short for a practical energy storage system. The **positronium negative ion** Ps^- ($e^-e^+e^-$), aka. “heavy positronium”, has a measured self-annihilation lifetime of 0.0005 μsec .¹⁵³⁷ the exotic molecule **dipositronium**¹⁵³⁸ (Ps_2) has also been fleetingly observed.¹⁵³⁹

Protonium¹⁵⁴⁰ – an antiproton orbiting a proton; an antiprotonic or hadronic atom.¹⁵⁴¹ Protonium has been observed experimentally¹⁵⁴² and is believed to have a self-annihilation lifetime of 0.1-10 μsec .¹⁵⁴³

Antiprotonic helium¹⁵⁴⁴ – an antiproton and an electron orbiting an ordinary helium nucleus. The observed lifetime of an antiprotonic helium-4 atom ($\bar{p}^4\text{He}^+$) is $\sim 1 \mu\text{sec}$,¹⁵⁴⁵ and similarly for

¹⁵³⁵ <https://en.wikipedia.org/wiki/Onium>.

¹⁵³⁶ <https://en.wikipedia.org/wiki/Positronium>.

¹⁵³⁷ Mills AP Jr. Measurement of the decay rate of the positronium negative ion. Phys Rev Lett. 1983 Feb 28;50(9):671-674;

<https://positron.ucr.edu/publications/1983measurementofthedecayrateofthepositroniumnegativeion.pdf>.

Fleisch F, *et al.* Measurement of the Decay Rate of the Negative Ion of Positronium (Ps^-). Phys Rev Lett. 2006 Feb 17;96(6):063401; <https://journals.aps.org/prl/abstract/10.1103/PhysRevLett.96.063401>.

¹⁵³⁸ <https://en.wikipedia.org/wiki/Di-positronium>.

¹⁵³⁹ Cassidy DB, Mills AP Jr. The production of molecular positronium. Nature 2007 Sep 13;449:195-7;

<https://positron.ucr.edu/publications/2007/2007theproductionofmolecularpositronium.pdf>.

¹⁵⁴⁰ <https://en.wikipedia.org/wiki/Protonium>.

¹⁵⁴¹ https://en.wikipedia.org/wiki/Exotic_atom#Hadronic_atoms.

¹⁵⁴² Zurlo N, *et al.* Production of slow protonium in vacuum. Hyperfine Interactions. 2006;172(1-3):97-105; <https://arxiv.org/pdf/0801.3193>.

¹⁵⁴³ <https://en.wikipedia.org/wiki/Protonium#Studies>.

¹⁵⁴⁴ https://en.wikipedia.org/wiki/Antiprotonic_helium.

¹⁵⁴⁵ Hayano RS. Spectroscopy of antiprotonic helium atoms and its contribution to the fundamental physical constants. Proc Jpn Acad Ser B Phys Biol Sci. 2010 Jan;86(1):1-10; <https://www.ncbi.nlm.nih.gov/pmc/articles/PMC3417566/>.

the antiprotonic helium-3 atom ($\bar{p}^3\text{He}^+$) atom;¹⁵⁴⁶ the lifetime of a cold antiprotonic helium ion (the electron has been removed) is $\sim 0.1 \mu\text{sec}$.¹⁵⁴⁷

Antiprotonic lithium – an antiproton and two electrons orbiting an ordinary lithium nucleus. Antiprotonic lithium has been observed experimentally,¹⁵⁴⁸ also with a lifetime in the $\sim \mu\text{sec}$ range.¹⁵⁴⁹

Hydrogen-antihydrogen molecule. The hypothetical hydrogen-antihydrogen molecule ($p^+e^- - p^-e^+$) has no stable bound state and must decay into protonium (p^+p^-) and positronium (e^-e^+); the hypothetical **muonium-antimuonium molecule** ($\mu^+e^- - \mu^-e^+$) is also unstable.¹⁵⁵⁰

True muonium, a muon and antimuon orbiting each other ($\mu^+\mu^-$), has yet to be observed but may have been generated in the collision of energetic electron and positron beams.¹⁵⁵¹ Its annihilation lifetime is estimated as 0.602×10^{-12} sec in the 1S_0 state (decaying to $\gamma\gamma$) and 1.81×10^{-12} sec in the 3S_1 state (decaying to e^+e^-).¹⁵⁵² The corresponding estimated annihilation lifetimes of **true tauonium** ($\tau^+\tau^-$) are only 0.0358×10^{-12} sec and 0.107×10^{-12} sec.¹⁵⁵³

Pionium is an experimentally observed bound state of a pion and an antipion ($\pi^+\pi^-$), decaying into two neutral pions ($2\pi^0$) in a lifetime of 2.89×10^{-15} sec.¹⁵⁵⁴

Kaonium is a hypothetical bound state of a kaon and an antikaon (K^+K^-), with a predicted lifetime of only $\sim 10^{-18}$ sec.¹⁵⁵⁵

¹⁵⁴⁶ Hori M, Sótér A, Barna D, Dax A, Hayano R, Friedreich S, Juhász B, Pask T, Widmann E, Horváth D, Venturelli L, Zurlo N. Two-photon laser spectroscopy of antiprotonic helium and the antiproton-to-electron mass ratio. *Nature*. 2011 Jul 27;475(7357):484-8; http://www.rmki.kfki.hu/sites/www.rmki.kfki.hu/files/documents/nature_2photon.pdf.

¹⁵⁴⁷ https://en.wikipedia.org/wiki/Antiprotonic_helium#Antiprotonic_helium_ions.

¹⁵⁴⁸ Sakimoto K. Long-lived states of antiprotonic lithium $p\text{Li}^+$ produced in $p^+\text{Li}$ collisions. *Phys Rev A*. 2011 Sep 2;84:032501; [http://antimatter.isas.jaxa.jp/publication/reprint/pa84\(2011\)032501.pdf](http://antimatter.isas.jaxa.jp/publication/reprint/pa84(2011)032501.pdf).

¹⁵⁴⁹ Ahlrichs R, Dumbrajs O, Pilkuhn H, Schlaile HG. Antiprotonic helium and lithium with one or two electrons. *Zeitschrift für Physik A Atoms and Nuclei* 1982 Dec;306(4):297-300; <https://link.springer.com/article/10.1007/BF01432369>.

¹⁵⁵⁰ Gridnev DK, Greiner C. Proof that the hydrogen-antihydrogen molecule is unstable. *Phys Rev Lett*. 2005 Jun 10;94(22):223402; <https://arxiv.org/pdf/math-ph/0502029.pdf>.

¹⁵⁵¹ <https://en.wikipedia.org/wiki/Muonium#Nomenclature>.

¹⁵⁵² Brodsky SJ, Lebed RF. Production of the smallest QED atom: True muonium ($\mu^+\mu^-$). *Phys Rev Lett*. 2009;102(21):213401; <https://arxiv.org/pdf/0904.2225.pdf>.

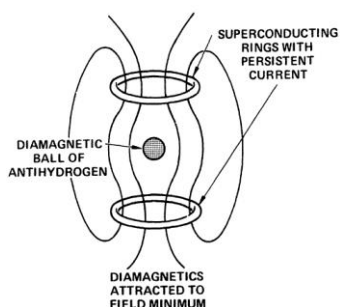
¹⁵⁵³ Brodsky SJ, Lebed RF. Production of the smallest QED atom: True muonium ($\mu^+\mu^-$). *Phys Rev Lett*. 2009;102(21):213401; <https://arxiv.org/pdf/0904.2225.pdf>.

¹⁵⁵⁴ <https://en.wikipedia.org/wiki/Pionium>.

¹⁵⁵⁵ <https://en.wikipedia.org/wiki/Kaonium>.

7.6.4 Antimatter Energy Storage

One of the most significant drawbacks to antimatter-based energy storage systems and antimatter rockets¹⁵⁵⁶ is the great difficulty in storing the antimatter component for subsequent or metered usage. Traditional antimatter such as molecular antihydrogen¹⁵⁵⁷ (a gas at room temperature) or antilithium antihydride (a diamagnetic ionic solid at room temperature) would annihilate on contact if stored in a container made of ordinary matter. Laser-pressure containment or magnetic confinement of charged antiprotons inside a completely evacuated vessel might suffice. Liquid or solid antihydrogen is diamagnetic, so levitation within a confining vessel could be provided by a magnet of modest size.¹⁵⁵⁸ Ionized molecular antihydrogen would be stable if formed and could be controlled and manipulated via magnetic, electrostatic, or RF techniques.¹⁵⁵⁹ Earnshaw's theorem¹⁵⁶⁰ proves that no set of static charges can be used to create a stable trap (they can only create a metastable trap), so nonstationary dynamic fields, as in a Penning Trap,¹⁵⁶¹ must be used.



Levitation of neutral antihydrogen ice would depend on its form – orthohydrogen (spins parallel) or parahydrogen (spins antiparallel) – as the latter is diamagnetic and might be stably levitated in a static field (image, left) as has been demonstrated with graphite of similar diamagnetic susceptibility.¹⁵⁶² According to one Masters Thesis written on the subject for a military audience: “If vacuum-chamber pressures as low as 10^{-18} torr can be reached ... milligram quantities of solid antimatter could be stored indefinitely at 1.5 K using cooling powers of less than a microwatt. The system

modeled is a sphere of solid anti-parahydrogen levitated in a spherical cryogenic vacuum chamber.”¹⁵⁶³ Active electrostatic levitation with feedback position control would require charging of the ice particles, e.g., by irradiation with UV light. An analogous trap has been

¹⁵⁵⁶ https://en.wikipedia.org/wiki/Antimatter_rocket.

¹⁵⁵⁷ Forward RL. Antiproton Annihilation Propulsion - Final Report. U.S. Air Force Rocket Propulsion Laboratory, AFRPL TR-85-034/055, 1985.

¹⁵⁵⁸ Paine CG, Seidel GM. Magnetic levitation of condensed hydrogen. Rev Sci Instrum. 1991;62(12):3022-3024; <https://aip.scitation.org/doi/abs/10.1063/1.1142148>.

¹⁵⁵⁹ Perkins LJ. Antiproton fast ignition for inertial confinement fusion. Lawrence Livermore National Laboratory, UCRL-ID-128923, 24 Oct 1997; <https://e-reports-ext.llnl.gov/pdf/232381.pdf>.

¹⁵⁶⁰ http://en.wikipedia.org/wiki/Earnshaw%27s_theorem.

¹⁵⁶¹ https://en.wikipedia.org/wiki/Penning_trap.

¹⁵⁶² Waldron RD. Diamagnetic levitation using pyrolytic graphite. Rev Sci Instr. 1966;37:29; <https://aip.scitation.org/doi/abs/10.1063/1.1719946>.

¹⁵⁶³ Michael J. MacLachlan, “Parametric Study of Radiative Cooling of Solid Antihydrogen,” Air Force Institute of Technology, AD-A206092, Mar 1989; <https://apps.dtic.mil/dtic/tr/fulltext/u2/a206092.pdf>.

constructed at JPL¹⁵⁶⁴ and has levitated a 20 mg ball of H₂O ice in the Earth's gravitational field.¹⁵⁶⁵

Another proposal by L. Serni¹⁵⁶⁶ for “safe” storage is that it may be possible “to create a structure¹⁵⁶⁷ (Dehmelt-Paul lattice)¹⁵⁶⁸ capable of trapping antimatter ions in a charged ionic lattice. Building it would require extreme tolerances, and the anti-ions' thermal energy must be lower enough than the lattice constraints that the lattice itself doesn't implode. We could imagine a metamaterial where a positively charged lattice held free antiprotons in crystal-like “cells” at room temperature for an indefinite time. When heated (e.g., by a laser), the lattice would start collapsing and freeing antiprotons towards the laser itself; these could be electrically accelerated and used to trigger a controlled series of annihilations. You would get lots of radiation and a staggering amount of thermal energy.... Once the nature of the magic crystals is discovered (that they are about 5% antimatter in mass), to exploit them you only need a tuned laser and to be able to control an electric field.... The crystals also double as fearsome weapons – crush a crystal with a powerful enough explosive, and enough of it will fracture and start an antimatter explosion, vaporizing the remainder of the crystal and instantly triggering an even larger reaction.” At 5% antimatter by weight, the specific energy of the loaded crystal might be of the order $E_{S,crystal} \sim 0.05 E_{S,p-ap} = 2.4 \times 10^9 \text{ MJ/kg}$. Other authors have addressed the possibility of designing a solid-state containment system that will safely hold antimatter in quantities dense enough to be of engineering utility.¹⁵⁶⁹

Another intriguing idea is the 1978 description of hypergolic antimatter by Freund and Hill:¹⁵⁷⁰ “Our proposal is based on the existence of two new, virtually stable, forms of matter that annihilate each other with enormous energy release, but neither of which annihilates ordinary

¹⁵⁶⁴ Rhim W. Development of an Electrostatic Levitator at JPL. In: Rindone G, ed., Material Processing in the Reduced Gravity Environment of Space, Elsevier, 1982, p. 115.

¹⁵⁶⁵ The vapor pressure of antihydrogen drops precipitously once the ice ball is cooled below 4 K, but even at a fraction above 0 K some antiatoms will evaporate off the ice ball, creating radiant heat when they strike the containment chamber walls. Molecules of ordinary matter can also be knocked off of the chamber walls and will create heat when they drift over and hit the antimatter ice ball. There is also the background flux of cosmic rays. These rays are made of matter and can easily penetrate the chamber and hit the ice ball. Hence the antimatter will have to be cooled, and with passive cooling, since active cooling won't work when the coolant is ordinary matter and the item to be cooled is antimatter.

http://www.projectrho.com/public_html/rocket/antimatterfuel.php.

¹⁵⁶⁶ <https://worldbuilding.stackexchange.com/questions/79194/high-energy-density-radioactive-materials-not-commonly-found-on-earth>.

¹⁵⁶⁷ https://en.wikipedia.org/wiki/Penning_trap.

¹⁵⁶⁸ <https://physics.aps.org/articles/v6/113>.

¹⁵⁶⁹ Rejcek JM, Browder MK, Fry JL, Koymen A, Weiss AH. Alternative pathways to antimatter containment. Radiation Physics and Chemistry 2003 Oct-Nov;68(3-4):655-661; <https://www.sciencedirect.com/science/article/abs/pii/S0969806X03001956>.

¹⁵⁷⁰ Freund PGO, Hill CT. A possible practical application of heavy quark physics. Nature 1978 Nov 16;276:250; <https://www.nature.com/articles/276250a0>.

matter (and can thus be stored easily).” Key to the proposal is the hypothetical existence of two stable hadrons – a $\bar{b}u$ meson they call M^+ [mass $\sim 4182 \text{ MeV}/c^2$] and a bu baryon they call B^+ . [mass $\sim 4185 \text{ MeV}/c^2$]. The authors then note: “(1) Neither M^+ nor B^+ contain \bar{u} or \bar{d} antiquarks and therefore do not annihilate ordinary matter. (2) The positively charged hadrons M^+ and B^+ can form hydrogenoid atoms, which we denote $M(M^+e^-)$ and $B(B^+e^-)$, with ordinary negative electrons. These electrically neutral atoms are stable and, as they contain electrons rather than positrons, they do not annihilate ordinary matter either. Hence they may participate in ordinary chemical reactions. (3) M^+ contains one \bar{b} antiquark but B^+ contains one b quark, so that M^+ can annihilate with B^+ . Assum[ing] stable M^+ and B^+ , the resulting hydrogenoid gases M_2 and B_2 may be stored in conventional containers and transported separately, or the compound MB may be formed and transported itself. These two new forms of matter M and B can be induced to annihilate with considerable release of energy....Stable quarks would, therefore, offer the possibility of storing very powerful energies within small volumes.” The b quark and the \bar{b} antiquark have a mass of $\sim 4180 \text{ MeV}/c^2$,¹⁵⁷¹ so the annihilation of two bottom quarks would release $\sim 8360 \text{ MeV}$ from each $M+B$ reaction of reactant mass $\sim 8367 \text{ MeV}/c^2$, giving a specific energy of $E_s \sim (1.35 \times 10^9 \text{ J}) / (1.49 \times 10^{-26} \text{ kg}) = \mathbf{9 \times 10^{10} \text{ MJ/kg}}$.¹⁵⁷²

Another amusing idea for antimatter collection and storage, albeit at only modest density, is the proposal to use the Van Allen radiation belt (created by the Earth’s magnetic field) to confine naturally-occurring 60-750 MeV antiparticles.¹⁵⁷³ The magnetic fields of Jupiter and Saturn are also viewed as possible antiproton sources to be harvested.¹⁵⁷⁴

¹⁵⁷¹ https://en.wikipedia.org/wiki/Quark#Table_of_properties.

¹⁵⁷² After more than 4 decades of further research following this 1978 proposal, it now appears that the two specified hadrons may not be stable, at least as isolated particles. The u or bottom Sigma (Σ_b^+) baryon (https://en.wikipedia.org/wiki/Sigma_baryon) is estimated to decay in 5.7×10^{-23} sec as calculated in 2012 from the resonance width (<http://pdg.lbl.gov/2013/listings/rpp2013-list-sigmab-star.pdf>), and the $u\bar{b}$ B^+ meson (https://en.wikipedia.org/wiki/B_meson) is estimated to decay in 1.6×10^{-12} sec as calculated in 2014 (<http://pdg.lbl.gov/2014/listings/rpp2014-list-B-plus-minus.pdf>) from earlier measurements. It also seems unlikely that adding an electron to the indicated baryon or meson will significantly increase particle lifetime, since, e.g., the lifetime of a muon (μ^+) and muonium (μ^+e^-) differ only by 1 part in 10^9 ; Czarnecki A, Lepage GP, Marciano WJ. Muonium decay. Phys Rev D 2000 Feb 17;61:073001; <https://arxiv.org/pdf/hep-ph/9908439.pdf>.

¹⁵⁷³ https://en.wikipedia.org/wiki/Van_Allen_radiation_belt#Antimatter_confinement.

¹⁵⁷⁴ James Bickford, Extraction of Antiparticles Concentrated in Planetary Magnetic Fields, NIAC Phase II, Year 1 Report, Draper Laboratory, August 2007; http://www.centauri-dreams.org/wp-content/Bickford_Phase_II.pdf.

Chapter 8. Gravitational Energy Storage

As far as we know, all objects in the universe that are composed of matter, antimatter, or energy experience the force of gravity. Gravity is perhaps the most “universal” force (though also the weakest), and hence may be widely applicable to energy storage.

Masses located near other masses, and masses orbiting or exhibiting constrained movement near other masses, create a gravitational potential that can be harnessed to store energy. Ordinary matter employed in this way can store only modest densities of energy (**Section 8.1**), but fully-degenerate matter can achieve extremely high energy storage densities (**Section 8.2**), and there may be some other unusual possibilities (**Section 8.3**).¹⁵⁷⁵

Gravitational energy storage is widely employed as a power source¹⁵⁷⁶ in mechanical clocks;¹⁵⁷⁷ in pumped-storage hydroelectricity;¹⁵⁷⁸ in raised-weight hydraulic accumulators;¹⁵⁷⁹ in counterweights for lifting elevators,¹⁵⁸⁰ cranes,¹⁵⁸¹ seabed winches,¹⁵⁸² bridges,¹⁵⁸³ and ski lifts;¹⁵⁸⁴ in energy storage schemes employing active mass transfer between different altitudes;¹⁵⁸⁵ in transportation systems to partially reclaim energy lost when traversing hills and valleys;¹⁵⁸⁶ in amusement park rides such as roller coasters;¹⁵⁸⁷ and in spacecraft exploiting tether-based orbit alteration¹⁵⁸⁸ or the gravitational slingshot maneuver.¹⁵⁸⁹

¹⁵⁷⁵ For example, Jupiter’s metallic layer is 90% H, 10% He, and well mixed. If all the helium could be induced to form droplets, fall as rain, and settle out on the bottom, with the lighter-atom H above and the heavier-atom He in a layer below it, this would release gravitational energy on the order of 3×10^{34} joules. If 10% of Jovian mass ($\sim 1.9 \times 10^{26}$ kg) settles out as “rain” as proposed here, then the energy density of this **gravitational rain** would be $E_D \sim (3 \times 10^{34} \text{ J}) / (1.9 \times 10^{26} \text{ kg}) = \mathbf{158 \text{ MJ/kg}}$. Salpeter EE. On convection and gravitational layering in Jupiter and in stars of low mass. *Astrophys J Lett* 1973;181:L83-L86; http://adsbit.harvard.edu/cgi-bin/nph-iarticle_query?1973ApJ...181L..83S&classic=YES.

¹⁵⁷⁶ https://en.wikipedia.org/wiki/Gravity_battery.

¹⁵⁷⁷ https://en.wikipedia.org/wiki/Clock#Power_source.

¹⁵⁷⁸ https://en.wikipedia.org/wiki/Pumped-storage_hydroelectricity.

¹⁵⁷⁹ https://en.wikipedia.org/wiki/Hydraulic_accumulator#Raised_weight.

¹⁵⁸⁰ <https://en.wikipedia.org/wiki/Counterweight>.

¹⁵⁸¹ <https://qz.com/1355672/stacking-concrete-blocks-is-a-surprisingly-efficient-way-to-store-energy/>.

¹⁵⁸² <http://www.stratosolar.com/gravity-energy-storage.html>.

¹⁵⁸³ https://en.wikipedia.org/wiki/Vertical_lift_bridge.

¹⁵⁸⁴ <https://web.archive.org/web/20180329054215/https://www.bloomberg.com/news/print/2012-08-27/ski-lifts-help-open-25-billion-market-for-storing-power-energy.html>.

¹⁵⁸⁵ <https://www.aresnorthamerica.com/grid-scale-energy-storage>, <http://fortune.com/2016/05/22/energy-storing-train-nevada/>.

¹⁵⁸⁶ https://en.wikipedia.org/wiki/Potential_energy#Uses.

¹⁵⁸⁷ https://en.wikipedia.org/wiki/Roller_coaster#Mechanics.

¹⁵⁸⁸ Landis GA, Hrach FJ. Satellite Relocation by Tether Deployment. NASA Technical Memorandum 101992, Apr 1989; <https://ntrs.nasa.gov/archive/nasa/casi.ntrs.nasa.gov/19890017506.pdf>.

¹⁵⁸⁹ https://en.wikipedia.org/wiki/Gravity_assist.

8.1 Masses, Orbits, and Pendulums

Gravitational energy may be stored by forcibly separating two masses in space. This requires work that increases the potential energy stored in the mutual gravitational attraction between the two bodies. The stored potential energy can then be released from storage by removing the separating restraint and allowing the two masses to approach each other once again, converting potential into kinetic energy. The change in potential energy stored in two spherical masses m_1 and m_2 of radius r_1 and r_2 whose opposing surfaces are separated by a distance X is:

$$\Delta E_{\text{pot}} = G m_1 m_2 [(r_1+r_2)^{-1} - (r_1+r_2+X)^{-1}]$$

where the gravitational constant¹⁵⁹⁰ $G = 6.67 \times 10^{-11} \text{ N}\cdot\text{m}^2/\text{kg}^2$. The specific energy attributable to the gravitational potential energy stored between the two masses is $E_{\text{S,pot}} = \Delta E_{\text{pot}} / (m_1 + m_2) = \mathbf{3.0 \times 10^{-16} \text{ MJ/kg}}$ for a separation distance of $X = 1$ meter, taking masses $m_1 = m_2 = m = 1 \text{ kg}$ of density $\rho = 1910 \text{ kg/m}^3$ with $r_1 = r_2 = (3m / 4\pi\rho)^{1/3} = 0.05$ meter; or $E_{\text{S,pot}} = \mathbf{3.3 \times 10^{-16} \text{ MJ/kg}}$ for $X = 1000$ meters. We can readily imagine a “gravitational battery” in which one gravitationally-bound mass linearly oscillates back and forth through a central hole in another mass, with r_1+r_2+X representing the maximum separation of the centers of the two masses during each oscillation.¹⁵⁹¹

In the case where the first mass is very large, e.g., the Earth, with $m_1 = M_{\text{Earth}} = 5.98 \times 10^{24} \text{ kg}$ and $r_1 = R_{\text{Earth}} = 6.37 \times 10^6$ meters ($\rho_1 = \rho_{\text{Earth}} = 5523 \text{ kg/m}^3$), then if the small mass m_2 is lifted $X = 1$ meter above the Earth’s surface, $E_{\text{S,pot}} = \mathbf{1.6 \times 10^{-30} \text{ MJ/kg}}$ for the entire system including both masses, but $E_{\text{S,pot}} = \mathbf{9.8 \times 10^{-6} \text{ MJ/kg}}$ if the gravitational energy storage system is viewed as including only the smaller lifted mass m_2 . Gravitational energy storage appears very modest using ordinary matter because gravity is the weakest force in physics.

As a convenient approximation near a planetary surface, the local gravity field can be regarded as nearly constant with altitude,¹⁵⁹² in which case the change in the gravitational potential energy of a small mass m ($\ll M_{\text{planet}}$) raised a height h above the surface of a planet is $\Delta E_{\text{pot}} \sim mgh$, where g is the acceleration of gravity¹⁵⁹³ at the planet’s surface. Regarding the small mass as the entire energy storage system (residing in a uniform gravitational field), the specific energy $E_{\text{S,pot}} \sim mgh/m = gh$, which is independent of the suspended mass. Thus any small mass suspended $h = 1$ meter above a planetary surface having $g = 9.81 \text{ m/sec}^2$ (i.e., the Earth) has $E_{\text{S,pot}} \sim \mathbf{9.8 \times 10^{-6}}$

¹⁵⁹⁰ https://en.wikipedia.org/wiki/Gravitational_constant.

¹⁵⁹¹ The period of each oscillation is independent of mass and given by $T = (3\pi / G \rho)^{1/2}$ sec, where ρ is the density of the mass with the central hole.

¹⁵⁹² The actual acceleration of gravity as a function of altitude on a planet of mass M_{planet} is $g = G M_{\text{planet}} / (R_{\text{planet}} + h)^2$. Taking $M_{\text{planet}} = M_{\text{Earth}} = 5.972 \times 10^{24} \text{ kg}$, $R_{\text{planet}} = R_{\text{Earth}} = 6.375 \times 10^6$ meters, and $G = 6.674 \times 10^{-11} \text{ N}\cdot\text{m}^2/\text{kg}^2$, then $g = 9.807 \text{ m/sec}^2$ for $h = 0$ meters and $g = 9.22 \text{ m/sec}^2$ for $h = 200 \text{ km}$ (Low Earth Orbit or LEO), but $g = 0.0026 \text{ m/sec}^2$ for $h = 384,000 \text{ km}$ (the mean orbital distance of the Moon from the Earth).

¹⁵⁹³ https://en.wikipedia.org/wiki/Gravitational_acceleration.

MJ/kg, and any small mass suspended at $h = 200$ km (e.g., LEO) above the Earth's surface has $E_{S,pot} \sim \mathbf{1.9\ MJ/kg}$. A hydroelectric dam¹⁵⁹⁴ provides another practical example of a “gravitational battery”,¹⁵⁹⁵ as, for instance: Hoover Dam¹⁵⁹⁶ stores a volume $V = 2.48 \times 10^6$ m³ of water ($m \sim 2.48 \times 10^9$ kg taking $\rho_{water} \sim 1000$ kg/m³) at an average height of $h = 90$ meters, hence the hydroelectric energy storage capacity of $\Delta E_{pot} \sim 2.19 \times 10^6$ MJ represents a specific energy of $E_{S,pot} \sim \mathbf{8.8 \times 10^{-4}\ MJ/kg}$ and an energy density of $E_{D,pot} \sim E_{pot} / V = \mathbf{8.8 \times 10^{-4}\ MJ/L}$.

Note that a $\eta_{car} \sim 70\%$ energy-efficient flying car¹⁵⁹⁷ of mass $m_{car} = 1000$ kg in principle would only require $E_{car} = m_{car} g h_{lift} / \eta_{car} = 14$ MJ to lift to $h_{lift} = 1000$ m (~ 3281 ft) altitude above Earth's surface, with a power requirement of $P_{car} = E_{car} / \tau_{lift} = 0.31$ MW during $\tau_{lift} = 45.2$ sec of ascent, holding vertical acceleration to a constant $a_{lift} = 2 h_{lift} / \tau_{lift}^2 = 0.981$ m/sec² = 0.1 gee. A car equipped with a “Mr. Fusion” power source¹⁵⁹⁸ containing 1 liter of pure fusion fuel having an energy density of $\sim 10^7$ MJ/L (**Section 7.3.1**) could perform this lift operation more than 700,000 times between refuelings.

The gravitational potential energy of a small mass m in a circular orbit of altitude h above a larger (e.g., planetary) mass M_{planet} of radius R_{planet} , with P.E. taken as zero at $h = 0$, is $E_{pot,orbit} = G M_{planet} m [(R_{planet})^{-1} - (R_{planet} + h)^{-1}] = 1.9 \times 10^6$ J, taking $m = 1$ kg, $M_{planet} = M_{Earth} = 5.98 \times 10^{24}$ kg, $h = 200$ km for LEO orbit, and $R_{planet} = R_{Earth} = 6.37 \times 10^6$ meters, representing a specific energy of $E_{S,pot,orbit} = E_{pot,orbit} / m = \mathbf{1.9\ MJ/kg}$. In addition to this gravitational potential energy, due to its stable orbit around the Earth the same small mass also possesses an orbital kinetic energy of $E_{kin} = G M_{planet} m / (2 (R_{planet} + h)) = 3.04 \times 10^7$ J, adding another $E_{S,kin} = E_{kin} / m = \mathbf{30\ MJ/kg}$ to the total specific energy stored by the orbiting mass.¹⁵⁹⁹

Similarly, for the gravitational specific energy of the Earth orbiting the Sun, $E_{pot,orbit} = G M_{Sun} M_{Earth} [(R_{Sun})^{-1} - (R_{Sun} + h)^{-1}] = 1.14 \times 10^{36}$ J, taking $M_{Sun} = 2 \times 10^{30}$ kg, $h = 1.49 \times 10^{11}$ meters and $R_{Sun} = 6.957 \times 10^8$ meters, representing a specific energy of $E_{S,pot,orbit} = E_{pot,orbit} / M_{Earth} = \mathbf{191,000\ MJ/kg}$, plus an orbital kinetic energy of $E_{kin} = G M_{Sun} M_{Earth} / (2 (R_{Sun} + h)) = 2.66 \times 10^{33}$ J, adding another $E_{S,kin} = E_{kin} / M_{Earth} = \mathbf{446\ MJ/kg}$ to the total specific energy stored by the orbiting planetary mass.

¹⁵⁹⁴ https://en.wikipedia.org/wiki/Pumped-storage_hydroelectricity.

¹⁵⁹⁵ Quartz, “The plan to turn Hoover Dam into a giant battery,” YouTube, 22 Aug 2018; https://www.youtube.com/watch?v=PRmDm_EusRU.

¹⁵⁹⁶ https://en.wikipedia.org/wiki/Hoover_Dam.

¹⁵⁹⁷ Kasliwal A, *et al.* Role of flying cars in sustainable mobility. Nat Commun. 2019 Apr 9; 10:1555; <https://www.nature.com/articles/s41467-019-09426-0.pdf>.

¹⁵⁹⁸ https://backtothefuture.fandom.com/wiki/Mr._Fusion.

¹⁵⁹⁹ The energy necessary for a mass m to achieve escape velocity to infinity from the surface of a planet of mass M_{planet} and radius R_{planet} is $E_{escape} = G M_{planet} m / R_{planet}$, requiring a specific energy of $E_{S,escape} = G M_{planet} / R_{planet} = \mathbf{63\ MJ/kg}$ to escape from the surface of Earth, taking $M_{planet} = M_{Earth} = 5.98 \times 10^{24}$ kg and $R_{planet} = R_{Earth} = 6.37 \times 10^6$ meters.

Gravitational energy can also be stored in a physical pendulum.¹⁶⁰⁰ A simple gravity pendulum might consist of a fixed pivot point to which is attached a cord of length L_{cord} from the end of which hangs a bob of mass M_{bob} that swings freely along its arc and is vertically displaced a height H_{bob} above the lowest point, making an angle θ from vertical-down. When released, the bob oscillates with a period of $T \sim 2\pi (L_{\text{cord}} / g)^{1/2}$ sec and stores a total energy of $E_{\text{total}} = g M_{\text{bob}} H_{\text{bob}}$ where $H_{\text{bob}} = L_{\text{cord}} [1 - \cos(\theta)]$.¹⁶⁰¹ The total energy remains constant but alternates between all-potential energy at the top of each swing and all-kinetic energy at the bottom of each swing. Taking $L_{\text{cord}} = 1$ meter, $M_{\text{bob}} = 1$ kg, and maximum $H_{\text{bob}} = 1$ meter (i.e., the cord is horizontal, a full $\theta = 90^\circ$ away from vertical-down), the pendulum has a specific energy of $E_S = E_{\text{total}} / M_{\text{bob}} = g H_{\text{bob}} = \mathbf{9.8 \times 10^{-6} \text{ MJ/kg}}$.

¹⁶⁰⁰ <https://en.wikipedia.org/wiki/Pendulum>.

¹⁶⁰¹ <https://blogs.bu.edu/ggarber/interlace/pendulum/energy-in-a-pendulum/>.

8.2 Extreme Gravity

A black hole is a region of spacetime exhibiting such strong gravitational effects that nothing – not even particles or electromagnetic radiation such as light – can escape from inside it.¹⁶⁰² The boundary of the region from which no escape is possible is called the event horizon.¹⁶⁰³

A stellar black hole¹⁶⁰⁴ (aka. stellar-mass black hole, or collapsar) is a black hole formed by the gravitational collapse of a star,¹⁶⁰⁵ which may be observed in our galaxy as a supernova explosion¹⁶⁰⁶ or in distant galaxies as a gamma ray burst.¹⁶⁰⁷ There are estimated to be as many as ~100 million stellar black holes in our galaxy alone.¹⁶⁰⁸ Stellar black holes have masses ranging from 5-50 M_{solar} . The event horizon of a nonrotating uncharged black hole of mass M_{BH} occurs at the Schwarzschild radius¹⁶⁰⁹ (R_{BH}) or:

$$R_{\text{BH}} = 2 G M_{\text{BH}} / c^2 = 1.48 \times 10^{-27} M_{\text{BH}} \text{ (meters)}$$

which implies that the mean density of a Schwarzschild (nonrotating uncharged) black hole is $\rho_{\text{BH}} \sim M_{\text{BH}} / V_{\text{BH}} = 3 c^6 / (32\pi G^3 M_{\text{BH}}^2) = 7.33 \times 10^{79} / M_{\text{BH}}^2 \text{ (kg/m}^3\text{)}$ for black hole volume $V_{\text{BH}} = 4/3 \pi R_{\text{BH}}^3$, with a rest-mass specific energy of $E_{\text{S,BH}} = M_{\text{BH}} c^2 / M_{\text{BH}} = c^2 \sim \mathbf{9 \times 10^{10} \text{ MJ/kg}}$. The rest-mass energy density of a Schwarzschild black hole with a mass equal to that of the Sun ($M_{\text{BH}} = M_{\text{solar}} = 2 \times 10^{30} \text{ kg}$) is then $E_{\text{D,BH}} = \rho_{\text{BH}} c^2 = \mathbf{1.65 \times 10^{27} \text{ MJ/L}}$, at a radius of $R_{\text{BH}} = 2960 \text{ m}$ and with a mean density of $\rho_{\text{BH}} = 1.83 \times 10^{19} \text{ kg/m}^3$.

¹⁶⁰² https://en.wikipedia.org/wiki/Black_hole.

¹⁶⁰³ https://en.wikipedia.org/wiki/Event_horizon.

¹⁶⁰⁴ https://en.wikipedia.org/wiki/Stellar_black_hole.

¹⁶⁰⁵ Celotti A, Miller JC, Sciamia DW. Astrophysical evidence for the existence of black holes. *Class Quant Grav.* 1999;16(12A):A3–A21; <https://arxiv.org/pdf/astro-ph/9912186>. Hughes SA. Trust but verify: The case for astrophysical black holes. Invited Lecture at the 2005 SLAC Summer Institute (SSI05-L006), 21 Nov 2005; <https://arxiv.org/pdf/hep-ph/0511217>.

¹⁶⁰⁶ https://en.wikipedia.org/wiki/Type_II_supernova.

¹⁶⁰⁷ https://en.wikipedia.org/wiki/Gamma-ray_burst.

¹⁶⁰⁸ Elbert OD, Bullock JS, Kaplinghat M. Counting black holes: The cosmic stellar remnant population and implications for LIGO. *Mon Not Roy Astron Soc.* 2018 Jan 1;473(1):1186-1194; <https://academic.oup.com/mnras/article/473/1/1186/4060726?guestAccessKey=d1a72ca6-9200-4dca-850a-f4c87663106e>.

¹⁶⁰⁹ https://en.wikipedia.org/wiki/Schwarzschild_metric.

8.2.1 Energy Extraction from Microscale Black Holes

If nothing can escape a black hole, how do we extract stored energy from a “black hole battery”? Quantum field theory in curved spacetime¹⁶¹⁰ predicts that event horizons emit Hawking radiation,¹⁶¹¹ with the same spectrum as a black body having a temperature (T_{BH}) that is inversely proportional to its mass, as: $T_{\text{BH}} = h c^3 / (16\pi^2 G M_{\text{BH}} k_B) = 1.23 \times 10^{23} / M_{\text{BH}}$ where $k_B = 1.38 \times 10^{-23}$ J/K (Boltzmann’s constant). For a black hole of solar mass ($M_{\text{BH}} = M_{\text{solar}}$), $T_{\text{BH}} = 62$ nanokelvins which is far colder than the 2.72548 K temperature of the cosmic microwave background radiation.¹⁶¹² As a result, stellar-mass black holes receive more mass-energy from the cosmic microwave background than they emit through Hawking radiation, and thus will grow instead of shrink (paradoxically, becoming even colder). Black holes with mass $M_{\text{BH}} < M_{\text{BH, equil}} = (1.23 \times 10^{23} \text{ K}\cdot\text{kg}) / (2.72548 \text{ K}) = 4.51 \times 10^{22} \text{ kg}$ are hotter than the cosmic microwave background temperature and will slowly evaporate. The maximum size threshold for a black hole capable of evaporation is therefore $R_{\text{BH, equil}} = 2 G M_{\text{BH, equil}} / c^2 = 67 \mu\text{m}$, a “microscale black hole” (μBH),¹⁶¹³ aka. a “quantum black hole”.

Given sufficient time, an evaporating Schwarzschild μBH will radiate away its entire rest mass. The physics of black hole evaporation depends on many assumptions and is difficult to calculate exactly. One early estimate¹⁶¹⁴ (that ignored the mass of neutrinos)¹⁶¹⁵ calculated an evaporation time for μBH s of $\tau_{\text{evap}} \sim k_{\text{evap}} M_{\text{BH}}^3$, where $k_{\text{evap}} \sim 8.66 \times 10^{-18}$ for $M_{\text{BH}} > 10^{14} \text{ kg}$ and $k_{\text{evap}} \sim 4.8 \times 10^{-18}$ for $M_{\text{BH}} < 10^{14} \text{ kg}$, in which the power output is 81% neutrinos (probably unrecoverable), 17% photons, and 2% gravitons (**Section 8.3**). A more recent crude estimate¹⁶¹⁶ of the Bekenstein-Hawking luminosity of a black hole (assuming pure photon emission, the horizon as the radiating surface, and no infalling cosmic background radiation) is $P_{\mu\text{BH}} = h c^6 / (30720\pi^2 G^2 M_{\mu\text{BH}}^2)$ watts = $3.56 \times 10^{32} / M_{\mu\text{BH}}^2$ watts, with a μBH evaporation time¹⁶¹⁷ of $\tau_{\text{evap}} \sim 10240 \pi^2 G^2 / h c^4 = 8.41 \times 10^{-17} M_{\mu\text{BH}}^3$.

By this latter calculation, an $M_{\mu\text{BH}} \sim 10^{20} \text{ kg}$ microscale black hole radiating an average of $P_{\mu\text{BH}} \sim 40 \text{ nanowatts}$ would evaporate in $\tau_{\text{evap}} \sim 3 \times 10^{36}$ years from a radius of $R_{\mu\text{BH}} = 0.148 \mu\text{m}$, volume $V_{\mu\text{BH}} = 0.0136 \mu\text{m}^3$, density $\rho_{\mu\text{BH}} = 7.33 \times 10^{39} \text{ kg/m}^3$, initial mass-energy density $E_{\text{D}, \mu\text{BH}} = \rho_{\mu\text{BH}} c^2$

¹⁶¹⁰ https://en.wikipedia.org/wiki/Quantum_field_theory_in_curved_spacetime.

¹⁶¹¹ https://en.wikipedia.org/wiki/Hawking_radiation.

¹⁶¹² https://en.wikipedia.org/wiki/Cosmic_microwave_background.

¹⁶¹³ https://en.wikipedia.org/wiki/Micro_black_hole.

¹⁶¹⁴ Page DN. Particle emission rates from a black hole: Massless particles from an uncharged, nonrotating hole. Phys Rev D. 1976 Jan 15;13(2):198-206; <https://journals.aps.org/prd/abstract/10.1103/PhysRevD.13.198>.

¹⁶¹⁵ https://en.wikipedia.org/wiki/Hawking_radiation#1976_Page_numerical_analysis.

¹⁶¹⁶ https://en.wikipedia.org/wiki/Hawking_radiation#A_crude_analytic_estimate.

¹⁶¹⁷ Hawking SW. Black hole explosions? Nature 1974;248:30-31; <https://www.nature.com/articles/248030a0>.

= 6.6×10^{47} MJ/L, initial specific power density of $P_{D,\mu\text{BH}} = P_{\mu\text{BH}} / V_{\mu\text{BH}} = 2900$ MW/L, and initial specific power of $P_{S,\mu\text{BH}} = P_{\mu\text{BH}} / M_{\mu\text{BH}} = 4 \times 10^{-34}$ MW/kg.

Similarly, an $M_{\mu\text{BH}} \sim 10^{10}$ kg microscale black hole radiating an average of 4×10^{12} watts might take $\tau_{\text{evap}} \sim 3$ million years to fully evaporate from a radius of $R_{\mu\text{BH}} = 1.48 \times 10^{-8}$ nm, volume $V_{\mu\text{BH}} = 1.36 \times 10^{-50}$ m³, density $\rho_{\mu\text{BH}} = 7.33 \times 10^{59}$ kg/m³, initial mass-energy density $E_{D,\mu\text{BH}} = \rho_{\mu\text{BH}} c^2 = 6.6 \times 10^{76}$ MJ/L, initial specific power density of $P_{D,\mu\text{BH}} = P_{\mu\text{BH}} / V_{\mu\text{BH}} = 2.9 \times 10^{53}$ MW/L, and initial specific power of $P_{S,\mu\text{BH}} = P_{\mu\text{BH}} / M_{\mu\text{BH}} = 4 \times 10^{-4}$ MW/kg. While in principle¹⁶¹⁸ a microscale black hole could have any mass at or above the Planck mass of 2.2×10^{-8} kg,¹⁶¹⁹ the limited spatial extent of fermions might restrict the minimum mass of a black hole to $\sim 10^{16}$ kg.¹⁶²⁰

Creating even a minimum-mass μBH would require compressing 2.2×10^{-8} kg or $\sim 10^{16}$ TeV (1.98×10^9 J) into a subatomic region the size of a single Planck length¹⁶²¹ (1.6×10^{-35} meter). The Large Hadron Collider can accelerate individual protons to 6.5 TeV,¹⁶²² and has also been used to accelerate atomic nuclei of lead to similar energies amounting to 1045 TeV per nucleon¹⁶²³ – but this is still 13 orders of magnitude below the energy of even the smallest possible microscopic black hole. One method for creating μBH s that has been proposed by science fiction writers is to axially accelerate several very long thin rods of high-density matter to relativistic speeds (shortening their length in the direction of motion) on trajectories that will bring them into collision at a precise location and instant of time after perhaps light-years of travel.¹⁶²⁴

Microscale black holes could provide an abundant energy source by capturing the accessible $\sim 17\%$ of their energy that is expected to be emitted as photons as they evaporate.¹⁶²⁵ Microscale black holes could be magnetically or electrostatically manipulated by injecting them with electrical charge, and μBH s could be refueled by feeding them a stream of matter, effectively turning them into 17% efficient “total conversion” engines similar to the matter-antimatter systems described earlier (**Section 7.6**). However, black hole emission energy cannot easily be throttled to match a load. Left to themselves, μBH s will emit harvestable radiation according to a fixed schedule, much like radionuclides (**Section 7.1**) – but unlike radionuclides, the rate of energy production increases rather than decreases over time. Absorbing matter that is fed to it will increase the μBH lifetime and decrease its rate of energy emission, but no method has yet

¹⁶¹⁸ Hawking SW. Gravitationally collapsed objects of very low mass. Mon Not Royal Astron Soc. 1971;152:75-78; <http://adsabs.harvard.edu/full/1971MNRAS.152...75H>.

¹⁶¹⁹ https://en.wikipedia.org/wiki/Planck_mass.

¹⁶²⁰ https://en.wikipedia.org/wiki/Micro_black_hole#Minimum_mass_of_a_black_hole.

¹⁶²¹ https://en.wikipedia.org/wiki/Planck_length.

¹⁶²² https://en.wikipedia.org/wiki/Large_Hadron_Collider#Design.

¹⁶²³ John Jowett, “A new energy frontier for heavy ions,” CERN News, 24 Nov 2015; <https://home.cern/news/opinion/physics/new-energy-frontier-heavy-ions>.

¹⁶²⁴ “Black Hole,” 8 Oct 2001; <http://www.orionsarm.com/eg-article/460e790e8b615>.

¹⁶²⁵ Page DN. Particle emission rates from a black hole: Massless particles from an uncharged, nonrotating hole. Phys Rev D. 1976 Jan 15;13(2):198-206; <https://journals.aps.org/prd/abstract/10.1103/PhysRevD.13.198>.

been proposed to alter the rate of increasing energy production of an otherwise undisturbed slowly-evaporating μBH . Lacking such methods, presumably a practical microscale black hole energy storage system would employ the μBH as a primary energy source to charge up a battery, capacitor, or some other secondary storage medium that is more easily throttled to match load demands.

8.2.2 Energy Extraction from Stellar Black Holes

There are proposals for harvesting energy from stellar-mass Schwarzschild black holes, including the Unruh-Wald suggestion of raising and lowering boxes full of radiation in the vicinity of black hole horizons¹⁶²⁶ (a proposal that has been challenged on technical grounds¹⁶²⁷) or, if string theory is correct, threading the black hole horizon with strings (e.g., a string dangled into a black hole wicks away Hawking radiation,¹⁶²⁸ and employing many strings kept far enough apart to prevent reconnection and expulsion from the hole may allow the systematic mining of black holes¹⁶²⁹) or mining black holes in more than 5-dimensional space.¹⁶³⁰ Unruh-Wald energy mining might also be applied to charged black holes.¹⁶³¹

Black holes can store significant amounts of rotational energy too. For instance, the gravitational potential energy of a stellar-mass Schwarzschild black hole (e.g., $M_{\text{BH}} = M_{\text{solar}} = 2 \times 10^{30}$ kg) of radius $R_{\text{BH}} = 2960$ meters in a closest-possible circular orbit of altitude $h = 2960$ m around an identical stellar-mass Schwarzschild black hole, which is $E_{\text{pot,orbit}} = G M_{\text{BH}}^2 [(R_{\text{BH}})^{-1} - (R_{\text{BH}} + h)^{-1}] = 4.5 \times 10^{46}$ J, represents a mass-independent specific energy of $E_{\text{S,pot,orbit}} = E_{\text{pot,orbit}} / M_{\text{BH}} = \mathbf{2.3 \times 10^{10} \text{ MJ/kg}}$, along with an orbital kinetic energy contribution of $E_{\text{kin}} = G M_{\text{BH}}^2 / (2 (R_{\text{BH}} + h)) = 2.3 \times 10^{46}$ J (classical orbital velocity $v_{\text{orb}} \sim (2 E / M_{\text{BH}})^{1/2} \sim 0.5 c$) that adds a mass-independent $E_{\text{S,kin}} = E_{\text{kin}} / M_{\text{BH}} = \mathbf{1.1 \times 10^{10} \text{ MJ/kg}}$ to the total specific energy stored by the orbiting mass. The existence of close-orbiting binary black holes¹⁶³² was apparently confirmed with the LIGO detection of the distinctive gravity wave signature of two merging co-orbiting black holes of $\sim 30 M_{\text{solar}}$ each, located ~ 1.3 billion light-years away, which released $\sim 3 M_{\text{solar}}$ of gravitational energy

¹⁶²⁶ Unruh WG, Wald RM. How to mine energy from a black hole. Gen Rel Grav D. 1983 Mar;15(3):195-199; <https://link.springer.com/article/10.1007/BF00759206>.

¹⁶²⁷ Brown AR. Tensile strength and the mining of black holes. Phys Rev Lett. 2013 Nov 22;111(21-22):211301; <https://arxiv.org/pdf/1207.3342v1.pdf>.

¹⁶²⁸ Lawrence AE, Martinec EJ. Black hole evaporation along macroscopic strings. Phys Rev D. 1994 Aug 15;50(4):2680-2691; <https://arxiv.org/pdf/hep-th/9312127>.

¹⁶²⁹ Frolov VP, Fursaev D. Mining energy from a black hole by strings. Phys Rev D. 2001 Jun 15;63(12):124010; <https://arxiv.org/pdf/hep-th/0012260.pdf>. Frolov VP. Cosmic strings and energy mining from black holes. Int J Mod Phys A. 2002;17(20):2673-2676; <https://www.worldscientific.com/doi/abs/10.1142/S0217751X0201159X>.

¹⁶³⁰ “Appendix B. Constraints on mining in $n + 1$ -dimensions,” in: Brown AR. Tensile strength and the mining of black holes. Phys Rev Lett. 2013 Nov 22;111(21-22):211301; <https://arxiv.org/pdf/1207.3342v1.pdf>.

¹⁶³¹ Roman TA. Mining a charged black hole and the third law of black hole thermodynamics. Gen Rel Grav. 1988 Apr;20(4):359-370; <https://link.springer.com/article/10.1007/BF00758960>.

¹⁶³² https://en.wikipedia.org/wiki/Binary_black_hole.

during the merger, peaking at 3.6×10^{49} watts during the last moments of the in-spiral and merger.¹⁶³³

A solitary black hole can also be rotating, making it a Kerr black hole.¹⁶³⁴ For example, the X-ray source GRS 1915+105 appears to be a $14 M_{\text{solar}}$ mass Kerr black hole with a near-theoretical-maximum spin rate of ~ 1000 Hz (equatorial velocity $\sim 0.87c$).¹⁶³⁵ A Kerr black hole of mass $M_{\text{KBH}} = M_{\text{solar}}$, volume $V_{\text{KBH}} \sim 4/3 \pi R_{\text{KBH}}^3 = 1.09 \times 10^{11} \text{ m}^3$ with core radius $R_{\text{KBH}} \sim 2960$ meters rotating with a near-maximum equatorial velocity of $0.5c$ has a rotation rate of $\omega = 0.5 c / R_{\text{KBH}} = 50,700$ rad/sec (~ 8070 Hz), rotational inertia $I_{\text{KBH}} \sim (2/5) M_{\text{KBH}} R_{\text{KBH}}^2 = 7 \times 10^{36} \text{ kg}\cdot\text{m}^2$, and rotational kinetic energy $K_{\text{KBH}} = (1/2) I \omega^2 = 2.3 \times 10^{44} \text{ J}$, providing a specific energy of $E_{\text{S,KBH}} = K_{\text{KBH}} / M_{\text{KBH}} = \mathbf{1.1 \times 10^8 \text{ MJ/kg}}$ and an energy density of $E_{\text{D,KBH}} = K_{\text{KBH}} / V_{\text{KBH}} = \mathbf{2.1 \times 10^{24} \text{ MJ/L}}$.

It has been suggested that rotational energy could be extracted from a rotating Kerr black hole, eventually converting it into a nonrotating Schwarzschild black hole, using the “Penrose process”¹⁶³⁶ (a proposal that has been challenged on technical grounds¹⁶³⁷) in which a lump of matter entering the ergosphere¹⁶³⁸ is triggered to split into two parts, with the momentum of the two parts arranged so that one piece escapes from the black hole with a greater mass-energy than the original piece of matter while the other piece falls past the event horizon into the black hole.¹⁶³⁹ Efficiency limits for this process have been estimated.¹⁶⁴⁰ Another proposal is to thread a rotating black hole with magnetic field lines supported by external currents flowing in an equatorial disc, inducing an electric potential difference which (if the field strength is large enough) will cause the vacuum to become unstable to a cascade production of electron-positron pairs, creating a surrounding force-free magnetosphere allowing energy and angular momentum

¹⁶³³ Abbott BP, *et al.* Observation of gravitational waves from a binary black hole merger. Phys Rev Lett. 2016 Feb 12;116(6):061102; <https://journals.aps.org/prl/pdf/10.1103/PhysRevLett.116.061102>. Abbott BP, *et al.* Properties of the binary black hole merger GW150914. Phys Rev Lett. 2016 Jun 14;116(24):241102; <https://journals.aps.org/prl/pdf/10.1103/PhysRevLett.116.241102>.

¹⁶³⁴ https://en.wikipedia.org/wiki/Kerr_metric.

¹⁶³⁵ McClintock JE, *et al.* The spin of the near-extreme Kerr black hole GRS 1915+105. Astrophys J 2006 Nov;652(1):518-539; <https://arxiv.org/pdf/astro-ph/0606076.pdf>.

¹⁶³⁶ Penrose R, Floyd RM. Extraction of rotational energy from a black hole. Nature Phys Sci. 1971 Feb;229(6):177-179; <https://www.nature.com/articles/physci229177a0>.

¹⁶³⁷ Bardeen JM, Press WH, Teukolsky SA. Rotating black holes: Locally nonrotating frames, energy extraction, and scalar synchrotron radiation. Astrophys J. 1972 Dec 1;178:347-369; <http://adsabs.harvard.edu/full/1972ApJ...178..347B>.

¹⁶³⁸ A region just outside the event horizon of a rotating black hole within which energy can be extracted from the black hole; <https://en.wikipedia.org/wiki/Ergosphere>.

¹⁶³⁹ https://en.wikipedia.org/wiki/Penrose_process.

¹⁶⁴⁰ Schnittman JD. Revised upper limit to energy extraction from a Kerr black hole. Phys Rev Lett 2014 Dec 30;113:261102; <https://arxiv.org/pdf/1410.6446.pdf>.

to be extracted electromagnetically.¹⁶⁴¹ In yet another proposal,¹⁶⁴² a charged wave field is amplified upon being scattered by a charged rotating black hole (aka., a Kerr-Newman black hole¹⁶⁴³) with consequent extraction of charge and Coulomb energy from the hole. Other wave analogs of the Penrose process have been discussed.¹⁶⁴⁴

There are at least two possible experimental observations of the extraction of energy from rotating Kerr black holes.¹⁶⁴⁵

¹⁶⁴¹ Blandford RD, Znajek RL. Electromagnetic extraction of energy from Kerr black holes. *Mon Not Royal Astron Soc.* 1977 Jul 1;179(3):433-456; <https://academic.oup.com/mnras/article/179/3/433/962905>. Ghosh P, Abramowicz MA. Electromagnetic extraction of rotational energy from disc-fed black holes: the strength of the Blandford-Znajek process. *Mon Not Royal Astron Soc.* 1997 Dec;292(4):887-895; <http://adsabs.harvard.edu/full/1997MNRAS.292..887G>.

¹⁶⁴² Bekenstein JD. Extraction of energy and charge from a black hole. *Phys Rev D.* 1973 Feb 15;7(4):949-953; <https://journals.aps.org/prd/abstract/10.1103/PhysRevD.7.949>.

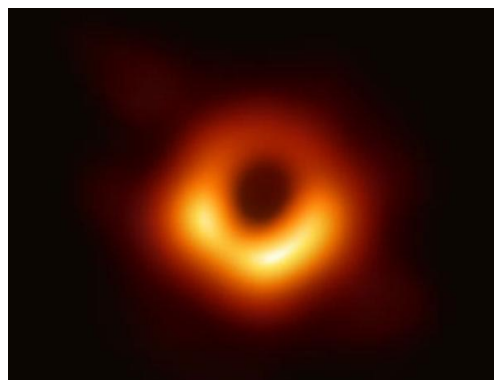
¹⁶⁴³ https://en.wikipedia.org/wiki/Kerr-Newman_metric.

¹⁶⁴⁴ Finster F, Kamran N, Smoller J, Yau ST. A rigorous treatment of energy extraction from a rotating black hole. *Commun Math Phys.* 2009 May;287(3):829-847; <https://arxiv.org/pdf/gr-qc/0701018.pdf>.

¹⁶⁴⁵ Wilms J, *et al.* XMM-EPIC observation of MCG-6-30-15: direct evidence for the extraction of energy from a spinning black hole? *Mon Not Royal Astron Soc.* 2001 Dec 11;328(3):L27-L31; <https://academic.oup.com/mnras/article/328/3/L27/1247476>. Miller JM, *et al.* Evidence of spin and energy extraction in a galactic black hole candidate: The XMM-Newton/EPIC-pn spectrum of XTE J1650-500. *Astrophys J Lett.* 2002 May 10;570(2):L69-L73; <https://iopscience.iop.org/article/10.1086/341099/pdf>.

8.2.3 Supermassive Black Holes

A supermassive black hole¹⁶⁴⁶ is the largest type of black hole, containing a mass of the order of 10^5 - $10^9 M_{\text{solar}}$. Observational evidence indicates that all, or nearly all, massive galaxies contain a supermassive black hole located at the galaxy's center.¹⁶⁴⁷ The first photograph of a supermassive black hole (image, right),¹⁶⁴⁸ located at the center of the supergiant elliptical galaxy M87,¹⁶⁴⁹ was published in April 2019.¹⁶⁵⁰ This black hole is estimated to have a mass of $\sim 6.5 \times 10^9 M_{\text{solar}}$ ($\sim 1.3 \times 10^{40}$ kg).



The supermassive black hole at the Galactic Core of the Milky Way,¹⁶⁵¹ located in the region called Sagittarius A* about 26,000 light-years from Earth, is believed on the basis of astronomical observations to have a mass of $\sim 4.1 \times 10^6 M_{\text{solar}}$ (8.2×10^{36} kg)¹⁶⁵² and a radius of less than 6.25 light-hours ($< 6.75 \times 10^{12}$ meters).¹⁶⁵³ Assuming the mass estimate is correct, this would imply that the Galactic Core supermassive black hole has a radius of $R_{\text{SBH,MW}} = 1.2 \times 10^{10}$ meters, a volume of $V_{\text{SBH,MW}} = 7.5 \times 10^{30} \text{ m}^3$, mean density of $\rho_{\text{SBH,MW}} = 1.09 \times 10^6 \text{ kg/m}^3$, a rest-mass specific energy of $E_{\text{S,SBH,MW}} \sim 9 \times 10^{10} \text{ MJ/kg}$ and a rest-mass energy density of $E_{\text{D,SBH,MW}} = 9.8 \times 10^{13} \text{ MJ/L}$.

¹⁶⁴⁶ https://en.wikipedia.org/wiki/Supermassive_black_hole.

¹⁶⁴⁷ Kormendy J, Richstone D. Inward bound – the search for supermassive black holes in galactic nuclei. *Ann Rev Astron Astrophys.* 1995;33:581-624; <http://adsabs.harvard.edu/full/1995ARA%26A..33..581K>. King A. Black Holes, Galaxy Formation, and the MBH- σ Relation. *Astrophys J Lett.* 2003 Sep 15;596:L27-L29; <https://arxiv.org/pdf/astro-ph/0308342.pdf>. Kormendy J, Ho L. Coevolution (Or Not) of Supermassive Black Holes and Host Galaxies. *Ann Rev Astron Astrophys.* 2013;51(1):511-653; <https://arxiv.org/pdf/1304.7762>.

¹⁶⁴⁸ <https://www.sciencenews.org/article/black-hole-first-picture-event-horizon-telescope>.

¹⁶⁴⁹ https://en.wikipedia.org/wiki/Messier_87.

¹⁶⁵⁰ Akiyama K, *et al.* First M87 event horizon telescope results. I. The shadow of the supermassive black hole. *Astrophys J Lett.* 2019 Apr 11;875(1); <https://iopscience.iop.org/article/10.3847/2041-8213/ab0ec7>.

¹⁶⁵¹ https://en.wikipedia.org/wiki/Supermassive_black_hole#In_the_Milky_Way.

¹⁶⁵² Ghez AM, *et al.* Measuring distance and properties of the milky way's central supermassive black hole with stellar orbits. *Astrophys J.* 2008 Dec 20; 689(2):1044-1062; <https://pdfs.semanticscholar.org/b1cf/4a7427a7b363fb415eebb6c8c5f3765ca026.pdf>.

¹⁶⁵³ Ghez AM, Salim S, Hornstein SD, Tanner A, Lu JR, Morris M, Becklin EE, Duchêne G. Stellar orbits around the galactic center black hole. *Astrophys J.* 2005 Feb 20;620(2):744-757; http://www.physics.sfsu.edu/~cool/TEACHING/a490/spring07/readings/ghez_galactic_ctr_2005.pdf.

Our neighboring Andromeda galaxy contains a $1.1\text{-}2.3 \times 10^8 M_{\text{solar}}$ supermassive black hole at its core,¹⁶⁵⁴ having a mean density of $346\text{-}1514 \text{ kg/m}^3$ or roughly the density of water. At least 129 supermassive black hole candidates have been discovered to date,¹⁶⁵⁵ of which the largest known is a quasar designated TON 618¹⁶⁵⁶ with a mass of $6.6 \times 10^{10} M_{\text{solar}}$, with a computed radius of $R_{\text{SBH}} = 1.95 \times 10^{14}$ meters (~ 0.02 light-year), volume $V_{\text{SBH}} = 3.11 \times 10^{43} \text{ m}^3$, density $\rho_{\text{SBH}} = 0.0042 \text{ kg/m}^3$ (~ 300 times less dense than STP air), and a rest-mass energy density of $E_{\text{D,SBH}} = \mathbf{8.8 \times 10^5 \text{ MJ/L}}$. Some galaxies, such as the galaxy 4C+37.11,¹⁶⁵⁷ appear to have two supermassive black holes at their centers, forming a binary system. Energy can be extracted from supermassive black holes in a similar manner as previously described for stellar-mass black holes (**Section 8.2.2**).

There is a physical limit to the mass of a supermassive black hole that grows by luminous accretion of gas – above this mass limit, it cannot appear as a quasar or active galactic nucleus and can only undergo nonluminous growth, e.g., by black hole mergers. The limit is $M_{\text{SBH,max}} \approx 5 \times 10^{10} M_{\text{solar}}$ ($= 1 \times 10^{41} \text{ kg}$) for typical parameters, but can reach $M_{\text{max}} \approx 27 \times 10^{10} M_{\text{solar}}$ ($= 5.4 \times 10^{41} \text{ kg}$) in extreme cases such as maximal prograde spin.¹⁶⁵⁸ The biggest supermassive black holes observed to date are very near these limits.

It is a perhaps amusing coincidence that a supermassive black hole equal in mass to the mass of the entire observable universe $M_{\text{SBH,U}} = M_{\text{universe}} \sim 1 \times 10^{53} \text{ kg}$ ordinary baryonic matter ($\sim 4.84\%$ of all mass)¹⁶⁵⁹ + $1.97 \times 10^{54} \text{ kg}$ nonbaryonic matter ($\sim 95.16\%$ of all mass)¹⁶⁶⁰ = $2.1 \times 10^{54} \text{ kg}$ (total mass of universe) would have a Schwarzschild radius of $R_{\text{SBH,U}} = \underline{3.1 \times 10^{27} \text{ meters}}$ (329×10^9 light-years), which is only slightly larger than the estimated $4.4 \times 10^{26} \text{ meter}$ (47×10^9 light-years) radius of the observable universe.¹⁶⁶¹ (The calculated mean black hole density of $\rho_{\text{SBH,U}} \sim 1.7 \times 10^{-29} \text{ kg/m}^3$ is also very close to the $\sim 0.99 \times 10^{-29} \text{ kg/m}^3$ conventional matter density estimate for the entire universe.¹⁶⁶²) The implication seems to be that we might be living inside a universe-size supermassive black hole.

¹⁶⁵⁴ Bender R, *et al.* HST STIS Spectroscopy of the triple nucleus of M31: two nested disks in Keplerian rotation around a supermassive black hole. *Astrophys J.* 2005 Sep 20;631(1):280-300; http://fifils.mpe-garching.mpg.de/~bender/m31_resub/m31bhp3.pdf.

¹⁶⁵⁵ https://en.wikipedia.org/wiki/List_of_most_massive_black_holes#List.

¹⁶⁵⁶ https://en.wikipedia.org/wiki/TON_618#Ultramassive_black_hole.

¹⁶⁵⁷ https://en.wikipedia.org/wiki/4C_%2B37.11.

¹⁶⁵⁸ King A. How big can a black hole grow? *Mon Not Roy Astron Soc.* 2016 Feb 11;456(1):L109-L112; <https://arxiv.org/pdf/1511.08502.pdf>.

¹⁶⁵⁹ Adam R, *et al.* Planck 2015 results. I. Overview of products and scientific results. *A&A* 2016;594:A1; <https://pdfs.semanticscholar.org/acd3/ac9cbc8f717e2c06626e58ccd8a0a0bab1b8.pdf>.

¹⁶⁶⁰ <https://en.wikipedia.org/wiki/Universe>.

¹⁶⁶¹ https://en.wikipedia.org/wiki/Observable_universe#Size.

¹⁶⁶² “What is the Universe made of?” NASA, 24 Jan 2014; https://map.gsfc.nasa.gov/universe/uni_matter.html.

8.2.4 White Holes

In general relativity, a white hole is a hypothetical region of spacetime which cannot be entered from the outside, although matter and light can escape from it – the reverse of a black hole, which can only be entered from the outside and from which matter and light cannot escape.¹⁶⁶³ It has been proposed that the Big Bang itself may have been one instance of a white hole.¹⁶⁶⁴ The existence of white holes is very speculative so their energy density is unknown, but one estimate¹⁶⁶⁵ for an “exploding primordial black hole” gives an energy of $E_{\text{WH}} = 1.7 \times 10^{40}$ J within a Schwarzschild radius of $R_{\text{WH}} \sim 0.02$ cm, which implies an energy density of $E_{\text{D,WH}} \sim 3 E_{\text{WH}} / 4\pi R_{\text{WH}}^3 = 5.1 \times 10^{41}$ MJ/L. Capturing a burst of energy of this magnitude will be technically challenging, and there are no proposed means for recharging a white hole energy store once it has been discharged.

¹⁶⁶³ https://en.wikipedia.org/wiki/White_hole.

¹⁶⁶⁴ Retter A, Heller S. The revival of white holes as Small Bangs. *New Astron.* 2012 Feb;17(2):73-75; <https://www.hamaraemet.org/wp-content/uploads/2014/07/white-holes-retter.pdf>.

¹⁶⁶⁵ Barrau A, Rovelli C, Vidotto F. Fast radio bursts and white hole signals. *Phys Rev D.* 2014 Dec 15;90(12-15):127503; <https://arxiv.org/pdf/1409.4031.pdf>.

8.3 Theoretical and Speculative Forms of Matter

Finally, it may be possible to store gravitational energy in various theoretical and speculative forms, assuming these forms exist and behave largely as anticipated once they are discovered.

Gravitons. Gravitational waves¹⁶⁶⁶ are disturbances in the curvature (fabric) of spacetime, generated by accelerated masses, that propagate as waves outward from their source at the speed of light. Gravitational waves transport energy as gravitational radiation, a form of radiant energy similar to electromagnetic radiation (whose forces are mediated by photons).¹⁶⁶⁷ In theories of quantum gravity, by analogy to the photon, the graviton is the hypothetical quantum of gravity, an elementary particle that mediates the force of gravity.¹⁶⁶⁸ Although the Standard Model assumes the existence of a graviton, all attempts to produce a consistent theory based on them have failed.

If gravitons exist, what might their energy density be? GW170104,¹⁶⁶⁹ the official name of a gravitational wave signal detected by the LIGO observatory in 2017, set a new upper bound on the mass of gravitons of $7.7 \times 10^{-29} \text{ MeV}/c^2$,¹⁶⁷⁰ a maximum rest-mass energy of $E_{\text{graviton}} \sim 1.2 \times 10^{-41} \text{ J}$. The frequency of this wave was measured as $\nu_{\text{graviton}} \sim 180 \pm 20 \text{ Hz}$. Following the method for calculating the energy density of a photon described in **Section 6**,¹⁶⁷¹ our estimate of the energy density of a 180 Hz graviton would be an extremely low $E_{\text{D,graviton}} \sim h\nu^4/c^3 = \mathbf{3 \times 10^{-59} \text{ MJ/L}}$. In order to concentrate these waves into a higher and more useful energy density, there is at least one proposal for a gravitational wave mirror using thin sheets of Type I superconductors.¹⁶⁷²

Geons and Neutrino Condensate. In theoretical general relativity, a geon¹⁶⁷³ is an electromagnetic wave which is held together in a confined region by the gravitational attraction of its own field energy – in essence, a blob of electromagnetic energy trapped by its own gravity.

¹⁶⁶⁶ https://en.wikipedia.org/wiki/Gravitational_wave.

¹⁶⁶⁷ Einstein A, Rosen N. On gravitational waves. J Franklin Institute. 1937 Jan;223(1):43-54; <https://www.sciencedirect.com/science/article/pii/S0016003237905830>.

¹⁶⁶⁸ <https://en.wikipedia.org/wiki/Graviton>.

¹⁶⁶⁹ <https://en.wikipedia.org/wiki/GW170104>.

¹⁶⁷⁰ Abbott BP, *et al.* GW170104: Observation of a 50-solar-mass binary black hole coalescence at redshift 0.2. Phys Rev Lett. 2017 Jun 2;118(22):221101; <https://journals.aps.org/prl/pdf/10.1103/PhysRevLett.118.221101>.

¹⁶⁷¹ Brian Koberlein, “That’s about the size of it,” 14 Apr 2015; <https://briankoberlein.com/2015/04/14/thats-about-the-size-of-it/>.

¹⁶⁷² Chiao RY, Minter SJ, Wegter-McNelly K. Laboratory-scale superconducting mirrors for gravitational microwaves. eprintarXiv :0903.3280, 2009 Mar 26; <https://arxiv.org/pdf/0903.3280.pdf>.

¹⁶⁷³ [https://en.wikipedia.org/wiki/Geon_\(physics\)](https://en.wikipedia.org/wiki/Geon_(physics)).

Geons were first investigated theoretically in 1955 by Wheeler who coined the term as a contraction of “gravitational electromagnetic entity”.¹⁶⁷⁴ Wheeler calculated that a simple toroidal electromagnetic geon would have a minor radius of $\sim 7.91 \times 10^8$ m and a mass density of $\rho_{\text{ToroidGeon}} \sim 2.16 \times 10^9$ kg/m³, which implies a rest-mass energy density of $E_{\text{D,geon-phot}} \sim \rho_{\text{ToroidGeon}} c^2 \sim \mathbf{1.9 \times 10^{17}}$ MJ/L. The question of whether geons are stable or must decay over time as the energy of the wave gradually leaks away has not yet been definitively answered, though the current consensus seems to be that they probably cannot be stable.¹⁶⁷⁵

According to Wheeler, “there is little difference between the theory of a geon built out of neutrinos, and one built out of electromagnetic fields...” He calculates that the smallest neutrino geon would have radius $\sim 2.83 \times 10^7$ m, a mass of 3.82×10^{33} kg, and an energy density of $E_{\text{D,geon-neut}} \sim \mathbf{3.62 \times 10^{21}}$ MJ/L. This suggests that it might be possible to create a liquid or solid phase of neutrinos that might be called “neutrinium”¹⁶⁷⁶ or “neutrino condensate”.¹⁶⁷⁷ There is also a mathematical proof that a neutrino superfluid can exist.¹⁶⁷⁸

Electroweak Matter and Preon Matter. An electroweak star is a theoretical type of exotic star, whereby the gravitational collapse of the star is prevented by radiation pressure resulting from electroweak burning (the energy released by conversion of quarks to leptons through the electroweak force), when quark degeneracy pressure is no longer able to withstand gravitational attraction but may still be withstood by electroweak burning radiation pressure.¹⁶⁷⁹ This process is expected to occur in a $V_{\text{ewstar}} \sim 0.1$ L volume at the star’s core, containing $M_{\text{ewstar}} \sim 10^{25}$ kg of hypothetical electroweak matter.¹⁶⁸⁰ Electroweak stars would be denser than quark stars, so electroweak matter, if it exists, should have a much higher energy density than the estimated 0.8-

¹⁶⁷⁴ Wheeler JA. Geons. Phys Rev. 1955 Jan 15;97(2):511-536; <http://mediathek.mpiwg-berlin.mpg.de/mediathekPublic/dms/mediathek/pdf/Department1/Quantum-Gravity-Workshop/o1955Geons.pdf>.

¹⁶⁷⁵ Perry GP, Cooperstock FI. Stability of gravitational and electromagnetic geons. Class Quant Grav. 1999;16(6):1889–1916; <https://arxiv.org/pdf/gr-qc/9810045>.

¹⁶⁷⁶ <https://plus.google.com/+johncbaz999/posts/L7mclBJuEAp>.

¹⁶⁷⁷ Barenboim G. Gravity triggered neutrino condensates. Phys Rev D. 2010;82:093014; <https://arxiv.org/pdf/1009.2504>.

¹⁶⁷⁸ Kapusta JJ. Neutrino superfluidity. Phys Rev Lett. 2004 Dec 17; 93(25):251801; <https://arxiv.org/pdf/hep-th/0407164.pdf>.

¹⁶⁷⁹ https://en.wikipedia.org/wiki/Electroweak_star.

¹⁶⁸⁰ Dai DC, Lue A, Starkman G, Stojkovic, D. Electroweak stars: how nature may capitalize on the standard model's ultimate fuel. J Cosmology and Astroparticle Phys. 2010(12):004; https://s3.amazonaws.com/academia.edu.documents/42479573/Electroweak_stars_how_nature_may_capitalize_on_the_standard_model's_ultimate_fuel.pdf?AWSAccessKeyId=AKIAIWOWYYGZ2Y53UL3A&Expires=1549264309&Signature=oWILkfCoGdW6LrD9nyv3Dw0ZxTo%3D&response-content-disposition=inline%3B%20filename%3DElectroweak_stars_how_nature_may_capital.pdf.

3×10^{26} MJ/L of quarkium (**Section 7.5.4.3**); assuming a mean density of $\rho_{\text{ewstar}} \sim M_{\text{ewstar}} / V_{\text{ewstar}} \sim 10^{29}$ kg/m³ and a rest-mass energy density of $E_{\text{D,ew}} \sim \rho_{\text{ewstar}}c^2 \sim 9 \times 10^{36}$ MJ/L.

A preon star¹⁶⁸¹ is another theoretical type of exotic star, composed of “preons” which are conceived to be the hypothetical subcomponents of quarks and leptons.¹⁶⁸² It is believed that primordial preon stars may still exist,¹⁶⁸³ and that new preon stars might arise from massive stars that collapse too unstably to become neutron stars but not enough to become black holes.¹⁶⁸⁴ Preon models represent an attempt to simplify the Standard Model. Interest peaked in the 1980s but slowed because the Standard Model of particle physics continued to describe the physics mostly successfully¹⁶⁸⁵ and because no direct experimental evidence for lepton and quark compositeness has yet been found.¹⁶⁸⁶ The maximum radius and mass of a preon star are predicted to be $R_{\text{pstar}} \sim 1$ meter and $M_{\text{pstar}} \sim 6 \times 10^{26}$ kg,¹⁶⁸⁷ which implies a mean density of $\rho_{\text{pstar}} \sim M_{\text{pstar}} / (4\pi R_{\text{pstar}}^3/3) = 1.4 \times 10^{26}$ kg/m³ and a rest-mass energy density of $E_{\text{D,preon}} \sim \rho_{\text{pstar}}c^2 \sim 1.3 \times 10^{34}$ MJ/L.

Planck Matter. In loop quantum gravity, a Planck star¹⁶⁸⁸ (composed of Planck matter) is a theoretically possible astronomical object that is created when the energy density of a collapsing star reaches the Planck energy density¹⁶⁸⁹ of $E_{\text{D,Planck}} = c^7/\hbar G^2 = 4.633 \times 10^{104}$ MJ/L, where $c = 3 \times 10^8$ m/sec (speed of light), $\hbar = h/2\pi = 1.06 \times 10^{-34}$ J-sec (reduced Planck’s constant) and $G = 6.67 \times 10^{-11}$ N-m²/kg² (gravitational constant). A repulsive force arises under these conditions, derived from Heisenberg’s uncertainty principle, assuming that gravity and spacetime are both quantized. In this case, the accumulation of mass-energy inside the Planck star cannot further collapse because it would violate the uncertainty principle for spacetime itself.¹⁶⁹⁰ This repulsive force arises from the energy density, not the Planck length, and is strong enough to stop the

¹⁶⁸¹ Hansson J, Sandin F. Preon stars: a new class of cosmic compact objects. Phys Lett B. 2005 Jun 9;616(1-2):1-7; <https://arxiv.org/abs/astro-ph/0410417>.

¹⁶⁸² D’Souza IA, Kalman CS. Preons: Models of Leptons, Quarks and Gauge Bosons as Composite Objects. World Scientific, 1992.

¹⁶⁸³ Philip Ball, “Splitting the quark,” Nature News, 30 Nov 2007; <http://www.nature.com/news/2007/071130/full/news.2007.292.html>.

¹⁶⁸⁴ https://en.wikipedia.org/wiki/Preon_star.

¹⁶⁸⁵ <https://en.wikipedia.org/wiki/Preon>.

¹⁶⁸⁶ Dorminey B. Focus: Nuggets of New Physics. Phys Rev Focus 2007 Nov 20;20:18; <https://physics.aps.org/story/v20/st18>.

¹⁶⁸⁷ Sandin F. Exotic Phases of Matter in Compact Stars. Thesis, Luleå University of Technology, OCLC 185216905, 2007; <http://epubl.ltu.se/1402-1544/2007/05/LTU-DT-0705-SE.pdf>.

¹⁶⁸⁸ https://en.wikipedia.org/wiki/Planck_star.

¹⁶⁸⁹ https://en.wikipedia.org/wiki/Planck_units#Derived_units.

¹⁶⁹⁰ Rovelli C, Vidotto F. Planck stars. Int J Mod Phys D. 2014 Dec;23(12):1442026; <https://arxiv.org/pdf/1401.6562>.

collapse of the Planck star at a diameter of ~ 1 pm (for a stellar mass), well before a singularity is formed.¹⁶⁹¹

Tachyons. A tachyon¹⁶⁹² is a hypothetical particle that always travels faster than light. The speed of a tachyon increases as its energy decreases, reaching infinite velocity (becoming a “transcendent tachyon” everywhere present on its worldline) at zero energy. To accomplish this, classical tachyons have an imaginary mass,¹⁶⁹³ although in some modern formulations of the theory the mass of tachyons is regarded as real.¹⁶⁹⁴ Most physicists believe that faster-than-light particles cannot exist because they are not consistent with the known laws of physics,¹⁶⁹⁵ including causality violations via the tachyon telephone paradox.¹⁶⁹⁶ No experimental evidence for the existence of such particles has been found, though tachyons have been considered as candidates for dark matter and dark energy,¹⁶⁹⁷ and tachyon condensation¹⁶⁹⁸ has been invoked in string theory.¹⁶⁹⁹ A recent paper describing a hypothetical Fermi gas of free tachyons¹⁷⁰⁰

¹⁶⁹¹ “New Type of Star Emerges From Inside Black Holes,” The Physics arXiv Blog, 5 Feb 2014; <https://medium.com/the-physics-arxiv-blog/new-type-of-star-emerges-from-inside-black-holes-6cf7ec0ed28b>.

¹⁶⁹² <https://en.wikipedia.org/wiki/Tachyon>.

¹⁶⁹³ Sommerfeld A. Simplified deduction of the field and the forces of an electron moving in any given way. *Knl. Acad. Wetensch.* 1904;7:345-367. Bilaniuk OMP, Deshpande VK, Sudarshan ECG. 'Meta' relativity. *Am J Phys.* 1962 Oct;30(10):718-723; <https://vdocuments.mx/omp-bilaniuk-vk-deshpande-ecg-sudarshan-meta-relativity.html>. Feinberg G. Possibility of faster-than-light particles. *Phys Rev.* 1967 Jul 25;159(5):1089-1105; http://relativityscience.com/images/superluminal_velocities/possibility_faster_than_light.pdf. Bilaniuk OMP, Sudarshan ECG. Particles beyond the light barrier. *Physics Today.* 1969;22(5):43-51; <http://www.santilli-foundation.org/docs/Sudarshan.pdf>.

¹⁶⁹⁴ Recami E. Classical tachyons and possible applications. *Rivista del Nuovo Cimento.* 2007 Oct 16;9(6):1-178; <http://cds.cern.ch/record/160441/files/CM-P00049220.pdf>. Vieira RS. An introduction to the theory of tachyons. *Rev Bras Ens Fis.* 2011 Dec;34(3); <http://www.academia.edu/download/41595643/causality.pdf>. Hill JM, Cox BJ. Einstein's special relativity beyond the speed of light. *Proc R Soc A.* 2012 Dec 8;468(2148):4174-4192; <http://citeseerx.ist.psu.edu/viewdoc/download?doi=10.1.1.681.8612&rep=rep1&type=pdf>.

¹⁶⁹⁵ Tipler PA, Llewellyn RA. *Modern Physics* (5th ed.), W.H. Freeman & Co, NY, 2008.

¹⁶⁹⁶ Benford GA, Book DL, Newcomb WA. The tachyonic antitelephone. *Phys Rev D.* 1970 Jul 15;2(2):263-265; <https://journals.aps.org/prd/abstract/10.1103/PhysRevD.2.263>.

¹⁶⁹⁷ Copeland EJ, Garousi MR, Sami M, Tsujikawa S. What is needed of a tachyon if it is to be the dark energy? *Phys Rev D.* 2005 Feb 10;71:043003; <http://www.academia.edu/download/45798530/0411192.pdf>. Debnath U. Classical and quantum gravity emergent universe and the phantom tachyon model. *Class Quant Grav.* 2008 Sep 30;25(20):205019; <http://citeseerx.ist.psu.edu/viewdoc/download?doi=10.1.1.314.3969&rep=rep1&type=pdf>.

¹⁶⁹⁸ https://en.wikipedia.org/wiki/Tachyon_condensation.

¹⁶⁹⁹ Sen A. Tachyon condensation on the brane antibrane system. *J High Energy Phys.* 1998 Sep 1;8(8):012; <https://arxiv.org/pdf/hep-th/9805170>.

concludes that stable nucleon-mass tachyon matter requires a critical density $n_T = 1.5$ tachyon-equivalent nucleons/fm³ with a nuclear energy density of $E_{D,tach} = 1.2 \times 10^{15}$ kg/L = **1.1 x 10²⁶ MJ/L**.

Negative Matter. Matter with negative mass¹⁷⁰¹ having negative gravitational, inertial, and rest masses would possess some strange properties, such as accelerating in the direction opposite of applied force. (Negative mass is not antimatter (**Section 7.6**), which is currently believed to have normal (positive) mass.¹⁷⁰²) A piece of negative matter placed near a chunk of positive matter of equal mass will repel the positive mass, while the positive mass will attract the negative mass, producing “an unlimited amount of unidirectional acceleration of the combination without the requirement for an energy source or reaction mass”.¹⁷⁰³ Despite being inconsistent with the expected behavior of “normal” matter, negative mass is claimed by advocates to be mathematically consistent and to introduce no violations of conservation of momentum or energy.¹⁷⁰⁴ The objection by cosmologists that negative mass is impossible because it would violate an “energy condition”¹⁷⁰⁵ has recently been overcome with a mathematical demonstration that negative mass can produce a reasonable Schwarzschild solution without violating the energy condition.¹⁷⁰⁶

The energy density of an isolated piece of negative matter, consisting of negative mass-energy¹⁷⁰⁷ trapped in a finite volume, would presumably also be negative,¹⁷⁰⁸ though of similar magnitude as ordinary matter of comparable substance. If it exists, negative mass could be used to warp spacetime around a spaceship according to an Alcubierre metric,¹⁷⁰⁹ achieving apparent faster-than-light travel if a configurable energy-density field lower than that of vacuum (that is, negative mass) could be created. Note that if the two objects described above start at rest with zero

¹⁷⁰⁰ Trojan E, Vlasov GV. Acoustics of tachyon Fermi gas. Phys Rev D. 2011 Jun 15;83(12):124013; <http://inspirehep.net/record/892347/files/arXiv%3A1103.2276.pdf>.

¹⁷⁰¹ https://en.wikipedia.org/wiki/Negative_mass.

¹⁷⁰² https://en.wikipedia.org/wiki/Gravitational_interaction_of_antimatter.

¹⁷⁰³ Forward RL. Negative matter propulsion. J Propulsion and Power. 1990;6(1):28–37; <https://arc.aiaa.org/doi/abs/10.2514/3.23219>.

¹⁷⁰⁴ Bondi H. Negative mass in general relativity. Rev Mod Phys. 1957 Jul;29(3):423-428; <http://ayuba.fr/pdf/bondi1957.pdf>. Forward RL. Negative matter propulsion. J Propulsion and Power. 1990;6(1):28–37; <https://arc.aiaa.org/doi/abs/10.2514/3.23219>. Compare: Bonnor WB. Negative mass in general relativity. Gen Rel and Gravitation. 1989 Nov;21(11):1143-1157; <https://link.springer.com/article/10.1007/BF00763458>.

¹⁷⁰⁵ https://en.wikipedia.org/wiki/Energy_condition.

¹⁷⁰⁶ Mbarek S, Paranjape MB. Negative mass bubbles in de Sitter space-time. Phys Rev D. 2014 Nov;90(10-15):101502(R); <https://arxiv.org/pdf/1407.1457.pdf>.

¹⁷⁰⁷ https://en.wikipedia.org/wiki/Negative_energy.

¹⁷⁰⁸ https://en.wikipedia.org/wiki/Negative_mass#In_Gauss's_law_of_gravity.

¹⁷⁰⁹ https://en.wikipedia.org/wiki/Alcubierre_drive.

combined kinetic energy, the system continues to maintain zero kinetic energy – hence **0 MJ/L** and **0 MJ/kg** – however long the two objects accelerate together because the piece of negative matter has negative energy.

Polariton quasiparticles (**Section 7.5.1**) with negative mass have been demonstrated experimentally,¹⁷¹⁰ and it has been claimed that acoustic phonons carry a negative gravitational mass.¹⁷¹¹

¹⁷¹⁰ Dhara S, Chakraborty C, Goodfellow KM, Qiu L, O’Loughlin TA, Wicks GW, Bhattacharjee S, Vamivakas AN. Anomalous dispersion of microcavity trion-polaritons. *Nat Phys*. 2018;14:130-133; <https://www.nature.com/articles/nphys4303>.

¹⁷¹¹ Esposito A, Krichevsky, Nicolis A. The mass of sound. arXiv, 2018 Jul 23; <https://arxiv.org/pdf/1807.08771.pdf>.

Chapter 9. Summary of the Data

This book surveys the energy densities available in all major fundamental classes of energy storage and primary power generation. Some of the results are summarized in the charts below.

The first five charts provide energy density (MJ/L) vs. specific energy (MJ/kg) for each of four energy storage modalities:

Figure 2. Thermochemical Energy Storage – range: **0.0001-20 MJ/L** and **0.01-50 MJ/kg**.

Figure 3. Chemical Energy Storage – range: **0.1-270 MJ/L** and **0.1-120 MJ/kg**.

Figure 4. Mechanical Energy Storage – range: **0.001-90 MJ/L** and **0.001-30 MJ/kg**.

Figure 5. Nuclear Energy Storage – range: **30,000-10¹⁰ MJ/L** and **5000-5 x 10¹⁰ MJ/kg**.

The four storage modalities are combined on a single chart in **Figure 6**. On all charts, the inscribed line represents the density (1 kg/L) where energy density (MJ/L) and specific energy (MJ/kg) are numerically equal – i.e., materials below the line are less dense than water, while those above the line are more dense than water.

In general, nuclear materials offer at least ~1000 times more energy storage capacity than a similar mass or volume of materials whose ability to store energy depends on chemical forces. The chemical and nuclear realms form two separate islands of energy density on the chart. A third smaller island in the uppermost right corner of **Figure 5** and **Figure 6** represents antimatter energy storage, ~100 times more energy dense than conventional fission/fusion-based materials.

Figure 2. Thermochemical Energy Storage
(human body ~10 MJ/L, ~10 MJ/kg)

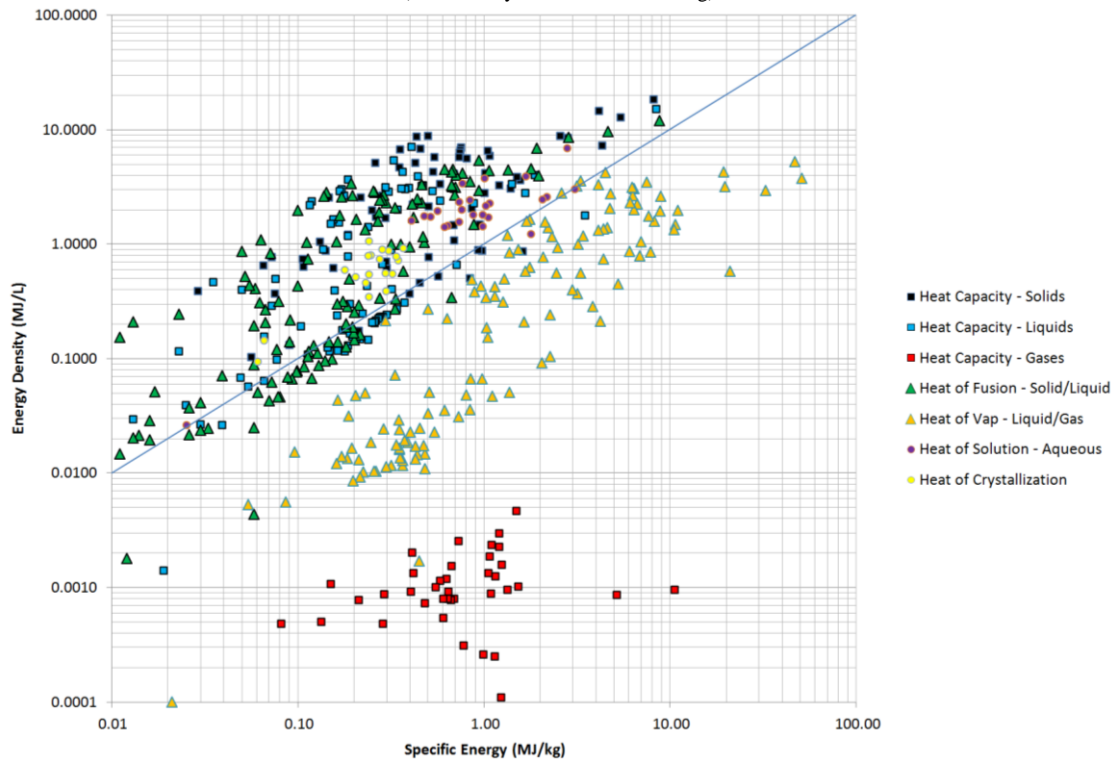


Figure 3. Chemical Energy Storage
(human body ~10 MJ/L, ~10 MJ/kg)

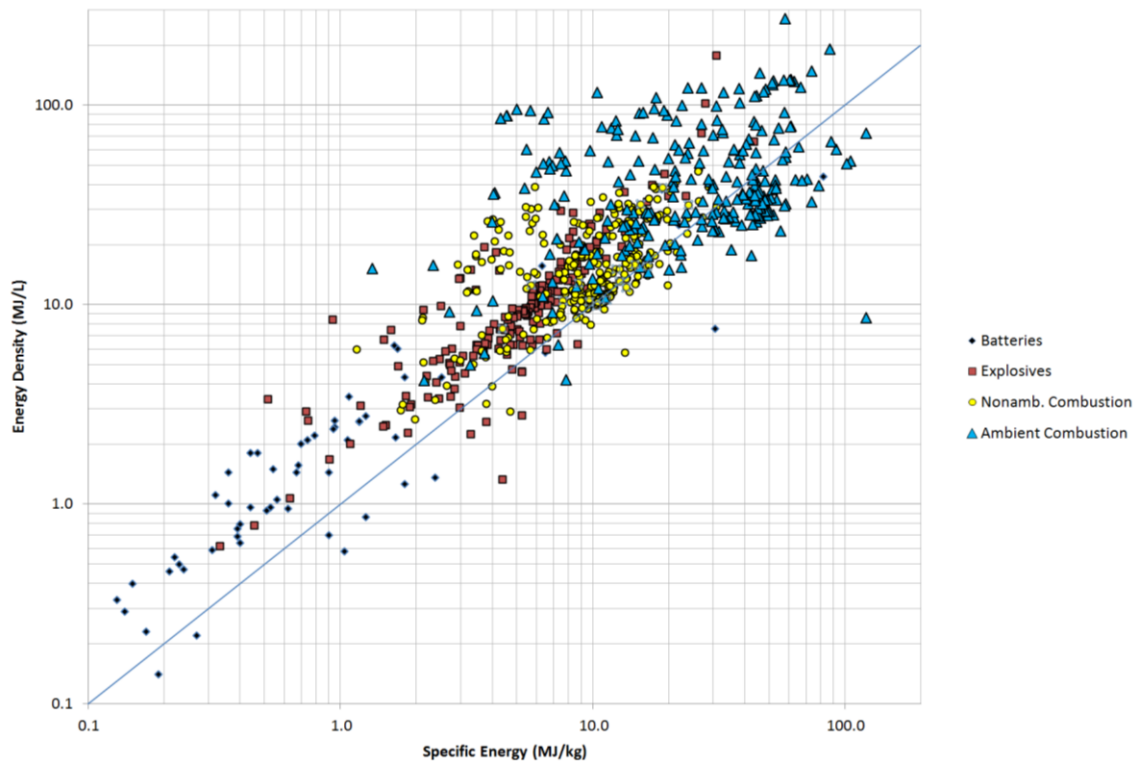


Figure 4. Mechanical Energy Storage
(human body ~10 MJ/L, ~10 MJ/kg)

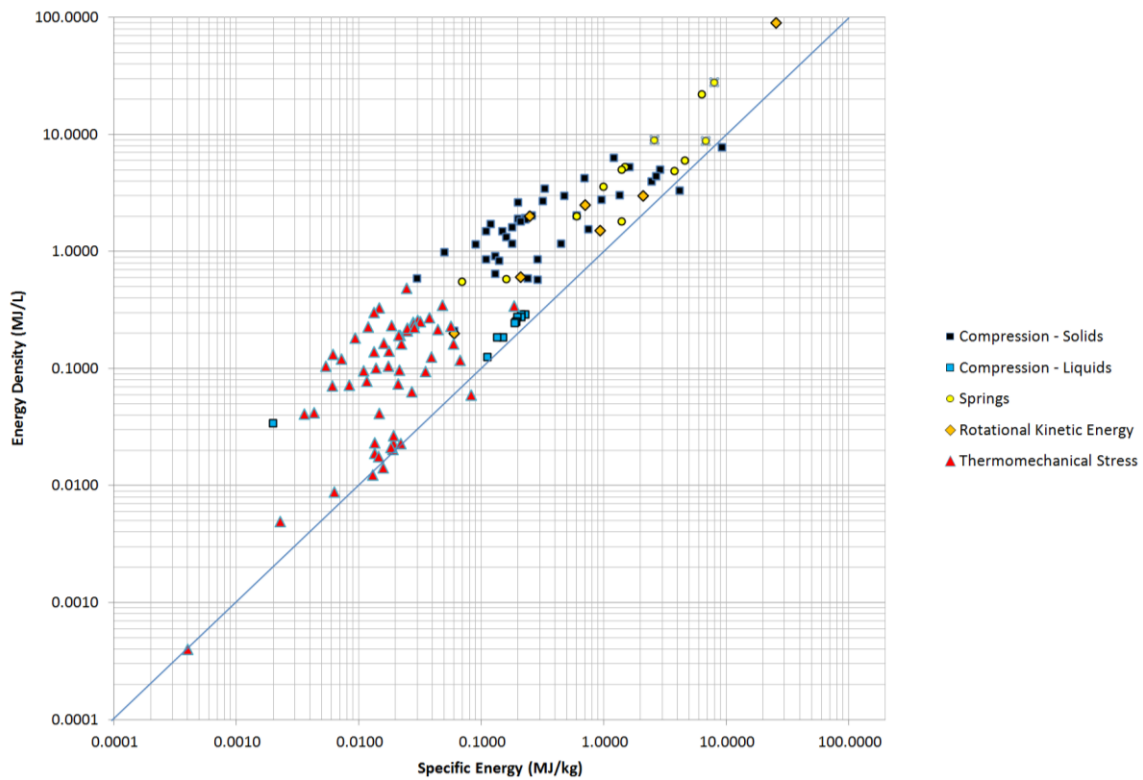


Figure 5. Nuclear Energy Storage
(human body ~10 MJ/L, ~10 MJ/kg)

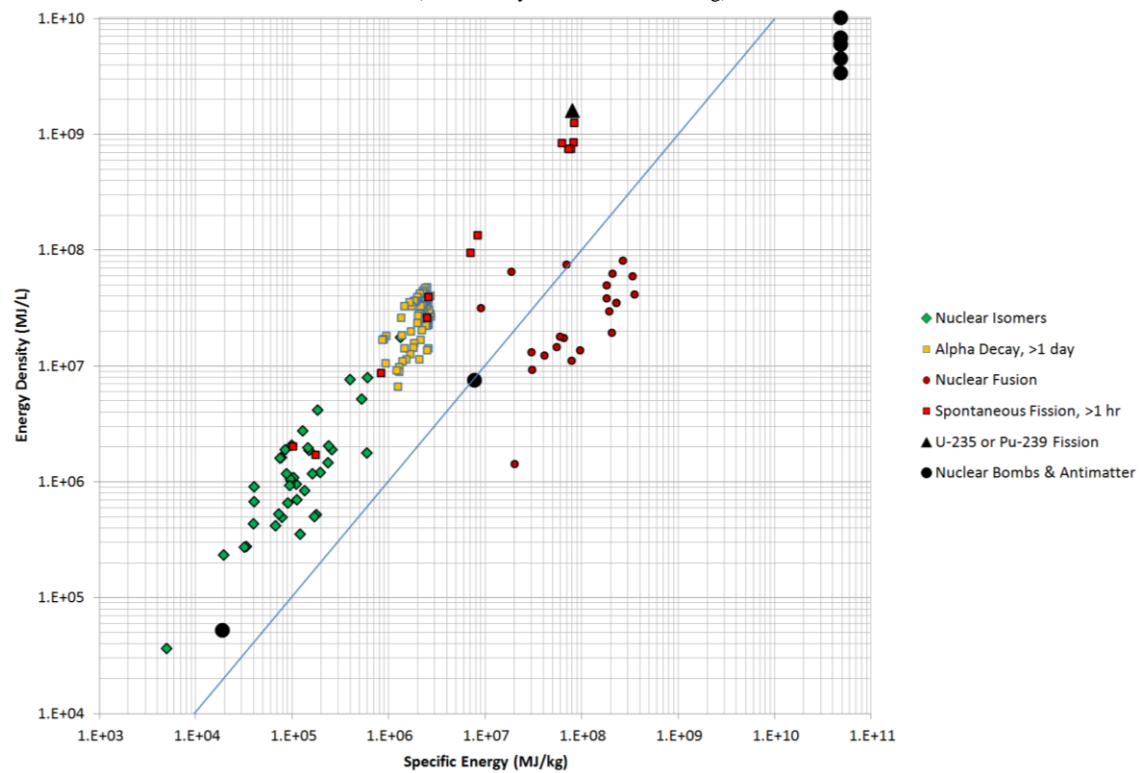
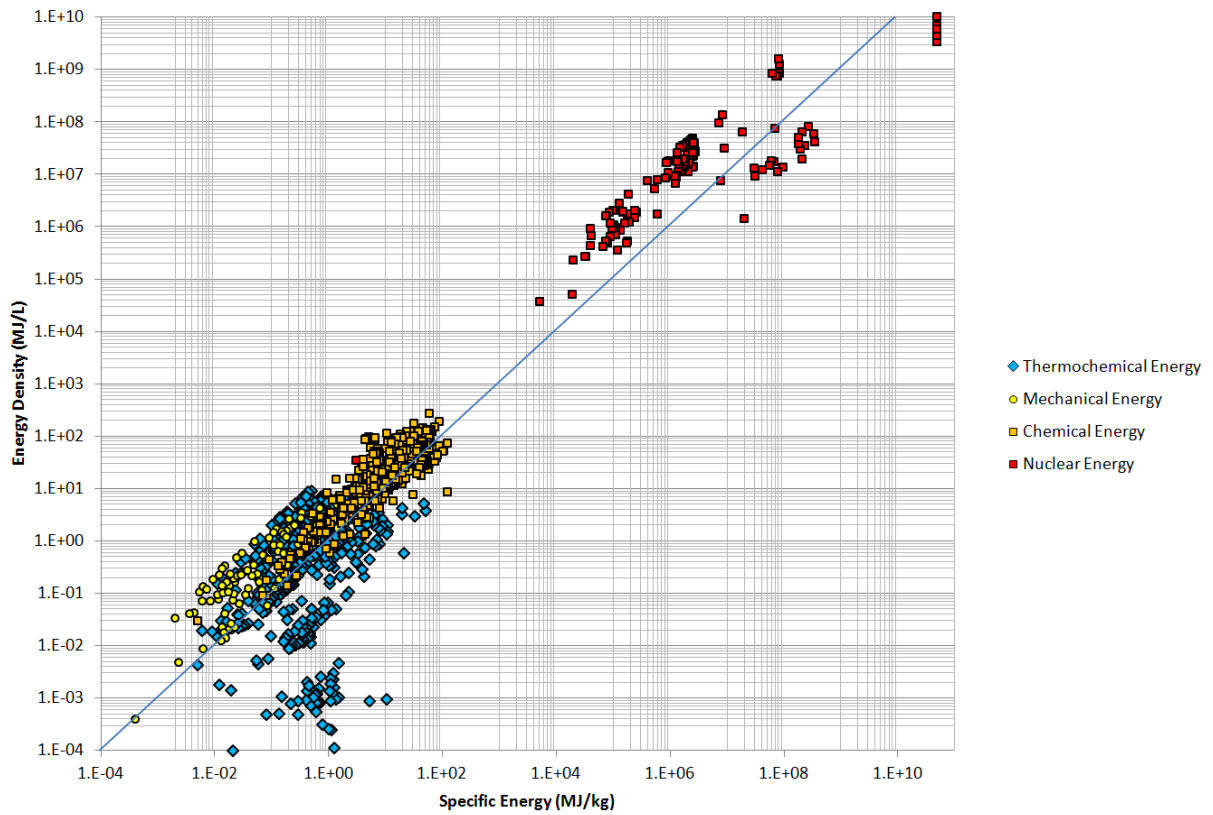


Figure 6. Summary of Energy Storage
(human body ~10 MJ/L, ~10 MJ/kg)



The next six charts provide power density (MW/L) vs. specific power (MW/kg) (aka. power-to-weight ratio) for each of several power storage modalities for which a well-defined output power can be specified:

Figure 7. Battery and Fuel Cell Power Storage – range: **0.00001-0.02 MW/L** and **0.00001-0.07 MW/kg**.

Figure 8. Nuclear Power Storage: α -Emitting Radionuclides – range: **10^{-20} - 10^2 MW/L** and **10^{-21} - 10^1 MW/kg**.

Figure 9. Nuclear Power Storage: Spontaneous Fission and Radioisotope Thermoelectric Generators (RTGs) – range: **10^{-9} - 10^5 MW/L** and **10^{-11} - 10^4 MW/kg**. The values for the solar core of the Sun (which produces ~99% of the energy) are included for comparison.

Figure 10. Nuclear Power Storage: Nuclear Isomers – range: **10^{-7} - 10^3 MW/L** and **10^{-8} - 10^2 MW/kg**.

Figure 11. Nuclear Power Storage: Nuclear Bombs (a fission bomb and a fusion bomb, whole-bomb and nuclear materials only) and Catalyzed Fusion – range: **10^{10} - 10^{15} MW/L** and **10^{10} - 10^{15} MW/kg**.

The five storage modalities are combined on a single specific power vs. power density chart in **Figure 12**. As before, the inscribed line divides materials that are more dense (above the line) or less dense (below the line) than water. The various forms of nuclear power span a vast range of 35 orders of magnitude, while batteries and fuel cells cluster within a few orders of magnitude in the middle over a not very impressive range.

Figure 13 compares specific energy and specific power, and **Figure 14** compares energy density and power density, for energy and power storage modalities for which well-defined data are available. Batteries and nuclear sources form two separate islands of specific energy, separated by 4-6 orders of magnitude in MJ/kg. Nuclear materials cluster in a fairly narrow range of specific energy, but span a very wide range of specific power because of the large variation in half-life of radioactive nuclear species.

Figure 15 lays out the various energy storage modalities according to the available ranges of specific energy (MJ/kg). **Figure 16** provides the same information for energy density (MJ/L). In the latter, fusion reactor energy density is estimated by multiplying the known specific energy of the nuclear materials by the currently available ion densities – 10^{10} cm⁻³ (1.7×10^{-14} kg/L) achieved for protons in magnetic Penning traps, 1.9×10^{14} cm⁻³ (3.2×10^{-10} kg/L) achieved for a proton beam, and 4.3×10^{14} cm⁻³ (1.8×10^{-9} kg/L) for a deuteron/triton mixture in the Alcator C-Mod tokamak fusion reactor at MIT in 2016 (**Section 4.3.1.4**) or prospective ion densities (e.g., 10^{19} - 10^{20} cm⁻³ or 1.7 - 17×10^{-5} kg/L for hydrogen; **Section 4.3.1.1** and **Section 4.3.1.2**).

Figure 7. Battery and Fuel Cell Power Storage
 (human body $1\text{-}24 \times 10^{-6}$ MW/L, $1\text{-}23 \times 10^{-6}$ MW/kg)

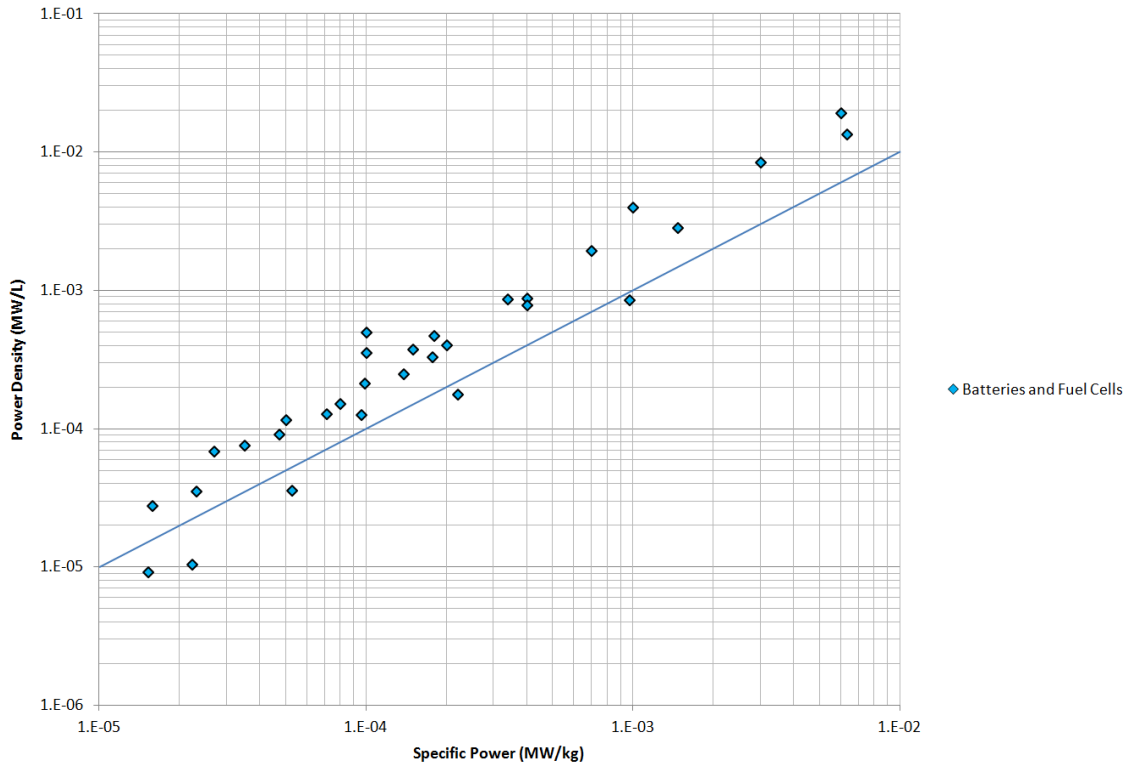


Figure 8. Nuclear Power Storage – Alpha Radionuclides
 (human body $1\text{-}24 \times 10^{-6}$ MW/L, $1\text{-}23 \times 10^{-6}$ MW/kg)

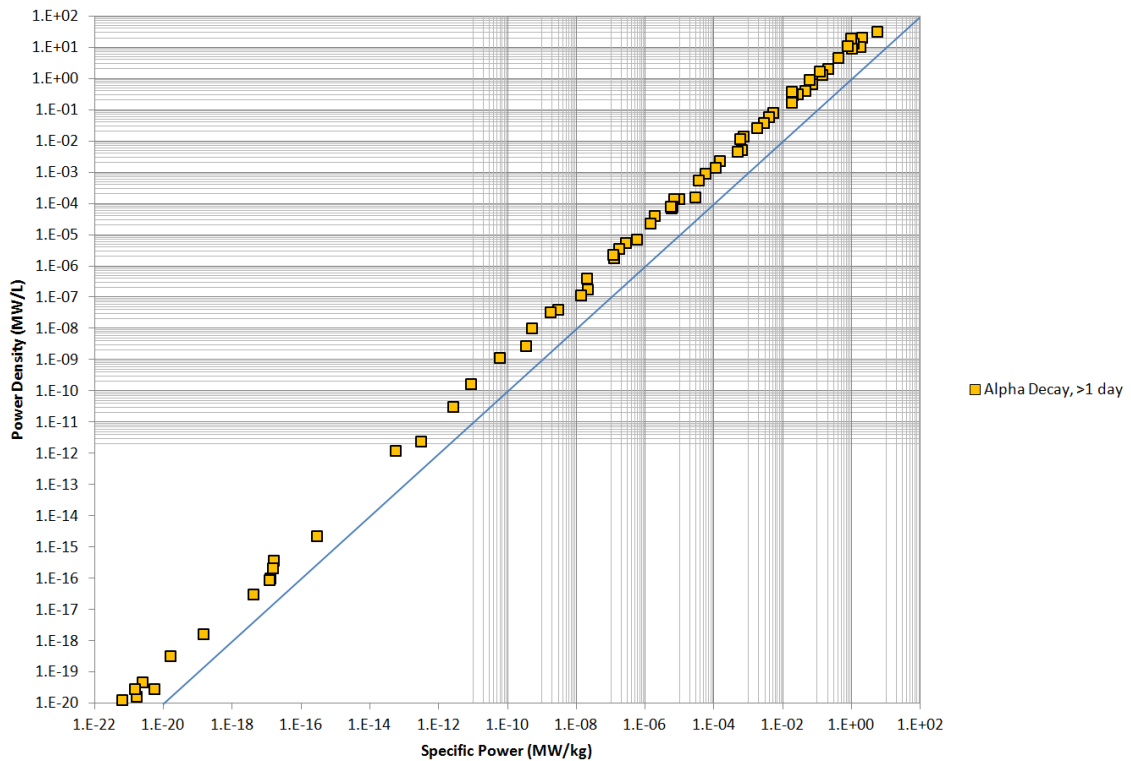


Figure 9. Nuclear Power Storage – Spontaneous Fission & RTGs
 (human body $1-24 \times 10^{-6}$ MW/L, $1-23 \times 10^{-6}$ MW/kg)

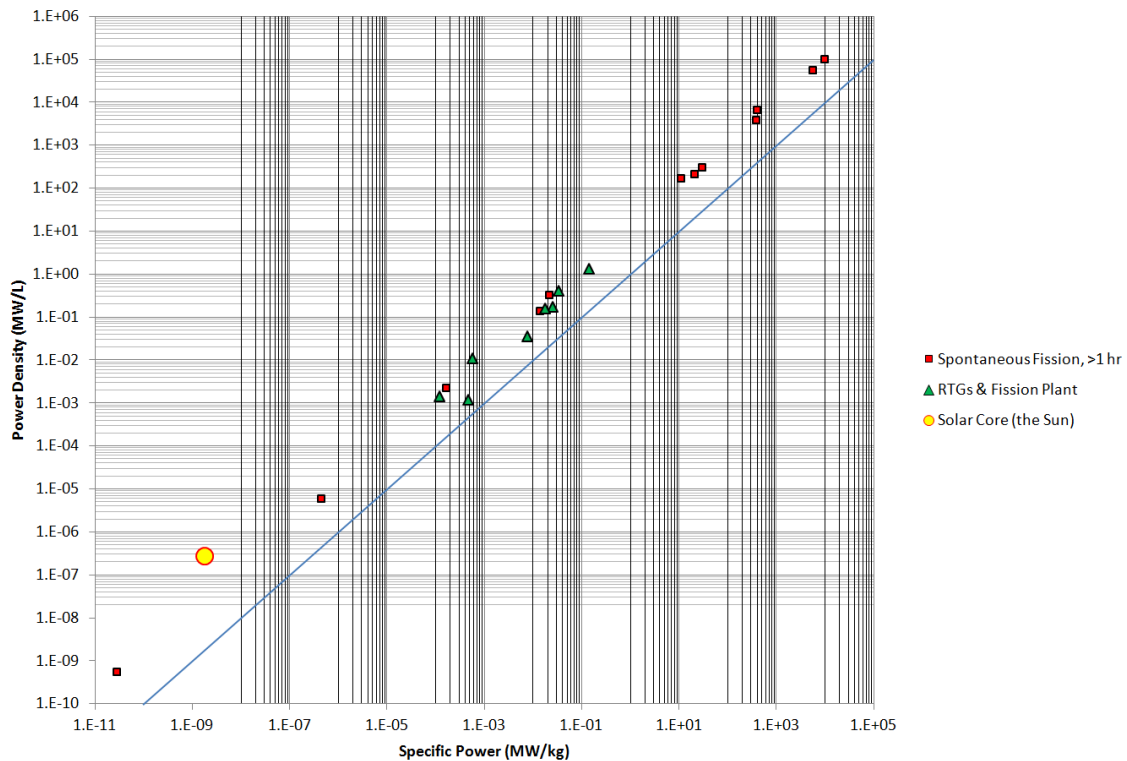


Figure 10. Nuclear Power Storage – Nuclear Isomers
 (human body $1-24 \times 10^{-6}$ MW/L, $1-23 \times 10^{-6}$ MW/kg)

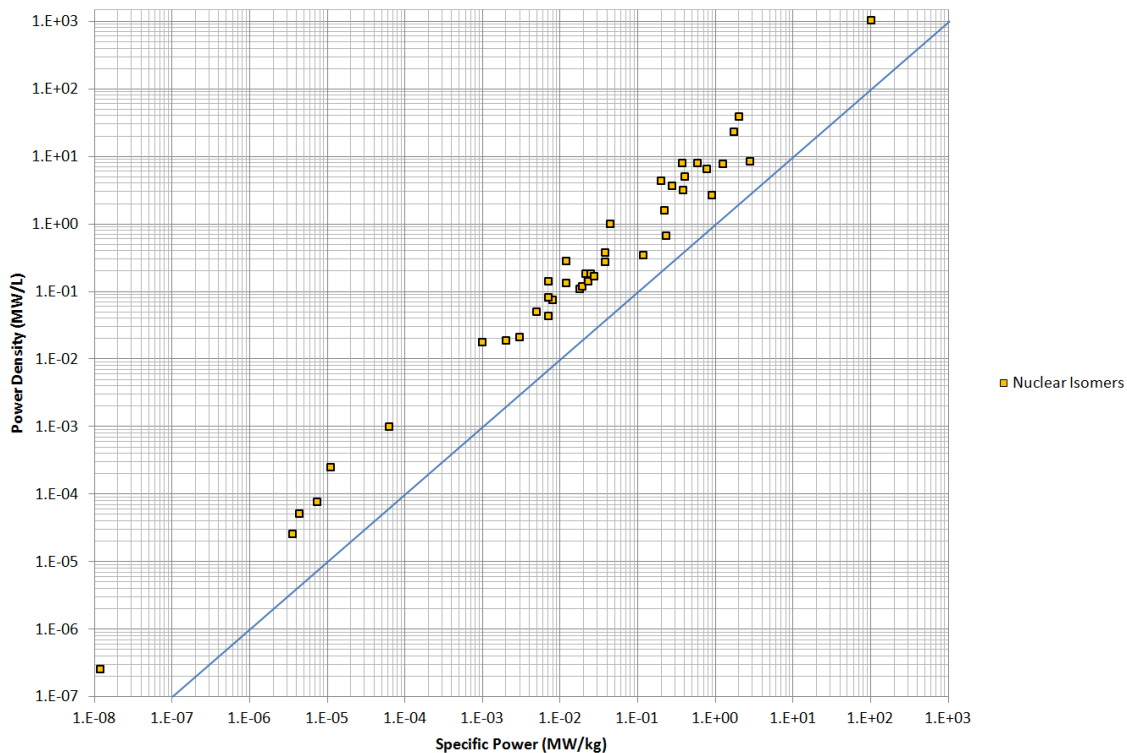


Figure 11. Nuclear Power Storage – Nuclear Bombs & Catalyzed Fusion
 (human body $1-24 \times 10^{-6}$ MW/L, $1-23 \times 10^{-6}$ MW/kg)

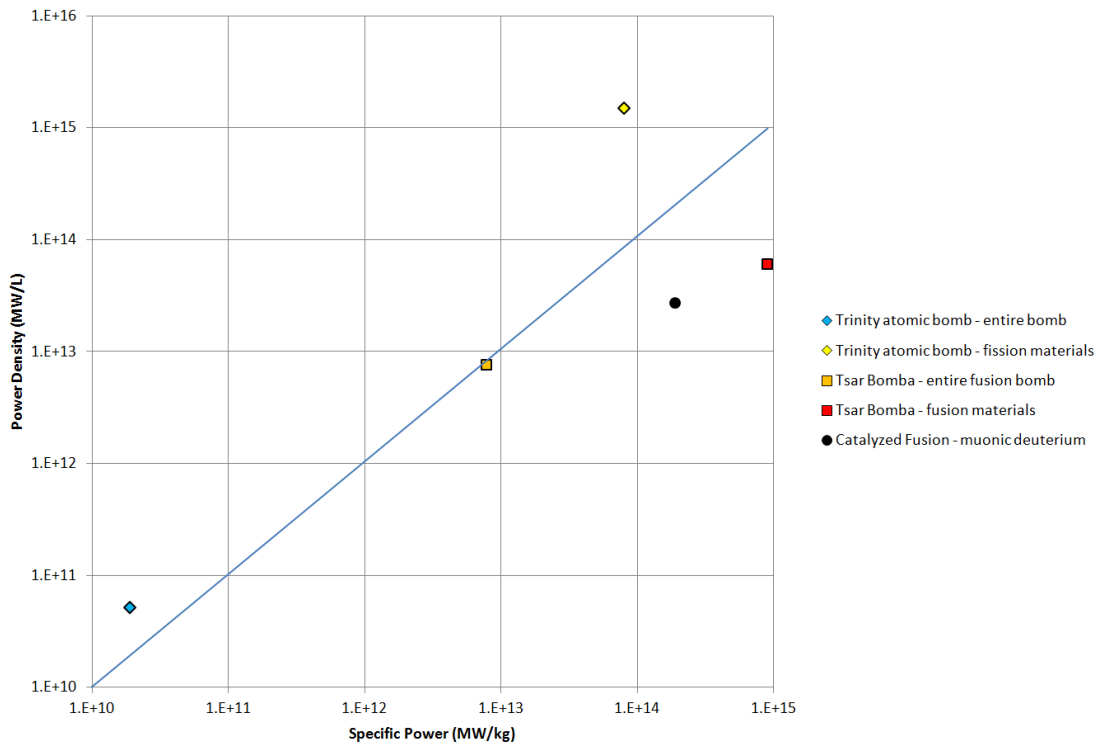


Figure 12. Summary of Power Storage
 (human body $1-24 \times 10^{-6}$ MW/L, $1-23 \times 10^{-6}$ MW/kg)

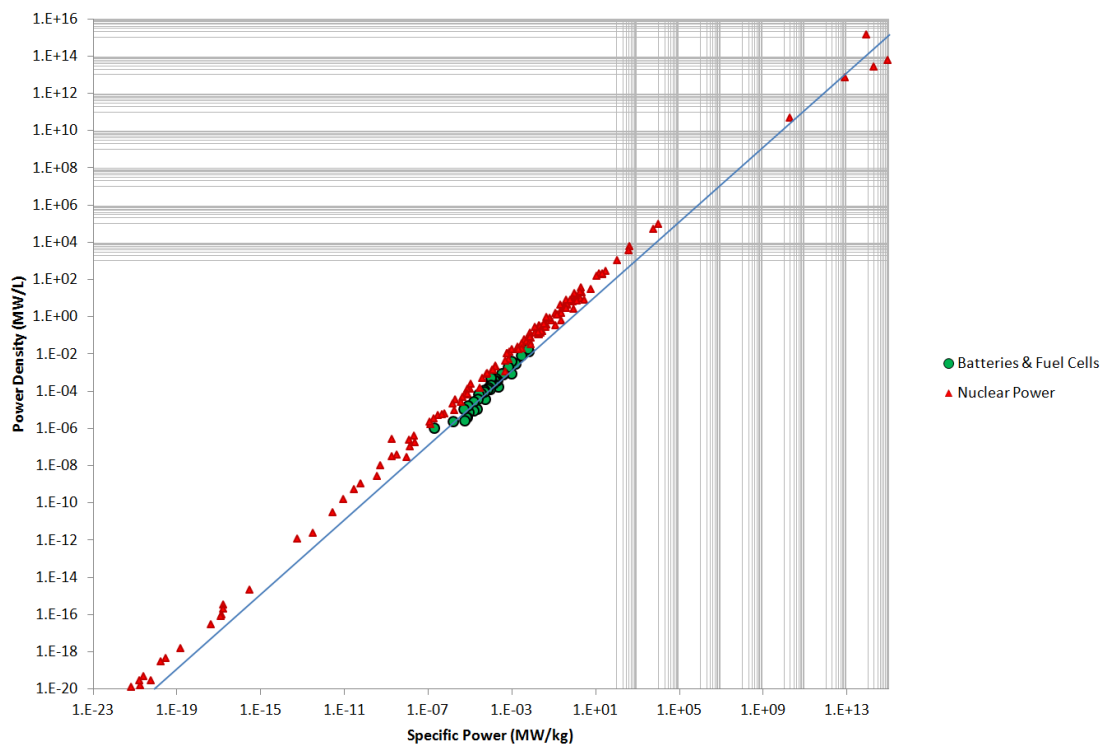


Figure 13. Specific Energy vs. Specific Power
(human body ~ 10 MJ/kg, $1-23 \times 10^{-6}$ MW/kg)

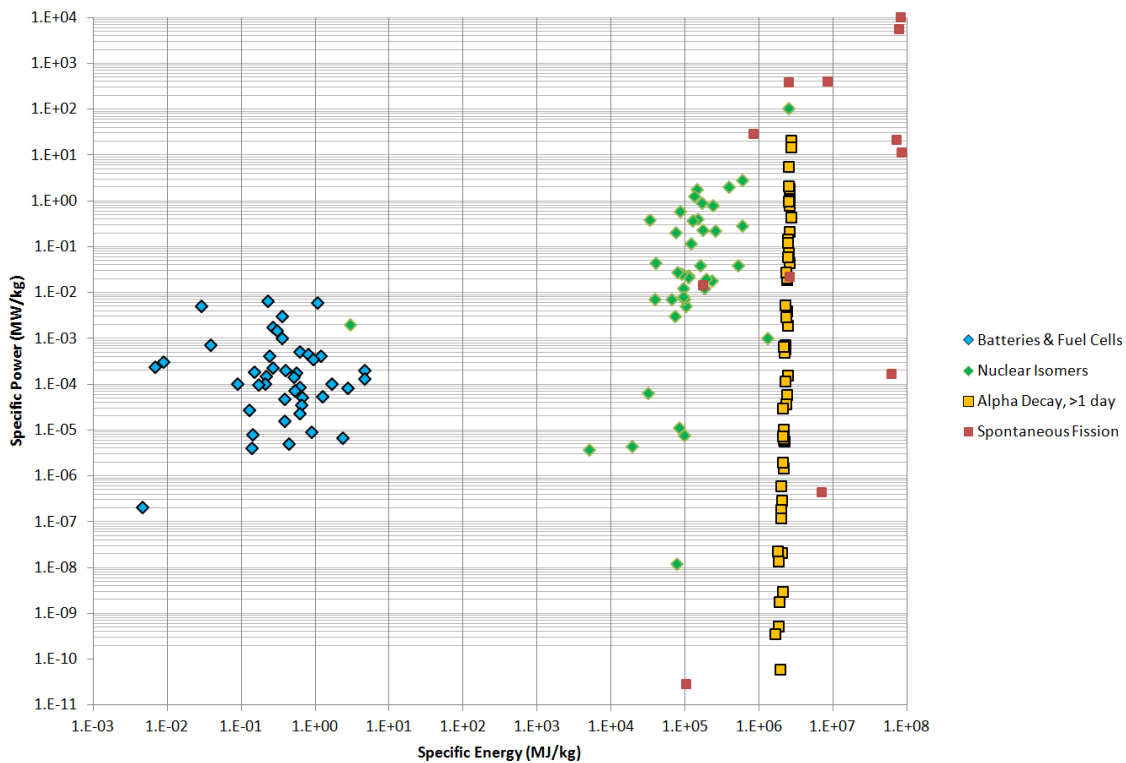


Figure 14. Energy Density vs. Power Density
(human body ~ 10 MJ/L, $1-24 \times 10^{-6}$ MW/L)

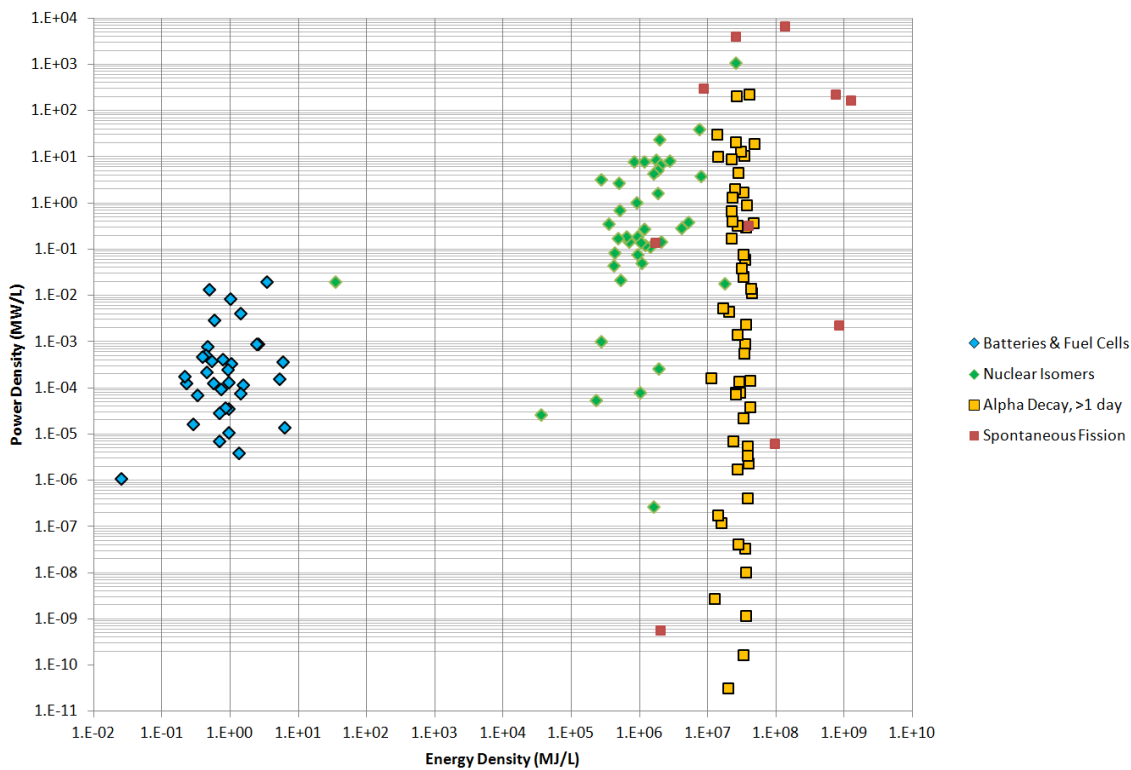


Figure 15. Specific Energy (MJ/kg) of Energy Storage Modalities
(human body ~10 MJ/kg)

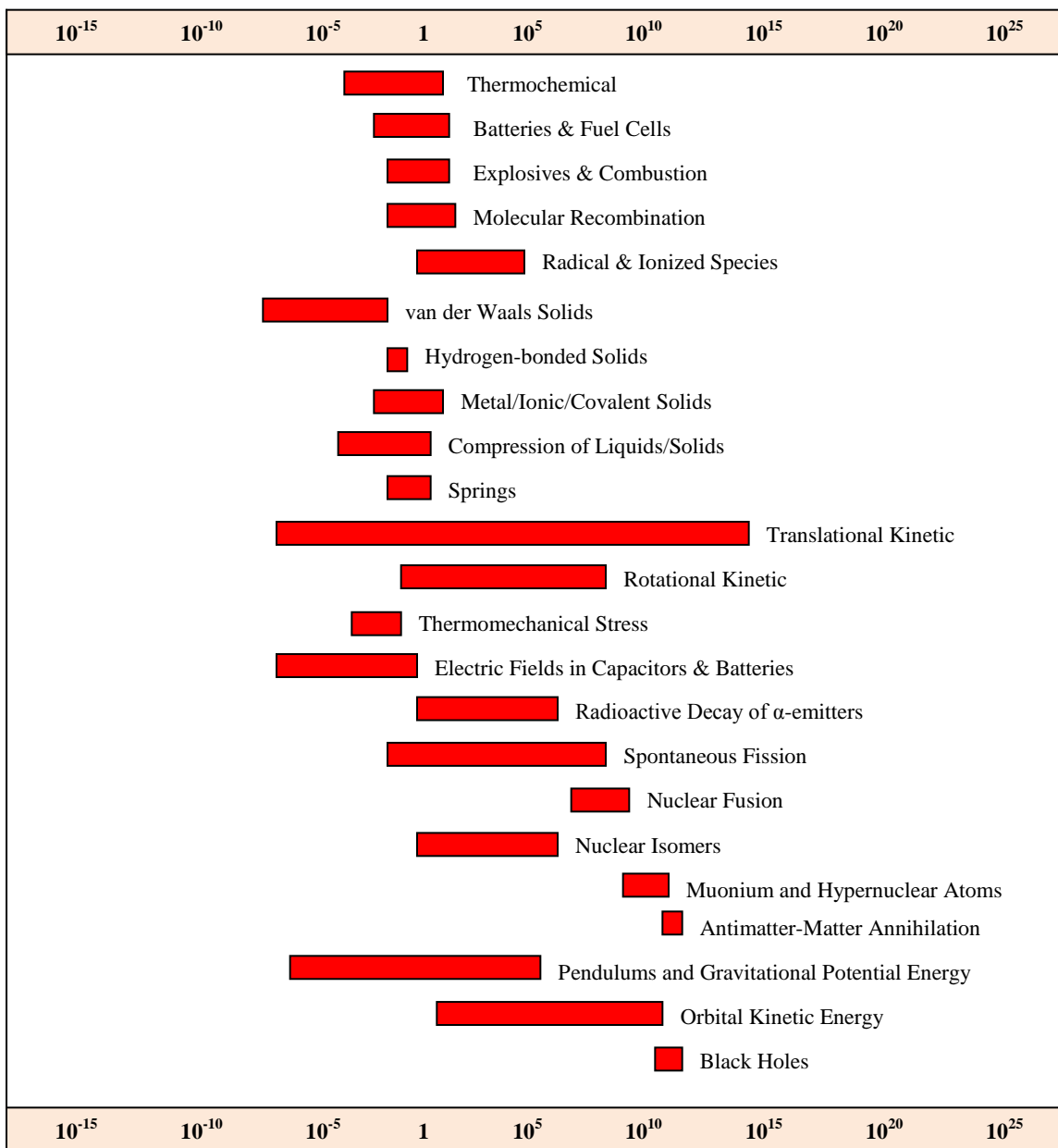
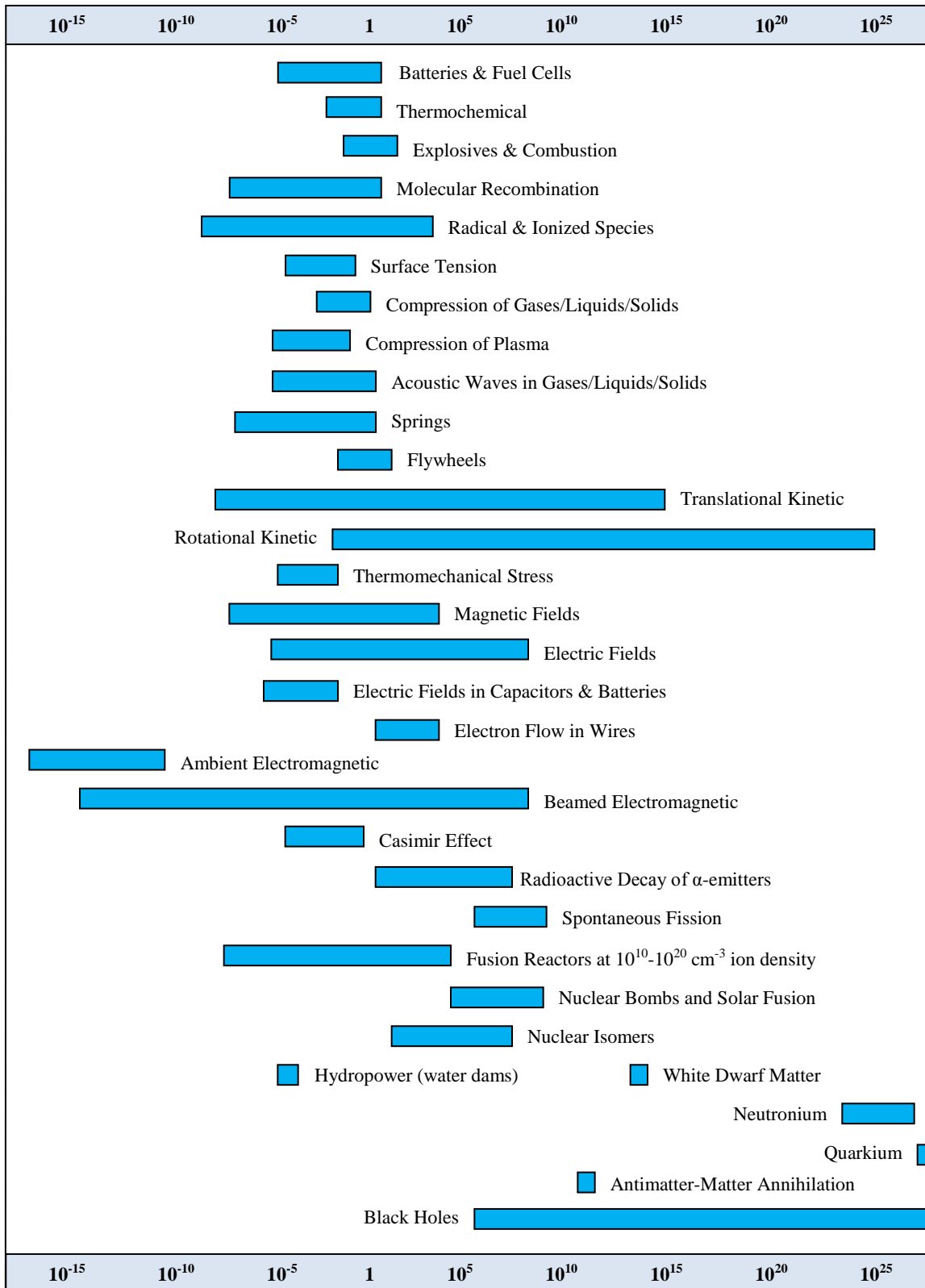


Figure 16. Energy Density (MJ/L) of Energy Storage Modalities
(human body ~10 MJ/L)



Appendix A. Compendium of Data Tables

This Appendix contains calculations and source data with literature references supporting the results recorded in several tables provided elsewhere in this book.

Table A1 in Appendix A.1 provides data on energy storage in nature, supporting the results reported in **Table 1** and **Table 2** in the main text.

Table A2 in Appendix A.2 provides data on power generation in nature, supporting the results reported in **Table 3** and **Table 4** in the main text.

Table A3 in Appendix A.3 provides data on energy storage in chemical decomposition, supporting the results reported in **Table 25** and **Table 26** in the main text.

Table A4 in Appendix A.4 provides data on energy storage in chemical combustion fuels, for both ambient and non-ambient combustion, supporting the results reported in **Table 27**, **Table 28**, **Table 29**, and **Table 30** in the main text.

Table A5 in Appendix A.5 provides power and energy storage data for radionuclides, supporting the results reported in **Table 50**, **Table 51**, **Table 52**, and **Table 53** in the main text.

Table A6 in Appendix A.6 provides power and energy storage data for spontaneous fission radionuclides, supporting the results reported in **Table 54** in the main text.

A.1 Data on Energy Storage in Nature

Table A1. Data on energy storage in nature.			
Energy Storage System	Energy (J)	Mass (kg)	Volume (m ³)
<u>Nuclear and Atomic</u>			
Thermal energy, H ₂ molecule at STP ¹⁷¹²	5.66 x 10 ⁻²¹	3.35 x 10 ⁻²⁷	3.72 x 10 ⁻²⁶
Chemical bond energy, H ₂ molecule at STP ¹⁷¹³	7.17 x 10 ⁻¹⁹	3.35 x 10 ⁻²⁷	3.72 x 10 ⁻²⁶
Neodymium-144 radionuclide ¹⁷¹⁴	2.93 x 10 ⁻¹³	2.39 x 10 ⁻²⁵	3.41 x 10 ⁻²⁹
Europium-147 radionuclide	4.66 x 10 ⁻¹³	2.44 x 10 ⁻²⁵	4.64 x 10 ⁻²⁹
Gadolinium-148 radionuclide	5.10 x 10 ⁻¹³	2.46 x 10 ⁻²⁵	3.11 x 10 ⁻²⁹
Polonium-210 radionuclide	8.50 x 10 ⁻¹³	3.49 x 10 ⁻²⁵	3.79 x 10 ⁻²⁹
Francium-215 radionuclide	1.75 x 10 ⁻¹²	3.57 x 10 ⁻²⁵	1.91 x 10 ⁻²⁸
Rest mass energy of one H ₂ molecule ¹⁷¹⁵	3.02 x 10 ⁻¹⁰	3.35 x 10 ⁻²⁷	3.72 x 10 ⁻²⁶
Most energetic cosmic ray known ¹⁷¹⁶	51	1.67 x 10 ⁻²⁷	2.8 x 10 ⁻⁴⁵
<u>Biological</u>			
Resilin pad of the flea (<i>Spilopsyllus</i>) ¹⁷¹⁷	4.2 x 10 ⁻⁷	1.86 x 10 ⁻¹⁰	1.4 x 10 ⁻¹³

¹⁷¹² A single hydrogen molecule has thermal energy $\sim (3/2) k_B T = (1.5) (1.381 \times 10^{-23} \text{ J/K}) (273.15 \text{ K}) = 5.66 \times 10^{-21}$ joules, mass $\sim 3.35 \times 10^{-27}$ kg, and volume $\sim 3.72 \times 10^{-26} \text{ m}^3$ at STP.

¹⁷¹³ Chemical energy of a single H-H bond in an H₂ molecule is 432 kJ/mole = 7.17 x 10⁻¹⁹ joules; http://www.wiredchemist.com/chemistry/data/bond_energies_lengths.html.

¹⁷¹⁴ Data from **Table A5** in **Appendix A**, and from Theodore Gray: <http://www.periodictable.com/Isotopes/001.1/index2.full.dm.prod.html>.

¹⁷¹⁵ $E = mc^2 = (3.35 \times 10^{-27} \text{ kg}) (3 \times 10^8 \text{ m/sec})^2 = 3.02 \times 10^{-10}$ joules.

¹⁷¹⁶ The most energetic cosmic ray ever detected was probably a single proton (mass = 1.67 x 10⁻²⁷ kg, volume = 2.8 x 10⁻⁴⁵ m³ based on 2014 CODATA charge radius of 0.8751 fm) traveling just below the speed of light with an energy of 51 joules (3.2 x 10²⁰ eV). Bird DJ *et al.* Detection of a cosmic ray with measured energy well beyond the expected spectral cutoff due to cosmic microwave radiation. *Astrophys J.* 1995 Mar; 441(1):144-150; <http://www.cosmic-ray.org/papers/1995ApJ...441..144B.pdf>.

¹⁷¹⁷ An example of mechanical energy storage in biology. Bennet-Clark HC, Lucey ECA. The jump of the flea: a study of the energetics and a model of the mechanism. *J Exp Biol.* 1967 Aug;47(1):59-67; <http://jeb.biologists.org/content/jexbio/47/1/59.full.pdf>. Elvin CM, Carr AG, Huson MG, Maxwell JM, Pearson RD, Vuocolo T, Liyou NE, Wong DC, Merritt DJ, Dixon NE. Synthesis and properties of crosslinked recombinant pro-resilin. *Nature.* 2005 Oct 13;437(7061):999-1002; https://www.researchgate.net/profile/Mickey_Huson/publication/7544512_Elvin_C_M_et_al_Synthesis_and_properties_of_crosslinked_recombinant_pro-resilin_Nature_437_999-1002/links/0c96051afbe2e420ec000000.pdf. "Resilin," <https://en.wikipedia.org/wiki/Resilin>.

Electric eel (<i>Electrophorus electricus</i>) ¹⁷¹⁸	1.2-1.7	20	2×10^{-2}
Apple falling from a tree ¹⁷¹⁹	2.9	0.15	3.3×10^{-4}
Glucose (oxidation, excluding O ₂) ¹⁷²⁰	16,000	0.001	6.49×10^{-7}
Glucose (oxidation, including O ₂ @ STP) ¹⁷²¹	16,000	0.00207	7.46×10^{-4}
Fat (oxidation, excluding O ₂) ¹⁷²²	37,000	0.001	$\sim 9 \times 10^{-7}$
Fat (oxidation, including O ₂ @ STP) ¹⁷²³	37,000	0.00387	2.01×10^{-3}
ATP (1 mole, full conversion to AMP) ¹⁷²⁴	76,100	0.50718	4.88×10^{-4}
Human body (typical, male, fasting) ¹⁷²⁵	6.476×10^8	70	6.73×10^{-2}
Planet-wide			

¹⁷¹⁸ An example of electrical energy storage in biology. “Electric eel,” https://en.wikipedia.org/wiki/Electric_eel. “Voltage of an Electric Eel,” The Physics Factbook; <http://hypertextbook.com/facts/BarryLajnwand.shtml>.

¹⁷¹⁹ An example of gravitational energy storage in biology. A typical apple weighs 1/3 pound or 0.15 kg (<https://www.reference.com/food/much-apple-weigh-2e062ed8710fd63>); the density of raw fuji apples is 461 kg/m³ (<http://www.aqua-calc.com/page/density-table/substance/apples>), giving a volume of 3.3×10^{-4} m³ per apple; and the energy released from a 2 meter fall to the ground at sea level on Earth is $E = mgh = (0.15 \text{ kg})(9.81 \text{ m/sec}^2)(2 \text{ m}) = 2.9 \text{ joules}$.

¹⁷²⁰ A representative carbohydrate. “Glucose,” <https://en.wikipedia.org/wiki/Glucose>.

¹⁷²¹ “Glucose,” <https://en.wikipedia.org/wiki/Glucose>; “Oxygen,” <https://en.wikipedia.org/wiki/Oxygen>.

¹⁷²² Biological fats are triglycerides, which are esters of the three-carbon chain alcohol glycerol and three fatty acids, e.g., palmitic acid (C₁₆H₃₂O₂), oleic acid (C₁₈H₃₄O₂), stearic acid (C₁₈H₃₆O₂), etc. “Fat,” <https://en.wikipedia.org/wiki/Fat>.

¹⁷²³ “Fatty acid metabolism,” https://en.wikipedia.org/wiki/Fatty_acid_metabolism; “Triglyceride,” <https://en.wikipedia.org/wiki/Triglyceride>; “Oxygen,” <https://en.wikipedia.org/wiki/Oxygen>. Assumes representative triglyceride (fat) C₅₅H₉₈O₆ completely oxidized to CO₂ and H₂O by application of O₂.

¹⁷²⁴ An example of intracellular nonoxygenic chemical energy storage in biology. “ATP,” https://en.wikipedia.org/wiki/Adenosine_triphosphate.

¹⁷²⁵ A “typical” fasting 70 kg male human body starts with 17.5 kg of fat (Body Fat Percentage ~ 25% of 70 kg; https://en.wikipedia.org/wiki/Body_fat_percentage), 4 gm of glucose (<http://www.ncbi.nlm.nih.gov/pmc/articles/PMC2636990/>), and 250 gm of ATP (https://en.wikipedia.org/wiki/Adenosine_triphosphate), an energy store of (17.5 kg fat)(37 x 10⁶ J/kg) + (0.004 kg glucose)(16 x 10⁶ J/kg) + (0.25 kg ATP)(1.5 x 10⁵ J/kg) = 6.476 x 10⁸ J, assuming no further caloric intake, which at the 100 W basal metabolic rate would allow survival for (6.476 x 10⁸ J) / (100 W) = 6.476 x 10⁶ sec = 75 days. There are many documented hunger-strike survivals at 40 days, and at least one report of other hunger strikers who “died after periods of between 46 and 73 days without food” (<http://www.scientificamerican.com/article/how-long-can-a-person-sur/>) which is not inconsistent with the above estimate. In 1967 the average density of human males aged 17-69 and weighing 47-79 kg was measured as 1.04 ± 0.02 kg/L (Krzywicki HJ, Chinn KSK. Human body density and fat of an adult male population as measured by water displacement. *Amer J Clin Nutrition*. 1967 Apr;20(4):305-310; <http://vorga.org/20-4-305.full.pdf>), though 21st century males are likely to be a bit less dense, having more fat than their forebears.

Lightning bolt (average negative discharge) ¹⁷²⁶	5×10^8	2-880	2-800
Tsunami (typical) ¹⁷²⁷	5×10^{14}	3.1×10^{16}	3×10^{13}
Hydroelectric dam reservoir ¹⁷²⁸	1.55×10^{16}	1.96×10^{13}	1.96×10^{10}
Tornado (maximum EF5) ¹⁷²⁹	4×10^{16}	4.6×10^{10}	4.2×10^{10}
Meteoroid impact (Meteor Crater, AZ) ¹⁷³⁰	6.3×10^{16}	2.9×10^8	3.9×10^4
Volcanic eruption, Class 5 (Mount St. Helens) ¹⁷³¹	1×10^{17}	1.1×10^{13}	4.2×10^9
Hurricane (typical) ¹⁷³²	2.1×10^{20}	1.9×10^{16}	1.7×10^{16}

¹⁷²⁶ An average bolt of negative lightning (>95% of all strikes) transfers 5×10^8 joules of energy in $\sim 5 \times 10^{-4}$ sec (15 coulombs / 30,000 amperes), giving a brief power surge of 1×10^{12} watts at ~ 33 megavolts (<https://en.wikipedia.org/wiki/Lightning>); if the bolt is ~ 1 km high and the channel is 0.05-1 m wide (<http://www.aharfield.co.uk/lightning-protection-services/about-lightning>), then its volume is 2-800 m³ and its mass is 2-880 kg (assuming ~ 1.1 kg/m³ for humid air).

¹⁷²⁷ The model tsunami analyzed by Dutykh assumes a block of seawater placed in motion by sea floor movement, of dimensions 150 km x 50 km and 4 km water depth (water volume $\sim 3 \times 10^{13}$ m³ and mass $\sim 3.1 \times 10^{16}$ kg assuming seawater density ~ 1040 kg/m³ at depth; <http://fermi.jhuapl.edu/denscalc.html>), producing a wave energy of $\sim 5 \times 10^{14}$ joules and power of 1×10^{13} watts assuming a 50 sec rise time. (Dutykh D, Dias F. Energy of tsunami waves generated by bottom motion. Proc R Soc A. 2009;465:725–744; <http://hal.univ-savoie.fr/hal-00311752v2/document>).

¹⁷²⁸ The active capacity of Hoover Dam (https://en.wikipedia.org/wiki/Hoover_Dam) stores 19.554×10^9 m³ of water in the associated Lake Mead reservoir with a maximum depth of 162 m, having a mean gravitational storage energy of $E = mg(h/2) \sim (19.554 \times 10^9 \text{ m}^3) (\sim 1000 \text{ kg/m}^3) (9.81 \text{ m/sec}^2) (162 \text{ m} / 2) = 1.55 \times 10^{16}$ joules.

¹⁷²⁹ One 2013 Oklahoma tornado of maximum severity “EF5” (https://en.wikipedia.org/wiki/Enhanced_Fujita_scale) with 340 kph wind speeds was believed to have up to 9.6 megatons (4×10^{16} joules) of energy, was measured 2.1 km wide, and lasted ~ 40 min (2400 sec) (<http://www.dailymail.co.uk/news/article-2328834/Oklahoma-tornado-600-TIMES-powerful-Hiroshima-atomic-bomb.html>), giving a continuous power of 1.7×10^{13} watts. If the height of the EF5 tornado includes the mesocyclonic updraft in the parent thunderstorm up to ~ 12 km, then its volume is $\sim 4.2 \times 10^{10}$ m³ and mass $\sim 4.6 \times 10^{10}$ kg (assuming ~ 1.1 kg/m³ for humid air).

¹⁷³⁰ The energy released by the impactor that created Meteor Crater in Arizona is estimated as ~ 15 megatons (6.3×10^{16} joules), with the impactor believed to be 42 m in spherical diameter (3.9×10^4 m³) with a mass of 2.9×10^8 kg (assuming 7500 kg/m³ for meteoritic iron) with an impact velocity of ~ 20 km/sec and an impact power of $\sim 3 \times 10^{19}$ watts during a ground impact time of (42 m) / (20 km/sec) ~ 0.0021 sec. Shoemaker EM. Asteroid and comet bombardment of the earth. Ann Rev Earth Planet Sci. 1983;11:461-494, <http://articles.adsabs.harvard.edu/full/1983AREPS..11..461S/0000470.000.html>.

¹⁷³¹ The eruption of Mount St. Helens, rated Class 5 on the Volcanic Explosivity Index (<http://www.unc.edu/~rowlett/units/scales/VEI.html>), released 24 megatons (1×10^{17} joules) of thermal energy and ~ 4.2 km³ (1.1×10^{13} kg @ ~ 2700 kg/m³) of ejecta. <http://science.howstuffworks.com/environmental/energy/energy-hurricane-volcano-earthquake2.htm> and lasted ~ 80 sec (https://en.wikipedia.org/wiki/1980_eruption_of_Mount_St._Helens), giving a blast power of 1.3×10^{15} watts.

Volcanic eruption, Class 8 (La Garita Caldera) ¹⁷³³	1×10^{21}	1.3×10^{16}	5×10^{12}
Earthquake, magnitude 9.5 (Valdivia, 1960) ¹⁷³⁴	2.2×10^{23}	7×10^{14}	2.6×10^{11}
Asteroid impact, extinction-level (Chicxulub) ¹⁷³⁵	4.2×10^{23}	3.4×10^{15}	1.5×10^{11}
<u>Astronomical</u>			
Solar flare (Sun) ¹⁷³⁶	1.9×10^{23}	1.6×10^{12}	1.1×10^9
Moon orbiting Earth (kinetic energy) ¹⁷³⁷	3.81×10^{28}	6.045×10^{24}	3.76×10^{24}

¹⁷³² Most (99.5%) of hurricane energy is released by water droplet condensation and not horizontal wind driving; estimated continuous power $\sim 6 \times 10^{14}$ watts for a typical hurricane of radius 665 km and altitude ~ 12 km, a volume of $1.7 \times 10^{16} \text{ m}^3$ (“How much energy does a hurricane release?” NOAA, 2014, <http://www.aoml.noaa.gov/hrd/tcfaq/D7.html>) and a mass of $1.9 \times 10^{16} \text{ kg}$ (assuming $\sim 1.1 \text{ kg/m}^3$ for humid air). A hurricane of this power that lasts for ~ 4 days ($3.5 \times 10^5 \text{ sec}$) has a total energy release of 2.1×10^{20} joules.

¹⁷³³ The La Garita event (https://en.wikipedia.org/wiki/La_Garita_Caldera) is one of the largest known eruptions in Earth’s history, rated Class 8 on the Volcanic Explosivity Index (https://en.wikipedia.org/wiki/Volcanic_explosivity_index), releasing $\sim 250,000$ megatons ($1 \times 10^{21} \text{ J}$) of energy displacing $\sim 5000 \text{ km}^3$ ($1.3 \times 10^{16} \text{ kg}$ @ $\sim 2500 \text{ kg/m}^3$) of rock.

¹⁷³⁴ The 1960 Valdivia earthquake (https://en.wikipedia.org/wiki/1960_Valdivia_earthquake) is the largest ever recorded, estimated at Magnitude 9.5 with a total seismic moment energy release of 2.2×10^{23} joules (<http://alabamaquake.com/energy.html>). The estimated rupture zone was 33 km deep and 800 km long; assuming a rupture width of ~ 10 m gives a rupture volume of $2.6 \times 10^{11} \text{ m}^3$ with a rupture mass of $7.0 \times 10^{14} \text{ kg}$ (assuming 2700 kg/m^3 for continental crustal rock). The quake had a rupture power of 3.7×10^{20} watts if the energy is viewed as having been released over the 10 min (600 sec) that the earthquake lasted.

¹⁷³⁵ The energy released by the dinosaur-extincting Chicxulub asteroid impact on Earth 65.5 million years ago was first estimated in 1980 as $\sim 10^8$ megatons of TNT ($4.184 \times 10^{15} \text{ joules/megaton}$) = 4.2×10^{23} joules, with the impactor having a diameter of $\sim 6.6 \text{ km}$ ($\sim 1.5 \times 10^{11} \text{ m}^3$ if spherical) and a mass of $3.4 \times 10^{14} \text{ kg}$; Alvarez LW, Alvarez W, Asaro F, Michel HV. Extraterrestrial cause for the cretaceous-tertiary extinction. Science. 1980 Jun 6;208(4448):1095-108; <http://citeseerx.ist.psu.edu/viewdoc/download?doi=10.1.1.126.8496&rep=rep1&type=pdf>. (A 1998 research group concluded the impactor was a $1.2 \times 10^{24} \text{ J}$, $1.8 \times 10^{15} \text{ kg}$, 16.5 km diameter ($\sim 2.4 \times 10^{12} \text{ m}^3$) comet (<http://sp.lyellcollection.org/content/140/1/155.short>), and there have been other estimates.) An impact velocity of $\sim 20 \text{ km/sec}$ yields an impact power of $\sim 1.3 \times 10^{24}$ watts during a ground impact time of $(6.6 \text{ km}) / (20 \text{ km/sec}) \sim 0.33 \text{ sec}$.

¹⁷³⁶ Solar flares with energies 10^{20} - 10^{25} J (https://en.wikipedia.org/wiki/Solar_flare) accompanied by coronal mass ejections averaging $1.6 \times 10^{12} \text{ kg}$ ($\sim 1.1 \times 10^9 \text{ m}^3$ taking mean solar density $\sim 1410 \text{ kg/m}^3$) with average ejection velocity 489 km/sec (https://en.wikipedia.org/wiki/Coronal_mass_ejection#Physical_properties) may have a kinetic energy of $E = (1/2) mv^2 = (0.5) (1.6 \times 10^{12} \text{ kg}) (4.89 \times 10^5 \text{ m/sec})^2 = 1.9 \times 10^{23}$ joules, a power output of 6×10^{19} watts assuming a flare ejection time of $\sim 3000 \text{ sec}$ (http://www.mssl.ucl.ac.uk/www_solar/PUS/PO/explosions.html).

¹⁷³⁷ Kinetic energy = $(1/2) GM_{\text{Earth}}M_{\text{Moon}}/R_{\text{Earth-Moon}} = 3.81 \times 10^{28}$ joules, taking $G = 6.674 \times 10^{-11} \text{ N-m}^2/\text{kg}^2$, $M_{\text{Earth}} = 5.972 \times 10^{24} \text{ kg}$, $M_{\text{Moon}} = 7.342 \times 10^{22} \text{ kg}$, and $R_{\text{Earth-Moon}} \sim 3.84 \times 10^8 \text{ m}$ (<https://en.wikipedia.org/wiki/Earth> and <https://en.wikipedia.org/wiki/Moon>). The system mass = $M_{\text{Earth}} + M_{\text{Moon}} = 6.045 \times 10^{24} \text{ kg}$, and the system volume is roughly a disk of volume $\sim \pi R_{\text{Earth-Moon}}^2 (R_{\text{Earth}} + R_{\text{Moon}}) = 3.76 \times 10^{24} \text{ m}^3$, where $R_{\text{Earth}} = 6.371 \times 10^6 \text{ m}$ and $R_{\text{Moon}} = 1.737 \times 10^6 \text{ m}$.

Earth rotational energy ¹⁷³⁸	2.56×10^{29}	5.972×10^{24}	1.083×10^{21}
Earth orbiting Sun (kinetic energy) ¹⁷³⁹	2.65×10^{33}	1.989×10^{30}	4.94×10^{31}
Sun rotational energy ¹⁷⁴⁰	1.63×10^{36}	1.989×10^{30}	1.41×10^{27}
Jupiter mass (as fusion fuel) ¹⁷⁴¹	1.7×10^{42}	1.8986×10^{27}	1.4313×10^{24}
Brown dwarf (W0607+24) ¹⁷⁴²	9.9×10^{43}	1.1×10^{29}	1.4×10^{24}
Type M9 star ¹⁷⁴³	1.3×10^{44}	1.49×10^{29}	9×10^{25}
Type Ia supernova ¹⁷⁴⁴	2×10^{44}	2.8×10^{30}	2×10^{21}
Sun (typical G2 star) ¹⁷⁴⁵	1.8×10^{45}	1.989×10^{30}	1.41×10^{27}
Type II supernova ¹⁷⁴⁶	1×10^{46}	$1.6-8 \times 10^{31}$	$0.3-1 \times 10^{30}$
Type O9 star ¹⁷⁴⁷	2.9×10^{46}	3.18×10^{31}	4.05×10^{29}

¹⁷³⁸ Rotational energy $\sim (1/2) I_{\text{Earth}} \omega_{\text{Earth}}^2 = (0.5) (9.696 \times 10^{37} \text{ kg}\cdot\text{m}^2) (2\pi / 86400 \text{ sec})^2 = 2.56 \times 10^{29}$ joules, where $\omega_{\text{Earth}} = 86400 \text{ sec/rotation}$, rotational inertia $I_{\text{Earth}} = (2/5) M_{\text{Earth}} R_{\text{Earth}}^2$ for solid sphere, $M_{\text{Earth}} = 5.972 \times 10^{24} \text{ kg}$, and $R_{\text{Earth}} = 6.371 \times 10^6 \text{ m}$ (<https://en.wikipedia.org/wiki/Earth>).

¹⁷³⁹ Kinetic energy $= (1/2) GM_{\text{Earth}}M_{\text{Sun}}/R_{\text{Earth-Sun}} = 3.81 \times 10^{28}$ joules, taking $G = 6.674 \times 10^{-11} \text{ N}\cdot\text{m}^2/\text{kg}^2$, $M_{\text{Earth}} = 5.972 \times 10^{24} \text{ kg}$, $M_{\text{Sun}} = 1.989 \times 10^{30} \text{ kg}$, and $R_{\text{Earth-Sun}} \sim 1.496 \times 10^{11} \text{ m}$ (<https://en.wikipedia.org/wiki/Earth> and <https://en.wikipedia.org/wiki/Sun>). The system mass $= M_{\text{Earth}} + M_{\text{Sun}} = 1.989 \times 10^{30} \text{ kg}$, and the system volume is roughly a disk of volume $\sim \pi R_{\text{Earth-Sun}}^2 (R_{\text{Earth}} + R_{\text{Sun}}) = 4.94 \times 10^{31} \text{ m}^3$, where $R_{\text{Earth}} = 6.371 \times 10^6 \text{ m}$ and $R_{\text{Sun}} = 6.957 \times 10^8 \text{ m}$.

¹⁷⁴⁰ Rotational energy $\sim (1/2) I_{\text{Solar}} \omega_{\text{Solar}}^2 = (0.5) (3.85 \times 10^{47} \text{ kg}\cdot\text{m}^2) (2\pi / 2.16 \times 10^6 \text{ sec})^2 = 1.63 \times 10^{36}$ joules, where $\omega_{\text{Solar}} = 2.16 \times 10^6 \text{ sec/rotation}$, rotational inertia $I_{\text{Solar}} \sim (2/5) M_{\text{Solar}} R_{\text{Solar}}^2$ assuming a solid sphere, $M_{\text{Solar}} = 1.989 \times 10^{30} \text{ kg}$, and $R_{\text{Solar}} = 6.957 \times 10^8 \text{ m}$ (<https://en.wikipedia.org/wiki/Sun>).

¹⁷⁴¹ Releasable energy as fusion assuming 1% mass-energy conversion of the planetary mass; “Jupiter,” <https://en.wikipedia.org/wiki/Jupiter>.

¹⁷⁴² Releasable energy as fusion assuming 1% mass-energy conversion of this nearby brown dwarf with mass $\sim 0.055 M_{\text{solar}} = 57.9 M_{\text{Jupiter}}$ and radius $\sim 0.1 R_{\text{solar}}$ (Gizis JE, Williams PK, Burgasser AJ, Libralato M, Nardiello D, Piotto G, Bedin LR, Berger E, Paudel R. WISEP J060738. 65+ 242953.4: A Nearby. Pole-On L8 Brown Dwarf with Radio Emission. arXiv preprint arXiv:1607.00943. 2016 Jul 4; <https://arxiv.org/pdf/1607.00943v1.pdf>), with $M_{\text{solar}} = 1.989 \times 10^{30} \text{ kg}$ and $R_{\text{solar}} = 6.957 \times 10^8 \text{ m}$.

¹⁷⁴³ Releasable energy as fusion assuming 1% mass-energy conversion of an M9 star with mass $\sim 0.075 M_{\text{solar}}$ and spherical radius $\sim 0.4 R_{\text{solar}}$, with $R_{\text{solar}} = 6.957 \times 10^8 \text{ m}$; https://en.wikipedia.org/wiki/Red_dwarf and https://en.wikipedia.org/wiki/Stellar_classification.

¹⁷⁴⁴ Fusion explosion in a binary star system, where the exploding star is a carbon-oxygen white dwarf of mass $\sim 1.39 M_{\text{solar}}$ and radius $\sim 0.011 R_{\text{solar}}$, releasing $\sim 2 \times 10^{44} \text{ J}$ in a few seconds; “Type Ia supernova,” https://en.wikipedia.org/wiki/Type_Ia_supernova.

¹⁷⁴⁵ Releasable energy as fusion assuming 1% mass-energy conversion, with $R_{\text{solar}} = 6.957 \times 10^8 \text{ m}$. Williams DR. Sun Fact Sheet. NASA Goddard Space Flight Center, 2016; <http://nssdc.gsfc.nasa.gov/planetary/factsheet/sunfact.html>.

¹⁷⁴⁶ Rapid collapse and violent fusion explosion of a massive ($8-40 M_{\text{solar}}$) star of radius $\sim 6-9 R_{\text{solar}}$, releasing $\sim 10^{46} \text{ J}$ in $\sim 10 \text{ sec}$, resulting in a neutron star below $20 M_{\text{solar}}$ and a black hole above $20 M_{\text{solar}}$; “Type II supernova,” https://en.wikipedia.org/wiki/Type_II_supernova.

Quark nova ¹⁷⁴⁸	1×10^{47}	$3\text{-}3.6 \times 10^{30}$	$\sim 1 \times 10^{10}$
Binary black hole merger ¹⁷⁴⁹	5.37×10^{47}	1.29×10^{32}	3.88×10^{16}
Globular cluster (M15) ¹⁷⁵⁰	1.0×10^{51}	1.1×10^{36}	2.4×10^{54}
Milky Way galaxy ¹⁷⁵¹	1.5×10^{57}	1.69×10^{42}	6.57×10^{60}
Universe ¹⁷⁵²	1.31×10^{68}	1.46×10^{53}	3.57×10^{80}
Rest mass energy of observable baryonic universe ¹⁷⁵³	1.31×10^{70}	1.46×10^{53}	3.57×10^{80}
Evaporating black hole ¹⁷⁵⁴ of mass:			
Galactic core ($\sim 10^6 M_{\text{solar}}$), $t_{\text{ev}} \sim 8.4 \times 10^{91}$ sec	9×10^{52}	1×10^{36}	1.4×10^{28}
Stellar ($\sim 1 M_{\text{solar}}$), $t_{\text{ev}} \sim 8.4 \times 10^{73}$ sec	9×10^{46}	1×10^{30}	1.4×10^{10}
Planetary ($\sim 10^{-6} M_{\text{solar}}$), $t_{\text{ev}} \sim 8.4 \times 10^{55}$ sec	9×10^{40}	1×10^{24}	1.4×10^{-8}
Asteroidal ($\sim 10^{-12} M_{\text{solar}}$), $t_{\text{ev}} \sim 8.4 \times 10^{37}$ sec	9×10^{34}	1×10^{18}	1.4×10^{-26}
~ 1 km meteor ($\sim 10^{-18} M_{\text{solar}}$), $t_{\text{ev}} \sim 8.4 \times 10^{19}$ sec	9×10^{28}	1×10^{12}	1.4×10^{-44}
~ 10 -meter boulder ($\sim 10^{-24} M_{\text{solar}}$), $t_{\text{ev}} \sim 84$ sec	9×10^{22}	1×10^6	1.4×10^{-62}
Ylem (cosmic egg) ¹⁷⁵⁵	1.31×10^{70}	1.46×10^{53}	4.22×10^{105}

¹⁷⁴⁷ Releasable energy as fusion assuming 1% mass-energy conversion of an O9 star with mass $\sim 16 M_{\text{solar}}$ and spherical radius $\sim 6.6 R_{\text{solar}}$, with $R_{\text{solar}} = 6.957 \times 10^8$ m; https://en.wikipedia.org/wiki/O-type_star and https://en.wikipedia.org/wiki/Stellar_classification.

¹⁷⁴⁸ Hypothetical violent explosion (<https://en.wikipedia.org/wiki/Quark-nova>) resulting from the conversion of a neutron star to a quark star in which the process of quark deconfinement creates quark matter (https://en.wikipedia.org/wiki/QCD_matter) in the 1.5-1.8 M_{solar} neutron star interior, releasing $\sim 10^{47}$ J on the average ~ 30 sec timescale of gamma-ray bursts (https://en.wikipedia.org/wiki/Gamma-ray_burst).

¹⁷⁴⁹ Observed merger of a binary black hole, involving two black holes of total mass $\sim 65 M_{\text{solar}}$ with a summed Schwarzschild radius for the binary components of ~ 210 km, produced a ~ 0.2 sec release of gravitational waves of energy $\sim 3 M_{\text{solar}} c^2$. Abbott BP *et al.* Observation of Gravitational Waves from a Binary Black Hole Merger. Phys Rev Lett. 2016 Feb 11;116, 061102; <http://journals.aps.org/prl/pdf/10.1103/PhysRevLett.116.061102>.

¹⁷⁵⁰ Releasable energy as fusion assuming 1% mass-energy conversion of the M15 globular cluster with mass $\sim 5.6 \times 10^5 M_{\text{solar}}$ and radius ~ 88 light-years = 8.3×10^{17} m; “Messier 15,” https://en.wikipedia.org/wiki/Messier_15.

¹⁷⁵¹ Releasable energy as fusion assuming 1% mass-energy conversion of the Milky Way galaxy with mass $\sim 8.5 \times 10^{11} M_{\text{solar}}$; “Milky Way,” https://en.wikipedia.org/wiki/Milky_Way.

¹⁷⁵² Releasable energy as fusion assuming 1% mass-energy conversion of all stellar mass in the Universe or $\sim (4.08 \times 10^{-28} \text{ kg/m}^3)(3.57 \times 10^{80} \text{ m}^3) = 1.46 \times 10^{53}$ kg; https://en.wikipedia.org/wiki/Observable_universe.

¹⁷⁵³ $E = mc^2 = (1.46 \times 10^{53})(3 \times 10^8 \text{ m/sec})^2 = 1.31 \times 10^{70}$ joules.

¹⁷⁵⁴ Black hole evaporation time $t_{\text{ev}} = 5120 \pi G^2 M_{\text{bh}}^3 / \hbar c^4$, black hole evaporative power output is $P_{\text{ev}} = \hbar c^6 / (15360 \pi G^2 M_{\text{bh}}^2)$, total black hole radiative energy $E_{\text{ev}} = M_{\text{bh}} c^2$ with average radiated power over the entire evaporation time $P_{\text{avg}} = E_{\text{ev}}/t_{\text{ev}}$, and black hole Schwarzschild radius $R_{\text{bh}} = 2 G M_{\text{bh}} / c^2$, where $G = 6.67 \times 10^{-11} \text{ N}\cdot\text{m}^2/\text{kg}^2$, M_{bh} = black hole mass (kg), $\hbar = h/2\pi = 1.055 \times 10^{-34}$ J-sec, $h = 6.63 \times 10^{-34}$ J-sec, and $c = 3 \times 10^8$ m/sec. “Hawking radiation,” https://en.wikipedia.org/wiki/Hawking_radiation.

Electromagnetic quantum vacuum energy(Compton) ¹⁷⁵⁶	1.3×10^{32}	1.4×10^{15}	1
Electromagnetic quantum vacuum energy (Planck) ¹⁷⁵⁷	5.8×10^{111}	6.4×10^{94}	1

¹⁷⁵⁵ The ylem (cosmic egg) is the hypothetical primordial singularity from which the entire universe expanded during the Big Bang, containing at least the entire mass of the observable universe ($M_U = 1.46 \times 10^{53}$ kg; https://en.wikipedia.org/wiki/Observable_universe#Estimates_based_on_critical_density) compressed into the smallest measurable volume ($V_{\text{Planck}} = 4.22 \times 10^{-105}$ m³), or “Planck volume,” the cube of the Planck length ($L_{\text{Planck}} = 1.616 \times 10^{-35}$ m) which has been hypothesized to be “the shortest measurable length” (https://en.wikipedia.org/wiki/Planck_length). The shortest measurable time over which this mass-energy ($M_U c^2 = 1.31 \times 10^{70}$ J) might be released may be the Planck time (https://en.wikipedia.org/wiki/Planck_time) or $t_{\text{Planck}} = 5.39 \times 10^{-44}$ sec, defining the maximum possible power development (2.43×10^{113} W).

¹⁷⁵⁶ aka. zero-point vacuum energy density, has been estimated (Davis EW, Teofilo VL, Haisch B, Puthoff HE, Nickisch LJ, Rueda A, Cole DC. Review of Experimental Concepts for Studying the Quantum Vacuum Field. AIP Conf. Proc. 2006;813:1390-1401; http://www.bu.edu/simulation/publications/dcole/PDF/Davis%20et%20al_STAIF06_Log063.pdf) by summing the zero-point energies of all the electromagnetic vibrational modes predicted to exist by quantum theory, giving $E_D = \hbar v^4 / 8\pi^2 c^3 \sim 1.3 \times 10^{32}$ J/m³ (mass-energy $\sim 1.4 \times 10^{15}$ kg/m³) when integrated over all frequency modes up to the proton Compton frequency ($\nu = m_p c^2 / h = 2.27 \times 10^{23}$ Hz; https://en.wikipedia.org/wiki/Compton_wavelength) as the cutoff, where $\hbar = h/2\pi = 1.055 \times 10^{-34}$ J-sec, $h = 6.63 \times 10^{-34}$ J-sec, $m_p = 1.67 \times 10^{-27}$ kg, and $c = 3 \times 10^8$ m/sec.

¹⁷⁵⁷ aka. zero-point vacuum energy density, has been estimated (Davis EW, Teofilo VL, Haisch B, Puthoff HE, Nickisch LJ, Rueda A, Cole DC. Review of Experimental Concepts for Studying the Quantum Vacuum Field. AIP Conf. Proc. 2006;813:1390-1401; http://www.bu.edu/simulation/publications/dcole/PDF/Davis%20et%20al_STAIF06_Log063.pdf) by summing the zero-point energies of all the electromagnetic vibrational modes predicted to exist by quantum theory, giving $E_D = \hbar v^4 / 8\pi^2 c^3 \sim 5.8 \times 10^{111}$ J/m³ (mass-energy 6.4×10^{94} kg/m³) when integrated over all frequency modes up to the Planck frequency ($\nu = 1.85 \times 10^{43}$ Hz; https://en.wikipedia.org/wiki/Planck_units#Derived_units) as the cutoff, where $\hbar = h/2\pi = 1.055 \times 10^{-34}$ J-sec, $h = 6.63 \times 10^{-34}$ J-sec, and $c = 3 \times 10^8$ m/sec.

A.2 Data on Power Generation in Nature

Table A2. Data on power generation in nature.			
Power Generation System	Power (W)	Mass (kg)	Volume (m ³)
Nuclear and Atomic ¹⁷⁵⁸			
Neodymium-144 radionuclide	2.81 x 10 ⁻³⁶	2.39 x 10 ⁻²⁵	3.41 x 10 ⁻²⁹
Gadolinium-148 radionuclide	1.50 x 10 ⁻²²	2.46 x 10 ⁻²⁵	3.11 x 10 ⁻²⁹
Polonium-210 radionuclide	4.93 x 10 ⁻²⁰	3.49 x 10 ⁻²⁵	3.79 x 10 ⁻²⁹
Europium-147 radionuclide	1.55 x 10 ⁻¹⁹	2.44 x 10 ⁻²⁵	4.64 x 10 ⁻²⁹
Francium-215 radionuclide	3.46 x 10 ⁻⁴	3.57 x 10 ⁻²⁵	1.91 x 10 ⁻²⁸
Biological			
Myosin muscle motor ¹⁷⁵⁹	1 x 10 ⁻¹⁸	~5 x 10 ⁻²²	5 x 10 ⁻²⁵
Bacterial flagellar motor ¹⁷⁶⁰	1 x 10 ⁻¹⁶	~5 x 10 ⁻²⁰	5 x 10 ⁻²³
<i>E. faecalis</i> bacterium (basal) ¹⁷⁶¹	3.5 x 10 ⁻¹⁶	~2 x 10 ⁻¹⁶	2 x 10 ⁻¹⁹
Platelet (resting) ¹⁷⁶²	3-90 x 10 ⁻¹⁵	3.2 x 10 ⁻¹⁵	3 x 10 ⁻¹⁸
Erythrocyte (red blood cell) ¹⁷⁶³	8 x 10 ⁻¹⁵	1.1 x 10 ⁻¹³	9.4 x 10 ⁻¹⁷

¹⁷⁵⁸ Data from **Table A5** in **Appendix A** and from Theodore Gray:
<http://www.periodictable.com/Isotopes/001.1/index2.full.dm.prod.html>.

¹⁷⁵⁹ James A. Spudich, "How molecular motors work," *Nature* 372(8 December 1994):515-518.

¹⁷⁶⁰ Christopher J. Jones, Shin-Ichi Aizawa, "The Bacterial Flagellum and Flagellar Motor: Structure, Assembly and Function," *Adv. Microbial Physiol.* 32(1991):109-172.

¹⁷⁶¹ W.W. Forrest, D.J. Walker, "Calorimetric Measurements of Energy of Maintenance of *Streptococcus faecalis*," *Biochem. Biophys. Res. Commun.* 13(1963):217-222.

¹⁷⁶² Polanowska-Grabowska R, Raha S, Gear AR. Adhesion efficiency, platelet density and size. *Br J Haematol.* 1992 Dec;82(4):715-20; <http://www.ncbi.nlm.nih.gov/pubmed/1282829>. Philip D. Ross, A.P. Fletcher, G.A. Jamieson, "Microcalorimetric Study of Isolated Blood Platelets in the Presence of Thrombin and Other Aggregating Agents," *Biochimica Biophysica Acta* 313(1973):106-118. K. Levin, "Heat Production by Leucocytes and Thrombocytes Measured with a Flow Microcalorimeter in Normal Man and During Thyroid Dysfunction," *Clinica Chimica Acta* 32(1971):87-94. K. Levin, "A Modified Flow Microcalorimeter Adapted for the Study of Human Leucocyte Phagocytosis," *Scand. J. Clin. Lab. Investig.* 32(1973):67-73.

¹⁷⁶³ M. Trumpa, B. Wendt, "Microcalorimetric Measurements of Heat Production in Human Erythrocytes with a Batch Calorimeter," in I. Lamprecht, B. Schaarschmidt, eds., *Application of Calorimetry in Life Sciences*, Walter de Gruyter, New York, 1977, pp. 241-249. "Density of blood," <http://hypertextbook.com/facts/2004/MichaelShmukler.shtml>.

Protists (phytoplankton, algae) ¹⁷⁶⁴	1.8×10^{-14}	$\sim 2 \times 10^{-13}$	2×10^{-16}
<i>E. coli</i> bacterium (basal) ¹⁷⁶⁵	5×10^{-14}	7.2×10^{-16}	6.5×10^{-19}
Mitochondrion organelle ¹⁷⁶⁶	$1-11 \times 10^{-13}$	1.19×10^{-15}	1×10^{-18}
<i>E. foecalis</i> bacterium (max. growth) ¹⁷⁶⁷	2.3×10^{-13}	$\sim 2 \times 10^{-16}$	2×10^{-19}
Chondrocyte ¹⁷⁶⁸	3×10^{-13}	$\sim 6.7 \times 10^{-13}$	6.7×10^{-16}
Platelet (activated) ¹⁷⁶⁹	$7-70 \times 10^{-13}$	3.2×10^{-15}	3×10^{-18}
Skin cell ¹⁷⁷⁰	$1-3 \times 10^{-12}$	1×10^{-12}	1×10^{-15}
Skeletal muscle cell (resting) ¹⁷⁷¹	$1-10 \times 10^{-12}$	2.2×10^{-12}	2×10^{-15}

¹⁷⁶⁴ “Chlorella,” <https://en.wikipedia.org/wiki/Chlorella>. Chaisson E. Energy Rate Density as a Complexity Metric and Evolutionary Driver. Complexity 2011;16:27–40; https://www.cfa.harvard.edu/~ejchaisson/reprints/EnergyRateDensity_I_FINAL_2011.pdf.

¹⁷⁶⁵ E.A. Dawes, D.W. Ribbons, “The Endogenous Metabolism of Microorganisms,” Ann. Rev. Microbiol. 16(1962):241-263. E Martínez-Salas, J A Martín, and M Vicente. Relationship of Escherichia coli density to growth rate and cell age. J Bacteriol. 1981 Jul; 147(1): 97–100; <http://www.ncbi.nlm.nih.gov/pmc/articles/PMC216012/>. “E. coli,” https://en.wikipedia.org/wiki/Escherichia_coli.

¹⁷⁶⁶ Freitas RA Jr. Nanomedicine, Volume I: Basic Capabilities. Landes Bioscience, Georgetown, TX, 1999, Table 8.17; <http://www.nanomedicine.com/NMI/Tables/8.17.jpg>. Robert E. Smith, “Quantitative Relations Between Liver Mitochondria Metabolism and Total Body Weight in Mammals,” Ann. N.Y. Acad. Sci. 62.17(31 January 1956):403-422. Jan Nedergaard, Barbara Cannon, “Chapter 10. Thermogenic mitochondria,” in L. Ernster, ed., Bioenergetics, Elsevier, New York, 1984, pp. 291-314.

¹⁷⁶⁷ W.W. Forrest, D.J. Walker, “Calorimetric Measurements of Energy of Maintenance of Streptococcus faecalis,” Biochem. Biophys. Res. Commun. 13(1963):217-222.

¹⁷⁶⁸ Knut Schmidt-Nielsen, Scaling: Why is Animal Size So Important? Cambridge University Press, Cambridge, 1984.

¹⁷⁶⁹ Polanowska-Grabowska R, Raha S, Gear AR. Adhesion efficiency, platelet density and size. Br J Haematol. 1992 Dec;82(4):715-20; <http://www.ncbi.nlm.nih.gov/pubmed/1282829>. J. Anthony Ware, Barry S. Collier, “Chapter 119. Platelet morphology, biochemistry, and function.” In Ernest Beutler, Marshall A. Lichtman, Barry S. Collier, Thomas J. Kipps, eds., William's Hematology, Fifth Edition, McGraw-Hill, New York, 1995, pp. 1161-1201.

¹⁷⁷⁰ Knut Schmidt-Nielsen, Scaling: Why is Animal Size So Important? Cambridge University Press, Cambridge, 1984. Roland A. Coulson, Thomas Hernandez, Jack D. Herbert, “Metabolic Rate, Enzyme Kinetics In Vivo,” Comp. Biochem. Physiol. 56A(1977):251-262. A. Anders, G. Welge, B. Schaarschmidt, I. Lamprecht, H. Schaefer, “Calorimetric Investigations of Metabolic Regulation in Human Skin,” in I. Lamprecht, B. Schaarschmidt, eds., Application of Calorimetry in Life Sciences, Walter de Gruyter, New York, 1977, pp. 199-208. K. Michael Sekins, Ashley F. Emery, “Chapter 2. Thermal Science for Physical Medicine,” in Justus F. Lehmann, ed., Therapeutic Heat and Cold, Fourth Edition, Williams & Wilkins, Baltimore MD, 1990, pp. 62-112.

¹⁷⁷¹ James A. Wilson, Principles of Animal Physiology, Macmillan Publishing Company, New York, 1972. Knut Schmidt-Nielsen, Scaling: Why is Animal Size So Important? Cambridge University Press, Cambridge, 1984. K. Michael Sekins, Ashley F. Emery, “Chapter 2. Thermal Science for Physical Medicine,” in Justus F. Lehmann, ed., Therapeutic Heat and Cold, Fourth Edition, Williams & Wilkins, Baltimore MD, 1990, pp. 62-112.

Neutrophil (white blood cell, resting) ¹⁷⁷²	$2-9 \times 10^{-12}$	1.25×10^{-12}	1.15×10^{-15}
Osteocyte (bone) ¹⁷⁷³	$2-38 \times 10^{-12}$	$\sim 3 \times 10^{-11}$	3×10^{-14}
Pancreatic cell ¹⁷⁷⁴	9×10^{-12}	$\sim 1 \times 10^{-15}$	1×10^{-15}
Heart muscle cell (resting) ¹⁷⁷⁵	1.6×10^{-11}	8.8×10^{-12}	8×10^{-15}
Diaphragm muscle cell ¹⁷⁷⁶	2×10^{-11}	$\sim 2 \times 10^{-12}$	2×10^{-15}
Hepatocyte (liver cell) ¹⁷⁷⁷	$4.5-11.5 \times 10^{-11}$	$\sim 2 \times 10^{-12}$	6.4×10^{-15}
Neutrophil (white blood cell, activated) ¹⁷⁷⁸	2.8×10^{-11}	1.25×10^{-12}	1.15×10^{-15}
Typical human tissue cell (basal) ¹⁷⁷⁹	3×10^{-11}	$\sim 8 \times 10^{-12}$	8×10^{-15}
T-cell lymphocyte (basal) ¹⁷⁸⁰	4×10^{-11}	2.1×10^{-13}	2×10^{-16}

¹⁷⁷² Pember SO, Barnes KC, Brandt SJ, Kinkade JM Jr. Density heterogeneity of neutrophilic polymorphonuclear leukocytes: gradient fractionation and relationship to chemotactic stimulation. *Blood*. 1983 Jun;61(6):1105-15; <http://www.bloodjournal.org/content/61/6/1105.full.pdf>. H. Hayatsu, T. Miyamae, M. Yamamura, "Heat production as a quantitative parameter of phagocytosis," *J. Immunol. Methods* 109(9 May 1988):157-160.

¹⁷⁷³ Knut Schmidt-Nielsen, *Scaling: Why is Animal Size So Important?* Cambridge University Press, Cambridge, 1984. K. Michael Sekins, Ashley F. Emery, "Chapter 2. Thermal Science for Physical Medicine," in Justus F. Lehmann, ed., *Therapeutic Heat and Cold, Fourth Edition*, Williams & Wilkins, Baltimore MD, 1990, pp. 62-112.

¹⁷⁷⁴ Martin Davies, "On Body Size and Tissue Respiration," *J. Cellular Comp. Physiol.* 57(1961):135-147.

¹⁷⁷⁵ C.L. Gibbs, W.F.H.M. Mommaerts, N.V. Ricchiuti, "Energetics of cardiac contractions," *J. Physiol. (London)* 191(1967):25-46.

¹⁷⁷⁶ Knut Schmidt-Nielsen, *Scaling: Why is Animal Size So Important?* Cambridge University Press, Cambridge, 1984.

¹⁷⁷⁷ Knut Schmidt-Nielsen, *Scaling: Why is Animal Size So Important?* Cambridge University Press, Cambridge, 1984. Martin Davies, "On Body Size and Tissue Respiration," *J. Cellular Comp. Physiol.* 57(1961):135-147. M.A. Holliday, D. Potter, A. Jarrah, S. Bearg, "The Relation of Metabolic Rate to Body Weight and Organ Size," *Pediatric Res.* 1(1967):185-195. Roland A. Coulson, Thomas Hernandez, Jack D. Herbert, "Metabolic Rate, Enzyme Kinetics In Vivo," *Comp. Biochem. Physiol.* 56A(1977):251-262. K. Michael Sekins, Ashley F. Emery, "Chapter 2. Thermal Science for Physical Medicine," in Justus F. Lehmann, ed., *Therapeutic Heat and Cold, Fourth Edition*, Williams & Wilkins, Baltimore MD, 1990, pp. 62-112.

¹⁷⁷⁸ Pember SO, Barnes KC, Brandt SJ, Kinkade JM Jr. Density heterogeneity of neutrophilic polymorphonuclear leukocytes: gradient fractionation and relationship to chemotactic stimulation. *Blood*. 1983 Jun;61(6):1105-15; <http://www.bloodjournal.org/content/61/6/1105.full.pdf>. H. Hayatsu, T. Miyamae, M. Yamamura, "Heat production as a quantitative parameter of phagocytosis," *J. Immunol. Methods* 109(9 May 1988):157-160.

¹⁷⁷⁹ Knut Schmidt-Nielsen, *Scaling: Why is Animal Size So Important?* Cambridge University Press, Cambridge, 1984. Martin Davies, "On Body Size and Tissue Respiration," *J. Cellular Comp. Physiol.* 57(1961):135-147. M.A. Holliday, D. Potter, A. Jarrah, S. Bearg, "The Relation of Metabolic Rate to Body Weight and Organ Size," *Pediatric Res.* 1(1967):185-195.

Bone marrow cell ¹⁷⁸¹	4.5×10^{-11}	$\sim 8 \times 10^{-12}$	8×10^{-15}
Intestine/stomach cell ¹⁷⁸²	$4.6-5.2 \times 10^{-11}$	$\sim 8 \times 10^{-12}$	8×10^{-15}
Testicular cell ¹⁷⁸³	$4.6-14.9 \times 10^{-11}$	$\sim 8 \times 10^{-12}$	8×10^{-15}
Lung cell ¹⁷⁸⁴	$5.6-7.8 \times 10^{-11}$	$\sim 8 \times 10^{-12}$	8×10^{-15}
Brown fat cell (resting) ¹⁷⁸⁵	6×10^{-11}	1.8×10^{-10}	2×10^{-13}
Spleen cell ¹⁷⁸⁶	$6-8 \times 10^{-11}$	$\sim 8 \times 10^{-12}$	8×10^{-15}
Neuron (basal) ¹⁷⁸⁷	$7-11 \times 10^{-11}$	$\sim 1.4 \times 10^{-11}$	$\sim 1.4 \times 10^{-14}$
Thymus cell ¹⁷⁸⁸	7.4×10^{-11}	$\sim 8 \times 10^{-12}$	8×10^{-15}
Heart muscle cell (typical) ¹⁷⁸⁹	$8.7-29 \times 10^{-11}$	$\sim 8 \times 10^{-12}$	8×10^{-15}

¹⁷⁸⁰ Claësson MH, Rodger MB, Johnson GR, Whittingham S, Metcalf D. Colony formation by human T lymphocytes in agar medium. *Clin Exp Immunol.* 1977 Jun;28(3):526-34; <http://www.ncbi.nlm.nih.gov/pmc/articles/PMC1541018/>. Augusto Cogoli, Birgitt Bechler, Marianne Cogoli-Greuter, Sue B. Criswell, Helen Joller, Peter Joller, Elisabeth Hunzinger, Otfried Muller, "Mitogenic signal transduction in T lymphocytes in microgravity," *J. Leukocyte Biol.* 53(May 1993):569-575. Dennis A. Carson, "Chapter 94. Composition and biochemistry of lymphocytes and plasma cells," in Ernest Beutler, Marshall A. Lichtman, Barry S. Collier, Thomas J. Kipps, eds., *William's Hematology*, Fifth Edition, McGraw-Hill, New York, 1995, pp. 916-921.

¹⁷⁸¹ Martin Davies, "On Body Size and Tissue Respiration," *J. Cellular Comp. Physiol.* 57(1961):135-147.

¹⁷⁸² Martin Davies, "On Body Size and Tissue Respiration," *J. Cellular Comp. Physiol.* 57(1961):135-147.

¹⁷⁸³ Martin Davies, "On Body Size and Tissue Respiration," *J. Cellular Comp. Physiol.* 57(1961):135-147.

¹⁷⁸⁴ Knut Schmidt-Nielsen, *Scaling: Why is Animal Size So Important?* Cambridge University Press, Cambridge, 1984. Martin Davies, "On Body Size and Tissue Respiration," *J. Cellular Comp. Physiol.* 57(1961):135-147. M.A. Holliday, D. Potter, A. Jarrah, S. Bearg, "The Relation of Metabolic Rate to Body Weight and Organ Size," *Pediatric Res.* 1(1967):185-195.

¹⁷⁸⁵ Martin Davies, "On Body Size and Tissue Respiration," *J. Cellular Comp. Physiol.* 57(1961):135-147. K. Michael Sekins, Ashley F. Emery, "Chapter 2. Thermal Science for Physical Medicine," in Justus F. Lehmann, ed., *Therapeutic Heat and Cold*, Fourth Edition, Williams & Wilkins, Baltimore MD, 1990, pp. 62-112.

¹⁷⁸⁶ Martin Davies, "On Body Size and Tissue Respiration," *J. Cellular Comp. Physiol.* 57(1961):135-147.

¹⁷⁸⁷ Knut Schmidt-Nielsen, *Scaling: Why is Animal Size So Important?* Cambridge University Press, Cambridge, 1984. Martin Davies, "On Body Size and Tissue Respiration," *J. Cellular Comp. Physiol.* 57(1961):135-147. R. Duara *et al.*, "Human Brain Glucose Utilization and Cognitive Function in Relation to Age," *Annals of Neurology* 16(1984):702-713. Louis Sokoloff, "Localization of Functional Activity in the Central Nervous System by Measurement of Glucose Utilization with Radioactive Deoxyglucose," *J. Cerebral Blood Flow and Metabolism* 1(1981):7-36. M.A. Holliday, D. Potter, A. Jarrah, S. Bearg, "The Relation of Metabolic Rate to Body Weight and Organ Size," *Pediatric Res.* 1(1967):185-195.

¹⁷⁸⁸ Martin Davies, "On Body Size and Tissue Respiration," *J. Cellular Comp. Physiol.* 57(1961):135-147.

Skeletal muscle cell (max. voluntary) ¹⁷⁹⁰	1.13×10^{-10}	2.2×10^{-12}	2×10^{-15}
Thyroid cell ¹⁷⁹¹	1.3×10^{-10}	$\sim 8 \times 10^{-12}$	8×10^{-15}
T-cell lymphocyte (antigen response) ¹⁷⁹²	1.3×10^{-10}	2.1×10^{-13}	2×10^{-16}
Adrenal cell ¹⁷⁹³	1.5×10^{-10}	$\sim 8 \times 10^{-12}$	8×10^{-15}
Kidney cell ¹⁷⁹⁴	$1.55-3.46 \times 10^{-10}$	$\sim 8 \times 10^{-12}$	8×10^{-15}
Neuron (max.) ¹⁷⁹⁵	$2.55-3.3 \times 10^{-10}$	$\sim 1.4 \times 10^{-11}$	$\sim 1.4 \times 10^{-14}$
Typical human tissue cell (max.) ¹⁷⁹⁶	4.8×10^{-10}	$\sim 8 \times 10^{-12}$	8×10^{-15}
Skeletal muscle cell (max. tetanic) ¹⁷⁹⁷	2.3×10^{-9}	2.2×10^{-12}	2×10^{-15}

¹⁷⁸⁹ Knut Schmidt-Nielsen, *Scaling: Why is Animal Size So Important?* Cambridge University Press, Cambridge, 1984. M.A. Holliday, D. Potter, A. Jarrah, S. Bearg, "The Relation of Metabolic Rate to Body Weight and Organ Size," *Pediatric Res.* 1(1967):185-195. Roland A. Coulson, Thomas Hernandez, Jack D. Herbert, "Metabolic Rate, Enzyme Kinetics In Vivo," *Comp. Biochem. Physiol.* 56A(1977):251-262. Beatrice A. Wittenberg, "Intracellular Oxygen Delivery in Heart Cells," in Arie Pinson, ed., *The Heart Cell in Culture*, Vol. III, CRC Press, Boca Raton, Florida, 1987, pp. 83-89. K. Michael Sekins, Ashley F. Emery, "Chapter 2. Thermal Science for Physical Medicine," in Justus F. Lehmann, ed., *Therapeutic Heat and Cold*, Fourth Edition, Williams & Wilkins, Baltimore MD, 1990, pp. 62-112.

¹⁷⁹⁰ K. Michael Sekins, Ashley F. Emery, "Chapter 2. Thermal Science for Physical Medicine," in Justus F. Lehmann, ed., *Therapeutic Heat and Cold*, Fourth Edition, Williams & Wilkins, Baltimore MD, 1990, pp. 62-112.

¹⁷⁹¹ Martin Davies, "On Body Size and Tissue Respiration," *J. Cellular Comp. Physiol.* 57(1961):135-147.

¹⁷⁹² Claësson MH, Rodger MB, Johnson GR, Whittingham S, Metcalf D. Colony formation by human T lymphocytes in agar medium. *Clin Exp Immunol.* 1977 Jun;28(3):526-34; <http://www.ncbi.nlm.nih.gov/pmc/articles/PMC1541018/>. Augusto Cogoli, Birgitt Bechler, Marianne Cogoli-Greuter, Sue B. Criswell, Helen Joller, Peter Joller, Elisabeth Hunzinger, Otfried Muller, "Mitogenic signal transduction in T lymphocytes in microgravity," *J. Leukocyte Biol.* 53(May 1993):569-575. Dennis A. Carson, "Chapter 94. Composition and biochemistry of lymphocytes and plasma cells," in Ernest Beutler, Marshall A. Lichtman, Barry S. Coller, Thomas J. Kipps, eds., *William's Hematology*, Fifth Edition, McGraw-Hill, New York, 1995, pp. 916-921.

¹⁷⁹³ Martin Davies, "On Body Size and Tissue Respiration," *J. Cellular Comp. Physiol.* 57(1961):135-147.

¹⁷⁹⁴ Knut Schmidt-Nielsen, *Scaling: Why is Animal Size So Important?* Cambridge University Press, Cambridge, 1984. Martin Davies, "On Body Size and Tissue Respiration," *J. Cellular Comp. Physiol.* 57(1961):135-147. M.A. Holliday, D. Potter, A. Jarrah, S. Bearg, "The Relation of Metabolic Rate to Body Weight and Organ Size," *Pediatric Res.* 1(1967):185-195. K. Michael Sekins, Ashley F. Emery, "Chapter 2. Thermal Science for Physical Medicine," in Justus F. Lehmann, ed., *Therapeutic Heat and Cold*, Fourth Edition, Williams & Wilkins, Baltimore MD, 1990, pp. 62-112.

¹⁷⁹⁵ Michel A. Hofman, "Energy Metabolism, Brain Size and Longevity in Mammals," *Quart. Rev. Biology* 58(December 1983):495-512. Louis Sokoloff, "Localization of Functional Activity in the Central Nervous System by Measurement of Glucose Utilization with Radioactive Deoxyglucose," *J. Cerebral Blood Flow and Metabolism* 1(1981):7-36.

¹⁷⁹⁶ Martin Davies, "On Body Size and Tissue Respiration," *J. Cellular Comp. Physiol.* 57(1961):135-147. J.F. Nunn, *Nunn's Applied Respiratory Physiology*, 4th Edition, Butterworth-Heinemann Ltd., London, 1993. M.A. Holliday, D. Potter, A. Jarrah, S. Bearg, "The Relation of Metabolic Rate to Body Weight and Organ Size," *Pediatric Res.* 1(1967):185-195.

Heart muscle cell (max.) ¹⁷⁹⁸	$3.5\text{-}5 \times 10^{-9}$	8.8×10^{-12}	8×10^{-15}
Pancreatic islet (multi-cell) ¹⁷⁹⁹	$5\text{-}9 \times 10^{-8}$	$\sim 8 \times 10^{-9}$	8×10^{-12}
Brown fat cell (thermogenic) ¹⁸⁰⁰	6.4×10^{-8}	1.8×10^{-10}	2×10^{-13}
Flea jumping ¹⁸⁰¹	3×10^{-4}	4.5×10^{-7}	$\sim 4.5 \times 10^{-10}$
Firefly (e.g., <i>Photinus pyralis</i>) ¹⁸⁰²	3.25×10^{-4}	$\sim 2 \times 10^{-4}$	2×10^{-7}
<i>A. maculatum</i> florets ¹⁸⁰³	0.4	1×10^{-3}	$\sim 1 \times 10^{-6}$
Bee hummingbird in flight ¹⁸⁰⁴	0.593	2.5×10^{-3}	4×10^{-6}
Temperate zone herbs (wheat, tomato) ¹⁸⁰⁵	1.35	1	$\sim 1 \times 10^{-3}$
Honeybee flight muscle ¹⁸⁰⁶	2.4	1×10^{-3}	9.1×10^{-7}
Tropical grasses (maize, sugarcane) ¹⁸⁰⁷	6.19	2.75	6.9×10^{-3}
<i>Philodendron</i> spadix at 10 °C ambient ¹⁸⁰⁸	9	1.25×10^{-1}	$\sim 1.25 \times 10^{-4}$

¹⁷⁹⁷ James A. Wilson, Principles of Animal Physiology, Macmillan Publishing Company, New York, 1972.

¹⁷⁹⁸ Roland A. Coulson, Thomas Hernandez, Jack D. Herbert, "Metabolic Rate, Enzyme Kinetics In Vivo," Comp. Biochem. Physiol. 56A(1977):251-262. Richard J. Kones, Glucose, Insulin, Potassium and the Heart: Selected Aspects of Cardiac Energy Metabolism, Futura Publishing Company, 1975.

¹⁷⁹⁹ E. Gylfe, B. Hellman, "The heat production of pancreatic beta-cells stimulated by glucose," Acta Physiol. Scand. 93(1975):179-183.

¹⁸⁰⁰ Jan Nedergaard, Barbara Cannon, "Chapter 10. Thermogenic mitochondria," in L. Ernster, ed., Bioenergetics, Elsevier, New York, 1984, pp. 291-314.

¹⁸⁰¹ Bennet-Clark HC, Lucey ECA. The jump of the flea: a study of the energetics and a model of the mechanism. J Exp Biol. 1967 Aug;47(1):59-67; <http://jeb.biologists.org/content/jexbio/47/1/59.full.pdf>.

¹⁸⁰² A $\sim 120 \text{ mm}^3$ firefly with 96.5% luminous efficiency (Ives HE, Coblenz WW. Luminous efficiency of the firefly. Bulletin of the Bureau of Standards 1910; 6(3):321-336; http://nvlpubs.nist.gov/nistpubs/bulletin/06/nbsbulletinv6n3p321_A2b.pdf) emits $\sim 1/400$ candlepower ("The Chemistry of the Luciferin-Luciferase Reaction," 19 Apr 2001; <http://web.archive.org/web/20040509205852/http://www.isat.jmu.edu/users/klevicca/isat453/Web/luciferase.e.htm>), equivalent to 0.0314 lumens or 0.000325 watts ("Lumens to watts calculator," <http://www.rapidtables.com/calc/light/lumen-to-watt-calculator.htm>).

¹⁸⁰³ Seymour RS. Plants that warm themselves. Sci Am. 1997 Mar;276:104-109.

¹⁸⁰⁴ Seymour RS. Plants that warm themselves. Sci Am. 1997 Mar;276:104-109. <https://en.wikipedia.org/wiki/Hummingbird>.

¹⁸⁰⁵ Chaisson E. Energy Rate Density as a Complexity Metric and Evolutionary Driver. Complexity 2011;16:27-40; https://www.cfa.harvard.edu/~ejchaisson/reprints/EnergyRateDensity_I_FINAL_2011.pdf.

¹⁸⁰⁶ Seymour RS. Plants that warm themselves. Sci Am. 1997 Mar;276:104-109.

¹⁸⁰⁷ "Sugarcane," <https://en.wikipedia.org/wiki/Sugarcane>. "Density of Sugar Factory Products," <http://www.sugartech.co.za/density/>. Chaisson E. Energy Rate Density as a Complexity Metric and Evolutionary Driver. Complexity 2011;16:27-40; https://www.cfa.harvard.edu/~ejchaisson/reprints/EnergyRateDensity_I_FINAL_2011.pdf.

Human brain ¹⁸⁰⁹	20	1.4	1.2×10^{-3}
Human body (basal) ¹⁸¹⁰	100	70	6.73×10^{-2}
Electric eel (<i>Electrophorus electricus</i>) ¹⁸¹¹	500-860	20	2×10^{-2}
Human body (max.) ¹⁸¹²	1600	70	6.73×10^{-2}
Evergreen trees (pine, fir, larch) ¹⁸¹³	2200	4000	8
Deciduous trees (oak, beech) ¹⁸¹⁴	5040	7000	10
Global photosynthesis (all plants) ¹⁸¹⁵	1.3×10^{14}	1.841×10^{15}	2.6×10^{12}
Animals ¹⁸¹⁶			

¹⁸⁰⁸ Seymour RS. Plants that warm themselves. *Sci Am.* 1997 Mar;276:104-109. The sterile male flowers produce and maintain a constant temperature that is 30 °C above that of the environment during the two days the flower structure is open; heat is produced by metabolizing fat, not carbohydrate.
https://en.wikipedia.org/wiki/Philodendron_bipinnatifidum.

¹⁸⁰⁹ Hofman MA. Energy Metabolism, Brain Size and Longevity in Mammals. *Quart Rev Biol.* 1983 Dec;58:495-512. Duara R, *et al.* Human Brain Glucose Utilization and Cognitive Function in Relation to Age. *Annals of Neurology* 1984;16:702-713. Mink JW, Blumenschine RJ, Adams DB. Ratio of central nervous system to body metabolism in vertebrates: its constancy and functional basis. *Amer J Physiol.* 1981;241:R203-R212. Mason GF, *et al.* Simultaneous Determination of the Rates of the TCA Cycle, Glucose Utilization, alpha-Ketoglutarate/Glutamate Exchange, and Glutamine Synthesis in Human Brain by NMR. *J Cerebral Blood Flow and Metabolism* 1995;15:12-25.

¹⁸¹⁰ J.F. Nunn, Nunn's Applied Respiratory Physiology, 4th Edition, Butterworth-Heinemann Ltd., London, 1993.

¹⁸¹¹ "Electric eel," https://en.wikipedia.org/wiki/Electric_eel. "Voltage of an Electric Eel," The Physics Factbook; <http://hypertextbook.com/facts/BarryLajnwand.shtml>.

¹⁸¹² J.F. Nunn, Nunn's Applied Respiratory Physiology, 4th Edition, Butterworth-Heinemann Ltd., London, 1993.

¹⁸¹³ "Physical Properties of Common Woods," <http://www.csudh.edu/oliver/chemdata/woods.htm>. Davis, S.C., Ed. Biomass Energy Data Book, Appendix B; U.S. Department of Energy: Washington, DC, 2009. Chaisson E. Energy Rate Density as a Complexity Metric and Evolutionary Driver. *Complexity* 2011;16:27-40; https://www.cfa.harvard.edu/~ejchaisson/reprints/EnergyRateDensity_I_FINAL_2011.pdf.

¹⁸¹⁴ "One Oak," https://sylva.org.uk/oneoak/tree_facts.php. "Physical Properties of Common Woods," <http://www.csudh.edu/oliver/chemdata/woods.htm>. Chaisson E. Energy Rate Density as a Complexity Metric and Evolutionary Driver. *Complexity* 2011;16:27-40; https://www.cfa.harvard.edu/~ejchaisson/reprints/EnergyRateDensity_I_FINAL_2011.pdf.

¹⁸¹⁵ The average global rate of photosynthesis is 130 terawatts; Steger U, Achterberg W, Blok K, Bode H, Frenz W, Gather C, Hanekamp G, Imboden D, Jahnke M, Kost M, Kurz R, Nutzinger HG, Ziesemer T. Sustainable development and innovation in the energy sector. Berlin: Springer, Berlin, 2005, p. 32. The mass of all photosynthetic plant biomass ~ 1.841×10^{15} kg (https://en.wikipedia.org/wiki/Primary_production#Estimates) and 2.6×10^{12} m³ assuming mean density ~700 kg/m³ (mostly wood; <http://www.fao.org/docrep/w4095e/w4095e0c.htm>).

Bacterium (<i>Sarcina lutea</i>)	3.8×10^{-14}	1×10^{-15}	1×10^{-18}
Fungi (<i>Saccharomyces</i> sp)	1.0×10^{-11}	1.8×10^{-13}	1.8×10^{-16}
Protozoa (<i>Chaos chaos</i>)	$4.6-7.0 \times 10^{-8}$	5×10^{-8}	5×10^{-11}
Nematode (<i>Plectus</i>)	$2.8-7.9 \times 10^{-6}$	$0.5-1 \times 10^{-6}$	$0.5-1 \times 10^{-9}$
Annelid (earthworm; <i>Lumbricus terrestris</i>)	1.7×10^{-4}	5×10^{-4}	5×10^{-7}
Diptera (flies; larvae of <i>Tipula</i> sp)	3.2×10^{-4}	2.75×10^{-4}	2.75×10^{-7}
Mollusc (garden snail; <i>Helix aspersa</i>)	$2.4-4.9 \times 10^{-3}$	1×10^{-2}	1×10^{-5}
Rat, adult male	1.5	0.2	2×10^{-4}
Guinea pig, adult male	2.4	0.8	8×10^{-4}
Chicken, adult male	12	2.6	2.6×10^{-3}
Goat, adult	140	70	7×10^{-2}
Pig, adult male	290	250	2.5×10^{-1}
Beef cattle, adult male	510	500	5×10^{-1}
Horse, adult male	790	650	6.5×10^{-1}
Planet-wide			
Lightning bolt (average negative discharge) ¹⁸¹⁷	1×10^{12}	2-880	2-800
Tsunami (typical) ¹⁸¹⁸	1×10^{13}	3.1×10^{16}	3×10^{13}
Tornado (maximum EF5) ¹⁸¹⁹	1.7×10^{13}	4.6×10^{10}	4.2×10^{10}
Hurricane (typical) ¹⁸²⁰	6×10^{14}	1.9×10^{16}	1.7×10^{16}

¹⁸¹⁶ Mass and power as metabolic rate from William S. Spector, ed.; Handbook of Biological Data, The Committee on the Handbook of Biological Data, Division of Biology and Agriculture, The National Academy of Sciences, The National Research Council, October 1956; Wright Air Development Center, WADC Technical Report 56-273, ASTIA Document No. AD 110501, pp. 255-258; volume estimated from mass assuming a density of $\sim 1000 \text{ kg/m}^3$.

¹⁸¹⁷ An average bolt of negative lightning (>95% of all strikes) transfers 5×10^8 joules of energy in $\sim 5 \times 10^{-4}$ sec (15 coulombs / 30,000 amperes), giving a brief power surge of 1×10^{12} watts at ~ 33 megavolts (<https://en.wikipedia.org/wiki/Lightning>); if the bolt is ~ 1 km high and the channel is 0.05-1 m wide (<http://www.aharfield.co.uk/lightning-protection-services/about-lightning>), then its volume is 2-800 m^3 and its mass is 2-880 kg (assuming $\sim 1.1 \text{ kg/m}^3$ for humid air).

¹⁸¹⁸ The model tsunami analyzed by Dutykh assumes a block of seawater placed in motion by sea floor movement, of dimensions 150 km x 50 km and 4 km water depth (water volume $\sim 3 \times 10^{13} \text{ m}^3$ and mass $\sim 3.1 \times 10^{16}$ kg assuming seawater density $\sim 1040 \text{ kg/m}^3$ at depth; <http://fermi.jhuapl.edu/denscalc.html>), producing a wave energy of $\sim 5 \times 10^{14}$ joules and power of 1×10^{13} watts assuming a 50 sec rise time. (Dutykh D, Dias F. Energy of tsunami waves generated by bottom motion. Proc R Soc A. 2009;465:725–744; <http://hal.univ-savoie.fr/hal-00311752v2/document>).

¹⁸¹⁹ One 2013 Oklahoma tornado of maximum severity “EF5” (https://en.wikipedia.org/wiki/Enhanced_Fujita_scale) with 340 kph wind speeds was believed to have up to 9.6 megatons (4×10^{16} joules) of energy, was measured 2.1 km wide, and lasted ~ 40 min (2400 sec) (<http://www.dailymail.co.uk/news/article-2328834/Oklahoma-tornado-600-TIMES-powerful-Hiroshima-atomic-bomb.html>), giving a continuous power of 1.7×10^{13} watts. If the height of the EF5 tornado includes the mesocyclonic updraft in the parent thunderstorm up to ~ 12 km, then its volume is $\sim 4.2 \times 10^{10} \text{ m}^3$ and mass $\sim 4.6 \times 10^{10}$ kg (assuming $\sim 1.1 \text{ kg/m}^3$ for humid air).

Volcanic eruption, Class 5 (Mount St. Helens) ¹⁸²¹	1.3×10^{15}	1.1×10^{13}	4.2×10^9
Meteoroid impact (Meteor Crater, AZ) ¹⁸²²	3×10^{19}	2.9×10^8	3.9×10^4
Earthquake, magnitude 9.5 (Valdivia, 1960) ¹⁸²³	3.7×10^{20}	7×10^{14}	2.6×10^{11}
Asteroid impact, extinction-level (Chicxulub) ¹⁸²⁴	1.3×10^{24}	3.4×10^{15}	1.5×10^{11}
<u>Astronomical</u>			
Marine tidal oscillations (Earth-Moon) ¹⁸²⁵	3.675×10^{12}	1.4×10^{21}	1.338×10^{18}

¹⁸²⁰ Most (99.5%) of hurricane energy is released by water droplet condensation and not horizontal wind driving; estimated continuous power $\sim 6 \times 10^{14}$ watts for a typical hurricane of radius 665 km and altitude ~ 12 km, a volume of $1.7 \times 10^{16} \text{ m}^3$ (“How much energy does a hurricane release?” NOAA, 2014, <http://www.aoml.noaa.gov/hrd/tcfaq/D7.html>) and a mass of $1.9 \times 10^{16} \text{ kg}$ (assuming $\sim 1.1 \text{ kg/m}^3$ for humid air). A hurricane of this power that lasts for ~ 4 days ($3.5 \times 10^5 \text{ sec}$) has a total energy release of 2.1×10^{20} joules.

¹⁸²¹ The eruption of Mount St. Helens, rated Class 5 on the Volcanic Explosivity Index (<http://www.unc.edu/~rowlett/units/scales/VEI.html>), released 24 megatons (1×10^{17} joules) of thermal energy and $\sim 4.2 \text{ km}^3$ ($1.1 \times 10^{13} \text{ kg}$ @ $\sim 2700 \text{ kg/m}^3$) of ejecta. <http://science.howstuffworks.com/environmental/energy/energy-hurricane-volcano-earthquake2.htm> and lasted $\sim 80 \text{ sec}$ (https://en.wikipedia.org/wiki/1980_eruption_of_Mount_St._Helens), giving a blast power of 1.3×10^{15} watts.

¹⁸²² The energy released by the impactor that created Meteor Crater in Arizona is estimated as ~ 15 megatons (6.3×10^{16} joules), with the impactor believed to be 42 m in spherical diameter ($3.9 \times 10^4 \text{ m}^3$) with a mass of $2.9 \times 10^8 \text{ kg}$ (assuming 7500 kg/m^3 for meteoritic iron) with an impact velocity of $\sim 20 \text{ km/sec}$ and an impact power of $\sim 3 \times 10^{19}$ watts during a ground impact time of (42 m) / (20 km/sec) $\sim 0.0021 \text{ sec}$. Shoemaker EM. Asteroid and comet bombardment of the earth. Ann Rev Earth Planet Sci. 1983;11:461-494, <http://articles.adsabs.harvard.edu/full/1983AREPS..11..461S/0000470.000.html>.

¹⁸²³ The 1960 Valdivia earthquake (https://en.wikipedia.org/wiki/1960_Valdivia_earthquake) is the largest ever recorded, estimated at Magnitude 9.5 with a total seismic moment energy release of 2.2×10^{23} joules (<http://alabamaquake.com/energy.html>). The estimated rupture zone was 33 km deep and 800 km long; assuming a rupture width of $\sim 10 \text{ m}$ gives a rupture volume of $2.6 \times 10^{11} \text{ m}^3$ with a rupture mass of $7.0 \times 10^{14} \text{ kg}$ (assuming 2700 kg/m^3 for continental crustal rock). The quake had a rupture power of 3.7×10^{20} watts if the energy is viewed as having been released over the 10 min (600 sec) that the earthquake lasted.

¹⁸²⁴ The energy released by the dinosaur-extincting Chicxulub asteroid impact on Earth 65.5 million years ago was first estimated in 1980 as $\sim 10^8$ megatons of TNT x (4.184×10^{15} joules/megaton) = 4.2×10^{23} joules, with the impactor having a diameter of $\sim 6.6 \text{ km}$ ($\sim 1.5 \times 10^{11} \text{ m}^3$ if spherical) and a mass of $3.4 \times 10^{14} \text{ kg}$; Alvarez LW, Alvarez W, Asaro F, Michel HV. Extraterrestrial cause for the cretaceous-tertiary extinction. Science. 1980 Jun 6;208(4448):1095-108; <http://citeseerx.ist.psu.edu/viewdoc/download?doi=10.1.1.126.8496&rep=rep1&type=pdf>. (A 1998 research group concluded the impactor was a $1.2 \times 10^{24} \text{ J}$, $1.8 \times 10^{15} \text{ kg}$, 16.5 km diameter ($\sim 2.4 \times 10^{12} \text{ m}^3$) comet (<http://sp.jvellingcollection.org/content/140/1/155.short>), and there have been other estimates.) An impact velocity of $\sim 20 \text{ km/sec}$ yields an impact power of $\sim 1.3 \times 10^{24}$ watts during a ground impact time of (6.6 km) / (20 km/sec) $\sim 0.33 \text{ sec}$.

¹⁸²⁵ Earth’s tidal oscillations dissipated about 3.75 terawatts, 98% of which is due to marine tidal movement. Munk, W.; Wunsch, C. (1998). “Abyssal recipes II: energetics of tidal and wind mixing”. Deep-Sea Research Part I 45 (12): 1977; <https://en.wikipedia.org/wiki/Tide#Dissipation>. All Earth’s oceans have a volume $\sim 1.338 \times 10^9 \text{ km}^3$ (<http://water.usgs.gov/edu/watercycleoceans.html>) and mass $\sim 1.4 \times 10^{21} \text{ kg}$ (<https://en.wikipedia.org/wiki/Ocean>).

Geothermal heat (whole planet, Earth) ¹⁸²⁶	4.42×10^{13}	5.972×10^{24}	1.083×10^{21}
Tidal heating of Jovian moon Io ¹⁸²⁷	$0.6\text{-}1.6 \times 10^{14}$	8.93×10^{22}	2.53×10^{19}
Jovothermal heat (whole planet, Jupiter) ¹⁸²⁸	3.35×10^{17}	1.8986×10^{27}	1.4313×10^{24}
Solar flare (Sun) ¹⁸²⁹	6×10^{19}	1.6×10^{12}	1.1×10^9
Brown dwarf (W0607+24) ¹⁸³⁰	8.4×10^{21}	1.1×10^{29}	1.4×10^{24}
Type M9 star ¹⁸³¹	5.74×10^{22}	1.49×10^{29}	9×10^{25}

¹⁸²⁶ Earth emits more radiation than it receives from the Sun, due to radioactive decay (~80%) and residual heat from planetary accretion (~20%), with thermal luminosity = 4.42×10^{13} watts, mass = 5.972×10^{24} kg, radius = 6.371×10^6 m. Pollack HN, Hurter SJ, Johnson JR. Heat flow from the Earth's interior: Analysis of the global data set. *Rev Geophysics* 1993 Aug;31(3):267-80. Turcotte DL, Schubert G. Chapter 4, *Geodynamics*, 2nd Ed., Cambridge University Press, Cambridge, England UK, 2002, pp. 136-137. "Earth," <https://en.wikipedia.org/wiki/Earth>.

¹⁸²⁷ Tidal heating of Io from differential gravitational forces produces a ~100 m bulge in the moon's surface, with moon mass ~ 8.93×10^{22} kg and volume ~ 2.53×10^{10} km³. Moore WB *et al.* The Interior of Io, in: Lopes RMC, Spencer JR, Io after Galileo, Springer-Praxis, 2007, pp. 89-108; [https://en.wikipedia.org/wiki/Io_\(moon\)#Tidal_heating](https://en.wikipedia.org/wiki/Io_(moon)#Tidal_heating).

¹⁸²⁸ Jupiter emits more radiation than it receives from the Sun, due to fusionless gravitational compression via the Kelvin-Helmholtz mechanism (https://en.wikipedia.org/wiki/Kelvin%E2%80%93Helmholtz_mechanism), with thermal luminosity ~ 8.7×10^{10} L_{solar} = 335 petawatts (<https://www.physicsforums.com/threads/computing-jupiters-thermal-time-scale.646615/>, https://books.google.com/books?id=jIB4MY50sIUC&pg=PA1129&lpg=PA1129&dq=jupiter+internal+heat+W/m2&source=bl&ots=woJ_a_u9O6&sig=ZICQmNzEFLstUe10PI8PAqhrhkg&hl=en&sa=X&ved=0ah_UKEwidoO-Z1-NAhVGID4KHb5ICuoQ6AEIOzAG#v=onepage&q=jupiter%20internal%20heat%20W%20m2&f=false), mass M_{Jupiter} = 1.8986×10^{27} kg, mean radius R_{Jupiter} = 6.9911×10^7 m. "Jupiter," <https://en.wikipedia.org/wiki/Jupiter>.

¹⁸²⁹ Solar flares with energies 10^{20} - 10^{25} J (https://en.wikipedia.org/wiki/Solar_flare) accompanied by coronal mass ejections averaging 1.6×10^{12} kg (~ 1.1×10^9 m³ taking mean solar density ~ 1410 kg/m³) with average ejection velocity 489 km/sec (https://en.wikipedia.org/wiki/Coronal_mass_ejection#Physical_properties) may have a kinetic energy of $E = (1/2)mv^2 = (0.5)(1.6 \times 10^{12} \text{ kg})(4.89 \times 10^5 \text{ m/sec})^2 = 1.9 \times 10^{23}$ joules, a power output of 6×10^{19} watts assuming a flare ejection time of ~3000 sec (http://www.mssl.ucl.ac.uk/www_solar/PUS/PO/explosions.html).

¹⁸³⁰ Nearby brown dwarf of luminosity ~ 0.000022 L_{solar}, mass ~ 0.055 M_{solar} = 57.9 M_{Jupiter}, and radius ~ 0.1 R_{solar} (Gizis JE, Williams PK, Burgasser AJ, Libralato M, Nardiello D, Piotto G, Bedin LR, Berger E, Paudel R. WISEP J060738.65+242953.4: A Nearby, Pole-On L8 Brown Dwarf with Radio Emission. arXiv preprint arXiv:1607.00943. 2016 Jul 4; <https://arxiv.org/pdf/1607.00943v1.pdf>). Brown dwarfs are not massive enough to sustain nuclear fusion of ordinary hydrogen to helium in their cores, but may be able to burn deuterium and lithium if their mass is above 13 M_{Jupiter} and 65 M_{Jupiter}, respectively; "Brown dwarf," https://en.wikipedia.org/wiki/Brown_dwarf.

¹⁸³¹ Power from fusion. An M9 star may have luminosity ~ 0.00015 L_{solar}, mass ~ 0.075 M_{solar}, and radius ~ 0.4 R_{solar}, with R_{solar} = 6.957×10^8 m; https://en.wikipedia.org/wiki/Red_dwarf and https://en.wikipedia.org/wiki/Stellar_classification.

Radio pulsar (first known, PSR B1919+21) ¹⁸³²	2.3×10^{24}	2.8×10^{30}	3.9×10^9
White dwarf star (Procyon B) ¹⁸³³	1.88×10^{23}	1.2×10^{30}	2.65×10^{21}
Sun (typical G2 star) ¹⁸³⁴	3.828×10^{26}	1.989×10^{30}	1.41×10^{27}
X-ray pulsar, excluding star (Centaurus X-3) ¹⁸³⁵	10^{26} - 10^{29}	2.4×10^{30}	3.4×10^9
Type O9 star ¹⁸³⁶	3.828×10^{30}	3.18×10^{31}	4.05×10^{29}
Red supergiant star (Betelgeuse) ¹⁸³⁷	3.4 - 5.7×10^{31}	2.3×10^{31}	1.2 - 2.4×10^{36}
Blue supergiant star (Deneb) ¹⁸³⁸	7.5×10^{31}	3.8×10^{31}	1.2×10^{34}
Globular cluster (M15) ¹⁸³⁹	1.4×10^{32}	1.1×10^{36}	2.4×10^{54}
Milky Way galaxy ¹⁸⁴⁰	1.76 - 2.46×10^{37}	1.69×10^{42}	6.57×10^{60}
Superluminous supernova (ASASSN-15lh) ¹⁸⁴¹	2.2×10^{38}	$\sim 8 \times 10^{31}$	$\sim 1 \times 10^{30}$
Hyperluminous quasar (S5 0014+81) ¹⁸⁴²	1×10^{41}	8×10^{40}	7×10^{42}

¹⁸³² Power from rotational slowing of neutron star. Luminosity $\sim 0.006 L_{\text{solar}}$, mass $\sim 1.4 M_{\text{solar}}$, radius $\sim 1.4 \times 10^6 R_{\text{solar}}$; “PSR B1919+21,” https://en.wikipedia.org/wiki/PSR_B1919%2B21.

¹⁸³³ Power from fusion. Luminosity $\sim 0.00049 L_{\text{solar}}$, mass $\sim 0.602 M_{\text{solar}}$, radius $\sim 0.01234 R_{\text{solar}}$; “Procyon,” https://en.wikipedia.org/wiki/Procyon#Procyon_B.

¹⁸³⁴ Power from fusion. “Sun,” <https://en.wikipedia.org/wiki/Sun>.

¹⁸³⁵ Power from infall of matter from Type O6 star onto a spinning neutron star, resulting in X-ray emission, e.g., “accretion-powered pulsar”. X-ray luminosity $\sim 10^{26}$ - 10^{29} watts; Trumper JE, Zezas A, Ertan U, Kylafis ND. The energy spectrum of anomalous X-ray pulsars and soft gamma-ray repeaters. *Astronomy & Astrophysics* 2010; A46:518; <http://research.sabanciuniv.edu/14354/1/aa11834-09.pdf>. Neutron star mass $\sim 1.21 M_{\text{solar}}$, Type O star luminosity $\sim 316,000 L_{\text{solar}}$, mass $\sim 20.5 M_{\text{solar}}$, radius $\sim 12 R_{\text{solar}}$; “Centaurus X-3,” https://en.wikipedia.org/wiki/Centaurus_X-3.

¹⁸³⁶ Power from fusion. An O9 star may have luminosity $\sim 10,000 L_{\text{solar}}$, mass $\sim 16 M_{\text{solar}}$, and spherical radius $\sim 6.6 R_{\text{solar}}$, with $R_{\text{solar}} = 6.957 \times 10^8$ m; https://en.wikipedia.org/wiki/O-type_star and https://en.wikipedia.org/wiki/Stellar_classification.

¹⁸³⁷ Power from fusion. Luminosity $\sim 90,000$ - $150,000 L_{\text{solar}}$, mass $\sim 11.6 M_{\text{solar}}$, radius ~ 955 - $1200 R_{\text{solar}}$; “Betelgeuse,” <https://en.wikipedia.org/wiki/Betelgeuse>.

¹⁸³⁸ Power from fusion. Luminosity $\sim 196,000 L_{\text{solar}}$, mass $\sim 19 M_{\text{solar}}$, radius $\sim 203 R_{\text{solar}}$; “Deneb,” <https://en.wikipedia.org/wiki/Deneb>.

¹⁸³⁹ Spherical cluster of $\sim 100,000$ stars powered by fusion, total luminosity $\sim 360,000 L_{\text{solar}}$, mass $\sim 5.6 \times 10^5 M_{\text{solar}}$, radius ~ 88 light-years = 8.3×10^{17} m; “Messier 15,” https://en.wikipedia.org/wiki/Messier_15.

¹⁸⁴⁰ Milky Way galaxy is approximately a disk 100,000 light-years in diameter and 1000 light-years thick, of mass $8.5 \times 10^{11} M_{\text{solar}}$, with fusion-derived luminosity 4.6 - $6.43 \times 10^{10} L_{\text{solar}}$; “Milky Way,” https://en.wikipedia.org/wiki/Milky_Way. $M_{\text{solar}} = 1.989 \times 10^{30}$ kg, $L_{\text{solar}} = 3.828 \times 10^{26}$ watts, 1 light-year = 9.42×10^{15} m.

¹⁸⁴¹ Most luminous supernova ever recorded with peak power output of 2.2×10^{38} watts; precursor may have been a rapidly rotating hot blue Type O or Wolf-Rayet star, perhaps with mass $\sim 40 M_{\text{solar}}$ and radius $\sim 10 R_{\text{solar}}$; “ASASSN-15lh,” <https://en.wikipedia.org/wiki/ASASSN-15lh>.

¹⁸⁴² Largest known hyperluminous quasar or “blazer”, driven by a supermassive black hole (https://en.wikipedia.org/wiki/Supermassive_black_hole); luminosity $\sim 3 \times 10^{14} L_{\text{solar}}$, mass $\sim 4 \times 10^{10} M_{\text{solar}}$, radius $\sim 1.18 \times 10^{14}$ m; “S5 0014+81,” https://en.wikipedia.org/wiki/S5_0014%2B81.

Type Ia supernova ¹⁸⁴³	$\sim 1 \times 10^{44}$	2.8×10^{30}	2×10^{21}
Type II supernova ¹⁸⁴⁴	$\sim 1 \times 10^{45}$	$1.6-8 \times 10^{31}$	$0.3-1 \times 10^{30}$
Quark nova ¹⁸⁴⁵	$\sim 3 \times 10^{45}$	$3-3.6 \times 10^{30}$	$\sim 1 \times 10^{10}$
Binary black hole merger ¹⁸⁴⁶	2.69×10^{48}	1.29×10^{32}	3.88×10^{16}
Universe ¹⁸⁴⁷	2.80×10^{49}	3.03×10^{54}	3.57×10^{80}
Evaporating black hole ¹⁸⁴⁸ of mass:			
Galactic core ($\sim 10^6 M_{\text{solar}}$), $t_{\text{ev}} \sim 8.4 \times 10^{91}$ sec	3.6×10^{-40}	1×10^{36}	1.4×10^{28}
Stellar ($\sim 1 M_{\text{solar}}$), $t_{\text{ev}} \sim 8.4 \times 10^{73}$ sec	3.6×10^{-28}	1×10^{30}	1.4×10^{10}
Planetary ($\sim 10^{-6} M_{\text{solar}}$), $t_{\text{ev}} \sim 8.4 \times 10^{55}$ sec	3.6×10^{-16}	1×10^{24}	1.4×10^{-8}
Asteroidal ($\sim 10^{-12} M_{\text{solar}}$), $t_{\text{ev}} \sim 8.4 \times 10^{37}$ sec	3.6×10^{-4}	1×10^{18}	1.4×10^{-26}
1 km meteor ($\sim 10^{-18} M_{\text{solar}}$), $t_{\text{ev}} \sim 8.4 \times 10^{19}$ sec	3.6×10^8	1×10^{12}	1.4×10^{-44}
10-meter boulder ($\sim 10^{-24} M_{\text{solar}}$), $t_{\text{ev}} \sim 84$ sec	3.6×10^{20}	1×10^6	1.4×10^{-62}
Ylem (cosmic egg) ¹⁸⁴⁹	2.43×10^{113}	1.46×10^{53}	4.22×10^{105}

¹⁸⁴³ Fusion explosion in a binary star system, where the exploding star is a carbon-oxygen white dwarf of mass $\sim 1.39 M_{\text{solar}}$ and radius $\sim 0.011 R_{\text{solar}}$, releasing $\sim 2 \times 10^{44}$ J in a few seconds; “Type Ia supernova,” https://en.wikipedia.org/wiki/Type_Ia_supernova.

¹⁸⁴⁴ Rapid collapse and violent fusion explosion of a massive ($8-40 M_{\text{solar}}$) star of radius $\sim 6-9 R_{\text{solar}}$, releasing $\sim 10^{46}$ J in ~ 10 sec, resulting in a neutron star below $20 M_{\text{solar}}$ and a black hole above $20 M_{\text{solar}}$; “Type II supernova,” https://en.wikipedia.org/wiki/Type_II_supernova.

¹⁸⁴⁵ Hypothetical violent explosion (<https://en.wikipedia.org/wiki/Quark-nova>) resulting from the conversion of a neutron star to a quark star in which the process of quark deconfinement creates quark matter (https://en.wikipedia.org/wiki/QCD_matter) in the $1.5-1.8 M_{\text{solar}}$ neutron star interior, releasing $\sim 10^{47}$ J on the average ~ 30 sec timescale of gamma-ray bursts (https://en.wikipedia.org/wiki/Gamma-ray_burst).

¹⁸⁴⁶ Observed merger of a binary black hole, involving two black holes of total mass $\sim 65 M_{\text{solar}}$ with a summed Schwarzschild radius for the binary components of ~ 210 km, produced a ~ 0.2 sec release of gravitational waves of energy $\sim 3 M_{\text{solar}} c^2$. Abbott BP *et al.* Observation of Gravitational Waves from a Binary Black Hole Merger. Phys Rev Lett. 2016 Feb 11;116, 061102; <http://journals.aps.org/prl/pdf/10.1103/PhysRevLett.116.061102>.

¹⁸⁴⁷ The diameter of the (assumed spherical) universe is 8.8×10^{26} light-years, volume $3.58 \times 10^{80} \text{ m}^3$, total mass is $(0.85 \times 10^{-26} \text{ kg/m}^3)(3.57 \times 10^{80} \text{ m}^3) = 3.03 \times 10^{54} \text{ kg}$, total stellar mass is $(4.08 \times 10^{-28} \text{ kg/m}^3)(3.57 \times 10^{80} \text{ m}^3) = 1.46 \times 10^{53} \text{ kg} = 7.32 \times 10^{22} M_{\text{solar}}$, and total luminosity ($7.32 \times 10^{22} M_{\text{solar}}$) (3.828×10^{26} watts) = 2.80×10^{49} watts; https://en.wikipedia.org/wiki/Observable_universe.

¹⁸⁴⁸ Black hole evaporation time $t_{\text{ev}} = 5120 \pi G^2 M_{\text{bh}}^3 / \hbar c^4$, black hole evaporative power output is $P_{\text{ev}} = \hbar c^6 / (15360 \pi G^2 M_{\text{bh}}^2)$, total black hole radiative energy $E_{\text{ev}} = M_{\text{bh}} c^2$ with average radiated power over the entire evaporation time $P_{\text{avg}} = E_{\text{ev}}/t_{\text{ev}}$, and black hole Schwarzschild radius $R_{\text{bh}} = 2 G M_{\text{bh}} / c^2$, where $G = 6.67 \times 10^{-11} \text{ N-m}^2/\text{kg}^2$, M_{bh} = black hole mass (kg), $\hbar = h/2\pi = 1.055 \times 10^{-34} \text{ J-sec}$ with $h = 6.63 \times 10^{-34} \text{ J-sec}$, and $c = 3 \times 10^8 \text{ m/sec}$. “Hawking radiation,” https://en.wikipedia.org/wiki/Hawking_radiation.

¹⁸⁴⁹ The ylem (cosmic egg) is the hypothetical primordial singularity from which the entire universe expanded during the Big Bang, containing at least the entire mass of the observable universe ($M_U = 1.46 \times 10^{53}$ kg) compressed into the smallest measurable volume ($V_{\text{planck}} = 4.22 \times 10^{-105}$ m³), which is the cube of the Planck length ($L_{\text{Planck}} = 1.616 \times 10^{-35}$ m) that has been hypothesized to be “the shortest measurable length” (https://en.wikipedia.org/wiki/Planck_length). The shortest measurable time over which this mass-energy ($M_U c^2 = 1.31 \times 10^{70}$ J) might be released may be the Planck time (https://en.wikipedia.org/wiki/Planck_time) or $t_{\text{Planck}} = 5.39 \times 10^{-44}$ sec, defining the maximum possible power development (2.43×10^{113} W).

A.3 Data on Energy Storage in Chemical Decomposition

Table A3. Data on energy storage in chemical decomposition.			
Energy Storage System	Energy (J)	Mass (kg)	Volume (m ³)
Monopropellants			
Ammonium dinitramide monopropellant ¹⁸⁵⁰	3.36 x 10 ⁵	0.124	6.58 x 10 ⁻⁵
Ammonium nitrate monopropellant ¹⁸⁵¹	3.64 x 10 ⁴	0.080	4.64 x 10 ⁻⁵
Cyclic ozone (O ₃) decomposition (theoretical) ¹⁸⁵²	2.73 x 10 ⁵	0.048	2.78 x 10 ⁻⁵
Guanidine nitrate monopropellant ¹⁸⁵³	8.75 x 10 ⁵	0.122	8.50 x 10 ⁻⁵

¹⁸⁵⁰ Ammonium dinitramide, aka. ADN or LMP-103S (NH₄⁺N(NO₂)₂⁻ or H₄N₄O₄, 0.124 kg/mole, solid density 1810 kg/m³; https://en.wikipedia.org/wiki/Ammonium_dinitramide), has been used as a satellite monopropellant and decomposes under heat to leave only nitrogen, oxygen, and water, according to: H₄N₄O₄ → 2N₂ + 2H₂O + O₂, taking the standard heats of formation as -148.1 kJ/mole for H₄N₄O₄ and -241.8 kJ/mole for H₂O (http://www.update.uu.se/~jolkkonen/pdf/CRC_TD.pdf), releasing 3.36 x 10⁵ J.

¹⁸⁵¹ Ammonium nitrate (NH₄NO₃, 0.080 kg/mole, 4.64 x 10⁻⁵ m³/mole) decomposes when heated according to: NH₄NO₃ → N₂O + 2H₂O, releasing its 3.64 x 10⁴ J/mole heat of formation (http://www.update.uu.se/~jolkkonen/pdf/CRC_TD.pdf) as a gaseous monopropellant (https://en.wikipedia.org/wiki/Ammonium_nitrate#Reactions).

¹⁸⁵² Cyclic ozone (O₃, 0.048 kg/mole, density ~ 1728 kg/m³ the same as solid “open” ozone) has not been detected in the free form, but has been detected on the surface of magnesium oxide crystals in air* and there has been at least one experimental attempt to create it.** Theoretical calculations indicate that free cyclic ozone should be stable, with a heat of formation +130 kJ/mole higher than “open” ozone and a barrier of 95 kJ/mole preventing conversion to the “open” form,*** although the most recent theoretical analysis suggests that free cyclic ozone might have a lifetime of only ~70 sec at 100 K.**** The decomposition to molecular oxygen via O₃ → 1.5O₂, should therefore release (130 kJ/mole + 142.7 kJ/mole) = 272.7 kJ/mole. *Plass R, *et al.* Cyclic ozone identified in magnesium oxide (111) surface reconstructions. Phys Rev Lett. 1998 Nov 30;81:4891; http://www.numis.northwestern.edu/Research/Articles/1998/98_PRL_Plass.pdf. ***Temple researcher attempting to create cyclic ozone,” ScienceDaily, 8 Feb 2005; <https://www.sciencedaily.com/releases/2005/02/050205122519.htm>. ****Roald Hoffmann. The story of O. Amer Sci. 2004 Jan-Feb; <http://www.americanscientist.org/issues/pub/the-story-of-o/99999>. ****Chen JL, Hu WP. Theoretical prediction on the thermal stability of cyclic ozone and strong oxygen tunneling. J Am Chem Soc. 2011 Oct 12;133(40):16045-53; http://140.123.79.88/~yach932/CH3_Reference/49.cyc-O3_JACS_2011.pdf.

Hydrazine (N ₂ H ₄) monopropellant ¹⁸⁵⁴	9.54 x 10 ⁴	0.032	3.14 x 10 ⁻⁵
Hydrogen peroxide monopropellant ¹⁸⁵⁵	1.06 x 10 ⁵	0.034	2.34 x 10 ⁻⁵
Hydroxylammonium nitrate ¹⁸⁵⁶	1.05 x 10 ⁵	0.096	5.25 x 10 ⁻⁵
Nitromethane monopropellant ¹⁸⁵⁷	6.30 x 10 ⁵	0.061	3.14 x 10 ⁻⁵
Nitrous oxide (N ₂ O) monopropellant ¹⁸⁵⁸	8.16 x 10 ⁴	0.044	3.58 x 10 ⁻⁵
Octaoxygen (O ₈) decomposition ¹⁸⁵⁹	3.93 x 10 ⁵	0.128	7.11 x 10 ⁻⁵

¹⁸⁵³ Guanidine nitrate, aka. guanidinium nitrate ([C(NH₂)₃]NO₃ or CH₆N₄O₃, 0.122 kg/mole, 1436 kg/m³) has been used as a monopropellant in the Jetex engine (<https://en.wikipedia.org/wiki/Jetex>) for model airplanes because it has a high gas output and low flame temperature (https://en.wikipedia.org/wiki/Guanidine_nitrate), releasing a combustion energy of 8.75 x 10⁵ J/mole (http://www.chemicalbook.com/productmsdsdetailcb9150870_en.htm).

¹⁸⁵⁴ Hydrazine, aka. diazane or diamine (N₂H₄, 0.032 kg/mole, 3.14 x 10⁻⁵ m³/mole) decomposes into the elements in the presence of iridium metal or other catalysts, releasing its 9.54 x 10⁴ J/mole heat of formation (http://www.update.uu.se/~jolkkonen/pdf/CRC_TD.pdf) as a gaseous monopropellant (https://en.wikipedia.org/wiki/Hydrazine#Rocket_fuel).

¹⁸⁵⁵ Hydrogen peroxide (H₂O₂, 0.034 kg/mole, 2.34 x 10⁻⁵ m³/mole) decomposes exothermically into the elements in the presence of a platinum mesh or other transition metal catalyst, releasing its 1.06 x 10⁵ J/mole heat of formation (http://www.update.uu.se/~jolkkonen/pdf/CRC_TD.pdf) as a gaseous monopropellant. “Because of the large heat release, the catalytic action rapidly becomes secondary as thermal autodecomposition becomes dominant” (https://en.wikipedia.org/wiki/Nitrous_oxide).

¹⁸⁵⁶ Hydroxylammonium nitrate, aka. HAN (NH₃OH⁺NO₃⁻ or H₄N₂O₄, 0.096 kg/mole, density 1830 kg/m³, heat of formation -333.4 kJ/mole (Khare P, *et al.* Thermal and electrolytic decomposition and ignition of HAN-water solutions. Combust Sci Technol. 2015;187:1065-1078; [http://www.yang.gatech.edu/publications/Journal/CST%20\(2015,%20HAN,%20Khare\).pdf](http://www.yang.gatech.edu/publications/Journal/CST%20(2015,%20HAN,%20Khare).pdf)) is being used as a fuel/oxidizer blend (monopropellant) for NASA’s Green Propellant Infusion Mission (https://en.wikipedia.org/wiki/Green_Propellant_Infusion_Mission). A stoichiometric reaction of the decomposition of HAN: H₄N₂O₄ [0.096 kg, 5.25 x 10⁻⁵ m³] → N₂ + 2H₂O + 1.5O₂, taking standard heat of formation as -241.8 kJ/mole for H₂O (http://www.update.uu.se/~jolkkonen/pdf/CRC_TD.pdf), releases 1.50 x 10⁵ J/mole of HAN.

¹⁸⁵⁷ Nitromethane or CH₃NO₂ (0.061 kg/mole, 5.36 x 10⁻⁵ m³/mole) burns without added oxygen as a monopropellant according to CH₃NO₂ → CO + H₂O + 0.5H₂ + 0.5N₂ releasing 6.30 x 10⁵ J/mole or 10.3 MJ/kg, although a relatively high 0.56 MJ/kg must be expended to vaporize the liquid (<https://en.wikipedia.org/wiki/Nitromethane>).

¹⁸⁵⁸ Nitrous oxide (N₂O, 0.044 kg/mole, 3.58 x 10⁻⁵ m³/mole taking liquid density as 1230 kg/m³; <http://encyclopedia.airliquide.com/Encyclopedia.asp?GasID=55>) decomposes exothermically into the elements in the presence of a heated catalyst, releasing its 8.16 x 10⁴ J/mole heat of formation (http://www.update.uu.se/~jolkkonen/pdf/CRC_TD.pdf) as a gaseous monopropellant. “Because of the large heat release, the catalytic action rapidly becomes secondary as thermal autodecomposition becomes dominant” (https://en.wikipedia.org/wiki/Nitrous_oxide).

Ozone (O ₃) decomposition ¹⁸⁶⁰	1.43 x 10 ⁵	0.048	2.78 x 10 ⁻⁵
Propylene glycol dinitrate monopropellant ¹⁸⁶¹	7.60 x 10 ⁵	0.166	1.35 x 10 ⁻⁴
Sodium ozonide decomposition ¹⁸⁶²	4.49 x 10 ⁵	0.071	4.44 x 10 ⁻⁵
<u>Polynitrogen and Binary Nitrogen Explosives</u>			
N ₄ , tetraazatetrahedrane (theoretical) ¹⁸⁶³	9.66 x 10 ⁵	0.056	2.43 x 10 ⁻⁵

¹⁸⁵⁹ Octaoxygen (O₈, 0.128 kg/mole), aka. “red oxygen,” is a rhomboid cluster of oxygen atoms that is obtained by compressing oxygen through 10 GPa at room temperature, producing a deep red solid ε-phase (https://en.wikipedia.org/wiki/Solid_oxygen#Red_oxygen) that is stable over a wide range of pressure range,* though it is not known whether O₈ remains metastable at lower pressures after formation. Its enthalpy of formation has been estimated as 393 kJ/mole**; its density is reported as being higher than conventional α-phase solid oxygen (1524 kg/m³), and is probably higher than solid ozone (1728 kg/m³), so ~1800 kg/m³ is assumed here for O₈. Octaoxygen decomposing to molecular oxygen via O₈ → 4O₂ should release 3.93 x 10⁵ J. * Lundegaard LF, *et al.* Observation of an O₈ molecular lattice in the ε phase of solid oxygen. Nature 2006 Sep 14;443:201-204; <http://www.nature.com/nature/journal/v443/n7108/full/nature05174.html>. ** Hernandez-Lamoned R, *et al.* Systematic *ab initio* calculations on the energetics and stability of covalent O₄. J Chem Phys. 2004 Jun 1;120(21):10084-8; <http://www.ncbi.nlm.nih.gov/pubmed/15268030>.

¹⁸⁶⁰ Ozone (O₃, 0.048 kg/mole) decomposing to molecular oxygen via O₃ → 1.5O₂, with standard heat of formation of +142.7 kJ/mole for O₃ (http://www.update.uu.se/~jolkkonen/pdf/CRC_TD.pdf), releases 1.427 x 10⁵ J. Solid ozone is a violet-black solid below 80 K with a density of 1728 kg/m³ and 0.048 kg/mole (<http://pubs.acs.org/doi/abs/10.1021/ja01513a012>); concentrated gaseous and liquid ozone can detonate (<https://en.wikipedia.org/wiki/Ozone>), and solid ozone will “detonate at the slightest provocation...with a bright, white flash, shattering glassware containing it to a fine powder” (<http://pubs.acs.org/doi/abs/10.1021/ja01513a012>).

¹⁸⁶¹ Propylene glycol dinitrate, aka. PGDN, 1,2-propanediol dinitrate, or “Otto fuel II” (C₃H₆(ONO₂)₂ or C₃H₆N₂O₆, 0.166 kg/mole, 1.35 x 10⁻⁴ m³/mole) decomposes at 394 K and is shock-sensitive, burning as a monopropellant with a clean flame by: C₃H₆N₂O₆ → 3CO + 3H₂O + N₂ (https://en.wikipedia.org/wiki/Propylene_glycol_dinitrate) and releasing a decomposition energy of 7.60 x 10⁵ J/mole, taking the solid PGDN heat of formation as -296.9 kJ/mole (<http://webbook.nist.gov/cgi/cbook.cgi?ID=C6423434&Mask=2>).

¹⁸⁶² Sodium ozonide (NaO₃, 0.071 kg/mole, 1600 kg/m³) decomposing via NaO₃ → NaO₂ + 0.5O₂, with standard heat of formation of +188.3 kJ/mole for O₃,* releases 4.49 x 10⁵ J. *Volnov II. Peroxides, Superoxides, and Ozonides of Alkali and Alkaline Earth Metals, Springer, 2012, p. 129.

N ₄ , tetrazete (theoretical) ¹⁸⁶⁴	7.47 x 10 ⁵	0.056	2.03 x 10 ⁻⁵
N ₄ , tetranitrogen ¹⁸⁶⁵	1.12 x 10 ⁶	0.056	3.20 x 10 ⁻⁵
N ₅ , pentanitrogen ¹⁸⁶⁶	1.469 x 10 ⁶	0.070	3.78 x 10 ⁻⁵
N ₆ , hexaazaprismane (theoretical) ¹⁸⁶⁷	1.38 x 10 ⁶	0.084	4.20 x 10 ⁻⁵

¹⁸⁶³ Tetraazetatetrahedrane, aka. “tetrahedral nitrogen” (N₄, 0.056 kg/mole, 2.43 x 10⁻⁵ m³/mole at density 2300 kg/m³),* is a tetrahedron (triangular pyramid) of N atoms that has not been synthesized by 2016 but is predicted to explosively decompose into the elements (N₄ → 2N₂) releasing its 7.33 x 10⁵ J/mole enthalpy of formation (Glukhovtsev MN, Laiter S. Thermochemistry of Tetrazete and Tetraazetatetrahedrane: A High-Level Computational Study. J Phys Chem. 1996;100(5):1569-1577; <http://pubs.acs.org/doi/abs/10.1021/jp952026w>) plus its estimated strain energy of 233 kJ/mole (Glukhovtsev MN, *et al.* Besides N₂, what is the most stable molecule composed only of nitrogen atoms? Inorg Chem. 1996;35(24):7124-7133; <http://pubs.acs.org/doi/abs/10.1021/ic9606237>). Tetrahedral N₄ is predicted to be metastable; “tetrahedral N₄ is forbidden by symmetry from decaying to ground state N₂ molecules”; Lauderdale WJ *et al.*, Stability and energetics of metastable molecules: tetraazetatetrahedrane (N₄), hexazabenzene (N₆), and actaazacubane (N₈). J Phys Chem. 1992;96(3):1173-1178; <http://pubs.acs.org/doi/abs/10.1021/j100182a029>. *Wallin S, *et al.* High Energy Density Materials Efforts to synthesize the pentazolite anion: Part 1, Technical Report FOI-R-1602-SE, March 2005; http://foi.se/ReportFiles/foir_1602.pdf.

¹⁸⁶⁴ Tetrazete (N₄, 0.056 kg/mole, 2.03 x 10⁻⁵ m³/mole at density* 2757 kg/m³), is a square ring of four nitrogen atoms with two double bonds on opposite sides that had not been synthesized by 2016, but is predicted to explosively decompose into the elements (N₄ → 2N₂) releasing its 7.47 x 10⁵ J/mole enthalpy of formation (Glukhovtsev MN, Laiter S. Thermochemistry of Tetrazete and Tetraazetatetrahedrane: A High-Level Computational Study. J Phys Chem. 1996;100(5):1569-1577; <http://pubs.acs.org/doi/abs/10.1021/jp952026w>). * Committee on Advanced Energetic Materials and Manufacturing Technologies, Board on Manufacturing and Engineering Design, Division on Engineering and Physical Sciences, National Research Council. Advanced Energetic Materials, National Academies Press, 2004, p. 13.

¹⁸⁶⁵ Tetranitrogen (N₄, 0.056 kg/mole, est. density 1752 kg/m³) is a linear chain of nitrogen atoms with a heat of formation of +1124 kJ/mole,* which is released when the molecule decomposes via N₄ → 2N₂; the molecule has been synthesized and is a gas at room temperature where it has a lifetime of only ~10⁻⁶ sec (<http://science.sciencemag.org/content/295/5554/480.full>). *Nair UR, *et al.* Advances in high energy materials. Defence Sci J. 2010 Mar;60(2):137-151; <http://publications.drdo.gov.in/ojs/index.php/dsj/article/viewFile/327/193>.

¹⁸⁶⁶ Pentanitrogen, aka. pentazenium cation, pentanitrogen cation (N₅⁺, 0.070 kg/mole; <https://en.wikipedia.org/wiki/Pentazenium>) and its salts have been reported; gaseous N₅⁺ as a linear chain of nitrogen atoms would have a heat of formation of +1469 kJ/mole, which would be released when the molecule decomposes via N₅ → 2.5N₂ (Christe KO, *et al.* N₅⁺: A Novel Homoleptic Polynitrogen Ion as a High Energy Density Material. Angew Chem Int Ed. 1999;38(13/14):2004-2009; http://www.chimdocet-inorganica.it/SITO_ESERCIZI/Complementi/COMP2/N5.pdf). A claimed density of 1850 kg/m³ for N₅ is mentioned by Nair UR, *et al.* Advances in high energy materials. Defence Sci J. 2010 Mar;60(2):137-151; <http://publications.drdo.gov.in/ojs/index.php/dsj/article/viewFile/327/193>, but its provenance is unclear.

¹⁸⁶⁷ Hexaazaprismane (N₆, 0.084 kg/mole, assumed density ~2000 kg/m³), a triangular prism with nitrogen atoms at the six vertices that had not been synthesized by 2016, is predicted to explosively decompose into the elements (N₆ → 3N₂) releasing its 1.38 x 10⁶ J/mole enthalpy of formation (estimated as 331 kcal/mole using the highest-theory (MP2/6-31G*) calculations; Engelke R. Ab-Initio correlated calculations of six N₆ isomers. J Phys Chem. 1992;96:10789-10792; <http://pubs.acs.org/doi/abs/10.1021/j100205a037>).

N ₆ , hexaazabenzene (theoretical) ¹⁸⁶⁸	9.114 x 10 ⁵	0.084	6.72 x 10 ⁻⁵
N ₆ , diazide (theoretical) ¹⁸⁶⁹	7.732 x 10 ⁵	0.084	4.00 x 10 ⁻⁵
N ₈ , azidopentazole (theoretical) ¹⁸⁷⁰	8.23 x 10 ⁵	0.112	---
N ₈ , cubic gauche nitrogen (theoretical at STP) ¹⁸⁷¹	3.127 x 10 ⁶	0.112	3.06 x 10 ⁻⁵
N ₈ , octaazacubane (theoretical) ¹⁸⁷²	3.02 x 10 ⁶	0.112	4.17 x 10 ⁻⁵

¹⁸⁶⁸ Hexaazabenzene, aka. hexazine (N₆, 0.084 kg/mole, assumed density ~1250 kg/m³), a predicted ring-shaped molecule analogous to benzene that had not been synthesized by 2016 (<https://en.wikipedia.org/wiki/Hexazine>), is predicted to have a very low barrier to explosive decomposition into the elements (N₆ → 3N₂) releasing (up to) 9.114 x 10⁵ J/mole as estimated using the highest-theory (MP2-based) calculations (Fabian J, Lewars E. Azabenzenes. *Ca J Chem* 2004;82:50-69; <http://web.archive.org/web/20050329185413/http://pubs.nrc-cnrc.gc.ca/rp/rpdf/v03-178.pdf>).

¹⁸⁶⁹ The open-chain diazide (N₆, 0.084 kg/mole, density ~66 Å³/molecule or ~2100 kg/m³), not yet synthesized in 2016, is predicted by one study to be more stable than the ring-shaped benzene analog motif, to form a stable crystal structure at 300 K, and to decompose into the elements (N₆ → 3N₂) releasing 7.732 x 10⁵ J/mole (Greschner MJ, *et al.* A new allotrope of nitrogen as high-energy density material. *J Phys Chem* 2016; 120:2920-2925; <http://pubs.acs.org/doi/abs/10.1021/acs.jpca.6b01655>).

¹⁸⁷⁰ Azidopentazole (N₅-NNN or N₈, 0.112 kg/mole), a five-membered ring with an azide side chain, is currently believed to be the lowest energy isomer of N₈ (Nguyen MT, Ha TK. Azidopentazole is Probably the Lowest-Energy N₈ Species – A Theoretical Study. *Eur J Inorg Chem.* 1996 Oct;129(10):1157-1159; <http://onlinelibrary.wiley.com/doi/10.1002/cber.19961291003/full>), and lies +823 kJ/mole higher in energy than four N₂ molecules at the B3LYP/6-311+G** level of theory (Glukhovtsev MN, *et al.* Besides N₂, what is the most stable molecule composed only of nitrogen atoms? *Inorg Chem.* 1996;35(24):7124-7133; <http://pubs.acs.org/doi/abs/10.1021/ic9606237>).

¹⁸⁷¹ Above 110 GPa and ~2000 K, nitrogen forms a network solid, bound by single covalent bonds in a “cubic-gauche” structure, abbreviated as cg-N. This substance has been synthesized under high pressure and is very stiff with a bulk modulus around 298 GPa, similar to diamond. It is the highest-energy non-nuclear pure material currently known and is being investigated for use in explosives and rocket fuel (https://en.wikipedia.org/wiki/Solid_nitrogen#Cubic_gauche). Cubic gauche N is metastable when pressure is released at least down to 25 GPa but is predicted possibly to be metastable down to atmospheric pressures (Eremets MI, Gavriluk AG, Trojan IA, Dzivenko DA, Boehler R. Single-bonded cubic form of nitrogen. *Nat Mater.* 2004 Aug;3(8):558-63; https://www.researchgate.net/profile/A_Gavriluk/publication/8472556_Single-bonded_cubic_form_of_nitrogen/links/0fcfd50a001fe74989000000.pdf). Decomposition to N₂ would release the entire +6673 kcal/kg (+27.92 MJ/kg) heat of formation with detonation velocity up to 19,740 m/sec (“Polymeric Nitrogen Poster,” <https://www.google.com/url?sa=t&rct=j&q=&esrc=s&source=web&cd=4&ved=0ahUKEwIjjqIpZPPAhXCZiYKHVGeC-cQFggzMAM&url=http%3A%2F%2Fwww.sciencemadness.org%2Ftalk%2Ffiles.php%3Fpid%3D314105%26aid%3D28461&usg=AFQjCNGRQL-IYxBYz9gSI01riPBFgymSAA&bvm=bv.133053837,d.eWE&cad=rja>), according to the decomposition reaction: N₈ [aka. cg-N, 0.112 kg/mole, 3.61 x 10⁻⁵ m³, HOF = 3127 kJ/mole of cg-N] → 4N₂. Density is estimated as 6.348 Å³/atom or 3665 kg/m³ (<https://pdfs.semanticscholar.org/7b5e/67fd020b0c2f17575622843bcea828dbddfe.pdf>).

¹⁸⁷² Octaazacubane (N₈, 0.112 kg/mole, 4.17 x 10⁻⁵ m³/mole based on predicted density of 2690 kg/m³) is a hypothetical allotrope of nitrogen in a cubane-type cluster where all eight corners are nitrogen atoms bonded along the edges. “It is predicted to be a metastable molecule; despite the thermodynamic instability caused by bond strain and the high energy of the N–N single bonds, the molecule remains kinetically stable

N ₈ , octanitrogen (theoretical) ¹⁸⁷³	1.088 x 10 ⁶	0.112	4.29 x 10 ⁻⁵
N ₈ , pentaazapentalene (theoretical) ¹⁸⁷⁴	9.41 x 10 ⁵	0.112	4.67 x 10 ⁻⁵
N ₁₀ , dipentazole (theoretical) ¹⁸⁷⁵	1.088 x 10 ⁶	0.140	7.37 x 10 ⁻⁵

for reasons of orbital symmetry” (<https://en.wikipedia.org/wiki/Octaazacubane>). Decomposition according to N₈ → 4N₂ would release its 2.22 x 10⁶ J/mole enthalpy of formation (estimated as 530 kcal/mole by Engelke R, Stine JR. Is N₈ cubane stable? J Phys Chem. 1990;94(15):5689-5694; <http://pubs.acs.org/doi/abs/10.1021/j100378a018>) plus its estimated strain energy of 805.8 kJ/mole (Glukhovtsev MN, *et al.* Besides N₂, what is the most stable molecule composed only of nitrogen atoms? Inorg Chem. 1996;35(24):7124-7133; <http://pubs.acs.org/doi/abs/10.1021/ic9606237>). Calculations at the MP2/6-31G(d) level of theory predict that the barrier to decomposition for octaazacubane is +64.4 kJ/mole which, while still positive, is asserted to be inadequate for safe bulk handling of high energy density materials which typically rely on a unimolecular decomposition barrier of 125-145 kJ/mole (Schmidt M., *et al.* Cubic fuels? Intl J Quantum Chem 2000;76:434-446; http://lib.dr.iastate.edu/cgi/viewcontent.cgi?article=1370&context=chem_pubs). Another group running similar calculations at the CASSCF/CASPT2 level of theory found 42-84 kJ/mole barriers to decomposition (Gagliardi L. A theoretical study of the N₈ cubane to N₈ pentalene isomerization reaction. Theor Chem Acc 1997;97:136-142; <http://archive-ouverte.unige.ch/unige:2950/ATTACHMENT01>). As of 2016, this molecule had not yet been synthesized.

¹⁸⁷³ Octanitrogen (N₈, 0.112 kg/mole, est. density 1752 kg/m³) has not been synthesized but is predicted to be a metastable molecular crystal of linear chains of nitrogen atoms with a heat of formation of +1088 kJ/mole, which would be released when the molecule decomposes via N₈ → 4N₂, with a minimum barrier of +92 kJ/mole against decomposition. Density is estimated as 8.897 Å³/atom or 2612 kg/m³. The structure is claimed to be more stable than cg-N below 20 GPa, with 0.5274 eV/atom stabilization relative to cg-N, and a possible preparation strategy has been proposed (Hirshberg B, Gerber RB, Krylov AI. Calculations predict a stable molecular crystal of N₈. Nat. Chem. 2014;6:52-56; <https://pdfs.semanticscholar.org/7b5e/67fd020b0c2f17575622843bcea828dbddf.pdf>). This molecule appears to be the same as, or similar to, the predicted acyclic diazidyldiimide (N₃-N=N-N₃) molecule (Nguyen MT, Ha TK. Azidopentazole is Probably the Lowest-Energy N₈ Species – A Theoretical Study. Eur J Inorg Chem. 1996 Oct;129(10):1157-1159; <http://onlinelibrary.wiley.com/doi/10.1002/cber.19961291003/full>). In case this molecule is not sufficiently stable at normal temperature and pressure, calculations suggest that ~linear single-bonded N₈ molecules could be stored stably inside carbon nanotubes; Abou-Rachid H, *et al.* Nanoscale High Energetic Materials: A Polymeric Nitrogen Chain N₈ Confined inside a Carbon Nanotube. Phys Rev Lett. 2008 May 16;100:196401; <http://journals.aps.org/prl/abstract/10.1103/PhysRevLett.100.196401>.

¹⁸⁷⁴ Pentaazapentalene, aka. azapentalene, octaazapentalene (N₈, 0.112 kg/mole, assumed density ~2400 kg/m³), a planar molecule with two fused aromatic 5-member pentazole rings sharing one common edge, had not been synthesized by 2016 but may decompose into the elements (N₈ → 4N₂) releasing its 9.41 x 10⁵ J/mole enthalpy of formation (Leininger ML, *et al.* N₈: A structure analogous to pentalene, and other high-energy density materials. J Phys Chem 1995;99(8):2324-2328; <http://pubs.acs.org/doi/abs/10.1021/j100008a013>). Calculations at the CASSCF/CASPT2 level of theory predict that the barrier to decomposition for azapentalene is +79.5 kJ/mole, which, while still positive, leads the authors to conclude that azapentalene “is not stable enough to be considered as a candidate for a high-energy density material” (Gagliardi L, *et al.* Dissociation Reaction of N₈ Azapentalene to 4N₂: A Theoretical Study. Intl J Quantum Chem 2000;77:311-315; <http://archive-ouverte.unige.ch/unige:3736/ATTACHMENT01>).

N ₁₀ , azaadamantane (theoretical) ¹⁸⁷⁶	4.324 x 10 ⁶	0.140	2.44 x 10 ⁻³
N ₁₀ , triazidamine (theoretical) ¹⁸⁷⁷	1.264 x 10 ⁶	0.140	8.86 x 10 ⁻⁵
N ₁₂ , cage isomer 2060 (theoretical) ¹⁸⁷⁸	2.225 x 10 ⁶	0.168	---
N ₁₈ , cage isomer 2063A (theoretical) ¹⁸⁷⁹	3.449 x 10 ⁶	0.252	---
N ₂₀ , eicosaza[20]fullerene (theoretical) ¹⁸⁸⁰	5.41 x 10 ⁶	0.280	1.20 x 10 ⁻⁴

¹⁸⁷⁵ Dipentazole, aka. bis-pentazole (N₅⁺N₅⁻ or N₁₀, 0.140 kg/mole), two 5-member pentazole rings linked by a single N-N bond and offset 90° axially, had not been synthesized by 2016, though the precursor 5-member ring ions N₅⁺ (<http://www.dtic.mil/cgi-bin/GetTRDoc?AD=ADA409721>) and N₅⁻ ([http://onlinelibrary.wiley.com/doi/10.1002/1521-3757\(20020816\)114:16%3C3177::AID-ANGE3177%3E3.0.CO;2-I/full](http://onlinelibrary.wiley.com/doi/10.1002/1521-3757(20020816)114:16%3C3177::AID-ANGE3177%3E3.0.CO;2-I/full)) have been produced. Dipentazole may decompose to the elements (N₁₀ → 5N₂) and lies +1088 kJ/mole higher in energy than five N₂ molecules at the B3LYP/6-311+G** level of theory (Glukhovtsev MN, *et al.* Besides N₂, what is the most stable molecule composed only of nitrogen atoms? *Inorg Chem.* 1996;35(24):7124-7133; <http://pubs.acs.org/doi/abs/10.1021/ic9606237>). The estimated density of N₅⁺N₅⁻ is 1900 kg/m³ (Fau S, *et al.* On the stability of N₅⁺N₅⁻. *J Phys Chem A.* 2002;106(18):4639-4644; <http://pubs.acs.org/doi/abs/10.1021/jp015564j>).

¹⁸⁷⁶ Azaadamantane (N₁₀, 0.140 kg/mole, density ~4.05 Å³/molecule or ~5740 kg/m³) is an all-nitrogen adamantane-analog cage molecule predicted to be stable above 263 GPa, with an enthalpy at ~100 GPa that lies +0.43 eV/atom or +415 kJ/mole above the enthalpy of cg-N (N₈, see above) at the same pressure (Wang X, *et al.* Cagelike diamondoid nitrogen at high pressures. *Phys Rev Lett.* 2012 Oct 26;109(17):175502; <http://www.ncbi.nlm.nih.gov/pubmed/23215200>). The decomposition energy of cg-N to N₂, from ~100 GPa down to ambient pressure, is ~390.9 kJ/mole per atom of cg-N, or +3909 kJ/mole for N₁₀, giving a total decomposition energy release for N₁₀, from 263 atm down to ambient pressure, of 4.324 x 10⁶ J/mole or 30.9 MJ/kg.

¹⁸⁷⁷ Triazidamine, aka. TAA monopropellant (N(N₃)₃ or N₁₀, 0.140 kg/mole, 1580 kg/m³), a theoretical polynitrogen azidamine, upon decomposing to the elements will release its +1264 kJ/mole heat of formation (Michels HH, *et al.* Structure, thermochemistry and performance of advanced propellants, in Thompson TL, Rodgers SL, eds., *Proc. HEDM Contractors Conference*, 5-7 Jun 1994, pp.154-171; <http://www.dtic.mil/cgi-bin/GetTRDoc?AD=ADA292988>).

¹⁸⁷⁸ Cage isomer 2060 is the most stable isomer of N₁₂ (0.168 kg/mole) (Bruney LY, Bledson TM, Strout DL. What makes an N₁₂ cage stable? *Inorg Chem.* 2003;42(24):8117-8120; <http://europepmc.org/abstract/MED/14632534>), with decomposition reaction (N₁₂ → 6N₂) energy reported as 2.225 x 10⁶ J/mole (Strout DL. Stabilization of Cylindrical N₁₂ and N₁₈ by Phosphorus Substitution. *J Chem Theory Comput* 2005 Jul;1(4):561-565; <http://europepmc.org/articles/pmc4674835>).

¹⁸⁷⁹ Cage isomer 2063A is the most stable isomer of N₁₈ (0.252 kg/mole) (Sturdivant SE, Nelson FA, Strout DL. Trends in Stability for N18 Cages. *J Phys Chem A.* 2004;108:7087-7090; https://www.researchgate.net/publication/231639366_Trends_in_Stability_for_N18_Cages), with decomposition reaction (N₁₂ → 6N₂) energy reported as 3.449 x 10⁶ J/mole (Strout DL. Stabilization of Cylindrical N₁₂ and N₁₈ by Phosphorus Substitution. *J Chem Theory Comput* 2005 Jul;1(4):561-565; <http://europepmc.org/articles/pmc4674835>).

N ₆₀ , hexacontaazo[60]fullerene (theoretical) ¹⁸⁸¹	6.79 x 10 ⁶	0.840	3.15 x 10 ⁻⁴
NAg ₃ , silver nitride ¹⁸⁸²	3.15 x 10 ⁵	0.338	3.75 x 10 ⁻⁵
NCl ₃ , nitrogen trichloride ¹⁸⁸³	2.30 x 10 ⁵	0.1204	7.28 x 10 ⁻⁵
NH, imidogen ¹⁸⁸⁴	3.515 x 10 ⁵	0.015	---
NI ₃ , nitrogen triiodide ¹⁸⁸⁵	2.90 x 10 ⁵	0.395	1 x 10 ⁻⁴

¹⁸⁸⁰ Eicosaza[20]fullerene, aka. N₂₀ dodecahedron (N₂₀, 0.280 kg/mole, 1.20 x 10⁻⁴ m³/mole if N₂₀ density is assumed to be 2340 kg/m³, the same as for compressed Phase I C₂₀ fullerene*). This molecule had not been synthesized as of 2016, but it should be less strained and therefore more stable than the N₈ cubane analog. Theoretical results suggest that the “highly constrained dodecahedral structure of this N₂₀ isomer suggests that a substantial barrier to fragmentation may exist,” but an activation barrier, once surmounted (e.g., via heat, friction, pressure, etc.), could lead to explosive decomposition (N₂₀ → 10N₂) releasing the entire 4.18 x 10⁶ J/mole estimated heat of formation (Bliznyuk AA, Shen M, Schaefer III HF. The dodecahedral N₂₀ molecule. Some theoretical predictions. Chem Phys Lett 1992;198:249-252; <http://www.sciencedirect.com/science/article/pii/000926149285046D>) plus its estimated strain energy of 1233 kJ/mole (Glukhovtsev MN, *et al.* Besides N₂, what is the most stable molecule composed only of nitrogen atoms? Inorg Chem. 1996;35(24):7124-7133; <http://pubs.acs.org/doi/abs/10.1021/ic9606237>). . *Claus D. Sattler, Carbon Nanomaterials Sourcebook, CRC Press, 2016, Table 8.1, p. 188; <https://books.google.com/books?id=eAnYCwAAQBAJ&pg=PA188>.

¹⁸⁸¹ An N₆₀ cage molecule, aka. hexacontaazo[60]fullerene, is predicted to be stable but had not yet been synthesized as of 2016; it would have a MW of 0.840 kg/mole and is predicted to release 6.79 x 10⁶ J/mole upon decomposition via N₆₀ → 30N₂ (Wang LJ, Zgierski MZ. Super-high energy-rich nitrogen cluster N₆₀. Chem Phys Lett. 2003 Jul 31;376(5-6):698-703; <http://www.sciencedirect.com/science/article/pii/S0009261403010583>); estimated (but un sourced) density is 2670 kg/m³ as listed in Nair UR, *et al.* Advances in high energy materials. Defence Sci J. 2010 Mar;60(2):137-151; <http://publications.drdo.gov.in/ojs/index.php/dsj/article/viewFile/327/193>.

¹⁸⁸² Silver nitride (NAg₃, 0.338 kg/mole, 3.75 x 10⁻⁵ m³/mole) slowly decomposes in air at room temperature and explodes upon heating to 438 K, releasing its standard free energy of 315 kJ/mole (https://en.wikipedia.org/wiki/Silver_nitride).

¹⁸⁸³ Nitrogen trichloride, aka. trichloramine, trichloroazane, trichlorine nitride, agene (NCl₃, 0.1204 kg/mole, 1653 kg/m³; https://en.wikipedia.org/wiki/Nitrogen_trichloride) is a yellow, oily, pungent-smelling liquid that can explode to give molecular nitrogen and chlorine gas (NCl₃ → 0.5N₂ + 1.5Cl₂, taking the standard heat of formation as +230 kJ/mole for NCl₃ (http://www.update.uu.se/~jolkkonen/pdf/CRC_TD.pdf), releasing 2.30 x 10⁵ J/mole.

¹⁸⁸⁴ Imidogen, aka. triplet nitrene (<https://en.wikipedia.org/wiki/Nitrene>), aminylene, or hydridonitrogen (NH, 0.015 kg/mole), has a more stable triplet ground state and polymerizes to metastable triazidine in sufficiently high concentrations (<https://en.wikipedia.org/wiki/Imidogen>). Decomposition to the elements (NH → 0.5N₂ + 0.5H₂) releases its 3.515 x 10⁵ J/mole heat of formation (http://www.update.uu.se/~jolkkonen/pdf/CRC_TD.pdf). The gas decomposes in ~3 μsec at room temperature, thus can only be stored for any length of time at cryogenic temperatures (<40 K) in, for example, a solid argon matrix (Wiberg E, Wiberg N. Inorganic Chemistry, Academic Press, 2001, p. 628; <https://books.google.com/books?id=Mth5g59dEIC&pg=PA628>).

N_2B_2 , dinitrogen diboride (theoretical) ¹⁸⁸⁶	2.16×10^5	0.0496	---
N_2Be_3 , beryllium nitride ¹⁸⁸⁷	5.87×10^5	0.0551	2.03×10^{-5}
N_2C , penta-CN ₂ (theoretical) ¹⁸⁸⁸	1.76×10^5	0.040	---
N_2C_4 , dicyanoacetylene ¹⁸⁸⁹	5.004×10^5	0.0761	8.39×10^{-5}
N_2H , polymeric hydronitrogen (theoretical) ¹⁸⁹⁰	1.28×10^5	0.029	---
N_2H_2 , diimine ¹⁸⁹¹	9.84×10^4	0.030	4.4×10^{-5}

¹⁸⁸⁵ Nitrogen triiodide (NI_3 , $\sim 4000 \text{ kg/m}^3$, 0.395 kg/mole , $\sim 1 \times 10^{-4} \text{ m}^3/\text{mole}$) is an extremely sensitive contact explosive. Small quantities explode with a loud, sharp snap when touched even lightly, releasing a purple cloud of iodine vapor, according to: $NI_3 \rightarrow 0.5N_2 + 1.5I_2$ with the release of -290 kJ/mole . “The instability of NI_3 can be attributed to the large steric strain caused by the three large iodine atoms being held in close proximity to each other around the relatively tiny nitrogen atom. This results in a very low activation energy for its decomposition, a reaction made even more favorable due to the great stability of N_2 ” (https://en.wikipedia.org/wiki/Nitrogen_triiodide). NI_3 is the only known chemical explosive that detonates when exposed to alpha particles and nuclear fission products (Bowden FP. Initiation of Explosion by Neutrons, α -Particles, and Fission Products. Proc Royal Soc London A. 1958;246(1245):216–219; <http://rspa.royalsocietypublishing.org/content/246/1245/216>).

¹⁸⁸⁶ Asymmetric dinitrogen diboride (N_2B_2 , 0.0496 kg/mole) has been considered theoretically at the SCF/6-31G* level of theory and appears to be stable with a specific enthalpy of 4.35 MJ/kg (Brener NE, Kestner NR, Callaway J. Theoretical studies of highly energetic CBES materials. AL-TR-90-060, Dec 1990, Table 2, p. 8; <http://www.dtic.mil/dtic/tr/fulltext/u2/a231340.pdf>).

¹⁸⁸⁷ Beryllium nitride (Be_3N_2 , 0.0551 kg/mole , 2710 kg/m^3) decomposes in vacuum to Be and N_2 (https://en.wikipedia.org/wiki/Beryllium_nitride). A stoichiometric decomposition ($Be_3N_2 \rightarrow 3Be + N_2$) releases the -587 kJ/mole heat of formation of Be_3N_2 (Yates RE, Greenbaum MA, Farber M. The Thermodynamic and Physical Properties of Beryllium Compounds. VI. The Heat of Formation of Beryllium Nitride. J Phys Chem. 1964;68(9):2682-2686; <http://pubs.acs.org/doi/abs/10.1021/j100791a051>).

¹⁸⁸⁸ Penta-CN₂ (0.040 kg/mole) is a kinetically stable two-dimensional sheet composed entirely of pentagonal units, predicted to have a specific energy of 4.41 MJ/kg or 176 kJ/mole (Zhang S, *et al.* Beyond Graphitic Carbon Nitride: Nitrogen-Rich Penta-CN₂ Sheet. J Phys Chem C 2016;120:3993-3998; <http://www2.coe.pku.edu.cn/tpic/file/20160521/20160521184956945694.pdf>).

¹⁸⁸⁹ Dicyanoacetylene, aka. carbon subnitride, but-2-ynedinitrile ($N\equiv C-C\equiv C-C\equiv N$ or N_2C_4 , 0.0761 kg/mole , $8.39 \times 10^{-5} \text{ m}^3/\text{mole}$), a clear liquid at room temperature that can explode to carbon powder and nitrogen gas with the release of $5.004 \times 10^5 \text{ J/mole}$, its enthalpy of formation ([https://en.wikipedia.org/wiki/Lead\(II\)_azide](https://en.wikipedia.org/wiki/Lead(II)_azide)).

¹⁸⁹⁰ According to a first-principles theoretical structure search, “this polymeric hydronitrogen [N_2H , 0.029 kg/mole] consists of quasi-one-dimensional infinite armchair-like polymeric N chains, where H atoms bond with two adjacent N located at one side of the armchair edge. It is energetically stable against decomposition above $\sim 33 \text{ GPa}$, and shows novel metallic feature as the result of pressure-enhanced charge transfer and delocalization of π electrons within the infinite nitrogen chains.” N-N and N=N bonds alternate in the chain. A high energy density is predicted, $\sim 4.40 \text{ MJ/kg}$ or $1.28 \times 10^5 \text{ J/mole}$. Yin K, *et al.* N_2H : a novel polymeric hydronitrogen as a high energy density material. J Mater Chem A. 2015;3:4188-4194; <https://arxiv.org/ftp/arxiv/papers/1503/1503.03988.pdf>.

N ₂ O ₂ , dinitrogen dioxide ¹⁸⁹²	5.00 x 10 ⁵	0.060	---
N ₂ O ₃ , dinitrogen trioxide (theoretical) ¹⁸⁹³	8.15 x 10 ⁵	0.076	---
N ₃ Ag, silver azide ¹⁸⁹⁴	6.21 x 10 ⁵	0.150	3.39 x 10 ⁻⁵
N ₃ Cl, chlorine azide ¹⁸⁹⁵	3.90 x 10 ⁵	0.0775	5.17 x 10 ⁻⁵
N ₃ B, boron azide (theoretical) ¹⁸⁹⁶	2.82 x 10 ⁵	0.0528	---
N ₃ F, fluorine azide ¹⁸⁹⁷	5.65 x 10 ⁵	0.061	4.69 x 10 ⁻⁵

¹⁸⁹¹ Diimine, aka. diimide or diazene (N₂H₂, 0.030 kg/mole, <https://en.wikipedia.org/wiki/Diazene>; assumed maximum density ~ 682 kg/m³ same as liquid ammonia), is a yellow gas. During thermolysis above 120 °C, N₂H₂ under goes both disproportionation (N₂H₂ → 0.5N₂ + 0.5N₂H₄, releasing 86 kJ/mole, ~77% of the time at 180 °C) and decomposition (N₂H₂ → N₂ + H₂, releasing 140 kJ/mole, ~23% of the time at 180 °C), for a net energy release of 98.4 kJ/mole at 180 °C, with higher temperatures producing more of the second reaction (Wiberg E, Wiberg N. Inorganic Chemistry, Academic Press, 2001, p. 631; <https://books.google.com/books?id=Mth5g59dEIC&pg=PA631>). “Gaseous diimine can be kept for long periods at pressures below 0.13 Pa, even at room temperature.”

¹⁸⁹² Asymmetric dinitrogen dioxide (a-N₂O₂, 0.060 kg/mole) has been studied theoretically and a stable near-linear non-ring isomer structure is predicted to exist, with a heat of formation of +500 kJ/mole and an activation barrier to the decomposition reaction [a-N₂O₂ → N₂ + O₂(singlet)] of 65 kJ/mole (Michels HH, Montgomery JA Jr. The electronic structure and stability of asymmetric dinitrogen dioxide. J Chem Phys 1988;88:7248; <http://scitation.aip.org/content/aip/journal/jcp/88/11/10.1063/1.454330>). At least one N₂O₂ isomer has been observed experimentally (Arnold DW, Neumark DM. Study of N₂O₂ by photoelectron spectroscopy of N₂O₂⁻. J Chem Phys 1995;102:7035; <http://scitation.aip.org/content/aip/journal/jcp/102/18/10.1063/1.469097>).

¹⁸⁹³ Dinitrogen trioxide (N₂O₃, 0.076 kg/mole) has been considered theoretically at the SCF/6-31G* level of theory and appears to be stable with a specific enthalpy of 10.72 MJ/kg (Brener NE, Kestner NR, Callaway J. Theoretical studies of highly energetic CBES materials. AL-TR-90-060, Dec 1990, Table 2, p. 8; <http://www.dtic.mil/dtic/tr/fulltext/u2/a231340.pdf>).

¹⁸⁹⁴ Silver azide (N₃Ag, 0.150 kg/mole, 3.39 x 10⁻⁵ m³/mole) decomposes explosively to the elements upon impact, exposure to UV light, or heating to 613 K (https://en.wikipedia.org/wiki/Silver_azide), releasing its heat of formation of 621 kJ/mole (Matayas R, Pachman J. Primary Explosives, Springer, 2013, p. 91).

¹⁸⁹⁵ Chlorine azide (ClN₃, 0.0775 kg/mole, with estimated density ~1500 kg/m³ assumed midway between liquid Cl₂ at 1468 kg/m³ and liquid NCl₃ at 1653 kg/m³) is a yellow-orange liquid or gas that is extremely shock- and friction-sensitive. Chlorine azide may be one of the most stable halogen azides (<https://books.google.com/books?id=xVTkMJDOulsC&pg=PA270>), but concentrated ClN₃ is “notoriously unstable and may spontaneously detonate at any temperature” (https://en.wikipedia.org/wiki/Chlorine_azide). Decomposition to molecular nitrogen and chlorine gas (ClN₃ → 1.5N₂ + 0.5Cl₂, would release 3.90 x 10⁵ J/mole, taking the standard heat of formation as 4.04 eV or 389.8 kJ/mole for ClN₃ (Hansen N, Wodtke AM. Velocity Map Ion Imaging of Chlorine Azide Photolysis: Evidence for Photolytic Production of Cyclic-N₃. J Phys Chem A 2003 Sep 30;107(49):10608-10614; <http://web.chem.ucsb.edu/~wodtke/groupwebpage/jpc%20cln3.pdf>).

¹⁸⁹⁶ Boron azide (N₃B, 0.0528 kg/mole) has been considered theoretically at the SCF/6-31G* level of theory and appears to be stable with a specific enthalpy of 5.35 MJ/kg (Brener NE, Kestner NR, Callaway J. Theoretical studies of highly energetic CBES materials. AL-TR-90-060, Dec 1990, Table 2, p. 8; <http://www.dtic.mil/dtic/tr/fulltext/u2/a231340.pdf>).

N ₃ H, hydrogen azide ¹⁸⁹⁸	2.64 x 10 ⁵	0.043	3.95 x 10 ⁻⁵
N ₃ H ₃ , triazene ¹⁸⁹⁹	1.92 x 10 ⁵	0.045	---
N ₃ H ₃ , triaziridine ¹⁹⁰⁰	3.65 x 10 ⁵	0.045	---
N ₃ Na, sodium azide ¹⁹⁰¹	2.17 x 10 ⁴	0.065	3.52 x 10 ⁻⁵
N ₄ H ₄ (theoretical) ¹⁹⁰²	5.03 x 10 ⁵	0.060	---
N ₄ O, nitrosyl azide (theoretical) ¹⁹⁰³	4.39 x 10 ⁵	0.072	4.68 x 10 ⁻⁵
N ₄ O ₂ , nitryl azide (theoretical) ¹⁹⁰⁴	3.77 x 10 ⁵	0.088	5.00 x 10 ⁻⁵

¹⁸⁹⁷ Fluorine azide (N₃F, 0.061 kg/mole, estimated solid density 1300 kg/m³; <http://www.dtic.mil/dtic/tr/fulltext/u2/a231340.pdf>) is a highly explosive and unstable yellow-green gas that liquefies at 191 K and solidifies at 121 K, but “solid or liquid FN₃ explodes... because the explosion hazard is great only very small quantities of this substance should be handled at a time” (https://en.wikipedia.org/wiki/Fluorine_azide). Decomposition to the elements releases the 5.65 x 10⁵ J/mole heat of formation energy (Patel D, *et al.* Photolysis of FN₃ at 193 nm. J Phys Chem 1986;90:1931-1934; <http://pubs.acs.org/doi/abs/10.1021/j100400a038>); “several spontaneous detonations occurred during our early attempts to produce a useable flow of the material...we carried out the FN₃ generation process inside a 1/4-in. lexan blast shield.”

¹⁸⁹⁸ Hydrogen azide, aka. hydrazoic acid or azoimide (N₃H, 0.043 kg/mole, 3.95 x 10⁻⁵ m³/mole at 1090 kg/m³) is a colorless, volatile, and explosive liquid at room temperature, with decomposition to the elements triggered by shock, friction, or spark with release of the 2.64 x 10⁵ J/mole heat of formation energy (https://en.wikipedia.org/wiki/Hydrazoic_acid).

¹⁸⁹⁹ Triazene, aka. triazanylene (linear H₂N-NH-N or N₃H₃, 0.045 kg/mole) is a gas at room temperature and is colored with a strong and unpleasant smell (<https://en.wikipedia.org/wiki/Triazene>). Decomposition to the elements according to N₃H₃ → 1.5N₂ + 1.5H₂ would release the 192 kJ/mole heat of formation for triazene (Haubold R, *et al.* N Nitrogen, Springer, 2013, p.159; <https://books.google.com/books?id=JWnwCAAQBAJ&pg=PA159>).

¹⁹⁰⁰ Triaziridine (cyclical (NH)₃ or N₃H₃, 0.045 kg/mole) upon decomposition to the elements according to N₃H₃ → 1.5N₂ + 1.5H₂ would release the 365 kJ/mole heat of formation for triaziridine (Haubold R, *et al.* N Nitrogen, Springer, 2013, p.159; <https://books.google.com/books?id=JWnwCAAQBAJ&pg=PA159>).

¹⁹⁰¹ Sodium azide (N₃Na → Na + 1.5N₂, 0.065 kg/mole, 3.52 x 10⁻⁵ m³/mole at 1846 kg/m³; https://en.wikipedia.org/wiki/Sodium_azide) is a weak explosive used in automobile airbags that can be triggered electrically or by heating to ~573 K, whereupon it releases its 2.17 x 10⁴ J/mole heat of formation (http://www.update.uu.se/~jolkkonen/pdf/CRC_TD.pdf).

¹⁹⁰² N₄H₄ (0.060 kg/mole) has been considered theoretically at the SCF/6-31G* level of theory and appears to be stable with a specific enthalpy of 8.39 MJ/kg (Brener NE, Kestner NR, Callaway J. Theoretical studies of highly energetic CBES materials. AL-TR-90-060, Dec 1990, Table 2, p. 8; <http://www.dtic.mil/dtic/tr/fulltext/u2/a231340.pdf>).

¹⁹⁰³ Nitrosyl azide (NON₃ or N₄O, 0.072 kg/mole, 1540 kg/m³), a theoretical polynitrogen azidamine, upon decomposing to the elements will release its +439 kJ/mole heat of formation (Michels HH, *et al.* Structure, thermochemistry and performance of advanced propellants, in Thompson TL, Rodgers SL, eds., Proc. HEDM Contractors Conference, 5-7 Jun 1994, pp.154-171; <http://www.dtic.mil/cgi-bin/GetTRDoc?AD=ADA292988>).

¹⁹⁰⁴ Nitryl azide (NO₂N₃ or N₄O₂, 0.088 kg/mole, 1760 kg/m³), a theoretical polynitrogen azidamine, upon decomposing to the elements will release its +377 kJ/mole heat of formation (Michels HH, *et al.* Structure, thermochemistry and performance of advanced propellants, in Thompson TL, Rodgers SL, eds., Proc.

N ₄ O ₆ , trinitramine (theoretical) ¹⁹⁰⁵	3.77 x 10 ⁵	0.152	7.07 x 10 ⁻⁵
N ₄ S ₄ , tetrasulfur tetranitride ¹⁹⁰⁶	4.80 x 10 ⁵	0.184	8.21 x 10 ⁻⁵
N ₅ B ₃ , triboron pentanitride (theoretical) ¹⁹⁰⁷	3.52 x 10 ⁵	0.1024	2.97 x 10 ⁻⁵
N ₅ H, hydrogen pentazole ¹⁹⁰⁸	4.09 x 10 ⁵	0.071	6.51 x 10 ⁻⁵
N ₅ H ₅ , hydrazinium azide ¹⁹⁰⁹	2.85 x 10 ⁵	0.075	1.10 x 10 ⁻⁴
N ₅ Li, lithium pentanitride (theoretical) ¹⁹¹⁰	2.09 x 10 ⁵	0.077	4.2 x 10 ⁻⁵

HEDM Contractors Conference, 5-7 Jun 1994, pp.154-171; <http://www.dtic.mil/cgi-bin/GetTRDoc?AD=ADA292988>).

¹⁹⁰⁵ Trinitramine (N(NO₂)₃ or N₄O₆, 0.152 kg/mole, 2150 kg/m³), upon decomposing to the elements, will release its +377 kJ/mole heat of formation (Michels HH, *et al.* Structure, thermochemistry and performance of advanced propellants, in Thompson TL, Rodgers SL, eds., Proc. HEDM Contractors Conference, 5-7 Jun 1994, pp.154-171; <http://www.dtic.mil/cgi-bin/GetTRDoc?AD=ADA292988>).

¹⁹⁰⁶ Tetrasulfur tetranitride, aka. tetranitrogen tetrasulfide (N₄S₄, 0.184 kg/mole, density 2240 kg/m³; https://www.webelements.com/compounds/sulfur/tetrasulphur_tetranitride.html) forms vivid orange opaque crystals that is stable to air but has a +480 kJ/mole heat of formation and is an explosive because one of its decomposition products (N₄S₄ → 2N₂ + 0.5S₈) is a gas (https://en.wikipedia.org/wiki/Tetrasulfur_tetranitride). Purer samples tend to be more explosive and shock-sensitive; “small samples can be detonated by striking with a hammer.” N₄S₄ can decompose to 2N₂S₂ (disulfur dinitride) as an intermediate reaction product, but S₂N₂, an unstable cyclic square planar molecule that explodes above 30 °C and is shock sensitive, can also decompose to the elements (https://en.wikipedia.org/wiki/Disulfur_dinitride).

¹⁹⁰⁷ N₅B₃, aka. triboron pentanitride or C222₁-B₃N₅ (0.1024 kg/mole, assumed density ~3450 kg/m³, the same as cubic boron nitride) is predicted to be formed at 15 GPa and to be metastable, able to be recovered under ambient conditions, with a specific energy of 3.44 MJ/kg or 3.52 x 10⁵ J/mole (Li Y, *et al.* High-energy density and superhard nitrogen-rich B-N compounds. Phys Rev Lett 2015 Sep 3;115:105502; <http://journals.aps.org/prl/abstract/10.1103/PhysRevLett.115.105502>).

¹⁹⁰⁸ Hydrogen pentazole, aka. pentazole (HN₅, 0.071 kg/mole; <https://en.wikipedia.org/wiki/Pentazole>; assumed density ~1090 kg/m³ same as N₃H, see above) has never been directly observed experimentally in isolation but “is likely to be metastable,” and phenyl derivatives have been synthesized; an *ab initio* quantum chemistry theoretical study found a decomposition energy of 409 kJ/mole (derived from 0.071 kg/mole and the computed I_{sp} of 346 sec) with an activation barrier of 83 kJ/mole (Bartlett RJ. Final Report: Air Force High Energy Density Materials (HEDM) Project. Air Force Office of Scientific Research, AFOSR-TR-96-0140, 31 Mar 1996, p. 4; <http://www.dtic.mil/cgi-bin/GetTRDoc?Location=U2&doc=GetTRDoc.pdf&AD=ADA306340>).

¹⁹⁰⁹ Hydrazinium azide (H₂NNH₃)⁺[N₃]⁻ or N₅H₅, 0.075 kg/mole, 680 kg/m³; <http://www.wydawnictwa.ipo.waw.pl/cejem/Vol-12-Number-4-2015/Kozyrev.pdf>) forms white crystals that explosively decompose with a measured 2.85 x 10⁵ J/mole heat of reaction (Haubold R, *et al.* N Nitrogen, Springer, 2013, p. 181; <https://books.google.com/books?id=JWnwCAAQBAJ&pg=PA181>).

¹⁹¹⁰ The lithium pentanitride crystal (LiN₅, 0.0770 kg/mole, density ~1830 kg/m³ assumed same as lithium azide LiN₃) is predicted to become energetically stable above 9.9 GPa of pressure, but is also predicted to exhibit mechanical stability at ambient pressure. The decomposition of LiN₅ is predicted to be highly exothermic, releasing an energy of approximately 2.72 MJ/kg or 2.09 x 10⁵ J/mole; Peng F, Yao Y, Liu H, Ma Y. Crystalline LiN₅ Predicted from First-Principles as a Possible High-Energy Material. J Phys Chem Lett. 2015 Jun 18;6(12):2363-6; <http://www.ncbi.nlm.nih.gov/pubmed/26266618>.

N ₅ Na, sodium pentazolate (theoretical) ¹⁹¹¹	8.44 x 10 ⁴	0.093	5.04 x 10 ⁻⁵
N ₆ Be, beryllium azide ¹⁹¹²	n/a	0.0931	n/a
N ₆ Cs, cesium pentanitride (theoretical) ¹⁹¹³	1.62 x 10 ⁵	0.217	6.2 x 10 ⁻⁵
N ₆ Cu, copper(II) azide ¹⁹¹⁴	~4.44 x 10 ⁵	0.148	5.69 x 10 ⁻⁵
N ₆ Cu ₂ , copper(I) azide ¹⁹¹⁵	2.531 x 10 ⁵	0.211	8.12 x 10 ⁻⁵
N ₆ O ₈ , tetranitrohydrazine (theoretical) ¹⁹¹⁶	5.86 x 10 ⁵	0.212	9.77 x 10 ⁻⁵

¹⁹¹¹ Solid sodium pentazolate (NaN₅, 0.0770 kg/mole, density ~1846 kg/m³ assumed same as sodium azide NaN₃) is composed of a 5-member ring pentazole anion (N₅⁻) predicted to be stabilized by a sodium Na⁺ cation above 20 GPa pressure, becoming metastable upon release of pressure, and upon decomposition releasing the +84.4 kJ/mole formation enthalpy at ambient pressure; Steele BA, Oleynik II. Sodium pentazolate: a nitrogen rich high energy density material. Chem Phys Lett. 2016;643:21-26; https://www.researchgate.net/publication/283532391_Sodium_Pentazolate_a_Nitrogen_Rich_High_Energy_Density_Material.

¹⁹¹² Solid beryllium azide (Be(N₃)₂ or BeN₆, 0.0931 kg/mole; https://en.wikipedia.org/wiki/Beryllium_azide) is a white solid that can be warmed to room temperature without decomposition, first prepared in 1954,* that is predicted** to consist of infinite chains with tetrahedrally coordinated Be²⁺ ions linked by end-on bridging N₃⁻ ions. The azide decomposes to the elements according to: BeN₆ [0.0931 kg] → Be + 3N₂, releasing its enthalpy of formation energy which apparently has not yet been reported in the literature. *Wiberg E, Horst M. Beryllium azide, Be(N₃)₂. Zeitschrift für Naturforschung B. 1954;9:502; <http://link.springer.com/article/10.1007%2FBF02873199>. **Klapötke TM, Schutt T. (1999). "Synthesis and spectroscopic characterization of beryllium azide and two derivatives". Main Group Metal Chemistry. 1999;22(6):357-360; <https://www.degruyter.com/view/j/mgmc.1999.22.6/mgmc.1999.22.6.357/mgmc.1999.22.6.357.xml>.

¹⁹¹³ Although cesium pentanitride (CsN₆, 0.217 kg/mole, density ~3500 kg/m³ assumed same as cesium azide CsN₃) is believed to be unstable, cesium azide (CsN₃) has been synthesized and is stable in ordinary conditions, and theoretical analysis suggests the decomposition reaction CsN₆ → 3N₂ + Cs would release ~0.24 eV/atom or 1.62 x 10⁵ J/mole; Peng F, Han Y, Liu H, Yao Y. Exotic stable cesium polynitrides at high pressure. Sci Rep. 2015 Nov 19;5:16902; <http://www.ncbi.nlm.nih.gov/pmc/articles/PMC4652274/>.

¹⁹¹⁴ Copper (II) azide, aka. cupric azide (Cu(N₃)₂ or CuN₆, 0.148 kg/mole, 2600 kg/m³; [https://en.wikipedia.org/wiki/Copper\(II\)_azide](https://en.wikipedia.org/wiki/Copper(II)_azide)) forms brownish red crystals. "Violent explosion can occur when this substance is subjected to shock or friction. Scratching the crystals out from the container may result in explosion. It can detonate when dry. It may even explode when moist." (Patnaik P. A Comprehensive Guide to the Hazardous Properties of Chemical Substances. John Wiley & Sons, 2007, p. 620; <https://books.google.com/books?id=-CRRJBVv5d0C&pg=PA620>). The enthalpy of formation of cupric azide in a metal-organic framework was ~3 MJ/kg (https://www.researchgate.net/publication/302591998_Metal-Organic_Framework_Templated_Synthesis_of_Copper_Azide_as_the_Primary_Explosive_with_Low_Electrostatic_Sensitivity_and_Excellent_Initiation_Ability).

¹⁹¹⁵ Copper (I) azide, aka. cuprous azide (Cu₂(N₃)₂ or Cu₂N₆, 0.211 kg/mole, heat of formation +253.1 kJ/mole) is a colorless crystalline solid, highly sensitive to impact, that explodes upon heating and decomposes at 205 °C to the elements (Patnaik P. A Comprehensive Guide to the Hazardous Properties of Chemical Substances. John Wiley & Sons, 2007, p. 620; <https://books.google.com/books?id=-CRRJBVv5d0C&pg=PA620>). Density assumed to be same as for copper (II) azide, 2600 kg/m³.

¹⁹¹⁶ Tetranitrohydrazine (N₂(NO₂)₄ or N₆O₈, 0.212 kg/mole, 2170 kg/m³), upon decomposing to the elements, will release its +586 kJ/mole heat of formation (Michels HH, *et al.* Structure, thermochemistry

N ₆ Pb, lead azide ¹⁹¹⁷	4.623 x 10 ⁵	0.291	6.18 x 10 ⁻⁵
N ₇ H, diazidamine (theoretical) ¹⁹¹⁸	8.33 x 10 ⁵	0.0991	6.35 x 10 ⁻⁵
N ₁₀ C ₂ , planar DAT ¹⁹¹⁹	1.088 x 10 ⁶	0.164	9.52 x 10 ⁻⁵
N ₁₀ C ₂ cage "Isomer B" (theoretical) ¹⁹²⁰	2.21 x 10 ⁶	0.164	9.52 x 10 ⁻⁵
N ₁₀ C ₃ , planar NAA (theoretical) ¹⁹²¹	1.21 x 10 ⁶	0.176	9.89 x 10 ⁻⁵
N ₁₂ C, tetraazidomethane ¹⁹²²	1.5 x 10 ⁶	0.180	1.1 x 10 ⁻⁴
N ₁₂ C ₃ , cyanuric triazide ¹⁹²³	7.40 x 10 ⁵	0.214	1.18 x 10 ⁻⁴

and performance of advanced propellants, in Thompson TL, Rodgers SL, eds., Proc. HEDM Contractors Conference, 5-7 Jun 1994, pp.154-171; <http://www.dtic.mil/cgi-bin/GetTRDoc?AD=ADA292988>).

¹⁹¹⁷ Lead azide (Pb(N₃)₂ or PbN₆, 0.291 kg/mole, 6.18 x 10⁻⁵ m³/mole at 4710 kg/m³), an explosive used in detonators, will explode after a fall of around 150 mm or in the presence of a static discharge of 7 millijoules, decomposing to the elements with the release of 4.623 x 10⁵ J/mole, its enthalpy of formation ([https://en.wikipedia.org/wiki/Lead\(II\)_azide](https://en.wikipedia.org/wiki/Lead(II)_azide)).

¹⁹¹⁸ Diazidamine (HN(N₃)₂ or N₇H, 0.0991 kg/mole, 1560 kg/m³), a theoretical polynitrogen azidamine, upon decomposing to the elements will release its +833 kJ/mole heat of formation (Michels HH, *et al.* Structure, thermochemistry and performance of advanced propellants, in Thompson TL, Rodgers SL, eds., Proc. HEDM Contractors Conference, 5-7 Jun 1994, pp.154-171; <http://www.dtic.mil/cgi-bin/GetTRDoc?AD=ADA292988>).

¹⁹¹⁹ N₁₀C₂, planar 3,6-diaza-1,2,4,5-tetrazine or DAT (N₃-CN₄C-N₃ or C₂N₁₀, 0.164 kg/mole, +1088 kJ/mole heat of formation, assume same density as N₁₄C₂ ~ 1723 kg/m³), a C₂N₄ ring with *para* carbons and with one N₃ chain on each carbon, was first synthesized in 2007, and its decomposition to the elements would release 1.088 x 10⁶ J/mole; Li XT, *et al.* Synthesis and theoretical studies of 3,6-diaza-1,2,4,5-tetrazine. Acta Chim Sinica 2007 May;65(10):971-976; http://sioc-journal.cn/Jwk_hxxb/EN/abstract/abstract328357.shtml.

¹⁹²⁰ N₁₀C₂ cage "Isomer B" (0.164 kg/mole, +2210 kJ/mole heat of formation, assume same density as N₁₄C₂ ~ 1723 kg/m³) had not been synthesized by 2014, but its decomposition to the elements would release 2.21 x 10⁶ J/mole; Strout DL. Effect of C-O Bonding on the Stability and Energetics of High-Energy Nitrogen-Carbon Molecules N₁₀C₂ and N₁₆C₂. Advances Chem. 2014;2014:175384; <https://www.hindawi.com/journals/ac/2014/175384/>.

¹⁹²¹ N₁₀C₃, planar 1,2,3,4,5,6,7,8,9-nonaazacycl[3.3.3]azine, or NAA (C₃N₁₀, 0.176 kg/mole, 1723 kg/m³) upon detonation is predicted to release a total explosive energy of 1.21 x 10⁶ J/mole (Wu Q, *et al.* Improving an insensitive low-energy compound, 1,3,4,6,7,9-hexaazacycl[3.3.3]azine, to be an insensitive high explosive by way of two-step structural modifications. Can J Chem 2014;92:1157-1161; http://www.nrcresearchpress.com/doi/abs/10.1139/cjc-2014-0396#.V_hT08mZPuN).

¹⁹²² Tetraazidomethane, aka. TAM, perazidomethane (C(N₃)₄ or N₁₂C, 0.180 kg/mole, ~1.1 x 10⁻⁴ m³/mole assuming ~1700 kg/m³ like CN₁₄) has been synthesized as a colorless highly explosive liquid at ambient temperature (<https://en.wikipedia.org/wiki/Tetraazidomethane>). It has the highest nitrogen content (93.33%) of any organic compound. Assuming about the same heat of formation as for C₂N₁₄ (see above), explosive decomposition to the elements would release ~1.50 MJ/mole. An explosion that caused serious laboratory damage has been attributed to diazidomethane, TAM's less-energetic cousin (<http://pubs.acs.org/doi/abs/10.1021/op8000977>).

$N_{12}P_6$ (N_{18} isomer 2063A analog) (theoretical) ¹⁹²⁴	2.069×10^6	0.354	---
$N_{14}C_2$, azidotetrazole ¹⁹²⁵	1.495×10^6	0.220	1.28×10^{-4}
$N_{16}C_2$ cage “Isomer B” (theoretical) ¹⁹²⁶	3.348×10^6	0.248	1.44×10^{-4}
$N_{17}B$ ¹⁹²⁷	2.08×10^6	0.249	7.22×10^{-5}
$N_{18}H_6$ (theoretical) ¹⁹²⁸	2.80×10^6	0.248	1.18×10^{-4}
$N_{20}C_6$ ¹⁹²⁹	2.171×10^6	0.352	2.05×10^{-4}

¹⁹²³ Cyanuric triazide, aka. 2,4,6-triazido-1,3,5-triazine ($(NCN_3)_3$ or $N_{12}C_3$, 0.214 kg/mole, 1.18×10^{-4} m³/mole at 1730 kg/m³) is an organic primary explosive with a detonation velocity of about 7,300 m/sec and an ignition temperature at 478 K, that is stable under standard conditions but extremely shock sensitive, e.g., violently decomposing when ground with a mortar, liberating 7.40×10^5 J/mole (https://en.wikipedia.org/wiki/Cyanuric_triazide).

¹⁹²⁴ $N_{12}P_6$ (0.354 kg/mole) is a cylindrical cage analog to N_{18} cage isomer 2063A, with phosphorus atoms substituted for N atoms in bonding positions that would be more prone to instability. The decomposition reaction ($N_{12}P_6 \rightarrow 6N_2 + 1.5P_4$) energy is 2.069×10^6 J/mole, calculated at the MP4(SDQ)/CCSD(T) level of theory (Strout DL. Stabilization of Cylindrical N_{12} and N_{18} by Phosphorus Substitution. J Chem Theory Comput 2005 Jul;1(4):561-565; <http://europepmc.org/articles/pmc4674835>). However, the weakest bond in the molecule dissociates at a relatively modest 105 kJ/mole, leading the authors to conclude: “The $N_{12}P_6$ may be more stable than its N_{18} analogue, but the viability of $N_{12}P_6$ as a stable HEDM is questionable.”

¹⁹²⁵ 1-diazidocarbamoyl-5-azidotetrazole (closed form), aka. “azidoazide azide” ($N_{14}C_2$, 0.220 kg/mole, 1.28×10^{-4} m³/mole at 1723 kg/m³) has the second-highest nitrogen content (89.08%) of any organic compound synthesized through 2016. The smallest possible loadings in shock and friction tests led to explosive decomposition to the elements, releasing the 1.495 MJ/mole heat of formation. (Klapotke TM *et al.* C_2N_{14} : An Energetic and Highly Sensitive Binary Azidotetrazole. Angew Chem Int Ed. 2011;50:4227-9; <http://onlinelibrary.wiley.com/doi/10.1002/anie.201100300/abstract>, <http://www.chtf.stuba.sk/~szolcsanyi/education/files/Chemia%20heterocyklickych%20zlucenin/Prednaska%203/Doplukove%20studijne%20materialy/Tetra-%20and%20Pentazoles/C2N14%20-%20An%20Energetic%20and%20Highly%20Sensitive%20Binary%20Azidotetrazole.pdf>) “The sensitivity of C_2N_{14} is beyond our capabilities of measurement.”

¹⁹²⁶ $N_{16}C_2$ cage “Isomer B” (0.248 kg/mole, +3348 kJ/mole heat of formation, assume same density as $N_{14}C_2 \sim 1723$ kg/m³) had not been synthesized by 2014, but its decomposition to the elements would release 3.348×10^6 J/mole; Strout DL. Effect of C-O Bonding on the Stability and Energetics of High-Energy Nitrogen-Carbon Molecules $N_{10}C_2$ and $N_{16}C_2$. Advances Chem. 2014;2014:175384; <https://www.hindawi.com/journals/ac/2014/175384/>.

¹⁹²⁷ $N_{17}B$, aka. $N_5B(N_3)_4$ (0.249 kg/mole, assumed density ~ 3450 kg/m³, the same as cubic boron nitride) has been prepared experimentally with a stated decomposition specific energy of ~ 8.37 MJ/kg, or 2.08×10^6 J/mole (Haiges R, *et al.* High-energy-density materials: synthesis and characterization of $N_5^+[P(N_3)_6]^-$, $N_5^+[B(N_3)_4]^-$, $N_5^+[HF_2] \cdot n HF$, $N_5^+[BF_4]^-$, $N_5^+[PF_6]^-$, and $N_5^+[SO_3F]^-$. Angew Chem Int Ed 2004;43:4919-4924; https://www.researchgate.net/publication/8341474_High-energy-density_materials_synthesis_and_characterization_of_N5PN36-N5BN34-N5HF2-n-HF-N5BF4-N5PF6-and-N5SO3F-).

¹⁹²⁸ $N_{18}H_6$ (0.258 kg/mole, 1.18×10^{-4} m³/mole at estimated density 2191 kg/m³), a theoretically-proposed mostly-nitrogen cage molecule, had not been synthesized by 2016 but might decompose to the elements ($N_{18}H_6 \rightarrow 9N_2 + 3H_2$) releasing its estimated +2799.6 kJ/mole heat of formation (Haskins PJ, Fellows J, Cook MD, Wood A. Molecular studies of poly-nitrogen explosives. QinetiQ Ltd., 2002; <http://www.intdetsymp.org/detsymp2002/PaperSubmit/FinalManuscript/pdf/Haskins-102.PDF>).

$N_{20}Ti$ (theoretical) ¹⁹³⁰	1.22×10^6	0.328	6.28×10^{-5}
$N_{23}P$ ¹⁹³¹	2.95×10^6	0.353	1.27×10^{-4}
<u>Decomposing Explosives</u>			
AAT ¹⁹³²	5.93×10^5	0.208	1.36×10^{-4}
Acetylene ¹⁹³³	2.269×10^5	0.026	3.57×10^{-5}

¹⁹²⁹ 4,4',6,6'-tetra(azido)azo-1,3,5-triazine ($N_3C_3(N_3)_2-N=N-C_3(N_3)_2N_3$ or C_6N_{20} , 0.352 kg/mole, 1720 kg/m³, heat of formation +2171 kJ/mole; Huynh MHV, *et al.* Polyazido High-Nitrogen Compounds: Hydrazo- and Azo-1,3,5-triazine. *Angew Chemie Intl Ed.* 2004 Sep 20;43(37):4924-4928; <http://onlinelibrary.wiley.com/doi/10.1002/anie.200460366/full>) consists of two CN-benzene analogs, each with two azide groups, joined by a pair of N atoms, that “has the highest experimentally measured heat of formation reported for organic compounds” and is released upon decomposition to the elements ($C_6N_{20} \rightarrow 10N_2 + 6C$).

¹⁹³⁰ $N_{20}Ti$, aka. $Ti(N_5)_4$ (0.328 kg/mole, assumed density ~5220 kg/m³, the same as titanium nitride) is predicted theoretically to be stable enough to synthesize, with a barrier of ~54 kJ/mole against decomposition to titanium tetraazide via $Ti(N_5)_4 \rightarrow Ti(N_3)_4 + 4N_2$ with the release of the dissociation energy of 7.24×10^5 J/mole (Choi C, *et al.* $Ti(N_5)_4$ as a Potential Nitrogen-Rich Stable High-Energy Density Material. *J Phys Chem A* 2016 Jun 6;120(24):4249-4255; <http://pubs.acs.org/doi/abs/10.1021/acs.jpca.6b04226>). But titanium tetraazide ($Ti(N_3)_4$) can further decompose, releasing more energy – it has been synthesized experimentally and is described as a “highly endothermic covalent polyazide species” that is “very shock sensitive and can explode violently when touched with a metal spatula or when exposed to a rapid change in temperature (e.g. freezing with liquid nitrogen)” (Haiges R, *et al.* The Binary Group 4 Azides [$Ti(N_3)_4$], [$P(C_6H_5)_4$][$Ti(N_3)_5$], and [$P(C_6H_5)_4$]₂[$Ti(N_3)_6$] and on Linear Ti-N-NN Coordination. *Angew Chemie Intl Ed.* 2004;43:3148-3152; <http://onlinelibrary.wiley.com/doi/10.1002/anie.200454156/full>). The reference provides no information on the decomposition energy of $Ti(N_3)_4$, but on the basis of other azides listed herein (200–600 kJ/mole) we may assume the decomposition energy for $Ti(N_3)_4$ may be ~500 kJ/mole, increasing our estimate of the total decomposition energy of $Ti(N_5)_4$ to 1.22×10^6 J/mole.

¹⁹³¹ $N_{23}P$, aka. $N_5P(N_3)_6$ (0.353 kg/mole, assumed density ~2770 kg/m³, the same as phosphorus pentanitride) is a “white solid” that has been prepared experimentally with a stated decomposition specific energy of ~8.37 MJ/kg, or 2.95×10^6 J/mole (Haiges R, *et al.* High-energy-density materials: synthesis and characterization of $N_5^+[P(N_3)_6]^-$, $N_5^+[B(N_3)_4]^-$, $N_5^+[HF_2]^- \cdot n HF$, $N_5^+[BF_4]^-$, $N_5^+[PF_6]^-$, and $N_5^+[SO_3F]^-$. *Angew Chem Intl Ed* 2004;43:4919-4924; https://www.researchgate.net/publication/8341474_High-energy-density_materials_synthesis_and_characterization_of_N5PN36-N5BN34-N5HF2-n-HF-N5BF4-N5PF6-and-N5SO3F-).

¹⁹³² AAT, aka. ammonium azotetrazolate ($C_2H_8N_{12}$, 0.208 kg/mole, 1.36×10^{-4} m³/mole at 1530 kg/m³) is a new explosive with a +443.9 kJ/kg heat of formation (Agrawal JP. *High Energy Materials: Propellants, Explosives and Pyrotechnics*, John Wiley & Sons, 2015, Table 1.5, p. 143). Taking the decomposition reaction as: $C_2H_8N_{12} \rightarrow 6N_2 + 2CH_4$, and taking the standard heat of formation as -74.6 kJ/mole for CH_4 (http://www.update.uu.se/~jolkkonen/pdf/CRC_TD.pdf), the decomposition energy is 5.93×10^5 J/mole of $C_2H_8N_{12}$.

ADNQ ¹⁹³⁴	8.34 x 10 ⁵	0.166	9.57 x 10 ⁻⁵
Aluminum pentazolate (theoretical) ¹⁹³⁵	1.011 x 10 ⁶	0.237	6.8 x 10 ⁻⁵
Ammonium permanganate ¹⁹³⁶	3.20 x 10 ⁵	0.137	6.14 x 10 ⁻⁵
ANG ¹⁹³⁷	5.79 x 10 ⁵	0.119	6.73 x 10 ⁻⁵
Antimony trisulfide ¹⁹³⁸	1.75 x 10 ⁵	0.340	5.23 x 10 ⁻⁵

¹⁹³³ Acetylene, aka. ethyne (H-C≡C-H or C₂H₂, 0.026 kg/mole, 3.57 x 10⁻⁵ m³/mole for solid density 729 kg/m³ below 192 K; <http://encyclopedia.airliquide.com/encyclopedia.asp?GasID=1>) is unstable in pure form and can decompose explosively, if initiated by intense heat or a shockwave, e.g., if the absolute pressure of the gas exceeds about 200 kPa or 29 psi; copper also catalyzes decomposition by formation of the acetylide which itself decomposes readily, detonating the pressurized C₂H₂ (<https://en.wikipedia.org/wiki/Acetylene>). Decomposition to the elements releases the heat of formation, which is 0.2269 MJ/mole or 8.73 MJ/kg for acetylene.

¹⁹³⁴ Ammonium dinitroguanidine, aka. ADNQ (CH₆N₆O₄, 0.166 kg/mole, 9.57 x 10⁻⁵ m³/mole at density 1735 kg/m³), if detonated via the highest-energy stoichiometric decomposition reaction as CH₆N₆O₄ → 3N₂ + CO + 3H₂O, taking the standard heats of formation as -110.5 kJ/mole for CO and -241.8 kJ/mole for H₂O (http://www.update.uu.se/~jolkkonen/pdf/CRC_TD.pdf) and -1.5 kJ/mole for CH₆N₆O₄ (Klapötke TM, Stierstorfer J. Potential Replacements of RDX with Low Sensitivities, 2002, http://www2.imemg.org/res/IMEMTS%202010/papers/Klapotke-10400_Potential%20Replacements%20of%20RDX%20with%20Low%20Sensitivities_IMEMTS2010-Paper.pdf), the decomposition energy is 8.34 x 10⁵ J/mole.

¹⁹³⁵ Aluminum pentazolate complex (Al(N₅)₃ or AlN₁₅, 0.237 kg/mole, ~6.8 x 10⁻⁵ m³/mole assuming (as yet unreported) density of ~3500 kg/m³, cf. 3260 kg/m³ for AlN and 2700 kg/m³ for Al) has not yet been synthesized. Given a decomposition reaction: AlN₁₅ → 7.5N₂ + Al, and taking the standard heat of formation as +1011 kJ/mole for AlN₁₅ (Straka M, Pyykkö P. One metal and forty nitrogens. Ab initio predictions for possible new high-energy pentazolides. Inorg Chem. 2003 Dec 15;42(25):8241-9; <http://www.ncbi.nlm.nih.gov/pubmed/14658874>), the decomposition energy is 1.011 x 10⁶ J/mole.

¹⁹³⁶ Ammonium permanganate (NH₄MnO₄, 0.137 kg/mole, 6.14 x 10⁻⁵ m³/mole) is a moderately strong explosive; the dry solid can detonate by heat, shock, or friction, and explode at temperatures above 333 K, via: NH₄MnO₄ → 0.5N₂ + 2H₂O + MnO₂ (https://en.wikipedia.org/wiki/Ammonium_permanganate), releasing 3.20 x 10⁵ J/mole, taking the NH₄MnO₄ heat of formation as -684 kJ/mole (Kotai L, *et al.* An Overview on the Synthesis and the Reactivity of Simple and Complex Permanganates. ChemInform 2011 Mar;11(13):25-104; https://www.researchgate.net/publication/257922081_ChemInform_Abstract_Beliefs_and_Facts_in_Permanganate_Chemistry_-_An_Overview_on_the_Synthesis_and_the_Reactivity_of_Simple_and_Complex_Permanganates).

¹⁹³⁷ Amino-nitro-guanidine, aka. ANG (CH₅N₅O₂, 0.119 kg/mole, 6.73 x 10⁻⁵ m³/mole at density 1767 kg/m³), if detonated via the highest-energy stoichiometric decomposition reaction as CH₅N₅O₂ → 2.5N₂ + 2H₂O + 0.25CH₄ + 0.75C, taking the standard heats of formation as -241.8 kJ/mole for H₂O and -74.5 kJ/mole for CH₄ (http://www.update.uu.se/~jolkkonen/pdf/CRC_TD.pdf) and +77.0 kJ/mole for CH₅N₅O₂ (Klapötke TM, Stierstorfer J. Potential Replacements of RDX with Low Sensitivities, 2002, http://www2.imemg.org/res/IMEMTS%202010/papers/Klapotke-10400_Potential%20Replacements%20of%20RDX%20with%20Low%20Sensitivities_IMEMTS2010-Paper.pdf), the decomposition energy is 5.79 x 10⁵ J/mole.

Argon hydrogen fluoride (theoretical) ¹⁹³⁹	5.75×10^5	0.060	---
1,1'-Azobis(tetrazole) ¹⁹⁴⁰	1.03×10^6	0.166	9.36×10^{-5}
1,1'-Azobis-1,2,3-triazole ¹⁹⁴¹	1.06×10^6	0.164	1.00×10^{-4}
BAFDAONAB ¹⁹⁴²	8.16×10^6	0.738	3.82×10^{-4}
BDNM-TN-TABO (theoretical) ¹⁹⁴³	3.34×10^6	0.498	2.39×10^{-4}
BHDBT ¹⁹⁴⁴	7.64×10^5	0.420	2.19×10^{-4}

¹⁹³⁸ Antimony trisulfide (Sb_2S_3 , 0.340 kg/mole, 6500 kg/m³) forms into grey-black orthorhombic crystals used in safety matches, military ammunition, explosives and fireworks (https://en.wikipedia.org/wiki/Antimony_trisulfide). Decomposition to the elements releases the 1.75×10^5 J/mole heat of formation (<https://toxnet.nlm.nih.gov/cgi-bin/sis/search/a?dbs+hsdb:@term+@DOCNO+1604>).

¹⁹³⁹ Argon hydrogen fluoride (HArF , 0.060 kg/mole) has not been synthesized experimentally but has been predicted theoretically to be a metastable chemically-bonded molecule with a +117.2 kJ/mole (+1.21 eV) barrier to decomposition and a decomposition energy of 5.75×10^5 J/mole via the reaction $\text{HArF} \rightarrow \text{HF} + \text{Ar}$ (Wong MW. Prediction of a metastable helium compound: HHeF . *J Am Chem Soc* 2000 Jul 5;122(26):6289-90; <http://140.123.79.88/~ppmpk/paper/44.pdf>).

¹⁹⁴⁰ 1,1'-Azobis(tetrazole) ($\text{HCN}_4\text{-N=N-N}_4\text{CH}$ or $\text{C}_2\text{H}_2\text{N}_{10}$, 0.166 kg/mole, 1774 kg/m³, heat of formation +1030 kJ/mole) has been synthesized but is thermally and physically unstable with a decomposition temperature of 80 °C, and decomposing in solution; the researchers reported “several inadvertent explosions during handling” (Klapötke TM, Piercey DG. 1,1'-azobis(tetrazole): a highly energetic nitrogen-rich compound with a N_{10} chain. *Inorg Chem*. 2011 Apr 4;50(7):2732-4; https://edoc.ub.uni-muenchen.de/15389/1/Piercey_Davin.pdf#page=93).

¹⁹⁴¹ 1,1'-Azobis-1,2,3-triazole ($\text{CHCHN}_3\text{-N=N-N}_3\text{CHCH}$ or $\text{C}_4\text{H}_4\text{N}_8$, 0.164 kg/mole, 1640 kg/m³, heat of formation +962 kJ/mole) is a yellow solid that undergoes thermal decomposition at 194 °C (Turker L. Azobridged triazoles: green energetic materials. *Defence Technol*. 2016 Feb;12(1):1-15; <http://www.sciencedirect.com/science/article/pii/S2214914715000768>); the most energetically favorable decomposition stoichiometry would be: $\text{C}_4\text{H}_4\text{N}_8 \rightarrow 4\text{N}_2 + \text{CH}_4 + 3\text{C}$, yielding 1.04×10^6 J/mole.

¹⁹⁴² BAFDAONAB, aka. N,N-bis(3-aminofurazan-4-yl)-4,4'-diamino-2,2',3,3',5,5',6,6'-octanitroazobenzene ($\text{C}_{16}\text{H}_6\text{N}_{18}\text{O}_{18}$, 0.738 kg/mole, 1930 kg/m³, heat of formation +4487.44 kJ/mole) has been synthesized; the most energetically favorable decomposition stoichiometry would be: $\text{C}_{16}\text{H}_6\text{N}_{18}\text{O}_{18} \rightarrow 9\text{N}_2 + 7.5\text{CO}_2 + 3\text{H}_2\text{O} + 8.5\text{C}$, yielding 8.16×10^6 J/mole (Jing S, *et al*. Synthesis and Theoretical Studies of a New High Explosive, N,N-Bis(3-aminofurazan-4-yl)-4,4'-diamino-2,2',3,3',5,5',6,6'-octanitroazobenzene. *Central Euro J Energetic Mater*. 2015;12(4):745-755; <http://www.wydawnictwa.ipw.waw.pl/cejem/Vol-12-Number-4-2015/Jing.pdf>).

¹⁹⁴³ 3,7-Bis(dinitromethylene)-2,4,6,8-tetranitro-2,4,6,8-tetraaza-bicyclo[3.3.0]octane ($\text{C}_6\text{H}_2\text{N}_{12}\text{O}_{16}$, 0.498 kg/mole, 2080 kg/m³, heat of formation +740.4 kJ/mole) is predicted to have “superior detonation properties compared to those of RDX and HMX” (Jin X, *et al*. Computational study on structure and properties of new energetic material 3,7-bis(dinitromethylene)-2,4,6,8-tetranitro-2,4,6,8-tetraaza-bicyclo[3.3.0]octane. *Quimica Nova* 2016 May;39(4); http://www.scielo.br/scielo.php?script=sci_arttext&pid=S0100-40422016000400467). The most energetically favorable decomposition stoichiometry would be: $\text{C}_6\text{H}_2\text{N}_{12}\text{O}_{16} \rightarrow 6\text{N}_2 + 6\text{CO}_2 + \text{H}_2\text{O} + 1.5\text{O}_2$, yielding 3.34×10^6 J/mole.

Bicyclo-dioxydiazamethane (theoretical) ¹⁹⁴⁵	7.95×10^5	0.072	6.00×10^{-3}
1,4-Bis(dihydroperoxymethyl)benzene ¹⁹⁴⁶	1.287×10^6	0.234	1.46×10^{-4}
BNCP ¹⁹⁴⁷	2.00×10^6	0.454	1.51×10^{-3}
BNO ₂ (theoretical) ¹⁹⁴⁸	4.20×10^5	0.0568	---
BTAT ¹⁹⁴⁹	2.83×10^6	0.438	2.32×10^{-4}
BTATz ¹⁹⁵⁰	9.58×10^5	0.248	1.41×10^{-4}
BTTN ¹⁹⁵¹	1.84×10^6	0.241	1.59×10^{-4}

¹⁹⁴⁴ BHDBT, aka. 2,3-bis-hydroxymethyl-2,3-dinitro-1,4-butanediol tetranitrate (C₆H₈N₆O₁₆, 0.420 kg/mole, 2.19×10^{-4} m³/mole at density 1917 kg/m³), claimed to have the highest density of any known nitrate ester composed only of CHNO, has a decomposition energy release of 1.818 MJ/kg, or 7.64×10^5 J/mole (Chavez DE, *et al.* Synthesis of a new energetic nitrate ester. *Angew Chemie* 2008 Oct 13;120(43):8431-8433; <http://permalink.lanl.gov/object/tr?what=info:lanl-repo/lareport/LA-UR-08-04925>).

¹⁹⁴⁵ Bicyclo-dioxydiazamethane (O₂CN₂, 0.072 kg/mole, density ~1200 kg/m³ assumed the same as nitrosyl cyanide OCN₂; <http://cris3.guidechem.com/dictionary/en/4343-68-4.html>) has high ring strain, a barrier to decomposition of 121 kJ/mole, and decomposes to the elements (O₂CN₂ → N₂ + CO₂) with the release of 7.95×10^5 kJ/mole (Korkin AA, *et al.* Theoretical Ab Initio Study of CN₂O₂ Structures: Prediction of Nitryl Cyanide as a High-Energy Molecule, in Carrick PG, Williams NT. Proceedings of the HEDM Contractors' Conference, Air Force Materiel Command, PL-TR-96-3037, March 1997, 204-210; <http://www.dtic.mil/cgi-bin/GetTRDoc?AD=ADA325307>).

¹⁹⁴⁶ 1,4-Bis(dihydroperoxymethyl)benzene (C₈H₁₀O₈, 0.234 kg/mole, 1600 kg/m³, heat of formation -418.2 kJ/mole) is a white solid with a measured heat of explosion of 5.498 MJ/kg or 1287 kJ/mole (http://digitalcommons.wayne.edu/cgi/viewcontent.cgi?article=2371&context=oa_dissertations).

¹⁹⁴⁷ BNCP, aka. tetraamine-cis-bis(5-nitro-2H-tetrazolato-N²) cobalt (III) perchlorate (CoC₂H₁₂N₁₄O₈Cl, 0.454 kg/mole, 300 kg/m³) is a new explosive with a 4406 kJ/kg heat of explosion (Agrawal JP. *High Energy Materials: Propellants, Explosives and Pyrotechnics*, John Wiley & Sons, 2015, Table 1.5, p. 137).

¹⁹⁴⁸ BNO₂ (0.0568 kg/mole) has been considered theoretically at the SCF/6-31G* level of theory and appears to be stable with a specific enthalpy of 7.39 MJ/kg (Brener NE, Kestner NR, Callaway J. Theoretical studies of highly energetic CBES materials. AL-TR-90-060, Dec 1990, Table 2, p. 8; <http://www.dtic.mil/dtic/tr/fulltext/u2/a231340.pdf>).

¹⁹⁴⁹ Bis(trinitroethyl)-1,2,4,5-tetrazine-3,6-diamine, aka. BTAT (C₆H₆N₁₂O₁₂, 0.438 kg/mole, 2.32×10^{-4} m³/mole at density 1886 kg/m³), if detonated via the highest-energy stoichiometric decomposition reaction as C₆H₆N₁₂O₁₂ → 6N₂ + 4.5CO₂ + 3H₂O + 1.5C, taking the standard heats of formation as -393.5 kJ/mole for CO₂ and -241.8 kJ/mole for H₂O (http://www.update.uu.se/~jolkkonen/pdf/CRC_TD.pdf) and +336 kJ/mole for C₆H₆N₁₂O₁₂ (Klapotke TM. *Chemistry of High-Energy Materials*, Walter de Gruyter GmbH, 2015, p. 169), the decomposition energy is 2.83×10^6 J/mole.

¹⁹⁵⁰ BTATz (C₄H₄N₁₄, 0.248 kg/mole, 1760 kg/m³, heat of formation +883 kJ/mole; Huynh MHV, *et al.* Polyazido High-Nitrogen Compounds: Hydrazo- and Azo-1,3,5-triazine. *Angew Chemie Intl Ed.* 2004 Sep 20;43(37):4924-4928; <http://onlinelibrary.wiley.com/doi/10.1002/anie.200460366/full>), if decomposed via the highest-energy stoichiometry (C₄H₄N₁₄ → 7N₂ + CH₄ + 3C), releases 9.58×10^5 J/mole.

Carbenium triazidoperchlorate ¹⁹⁵²	2.34×10^6	0.237	9.48×10^{-3}
Carbon tetroxide, monocyclic ¹⁹⁵³	1.891×10^5	0.076	---
Carbon tetroxide, bicyclic (theoretical) ¹⁹⁵⁴	3.318×10^6	0.076	---
Carbonyl oxide ¹⁹⁵⁵	5.197×10^5	0.046	---

¹⁹⁵¹ BTTN, aka. 1,2,4-butanetriol trinitrate ($C_4H_7N_3O_9$, 0.241 kg/mole, $1.59 \times 10^{-4} \text{ m}^3/\text{mole}$; https://en.wikipedia.org/wiki/1,2,4-Butanetriol_trinitrate) is used as a propellant in virtually all single-stage missiles used by the United States, including the Hellfire, and is less volatile, less sensitive to shock, and more thermally stable than nitroglycerine. Taking the decomposition reaction as: $C_4H_7N_3O_9 \rightarrow 1.5N_2 + 2.75CO_2 + 3.5H_2O + 1.25C$, and taking standard heats of formation as -393.5 kJ/mole for CO_2 and -241.8 kJ/mole for H_2O (http://www.update.uu.se/~jolkkonen/pdf/CRC_TD.pdf) and -91.42 kJ/mole for $C_4H_7N_3O_9$ (Nair UR, *et al.* Advances in high energy materials. Defence Sci J. 2010 Mar;60(2):137-151; <http://publications.drdo.gov.in/ojs/index.php/dsj/article/viewFile/327/193>), the decomposition energy is $1.84 \times 10^6 \text{ J/mole}$ of $C_4H_7N_3O_9$.

¹⁹⁵² Solid carbenium triazidoperchlorate ($C(N_3)_3ClO_4$, 0.237 kg/mole, assumed density $\sim 2500 \text{ kg/m}^3$, +1946 kJ/mole heat of formation) is “extremely shock sensitive and a highly energetic explosive” (Christe KO, *et al.* Recent progress in the theory and synthesis of novel high energy density materials, in Carrick PG, Williams NT. Proceedings of the HEDM Contractors’ Conference, Air Force Materiel Command, PL-TR-96-3037, March 1997, 152-155; <http://www.dtic.mil/cgi-bin/GetTRDoc?AD=ADA325307>) that might decompose according to: $C(N_3)_3ClO_4 \rightarrow 4.5N_2 + CO_2 + 0.25O_2 + 0.5Cl_2$, giving an energy release of $2.34 \times 10^6 \text{ J/mole}$, taking the heat of formation as -393.5 kJ/mole for CO_2 (http://www.update.uu.se/~jolkkonen/pdf/CRC_TD.pdf).

¹⁹⁵³ Monocyclic carbon tetroxide (CO_4 , 0.076 kg/mole) is a high-order carboxide with potential as an energetic molecule that has been detected experimentally* and exists as a metastable molecule (at least in the gas phase) that shows a very exothermic dissociation reaction with a consistent activation barrier. Monocyclic CO_4 is a “kinetically stable energetic molecule” calculated to release 189.1 kJ/mole upon dissociation as $CO_4 \rightarrow CO_2 + O_2$, with a rate-determining barrier to dissociation of 120.1 kJ/mole barrier at 298 K, at the CASPT2(18e,12o)/CBS level of theory (He F, Gao S, de Petris G, Ding Y. Monocyclic and bicyclic CO_4 : How stable can they be? RSC Advances 2015 Oct;5(111); <http://pubs.rsc.org/en/content/articlelanding/ra/2015/c5ra19895j>). *Cacace F, de Petris G, Rosi M, Troiani A. Carbon tetroxide: theoretically predicted and experimentally detected. Angew Chem Int Ed. 2003;42:2985-2990.

¹⁹⁵⁴ Bicyclic carbon tetroxide (CO_4 , 0.076 kg/mole) is a high-order carboxide with potential as an energetic metastable molecule (at least in the gas phase) that shows a very exothermic dissociation reaction with a consistent activation barrier. Bicyclic CO_4 is a “kinetically stable energetic molecule” calculated to release 331.8 kJ/mole upon dissociation as $CO_4 \rightarrow CO_2 + O_2$, with a rate-determining barrier to dissociation of 61.5 kJ/mole barrier at 298 K, at the CASPT2(18e,12o)/CBS level of theory (He F, Gao S, de Petris G, Ding Y. Monocyclic and bicyclic CO_4 : How stable can they be? RSC Advances 2015 Oct;5(111); <http://pubs.rsc.org/en/content/articlelanding/ra/2015/c5ra19895j>). Because the bicyclic form has a lower dissociation barrier, it seems likely that the molecule that has been detected experimentally* is most likely the monocyclic form; there is no confirmed experimental detection of the bicyclic form to date, which is why its existence remains theoretical as of 2016. *Cacace F, de Petris G, Rosi M, Troiani A. Carbon tetroxide: theoretically predicted and experimentally detected. Angew Chem Int Ed. 2003;42:2985-2990.

Carboxycubane, C ₄ O ₄ (theoretical) ¹⁹⁵⁶	1.464 x 10 ⁶	0.112	---
Chlorine dioxide ¹⁹⁵⁷	1.025 x 10 ⁵	0.0675	4.11 x 10 ⁻⁵
Chromium pentazolate (theoretical) ¹⁹⁵⁸	3.536 x 10 ⁶	0.612	1.53 x 10 ⁻⁴
CL-20 ¹⁹⁵⁹	3.28 x 10 ⁶	0.438	2.14 x 10 ⁻⁴

¹⁹⁵⁵ Carbonyl oxide, aka. formaldehyde oxide or Criegee intermediate (H₂COO, 0.046 kg/mole) is the noncyclical form that decomposes according to: H₂COO → H₂ + CO₂ to yield the largest possible reaction enthalpy of 519.7 kJ/mole, with a barrier of 80.3 kJ/mole against isomerization to the cyclical dioxirane (H₂CO₂) form (Cremer D *et al.* A CCSD(T) Investigation of Carbonyl Oxide and Dioxirane. Equilibrium Geometries, Dipole Moments, Infrared Spectra, Heats of Formation and Isomerization Energies. Chem Phys Lett. 1993;209:547; https://sites.smu.edu/dedman/catco/publications/pdf/ChemPhysLett_209_547_1993.pdf). The carbonyl oxide was first observed experimentally in 2012 with a lifetime of only 2 msec,* despite earlier predictions of an upper limit of 3 sec (Olzmann M, *et al.* Energetics, kinetics, and product distributions of the reactions of ozone with ethene and 2,3-dimethyl-2-butene. J Phys Chem A 1997;101:9421; <http://citeseerx.ist.psu.edu/viewdoc/download?doi=10.1.1.532.2041&rep=rep1&type=pdf>). *Welz O, *et al.*, Direct kinetic measurements of Criegee intermediate (CH₂OO) formed by reaction of CH₂I with O₂. Science 2012;335:204; <http://science.sciencemag.org/content/335/6065/204.full>.

¹⁹⁵⁶ Carboxycubane (C₄O₄, 0.112 kg/mole) is a theoretical nearly-cubic molecule first proposed in 1996, with a calculated dissociation energy (C₄O₄ → 4CO) of ~1464 kJ/mole (Evangelisti S. Ab initio study of C₄O₄ in T_d symmetry. Chem Phys Lett. 1996 Sep 6;259(3-4):261-264; <http://www.sciencedirect.com/science/article/pii/0009261496007488>). Subsequent more detailed analysis suggests that the dissociation barrier is only 0.008 kJ/mole, but that the lowest vibrational frequency lies at 167.3 cm⁻¹ or 2.01 kJ/mole, which if correct would imply that carboxycubane is unstable and “not an observable molecule” (Schmidt M., *et al.* Cubic fuels? Intl J Quantum Chem 2000;76:434-446; http://lib.dr.iastate.edu/cgi/viewcontent.cgi?article=1370&context=chem_pubs).

¹⁹⁵⁷ Chlorine dioxide (ClO₂, 0.0675 kg/mole, 4.11 x 10⁻⁵ m³/mole taking liquid density as 1642 kg/m³; https://pubchem.ncbi.nlm.nih.gov/compound/chlorine_dioxide#section=Experimental-Properties) can explosively decompose to the elements (ClO₂ → 0.5Cl₂ + O₂), initiated by light, hot spots, chemical reaction, or pressure shock (https://en.wikipedia.org/wiki/Chlorine_dioxide#Handling_properties), releasing the 1.025 x 10⁵ J/mole heat of formation (http://www.update.uu.se/~jolkkonen/pdf/CRC_TD.pdf).

¹⁹⁵⁸ Chromium pentazolate complex (Cr(N₅)₈²⁻ or CrN₄₀, 0.612 kg/mole, ~1.53 x 10⁻⁴ m³/mole assuming (as yet unreported) density of ~4000 kg/m³, cf. 1770 kg/m³ for Cr(CO)₆, 5900 kg/m³ for CrN, and 7190 kg/m³ for Cr) has not yet been synthesized but has been theoretically predicted to be stable. Given a decomposition reaction: CrN₄₀ → 20N₂ + Cr, and taking the standard heat of formation as +3536 kJ/mole for CrN₄₀ (Straka M, Pyykkö P. One metal and forty nitrogens. Ab initio predictions for possible new high-energy pentazolides. Inorg Chem. 2003 Dec 15;42(25):8241-9; <http://www.ncbi.nlm.nih.gov/pubmed/14658874>; as cited in Table 3 of Wallin S, *et al.* High Energy Density Materials Efforts to synthesize the pentazolate anion: Part 1, Technical Report FOI-R-1602-SE, March 2005; http://foi.se/ReportFiles/foir_1602.pdf), the decomposition energy is 3.536 x 10⁶ J/mole.

CLCP ¹⁹⁶⁰	1.814 x 10 ⁶	0.4465	2.27 x 10 ⁻⁴
Composition B ¹⁹⁶¹	5.56 x 10 ⁶	1	6.06 x 10 ⁻⁴
Composition C-4 ¹⁹⁶²	5.90 x 10 ⁶	1	5.79 x 10 ⁻⁴
Composition H6 ¹⁹⁶³	5.65 x 10 ⁶	1	5.81 x 10 ⁻⁴
Copper acetylide ¹⁹⁶⁴	5.78 x 10 ⁵	0.151	---
CTA ¹⁹⁶⁵	7.40 x 10 ⁵	0.214	1.24 x 10 ⁻⁴
DAAF ¹⁹⁶⁶	1.123 x 10 ⁶	0.212	1.21 x 10 ⁻⁴

¹⁹⁵⁹ Hexanitrohexaazaisowurtzitane, aka. HNIW, China Lake compound #20 or CL-20 ((CH)₆(NNO₂)₆ or C₆H₆N₁₂O₁₂, 0.438 kg/mole, 2.14 x 10⁻⁴ m³/mole at 2044 kg/m³; <https://en.wikipedia.org/wiki/Hexanitrohexaazaisowurtzitane>) is a nitroamine explosive developed as a propellant in the 1980s. Taking the decomposition reaction as: C₆H₆N₁₂O₁₂ → 6N₂ + 4.5CO₂ + 3H₂O + 1.5C, and taking the standard heats of formation as -393.5 kJ/mole for CO₂ and -241.8 kJ/mole for H₂O (http://www.update.uu.se/~jolkkonen/pdf/CRC_TD.pdf) and +460 kJ/mole for C₆H₆N₁₂O₁₂ (Agrawal JP. High Energy Materials: Propellants, Explosives and Pyrotechnics, John Wiley & Sons, 2015, Table 1.5, p. 26), the decomposition energy is 2.96 x 10⁶ J/mole of C₆H₆N₁₂O₁₂. plus ~319 kJ/mole of “conventional ring strain energy” (Bumpus JA. A Theoretical Investigation of the Ring Strain Energy, Destabilization Energy, and Heat of Formation of CL-20. Adv Phys Chem 2012:175146; <http://downloads.hindawi.com/journals/apc/2012/175146.pdf>).

¹⁹⁶⁰ CLCP, aka. (2-(5-chlorotetrazolato)pentaamine-cobalt(III) perchlorate (CoCH₁₅N₉Cl₃O₈, 0.4465 kg/mole, 1970 kg/m³, heat of formation -543.9 kJ/mole) decomposes explosively with the release of 971 kcal/kg or 1.814 x 10⁶ J/mole of CLCP (<http://www.ocsresponds.com/ref/hazlist/TechSpecs.pdf>).

¹⁹⁶¹ Composition B is a castable military explosive composed of 59.5% RDX and 39.4% TNT with a density of 1650 kg/m³ (https://en.wikipedia.org/wiki/Composition_B); its RE Factor of 1.33 x TNT (https://en.wikipedia.org/wiki/Relative_effectiveness_factor) implies a detonation energy of 5.56 MJ/kg. Cyclotol (<https://en.wikipedia.org/wiki/Cyclotol>) is a similar mixture, with RDX ranging from 60%-80%.

¹⁹⁶² C-4 is a common variety of the plastic explosive family known as Composition C, containing 91% RDX with density 1727 kg/m³ and a maximum heat of detonation of 5.9 MJ/kg ([https://en.wikipedia.org/wiki/C-4_\(explosive\)](https://en.wikipedia.org/wiki/C-4_(explosive))).

¹⁹⁶³ Composition H6 is a castable military explosive composed primarily of 44.0% RDX and nitrocellulose, 29.5% TNT, and 21% powdered aluminum, with a density of 1720 kg/m³ and an RE Factor of ~1.35 x TNT (https://en.wikipedia.org/wiki/Composition_H6), giving a detonation energy of ~5.65 MJ/kg.

¹⁹⁶⁴ Copper acetylide, aka. copper (I) acetylide or cuprous acetylide (Cu-C≡C-Cu or Cu₂C₂, 0.151 kg/mole) is reddish solid that is heat- and shock-sensitive and easily explodes when dry ([https://en.wikipedia.org/wiki/Copper\(I\)_acetylide](https://en.wikipedia.org/wiki/Copper(I)_acetylide)). It is one of the few explosives that do not liberate any gases upon detonation via Cu₂C₂ → 2Cu + 2C. If the detonation energy is ~47% of TNT (<http://www.powerlabs.org/chemlabs/acetylide.htm>), this would release ~578 kJ/mole.

¹⁹⁶⁵ CTA, aka. cyanuric triazide or 2,4,6-triazido-1,3,5-triazine, triazine triazide or TTA ((NCN₃)₃ or C₃N₁₂, 0.214 kg/mole, 1.24 x 10⁻⁴ m³/mole at 1730 kg/m³) under detonation conditions liberates 7.40 x 10⁵ J/mole (https://en.wikipedia.org/wiki/Cyanuric_triazide).

¹⁹⁶⁶ DAAF or 3,3'-diamino-4,4'-azoxyfurazan (C₄H₄N₈O₃, 0.212 kg/mole, 1747 kg/m³, heat of formation +443 kJ/mole; <http://permalink.lanl.gov/object/tr?what=info:lanl-repo/lareport/LA-UR-01-1493>) consists of solid orange-yellow crystals that if decomposed to products that evolve maximum energy (C₄H₄N₈O₃ → 4N₂ + 0.5CO₂ + 2H₂O + 3.5C) would release 1.123 x 10⁶ J/mole.

DAAT ¹⁹⁶⁷	1.11×10^6	0.220	1.24×10^{-4}
DAB ¹⁹⁶⁸	4.52×10^5	0.0959	6.31×10^{-5}
DADP ¹⁹⁶⁹	4.20×10^5	0.148	1.11×10^{-4}
DDNP ¹⁹⁷⁰	1.24×10^6	0.210	1.29×10^{-4}
DEGDN ¹⁹⁷¹	1.14×10^6	0.196	1.39×10^{-4}

¹⁹⁶⁷ DAAT (diamino azobis tetrazine), aka. 3,3'-azobis(6-amino-1,2,4,5-tetrazine) ($\text{H}_2\text{N}-\text{C}_2\text{N}_4-\text{N}_2-\text{C}_2\text{N}_4-\text{NH}_2$ or $\text{C}_4\text{H}_4\text{N}_{12}$, 0.220 kg/mole) is considered as a potential high energy material to be used in rocket propellants and insensitive high-explosive formulations. Given a decomposition reaction: $\text{C}_4\text{H}_4\text{N}_{12} \rightarrow 6\text{N}_2 + \text{CH}_4 + 3\text{C}$, and taking the standard heats of formation as -74.6 kJ/mole for CH_4 (http://www.update.uu.se/~jolkkonen/pdf/CRC_TD.pdf) and $+1032$ kJ/mole for $\text{C}_4\text{H}_4\text{N}_{12}$ (Kerth J, Lobbecke S. Synthesis and characterization of 3,3'-azobis(6-amino-1,2,4,5-tetrazine) DAAT: A new promising nitrogen-rich compound. *Propellants Explos Pyrotech.* 2002;27:111-118; [http://onlinelibrary.wiley.com/doi/10.1002/1521-4087\(200206\)27:3%3C111::AID-PREP111%3E3.0.CO;2-O/full](http://onlinelibrary.wiley.com/doi/10.1002/1521-4087(200206)27:3%3C111::AID-PREP111%3E3.0.CO;2-O/full)), the decomposition energy is 1.11×10^6 J/mole, with density reported as 1780 kg/m³ by Huynh MHV, *et al.* Polyazido High-Nitrogen Compounds: Hydrazo- and Azo-1,3,5-triazine. *Angew Chemie Intl Ed.* 2004 Sep 20;43(37):4924-4928; <http://onlinelibrary.wiley.com/doi/10.1002/anie.200460366/full>. * De Luca LL, Shimada T, Sinditskii VP, Calabro M. *Chemical Rocket Propulsion: A Comprehensive Survey of Energetic Materials*, Springer, 2016, p. 109; <https://books.google.com/books?id=9XbhDAAAQBAJ&pg=PA109>.

¹⁹⁶⁸ Diazidoborane, aka. DAB ($\text{HB}(\text{N}_3)_2$, 0.0959 kg/mole, 1520 kg/m³), a theoretical azidoborane, upon decomposing to the elements will release its $+452$ kJ/mole heat of formation (Michels HH, *et al.* Structure, thermochemistry and performance of advanced propellants, in Thompson TL, Rodgers SL, eds., *Proc. HEDM Contractors Conference*, 5-7 Jun 1994, pp.154-171; <http://www.dtic.mil/cgi-bin/GetTRDoc?AD=ADA292988>).

¹⁹⁶⁹ DADP, aka. diacetone diperoxide ($\text{C}_6\text{H}_{12}\text{O}_4$, 0.148 kg/mole, 1.11×10^{-4} m³/mole at a density of 1331 kg/m³; http://digitalcommons.wayne.edu/cgi/viewcontent.cgi?article=2371&context=oa_dissertations) is an organic peroxide and a non-nitrogenous high explosive, sometimes called a "peroxo-based homemade explosive" because of its ease of manufacture. The most recent calorimetric work finds that the heat of explosion for TATP is 2.837 MJ/kg or 4.20×10^5 J/mole (Sinditskii VP, *et al.* Thermochemistry of cyclic acetone peroxides. *Thermochim Acta* 2014;585:10-15; http://www.academia.edu/download/40203159/Thermochemistry_of_Cyclic_Acetone_Peroxi20151120-29225-mrexfo.pdf).

¹⁹⁷⁰ Diazodinitrophenol, aka. 6-diazo-2,4-dinitrocyclohexa-2,4-dien-1-one, Dinol, or DDNP ($\text{C}_6\text{H}_2(\text{NO}_2)_2\text{ONN}$ or $\text{C}_6\text{H}_2\text{N}_4\text{O}_5$, 0.210 kg/mole, 1.29×10^{-4} m³/mole at 1630 kg/m³; <https://de.wikipedia.org/wiki/Diazodinitrophenol>) is often used as an initiating explosive in propellant primer devices. Taking the decomposition reaction as: $\text{C}_6\text{H}_2\text{N}_4\text{O}_5 \rightarrow 2\text{N}_2 + 2\text{CO}_2 + \text{H}_2\text{O} + 4\text{C}$, and taking the standard heats of formation as -393.5 kJ/mole for CO_2 and -241.8 kJ/mole for H_2O (http://www.update.uu.se/~jolkkonen/pdf/CRC_TD.pdf) and $+207$ kJ/mole for $\text{C}_6\text{H}_2\text{N}_4\text{O}_5$ (Agrawal JP. *High Energy Materials: Propellants, Explosives and Pyrotechnics*, John Wiley & Sons, 2015, Table 1.5, p. 26), the decomposition energy is 1.24×10^6 J/mole of $\text{C}_6\text{H}_2\text{N}_4\text{O}_5$.

¹⁹⁷¹ Diethylene glycol dinitrate, aka. oxydiethylene dinitrate, or DEGDN ($(\text{CH}_2)_4(\text{ONO}_2)_2\text{O}$ or $\text{C}_4\text{H}_8\text{N}_2\text{O}_7$, 0.196 kg/mole, 1.39×10^{-4} m³/mole; https://en.wikipedia.org/wiki/Diethylene_glycol_dinitrate) is an oily explosive liquid. Taking the decomposition reaction as: $\text{C}_4\text{H}_8\text{N}_2\text{O}_7 \rightarrow \text{N}_2 + 1.5\text{CO}_2 + 4\text{H}_2\text{O} + 2.5\text{C}$, and taking the standard heats of formation as -393.5 kJ/mole for CO_2 and -241.8 kJ/mole for H_2O (http://www.update.uu.se/~jolkkonen/pdf/CRC_TD.pdf) and -415.7 kJ/mole for $\text{C}_4\text{H}_8\text{N}_2\text{O}_7$ (Agrawal JP. *High Energy Materials: Propellants, Explosives and Pyrotechnics*, John Wiley & Sons, 2015, Table 1.5, p. 26), the decomposition energy is 1.14×10^6 J/mole of $\text{C}_4\text{H}_8\text{N}_2\text{O}_7$.

Diazirinone ¹⁹⁷²	4.18×10^5	0.056	2.55×10^{-3}
Dihydrazinium 5,5'-azotetrazolate dihydrazinate ¹⁹⁷³	1.105×10^6	0.230	2.34×10^{-4}
3,5-Dihydroperoxy-3,5-dimethyl-1,2-dioxolane ¹⁹⁷⁴	8.521×10^5	0.166	1.16×10^{-4}
DNAF/DDF ¹⁹⁷⁵	2.24×10^6	0.288	1.43×10^{-4}
DNAN ¹⁹⁷⁶	9.32×10^5	0.198	1.48×10^{-4}
DNBT ¹⁹⁷⁷	1.57×10^6	0.254	1.95×10^{-4}

¹⁹⁷² Diazirinone (N_2CO , 0.056 kg/mole) gas dissociation ($N_2CO \rightarrow N_2 + CO$) is exothermic by 96-100 kcal/mole (418 kJ/mole) with a 27 kcal/mole (113 kJ/mole) barrier that is “sufficiently high to permit observation” (Korkin AA, Schleyer PV, Boyd RJ. Theoretical-Study of Metastable N_2CO Isomers - New Candidates for High-Energy Materials. Chem Phys Lett. 1994;227(3):312-320; <https://dalspace.library.dal.ca/handle/10222/35839>). Diazirinone has been synthesized as a yellow solid at 77 K (Zeng X, *et al.* Elusive diazirinone, N_2CO . Angew Chem Int Ed. 2011 Feb 11;50(7):1720-1723; <http://onlinelibrary.wiley.com/doi/10.1002/anie.201006745/abstract>) with an estimated density of 2200 kg/m³ (<http://www.chemspider.com/Chemical-Structure.9449962.html>).

¹⁹⁷³ Dihydrazinium 5,5'-azotetrazolate dihydrazinate ($[N_2H_5]_2^+[N_4C-N=N-CN_4]^{2-}$ or $C_2H_{10}N_{14}$, 0.230 kg/mole, 983 kg/m³ based on calculated molecular volume of 0.3345 nm³/molecule) is a high-nitrogen high-energy material that derives most of its energy from its very high heat of formation, in this case +264 kcal/mole or 4.80 MJ/kg (Hammerl A, Klapötke TM, Nöth H, Warchhold M, Holl G, Kaiser M, Ticmanis U. [N(2)H(5)](+) (2)[N(4)C-N=N-CN(4)](2-): a new high-nitrogen high-energetic material. Inorg Chem. 2001 Jul 2;40(14):3570-5; <http://www.ncbi.nlm.nih.gov/pubmed/11421707>). The compound is “stable at room temperature, almost insensitive to friction and impact, but detonates violently when the explosion is initiated.”

¹⁹⁷⁴ 3,5-Dihydroperoxy-3,5-dimethyl-1,2-dioxolane ($C_5H_{10}O_6$, 0.166 kg/mole, 1430 kg/m³, heat of formation -509.1 kJ/mole, heat of explosion 5.133 MJ/kg or 852.1 kJ/mole) is a colorless polygonal crystalline solid and is one of the highest-energy cyclic dihydroperoxy compounds due to high density and high oxygen content, but impact and friction sensitivities are high (http://digitalcommons.wayne.edu/cgi/viewcontent.cgi?article=2371&context=oa_dissertations).

¹⁹⁷⁵ DNAF, aka. 4,4'-dinitro-3,3'-diazonofuroxan, dinitroazofuroxane, or DDF ($C_4N_8O_8$, 0.288 kg/mole, 1.43×10^{-4} m³/mole; <https://en.wikipedia.org/wiki/4,4%27-Dinitro-3,3%27-diazonofuroxan>) is a high detonation velocity (~10,000 m/sec) explosive. Taking the decomposition reaction as: $C_4N_8O_8 \rightarrow 4N_2 + 4CO_2$, and taking the standard heats of formation as -393.5 kJ/mole for CO_2 (http://www.update.uu.se/~jolkkonen/pdf/CRC_TD.pdf) and +668 kJ/mole for $C_4N_8O_8$ (Nair UR, *et al.* Advances in high energy materials. Defence Sci J. 2010 Mar;60(2):137-151; <http://publications.drdo.gov.in/ojs/index.php/dsj/article/viewFile/327/193>), the decomposition energy is 2.24×10^6 J/mole of $C_4N_8O_8$.

¹⁹⁷⁶ DNAN or 2,4-dinitroanisole ($C_7H_6N_2O_5$, 0.198 kg/mole, 1.48×10^{-4} m³/mole; <https://en.wikipedia.org/wiki/2,4-Dinitroanisole>) is a low-sensitivity explosive organic compound that is a key ingredient in the new IMX class explosives (<https://en.wikipedia.org/wiki/IMX-101>). Taking the decomposition reaction as: $C_7H_6N_2O_5 \rightarrow N_2 + CO_2 + 3H_2O + 6C$, and taking the standard heats of formation as -393.5 kJ/mole for CO_2 and -241.8 kJ/mole for H_2O (http://www.update.uu.se/~jolkkonen/pdf/CRC_TD.pdf) and -186.65 kJ/mole for $C_7H_6N_2O_5$ (Meyer R, Kohler J, Homburg A. Explosives. John Wiley & Sons, 2016), the decomposition energy is 9.32×10^5 J/mole of $C_7H_6N_2O_5$.

DTTO (theoretical) ¹⁹⁷⁸	1.264 x 10 ⁶	0.200	1.01 x 10 ⁻⁴
Dynamite ¹⁹⁷⁹	1.0 x 10 ⁶	0.19	1.6 x 10 ⁻⁴
EGDN ¹⁹⁸⁰	1.01 x 10 ⁶	0.152	1.02 x 10 ⁻⁴
Erythritol tetranitrate ¹⁹⁸¹	2.81 x 10 ⁶	0.302	1.89 x 10 ⁻⁴
FNO ₂ (theoretical) ¹⁹⁸²	3.30 x 10 ⁵	0.065	---
FOX-7 ¹⁹⁸³	8.69 x 10 ⁵	0.148	7.86 x 10 ⁻⁵

¹⁹⁷⁷ DNBT or dinitro-bis-triazolo-tetrazine (C₄H₂N₁₀O₄, 0.254 kg/mole, 1.95 x 10⁻⁴ m³/mole assuming ~1300 kg/m³) is a low-sensitivity explosive. Taking the decomposition reaction as: C₄H₂N₁₀O₄ → 5N₂ + 1.5CO₂ + H₂O + 2.5C, and taking the standard heats of formation as -393.5 kJ/mole for CO₂ and -241.8 kJ/mole for H₂O (http://www.update.uu.se/~jolkkonen/pdf/CRC_TD.pdf) and +741.0 kJ/mole for C₄H₂N₁₀O₄ (Tsyshevskiy R, *et al.* Computational Design of Novel Energetic Materials: Dinitro-bis-triazolo-tetrazine. J Phys Chem. 2015;119:8512-8521; https://www.researchgate.net/publication/275230056_Computational_Design_of_Novel_Energetic_Materials_Dinitro-bis-triazolo-tetrazine), the decomposition energy is 1.57 x 10⁶ J/mole of C₄H₂N₁₀O₄.

¹⁹⁷⁸ DTTO, aka. di-tetrazine-tetroxide or tetrazino-tetrazine-tetraoxide (C₂N₈O₄, 0.200 kg/mole, 1980 kg/m³) has not yet been synthesized but is predicted to have a decomposition energy of 6.32 MJ/kg or 1.264 x 10⁶ J/mole (Mendoza-Cortes JL, *et al.* Prediction of the Crystal Packing of Di-Tetrazine-Tetroxide (DTTO) Energetic Material. J Comp Chem 2016;37:163-167; <http://www.wag.caltech.edu/publications/sup/pdf/1141.pdf>).

¹⁹⁷⁹ Dynamite is an explosive made of nitroglycerin, sorbents (such as powdered shells or clay) and stabilizers. A cylindrical stick of dynamite 20 cm long and 3.2 cm in diameter (~1.6 x 10⁻⁴ m³) contains 0.19 kg of explosive material, producing ~1 x 10⁶ J upon detonation (<https://en.wikipedia.org/wiki/Dynamite#Form>).

¹⁹⁸⁰ Ethylene glycol dinitrate, aka. EGDN, NGc, or nitroglycol ((CH₂)₂(ONO₂)₂ or C₂H₄N₂O₆, 0.152 kg/mole, 1.02 x 10⁻⁴ m³/mole; https://en.wikipedia.org/wiki/Ethylene_glycol_dinitrate) is an oily explosive liquid. Taking the perfectly oxygen-balanced decomposition reaction as: C₂H₄N₂O₆ → N₂ + 2CO₂ + 2H₂O, and taking the standard heats of formation as -393.5 kJ/mole for CO₂ and -241.8 kJ/mole for H₂O (http://www.update.uu.se/~jolkkonen/pdf/CRC_TD.pdf) and -259 kJ/mole for C₂H₄N₂O₆ (Agrawal JP. High Energy Materials: Propellants, Explosives and Pyrotechnics, John Wiley & Sons, 2015, Table 1.5, p. 26), the decomposition energy is 1.01 x 10⁶ J/mole of C₂H₄N₂O₆.

¹⁹⁸¹ Erythritol tetranitrate, aka. ETN, erythryl tetranitrate, or nitroglyc (C₄H₆N₄O₁₂, 0.302 kg/mole, 1.89 x 10⁻⁴ m³/mole; https://en.wikipedia.org/wiki/Erythritol_tetranitrate) is an explosive solid similar to PETN, but one-third more sensitive to friction and impact. ETN releases 0.5 mole of free O₂ per mole of ETN upon detonation, which can be used to oxidize an added metal dust or an oxygen deficient explosive such as TNT or PETN. Taking the decomposition reaction as: C₄H₆N₄O₁₂ → 2N₂ + 4CO₂ + 3H₂O + 0.5O₂, and taking the standard heats of formation as -393.5 kJ/mole for CO₂ and -241.8 kJ/mole for H₂O (http://www.update.uu.se/~jolkkonen/pdf/CRC_TD.pdf) and +506.9 kJ/mole for C₄H₆N₄O₁₂ (https://www.researchgate.net/publication/287410480_Synthesis_characterization_of_1_2_3_4-Erythryl_tetranitrate), the decomposition energy is 2.81 x 10⁶ J/mole of C₄H₆N₄O₁₂.

¹⁹⁸² FNO₂ (0.065 kg/mole) has been considered theoretically at the SCF/6-31G* level of theory and appears to be stable with a specific enthalpy of 5.08 MJ/kg (Brener NE, Kestner NR, Callaway J. Theoretical studies of highly energetic CBES materials. AL-TR-90-060, Dec 1990, Table 2, p. 8; <http://www.dtic.mil/dtic/tr/fulltext/u2/a231340.pdf>).

GAT ¹⁹⁸⁴	6.34×10^5	0.284	1.85×10^{-4}
HAA ¹⁹⁸⁵	4.15×10^5	0.173	1.02×10^{-4}
Helium hydrogen fluoride (theoretical) ¹⁹⁸⁶	6.755×10^5	0.024	---
Heptanitrocubane ¹⁹⁸⁷	4.346×10^6	0.419	2.07×10^{-4}

¹⁹⁸³ FOX-7, aka. DADNE or 1,1-diamino-2,2-dinitroethene ($C_2(NH_2)_2(NO_2)_2$ or $C_2H_4N_4O_4$, 0.148 kg/mole, $7.86 \times 10^{-5} m^3/mole$; <https://en.wikipedia.org/wiki/FOX-7>) is an impact- and friction-insensitive high explosive. Taking the decomposition reaction as: $C_2H_4N_4O_4 \rightarrow 2N_2 + CO_2 + 2H_2O + C$, and taking standard heats of formation as -393.5 kJ/mole for CO_2 and -241.8 kJ/mole for H_2O (http://www.update.uu.se/~jolkkonen/pdf/CRC_TD.pdf) and -8 kJ/mole for $C_2H_4N_4O_4$ (<http://www.eurenc.com/wp-content/uploads/2013/07/FOX-7-DADNE.pdf>), the decomposition energy is $8.69 \times 10^5 J/mole$ of $C_2H_4N_4O_4$.

¹⁹⁸⁴ GAT, aka. guanidinium azotetrazolate ($C_4H_{12}N_{16}$, 0.284 kg/mole, $1.85 \times 10^{-4} m^3/mole$ at $1538 kg/m^3$) is a new explosive with a +410.0 kJ/kg heat of formation (Agrawal JP. High Energy Materials: Propellants, Explosives and Pyrotechnics, John Wiley & Sons, 2015, Table 1.5, p. 143). Taking the decomposition reaction as: $C_4H_{12}N_{16} \rightarrow 8N_2 + 3CH_4 + C$, and taking the standard heat of formation as -74.6 kJ/mole for CH_4 (http://www.update.uu.se/~jolkkonen/pdf/CRC_TD.pdf), the decomposition energy is $6.34 \times 10^5 J/mole$ of $C_4H_{12}N_{16}$.

¹⁹⁸⁵ HAA, aka. planar 1,3,4,6,7,9-hexaazacycl[3.3.3]azine ($C_6N_7H_3$, 0.173 kg/mole, $1690 kg/m^3$) upon detonation is predicted to release a total explosive energy of $4.15 \times 10^5 J/mole$ (Wu Q, *et al.* Improving an insensitive low-energy compound, 1,3,4,6,7,9-hexaazacycl[3.3.3]azine, to be an insensitive high explosive by way of two-step structural modifications. Can J Chem 2014;92:1157-1161; http://www.nrcresearchpress.com/doi/abs/10.1139/cjc-2014-0396#.V_hT08mZPuN).

¹⁹⁸⁶ Helium hydrogen fluoride (HHeF, 0.024 kg/mole) has not been synthesized experimentally but has been predicted theoretically to be a metastable chemically-bonded molecule with a +36.4 kJ/mole (+0.38 eV) barrier to decomposition and a decomposition energy of $6.755 \times 10^5 J/mole$ via the reaction $HHeF \rightarrow HF + He$ (Wong MW. Prediction of a metastable helium compound: HHeF. J Am Chem Soc 2000 Jul 5;122(26):6289-90; <http://140.123.79.88/~ppmpk/paper/44.pdf>). Subsequent calculations suggested that the molecule might have a very short lifetime, but that it might be possible to stabilize it against decomposition (e.g., by high pressure, complexation, embedding in cold xenon matrix, or substituting deuterium for hydrogen) in order to extend the lifetime (https://pl.wikipedia.org/wiki/Fluorowodorek_helu).

Hexamine peroxide ¹⁹⁸⁸	1.09×10^6	0.208	2.37×10^{-4}
Hexanitrobenzene ¹⁹⁸⁹	2.56×10^6	0.348	1.75×10^{-4}
Hexanitroprismane (theoretical) ¹⁹⁹⁰	3.39×10^6	0.348	1.74×10^{-4}

¹⁹⁸⁷ Heptanitrocubane, aka. HNC, HpNC, or 7-CUB ($C_8H_7N_7O_{14}$, 0.419 kg/mole, and 2.07×10^{-4} m³/mole using a calculated density of 2028 kg/m³; Zhang MX, Eaton PE, Gilardi R. Hepta- and Octanitrocubanes. *Angew Chem Int Ed.* 2000;39(2):401-404; <http://ramsey1.chem.uic.edu/chem494/downloads-2/files/Zhang%20et%20al%202000.pdf>) has 7 of the 8 corners of cubane terminated with NO₂ instead of H; HNC is very similar in structure to octanitrocubane (<https://en.wikipedia.org/wiki/Heptanitrocubane>). Theory calculations indicate that HNC stores 4346 kJ/mole of free energy (Chaban VV, Prezhdov OV. Energy Storage in Cubane Derivatives and Their Real-Time Decomposition: Computational Molecular Dynamics and Thermodynamics. *ACS Energy Lett.* 2016;1(1):189–194; <http://pubs.acs.org/doi/abs/10.1021/acseenergylett.6b00075>). Related high-energy explosive compounds including **dinitrocubane** (Eaton PE, Shankar BKR, Price GD, Pluth JJ, Gilbert EE, Alster J, Sandus O. Synthesis of 1,4-dinitrocubane. *J Org Chem.* 1984;49(1):185-186; <https://pubs.acs.org/doi/abs/10.1021/jo00175a044>), **trinitrocubane** and **tetranitrocubane** (Eaton PE, Xiong Y, Gilardi R. Systematic substitution on the cubane nucleus. Synthesis and properties of 1,3,5-trinitrocubane and 1,3,5,7-tetranitrocubane. *J Am Chem Soc.* 1993;115(22):10195-10202; <https://pubs.acs.org/doi/abs/10.1021/ja00075a039>), **pentanitrocubane** (Lukin K, Li J, Gilardi R, Eaton PE. Anions Stabilized by β -Nitro Groups: The Acidity and ortho-Metalation of Nitrocubanes – Penta- and Hexanitrocubanes. *Angew Chemie Intl Ed.* 1996 May 3;35(8):864-866; <https://onlinelibrary.wiley.com/doi/abs/10.1002/anie.199608641>), and **hexanitrocubane** (Gilardi R, Butcher RJ, Zhang MX. 1,2,3,4,5,7-Hexanitrocubane. *Acta Cryst E.* 2002;58:0978-0980; <https://scripts.iucr.org/cgi-bin/paper?ac6009>) have also been synthesized.

¹⁹⁸⁸ Hexamine peroxide, aka. hexamethylene triperoxide diamine or HMTD ($C_6H_{12}N_2O_6$, 0.208 kg/mole, 2.37×10^{-4} m³/mole; https://en.wikipedia.org/wiki/Hexamethylene_triperoxide_diamine) is unstable and detonates upon exposure to heat, friction or shock. The reaction products can vary significantly depending upon temperature and the presence or absence of oxygen ([http://cnqzu.com/library/Anarchy%20Folder/Explosives/Explosive%20Compounds/Peroxides/Decomposition%20of%20multi-peroxidic%20compounds%20Part%20II.%20Hexamethylene%20triperoxide%20diamine%20\(HMTD\).pdf](http://cnqzu.com/library/Anarchy%20Folder/Explosives/Explosive%20Compounds/Peroxides/Decomposition%20of%20multi-peroxidic%20compounds%20Part%20II.%20Hexamethylene%20triperoxide%20diamine%20(HMTD).pdf)), but the highest energy-yielding decomposition reaction is: $C_6H_{12}N_2O_6 \rightarrow 6H_2O + N_2 + 6C$; taking the standard heats of formation as -241.8 kJ/mole for H₂O (http://www.update.uu.se/~jolkkonen/pdf/CRC_TD.pdf) and -360 kJ/mole for C₆H₁₂N₂O₆ (<https://books.google.com/books?id=hX3mBgAAQBAJ&pg=PA519>), the decomposition energy would be 1.09×10^6 J/mole of C₆H₁₂N₂O₆.

¹⁹⁸⁹ Hexanitrobenzene, aka. HNB ($C_6(NO_2)_6$ or $C_6N_6O_{12}$, 0.348 kg/mole, 1.75×10^{-4} m³/mole; <https://en.wikipedia.org/wiki/Hexanitrobenzene>) is a high-density, moderately light-sensitive explosive compound. Given the stoichiometric decomposition reaction as $C_6N_6O_{12} \rightarrow 3N_2 + 6CO_2$, and taking the standard heats of formation as -393.5 kJ/mole for CO₂ (http://www.update.uu.se/~jolkkonen/pdf/CRC_TD.pdf) and +200 kJ/mole for C₆N₆O₁₂ (Talawar MB, *et al.* Novel ultrahigh-energy materials. *Combust Explos Shock Waves* 2005;41:264-277; http://www14.atpages.jp/highenergy/hb_jx/File-hb-005-CESW2005-EMs.pdf), the decomposition energy is 2.56×10^6 J/mole.

Hexanitrostilbene ¹⁹⁹¹	2.55×10^6	0.450	2.65×10^{-4}
HHTDD ¹⁹⁹²	2.72×10^6	0.468	2.26×10^{-4}
HMTD ¹⁹⁹³	1.09×10^6	0.208	2.36×10^{-4}
HMX ¹⁹⁹⁴	1.83×10^6	0.296	1.55×10^{-4}
HNF ¹⁹⁹⁵	9.26×10^5	0.183	9.84×10^{-5}

¹⁹⁹⁰ Hexanitroprismane, aka. 1,2,3,4,5,6-hexanitroprismane ($C_6(NO_2)_6$ or $C_6N_6O_{12}$, 0.348 kg/mole, $1.74 \times 10^{-4} \text{ m}^3/\text{mole}$) is perfectly oxygen balanced and will decompose according to $C_6N_6O_{12} \rightarrow 3N_2 + 6CO_2$ releasing $3.39 \times 10^6 \text{ J/mole}$ (taking the estimated heat of formation for $C_6N_6O_{12}$ as $+1026.13 \text{ kJ/mole}$; Chi WJ, Li LL, Li BT, Wu HS. Density functional calculations for a high energy density compound of formula $C_6H_6-n(NO_2)_n$. J Mol Model. 2012 Aug;18(8):3695-704; <http://www.ncbi.nlm.nih.gov/pubmed/22382574>). This molecule had not yet been synthesized as of 2016.

¹⁹⁹¹ 2,2',4,4',6,6'-hexanitrostilbene, aka. HNS, JD-X or 1,3,5-trinitro-2-[2-(2,4,6-trinitrophenyl)ethenyl]benzene ($(C_6H_2)_2(CH)_2(NO_2)_6$ or $C_{14}H_6N_6O_{12}$, 0.450 kg/mole, $2.65 \times 10^{-4} \text{ m}^3/\text{mole}$; <https://en.wikipedia.org/wiki/Hexanitrostilbene>) is a heat-resistant high explosive reportedly used in achieving stage separation in space rockets and also as a component of heat-resistant compositions employed in the Apollo spaceship and for seismic experiments on the moon. Taking the decomposition reaction as: $C_{14}H_6N_6O_{12} \rightarrow 3N_2 + 4.5CO_2 + 3H_2O + 9.5C$, and taking the standard heats of formation as -393.5 kJ/mole for CO_2 and -241.8 kJ/mole for H_2O (http://www.update.uu.se/~jolkkonen/pdf/CRC_TD.pdf) and $+58 \text{ kJ/mole}$ for $C_{14}H_6N_6O_{12}$ (Agrawal JP. High Energy Materials: Propellants, Explosives and Pyrotechnics, John Wiley & Sons, 2015, Table 1.5, p. 26), the decomposition energy is $2.55 \times 10^6 \text{ J/mole}$ of $C_{14}H_6N_6O_{12}$.

¹⁹⁹² HHTDD, aka. Ex144 or octahydro-1,3,4,5,7,8-hexanitro-diimidazo[4,5-b:4',5'-e]pyrazine-2,6(1H,3H)-dione ($C_6H_4N_{12}O_{14}$, 0.468 kg/mole, 2070 kg/m^3 , and heat of explosion is 5.81 MJ/kg or $2.72 \times 10^6 \text{ J/mole}$ (<http://www.sciencemadness.org/talk/viewthread.php?tid=5997#pid150672>). HHTDD “is a powerful but moisture sensitive explosive compound with detonation velocity even higher than that of CL-20, but readily decomposes in the presence of even trace amounts of water” (<https://en.wikipedia.org/wiki/HHTDD>).

¹⁹⁹³ HMTD, aka. hexamethylene triperoxide diamine or hexamine peroxide ($C_6H_{12}N_2O_6$, 0.208 kg/mole, $2.36 \times 10^{-4} \text{ m}^3/\text{mole}$ at 880 kg/m^3 ; https://en.wikipedia.org/wiki/Hexamethylene_triperoxide_diamine), taking the ideal decomposition reaction as: $C_6H_{12}N_2O_6 \rightarrow N_2 + 6H_2O + 6C$, and taking the standard heats of formation as -241.8 kJ/mole for H_2O (http://www.update.uu.se/~jolkkonen/pdf/CRC_TD.pdf) and -360 kJ/mole for $C_6H_{12}N_2O_6$ (<https://books.google.com/books?id=hX3mBgAAQBAJ&pg=PA519>), releases $1.09 \times 10^6 \text{ J/mole}$ of $C_6H_{12}N_2O_6$. HMTD is sometimes called a “peroxo-based homemade explosive” because of its ease of manufacture.

¹⁹⁹⁴ HMX, aka. “high melting explosive,” octogen, tetranitro tetramethylene cyclooctane, or cyclotetramethylene-tetranitramine, or $((CH_2)_4(NNO_2)_4$ or $C_4H_8N_8O_8$, 0.296 kg/mole, $1.55 \times 10^{-4} \text{ m}^3/\text{mole}$ at 1910 kg/m^3 ; <https://en.wikipedia.org/wiki/HMX>) is one of the most potent chemical explosives. Taking the decomposition reaction as: $C_4H_8N_8O_8 \rightarrow 4N_2 + 2CO_2 + 4H_2O + 2C$, and taking the standard heats of formation as -393.5 kJ/mole for CO_2 and -241.8 kJ/mole for H_2O (http://www.update.uu.se/~jolkkonen/pdf/CRC_TD.pdf) and $+75 \text{ kJ/mole}$ for $C_4H_8N_8O_8$ (Agrawal JP. High Energy Materials: Propellants, Explosives and Pyrotechnics, John Wiley & Sons, 2015, Table 1.5, p. 26), the decomposition energy is $1.83 \times 10^6 \text{ J/mole}$ of $C_4H_8N_8O_8$.

HNO ₂ (theoretical) ¹⁹⁹⁶	3.97 x 10 ⁵	0.047	---
HN ₃ O (theoretical) ¹⁹⁹⁷	5.99 x 10 ⁵	0.059	---
Hydrazine mononitrate ¹⁹⁹⁸	3.64 x 10 ⁵	0.095	5.79 x 10 ⁻⁵
Hydroperoxymethane ¹⁹⁹⁹	3.46 x 10 ⁵	0.048	4.81 x 10 ⁻⁵
Hydroxylammonium azidotetrazolate ²⁰⁰⁰	6.83 x 10 ⁵	0.144	8.73 x 10 ⁻⁵
Krypton hydrogen fluoride (theoretical) ²⁰⁰¹	4.783 x 10 ⁵	0.104	---
Lead styphnate ²⁰⁰²	7.62 x 10 ⁵	0.450	1.55 x 10 ⁻⁴

¹⁹⁹⁵ Hydrazinium nitroformate, aka. HNF (N₂H₅⁺C(NO₂)₃⁻ or CH₅N₅O₆, 0.183 kg/mole, density 1860 kg/m³, heat of formation -72.0 kJ/mole (Sarner HF. Propellant Chemistry, Reinhold Publishing, 1966; http://yarchive.net/space/rocket/fuels/hydrazinium_nitroformate.html) is a yellow crystalline solid with moderate friction- and thermal sensitivity. A stoichiometric decomposition as: CH₅N₅O₆ → 2.5N₂ + CO₂ + 2.5H₂O + 0.75O₂, taking standard heats of formation as -393.5 kJ/mole for CO₂ and -241.8 kJ/mole for H₂O (http://www.update.uu.se/~jolkkonen/pdf/CRC_TD.pdf), releases 9.26 x 10⁵ J/mole of HNF.

¹⁹⁹⁶ HNO₂ (0.047 kg/mole) has been considered theoretically at the SCF/6-31G* level of theory and appears to be stable with a specific enthalpy of 8.44 MJ/kg (Brener NE, Kestner NR, Callaway J. Theoretical studies of highly energetic CBES materials. AL-TR-90-060, Dec 1990, Table 2, p. 8; <http://www.dtic.mil/dtic/tr/fulltext/u2/a231340.pdf>).

¹⁹⁹⁷ HN₃O (0.059 kg/mole) has been considered theoretically at the SCF/6-31G* level of theory and appears to be stable with a specific enthalpy of 10.15 MJ/kg (Brener NE, Kestner NR, Callaway J. Theoretical studies of highly energetic CBES materials. AL-TR-90-060, Dec 1990, Table 2, p. 8; <http://www.dtic.mil/dtic/tr/fulltext/u2/a231340.pdf>).

¹⁹⁹⁸ Hydrazine mononitrate, aka. hydrazine nitrate (H₅N₃O₃, 0.095 kg/mole, 5.79 x 10⁻⁵ m³/mole at 1640 kg/m³) explodes at 580 K and has an explosion heat of 3.829 MJ/kg, or 3.64 x 10⁵ J/mole; https://en.wikipedia.org/wiki/Hydrazine_nitrate.

¹⁹⁹⁹ Hydroperoxymethane, aka. methyl hydroperoxide (CH₃OOH or CH₄O₂, 0.048 kg/mole, 997 kg/m³; <http://www.syntechem.com/prod/STP216879/>) if undergoing a stoichiometric combustion (CH₄O₂ → 2H₂O + C) would release 3.46 x 10⁵ J/mole of CH₄O₂, taking the standard heats of formation as -241.8 kJ/mole for H₂O (http://www.update.uu.se/~jolkkonen/pdf/CRC_TD.pdf) and -138.1 kJ/mole for CH₄O₂ (<https://www3.nd.edu/~powers/ame.60636/baulch2005.pdf>).

²⁰⁰⁰ Hydroxylammonium azidotetrazolate, aka. HxAzTz (CH₄N₈O, 0.144 kg/mole, 1649 kg/m³, heat of formation +608.8 kJ/mole)* if decomposing efficiently (CH₄N₈O → 4N₂ + CH₄ + 0.5O₂) should release 6.83 x 10⁵ J/mole, taking the standard heat of formation as -74.6 kJ/mole for CH₄ (http://www.update.uu.se/~jolkkonen/pdf/CRC_TD.pdf). *Klapotke TM, *et al.* The taming of CN₇⁻: the azidotetrazolate 2-oxide anion. Chem Euro J 2011;17:13068-13077; https://edoc.ub.uni-muenchen.de/15389/1/Piercey_Davin.pdf#page=160.

²⁰⁰¹ Krypton hydrogen fluoride (HKrF, 0.104 kg/mole) has not been synthesized experimentally but has been predicted theoretically to be a metastable chemically-bonded molecule with a +145.0 kJ/mole (+1.50 eV) barrier to decomposition and a decomposition energy of 4.783 x 10⁵ J/mole via the reaction HKrF → HF + Kr (Wong MW. Prediction of a metastable helium compound: HHeF. J Am Chem Soc 2000 Jul 5;122(26):6289-90; <http://140.123.79.88/~ppmpk/paper/44.pdf>).

LLM-105 ²⁰⁰³	1.24×10^6	0.216	1.13×10^{-4}
Mannitol hexanitrate ²⁰⁰⁴	2.65×10^6	0.452	2.61×10^{-4}
MEKP ²⁰⁰⁵	1.19×10^6	0.210	1.79×10^{-4}
Mercury fulminate ²⁰⁰⁶	6.07×10^5	0.285	6.44×10^{-5}
Methylammonium nitrate ²⁰⁰⁷	3.977×10^5	0.094	6.62×10^{-5}

²⁰⁰² Lead styphnate, aka. lead tricininate, lead trinitroresorcinat (PbC₆HN₃O₈, 0.450 kg/mole, 1.55×10^{-4} m³/mole; https://en.wikipedia.org/wiki/Lead_styphnate) is an explosive used as a component in primer and detonator mixtures. Taking the stoichiometric decomposition reaction as PbC₆HN₃O₈ → 1.5N₂ + 3.75CO₂ + 0.5H₂O + 2.25C + Pb, and taking the standard heats of formation as -393.5 kJ/mole for CO₂ and -241.8 kJ/mole for H₂O (http://www.update.uu.se/~jolkkonen/pdf/CRC_TD.pdf) and -835 kJ/mole for PbC₆HN₃O₈ (https://en.wikipedia.org/wiki/Lead_styphnate), the decomposition energy is 7.62×10^5 J/mole of PbC₆HN₃O₈.

²⁰⁰³ LLM-105, aka. ANPZO or 2,6-diamino-3,5-dinitropyrazine-1-oxide (C₄H₄N₆O₅, 0.216 kg/mole, 1.13×10^{-4} m³/mole; <http://www.sciencedirect.com/science/article/pii/S2214914714000774>) is said to possess 81% of the energy of HMX (<http://www.osti.gov/scitech/servlets/purl/672328>) or 0.81×7.11 MJ/kg = 5.76 MJ/kg, or 1.24×10^6 J/mole.

²⁰⁰⁴ Mannitol hexanitrate, aka. MHN, nitromannite, nitromannitol, Nitranitol, or Mannitrin (C₆H₈N₆O₁₈, 0.452 kg/mole, 2.61×10^{-4} m³/mole; https://en.wikipedia.org/wiki/Mannitol_hexanitrate) is a secondary explosive more stable than nitroglycerin, used in detonators. Taking the stoichiometric decomposition reaction as C₆H₈N₆O₁₈ → 3N₂ + 6CO₂ + 4H₂O + O₂, and taking the standard heats of formation as -393.5 kJ/mole for CO₂ and -241.8 kJ/mole for H₂O (http://www.update.uu.se/~jolkkonen/pdf/CRC_TD.pdf) and -675.7 kJ/mole for C₆H₈N₆O₁₈ (http://www.academia.edu/8708518/Prediction_of_heat_of_formation_and_related_parameters_of_high_energy_materials), the decomposition energy is 2.65×10^6 J/mole of C₆H₈N₆O₁₈.

²⁰⁰⁵ MEKP, aka. methyl ethyl ketone peroxide (C₈H₁₈O₆, 0.210 kg/mole, 1170 kg/m³) is a colorless oily liquid and high explosive similar to acetone peroxide (https://en.wikipedia.org/wiki/Methyl_ethyl_ketone_peroxide). MEKP is sometimes called a “peroxo-based homemade explosive” because of its ease of manufacture. Taking the stoichiometric decomposition reaction as C₈H₁₈O₆ → 6H₂O + 1.5CH₄ + 6.5C, and taking the standard heats of formation as -241.8 kJ/mole for H₂O and -74.6 kJ/mole for CH₄ (http://www.update.uu.se/~jolkkonen/pdf/CRC_TD.pdf) and -372.4 kJ/mole for C₈H₁₈O₆ (http://digitalcommons.wayne.edu/cgi/viewcontent.cgi?article=2371&context=oa_dissertations), the decomposition energy is 1.19×10^6 J/mole of C₈H₁₈O₆.

²⁰⁰⁶ Mercury fulminate (Hg(CNO)₂, 0.285 kg/mole, 6.44×10^{-5} m³/mole) is highly sensitive to friction and shock, and is mainly used as a trigger for other explosives in percussion caps and blasting caps ([https://en.wikipedia.org/wiki/Mercury\(II\)_fulminate](https://en.wikipedia.org/wiki/Mercury(II)_fulminate)). Explosive decomposition to mercury, nitrogen, and carbon dioxide releases 6.07×10^5 J/mole, taking the heat of formation as +386 kJ/mole (Agrawal JP. High Energy Materials: Propellants, Explosives and Pyrotechnics, John Wiley & Sons, 2015, Table 1.5, p. 26).

²⁰⁰⁷ Methylammonium nitrate, aka. MAN, methanaminium nitrate, methylamine nitrate, or monomethylamine nitrate ([H₃C-NH₃]⁺[NO₃]⁻ or CH₆N₂O₃, 0.094 kg/mole, 1420 kg/m³) is an explosive first used in World War II (https://en.wikipedia.org/wiki/Methylammonium_nitrate) and has a measured decomposition energy of 1011.2 cal/gm or 397.7 kJ/mole, with an activation energy of 59.8 kJ/mole (Hershkowitz J, Akst I. A new approach to improving the performance of non-ideal explosives containing ammonium nitrate, Picatinny Arsenal, Dover NJ, Technical Report 4789, March 1975, pp. 34, 46; <http://www.dtic.mil/cgi-bin/GetTRDoc?Location=U2&doc=GetTRDoc.pdf&AD=ADB004532>).

Methylene dinitramine ²⁰⁰⁸	9.25×10^5	0.136	8.82×10^{-5}
MTO3N (theoretical) ²⁰⁰⁹	5.907×10^6	1	4.76×10^{-4}
NAATO (theoretical) ²⁰¹⁰	1.52×10^6	0.224	1.18×10^{-4}
Nitramide ²⁰¹¹	1.523×10^5	0.062	4.50×10^{-5}
Nitrocellulose ²⁰¹²	1.61×10^6	0.297	1.80×10^{-4}
Nitroglycerine ²⁰¹³	1.41×10^6	0.227	1.42×10^{-4}
Nitroguanidine ²⁰¹⁴	3.89×10^5	0.104	6.09×10^{-5}

²⁰⁰⁸ Methylene dinitramine, aka. MEDINA, methylene dinitroamine, N,N'-dinitromethanediamine, or 1,3-dinitro-1,3-diazapropane ($\text{O}_2\text{N-NH-CH}_2\text{-NH-NO}_2$ or $\text{CH}_4\text{N}_4\text{O}_4$, 0.136 kg/mole, 8.82×10^{-5} m³/mole; <http://www.lookchem.com/Methylene-dinitramine/>) explodes when heated to 490 K. The “heat of combustion” where no oxygen need be added ($\text{CH}_4\text{N}_4\text{O}_4 \rightarrow 2\text{N}_2 + \text{CO}_2 + 2\text{H}_2\text{O}$) was measured* as 6.803 MJ/kg, or 9.25×10^5 J/mole. *Helf S, Ottoson KG. Test of Explosive Compounds. Technical Report ARMET-TR-10015, Oct 1949; <http://handle.dtic.mil/100.2/ADA526427>.

²⁰⁰⁹ 2,4,6-trinitro-1,3,5-triazine-1,3,5-trioxide, aka. MTO3N, is predicted to have a density of 2100 kg/m³ and a decomposition reaction energy of 5.907 MJ/kg (Naserifar S, *et al.* Prediction of structures and properties of 2,4,6-triamino-1,3,5-triazine-1,3,5-trioxide (MTO) and 2,4,6-trinitro-1,3,5-triazine-1,3,5-trioxide (MTO3N) green energetic materials from DFT and ReaxFF molecular modeling. J Mater Chem A 2016;4:1264-1276; <http://pubs.rsc.org/en/content/articlelanding/2016/TA/c5ta06426k>).

²⁰¹⁰ NAATO, aka. planar 1,2,3,4,5,6,7,8,9-nonaaazacycl[3.3.3]azine-2,5,8-trioxides ($\text{C}_3\text{N}_{10}\text{O}_3$, 0.224 kg/mole, 1900 kg/m³) upon detonation is predicted to release a total explosive energy of 1.52×10^6 J/mole (Wu Q, *et al.* Improving an insensitive low-energy compound, 1,3,4,6,7,9-hexaazacycl[3.3.3]azine, to be an insensitive high explosive by way of two-step structural modifications. Can J Chem 2014;92:1157-1161; http://www.nrcresearchpress.com/doi/abs/10.1139/cjc-2014-0396#.V_hT08mZPuN).

²⁰¹¹ Nitramide, aka. nitramine ($\text{H}_2\text{N-NO}_2$ or $\text{H}_2\text{N}_2\text{O}_2$, 0.062 kg/mole, 1378 kg/m³; http://www.chemsrc.com/en/cas/7782-94-7_283885.html) is a colorless solid explosive that can decompose according to $\text{H}_2\text{N}_2\text{O}_2 \rightarrow \text{N}_2 + \text{H}_2\text{O} + 0.5\text{O}_2$, releasing 1.523×10^5 J/mole, taking standard heats of formation as -89.5 kJ/mole for solid nitramide and -241.8 kJ/mole for H₂O (http://www.update.uu.se/~jolkkonen/pdf/CRC_TD.pdf).

²⁰¹² Nitrocellulose, aka. guncotton, NC, cellulose nitrate, flash cotton, flash paper, or flash string (e.g., $\text{C}_6\text{H}_7(\text{NO}_2)_3\text{O}_5$, 0.297 kg/mole, 1.80×10^{-4} m³/mole at density of 1650 kg/m³) is a highly flammable compound formed by nitrating cellulose via exposure to nitric acid or other powerful nitrating agents. Nitrocellulose needs no air to keep burning as the reaction produces oxygen (<https://en.wikipedia.org/wiki/Nitrocellulose>). Taking the stoichiometric decomposition reaction as $\text{C}_6\text{H}_7\text{N}_3\text{O}_{11} \rightarrow 1.5\text{N}_2 + 3.75\text{CO}_2 + 3.5\text{H}_2\text{O} + 2.25\text{C}$, and taking the standard heats of formation as -393.5 kJ/mole for CO₂ and -241.8 kJ/mole for H₂O (http://www.update.uu.se/~jolkkonen/pdf/CRC_TD.pdf), and -708.0 kJ/mole for $\text{C}_6\text{H}_7\text{N}_3\text{O}_{11}$ (Wallin S, *et al.* High Energy Density Materials Efforts to synthesize the pentazolate anion: Part 1, Technical Report FOI-R-1602-SE, March 2005; http://foi.se/ReportFiles/foir_1602.pdf), the decomposition energy is 1.61×10^6 J/mole.

²⁰¹³ Nitroglycerine, aka. NG, trinitroglycerin (TNG), nitro, glyceryl trinitrate (GTN), or 1,2,3-trinitropropane ($\text{C}_3\text{H}_5(\text{ONO}_2)_3$ or $\text{C}_3\text{H}_5\text{N}_3\text{O}_9$, 0.227 kg/mole, 1.42×10^{-4} m³/mole) was the first practical explosive produced that was stronger than black powder. Taking the decomposition reaction as: $\text{C}_3\text{H}_5\text{N}_3\text{O}_9 \rightarrow 1.5\text{N}_2 + 3\text{CO}_2 + 2.5\text{H}_2\text{O} + 0.25\text{O}_2$, and taking the standard heats of formation as -393.5 kJ/mole for CO₂ and -241.8 kJ/mole for H₂O (http://www.update.uu.se/~jolkkonen/pdf/CRC_TD.pdf) and -380 kJ/mole for $\text{C}_3\text{H}_5\text{N}_3\text{O}_9$ (Agrawal JP. High Energy Materials: Propellants, Explosives and Pyrotechnics, John Wiley & Sons, 2015, Table 1.5, p. 26), the decomposition energy is 1.41×10^6 J/mole of $\text{C}_3\text{H}_5\text{N}_3\text{O}_9$.

Nitrourea ²⁰¹⁵	3.894×10^5	0.105	6.74×10^{-5}
NONA ²⁰¹⁶	2.229×10^6	0.635	3.56×10^{-4}
NTO (nitrotriazolon) ²⁰¹⁷	5.06×10^5	0.130	6.81×10^{-5}
ONC (octanitrocubane) ²⁰¹⁸	4.81×10^6	0.464	2.34×10^{-4}
PETN ²⁰¹⁹	1.98×10^6	0.316	1.78×10^{-4}

²⁰¹⁴ Nitroguanidine, aka. NQ, picrite, N-nitro-guanidine ($C=NHNH_2NHNO_2$ or $CH_4N_4O_2$, 0.104 kg/mole, 6.09×10^{-5} m³/mole; <https://en.wikipedia.org/wiki/Nitroguanidine>) is an explosive used in automobile airbags. Taking the decomposition reaction as: $CH_4N_4O_2 \rightarrow 2N_2 + 2H_2O + C$, and taking the standard heats of formation as -241.8 kJ/mole for H₂O (http://www.update.uu.se/~jolkkonen/pdf/CRC_TD.pdf) and -95 kJ/mole for CH₄N₄O₂ (Agrawal JP. High Energy Materials: Propellants, Explosives and Pyrotechnics, John Wiley & Sons, 2015, Table 1.5, p. 26), the decomposition energy is 3.89×10^5 J/mole of CH₄N₄O₂.

²⁰¹⁵ Nitrourea, aka. N-nitrourea, 1-nitrourea, or N-nitrocarbamide ($CH_3N_3O_3$, 0.105 kg/mole, 1557 kg/m³; http://www.chemsrc.com/en/cas/556-89-8_954381.html) is an explosive compound that degrades quickly in contact with moisture, thus is not widely used commercially. Taking the decomposition reaction as: $CH_3N_3O_3 \rightarrow 1.5N_2 + 0.75CO_2 + 1.5H_2O + 0.25C$, and taking the standard heats of formation as -393.5 kJ/mole for CO₂, -241.8 kJ/mole for H₂O (http://www.update.uu.se/~jolkkonen/pdf/CRC_TD.pdf), and -268.4 kJ/mole for CH₃N₃O₃ (<https://engineering.purdue.edu/~propulsi/propulsion/comb/propellants.html>), the decomposition energy is 3.894×10^5 J/mole for CH₃N₃O₃.

²⁰¹⁶ NONA, aka. 2,2',2''-4,4',4''-6,6',6''-nonanitroterphenyl ($C_{18}H_5N_9O_{18}$, 0.635 kg/mole, 1780 kg/m³, heat of formation +132.2 kJ/mole) decomposes explosively with the release of 839 kcal/kg or 2.229×10^6 J/mole of NONA (<http://www.ocsresponds.com/ref/hazlist/TechSpecs.pdf>).

²⁰¹⁷ Nitrotriazolon, aka. NTO, oxynitrotriazol (ONTA), or 3-nitro-1,2,4-triazol-5-one ($C_2H_2N_4O_3$, 0.130 kg/mole, 6.81×10^{-5} m³/mole, heat of formation -129.5 kJ/mole; <https://de.wikipedia.org/wiki/Nitrotriazolon>) is an explosive additive that can reduce sensitivity, but not performance, of the mixture when cast with TNT or IMX explosives. Taking the decomposition reaction as: $C_2H_2N_4O_3 \rightarrow 2N_2 + CO_2 + H_2O + C$, and taking the standard heats of formation as -393.5 kJ/mole for CO₂ and -241.8 kJ/mole for H₂O (http://www.update.uu.se/~jolkkonen/pdf/CRC_TD.pdf), the decomposition energy is 5.06×10^5 J/mole of C₂H₂N₄O₃.

²⁰¹⁸ Octanitrocubane, aka. ONC or 8-CUB ($C_8(NO_2)_8$ or $C_8N_8O_{16}$, 0.464 kg/mole, 2.21×10^{-4} m³/mole at a density of 1980 kg/m³ for the most stable polymorph of ONC) has the same chemical structure as cubane (C_8H_8) except that each of the eight hydrogen atoms is replaced by a nitro group (NO₂) (<https://en.wikipedia.org/wiki/Octanitrocubane>). Given the perfectly oxygen-balanced decomposition reaction: $C_8N_8O_{16} \rightarrow 4N_2 + 8CO_2$, and taking the standard heats of formation as -393.5 kJ/mole for CO₂ (http://www.update.uu.se/~jolkkonen/pdf/CRC_TD.pdf) and +594 kJ/mole for C₈N₈O₁₆ (Astakhov AM, Stepanov RS, Babushkin AY. On the detonation parameters of octanitrocubane. Combust Explos Shock Waves 1998;34(1):85-87; <http://link.springer.com/article/10.1007/BF02671823>), the decomposition energy is 3.72×10^6 J/mole plus 1093 kJ/mole of "conventional ring strain energy" (Bumpus JA. A Theoretical Investigation of the Ring Strain Energy, Destabilization Energy, and Heat of Formation of CL-20. Adv Phys Chem 2012;175146; <http://downloads.hindawi.com/journals/apc/2012/175146.pdf>). A proposed alternative synthesis pathway for ONC (<https://apps.dtic.mil/dtic/tr/fulltext/u2/a364287.pdf>) leads through the cyclooligomerization of dinitroacetylene ($O_2N-C\equiv C-NO_2$), an even more unstable compound that has yet to be synthesized (Dewar MJS. Dinitroacetylene and related compounds. DTIC Final Report DAAG29-81-K-0008, 20 Apr 1983; <https://apps.dtic.mil/dtic/tr/fulltext/u2/a128954.pdf>. Windler GK, Zhang MX, Zitterbart R, Pagoria PF, Vollhardt KP. En route to dinitroacetylene: nitro(trimethylsilyl)acetylene and nitroacetylene harnessed by dicobalt hexacarbonyl. Chemistry. 2012 May 21;18(21):6588-603; <https://onlinelibrary.wiley.com/doi/abs/10.1002/chem.201200473>).

sil-a-PETN ²⁰²⁰	1.49 x 10 ⁶	0.332	2.00 x 10 ⁻⁴
PETNC ²⁰²¹	2.11 x 10 ⁶	0.488	2.77 x 10 ⁻⁴
sil-a-PETNC ²⁰²²	1.70 x 10 ⁶	0.504	3.07 x 10 ⁻⁴
Picric acid ²⁰²³	1.22 x 10 ⁶	0.229	1.30 x 10 ⁻⁴

²⁰¹⁹ Pentaerythritol tetranitrate, aka. PETN, PENT, PENTA, TEN, corpent, penthrite, or Nitropenta, and the detonating cords Cordtex and Primacord (C(CH₂)₄(ONO₂)₄ or C₅H₈N₄O₁₂, 0.316 kg/mole, 1.78 x 10⁻⁴ m³/mole at 1780 kg/m³) is structurally similar to nitroglycerin and is claimed to be one of the most powerful explosive materials known (https://en.wikipedia.org/wiki/Pentaerythritol_tetranitrate). The well-known plastic explosive Semtex is a mixture of PETN (41%-76%) and RDX (41%-5%), plus plasticizer (<https://en.wikipedia.org/wiki/Semtex>). Taking the decomposition reaction as: C₅H₈N₄O₁₂ → 2N₂ + 4CO₂ + 4H₂O + C, and taking the standard heats of formation as -393.5 kJ/mole for CO₂ and -241.8 kJ/mole for H₂O (http://www.update.uu.se/~jolkkonen/pdf/CRC_TD.pdf) and -561 kJ/mole for C₅H₈N₄O₁₂ (Axthammer QJ, *et al.* Energetic Sila-Nitrocarbamates: Silicon Analogues of Neo-Pentane Derivatives. Inorg Chem 2016;55:4683-4692; <http://pubs.acs.org/doi/abs/10.1021/acs.inorgchem.6b00602>), the decomposition energy is 1.98 x 10⁶ J/mole of C₅H₈N₄O₁₂.

²⁰²⁰ The silicon analog to PETN (C₄H₈N₄O₁₂Si, 0.332 kg/mole, 2.00 x 10⁻⁴ m³/mole at density 1660 kg/m³), if fully decomposed for maximum energy according to: C₄H₈N₄O₁₂Si → 2N₂ + 3CO₂ + 4H₂O + SiO₂ + C, and taking the standard heats of formation as -393.5 kJ/mole for CO₂, -241.8 kJ/mole for H₂O, and -910.7 for SiO₂ (http://www.update.uu.se/~jolkkonen/pdf/CRC_TD.pdf) and -1568 kJ/mole for C₄H₈N₄O₁₂Si (Axthammer QJ, *et al.* Energetic Sila-Nitrocarbamates: Silicon Analogues of Neo-Pentane Derivatives. Inorg Chem 2016;55:4683-4692; <http://pubs.acs.org/doi/abs/10.1021/acs.inorgchem.6b00602>), the decomposition energy is 1.49 x 10⁶ J/mole of C₄H₈N₄O₁₂Si.

²⁰²¹ Pentaerythritol tetranitrocarbamate, aka. PETNC (C₉H₁₂N₈O₁₆, 0.488 kg/mole, 2.77 x 10⁻⁴ m³/mole at density 1760 kg/m³) “shows an increased thermal stability as well as lower sensitivities against friction and impact” compared to PETN. If PETNC is fully decomposed for maximum energy according to: C₉H₁₂N₈O₁₆ → 4N₂ + 5CO₂ + 6H₂O + 4C, and taking the standard heats of formation as -393.5 kJ/mole for CO₂ and -241.8 kJ/mole for H₂O (http://www.update.uu.se/~jolkkonen/pdf/CRC_TD.pdf) and -1311 kJ/mole for C₉H₁₂N₈O₁₆ (Axthammer QJ, *et al.* Energetic Sila-Nitrocarbamates: Silicon Analogues of Neo-Pentane Derivatives. Inorg Chem 2016;55:4683-4692; <http://pubs.acs.org/doi/abs/10.1021/acs.inorgchem.6b00602>), the detonation energy is 2.11 x 10⁶ J/mole of PETNC.

²⁰²² The silicon analog to PETNC (C₈H₁₂N₈O₁₆Si, 0.504 kg/mole, 3.07 x 10⁻⁴ m³/mole at density 1640 kg/m³), if fully decomposed for maximum energy according to: C₈H₁₂N₈O₁₆Si → 4N₂ + 4CO₂ + 6H₂O + SiO₂ + 4C, and taking the standard heats of formation as -393.5 kJ/mole for CO₂, -241.8 kJ/mole for H₂O, and -910.7 for SiO₂ (http://www.update.uu.se/~jolkkonen/pdf/CRC_TD.pdf) and -2240 kJ/mole for C₈H₁₂N₈O₁₆Si (Axthammer QJ, *et al.* Energetic Sila-Nitrocarbamates: Silicon Analogues of Neo-Pentane Derivatives. Inorg Chem 2016;55:4683-4692; <http://pubs.acs.org/doi/abs/10.1021/acs.inorgchem.6b00602>), the decomposition energy is 1.70 x 10⁶ J/mole of C₈H₁₂N₈O₁₆Si.

²⁰²³ Picric acid, aka. 2,4,6-trinitrophenol or TNP (C₆H₂(NO₂)₃OH or C₆H₃N₃O₇, 0.229 kg/mole, 1.30 x 10⁻⁴ m³/mole; https://en.wikipedia.org/wiki/Picric_acid) is an explosive sensitive to shock and friction. Taking the decomposition reaction as: C₆H₃N₃O₇ → 1.5N₂ + 2.75CO₂ + 1.5H₂O + 3.25C, and taking the standard heats of formation as -393.5 kJ/mole for CO₂ and -241.8 kJ/mole for H₂O (http://www.update.uu.se/~jolkkonen/pdf/CRC_TD.pdf) and -224 kJ/mole for C₆H₃N₃O₇ (Agrawal JP. High Energy Materials: Propellants, Explosives and Pyrotechnics, John Wiley & Sons, 2015, p. 25; <https://books.google.com/books?id=z25cCwAAQBAJ&pg=PA25>), the decomposition energy is 1.22 x 10⁶ J/mole of C₆H₃N₃O₇.

Polymeric CNO (theoretical) ²⁰²⁴	2.2×10^6	1	5×10^{-4}
Polymeric CO ²⁰²⁵	8×10^6	1	6.06×10^{-4}
Prismane ²⁰²⁶	5.672×10^5	0.0781	4.88×10^{-5}
Propyne (methylacetylene) ²⁰²⁷	2.10×10^5	0.0401	7.57×10^{-5}
PYX ²⁰²⁸	3.375×10^6	0.621	3.51×10^{-4}
RDX ²⁰²⁹	1.38×10^6	0.222	1.22×10^{-4}

²⁰²⁴ At high pressure, CO catalyzes the molecular dissociation of N₂, allowing a polymeric form of (CNO)_n to form above 52 GPa. At ambient pressure, the metastable polymer is expected to decompose exothermically as: $4\text{CNO} \rightarrow 2\text{CO}_2 + 2\text{C} + 2\text{N}_2 + 4.1 \text{ eV}$, corresponding to a specific energy of 2.2 MJ/kg, according to one theoretical analysis (Raza Z, Pickard CJ, Pinilla C, Saitta AM. A High Energy Density Mixed Polymeric Phase From Carbon Monoxide and Nitrogen. Phys Rev Lett. 2013;111:235501; https://www.researchgate.net/profile/Zamaan_Raza/publication/259984326_High_Energy_Density_Mixed_Polymeric_Phase_from_Carbon_Monoxide_and_Nitrogen/links/00b7d52a1c0cc23a64000000.pdf). A CNO polymer density of $\sim 2000 \text{ kg/m}^3$ would imply an energy density of $\sim 4.4 \text{ MJ/liter}$.

²⁰²⁵ Carbon monoxide gas has a metastable solid phase that forms at 5 GPa and 300 K, which can be recovered to ambient conditions. Polymeric CO is an orange-yellow solid with density 1650 kg/m^3 , which decomposes steadily while releasing CO₂ and at an increased rate when exposed to light, becoming sticky after exposure to air for several days. Solid p-CO explosively decomposes to CO₂ and a small residue of glassy carbon, with measured detonation energy density up to 8 MJ/kg. “p-CO could be synthesized in carbon foam to reduce its sensitivity, similar to the way highly sensitive TNT was developed into dynamite.” Lipp MJ, Evans WJ, Baer BJ, Yoo CS. High-energy-density extended CO solid. Nat Mater. 2005 Mar;4(3):211-5; https://www.researchgate.net/profile/William_Evans9/publication/8020770_High-energy-density_extended_CO_solid/links/0fcfd508848afe95ec000000.pdf.

²⁰²⁶ Prismane, aka. tetracyclo[2.2.0.0.2,6.0.3,5]hexane (C₆H₆, 0.0781 kg/mole, $4.88 \times 10^{-5} \text{ m}^3/\text{mole}$ taking density as 1600 kg/m^3 ; <http://www.chemspider.com/Chemical-Structure.16736515.html>), is a triangular prism with carbon atoms at the six vertices, each terminated by one hydrogen. “Prismane is a colourless liquid at room temperature. The deviation of the carbon-carbon bond angle from 109° to 60° in a triangle leads to a high ring strain, reminiscent of that of cyclopropane but greater. The compound is explosive, which is unusual for a hydrocarbon.” (<https://en.wikipedia.org/wiki/Prismane>) Decomposition to the elements yields $5.672 \times 10^5 \text{ J/mole}$, the enthalpy of formation; Allison TC, Burgess DR Jr. First-Principles Prediction of Enthalpies of Formation for Polycyclic Aromatic Hydrocarbons and Derivatives. J Phys Chem A. 2015 Nov 19;119(46):11329-65; <http://pubs.acs.org/doi/abs/10.1021/acs.jpca.5b07908>.

²⁰²⁷ Propyne, aka. methylacetylene (H-C≡C-CH₃ or C₃H₄, 0.0401 kg/mole, $7.57 \times 10^{-5} \text{ m}^3/\text{mole}$; <https://en.wikipedia.org/wiki/Propyne>) in pure form at room temperature decomposes explosively at 4.5-5.6 atm pressure,* according to: $\text{C}_3\text{H}_4 \rightarrow 2.67\text{C} + 1.33 \text{ H}_2 + 0.33 \text{ CH}_4$,** liberating $2.10 \times 10^5 \text{ J/mole}$ based on the relevant heats of formation (http://www.update.uu.se/~jolkkonen/pdf/CRC_TD.pdf). *Rutledge TF. Acetylenic Compounds: Preparation and Substitution Reactions, Reinhold Book Corp., New York, 1968. **Kuchta JM, Spolan I, Zabetakis MG. Flammability characteristics of methylacetylene, propadiene (allene), and propylene. J Chem Eng Data, 1964; 9(3):467-472; https://web.anl.gov/PCS/acsfuel/preprint%20archive/Files/07_2_NEW%20YORK_09-63_0193.pdf.

²⁰²⁸ PYX, aka. 2,6-bis(picrylamino)-3,5-dinitropyridine (C₁₇H₇N₁₁O₁₆, 0.621 kg/mole, 1770 kg/m^3 , heat of formation +69.4 kJ/mole) decomposes explosively with the release of 1299 kcal/kg or $3.375 \times 10^6 \text{ J/mole}$ of PYX (<http://www.ocsresponds.com/ref/hazlist/TechSpecs.pdf>).

Silver acetylide ²⁰³⁰	3.58×10^5	0.240	5.37×10^{-5}
Silver fulminate ²⁰³¹	3.76×10^5	0.150	3.81×10^{-5}
TACOT ²⁰³²	3.36×10^6	0.388	2.10×10^{-4}
TAG-AT ²⁰³³	1.37×10^6	0.374	2.33×10^{-4}
TATB ²⁰³⁴	1.16×10^6	0.258	1.34×10^{-4}

²⁰²⁹ RDX (Research Department Formula X), aka. cyclotrimethylene trinitramine, cyclonite, hexogen, or T4 ((CH₂)₃(NNO₂)₃ or C₃H₆N₆O₆, 0.222 kg/mole, 1.22×10^{-4} m³/mole at 1820 kg/m³; <https://en.wikipedia.org/wiki/RDX>) is a white solid widely used as an explosive. Taking the most energetic decomposition reaction as: C₃H₆N₆O₆ → 3N₂ + 1.5CO₂ + 3H₂O + 1.5C, and taking the standard heats of formation as -393.5 kJ/mole for CO₂ and -241.8 kJ/mole for H₂O (http://www.update.uu.se/~jolkkonen/pdf/CRC_TD.pdf) and +62 kJ/mole for C₃H₆N₆O₆ (Agrawal JP. High Energy Materials: Propellants, Explosives and Pyrotechnics, John Wiley & Sons, 2015, Table 1.5, p. 26), the decomposition energy is 1.38×10^6 J/mole of C₃H₆N₆O₆.

²⁰³⁰ Silver acetylide (Ag-C≡C-Ag or Ag₂C₂, 0.240 kg/mole, 5.37×10^{-5} m³/mole at 4470 kg/m³) is a heat- and shock-sensitive explosive with a detonation velocity of 4000 m/sec. It decomposes above 442 K to the elements (Ag₂C₂ → 2Ag + 2C), evolving no gases upon detonation, and releasing its 3.58×10^5 J/mole heat of formation (Matyas R, Pachman J, Primary Explosives, Spinger-Verlag, 2013, p. 304; http://link.springer.com/chapter/10.1007%2F978-3-642-28436-6_12#page-1).

²⁰³¹ Silver fulminate (AgCNO, 0.150 kg/mole, 3.81×10^{-5} m³/mole at 3938 kg/m³) is a white crystalline material that is extremely sensitive to impact, heat, pressure and electricity, with an autoignition temperature of 170 °C (https://en.wikipedia.org/wiki/Silver_fulminate). “The touch of a falling feather, the impact of a single water droplet or a small static discharge are all capable of explosively detonating an unconfined pile of silver fulminate no larger than a dime and no heavier than a few milligrams. Aggregation of larger quantities is impossible due to the compound’s tendency to self-detonate under its own weight.” Explosive decomposition to silver, nitrogen, and carbon dioxide (AgCNO → Ag + 0.5N₂ + 0.5CO₂ + 0.5C) releases 3.76×10^5 J/mole, taking the heat of formation as +179 kJ/mole (Matyas R, Pachman J, Primary Explosives, Spinger-Verlag, 2013, p. 58; <https://books.google.com/books?id=wFJHAAAQBAJ&pg=PA58>).

²⁰³² TACOT, aka. tetranitro-dibenzo-1,3a,4,4a-tetraazapentalene ((C₆H₂)₂(NO₂)₄N₄ or C₁₂H₄N₈O₈, 0.388 kg/mole, 2.10×10^{-4} m³/mole at 1850 kg/m³) heat-resistant explosive for guided missiles. Taking the ideal decomposition reaction as: C₁₂H₄N₈O₈ → 4N₂ + 3CO₂ + 2H₂O + 9C, and taking the standard heats of formation as -393.5 kJ/mole for CO₂ and -241.8 kJ/mole for H₂O (http://www.update.uu.se/~jolkkonen/pdf/CRC_TD.pdf) and +1592.8 kJ/mole for C₁₂H₄N₈O₈ (Agrawal JP. High Energy Materials: Propellants, Explosives and Pyrotechnics, John Wiley & Sons, 2015, Table 1.5, p. 26), the decomposition energy is 3.36×10^6 J/mole of C₁₂H₄N₈O₈. (One Navy report of early experiments with this explosive measured a total detonation energy of only 1.20×10^6 J/mole; “A preliminary evaluation of TACOT, a new heat resistant explosive,” Naval Ordnance Laboratory, 14 Nov 1961; <http://www.dtic.mil/dtic/tr/fulltext/u2/329452.pdf>.)

²⁰³³ TAG-AT, aka. triaminoguanidinium azotetrazolate (C₄H₁₈N₂₂, 0.374 kg/mole, 2.33×10^{-4} m³/mole at 1602 kg/m³) is a new explosive with a +1075.3 kJ/kg heat of formation (Agrawal JP. High Energy Materials: Propellants, Explosives and Pyrotechnics, John Wiley & Sons, 2015, Table 1.5, p. 143). Taking the decomposition reaction as: C₄H₁₈N₂₂ → 11N₂ + 4CH₄ + H₂, and taking the standard heat of formation as -74.6 kJ/mole for CH₄ (http://www.update.uu.se/~jolkkonen/pdf/CRC_TD.pdf), the decomposition energy is 1.37×10^6 J/mole of TAGAT.

TATP ²⁰³⁵	6.09×10^5	0.222	1.76×10^{-4}
TEGDN ²⁰³⁶	1.24×10^6	0.240	1.80×10^{-4}
Tetradecanitrobicubane (theoretical) ²⁰³⁷	3.77×10^6	0.514	2.84×10^{-4}
Tetradecanitrofullerene ²⁰³⁸	2.02×10^6	1.364	8.27×10^{-4}
Tetranitratocarbon (theoretical) ²⁰³⁹	1.326×10^6	0.308	2×10^{-4}

²⁰³⁴ 1,3,5-Triamino-2,4,6-trinitrobenzene, aka. TATB ($C_6(NH_2)_3(NO_2)_3$ or $C_6H_6N_6O_6$, 0.258 kg/mole, $1.34 \times 10^{-4} m^3/mole$; <https://en.wikipedia.org/wiki/TATB>) is an impact- and friction-insensitive explosive – TATB will not explode when burnt or hit by a shell splinter. Taking the decomposition reaction as: $C_6H_6N_6O_6 \rightarrow 3N_2 + 1.5CO_2 + 3H_2O + 4.5C$, and taking the standard heats of formation as -393.5 kJ/mole for CO_2 and -241.8 kJ/mole for H_2O (http://www.update.uu.se/~jolkkonen/pdf/CRC_TD.pdf) and -154 kJ/mole for $C_6H_6N_6O_6$ (Agrawal JP. High Energy Materials: Propellants, Explosives and Pyrotechnics, John Wiley & Sons, 2015, Table 1.5, p. 26), the decomposition energy is $1.16 \times 10^6 J/mole$ of $C_6H_6N_6O_6$.

²⁰³⁵ TATP (triacetone triperoxide), aka. acetone peroxide or TCAP (tri-cyclic acetone peroxide) ($C_9H_{18}O_6$, 0.222 kg/mole, $1.76 \times 10^{-4} m^3/mole$ at a density of $1260 kg/m^3$) is an organic peroxide and a non-nitrogenous high explosive, produced by the oxidation of acetone to yield a cyclic trimer (triacetone triperoxide or tri-cyclic acetone peroxide) that is a white crystalline powder with a distinctive bleach-like odor that can explode if subjected to heat, friction, or shock (https://en.wikipedia.org/wiki/Acetone_peroxide). TATP, aka. “white snow,” is sometimes called a “peroxo-based homemade explosive” because of its ease of manufacture (<https://info.publicintelligence.net/IslamicTerroristExplosivesManual.pdf>). The most recent calorimetric work finds that the heat of explosion for TATP is 2.745 MJ/kg or $6.09 \times 10^5 J/mole$ (Sinditskii VP, *et al.* Thermochemistry of cyclic acetone peroxides. Thermochim Acta 2014;585:10-15; http://www.academia.edu/download/40203159/Thermochemistry_of_Cyclic_Acetone_Peroxi20151120-29225-mrexf.pdf).

²⁰³⁶ Triethylene glycol dinitrate, aka. oxydiethylene dinitrate, or TEGDN ($(CH_2)_6(ONO_2)_2O_2$ or $C_6H_{12}N_2O_8$, 0.196 kg/mole, $1.39 \times 10^{-4} m^3/mole$; https://en.wikipedia.org/wiki/Triethylene_glycol_dinitrate) is used as an energetic plasticizer in explosives and propellants. Taking the decomposition reaction as: $C_6H_{12}N_2O_8 \rightarrow N_2 + CO_2 + 6H_2O + 5C$, and taking the standard heats of formation as -393.5 kJ/mole for CO_2 and -241.8 kJ/mole for H_2O (http://www.update.uu.se/~jolkkonen/pdf/CRC_TD.pdf) and -601.7 kJ/mole for $C_6H_{12}N_2O_8$ (Agrawal JP. High Energy Materials: Propellants, Explosives and Pyrotechnics, John Wiley & Sons, 2015, Table 1.5, p. 26), the decomposition energy is $1.24 \times 10^6 J/mole$ of $C_6H_{12}N_2O_8$.

²⁰³⁷ Tetradecanitrobicubane ($(NO_2)_7C_8-C_8(NO_2)_7$ or $C_{16}N_7O_{14}$, 0.514 kg/mole, estimated density $1810 kg/m^3$) is a theoretical fully-nitrated cubane dimer with an estimated +1013 kJ/mole heat of formation (Rice BM. Theoretical chemistry: Applications in energetic materials research, U.S. Army Research Laboratory, 2002; http://www.chem.missouri.edu/Thompson/MURI02/extended/Betsy_Rice.ppt). Taking the decomposition reaction as: $C_{16}N_7O_{14} \rightarrow 3.5N_2 + 7CO_2 + 9C$, and taking the standard heat of formation as -393.5 kJ/mole for CO_2 (http://www.update.uu.se/~jolkkonen/pdf/CRC_TD.pdf), the decomposition energy is $3.77 \times 10^6 J/mole$ of $C_{16}N_7O_{14}$.

²⁰³⁸ Tetradecanitrofullerene, aka. polynitro[60]fullerene ($C_{60}(NO_2)_{14}$, 1.364 kg/mole, $8.27 \times 10^{-4} m^3/mole$ assuming $\sim 1650 kg/m^3$, the same as uncompressed buckyballs) has been synthesized. It deflagrates above 443 K under nitrogen or air, and releases $2.02 \times 10^6 J/kg$ during explosive decomposition in the absence of air (Cataldo F, Ursini O, Angelini G. Synthesis and explosive decomposition of polynitro[60]fullerene. Carbon 2013 Oct;62:413-421; <http://www.sciencedirect.com/science/article/pii/S0008622313005356>).

Tetranitromethane ²⁰⁴⁰	3.70×10^5	0.196	1.21×10^{-4}
Tetranitrotetrahdrane (C ₄ (NO ₂) ₄) ²⁰⁴¹	1.13×10^6	0.232	1.8×10^{-4}
Tetrazene ²⁰⁴²	1.17×10^5	0.185	1.09×10^{-4}
Tetryl ²⁰⁴³	1.72×10^6	0.287	1.66×10^{-4}
TEX ²⁰⁴⁴	1.26×10^6	0.262	1.32×10^{-4}

²⁰³⁹ Tetranitratocarbon, aka. tetrakis(nitratocarbon)methane (C(CO₃N)₄, 0.308 kg/mole, $\sim 2 \times 10^{-4}$ m³/mole arbitrarily assuming ~ 1500 kg/m³, not yet reported) is predicted to have explosive properties but might be too thermally unstable for practical use (Zoellner RW, Lazen CL, Boehr KM. A computational study of novel nitratocarbon, nitritocarbonyl, and nitrate compounds and their potential as high energy materials. *Comput Theoret Chem* 2012 Jan 1;979:33-37; <http://www.sciencedirect.com/science/article/pii/S2210271X11005433>). The predicted decomposition reaction: C(CO₃N)₄ → 5CO₂ + O₂ + 2N₂ has a predicted enthalpy change of -1.326×10^6 J/mole (<https://en.wikipedia.org/wiki/Tetranitratocarbon>). The molecule had not been synthesized as of 2016.

²⁰⁴⁰ Tetranitromethane, aka. TNM (C(NO₂)₄, 0.196 kg/mole, 1.21×10^{-4} m³/mole; <https://en.wikipedia.org/wiki/Tetranitromethane>) has been investigated for use as an oxidizer in bipropellant rockets and has the ability to detonate with an explosive energy release of 1.89 MJ/kg (Jiping Liu, *Liquid Explosives*, Springer, 2015, p. 158), or 3.70×10^5 J/mole.

²⁰⁴¹ Tetranitrotetrahdrane (C₄(NO₂)₄, 0.232 kg/mole, $\sim 1.8 \times 10^{-4}$ m³/mole assuming the same density as cubane ~ 1290 kg/m³) had not been synthesized by 2016, but would decompose according to C₄(NO₂)₄ → 4CO₂ + 2N₂ with the release of 1.13×10^6 J/mole, taking estimated heat of formation for C₄(NO₂)₄ as +685.75 kJ/mole; Zhou G *et al.* Computational studies on a kind of novel energetic materials tetrahdrane and nitro derivatives. *J Mol Struct: THEOCHEM* 2004 Jan;668(2-3):189-195; <http://www.sciencedirect.com/science/article/pii/S0166128003008972>. “Due to its bond strain and perfect oxygen balance, tetranitrotetrahdrane, an analogue of tetrahdrane with four nitro group substituents, has potential as a high-performance energetic material. The addition of these nitro groups is likely to reduce tetranitrohdrane’s stability.”

²⁰⁴² Tetrazine, aka. 1-(5-tetrazolyl)-3-guanyl tetrazene hydrate (C₂H₆N₁₀, 0.185 kg/mole, 1.09×10^{-4} m³/mole) decomposes autocatalytically and rapidly over 363 K, explodes in contact with fire, and is slightly more impact sensitive than mercury fulminate (https://en.wikipedia.org/wiki/Tetrazene_explosive). The exothermic decomposition reaction releases 6.30×10^5 J/kg or 1.17×10^5 J/mole (<http://dspace.dsto.defence.gov.au/dspace/bitstream/1947/4229/1/DSTO-TR-0450%20PR.pdf>).

²⁰⁴³ Tetryl, aka. nitramine, tetralite, tetryl, or 2,4,6-trinitrophenylmethylnitramine (C₆H₂(NO₂)₃NNO₂CH₃ or C₇H₅N₅O₈, 0.287 kg/mole, 1.66×10^{-4} m³/mole; <https://en.wikipedia.org/wiki/Tetryl>) is an explosive crystalline powder used to make detonators and explosive booster charges. Taking the decomposition reaction as: C₇H₅N₅O₈ → 2.5N₂ + 2.75CO₂ + 2.5H₂O + 4.25C, and taking the standard heats of formation as -393.5 kJ/mole for CO₂ and -241.8 kJ/mole for H₂O (http://www.update.uu.se/~jolkkonen/pdf/CRC_TD.pdf) and +34 kJ/mole for C₇H₅N₅O₈ (Agrawal JP. *High Energy Materials: Propellants, Explosives and Pyrotechnics*, John Wiley & Sons, 2015, Table 1.5, p. 26), the decomposition energy is 1.72×10^6 J/mole of C₇H₅N₅O₈.

TKX-50 ²⁰⁴⁵	1.41 x 10 ⁶	0.236	1.26 x 10 ⁻⁴
TMETN ²⁰⁴⁶	1.56 x 10 ⁶	0.255	1.72 x 10 ⁻⁴
TNAZ ²⁰⁴⁷	1.38 x 10 ⁶	0.192	1.03 x 10 ⁻⁴
TNB ²⁰⁴⁸	1.22 x 10 ⁶	0.213	1.21 x 10 ⁻⁴
TNGU ²⁰⁴⁹	1.87 x 10 ⁶	0.322	1.60 x 10 ⁻⁴

²⁰⁴⁴ TEX, aka. 4,10-dinitro-2,6,8,12-tetraoxa-4,10-diazatetracyclo[5.5.0.0^{5,9}.0^{3,11}]-dodecane, or 4,10-dinitro-2,6,8,12-tetraoxa-4,10-diazaisowurtzitane (C₆H₆N₄O₈, 0.262 kg/mole, 1.32 x 10⁻⁴ m³/mole; <https://en.wikipedia.org/wiki/TEX-explosive>) is an impact- and friction-insensitive explosive. Taking the decomposition reaction as: C₆H₆N₄O₈ → 2N₂ + 2.5CO₂ + 3H₂O + 3.5C, and taking the standard heats of formation as -393.5 kJ/mole for CO₂ and -241.8 kJ/mole for H₂O (http://www.update.uu.se/~jolkkonen/pdf/CRC_TD.pdf) and -445.6 kJ/mole for C₆H₆N₄O₈ (Talwar MB *et al.* TEX: The new insensitive high explosive. Defence Sci J. 2002 Apr;52(2):157-163; <http://www.publications.drdo.gov.in/ojs/index.php/dsj/article/viewFile/2160/1141>), the decomposition energy is 1.26 x 10⁶ J/mole of C₆H₆N₄O₈.

²⁰⁴⁵ TKX-50, aka. dihydroxylammonium 5,5'-bistetrazole-1,1'-diolate (C₂H₈N₁₀O₄, 0.236 kg/mole, 1.26 x 10⁻⁴ m³/mole at 1877 kg/m³) is a new high-performance, low-sensitivity explosive. Taking the decomposition reaction as: C₂H₈N₁₀O₄ → 5N₂ + 4H₂O + 2C, and taking the standard heats of formation as -241.8 kJ/mole for H₂O (http://www.update.uu.se/~jolkkonen/pdf/CRC_TD.pdf) and +446.6 kJ/mole for C₂H₈N₁₀O₄ (Fischer N, *et al.* Pushing the limits of energetic materials. J Mater Chem. 2012;22:20418; https://epub.ub.uni-muenchen.de/18075/1/oa_18075.pdf), the decomposition energy is 1.41 x 10⁶ J/mole of C₂H₈N₁₀O₄.

²⁰⁴⁶ TMETN, aka. trimethylolethane trinitrate, metriol trinitrate (METN, MTN, METRTN), or nitropentaglycerin (CH₃-C(CH₂-O-NO₂)₃ or C₅H₉N₃O₉, 0.255 kg/mole, 1.72 x 10⁻⁴ m³/mole; https://en.wikipedia.org/wiki/Trimethylolethane_trinitrate) is a high explosive similar to nitroglycerin used in some solid propellants, smokeless powders as a plasticizer, and as a monopropellant, and can be initiated by friction, impact, or electrostatic discharge. Taking the decomposition reaction as: C₅H₉N₃O₉ → 1.5N₂ + 2.25CO₂ + 4.5H₂O + 2.75C, and taking standard heats of formation as -393.5 kJ/mole for CO₂ and -241.8 kJ/mole for H₂O (http://www.update.uu.se/~jolkkonen/pdf/CRC_TD.pdf) and -411 kJ/mole for C₅H₉N₃O₉ (Nair UR, *et al.* Advances in high energy materials. Defence Sci J. 2010 Mar;60(2):137-151; <http://publications.drdo.gov.in/ojs/index.php/dsj/article/viewFile/327/193>), the decomposition energy is 1.56 x 10⁶ J/mole of C₅H₉N₃O₉.

²⁰⁴⁷ TNAZ or 1,3,3-trinitroazetidine (C₃H₄N₄O₆, 0.192 kg/mole, 1.03 x 10⁻⁴ m³/mole at 1860 kg/m³) is a strained-ring heterocyclic nitramine melt-cast explosive that is less shock-sensitive than HMX. Taking the decomposition reaction as: C₃H₄N₄O₆ → 2N₂ + 2CO₂ + 2H₂O + C, and taking the standard heats of formation as -393.5 kJ/mole for CO₂ and -241.8 kJ/mole for H₂O (http://www.update.uu.se/~jolkkonen/pdf/CRC_TD.pdf) and +110.9 kJ/mole for C₃H₄N₄O₆ ([http://www.yang.gatech.edu/publications/Journal/C&F\(2007,%20Catoire\).pdf](http://www.yang.gatech.edu/publications/Journal/C&F(2007,%20Catoire).pdf)), the decomposition energy is 1.38 x 10⁶ J/mole of C₃H₄N₄O₆.

²⁰⁴⁸ TNB, aka. 1,3,5-trinitrobenzene (C₆H₃(NO₂)₃ or C₆H₃N₃O₆, 0.213 kg/mole, 1.21 x 10⁻⁴ m³/mole; <https://en.wikipedia.org/wiki/1,3,5-Trinitrobenzene>) is a high explosive that detonates with heat or shock. Taking the decomposition reaction as: C₆H₃N₃O₆ → 1.5N₂ + 2.25CO₂ + 1.5H₂O + 3.75C, and taking the standard heats of formation as -393.5 kJ/mole for CO₂ and -241.8 kJ/mole for H₂O (http://www.update.uu.se/~jolkkonen/pdf/CRC_TD.pdf) and -28.7 kJ/mole for C₆H₃N₃O₆ (Agrawal JP. High Energy Materials: Propellants, Explosives and Pyrotechnics, John Wiley & Sons, 2015, Table 1.5, p. 26), the decomposition energy is 1.22 x 10⁶ J/mole of C₆H₃N₃O₆.

TNT ²⁰⁵⁰	1.23 x 10 ⁶	0.227	1.37 x 10 ⁻⁴
TNTA ²⁰⁵¹	1.272 x 10 ⁶	0.216	1.03 x 10 ⁻⁴
TTD ²⁰⁵²	1.65 x 10 ⁶	0.359	1.96 x 10 ⁻⁴

²⁰⁴⁹ Tetranitroglycoluril, aka. TNGU (C₄H₂N₈O₁₀, 0.322 kg/mole, 2010 kg/m³, heat of formation +50 kJ/mole; Sherrill WM, Johnson EC. A new method for the production of tetranitroglycoluril... Army Research Laboratory, ARL-TR-6829, Feb 2014; <https://www.google.com/url?sa=t&rct=j&q=&esrc=s&source=web&cd=4&ved=0ahUKEwjMrLGGiJPPA hVJ1R4KHR3NA0EQFggxMAM&url=http%3A%2F%2Fwww.dtic.mil%2Fcgi-bin%2FGetTRDoc%3FAD%3DADA598881&usq=AFOjCNFKUXz3GzsbYeYkflEmsjin4zcwLg&cad=rja>) is a powerful high explosive similar to RDX and HMX. Taking the decomposition reaction as: C₄H₂N₈O₁₀ → 4N₂ + 4CO₂ + H₂O + 0.5O₂, and taking the standard heats of formation as -393.5 kJ/mole for CO₂ and -241.8 kJ/mole for H₂O (http://www.update.uu.se/~jolkkonen/pdf/CRC_TD.pdf), the decomposition energy is 1.87 x 10⁶ J/mole of C₄H₂N₈O₁₀.

²⁰⁵⁰ Trinitrotoluene or TNT (C₆H₂(NO₂)₃CH₃ or C₇H₅N₃O₆, 0.227 kg/mole, 1.37 x 10⁻⁴ m³/mole at 1654 kg/m³; <https://en.wikipedia.org/wiki/Trinitrotoluene>) is a yellow-colored solid explosive material with convenient handling properties. Taking the most energetic decomposition reaction as: C₇H₅N₃O₆ → 1.5N₂ + 1.75CO₂ + 2.5H₂O + 5.25C, and taking the standard heats of formation as -393.5 kJ/mole for CO₂ and -241.8 kJ/mole for H₂O (http://www.update.uu.se/~jolkkonen/pdf/CRC_TD.pdf) and -63.2 kJ/mole for C₇H₅N₃O₆ (Rouse PE Jr. Enthalpies of formation and calculated detonation properties of some thermally stable explosives. J Chem Eng Data 1976;21:16-20; <http://webbook.nist.gov/cgi/inchi?ID=C118967&Mask=2#Thermo-Condensed>), the decomposition energy is 1.23 x 10⁶ J/mole of C₇H₅N₃O₆. (An oft-cited alternative decomposition reaction: C₇H₅N₃O₆ → 1.5N₂ + 2.5H₂O + 3.5CO + 3.5C would produce a 25% lower energy release of 9.28 x 10⁵ J/mole, taking the standard heat of formation as -110.5 kJ/mole for CO.) Due to the production of large amounts of elemental carbon during detonation, explosive mixtures with oxygen-rich compounds can yield more energy per kilogram than TNT alone – e.g., the heat of combustion of TNT in oxygen (3.30 MJ/mole) is several times higher than its heat of detonation *in vacuo* (1.23 MJ/mole).

Note that for historical reasons the explosive yield of TNT was widely considered to be the standard measure of explosive power for bombs and other explosives. For this purpose, the energy liberated by 1 gram of TNT was arbitrarily defined by convention to be 4184 J, exactly one kilocalorie, for convenient use as a reference standard for many other explosives, including nuclear weapons. (Isabelle Sochet. Blast effects of external explosions. Eighth International Symposium on Hazards, Prevention, and Mitigation of Industrial Explosions, Sep 2010, Yokohama, Japan, “Section 4.8. Limitations of the TNT equivalent method”; <http://hal.archives-ouvertes.fr/hal-00629253/document>.) For this limited purpose, NIST uses 4.184 MJ/kg, or 9.503 x 10⁵ J/mole, as its arbitrary standard (https://en.wikipedia.org/wiki/Trinitrotoluene#Energy_content).

Solid TNT requires an activation energy of ~0.146 MJ/mole to initiate the decomposition reaction (Furman D *et al.* Decomposition of Condensed Phase Energetic Materials: Interplay between Uni- and Bimolecular Mechanisms. J Am Chem Soc. 2014;136(11):4192-4200; <http://pubs.acs.org/doi/abs/10.1021/ja410020f>).

²⁰⁵¹ 2,4,6-Trinitro-1,3,5-triazine, aka. TNTA (C₃N₃(NO₂)₃ or C₃N₆O₆, 0.216 kg/mole, 2100 kg/m³), if detonated via the highest-energy stoichiometric decomposition reaction as C₃N₆O₆ → 3N₂ + 3CO₂, would yield a decomposition energy of 1.272 x 10⁶ J/mole (Korkin AA, Bartlett RJ. Theoretical prediction of 2,4,6-trinitro-1,3,5-triazine (TNTA). A new, powerful, high-energy density material. J Am Chem Soc. 1996;118:12244-12245; <http://pubs.acs.org/doi/abs/10.1021/ja962744b>).

TTTO ²⁰⁵³	1.58×10^6	0.200	8.40×10^{-5}
Urea nitrate ²⁰⁵⁴	3.39×10^5	0.123	7.28×10^{-5}
Xenon dioxide ²⁰⁵⁵	4.87×10^5	0.163	3.6×10^{-5}
Xenon tetroxide ²⁰⁵⁶	6.43×10^5	0.195	4.3×10^{-5}
Xenon trioxide ²⁰⁵⁷	5.28×10^5	0.179	3.93×10^{-5}

²⁰⁵² Trinitroethyl-tetrazol-1,5-diamine, aka. TTD ($C_3H_5N_9O_6$, 0.359 kg/mole, $1.96 \times 10^{-4} \text{ m}^3/\text{mole}$ at density 1831 kg/m^3), if detonated via the highest-energy stoichiometric decomposition reaction as $C_3H_5N_9O_6 \rightarrow 4.5N_2 + 1.75CO_2 + 2.5H_2O + 1.25C$, taking the standard heats of formation as -393.5 kJ/mole for CO_2 and -241.8 kJ/mole for H_2O (http://www.update.uu.se/~jolkkonen/pdf/CRC_TD.pdf) and $+356 \text{ kJ/mole}$ for $C_3H_5N_9O_6$ (Klapotke TM. Chemistry of High-Energy Materials, Walter de Gruyter GmbH, 2015, p. 169), the decomposition energy is $1.65 \times 10^6 \text{ J/mole}$.

²⁰⁵³ Tetrazino-tetrazine 1,3,6,8-tetraoxide, aka. 1,2,3,4]tetrazino[5,6-e][1,2,3,4]tetrazine 1,3,6,8-tetraoxide or TTTO ($C_2N_8O_4$, 0.200 kg/mole, $8.40 \times 10^{-5} \text{ m}^3/\text{mole}$ at density 2380 kg/m^3) has perfect oxygen balance and was first synthesized in 2016 (<http://onlinelibrary.wiley.com/doi/10.1002/anie.201605611/abstract>). Taking the stoichiometric decomposition reaction as $C_2N_8O_4 \rightarrow 4N_2 + 2CO_2$, and taking the standard heats of formation as -393.5 kJ/mole for CO_2 (http://www.update.uu.se/~jolkkonen/pdf/CRC_TD.pdf) and $+795 \text{ kJ/mole}$ for $C_2N_8O_4$ (Wallin S, *et al.* High Energy Density Materials Efforts to synthesize the pentazolate anion: Part 1, Technical Report FOI-R-1602-SE, March 2005; http://foi.se/ReportFiles/foir_1602.pdf), the decomposition energy is $1.58 \times 10^6 \text{ J/mole}$.

²⁰⁵⁴ Urea nitrate ($[(NH_2)_2C=OH]^+[NO_3]^-$ or $CH_5N_3O_4$, 0.123 kg/mole, 1690 kg/m^3 ; https://en.wikipedia.org/wiki/Urea_nitrate) is a fertilizer-based high explosive that has been used in improvised explosive devices. The decomposition reaction that yields the most energy ($CH_5N_3O_4 \rightarrow 1.5N_2 + 0.75CO_2 + 2.5H_2O + 0.25C$) would release $3.39 \times 10^5 \text{ J/mole}$, taking heats of formation as -393.5 kJ/mole for CO_2 , -241.8 kJ/mole for H_2O (http://www.update.uu.se/~jolkkonen/pdf/CRC_TD.pdf), and -560.7 kJ/mole for $CH_5N_3O_4$ (Hiyoshi RI, *et al.* Experimental and computational study of the thermal decomposition of uronium nitrate (urea nitrate). 12th Intl. Detonation Symposium, 11-16 Aug 2002, San Diego CA; <http://www.intdetsymp.org/detsymp2002/PaperSubmit/FinalManuscript/pdf/Hiyoshi-30.pdf>).

²⁰⁵⁵ XeO_2 ($\sim 4500 \text{ kg/m}^3$, 0.163 kg/mole, $\sim 3.6 \times 10^{-5} \text{ m}^3/\text{mole}$) is an unstable yellow-orange solid with a half-life of about two minutes, disproportionating into XeO_3 and xenon gas (https://en.wikipedia.org/wiki/Xenon_dioxide): $XeO_2 \rightarrow 1/3 Xe + 2/3 XeO_3$, releasing an estimated $4.87 \times 10^5 \text{ J}$ (https://www.researchgate.net/profile/Pekka_Pyykkoe/publication/228495220_Calculations_for_XeO_n_n_2-4_Could_the_Xenon_Dioxide_Molecule_Exist/links/0deec52bd2f729b9b2000000.pdf).

²⁰⁵⁶ XeO_4 ($\sim 4500 \text{ kg/m}^3$, 0.195 kg/mole, $\sim 4.3 \times 10^{-5} \text{ m}^3/\text{mole}$) is a yellow crystalline solid very prone to explosion at temperatures above 237 K (https://en.wikipedia.org/wiki/Xenon_tetroxide), decomposing into xenon gas and oxygen via: $XeO_4 \rightarrow Xe + 2O_2$, releasing $6.43 \times 10^5 \text{ J}$ (https://www.researchgate.net/profile/Pekka_Pyykkoe/publication/228495220_Calculations_for_XeO_n_n_2-4_Could_the_Xenon_Dioxide_Molecule_Exist/links/0deec52bd2f729b9b2000000.pdf).

²⁰⁵⁷ XeO_3 (4550 kg/m^3 , 0.179 kg/mole, $3.93 \times 10^{-5} \text{ m}^3/\text{mole}$) is a colorless crystalline solid very prone to violent explosion at temperatures above 298 K (https://en.wikipedia.org/wiki/Xenon_trioxide), decomposing into xenon gas and oxygen via: $XeO_3 \rightarrow Xe + 1.5O_2$, releasing $5.28 \times 10^5 \text{ J}$ (https://www.researchgate.net/profile/Pekka_Pyykkoe/publication/228495220_Calculations_for_XeO_n_n_2-4_Could_the_Xenon_Dioxide_Molecule_Exist/links/0deec52bd2f729b9b2000000.pdf).

A.4 Data on Energy Storage in Chemical Combustion Fuels

Table A4. Data on energy storage in chemical combustion fuels.			
Energy Storage System	Energy (J)	Mass (kg)	Volume (m ³)
Metals and Elements			
Solid hydrogen H ₂ (excluding O ₂) ²⁰⁵⁸	2.42 x 10 ⁵	0.002	3.33 x 10 ⁻⁶
Solid hydrogen H ₂ (with solid O ₂)	2.42 x 10 ⁵	0.018	1.37 x 10 ⁻⁵
Liquid molecular hydrogen H ₂ (excluding O ₂) ²⁰⁵⁹	2.42 x 10 ⁵	0.002	2.82 x 10 ⁻⁵
Liquid molecular hydrogen H ₂ (with LOX)	2.42 x 10 ⁵	0.018	4.22 x 10 ⁻⁵
Lithium Li (excluding O ₂) ²⁰⁶⁰	5.958 x 10 ⁵	0.014	3.37 x 10 ⁻⁵
Lithium Li (with LOX)	5.958 x 10 ⁵	0.030	4.77 x 10 ⁻⁵
Sodium Na (excluding O ₂) ²⁰⁶¹	5.15 x 10 ⁵	0.046	4.75 x 10 ⁻⁵

²⁰⁵⁸ Assuming a density of 600 kg/m³ with a MW of 0.002 kg/mole for compressed solid hydrogen (H₂),* and a density of 1540 kg/m³ with a MW of 0.032 kg/mole for solid oxygen (O₂),** a stoichiometric combustion (H₂ + 0.5O₂ → H₂O) consumes 0.002 kg of H₂ and 0.016 kg of O₂ and releases 2.42 x 10⁵ J/mole of H₂O(g) (standard heat of formation). *Mao HK, Bell PM. Observations of Hydrogen at Room Temperature (25 {degrees}C) and High Pressure (to 500 Kilobars). Science. 1979 Mar 9;203(4384):1004-6; <http://science.sciencemag.org/content/203/4384/1004.full.pdf+html>. **Roder HM. The molar volume (density) of solid oxygen in equilibrium with vapor. J Phys Chem Ref Data 1978;7(3):949-957; <https://srd.nist.gov/JPCRD/jpcrd122.pdf>.

²⁰⁵⁹ Liquid H₂ at 20 K has a density of 70.85 kg/m³; https://en.wikipedia.org/wiki/Liquid_hydrogen. Liquid O₂ (aka. LOX) at 50 K has a density of 1141 kg/m³; https://en.wikipedia.org/wiki/Liquid_oxygen. The same stoichiometric combustion formula (H₂ + 0.5O₂ → H₂O) applies.

²⁰⁶⁰ Solid lithium (Li) has a density of 534 kg/m³ with MW of 0.007 kg/mole; a stoichiometric combustion (2Li + 0.5O₂ → Li₂O) using liquid oxygen (LOX: density 1141 kg/m³, MW 0.032 kg/mole) consumes 0.014 kg of Li and 0.016 kg of O₂ and releases 5.958 x 10⁵ J/mole of Li₂O (standard enthalpy of formation); <https://en.wikipedia.org/wiki/Lithium> and https://en.wikipedia.org/wiki/Beryllium_oxide.

Sodium Na (with LOX)	5.15×10^5	0.078	7.56×10^{-5}
Potassium K (excluding O ₂) ²⁰⁶²	2.85×10^5	0.0391	4.54×10^{-5}
Potassium K (with LOX)	2.85×10^5	0.0711	7.34×10^{-5}
Rubidium Rb (excluding O ₂) ²⁰⁶³	2.787×10^5	0.0855	5.58×10^{-5}
Rubidium Rb (with LOX)	2.787×10^5	0.1175	8.39×10^{-5}
Cesium Cs (excluding O ₂) ²⁰⁶⁴	2.862×10^5	0.1329	6.89×10^{-5}
Cesium Cs (with LOX)	2.862×10^5	0.1649	9.69×10^{-5}
Beryllium Be (excluding O ₂) ²⁰⁶⁵	5.99×10^5	0.009	4.87×10^{-6}
Beryllium Be (with LOX)	5.99×10^5	0.025	1.89×10^{-5}

²⁰⁶¹ Solid sodium (Na) has a density of 968 kg/m³ with MW of 0.023 kg/mole; a stoichiometric combustion ($2\text{Na} + \text{O}_2 \rightarrow \text{Na}_2\text{O}_2$) using liquid oxygen (LOX: density 1141 kg/m³, MW 0.032 kg/mole) consumes 0.046 kg of Na and 0.032 kg of O₂ and releases 5.15×10^5 J/mole of Na₂O₂ (standard enthalpy of formation); https://en.wikipedia.org/wiki/Sodium_hydride and https://en.wikipedia.org/wiki/Sodium_peroxide. Sodium peroxide (Na₂O₂) is the product of sodium ignited in excess oxygen.” Harald Jakob, Stefan Leininger, Thomas Lehmann, Sylvia Jacobi, Sven Gutewort, “Peroxo Compounds, Inorganic,” Ullmann's Encyclopedia of Industrial Chemistry, 2007, Wiley-VCH, Weinheim. However, “[cold] sodium hydride is not attacked by liquid oxygen” [Mellor JW, A Comprehensive Treatise on Inorganic and Theoretical Chemistry, 1922, p. 483], so the LOX may need preheating.

²⁰⁶² Solid potassium (K) has a density of 862 kg/m³ with MW of 0.0391 kg/mole; a stoichiometric combustion ($\text{K} + \text{O}_2 \rightarrow \text{KO}_2$) using liquid oxygen (LOX: density 1141 kg/m³, MW 0.032 kg/mole) consumes 0.0391 kg of K and 0.032 kg of O₂ and releases 2.85×10^5 J/mole of KO₂ (standard enthalpy of formation); <https://en.wikipedia.org/wiki/Potassium> and http://www.update.uu.se/~jolkkonen/pdf/CRC_TD.pdf. “Potassium superoxide (KO₂) is produced by burning molten potassium in an atmosphere of oxygen.” Harald Jakob, Stefan Leininger, Thomas Lehmann, Sylvia Jacobi, Sven Gutewort, “Peroxo Compounds, Inorganic,” Ullmann's Encyclopedia of Industrial Chemistry, 2007, Wiley-VCH, Weinheim. “Potassium hydride will ignite at room temperature in dry oxygen and air.” Mueller WM, Blackledge JP, Libowitz GG. Metal Hydrides, Academic Press, 2013, p. 122.

²⁰⁶³ Solid rubidium (Rb) has a density of 1532 kg/m³ with MW of 0.0855 kg/mole; a stoichiometric combustion ($\text{Rb} + \text{O}_2 \rightarrow \text{RbO}_2$) using liquid oxygen (LOX: density 1141 kg/m³, MW 0.032 kg/mole) consumes 0.0855 kg of Rb and 0.032 kg of O₂ and releases 2.787×10^5 J/mole of RbO₂ (standard enthalpy of formation); <https://en.wikipedia.org/wiki/Rubidium> and http://www.update.uu.se/~jolkkonen/pdf/CRC_TD.pdf.

²⁰⁶⁴ Solid cesium (Cs) has a density of 1930 kg/m³ with MW of 0.1329 kg/mole; a stoichiometric combustion ($\text{Cs} + \text{O}_2 \rightarrow \text{CsO}_2$) using liquid oxygen (LOX: density 1141 kg/m³, MW 0.032 kg/mole) consumes 0.1329 kg of Cs and 0.032 kg of O₂ and releases 2.862×10^5 J/mole of CsO₂ (standard enthalpy of formation); <https://en.wikipedia.org/wiki/Caesium> and http://www.update.uu.se/~jolkkonen/pdf/CRC_TD.pdf.

²⁰⁶⁵ Solid beryllium (Be) has a density of 1850 kg/m³ with MW of 0.009 kg/mole; a stoichiometric combustion ($\text{Be} + 0.5\text{O}_2 \rightarrow \text{BeO}$) using liquid oxygen (LOX: density 1141 kg/m³, MW 0.032 kg/mole) consumes 0.009 kg of Be and 0.016 kg of O₂ and releases 5.99×10^5 J/mole of BeO (standard enthalpy of formation); <https://en.wikipedia.org/wiki/Beryllium> and https://en.wikipedia.org/wiki/Beryllium_oxide.

Magnesium Mg (excluding O ₂) ²⁰⁶⁶	5.966 x 10 ⁵	0.0243	1.40 x 10 ⁻⁵
Magnesium Mg (with LOX)	5.966 x 10 ⁵	0.0403	2.80 x 10 ⁻⁵
Calcium Ca (excluding O ₂) ²⁰⁶⁷	6.35 x 10 ⁵	0.040	2.58 x 10 ⁻⁵
Calcium Ca (with LOX)	6.35 x 10 ⁵	0.056	3.98 x 10 ⁻⁵
Strontium Sr (excluding O ₂) ²⁰⁶⁸	5.92 x 10 ⁵	0.0876	3.32 x 10 ⁻⁵
Strontium Sr (with LOX)	5.92 x 10 ⁵	0.1036	4.72 x 10 ⁻⁵
Scandium Sc (excluding O ₂) ²⁰⁶⁹	1.91 x 10 ⁶	0.090	3.02 x 10 ⁻⁵
Scandium Sc (with LOX)	1.91 x 10 ⁶	0.138	7.22 x 10 ⁻⁵
Cerium Ce (excluding O ₂) ²⁰⁷⁰	1.09 x 10 ⁶	0.140	2.07 x 10 ⁻⁵
Cerium Ce (with LOX)	1.09 x 10 ⁶	0.172	4.87 x 10 ⁻⁵
Uranium U (excluding O ₂) ²⁰⁷¹	3.575 x 10 ⁶	0.714	3.74 x 10 ⁻⁵

²⁰⁶⁶ Solid magnesium (Mg) has a density of 1738 kg/m³ with MW of 0.0243 kg/mole; a stoichiometric combustion ($\text{Mg} + 0.5\text{O}_2 \rightarrow \text{MgO}$) using liquid oxygen (LOX: density 1141 kg/m³, MW 0.032 kg/mole) consumes 0.0243 kg of Mg and 0.016 kg of O₂ and releases 5.966 x 10⁵ J/mole of MgO (standard enthalpy of formation); <https://en.wikipedia.org/wiki/Magnesium> and https://en.wikipedia.org/wiki/Magnesium_oxide.

²⁰⁶⁷ Solid calcium (Ca) has a density of 1550 kg/m³ with MW of 0.040 kg/mole; a stoichiometric combustion ($\text{Ca} + 0.5\text{O}_2 \rightarrow \text{CaO}$) using liquid oxygen (LOX: density 1141 kg/m³, MW 0.032 kg/mole) consumes 0.040 kg of Ca and 0.016 kg of O₂ and releases 6.35 x 10⁵ J/mole of CaO (standard enthalpy of formation); <https://en.wikipedia.org/wiki/Calcium> and https://en.wikipedia.org/wiki/Calcium_oxide.

²⁰⁶⁸ Solid strontium (Sr) has a density of 2640 kg/m³ with MW of 0.0876 kg/mole; a stoichiometric combustion ($\text{Sr} + 0.5\text{O}_2 \rightarrow \text{SrO}$) using liquid oxygen (LOX: density 1141 kg/m³, MW 0.032 kg/mole) consumes 0.0876 kg of Sr and 0.016 kg of O₂ and releases 5.92 x 10⁵ J/mole of SrO (standard enthalpy of formation); <https://en.wikipedia.org/wiki/Strontium> and https://en.wikipedia.org/wiki/Strontium_oxide.

²⁰⁶⁹ Solid scandium (Sc) has a density of 2985 kg/m³ with MW of 0.045 kg/mole; a stoichiometric combustion ($2\text{Sc} + 1.5\text{O}_2 \rightarrow \text{Sc}_2\text{O}_3$) using liquid oxygen (LOX: density 1141 kg/m³, MW 0.032 kg/mole) consumes 0.090 kg of Sc and 0.048 kg of O₂ and releases 1.91 x 10⁶ J/mole of Sc₂O₃ (standard enthalpy of formation); <https://en.wikipedia.org/wiki/Scandium> and Huber EJ Jr, Fitzgibbon GC, Head EL, Holley CE Jr. The heat of formation of scandium oxide. J Phys Chem 1963;67(8):1731-1733; <http://pubs.acs.org/doi/abs/10.1021/j100802a511>.

²⁰⁷⁰ Solid cerium (Ce) has a density of 6770 kg/m³ with MW of 0.140 kg/mole; a stoichiometric combustion ($\text{Ce} + \text{O}_2 \rightarrow \text{CeO}_2$) using liquid oxygen (LOX: density 1141 kg/m³, MW 0.032 kg/mole) consumes 0.140 kg of Ce and 0.032 kg of O₂ and releases 1.09 x 10⁶ J/mole of CeO₂ (standard enthalpy of formation); <https://en.wikipedia.org/wiki/Cerium> and http://www.update.uu.se/~jolkkonen/pdf/CRC_TD.pdf.

Uranium U (with LOX)	3.575×10^6	0.842	1.50×10^{-4}
Neptunium Np (excluding O ₂) ²⁰⁷²	1.079×10^6	0.237	1.22×10^{-5}
Neptunium Np (with LOX)	1.079×10^6	0.269	4.03×10^{-5}
Plutonium Pu (excluding O ₂) ²⁰⁷³	1.056×10^6	0.244	1.23×10^{-5}
Plutonium Pu (with LOX)	1.056×10^6	0.276	4.04×10^{-5}
Titanium Ti (excluding O ₂) ²⁰⁷⁴	9.45×10^5	0.0479	1.06×10^{-5}
Titanium Ti (with LOX)	9.45×10^5	0.0799	3.87×10^{-5}
Zirconium Zr (excluding O ₂) ²⁰⁷⁵	1.080×10^6	0.0912	1.40×10^{-5}
Zirconium Zr (with LOX)	1.080×10^6	0.1232	4.20×10^{-5}
Hafnium Hf (excluding O ₂) ²⁰⁷⁶	1.145×10^6	0.1785	1.34×10^{-5}

²⁰⁷¹ Solid uranium (U), a pyrophoric radioactive metal, has a density of $19,100 \text{ kg/m}^3$ with MW of 0.238 kg/mole; a stoichiometric combustion ($3\text{U} + 4\text{O}_2 \rightarrow \text{U}_3\text{O}_8$) using liquid oxygen (LOX: density 1141 kg/m^3 , MW 0.032 kg/mole) consumes 0.714 kg of U and 0.128 kg of O₂ and releases $3.575 \times 10^6 \text{ J/mole}$ of U₃O₈ (standard enthalpy of formation); <https://en.wikipedia.org/wiki/Uranium> and Konings RJM *et al.* The Thermodynamic Properties of the f-Elements and their Compounds. Part 2. The Lanthanide and Actinide Oxides. J Phys Chem Ref Data 2014;43:013101; http://thermophysics.ru/pdf_doc/konings2014.pdf. “Powdered uranium burns with a bright glow.” J.J. Katz, Eugene Rabinowitch, The Chemistry of Uranium, 1961, p. 166.

²⁰⁷² Solid neptunium (Np), a pyrophoric radioactive metal, has a density of $19,380 \text{ kg/m}^3$ with MW of 0.237 kg/mole; a stoichiometric combustion ($\text{Np} + \text{O}_2 \rightarrow \text{NpO}_2$) using liquid oxygen (LOX: density 1141 kg/m^3 , MW 0.032 kg/mole) consumes 0.237 kg of Np and 0.032 kg of O₂ and releases $1.079 \times 10^6 \text{ J/mole}$ of NpO₂ (standard enthalpy of formation); <https://en.wikipedia.org/wiki/Neptunium> and Konings RJM *et al.* The Thermodynamic Properties of the f-Elements and their Compounds. Part 2. The Lanthanide and Actinide Oxides. J Phys Chem Ref Data 2014;43:013101; http://thermophysics.ru/pdf_doc/konings2014.pdf.

²⁰⁷³ Solid plutonium (Pu), a pyrophoric radioactive metal, has a density of $19,816 \text{ kg/m}^3$ with MW of 0.244 kg/mole; a stoichiometric combustion ($\text{Pu} + \text{O}_2 \rightarrow \text{PuO}_2$) using liquid oxygen (LOX: density 1141 kg/m^3 , MW 0.032 kg/mole) consumes 0.244 kg of Pu and 0.032 kg of O₂ and releases $1.056 \times 10^6 \text{ J/mole}$ of PuO₂ (standard enthalpy of formation); <https://en.wikipedia.org/wiki/Plutonium> and Konings RJM *et al.* The Thermodynamic Properties of the f-Elements and their Compounds. Part 2. The Lanthanide and Actinide Oxides. J Phys Chem Ref Data 2014;43:013101; http://thermophysics.ru/pdf_doc/konings2014.pdf.

²⁰⁷⁴ Solid titanium (Ti) has a density of 4506 kg/m^3 with MW of 0.0479 kg/mole; a stoichiometric combustion ($\text{Ti} + \text{O}_2 \rightarrow \text{TiO}_2$) using liquid oxygen (LOX: density 1141 kg/m^3 , MW 0.032 kg/mole) consumes 0.0479 kg of Ti and 0.032 kg of O₂ and releases $9.45 \times 10^5 \text{ J/mole}$ of TiO₂ (standard enthalpy of formation); <https://en.wikipedia.org/wiki/Titanium> and https://en.wikipedia.org/wiki/Titanium_dioxide.

²⁰⁷⁵ Solid zirconium (Zr) has a density of 6520 kg/m^3 with MW of 0.0912 kg/mole; a stoichiometric combustion ($\text{Zr} + \text{O}_2 \rightarrow \text{ZrO}_2$) using liquid oxygen (LOX: density 1141 kg/m^3 , MW 0.032 kg/mole) consumes 0.0912 kg of Zr and 0.032 kg of O₂ and releases $1.080 \times 10^6 \text{ J/mole}$ of ZrO₂ (standard enthalpy of formation); <https://en.wikipedia.org/wiki/Zirconium> and https://en.wikipedia.org/wiki/Zirconium_dioxide. The combustion temperature can reach 4930 K (<http://www.sciencedirect.com/science/article/pii/0022190258800597>).

Hafnium Hf (with LOX)	1.145×10^6	0.2105	4.15×10^{-5}
Vanadium V (excluding O ₂) ²⁰⁷⁷	1.557×10^6	0.1018	1.70×10^{-5}
Vanadium V (with LOX)	1.557×10^6	0.1818	8.71×10^{-5}
Tantalum Ta (excluding O ₂) ²⁰⁷⁸	2.046×10^6	0.3618	2.17×10^{-5}
Tantalum Ta (with LOX)	2.046×10^6	0.4418	9.18×10^{-5}
Chromium Cr (excluding O ₂) ²⁰⁷⁹	1.128×10^6	0.104	1.45×10^{-5}
Chromium Cr (with LOX)	1.128×10^6	0.152	5.65×10^{-5}
Tungsten W (excluding O ₂) ²⁰⁸⁰	8.429×10^5	0.1838	9.55×10^{-6}
Tungsten W (with LOX)	8.429×10^5	0.2318	5.16×10^{-5}
Iron Fe (excluding O ₂) ²⁰⁸¹	8.242×10^5	0.1117	1.42×10^{-5}

²⁰⁷⁶ Solid hafnium (Hf) has a density of 13,310 kg/m³ with MW of 0.1785 kg/mole; a stoichiometric combustion ($\text{Hf} + \text{O}_2 \rightarrow \text{HfO}_2$) using liquid oxygen (LOX: density 1141 kg/m³, MW 0.032 kg/mole) consumes 0.1785 kg of Hf and 0.032 kg of O₂ and releases 1.145×10^6 J/mole of HfO₂ (standard enthalpy of formation); <https://en.wikipedia.org/wiki/Hafnium> and http://www.update.uu.se/~jolkkonen/pdf/CRC_TD.pdf. “Hafnium burns with very little flame, but it releases large quantities of heat. Hafnium in sponge form may ignite spontaneously.” Primer on Spontaneous Heating and Pyrophoricity, DOE-HDBK-1081-94, FSC-6910, Dec 1994; <http://web.archive.org/web/20100527183802/http://www.hss.energy.gov/nuclearsafety/ns/techstds/standard/hdbk1081/hdbk1081.pdf>.

²⁰⁷⁷ Solid vanadium (V) has a density of 6000 kg/m³ with MW of 0.0509 kg/mole; a stoichiometric combustion ($2\text{V} + 2.5\text{O}_2 \rightarrow \text{V}_2\text{O}_5$) using liquid oxygen (LOX: density 1141 kg/m³, MW 0.032 kg/mole) consumes 0.1018 kg of V and 0.080 kg of O₂ and releases 1.557×10^6 J/mole of V₂O₅ (standard enthalpy of formation); <https://en.wikipedia.org/wiki/Vanadium> and Lavut EG, Chelovskaya NV. Use of an electric furnace in a calorimetric bomb for combustion in oxygen. Determination of the standard molar enthalpy of formation of V₂O₅. J Chem Thermodyn. 1989 Jul;21(7):765-771; <http://www.sciencedirect.com/science/article/pii/002196148990061X>.

²⁰⁷⁸ Solid tantalum (Ta) has a density of 16,690 kg/m³ with MW of 0.1809 kg/mole; a stoichiometric combustion ($2\text{Ta} + 2.5\text{O}_2 \rightarrow \text{Ta}_2\text{O}_5$) using liquid oxygen (LOX: density 1141 kg/m³, MW 0.032 kg/mole) consumes 0.3618 kg of Ta and 0.080 kg of O₂ and releases 2.046×10^6 J/mole of Ta₂O₅ (standard enthalpy of formation); <https://en.wikipedia.org/wiki/Tantalum> and http://chemistry-reference.com/q_compounds.asp?CAS=1314-61-0&language=en.

²⁰⁷⁹ Solid chromium (Cr) has a density of 7190 kg/m³ with MW of 0.052 kg/mole; a stoichiometric combustion ($2\text{Cr} + 1.5\text{O}_2 \rightarrow \text{Cr}_2\text{O}_3$) using liquid oxygen (LOX: density 1141 kg/m³, MW 0.032 kg/mole) consumes 0.104 kg of Cr and 0.048 kg of O₂ and releases 1.128×10^6 J/mole of Cr₂O₃ (standard enthalpy of formation); <https://en.wikipedia.org/wiki/Chromium> and [https://en.wikipedia.org/wiki/Chromium\(III\)_oxide](https://en.wikipedia.org/wiki/Chromium(III)_oxide).

²⁰⁸⁰ Solid tungsten (W) has a density of 19,250 kg/m³ with MW of 0.1838 kg/mole; a stoichiometric combustion ($\text{W} + 1.5\text{O}_2 \rightarrow \text{WO}_3$) using liquid oxygen (LOX: density 1141 kg/m³, MW 0.032 kg/mole) consumes 0.1838 kg of Ta and 0.048 kg of O₂ and releases 8.429×10^5 J/mole of WO₃ (standard enthalpy of formation); <https://en.wikipedia.org/wiki/Tungsten> and http://chemistry-reference.com/q_compounds.asp?CAS=1314-35-8&language=en.

Iron Fe (with LOX)	8.242×10^5	0.1597	5.63×10^{-3}
Cobalt Co (excluding O ₂) ²⁰⁸²	2.38×10^5	0.0589	6.62×10^{-6}
Cobalt Co (with LOX)	2.38×10^5	0.0749	2.06×10^{-5}
Nickel Ni (excluding O ₂) ²⁰⁸³	2.40×10^5	0.0587	6.59×10^{-6}
Nickel Ni (with LOX)	2.40×10^5	0.0747	2.06×10^{-5}
Zinc Zn (excluding O ₂) ²⁰⁸⁴	3.505×10^5	0.0654	9.16×10^{-6}
Zinc Zn (with LOX)	3.505×10^5	0.0814	2.32×10^{-5}
Boron B (excluding O ₂) ²⁰⁸⁵	1.254×10^6	0.0216	4.62×10^{-6}
Boron B (with LOX)	1.254×10^6	0.0696	4.67×10^{-5}
Aluminum Al (excluding O ₂) ²⁰⁸⁶	1.676×10^6	0.054	2.00×10^{-5}
Aluminum Al (with LOX)	1.676×10^6	0.102	6.21×10^{-5}

²⁰⁸¹ Solid iron (Fe) has a density of 7874 kg/m^3 with MW of 0.05585 kg/mole , and when burned in the presence of excess O₂ becomes Fe₂O₃, the maximally oxidized oxide of iron; <https://www.airproducts.com/~media/Files/PDF/industries/metals-discussion-steel-burning-oxygen-steelmaking-metallurgist-perspective.pdf>. A stoichiometric combustion ($2\text{Fe} + 1.5\text{O}_2 \rightarrow \text{Fe}_2\text{O}_3$) using liquid oxygen (LOX: density 1141 kg/m^3 , MW 0.032 kg/mole) consumes 0.1117 kg of Fe and 0.048 kg of O₂ and releases $8.242 \times 10^5 \text{ J/mole}$ of Fe₂O₃ (standard enthalpy of formation); <https://en.wikipedia.org/wiki/Iron> and https://en.wikipedia.org/wiki/Iron%28III%29_oxide.

²⁰⁸² Solid cobalt (Co) has a density of 8900 kg/m^3 with MW of 0.0589 kg/mole ; a stoichiometric combustion ($\text{Co} + 0.5\text{O}_2 \rightarrow \text{CoO}$) using liquid oxygen (LOX: density 1141 kg/m^3 , MW 0.032 kg/mole) consumes 0.0587 kg of Co and 0.016 kg of O₂ and releases $2.38 \times 10^5 \text{ J/mole}$ of CoO (standard enthalpy of formation); <https://en.wikipedia.org/wiki/Cobalt> and [https://en.wikipedia.org/wiki/Cobalt\(II\)_oxide](https://en.wikipedia.org/wiki/Cobalt(II)_oxide), and http://www.update.uu.se/~jolkkonen/pdf/CRC_TD.pdf.

²⁰⁸³ Solid nickel (Ni) has a density of 8908 kg/m^3 with MW of 0.0587 kg/mole ; a stoichiometric combustion ($\text{Ni} + 0.5\text{O}_2 \rightarrow \text{NiO}$) using liquid oxygen (LOX: density 1141 kg/m^3 , MW 0.032 kg/mole) consumes 0.0587 kg of Ni and 0.016 kg of O₂ and releases $2.40 \times 10^5 \text{ J/mole}$ of NiO (standard enthalpy of formation); <https://en.wikipedia.org/wiki/Nickel> and [https://en.wikipedia.org/wiki/Nickel\(II\)_oxide](https://en.wikipedia.org/wiki/Nickel(II)_oxide).

²⁰⁸⁴ Solid zinc (Zn) has a density of 7140 kg/m^3 with MW of 0.0654 kg/mole ; a stoichiometric combustion ($\text{Zn} + 0.5\text{O}_2 \rightarrow \text{ZnO}$) using liquid oxygen (LOX: density 1141 kg/m^3 , MW 0.032 kg/mole) consumes 0.0654 kg of Zn and 0.016 kg of O₂ and releases $3.505 \times 10^5 \text{ J/mole}$ of ZnO (standard enthalpy of formation); <https://en.wikipedia.org/wiki/Zinc> and http://www.update.uu.se/~jolkkonen/pdf/CRC_TD.pdf.

²⁰⁸⁵ Solid boron (B) has a density of 2340 kg/m^3 with MW of 0.0108 kg/mole ; a stoichiometric combustion ($2\text{B} + 1.5\text{O}_2 \rightarrow \text{B}_2\text{O}_3$) using liquid oxygen (LOX: density 1141 kg/m^3 , MW 0.032 kg/mole) consumes 0.0216 kg of B and 0.048 kg of O₂ and releases $1.254 \times 10^6 \text{ J/mole}$ of B₂O₃ (standard enthalpy of formation); <http://www.rsc.org/periodic-table/element/5/boron> and https://en.wikipedia.org/wiki/Boron_trioxide.

²⁰⁸⁶ Solid aluminum (Al) has a density of 2700 kg/m^3 with MW of 0.027 kg/mole ; a stoichiometric combustion ($2\text{Al} + 1.5\text{O}_2 \rightarrow \text{Al}_2\text{O}_3$) using liquid oxygen (LOX: density 1141 kg/m^3 , MW 0.032 kg/mole) consumes 0.054 kg of Al and 0.048 kg of O₂ and releases $1.676 \times 10^6 \text{ J/mole}$ of Al₂O₃ (standard enthalpy of formation); <https://en.wikipedia.org/wiki/Aluminium> and https://en.wikipedia.org/wiki/Aluminium_oxide.

Carbon, as diamond C (excluding O ₂) ²⁰⁸⁷	3.953 x 10 ⁵	0.012	3.42 x 10 ⁻⁶
Carbon, as diamond C (with LOX)	3.953 x 10 ⁵	0.044	3.15 x 10 ⁻⁵
Carbon, as graphite C (excluding O ₂) ²⁰⁸⁸	3.935 x 10 ⁵	0.012	5.38 x 10 ⁻⁶
Carbon, as graphite C (with LOX)	3.935 x 10 ⁵	0.044	3.34 x 10 ⁻⁵
Carbon, as C ₆₀ fullerene (excluding O ₂) ²⁰⁸⁹	2.611 x 10 ⁷	0.721	4.37 x 10 ⁻⁴
Carbon, as C ₆₀ fullerene (with LOX)	2.611 x 10 ⁷	2.641	2.12 x 10 ⁻³
Carbon, as C ₂₀ fullerene (excluding O ₂) ²⁰⁹⁰	1.103 x 10 ⁷	0.240	7.59 x 10 ⁻⁵
Carbon, as C ₂₀ fullerene (with LOX)	1.103 x 10 ⁷	0.880	6.37 x 10 ⁻⁴
Silicon Si (excluding O ₂) ²⁰⁹¹	9.11 x 10 ⁵	0.028	1.20 x 10 ⁻⁵

²⁰⁸⁷ Solid diamond (C) has a density of 3510 kg/m³ with MW of 0.012 kg/mole; a stoichiometric combustion (C_{diamond} + O₂ → CO₂) using liquid oxygen (LOX: density 1141 kg/m³, MW 0.032 kg/mole) consumes 0.012 kg of C_{diamond} and 0.032 kg of O₂ and releases 3.953 x 10⁵ J/mole of C_{diamond} (standard enthalpy of combustion); Hawtin P, Lewis JB, Moul N, Phillips RH. The Heats of Combustion of Graphite, Diamond and Some Non-Graphitic Carbons. Phil Trans R Soc London Ser A. 1966 Nov 17;261:67-95; <http://www.jstor.org/pss/73489>. Diamond burns readily in LOX (e.g., <https://www.youtube.com/watch?v=0tcP9SLKEG4>).

²⁰⁸⁸ Solid graphite (C) has a density of 2230 kg/m³ with MW of 0.012 kg/mole; a stoichiometric combustion (C_{graphite} + O₂ → CO₂) using liquid oxygen (LOX: density 1141 kg/m³, MW 0.032 kg/mole) consumes 0.012 kg of C_{graphite} and 0.032 kg of O₂ and releases 3.935 x 10⁵ J/mole of C_{graphite} (standard enthalpy of combustion); <https://en.wikipedia.org/wiki/Graphite> and Hawtin P, Lewis JB, Moul N, Phillips RH. The Heats of Combustion of Graphite, Diamond and Some Non-Graphitic Carbons. Phil Trans R Soc London Ser A. 1966 Nov 17;261:67-95; <http://www.jstor.org/pss/73489>. A mixture of liquid oxygen with a suitable fuel such as carbon lampblack is called an oxyliquid, aka liquid air explosive or liquid oxygen explosive (<https://en.wikipedia.org/wiki/Oxyliquid>).

²⁰⁸⁹ Solid fullerene (C₆₀) has a density of 1650 kg/m³ with MW of 0.721 kg/mole; a stoichiometric combustion (C₆₀ + 6O₂ → 6CO₂) using liquid oxygen (LOX: density 1141 kg/m³, MW 0.032 kg/mole) consumes 0.721 kg of C₆₀ and 1.92 kg of O₂ and releases 2.611 x 10⁷ J/mole of C₆₀ (standard heat of formation); http://www.update.uu.se/~jolkkonen/pdf/CRC_TD.pdf.

²⁰⁹⁰ Solid C₂₀ fullerene (the smallest possible fullerene) has a density of 3160 kg/m³,* with MW of 0.240 kg/mole; a stoichiometric combustion (C₂₀ + 20O₂ → 20CO₂) using liquid oxygen (LOX: density 1141 kg/m³, MW 0.032 kg/mole) consumes 0.240 kg of C₆₀ and 0.640 kg of O₂ and releases 1.103 x 10⁷ J/mole of C₂₀ taking the estimated heat of formation for C₂₀ as +3156.8 kJ/mole (Popov AP, Bazhin IV, in Veziroglu TN *et al.*, eds. Hydrogen Materials Science and Chemistry of Carbon Nanomaterials, Springer, 2007, p. 715, Table 1). The C₂₀ molecule was first synthesized in 2000; Prinzbach H *et al.* Gas-phase production and photoelectron spectroscopy of the smallest fullerene, C₂₀. Nature. 2000 Sep 7;407(6800):60-3; <http://cluster.physik.uni-freiburg.de/lit/preprints/NATC20.PDF>. *The density figure is for Phase III C₂₀ that has been inelastically compressed to ~290 GPa, then decompressed back to 0 GPa. Claus D. Sattler, Carbon Nanomaterials Sourcebook, CRC Press, 2016, Table 8.1, p. 188; <https://books.google.com/books?id=eAnYCwAAQBAJ&pg=PA188>.

Silicon Si (with LOX)	9.11×10^5	0.060	4.01×10^{-5}
Lead Pb (excluding O ₂) ²⁰⁹²	2.77×10^5	0.2072	1.83×10^{-5}
Lead Pb (with LOX)	2.77×10^5	0.2392	4.63×10^{-5}
Sulfur S (excluding O ₂) ²⁰⁹³	2.97×10^5	0.0321	1.55×10^{-5}
Sulfur S (with LOX)	2.97×10^5	0.0641	4.36×10^{-5}
Phosphorus P (excluding O ₂) ²⁰⁹⁴	2.984×10^6	0.124	4.61×10^{-5}
Phosphorus P (with LOX)	2.984×10^6	0.284	1.86×10^{-4}
Hydrides ²⁰⁹⁵			

²⁰⁹¹ Solid silicon (Si) has a density of 2329 kg/m³ with MW of 0.028 kg/mole; a stoichiometric combustion ($\text{Si} + \text{O}_2 \rightarrow \text{SiO}_2$) using liquid oxygen (LOX: density 1141 kg/m³, MW 0.032 kg/mole) consumes 0.028 kg of Si and 0.032 kg of O₂ and releases 9.11×10^5 J/mole of SiO₂ (standard enthalpy of formation); <https://en.wikipedia.org/wiki/Silicon> and https://en.wikipedia.org/wiki/Silicon_dioxide. Observed explosions when LOX is applied to hydrogen-terminated porous silicon with atomic-scale spacing between interacting surface Si atoms generate energy releases on the order of 12-28 MJ/kg; Kovalev D, *et al.* Strong explosive interaction of hydrogenated porous silicon with oxygen at cryogenic temperatures. *Phys Rev Lett.* 2001 Aug 6;87(6):068301; <http://journals.aps.org/prl/abstract/10.1103/PhysRevLett.87.068301>. See also: <https://www.newscientist.com/article/dn1103-superpowerful-explosive-arrives-with-a-bang/>.

²⁰⁹² Solid lead (Pb) has a density of 11,340 kg/m³ with MW of 0.2072 kg/mole; a stoichiometric combustion ($\text{Pb} + \text{O}_2 \rightarrow \text{PbO}_2$) using liquid oxygen (LOX: density 1141 kg/m³, MW 0.032 kg/mole) consumes 0.2072 kg of Pb and 0.032 kg of O₂ and releases 2.77×10^5 J/mole of PbO₂ (standard enthalpy of formation); <https://en.wikipedia.org/wiki/Lead>, https://en.wikipedia.org/wiki/Lead_dioxide, and http://www.update.uu.se/~jolkkonen/pdf/CRC_TD.pdf. “Powdered lead burns with a bluish-white flame. As with many metals, finely divided powdered lead exhibits pyrophoricity.” Charles J, Kopf PW, Toby S. The reaction of pyrophoric lead with oxygen. *J Phys Chem.* 1966;70(5):1478-1482; <http://pubs.acs.org/doi/abs/10.1021/j100877a023>.

²⁰⁹³ Sulfur has a density of 2070 kg/m³ with MW of 0.0321 kg/mole; a stoichiometric combustion ($\text{S} + \text{O}_2 \rightarrow \text{SO}_2$) using liquid oxygen (LOX: density 1141 kg/m³, MW 0.032 kg/mole) consumes 0.0321 kg of S and 0.032 kg of O₂ and releases 2.97×10^5 J/mole of S (standard heat of formation); http://www.update.uu.se/~jolkkonen/pdf/CRC_TD.pdf.

²⁰⁹⁴ Solid black phosphorus (P), with a density of 2690 kg/m³ and MW of 0.031 kg/mole, is the most chemically stable and dense allotrope but is still oxidized by O₂; Huang Y, He K, Bliznakov S, Sutter E, Meng F, Su D, Sutter P. Degradation of Black Phosphorus: The Role of Oxygen and Water, 2015; <https://arxiv.org/ftp/arxiv/papers/1511/1511.09201.pdf>. A stoichiometric combustion ($4\text{P} + 5\text{O}_2 \rightarrow \text{P}_4\text{O}_{10}$) using liquid oxygen (LOX: density 1141 kg/m³, MW 0.032 kg/mole) consumes 0.124 kg of P and 0.16 kg of O₂ and releases 2.984×10^6 J/mole of P₄O₁₀ (standard enthalpy of formation); <https://en.wikipedia.org/wiki/Phosphorus> and Holmes WS. Heat of combustion of phosphorus and the enthalpies of formation of P₄O₁₀ and H₃PO₄. *Trans Faraday Soc.* 1962;58:1916-1925; <http://pubs.rsc.org/en/Content/ArticleLanding/1962/TF/TF9625801916#!divAbstract>.

²⁰⁹⁵ For items without reference tags: Gany A, Netzer DW. Fuel performance evaluation for the solid-fueled ramjet. Naval Postgraduate School, 1984-10; <http://calhoun.nps.edu/bitstream/handle/10945/29887/fuelperformance00gany.pdf?sequence=1>.

Lithium hydride LiH (excluding O ₂) ²⁰⁹⁶	3.28 x 10 ⁵	0.00795	1.02 x 10 ⁻⁵
Lithium hydride LiH (with LOX)	3.28 x 10 ⁵	0.02395	2.42 x 10 ⁻⁵
Lithium octahydride LiH ₈ (theoretical) (excluding O ₂) ²⁰⁹⁷	1.31 x 10 ⁶	0.0149	---
Lithium octahydride LiH ₈ (theoretical) (with LOX)	1.31 x 10 ⁶	0.0869	---
Lithium borohydride LiBH ₄ (excluding O ₂) ²⁰⁹⁸	1.386 x 10 ⁶	0.0218	3.27 x 10 ⁻⁵
Lithium borohydride LiBH ₄ (with LOX)	1.386 x 10 ⁶	0.0698	7.48 x 10 ⁻⁵
Lithium aluminum hydride LiAlH ₄ (excluding O ₂)	1.49 x 10 ⁶	0.037951	4.13 x 10 ⁻⁵
Sodium hydride NaH (excluding O ₂) ²⁰⁹⁹	3.22 x 10 ⁵	0.024	1.72 x 10 ⁻⁵

²⁰⁹⁶ Solid lithium hydride (LiH) has a density of 780 kg/m³ with MW of 0.00795 kg/mole; a stoichiometric combustion (LiH + 0.5O₂ → 0.5Li₂O + 0.5H₂O) using liquid oxygen (LOX: density 1141 kg/m³, MW 0.032 kg/mole) consumes 0.00795 kg of LiH and 0.016 kg of O₂ and releases 3.28 x 10⁵ J/mole of LiH (taking heats of formation of -90.65 kJ/mole for LiH, -595.8 kJ/mole for Li₂O, and -241.8 kJ/mole for H₂O(g)); https://en.wikipedia.org/wiki/Lithium_hydride and https://en.wikipedia.org/wiki/Lithium_oxide. “Dry oxygen does not react with crystalline LiH unless heated strongly, when an almost explosive combustion occurs.” https://en.wikipedia.org/wiki/Lithium_hydride#cite_note-Smith-3. “The ignition temperature for LiH is around 200 °C.”, Mueller WM, Blackledge JP, Libowitz GG. Metal Hydrides, Academic Press, 2013, p. 122.

²⁰⁹⁷ Lithium octahydride (LiH₈) has been predicted to be stable at very high pressure (>100 GPa) with a MW of 0.0149 kg/mole; a stoichiometric combustion (LiH₈ + 2.25O₂ → 0.5Li₂O + 4H₂O) using liquid oxygen (LOX: density 1141 kg/m³, MW 0.032 kg/mole) consumes 0.0149 kg of LiH and 0.072 kg of O₂ and releases 1.31 x 10⁶ J/mole of LiH₈, taking heats of formation as -597.9 kJ/mole for Li₂O and -241.8 kJ/mole for H₂O (http://www.update.uu.se/~jolkkonen/pdf/CRC_TD.pdf) and an estimated +43.42 kJ/mole for LiH₈ at 50 GPa (<http://uspex-team.org/file/ogonov/Zurek-LiHn-PNAS-2009.pdf>). No density information was provided.

²⁰⁹⁸ Solid lithium borohydride (LiBH₄) has a density of 666 kg/m³ with MW of 0.0218 kg/mole; a stoichiometric combustion (LiBH₄ + 1.5O₂ → LiOH + H₃BO₂) using liquid oxygen (LOX: density 1141 kg/m³, MW 0.032 kg/mole) consumes 0.0218 kg of LiBH₄ and 0.048 kg of O₂ and releases 1.386 x 10⁶ J/mole of LiBH₄ (standard enthalpy of combustion); https://en.wikipedia.org/wiki/Lithium_borohydride and Brinkman KS, Gray JR, Hardy B, Anton DL, The Hydrolysis and Oxidation Behavior of Lithium Borohydride and Magnesium Hydride (LiBH₄-MgH₂) Determined by Calorimetry, Savannah River National Laboratory, DOE, WSRC-STI-2008-00155, 2008; <http://sti.srs.gov/fulltext/WSRC-STI-2008-00155.pdf>.

²⁰⁹⁹ Solid sodium hydride (NaH) has a density of 1396 kg/m³ with MW of 0.024 kg/mole; a stoichiometric combustion (assumed NaH + 0.75O₂ → 0.5Na₂O₂ + 0.5H₂O) using liquid oxygen (LOX: density 1141 kg/m³, MW 0.032 kg/mole) consumes 0.024 kg of NaH and 0.024 kg of O₂ and releases 3.22 x 10⁵ J/mole of NaH (taking heats of formation of -56.4 kJ/mole for NaH, -515 kJ/mole for Na₂O₂, and -241.8 kJ/mole for H₂O(g)); https://en.wikipedia.org/wiki/Sodium_hydride and https://en.wikipedia.org/wiki/Sodium_peroxide. “Sodium hydride is stable in dry air but ignites above 230 °C, burning to form sodium oxide (Na₂O)...Sodium peroxide (Na₂O₂) is the product of sodium ignited in excess oxygen.” Harald Jakob, Stefan Leininger, Thomas Lehmann, Sylvia Jacobi, Sven Gutewort, “Peroxo Compounds, Inorganic,” Ullmann's Encyclopedia of Industrial Chemistry, 2007, Wiley-VCH, Weinheim. “[Cold] sodium hydride is not attacked by liquid oxygen,” Mellor JW, A Comprehensive Treatise on Inorganic and Theoretical Chemistry, 1922, p. 483.

Sodium hydride NaH (with LOX)	3.22×10^5	0.048	3.82×10^{-5}
Potassium hydride KH (excluding O ₂) ²¹⁰⁰	3.46×10^5	0.0401	2.80×10^{-5}
Potassium hydride KH (with LOX)	3.46×10^5	0.0761	5.96×10^{-5}
Rubidium hydride RbH (excluding O ₂) ²¹⁰¹	3.47×10^5	0.0865	3.33×10^{-5}
Rubidium hydride RbH (with LOX)	3.47×10^5	0.1225	6.48×10^{-5}
Cesium hydride CsH (excluding O ₂) ²¹⁰²	3.62×10^5	0.1339	3.92×10^{-5}
Cesium hydride CsH (with LOX)	3.62×10^5	0.1699	7.07×10^{-5}
Beryllium monohydride BeH (excluding O ₂) ²¹⁰³	1.052×10^6	0.010	---

²¹⁰⁰ Solid potassium hydride (KH) has a density of 1430 kg/m^3 with MW of 0.0401 kg/mole ; a stoichiometric combustion (assumed $\text{KH} + 1.25\text{O}_2 \rightarrow \text{KO}_2 + 0.5\text{H}_2\text{O}$) using liquid oxygen (LOX: density 1141 kg/m^3 , MW 0.032 kg/mole) consumes 0.0401 kg of KH and 0.036 kg of O₂ and releases $3.22 \times 10^5 \text{ J/mole}$ of KH (taking heats of formation of -57.82 kJ/mole for KH, -283 kJ/mole for KO₂, and -241.8 kJ/mole for H₂O(g)); https://en.wikipedia.org/wiki/Potassium_hydride and https://en.wikipedia.org/wiki/Potassium_superoxide. “Potassium superoxide is produced by burning molten potassium in an atmosphere of oxygen.” Harald Jakob, Stefan Leininger, Thomas Lehmann, Sylvia Jacobi, Sven Gutewort, “Peroxo Compounds, Inorganic,” Ullmann's Encyclopedia of Industrial Chemistry, 2007, Wiley-VCH, Weinheim. “Potassium hydride will ignite at room temperature in dry oxygen and air.” Mueller WM, Blackledge JP, Libowitz GG. Metal Hydrides, Academic Press, 2013, p. 122.

²¹⁰¹ Solid rubidium hydride (RbH) has a density of 2600 kg/m^3 with MW of 0.0865 kg/mole ; a stoichiometric combustion (assumed $\text{RbH} + 1.25\text{O}_2 \rightarrow \text{RbO}_2 + 0.5\text{H}_2\text{O}$) using liquid oxygen (LOX: density 1141 kg/m^3 , MW 0.032 kg/mole) consumes 0.0865 kg of RbH and 0.036 kg of O₂ and releases $3.47 \times 10^5 \text{ J/mole}$ of RbH (taking heats of formation of -52.3 kJ/mole for RbH, -278.7 kJ/mole for RbO₂, and -241.8 kJ/mole for H₂O(g)); https://en.wikipedia.org/wiki/Rubidium_hydride and http://www.update.uu.se/~jolkkonen/pdf/CRC_TD.pdf. “The final product of oxygenation of Rb is principally RbO₂, rubidium superoxide”; https://en.wikipedia.org/wiki/Rubidium_oxide. “Rubidium hydride will burn in dry oxygen at ordinary temperatures.” Mueller WM, Blackledge JP, Libowitz GG. Metal Hydrides, Academic Press, 2013, p. 122.

²¹⁰² Solid cesium hydride (CsH) has a density of 3420 kg/m^3 with MW of 0.1339 kg/mole ; a stoichiometric combustion (assumed $\text{CsH} + 1.25\text{O}_2 \rightarrow \text{CsO}_2 + 0.5\text{H}_2\text{O}$) using liquid oxygen (LOX: density 1141 kg/m^3 , MW 0.032 kg/mole) consumes 0.1339 kg of CsH and 0.036 kg of O₂ and releases $3.62 \times 10^5 \text{ J/mole}$ of CsH (taking heats of formation of -45 kJ/mole for CsH (calculated), -286.2 kJ/mole for CsO₂, and -241.8 kJ/mole for H₂O(g)); https://en.wikipedia.org/wiki/Caesium_hydride, http://www.update.uu.se/~jolkkonen/pdf/CRC_TD.pdf, and Anders Andreasen, “Predicting formation enthalpies of metal hydrides,” Risø National Laboratory, Roskilde, Denmark, Oct 2004, http://orbit.dtu.dk/fedora/objects/orbit:88288/datastreams/file_7711359/content. “If caesium is burned in air, the result is mainly formation of orange caesium superoxide, CsO₂”; https://www.webelements.com/compounds/caesium/caesium_superoxide.html.

Beryllium monohydride BeH (with LOX)	1.052×10^6	0.034	---
Beryllium dihydride BeH ₂ (excluding O ₂) ²¹⁰⁴	1.017×10^6	0.011	1.69×10^{-5}
Beryllium dihydride BeH ₂ (with LOX)	1.017×10^6	0.043	4.49×10^{-5}
Beryllium borohydride Be(BH ₄) ₂ (excluding O ₂) ²¹⁰⁵	2.74×10^6	0.0387	6.41×10^{-5}
Beryllium borohydride Be(BH ₄) ₂ (with LOX)	2.74×10^6	0.1667	1.76×10^{-4}
Magnesium borohydride Mg(BH ₄) ₂ (excluding O ₂) ²¹⁰⁶	2.56×10^6	0.0539	5.45×10^{-5}
Magnesium borohydride Mg(BH ₄) ₂ (with LOX)	2.56×10^6	0.182	1.67×10^{-4}
Magnesium hydride MgH ₂ (excluding O ₂)	7.67×10^5	0.026328	1.85×10^{-5}

²¹⁰³ Beryllium monohydride (BeH, 0.010 kg/mole, +321.2 kJ/mole heat of formation; https://en.wikipedia.org/wiki/Beryllium_monohydride) is a metastable monoradical species that has only been observed in gas phase (Dattani NS. Beryllium monohydride (BeH). J Molec Spectroscopy. 2015 May;311:76–83; https://www.academia.edu/12040610/Beryllium_monohydride_BeH_Where_we_are_now_after_86_years_of_spectroscopy) A stoichiometric combustion ($\text{BeH} + 0.75\text{O}_2 \rightarrow \text{BeO} + 0.5\text{H}_2\text{O}$) using liquid oxygen (LOX: density 1141 kg/m³, MW 0.032 kg/mole) consumes 0.010 kg of Be(BH₄)₂ and 0.024 kg of O₂ and releases 1.052×10^6 J/mole of BeH, taking heats of formation of -609.4 kJ/mole for BeO and -241.8 kJ/mole for H₂O (http://www.update.uu.se/~jolkkonen/pdf/CRC_TD.pdf). The dimeric molecule Be₂H₂ has also been observed in an argon matrix at 10 K (Tague TJ Jr, Andrews L. Reactions of beryllium atoms with hydrogen. Matrix infrared spectra of novel product molecules. J Am Chem Soc. 1993;115(25):12111-12116; <http://pubs.acs.org/doi/abs/10.1021/ja00078a057>).

²¹⁰⁴ Beryllium dihydride (BeH₂, 0.011 kg/mole, 650 kg/m³) is an amorphous white solid that decomposes above 523 K (https://en.wikipedia.org/wiki/Beryllium_hydride). A stoichiometric combustion ($\text{BeH}_2 + \text{O}_2 \rightarrow \text{BeO} + \text{H}_2\text{O}$) using liquid oxygen (LOX: density 1141 kg/m³, MW 0.032 kg/mole) consumes 0.011 kg of BeH₂ and 0.032 kg of O₂ and releases 1.017×10^6 J/mole of BeH₂, taking heats of formation as -609.4 kJ/mole for BeO, -241.8 kJ/mole for H₂O (http://www.update.uu.se/~jolkkonen/pdf/CRC_TD.pdf), and a predicted +165.3 kJ/mole for BeH₂ (Pople JA, *et al.* Theoretical thermochemistry. J Phys Chem 1985;89:2198-2203; <http://pubs.acs.org/doi/abs/10.1021/j100257a013>).

²¹⁰⁵ Solid beryllium borohydride (Be(BH₄)₂) has a density of 604 kg/m³ with MW of 0.0387 kg/mole; a stoichiometric combustion ($\text{Be}(\text{BH}_4)_2 + 4\text{O}_2 \rightarrow \text{BeO} + \text{B}_2\text{O}_3 + 4\text{H}_2\text{O}$) using liquid oxygen (LOX: density 1141 kg/m³, MW 0.032 kg/mole) consumes 0.0387 kg of Be(BH₄)₂ and 0.128 kg of O₂ and releases 2.74×10^6 J/mole of Be(BH₄)₂ (taking heats of formation of -108 kJ/mole for Be(BH₄)₂, -609.4 kJ/mole for BeO, -1273.5 kJ/mole for B₂O₃, and -241.8 kJ/mole for H₂O); https://en.wikipedia.org/wiki/Beryllium_borohydride, http://www.update.uu.se/~jolkkonen/pdf/CRC_TD.pdf, and <http://www.ncbi.nlm.nih.gov/pmc/articles/PMC3956662/>.

²¹⁰⁶ Solid magnesium borohydride (Mg(BH₄)₂) has a density of 989 kg/m³ with MW of 0.0539 kg/mole (<http://link.springer.com/article/10.1007/BF00849335>); a stoichiometric combustion ($\text{Mg}(\text{BH}_4)_2 + 4\text{O}_2 \rightarrow \text{MgO} + \text{B}_2\text{O}_3 + 4\text{H}_2\text{O}$) using liquid oxygen (LOX: density 1141 kg/m³, MW 0.032 kg/mole) consumes 0.0539 kg of Mg(BH₄)₂ and 0.128 kg of O₂ and releases 2.56×10^6 J/mole of Mg(BH₄)₂, taking heats of formation of -601.6 kJ/mole for MgO, -1273.5 kJ/mole for B₂O₃, and -241.8 kJ/mole for H₂O (http://www.update.uu.se/~jolkkonen/pdf/CRC_TD.pdf) and -282 kJ/mole for Mg(BH₄)₂ (Reed DR. An Investigation into the Synthesis and Characterisation of Metal Borohydrides for Hydrogen Storage. PhD thesis, University of Birmingham, Oct 2009, p.37; <http://etheses.bham.ac.uk/1008/1/Reed10PhD.pdf>).

Titanium dihydride TiH_2 (excluding O_2)	1.07×10^6	0.049916	1.28×10^{-3}
Zirconium hydride ZrH_2 (excluding O_2)	1.16×10^6	0.093236	1.64×10^{-5}
Aluminum borohydride $\text{Al}(\text{BH}_4)_3$, liquid (excluding O_2)	4.13×10^6	0.07154	1.32×10^{-4}
Dialuminum borohydride $\text{Al}_2\text{H}_2(\text{BH}_4)_4$ (excluding O_2) ²¹⁰⁷	6.69×10^6	0.115	2.08×10^{-4}
Boron monohydride BH (excluding O_2) ²¹⁰⁸	1.20×10^6	0.0118	---
Boron monohydride BH (with LOX)	1.20×10^6	0.0438	---
Aluminum monohydride AlH (excluding O_2) ²¹⁰⁹	1.22×10^6	0.028	---
Aluminum monohydride AlH (with LOX)	1.22×10^6	0.060	---
Alane AlH_3 (excluding O_2) ²¹¹⁰	1.15×10^6	0.030	2.03×10^{-5}

²¹⁰⁷ Dialuminum borohydride ($\text{Al}_2\text{H}_2(\text{BH}_4)_4$ or $\text{Al}_2\text{B}_4\text{H}_{18}$, 0.115 kg/mole, density 554 kg/m³; <http://chemister.ru/Database/properties-en.php?dbid=1&id=2121>) is readily synthesized from aluminum borohydride and has a calculated +272 kJ/mole heat of formation and a calculated combustion reaction energy of 6.69×10^6 J/mole (Bartlett RJ. Metastability in Molecules. Air Force Office of Scientific Research, AFOSR-89-0207, 5 Mar 1993, p.14; <http://www.dtic.mil/cgi-bin/GetTRDoc?AD=ADA264344>).

²¹⁰⁸ Gaseous boron monohydride radical (BH , 0.0118 kg/mole), upon undergoing stoichiometric combustion ($\text{BH} + \text{O}_2 \rightarrow 0.5\text{B}_2\text{O}_3 + 0.5\text{H}_2\text{O}$) using liquid oxygen (LOX: density 1141 kg/m³, MW 0.032 kg/mole) consumes 0.0118 kg of BH and 0.032 kg of O_2 and releases 1.20×10^6 J/mole of BH , taking heats of formation of +442.7 kJ/mole for BH , -1273.5 kJ/mole for B_2O_3 , and -241.8 kJ/mole for H_2O (http://www.update.uu.se/~jolkkonen/pdf/CRC_TD.pdf), with an activation energy of only 10 kJ/mole for BH reaction with O_2 (Garland NL, *et al.* BH reaction kinetics studied with a high-temperature reactor. *J Phys Chem.* 1990;94:4952-4956; <http://pubs.acs.org/doi/abs/10.1021/j100375a036>) and a dissociation energy of 330.1 kJ/mole for BH (Huber K, Herzberg G. *Molecular Spectra and Molecular Structure 4. Constants of Diatomic Molecules*, Van Nostrand, Princeton, 1979). The rate constants for initial reaction with O_2 have been measured at pressures of $\sim 10^{-8}$ atm, the BH being produced via excimer photodissociation of borane carbonyl (Rice JK, *et al.* Gas-phase reaction kinetics of BH . *J Phys Chem.* 1989;93:3600-3605; <http://pubs.acs.org/doi/abs/10.1021/j100346a045>).

²¹⁰⁹ Aluminum monohydride radical (AlH , 0.028 kg/mole), upon undergoing stoichiometric combustion ($\text{AlH} + \text{O}_2 \rightarrow 0.5\text{Al}_2\text{O}_3 + 0.5\text{H}_2\text{O}$) using liquid oxygen (LOX: density 1141 kg/m³, MW 0.032 kg/mole) consumes 0.028 kg of AlH and 0.032 kg of O_2 and releases 1.19×10^6 J/mole of AlH , taking heats of formation of -1675.7 kJ/mole for Al_2O_3 , -241.8 kJ/mole for H_2O (http://www.update.uu.se/~jolkkonen/pdf/CRC_TD.pdf), and +240.6 kJ/mole for AlH (Cobos CJ. Heats of formation for AlH , AlOH , OAlH and OAlOH and their monocations. *J Molec Struct (THEOCHEM)*. 2002 Apr 5;581(1-3):17-29; http://www.academia.edu/21928198/Heats_of_formation_for_AlH_AlOH_OAlH_and_OAlOH_and_their_monocations). This reactive gas has been used as the active medium in a metal-hydride photodissociation laser (Erlandson AC, Cool TA. Metal hydride photodissociation lasers: Laser operation for Al and In photofragments. *J Appl Phys.* 1984;56:1325; <http://scitation.aip.org/content/aip/journal/jap/56/5/10.1063/1.334121>) and the rate constants for initial reaction with O_2 have been measured at pressures of $<10^{-6}$ atm, the AlH being produced via excimer photodissociation of triethylaluminum (Pasternack L, Rice JK. AlH gas-phase reaction kinetics. *J Phys Chem.* 1991;95:8701-8706; <http://pubs.acs.org/doi/abs/10.1021/j100175a052>).

Alane AlH_3 (with LOX)	1.15×10^6	0.078	6.24×10^{-5}
Silane SiH_4 (excluding O_2) ²¹¹¹	1.43×10^6	0.0321	5.51×10^{-5}
Silane SiH_4 (with LOX)	1.43×10^6	0.0961	1.11×10^{-4}
Germane GeH_4 (excluding O_2) ²¹¹²	1.15×10^6	0.0766	5.63×10^{-5}
Germane GeH_4 (with LOX)	1.15×10^6	0.1406	1.12×10^{-4}
Arsine AsH_3 (excluding O_2) ²¹¹³	7.58×10^5	0.0779	4.75×10^{-5}
Arsine AsH_3 (with LOX)	7.58×10^5	0.1259	8.96×10^{-5}
Sulfanyl HS (excluding O_2) ²¹¹⁴	6.59×10^5	0.0331	---
Sulfanyl HS (with LOX)	6.59×10^5	0.0891	---
Uranium hydride UH_3 (excluding O_2) ²¹¹⁵	1.32×10^6	0.241	2.20×10^{-5}

²¹¹⁰ Alane, aka. aluminum hydride or alumane (AlH_3 , 0.030 kg/mole, density 1477 kg/m³; https://en.wikipedia.org/wiki/Aluminium_hydride) is a colorless pyrophoric solid. A stoichiometric combustion ($\text{AlH}_3 + 1.5\text{O}_2 \rightarrow 0.5\text{Al}_2\text{O}_3 + 1.5\text{H}_2\text{O}$) using liquid oxygen (LOX: density 1141 kg/m³, MW 0.032 kg/mole) consumes 0.030 kg of AlH_3 and 0.048 kg of O_2 and releases 1.15×10^6 J/mole of AlH_3 , taking heats of formation of -46.0 kJ/mole for AlH_3 , -1675.7 kJ/mole for Al_2O_3 , and -241.8 kJ/mole for H_2O (http://www.update.uu.se/~jolkkonen/pdf/CRC_TD.pdf).

²¹¹¹ Liquid silane (SiH_4) has a density of 583 kg/m³ with MW of 0.0321 kg/mole; a stoichiometric combustion ($\text{SiH}_4 + 2\text{O}_2 \rightarrow \text{SiO}_2 + 2\text{H}_2\text{O}$) using liquid oxygen (LOX: density 1141 kg/m³, MW 0.032 kg/mole) consumes 0.0321 kg of SiH_4 and 0.064 kg of O_2 and releases 1.43×10^6 J/mole of SiH_4 (taking heats of formation of +34.3 kJ/mole for SiH_4 , -910.7 kJ/mole for SiO_2 , and -241.8 kJ/mole for $\text{H}_2\text{O}(\text{g})$); <https://en.wikipedia.org/wiki/Silane>, <http://encyclopedia.airliquide.com/Encyclopedia.asp?GasID=57>, and http://www.update.uu.se/~jolkkonen/pdf/CRC_TD.pdf.

²¹¹² Liquid germane (GeH_4) has a density of 1360 kg/m³ with MW of 0.0766 kg/mole; a stoichiometric combustion ($\text{GeH}_4 + 2\text{O}_2 \rightarrow \text{GeO}_2 + 2\text{H}_2\text{O}$) using liquid oxygen (LOX: density 1141 kg/m³, MW 0.032 kg/mole) consumes 0.0766 kg of GeH_4 and 0.064 kg of O_2 and releases 1.15×10^6 J/mole of GeH_4 (taking heats of formation of +90.8 kJ/mole for GeH_4 , -580.0 kJ/mole for GeO_2 , and -241.8 kJ/mole for $\text{H}_2\text{O}(\text{g})$); <https://en.wikipedia.org/wiki/Germane>, <http://encyclopedia.airliquide.com/Encyclopedia.asp?GasID=31>, and http://www.update.uu.se/~jolkkonen/pdf/CRC_TD.pdf.

²¹¹³ Liquid arsine (AsH_3) has a density of 1640 kg/m³ with MW of 0.0779 kg/mole; a stoichiometric combustion ($\text{AsH}_3 + 1.5\text{O}_2 \rightarrow 0.5\text{As}_2\text{O}_3 + 1.5\text{H}_2\text{O}$) using liquid oxygen (LOX: density 1141 kg/m³, MW 0.032 kg/mole) consumes 0.0779 kg of AsH_3 and 0.048 kg of O_2 and releases 7.58×10^5 J/mole of AsH_3 (taking heats of formation of +66.4 kJ/mole for AsH_3 , -657.4 kJ/mole for As_2O_3 , and -241.8 kJ/mole for $\text{H}_2\text{O}(\text{g})$); <https://en.wikipedia.org/wiki/Arsine>, https://en.wikipedia.org/wiki/Arsenic_trioxide, and http://www.update.uu.se/~jolkkonen/pdf/CRC_TD.pdf.

²¹¹⁴ Sulfanyl, aka. mercapto radical or hydridosulfur (HS, 0.0331 kg/mole) is a reactive yellow gas (<https://en.wikipedia.org/wiki/Sulfanyl>). A stoichiometric combustion ($\text{HS} + 1.75\text{O}_2 \rightarrow \text{SO}_3 + 0.5\text{H}_2\text{O}$) using liquid oxygen (LOX: density 1141 kg/m³, MW 0.032 kg/mole) consumes 0.0331 kg of HS and 0.056 kg of O_2 and releases 6.59×10^5 J/mole of HS, taking heats of formation as +142.7 kJ/mole for HS, -395.7 kJ/mole for SO_3 , and -241.8 kJ/mole for H_2O (http://www.update.uu.se/~jolkkonen/pdf/CRC_TD.pdf).

Uranium hydride UH ₃ (with LOX)	1.32 x 10 ⁶	0.297	7.11 x 10 ⁻⁵
<u>Boranes and Carboranes</u>			
Borane BH ₃ (excluding O ₂) ²¹¹⁶	1.09 x 10 ⁶	0.0138	---
Borane BH ₃ (with LOX)	1.09 x 10 ⁶	0.0618	---
Diborane B ₂ H ₆ (excluding O ₂) ²¹¹⁷	2.04 x 10 ⁶	0.0277	6.20 x 10 ⁻⁵
Diborane B ₂ H ₆ (with LOX)	2.04 x 10 ⁶	0.1237	1.46 x 10 ⁻⁴
Pentaborane B ₅ H ₉ (excluding O ₂) ²¹¹⁸	4.27 x 10 ⁶	0.0631	1.02 x 10 ⁻⁴
Pentaborane B ₅ H ₉ (with LOX)	4.27 x 10 ⁶	0.2551	2.70 x 10 ⁻⁴
Decaborane B ₁₀ H ₁₄ (excluding O ₂) ²¹¹⁹	8.02 x 10 ⁶	0.1222	1.30 x 10 ⁻⁴

²¹¹⁵ Solid uranium hydride (UH₃) has a density of 10,950 kg/m³ with MW of 0.241 kg/mole; a stoichiometric combustion (UH₃ + 1.75O₂ → UO₂ + 1.5H₂O) using liquid oxygen (LOX: density 1141 kg/m³, MW 0.032 kg/mole) consumes 0.241 kg of UH₃ and 0.056 kg of O₂ and releases 1.32 x 10⁶ J/mole of UH₃ (taking heats of formation of -127.2 kJ/mole for UH₃, -1085.0 kJ/mole for UO₂, and -241.8 kJ/mole for H₂O(g));

https://en.wikipedia.org/wiki/Uranium_hydride and http://www.update.uu.se/~jolkkonen/pdf/CRC_TD.pdf.

²¹¹⁶ Borane (BH₃) has a MW of 0.0138 kg/mole but cannot be concentrated in pure form and has only been detected in the gaseous state (<https://en.wikipedia.org/wiki/Borane>), so any density or volumetric calculation would be meaningless. A stoichiometric combustion (BH₃ + 1.5O₂ → 0.5B₂O₃ + 1.5H₂O) using liquid oxygen (LOX: density 1141 kg/m³, MW 0.032 kg/mole) consumes 0.0138 kg of BH₃ and 0.048 kg of O₂ and releases 1.09 x 10⁶ J/mole of BH₃ (heat of combustion);

http://www.update.uu.se/~jolkkonen/pdf/CRC_TD.pdf.

²¹¹⁷ Liquid diborane (B₂H₆) has a MW of 0.0277 kg/mole and a density of 447 kg/m³ (<https://pubchem.ncbi.nlm.nih.gov/compound/diborane#section=Density>); a stoichiometric combustion (B₂H₆ + 3O₂ → B₂O₃ + 3H₂O) using liquid oxygen (LOX: density 1141 kg/m³, MW 0.032 kg/mole) consumes 0.0277 kg of B₂H₆ and 0.096 kg of O₂ and releases 2.04 x 10⁶ J/mole of B₂H₆ (heat of combustion); http://www.update.uu.se/~jolkkonen/pdf/CRC_TD.pdf.

²¹¹⁸ Liquid pentaborane (B₅H₉) has a density of 618 kg/m³ with MW of 0.0631 kg/mole; a stoichiometric combustion (B₅H₉ + 6O₂ → 2.5B₂O₃ + 4.5H₂O) using liquid oxygen (LOX: density 1141 kg/m³, MW 0.032 kg/mole) consumes 0.0631 kg of B₅H₉ and 0.192 kg of O₂ and releases 4.27 x 10⁶ J/mole of B₅H₉ (heat of combustion); <https://en.wikipedia.org/wiki/Pentaborane> and Altshuller AP. Calculated heats of formation and combustion of boron compounds (boron, hydrogen, carbon, silicon), NACA Research Memorandum, Washington DC, 4 Oct 1955;

http://digital.library.unt.edu/ark:/67531/metadc61577/m2/1/high_res_d/19930088850.pdf.

²¹¹⁹ Solid decaborane (B₁₀H₁₄) is a small cage cluster with a density of 940 kg/m³ and MW of 0.1222 kg/mole; a stoichiometric combustion (B₁₀H₁₄ + 11O₂ → 5B₂O₃ + 7H₂O) using liquid oxygen (LOX: density 1141 kg/m³, MW 0.032 kg/mole) consumes 0.1222 kg of B₁₀H₁₄ and 0.352 kg of O₂ and releases 8.02 x 10⁶ J/kg of B₁₀H₁₄ (heat of combustion); <https://en.wikipedia.org/wiki/Decaborane> and Altshuller AP. Calculated heats of formation and combustion of boron compounds (boron, hydrogen, carbon, silicon), NACA Research Memorandum, Washington DC, 4 Oct 1955;

http://digital.library.unt.edu/ark:/67531/metadc61577/m2/1/high_res_d/19930088850.pdf.

Decaborane B ₁₀ H ₁₄ (with LOX)	8.02 x 10 ⁶	0.4742	4.39 x 10 ⁻⁴
Iminoborane HNBH (excluding O ₂) ²¹²⁰	9.35 x 10 ⁵	0.0268	---
Iminoborane HNBH (with LOX)	9.35 x 10 ⁵	0.0668	---
Ammonia borane H ₃ NBH ₃ (excluding O ₂) ²¹²¹	1.11 x 10 ⁶	0.0309	3.96 x 10 ⁻⁵
Ammonia borane H ₃ NBH ₃ (with LOX)	1.11 x 10 ⁶	0.1029	1.03 x 10 ⁻⁴
Trimethylborane B(CH ₃) ₃ (excluding O ₂) ²¹²²	2.99 x 10 ⁶	0.0559	8.94 x 10 ⁻⁵
Trimethylborane B(CH ₃) ₃ (with LOX)	2.99 x 10 ⁶	0.2479	2.58 x 10 ⁻⁴
Triethylborane B(C ₂ H ₅) ₃ (excluding O ₂) ²¹²³	4.98 x 10 ⁶	0.098	1.45 x 10 ⁻⁴
Triethylborane B(C ₂ H ₅) ₃ (with LOX)	4.98 x 10 ⁶	0.434	4.39 x 10 ⁻⁴

²¹²⁰ Iminoborane (H-N≡B-H or HNBH, 0.0268 kg/mole) has been observed experimentally, is isoelectronic with and more reactive than acetylene, and trimerizes readily to borazine. A stoichiometric combustion (NBH₂ + 1.25O₂ → 0.5N₂ + 0.5B₂O₃ + H₂O) using liquid oxygen (LOX: density 1141 kg/m³, MW 0.032 kg/mole) consumes 0.0268 kg of NBH₂ and 0.040 kg of O₂ and releases 9.35 x 10⁵ J/mole of NBH₂, taking heats of formation as -1273.5 kJ/mole for B₂O₃ and -241.8 kJ/mole for H₂O (http://www.update.uu.se/~jolkkonen/pdf/CRC_TD.pdf) and +56.9 kJ/mole for HNBH (Dixon DA, Gutowski M. Thermodynamic properties of molecular borane amines and the [BH₄][NH₄⁺] salt for chemical hydrogen storage systems from ab initio electronic structure theory. J Phys Chem A. 2005 Jun 16;109(23):5129-35; <https://www.ncbi.nlm.nih.gov/pubmed/16833867>).

²¹²¹ Solid ammonia borane (NBH₆) has a density of 780 kg/m³ with MW of 0.0309 kg/mole (https://en.wikipedia.org/wiki/Ammonia_borane); a stoichiometric combustion (NBH₆ + 2.25O₂ → 0.5N₂ + BHO₂ + 2.5H₂O) using liquid oxygen (LOX: density 1141 kg/m³, MW 0.032 kg/mole) consumes 0.0309 kg of NBH₆ and 0.072 kg of O₂ and releases 1.11 x 10⁶ J/mole of NBH₆ (heat of combustion), taking NBH₆ heat of formation at -56.4 kJ/mole and BHO₂ as the final boron compound in the combustion of NBH₆ in oxygen (Weismiller M. Characterization of ammonia borane for chemical propulsion applications. PhD dissertation, Aug 2012, pp. 131, 138; https://etda.libraries.psu.edu/files/final_submissions/7560), and the heats of formation as -561.9 kJ/mole for BHO₂(g) and -241.8 kJ/mole for H₂O(g) (http://www.update.uu.se/~jolkkonen/pdf/CRC_TD.pdf).

²¹²² Liquid trimethylborane (B(CH₃)₃) has a density of 625 kg/m³ with MW of 0.0559 kg/mole; a stoichiometric combustion (B(CH₃)₃ + 6O₂ → 0.5B₂O₃ + 3CO₂ + 4.5H₂O) using liquid oxygen (LOX: density 1141 kg/m³, MW 0.032 kg/mole) consumes 0.0559 kg of B(CH₃)₃ and 0.192 kg of O₂ and releases 2.99 x 10⁶ J/mole of B(CH₃)₃ (heat of combustion); <https://en.wikipedia.org/wiki/Trimethylborane> and Johnson WH, Kilday MV, Prosen EJ. Heats of combustion and formation of trimethylborane, triethylborane, and tri-n-butylborane. J Res NBS. 1961 May-Jun;65A(3):215-219; http://nvlpubs.nist.gov/nistpubs/jres/65A/jresv65An3p215_A1b.pdf.

²¹²³ Liquid triethylborane (B(C₂H₅)₃), used as a pyrophoric ignitor in the Pratt & Whitney J58 turbojet/ramjet engines on the Lockheed SR-71 spy plane, has a density of 677 kg/m³ with MW of 0.098 kg/mole; a stoichiometric combustion (B(C₂H₅)₃ + 10.5O₂ → 0.5B₂O₃ + 6CO₂ + 7.5H₂O) using liquid oxygen (LOX: density 1141 kg/m³, MW 0.032 kg/mole) consumes 0.098 kg of B(C₂H₅)₃ and 0.336 kg of O₂ and releases 4.98 x 10⁶ J/mole of B(C₂H₅)₃ (heat of combustion); <https://en.wikipedia.org/wiki/Triethylborane> and Johnson WH, Kilday MV, Prosen EJ. Heats of combustion and formation of trimethylborane, triethylborane, and tri-n-butylborane. J Res NBS. 1961 May-Jun;65A(3):215-219; http://nvlpubs.nist.gov/nistpubs/jres/65A/jresv65An3p215_A1b.pdf.

closo-2,4-C ₂ B ₅ H ₇ carborane (excluding O ₂) ²¹²⁴	4.96 x 10 ⁶	0.0851	9.05 x 10 ⁻⁵
closo-2,4-C ₂ B ₅ H ₇ carborane (with LOX)	4.96 x 10 ⁶	0.3251	3.01 x 10 ⁻⁴
1,7-C ₂ B ₁₀ H ₁₁ -1-CH ₃ carborane (excluding O ₂) ²¹²⁵	8.92 x 10 ⁶	0.158	1.68 x 10 ⁻⁴
1,7-C ₂ B ₁₀ H ₁₁ -1-CH ₃ carborane (with LOX)	8.92 x 10 ⁶	0.606	5.61 x 10 ⁻⁴
Silanes			
Silane SiH ₄ (excluding O ₂) ²¹²⁶	1.43 x 10 ⁶	0.0331	5.68 x 10 ⁻⁵
Silane SiH ₄ (with LOX)	1.43 x 10 ⁶	0.0971	1.13 x 10 ⁻⁴
Disilane Si ₂ H ₆ (excluding O ₂) ²¹²⁷	2.63 x 10 ⁶	0.0622	9.15 x 10 ⁻⁵
Disilane Si ₂ H ₆ (with LOX)	2.63 x 10 ⁶	0.1742	1.90 x 10 ⁻⁴
Phosphanes			
Phosphine PH ₃ (excluding O ₂) ²¹²⁸	1.11 x 10 ⁶	0.0551	7.44 x 10 ⁻⁵

²¹²⁴ closo-2,4-C₂B₅H₇ carborane (C₂B₅H₇, 0.0851 kg/mole, density assumed same as decaborane ~ 940 kg/m³), heat of formation* +141 kJ/mole); a stoichiometric combustion (C₂B₅H₇ + 7.5O₂ → 2.5B₂O₃ + 2CO₂ + 3.5H₂O) using liquid oxygen (LOX: density 1141 kg/m³, MW 0.032 kg/mole) consumes 0.0851 kg of C₂B₅H₇ and 0.240 kg of O₂ and releases 4.96 x 10⁶ J/mole of C₂B₅H₇ (heat of combustion).

* Karl Beeker, Thomas Onak, B Boron Compounds: Boron and Chalcogens. Carboranes. Formula Index for 1st Suppl. Vol. 1 to 3, Springer, 2013, p. 144;

<https://books.google.com/books?id=TvXxCAAQBAJ&pg=PA144>.

²¹²⁵ 1,7-C₂B₁₀H₁₁-1-CH₃ carborane (C₃B₁₀H₁₄, 0.158 kg/mole, density assumed same as decaborane ~ 940 kg/m³), heat of formation* -311.6 kJ/mole); a stoichiometric combustion (C₃B₁₀H₁₄ + 14O₂ → 5B₂O₃ + 3CO₂ + 7H₂O) using liquid oxygen (LOX: density 1141 kg/m³, MW 0.032 kg/mole) consumes 0.158 kg of C₃B₁₀H₁₄ and 0.448 kg of O₂ and releases 8.93 x 10⁶ J/mole of C₃B₁₀H₁₄ (heat of combustion).

* Karl Beeker, Thomas Onak, B Boron Compounds: Boron and Chalcogens. Carboranes. Formula Index for 1st Suppl. Vol. 1 to 3, Springer, 2013, p. 230;

<https://books.google.com/books?id=TvXxCAAQBAJ&pg=PA230>.

²¹²⁶ Liquid silane (SiH₄) has a density of 583 kg/m³ with MW of 0.0331 kg/mole; a stoichiometric combustion (SiH₄ + 2O₂ → SiO₂ + 2H₂O) using liquid oxygen (LOX: density 1141 kg/m³, MW 0.032 kg/mole) consumes 0.0331 kg of SiH₄ and 0.064 kg of O₂ and releases 1.43 x 10⁶ J/mole of SiH₄ (taking heats of formation of +34.31 kJ/mole for SiH₄, -911 kJ/mole for SiO₂, and -241.8 kJ/mole for H₂O(g));

<https://en.wikipedia.org/wiki/Silane>, https://en.wikipedia.org/wiki/Silicon_dioxide, and

<http://encyclopedia.airliquide.com/Encyclopedia.asp?GasID=57>.

²¹²⁷ Liquid disilane (Si₂H₆) has a density of 680 kg/m³ with MW of 0.0622 kg/mole; a stoichiometric combustion (Si₂H₆ + 3.5O₂ → 2SiO₂ + 3H₂O) using liquid oxygen (LOX: density 1141 kg/m³, MW 0.032 kg/mole) consumes 0.0622 kg of Si₂H₆ and 0.112 kg of O₂ and releases 2.63 x 10⁶ J/mole of Si₂H₆ (taking heats of formation of +80.3 kJ/mole for Si₂H₆, -911 kJ/mole for SiO₂, and -241.8 kJ/mole for H₂O(g));

<https://en.wikipedia.org/wiki/Disilane>, http://www.concoa.com/silane_properties.html, and "Standard Thermodynamic Properties of Chemical Substances"

http://www.update.uu.se/~jolkkonen/pdf/CRC_TD.pdf.

Phosphine PH ₃ (with LOX)	1.11 x 10 ⁶	0.0791	9.55 x 10 ⁻⁵
Diphosphane P ₂ H ₆ (excluding O ₂) ²¹²⁹	1.97 x 10 ⁶	0.065	8.13 x 10 ⁻⁵
Diphosphane P ₂ H ₆ (with LOX)	1.97 x 10 ⁶	0.177	1.79 x 10 ⁻⁴
Trisilylphosphine P(SiH ₃) ₃ (excluding O ₂) ²¹³⁰	4.64 x 10 ⁶	0.1243	1.12 x 10 ⁻⁴
Trisilylphosphine P(SiH ₃) ₃ (with LOX)	4.64 x 10 ⁶	0.3323	2.94 x 10 ⁻⁴
<u>Metal Borides</u> ²¹³¹			
Be ₂ B (excluding O ₂)	1.74 x 10 ⁶	0.02884	1.3 x 10 ⁻⁵
Be ₅ B (excluding O ₂)	3.51 x 10 ⁶	0.05587	2.66 x 10 ⁻⁵
BeB ₆ (excluding O ₂)	4.23 x 10 ⁶	0.07388	3.17 x 10 ⁻⁵
MgB ₂ (excluding O ₂)	1.76 x 10 ⁶	0.04593	1.71 x 10 ⁻⁵
MgB ₄ (excluding O ₂)	3.01 x 10 ⁶	0.06756	2.70 x 10 ⁻⁵
MgB ₆ (excluding O ₂)	4.25 x 10 ⁶	0.08918	3.63 x 10 ⁻⁵
MgB ₁₂ (excluding O ₂)	7.99 x 10 ⁶	0.15404	6.31 x 10 ⁻⁵
TiB ₂ (excluding O ₂)	1.88 x 10 ⁶	0.06952	1.54 x 10 ⁻⁵
ZrB ₂ (excluding O ₂)	2.02 x 10 ⁶	0.11284	1.85 x 10 ⁻⁵
VB ₂ (excluding O ₂)	1.73 x 10 ⁶	0.07256	1.42 x 10 ⁻⁵
TaB ₂ (excluding O ₂)	2.11 x 10 ⁶	0.20257	1.82 x 10 ⁻⁵

²¹²⁸ Liquid phosphine (PH₃) has a density of 740 kg/m³ with MW of 0.0321 kg/mole; a stoichiometric combustion (PH₃ + 2O₂ → 0.5P₂O₅ + 1.5H₂O) using liquid oxygen (LOX: density 1141 kg/m³, MW 0.032 kg/mole) consumes 0.0321 kg of PH₃ and 0.064 kg of O₂ and releases 1.11 x 10⁶ J/mole of PH₃ (taking heats of formation of +5.4 kJ/mole for PH₃, -1492 kJ/mole for P₂O₅, and -241.8 kJ/mole for H₂O(g)); <https://en.wikipedia.org/wiki/Phosphine> and <http://encyclopedia.airliquide.com/Encyclopedia.asp?GasID=51>.

²¹²⁹ Liquid diphosphane (P₂H₆) has a density of ~800 kg/m³ with MW of 0.065 kg/mole; a stoichiometric combustion (P₂H₆ + 3.5O₂ → 5P₂O₅ + 2H₂O) using liquid oxygen (LOX: density 1141 kg/m³, MW 0.032 kg/mole) consumes 0.065 kg of P₂H₆ and 0.112 kg of O₂ and releases 1.97 x 10⁶ J/mole of P₂H₆ (taking heats of formation of -5.0 kJ/mole for P₂H₆ (liq), -1492 kJ/mole for P₂O₅, and -241.8 kJ/mole for H₂O(g)); <https://en.wikipedia.org/wiki/Diphosphane> and http://www.update.uu.se/~jolkkonen/pdf/CRC_TD.pdf.

²¹³⁰ Liquid trisilylphosphine (P(SiH₃)₃) has a density of 1112 kg/m³ with MW of 0.1243 kg/mole; a stoichiometric combustion (herein arbitrarily assumed to be P(SiH₃)₃ + 6.5O₂ → 0.5P₂O₅ + 3SiO₂ + 4.5H₂O(g)) using liquid oxygen (LOX: density 1141 kg/m³, MW 0.032 kg/mole) consumes 0.1243 kg of P(SiH₃)₃ and 0.208 kg of O₂ and releases 4.64 x 10⁶ J/mole of P(SiH₃)₃ (taking heats of formation of +69 kJ/mole for P(SiH₃)₃, -1492 kJ/mole for P₂O₅, -910.86 kJ/mole for SiO₂, and -241.8 kJ/mole for H₂O); https://www.researchgate.net/publication/250431206_Structure_of_Trisilylphosphine_PSiH33_at_100_K and Baboul AG, Schlegel HB. Structures and Energetics of Some Silicon–Phosphorus Compounds: SiHmPHn, SiHmPHnSiHo, and (SiH₃)₃P. An ab Initio Molecular Orbital Study. J Am Chem Soc. 1996;118(35):8444-8451; http://www.chem.wayne.edu/schlegel/Pub_folder/186.pdf. P(SiH₃)₃ is described as “a colorless liquid that ignites spontaneously in air.” Amberger E, Boeters H. The preparation of trisilylphosphine. Angew Chemie 1962 Jan 27;74:32-3.

²¹³¹ For items without reference tags: Gany A, Netzer DW. Fuel performance evaluation for the solid-fueled ramjet. Naval Postgraduate School, 1984-10; <http://calhoun.nps.edu/bitstream/handle/10945/29887/fuelperformance00gany.pdf?sequence=1>.

B ₃ Si (excluding O ₂)	2.66 x 10 ⁶	0.06052	2.40 x 10 ⁻⁵
B ₆ Si (excluding O ₂)	4.51 x 10 ⁶	0.09295	3.76 x 10 ⁻⁵
AlB ₂ (excluding O ₂)	1.77 x 10 ⁶	0.0466	1.46 x 10 ⁻⁵
AlB ₁₂ (excluding O ₂)	8.16 x 10 ⁶	0.15671	6.15 x 10 ⁻⁵
Beryllium diboride BeB ₂ (excluding O ₂) ²¹³²	1.87 x 10 ⁶	0.0306	1.39 x 10 ⁻⁵
Beryllium diboride BeB ₂ (with LOX)	1.87 x 10 ⁶	0.0946	7.00 x 10 ⁻⁵
Diberyllium diboride Be ₂ B ₂ (theoretical) (excluding O ₂) ²¹³³	3.44 x 10 ⁶	0.0396	1.80 x 10 ⁻⁵
Diberyllium diboride Be ₂ B ₂ (theoretical) (with LOX)	3.44 x 10 ⁶	0.1196	8.81 x 10 ⁻⁵
Dilithium diboride Li ₂ B ₂ (theoretical) (excluding O ₂) ²¹³⁴	2.62 x 10 ⁶	0.0354	---
Dilithium diboride Li ₂ B ₂ (theoretical) (with LOX)	2.62 x 10 ⁶	0.0994	---
<u>Intermetallics</u> ²¹³⁵			
Al ₃ Mg ₄ (excluding O ₂)	4.90 x 10 ⁶	0.17819	8.29 x 10 ⁻⁵
Mg ₂ Si (excluding O ₂)	2.03 x 10 ⁶	0.07671	3.95 x 10 ⁻⁵
VS ₂ (excluding O ₂)	2.42 x 10 ⁶	0.10711	2.42 x 10 ⁻⁵
V ₂ Si (excluding O ₂)	2.28 x 10 ⁶	0.12997	2.37 x 10 ⁻⁵
<u>Solid Carbides</u> ²¹³⁶			

²¹³² Beryllium diboride (BeB₂, 0.0306 kg/mole, 2206 kg/m³ density and -16.2 kJ/mole heat of formation for the most stable Cmc_m phase; Fan C, *et al.* A stable binary BeB₂ phase. Sci Reports 2014;4:6993; <http://www.nature.com/articles/srep06993>) with a stoichiometric combustion (BeB₂ + 2O₂ → BeO + B₂O₃) using liquid oxygen (LOX: density 1141 kg/m³, MW 0.032 kg/mole) consumes 0.0306 kg of BeB₂ and 0.064 kg of O₂, releasing 1.87 x 10⁶ J/mole of BeB₂, taking heats of formation of -609.4 kJ/mole for BeO and -1273.5 kJ/mole for Be₂O₃ (http://www.update.uu.se/~jolkkonen/pdf/CRC_TD.pdf).

²¹³³ Diberyllium diboride (Be₂B₂, 0.0396 kg/mole, density 2206 kg/m³ assumed same as BeB₂, and predicted +949.3 kJ/mole heat of formation at the MP4/6-31G* level of theory*) has been elusive experimentally, but a stoichiometric combustion (Be₂B₂ + 2.5O₂ → 2BeO + B₂O₃) using liquid oxygen (LOX: density 1141 kg/m³, MW 0.032 kg/mole) would consume 0.0396 kg of Be₂B₂ and 0.080 kg of O₂, and would release 3.44 x 10⁶ J/mole of Be₂B₂, taking heats of formation of -609.4 kJ/mole for BeO and -1273.5 kJ/mole for Be₂O₃ (http://www.update.uu.se/~jolkkonen/pdf/CRC_TD.pdf). *Guner OF, Lammertsma K. Structural and electronic properties of the tetraatomic B₂Be₂ cluster. J Am Chem Soc 1990;112:508-516; <http://pubs.acs.org/doi/abs/10.1021/ja00158a006>.

²¹³⁴ Dilithium diboride (Li₂B₂, 0.0354 kg/mole, and +746.8 kJ/mole heat of formation; Lammertsma K. New high energy density small ring systems. AL-TR-90-004, Dec 1990; <http://handle.dtic.mil/100.2/ADA231309>) with a stoichiometric combustion (Li₂B₂ + 2O₂ → Li₂O + B₂O₃) using liquid oxygen (LOX: density 1141 kg/m³, MW 0.032 kg/mole) consumes 0.0354 kg of Be₂B₂ and 0.064 kg of O₂, releasing 2.62 x 10⁶ J/mole of Be₂B₂, taking heats of formation of -597.9 kJ/mole for Li₂O and -1273.5 kJ/mole for Be₂O₃ (http://www.update.uu.se/~jolkkonen/pdf/CRC_TD.pdf).

²¹³⁵ For items without reference tags: Gany A, Netzer DW. Fuel performance evaluation for the solid-fueled ramjet. Naval Postgraduate School, 1984-10; <http://calhoun.nps.edu/bitstream/handle/10945/29887/fuelperformance00gany.pdf?sequence=1>.

Li ₂ C ₂ (excluding O ₂)	1.28 x 10 ⁶	0.03790	2.92 x 10 ⁻⁵
Be ₂ C (excluding O ₂)	1.47 x 10 ⁶	0.03363	1.77 x 10 ⁻⁵
CaC ₂ (excluding O ₂)	1.36 x 10 ⁶	0.06410	2.89 x 10 ⁻⁵
TiC (excluding O ₂)	1.15 x 10 ⁶	0.05991	1.22 x 10 ⁻⁵
ZrC (excluding O ₂)	1.28 x 10 ⁶	0.10323	1.53 x 10 ⁻⁵
VC (excluding O ₂)	1.00 x 10 ⁶	0.06295	1.09 x 10 ⁻⁵
TaC (excluding O ₂)	1.28 x 10 ⁶	0.19296	1.39 x 10 ⁻⁵
Fe ₃ C (excluding O ₂)	1.21 x 10 ⁶	0.17955	2.33 x 10 ⁻⁵
Ni ₃ C (excluding O ₂)	1.20 x 10 ⁶	0.18814	2.36 x 10 ⁻⁵
B ₄ C (excluding O ₂)	2.85 x 10 ⁶	0.05526	2.19 x 10 ⁻⁵
Al ₄ C ₃ (excluding O ₂)	4.32 x 10 ⁶	0.14395	6.10 x 10 ⁻⁵
SiC (excluding O ₂)	1.24 x 10 ⁶	0.04010	1.25 x 10 ⁻⁵
<u>Solid Nitrides</u>			
Lithium nitride Li ₃ N (excluding O ₂) ²¹³⁷	7.29 x 10 ⁵	0.0348	2.74 x 10 ⁻⁵
Lithium nitride Li ₃ N (with LOX)	7.29 x 10 ⁵	0.0588	4.84 x 10 ⁻⁵
Beryllium nitride Be ₃ N ₂ (excluding O ₂) ²¹³⁸	1.21 x 10 ⁶	0.0551	2.03 x 10 ⁻⁵
Beryllium nitride Be ₃ N ₂ (with LOX)	1.21 x 10 ⁶	0.0791	4.14 x 10 ⁻⁵
Boron nitride BN (excluding O ₂) ²¹³⁹	3.77 x 10 ⁵	0.0248	7.19 x 10 ⁻⁶

²¹³⁶ For items without reference tags: Gany A, Netzer DW. Fuel performance evaluation for the solid-fueled ramjet. Naval Postgraduate School, 1984-10;
<http://calhoun.nps.edu/bitstream/handle/10945/29887/fuelperformance00gany.pdf?sequence=1>.

²¹³⁷ Solid lithium nitride (Li₃N) has a density of 1270 kg/m³ with MW of 0.0348 kg/mole; a stoichiometric combustion (Li₃N + 0.75O₂ → 1.5Li₂O + 0.5N₂) using liquid oxygen (LOX: density 1141 kg/m³, MW 0.032 kg/mole) consumes 0.0348 kg of Li₃N and 0.024 kg of O₂ and releases 7.29 x 10⁵ J/mole of Li₃N (taking heats of formation of -164.56 kJ/mole for Li₃N and -595.8 kJ/mole for Li₂O);
https://en.wikipedia.org/wiki/Lithium_nitride, https://en.wikipedia.org/wiki/Lithium_oxide, and Osborne DW, Flotow HE. Lithium nitride (Li₃N): heat capacity from 5 to 350 K and thermochemical properties to 1086 K. J Chem Thermodyn. 1978 Jul;10(7):675-682;
<http://www.sciencedirect.com/science/article/pii/002196147890109X>.

²¹³⁸ Solid beryllium nitride (αBe₃N₂) has a density of 2710 kg/m³ with MW of 0.0551 kg/mole; a stoichiometric combustion (Be₃N₂ + 0.75O₂ → 3BeO + N₂) using liquid oxygen (LOX: density 1141 kg/m³, MW 0.032 kg/mole) consumes 0.0551 kg of Be₃N₂ and 0.024 kg of O₂ and releases 1.21 x 10⁶ J/mole of Be₃N₂ (taking heats of formation of -587 kJ/mole for Be₃N₂ and -599 kJ/mole for BeO);
https://en.wikipedia.org/wiki/Beryllium_nitride, https://en.wikipedia.org/wiki/Beryllium_oxide, and Yates RE, Greenbaum MA, Farber M. The Thermodynamic and Physical Properties of Beryllium Compounds. VI. The Heat of Formation of Beryllium Nitride. J Phys Chem. 1964;68(9):2682-2686;
<http://pubs.acs.org/doi/abs/10.1021/j100791a051>.

Boron nitride BN (with LOX)	3.77×10^5	0.0488	2.82×10^{-5}
Aluminum nitride AlN (excluding O ₂) ²¹⁴⁰	5.20×10^5	0.041	1.26×10^{-5}
Aluminum nitride AlN (with LOX)	5.20×10^5	0.065	3.36×10^{-5}
Silicon nitride Si ₃ N ₄ (excluding O ₂) ²¹⁴¹	1.97×10^6	0.140	4.38×10^{-5}
Silicon nitride Si ₃ N ₄ (with LOX)	1.97×10^6	0.236	1.28×10^{-4}
<u>Metal Phosphides</u> ²¹⁴²			
MgP ₂ (excluding O ₂)	1.80×10^6	0.08626	4.31×10^{-5}
Mg ₃ P ₂ (excluding O ₂)	2.88×10^6	0.13488	6.56×10^{-5}
TiP (excluding O ₂)	1.37×10^6	0.07887	2.00×10^{-5}
ZrP ₂ (excluding O ₂)	2.26×10^6	0.15317	3.21×10^{-5}
FeP (excluding O ₂)	8.46×10^5	0.08682	1.43×10^{-5}
FeP ₂ (excluding O ₂)	1.48×10^6	0.11780	1.96×10^{-5}
Fe ₂ P (excluding O ₂)	1.07×10^6	0.14267	2.10×10^{-5}
Fe ₃ P (excluding O ₂)	1.34×10^6	0.19851	2.79×10^{-5}
Ni ₃ P (excluding O ₂)	1.24×10^6	0.20710	2.69×10^{-5}
Ni ₂ P (excluding O ₂)	1.03×10^6	0.14839	2.06×10^{-5}
Ni ₃ P ₂ (excluding O ₂)	1.87×10^6	0.23808	3.97×10^{-5}
Zn ₃ P ₂ (excluding O ₂)	1.99×10^6	0.25806	5.67×10^{-5}
BP (excluding O ₂)	1.13×10^6	0.04178	1.41×10^{-5}

²¹³⁹ Solid cubic boron nitride (c-BN) has a density of 3450 kg/m³ with MW of 0.0248 kg/mole; a stoichiometric combustion (BN + 0.75O₂ → 0.5B₂O₃ + 0.5N₂) using liquid oxygen (LOX: density 1141 kg/m³, MW 0.032 kg/mole) consumes 0.0248 kg of BN and 0.024 kg of O₂ and releases 3.77 x 10⁵ J/mole of BN (standard enthalpy of combustion); https://en.wikipedia.org/wiki/Boron_nitride and Dworkin AS, Sasmor DJ, Van Artsdalen ER. The Thermodynamics of Boron Nitride; Low-Temperature Heat Capacity and Entropy; Heats of Combustion and Formation. J Chem Phys. 1954;22:837; <http://scitation.aip.org/content/aip/journal/jcp/22/5/10.1063/1.1740199>.

²¹⁴⁰ Solid aluminum nitride (AlN) has a density of 3260 kg/m³ with MW of 0.0410 kg/mole; a stoichiometric combustion (AlN + 0.75O₂ → 0.5Al₂O₃ + 0.5N₂) using liquid oxygen (LOX: density 1141 kg/m³, MW 0.032 kg/mole) consumes 0.041 kg of AlN and 0.024 kg of O₂ and releases 5.20 x 10⁵ J/mole of AlN (taking heats of formation of -318 kJ/mole for AlN and -1675.7 kJ/mole for Al₂O₃ (http://www.update.uu.se/~jolkkonen/pdf/CRC_TD.pdf); https://en.wikipedia.org/wiki/Aluminium_nitride and https://en.wikipedia.org/wiki/Aluminium_oxide).

²¹⁴¹ Solid silicon nitride (Si₃N₄) has a density of 3200 kg/m³ with MW of 0.140 kg/mole; a stoichiometric combustion (Si₃N₄ + 3O₂ → 3SiO₂ + 2N₂) using liquid oxygen (LOX: density 1141 kg/m³, MW 0.032 kg/mole) consumes 0.140 kg of Si₃N₄ and 0.096 kg of O₂ and releases 1.97 x 10⁶ J/mole of Si₃N₄ (taking heats of formation of -760 kJ/mole for amorphous Si₃N₄ and -910.86 kJ/mole for SiO₂); https://en.wikipedia.org/wiki/Silicon_nitride and Tomaszkiwicz I. Thermodynamics of silicon nitride: Standard molar enthalpy of formation of amorphous Si₃N₄ at 298.15 K. J Thermal Anal Calorimetry 2001 Aug;65(2):425-433; <http://link.springer.com/article/10.1023/A:1012472801483>.

²¹⁴² For items without reference tags: Gany A, Netzer DW. Fuel performance evaluation for the solid-fueled ramjet. Naval Postgraduate School, 1984-10; <http://calhoun.nps.edu/bitstream/handle/10945/29887/fuelperformance00gany.pdf?sequence=1>.

AIP (excluding O ₂)	1.38 x 10 ⁶	0.05796	2.40 x 10 ⁻³
<u>Organics</u>			
Methane CH ₄ , liquid (excluding O ₂) ²¹⁴³	8.91 x 10 ⁵	0.016	3.79 x 10 ⁻⁵
Methane CH ₄ , liquid (with LOX)	8.91 x 10 ⁵	0.080	9.40 x 10 ⁻⁵
Ethane C ₂ H ₆ , liquid (excluding O ₂) ²¹⁴⁴	1.561 x 10 ⁶	0.03007	5.52 x 10 ⁻⁵
Ethane C ₂ H ₆ , liquid (with LOX)	1.561 x 10 ⁶	0.14207	1.53 x 10 ⁻⁴
Propane C ₃ H ₈ , liquid (excluding O ₂) ²¹⁴⁵	2.22 x 10 ⁶	0.0441	7.59 x 10 ⁻⁵
Propane C ₃ H ₈ , liquid (with LOX)	2.22 x 10 ⁶	0.2041	2.16 x 10 ⁻⁴
Butane C ₄ H ₁₀ , liquid (excluding O ₂) ²¹⁴⁶	2.87 x 10 ⁶	0.0581	9.78 x 10 ⁻⁵
Butane C ₄ H ₁₀ , liquid (with LOX)	2.87 x 10 ⁶	0.2661	2.80 x 10 ⁻⁴
Octane C ₈ H ₁₈ ~ gasoline (excluding O ₂) ²¹⁴⁷	5.46 x 10 ⁶	0.114	1.65 x 10 ⁻⁴
Octane C ₈ H ₁₈ ~ gasoline (with LOX)	5.46 x 10 ⁶	0.514	5.15 x 10 ⁻⁴
Diesel fuel ~C ₁₂ H ₂₃ (excluding O ₂) ²¹⁴⁸	7.20 x 10 ⁶	0.167	2.01 x 10 ⁻⁴

²¹⁴³ Liquid methane (CH₄) has a density of 422.6 kg/m³ with MW of 0.016 kg/mole; a stoichiometric combustion (CH₄ + 2O₂ → CO₂ + 2H₂O) using liquid oxygen (LOX: density 1141 kg/m³, MW 0.032 kg/mole) consumes 0.016 kg of CH₄ and 0.064 kg of O₂ and releases 8.91 x 10⁵ J/mole of CH₄ (standard enthalpy of combustion); <https://en.wikipedia.org/wiki/Methane>.

²¹⁴⁴ Liquid ethane (C₂H₆) has a density of 544.6 kg/m³ with MW of 0.03007 kg/mole; a stoichiometric combustion (C₂H₆ + 3.5O₂ → 2CO₂ + 3H₂O) using liquid oxygen (LOX: density 1141 kg/m³, MW 0.032 kg/mole) consumes 0.03007 kg of C₂H₆ and 0.112 kg of O₂ and releases 1.561 x 10⁶ J/mole of C₂H₆ (standard enthalpy of combustion); <https://en.wikipedia.org/wiki/Ethane>.

²¹⁴⁵ Liquid propane (C₃H₈) has a density of 581 kg/m³ with MW of 0.0441 kg/mole; a stoichiometric combustion (C₃H₈ + 5O₂ → 3CO₂ + 4H₂O) using liquid oxygen (LOX: density 1141 kg/m³, MW 0.032 kg/mole) consumes 0.0441 kg of C₃H₈ and 0.160 kg of O₂ and releases 2.22 x 10⁶ J/mole of C₃H₈ (standard enthalpy of combustion); <https://en.wikipedia.org/wiki/Propane> and <http://encyclopedia.airliquide.com/Encyclopedia.asp?GasID=53>.

²¹⁴⁶ Liquid iso-butane (C₄H₁₀) has a density of 594 kg/m³ with MW of 0.0581 kg/mole; a stoichiometric combustion (C₄H₁₀ + 6.5O₂ → 4CO₂ + 5H₂O) using liquid oxygen (LOX: density 1141 kg/m³, MW 0.032 kg/mole) consumes 0.0581 kg of C₄H₁₀ and 0.208 kg of O₂ and releases 2.87 x 10⁶ J/mole of C₄H₁₀ (standard enthalpy of combustion); <https://en.wikipedia.org/wiki/Isobutane> and <http://encyclopedia.airliquide.com/Encyclopedia.asp?GasID=38>.

²¹⁴⁷ Liquid iso-octane or 2,2,4-trimethylpentane (C₈H₁₈), a main component of gasoline, has a density of 692 kg/m³ with MW of 0.114 kg/mole; a stoichiometric combustion (C₈H₁₈ + 12.5O₂ → 8CO₂ + 9H₂O) using liquid oxygen (LOX: density 1141 kg/m³, MW 0.032 kg/mole) consumes 0.114 kg of C₈H₁₈ and 0.4 kg of O₂ and releases 5.46 x 10⁶ J/mole of C₈H₁₈ (standard enthalpy of combustion); <https://en.wikipedia.org/wiki/2,2,4-Trimethylpentane>.

Diesel fuel ~C ₁₂ H ₂₃ (with LOX)	7.20 x 10 ⁶	0.735	6.99 x 10 ⁻⁴
Dodecane C ₁₂ H ₂₆ (excluding O ₂) ²¹⁴⁹	7.90 x 10 ⁶	0.1703	2.27 x 10 ⁻⁴
Dodecane C ₁₂ H ₂₆ (with LOX)	7.90 x 10 ⁶	0.7623	7.46 x 10 ⁻⁴
Adamantane C ₁₀ H ₁₆ (excluding O ₂) ²¹⁵⁰	6.03 x 10 ⁶	0.1362	1.26 x 10 ⁻⁴
Adamantane C ₁₀ H ₁₆ (with LOX)	6.03 x 10 ⁶	0.5842	5.19 x 10 ⁻⁴
Ethylene C ₂ H ₄ (excluding O ₂) ²¹⁵¹	1.39 x 10 ⁶	0.0281	4.95 x 10 ⁻⁵
Ethylene C ₂ H ₄ (with LOX)	1.39 x 10 ⁶	0.1241	1.34 x 10 ⁻⁴
Propylene C ₃ H ₆ (excluding O ₂) ²¹⁵²	1.93 x 10 ⁶	0.0421	6.86 x 10 ⁻⁵
Propylene C ₃ H ₆ (with LOX)	1.93 x 10 ⁶	0.1861	1.95 x 10 ⁻⁴
Acetylene C ₂ H ₂ (excluding O ₂) ²¹⁵³	1.254 x 10 ⁶	0.026	4.24 x 10 ⁻⁵

²¹⁴⁸ Liquid diesel fuel of average chemical formula C₁₂H₂₃ has a density of 832 kg/m³ with MW of 0.167 kg/mole; a stoichiometric combustion (C₁₂H₂₃ + 17.75O₂ → 12CO₂ + 11.5H₂O) using liquid oxygen (LOX: density 1141 kg/m³, MW 0.032 kg/mole) consumes 0.167 kg of C₁₂H₂₃ and 0.568 kg of O₂ and releases 7.20 x 10⁶ J/mole of C₁₂H₂₃ (assuming ~43.1 MJ/kg); https://en.wikipedia.org/wiki/Diesel_fuel.

²¹⁴⁹ Liquid n-dodecane (C₁₂H₂₆) has a density of 750 kg/m³ with MW of 0.1703 kg/mole; a stoichiometric combustion (C₁₂H₂₆ + 18.5O₂ → 12CO₂ + 13H₂O) using liquid oxygen (LOX: density 1141 kg/m³, MW 0.032 kg/mole) consumes 0.1703 kg of C₁₂H₂₆ and 0.592 kg of O₂ and releases 7.90 x 10⁶ J/mole of C₁₂H₂₆ (standard enthalpy of combustion); <https://en.wikipedia.org/wiki/Dodecane>. “In recent years, n-dodecane has garnered attention as a possible surrogate for kerosene-based fuels such as Jet-A, S-8, and other conventional aviation fuels.”

²¹⁵⁰ Solid adamantane (C₁₀H₁₆) has a density of 1080 kg/m³ with MW of 0.1362 kg/mole; a stoichiometric combustion (C₁₀H₁₆ + 14O₂ → 10CO₂ + 8H₂O) using liquid oxygen (LOX: density 1141 kg/m³, MW 0.032 kg/mole) consumes 0.1362 kg of C₁₀H₁₆ and 0.448 kg of O₂ and releases 6.0304 x 10⁶ J/mole of C₁₀H₁₆ (standard enthalpy of combustion); <https://en.wikipedia.org/wiki/Adamantane> and Bazyleva AB *et al.* Thermodynamic properties of adamantane revisited. J Phys Chem B 2011;115:10064-10072; <http://www.chemie1.uni-rostock.de/pci/emelyanenko/publications/75.pdf>.

²¹⁵¹ Liquid ethylene (H₂C=CH₂ or C₂H₄), aka. ethene, has a density of 568 kg/m³ with MW of 0.0281 kg/mole; a stoichiometric combustion (C₂H₄ + 3O₂ → 2CO₂ + 2H₂O) using liquid oxygen (LOX: density 1141 kg/m³, MW 0.032 kg/mole) consumes 0.0281 kg of C₂H₄ and 0.096 kg of O₂ and releases 1.39 x 10⁶ J/mole of C₂H₄ (standard enthalpy of combustion); [https://en.wikipedia.org/wiki/Ethylene_\(data_page\)](https://en.wikipedia.org/wiki/Ethylene_(data_page)), <http://encyclopedia.airliquide.com/Encyclopedia.asp?GasID=29>, and http://www.update.uu.se/~jolkkonen/pdf/CRC_TD.pdf.

²¹⁵² Liquid propylene (H₃C-CH=CH₂ or C₃H₆), aka. propene, has a density of 614 kg/m³ with MW of 0.0421 kg/mole; a stoichiometric combustion (C₃H₆ + 4.5O₂ → 3CO₂ + 3H₂O) using liquid oxygen (LOX: density 1141 kg/m³, MW 0.032 kg/mole) consumes 0.0421 kg of C₃H₆ and 0.144 kg of O₂ and releases 45.799 MJ/kg = 1.93 x 10⁶ J/mole of C₃H₆ (standard enthalpy of combustion); <https://en.wikipedia.org/wiki/Propene> and https://en.wikipedia.org/wiki/Heat_of_combustion.

Acetylene C ₂ H ₂ (with LOX)	1.254 x 10 ⁶	0.106	1.13 x 10 ⁻⁴
Propadiene C ₃ H ₄ (excluding O ₂) ²¹⁵⁴	1.85 x 10 ⁶	0.0401	6.09 x 10 ⁻⁵
Propadiene C ₃ H ₄ (with LOX)	1.85 x 10 ⁶	0.168	1.73 x 10 ⁻⁴
Diacetylene C ₄ H ₂ (excluding O ₂) ²¹⁵⁵	2.27 x 10 ⁶	0.050	8.16 x 10 ⁻⁵
Diacetylene C ₄ H ₂ (with LOX)	2.27 x 10 ⁶	0.194	2.08 x 10 ⁻⁴
Butatriene C ₄ H ₄ (excluding O ₂) ²¹⁵⁶	2.41 x 10 ⁶	0.052	8.84 x 10 ⁻⁵
Butatriene C ₄ H ₄ (with LOX)	2.41 x 10 ⁶	0.212	2.28 x 10 ⁻⁴
Triacetylene C ₆ H ₂ (excluding O ₂) ²¹⁵⁷	3.25 x 10 ⁶	0.074	8.22 x 10 ⁻⁵

²¹⁵³ Liquid acetylene (HC≡CH or C₂H₂), regarded as highly explosive if any oxygen is present, can only exist above 1.27 atm pressure and has a density of 613 kg/m³ at -80 °C with MW of 0.026 kg/mole; a stoichiometric combustion (C₂H₂ + 2.5O₂ → 2CO₂ + H₂O) using liquid oxygen (LOX: density 1141 kg/m³, MW 0.032 kg/mole) consumes 0.026 kg of C₂H₂ and 0.080 kg of O₂ and releases 48.241 MJ/kg = 1.254 x 10⁶ J/mole of C₂H₂ (heat of combustion); <https://en.wikipedia.org/wiki/Acetylene>, https://en.wikipedia.org/wiki/Heat_of_combustion, and http://carbon.atomistry.com/physical_properties_acetylene.html.

²¹⁵⁴ Propadiene, aka. allene (H₂C=C=CH₂ or C₃H₄, 0.0401 kg/mole, liquid density 658 kg/m³; <http://encyclopedia.airliquide.com/Encyclopedia.asp?GasID=52#GeneralData>) exists in equilibrium with propyne, the mixture being sold as MAPP gas, a fuel for specialized welding (<https://en.wikipedia.org/wiki/Propadiene>). Stoichiometric combustion (C₃H₄ + 4O₂ → 3CO₂ + 2H₂O) using liquid oxygen (LOX: density 1141 kg/m³, MW 0.032 kg/mole), consumes 0.0401 kg of C₃H₄ and 0.128 kg of O₂ and releases 1.85 x 10⁶ J/mole of C₃H₄, taking the heat of formation for C₃H₄ as +190.5 kJ/mole (http://www.update.uu.se/~jolkkonen/pdf/CRC_TD.pdf).

²¹⁵⁵ Diacetylene, aka. butadiyne (HC≡C-C≡CH or C₄H₂, 0.050 kg/mole, density ~ 613 kg/m³, assumed same as liquid acetylene) may undergo stoichiometric combustion (C₄H₂ + 4.5O₂ → 4CO₂ + H₂O) using liquid oxygen (LOX: density 1141 kg/m³, MW 0.032 kg/mole), consuming 0.050 kg of C₄H₂ and 0.144 kg of O₂ and releasing 2.27 x 10⁶ J/mole of C₄H₂, taking the heat of formation for C₄H₂ as +456.1 kJ/mole; Wodrich MD, *et al.* How strained are carbomeric-cycloalkanes? J Phys Chem. 2010 May 20;114(24):6705-6712.

²¹⁵⁶ Butatriene, aka. cumulene* (H₂C=C=C=CH₂ or C₄H₄, 0.052 kg/mole, liquid density 588 kg/m³; <http://www.guidechem.com/dictionary/en/2873-50-9.html>), upon undergoing stoichiometric combustion (C₄H₄ + 5O₂ → 4CO₂ + 2H₂O) using liquid oxygen (LOX: density 1141 kg/m³, MW 0.032 kg/mole), consumes 0.052 kg of C₃H₄ and 0.160 kg of O₂ and releases 2.41 x 10⁶ J/mole of C₃H₄, taking the heat of formation for C₄H₄ as +349 kJ/mole (Yung YL, DeMore WB, Photochemistry of Planetary Atmospheres, Oxford University Press, 1999, Table 5.9, p. 145; <https://books.google.com/books?id=FY3mCwAAQBAJ&pg=PA145>). *”Cumulene,” <https://en.wikipedia.org/wiki/Cumulene>.

Triacetylene C ₆ H ₂ (with LOX)	3.25 x 10 ⁶	0.282	2.64 x 10 ⁻⁴
Tetraacetylene C ₈ H ₂ (excluding O ₂) ²¹⁵⁸	4.25 x 10 ⁶	0.098	9.80 x 10 ⁻⁵
Tetraacetylene C ₈ H ₂ (with LOX)	4.25 x 10 ⁶	0.370	3.36 x 10 ⁻⁴
Propyne C ₃ H ₄ (excluding O ₂) ²¹⁵⁹	1.85 x 10 ⁶	0.0401	5.95 x 10 ⁻⁵
Propyne C ₃ H ₄ (with LOX)	1.85 x 10 ⁶	0.1681	1.72 x 10 ⁻⁴
Butyne C ₄ H ₆ (excluding O ₂) ²¹⁶⁰	2.45 x 10 ⁶	0.0541	7.98 x 10 ⁻⁵
Butyne C ₄ H ₆ (with LOX)	2.45 x 10 ⁶	0.2301	2.34 x 10 ⁻⁴
Cyclopropane C ₃ H ₆ , liquid (excluding O ₂) ²¹⁶¹	2.08 x 10 ⁶	0.0421	6.21 x 10 ⁻⁵
Cyclopropane C ₃ H ₆ , liquid (with LOX)	2.08 x 10 ⁶	0.1861	1.88 x 10 ⁻⁴
Cyclobutadiene C ₄ H ₄ , liquid (excluding O ₂) ²¹⁶²	2.76 x 10 ⁶	0.0521	---

²¹⁵⁷ Triacetylene, aka. 1,3,5-hexatriyne (HC≡C-C≡C-C≡CH or C₆H₂, 0.074 kg/mole, density ~ 900 kg/m³; <http://www.chemspider.com/Chemical-Structure.121493.html?rid=f3695b2f-1550-42fd-a149-7021bd5ba3b1>) may undergo stoichiometric combustion (C₆H₂ + 6.5O₂ → 6CO₂ + H₂O) using liquid oxygen (LOX: density 1141 kg/m³, MW 0.032 kg/mole), consuming 0.074 kg of C₆H₂ and 0.208 kg of O₂ and releasing 3.25 x 10⁶ J/mole of C₆H₂, taking the heat of formation for C₆H₂ as +644 kJ/mole; Sorkhabi O, Qi F, Rizvi AH, Suits AG. The ultraviolet photochemistry of phenylacetylene and the enthalpy of formation of 1,3,5-hexatriyne. J Am Chem Soc. 2001 Jan 31;123(4):671-6; <https://publications.lbl.gov/islandora/object/ir%3A115749/datastream/PDF/download/citation.pdf>.

²¹⁵⁸ Tetraacetylene, aka. 1,3,5,7-octatetrayne (HC≡C-C≡C-C≡C-C≡CH or C₈H₂, 0.098 kg/mole, density ~ 1000 kg/m³; <http://www.chemspider.com/Chemical-Structure.122295.html>) may undergo stoichiometric combustion (C₈H₂ + 8.5O₂ → 8CO₂ + H₂O) using liquid oxygen (LOX: density 1141 kg/m³, MW 0.032 kg/mole), consuming 0.098 kg of C₈H₂ and 0.272 kg of O₂ and releasing 4.25 x 10⁶ J/mole of C₈H₂, taking the heat of formation for C₈H₂ as +864.0 kJ/mole; <http://udfa.ajmarkwick.net/index.php?species=425>.

²¹⁵⁹ Liquid propyne (H₃C-C≡CH or C₃H₄), which unlike C₂H₂ can be safely condensed, has a density of 674 kg/m³ at -25 °C with MW of 0.0401 kg/mole; a stoichiometric combustion (C₃H₄ + 4O₂ → 3CO₂ + 2H₂O) using liquid oxygen (LOX: density 1141 kg/m³, MW 0.032 kg/mole) consumes 0.0401 kg of C₃H₄ and 0.128 kg of O₂ and releases 46.194 MJ/kg = 1.85 x 10⁶ J/mole of C₃H₄ (heat of combustion); <https://en.wikipedia.org/wiki/Propyne>, https://en.wikipedia.org/wiki/Heat_of_combustion, and <http://encyclopedia.airliquide.com/Encyclopedia.asp?GasID=72>.

²¹⁶⁰ Liquid 1-butyne (H₃C-CH₂-C≡CH or C₄H₆), aka. ethylacetylene, has a density of 678 kg/m³ with MW of 0.0541 kg/mole; a stoichiometric combustion (C₄H₆ + 5.5O₂ → 4CO₂ + 3H₂O) using liquid oxygen (LOX: density 1141 kg/m³, MW 0.032 kg/mole) consumes 0.0541 kg of C₄H₆ and 0.176 kg of O₂ and releases 45.334 MJ/kg = 2.45 x 10⁶ J/mole of C₄H₆ (heat of combustion); <https://en.wikipedia.org/wiki/1-Butyne> and https://en.wikipedia.org/wiki/Heat_of_combustion.

²¹⁶¹ Liquid cyclopropane (C₃H₆), with the highest ring strain of the cycloalkanes, has a density of 678 kg/m³ with MW of 0.0421 kg/mole; a stoichiometric combustion (C₃H₆ + 4.5O₂ → 3CO₂ + 3H₂O) using liquid oxygen (LOX: density 1141 kg/m³, MW 0.032 kg/mole) consumes 0.0421 kg of C₃H₆ and 0.144 kg of O₂ and releases 1.96 x 10⁶ J/mole of C₃H₆ (http://chem.libretexts.org/Core/Organic_Chemistry/Hydrocarbons/Alkanes/Reactivity_of_Alkanes/Alkane_Heats_of_Combustion) plus 115.5 kJ/mole of strain energy (<https://en.wikipedia.org/wiki/Cyclopropane>).

Cyclobutadiene C ₄ H ₄ , liquid (with LOX)	2.76 x 10 ⁶	0.212	---
Cyclobutene C ₄ H ₆ , liquid (excluding O ₂) ²¹⁶³	2.58 x 10 ⁶	0.0541	7.38 x 10 ⁻⁵
Cyclobutene C ₄ H ₆ , liquid (with LOX)	2.58 x 10 ⁶	0.230	2.28 x 10 ⁻⁴
Bicyclobutane C ₄ H ₆ , liquid (excluding O ₂) ²¹⁶⁴	2.79 x 10 ⁶	0.0541	7.38 x 10 ⁻⁵
Bicyclobutane C ₄ H ₆ , liquid (with LOX)	2.79 x 10 ⁶	0.230	2.28 x 10 ⁻⁴
Cyclobutane C ₄ H ₈ , liquid (excluding O ₂) ²¹⁶⁵	2.68 x 10 ⁶	0.0561	7.79 x 10 ⁻⁵
Cyclobutane C ₄ H ₈ , liquid (with LOX)	2.68 x 10 ⁶	0.2481	2.46 x 10 ⁻⁴
Cyclopentane C ₅ H ₁₀ , liquid (excluding O ₂) ²¹⁶⁶	3.13 x 10 ⁶	0.0701	9.33 x 10 ⁻⁵

²¹⁶² Cyclobutadiene, aka. 1,3-cyclobutadiene or [4]annulene (C₄H₄, 0.0521 kg/mole) is “an extremely unstable hydrocarbon having a lifetime shorter than five seconds in the free state” (<https://en.wikipedia.org/wiki/Cyclobutadiene>). A stoichiometric combustion (C₄H₄ + 5O₂ → 4CO₂ + 2H₂O) using liquid oxygen (LOX: density 1141 kg/m³, MW 0.032 kg/mole) consumes 0.0521 kg of C₄H₄ and 0.160 kg of O₂ and releases 2.49 x 10⁶ J/mole of C₄H₄, taking the standard heats of formation as -393.5 kJ/mole for CO₂, -241.8 kJ/mole for H₂O (http://www.update.uu.se/~jolkkonen/pdf/CRC_TD.pdf), and +431.0 kJ/mole for cyclobutadiene (Lammertsma K. New high energy density small ring systems. AL-TR-90-004, Dec 1990; <http://handle.dtic.mil/100.2/ADA231309>) plus 272 kJ/mole of strain energy.

²¹⁶³ Liquid cyclobutene (C₄H₆, 0.0541 kg/mole, 733 kg/m³; <https://en.wikipedia.org/wiki/Cyclobutene>), with a stoichiometric combustion (C₄H₆ + 5.5O₂ → 4CO₂ + 3H₂O) using liquid oxygen (LOX: density 1141 kg/m³, MW 0.032 kg/mole) consumes 0.0541 kg of C₄H₆ and 0.176 kg of O₂ and releases 2.46 x 10⁶ J/mole of C₄H₆, taking the standard heats of formation as -393.5 kJ/mole for CO₂, -241.8 kJ/mole for H₂O (http://www.update.uu.se/~jolkkonen/pdf/CRC_TD.pdf) and +156.9 kJ/mole for C₄H₆ (Lammertsma K. New high energy density small ring systems. AL-TR-90-004, Dec 1990; <http://handle.dtic.mil/100.2/ADA231309>) plus 121.3 kJ/mole of strain energy.

²¹⁶⁴ Bicyclobutane, aka. bicyclo[1.1.0]butane (C₄H₆, 0.0541 kg/mole, assumed ~733 kg/m³ in liquid form) “is one of the most strained compounds isolatable on a large scale” (<https://en.wikipedia.org/wiki/Bicyclobutane>). A stoichiometric combustion (C₄H₆ + 5.5O₂ → 4CO₂ + 3H₂O) using liquid oxygen (LOX: density 1141 kg/m³, MW 0.032 kg/mole) consumes 0.0541 kg of C₄H₆ and 0.176 kg of O₂ and releases 2.52 x 10⁶ J/mole of C₄H₆, taking the standard heats of formation as -393.5 kJ/mole for CO₂, -241.8 kJ/mole for H₂O (http://www.update.uu.se/~jolkkonen/pdf/CRC_TD.pdf), and +217.1 kJ/mole for bicyclobutane (Lammertsma K. New high energy density small ring systems. AL-TR-90-004, Dec 1990; <http://handle.dtic.mil/100.2/ADA231309>) plus 272 kJ/mole of strain energy.

²¹⁶⁵ Liquid cyclobutane (C₄H₈), with the second highest ring strain of the cycloalkanes, has a density of 720 kg/m³ with MW of 0.0561 kg/mole (<https://en.wikipedia.org/wiki/Cyclobutane>); a stoichiometric combustion (C₄H₈ + 6O₂ → 4CO₂ + 4H₂O) using liquid oxygen (LOX: density 1141 kg/m³, MW 0.032 kg/mole) consumes 0.0561 kg of C₄H₈ and 0.192 kg of O₂ and releases 2.57 x 10⁶ J/mole of C₄H₈ (http://chem.libretexts.org/Core/Organic_Chemistry/Hydrocarbons/Alkanes/Reactivity_of_Alkanes/Alkane_Heats_of_Combustion) plus 109.6 kJ/mole of strain energy (<https://en.wikipedia.org/wiki/Cyclopropane>).

²¹⁶⁶ Liquid cyclopentane (C₅H₁₀, 0.0701 kg/mole, 751 kg/m³; <https://en.wikipedia.org/wiki/Cyclopentane>) in a stoichiometric combustion (C₅H₁₀ + 7.5O₂ → 5CO₂ + 5H₂O) using liquid oxygen (LOX: density 1141 kg/m³, MW 0.032 kg/mole) consumes 0.0701 kg of C₅H₁₀ and 0.240 kg of O₂ and releases 3.10 x 10⁶ J/mole of C₅H₁₀, plus 29 kJ/mole of strain energy (<https://openresearch-repository.anu.edu.au/bitstream/1885/48020/19/07Chapter4b.pdf>).

Cyclopentane C ₅ H ₁₀ , liquid (with LOX)	3.13 x 10 ⁶	0.3101	3.03 x 10 ⁻⁴
Benzene C ₆ H ₆ , liquid (excluding O ₂) ²¹⁶⁷	3.268 x 10 ⁶	0.0781	8.91 x 10 ⁻⁵
Benzene C ₆ H ₆ , liquid (with LOX)	3.268 x 10 ⁶	0.3181	2.99 x 10 ⁻⁴
Benzvalene C ₆ H ₆ (excluding O ₂) ²¹⁶⁸	3.465 x 10 ⁶	0.0781	6.01 x 10 ⁻⁵
Benzvalene C ₆ H ₆ (with LOX)	3.465 x 10 ⁶	0.3181	2.70 x 10 ⁻⁴
Benzyne C ₆ H ₄ (theoretical) (excluding O ₂) ²¹⁶⁹	4.43 x 10 ⁶	0.076	7.60 x 10 ⁻⁵
Benzyne C ₆ H ₄ (theoretical) (with LOX)	4.43 x 10 ⁶	0.524	4.69 x 10 ⁻⁴
1,3-Butadiene C ₄ H ₆ (excluding O ₂) ²¹⁷⁰	2.39 x 10 ⁶	0.0541	8.45 x 10 ⁻⁵
1,3-Butadiene C ₄ H ₆ (with LOX)	2.39 x 10 ⁶	0.2301	2.39 x 10 ⁻⁴
1,2-Butadiene C ₄ H ₆ (excluding O ₂) ²¹⁷¹	2.44 x 10 ⁶	0.0541	8.00 x 10 ⁻⁵

²¹⁶⁷ Liquid benzene (C₆H₆) has a density of 877 kg/m³ with MW of 0.0781 kg/mole; a stoichiometric combustion (C₆H₆ + 7.5O₂ → 6CO₂ + 3H₂O) using liquid oxygen (LOX: density 1141 kg/m³, MW 0.032 kg/mole) consumes 0.0781 kg of C₆H₆ and 0.240 kg of O₂ and releases 3.268 x 10⁶ J/mole of C₆H₆ (standard enthalpy of combustion); <https://en.wikipedia.org/wiki/Benzene>.

²¹⁶⁸ Benzvalene (C₆H₆, 0.0781 kg/mole, 1300 kg/m³; <http://www.chemspider.com/Chemical-Structure.120239.html>) is an isomer of benzene that easily detonates (e.g., by scratching) when in pure form, and converts to benzene with a chemical half-life of ~10 days (<https://en.wikipedia.org/wiki/Benzvalene>). A stoichiometric combustion (C₆H₆ + 7.5O₂ → 6CO₂ + 3H₂O) using liquid oxygen (LOX: density 1141 kg/m³, MW 0.032 kg/mole) consumes 0.0781 kg of C₆H₆ and 0.240 kg of O₂ and releases 3.465 x 10⁶ J/mole of C₆H₆, given a heat of formation of +378.1 kJ/mole for benzvalene (<https://en.wikipedia.org/wiki/Bicyclopropenyl>).

²¹⁶⁹ Liquid benzyne (C₆H₄), a ring molecule incorporating one C≡C bond, has a putative density of 1000 kg/m³ (<http://www.chemspider.com/Chemical-Structure.109690.html>) with MW of 0.076 kg/mole; a stoichiometric combustion (C₆H₄ + 14O₂ → 6CO₂ + 2H₂O) using liquid oxygen (LOX: density 1141 kg/m³, MW 0.032 kg/mole) consumes 0.076 kg of C₆H₄ and 0.448 kg of O₂ and releases 4.43 x 10⁶ J/mole of C₆H₄ taking the C₆H₄ heat of formation as +1584 kJ/mole (<http://webbook.nist.gov/cgi/inchi?ID=C462806&Mask=8>). Unfortunately, its use is theoretical because even gas phase benzyne is highly unstable with a lifetime of 2 x 10⁻⁸ sec (<http://www.omicsonline.org/formation-and-trapping-of-benzyne-2153-2435.1000137.php?aid=1966>).

²¹⁷⁰ Liquid 1,3-butadiene (H₂C=CH-CH=CH₂ or C₄H₆), aka. ethylacetylene, has a density of 640 kg/m³ with MW of 0.0541 kg/mole (<https://en.wikipedia.org/wiki/1,3-Butadiene>); a stoichiometric combustion (C₄H₆ + 5.5O₂ → 4CO₂ + 3H₂O) using liquid oxygen (LOX: density 1141 kg/m³, MW 0.032 kg/mole) consumes 0.0541 kg of C₄H₆ and 0.176 kg of O₂ and releases 2.39 x 10⁶ J/mole, taking the standard heats of formation as +88.5 kJ/mole for C₄H₆, -393.5 kJ/mole for CO₂ and -241.8 kJ/mole for H₂O (http://www.update.uu.se/~jolkkonen/pdf/CRC_TD.pdf).

²¹⁷¹ Liquid 1,2-butadiene (C₄H₆, 0.0541 kg/mole, 676 kg/m³; https://pubchem.ncbi.nlm.nih.gov/compound/1_2-butadiene) is slightly denser with a slightly higher heat of formation (+138.6 kJ/mole) than its 1,3 isomer (+88.5 kJ/mole). A stoichiometric combustion (C₄H₆ + 5.5O₂ → 4CO₂ + 3H₂O) using liquid oxygen (LOX: density 1141 kg/m³, MW 0.032 kg/mole) consumes 0.0541 kg of C₄H₆ and 0.176 kg of O₂ and releases 2.44 x 10⁶ J/mole, taking the standard heats of formation as -393.5 kJ/mole for CO₂ and -241.8 kJ/mole for H₂O (http://www.update.uu.se/~jolkkonen/pdf/CRC_TD.pdf).

1,2-Butadiene C ₄ H ₆ (with LOX)	2.44 x 10 ⁶	0.2301	2.34 x 10 ⁻⁴
[1.1.1]Propellane C ₅ H ₆ (excluding O ₂) ²¹⁷²	3.50 x 10 ⁶	0.066	8.25 x 10 ⁻⁵
[1.1.1]Propellane C ₅ H ₆ (with LOX)	3.50 x 10 ⁶	0.274	2.65 x 10 ⁻⁴
Methylcyclohexane C ₇ H ₁₄ , liquid (excluding O ₂) ²¹⁷³	4.257 x 10 ⁶	0.0982	1.28 x 10 ⁻⁴
Methylcyclohexane C ₇ H ₁₄ , liquid (with LOX)	4.257 x 10 ⁶	0.4342	4.22 x 10 ⁻⁴
Tetracene C ₁₈ H ₁₂ , solid (excluding O ₂) ²¹⁷⁴	8.705 x 10 ⁶	0.228	1.69 x 10 ⁻⁴
Tetracene C ₁₈ H ₁₂ , solid (with LOX)	8.705 x 10 ⁶	0.900	7.58 x 10 ⁻⁴
Methanol CH ₃ OH, liquid (excluding O ₂) ²¹⁷⁵	7.15 x 10 ⁵	0.032	4.04 x 10 ⁻⁵
Methanol CH ₃ OH, liquid (with LOX)	7.15 x 10 ⁵	0.080	8.24 x 10 ⁻⁵
Ethanol C ₂ H ₅ OH, liquid (excluding O ₂) ²¹⁷⁶	1.37 x 10 ⁶	0.046	5.83 x 10 ⁻⁵
Ethanol C ₂ H ₅ OH, liquid (with LOX)	1.37 x 10 ⁶	0.126	1.28 x 10 ⁻⁴
Propanol C ₃ H ₇ OH, liquid (excluding O ₂) ²¹⁷⁷	2.02 x 10 ⁶	0.0601	7.48 x 10 ⁻⁵

²¹⁷² [1.1.1]Propellane (C₅H₆, 0.0661 kg/mole, assumed density ~800 kg/m³) is a highly strained molecule (<https://en.wikipedia.org/wiki/1.1.1-Propellane>). A stoichiometric combustion (C₅H₆ + 6.5O₂ → 5CO₂ + 3H₂O) using liquid oxygen (LOX: density 1141 kg/m³, MW 0.032 kg/mole) consumes 0.066 kg of C₅H₆ and 0.208 kg of O₂ and releases 3.07 x 10⁶ J/mole of C₅H₆, taking the standard heats of formation as -393.5 kJ/mole for CO₂, -241.8 kJ/mole for H₂O (http://www.update.uu.se/~jolkkonen/pdf/CRC_TD.pdf), and +372.4 kJ/mole for propellane (Lammertsma K. New high energy density small ring systems. AL-TR-90-004, Dec 1990; <http://handle.dtic.mil/100.2/ADA231309>) plus 431 kJ/mole of strain energy.

²¹⁷³ Liquid methylcyclohexane (CH₃C₆H₁₁ or C₇H₁₄, 0.0982 kg/mole, 770 kg/m³; <https://en.wikipedia.org/wiki/Methylcyclohexane>) is a flammable hydrocarbon considered “very toxic to aquatic life.” A stoichiometric combustion (C₇H₁₄ + 10.5O₂ → 7CO₂ + 7H₂O) using liquid oxygen (LOX: density 1141 kg/m³, MW 0.032 kg/mole) consumes 0.0982 kg of C₇H₁₄ and 0.336 kg of O₂ and releases 4.257 x 10⁶ J/mole of methylcyclohexane (standard enthalpy of combustion).

²¹⁷⁴ Tetracene, aka. naphthacene, benz[b]anthracene, 2,3-benzanthracene (C₁₈H₁₂, 0.228 kg/mole, 1350 kg/m³; <https://en.wikipedia.org/wiki/Tetracene>) is a polycyclic aromatic hydrocarbon and a yellow-orange powder. A stoichiometric combustion (C₁₈H₁₂ + 21O₂ → 18CO₂ + 6H₂O) using liquid oxygen (LOX: density 1141 kg/m³, MW 0.032 kg/mole) consumes 0.228 kg of C₁₈H₁₂ and 0.672 kg of O₂ and releases 8.705 x 10⁶ J/mole of C₁₈H₁₂, taking standard heats of formation as +170.8 kJ/mole for solid C₁₈H₁₂, -393.5 kJ/mole for CO₂, and -241.8 kJ/mole for H₂O (http://www.update.uu.se/~jolkkonen/pdf/CRC_TD.pdf).

²¹⁷⁵ Liquid methanol (CH₄O) has a density of 792 kg/m³ with a MW of 0.032 kg/mole; a stoichiometric combustion (CH₄O + 1.5O₂ → CO₂ + 2H₂O) using liquid oxygen (LOX: density 1141 kg/m³, MW 0.032 kg/mole) consumes 0.032 kg of CH₄O and 0.048 kg of O₂ and releases 7.15 x 10⁵ J/mole of CH₄O (standard enthalpy of combustion); <https://en.wikipedia.org/wiki/Methanol> and [https://en.wikipedia.org/wiki/Methanol_\(data_page\)](https://en.wikipedia.org/wiki/Methanol_(data_page)).

²¹⁷⁶ Liquid ethanol (C₂H₆O) has a density of 789 kg/m³ with a MW of 0.046 kg/mole; a stoichiometric combustion (C₂H₆O + 2.5O₂ → 2CO₂ + 3H₂O) using liquid oxygen (LOX: density 1141 kg/m³, MW 0.032 kg/mole) consumes 0.046 kg of C₂H₆O and 0.080 kg of O₂ and releases 1.37 x 10⁶ J/mole of C₂H₆O (standard enthalpy of combustion); [https://en.wikipedia.org/wiki/Ethanol_\(data_page\)](https://en.wikipedia.org/wiki/Ethanol_(data_page)).

Propanol C ₃ H ₇ OH, liquid (with LOX)	2.02 x 10 ⁶	0.2041	2.01 x 10 ⁻⁴
Butanol C ₄ H ₉ OH, liquid (excluding O ₂) ²¹⁷⁸	2.67 x 10 ⁶	0.0741	9.15 x 10 ⁻⁵
Butanol C ₄ H ₉ OH, liquid (with LOX)	2.67 x 10 ⁶	0.2661	2.60 x 10 ⁻⁴
Octanol C ₈ H ₁₇ OH, liquid (excluding O ₂) ²¹⁷⁹	5.29 x 10 ⁶	0.1302	1.56 x 10 ⁻⁴
Octanol C ₈ H ₁₇ OH, liquid (with LOX)	5.29 x 10 ⁶	0.5142	4.93 x 10 ⁻⁴
Propargyl alcohol C ₃ H ₄ O, liquid (excluding O ₂) ²¹⁸⁰	1.732 x 10 ⁶	0.0561	5.97 x 10 ⁻⁵
Propargyl alcohol C ₃ H ₄ O, liquid (with LOX)	1.732 x 10 ⁶	0.1841	1.70 x 10 ⁻⁴
Acetone C ₃ H ₆ O, liquid (excluding O ₂) ²¹⁸¹	1.772 x 10 ⁶	0.0581	7.41 x 10 ⁻⁵
Acetone C ₃ H ₆ O, liquid (with LOX)	1.772 x 10 ⁶	0.1861	1.86 x 10 ⁻⁴
Ethylene oxide C ₂ H ₄ O, liquid (excluding O ₂) ²¹⁸²	1.306 x 10 ⁶	0.0441	5.00 x 10 ⁻⁵

²¹⁷⁷ Liquid n-propanol (C₃H₈O) has a density of 803 kg/m³ with a MW of 0.0601 kg/mole; a stoichiometric combustion (C₃H₈O + 4.5O₂ → 3CO₂ + 4H₂O) using liquid oxygen (LOX: density 1141 kg/m³, MW 0.032 kg/mole) consumes 0.0601 kg of C₃H₈O and 0.144 kg of O₂ and releases 2.02 x 10⁶ J/mole of C₃H₈O (standard enthalpy of combustion); <https://en.wikipedia.org/wiki/1-Propanol>.

²¹⁷⁸ Liquid n-butanol (C₄H₁₀O) has a density of 810 kg/m³ with a MW of 0.0741 kg/mole; a stoichiometric combustion (C₄H₁₀O + 6O₂ → 4CO₂ + 5H₂O) using liquid oxygen (LOX: density 1141 kg/m³, MW 0.032 kg/mole) consumes 0.0741 kg of C₄H₁₀O and 0.192 kg of O₂ and releases 2.67 x 10⁶ J/mole of C₄H₁₀O (standard enthalpy of combustion); <https://en.wikipedia.org/wiki/1-Propanol>.

²¹⁷⁹ Liquid iso-octanol (C₈H₁₈O), aka. 2-ethylhexanol, has a density of 833 kg/m³ with a MW of 0.1302 kg/mole; a stoichiometric combustion (C₈H₁₈O + 12O₂ → 8CO₂ + 9H₂O) using liquid oxygen (LOX: density 1141 kg/m³, MW 0.032 kg/mole) consumes 0.1302 kg of C₈H₁₈O and 0.384 kg of O₂ and releases 5.29 x 10⁶ J/mole of C₈H₁₈O (standard enthalpy of combustion); <https://en.wikipedia.org/wiki/2-Ethylhexanol>.

²¹⁸⁰ Liquid propargyl alcohol, aka. 2-propyn-1-ol (C₃H₄O, 0.0561 kg/mole, 972 kg/m³; https://en.wikipedia.org/wiki/Propargyl_alcohol) is a “flammable liquid, toxic by inhalation, highly toxic by ingestion, toxic by skin absorption, and corrosive.” A stoichiometric combustion (C₃H₄O + 4O₂ → 3CO₂ + 2H₂O) using liquid oxygen (LOX: density 1141 kg/m³, MW 0.032 kg/mole) consumes 0.0561 kg of C₃H₄O and 0.128 kg of O₂ and releases 1.732 x 10⁶ J/mole of C₃H₄O, taking the standard heats of formation as -393.5 kJ/mole for CO₂ and -241.8 kJ/mole for H₂O (http://www.update.uu.se/~jolkkonen/pdf/CRC_TD.pdf) and +67.9 kJ/mole for C₃H₄O as estimated from the 7378 cal/gm heat of combustion (NPCS Board of Consultants and Engineers, Industrial Alcohol Technology Handbook, Asia Pacific Business Press, 2010, Table 43, p. 285; <https://books.google.com/books?id=cXFPAQAAQBAJ&pg=PT150>).

²¹⁸¹ Liquid acetone (C₃H₆O), aka. methoxymethane, has a density of 784 kg/m³ with a MW of 0.0581 kg/mole; a stoichiometric combustion (C₃H₆O + 4O₂ → 3CO₂ + 3H₂O) using liquid oxygen (LOX: density 1141 kg/m³, MW 0.032 kg/mole) consumes 0.0581 kg of C₃H₆O and 0.128 kg of O₂ and releases 1.772 x 10⁶ J/mole of C₃H₆O (standard enthalpy of combustion); <https://en.wikipedia.org/wiki/Acetone>.

Ethylene oxide C ₂ H ₄ O, liquid (with LOX)	1.306 x 10 ⁶	0.1241	1.20 x 10 ⁻⁴
Propylene oxide C ₃ H ₆ O, liquid (excluding O ₂) ²¹⁸³	1.92 x 10 ⁶	0.0581	7.08 x 10 ⁻⁵
Propylene oxide C ₃ H ₆ O, liquid (with LOX)	1.92 x 10 ⁶	0.1861	1.83 x 10 ⁻⁴
Dimethylfuran C ₆ H ₈ O, liquid (excluding O ₂) ²¹⁸⁴	3.20 x 10 ⁶	0.0961	1.08 x 10 ⁻⁴
Dimethylfuran C ₆ H ₈ O, liquid (with LOX)	3.20 x 10 ⁶	0.3521	3.32 x 10 ⁻⁴
Dimethyl ether H ₃ COCH ₃ , liquid (excluding O ₂) ²¹⁸⁵	1.46 x 10 ⁶	0.046	6.26 x 10 ⁻⁵
Dimethyl ether H ₃ COCH ₃ , liquid (with LOX)	1.46 x 10 ⁶	0.142	1.47 x 10 ⁻⁴
Diethyl ether C ₄ H ₁₀ O, liquid (excluding O ₂) ²¹⁸⁶	2.73 x 10 ⁶	0.0741	1.04 x 10 ⁻⁴
Diethyl ether C ₄ H ₁₀ O, liquid (with LOX)	2.73 x 10 ⁶	0.2661	2.72 x 10 ⁻⁴
Dipropyl ether C ₆ H ₁₄ O, liquid (excluding O ₂) ²¹⁸⁷	3.72 x 10 ⁶	0.1022	1.36 x 10 ⁻⁴
Dipropyl ether C ₆ H ₁₄ O, liquid (with LOX)	3.72 x 10 ⁶	0.3902	3.89 x 10 ⁻⁴

²¹⁸² Ethylene oxide (C₂H₄O), aka. oxirane and a fuel-air explosive, has a density of 882 kg/m³ with a MW of 0.0441 kg/mole; a stoichiometric combustion (C₂H₄O + 2.5O₂ → 2CO₂ + 2H₂O) using liquid oxygen (LOX: density 1141 kg/m³, MW 0.032 kg/mole) consumes 0.0441 kg of C₂H₄O and 0.080 kg of O₂ and releases 1.306 x 10⁶ J/mole of C₂H₄O (standard enthalpy of combustion); https://en.wikipedia.org/wiki/Ethylene_oxide.

²¹⁸³ Propylene oxide (C₃H₆O) has a density of 821 kg/m³ with a MW of 0.0581 kg/mole; a stoichiometric combustion (C₃H₆O + 4O₂ → 3CO₂ + 3H₂O) using liquid oxygen (LOX: density 1141 kg/m³, MW 0.032 kg/mole) consumes 0.0581 kg of C₃H₆O and 0.128 kg of O₂ and releases 1.92 x 10⁶ J/mole of C₃H₆O (standard enthalpy of combustion); <http://www.dow.com/propyleneoxide/about/prop.htm>.

²¹⁸⁴ Liquid 2,5-dimethylfuran (C₆H₈O) has a density of 890 kg/m³ with a MW of 0.0961 kg/mole (<https://en.wikipedia.org/wiki/2,5-Dimethylfuran>); a stoichiometric combustion (C₆H₈O + 8O₂ → 6CO₂ + 4H₂O) using liquid oxygen (LOX: density 1141 kg/m³, MW 0.032 kg/mole) consumes 0.0961 kg of C₆H₈O and 0.256 kg of O₂ and releases 3.20 x 10⁶ J/mole of C₆H₈O (standard enthalpy of combustion); <http://pubs.acs.org/doi/abs/10.1021/jp3095984>).

²¹⁸⁵ Liquid dimethyl ether (C₂H₆O), aka. methoxymethane or DME, has a density of 735 kg/m³ with a MW of 0.046 kg/mole; a stoichiometric combustion (C₂H₆O + 3O₂ → 2CO₂ + 3H₂O) using liquid oxygen (LOX: density 1141 kg/m³, MW 0.032 kg/mole) consumes 0.046 kg of C₂H₆O and 0.096 kg of O₂ and releases 1.46 x 10⁶ J/mole of C₂H₆O (standard enthalpy of combustion); https://en.wikipedia.org/wiki/Dimethyl_ether.

²¹⁸⁶ Liquid diethyl ether (C₄H₁₀O), aka. ethoxyethane and once used as an anesthetic, has a density of 713 kg/m³ with a MW of 0.0741 kg/mole; a stoichiometric combustion (C₄H₁₀O + 6O₂ → 4CO₂ + 5H₂O) using liquid oxygen (LOX: density 1141 kg/m³, MW 0.032 kg/mole) consumes 0.0741 kg of C₄H₁₀O and 0.192 kg of O₂ and releases 2.73 x 10⁶ J/mole of C₄H₁₀O (standard enthalpy of combustion); https://en.wikipedia.org/wiki/Diethyl_ether.

²¹⁸⁷ Liquid dipropyl ether (C₆H₁₄O), aka. propoxypropane, has a density of 750 kg/m³ with a MW of 0.1022 kg/mole; a stoichiometric combustion (C₆H₁₄O + 9O₂ → 6CO₂ + 7H₂O) using liquid oxygen (LOX: density 1141 kg/m³, MW 0.032 kg/mole) consumes 0.1022 kg of C₆H₁₄O and 0.288 kg of O₂ and releases 36.355 MJ/kg = 3.72 x 10⁶ J/mole of C₆H₁₄O (standard enthalpy of combustion); https://en.wikipedia.org/wiki/Dipropyl_ether and https://en.wikipedia.org/wiki/Heat_of_combustion.

Butyraldehyde C ₄ H ₈ O, liquid (excluding O ₂) ²¹⁸⁸	2.49 x 10 ⁶	0.0721	8.99 x 10 ⁻⁵
Butyraldehyde C ₄ H ₈ O, liquid (with LOX)	2.49 x 10 ⁶	0.2481	2.44 x 10 ⁻⁴
Hydroperoxymethane CH ₄ O ₂ (excluding O ₂) ²¹⁸⁹	7.39 x 10 ⁵	0.048	4.81 x 10 ⁻⁵
Hydroperoxymethane CH ₄ O ₂ (with LOX)	7.39 x 10 ⁵	0.080	7.61 x 10 ⁻⁵
RP-1 rocket fuel ~kerosene (excluding O ₂) ²¹⁹⁰	7.54 x 10 ⁶	0.175	2.16 x 10 ⁻⁴
RP-1 rocket fuel ~kerosene (with LOX)	7.54 x 10 ⁶	0.623	6.09 x 10 ⁻⁴
Syntin rocket fuel C ₁₀ H ₁₆ (excluding O ₂) ²¹⁹¹	6.00 x 10 ⁶	0.136	1.60 x 10 ⁻⁴
Syntin rocket fuel C ₁₀ H ₁₆ (with LOX)	6.00 x 10 ⁶	0.584	5.53 x 10 ⁻⁴
Fuel Oil #2, liquid (excluding O ₂) ²¹⁹²	1.003 x 10 ⁷	0.226	2.38 x 10 ⁻⁴

²¹⁸⁸ Liquid butyraldehyde (C₄H₈O) has a density of 802 kg/m³ with a MW of 0.0721 kg/mole; a stoichiometric combustion (C₄H₈O + 5.5O₂ → 4CO₂ + 4H₂O) using liquid oxygen (LOX: density 1141 kg/m³, MW 0.032 kg/mole) consumes 0.0721 kg of C₄H₈O and 0.176 kg of O₂ and releases 2.49 x 10⁶ J/mole of C₄H₈O (standard enthalpy of combustion); <https://en.wikipedia.org/wiki/Butyraldehyde>.

²¹⁸⁹ Hydroperoxymethane, aka. methyl hydroperoxide (CH₃OOH or CH₄O₂, 0.048 kg/mole, 997 kg/m³; <http://www.syntechem.com/prod/STP216879/>) if undergoing a stoichiometric combustion (CH₄O₂ + O₂ → CO₂ + 2H₂O) using liquid oxygen (LOX: density 1141 kg/m³, MW 0.032 kg/mole) consumes 0.048 kg of CH₄O₂ and 0.032 kg of O₂ and releases 7.39 x 10⁵ J/mole of CH₄O₂, taking the standard heats of formation as -241.8 kJ/mole for H₂O and -393.5 kJ/mole for CO₂ (http://www.update.uu.se/~jolkkonen/pdf/CRC_TD.pdf) and -138.1 kJ/mole for CH₄O₂ (<https://www3.nd.edu/~powers/ame.60636/baulch2005.pdf>).

²¹⁹⁰ Liquid RP-1 is a highly refined form of kerosene similar to jet fuel, used as rocket fuel (<https://en.wikipedia.org/wiki/RP-1>), containing at least 87 identifiable hydrocarbons with density 810 kg/m³, an oxidizer/fuel ratio of 2.56, MW ~ 0.175 kg/mole, and heat of combustion of ~43.1 MJ/kg ~ 7.54 x 10⁶ J/mole of RP-1 (<http://ntrs.nasa.gov/archive/nasa/casi.ntrs.nasa.gov/20000065620.pdf>); combustion with liquid oxygen (LOX: density 1141 kg/m³, MW 0.032 kg/mole) thus consumes 0.175 kg of RP-1 and 0.448 kg of O₂.

²¹⁹¹ Liquid syntin, aka. 1'-Methyl-1,1':2',1''-tercyclopropane (C₁₀H₁₆) has a density of 851 kg/m³ with MW of 0.136 kg/mole, and includes three strained cyclopropane rings, giving the molecule a +133 kJ/mole enthalpy of formation (<https://en.wikipedia.org/wiki/Syntin>). It was first synthesized in the USSR in the 1960s, brought to mass production in the 1970s, then used in the Soviet Union and later Russia in the 1980s and 1990s as fuel for the Soyuz-U2 rocket. A stoichiometric combustion (C₁₀H₁₆ + 14O₂ → 10CO₂ + 8H₂O) using liquid oxygen (LOX: density 1141 kg/m³, MW 0.032 kg/mole) consumes 0.136 kg of C₁₀H₁₆ and 0.448 kg of O₂ and releases 6.00 x 10⁶ J/mole of C₁₀H₁₆ (standard enthalpy of combustion; http://www.update.uu.se/~jolkkonen/pdf/CRC_TD.pdf).

²¹⁹² Fuel Oil #2, aka. Home Heating Oil (HHO) with hydrocarbons in the 14- to 20-carbon atom range, has a density of 950 kg/m³ (https://en.wikipedia.org/wiki/Heating_oil) with a MW of 0.226 kg/mole if we use hexadecane (C₁₆H₃₄) as our proxy for the hydrocarbon energetics; a stoichiometric combustion (C₁₆H₃₄ + 24.5O₂ → 16CO₂ + 17H₂O) using liquid oxygen (LOX: density 1141 kg/m³, MW 0.032 kg/mole) consumes 0.226 kg of C₁₆H₃₄ and 0.784 kg of O₂ and releases 1.003 x 10⁷ J/mole of C₁₆H₃₄, taking standard heats of formation as -374.8 kJ/mole for C₁₆H₃₄, -393.5 kJ/mole for CO₂, and -241.8 kJ/mole for H₂O (http://www.update.uu.se/~jolkkonen/pdf/CRC_TD.pdf).

Fuel Oil #2, liquid (with LOX)	1.003×10^7	1.010	9.25×10^{-4}
Napalm-B, liquid (excluding O ₂) ²¹⁹³	4.175×10^7	1	1.175×10^{-3}
Napalm-B, liquid (with LOX)	4.175×10^7	4.216	3.995×10^{-3}
Pyramidane C ₅ H ₄ (theoretical) (excluding O ₂) ²¹⁹⁴	3.90×10^6	0.064	4.96×10^{-5}
Pyramidane C ₅ H ₄ (theoretical) (with LOX)	3.90×10^6	0.256	2.18×10^{-4}
Tetrahydrane C ₄ H ₄ (theoretical) (excluding O ₂) ²¹⁹⁵	3.16×10^6	0.052	4.04×10^{-5}
Tetrahydrane C ₄ H ₄ (theoretical) (with LOX)	3.16×10^6	0.212	1.81×10^{-4}
Diazatetrahydrane C ₂ N ₂ H ₂ (theoretical) (excluding O ₂) ²¹⁹⁶	1.61×10^6	0.054	4.2×10^{-5}

²¹⁹³ The original napalm, used in flamethrowers and incendiary bombs, was composed of a mixture of powdered aluminum soap of naphtenic acids (corrosives found in crude oil) and palmitic acid (a 16-carbon saturated fatty acid found in coconut oil), from whence the name derives. Modern napalm-B is a mixture of 33% gasoline [proxied by iso-octane C₈H₁₈, 0.114 kg/mole, 692 kg/m³, -250.1 kJ/mole heat of formation], 21% benzene [C₆H₆, 0.0781 kg/mole, 877 kg/m³, +49.1 kJ/mole], and 46% polystyrene [C₈H₈, 0.104 kg/mole, ~1000 kg/m³, +103.8 kJ/mole] by weight (<https://uscrow.org/2015/07/16/how-to-make-napalm-b/>, http://www.update.uu.se/~jolkkonen/pdf/CRC_TD.pdf). A combustion reaction (2.89C₈H₁₈ + 2.69C₆H₆ + 4.42C₈H₈ + 100.5O₂ → 74.62CO₂ + 51.76H₂O) using liquid oxygen (LOX: density 1141 kg/m³, MW 0.032 kg/mole) consumes 1 kg of liquid hydrocarbons and 3.216 kg of O₂, releasing 4.175 x 10⁷ J/mole.

²¹⁹⁴ Pyramidane, aka. tetracyclo-[2.1.0.0^{1,3}.0^{2,5}]pentane or [3.3.3.3]fenestrane (C₅H₄, 0.0641 kg/mole, assumed same density of cubane ~1290 kg/m³), while not yet synthesized by 2016, “is characterised by high kinetic stability with respect to the possible decomposition and rearrangement reactions [and is] separated from more stable isomers...by relatively high barriers corresponding to a half-life of more than 4 hours at room temperature....thus, synthesis of pyramidane should be possible.”* The estimated energy of the pyramidane molecule is +804.6 kJ/mole,* so a combustion reaction (C₅H₄ + 6O₂ → 5CO₂ + 2H₂O) using liquid oxygen (LOX: density 1141 kg/m³, MW 0.032 kg/mole) consumes 0.0641 kg of C₅H₄ and 0.192 kg of O₂, releasing 3.26 x 10⁶ J/mole of C₅H₄, plus 644 kJ/mole of strain energy (<https://openresearch-repository.anu.edu.au/bitstream/1885/48020/19/07Chapter4b.pdf>). *Minkin VI, Minyaev RM, Hoffmann R. Non-classical structures of organic compounds: unusual stereochemistry and hypercoordination. Russian Chem Rev. 2002;71(11):869-892, pp. 877, 878; http://www.roaldhoffmann.com/sites/all/files/485s_0.pdf.

²¹⁹⁵ Tetrahydrane (C₄H₄, 0.0521 kg/mole, assumed same density of cubane ~1290 kg/m³) had not been synthesized by 2016, but once formed should be kinetically stable* (<https://en.wikipedia.org/wiki/Tetrahydrane>). It is the smallest “platonic hydrocarbon” with a tetrahedral cage structure. A stoichiometric combustion (C₄H₄ + 5O₂ → 4CO₂ + 2H₂O) using liquid oxygen (LOX: density 1141 kg/m³, MW 0.032 kg/mole) consumes 0.0521 kg of C₄H₄ and 0.160 kg of O₂ and releases 2.59 x 10⁶ J/mole of C₄H₄ (standard enthalpy of combustion, using +535.6 kJ/mole for tetrahydrane; Glukhovtsev MN, Laiter S, Pross A. Thermochemistry of Cyclobutadiene and Tetrahydrane – A High-Level Computational Study. J Phys Chem. 1995;99:6828-6831; <http://pubs.acs.org/doi/abs/10.1021/j100018a012>) plus 571 kJ/mole of strain energy. *Nemirowski A, Reisenauer HP, Schreiner PR. Tetrahydrane – Dossier of an Unknown. Chem Eur J. 2006;12:7411-7420; <http://onlinelibrary.wiley.com/doi/10.1002/chem.200600451/abstract>.

Diazatetrahedrane C ₂ N ₂ H ₂ (theoretical) (with LOX)	1.61 x 10 ⁶	0.134	1.12 x 10 ⁻⁴
Prismane C ₆ H ₆ , liquid (excluding O ₂) ²¹⁹⁷	3.654 x 10 ⁶	0.0781	4.88 x 10 ⁻⁵
Prismane C ₆ H ₆ , liquid (with LOX)	3.654 x 10 ⁶	0.3181	2.59 x 10 ⁻⁴
1-Nitroprismane C ₆ H ₅ NO ₂ (theoretical) (excl. O ₂) ²¹⁹⁸	3.55 x 10 ⁶	0.123	8.31 x 10 ⁻⁵
1-Nitroprismane C ₆ H ₅ NO ₂ (theoretical) (with LOX)	3.55 x 10 ⁶	0.523	4.34 x 10 ⁻⁴
1,2-Nitroprismane C ₆ H ₄ (NO ₂) ₂ (theoretical) (excl. O ₂) ²¹⁹⁹	3.49 x 10 ⁶	0.168	1.00 x 10 ⁻⁴
1,2-Nitroprismane C ₆ H ₄ (NO ₂) ₂ (theoretical) (with LOX)	3.49 x 10 ⁶	0.328	2.40 x 10 ⁻⁴
1,2,3-Nitroprismane C ₆ H ₃ (NO ₂) ₃ (theoretical) (excl. O ₂) ²²⁰⁰	3.46 x 10 ⁶	0.213	1.20 x 10 ⁻⁴

²¹⁹⁶ Diazatetrahedrane (C₂N₂H₂, 0.054 kg/mole, 4.2 x 10⁻⁵ m³/mole assuming same density of cubane ~1290 kg/m³), a tetrahedral-shaped cage molecule, had not been synthesized by 2016. A stoichiometric combustion (C₂N₂H₂ + 2.5O₂ → N₂ + 2CO₂ + H₂O) using liquid oxygen (LOX: density 1141 kg/m³, MW 0.032 kg/mole) consumes 0.054 kg of C₂N₂H₂ and 0.080 kg of O₂ and releases 1.61 x 10⁶ J/mole of C₂N₂H₂ (standard enthalpy of combustion, using +577.0 kJ/mole for C₂N₂H₂; Jursic BS. Structures and properties of nitrogen derivatives of tetrahedrane. J Mol Struct (Theochem) 2001;536:143-154; <http://www.sciencedirect.com/science/article/pii/S0166128000006199>).

²¹⁹⁷ Liquid prismane (C₆H₆; <https://en.wikipedia.org/wiki/Prismane>) has a density of 1600 kg/m³ with MW of 0.0781 kg/mole; a stoichiometric combustion (C₆H₆ + 7.5O₂ → 6CO₂ + 3H₂O) using liquid oxygen (LOX: density 1141 kg/m³, MW 0.032 kg/mole) consumes 0.0781 kg of C₆H₆ and 0.240 kg of O₂ and releases 3.654 x 10⁶ J/mole of C₆H₆ (standard enthalpy of combustion, taking estimated heat of formation of +567.7 kJ/mole for prismane; Chi WJ, Li LL, Li BT, Wu HS. Density functional calculations for a high energy density compound of formula C₆H_{6-n}(NO₂)_n. J Mol Model. 2012 Aug;18(8):3695-704; <http://www.ncbi.nlm.nih.gov/pubmed/22382574>).

²¹⁹⁸ 1-Nitroprismane (C₆H₅NO₂, 0.123 kg/mole, 1480 kg/m³) in stoichiometric combustion (C₆H₅NO₂ + 12.5O₂ → 0.5N₂ + 6CO₂ + 2.5H₂O) using liquid oxygen (LOX: density 1141 kg/m³, MW 0.032 kg/mole) would consume 0.123 kg of C₆H₅NO₂ and 0.400 kg of O₂ and release 3.55 x 10⁶ J/mole of C₆H₅NO₂ (standard enthalpy of combustion, using estimated heat of formation +585.84 kJ/mole for C₆H₅NO₂; Chi WJ, Li LL, Li BT, Wu HS. Density functional calculations for a high energy density compound of formula C₆H_{6-n}(NO₂)_n. J Mol Model. 2012 Aug;18(8):3695-3704; <http://www.ncbi.nlm.nih.gov/pubmed/22382574>), but had not been synthesized by 2016.

²¹⁹⁹ 1,2-Nitroprismane (C₆H₄(NO₂)₂, 0.168 kg/mole, 1680 kg/m³) in stoichiometric combustion (C₆H₄(NO₂)₂ + 5O₂ → N₂ + 6CO₂ + 2H₂O) using liquid oxygen (LOX: density 1141 kg/m³, MW 0.032 kg/mole) would consume 0.168 kg of C₆H₄(NO₂)₂ and 0.160 kg of O₂ and release 3.49 x 10⁶ J/mole of C₆H₄(NO₂)₂ (standard enthalpy of combustion, using estimated heat of formation +646.19 kJ/mole for C₆H₄(NO₂)₂; Chi WJ, Li LL, Li BT, Wu HS. Density functional calculations for a high energy density compound of formula C₆H_{6-n}(NO₂)_n. J Mol Model. 2012 Aug;18(8):3695-3704; <http://www.ncbi.nlm.nih.gov/pubmed/22382574>), but had not been synthesized by 2016.

²²⁰⁰ 1,2,3-Nitroprismane (C₆H₃(NO₂)₃, 0.213 kg/mole, 1780 kg/m³) in stoichiometric combustion (C₆H₃(NO₂)₃ + 7.5O₂ → 1.5N₂ + 6CO₂ + 1.5H₂O) using liquid oxygen (LOX: density 1141 kg/m³, MW 0.032 kg/mole) would consume 0.213 kg of C₆H₃(NO₂)₃ and 0.240 kg of O₂ and release 3.46 x 10⁶ J/mole of C₆H₃(NO₂)₃ (standard enthalpy of combustion, using estimated heat of formation +733.95 kJ/mole for C₆H₃(NO₂)₃; Chi WJ, Li LL, Li BT, Wu HS. Density functional calculations for a high energy density compound of formula C₆H_{6-n}(NO₂)_n. J Mol Model. 2012 Aug;18(8):3695-3704; <http://www.ncbi.nlm.nih.gov/pubmed/22382574>), but had not been synthesized by 2016.

1,2,3-Nitroprismane $C_6H_3(NO_2)_3$ (theoretical) (with LOX)	3.46×10^6	0.453	3.30×10^{-4}
1,2,4,5-Nitroprismane $C_6H_2(NO_2)_4$ (theor.) (excl. O_2) ²²⁰¹	3.41×10^6	0.258	1.38×10^{-4}
1,2,4,5-Nitroprismane $C_6H_2(NO_2)_4$ (theor.) (with LOX)	3.41×10^6	0.338	2.08×10^{-4}
1,2,3,4,5-Nitroprismane $C_6H(NO_2)_5$ (theor.) (excl. O_2) ²²⁰²	3.39×10^6	0.303	1.57×10^{-4}
1,2,3,4,5-Nitroprismane $C_6H(NO_2)_5$ (theor.) (with LOX)	3.39×10^6	0.343	1.92×10^{-4}
Cubane C_8H_8 , solid (excluding O_2) ²²⁰³	5.432×10^6	0.104	8.06×10^{-5}
Cubane C_8H_8 , solid (with LOX)	5.432×10^6	0.424	3.61×10^{-4}
Heptanitrocubane $C_8HN_7O_{14}$ (excluding O_2) ²²⁰⁴	3.91×10^6	0.419	2.07×10^{-4}
Heptanitrocubane $C_8HN_7O_{14}$ (with LOX)	3.91×10^6	0.459	2.42×10^{-4}

²²⁰¹ 1,2,4,5-Nitroprismane ($C_6H_2(NO_2)_4$, 0.258 kg/mole, 1870 kg/m³) in stoichiometric combustion ($C_6H_2(NO_2)_4 + 2.5O_2 \rightarrow 2N_2 + 6CO_2 + H_2O$) using liquid oxygen (LOX: density 1141 kg/m³, MW 0.032 kg/mole) would consume 0.258 kg of $C_6H_2(NO_2)_4$ and 0.080 kg of O_2 and release 3.41×10^6 J/mole of $C_6H_2(NO_2)_4$ (standard enthalpy of combustion, using estimated heat of formation +808.79 kJ/mole for $C_6H_2(NO_2)_4$; Chi WJ, Li LL, Li BT, Wu HS. Density functional calculations for a high energy density compound of formula $C_6H_{6-n}(NO_2)_n$. J Mol Model. 2012 Aug;18(8):3695-3704; <http://www.ncbi.nlm.nih.gov/pubmed/22382574>), but had not been synthesized by 2016.

²²⁰² 1,2,3,4,5-Nitroprismane ($C_6H(NO_2)_5$, 0.303 kg/mole, 1930 kg/m³) in stoichiometric combustion ($C_6H(NO_2)_5 + 1.25O_2 \rightarrow 2.5N_2 + 6CO_2 + 0.5H_2O$) using liquid oxygen (LOX: density 1141 kg/m³, MW 0.032 kg/mole) would consume 0.303 kg of $C_6H(NO_2)_5$ and 0.040 kg of O_2 and release 3.39×10^6 J/mole of $C_6H(NO_2)_5$ (standard enthalpy of combustion, using estimated heat of formation +906.77 kJ/mole for $C_6H(NO_2)_5$; Chi WJ, Li LL, Li BT, Wu HS. Density functional calculations for a high energy density compound of formula $C_6H_{6-n}(NO_2)_n$. J Mol Model. 2012 Aug;18(8):3695-3704; <http://www.ncbi.nlm.nih.gov/pubmed/22382574>), but had not been synthesized by 2016.

²²⁰³ Solid cubane (C_8H_8), once formed, is quite kinetically stable due to a lack of readily available decomposition paths (<https://en.wikipedia.org/wiki/Cubane>). Cubane has a density of 1290 kg/m³ with MW of 0.104 kg/mole; a stoichiometric combustion ($C_8H_8 + 10O_2 \rightarrow 8CO_2 + 4H_2O$) using liquid oxygen (LOX: density 1141 kg/m³, MW 0.032 kg/mole) consumes 0.104 kg of C_8H_8 and 0.320 kg of O_2 and releases 5.432×10^6 J/mole of C_8H_8 (standard enthalpy of combustion, using +622.2 kJ/mole for gaseous cubane; Kybett BD, Carroll S, Natalis P, Bonnell DW, Margrave JL, Franklin JL. Thermodynamic properties of cubane. J Am Chem Soc 1966;88:626; <http://pubs.acs.org/doi/abs/10.1021/ja00955a056>), plus 166 kcal/mole or 695 kJ/mole of strain energy (https://books.google.com/books?id=gY-Sxijk_tMC&pg=PA126).

²²⁰⁴ Heptanitrocubane ($C_8H(NO_2)_7$ or $C_8HN_7O_{14}$, 0.419 kg/mole, and density* of 2028 kg/m³; <https://en.wikipedia.org/wiki/Cubane>) in stoichiometric combustion ($C_8HN_7O_{14} + 1.25O_2 \rightarrow 3.5N_2 + 8CO_2 + 0.5H_2O$) using liquid oxygen (LOX: density 1141 kg/m³, MW 0.032 kg/mole) would consume 0.419 kg of $C_8HN_7O_{14}$ and 0.040 kg of O_2 and release 3.91×10^6 J/mole of $C_8HN_7O_{14}$ (standard enthalpy of combustion, using estimated heat of formation +644.3 kJ/mole for $C_8HN_7O_{14}$; http://www.chemistry.illinois.edu/research/organic/seminar_extracts/2004_2005/8_LaFrate_Abstract_SP05.pdf). *Zhang MX, Eaton PE, Gilardi R. Hepta- and Octanitrocubanes. Angew Chem Int Ed. 2000;39(2):401-404; <http://ramsey1.chem.uic.edu/chem494/downloads-2/files/Zhang%20et%20al%202000.pdf>.

Quadricyclane C ₇ H ₈ , liquid (excluding O ₂) ²²⁰⁵	3.97 x 10 ⁶	0.0921	9.38 x 10 ⁻³
Quadricyclane C ₇ H ₈ , liquid (with LOX)	3.97 x 10 ⁶	0.380	3.46 x 10 ⁻⁴
Pagodane C ₂₀ H ₂₀ (excluding O ₂) ²²⁰⁶	1.08 x 10 ⁷	0.260	1.60 x 10 ⁻⁴
Pagodane C ₂₀ H ₂₀ (with LOX)	1.08 x 10 ⁷	1.060	8.61 x 10 ⁻⁴
Bihexaplane C ₁₇ H ₁₆ (excluding O ₂) ²²⁰⁷	1.203 x 10 ⁷	0.220	1.57 x 10 ⁻⁴
Bihexaplane C ₁₇ H ₁₆ (with LOX)	1.203 x 10 ⁷	0.892	7.46 x 10 ⁻⁴
[3.3.3]fenestrane C ₅ H ₆ (excluding O ₂) ²²⁰⁸	3.80 x 10 ⁶	0.066	4.13 x 10 ⁻⁵
[3.3.3]fenestrane C ₅ H ₆ (with LOX)	3.80 x 10 ⁶	0.274	2.23 x 10 ⁻⁴
Glucose C ₆ H ₁₂ O ₆ , solid (excluding O ₂) ²²⁰⁹	2.81 x 10 ⁶	0.180	1.17 x 10 ⁻⁴

²²⁰⁵ Liquid quadricyclane (C₇H₈, 0.0921 kg/mole, 982 kg/m³) is a strained, multi-cyclic hydrocarbon cage molecule with potential uses as an additive for rocket propellants (<https://en.wikipedia.org/wiki/Quadricyclane>). A stoichiometric combustion (C₇H₈ + 9O₂ → 7CO₂ + 4H₂O) using liquid oxygen (LOX: density 1141 kg/m³, MW 0.032 kg/mole) consumes 0.0921 kg of C₇H₈ and 0.288 kg of O₂ and releases 3.97 x 10⁶ J/mole of C₇H₈, taking heats of formation as -393.5 kJ/mole for CO₂ and -241.8 kJ/mole for H₂O (http://www.update.uu.se/~jolkkonen/pdf/CRC_TD.pdf) and +253 kJ/mole for C₇H₈ (Schmitt RJ, *et al.* Synthesis of New High Energy Density Matter (HEDM): Extra High Energy Oxidizers and Fuels, SRI International, AFRL-PR-ED-TR-1998-0023, Sep 2000, p.3.).

²²⁰⁶ Pagodane (C₂₀H₂₀, 0.260 kg/mole, 1629 kg/m³; <https://en.wikipedia.org/wiki/Pagodane>) undergoing stoichiometric combustion (C₂₀H₂₀ + 25O₂ → 20CO₂ + 10H₂O) using liquid oxygen (LOX: density 1141 kg/m³, MW 0.032 kg/mole) consumes 0.260 kg of C₂₀H₂₀ and 0.800 kg of O₂ and releases 1.045 x 10⁷ J/mole of C₂₀H₂₀, taking the standard heats of formation as -393.5 kJ/mole for CO₂, -241.8 kJ/mole for H₂O (http://www.update.uu.se/~jolkkonen/pdf/CRC_TD.pdf), and +163 kJ/mole for C₂₀H₂₀, plus 348 kJ/mole of strain energy (<https://openresearch-repository.anu.edu.au/bitstream/1885/48020/19/07Chapter4b.pdf>).

²²⁰⁷ Bihexaplane (C₁₇H₁₆, 0.220 kg/mole, assumed density ~1400 kg/m³; <https://openresearch-repository.anu.edu.au/bitstream/1885/48020/24/06Chapter4a.pdf>) is a representative member of the strained alkylanes. A stoichiometric combustion (C₁₇H₁₆ + 21O₂ → 17CO₂ + 8H₂O) using liquid oxygen (LOX: density 1141 kg/m³, MW 0.032 kg/mole) consumes 0.220 kg of C₁₇H₁₆ and 0.672 kg of O₂ and releases 1.026 x 10⁷ J/mole of C₁₇H₁₆, taking the standard heats of formation as -393.5 kJ/mole for CO₂, -241.8 kJ/mole for H₂O (http://www.update.uu.se/~jolkkonen/pdf/CRC_TD.pdf), and +1637 kJ/mole for C₁₇H₁₆, plus 1772 kJ/mole of strain energy (<https://openresearch-repository.anu.edu.au/bitstream/1885/48020/19/07Chapter4b.pdf>).

²²⁰⁸ [3.3.3]fenestrane, aka. tricyclo[2.1.0.0^{1,3}]pentane (C₅H₆, 0.066 kg/mole, density ~1600 kg/m³ assumed same as prismane) is believed to have the highest strain energy per carbon atom of any observed hydrocarbon. A stoichiometric combustion (C₅H₆ + 6.5O₂ → 5CO₂ + 3H₂O) using liquid oxygen (LOX: density 1141 kg/m³, MW 0.032 kg/mole) consumes 0.066 kg of C₅H₆ and 0.208 kg of O₂ and releases 3.22 x 10⁶ J/mole of C₅H₆, taking the standard heats of formation as -393.5 kJ/mole for CO₂, -241.8 kJ/mole for H₂O (http://www.update.uu.se/~jolkkonen/pdf/CRC_TD.pdf), and +526 kJ/mole for C₅H₆, plus 585 kJ/mole of strain energy (Danne Rene Rasmussen. A Theoretical Approach to Molecular Design: Planar-Tetracoordinate Carbon. Ph.D. thesis, Research School of Chemistry, Australian National University, April 2000, Table 4-14, p. 187; <https://openresearch-repository.anu.edu.au/bitstream/1885/48020/19/07Chapter4b.pdf>).

Glucose C ₆ H ₁₂ O ₆ , solid (with LOX)	2.81 x 10 ⁶	0.372	2.85 x 10 ⁻⁴
Fat (oxidation, excluding O ₂) ²²¹⁰	3.2 x 10 ⁷	0.854	9.5 x 10 ⁻⁴
Fat (oxidation, with LOX)	3.2 x 10 ⁷	3.302	3.1 x 10 ⁻³
Cholesterol C ₂₇ H ₄₆ O (excluding O ₂) ²²¹¹	1.6524 x 10 ⁷	0.3867	3.68 x 10 ⁻⁴
Cholesterol C ₂₇ H ₄₆ O (with LOX)	1.6524 x 10 ⁷	1.6187	1.45 x 10 ⁻³
Dietary carbohydrate ²²¹²	1.76 x 10 ⁷	1	6.49 x 10 ⁻⁴
Dietary lipid	3.95 x 10 ⁷	1	1.11 x 10 ⁻³
Dietary protein	2.36 x 10 ⁷	1	8.20 x 10 ⁻⁴
TNT, burned (excluding O ₂) ²²¹³	3.30 x 10 ⁶	0.227	1.37 x 10 ⁻⁴

²²⁰⁹ Solid glucose (C₆H₁₂O₆), a representative simple carbohydrate, has a density of 1540 kg/m³ with MW of 0.180 kg/mole; a stoichiometric combustion (C₆H₁₂O₆ + 6O₂ → 6CO₂ + 6H₂O) using liquid oxygen (LOX: density 1141 kg/m³, MW 0.032 kg/mole) consumes 0.180 kg of C₆H₁₂O₆ and 0.192 kg of O₂ and releases 2.81 x 10⁶ J/mole of C₆H₁₂O₆ (standard enthalpy of combustion); <https://en.wikipedia.org/wiki/Glucose>. Polysaccharides such as cellulose, paper, wood, and cotton have similar energy densities.

²²¹⁰ Biological fats are triglycerides, which are esters of the three-carbon chain alcohol glycerol and three fatty acids, e.g., palmitic acid (C₁₆H₃₂O₂), oleic acid (C₁₈H₃₄O₂), stearic acid (C₁₈H₃₆O₂), etc.; <https://en.wikipedia.org/wiki/Fat> and <https://en.wikipedia.org/wiki/Triglyceride>. We assume representative triglyceride (fat) C₅₅H₉₈O₆ (MW = 0.854 kg/mole) with density ~ 900 kg/m³ (https://en.wikipedia.org/wiki/Adipose_tissue) completely oxidized by application of liquid O₂ to CO₂ and H₂O. A stoichiometric combustion (C₅₅H₉₈O₆ + 76.5O₂ → 55CO₂ + 49H₂O) using liquid oxygen (LOX: density 1141 kg/m³, MW 0.032 kg/mole) consumes 0.854 kg of C₅₅H₉₈O₆ and 2.448 kg of O₂ and releases ~3.7 x 10⁷ J/kg of C₅₅H₉₈O₆ or 3.2 x 10⁷ J/mole (standard enthalpy of combustion); https://en.wikipedia.org/wiki/Fatty_acid_metabolism.

²²¹¹ Solid cholesterol has a density of 1052 kg/m³ with MW of 0.3867 kg/mole; a stoichiometric combustion (C₂₇H₄₆O + 38.5O₂ → 27CO₂ + 23H₂O) using liquid oxygen (LOX: density 1141 kg/m³, MW 0.032 kg/mole) consumes 0.3867 kg of C₂₇H₄₆O and 1.232 kg of O₂ and releases 1.6524 x 10⁷ J/mole of C₂₇H₄₆O (standard enthalpy of combustion); <https://en.wikipedia.org/wiki/Cholesterol> and Johnson WH. The enthalpies of combustion and formation of cholesterol [cholest-5-en-3-ol(3b)]. J Research NBS 1975 May-Jun;79A(3):493-496; http://nvlpubs.nist.gov/nistpubs/jres/79A/jresv79An3p493_A1b.pdf.

²²¹² The heat liberated by burning food in oxygen in a bomb calorimeter amounts to 4.20 Kcal/gm for pure **dietary carbohydrate**, 9.45 Kcal/gm for pure **dietary lipid**, and 5.65 Kcal/gm for pure **dietary protein**. McArdle WD, Katch FI, Katch VL, Essentials of Exercise Physiology, Third Edition, Lippincott Williams & Wilkins, 2006, p. 94. Densities are assumed to be 1540 kg/m³ for carbohydrate (<https://en.wikipedia.org/wiki/Glucose>), ~900 kg/m³ for fat (https://en.wikipedia.org/wiki/Adipose_tissue), and 1220 kg/m³ for protein (<http://www.ncbi.nlm.nih.gov/pubmed/10930825>),

TNT, burned (with LOX)	3.30×10^6	0.395	2.84×10^{-4}
Nitromethane CH_3NO_2 , liquid (excluding O_2) ²²¹⁴	6.436×10^5	0.0610	5.36×10^{-5}
Nitromethane CH_3NO_2 , liquid (with LOX)	6.436×10^5	0.0850	7.46×10^{-5}
Nitroethane $\text{C}_2\text{H}_5\text{NO}_2$, liquid (excluding O_2) ²²¹⁵	1.248×10^6	0.0751	7.13×10^{-5}
Nitroethane $\text{C}_2\text{H}_5\text{NO}_2$, liquid (with LOX)	1.248×10^6	0.1471	1.34×10^{-4}
Pyridine $\text{C}_5\text{H}_5\text{N}$, liquid (excluding O_2) ²²¹⁶	2.67×10^6	0.0791	8.06×10^{-5}
Pyridine $\text{C}_5\text{H}_5\text{N}$, liquid (with LOX)	2.67×10^6	0.2791	2.56×10^{-4}
1,1-dinitropropane $\text{C}_3\text{H}_6\text{N}_2\text{O}_4$, liquid (excluding O_2) ²²¹⁷	1.88×10^6	0.134	9.52×10^{-5}

²²¹³ Trinitrotoluene or TNT ($\text{C}_7\text{H}_5\text{N}_3\text{O}_6$) will burn in oxygen with a combustion energy greater than its detonation energy, stoichiometrically according to $\text{C}_7\text{H}_5\text{N}_3\text{O}_6$ [0.227 kg , $1.37 \times 10^{-4} \text{ m}^3$] + 5.25O_2 [0.168 kg , $1.47 \times 10^{-4} \text{ m}^3$] \rightarrow $1.5\text{N}_2 + 7\text{CO}_2 + 2.5\text{H}_2\text{O}$ (<https://en.wikipedia.org/wiki/Trinitrotoluene>), and taking standard heats of formation as -63.2 kJ/mole for $\text{C}_7\text{H}_5\text{N}_3\text{O}_6$ (Rouse PE Jr. Enthalpies of formation and calculated detonation properties of some thermally stable explosives. J Chem Eng Data 1976;21:16-20; <http://webbook.nist.gov/cgi/inchi?ID=C118967&Mask=2#Thermo-Condensed>), -393.5 kJ/mole for CO_2 , and -241.8 kJ/mole for H_2O (http://www.update.uu.se/~jolkkonen/pdf/CRC_TD.pdf), releasing $3.30 \times 10^6 \text{ J/mole TNT}$.

²²¹⁴ Nitromethane (CH_3NO_2 , 0.0610 kg/mole , 1137 kg/m^3 , -112.6 kJ/mole heat of formation; http://www.update.uu.se/~jolkkonen/pdf/CRC_TD.pdf), in a stoichiometric combustion ($\text{CH}_3\text{NO}_2 + 0.75\text{O}_2 \rightarrow 0.5\text{N}_2 + \text{CO}_2 + 1.5\text{H}_2\text{O}$) using liquid oxygen (LOX: density 1141 kg/m^3 , MW 0.032 kg/mole) consumes 0.0610 kg of CH_3NO_2 and 0.024 kg of O_2 and releases $6.436 \times 10^5 \text{ J/mole}$ of CH_3NO_2 (standard enthalpy of combustion); <https://en.wikipedia.org/wiki/Nitromethane>. “Nitromethane is used by hobbyists as a fuel in motor racing, particularly drag racing, as well as for radio-controlled models, and is commonly referred to in this context as ‘nitro’. The oxygen content of nitromethane enables it to burn with much less atmospheric oxygen.”

²²¹⁵ Nitroethane ($\text{C}_2\text{H}_5\text{NO}_2$, 0.0751 kg/mole , 1054 kg/m^3 ; <https://en.wikipedia.org/wiki/Nitroethane>) is a colorless oily liquid at STP with a fruity odor, sometimes used as an additive in racing fuels. A stoichiometric combustion ($\text{C}_2\text{H}_5\text{NO}_2 + 2.25\text{O}_2 \rightarrow 0.5\text{N}_2 + 2\text{CO}_2 + 2.5\text{H}_2\text{O}$) using liquid oxygen (LOX: density 1141 kg/m^3 , MW 0.032 kg/mole) consumes 0.0751 kg of $\text{C}_2\text{H}_5\text{NO}_2$ and 0.072 kg of O_2 and releases $1.248 \times 10^6 \text{ J/mole}$ of $\text{C}_2\text{H}_5\text{NO}_2$, taking taking the standard heats of formation as -143.9 kJ/mole for liquid $\text{C}_2\text{H}_5\text{NO}_2$, -393.5 kJ/mole for CO_2 , and -241.8 kJ/mole for H_2O (http://www.update.uu.se/~jolkkonen/pdf/CRC_TD.pdf).

²²¹⁶ Pyridine ($\text{C}_5\text{H}_5\text{N}$, 0.0791 kg/mole , 982 kg/m^3 ; <https://en.wikipedia.org/wiki/Pyridine>) is a colorless liquid; a stoichiometric combustion ($\text{C}_5\text{H}_5\text{N} + 6.25\text{O}_2 \rightarrow 0.5\text{N}_2 + 5\text{CO}_2 + 2.5\text{H}_2\text{O}$) using liquid oxygen (LOX: density 1141 kg/m^3 , MW 0.032 kg/mole) consumes 0.0751 kg of $\text{C}_5\text{H}_5\text{N}$ and 0.200 kg of O_2 and releases $2.67 \times 10^6 \text{ J/mole}$ of $\text{C}_5\text{H}_5\text{N}$, taking taking the standard heats of formation as $+100.2 \text{ kJ/mole}$ for liquid $\text{C}_5\text{H}_5\text{N}$, -393.5 kJ/mole for CO_2 , and -241.8 kJ/mole for H_2O (http://www.update.uu.se/~jolkkonen/pdf/CRC_TD.pdf).

²²¹⁷ 1,1-dinitropropane ($\text{C}_3\text{H}_6\text{N}_2\text{O}_4$) has an approximate density of 1408 kg/m^3 with a MW of 0.134 kg/mole ; a stoichiometric combustion ($\text{C}_3\text{H}_6\text{N}_2\text{O}_4 + 4.5\text{O}_2 \rightarrow \text{N}_2 + 3\text{H}_2\text{O} + 3\text{CO}_2$) using liquid oxygen (LOX: density 1141 kg/m^3 , MW 0.032 kg/mole) consumes 0.134 kg of $\text{C}_3\text{H}_6\text{N}_2\text{O}_4$ and 0.144 kg of O_2 and releases $1.88 \times 10^6 \text{ J/mole}$ of $\text{C}_3\text{H}_6\text{N}_2\text{O}_4$ (standard enthalpy of combustion); Helf S, Ottoson KG. Test of Explosive Compounds. Technical Report ARMET-TR-10015, Oct 1949, Table 1, p. 2; <http://handle.dtic.mil/100.2/ADA526427>.

1,1-dinitropropane $C_3H_6N_2O_4$, liquid (with LOX)	1.88×10^6	0.278	2.21×10^{-4}
Picryl propyl ether $C_9H_9N_3O_7$ (excluding O_2) ²²¹⁸	4.62×10^6	0.271	1.59×10^{-4}
Picryl propyl ether $C_9H_9N_3O_7$ (with LOX)	4.62×10^6	0.519	3.77×10^{-4}
Diethylenetriamine $C_4H_{13}N_3$ (excluding O_2) ²²¹⁹	3.08×10^6	0.103	1.08×10^{-4}
Diethylenetriamine $C_4H_{13}N_3$ (with LOX)	3.08×10^6	0.335	3.11×10^{-4}
DMAZ $C_4H_{10}N_4$ (excluding O_2) ²²²⁰	3.08×10^6	0.114	1.15×10^{-4}
DMAZ $C_4H_{10}N_4$ (with LOX)	3.08×10^6	0.322	2.97×10^{-4}
DNAN $C_7H_6N_2O_5$ (excluding O_2) ²²²¹	3.29×10^6	0.198	1.48×10^{-4}
DNAN $C_7H_6N_2O_5$ (with LOX)	3.29×10^6	0.390	3.16×10^{-4}
HMTD $C_6H_{12}N_2O_6$ (excluding O_2) ²²²²	3.45×10^6	0.208	2.37×10^{-4}

²²¹⁸ Picryl propyl ether, aka. 1,3,5-trinitro-2-propoxybenzene ($C_9H_9N_3O_7$) has an approximate density of 1700 kg/m^3 with a MW of 0.271 kg/mole ; a stoichiometric combustion ($C_9H_9N_3O_7 + 7.75O_2 \rightarrow 1.5N_2 + 4.5H_2O + 9CO_2$) using liquid oxygen (LOX: density 1141 kg/m^3 , MW 0.032 kg/mole) consumes 0.271 kg of $C_9H_9N_3O_7$ and 0.248 kg of O_2 and releases $4.62 \times 10^6 \text{ J/mole}$ of $C_9H_9N_3O_7$ (standard enthalpy of combustion); Helf S, Ottoson KG. Test of Explosive Compounds. Technical Report ARMET-TR-10015, Oct 1949, Table 1, p. 2; <http://handle.dtic.mil/100.2/ADA526427>.

²²¹⁹ Diethylenetriamine, aka. DETA ($C_4H_{13}N_3$) has a density of 955 kg/m^3 with a MW of 0.103 kg/mole ; a stoichiometric combustion ($C_4H_{13}N_3 + 7.25O_2 \rightarrow 1.5N_2 + 4CO_2 + 6.5H_2O$) using liquid oxygen (LOX: density 1141 kg/m^3 , MW 0.032 kg/mole) consumes 0.103 kg of $C_4H_{13}N_3$ and 0.232 kg of O_2 and releases $3.08 \times 10^6 \text{ J/mole}$ of $C_4H_{13}N_3$ (standard enthalpy of combustion); <https://en.wikipedia.org/wiki/Diethylenetriamine>.

²²²⁰ 2-Dimethylaminoethylazide, aka. DMAZ ($C_4H_{10}N_4$) has a density of 955 kg/m^3 with a MW of 0.114 kg/mole ; a stoichiometric combustion ($C_4H_{10}N_4 + 6.5O_2 \rightarrow 2N_2 + 4CO_2 + 5H_2O$) using liquid oxygen (LOX: density 1141 kg/m^3 , MW 0.032 kg/mole) consumes 0.114 kg of $C_4H_{10}N_4$ and 0.208 kg of O_2 and releases $3.08 \times 10^6 \text{ J/mole}$ of $C_4H_{10}N_4$ (standard enthalpy of combustion); <https://en.wikipedia.org/wiki/2-Dimethylaminoethylazide>.

²²²¹ DNAN, aka. 2,4-dinitroanisole ($C_7H_6N_2O_5$, 0.198 kg/mole , $1.48 \times 10^{-4} \text{ m}^3/\text{mole}$; <https://en.wikipedia.org/wiki/2,4-Dinitroanisole>), taking the ideal combustion reaction as: $C_7H_6N_2O_5 + 6O_2 \rightarrow N_2 + 7CO_2 + 3H_2O$, using liquid oxygen (LOX: density 1141 kg/m^3 , MW 0.032 kg/mole), and taking the standard heats of formation as -393.5 kJ/mole for CO_2 and -241.8 kJ/mole for H_2O (http://www.update.uu.se/~jolkkonen/pdf/CRC_TD.pdf) and -186.65 kJ/mole for $C_7H_6N_2O_5$ (Meyer R, Kohler J, Homburg A. Explosives. John Wiley & Sons, 2016), the combustion energy would be $3.29 \times 10^6 \text{ J/mole}$ of $C_7H_6N_2O_5$.

²²²² HMTD, aka. hexamine peroxide ($C_6H_{12}N_2O_6$, 0.208 kg/mole , $2.37 \times 10^{-4} \text{ m}^3/\text{mole}$; https://en.wikipedia.org/wiki/Hexamethylene_tri-peroxide_diamine), taking the ideal combustion reaction as: $C_6H_{12}N_2O_6 + 6O_2 \rightarrow N_2 + 6CO_2 + 6H_2O$, using liquid oxygen (LOX: density 1141 kg/m^3 , MW 0.032 kg/mole), and taking the standard heats of formation as -393.5 kJ/mole for CO_2 and -241.8 kJ/mole for H_2O (http://www.update.uu.se/~jolkkonen/pdf/CRC_TD.pdf) and -360 kJ/mole for $C_6H_{12}N_2O_6$ (<https://books.google.com/books?id=hX3mBgAAQBAJ&pg=PA519>), the combustion energy would be $3.45 \times 10^6 \text{ J/mole}$ of $C_6H_{12}N_2O_6$. HMTD is sometimes called a “peroxo-based homemade explosive” because of its ease of manufacture.

HMTD $C_6H_{12}N_2O_6$ (with LOX)	3.45×10^6	0.400	4.05×10^{-4}
HNS $C_{14}H_6N_6O_{12}$ (excluding O_2) ²²²³	6.29×10^6	0.450	2.65×10^{-4}
HNS $C_{14}H_6N_6O_{12}$ (with LOX)	6.29×10^6	0.754	5.31×10^{-4}
TACOT $C_{12}H_4N_8O_8$ (excluding O_2) ²²²⁴	5.26×10^6	0.388	2.10×10^{-4}
TACOT $C_{12}H_4N_8O_8$ (with LOX)	5.26×10^6	0.676	4.62×10^{-4}
UDMH $C_2H_8N_2$ (excluding O_2) ²²²⁵	1.80×10^6	0.0601	7.60×10^{-5}
UDMH $C_2H_8N_2$ (with LOX)	1.80×10^6	0.1881	1.88×10^{-4}
Cyanogen C_2N_2 , liquid (excluding O_2) ²²²⁶	1.10×10^6	0.052	5.47×10^{-5}
Cyanogen C_2N_2 , liquid (with LOX)	1.10×10^6	0.116	1.11×10^{-4}
Dicyanoacetylene C_4N_2 , liquid (excluding O_2) ²²²⁷	2.07×10^6	0.0761	8.39×10^{-5}

²²²³ HNS, aka. 2,2',4,4',6,6'-hexanitrostilbene ($(C_6H_2)_2(CH)_2(NO_2)_6$ or $C_{14}H_6N_6O_{12}$, 0.450 kg/mole, $2.65 \times 10^{-4} \text{ m}^3/\text{mole}$; <https://en.wikipedia.org/wiki/Hexanitrostilbene>), taking the ideal combustion reaction as: $C_{14}H_6N_6O_{12} + 9.5O_2 \rightarrow 3N_2 + 14CO_2 + 3H_2O$, using liquid oxygen (LOX: density 1141 kg/m^3 , MW 0.032 kg/mole), and taking the standard heats of formation as -393.5 kJ/mole for CO_2 and -241.8 kJ/mole for H_2O (http://www.update.uu.se/~jolkkonen/pdf/CRC_TD.pdf) and $+58 \text{ kJ/mole}$ for $C_{14}H_6N_6O_{12}$ (Agrawal JP. High Energy Materials: Propellants, Explosives and Pyrotechnics, John Wiley & Sons, 2015, Table 1.5, p. 26), the combustion energy is $6.29 \times 10^6 \text{ J/mole}$ of $C_{14}H_6N_6O_{12}$.

²²²⁴ TACOT, aka. tetranitro-dibenzo-1,3a,4,4a-tetraazapentalene ($(C_6H_2)_2(NO_2)_4N_4$ or $C_{12}H_4N_8O_8$, 0.388 kg/mole, $2.10 \times 10^{-4} \text{ m}^3/\text{mole}$ at 1850 kg/m^3), taking the ideal combustion reaction as: $C_{12}H_4N_8O_8 + 9O_2 \rightarrow 4N_2 + 12CO_2 + 2H_2O$, using liquid oxygen (LOX: density 1141 kg/m^3 , MW 0.032 kg/mole), and taking the standard heats of formation as -393.5 kJ/mole for CO_2 and -241.8 kJ/mole for H_2O (http://www.update.uu.se/~jolkkonen/pdf/CRC_TD.pdf) and $+1592.8 \text{ kJ/mole}$ for $C_{12}H_4N_8O_8$ (Agrawal JP. High Energy Materials: Propellants, Explosives and Pyrotechnics, John Wiley & Sons, 2015, Table 1.5, p. 26), the combustion energy would be $5.26 \times 10^6 \text{ J/mole}$ of $C_{12}H_4N_8O_8$.

²²²⁵ UDMH, aka. unsymmetrical dimethylhydrazine ($C_2H_8N_2$, 0.0601 kg/mole, 791 kg/m^3 ; https://en.wikipedia.org/wiki/Unsymmetrical_dimethylhydrazine) is sometimes used as a rocket fuel with liquid oxygen (LOX: density 1141 kg/m^3 , MW 0.032 kg/mole). The stoichiometric combustion is: $C_2H_8N_2 [0.0601 \text{ kg}, 7.60 \times 10^{-5} \text{ m}^3] + O_2 [0.128 \text{ kg}, 1.12 \times 10^{-4} \text{ m}^3] \rightarrow N_2 + 2CO_2 + 4H_2O$, taking standard heats of formation as $+48.3 \text{ kJ/mole}$ for $C_2H_8N_2$, -393.5 kJ/mole for CO_2 , and -241.8 kJ/mole for H_2O (http://www.update.uu.se/~jolkkonen/pdf/CRC_TD.pdf), releasing $1.80 \times 10^6 \text{ J/mole}$ of UDMH.

²²²⁶ Liquid cyanogen (C_2N_2) has a density of 950 kg/m^3 with a MW of 0.052 kg/mole; a stoichiometric combustion ($C_2N_2 + 2O_2 \rightarrow N_2 + 2CO_2$) using liquid oxygen (LOX: density 1141 kg/m^3 , MW 0.032 kg/mole) consumes 0.052 kg of C_2N_2 and 0.064 kg of O_2 and releases $1.10 \times 10^6 \text{ J/mole}$ of C_2N_2 (standard enthalpy of combustion); <https://en.wikipedia.org/wiki/Cyanogen>.

²²²⁷ Liquid dicyanoacetylene (C_4N_2) has a density of 907 kg/m^3 with a MW of 0.0761 kg/mole; a stoichiometric combustion ($C_4N_2 + 4O_2 \rightarrow N_2 + 4CO_2$) using liquid oxygen (LOX: density 1141 kg/m^3 , MW 0.032 kg/mole) consumes 0.0761 kg of C_4N_2 and 0.128 kg of O_2 and releases $2.07 \times 10^6 \text{ J/mole}$ of C_4N_2 (standard enthalpy of combustion); <https://en.wikipedia.org/wiki/Dicyanoacetylene>. "It burns in oxygen with a bright blue-white flame at a temperature of 5260 K ($4990 \text{ }^\circ\text{C}$, $9010 \text{ }^\circ\text{F}$), which is the hottest flame of any known chemical reaction."

Dicyanoacetylene C ₄ N ₂ , liquid (with LOX)	2.07 x 10 ⁶	0.2041	1.96 x 10 ⁻⁴
Tetranitratocarbon (theoretical) (excluding O ₂) ²²²⁸	1.144 x 10 ⁶	0.308	2 x 10 ⁻⁴
Tetranitratocarbon (theoretical) (with LOX)	1.144 x 10 ⁶	0.340	2.28 x 10 ⁻⁴
Dipropargylammonium C ₆ H ₇ N (excluding O ₂) ²²²⁹	3.67 x 10 ⁶	0.093	6.20 x 10 ⁻⁵
Dipropargylammonium C ₆ H ₇ N (with LOX)	3.67 x 10 ⁶	0.341	2.79 x 10 ⁻⁴
Tripropargyl amine C ₉ H ₉ N (excluding O ₂) ²²³⁰	5.33 x 10 ⁶	0.131	8.33 x 10 ⁻⁵
Tripropargyl amine C ₉ H ₉ N (with LOX)	5.33 x 10 ⁶	0.491	3.99 x 10 ⁻⁴
Tetrapropargylammonium tetraethynylborate (excl. O ₂) ²²³¹	1.245 x 10 ⁷	0.281	1.56 x 10 ⁻⁴

²²²⁸ Tetranitratocarbon, aka. tetrakis(nitratocarbon)methane (C(CO₃N)₄, 0.308 kg/mole, ~2 x 10⁻⁴ m³/mole arbitrarily assuming ~1500 kg/m³, not yet reported) is predicted to have explosive properties but might be too thermally unstable for practical use (Zoellner RW, Lazen CL, Boehr KM. A computational study of novel nitratocarbon, nitritocarbonyl, and nitrate compounds and their potential as high energy materials. *Comput Theoret Chem* 2012 Jan 1;979:33-37; <http://www.sciencedirect.com/science/article/pii/S2210271X11005433>). The predicted combustion reaction with oxygen: C(CO₃N)₄ + O₂ → 5CO₂ + 2NO₂ + N₂ has a predicted enthalpy change of -1.144 x 10⁶ J/mole (<https://en.wikipedia.org/wiki/Tetranitratocarbon>), and would require 1 mole of oxygen (LOX: density 1141 kg/m³, MW 0.032 kg/mole) per mole of (C(CO₃N)₄ consumed. The molecule had not been synthesized as of 2016.

²²²⁹ Dipropargylammonium (HN(CH₂C≡CH)₂ or C₆H₇N, 0.093 kg/mole, heat of formation +464.4 kJ/mole; Schmitt RJ, Bottaro JC, Petrie M, Penwell PE. Synthesis of new High Energy Density Matter (HEDM): Extra high energy oxidizers and fuels. Air Force Research laboratory (AFMC), AFRL-PR-ED-TR-1998-0023, 27 Jan 1998, <http://docslide.us/documents/robert-j-schmitt-et-al-synthesis-of-new-high-energy-density-matter-hedm-extra-high-energy-oxidizers-and-fuels.html>) if fully combusted in oxygen (C₆H₇N + 7.75O₂ → 0.5N₂ + 6CO₂ + 3.5H₂O) would release 3.67 x 10⁶ J/mole, using liquid oxygen (LOX: density 1141 kg/m³, MW 0.032 kg/mole) and taking heats of formation of -393.5 kJ/mole for CO₂ and -241.8 kJ/mole for H₂O (http://www.update.uu.se/~jolkkonen/pdf/CRC_TD.pdf). A density of ~1500 kg/m³ is assumed.

²²³⁰ Tripropargyl amine (N(CH₂C≡CH)₃ or C₉H₉N, 0.131 kg/mole, heat of formation +702.9 kJ/mole; Schmitt RJ, Bottaro JC, Petrie M, Penwell PE. Synthesis of new High Energy Density Matter (HEDM): Extra high energy oxidizers and fuels. Air Force Research laboratory (AFMC), AFRL-PR-ED-TR-1998-0023, 27 Jan 1998, <http://docslide.us/documents/robert-j-schmitt-et-al-synthesis-of-new-high-energy-density-matter-hedm-extra-high-energy-oxidizers-and-fuels.html>) if fully combusted in oxygen (C₉H₉N + 11.25O₂ → 0.5N₂ + 9CO₂ + 4.5H₂O) would release 5.33 x 10⁶ J/mole, using liquid oxygen (LOX: density 1141 kg/m³, MW 0.032 kg/mole) and taking heats of formation of -393.5 kJ/mole for CO₂ and -241.8 kJ/mole for H₂O (http://www.update.uu.se/~jolkkonen/pdf/CRC_TD.pdf). A density of ~1500 kg/m³ is assumed.

Tetrapropargylammonium tetraethynylborate (with LOX)	1.245×10^7	1.073	8.50×10^{-4}
Hexamine $C_6H_{12}N_4$, solid (excluding O_2) ²²³²	4.2×10^6	0.140	1.05×10^{-4}
Cyanuric triazide C_3N_3 , solid (excluding O_2) ²²³³	2.234×10^6	0.214	1.24×10^{-4}
<u>Organometallics</u>			
Methylithium $LiCH_3$ (excluding O_2) ²²³⁴	1.17×10^6	0.022	3.06×10^{-5}
Methylithium $LiCH_3$ (with LOX)	1.17×10^6	0.086	8.66×10^{-5}
Ethyllithium LiC_2H_5 (excluding O_2) ²²³⁵	1.74×10^6	0.036	4.18×10^{-5}
Ethyllithium LiC_2H_5 (with LOX)	1.74×10^6	0.148	1.40×10^{-4}
Butyllithium LiC_4H_9 (excluding O_2) ²²³⁶	3.025×10^6	0.0641	9.43×10^{-5}

²²³¹ Tetrapropargylammonium tetraethynylborate ($[N(CH_2C\equiv CH)_4]^+[B(C\equiv CH)_4]^-$ or $C_{20}H_{16}NB$, 0.281 kg/mole, heat of formation +2008.3 kJ/mole; Schmitt RJ, Bottaro JC, Petrie M, Penwell PE. Synthesis of new High Energy Density Matter (HEDM): Extra high energy oxidizers and fuels. Air Force Research laboratory (AFMC), AFRL-PR-ED-TR-1998-0023, 27 Jan 1998, <http://docslide.us/documents/robert-j-schmitt-et-al-synthesis-of-new-high-energy-density-matter-hedm-extra-high-energy-oxidizers-and-fuels.html>) if fully combusted in oxygen ($C_{20}H_{16}NB + 24.75O_2 \rightarrow 0.5N_2 + 0.5B_2O_3 + 20CO_2 + 8H_2O$) would release 1.245×10^7 J/mole, using liquid oxygen (LOX: density 1141 kg/m³, MW 0.032 kg/mole) and taking heats of formation of 1273.5 for B_2O_3 , -393.5 kJ/mole for CO_2 and -241.8 kJ/mole for H_2O (http://www.update.uu.se/~jolkkonen/pdf/CRC_TD.pdf). A density of ~1800 kg/m³ is assumed.

²²³² Hexamine, aka. methenamine, hexamethylenetetramine, or 1,3,5,7-tetraazaadamantane ($C_6H_{12}N_4$, 0.140 kg/mole, 1330 kg/m³) is used in fuel tablets (https://en.wikipedia.org/wiki/Hexamine_fuel_tablet) that burn smokelessly in air, releasing 30.0 MJ/kg of heat (<https://en.wikipedia.org/wiki/Hexamethylenetetramine>) or 4.2×10^6 J/mole.

²²³³ Cyanuric triazide, aka. CTA, 2,4,6-triazido-1,3,5-triazine, triazine triazide, or TTA ($(NCN_3)_3$ or C_3N_3 , 0.214 kg/mole, 1.24×10^4 m³/mole at 1730 Kg/m³) under combustion conditions liberates 2.234×10^6 J/mole (https://en.wikipedia.org/wiki/Cyanuric_triazide).

²²³⁴ Methylithium ($LiCH_3$) has a density of ~720 kg/m³ with a MW of 0.022 kg/mole; a complete stoichiometric combustion ($LiCH_3 + 2O_2 \rightarrow 0.5Li_2O + CO_2 + 1.5H_2O$) using liquid oxygen (LOX: density 1141 kg/m³, MW 0.032 kg/mole) consumes 0.022 kg of $LiCH_3$ and 0.064 kg of O_2 and releases 1.17×10^6 J/mole of $LiCH_3$ (taking heats of formation of +113 kJ/mole for $LiCH_3$, -597.9 kJ/mole for Li_2O , -393.5 kJ/mole for CO_2 , and -241.8 kJ/mole for $H_2O(g)$); <https://en.wikipedia.org/wiki/Methylithium>, https://en.wikipedia.org/wiki/Carbon_dioxide, http://www.update.uu.se/~jolkkonen/pdf/CRC_TD.pdf, <http://www.sigmaaldrich.com/catalog/product/aldrich/197343?lang=en®ion=US>, and Kaufmann E *et al.* Methylithium and its oligomers. Structural and energetic relationships. *Organometallics* 1988;7:1597-1607; <http://pubs.acs.org/doi/abs/10.1021/om00097a024?journalCode=orgnd7>.

²²³⁵ Ethyllithium (LiC_2H_5) has a density of 862 kg/m³ with a MW of 0.036 kg/mole; a complete stoichiometric combustion ($LiC_2H_5 + 3.5O_2 \rightarrow 0.5Li_2O + 2CO_2 + 2.5H_2O$) using liquid oxygen (LOX: density 1141 kg/m³, MW 0.032 kg/mole) consumes 0.036 kg of LiC_2H_5 and 0.112 kg of O_2 and releases 1.74×10^6 J/mole of LiC_2H_5 (standard enthalpy of combustion); http://www.chemicalbook.com/ChemicalProductProperty_US_CB5753039.aspx and <http://webbook.nist.gov/cgi/cbook.cgi?ID=C811494&Mask=E>.

Butyllithium LiC_4H_9 (with LOX)	3.025×10^6	0.2721	2.77×10^{-4}
Dimethylberyllium $\text{Be}(\text{CH}_3)_2$ (excluding O_2) ²²³⁷	1.88×10^6	0.0391	5.59×10^{-5}
Dimethylberyllium $\text{Be}(\text{CH}_3)_2$ (with LOX)	1.88×10^6	0.1671	1.68×10^{-4}
Dimethylmercury $\text{Hg}(\text{CH}_3)_2$ (excluding O_2) ²²³⁸	1.663×10^6	0.2307	7.79×10^{-5}
Dimethylmercury $\text{Hg}(\text{CH}_3)_2$ (with LOX)	1.663×10^6	0.3587	1.90×10^{-4}
Dimethylzinc $\text{Zn}(\text{CH}_3)_2$ (excluding O_2) ²²³⁹	2.02×10^6	0.0955	7.27×10^{-5}
Dimethylzinc $\text{Zn}(\text{CH}_3)_2$ (with LOX)	2.02×10^6	0.2235	1.85×10^{-4}
Diethylzinc $\text{Zn}(\text{C}_2\text{H}_5)_2$, liquid (excluding O_2) ²²⁴⁰	3.372×10^6	0.1235	1.02×10^{-4}

²²³⁶ *n*-butyllithium (*n*- LiC_4H_9) – “main hazard: pyrophoric (inflames in air)” – has a density of 680 kg/m^3 with a MW of 0.0641 kg/mole ; a complete stoichiometric combustion ($\text{LiC}_4\text{H}_9 + 6.5\text{O}_2 \rightarrow 0.5\text{Li}_2\text{O} + 4\text{CO}_2 + 4.5\text{H}_2\text{O}$) using liquid oxygen (LOX: density 1141 kg/m^3 , MW 0.032 kg/mole) consumes 0.0641 kg of LiC_4H_9 and 0.208 kg of O_2 and releases $3.025 \times 10^6 \text{ J/mole}$ of LiC_4H_9 (standard enthalpy of combustion); <https://en.wikipedia.org/wiki/N-Butyllithium> and <http://webbook.nist.gov/cgi/cbook.cgi?ID=C109728&Mask=1A8F>. *tert*-butyllithium (*t*- $\text{C}_4\text{H}_9\text{Li}$) is also a pyrophoric orangolithium compound with a cubane structure “that easily catches fire on exposure to air” ($\text{t-BuLi} + \text{O}_2 \rightarrow \text{t-BuOOLi}$), with density 660 kg/m^3 and MW of 0.0641 kg/mole ; <https://en.wikipedia.org/wiki/Tert-Butyllithium>.

²²³⁷ Dimethylberyllium ($\text{Be}(\text{CH}_3)_2$) has an estimated density of $\sim 700 \text{ kg/m}^3$ with a MW of 0.0391 kg/mole ; a complete stoichiometric combustion ($\text{Be}(\text{CH}_3)_2 + 4\text{O}_2 \rightarrow \text{BeO} + 2\text{CO}_2 + 3\text{H}_2\text{O}$) using liquid oxygen (LOX: density 1141 kg/m^3 , MW 0.032 kg/mole) consumes 0.0391 kg of $\text{Be}(\text{CH}_3)_2$ and 0.128 kg of O_2 and releases $1.88 \times 10^6 \text{ J/mole}$ of $\text{Be}(\text{CH}_3)_2$ (taking heats of formation of -237.7 kJ/mole for $\text{Be}(\text{CH}_3)_2$, -609.4 kJ/mole for BeO , -393.5 kJ/mole for CO_2 , and -241.8 kJ/mole for $\text{H}_2\text{O}(\text{g})$); <https://pqr.pitt.edu/mol/RPUYWDQUQHEHSQ-UHFFFAOYSA-N> and http://www.update.uu.se/~jolkkonen/pdf/CRC_TD.pdf.

²²³⁸ Liquid dimethylmercury ($\text{Hg}(\text{CH}_3)_2$), an extremely toxic* organometallic compound (<https://en.wikipedia.org/wiki/Dimethylmercury>), has a density of 2961 kg/m^3 with a MW of 0.23066 kg/mole ; a complete stoichiometric combustion ($\text{Hg}(\text{CH}_3)_2 + 4\text{O}_2 \rightarrow \text{HgO} + 2\text{CO}_2 + 3\text{H}_2\text{O}$) using liquid oxygen (LOX: density 1141 kg/m^3 , MW 0.032 kg/mole) consumes 0.2307 kg of $\text{Hg}(\text{CH}_3)_2$ and 0.128 kg of O_2 and releases $1.663 \times 10^6 \text{ J/mole}$ of $\text{Hg}(\text{CH}_3)_2$ (standard enthalpy of combustion); http://www.update.uu.se/~jolkkonen/pdf/CRC_TD.pdf. * https://en.wikipedia.org/wiki/Karen_Wetterhahn.

²²³⁹ Liquid dimethylzinc ($\text{Zn}(\text{CH}_3)_2$), a pyrophoric organometallic, has a density of 1313 kg/m^3 with a MW of 0.0955 kg/mole ; a complete stoichiometric combustion ($\text{Zn}(\text{CH}_3)_2 + 4\text{O}_2 \rightarrow \text{ZnO} + 2\text{CO}_2 + 3\text{H}_2\text{O}$) using liquid oxygen (LOX: density 1141 kg/m^3 , MW 0.032 kg/mole) consumes 0.0955 kg of $\text{Zn}(\text{CH}_3)_2$ and 0.128 kg of O_2 and releases $2.02 \times 10^6 \text{ J/mole}$ of $\text{Zn}(\text{CH}_3)_2$ (standard enthalpy of combustion); <https://en.wikipedia.org/wiki/Dimethylzinc>, <https://www.akzonobel.com/hpmo/products/dimethylzinc/>, and <http://webbook.nist.gov/cgi/cbook.cgi?ID=C544978&Mask=3EFF>.

²²⁴⁰ Liquid diethylzinc ($\text{Zn}(\text{C}_2\text{H}_5)_2$), used in small quantities as a hypergolic or “self igniting” liquid rocket fuel because it ignites on contact with oxidizer (the rocket motor need only contain a pump without a spark source for ignition), has a density of 1205 kg/m^3 with a MW of 0.1235 kg/mole ; a complete stoichiometric combustion ($\text{Zn}(\text{C}_2\text{H}_5)_2 + 7\text{O}_2 \rightarrow \text{ZnO} + 4\text{CO}_2 + 5\text{H}_2\text{O}$) using liquid oxygen (LOX: density 1141 kg/m^3 , MW 0.032 kg/mole) consumes 0.1235 kg of $\text{Zn}(\text{C}_2\text{H}_5)_2$ and 0.224 kg of O_2 and releases $3.372 \times 10^6 \text{ J/mole}$ of $\text{Zn}(\text{C}_2\text{H}_5)_2$ (standard enthalpy of combustion); <https://en.wikipedia.org/wiki/Diethylzinc>, <http://webbook.nist.gov/cgi/cbook.cgi?ID=C557200&Units=SI&Mask=FFF>.

Diethylzinc $Zn(C_2H_5)_2$, liquid (with LOX)	3.372×10^6	0.3475	2.99×10^{-4}
Trimethylaluminum $Al(CH_3)_3$, liquid (excluding O_2) ²²⁴¹	3.182×10^6	0.0721	9.59×10^{-5}
Trimethylaluminum $Al(CH_3)_3$, liquid (with LOX)	3.182×10^6	0.2641	2.64×10^{-4}
Diethylethoxyaluminum $(C_6H_{15}AlO)$ ²²⁴²	n/a		
Diethylaluminum chloride $(C_2H_5)_2AlCl$ (excluding O_2) ²²⁴³	3.577×10^6	0.1206	1.25×10^{-4}
Triethylaluminum $Al_2(C_2H_5)_6$, liquid (excluding O_2) ²²⁴⁴	5.11×10^6	0.2283	2.74×10^{-4}
Triethylaluminum $Al_2(C_2H_5)_6$, liquid (with LOX)	5.11×10^6	0.9003	8.63×10^{-4}
Diisobutylaluminum hydride $(i-C_4H_9)_2AlH$ (excl. O_2) ²²⁴⁵	6.412×10^6	0.1422	1.78×10^{-4}
Tributylaluminum $Al(C_4H_9)_3$ (excluding O_2) ²²⁴⁶	9.046×10^6	0.1983	2.43×10^{-4}

²²⁴¹ Liquid trimethylaluminum ($Al(CH_3)_3$), aka. TMA, a pyrophoric organoaluminum compound, has a density of 752 kg/m^3 with a MW of 0.0721 kg/mole ; a complete stoichiometric combustion ($Al(CH_3)_3 + 6O_2 \rightarrow 0.5Al_2O_3 + 3CO_2 + 4.5H_2O$) using liquid oxygen (LOX: density 1141 kg/m^3 , MW 0.032 kg/mole) consumes 0.0721 kg of $Al(CH_3)_3$ and 0.192 kg of O_2 and releases $3.182 \times 10^6 \text{ J/mole}$ of $Al(CH_3)_3$ (standard enthalpy of combustion); <https://en.wikipedia.org/wiki/Trimethylaluminium>, http://webcache.googleusercontent.com/search?q=cache:tQbw59B7HygJ:chemtura-organometallics.com/deployedfiles/Chemturav8/OMS/Service%2520and%2520Logistics/Chemical%2520and%2520Physical%2520Properties_ver.20131016.pdf+&cd=15&hl=en&ct=clnk&gl=us.

²²⁴² “The pure material ignites in air”; Peter Urben, Bretherick’s Handbook of Reactive Chemical Hazards, Elsevier, 1995, p. 831. Diethylethoxyaluminum has a density of 862 kg/m^3 with MW of 0.1292 kg/mole , and “ignites spontaneously in air in the pure form”; <http://www.lookchem.com/Ethoxy-diethyl-aluminum/>.

²²⁴³ Liquid diethylaluminum chloride ($(C_2H_5)_2AlCl$), aka. DEAC, “ignites upon exposure...neat pyrophoric liquid” to air, has a density of 962 kg/m^3 with a MW of 0.1206 kg/mole ; combustion consumes 0.1206 kg of $C_{12}H_{30}Al_2$ and releases $3.577 \times 10^6 \text{ J/mole}$ of $(C_2H_5)_2AlCl$ (standard enthalpy of combustion); http://www.pcpds.akzonobel.com/PolymerChemicalsPDS/showPDF.aspx?pds_id=413.

²²⁴⁴ Liquid triethylaluminum ($C_{12}H_{30}Al_2$), aka. TEA, one of the few substances pyrophoric enough to easily ignite on contact with cryogenic LOX (making it particularly desirable as a rocket engine ignitor), has a density of 832 kg/m^3 with a MW of 0.2283 kg/mole ; a complete stoichiometric combustion ($C_{12}H_{30}Al_2 + 21O_2 \rightarrow Al_2O_3 + 12CO_2 + 15H_2O$) using liquid oxygen (LOX: density 1141 kg/m^3 , MW 0.032 kg/mole) consumes 0.2283 kg of $C_{12}H_{30}Al_2$ and 0.672 kg of O_2 and releases $5.11 \times 10^6 \text{ J/mole}$ of $C_{12}H_{30}Al_2$ (standard enthalpy of combustion); <https://en.wikipedia.org/wiki/Triethylaluminium>, <http://webbook.nist.gov/cgi/cbook.cgi?ID=C97938&Mask=1A8F>.

²²⁴⁵ Diisobutylaluminum hydride ($(i-C_4H_9)_2AlH$), aka. DIBAL or DIBAH, has a density of 801 kg/m^3 with a MW of 0.1422 kg/mole ; combustion consumes 0.1422 kg of $(i-C_4H_9)_2AlH$ and releases $6.412 \times 10^6 \text{ J/mole}$ of $(i-C_4H_9)_2AlH$ (standard enthalpy of combustion); http://webcache.googleusercontent.com/search?q=cache:tQbw59B7HygJ:chemtura-organometallics.com/deployedfiles/Chemturav8/OMS/Service%2520and%2520Logistics/Chemical%2520and%2520Physical%2520Properties_ver.20131016.pdf+&cd=15&hl=en&ct=clnk&gl=us. “DIBAL...reacts violently with air and water...ignites in air.” https://en.wikipedia.org/wiki/Diisobutylaluminium_hydride.

Trimethylgallium Ga(CH ₃) ₃ (excluding O ₂) ²²⁴⁷	2.933 x 10 ⁶	0.1148	1.01 x 10 ⁻⁴
Triethylgallium Ga(C ₂ H ₅) ₃ (excluding O ₂) ²²⁴⁸	4.95 x 10 ⁶	0.1569	1.47 x 10 ⁻⁴
Trimethylamine N(CH ₃) ₃ (excluding O ₂) ²²⁴⁹	2.484 x 10 ⁶	0.0591	8.82 x 10 ⁻⁵
Triethylphosphine P(C ₂ H ₅) ₃ (excluding O ₂) ²²⁵⁰	5.176 x 10 ⁶	0.1182	1.47 x 10 ⁻⁴
Trimethylarsine As(CH ₃) ₃ (excluding O ₂) ²²⁵¹	2.779 x 10 ⁶	0.120	1.07 x 10 ⁻⁴
Trimethylstibine Sb(CH ₃) ₃ (excluding O ₂) ²²⁵²	2.921 x 10 ⁶	0.1669	1.10 x 10 ⁻⁴
Trimethylbismuthine Bi(CH ₃) ₃ (excluding O ₂) ²²⁵³	2.912 x 10 ⁶	0.2541	1.10 x 10 ⁻⁴

²²⁴⁶ Tributylaluminum (Al(n-C₄H₉)₃), aka. TBA, has a density of 816 kg/m³ with a MW of 0.1983 kg/mole; combustion consumes 0.1983 kg of Al(n-C₄H₉)₃ and releases 9.046 x 10⁶ J/mole of Al(n-C₄H₉)₃ (standard enthalpy of combustion); http://webcache.googleusercontent.com/search?q=cache:tQbw59B7HygJ:chemtura-organometallics.com/deployedfiles/Chemturav8/OMS/Service%2520and%2520Logistics/Chemical%2520and%2520Physical%2520Properties_ver.20131016.pdf+&cd=15&hl=en&ct=clnk&gl=us.

²²⁴⁷ Trimethylgallium (Ga(CH₃)₃), aka. TMG or TMGa, “a clear, colorless, pyrophoric liquid...known to catch fire on exposure to air,” has a density of 1132 kg/m³ with a MW of 0.1148 kg/mole; combustion consumes 0.1148 kg of Ga(CH₃)₃ and releases 2.933 x 10⁶ J/mole of Ga(CH₃)₃ (standard enthalpy of combustion); <https://en.wikipedia.org/wiki/Trimethylgallium>, <http://www.sigmaaldrich.com/catalog/product/aldrich/j100015?lang=en®ion=US>, and <http://webbook.nist.gov/cgi/cbook.cgi?ID=C1445790&Mask=1A8F>.

²²⁴⁸ Triethylgallium (Ga(C₂H₅)₃), aka. TEGa, “a clear, colorless, pyrophoric liquid,” has a density of 1067 kg/m³ with a MW of 0.1569 kg/mole; combustion consumes 0.1569 kg of Ga(C₂H₅)₃ and releases 4.95 x 10⁶ J/mole of Ga(C₂H₅)₃ (standard enthalpy of combustion); <https://en.wikipedia.org/wiki/Triethylgallium>, <http://www.sigmaaldrich.com/catalog/product/aldrich/j100017?lang=en®ion=US>, and <http://webbook.nist.gov/cgi/cbook.cgi?ID=C1115997&Units=SI&Mask=FFFF>.

²²⁴⁹ Trimethylamine (N(CH₃)₃) has a density of 670 kg/m³ with a MW of 0.0591 kg/mole; combustion consumes 0.0591 kg of N(CH₃)₃ and releases 2.484 x 10⁶ J/mole of N(CH₃)₃ (standard enthalpy of combustion); <https://en.wikipedia.org/wiki/Trimethylamine> and Ovchinnikov VV. Thermochemistry of heteroatomic compounds. Amer J Phys Chem. 2013;2(4):60-71; <http://article.sciencepublishinggroup.com/pdf/10.11648.j.ajpc.20130204.11.pdf>.

²²⁵⁰ Triethylphosphine (P(C₂H₅)₃) has a density of 802 kg/m³ with a MW of 0.1182 kg/mole; combustion consumes 0.1182 kg of P(C₂H₅)₃ and releases 5.176 x 10⁶ J/mole of P(C₂H₅)₃ (standard enthalpy of combustion); <http://www.sigmaaldrich.com/catalog/product/aldrich/245275?lang=en®ion=US> and Ovchinnikov VV. Thermochemistry of heteroatomic compounds. Amer J Phys Chem. 2013;2(4):60-71; <http://article.sciencepublishinggroup.com/pdf/10.11648.j.ajpc.20130204.11.pdf>.

²²⁵¹ Trimethylarsine (As(CH₃)₃), aka. TMA or TMAs and a pyrophoric liquid, has a density of 1124 kg/m³ with a MW of 0.120 kg/mole; combustion consumes 0.120 kg of As(CH₃)₃ and releases 2.779 x 10⁶ J/mole of As(CH₃)₃ (standard enthalpy of combustion); <https://en.wikipedia.org/wiki/Trimethylarsine> and Ovchinnikov VV. Thermochemistry of heteroatomic compounds. Amer J Phys Chem. 2013;2(4):60-71; <http://article.sciencepublishinggroup.com/pdf/10.11648.j.ajpc.20130204.11.pdf>.

²²⁵² Trimethylstibine (Sb(CH₃)₃), “a colorless pyrophoric liquid,” has a density of 1523 kg/m³ with a MW of 0.1669 kg/mole; combustion consumes 0.1669 kg of Sb(CH₃)₃ and releases 2.921 x 10⁶ J/mole of Sb(CH₃)₃ (standard enthalpy of combustion); <https://en.wikipedia.org/wiki/Trimethylstibine> and Ovchinnikov VV. Thermochemistry of heteroatomic compounds. Amer J Phys Chem. 2013;2(4):60-71; <http://article.sciencepublishinggroup.com/pdf/10.11648.j.ajpc.20130204.11.pdf>.

<u>Other Oxygen Combustibles</u>			
Nickel tetracarbonyl Ni(CO) ₄ (excluding O ₂) ²²⁵⁴	1.18 x 10 ⁶	0.1707	1.29 x 10 ⁻⁴
Nickel tetracarbonyl Ni(CO) ₄ (with LOX)	1.18 x 10 ⁶	0.2027	1.57 x 10 ⁻⁴
Cobalt octacarbonyl Co ₂ (CO) ₈ (excluding O ₂) ²²⁵⁵	2.37 x 10 ⁶	0.342	1.83 x 10 ⁻⁴
Cobalt octacarbonyl Co ₂ (CO) ₈ (with LOX)	2.37 x 10 ⁶	0.630	4.35 x 10 ⁻⁴
Hydrazine N ₂ H ₄ , liquid (excluding O ₂) ²²⁵⁶	6.221 x 10 ⁵	0.032	3.13 x 10 ⁻⁵
Hydrazine N ₂ H ₄ , liquid (with LOX)	6.221 x 10 ⁵	0.064	5.94 x 10 ⁻⁵
Ammonia NH ₃ , liquid (excluding O ₂) ²²⁵⁷	3.83 x 10 ⁵	0.017	2.49 x 10 ⁻⁵

²²⁵³ Trimethylbismuthine (Bi(CH₃)₃) has a density of 2300 kg/m³ with a MW of 0.2541 kg/mole; combustion consumes 0.2541 kg of Bi(CH₃)₃ and releases 2.912 x 10⁶ J/mole of Bi(CH₃)₃ (standard enthalpy of combustion); <https://www.americanelements.com/trimethylbismuth-593-91-9> and Ovchinnikov VV. Thermochemistry of heteroatomic compounds. Amer J Phys Chem. 2013;2(4):60-71; <http://article.sciencepublishinggroup.com/pdf/10.11648.j.ajpc.20130204.11.pdf>.

²²⁵⁴ Liquid nickel tetracarbonyl (Ni(CO)₄) has a density of 1319 kg/m³ with MW of 0.1707 kg/mole; a stoichiometric combustion (Ni(CO)₄ + O₂ → Ni(CO)O + 2CO + CO₂) using liquid oxygen (LOX: density 1141 kg/m³, MW 0.032 kg/mole) consumes 0.1707 kg of Ni(CO)₄ and 0.032 kg of O₂ and releases 1.18 x 10⁶ J/mole of Ni(CO)₄ (standard enthalpy of combustion); https://en.wikipedia.org/wiki/Nickel_tetracarbonyl and Stedman DH, Hikade DA, Pearson R Jr, Yalvac ED. Nickel carbonyl: decomposition in air and related kinetic studies. Science. 1980 May 30;208(4447):1029-31; <http://science.sciencemag.org/content/sci/208/4447/1029.full.pdf>.

²²⁵⁵ Solid dicobalt octacarbonyl (Co₂(CO)₈) has a density of 1870 kg/m³ with MW of 0.342 kg/mole; a complete stoichiometric combustion (assumed Co₂(CO)₈ + 9O₂ → 2CoO + 8CO₂) using liquid oxygen (LOX: density 1141 kg/m³, MW 0.032 kg/mole) consumes 0.342 kg of Co₂(CO)₈ and 0.288 kg of O₂ and releases 2.37 x 10⁶ J/mole of Co₂(CO)₈ (taking heats of formation of -1249 kJ/mole for Co₂(CO)₈, -237.9 kJ/mole for CoO, and -393.5 kJ/mole for CO₂); https://en.wikipedia.org/wiki/Dicobalt_octacarbonyl, <http://webbook.nist.gov/cgi/cbook.cgi?ID=C10210681&Mask=2#Thermo-Condensed>, and http://www.update.uu.se/~jolkkonen/pdf/CRC_TD.pdf.

²²⁵⁶ Liquid hydrazine (N₂H₄) has a density of 1021 kg/m³ with a MW of 0.032 kg/mole; a stoichiometric combustion (N₂H₄ + O₂ → 2N₂ + 2H₂O) using liquid oxygen (LOX: density 1141 kg/m³, MW 0.032 kg/mole) consumes 0.032 kg of N₂H₄ and 0.032 kg of O₂ and releases 6.221 x 10⁵ J/mole of N₂H₄ (standard enthalpy of combustion); <https://en.wikipedia.org/wiki/Hydrazine> and Cole LG, Gilbert EC. The heats of combustion of some nitrogen compounds and the apparent energy of the N-N bond. J Am Chem Soc. 1951;73:5423-5427. "Hydrazine ignites in air at room temperature when exposed to metal oxide surfaces and in a wide variety of porous materials." Primer on Spontaneous Heating and Pyrophoricity, DOE-HDBK-1081-94, FSC-6910, Dec 1994; <http://web.archive.org/web/20100527183802/http://www.hss.energy.gov/nuclearsafety/ns/techstds/standard/hdbk1081/hdbk1081.pdf>.

Ammonia NH ₃ , liquid (with LOX)	3.83 x 10 ⁵	0.041	4.60 x 10 ⁻⁵
Ammonium azide NH ₄ N ₃ solid (excluding O ₂) ²²⁵⁸	5.99 x 10 ⁵	0.060	4.46 x 10 ⁻⁵
Ammonium azide NH ₄ N ₃ solid (with LOX)	5.99 x 10 ⁵	0.092	7.26 x 10 ⁻⁵
Tetrazene H ₂ N-NH-N=NH solid (excluding O ₂) ²²⁵⁹	7.85 x 10 ⁵	0.060	4.46 x 10 ⁻⁵
Tetrazene H ₂ N-NH-N=NH solid (with LOX)	7.85 x 10 ⁵	0.092	7.26 x 10 ⁻⁵
Hydronitrogen polymer N ₁₀ H ₁₂ (excluding O ₂) ²²⁶⁰	2.20 x 10 ⁶	0.152	7.6 x 10 ⁻⁵
Hydronitrogen polymer N ₁₀ H ₁₂ (with LOX)	2.20 x 10 ⁶	0.248	1.6 x 10 ⁻⁴
N ₁₈ H ₆ (theoretical) (excluding O ₂) ²²⁶¹	3.525 x 10 ⁶	0.258	1.18 x 10 ⁻⁴

²²⁵⁷ Liquid ammonia (NH₃) has a density of 681.9 kg/m³ with a MW of 0.017 kg/mole; a stoichiometric combustion (NH₃ + 0.75O₂ → 0.5N₂ + 1.5H₂O) using liquid oxygen (LOX: density 1141 kg/m³, MW 0.032 kg/mole) consumes 0.017 kg of NH₃ and 0.024 kg of O₂ and releases 22.5 MJ/kg = 3.83 x 10⁵ J/mole of NH₃ (standard enthalpy of combustion); <https://en.wikipedia.org/wiki/Ammonia> and Zamfirescu C, Dincer I. Using ammonia as a sustainable fuel. J Power Sources 2008;185(1):459-465; <http://www.torium.se/res/Documents/dincer2008.pdf>. “When mixed with oxygen, it burns with a pale yellowish-green flame.”

²²⁵⁸ Solid ammonium azide (NH₄N₃ or N₄H₄, 0.060 kg/mole, 1346 kg/m³, a structural isomer of tetrazene, H₂N-NH-N=NH; https://en.wikipedia.org/wiki/Ammonium_azide) with a stoichiometric combustion (N₄H₄ + O₂ → 2N₂ + 2H₂O) using liquid oxygen (LOX: density 1141 kg/m³, MW 0.032 kg/mole) consumes 0.060 kg of N₄H₄ and 0.032 kg of O₂ and releases 5.99 x 10⁵ J/mole of N₄H₄ taking heats of formation +115.5 kJ/mole for N₄H₄ and -241.8 kJ/mole for H₂O (http://www.update.uu.se/~jolkkonen/pdf/CRC_TD.pdf). However, tetrazene has a higher heat of formation (+301.3 kJ/mole; <https://en.wikipedia.org/wiki/Tetrazene>), yielding a higher combustion energy of 7.85 x 10⁵ J/mole.

²²⁵⁹ Solid ammonium azide (NH₄N₃ or N₄H₄, 0.060 kg/mole, 1346 kg/m³, a structural isomer of tetrazene, H₂N-NH-N=NH; https://en.wikipedia.org/wiki/Ammonium_azide) with a stoichiometric combustion (N₄H₄ + O₂ → 2N₂ + 2H₂O) using liquid oxygen (LOX: density 1141 kg/m³, MW 0.032 kg/mole) consumes 0.060 kg of N₄H₄ and 0.032 kg of O₂ and releases 5.99 x 10⁵ J/mole of N₄H₄ taking heats of formation +115.5 kJ/mole for N₄H₄ and -241.8 kJ/mole for H₂O (http://www.update.uu.se/~jolkkonen/pdf/CRC_TD.pdf). However, tetrazene has a higher heat of formation (+301.3 kJ/mole; <https://en.wikipedia.org/wiki/Tetrazene>), yielding a higher combustion energy of 7.849 x 10⁵ J/mole.

²²⁶⁰ There has been at least one attempt to synthesize hydronitrogen polymer, aka. polyazanes or N_xH_{x+2}, at pressures up to 70 GPa, with inconclusive results, but theoretical calculations suggest that all polyazane variants from x = 2-10 could be stable and that N₁₀H₁₂ (0.152 kg/mole, assumed solid density ~2000 kg/m³) has the highest 0 K heat of formation at +745.6 kJ/mole (Wang H, *et al.* Nitrogen backbone oligomers. Sci Rep 2015;5:13239; <https://www.ncbi.nlm.nih.gov/pmc/articles/PMC4541254/>). The combustion reaction for: N₁₀H₁₂ + 3O₂ → 5N₂ + 6H₂O, using liquid oxygen (LOX: density 1141 kg/m³, MW 0.032 kg/mole) and consuming 0.152 kg of N₁₀H₁₂ and 0.096 kg of O₂, would release 2.20 x 10⁶ J/mole, taking the standard heat of formation of -241.8 kJ/mole for H₂O (http://www.update.uu.se/~jolkkonen/pdf/CRC_TD.pdf).

$N_{18}H_6$ (theoretical) (with LOX)	3.525×10^6	0.306	1.60×10^{-4}
Borazine $B_3N_3H_6$, liquid (excluding O_2) ²²⁶²	2.10×10^6	0.0805	9.94×10^{-5}
Borazine $B_3N_3H_6$, liquid (with LOX)	2.10×10^6	0.2005	2.04×10^{-4}
BN-prismane $B_3N_3H_6$ (theoretical) (excluding O_2) ²²⁶³	2.79×10^6	0.0805	5.37×10^{-5}
BN-prismane $B_3N_3H_6$ (theoretical) (with LOX)	2.79×10^6	0.2005	1.59×10^{-4}
Diborane + Hydrazine (excluding O_2) ²²⁶⁴	2.33×10^6	0.0597	9.33×10^{-5}
Diborane + Hydrazine (with LOX)	2.33×10^6	0.1717	1.91×10^{-4}
Octasilacubane Si_8H_8 (theoretical) (excluding O_2) ²²⁶⁵	8.464×10^6	0.233	1.41×10^{-4}

²²⁶¹ $N_{18}H_6$ (0.258 kg/mole, $1.18 \times 10^{-4} \text{ m}^3/\text{mole}$ at estimated density 2191 kg/m^3), a theoretically-proposed mostly-nitrogen cage molecule, had not been synthesized by 2016 but could be burned in oxygen according to: $N_{18}H_6 + 1.5O_2 \rightarrow 9N_2 + 3H_2O$, using liquid oxygen (LOX: density 1141 kg/m^3 , MW 0.032 kg/mole) and consuming 0.258 kg of $N_{18}H_6$ and 0.048 kg of O_2 to release $3.525 \times 10^6 \text{ J/mole}$, taking the standard heat of formation of -241.8 kJ/mole for H_2O (http://www.update.uu.se/~jolkkonen/pdf/CRC_TD.pdf) and $+2799.6 \text{ kJ/mole}$ for $N_{18}H_6$ (Haskins PJ, Fellows J, Cook MD, Wood A. Molecular studies of poly-nitrogen explosives. QinetiQ Ltd., 2002; <http://www.intdetsymp.org/detsymp2002/PaperSubmit/FinalManuscript/pdf/Haskins-102.PDF>).

²²⁶² Liquid borazine ($B_3N_3H_6$, 0.0805 kg/mole , 810 kg/m^3 , heat of formation -531 kJ/mole ; <https://en.wikipedia.org/wiki/Borazine>) is the BN analog of benzene. A stoichiometric combustion ($B_3N_3H_6 + 3.75O_2 \rightarrow 1.5N_2 + 1.5B_2O_3 + 3H_2O$) using liquid oxygen (LOX: density 1141 kg/m^3 , MW 0.032 kg/mole) consumes 0.0805 kg of $B_3N_3H_6$ and 0.120 kg of O_2 and releases $2.10 \times 10^6 \text{ J/mole}$ of $B_3N_3H_6$ taking heats of formation -1273.5 kJ/mole for B_2O_3 and -241.8 kJ/mole for H_2O (http://www.update.uu.se/~jolkkonen/pdf/CRC_TD.pdf).

²²⁶³ Boron-nitrogen prismane ($B_3N_3H_6$, 0.0805 kg/mole), if it can be synthesized, is predicted to lie $+682 \text{ kJ/mole}$ higher in energy than borazine (Matsunaga N, Gordon MS. Stabilities and energetics of inorganic benzene isomers: prismanes. J Am Chem Soc. 1994;116:11407-11419; http://lib.dr.iastate.edu/cgi/viewcontent.cgi?article=1265&context=chem_pubs), implying a heat of formation of $+151 \text{ kJ/mole}$. The prismane and benzene densities of 1600 kg/m^3 and 877 kg/m^3 suggest a plausible $\sim 1500 \text{ kg/m}^3$ density for BN-prismane, given 810 kg/m^3 for borazine. A stoichiometric combustion ($B_3N_3H_6 + 3.75O_2 \rightarrow 1.5N_2 + 1.5B_2O_3 + 3H_2O$) using liquid oxygen (LOX: density 1141 kg/m^3 , MW 0.032 kg/mole) consumes 0.0805 kg of $B_3N_3H_6$ and 0.120 kg of O_2 and releases $2.79 \times 10^6 \text{ J/mole}$ of $B_3N_3H_6$ taking heats of formation -1273.5 kJ/mole for B_2O_3 and -241.8 kJ/mole for H_2O (http://www.update.uu.se/~jolkkonen/pdf/CRC_TD.pdf).

²²⁶⁴ Liquid diborane (B_2H_6 , 0.0277 kg/mole , 447 kg/m^3) plus liquid hydrazine (N_2H_4 , 0.032 kg/mole , 1021 kg/m^3), in the most energetically favorable combustion ($B_2H_6 + N_2H_4 + 3.5O_2 \rightarrow N_2 + B_2O_3 + 4H_2O$) using liquid oxygen (LOX: density 1141 kg/m^3 , MW 0.032 kg/mole), would consume 0.0277 kg of B_2H_6 , 0.032 kg of N_2H_4 , and 0.112 kg of O_2 and release $2.33 \times 10^6 \text{ J}$, taking heats of formation as $+36.4 \text{ kJ/mole}$ for B_2H_6 , -1273.5 kJ/mole for B_2O_3 and -241.8 kJ/mole for H_2O (http://www.update.uu.se/~jolkkonen/pdf/CRC_TD.pdf) and $+50.63 \text{ kJ/mole}$ for N_2H_2 (<https://en.wikipedia.org/wiki/Hydrazine>).

Octasilacubane Si ₈ H ₈ (theoretical) (with LOX)	8.464 x 10 ⁶	0.553	4.21 x 10 ⁻⁴
Methyl tellurol CH ₃ TeH (excluding O ₂) ²²⁶⁶	n/a	n/a	n/a
<u>Nitrogen Combustibles</u>			
Lithium Li (excluding N ₂) ²²⁶⁷	1.646 x 10 ⁵	0.021	3.93 x 10 ⁻⁵
Lithium Li (with LN ₂)	1.646 x 10 ⁵	0.035	5.66 x 10 ⁻⁵
Beryllium Be (excluding N ₂) ²²⁶⁸	5.67 x 10 ⁵	0.027	1.46 x 10 ⁻⁵
Beryllium Be (with LN ₂)	5.67 x 10 ⁵	0.055	4.93 x 10 ⁻⁵
Magnesium Mg (excluding N ₂) ²²⁶⁹	4.61 x 10 ⁵	0.0729	4.19 x 10 ⁻⁵

²²⁶⁵ Octasilacubane (Si₈H₈, 0.233 kg/mole) had not been synthesized by 2016, although several variants of the molecule with large functional groups have been reported. Clean Si₈H₈ is predicted to exist in stable form with a calculated density of 1652 kg/m³ and heat of formation +211.2 kJ/mole at the B3LYP/CBSB7 level of theory (Nabati M, Mahkam M. Computational study of octasilacubane: structural properties with density functional theory method. Silicon 2016;8:461-465; <http://link.springer.com/article/10.1007/s12633-014-9276-1>). In the most energetically favorable combustion (Si₈H₈ + 10O₂ → 8SiO₂ + 4H₂O) using liquid oxygen (LOX: density 1141 kg/m³, MW 0.032 kg/mole), would consume 0.233 kg of Si₈H₈ and 0.320 kg of O₂ and release 8.464 x 10⁶ J, taking heats of formation as -910.7 kJ/mole for SiO₂ and -241.8 kJ/mole for H₂O (http://www.update.uu.se/~jolkkonen/pdf/CRC_TD.pdf).

²²⁶⁶ Methyl tellurol (CH₃TeH), an analog of methanol where Te replaces O, reportedly “explodes on contact with oxygen and is unstable above 0 °C.” Hamada K, Morishita H. The synthesis and the Raman and infrared spectra of methanetellurol. Synth Reactivity Inorg Metal-Org Chem. 1977;7(4):355-366; <http://www.tandfonline.com/doi/abs/10.1080/00945717708069709>.

²²⁶⁷ Solid lithium (Li) has a density of 534 kg/m³ with MW of 0.007 kg/mole; a stoichiometric combustion (3Li + 0.5N₂ → Li₃N) using liquid nitrogen (LN₂: density 807 kg/m³, MW 0.028 kg/mole) consumes 0.021 kg of Li and 0.014 kg of N₂ and releases 1.646 x 10⁵ J/mole of Li₃N (standard enthalpy of formation); <https://en.wikipedia.org/wiki/Lithium>, https://en.wikipedia.org/wiki/Lithium_nitride, and <http://webbook.nist.gov/cgi/inchi?ID=C26134623&Mask=2>. “Lithium nitride is prepared by direct combination of elemental lithium with nitrogen gas...burning lithium metal in an atmosphere of nitrogen.”

²²⁶⁸ Solid beryllium (Be) has a density of 1850 kg/m³ with MW of 0.009 kg/mole; a stoichiometric combustion (3Be + N₂ → Be₃N₂) using liquid nitrogen (LN₂: density 807 kg/m³, MW 0.028 kg/mole) consumes 0.027 kg of Be and 0.028 kg of N₂ and releases 5.67 x 10⁵ J/mole of Be₃N₂ (standard enthalpy of formation); <https://en.wikipedia.org/wiki/Beryllium> and <https://engineering.purdue.edu/~propulsi/propulsion/comb/propellants.html>. Be₃N₂ “can be prepared from the elements at high temperature (1100-1500 °C) [but] it decomposes in vacuum into beryllium and nitrogen.” https://en.wikipedia.org/wiki/Beryllium_nitride.

²²⁶⁹ Solid magnesium (Mg) has a density of 1738 kg/m³ with MW of 0.0243 kg/mole; a stoichiometric combustion (3Mg + N₂ → Mg₃N₂) using liquid nitrogen (LN₂: density 807 kg/m³, MW 0.028 kg/mole) consumes 0.0729 kg of Mg and 0.028 kg of N₂ and releases 4.61 x 10⁵ J/mole of Mg₃N₂ (standard enthalpy of formation); <https://en.wikipedia.org/wiki/Magnesium>, https://en.wikipedia.org/wiki/Magnesium_nitride, and “Selected values of chemical thermodynamic properties,” Natl. Bur Stand. (U.S.) 1952; Circ. 500. p. 374.

Magnesium Mg (with LN ₂)	4.61 x 10 ⁵	0.1009	7.66 x 10 ⁻⁵
Cerium Ce (excluding N ₂) ²²⁷⁰	3.27 x 10 ⁵	0.140	2.07 x 10 ⁻⁵
Cerium Ce (with LN ₂)	3.27 x 10 ⁵	0.154	3.80 x 10 ⁻⁵
Titanium Ti (excluding N ₂) ²²⁷¹	3.38 x 10 ⁵	0.0479	1.06 x 10 ⁻⁵
Titanium Ti (with LN ₂)	3.38 x 10 ⁵	0.0619	2.80 x 10 ⁻⁵
Zirconium Zr (excluding N ₂) ²²⁷²	3.65 x 10 ⁵	0.0912	1.40 x 10 ⁻⁵
Zirconium Zr (with LN ₂)	3.65 x 10 ⁵	0.1052	3.13 x 10 ⁻⁵
Boron B (excluding N ₂) ²²⁷³	2.52 x 10 ⁵	0.0108	4.62 x 10 ⁻⁶
Boron B (with LN ₂)	2.52 x 10 ⁵	0.0248	2.20 x 10 ⁻⁵
Aluminum Al (excluding N ₂) ²²⁷⁴	3.18 x 10 ⁵	0.027	1.00 x 10 ⁻⁵

²²⁷⁰ Solid cerium (Ce) has a density of 6770 kg/m³ with MW of 0.140 kg/mole; a stoichiometric combustion ($\text{Ce} + 0.5\text{N}_2 \rightarrow \text{CeN}$) using liquid nitrogen (LN₂: density 807 kg/m³, MW 0.028 kg/mole) consumes 0.140 kg of Ce and 0.014 kg of N₂ and releases 3.27 x 10⁵ J/mole of CeN (standard enthalpy of formation); <https://en.wikipedia.org/wiki/Cerium>, <https://engineering.purdue.edu/~propulsi/propulsion/comb/propellants.html>, and Muthmann W, Kraft K. Cerium and Lanthanum. *Annalen* 1902;325:261-278: “Cerium burns in nitrogen with a brilliant, white light.”

²²⁷¹ Solid titanium (Ti) has a density of 4506 kg/m³ with MW of 0.0479 kg/mole; a stoichiometric combustion ($\text{Ti} + 0.5\text{N}_2 \rightarrow \text{TiN}$) using liquid nitrogen (LN₂: density 807 kg/m³, MW 0.028 kg/mole) consumes 0.0479 kg of Ti and 0.014 kg of N₂ and releases 3.38 x 10⁵ J/mole of TiN (standard enthalpy of formation); <https://en.wikipedia.org/wiki/Titanium> and <http://webbook.nist.gov/cgi/inchi?ID=C25583204&Mask=2>. “Titanium is one of the few elements that burns in pure nitrogen gas, reacting at 800 °C (1,470 °F) to form titanium nitride.”

²²⁷² Solid zirconium (Zr) has a density of 6520 kg/m³ with MW of 0.0912 kg/mole; a stoichiometric combustion ($\text{Zr} + 0.5\text{N}_2 \rightarrow \text{ZrN}$) using liquid nitrogen (LN₂: density 807 kg/m³, MW 0.028 kg/mole) consumes 0.0912 kg of Zr and 0.014 kg of N₂ and releases 3.65 x 10⁵ J/mole of ZrN (standard enthalpy of formation); <https://en.wikipedia.org/wiki/Zirconium> and https://en.wikipedia.org/wiki/Zirconium_nitride. “Zirconium dust will ignite in nitrogen at approximately 788 °C.” Primer on Spontaneous Heating and Pyrophoricity, DOE-HDBK-1081-94, FSC-6910, Dec 1994; <http://web.archive.org/web/20100527183802/http://www.hss.energy.gov/nuclearsafety/ns/techstds/standard/hdbk1081/hdbk1081.pdf>.

²²⁷³ Solid boron (B) has a density of 2340 kg/m³ with MW of 0.0108 kg/mole; a stoichiometric combustion ($\text{B} + 0.5\text{N}_2 \rightarrow \text{BN}$) using liquid nitrogen (LN₂: density 807 kg/m³, MW 0.028 kg/mole) consumes 0.0108 kg of B and 0.014 kg of N₂ and releases 2.52 x 10⁵ J/mole of BN (standard enthalpy of formation); <http://www.rsc.org/periodic-table/element/5/boron> and <https://engineering.purdue.edu/~propulsi/propulsion/comb/propellants.html>. “Combustion of boron powder in nitrogen plasma at 5500 °C yields ultrafine boron nitride.” https://en.wikipedia.org/wiki/Boron_nitride.

²²⁷⁴ Solid aluminum (Al) has a density of 2700 kg/m³ with MW of 0.027 kg/mole; a stoichiometric combustion ($\text{Al} + 0.5\text{N}_2 \rightarrow \text{AlN}$) using liquid nitrogen (LN₂: density 807 kg/m³, MW 0.028 kg/mole) consumes 0.027 kg of Al and 0.014 kg of N₂ and releases 3.18 x 10⁵ J/mole of AlN (standard enthalpy of formation); <https://en.wikipedia.org/wiki/Aluminium>, https://en.wikipedia.org/wiki/Aluminium_nitride, and http://www.update.uu.se/~jolkkonen/pdf/CRC_TD.pdf.

Aluminum Al (with LN ₂)	3.18 x 10 ⁵	0.041	2.73 x 10 ⁻⁵
Silicon Si (excluding N ₂) ²²⁷⁵	7.435 x 10 ⁵	0.084	3.61 x 10 ⁻⁵
Silicon Si (with LN ₂)	7.435 x 10 ⁵	0.140	1.05 x 10 ⁻⁴
Phosphorus P (excluding N ₂) ²²⁷⁶	3.230 x 10 ⁵	0.093	3.46 x 10 ⁻⁵
Phosphorus P (with LN ₂)	3.230 x 10 ⁵	0.163	1.21 x 10 ⁻⁴
<u>Carbon Dioxide Combustibles</u>			
Magnesium Mg (excluding CO ₂) ²²⁷⁷	4.05 x 10 ⁵	0.0243	1.40 x 10 ⁻⁵
Magnesium Mg (with CO ₂ (s))	4.05 x 10 ⁵	0.0463	2.81 x 10 ⁻⁵
Titanium Ti (excluding CO ₂) ²²⁷⁸	5.52 x 10 ⁵	0.0479	1.06 x 10 ⁻⁵

²²⁷⁵ Solid silicon (Si) has a density of 2329 kg/m³ with MW of 0.028 kg/mole; a stoichiometric combustion (3Si + 2N₂ → Si₃N₄) using liquid nitrogen (LN₂: density 807 kg/m³, MW 0.028 kg/mole) consumes 0.084 kg of Si and 0.056 kg of N₂ and releases 7.435 x 10⁵ J/mole of Si₃N₄ (standard enthalpy of formation); <https://en.wikipedia.org/wiki/Silicon>, https://en.wikipedia.org/wiki/Silicon_nitride, and http://www.update.uu.se/~jolkkonen/pdf/CRC_TD.pdf.

²²⁷⁶ Solid black phosphorus (P) has a density of 2690 kg/m³ and MW of 0.031 kg/mole; a stoichiometric combustion (3P + 2.5N₂ → P₃N₅) using liquid nitrogen (LN₂: density 807 kg/m³, MW 0.028 kg/mole) consumes 0.093 kg of P and 0.070 kg of N₂ and releases 3.20 x 10⁵ J/mole of P₃N₅ (standard enthalpy of formation); <https://en.wikipedia.org/wiki/Phosphorus>, https://en.wikipedia.org/wiki/Triphosphorus_pentanitride, and <http://webbook.nist.gov/cgi/cbook.cgi?ID=C12136913&Mask=2>. “Triphosphorus pentanitride can be produced by...a reaction between the elements.” Vepřek S, Iqbal Z, Brunner J, Schärli M. Preparation and properties of amorphous phosphorus nitride prepared in a low-pressure plasma. *Phil Mag B* 1981 Mar 1;43(3):527–547; <http://www.tandfonline.com/doi/abs/10.1080/01418638108222114>.

²²⁷⁷ Solid magnesium (Mg) has a density of 1738 kg/m³ with MW of 0.0243 kg/mole; a stoichiometric combustion (Mg + 0.5CO₂ → MgO + 0.5C) using solid carbon dioxide (CO₂(s): density 1562 kg/m³, MW 0.044 kg/mole) consumes 0.0243 kg of Mg and 0.022 kg of CO₂ and releases 4.05 x 10⁵ J/mole of Mg (taking heats of formation of -393.5 kJ/mole for CO₂ and -601.6 kJ/mole for MgO); <https://en.wikipedia.org/wiki/Magnesium>, https://en.wikipedia.org/wiki/Carbon_dioxide, and http://www.update.uu.se/~jolkkonen/pdf/CRC_TD.pdf. “Magnesium burns in dry ice.” <https://practicum.melscience.com/experiments/magnesium-burning-in-dry-ice.html>.

²²⁷⁸ Solid titanium (Ti) has a density of 4506 kg/m³ with MW of 0.0479 kg/mole; a stoichiometric combustion (Ti + CO₂ → TiO₂ + C) using solid carbon dioxide (CO₂(s): density 1562 kg/m³, MW 0.044 kg/mole) consumes 0.0479 kg of Ti and 0.044 kg of CO₂ and releases 5.52 x 10⁵ J/mole of Ti (taking heats of formation of -393.5 kJ/mole for CO₂ and -601.6 kJ/mole for TiO₂); <https://en.wikipedia.org/wiki/Titanium>, https://en.wikipedia.org/wiki/Titanium_dioxide, and https://en.wikipedia.org/wiki/Carbon_dioxide. “[Powdered] titanium burns in carbon dioxide, when pure or diluted by nitrogen. If there is titanium dust in suspension in carbon dioxide, the mixture detonates when it is exposed to a flame or heat.” Bernard Martel, *Chemical Risk Analysis: A Practical Handbook*, Butterworth-Heinemann, 2004, p. 198. “Titanium burns in carbon dioxide above 550 °C.” Safety Data Sheet, https://www.3dsystems.com/sites/www.3dsystems.com/files/151806-7-s12-00-a_sds_ghs_english_laserform_ti_gr_5-23_type_a.pdf.

Titanium Ti (with CO ₂ (s))	5.52 x 10 ⁵	0.0919	3.88 x 10 ⁻⁵
Aluminum Al (excluding CO ₂) ²²⁷⁹	5.43 x 10 ⁵	0.027	1.00 x 10 ⁻⁵
Aluminum Al (with CO ₂ (s))	5.43 x 10 ⁵	0.060	3.11 x 10 ⁻⁵
<u>Water Combustibles</u>			
Lithium Li (excluding H ₂ O) ²²⁸⁰	2.46 x 10 ⁵	0.00694	1.30 x 10 ⁻⁵
Lithium Li (with H ₂ O)	2.46 x 10 ⁵	0.0250	3.10 x 10 ⁻⁵
Cesium Cs (excluding H ₂ O) ²²⁸¹	1.75 x 10 ⁵	0.133	6.89 x 10 ⁻⁵
Cesium Cs (with H ₂ O)	1.75 x 10 ⁵	0.151	8.69 x 10 ⁻⁵
Aluminum Al (excluding H ₂ O) ²²⁸²	4.75 x 10 ⁵	0.027	1.00 x 10 ⁻⁵
Aluminum Al (with H ₂ O)	4.75 x 10 ⁵	0.054	3.70 x 10 ⁻⁵
Magnesium Mg (excluding H ₂ O) ²²⁸³	3.60 x 10 ⁵	0.0243	1.40 x 10 ⁻⁵

²²⁷⁹ Solid aluminum (Al) has a density of 2700 kg/m³ with MW of 0.027 kg/mole; a stoichiometric combustion ($\text{Al} + 0.75\text{CO}_2 \rightarrow 0.5\text{Al}_2\text{O}_3 + 0.75\text{C}$) using solid carbon dioxide (CO₂(s); density 1562 kg/m³, MW 0.044 kg/mole) consumes 0.027 kg of Al and 0.033 kg of CO₂ and releases 5.43 x 10⁵ J/mole of Al (taking heats of formation of -393.5 kJ/mole for CO₂ and -1675.7 kJ/mole for Al₂O₃); <https://en.wikipedia.org/wiki/Aluminium>, https://en.wikipedia.org/wiki/Carbon_dioxide, and http://www.update.uu.se/~jolkkonen/pdf/CRC_TD.pdf. “Aluminum powder burns when heated in carbon dioxide.” <https://toxnet.nlm.nih.gov/cgi-bin/sis/search/a?dbs+hsdb:@term+@DOCNO+516>.

²²⁸⁰ Solid lithium (Li) has a density of 534 kg/m³ with MW of 0.00694 kg/mole; a stoichiometric combustion ($\text{Li} + \text{H}_2\text{O} \rightarrow \text{LiOH} + 0.5\text{H}_2$) using liquid water (H₂O(liq); density 1000 kg/m³, MW 0.018 kg/mole) consumes 0.00694 kg of Li and 0.018 kg of H₂O and releases 2.46 x 10⁵ J/mole of Li (taking heats of formation of -241.8 kJ/mole for H₂O and -487.6 kJ/mole for LiOH) (http://www.update.uu.se/~jolkkonen/pdf/CRC_TD.pdf).

²²⁸¹ Solid cesium (Cs) has a density of 1930 kg/m³ with MW of 0.1329 kg/mole; a stoichiometric combustion ($\text{Cs} + \text{H}_2\text{O} \rightarrow \text{CsOH} + 0.5\text{H}_2$) using liquid water (H₂O(liq); density 1000 kg/m³, MW 0.018 kg/mole) consumes 0.1329 kg of Cs and 0.018 kg of H₂O and releases 1.75 x 10⁵ J/mole of Cs (taking heats of formation of -241.8 kJ/mole for H₂O and -417.2 kJ/mole for CsOH) (http://www.update.uu.se/~jolkkonen/pdf/CRC_TD.pdf).

²²⁸² Solid aluminum (Al) has a density of 2700 kg/m³ with MW of 0.027 kg/mole; a stoichiometric combustion ($\text{Al} + 1.5\text{H}_2\text{O} \rightarrow 0.5\text{Al}_2\text{O}_3 + 1.5\text{H}_2$) using liquid water (H₂O(liq); density 1000 kg/m³, MW 0.018 kg/mole) consumes 0.027 kg of Al and 0.027 kg of H₂O and releases 4.75 x 10⁵ J/mole of Al (taking heats of formation of -241.8 kJ/mole for H₂O and -1675.7 kJ/mole for Al₂O₃) (http://www.update.uu.se/~jolkkonen/pdf/CRC_TD.pdf).

²²⁸³ Solid magnesium (Mg) has a density of 1738 kg/m³ with MW of 0.0243 kg/mole; a stoichiometric combustion ($\text{Mg} + \text{H}_2\text{O} \rightarrow \text{MgO} + \text{H}_2$) using liquid water (H₂O(liq); density 1000 kg/m³, MW 0.018 kg/mole) consumes 0.0243 kg of Mg and 0.018 kg of H₂O and releases 3.60 x 10⁵ J/mole of Mg (taking heats of formation of -241.8 kJ/mole for H₂O and -601.6 kJ/mole for MgO); <https://en.wikipedia.org/wiki/Magnesium>, https://en.wikipedia.org/wiki/Carbon_dioxide, and http://www.update.uu.se/~jolkkonen/pdf/CRC_TD.pdf.

Magnesium Mg (with H ₂ O)	3.60 x 10 ⁵	0.0423	3.20 x 10 ⁻⁵
Chlorine trifluoride ClF ₃ (excluding H ₂ O) ²²⁸⁴	2.654 x 10 ⁵	0.0925	5.22 x 10 ⁻⁵
Chlorine trifluoride ClF ₃ (with H ₂ O)	2.654 x 10 ⁵	0.1285	8.22 x 10 ⁻⁵
<u>Nonambient Combustibles: Halogen Oxidants</u>			
Aluminum + Chlorine trifluoride (ClF ₃) ²²⁸⁵	1.625 x 10 ⁶	0.12845	6.25 x 10 ⁻⁵
Aluminum + Dibromine pentoxide (Br ₂ O ₅) ²²⁸⁶	1.95 x 10 ⁶	0.198	5.95 x 10 ⁻⁵
Aluminum + Dichlorine heptoxide (Cl ₂ O ₇) ²²⁸⁷	1.79 x 10 ⁶	0.132	6.13 x 10 ⁻⁵

²²⁸⁴ Liquid chlorine trifluoride (ClF₃) has a density of 1770 kg/m³ with MW of 0.09245 kg/mole; a stoichiometric combustion (ClF₃ + 2H₂O → 3HF + HCl + O₂) using liquid water (H₂O(liq): density 1000 kg/m³, MW 0.018 kg/mole) consumes 0.09245 kg of ClF₃ and 0.036 kg of H₂O and releases 2.654 x 10⁵ J/mole of ClF₃ (taking heats of formation of -241.8 kJ/mole for H₂O and -163.2 kJ/mole for ClF₃); http://www.update.uu.se/~jolkkonen/pdf/CRC_TD.pdf.

²²⁸⁵ Assuming a density of 2700 kg/m³ with a MW of 0.0270 kg/mole for aluminum (Al) (<https://en.wikipedia.org/wiki/Aluminium>) and a density of 1880 kg/m³ with a MW of 0.09245 kg/mole for liquid ClF₃ (<http://pubs.rsc.org/en/Content/ArticleLanding/1950/JR/jr9500000191>), a stoichiometric combustion (4/3Al + ClF₃ → 1/3AlCl₃ + AlF₃) consumes 0.036 kg of Al and 0.09245 kg of ClF₃ and releases (1/3) 5.832 x 10⁵ J/mole of AlCl₃(g) plus 1.205 x 10⁶ J/mole of AlF₃(g) less 1.632 x 10⁵ J/mole for ClF₃ (standard heats of formation); http://www.update.uu.se/~jolkkonen/pdf/CRC_TD.pdf. “Chlorine trifluoride has been investigated as a high-performance storable oxidizer in rocket propellant systems. Handling concerns, however, prevented its use. John Drury Clark summarized the difficulties: ‘It is, of course, extremely toxic, but that’s the least of the problem. It is hypergolic with every known fuel, and so rapidly hypergolic that no ignition delay has ever been measured. It is also hypergolic with such things as cloth, wood, and test engineers, not to mention asbestos, sand, and water – with which it reacts explosively. It can be kept in some of the ordinary structural metals – steel, copper, aluminum, etc. – because of the formation of a thin film of insoluble metal fluoride which protects the bulk of the metal, just as the invisible coat of oxide on aluminum keeps it from burning up in the atmosphere. If, however, this coat is melted or scrubbed off, and has no chance to reform, the operator is confronted with the problem of coping with a metal-fluorine fire. For dealing with this situation, I have always recommended a good pair of running shoes.’” https://en.wikipedia.org/wiki/Chlorine_trifluoride.

²²⁸⁶ Dibromine pentoxide (Br₂O₅, 0.240 kg/mole; https://en.wikipedia.org/wiki/Dibromine_pentoxide), with a density assumed to lie midway between the densities of Cl₂O₇ and I₂O₆ (see below), at 3650 kg/m³. Br₂O₅ is a colorless solid, stable below -20 °C. Assuming a density of 2700 kg/m³ with a MW of 0.0270 kg/mole for aluminum (Al) (<https://en.wikipedia.org/wiki/Aluminium>), a stoichiometric combustion (2Al + 3/5 Br₂O₅ → Al₂O₃ + 3/5 Br₂) consumes 0.054 kg of Al and 0.144 kg of Br₂O₅ and releases 1.95 x 10⁶ J, taking the estimated heat of formation as +449.8 kJ/mole for Br₂O₅ (Li Z, Francisco JS. A density functional study of structure and heat of formation for Br₂O₄ and Br₂O₅. Chem Phys Lett. 2002 Mar 5;354(1-2):109-119; <http://www.sciencedirect.com/science/article/pii/S0009261402001173>).

Aluminum + Diiodine hexoxide (I ₂ O ₆) ²²⁸⁸	1.63 x 10 ⁶	0.229	5.24 x 10 ⁻⁵
Aluminum + Dioxygen difluoride (O ₂ F ₂) ²²⁸⁹	1.70 x 10 ⁶	0.159	9.24 x 10 ⁻⁵
Aluminum + Fluorine ²²⁹⁰	1.205 x 10 ⁶	0.084	3.89 x 10 ⁻⁵
Aluminum + Fluorine perchlorate (FClO ₄) ²²⁹¹	3.01 x 10 ⁶	0.2084	1.18 x 10 ⁻⁴
Aluminum + Oxygen difluoride (OF ₂) ²²⁹²	1.75 x 10 ⁶	0.216	1.05 x 10 ⁻⁴
Aluminum + Tetrafluorohydrazine (N ₂ F ₄) ²²⁹³	2.01 x 10 ⁶	0.140	7.83 x 10 ⁻⁵

²²⁸⁷ Dichlorine heptoxide (Cl₂O₇, 0.1829 kg/mole, 1900 kg/m³ liquid density; https://en.wikipedia.org/wiki/Dichlorine_heptoxide) is the most stable chlorine oxide but also a strong oxidizer and explosive that can be set off with flame, mechanical shock, or by contact with iodine. Assuming a density of 2700 kg/m³ with a MW of 0.0270 kg/mole for aluminum (Al) (<https://en.wikipedia.org/wiki/Aluminium>), a stoichiometric combustion (2Al + 3/7 Cl₂O₇ → Al₂O₃ + 3/7 Cl₂) consumes 0.054 kg of Al and 0.0784 kg of Cl₂O₇ and releases 1.79 x 10⁶ J, taking the heat of formation as +272 kJ/mole for Cl₂O₇ (Wiberg E, Wiberg N. Inorganic Chemistry, Academic Press, 2001, p. 464; <https://books.google.com/books?id=Mtth5g59dEIC&pg=PA464>).

²²⁸⁸ Diiodine hexoxide (I₂O₆, 0.350 kg/mole, 5400 kg/m³, HOF = -90.2 kJ/mole; <http://www.dtic.mil/cgi-bin/GetTRDoc?AD=ADA584359>) is stable up to 187 °C and is one of several “novel halogen oxidizers for formulation with high-performance explosives (HMX or RDX) to produce over-oxidized explosives for destruction of chemical and biological agents.” Assuming a density of 2700 kg/m³ with a MW of 0.0270 kg/mole for aluminum (Al) (<https://en.wikipedia.org/wiki/Aluminium>), a stoichiometric combustion (2Al + 0.5I₂O₆ → Al₂O₃ + 0.5I₂) consumes 0.054 kg of Al and 0.175 kg of I₂O₆ and releases 1.63 x 10⁶ J.

²²⁸⁹ Dioxygen difluoride (O₂F₂, aka. FOOF, 0.070 kg/mole, 1450 kg/m³ liquid density at 216 K, HOF = +18.0 kJ/mole; http://www.update.uu.se/~jolkkonen/pdf/CRC_TD.pdf) is strong oxidizer but readily decomposes into oxygen and fluorine (https://en.wikipedia.org/wiki/Dioxygen_difluoride). Assuming a density of 2700 kg/m³ with a MW of 0.0270 kg/mole for aluminum (Al) (<https://en.wikipedia.org/wiki/Aluminium>), a stoichiometric combustion (2Al + 1.5O₂F₂ → Al₂O₃ + 1.5F₂) consumes 0.054 kg of Al and 0.105 kg of O₂F₂ and releases 1.70 x 10⁶ J.

²²⁹⁰ Assuming a density of 2700 kg/m³ with a MW of 0.0270 kg/mole for aluminum (Al) (<https://en.wikipedia.org/wiki/Aluminium>) and a density of 1970 kg/m³ with a MW of 0.038 kg/mole for solid α-F₂ (https://en.wikipedia.org/wiki/Phases_of_fluorine), a stoichiometric combustion (Al + 1.5F₂ → AlF₃) consumes 0.0270 kg of Al and 0.057 kg of F₂ and releases 1.205 x 10⁶ J/mole of AlF₃(g) (standard heat of formation); http://www.update.uu.se/~jolkkonen/pdf/CRC_TD.pdf.

²²⁹¹ Assuming a density of 2700 kg/m³ with a MW of 0.0270 kg/mole for aluminum (Al) (<https://en.wikipedia.org/wiki/Aluminium>) and a density of ~1400 kg/m³ with a MW of 0.1184 kg/mole for fluorine perchlorate (FClO₄), a stoichiometric combustion (10/3 Al + FClO₄ → 1/3 AlF₃ + 1/3 AlCl₃ + 4/3 Al₂O₃) consumes 0.090 kg of Al and 0.1184 kg of FClO₄ and releases 3.01 x 10⁶ J/mole of FClO₄ (standard heat of formation).

²²⁹² Oxygen difluoride (OF₂, 0.054 kg/mole, 1900 kg/m³ liquid density at 49 K, HOF = +24.7 kJ/mole; http://www.update.uu.se/~jolkkonen/pdf/CRC_TD.pdf) is strong oxidizer (https://en.wikipedia.org/wiki/Oxygen_difluoride). Assuming a density of 2700 kg/m³ with a MW of 0.0270 kg/mole for aluminum (Al) (<https://en.wikipedia.org/wiki/Aluminium>), a stoichiometric combustion (2Al + 3OF₂ → Al₂O₃ + 3F₂) consumes 0.054 kg of Al and 0.162 kg of OF₂ and releases 1.75 x 10⁶ J/mole.

Beryllium + Chlorine trifluoride (ClF ₃) ²²⁹⁴	8.56 x 10 ⁵	0.1105	5.89 x 10 ⁻⁵
Beryllium + Chlorine pentafluoride (ClF ₅) ²²⁹⁵	1.29 x 10 ⁶	0.157	8.30 x 10 ⁻⁵
Beryllium + Dioxygen difluoride (O ₂ F ₂) ²²⁹⁶	1.75 x 10 ⁶	0.097	6.29 x 10 ⁻⁵
Beryllium + Fluorine ²²⁹⁷	1.01 x 10 ⁶	0.047	2.42 x 10 ⁻⁵
Beryllium + Fluorine perchlorate (FClO ₄) ²²⁹⁸	3.23 x 10 ⁶	0.1634	1.09 x 10 ⁻⁴
Beryllium + Nitrosyl tetrafluorochlorate (NOClF ₄) ²²⁹⁹	1.59 x 10 ⁶	0.173	9.23 x 10 ⁻⁵

²²⁹³ Assuming a density of 2700 kg/m³ with a MW of 0.0270 kg/mole for aluminum (Al) (<https://en.wikipedia.org/wiki/Aluminium>) and a density of 1600 kg/m³ with a MW of 0.104 kg/mole for liquid tetrafluorohydrazine (N₂F₄; <https://en.wikipedia.org/wiki/Tetrafluorohydrazine>, <http://www.chemspider.com/Chemical-Structure.23228.html>), a stoichiometric combustion (4/3 Al + N₂F₄ → 4/3 AlF₃ + N₂) consumes 0.036 kg of Al and 0.104 kg of N₂F₄ and releases 2.01 x 10⁶ J/mole of N₂F₄ (standard heat of formation); http://www.update.uu.se/~jolkkonen/pdf/CRC_TD.pdf.

²²⁹⁴ Assuming a density of 1850 kg/m³ with a MW of 0.009 kg/mole for beryllium (Be) (<https://en.wikipedia.org/wiki/Beryllium>) and a density of 1880 kg/m³ with a MW of 0.09245 kg/mole for liquid ClF₃ (<http://pubs.rsc.org/en/Content/ArticleLanding/1950/JR/jr950000191>), a stoichiometric combustion (2Be + ClF₃ → 1.5BeF₂ + 0.5BeCl₂) consumes 0.018 kg of Be and 0.09245 kg of ClF₃ and releases 8.56 x 10⁵ J/mole for ClF₃ (standard heats of formation; https://en.wikipedia.org/wiki/Chlorine_trifluoride and http://www.update.uu.se/~jolkkonen/pdf/CRC_TD.pdf).

²²⁹⁵ Assuming a density of 1850 kg/m³ with a MW of 0.009 kg/mole for beryllium (Be) (<https://en.wikipedia.org/wiki/Beryllium>) and a density of 1900 kg/m³ with a MW of 0.130445 kg/mole for liquid ClF₅ (<http://encyclopedia.airliquide.com/Encyclopedia.asp?GasID=128>), a stoichiometric combustion (3Be + ClF₅ → 2.5BeF₂ + 0.5BeCl₂) consumes 0.027 kg of Be and 0.130 kg of ClF₅ and releases 1.29 x 10⁶ J/mole for ClF₅ (standard heats of formation; https://en.wikipedia.org/wiki/Chlorine_pentafluoride and http://www.update.uu.se/~jolkkonen/pdf/CRC_TD.pdf).

²²⁹⁶ Dioxygen difluoride (O₂F₂, aka. FOOF, 0.070 kg/mole, 1450 kg/m³ liquid density at 216 K) is strong oxidizer but readily decomposes into oxygen and fluorine (https://en.wikipedia.org/wiki/Dioxygen_difluoride). Assuming a density of 1850 kg/m³ with a MW of 0.009 kg/mole for beryllium (Be) (<https://en.wikipedia.org/wiki/Beryllium>), a stoichiometric combustion (3Be + O₂F₂ → BeF₂ + 2BeO) consumes 0.027 kg of Be and 0.070 kg of O₂F₂ and releases 1.75 x 10⁶ J/mole of O₂F₂ (standard heat of formation).

²²⁹⁷ Assuming a density of 1850 kg/m³ with a MW of 0.009 kg/mole for beryllium (Be) (<https://en.wikipedia.org/wiki/Beryllium>) and a density of 1970 kg/m³ with a MW of 0.038 kg/mole for solid α-F₂ (https://en.wikipedia.org/wiki/Phases_of_fluorine), a stoichiometric combustion (Be + F₂ → BeF₂) consumes 0.009 kg of Be and 0.038 kg of F₂ and releases 1.01 x 10⁶ J/mole of BeF₂ (standard heat of formation); https://en.wikipedia.org/wiki/Beryllium_fluoride.

²²⁹⁸ Fluorine perchlorate (FClO₄, 0.1184 kg/mole, ~1400 kg/m³ liquid density assumed same as FClO₃) is an unstable gas that explodes spontaneously (https://en.wikipedia.org/wiki/Fluorine_perchlorate). Assuming a density of 1850 kg/m³ with a MW of 0.009 kg/mole for beryllium (Be) (<https://en.wikipedia.org/wiki/Beryllium>), a stoichiometric combustion (5Be + FClO₄ → 0.5BeF₂ + 0.5BeCl₂ + 4BeO) consumes 0.045 kg of Be and 0.1184 kg of FClO₄ and releases 3.23 x 10⁶ J/mole of FClO₄ (standard heat of formation).

Beryllium + Oxygen difluoride (OF ₂) ²³⁰⁰	1.15 x 10 ⁶	0.072	3.82 x 10 ⁻⁵
Beryllium + Perchloryl fluoride (FCIO ₃) ²³⁰¹	2.56 x 10 ⁶	0.1384	9.09 x 10 ⁻⁵
Beryllium + Tetrafluorohydrazine (N ₂ F ₄) ²³⁰²	2.05 x 10 ⁶	0.122	7.47 x 10 ⁻⁵
Boron + Fluorine ²³⁰³	1.137 x 10 ⁶	0.0678	3.35 x 10 ⁻⁵
Boron + Chlorine ²³⁰⁴	4.27 x 10 ⁵	0.1172	7.27 x 10 ⁻⁵
Boron + Fluorine perchlorate (FCIO ₄) ²³⁰⁵	2.25 x 10 ⁶	0.1544	1.02 x 10 ⁻⁴

²²⁹⁹ Nitrosyl tetrafluorochlorate (NOClF₄, 0.1415 kg/mole, ~1880 kg/m³ liquid density assumed same as ClF₃) is an unstable strong oxidizer with a heat of formation of -287 kJ/mole; Whitney ED, *et al.* Preparation of nitrosyl tetrafluorochlorate. J Am Chem Soc. 1964 Oct;86(20):4340-4342; <http://pubs.acs.org/doi/abs/10.1021/ja01074a021>). Assuming a density of 1850 kg/m³ with a MW of 0.009 kg/mole for beryllium (Be) (<https://en.wikipedia.org/wiki/Beryllium>), a stoichiometric combustion (3.5Be + NOClF₄ → 2BeF₂ + 0.5BeCl₂ + BeO + 0.5N₂) consumes 0.0315 kg of Be and 0.1415 kg of NOClF₄ and releases 1.59 x 10⁶ J/mole of NOClF₄ (standard heat of formation).

²³⁰⁰ Oxygen difluoride (OF₂, 0.054 kg/mole, 1900 kg/m³ liquid density at 49 K) is strong oxidizer (https://en.wikipedia.org/wiki/Oxygen_difluoride). Assuming a density of 1850 kg/m³ with a MW of 0.009 kg/mole for beryllium (Be) (<https://en.wikipedia.org/wiki/Beryllium>), a stoichiometric combustion (2Be + OF₂ → BeF₂ + 4BeO) consumes 0.018 kg of Be and 0.054 kg of OF₂ and releases 1.15 x 10⁶ J/mole of OF₂ (standard heat of formation).

²³⁰¹ Perchloryl fluoride (FCIO₃, 0.1024 kg/mole, 1434 kg/m³ liquid density) is a reactive but stable gas (https://en.wikipedia.org/wiki/Perchloryl_fluoride). Assuming a density of 1850 kg/m³ with a MW of 0.009 kg/mole for beryllium (Be) (<https://en.wikipedia.org/wiki/Beryllium>), a stoichiometric combustion (4Be + FCIO₃ → 0.5BeF₂ + 0.5BeCl₂ + 3BeO) consumes 0.036 kg of Be and 0.1024 kg of FCIO₃ and releases 2.56 x 10⁶ J/mole of FCIO₃ (standard heat of formation).

²³⁰² Assuming a density of 1850 kg/m³ with a MW of 0.009 kg/mole for beryllium (Be) (<https://en.wikipedia.org/wiki/Beryllium>) and a density of 1600 kg/m³ with a MW of 0.104 kg/mole for liquid tetrafluorohydrazine (N₂F₄; <https://en.wikipedia.org/wiki/Tetrafluorohydrazine>, <http://www.chemspider.com/Chemical-Structure.23228.html>), a stoichiometric combustion (2Be + N₂F₄ → 2BeF₂ + N₂) consumes 0.018 kg of Be and 0.104 kg of N₂F₄ and releases 2.05 x 10⁶ J/mole of N₂F₄ (standard heat of formation); http://www.update.uu.se/~jolkkonen/pdf/CRC_TD.pdf.

²³⁰³ Assuming a density of 2340 kg/m³ with a MW of 0.0108 kg/mole for boron (B) (<http://www.rsc.org/periodic-table/element/5/boron>) and a density of 1970 kg/m³ with a MW of 0.038 kg/mole for solid α-F₂ (https://en.wikipedia.org/wiki/Phases_of_fluorine), a stoichiometric combustion (B + 1.5F₂ → BF₃) consumes 0.0108 kg of B and 0.057 kg of F₂ and releases 1.137 x 10⁶ J/mole of BF₃(g) (standard heat of formation); https://en.wikipedia.org/wiki/Boron_trifluoride. "Fluorine attacks boron at ordinary temperatures, the resulting mass becoming incandescent." Fire Protection Guide to Hazardous Materials, 13th Ed., Quincy MA, National Fire Protection Association, 2002, p.491-31; <https://pubchem.ncbi.nlm.nih.gov/compound/boron#section=Other-Occupational-Permissible-Levels>.

²³⁰⁴ Assuming a density of 2340 kg/m³ with a MW of 0.0108 kg/mole for boron (B) (<http://www.rsc.org/periodic-table/element/5/boron>) and a density of 1563 kg/m³ with a MW of 0.0709 kg/mole for liquid Cl₂ (<https://en.wikipedia.org/wiki/Chlorine>), a stoichiometric combustion (B + 1.5Cl₂ → BCl₃) consumes 0.0108 kg of B and 0.1064 kg of Cl₂ and releases 4.27 x 10⁵ J/mole of BCl₃ (standard heat of formation); https://en.wikipedia.org/wiki/Boron_trichloride. "Boron ignites in chlorine at 410 °C"; <http://webwiser.nlm.nih.gov/WebWISER/pda/getSubstanceData.do?substanceId=338&menuItemID=7&identifier=Chlorine&identifierType=Name>.

Carbon + Fluorine ²³⁰⁶	9.336×10^5	0.088	4.20×10^{-5}
Cesium + Fluorine ²³⁰⁷	5.54×10^5	0.152	7.85×10^{-5}
Chlorine + Fluorine ²³⁰⁸	1.632×10^5	0.0925	5.16×10^{-5}
Hydrazine + Fluorine ²³⁰⁹	1.45×10^6	0.222	1.28×10^{-4}
Hydrogen + Chlorine ²³¹⁰	9.531×10^4	0.036	2.43×10^{-5}
Hydrogen + Chlorine trifluoride (ClF ₃) ²³¹¹	1.41×10^5	0.03215	1.86×10^{-5}
Hydrogen + Fluorine ²³¹²	2.733×10^5	0.020	1.13×10^{-5}

²³⁰⁵ Assuming a density of 2340 kg/m³ with a MW of 0.0108 kg/mole for boron (B) (<http://www.rsc.org/periodic-table/element/5/boron>) and a density of ~1400 kg/m³ with a MW of 0.1184 kg/mole for fluorine perchlorate (FClO₄), a stoichiometric combustion ($10/3 \text{ B} + \text{FClO}_4 \rightarrow 1/3 \text{ BF}_3 + 1/3 \text{ BCl}_3 + 4/3 \text{ B}_2\text{O}_3$) consumes 0.036 kg of B and 0.1184 kg of FClO₄ and releases 2.25×10^6 J/mole of FClO₄ (standard heat of formation).

²³⁰⁶ Assuming a density of 3510 kg/m³ with a MW of 0.012 kg/mole for carbon as diamond (C) (<https://en.wikipedia.org/wiki/Carbon>) and a density of 1970 kg/m³ with a MW of 0.038 kg/mole for solid α -F₂ (https://en.wikipedia.org/wiki/Phases_of_fluorine), a stoichiometric combustion ($\text{C} + 2\text{F}_2 \rightarrow \text{CF}_4$) consumes 0.012 kg of C and 0.076 kg of F₂ and releases 9.34×10^5 J/mole of CF₄(g) (standard heat of formation); http://www.update.uu.se/~jolkkonen/pdf/CRC_TD.pdf. “Carbon burns in fluorine”; William Ramsay, Modern Chemistry Systematic, 4th Ed., J.M. Dent & Company, 1907, p. 58.

²³⁰⁷ Assuming a density of 1930 kg/m³ with a MW of 0.1329 kg/mole for cesium metal (<https://en.wikipedia.org/wiki/Caesium>) and a density of 1970 kg/m³ with a MW of 0.038 kg/mole for solid α -F₂ (https://en.wikipedia.org/wiki/Phases_of_fluorine), a stoichiometric combustion ($\text{Cs} + 0.5\text{F}_2 \rightarrow \text{CsF}$) consumes 0.1329 kg of Cs and 0.019 kg of F₂ and releases 5.54×10^5 J/mole of CsF (standard heat of formation); http://www.update.uu.se/~jolkkonen/pdf/CRC_TD.pdf.

²³⁰⁸ Assuming a density of 1563 kg/m³ with a MW of 0.0709 kg/mole for liquid Cl₂ (<https://en.wikipedia.org/wiki/Chlorine>) and a density of 1970 kg/m³ with a MW of 0.038 kg/mole for solid α -F₂ (https://en.wikipedia.org/wiki/Phases_of_fluorine), a stoichiometric combustion ($0.5\text{Cl}_2 + 1.5\text{F}_2 \rightarrow \text{ClF}_3$) consumes 0.03545 kg of Cl and 0.057 kg of F₂ and releases 1.632×10^5 J/mole of ClF₃(g) (standard heat of formation); http://www.update.uu.se/~jolkkonen/pdf/CRC_TD.pdf.

²³⁰⁹ Hydrazine burns in excess fluorine gas according to $\text{N}_2\text{H}_4 [0.032 \text{ kg}, 3.13 \times 10^{-5} \text{ m}^3] + 5\text{F}_2 [0.190 \text{ kg}, 9.64 \times 10^{-5} \text{ m}^3] \rightarrow 2\text{NF}_3 + 4\text{HF}$; with a density of 1970 kg/m³ and a MW of 0.038 kg/mole for solid α -F₂ (https://en.wikipedia.org/wiki/Phases_of_fluorine) and standard heats of formation +95.4 kJ/mole for N₂H₄, -132.1 kJ/mole for NF₃, and -273.3 kJ/mole for HF (http://www.update.uu.se/~jolkkonen/pdf/CRC_TD.pdf), the combustion releases 1.45×10^6 J.

²³¹⁰ Assuming a density of 600 kg/m³ with a MW of 0.002 kg/mole for compressed solid H₂ and a density of 1563 kg/m³ with a MW of 0.0709 kg/mole for liquid Cl₂ (<https://en.wikipedia.org/wiki/Chlorine>), a stoichiometric combustion ($0.5\text{H}_2 + 0.5\text{Cl}_2 \rightarrow \text{HCl}$) consumes 0.001 kg of H₂ and 0.03545 kg of Cl₂ and releases 9.531×10^4 J/mole of HCl(g) (standard enthalpy of combustion); https://en.wikipedia.org/wiki/Hydrogen_chloride.

²³¹¹ Assuming a density of 600 kg/m³ with a MW of 0.002 kg/mole for compressed solid H₂ and a density of 1880 kg/m³ with a MW of 0.09245 kg/mole for liquid ClF₃ (<http://pubs.rsc.org/en/Content/ArticleLanding/1950/JR/jr9500000191>), a stoichiometric combustion ($2/3\text{H}_2 + 1/3\text{ClF}_3 \rightarrow 1/3\text{HCl} + \text{HF}$) consumes 0.00133 kg of H₂ and 0.03082 kg of ClF₃ and releases (1/3) 9.23×10^4 J/mole of HCl(g) plus 2.733×10^5 J/mole of HF(g) less (1/3) 1.632×10^5 J/mole for ClF₃ (standard heats of formation); http://www.update.uu.se/~jolkkonen/pdf/CRC_TD.pdf.

Lithium + Fluorine ²³¹³	6.16×10^5	0.0259	2.26×10^{-5}
Lithium + Fluorine perchlorate (FCIO ₄) ²³¹⁴	3.45×10^6	0.1878	2.15×10^{-4}
Magnesium + Fluorine ²³¹⁵	1.124×10^6	0.0623	3.33×10^{-5}
Dimethylmercury (HgC ₂ H ₆) + Dioxygen difluoride (O ₂ F ₂) ²³¹⁶	5.263×10^6	0.8813	4.455×10^{-4}
Scandium + Fluorine ²³¹⁷	1.247×10^6	0.102	4.40×10^{-5}
Silicon + Fluorine ²³¹⁸	1.615×10^6	0.1041	5.06×10^{-5}

²³¹² Assuming a density of 600 kg/m³ with a MW of 0.002 kg/mole for compressed solid H₂ and a density of 1970 kg/m³ with a MW of 0.038 kg/mole for solid α-F₂

(https://en.wikipedia.org/wiki/Phases_of_fluorine), a stoichiometric combustion (0.5H₂ + 0.5F₂ → HF) consumes 0.001 kg of H₂ and 0.019 kg of F₂ and releases 2.733 x 10⁵ J/mole of HF(g) (standard heat of formation); http://www.update.uu.se/~jolkkonen/pdf/CRC_TD.pdf.

²³¹³ The highest specific impulse chemistry ever test-fired in a rocket engine was lithium and fluorine, with hydrogen added to improve the exhaust thermodynamics (all propellants had to be kept in their own tanks, making this a tripropellant; http://archive.org/stream/nasa_techdoc_19700018655/19700018655_djvu.txt).

Assuming a density of 534 kg/m³ with a MW of 0.00694 kg/mole for lithium (Li) (<https://en.wikipedia.org/wiki/Lithium>) and a density of 1970 kg/m³ with a MW of 0.038 kg/mole for solid α-F₂ (https://en.wikipedia.org/wiki/Phases_of_fluorine), a stoichiometric combustion (Li + 0.5F₂ → LiF) consumes 0.00694 kg of Li and 0.019 kg of F₂ and releases 6.16 x 10⁵ J/mole of LiF (standard heat of formation); https://en.wikipedia.org/wiki/Lithium_fluoride.

²³¹⁴ Assuming a density of 534 kg/m³ with a MW of 0.00694 kg/mole for lithium (Li) (<https://en.wikipedia.org/wiki/Lithium>) and a density of ~1400 kg/m³ with a MW of 0.1184 kg/mole for fluorine perchlorate (FCIO₄), a stoichiometric combustion (10Li + FCIO₄ → LiF + LiCl + 4Li₂O) consumes 0.0694 kg of Li and 0.1184 kg of FCIO₄ and releases 3.45 x 10⁶ J/mole of FCIO₄ (standard heat of formation).

²³¹⁵ Assuming a density of 1738 kg/m³ with a MW of 0.0243 kg/mole for magnesium (Mg) (<https://en.wikipedia.org/wiki/Magnesium>) and a density of 1970 kg/m³ with a MW of 0.038 kg/mole for solid α-F₂ (https://en.wikipedia.org/wiki/Phases_of_fluorine), a stoichiometric combustion (Mg + F₂ → MgF₂) consumes 0.0243 kg of Mg and 0.038 kg of F₂ and releases 1.124 x 10⁶ J/mole of MgF₂ (standard heat of formation); http://www.update.uu.se/~jolkkonen/pdf/CRC_TD.pdf.

²³¹⁶ Dioxygen difluoride (O₂F₂, aka. FOOF, 0.070 kg/mole, 1450 kg/m³ liquid density at 216 K) is strong oxidizer but readily decomposes into oxygen and fluorine (https://en.wikipedia.org/wiki/Dioxygen_difluoride). Assuming a density of 2961 kg/m³ with a MW of 0.23066 kg/mole for dimethylmercury (HgC₂H₆) (<https://en.wikipedia.org/wiki/Dimethylmercury>), a stoichiometric combustion (2HgC₂H₆ + 6O₂F₂ → 12HF + 4CO₂ + 2HgO + O₂) consumes 0.4613 kg of HgC₂H₆ and 0.420 kg of O₂F₂ and releases 5.263 x 10⁶ J (standard heat of formation; http://www.update.uu.se/~jolkkonen/pdf/CRC_TD.pdf). This fuel/oxidant mixture was rumored to have been suggested as a purposely dangerous powerful rocket fuel combination as part of a disinformation campaign; <http://www.tor.com/2012/07/20/a-tall-tail/>.

²³¹⁷ Assuming a density of 2985 kg/m³ with a MW of 0.045 kg/mole for scandium (Sc) (<https://en.wikipedia.org/wiki/Scandium>) and a density of 1970 kg/m³ with a MW of 0.038 kg/mole for solid α-F₂ (https://en.wikipedia.org/wiki/Phases_of_fluorine), a stoichiometric combustion (Sc + 1.5F₂ → ScF₃) consumes 0.045 kg of Sc and 0.057 kg of F₂ and releases 1.247 x 10⁶ J/mole of ScF₃(g) (standard heat of formation); http://www.update.uu.se/~jolkkonen/pdf/CRC_TD.pdf.

Sodium + Fluorine ²³¹⁹	5.74×10^5	0.042	3.34×10^{-5}
Thorium + Fluorine ²³²⁰	1.759×10^6	0.308	5.84×10^{-5}
Tungsten + Fluorine ²³²¹	1.723×10^6	0.298	6.74×10^{-5}
Uranium + Fluorine ²³²²	2.147×10^6	0.352	7.03×10^{-5}
<u>Nonambient Combustibles: O_n-allotrope Oxidants</u>			
Acetylene + Ozone (O ₃) ²³²³	1.49×10^6	0.106	8.87×10^{-5}

²³¹⁸ Assuming a density of 2329 kg/m³ with a MW of 0.0281 kg/mole for silicon (Si) (<https://en.wikipedia.org/wiki/Silicon>) and a density of 1970 kg/m³ with a MW of 0.038 kg/mole for solid α -F₂ (https://en.wikipedia.org/wiki/Phases_of_fluorine), a stoichiometric combustion ($\text{Si} + 2\text{F}_2 \rightarrow \text{SiF}_4$) consumes 0.0281 kg of Si and 0.076 kg of F₂ and releases 1.615×10^6 J/mole of SiF₄ (standard heat of formation); http://www.update.uu.se/~jolkkonen/pdf/CRC_TD.pdf.

²³¹⁹ Assuming a density of 968 kg/m³ with a MW of 0.0230 kg/mole for sodium (Na) (<https://en.wikipedia.org/wiki/Sodium>) and a density of 1970 kg/m³ with a MW of 0.038 kg/mole for solid α -F₂ (https://en.wikipedia.org/wiki/Phases_of_fluorine), a stoichiometric combustion ($\text{Na} + 0.5\text{F}_2 \rightarrow \text{NaF}$) consumes 0.023 kg of Na and 0.019 kg of F₂ and releases 5.74×10^5 J/mole of NaF (standard heat of formation); https://en.wikipedia.org/wiki/Sodium_fluoride.

²³²⁰ Assuming a density of 11,724 kg/m³ with a MW of 0.232 kg/mole for thorium (Th) (<https://en.wikipedia.org/wiki/Thorium>) and a density of 1970 kg/m³ with a MW of 0.038 kg/mole for solid α -F₂ (https://en.wikipedia.org/wiki/Phases_of_fluorine), a stoichiometric combustion ($\text{Th} + 2\text{F}_2 \rightarrow \text{ThF}_4$) consumes 0.232 kg of Th and 0.076 kg of F₂ and releases 1.759×10^6 J/mole of ThF₄ (standard heat of formation); http://www.update.uu.se/~jolkkonen/pdf/CRC_TD.pdf.

²³²¹ Assuming a density of 19,250 kg/m³ with a MW of 0.1838 kg/mole for tungsten (W) (<https://en.wikipedia.org/wiki/Tungsten>) and a density of 1970 kg/m³ with a MW of 0.038 kg/mole for solid α -F₂ (https://en.wikipedia.org/wiki/Phases_of_fluorine), a stoichiometric combustion ($\text{W} + 3\text{F}_2 \rightarrow \text{WF}_6$) consumes 0.1838 kg of W and 0.114 kg of F₂ and releases 1.723×10^6 J/mole of WF₆ (standard heat of formation); http://www.update.uu.se/~jolkkonen/pdf/CRC_TD.pdf.

²³²² Assuming a density of 19,100 kg/m³ with a MW of 0.238 kg/mole for uranium (U) (<https://en.wikipedia.org/wiki/Uranium>) and a density of 1970 kg/m³ with a MW of 0.038 kg/mole for solid α -F₂ (https://en.wikipedia.org/wiki/Phases_of_fluorine), a stoichiometric combustion ($\text{U} + 3\text{F}_2 \rightarrow \text{UF}_6$) consumes 0.238 kg of U and 0.114 kg of F₂ and releases 2.147×10^6 J/mole of UF₆ (standard heat of formation); http://www.update.uu.se/~jolkkonen/pdf/CRC_TD.pdf. "Fluorine reacts vigorous with metallic uranium at room temperature...the metal may become incandescent if it is finely divided." J.J. Katz, Eugene Rabinowitch, The Chemistry of Uranium, 1961, p. 166.

²³²³ A stoichiometric reaction of acetylene and ozone, as C_2H_2 [$0.026 \text{ kg}, 4.24 \times 10^{-5} \text{ m}^3$] + $5/3 \text{ O}_3$ [$0.080 \text{ kg}, 4.63 \times 10^{-5} \text{ m}^3$] $\rightarrow 2\text{CO}_2 + \text{H}_2\text{O}$, taking standard heats of formation as +227.2 kJ/mole for C₂H₂, +142.7 kJ/mole for O₃, -393.5 kJ/mole for CO₂, and -241.8 kJ/mole for H₂O (http://www.update.uu.se/~jolkkonen/pdf/CRC_TD.pdf), releases 1.49×10^6 J. Liquid acetylene, regarded as highly explosive if any oxygen is present, can only exist above 1.27 atm pressure and has a density of 613 kg/m³ at -80 °C with MW of 0.026 kg/mole. Solid ozone is a violet-black solid below 80 K with a density of 1728 kg/m³ (<http://pubs.acs.org/doi/abs/10.1021/ja01513a012>); concentrated gaseous and liquid ozone can detonate (<https://en.wikipedia.org/wiki/Ozone>), and solid ozone will "detonate at the slightest provocation...with a bright, white flash, shattering glassware containing it to a fine powder" (<http://pubs.acs.org/doi/abs/10.1021/ja01513a012>).

Acetylene + Octaoxygen (O ₈) ²³²⁴	1.50 x 10 ⁶	0.106	8.68 x 10 ⁻⁵
Aluminum + Ozone ²³²⁵	9.09 x 10 ⁵	0.051	2.39 x 10 ⁻⁵
Aluminum + Octaoxygen ²³²⁶	1.82 x 10 ⁶	0.102	4.67 x 10 ⁻⁵
Beryllium + Ozone ²³²⁷	6.57 x 10 ⁵	0.025	1.41 x 10 ⁻⁵
Beryllium + Octaoxygen ²³²⁸	6.59 x 10 ⁵	0.025	1.38 x 10 ⁻⁵
Beryllium nitride + Ozone ²³²⁹	1.83 x 10 ⁶	0.1031	4.81 x 10 ⁻⁵
Boron + Ozone ²³³⁰	7.08 x 10 ⁵	0.0348	1.91 x 10 ⁻⁵
Hafnium + Ozone ²³³¹	1.24 x 10 ⁶	0.2105	3.19 x 10 ⁻⁵

²³²⁴ A stoichiometric reaction of acetylene and octaoxygen, as C₂H₂ [0.026 kg, 4.24 x 10⁻⁵ m³] + 5/8 O₈ [0.080 kg, 4.44 x 10⁻⁵ m³] → 2CO₂ + H₂O, taking standard heats of formation as +227.2 kJ/mole for C₂H₂, +393.0 kJ/mole for O₈, -393.5 kJ/mole for CO₂, and -241.8 kJ/mole for H₂O (http://www.update.uu.se/~jolkkonen/pdf/CRC_TD.pdf), releases 1.50 x 10⁶ J. Octaoxygen (O₈), aka. “red oxygen,” is a rhomboid cluster of oxygen atoms that is obtained by compressing oxygen through 10 GPa at room temperature, producing a deep red solid ε-phase (https://en.wikipedia.org/wiki/Solid_oxygen#Red_oxygen) that is stable over a wide pressure range,* though it is not known whether O₈ remains metastable at lower pressures after formation. Its enthalpy of formation has been estimated as 393 kJ/mole**; its density is reported as being higher than conventional α-phase solid oxygen (1524 kg/m³), and is probably higher than solid ozone (1728 kg/m³), so ~1800 kg/m³ is assumed here for O₈. * Lundegaard LF, *et al.* Observation of an O₈ molecular lattice in the ε phase of solid oxygen. Nature 2006 Sep 14;443:201-204; <http://www.nature.com/nature/journal/v443/n7108/full/nature05174.html>. ** Hernandez-Lamonedea R, *et al.* Systematic ab initio calculations on the energetics and stability of covalent O₄. J Chem Phys. 2004 Jun 1;120(21):10084-8; <http://www.ncbi.nlm.nih.gov/pubmed/15268030>.

²³²⁵ A stoichiometric reaction of aluminum and ozone, as Al [0.027 kg, 1 x 10⁻⁵ m³] + 0.5O₃ [0.024 kg, 1.39 x 10⁻⁵ m³] → 0.5Al₂O₃, taking standard heats of formation as +142.7 kJ/mole for O₃ and -1675.7 kJ/mole for Al₂O₃ (http://www.update.uu.se/~jolkkonen/pdf/CRC_TD.pdf), releases 9.09 x 10⁵ J.

²³²⁶ A stoichiometric reaction of aluminum and octaoxygen, as 2Al [0.054 kg, 2 x 10⁻⁵ m³] + 0.375O₈ [0.048 kg, 2.67 x 10⁻⁵ m³] → Al₂O₃, taking standard heats of formation as +393.0 kJ/mole for O₈ (see above) and -1675.7 kJ/mole for Al₂O₃ (http://www.update.uu.se/~jolkkonen/pdf/CRC_TD.pdf), releases 1.82 x 10⁶ J.

²³²⁷ A stoichiometric reaction of beryllium and ozone, as Be [0.009 kg, 4.87 x 10⁻⁶ m³] + 1/3 O₃ [0.016 kg, 9.26 x 10⁻⁶ m³] → BeO, taking standard heats of formation as +142.7 kJ/mole for O₃ and -609.4 kJ/mole for BeO (http://www.update.uu.se/~jolkkonen/pdf/CRC_TD.pdf), releases 6.57 x 10⁵ J.

²³²⁸ A stoichiometric reaction of beryllium and octaoxygen, as Be [0.009 kg, 4.87 x 10⁻⁶ m³] + 1/8 O₈ [0.016 kg, 8.89 x 10⁻⁶ m³] → BeO, taking standard heats of formation as +393.0 kJ/mole for O₈ and -609.4 kJ/mole for BeO (http://www.update.uu.se/~jolkkonen/pdf/CRC_TD.pdf), releases 6.59 x 10⁵ J.

²³²⁹ A stoichiometric reaction of beryllium nitride and ozone, as Be₃N₂ [0.0551 kg, 2.03 x 10⁻⁵ m³] + O₃ [0.048 kg, 2.78 x 10⁻⁵ m³] → 3BeO + N₂, taking standard heats of formation as -140.3 kJ/mole for Be₃N₂, +142.7 kJ/mole for O₃ and -609.4 kJ/mole for BeO (http://www.update.uu.se/~jolkkonen/pdf/CRC_TD.pdf), releases 1.83 x 10⁶ J.

²³³⁰ A stoichiometric reaction of boron and ozone, as B [0.0108 kg, 5.19 x 10⁻⁶ m³] + 0.5O₃ [0.024 kg, 1.39 x 10⁻⁵ m³] → 0.5B₂O₃, taking standard heats of formation as +142.7 kJ/mole for O₃ and -1273.5 kJ/mole for B₂O₃ (http://www.update.uu.se/~jolkkonen/pdf/CRC_TD.pdf), releases 7.08 x 10⁵ J.

Hydrogen + Ozone ²³³²	2.89×10^5	0.018	1.26×10^{-5}
Lithium + Ozone ²³³³	3.23×10^5	0.015	1.77×10^{-5}
Lithium borohydride + Ozone ²³³⁴	6.36×10^5	0.0698	6.05×10^{-5}
Magnesium + Ozone ²³³⁵	6.49×10^5	0.0403	2.33×10^{-5}
<u>Nonambient Combustibles: Nitrate Oxidants</u>			
Aluminum + Trinitramide ²³³⁶	9.00×10^5	0.065	2.81×10^{-5}
Beryllium + Hydrazinium nitroformate ²³³⁷	1.23×10^6	0.131	7.05×10^{-5}

²³³¹ A stoichiometric reaction of hafnium and ozone, as Hf [0.1785 kg, $1.34 \times 10^{-5} \text{ m}^3$] + $2/3 \text{ O}_3$ [0.032 kg, $1.85 \times 10^{-5} \text{ m}^3$] $\rightarrow \text{HfO}_2$, taking standard heats of formation as +142.7 kJ/mole for O_3 and -1144.7 kJ/mole for HfO_2 (http://www.update.uu.se/~jolkkonen/pdf/CRC_TD.pdf), releases $1.24 \times 10^6 \text{ J}$.

²³³² A stoichiometric reaction of solid hydrogen and ozone, as H_2 [0.002 kg, $3.33 \times 10^{-6} \text{ m}^3$] + $1/3 \text{ O}_3$ [0.016 kg, $9.26 \times 10^{-6} \text{ m}^3$] $\rightarrow \text{H}_2\text{O}$, taking standard heats of formation as +142.7 kJ/mole for O_3 and -241.8 kJ/mole for H_2O (http://www.update.uu.se/~jolkkonen/pdf/CRC_TD.pdf), releases $2.89 \times 10^5 \text{ J}$.

²³³³ A stoichiometric reaction of lithium and ozone, as Li [0.007 kg, $1.31 \times 10^{-5} \text{ m}^3$] + $1/6 \text{ O}_3$ [0.008 kg, $4.63 \times 10^{-6} \text{ m}^3$] $\rightarrow \text{Li}_2\text{O}$, taking standard heats of formation as +142.7 kJ/mole for O_3 and -597.9 kJ/mole for Li_2O (http://www.update.uu.se/~jolkkonen/pdf/CRC_TD.pdf), releases $3.23 \times 10^5 \text{ J}$.

²³³⁴ A stoichiometric reaction of lithium borohydride and ozone, as LiBH_4 [0.0551 kg, $2.03 \times 10^{-5} \text{ m}^3$] + O_3 [0.048 kg, $2.78 \times 10^{-5} \text{ m}^3$] $\rightarrow \text{LiOH} + \text{H}_3\text{BO}_2$, taking standard heats of formation as -190.8 kJ/mole for LiBH_4 , +142.7 kJ/mole for O_3 , -484.9 kJ/mole for LiOH , and -198.8.4 kJ/mole for H_3BO_2 (http://www.update.uu.se/~jolkkonen/pdf/CRC_TD.pdf), releases $6.36 \times 10^5 \text{ J}$.

²³³⁵ A stoichiometric reaction of magnesium and ozone, as Mg [0.0243 kg, $1.40 \times 10^{-5} \text{ m}^3$] + $1/3 \text{ O}_3$ [0.016 kg, $9.26 \times 10^{-6} \text{ m}^3$] $\rightarrow \text{MgO}$, taking standard heats of formation as +142.7 kJ/mole for O_3 and -601.6 kJ/mole for MgO (http://www.update.uu.se/~jolkkonen/pdf/CRC_TD.pdf), releases $6.49 \times 10^5 \text{ J}$.

²³³⁶ Trinitramide, aka. TNA, trinitroamine, or *N,N*-dinitronitramide ($\text{N}(\text{NO}_2)_3$ or N_4O_6 , 0.152 kg/mole; <http://en.wikipedia.org/wiki/Trinitramide>), with estimated density 2100 kg/m^3 (<http://www.chemspider.com/Chemical-Structure.24751851.html>) and predicted heat of formation +246.9 kJ/mole,* was first synthesized in 2010** and is expected to be an efficient rocket propellant oxidizer. A stoichiometric reaction of aluminum and trinitramide, as Al [0.027 kg, $1.00 \times 10^{-5} \text{ m}^3$] + $0.25\text{N}_4\text{O}_6$ [0.038 kg, $1.81 \times 10^{-5} \text{ m}^3$] $\rightarrow 0.5\text{N}_2 + 0.5\text{Al}_2\text{O}_3$, taking standard heat of formation as -1675.7 kJ/mole for Al_2O_3 (http://www.update.uu.se/~jolkkonen/pdf/CRC_TD.pdf), releases $9.00 \times 10^5 \text{ J}$ of Al. * Montgomery Jr JA, Michels HH. Structure and stability of trinitramide. J Phys Chem. 1993 Jul;97(26):6774-6775; <http://pubs.acs.org/doi/abs/10.1021/j100128a005>. ** Rahm M, Dvinskikh SV, Furó I, Brinck T. Experimental detection of trinitramide, $\text{N}(\text{NO}_2)_3$. Angew Chem Int Ed Engl. 2011 Feb 1;50(5):1145-8; <http://onlinelibrary.wiley.com/doi/10.1002/anie.201007047/abstract>.

²³³⁷ Hydrazinium nitroformate, aka. HNF ($\text{N}_2\text{H}_5^+\text{C}(\text{NO}_2)_3^-$ or $\text{CH}_5\text{N}_5\text{O}_6$, 0.183 kg/mole, density 1860 kg/m^3 , heat of formation -72.0 kJ/mole (Sarner HF. Propellant Chemistry, Reinhold Publishing, 1966; http://yarchive.net/space/rocket/fuels/hydrazinium_nitroformate.html) is an oxidizer being considered for use in solid rocket propellants. A stoichiometric reaction of beryllium and HNF, as Be [0.009 kg, $4.87 \times 10^{-6} \text{ m}^3$] + $2/3 \text{ CH}_5\text{N}_5\text{O}_6$ [0.122 kg, $6.56 \times 10^{-5} \text{ m}^3$] $\rightarrow 5/3 \text{ N}_2 + 2/3 \text{ CO}_2 + \text{BeO} + 5/3 \text{ H}_2\text{O}$, taking standard heats of formation as -393.5 kJ/mole for CO_2 , -609.4 kJ/mole for BeO , and -241.8 kJ/mole for H_2O (http://www.update.uu.se/~jolkkonen/pdf/CRC_TD.pdf), releases $1.23 \times 10^6 \text{ J}$ of Be.

Beryllium + Hydroxylammonium nitrate ²³³⁸	6.85×10^5	0.057	3.11×10^{-5}
Beryllium + Trinitramide ²³³⁹	6.51×10^5	0.0343	1.69×10^{-5}
Boron + Trinitramide ²³⁴⁰	6.98×10^5	0.0488	2.33×10^{-5}
Hydrogen + Trinitramide ²³⁴¹	2.83×10^5	0.0273	1.54×10^{-5}
Lithium + Trinitramide ²³⁴²	3.20×10^5	0.0196	1.90×10^{-5}
<u>Nonambient Combustibles: Thermite or Thermitic</u>			
Ag ₂ O ₂ + Al ²³⁴³	1.64×10^6	0.302	5.33×10^{-5}
BO + Al (theoretical) ²³⁴⁴	1.75×10^6	0.134	---

²³³⁸ Hydroxylammonium nitrate, aka. HAN (NH₃OH⁺NO₃⁻ or H₄N₂O₄, 0.096 kg/mole, density 1830 kg/m³, heat of formation -333.4 kJ/mole (Khare P, *et al.* Thermal and electrolytic decomposition and ignition of HAN-water solutions. *Combust Sci Technol.* 2015;187:1065-1078; [http://www.yang.gatech.edu/publications/Journal/CST%20\(2015,%20HAN,%20Khare\).pdf](http://www.yang.gatech.edu/publications/Journal/CST%20(2015,%20HAN,%20Khare).pdf)) is a potential solid rocket propellant oxidizer. A stoichiometric reaction of beryllium and HAN, as Be [0.009 kg, 4.87×10^{-6} m³] + 0.5H₄N₂O₄ [0.048 kg, 2.62×10^{-5} m³] → 0.5N₂ + H₂O + BeO, taking standard heats of formation as -241.8 kJ/mole for H₂O and -609.4 kJ/mole for BeO (http://www.update.uu.se/~jolkkonen/pdf/CRC_TD.pdf), releases 6.85×10^5 J/mole of Be.

²³³⁹ A stoichiometric reaction of beryllium and trinitramide, as Be [0.009 kg, 4.87×10^{-6} m³] + 1/6 N₄O₆ [0.0253 kg, 1.20×10^{-5} m³] → 1/3 N₂ + BeO, taking standard heats of formation as +246.9 kJ/mole for N₄O₆ and -609.4 kJ/mole for BeO (http://www.update.uu.se/~jolkkonen/pdf/CRC_TD.pdf), releases 6.51×10^5 J/mole of Be.

²³⁴⁰ A stoichiometric reaction of boron and trinitramide, as B [0.0108 kg, 5.19×10^{-6} m³] + 0.25N₄O₆ [0.038 kg, 1.81×10^{-5} m³] → 0.5N₂ + 0.5B₂O₃, taking standard heats of formation as +246.9 kJ/mole for N₄O₆ and -1273.5 kJ/mole for B₂O₃ (http://www.update.uu.se/~jolkkonen/pdf/CRC_TD.pdf), releases 6.98×10^5 J/mole of B.

²³⁴¹ A stoichiometric reaction of solid hydrogen and trinitramide, as H₂ [0.002 kg, 3.33×10^{-6} m³] + 1/6 N₄O₆ [0.0253 kg, 1.20×10^{-5} m³] → 1/3 N₂ + H₂O, taking standard heats of formation as +246.9 kJ/mole for N₄O₆ and -241.8 kJ/mole for H₂O (http://www.update.uu.se/~jolkkonen/pdf/CRC_TD.pdf), releases 2.83×10^5 J/mole of H₂.

²³⁴² A stoichiometric reaction of lithium and trinitramide, as Li [0.00694 kg, 1.30×10^{-5} m³] + 1/12 N₄O₆ [0.0127 kg, 6.05×10^{-6} m³] → 1/6 N₂ + 0.5Li₂O, taking standard heats of formation as +246.9 kJ/mole for N₄O₆ and -597.9 kJ/mole for Li₂O (http://www.update.uu.se/~jolkkonen/pdf/CRC_TD.pdf), releases 3.20×10^5 J/mole of Li.

²³⁴³ “Silver peroxide” (Ag₂O₂) is a high-density gray-black powder ([https://en.wikipedia.org/wiki/Silver\(I,III\)_oxide](https://en.wikipedia.org/wiki/Silver(I,III)_oxide)). The stoichiometry of the thermite-like reaction: 1.5Ag₂O₂ [0.248 kg, 3.33×10^{-5} m³] + 2Al [0.054 kg, 2.00×10^{-5} m³] → Al₂O₃ + 3Ag releases 1.64×10^6 J, taking standard heats of formation as -1675.7 kJ/mole for Al₂O₃ (http://www.update.uu.se/~jolkkonen/pdf/CRC_TD.pdf) and -26.4 kJ/mole for Ag₂O₂ (Hermann WA. *Synthetic Methods of Organometallic and Inorganic Chemistry*, Georg Thieme Verlag, 1996, p. 34).

$B_2O_2 + Al^{2345}$	9.94×10^5	0.134	---
$CO + Al^{2346}$	1.34×10^6	0.138	1.26×10^{-4}
$CO_2 + Al^{2347}$	1.086×10^6	0.120	6.23×10^{-5}
$C_3O_2 + Al^{2348}$	1.54×10^6	0.156	---
$CoO + Al^{2349}$	9.62×10^5	0.279	5.49×10^{-5}
$CuO + Al$ (Copper Thermite) ²³⁵⁰	1.20×10^6	0.293	5.79×10^{-5}
$FeO + Al^{2351}$	8.60×10^5	0.269	5.75×10^{-5}

²³⁴⁴ Boron monoxide (BO) is a reactive gaseous radical that probably cannot be stably condensed to liquid or solid form. But if it can be made to react, the stoichiometry of the thermite-like reaction: $3BO(g)$ [0.0804 kg] + $2Al$ [0.054 kg] $\rightarrow Al_2O_3 + 3B$ should release 1.75×10^6 J, taking standard heats of formation as +25.0 kJ/mole for BO and -1675.7 kJ/mole for Al_2O_3 (http://www.update.uu.se/~jolkkonen/pdf/CRC_TD.pdf).

²³⁴⁵ Diboron dioxide (B_2O_2) is a reactive gas but relatively unstudied gas that can be obtained both in liquid and solid form that may be available in liquid form (e.g., " B_2O_2 condenses to a deep brown amorphous solid on the cold walls of the condenser").* The stoichiometry of the thermite-like reaction: $1.5B_2O_2(g)$ [0.0804 kg] + $2Al$ [0.054 kg] $\rightarrow Al_2O_3 + 3B$ should release 9.94×10^5 J, taking standard heats of formation as -454.8 kJ/mole for B_2O_2 and -1675.7 kJ/mole for Al_2O_3 (http://www.update.uu.se/~jolkkonen/pdf/CRC_TD.pdf). *Rentzepis P, White D, Walsh PN. The reaction between $B_2O_3(l)$ and $C(s)$: Heat of formation of $B_2O_2(g)$. J Phys Chem 1960 Nov;64(11):1784-1787; <http://pubs.acs.org/doi/abs/10.1021/j100840a519>.

²³⁴⁶ Aluminum will burn (<http://dtic.mil/cgi-bin/GetTRDoc?AD=ADA425147>) in a flame of carbon monoxide according to the stoichiometric combustion formula: $3CO$ [0.028 kg/mole, liquid density 793 kg/m³; <http://encyclopedia.airliquide.com/Encyclopedia.asp?GasID=45>] + $2Al$ [0.054 kg/mole, 2700 kg/m³] $\rightarrow Al_2O_3 + 3C$, taking the standard heats of formation as -110.5 kJ/mole for CO and -1675.7 kJ/mole for Al_2O_3 (http://www.update.uu.se/~jolkkonen/pdf/CRC_TD.pdf), releasing 1.34×10^6 J.

²³⁴⁷ Solid aluminum (Al) has a density of 2700 kg/m³ with MW of 0.027 kg/mole; a stoichiometric combustion ($1.5CO_2 + 2Al \rightarrow Al_2O_3 + 1.5C$) using solid carbon dioxide ($CO_2(s)$: density 1562 kg/m³, MW 0.044 kg/mole; https://en.wikipedia.org/wiki/Carbon_dioxide) consumes 0.054 kg of Al and 0.066 kg of CO_2 and releases 1.086×10^6 J/mole of Al, taking heats of formation of -393.5 kJ/mole for CO_2 and -1675.7 kJ/mole for Al_2O_3 (http://www.update.uu.se/~jolkkonen/pdf/CRC_TD.pdf).

²³⁴⁸ Carbon suboxide (O=C=C=O or C_3O_2) is a colorless oily pungent liquid below 280 K (https://en.wikipedia.org/wiki/Carbon_suboxide). The stoichiometry of the thermite-like reaction: $1.5C_3O_2$ [0.102 kg] + $2Al$ [0.054 kg] $\rightarrow Al_2O_3 + 4.5C$ releases 1.54×10^6 J, taking standard heats of formation as -93.6 kJ/mole for C_3O_2 and -1675.7 kJ/mole for Al_2O_3 (http://www.update.uu.se/~jolkkonen/pdf/CRC_TD.pdf).

²³⁴⁹ Cobalt monoxide (CoO) is a high-density black powder used as a colorant in the ceramics industry ([https://en.wikipedia.org/wiki/Cobalt\(II\)_oxide](https://en.wikipedia.org/wiki/Cobalt(II)_oxide)). The stoichiometry of the thermite-like reaction: $3CoO$ [0.225 kg, 3.49×10^{-5} m³] + $2Al$ [0.054 kg, 2.00×10^{-5} m³] $\rightarrow Al_2O_3 + 3Co$ releases 9.62×10^5 J, taking standard heats of formation as -237.9 kJ/mole for CoO and -1675.7 kJ/mole for Al_2O_3 (http://www.update.uu.se/~jolkkonen/pdf/CRC_TD.pdf).

²³⁵⁰ The stoichiometric reaction of copper thermite, $3CuO$ [0.239 kg, 3.79×10^{-5} m³] + $2Al$ [0.054 kg, 2.00×10^{-5} m³] $\rightarrow Al_2O_3 + 3Cu$ (<https://en.wikipedia.org/wiki/Thermite>), taking standard heats of formation as -157.3 kJ/mole for CuO and -1675.7 kJ/mole for Al_2O_3 (http://www.update.uu.se/~jolkkonen/pdf/CRC_TD.pdf), releases 1.20×10^6 J.

$\text{Fe}_2\text{O}_3 + \text{Al}$ (Iron Thermite) ²³⁵²	8.52×10^5	0.214	5.05×10^{-5}
H_2O (ice) + Al ²³⁵³	4.75×10^5	0.054	3.70×10^{-5}
$\text{H}_2\text{O}_2 + \text{Al}$ ²³⁵⁴	1.39×10^6	0.105	5.52×10^{-5}
$\text{Li}_2\text{O}_2 + \text{Al}$ ²³⁵⁵	7.24×10^5	0.123	4.98×10^{-5}
$\text{MgO}_2 + \text{Al}$ ²³⁵⁶	1.76×10^6	0.1385	4.82×10^{-5}
$\text{Mn}_2\text{O}_7 + \text{Al}$ ²³⁵⁷	1.36×10^6	0.149	5.41×10^{-5}

²³⁵¹ The stoichiometric reaction of ferrous oxide, 3FeO [0.215 kg, $3.75 \times 10^{-5} \text{ m}^3$] + 2Al [0.054 kg, $2.00 \times 10^{-5} \text{ m}^3$] $\rightarrow \text{Al}_2\text{O}_3 + 3\text{Fe}$ (<https://en.wikipedia.org/wiki/Thermite>), taking standard heats of formation as -272.0 kJ/mole for FeO and -1675.7 kJ/mole for Al_2O_3 (http://www.update.uu.se/~jolkkonen/pdf/CRC_TD.pdf), releases $8.60 \times 10^5 \text{ J}$.

²³⁵² The stoichiometric reaction of iron thermite, Fe_2O_3 [aka. ferric oxide, 0.160 kg, $3.05 \times 10^{-5} \text{ m}^3$] + 2Al [0.054 kg, $2.00 \times 10^{-5} \text{ m}^3$] $\rightarrow \text{Al}_2\text{O}_3 + 2\text{Fe}$ (<https://en.wikipedia.org/wiki/Thermite>), taking standard heats of formation as -824.2 kJ/mole for Fe_2O_3 and -1675.7 kJ/mole for Al_2O_3 (http://www.update.uu.se/~jolkkonen/pdf/CRC_TD.pdf), releases $8.52 \times 10^5 \text{ J}$.

²³⁵³ Nanopowdered aluminum + water-ice, aka. ALuminum ICE rocket propellant or ALICE, has been proposed as a propellant well suited for in-situ production on outer space bodies such as the moon (<http://www.dtic.mil/dtic/tr/fulltext/u2/a546818.pdf>). Aluminum has a stronger affinity for oxygen than most elements, which allows Al to burn with a large release of heat in substances normally considered inert (e.g., carbon dioxide and water). Al combustion is usually hindered by the presence of a durable oxide layer on the surface of Al particles, but the oxide layer in nano-aluminum powder is thinner and easier to overcome than in that of larger particles ([https://en.wikipedia.org/wiki/ALICE_\(propellant\)](https://en.wikipedia.org/wiki/ALICE_(propellant))). A stoichiometric combustion according to Al [0.027 kg, $1.00 \times 10^{-5} \text{ m}^3$] + $1.5\text{H}_2\text{O}$ [0.027 kg, $2.70 \times 10^{-5} \text{ m}^3$] $\rightarrow 0.5\text{Al}_2\text{O}_3 + 1.5\text{H}_2$, taking the standard heats of formation as -241.8 kJ/mole for H_2O and -1675.7 kJ/mole for Al_2O_3 (http://www.update.uu.se/~jolkkonen/pdf/CRC_TD.pdf), releases $4.75 \times 10^5 \text{ J}$ for 0.054 kg or $3.70 \times 10^{-5} \text{ m}^3$ of propellants.

²³⁵⁴ Hydrogen peroxide (H_2O_2) in pure form is rocket propellant that explodes when heated to boiling (https://en.wikipedia.org/wiki/Hydrogen_peroxide). The stoichiometry of the thermite-like reaction: $1.5\text{H}_2\text{O}_2$ [0.051 kg, $3.52 \times 10^{-5} \text{ m}^3$] + 2Al [0.054 kg, $2.00 \times 10^{-5} \text{ m}^3$] $\rightarrow \text{Al}_2\text{O}_3 + 3\text{H}_2$ releases $1.39 \times 10^6 \text{ J}$, taking standard heats of formation as -187.8 kJ/mole for liquid H_2O_2 and -1675.7 kJ/mole for Al_2O_3 (http://www.update.uu.se/~jolkkonen/pdf/CRC_TD.pdf).

²³⁵⁵ Lithium peroxide (Li_2O_2) is a low-density white solid used to remove CO_2 in manned spacecraft (https://en.wikipedia.org/wiki/Lithium_peroxide). The stoichiometry of the thermite-like reaction: $1.5\text{Li}_2\text{O}_2$ [0.0689 kg, $2.98 \times 10^{-5} \text{ m}^3$] + 2Al [0.054 kg, $2.00 \times 10^{-5} \text{ m}^3$] $\rightarrow \text{Al}_2\text{O}_3 + 3\text{Li}$ releases $7.24 \times 10^5 \text{ J}$, taking standard heats of formation as -634.3 kJ/mole for Li_2O_2 and -1675.7 kJ/mole for Al_2O_3 (http://www.update.uu.se/~jolkkonen/pdf/CRC_TD.pdf).

²³⁵⁶ Magnesium peroxide (MgO_2) is an odorless white powder (https://en.wikipedia.org/wiki/Magnesium_peroxide). The stoichiometry of the thermite-like reaction: 1.5MgO_2 [0.0845 kg, $2.82 \times 10^{-5} \text{ m}^3$] + 2Al [0.054 kg, $2.00 \times 10^{-5} \text{ m}^3$] $\rightarrow \text{Al}_2\text{O}_3 + 1.5\text{Mg}$ releases $1.76 \times 10^6 \text{ J}$, taking standard heats of formation as -1675.7 kJ/mole for Al_2O_3 (http://www.update.uu.se/~jolkkonen/pdf/CRC_TD.pdf) and +57.89 kJ/mole for MgO_2 (<https://arxiv.org/pdf/1211.6521.pdf>).

MoO ₃ + Al ²³⁵⁸	9.31 x 10 ⁵	0.198	5.07 x 10 ⁻⁵
NaO ₂ + Al ²³⁵⁹	1.29 x 10 ⁶	0.1365	5.75 x 10 ⁻⁵
NO + Al ²³⁶⁰	1.95 x 10 ⁶	0.144	9.03 x 10 ⁻⁵
NO ₂ + Al ²³⁶¹	1.73 x 10 ⁶	0.123	6.77 x 10 ⁻⁵
NO ₂ + Sc ²³⁶²	1.96 x 10 ⁶	0.159	7.79 x 10 ⁻⁵
NiO + Al ²³⁶³	9.56 x 10 ⁵	0.278	5.36 x 10 ⁻⁵
OsO ₄ + Al ²³⁶⁴	1.38 x 10 ⁶	0.245	5.90 x 10 ⁻⁵

²³⁵⁷ Manganese heptoxide (Mn₂O₇) is a volatile reactive liquid that decomposes near room temperature, explosively so about 55 °C (https://en.wikipedia.org/wiki/Manganese_heptoxide). The stoichiometry of the thermite-like reaction: 3/7 Mn₂O₇ [0.0951 kg, 3.41 x 10⁻⁵ m³] + 2Al [0.054 kg, 2.00 x 10⁻⁵ m³] → Al₂O₃ + 6/7 Mn, releases 1.36 x 10⁶ J, taking standard heats of formation as -1675.7 kJ/mole for Al₂O₃ (http://www.update.uu.se/~jolkkonen/pdf/CRC_TD.pdf) and -742.2 kJ/mole for Mn₂O₇ (<http://onlinelibrary.wiley.com/doi/10.1002/zaac.19532710507/abstract>).

²³⁵⁸ Molybdenum trioxide (MoO₃) is a yellow or light blue solid that is unstable to the dioxide (https://en.wikipedia.org/wiki/Molybdenum_trioxide). The stoichiometry of the thermite-like reaction: MoO₃ [0.144 kg, 3.07 x 10⁻⁵ m³] + 2Al [0.054 kg, 2.00 x 10⁻⁵ m³] → Al₂O₃ + Mo, releases 9.31 x 10⁵ J, taking standard heats of formation as -745.1 kJ/mole for MoO₃ and -1675.7 kJ/mole for Al₂O₃ (http://www.update.uu.se/~jolkkonen/pdf/CRC_TD.pdf).

²³⁵⁹ Sodium superoxide (NaO₂) is a low-density yellow-orange solid (https://en.wikipedia.org/wiki/Sodium_superoxide). The stoichiometry of the thermite-like reaction: 1.5NaO₂ [0.0825 kg, 3.75 x 10⁻⁵ m³] + 2Al [0.054 kg, 2.00 x 10⁻⁵ m³] → Al₂O₃ + 1.5Na releases 1.29 x 10⁶ J, taking standard heats of formation as -260.2 kJ/mole for NaO₂ and -1675.7 kJ/mole for Al₂O₃ (http://www.update.uu.se/~jolkkonen/pdf/CRC_TD.pdf).

²³⁶⁰ Nitric oxide (NO, 0.030 kg/mole, liquid density 1281 kg/m³; <http://encyclopedia.airliquide.com/Encyclopedia.asp?GasID=44#GeneralData>), when combined with aluminum as 3NO [0.090 kg, 7.03 x 10⁻⁵ m³] + 2Al [0.054 kg, 2.00 x 10⁻⁵ m³] → Al₂O₃ + 1.5N₂, taking standard heat of formation as +91.3 kJ/mole for NO and -1675.7 kJ/mole for Al₂O₃ (http://www.update.uu.se/~jolkkonen/pdf/CRC_TD.pdf), can release 1.95 x 10⁶ J.

²³⁶¹ Nitrogen dioxide (NO₂, 0.046 kg/mole, liquid density 1448 kg/m³; <http://encyclopedia.airliquide.com/Encyclopedia.asp?GasID=25#GeneralData>), when combined with aluminum as 1.5NO₂ [0.069 kg, 4.77 x 10⁻⁵ m³] + 2Al [0.054 kg, 2.00 x 10⁻⁵ m³] → Al₂O₃ + 0.75N₂, taking standard heat of formation as +33.2 kJ/mole for NO₂ and -1675.7 kJ/mole for Al₂O₃ (http://www.update.uu.se/~jolkkonen/pdf/CRC_TD.pdf), can release 1.73 x 10⁶ J.

²³⁶² Nitrogen dioxide (NO₂, 0.046 kg/mole, liquid density 1448 kg/m³; <http://encyclopedia.airliquide.com/Encyclopedia.asp?GasID=25#GeneralData>), when combined with scandium as 1.5NO₂ [0.069 kg, 4.77 x 10⁻⁵ m³] + 2Sc [0.090 kg, 3.02 x 10⁻⁵ m³] → Sc₂O₃ + 0.75N₂, taking standard heat of formation as +33.2 kJ/mole for NO₂ and -1908.8 kJ/mole for Sc₂O₃ (http://www.update.uu.se/~jolkkonen/pdf/CRC_TD.pdf), can release 1.96 x 10⁶ J.

²³⁶³ Nickel oxide (NiO) is a high-density green solid ([https://en.wikipedia.org/wiki/Nickel\(II\)_oxide](https://en.wikipedia.org/wiki/Nickel(II)_oxide)). The stoichiometry of the thermite-like reaction: 3NiO [0.224 kg, 3.36 x 10⁻⁵ m³] + 2Al [0.054 kg, 2.00 x 10⁻⁵ m³] → Al₂O₃ + 3Ni releases 9.56 x 10⁵ J, taking standard heats of formation as -240.0 kJ/mole for NiO and -1675.7 kJ/mole for Al₂O₃ (http://www.update.uu.se/~jolkkonen/pdf/CRC_TD.pdf).

$P_2O_5 + Al^{2365}$	1.53×10^6	0.139	4.43×10^{-5}
$PdO + Al^{2366}$	1.42×10^6	0.420	6.41×10^{-5}
$RaO_2 + Al$ (theoretical) ²³⁶⁷	2.62×10^6	0.441	9.74×10^{-5}
$Rh_2O_3 + Al^{2368}$	1.33×10^6	0.308	5.10×10^{-5}
$RuO_4 + Al^{2369}$	1.50×10^6	0.178	5.76×10^{-5}
$SeO_3 + Al^{2370}$	1.16×10^6	0.181	5.69×10^{-5}

²³⁶⁴ Osmium tetroxide (OsO_4) is a volatile crystalline toxic solid with a pungent odor (https://en.wikipedia.org/wiki/Osmium_tetroxide). The stoichiometry of the thermite-like reaction: $0.75OsO_4$ [0.191 kg, $3.90 \times 10^{-5} m^3$] + $2Al$ [0.054 kg, $2.00 \times 10^{-5} m^3$] $\rightarrow Al_2O_3 + 0.75Os$ releases 1.38×10^5 J, taking standard heats of formation as -394.1 kJ/mole for OsO_4 and -1675.7 kJ/mole for Al_2O_3 (http://www.update.uu.se/~jolkkonen/pdf/CRC_TD.pdf).

²³⁶⁵ The stoichiometry of the thermite-like reaction: $0.6P_2O_5$ [0.0851 kg, $2.43 \times 10^{-5} m^3$] + $2Al$ [0.054 kg, $2.00 \times 10^{-5} m^3$] $\rightarrow Al_2O_3 + 0.6P$, taking standard heats of formation as -254.12 kJ/mole for P_2O_5 (see above), -166.5 kJ/mole for AlP and -1675.7 kJ/mole for Al_2O_3 (http://www.update.uu.se/~jolkkonen/pdf/CRC_TD.pdf), releases 1.53×10^6 J. (An alternative plausible reaction in which the free phosphorus combines with excess Al to produce AlP (HOF = -166.5 kJ/mole), energetically preferred to free P (HOF = 0 kJ/mole), nevertheless produces 5% less specific energy, in MJ/kg.)

²³⁶⁶ Palladium oxide (PdO) is a high-density greenish-black powder ([https://en.wikipedia.org/wiki/Palladium\(II\)_oxide](https://en.wikipedia.org/wiki/Palladium(II)_oxide)). The stoichiometry of the thermite-like reaction: $3PdO$ [0.366 kg, $4.41 \times 10^{-5} m^3$] + $2Al$ [0.054 kg, $2.00 \times 10^{-5} m^3$] $\rightarrow Al_2O_3 + 3Pd$ releases 1.42×10^5 J, taking standard heats of formation as -85.0 kJ/mole for PdO and -1675.7 kJ/mole for Al_2O_3 (http://www.update.uu.se/~jolkkonen/pdf/CRC_TD.pdf).

²³⁶⁷ Radium peroxide (RaO_2), 0.258 kg/mole, density ~ 5000 kg/ m^3) would be radioactive and is alleged to be capable of synthesis, but “there is no record of this compound ever having been prepared because of the lack of interest by industry and academia” (Ropp RC, Encyclopedia of the Alkaline Earth Compounds, Newnes, 2012, p. 130). The stoichiometry of the thermite-like reaction: $1.5RaO_2$ [0.387 kg, $7.74 \times 10^{-5} m^3$] + $2Al$ [0.054 kg, $2.00 \times 10^{-5} m^3$] $\rightarrow Al_2O_3 + 1.5Ra$ releases 2.62×10^6 J, taking standard heats of formation as -1675.7 kJ/mole for Al_2O_3 (http://www.update.uu.se/~jolkkonen/pdf/CRC_TD.pdf) and +627.6 kJ/mole for RaO_2 (Volnov II. Peroxides, Superoxides, and Ozonides of Alkali and Alkaline Earth Metals, Springer, 2012, p. 57; http://link.springer.com/chapter/10.1007/978-1-4684-8252-2_4#page-1).

²³⁶⁸ Rhodium sesquioxide (Rh_2O_3) is a dark gray odorless powder ([https://en.wikipedia.org/wiki/Rhodium\(III\)_oxide](https://en.wikipedia.org/wiki/Rhodium(III)_oxide)). The stoichiometry of the thermite-like reaction: Rh_2O_3 [0.254 kg, $3.10 \times 10^{-5} m^3$] + $2Al$ [0.054 kg, $2.00 \times 10^{-5} m^3$] $\rightarrow Al_2O_3 + 2Rh$ releases 1.33×10^5 J, taking standard heats of formation as -343.0 kJ/mole for Rh_2O_3 and -1675.7 kJ/mole for Al_2O_3 (http://www.update.uu.se/~jolkkonen/pdf/CRC_TD.pdf).

²³⁶⁹ Ruthenium tetroxide (RuO_4) is a colorless volatile liquid that is a very aggressive oxidant (https://en.wikipedia.org/wiki/Ruthenium_tetroxide). The stoichiometry of the thermite-like reaction: $0.75RuO_4$ [0.124 kg, $3.76 \times 10^{-5} m^3$] + $2Al$ [0.054 kg, $2.00 \times 10^{-5} m^3$] $\rightarrow Al_2O_3 + 0.75Ru$ releases 1.50×10^5 J, taking standard heats of formation as -239.3 kJ/mole for RuO_4 and -1675.7 kJ/mole for Al_2O_3 (http://www.update.uu.se/~jolkkonen/pdf/CRC_TD.pdf).

SO ₃ + Al ²³⁷¹	1.22 x 10 ⁶	0.134	6.13 x 10 ⁻⁵
WO ₃ + Al ²³⁷²	8.33 x 10 ⁵	0.286	5.24 x 10 ⁻⁵
ZnO ₂ + Al ²³⁷³	1.24 x 10 ⁶	0.200	1.13 x 10 ⁻⁴
<u>Nonambient Combustibles: Propellants & Explosives</u>			
Acetylene + Nitrogen tetroxide ²³⁷⁴	1.27 x 10 ⁶	0.141	1.22 x 10 ⁻⁴
Aerozine 50 + Nitrogen tetroxide ²³⁷⁵	2.88 x 10 ⁶	0.216	2.03 x 10 ⁻⁴

²³⁷⁰ Selenium trioxide (SeO₃) is a white solid that is unstable to the dioxide (https://en.wikipedia.org/wiki/Selenium_trioxide). The stoichiometry of the thermite-like reaction: SeO₃ [0.127 kg, 3.69 x 10⁻⁵ m³] + 2Al [0.054 kg, 2.00 x 10⁻⁵ m³] → Al₂O₃ + Se, releases 1.16 x 10⁶ J, taking standard heats of formation as -1675.7 kJ/mole for Al₂O₃ (http://www.update.uu.se/~jolkkonen/pdf/CRC_TD.pdf) and -514.6 kJ/mole for SeO₃ (Ganesan AS, Raman effect in selenic acid and some selenates, 1934, p. 160; <http://www-old.ias.ac.in/jarch/proca/1/156-162.pdf>). (The more stable SeO₂ can also be used but provides 6% less specific energy, in MJ/kg.)

²³⁷¹ Sulfur trioxide (SO₃) is a white crystalline solid, under 290 K, that fumes in air (https://en.wikipedia.org/wiki/Sulfur_trioxide). The stoichiometry of the thermite-like reaction: SO₃ [0.0801 kg, 4.17 x 10⁻⁵ m³] + 2Al [0.054 kg, 2.00 x 10⁻⁵ m³] → Al₂O₃ + S, releases 1.22 x 10⁶ J, taking standard heats of formation as -454.5 kJ/mole for solid SO₃ and -1675.7 kJ/mole for Al₂O₃ (http://www.update.uu.se/~jolkkonen/pdf/CRC_TD.pdf).

²³⁷² Tungsten trioxide (WO₃) is a dense yellow powder (https://en.wikipedia.org/wiki/Tungsten_trioxide). The stoichiometry of the thermite-like reaction: WO₃ [0.232 kg, 3.24 x 10⁻⁵ m³] + 2Al [0.054 kg, 2.00 x 10⁻⁵ m³] → Al₂O₃ + W, releases 8.33 x 10⁵ J, taking standard heats of formation as -842.9 kJ/mole for WO₃ and -1675.7 kJ/mole for Al₂O₃ (http://www.update.uu.se/~jolkkonen/pdf/CRC_TD.pdf).

²³⁷³ Zinc peroxide (ZnO₂) is a bright yellow powder used as an oxidant in explosives and pyrotechnic mixtures (https://en.wikipedia.org/wiki/Zinc_peroxide). The stoichiometry of the thermite-like reaction: 1.5ZnO₂ [0.146 kg, 9.31 x 10⁻⁵ m³] + 2Al [0.054 kg, 2.00 x 10⁻⁵ m³] → Al₂O₃ + 1.5Zn releases 1.24 x 10⁶ J, taking standard heats of formation as -1675.7 kJ/mole for Al₂O₃ (http://www.update.uu.se/~jolkkonen/pdf/CRC_TD.pdf) and -292.1 kJ/mole for ZnO₂ (<http://pubs.acs.org/doi/abs/10.1021/es4020629>).

²³⁷⁴ A stoichiometric reaction of acetylene and nitrogen tetroxide, as C₂H₂ [0.026 kg, 4.24 x 10⁻⁵ m³] + 1.25N₂O₄ [0.115 kg, 7.98 x 10⁻⁵ m³] → 1.25N₂ + 2CO₂ + H₂O, taking standard heats of formation as +227.2 kJ/mole for C₂H₂, +11.1 kJ/mole for N₂O₄, -393.5 kJ/mole for CO₂, and -241.8 kJ/mole for H₂O (http://www.update.uu.se/~jolkkonen/pdf/CRC_TD.pdf), releases 1.27 x 10⁶ J. Liquid acetylene, regarded as highly explosive if any oxygen is present, can only exist above 1.27 atm pressure and has a density of 613 kg/m³ at -80 °C with MW of 0.026 kg/mole.

AgClO ₄ + Be ²³⁷⁶	2.53 x 10 ⁶	0.243	9.33 x 10 ⁻⁵
Ammonal ²³⁷⁷	4.78 x 10 ⁶	0.568	3.02 x 10 ⁻⁴
Aluminum + Ammonium dinitramide ²³⁷⁸	1.45 x 10 ⁶	0.160	8.18 x 10 ⁻⁵
Aluminum + Carbenium triazidoperchlorate ²³⁷⁹	3.18 x 10 ⁶	0.264	1.05 x 10 ⁻⁴
ANFO ²³⁸⁰	1.42 x 10 ⁷	3.748	4.46 x 10 ⁻³

²³⁷⁵ Aerozine 50 + nitrogen tetroxide are the fuel and oxidizer components of a hypergolic rocket propellant whose components spontaneously ignite when they come into contact with each other, that was used to power the Titan II ICBM rocket engines and also the engines of the Apollo Lunar Module and the Service Propulsion System engine in the Apollo CSM during the first Moon landing. Aerozine 50 is a mix of 50% hydrazine (N₂H₄) and 50% UDMH (unsymmetrical dimethylhydrazine, C₂H₈N₂) by weight (https://en.wikipedia.org/wiki/Aerozine_50). The stoichiometric combustion is: 2N₂H₄ [0.064 kg, 6.27 x 10⁻⁵ m³] + C₂H₈N₂ [0.0601 kg, 7.60 x 10⁻⁵ m³] + N₂O₄ [0.0920 kg, 6.38 x 10⁻⁵ m³] → 4N₂ + 2CO₂ + 8H₂O, taking standard heats of formation as +95.4 kJ/mole for N₂H₄, +48.3 kJ/mole for C₂H₈N₂, +11.1 kJ/mole for N₂O₄, -393.5 kJ/mole for CO₂, and -241.8 kJ/mole for H₂O (http://www.update.uu.se/~jolkkonen/pdf/CRC_TD.pdf), releasing 2.88 x 10⁶ J for every 0.216 kg or 2.03 x 10⁻⁴ m³ of propellant.

²³⁷⁶ The stoichiometric reaction of AgClO₄ [0.207 kg, 7.38 x 10⁻⁵ m³] + 4Be [0.036 kg, 1.95 x 10⁻⁵ m³] → 4BeO + AgCl releases 2.53 x 10⁶ J, taking standard heats of formation as -609.4 kJ/mole for BeO, -127.0 kJ/mole for AgCl (http://www.update.uu.se/~jolkkonen/pdf/CRC_TD.pdf), and -32.4 kJ/mole for AgClO₄ (Hermann WA. Synthetic Methods of Organometallic and Inorganic Chemistry, Georg Thieme Verlag, 1996, pp. 32-33).

²³⁷⁷ The assumed stoichiometric reaction of 6NH₄NO₃ [0.480 kg, 2.78 x 10⁻⁴ m³] + 6Al [0.162 kg, 6.0 x 10⁻⁵ m³] → 5N₂ + 3Al₂O₃ + 9H₂O + 2NH₃ (<https://en.wikipedia.org/wiki/Ammonal>), taking standard heats of formation as -365.6 kJ/mole for NH₄NO₃, -1675.7 kJ/mole for Al₂O₃, -241.8 kJ/mole for H₂O, and -45.9 kJ for NH₃ (http://www.update.uu.se/~jolkkonen/pdf/CRC_TD.pdf), releases 5.10 x 10⁶ J. Ignoring the ~3% charcoal component, ammonal is approximately 82% (NH₄NO₃ + Al) plus 18% TNT (see above), giving a total combustion energy of 4.78 x 10⁶ J using 0.568 kg of reactants of volume 3.02 x 10⁻⁴ m³.

²³⁷⁸ Ammonium dinitramide, aka. ADN (NH₄⁺N(NO₂)₂⁻, 0.124 kg/mole, solid density 1810 kg/m³, heat of formation -148.1 kJ/mole), “is a chlorine free oxidizer that has been considered a possible ammonium perchlorate replacement for the last 20 years....ADN was secretly discovered in 1971 in the former USSR, and is believed to have been used in operational missile systems.” (<https://www.diva-portal.org/smash/get/diva2:360054/FULLTEXT01.pdf>). A stoichiometric combustion according to NH₄⁺N(NO₂)₂⁻ + 4/3 Al [0.027 kg/mole, 2700 kg/m³] → 2N₂ + 2H₂O + 2/3 Al₂O₃, taking the standard heats of formation as -148.1 kJ/mole for NH₄⁺N(NO₂)₂⁻, -241.8 kJ/mole for H₂O, and -1675.7 kJ/mole for Al₂O₃ (http://www.update.uu.se/~jolkkonen/pdf/CRC_TD.pdf), releases 1.45 x 10⁶ J.

²³⁷⁹ Solid carbenium triazidoperchlorate (C(N₃)₃ClO₄, 0.237 kg/mole, assumed density ~2500 kg/m³, +1946 kJ/mole heat of formation; Christie KO, *et al.* Recent progress in the theory and synthesis of novel high energy density materials, in Carrick PG, Williams NT. Proceedings of the HEDM Contractors' Conference, Air Force Materiel Command, PL-TR-96-3037, March 1997, 152-155; <http://www.dtic.mil/cgi-bin/GetTRDoc?AD=ADA325307>). Assuming the stoichiometric reaction: C(N₃)₃ClO₄ [0.237 kg] + Al [0.027 kg] → 4.5N₂ + 0.5Al₂O₃ + CO₂ + 0.5Cl₂ + 0.25O₂, the energy release is 3.18 x 10⁶ J/mole, taking heats of formation as -1675.7 kJ/mole for Al₂O₃ and -393.5 kJ/mole for CO₂ (http://www.update.uu.se/~jolkkonen/pdf/CRC_TD.pdf).

ANNM ²³⁸¹	1.64×10^6	0.362	2.46×10^{-4}
Armstrong's mixture ²³⁸²	2.10×10^6	0.381	1.52×10^{-4}
Diborane + Nitric oxide ²³⁸³	2.656×10^6	0.2077	2.03×10^{-4}

²³⁸⁰ ANFO, or Ammonium Nitrate (94% by wt.) + #2 Fuel Oil (6% by wt.), accounts for an estimated 80% of the 2.7 million tonnes of explosives used annually in North America (<https://en.wikipedia.org/wiki/ANFO>). #2 fuel oil is a distillate Home Heating Oil (HHO) with hydrocarbons in the 14- to 20-carbon atom range, energy density of ~38.6 MJ/liter, and density ~950 kg/m³ (https://en.wikipedia.org/wiki/Heating_oil). A 94%/6% stoichiometric combustion of ammonium nitrate and HHO (proxied by hexadecane), crudely approximated by $44\text{NH}_4\text{NO}_3 [3.522 \text{ kg}] + \text{C}_{16}\text{H}_{34} [0.226 \text{ kg}] \rightarrow 44\text{N}_2 + 13.5\text{CO}_2 + 105\text{H}_2\text{O} + 2.5\text{C}$, taking the standard heats of formation as -365.6 kJ/mole for NH₄NO₃, -374.8 kJ/mole for C₁₆H₃₄, -393.5 kJ/mole for CO₂, and -241.8 kJ/mole for H₂O (http://www.update.uu.se/~jolkkonen/pdf/CRC_TD.pdf), releases 1.42×10^7 J. Working ANFO is loosely packed to a density of only ~840 kg/m³, so we apply that density to obtain the volume estimate.

²³⁸¹ The stoichiometric reaction of Ammonium Nitrate and NitroMethane (ANNM) is $3\text{NH}_4\text{NO}_3 [0.240 \text{ kg}, 1.39 \times 10^{-4} \text{ m}^3] + 2\text{CH}_3\text{NO}_2 [0.122 \text{ kg}, 1.07 \times 10^{-4} \text{ m}^3] \rightarrow 4\text{N}_2 + 2\text{CO}_2 + 9\text{H}_2\text{O}$ (<https://en.wikipedia.org/wiki/ANFO#ANNM>), taking standard heats of formation as -365.6 kJ/mole for NH₄NO₃, -112.6 kJ/mole for CH₃NO₂, -393.5 kJ/mole for CO₂, and -241.8 kJ/mole for H₂O (http://www.update.uu.se/~jolkkonen/pdf/CRC_TD.pdf), releases 1.64×10^6 J.

²³⁸² Armstrong's mixture is a highly sensitive primary explosive whose primary ingredients are red phosphorus and strong oxidizer such as potassium chlorate or potassium perchlorate. Because of its sensitivity to shock, friction and flame, Armstrong's mixture is an extremely dangerous contact explosive that can explode violently in an enclosed space, depending on composition, conditions and quantity (https://en.wikipedia.org/wiki/Armstrong%27s_mixture). In his teenage pyrotechnic years, the author accidentally blew up the chemistry lab while mixing up a rather large batch of one favored variant having the approximate stoichiometry: $2\text{KClO}_4 [0.277 \text{ kg}, 1.10 \times 10^{-4} \text{ m}^3] + 2\text{Al} [0.054 \text{ kg}, 2 \times 10^{-5} \text{ m}^3] + 1.6\text{P}(\text{red}) [0.050 \text{ kg}, 2.17 \times 10^{-5} \text{ m}^3] \rightarrow \text{K}_2\text{O} + \text{Al}_2\text{O}_3 + 0.8\text{P}_2\text{O}_5 + \text{Cl}_2$, which, taking the standard heats of formation for components as -432.8 kJ/mole for KClO₄, -361.5 kJ/mole for K₂O, -1675.7 kJ/mole for Al₂O₃, and -254.12 kJ/mole for P₂O₅ (http://www.update.uu.se/~jolkkonen/pdf/CRC_TD.pdf), releases 2.10×10^6 J, or 5.51 MJ/kg of reactants. (One possible alternative reaction that avoids generating free chlorine, or $2\text{KClO}_4 + 2\text{Al} + 2\text{P}(\text{red}) \rightarrow \text{Al}_2\text{O}_3 + \text{P}_2\text{O}_5 + 2\text{KCl}$, yields a slightly lower specific energy at 4.93 MJ/kg.) The heat of formation used here for P₂O₅, the phosphorus oxide generated when a sufficiency of oxygen is present, is the dense α -orthorhombic form (3500 kg/m³) whose heat of formation lies -14.84 kJ/mole lower in energy than the -239.28 kJ/mole heat of formation for the less-dense, most common metastable hexagonal form (2300 kg/m³); Rustad JR. Density functional calculations of the enthalpies of formation of rare-earth orthophosphates. Amer Mineralogist 2012;97:791-799; http://minsocam.org/MSA/AmMin/toc/Abstracts/2012_Abstracts/MJ12_Abstracts/Rustad_p791-799_12.pdf.

Gunpowder (black powder) ²³⁸⁴	3.0×10^6	1	5.71×10^{-4}
Hydrazine + Nitrogen tetroxide ²³⁸⁵	1.17×10^6	0.156	1.27×10^{-4}
Hydrogen + Nitrous oxide ²³⁸⁶	3.23×10^5	0.046	3.91×10^{-5}
KClO ₃ + Al (Flash powder) ²³⁸⁷	1.71×10^6	0.1766	7.28×10^{-5}

²³⁸³ Liquid diborane (B₂H₆, 0.0277 kg/mole, 447 kg/m³; <https://pubchem.ncbi.nlm.nih.gov/compound/diborane#section=Density>) plus liquid nitric oxide (NO, 0.030 kg/mole, 1281 kg/m³; <http://encyclopedia.airliquide.com/Encyclopedia.asp?GasID=44#GeneralData>), in the most energetically favorable combustion (B₂H₆ + 6NO → 3N₂ + 2HBO₂ + 2H₂O) using liquid oxygen (LOX: density 1141 kg/m³, MW 0.032 kg/mole), would consume 0.0277 kg of B₂H₆ and 0.180 kg of NO, and release 2.656×10^6 J, taking heats of formation as +36.4 kJ/mole for B₂H₆, +91.3 kJ/mole for NO, -794.3 kJ/mole for HBO₂ (metaboric acid), and -241.8 kJ/mole for H₂O (http://www.update.uu.se/~jolkkonen/pdf/CRC_TD.pdf). An extensive analysis of this particular reaction found that the principal boron-containing product in the burnt gases was HBO₂, not B₂O₃ (whose stoichiometry indeed produces slightly less energy, 2.583×10^6 J/mole of diborane); Wolfhard HG, Clark AH, Vanpee M. Characteristics of diborane flames. AIAA Prog Astronautics Aeronautics: Heterog. Combust. 1964:327-343.

²³⁸⁴ Gunpowder, aka. black powder, is composed of 75% potassium nitrate, 15% charcoal, and 10% sulfur by weight, with a mass density of ~1750 kg/m³ (<http://www.lr.tudelft.nl/en/organisation/departments/space-engineering/space-systems-engineering/expertise-areas/space-propulsion/design-of-elements/rocket-propellants/solids/>) with an energy content of ~3 MJ/kg (https://en.wikipedia.org/wiki/Gunpowder#Combustion_characteristics). Charcoal is a partially pyrolyzed cellulose, not pure carbon, which leads to many reaction complexities; a simplistic stoichiometric equation that preserves the 75%/15%/10% mixture by weight while using pure amorphous carbon (30KNO₃ [3.033 kg] + 50C [0.600 kg] + 11S [0.396 kg] → 11K₂S + 4K₂CO₃ + 32CO₂ + 14CO + 15N₂) yields only 2 MJ/kg using the standard heats of formation for these compounds (http://www.update.uu.se/~jolkkonen/pdf/CRC_TD.pdf), so the influence of the charcoal composition is apparently substantial.

²³⁸⁵ Hydrazine and nitrogen tetroxide are the fuel and oxidizer components of a common hypergolic rocket propellant whose components spontaneously ignite when they come into contact with each other. The stoichiometric combustion of N₂O₄ [0.092 kg, 6.38×10^{-5} m³] + 2N₂H₄ [0.064 kg, 6.27×10^{-5} m³] → 3N₂ + 4H₂O, taking standard heats of formation as +11.1 kJ/mole for N₂O₄, +95.4 kJ/mole for N₂H₄, and -241.8 kJ/mole for H₂O (http://www.update.uu.se/~jolkkonen/pdf/CRC_TD.pdf), releases 1.17×10^6 J.

²³⁸⁶ Assuming a density of 600 kg/m³ with a MW of 0.002 kg/mole for compressed solid H₂ and a density of 1230 kg/m³ with a MW of 0.044 kg/mole for liquid N₂O (<http://encyclopedia.airliquide.com/Encyclopedia.asp?GasID=55>), a stoichiometric reaction (H₂ + N₂O → H₂O + N₂) consumes 0.002 kg of H₂ and 0.044 kg of N₂O and releases 2.418×10^5 J/mole of H₂O(g) plus 8.16×10^4 J/mole of N₂O (standard heats of formation); http://www.update.uu.se/~jolkkonen/pdf/CRC_TD.pdf. “Nitrous oxide can be used as an oxidizer in a rocket motor. This has the advantages over other oxidisers in that it is not only non-toxic, but also, due to its stability at room temperature, easy to store and relatively safe to carry on a flight.” https://en.wikipedia.org/wiki/Nitrous_oxide.

²³⁸⁷ The stoichiometric reaction of KClO₃ [0.1226 kg, 5.28×10^{-5} m³] + 2Al [0.054 kg, 2.0×10^{-5} m³] → Al₂O₃ + KCl, taking standard heats of formation as -397.7 kJ/mole for KClO₃, -1675.7 kJ/mole for Al₂O₃, and -436.5 kJ/mole for KCl (http://www.update.uu.se/~jolkkonen/pdf/CRC_TD.pdf), releases 1.71×10^6 J, or 9.71 MJ/kg of reactants. (One source (https://en.wikipedia.org/wiki/Flash_powder) claims the correct stoichiometry is 6KClO₃ + 10Al → 3K₂O + 5Al₂O₃ + 3Cl₂, but this reaction only yields 7.04 MJ/kg.)

KClO ₄ + Al (Flash powder) ²³⁸⁸	6.71 x 10 ⁶	0.632	2.45 x 10 ⁻⁴
KNO ₃ + Mg (Flash powder) ²³⁸⁹	2.38 x 10 ⁶	0.324	1.66 x 10 ⁻⁴
LiClO ₄ + Al ²³⁹⁰	1.70 x 10 ⁶	0.134	5.29 x 10 ⁻⁵
LiClO ₄ + B ²³⁹¹	1.29 x 10 ⁶	0.101	4.21 x 10 ⁻⁵
LiClO ₄ + Be ²³⁹²	2.47 x 10 ⁶	0.142	6.33 x 10 ⁻⁵
Panclastites ²³⁹³	7.21 x 10 ⁵	0.168	1.23 x 10 ⁻⁴
Rocket candy ²³⁹⁴	2.13 x 10 ⁶	0.978	5.17 x 10 ⁻⁴

²³⁸⁸ The stoichiometric reaction of 3KClO₄ [0.416 kg, 1.65 x 10⁻⁴ m³] + 8Al [0.216 kg, 8.0 x 10⁻⁵ m³] → 4Al₂O₃ + 3KCl, taking standard heats of formation as -432.8 kJ/mole for KClO₄, -1675.7 kJ/mole for Al₂O₃, and -436.5 kJ/mole for KCl (http://www.update.uu.se/~jolkkonen/pdf/CRC_TD.pdf), releases 6.71 x 10⁶ J, or 10.62 MJ/kg of reactants. (One source (https://en.wikipedia.org/wiki/Flash_powder) claims the correct stoichiometry is 6KClO₄ + 14Al → 3K₂O + 7Al₂O₃ + 3Cl₂, but this reaction only yields 8.45 MJ/kg.)

²³⁸⁹ The stoichiometric reaction of 2KNO₃ [0.2022 kg, 9.59 x 10⁻⁵ m³] + 5Mg [0.1215 kg, 6.99 x 10⁻⁵ m³] → K₂O + N₂ + 5MgO (https://en.wikipedia.org/wiki/Flash_powder), taking standard heats of formation as -494.6 kJ/mole for KNO₃, -361.5 kJ/mole for K₂O, and -601.6 kJ/mole for MgO (http://www.update.uu.se/~jolkkonen/pdf/CRC_TD.pdf), releases 2.38 x 10⁶ J.

²³⁹⁰ The stoichiometric reaction of 0.75LiClO₄ [0.0795 kg, 3.29 x 10⁻⁵ m³] + 2Al [0.054 kg, 2.0 x 10⁻⁵ m³] → Al₂O₃ + 0.75LiCl, taking standard heats of formation as -381.0 kJ/mole for LiClO₄, -1675.7 kJ/mole for Al₂O₃, and -408.6 kJ/mole for LiCl (http://www.update.uu.se/~jolkkonen/pdf/CRC_TD.pdf), releases 1.70 x 10⁶ J.

²³⁹¹ The stoichiometric reaction of 0.75LiClO₄ [0.0795 kg, 3.29 x 10⁻⁵ m³] + 2B [0.0216 kg, 9.23 x 10⁻⁶ m³] → B₂O₃ + 0.75LiCl, taking standard heats of formation as -381.0 kJ/mole for LiClO₄, -1273.5 kJ/mole for B₂O₃, and -408.6 kJ/mole for LiCl (http://www.update.uu.se/~jolkkonen/pdf/CRC_TD.pdf), releases 1.29 x 10⁶ J.

²³⁹² The stoichiometric reaction of LiClO₄ [0.106 kg, 4.38 x 10⁻⁵ m³] + 4Be [0.036 kg, 1.95 x 10⁻⁵ m³] → 4BeO + LiCl, taking standard heats of formation as -381.0 kJ/mole for LiClO₄, -609.4 kJ/mole for BeO, and -408.6 kJ/mole for LiCl (http://www.update.uu.se/~jolkkonen/pdf/CRC_TD.pdf), releases 2.47 x 10⁶ J.

²³⁹³ Panclastites are a mixture of liquid nitrogen tetroxide serving as oxidizer with a suitable fuel, e.g. carbon disulfide (<https://en.wikipedia.org/wiki/Panclastite>). The assumed stoichiometric reaction of N₂O₄ [0.092 kg, 6.38 x 10⁻⁵ m³] + CS₂ [0.076 kg, 5.89 x 10⁻⁵ m³] → C + 2SO₂ + 5N₂, taking standard heats of formation as +11.1 kJ/mole for N₂O₄, +116.7 kJ/mole for CS₂, and -296.8 kJ/mole for SO₂ (http://www.update.uu.se/~jolkkonen/pdf/CRC_TD.pdf), releases 7.21 x 10⁵ J.

²³⁹⁴ Rocket candy, aka. R-Candy, caramel candy, candy rocket, or KNSU (https://en.wikipedia.org/wiki/Rocket_candy), is a rocket fuel once used by the author and many other pyrotechnic hobbyists and amateur rocketry enthusiasts, consisting of 65% potassium nitrate (KNO₃, 0.1011 kg/mole, 2109 kg/m³) + 35% sucrose or table sugar (C₁₂H₂₂O₁₁, 0.3423 kg/mole, 1587 kg/m³) by weight (<http://www.nakka-rocketry.net/sucrose.html>) that burns at ~1700 K and ~1000 psi. According to one serious hobbyist (<http://www.nakka-rocketry.net/succhem.html>), the complete theoretical combustion formula is: C₁₂H₂₂O₁₁ + 6.288 KNO₃ → 3.796 CO₂ + 5.205 CO + 7.794 H₂O + 3.065 H₂ + 3.143 N₂ + 2.998 K₂CO₃ + 0.274 KOH; using standard heats of formation (http://www.update.uu.se/~jolkkonen/pdf/CRC_TD.pdf), the combustion of 0.978 kg of propellant having a volume of 5.17 x 10⁻⁴ m³ releases 2.13 x 10⁶ J of combustion energy.

Space Shuttle Solid Rocket Booster (SRB) propellant ²³⁹⁵	2.61×10^6	0.307	1.48×10^{-4}
UDMH + Nitrogen tetroxide ²³⁹⁶	1.82×10^6	0.244	2.04×10^{-4}
ZS propellants ²³⁹⁷	2.06×10^5	0.0975	2.47×10^{-5}

²³⁹⁵ The rocket propellant mixture in each Space Shuttle solid rocket booster, commonly referred to as Ammonium Perchlorate Composite Propellant or APCP, consisted of ammonium perchlorate (oxidizer, 69.8% by weight), atomized aluminum powder (fuel, 16%), iron oxide (catalyst, 0.2%), PBAN (binder, also acts as fuel, 12%), and an epoxy curing agent (2%) (https://en.wikipedia.org/wiki/Space_Shuttle_Solid_Rocket_Booster). The stoichiometric reaction of $2\text{NH}_4\text{ClO}_4$ [0.235 kg , $1.21 \times 10^{-4} \text{ m}^3$] + $8/3 \text{ Al}$ [0.072 kg , $2.67 \times 10^{-5} \text{ m}^3$] $\rightarrow \text{N}_2 + 4/3 \text{ Al}_2\text{O}_3 + 4\text{H}_2\text{O} + \text{Cl}_2$, a good proxy for the APCP mixture, and taking the standard heats of formation as -295.3 kJ/mole for NH_4ClO_4 , -1675.7 kJ/mole for Al_2O_3 , and -241.8 kJ/mole for H_2O (http://www.update.uu.se/~jolkkonen/pdf/CRC_TD.pdf), releases $2.61 \times 10^6 \text{ J}$. The SRB contains $\sim 500,000 \text{ kg}$ of APCP which is consumed during a 127 sec burn time, generating ~ 33.5 gigawatts.

²³⁹⁶ UDMH (unsymmetrical dimethylhydrazine, $\text{C}_2\text{H}_8\text{N}_2$; https://en.wikipedia.org/wiki/Unsymmetrical_dimethylhydrazine) + nitrogen tetroxide are the fuel and oxidizer components of a hypergolic rocket propellant that is used in the three first stages of the Russian Proton booster, the Indian Vikas engine for PSLV and GSLV rockets, and most Chinese boosters. The stoichiometric combustion is: $\text{C}_2\text{H}_8\text{N}_2$ [0.0601 kg , $7.60 \times 10^{-5} \text{ m}^3$] + $2\text{N}_2\text{O}_4$ [0.184 kg , $1.28 \times 10^{-4} \text{ m}^3$] $\rightarrow 3\text{N}_2 + 2\text{CO}_2 + 4\text{H}_2\text{O}$, taking standard heats of formation as $+48.3 \text{ kJ/mole}$ for $\text{C}_2\text{H}_8\text{N}_2$, $+11.1 \text{ kJ/mole}$ for N_2O_4 , -393.5 kJ/mole for CO_2 , and -241.8 kJ/mole for H_2O (http://www.update.uu.se/~jolkkonen/pdf/CRC_TD.pdf), releasing $1.82 \times 10^6 \text{ J}$ for every 0.244 kg or $2.04 \times 10^{-4} \text{ m}^3$ of propellant.

²³⁹⁷ The stoichiometric reaction of Zn [0.0654 kg/mole , $9.16 \times 10^{-6} \text{ m}^3/\text{mole}$] + S [0.0321 kg/mole , $1.55 \times 10^{-5} \text{ m}^3/\text{mole}$] $\rightarrow \text{ZnS}$, taking standard heats of formation as -206.0 kJ/mole for ZnS (http://www.update.uu.se/~jolkkonen/pdf/CRC_TD.pdf), releases $2.06 \times 10^5 \text{ J}$. “Composed of powdered zinc metal and powdered sulfur (oxidizer), ZS or ‘micrograin’ is another pressed propellant that does not find any practical application outside specialized amateur rocketry circles due to its poor performance (as most ZS burns outside the combustion chamber) and incredibly fast linear burn rates on the order of 2 m/s . ZS is most often employed as a novelty propellant as the rocket accelerates extremely quickly leaving a spectacular large orange fireball behind it” (https://en.wikipedia.org/wiki/Solid-fuel_rocket#Zinc.E2.80.93sulfur_.28ZS.29_propellants).

A.5 Data on Energy Storage in Radionuclides²³⁹⁸

Table A5. Power and energy data for α -emitting radionuclides with half-life ≥ 1 day						
Element	Atomic Number (# of protons)	Mass Number (gm/mole)	Half-Life (sec)	α Decay Energy (MeV)	Density (kg/m ³)	Nuclear Decay Products
Nd	60	144	7.22×10^{22}	1.9052	7010	α (100%)
Sm	62	146	3.25×10^{15}	2.5284	7520	α (100%)
Sm	62	147	3.34×10^{18}	2.31046	7520	α (100%)
Sm	62	148	2.20×10^{23}	1.98608	7520	α (100%)
Sm	62	149	6.31×10^{22}	1.8703	7520	α (100%), predicted
Eu	63	151	1.58×10^{26}	1.964	5264	α (100%)
Gd	64	148	2.24×10^9	3.27121	7900	α (100%) + $2\beta^+$ (rare)
Gd	64	150	5.64×10^{13}	2.80819	7900	α (100%) + $2\beta^+$ (rare)
Gd	64	152	3.41×10^{21}	2.20305	7900	α (100%) + $2\beta^+$ (rare)
Dy	66	154	9.50×10^{13}	2.94569	8540	α (100%) + $2\beta^+$ (rare)
Hf	72	174	6.30×10^{22}	2.49742	13,310	α (100%) + $2\beta^+$ (rare)
W	74	180	5.68×10^{25}	2.50812	19,300	α (100%) + $2\beta^+$ (rare)
W	74	182	2.62×10^{26}	1.77183	19,300	α (100%), predicted
W	74	183	4.10×10^{26}	1.68	19,300	α (100%), predicted
W	74	184	9.15×10^{26}	1.65618	19,300	α (100%), predicted
Os	76	186	6.30×10^{22}	2.82312	22,590	α (100%)
Pt	78	190	2.05×10^{19}	3.25114	21,450	α (100%) + $2\beta^+$ (rare)
Pb	82	204	4.42×10^{24}	1.96949	11,340	α (100%), predicted
Bi	83	209	5.99×10^{26}	3.13721	9780	α (100%)
Po	84	208	9.14×10^7	5.2153	9196	α (100%) + β^+ (0.00223%)
Po	84	209	3.22×10^9	4.79723	9196	α (100%) + β^+ (0.47%)
Po	84	210	1.20×10^7	5.40745	9196	α (100%)
Ra	88	223	9.87×10^5	5.97899	5500	α (100%) + ^{14}C (8.9×10^{-8} %)
Ra	88	224	3.14×10^5	5.78885	5500	α (100%) + ^{14}C (4×10^{-9} %)
Ra	88	226	5.00×10^{10}	4.87062	5500	α (100%) + ^{14}C (2.6×10^{-9} %) + $2\beta^-$ (1.89×10^{-6} %)
Ac	89	225	8.60×10^5	5.93508	10,000	α (100%) + ^{14}C (6×10^{-10} %)
Th	90	227	1.61×10^6	6.1466	11,700	α (100%)
Th	90	228	6.03×10^7	5.52008	11,700	α (100%) + ^{20}O (1.13×10^{-11} %)
Th	90	229	2.49×10^{11}	5.16757	11,700	α (100%)
Th	90	230	2.38×10^{12}	4.76996	11,700	α (100%) + ^{24}Ne (5.6×10^{-11} %) + SF (5×10^{-11} %)
Th	90	232	4.43×10^{17}	4.0816	11,700	α (100%) + SF (1.1×10^{-9} %) + $^{24}\text{Ne}/^{26}\text{Ne}$ (2.78×10^{-10} %) + $2\beta^-$ (rare)

²³⁹⁸ Data from Theodore Gray: <http://www.periodictable.com/Isotopes/001.1/index2.full.dm.prod.html>.

Pa	91	231	1.03×10^{12}	5.14987	15,370	α (100%) + ^{24}Ne (1.34×10^{-9} %) + SF (3×10^{-10} %) + ^{23}F (9.9×10^{-13} %)
U	92	230	1.80×10^6	5.99273	19,100	α (100%) + SF (1.4×10^{-10} %) + ^{22}Ne (4.8×10^{-12} %) + $2\beta^+$ (rare)
U	92	232	2.17×10^9	5.41363	19,100	α (100%) + ^{24}Ne (8.9×10^{-10} %) + ^{28}Mg (5×10^{-12} %) + SF (1×10^{-12} %)
U	92	233	5.02×10^{12}	4.90853	19,100	α (100%) + SF (6×10^{-9} %) + ^{24}Ne (7.2×10^{-11} %) + ^{28}Mg (1.3×10^{-13} %)
U	92	234	7.74×10^{12}	4.85773	19,100	α (100%) + SF (1.73×10^{-9} %) + ^{28}Mg (1.4×10^{-11} %) + $^{24}\text{Ne}/^{26}\text{Ne}$ (9×10^{-12} %)
U	92	235	2.22×10^{16}	4.67826	19,100	α (100%) + SF (7×10^{-9} %) + ^{28}Mg (8×10^{-10} %) + ^{25}Ne (8×10^{-10} %) + ^{20}Ne (8×10^{-10} %)
U	92	236	7.39×10^{14}	4.5731	19,100	α (100%) + SF (9.6×10^{-8} %)
U	92	238	1.41×10^{17}	4.26975	19,100	α (100%) + SF (5.45×10^{-5} %) + $2\beta^-$ (2.2×10^{-10} %)
Np	93	237	6.76×10^{13}	4.95826	19,380	α (100%) + SF (2×10^{-10} %) + ^{30}Mg (4×10^{-12} %)
Pu	94	236	9.01×10^7	5.86707	19,816	α (100%) + SF (1.36×10^{-7} %) + ^{28}Mg (2×10^{-12} %) + $2\beta^+$ (rare)
Pu	94	238	2.77×10^9	5.5932	19,816	α (100%) + SF (1.9×10^{-7} %) + ^{32}Si (1.4×10^{-14} %) + $^{28}\text{Mg}/^{30}\text{Mg}$ (6×10^{-15} %)
Pu	94	239	7.60×10^{11}	5.24451	19,816	α (100%) + SF (3.1×10^{-10} %)
Pu	94	240	2.07×10^{11}	5.25575	19,816	α (100%) + SF (5.7×10^{-6} %) + ^{34}Si (1.3×10^{-13} %)
Pu	94	242	1.18×10^{13}	4.98453	19,816	α (100%) + SF (5.5×10^{-4} %)
Pu	94	244	2.50×10^{15}	4.66554	19,816	α (100%) + SF (0.121 %) + $2\beta^-$ (7.3×10^{-9} %)
Am	95	241	1.36×10^{10}	5.63782	12,000	α (100%) + SF (4.3×10^{-10} %) + ^{34}Si (7.4×10^{-14} %)
Am	95	243	2.33×10^{11}	5.43881	12,000	α (100%) + SF (3.7×10^{-9} %)
Cm	96	240	2.30×10^6	6.3978	13,510	α (100%) + EC (0.5 %) + SF (3.9×10^{-6} %)
Cm	96	242	1.41×10^7	6.21556	13,510	α (100%) + SF (6.2×10^{-6} %) + ^{34}Si (1.1×10^{-14} %) + $2\beta^+$ (rare)
Cm	96	243	9.18×10^8	6.1688	13,510	α (100%) + EC (0.29 %) + SF (5.3×10^{-9} %)
Cm	96	244	5.71×10^8	5.90174	13,510	α (100%) + SF (1.37×10^{-4} %)
Cm	96	245	2.70×10^{11}	5.623	13,510	α (100%) + SF (6.1×10^{-7} %)
Cm	96	246	1.50×10^{11}	5.47513	13,510	α (100%) + SF (0.02615 %)
Cm	96	247	4.92×10^{14}	5.35348	13,510	α (100%)
Cm	96	248	1.10×10^{13}	5.16173	13,510	α (91.61 %) + SF (8.39 %) + $2\beta^-$ (rare)
Bk	97	247	4.35×10^{10}	5.8896	14,780	α (100%) + SF (rare)
Bk	97	248	3.00×10^8	5.774	14,780	α (~100%)
Cf	98	246	1.29×10^5	6.8616	15,100	α (100%) + EC (0.004 %) + SF (2.5×10^{-4} %)
Cf	98	248	2.88×10^7	6.3612	15,100	α (100%) + SF (0.0029 %)
Cf	98	249	1.11×10^{10}	6.296	15,100	α (100%) + SF (5×10^{-7} %)
Cf	98	250	4.18×10^8	6.12844	15,100	α (100%) + SF (0.077 %)
Cf	98	251	2.83×10^{10}	6.1758	15,100	α (100%) + SF (rare)

Cf	98	252	8.34×10^7	6.21687	15,100	α (96.908 %) + SF (3.092 %)
Es	99	252	4.07×10^7	6.789	8840	α (78 %) + EC (22 %)
Es	99	253	1.77×10^6	6.73916	8840	α (100%) + SF (8.7×10^{-6} %)
Es	99	254	2.38×10^7	6.6157	8840	α (100%) + EC (0.03 %) + β^- (1.74×10^{-4} %) + SF (3×10^{-6} %)
Fm	100	252	9.14×10^4	7.1527	9700	α (100%) + SF (0.0023 %) + $2\beta^+$ (rare)
Fm	100	257	8.68×10^6	6.86355	9700	α (100%) + SF (0.21 %)
Md	101	258	4.45×10^6	7.27128	10,300	α (100%) + β^- (0.0015 %) + β^+ (0.0015 %)
SF = Spontaneous Fission EC = Electron Capture						

A.6 Data on Energy Storage in Spontaneous Fission²³⁹⁹

Table A6. Power and energy data for spontaneous fission (SF) radionuclides with SF branch ratio $\geq 0.1\%$ and half-life ≥ 1 day

Element	Atomic Number (# of protons)	Mass Number (gm/mole)	Half-Life (sec)	SF Decay Energy (MeV)	Density (kg/m ³)	SF Branch Ratio	Specific Power (MW/kg)
Pu	94	244	2.50×10^{15}	212.28	19,816	0.121	2.82×10^{-11}
Cm	96	234	5.10×10^1	203.58	13,510	3	3.42×10^4
Cm	96	248	1.10×10^{13}	215.76	13,510	8.39	4.44×10^{-7}
Cm	96	250	2.61×10^{11}	217.5	13,510	74	1.65×10^{-4}
Cf	98	252	8.34×10^7	219.24	15,100	3.092	2.16×10^{-2}
Cf	98	254	5.23×10^6	220.98	15,100	99.69	1.11×10^1
Cf	98	237	2.10	206.19	15,100	10	2.77×10^6
Cf	98	238	2.11×10^{-2}	207.06	15,100	100	2.76×10^9
Cf	98	240	5.76×10^1	208.8	15,100	2	2.02×10^4
Cf	98	256	7.38×10^2	222.72	15,100	100	7.88×10^4
Es	99	242	1.35×10^1	210.54	8840	0.6	2.59×10^4
Fm	100	241	7.30×10^{-4}	209.67	9700	78	6.22×10^{10}
Fm	100	242	8.00×10^{-4}	210.54	9700	100	7.27×10^{10}
Fm	100	243	2.31×10^{-1}	211.41	9700	0.57	1.44×10^6
Fm	100	244	3.12×10^{-3}	212.28	9700	99.6	1.86×10^{10}
Fm	100	245	4.20	213.15	9700	0.13	1.80×10^4
Fm	100	246	1.54	214.02	9700	4.5	1.70×10^6
Fm	100	248	3.51×10^1	215.76	9700	0.1	1.66×10^3
Fm	100	256	9.46×10^3	222.72	9700	91.9	5.65×10^3
Fm	100	257	8.68×10^6	223.59	9700	0.21	1.41×10^{-2}
Fm	100	258	3.70×10^{-4}	224.46	9700	100	1.57×10^{11}
Md	101	245	9.00×10^{-4}	213.15	10,300	100	6.46×10^{10}
Md	101	247	1.12	214.89	10,300	100	5.20×10^7
Md	101	255	1.62×10^3	221.85	10,300	0.15	5.39×10^1
Md	101	256	4.60×10^3	222.72	10,300	3	3.79×10^2
Md	101	257	1.99×10^4	223.59	10,300	4	1.17×10^2
Md	101	258m	3.42×10^3	224.46	10,300	20	3.40×10^3
Md	101	259	5.80×10^3	225.33	10,300	98.7	9.90×10^3
Md	101	260	2.40×10^6	226.2	10,300	86.5	2.10×10^1
No	102	250	4.20×10^{-6}	217.5	9900	99.9	1.38×10^{13}
No	102	251	8.00×10^{-1}	218.37	9900	0.3	2.18×10^5
No	102	252	2.44	219.24	9900	32.2	7.68×10^6
No	102	254	5.10×10^1	220.98	9900	0.17	1.94×10^3
No	102	256	2.91	222.72	9900	0.53	1.06×10^5

²³⁹⁹ Data from Theodore Gray: <http://www.periodictable.com/Isotopes/001.1/index2.full.dm.prod.html>.

No	102	258	1.20×10^{-3}	224.46	9900	100	4.85×10^{10}
No	102	259	3.50×10^{-3}	225.33	9900	10	1.66×10^3
No	102	262	5.00×10^{-3}	227.94	9900	100	1.16×10^{10}
Lr	103	252	3.60×10^{-1}	219.24	16,100	1	1.62×10^6
Lr	103	253	5.70×10^{-1}	220.11	16,100	2.6	2.65×10^6
Lr	103	255	2.20×10^1	221.85	16,100	1	2.64×10^4
Lr	103	259	6.20	225.33	16,100	22	2.06×10^6
Lr	103	262	1.44×10^4	227.94	16,100	10	4.04×10^2
Rf	104	253	1.30×10^{-2}	220.11	23,200	50	2.24×10^9
Rf	104	254	2.30×10^{-5}	220.98	23,200	98.5	2.49×10^{12}
Rf	104	255	1.68	221.85	23,200	52	1.80×10^7
Rf	104	256	6.45×10^{-3}	222.72	23,200	99.68	8.99×10^9
Rf	104	257	4.70	223.59	23,200	1.4	1.73×10^5
Rf	104	258	1.20×10^{-2}	224.46	23,200	87	4.22×10^9
Rf	104	259	3.20	225.33	23,200	8	1.45×10^6
Rf	104	260	2.10×10^{-2}	226.2	23,200	98	2.72×10^9
Rf	104	261	6.50×10^1	227.07	23,200	40	3.58×10^5
Rf	104	262	2.30	227.94	23,200	99.2	2.51×10^7
Rf	104	263	6.00×10^2	228.81	23,200	70	6.79×10^4
Db	105	255	1.59	221.85	29,300	20	7.33×10^6
Db	105	257	1.50	223.59	29,300	6	2.33×10^6
Db	105	258	4.00	224.46	29,300	1	1.45×10^5
Db	105	260	1.52	226.2	29,300	9.6	3.67×10^6
Db	105	261	1.80	227.07	29,300	18	5.82×10^6
Db	105	262	3.50×10^1	227.94	29,300	30	4.99×10^5
Db	105	263	2.70×10^1	228.81	29,300	56	1.21×10^6
Sg	106	258	2.90×10^{-3}	224.46	35,000	80	1.61×10^{10}
Sg	106	259	4.80×10^{-1}	225.33	35,000	20	2.42×10^7
Sg	106	260	3.60×10^{-3}	226.2	35,000	60	9.70×10^9
Sg	106	261	2.30×10^{-1}	227.07	35,000	1	2.53×10^6
Sg	106	262	6.90×10^{-3}	227.94	35,000	78	6.58×10^9
Sg	106	266	2.10×10^1	231.42	35,000	66	1.83×10^6
Bh	107	262	2.90×10^{-1}	227.94	37,100	20	4.01×10^7
Bh	107	264	1.07	229.68	37,100	14	7.61×10^6